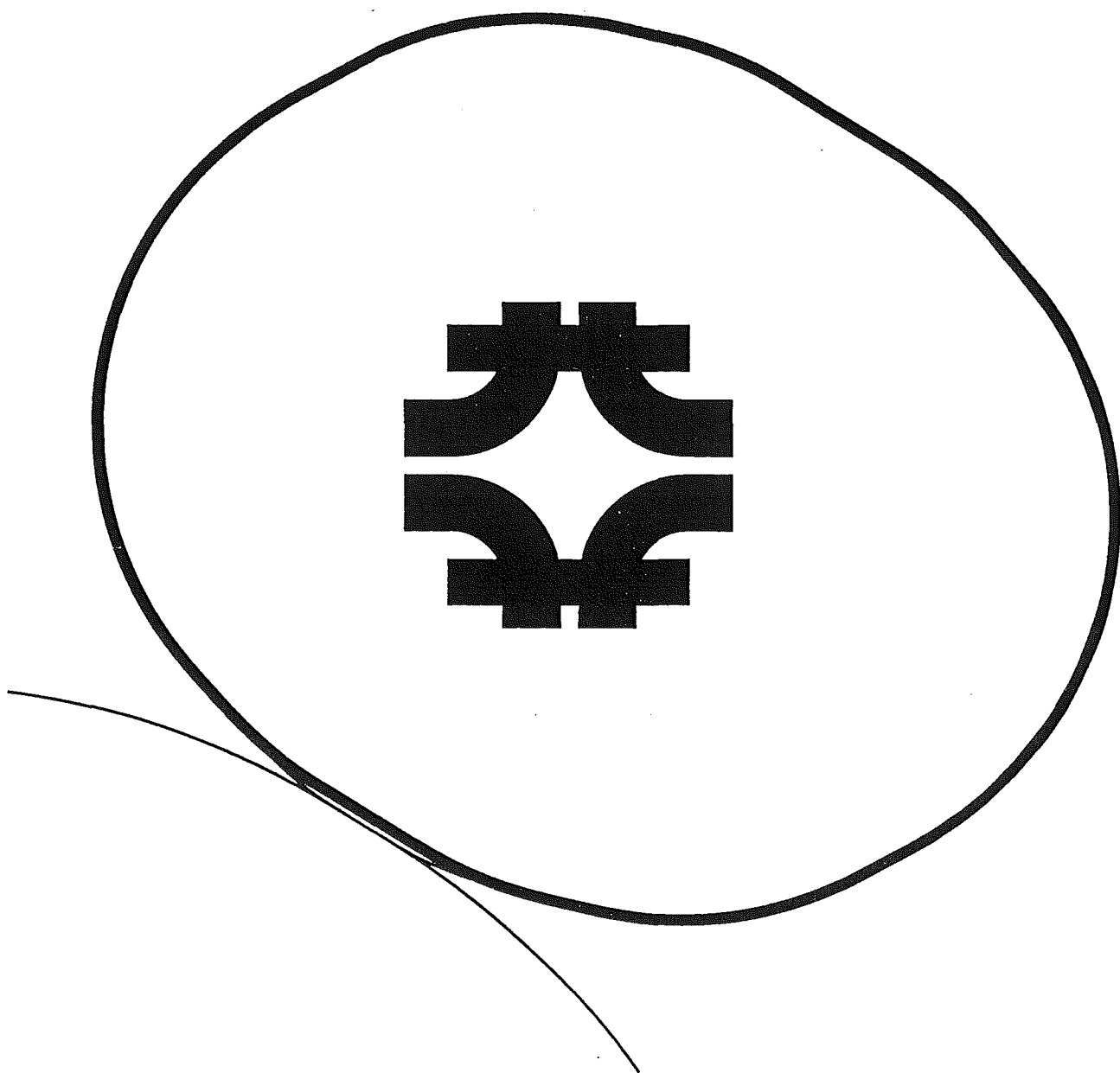


The Fermilab Main Injector



Technical Design Handbook

TABLE OF CONTENTS

	CHAPTER
INTRODUCTION	1
1.1. Role In The Fermilab III Program	
1.2. Performance	
1.3. Operational Modes	
1.4. Organization Of This Report	
ACCELERATOR PHYSICS	2
2.1. Overview	
2.2. Acceleration Cycles	
2.3. Tracking Studies	
2.4 Beamlines And Beam Transfers	
2.5 Transition Crossing	
2.6 Coalescing	
2.7 Slow Extraction	
2.8 Emittance Growth Issues	
2.9 Impedances And Instabilities	
TECHNICAL COMPONENTS	3
WBS 1.1.1. Magnets	3.1
WBS 1.1.2. Vacuum	3.2
WBS 1.1.3. Power Supplies	3.3
WBS 1.1.4. Rf Systems	3.4
WBS 1.1.6. Extraction	3.5
WBS 1.1.8. Instrumentation	3.6
WBS 1.1.9. Controls	3.7
WBS 1.1.10. Safety System	3.8
WBS 1.1.12. Utilities and Abort	3.9
WBS 1.1.13. Installation	3.10
CIVIL CONSTRUCTION	4
APPENDICES	
SCHEDULE 44	
SUMMARY SCHEDULES	
LATTICE FILES	
CONSTRUCTION DRAWINGS	

1. INTRODUCTION

This report contains a description of the design, cost estimate, and construction schedule of the Fermilab Main Injector (FMI) Project. The technical, cost, and schedule baselines for the FMI Project have already been established and may be found in the Fermilab Main Injector Title I Design Report, issued in August 1992. This report updates and expands upon the design and schedule for construction of all subsystem components and associated civil construction described in the Title I Design Report. The facilities described have been designed in conformance with DOE 6430.1A, "United States Department of Energy General Design Criteria."

The purpose of the Fermilab Main Injector Project is to construct a new 150 GeV accelerator, and all required interconnections and interfaces to the existing accelerator complex, on the Fermilab site in support of the Fermilab High Energy Physics (HEP) research program. The construction of this accelerator will result simultaneously in significant enhancements to both the Fermilab collider and fixed target programs. The FMI is to be located south of the Antiproton Source and tangent to the Tevatron ring at the F0 straight section, as shown in Figure 1-1. The FMI will perform all duties currently required of the existing Main Ring. Consequently, operation of the Main Ring will cease following commissioning of the FMI, with a concurrent reduction in the background rates seen in the colliding beam detectors. The performance of the FMI, as measured in terms of protons per second delivered to the antiproton production target or total protons delivered to the Tevatron, is expected to exceed that of the Main Ring by a factor of two to three. In addition the FMI will provide high duty factor 120 GeV beam to the experimental areas during collider operation, a capability which does not presently exist in the Main Ring.

The location, operating energy, and mode of construction of the FMI are chosen to minimize operational impacts on Fermilab's ongoing High Energy Physics program. The area in which the FMI is to be situated is devoid of any underground utilities that might be disturbed during construction, while the separation between the FMI and Tevatron is sufficient to allow construction concurrent with Tevatron operations. The energy capability of the FMI is chosen to match the antiproton production and Tevatron injection energies presently used in the Fermilab complex. The FMI will be built from newly constructed dipole magnets allowing a large portion of the installation process to proceed independent of Tevatron operations. The use of newly designed dipoles is also desirable from the standpoint of enhanced performance and reliability, and results in a reduction of the operating costs by 33% relative to what would be obtained by recycling existing Main Ring magnets.

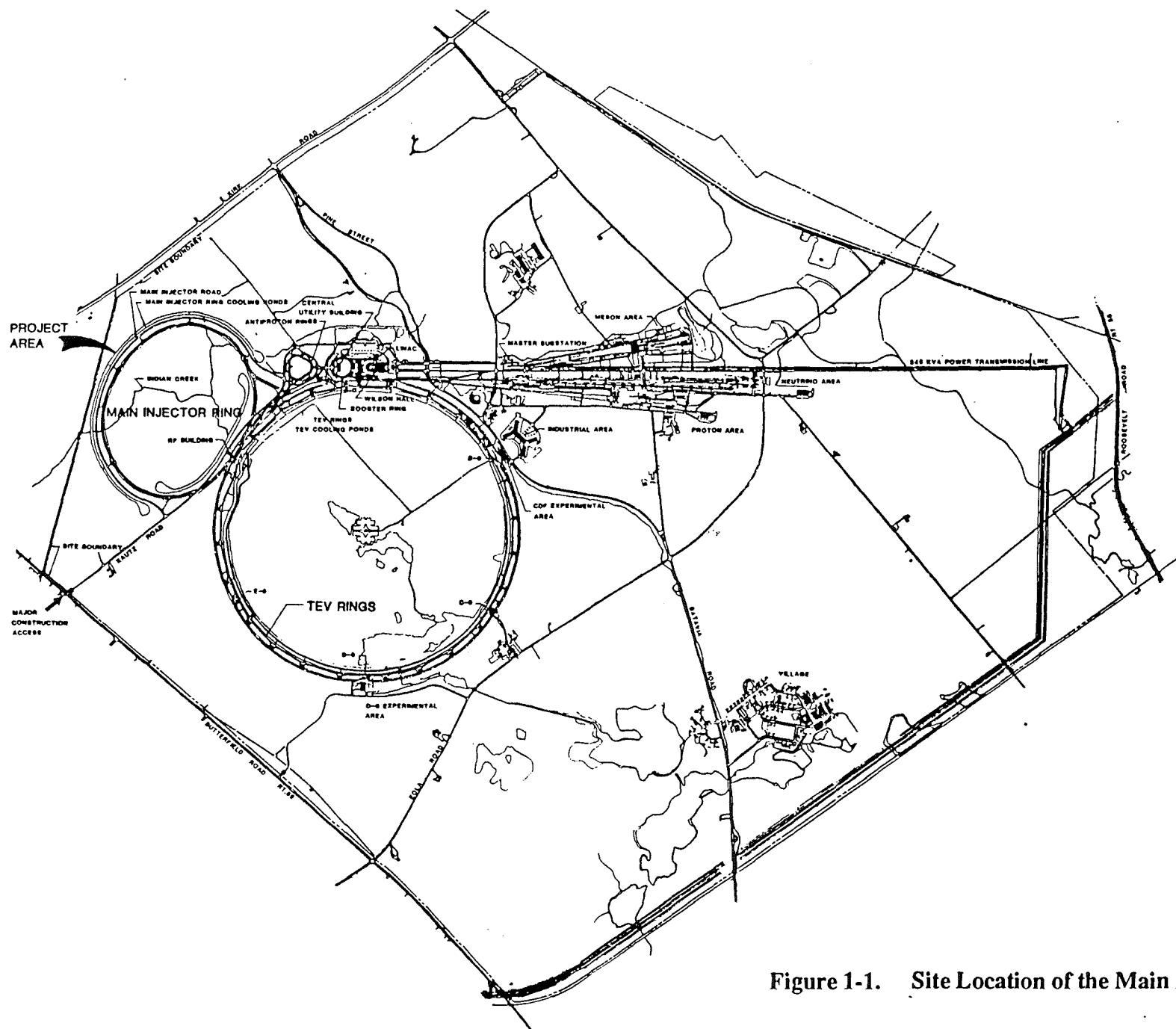


Figure 1-1. Site Location of the Main Injector.

The Total Project Cost (TPC) of the FMI is estimated to be \$259,300,000 including a Total Estimated Construction Cost (TEC) of \$229,600,000 and \$29,700,000 in associated R&D, pre-operating, capital equipment, conceptual design, and spares costs. Included within the scope of the project are all technical and civil construction components associated with the ring itself, with beamlines needed to tie the ring into the existing accelerator complex, and with modifications to the Tevatron and switchyard required to accommodate the relocated injections. The project involves the construction of 15,000 ft of tunnel enclosures, 11 service buildings, and a new 345 kV substation. The FMI ring and all beamline interconnections to existing facilities are shown schematically in Figure 1-2. Construction on the FMI project was initiated in June, 1992. Construction is expected to be completed over a six year period. Title II design of civil construction has been completed by an outside Architectural Engineering firm, Fluor Daniel, with support from the Accelerator Division and from Fermilab Engineering Support Section. Design, assembly, and installation of technical components is being done by Accelerator Division and Technical Support Section personnel. It is anticipated that construction and operation of the new FMI will not require any expansion of the Fermilab permanent staff.

1.1. ROLE IN THE FERMILAB III PROGRAM

The Fermilab Main Injector is the centerpiece of Fermilab's initiative for the 1990s, known as Fermilab III. Some of the more important goals of Fermilab III are to illuminate the properties of the top quark, the most recently discovered fundamental building block of matter, to provide a factor of two increase in the mass scales characterizing possible extensions to the Standard Model, and to support new initiatives in neutral kaon physics and neutrino oscillation investigations. In order to attain these goals Fermilab is planning to attain by the end of the decade a luminosity in excess of $5 \times 10^{31} \text{ cm}^{-2} \text{ sec}^{-1}$ in the Tevatron \bar{p} -p collider.

Several projects completed over the past four years have resulted in a factor of fifteen improvement over the initial $1.0 \times 10^{30} \text{ cm}^{-2} \text{ sec}^{-1}$ luminosity goal of the Tevatron collider. These include upgrades to the Antiproton Source, development of new low- β systems, implementation of a second high luminosity interaction region, development of electrostatic separators, an upgrade of the linac energy from 200 MeV to 400 MeV, and the installation of cold compressors to lower the temperature of the Tevatron. As a result of these enhancements, the Tevatron currently operates with initial luminosities in the range of 1.5 - $2.5 \times 10^{31} \text{ cm}^{-2} \text{ sec}^{-1}$. It is also anticipated that these developments will increase the number of protons delivered from the Tevatron for fixed target physics up to 3×10^{13} per minute.

Further performance improvements require the construction of the FMI. The present bottleneck in the production of antiprotons and in the delivery of intense beams to the Tevatron is

FERMILAB TEVATRON ACCELERATOR WITH MAIN INJECTOR

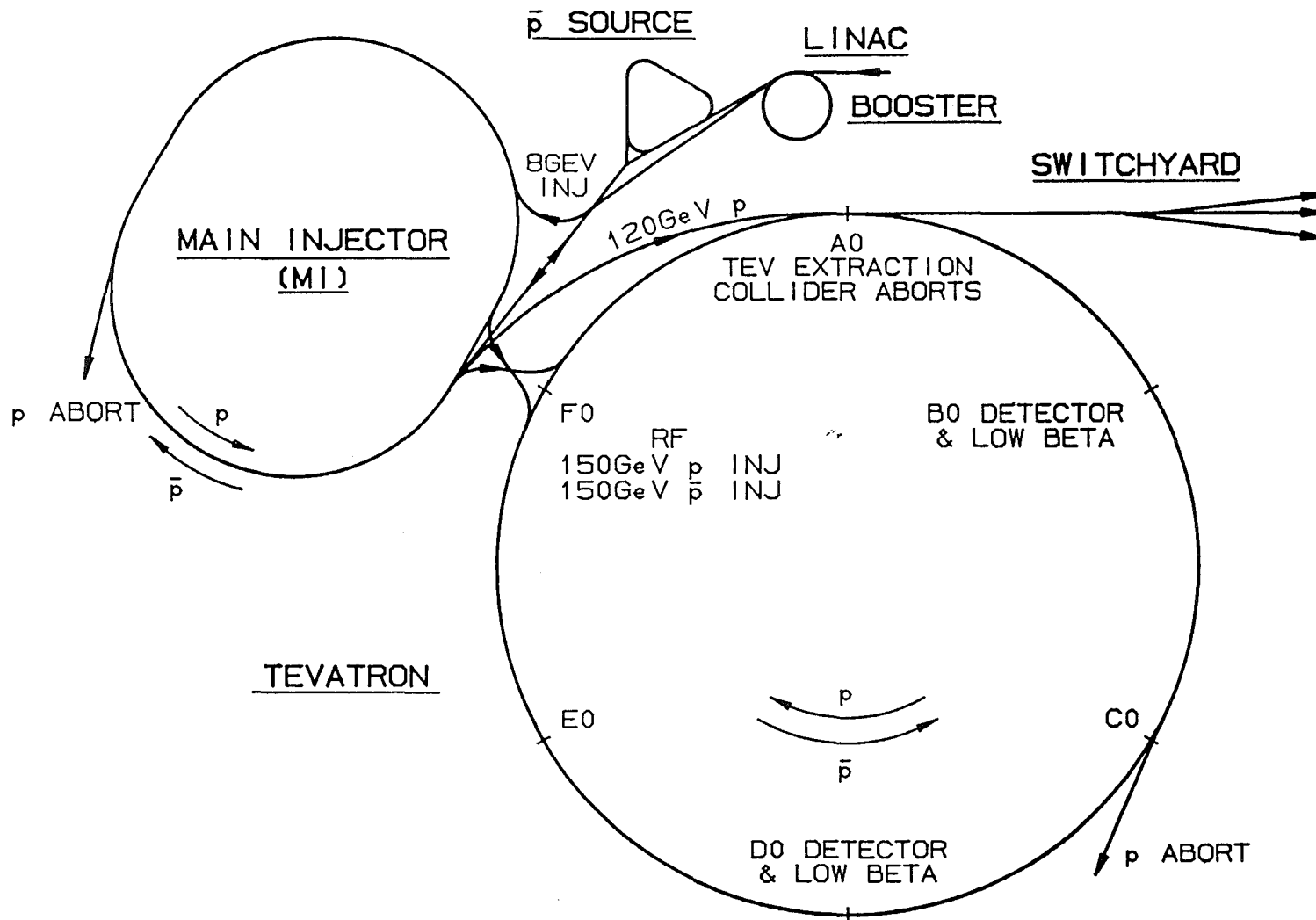


Figure 1-2. Schematic View of the Main Injector Connections to the Booster, Antiproton Source, Tevatron and Switchyard.

the Main Ring. The Main Ring is not capable of accelerating the quantity of protons that can be provided at injection by the 8 GeV Booster. This is for the simple reason that the aperture of the Main Ring ($\sim 12\pi$ mm-mr) is significantly smaller than the beam delivered from the Booster at full intensity. (All emittances in this report are quoted as 95% normalized values.) As a result the full intensity delivered from the Booster cannot be efficiently transmitted through the Main Ring and onto the antiproton production target or into the Tevatron. The restricted aperture in the Main Ring is due to perturbations to the ring that were required for the integration of overpasses and new injection and extraction systems related to operations with antiprotons. With the 400 MeV Linac upgrade the Booster intensities have increased through the Booster/Main Ring combination and the ability to produce large antiproton stacks has been improved. However, the mismatches between Booster/Antiproton Source and Main Ring capabilities remain acute. Only with the construction of the FMI will these mismatches be removed, and the full benefit to the collider and fixed target programs of the recently completed upgrade projects be realized.

The construction of the FMI will also provide beams of up to 3×10^{13} protons at 120 GeV to the experimental areas during collider runs. Such beams are envisioned as being used for supporting certain specialized rare K decay and neutrino experiments which can benefit from the high average intensity deliverable from the FMI, for detector development, and for the debugging and shakedown of fixed target experiments prior to commencement of 1 TeV fixed target runs. The Main Ring as presently configured does not support a slow spill, nor is it felt that implementation of a high intensity slow spill in the existing ring would be feasible in light of the small machine aperture and the need to minimize backgrounds in the collider experiments.

Specifically, benefits expected from the construction of the FMI include:

1. An increase in the number of protons targeted for \bar{p} production from 4.5×10^{15} /hour (current) to 1.2×10^{16} /hour.
2. An increase in the total number of protons which can be delivered to the Tevatron to 6×10^{13} .
3. The ability to accelerate efficiently antiprotons originating in stacks containing in excess of 2×10^{12} antiprotons for injection into the Tevatron collider.
4. The ability to produce proton bunches containing up to 3×10^{11} protons for injection into the Tevatron collider.
5. The reduction of backgrounds and dead time at the CDF and D0 detectors through removal of the Main Ring from the Tevatron enclosure.
6. Provision for slow extracted beams at 120 GeV year-round and potential development of very high intensity, high duty factor (1×10^{13} protons/sec at 120

GeV with 34% duty factor) beams for use in high sensitivity K decay and neutrino experiments.

It is expected that with the construction of the FMI and the completion of planned improvements to the Antiproton Source the antiproton production rate will exceed 1.5×10^{11} antiprotons/hour, and that a luminosity in excess of $5 \times 10^{31} \text{cm}^{-2} \text{sec}^{-1}$ will be supportable in the existing collider.

1.2 PERFORMANCE

The FMI parameter list is given in Table 1-1. It is anticipated that the FMI will perform at a significantly higher level than the existing Main Ring as measured either in terms of protons delivered per cycle, protons delivered per second, or transmission efficiency. For the most part expected improvements in performance are directly related to the optics of the ring. The FMI ring lies in a plane with stronger focusing per unit length than the Main Ring. This means that the maximum β -functions are half as large and the maximum (horizontal) dispersion only a third of the Main Ring, while vertical dispersion is nonexistent. As a result physical beam sizes associated with given transverse and longitudinal emittances are significantly reduced compared to the Main Ring. The elimination of dispersion in the rf regions, raising the level of the injection field, elimination of sagitta, and improved field quality in the dipoles will all have a beneficial impact on beam dynamics. The construction of new, mechanically simpler magnets is expected to yield a highly reliable machine.

The FMI is seven times the circumference of the Booster and slightly more than half the circumference of the existing Main Ring and Tevatron. Six Booster cycles will be required to fill the FMI and two FMI cycles to fill the Tevatron. The FMI is designed to have a transverse admittance of 40p mm-mr (both planes, normalized at 8.9 GeV/c). This is a factor of three larger than that of the existing Main Ring. It is expected that the Linac upgrade will ultimately yield a beam intensity out of the Booster of $5\text{-}7 \times 10^{12}$ protons per batch with $20\text{-}30\pi$ mm-mr transverse and ~ 0.2 eV-sec longitudinal emittance. A single Booster batch needs to be accelerated for antiproton production while six such batches are required to fill the FMI. The FMI should be capable of accepting and accelerating these protons without significant beam loss or degradation of beam quality. Yields out of the FMI for a full ring are expected to lie in the range $3\text{-}4 \times 10^{13}$ protons ($6\text{-}8 \times 10^{13}$ delivered to the Tevatron.) By way of contrast the existing Main Ring is capable of accelerating 1.8×10^{13} protons in 12 batches for delivery to the Tevatron.

Table 1-1: Main Injector Parameter List

Circumference	3319.419	m
Injection Momentum	8.9	GeV/c
Peak Momentum	150	GeV/c
Minimum Cycle Time (@ 120 GeV)	< 1.5	s
Minimum Cycle Time (@ 150 GeV)	2.4	s
Number of Protons	3×10^{13}	
Number of Bunches	498	
Protons/Bunch	6×10^{10}	
Max. Courant-Snyder Amplitude Function (β_{\max})	57	m
Maximum Dispersion Function	1.9	m
Phase Advance per Cell	90	degrees
Nominal Horizontal Tune	26.425	
Nominal Vertical Tune	25.415	
Natural Chromaticity (H)	-33.6	
Natural Chromaticity (V)	-33.9	
Transverse Admittance (@ 8.9 GeV)	$> 40\pi$	mm-mr
Longitudinal Admittance	> 0.5	eVs
Transverse Emittance (Normalized)	12π	mm-mr
Longitudinal Emittance	0.2	eVs
Harmonic Number (@ 53 MHz)	588	
RF Frequency (Injection)	52.8	MHz
RF Frequency (Extraction)	53.1	MHz
RF Voltage	4	MV
Transition Gamma	21.8	
Superperiodicity	2	
Number of Straight Sections	8	
Length of Standard Cell	34.5772	m
Length of Dispersion-Suppressor Cell	25.9330	m
Number of Dipoles	216/128	
Dipole Lengths	6.1/4.1	m
Dipole Field (@ 150 GeV)	17.2	kG
Dipole Field (@ 8.9 GeV)	1.0	kG
Number of Quadrupoles	128/32/48	
Quadrupole Lengths	2.13/2.54/2.95	m
Quadrupole Gradient at 150 GeV	200	kG/m
Number of Quadrupole Busses	2	

The power supply and magnet system is designed to allow a significant increase in the number of 120 GeV acceleration cycles that can be run each hour for antiproton production, as well as to allow a 120 GeV slow spill with a 35% duty factor. The cycle time at 120 GeV can be as low as 1.5 seconds. This is believed to represent the maximum rate at which the Antiproton Source could ultimately stack antiprotons, and is to be compared to the current Main Ring capability of 2.4 seconds. The FMI dipole magnets are designed with twice the total cross section of copper and half as many turns as existing Main Ring dipoles. This keeps the total power dissipated in the dipoles during antiproton production at roughly the same level as in present operations while keeping the number of power supplies and service buildings low.

1.3 OPERATIONAL MODES

At least four distinct roles for the FMI have been identified along with five corresponding acceleration cycles. These are listed in Table 1-2. More detailed description of the acceleration cycles and power supply requirements are given in Chapter 2 of this report.

Table 1-2: Main Injector Operational Modes

	<u>Operational Mode</u>	<u>Energy</u>	<u>Cycle</u>	<u>Flattop</u>	<u>Protons</u>
1)	Antiproton Production	120 GeV	1.5 sec	0.04 sec	5×10^{12}
2)	Fixed Target Injection	150	2.4	0.25	3×10^{12}
3)	Collider Injection	150	4.0	1.45	5×10^{12}
4a)	High Intensity Slow Spill	120	2.9	1.0	3×10^{13}
4b)	High Intensity Fast Spill	120	1.9	0.04	3×10^{13}

1) In the antiproton production mode a single Booster batch containing 5×10^{12} protons is injected into the FMI at 8.9 GeV. These protons are accelerated to 120 GeV and extracted in a single turn for delivery to the antiproton production target. As mentioned earlier, it is anticipated that with this flux of protons onto the target and expected improvements in the Antiproton Source the antiproton production rate will exceed 1.5×10^{11} /hour.

- 2) For fixed target injection the FMI is filled with six Booster batches, each containing 5×10^{12} protons at 8.9 GeV. Since the Booster cycles at 15 Hz, 0.4 seconds are required to fill the FMI. The beam is accelerated to 150 GeV, clogged, and extracted in a single turn for delivery to the Tevatron. The FMI is capable of cycling to 150 GeV every 2.4 seconds for short periods of time. Two FMI cycles are required to fill the Tevatron at 150 GeV at one minute intervals.
- 3) The FMI operates on a 4 second, 150 GeV cycle for delivery of beam to the Tevatron for collider operations. The acceleration cycle and beam manipulations are the similar for protons and antiprotons. A 1.45 second flat-top is required for bunch coalescing and clogging of the beams prior to injection into the Tevatron. Under the currently envisioned filling scenario a maximum of 12 cycles of the FMI are required to load the Tevatron with protons and antiprotons. Assuming a one minute Antiproton Source cycle time, this results in a 10 minute collider fill time. It is anticipated that the collider will require filling approximately every 20 hours.
- 4) A much higher intensity, high duty factor (34%) beam can be delivered at 120 GeV with a 2.9 second cycle time. The average proton current delivered is about $2 \mu\text{A}$ (3×10^{13} protons/2.9 seconds). Running in this mode does not put any peak power demands on the power supply system beyond those imposed by the antiproton production cycle, but it does expend 67% more average power. This cycle can also be used to provide test beams to the experimental areas during collider running. In this instance it is likely that a much lower cycle rate, accompanied by a much lower average power, would satisfy experimenters' needs. Additionally, a high intensity, low duty factor beam can be delivered at 120 GeV with a 1.9 second cycle time for the production of high flux neutrino beams.

Combinations of the above operational modes are also possible. One such example is simultaneous operation for antiproton production and high intensity slow spill. One could load the FMI with six Booster batches containing 3×10^{13} protons, accelerate to 120 GeV, fast extract one batch to the antiproton production target, and resonantly extract the remainder of the beam over a period ranging from a few milliseconds to a second. This would produce a correspondingly lower average antiproton flux into the Source and 83% of the average intensity of the dedicated scenarios listed in Table 1-2.

1.4 ORGANIZATION OF THIS REPORT

This report is organized into four chapters with several appendices. Chapter 1 is the Introduction. Chapter 2 is a summary of the accelerator physics issues of the FMI: lattice description, accelerator cycles, tracking studies, impedance calculations, beamline design, etc. Chapter 3 contains a description of the technical component subsystems as well as overviews of the performance objectives and design specifications. Discussion and descriptions of technical component subsystems are organized to follow the Work Breakdown Structure (WBS) of the project. Chapter 4 summarizes the civil construction for the Main Injector. The Appendices contain the current Construction Project Data Sheet (Schedule 44) for the FMI (with information on the current cost estimate and funding profile); lattice files for the ring and beamlines; detailed project schedule summaries produced from the Microsoft Project[®] detailed schedules for the civil construction and each Level 3 WBS; and a combination of the original Title 1 drawings (including revisions for the 8 GeV line) and copies of selected drawings from the construction package bid sets.

WBS Organization

Chapter 3 is organized according to the Work Breakdown Structure (WBS) that has been adopted for the FMI project. All technical components are contained in WBS category 1.1. The third digit of the WBS describes the component type: 1 = magnet, 2 = vacuum, 3 = power supply, etc. The fourth digit indicates the location in which that component will be used: 1 = Main Injector ring, 2 = 8 GeV line, 3 = 150 GeV proton transfer line, etc. To describe a general system which is used throughout the Main Injector, or in a number of different beamlines, the fourth digit is set to 10. The fifth level provides further definition of system or component subtype. Schedules for the design, procurement, fabrication and installation of major systems are included as figures in Chapter 3.

CHAPTER 2. ACCELERATOR PHYSICS

2.1. OVERVIEW

2.2. ACCELERATION CYCLES

2.3 TRACKING STUDIES

2.4. BEAMLINES AND BEAM TRANSFERS

2.5 TRANSITION CROSSING

2.6 COALESCING

2.7 SLOW EXTRACTION

2.8 EMITTANCE GROWTH ISSUES

2.9 IMPEDANCES AND INSTABILITIES

2.1. OVERVIEW

The FMI is a 150 GeV accelerator with a circumference 28/53 times that of the existing Main Ring. The primary design goals are to increase the admittance to 40π mm-mr and lower the cycle time to 1.5 sec. The FMI will be situated tangent to the Tevatron at the F0 straight section on the southwest side of the Fermilab site. Other possible sites have been considered, including locations inside the existing Tevatron ring, but these were deemed less desirable than the site shown in this report. The FMI, as described here, is constructed using newly designed (conventional) dipole magnets. The decision to build new magnets is based on considerations of field quality, aperture, and reliability. With the major exception of the dipoles, existing components from the Main Ring are for the most part recycled. Such components specifically include quadrupoles and the radio frequency (rf) systems. The use of all 18 existing rf cavities in a ring roughly half the size of the Main Ring will support an acceleration rate of 240 GeV/sec as compared to 120 GeV/sec in the present Main Ring. The FMI power supply systems are designed to support this rate.

Lattice

The design of the FMI is driven by a number of considerations. Given the preferred site, a maximum physical size of the ring is established by the proximity of the Fermilab site boundary. This in turn leads to a minimum needed field strength in the magnets. The number and location of the straight sections is determined by the roles the ring is required to play. In all phases of design the motivation has been to produce a lattice in which the transverse beam size is smaller than in the Main Ring over the energy range 8 to 150 GeV. The two lattice parameters which affect beam size are the beta function, β , and the dispersion, η . In this design β is kept small by the short distance between quadrupoles. This is a cost effective approach because the quadrupoles will be

taken from the existing Main Ring. The η is kept smaller in the FMI than in the Main Ring by carefully matching dispersion around all straight section insertions. Dispersion matching ensures that the maximum dispersion in the ring is no larger than the maximum dispersion in the standard cell. The FMI will not have overpasses, in contrast to the present Main Ring, and therefore, the vertical dispersion is zero.

Lattice Design

Figure 2.1-1 shows the FMI geometric layout. The standard cell of the FMI is, like the Main Ring, a FODO design but with two dipoles between the quadrupoles as shown in Figure 2.1-2. (The Main Ring has four dipoles between quadrupoles.) The interelement spacing is the same as in the present Main Ring so that the length of the half-cell is shorter by the length of two dipoles and the short drift spaces which follow them, i.e. by about half. Because of the shorter circumference, there are fewer than half as many dipoles as in the Main Ring.

The lattice incorporates two different types of cells, the normal 17.2886-m FODO cells and the 12.9665-m FODO dispersion-suppressor cells. The dispersion-suppressor cells feature shorter dipoles, and match the horizontal dispersion to zero in the straight sections. There are 72 normal cells (54 in the arcs and 18 within the straight sections), and 32 dispersion suppressing cells. The advantages of the lattice include:

- i. Zero dispersion in the straight sections. This reduces the horizontal beam size, which in turn makes beam transfers easier to accomplish.
- ii. The β -functions in the straight sections and in the dipoles surrounding the straight sections are the same as, or less than, those in the normal FODO cells, affording more clearance for the beam and tolerance in steering at transfer time.
- iii. A 136-m long rf straight.
- iv. A lattice which accommodates transfer lines to the Tevatron that match the vertical dispersion exactly.
- v. A separation of 11.8 m between the FMI and the Tevatron, which permits phased construction of the FMI enclosure.

Having fewer dipoles than the Main Ring leads to higher fields and a larger bending angle. The resulting sagitta in a 6 m dipole is 16 mm. The new dipoles will be built with a curvature which eliminates loss of aperture due to sagitta. A 90° phase advance per cell is chosen, resulting in a maximum β in the cells of 58 meters and a maximum η in the cells of 1.9 meters. By comparison the Main Ring has maximum β and η of 110 m and 6.6 m, respectively. Thus the beam size due to transverse emittance is only 70% of what it is presently, and the maximum beam

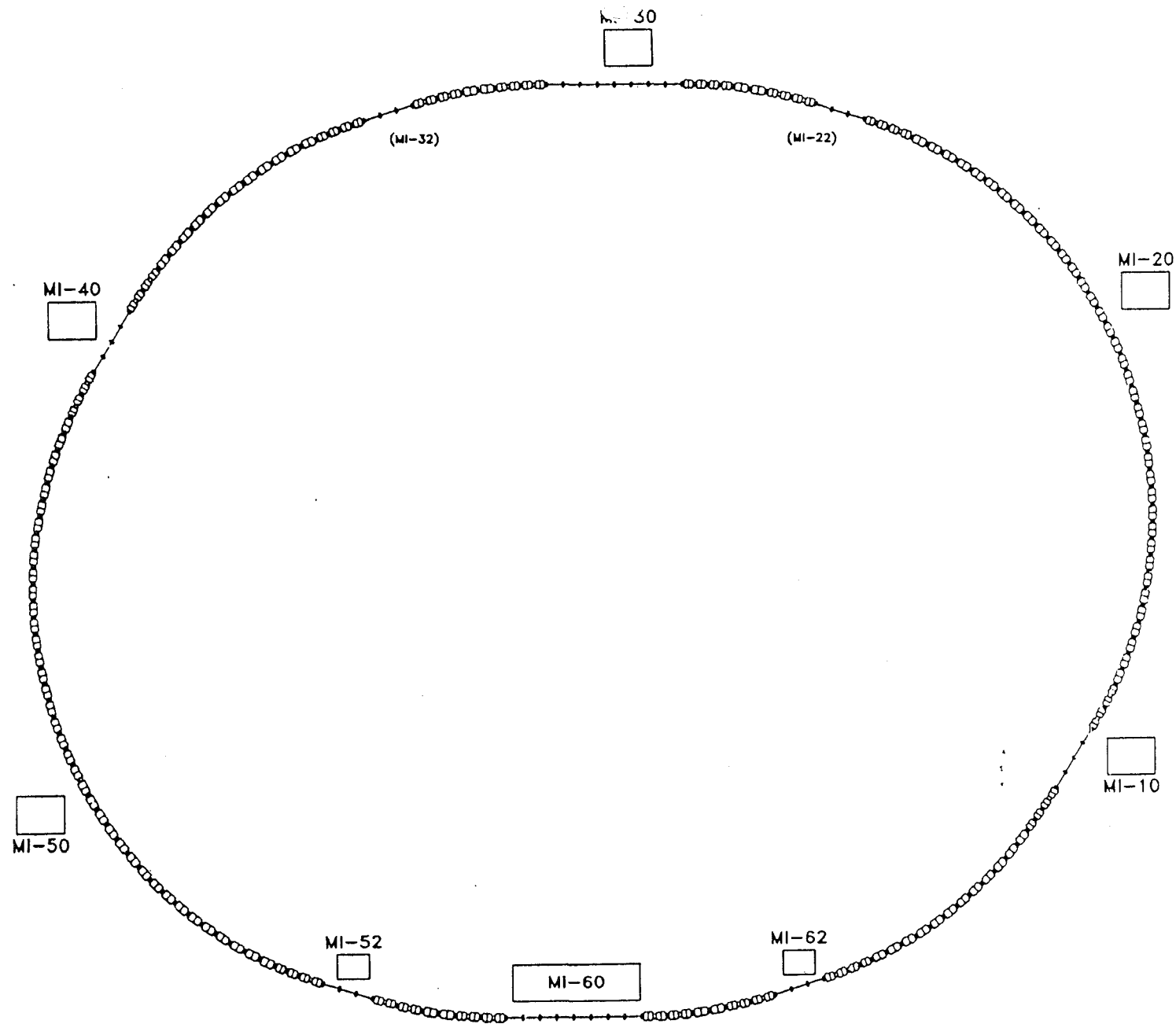


Figure 2.1-1. Main Injector Geometric Layout Showing Locations of Service Buildings and Straight Sections.

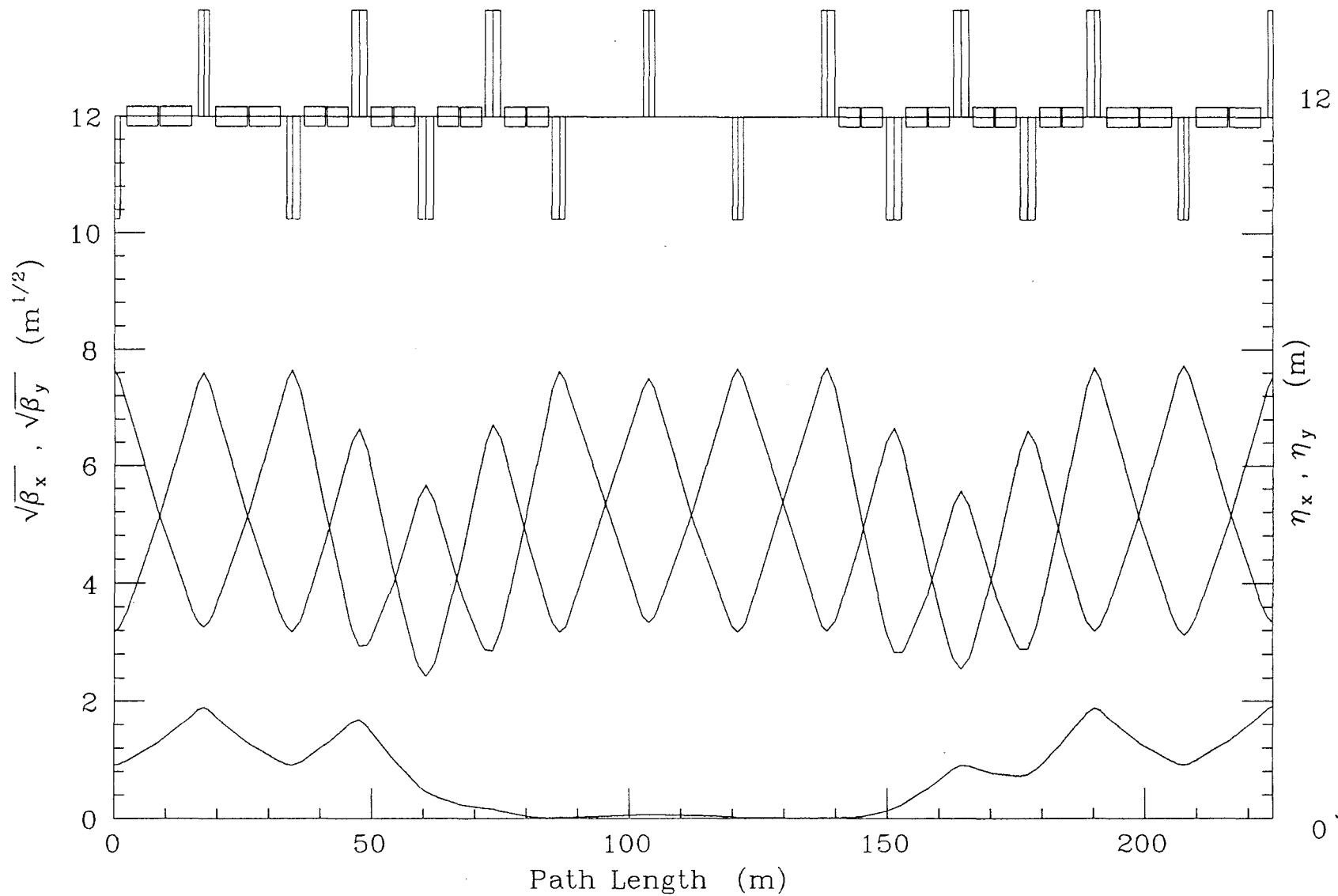


Figure 2.1-2. Main Injector FODO Lattice Showing (Left to Right) One Normal Cell, Two Dispersion-Suppressor Cells, Three Straight-Section Half-Cells, Two Dispersion-Suppressor Cells, and One Normal Cell.

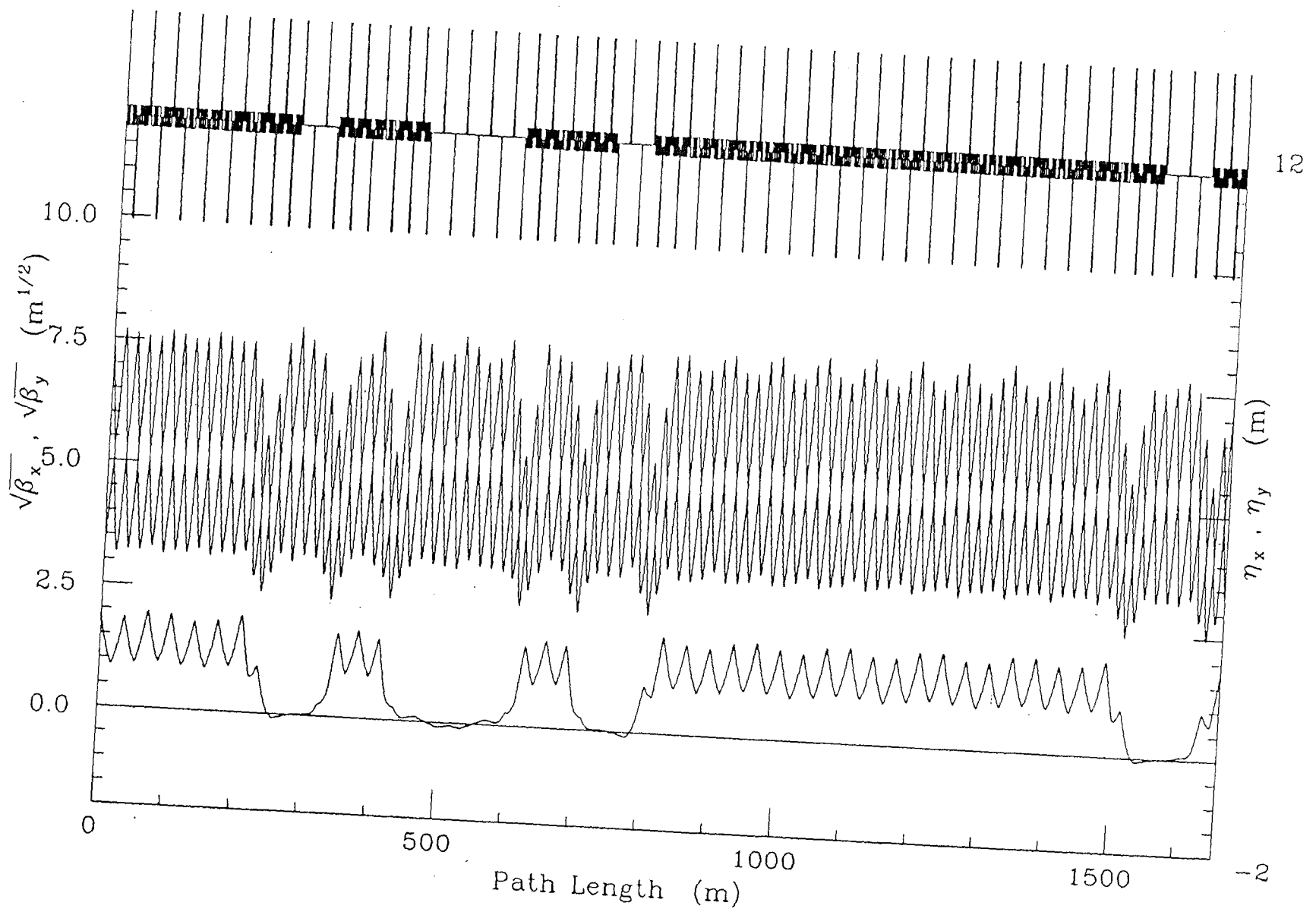


Figure 2.1-3. Main Injector Lattice Functions for One-Half the Ring.

size due to momentum spread is down by a factor of 3 from the Main Ring. The ring is designed to have twofold rotational symmetry; Figure 2.1-3 shows the FMI lattice functions for one-half the ring. Lattice functions, as generated by the program MAD, are tabulated in Appendix A.

The 344 dipoles are excited by 12 power supplies located in six service buildings; the locations of these service buildings are used as the basis for numbering locations in the FMI ring.

The FMI contains eight straight sections, as shown in Figure 2.1-1. Their numbering and their functions are as follows:

- MI-10 - 8 GeV proton injection
- MI-22 - (unused)
- MI-30 - (unused)
- MI-32 - (unused)
- MI-40 - proton abort
- MI-52 - 150/120 GeV proton extraction; 8 GeV antiproton injection
- MI-60 - FMI rf section
- MI-62 - 150 GeV antiproton extraction

All straight sections are obtained by omitting dipoles while retaining the standard 17.29-m quadrupole spacing. There are three different lengths of straight sections. Straight sections MI-10 and MI-40 are 69 m long (two cells), straight sections MI-22, -32, -52, and -62 are 52 m long (one and one half cells), and straight sections MI-30 and MI-60 are 138 m long (four cells). Straight section MI-60 is used for the rf; its length will allow flexible spacing of the rf cavities and provide generous free space for diagnostic beam pickups.

Three different quadrupole lengths are required: 2.13-m quadrupoles for the normal cells, 2.95-m quadrupoles for the dispersion-suppressor cells, and 2.54-m quadrupoles at the boundary between the two types of cells. The lengths are such that all quadrupoles are powered off two main quadrupoles busses. All straight section insertions are dispersion matched to the cells. With at least 135° of phase advance in each straight section, there is space within the long straight for kickers and septa, a situation not provided for in the present Main Ring lattice.

The long straight sections are capable of beam extraction at the highest FMI energy. Due to the fact the ring lies 11 meters from the Tevatron, two of these (MI-52, MI-62) are required to provide injection into the Tevatron, one each for protons and antiprotons. On the opposite side of the ring two straight sections (MI-22, MI-32) are added for symmetry. MI-10 is necessary for injection of protons from the Booster, and MI-40 is placed symmetrically for the proton abort.

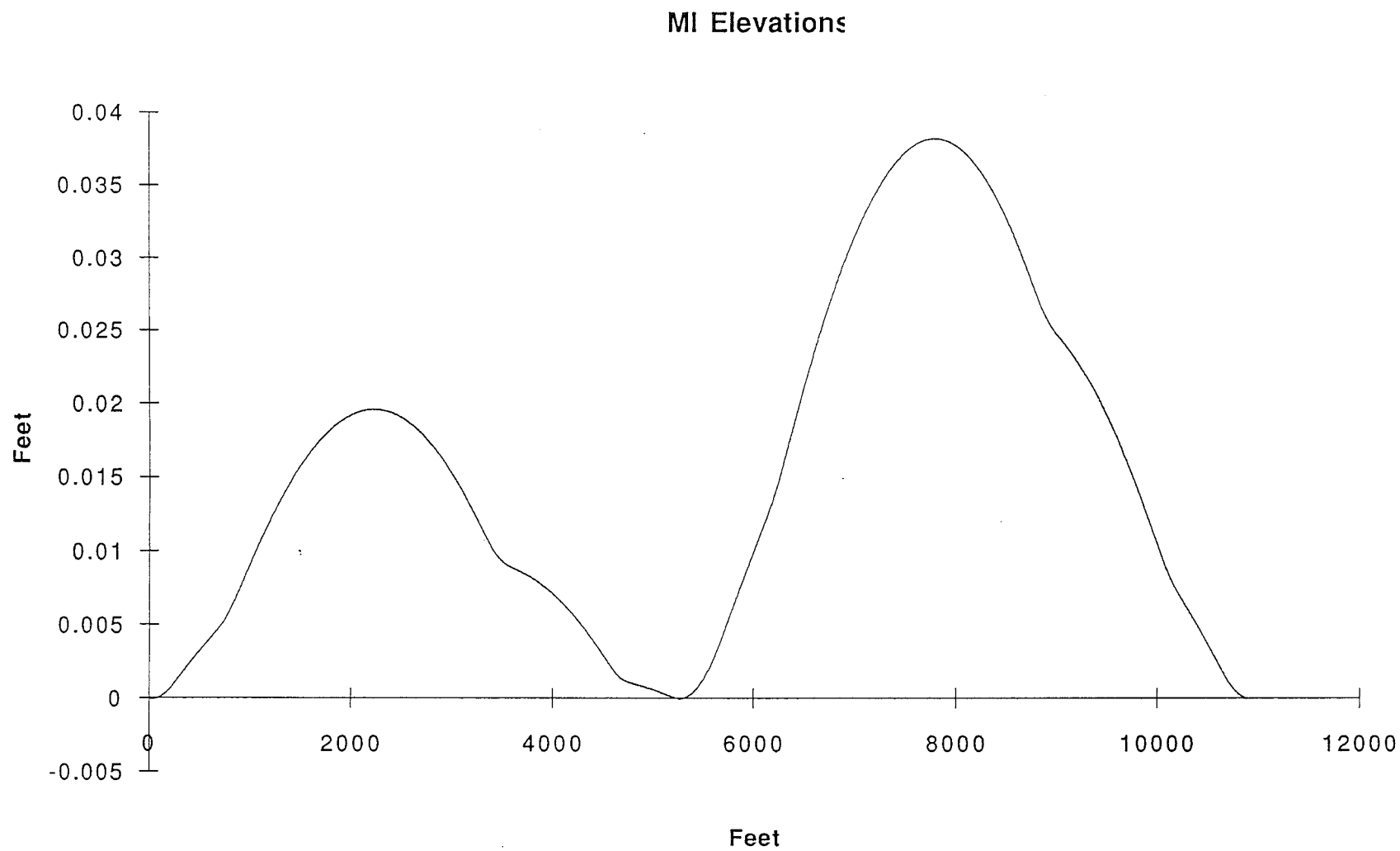


Figure 2.1-4. Variation of Main Injector Beam Height vs. Position

The FMI is situated in the southwest corner of the Fermilab site. The details of its location are determined by requirements for transfers of both protons and antiprotons into the Tevatron. The MI-60 straight section is parallel to the Tevatron F0 straight section, separated from it by 11.823 m (38' 9.5") horizontally and 2.3253 m (7' 7.5") vertically. The reference point defining the plane containing the Main Injector design orbit lies at the intersection of a line from the center of the Tevatron ring and passing near F0 normal to the F0 straight section, and a line parallel to the MI-60 straight section and equidistant from the MI-60 and MI-30 straight sections. Gravity at this point defines the normal to the plane. The plane containing the Main Injector orbit dips at an angle of 0.231 milliradians (47.65") toward the southwest corner (project coordinates) of the site.

The nominal elevation of the FMI was specified in earlier design reports to be 2.332 m below the Tevatron beam. To account for the relative tilt of the Tevatron and the FMI, it is now specified that MI-52 and MI-62 are placed at this elevation. The line from MI-52 to MI-62 is offset 28.789277 m from the MI-60 straight section and parallel to it. The tilt of the FMI then places the MI-60 straight section 2.3253 m below the Tevatron beanline.

The FMI is designed to be a planar machine, but because the ring is eccentric, the elevation varies around the ring. The minimum elevation is in the MI-30 and MI-60 straight sections and is about 11.6 mm below the maximum which occurs in the 100 arc near Q123 (northwest). A second elevation maximum, about 6.0 mm above the minimum, occurs in the 400 arc near Q425 (southeast). The variation in beam elevation, relative to a surface which follows the curvature of the earth, is shown in Figure 2.1-4. The elevation of the MI-60 and MI-30 straight sections is 715' 8.953", 2.3253 m below the elevation of the Tevatron (723' 4.5"). The center of the MI-60 straight section lies directly opposite the transfer point into the Tevatron, which is 13.222 m (43' 4.6") downstream of the center of the F0 straight section. For reference, the FMI tunnel floor is at a constant (locally-defined) elevation of 713' 6", and the MR/Tevatron tunnel floor is at 722' 6".

2.2. ACCELERATION CYCLES

There are four basic types of acceleration cycle, one for each of the four operational modes for the FMI:

1. Antiproton production

120 GeV top energy, 40 ms flattop

1 Booster batch, 5×10^{12} protons

single turn extraction

1.467 s cycle

2. FMI fixed target experiments

120 GeV top energy, 1 s flattop

6 Booster batches, 3×10^{13} protons

resonant extraction

a) slow spill, 1 s

2.867 s cycle

b) fast spill, ~ 1 ms

1.867 s cycle

3. Tevatron injection for fixed target experiments

Two Main Injector cycles per Tevatron cycle

150 GeV top energy, 250 ms flattop

6 Booster batches, 3×10^{13} protons

single turn extraction

2.4 s cycle

4. Tevatron Collider injection

150 GeV top energy, 1.4 s flattop

single turn extraction

4 s cycle

a) proton injection

3 Main Injector cycles to fill Tevatron

12 Booster batches, 4.6×10^{12} protons

b) antiproton injection

9 Main Injector cycles to fill Tevatron

1 Accumulator batch, 1.5×10^{11} antiprotons

Figure 2.2-1 gives a momentum program and the resulting total dipole bus voltage for each basic type. These examples embody conservative extrapolations from Main Ring practice and do not require rf or power supplies to run close to design limits. The ramps incorporate the changes in bend bus resistance and inductance discussed in Chapter 3.3. The bus resistance is assumed to be 0.30Ω , and the inductance is 0.67 H. The lower resistance (relative to the value used in Title 1 of 0.32Ω) allows increasing the ramp rate to 270 GeV/c/s while limiting the power supply voltage to $\sim 11,500$ V. On the other hand, the smaller resistance requires a slower invert; the power supply voltage during invert is $\sim 10,700$ V. The gain during convert does not quite offset the increase in the invert time, and the injection dwell period has been decreased by 0.008 s in order to keep the cycle time 1.4667 s for the pbar production cycle. The 2.8667 s, 120 GeV cycle has been assumed to be run in rapid succession for calculations of rms power when

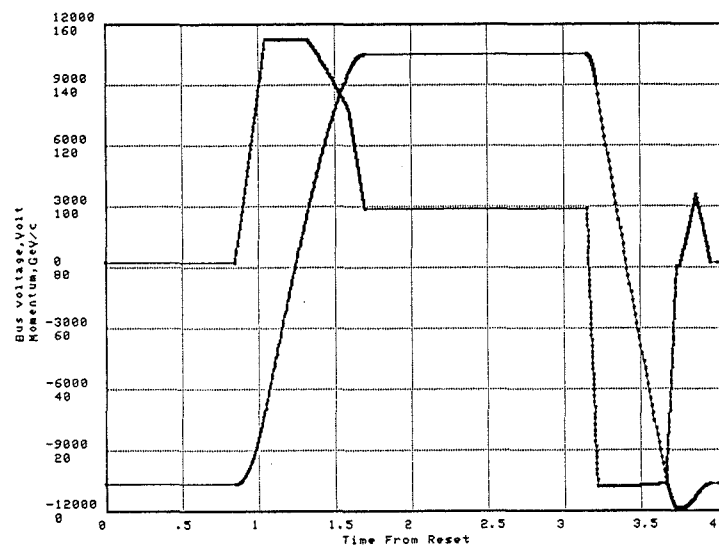
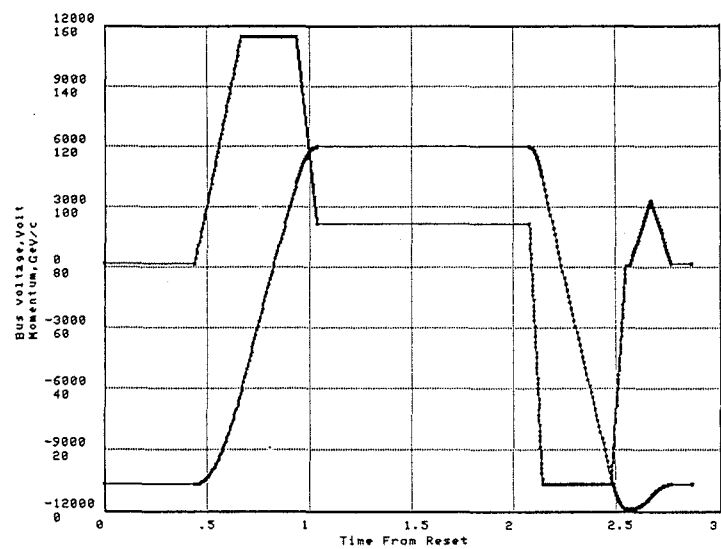
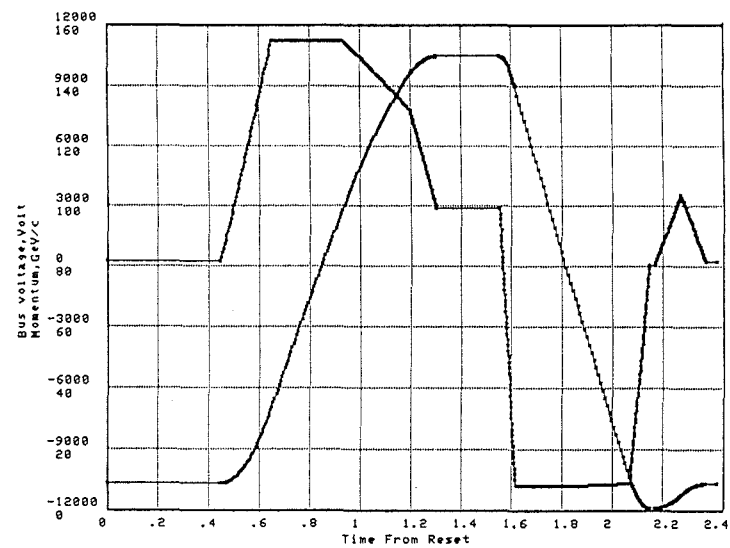
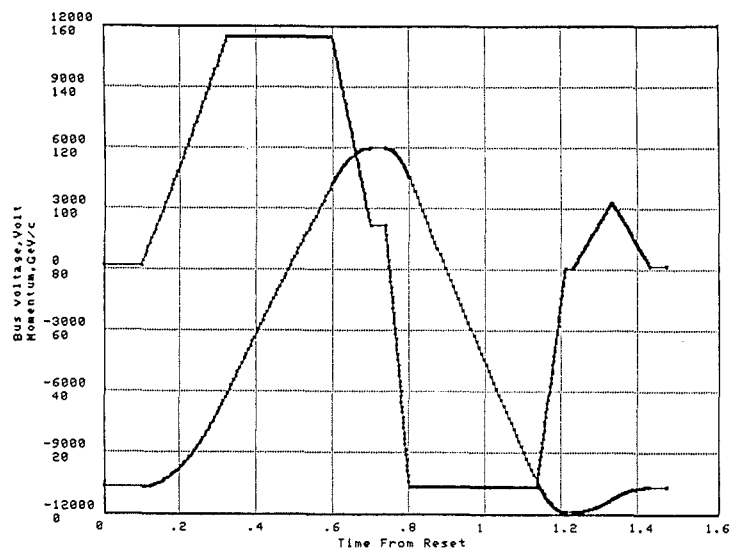


Figure 2.2-1. Acceleration Cycles:

- a. 120 GeV Antiproton Production
- b. 120 GeV Slow Spill

- c. 150 GeV Fixed Target Injection
- d. 150 GeV Collider Injection.

designing the cooling systems and pond sizes, and for determining feeder currents and capacities. The cycle times are required to be a multiple of the Booster 15-Hz repetition rate, 0.667 s.

A useful variant on the 120 GeV fixed target cycles is to fast extract one Booster batch for antiproton production before resonantly extracting to the target. This approach, referred to as "mixed mode", is extremely attractive for fulfilling the demand for protons per hour. The sixth Booster batch is injected into the center of the 3.2 μ sec gap that exists after the first five batches are injected. The beam is accelerated to 120 GeV, the sixth batch is extracted in a single turn to the antiproton production target, and then the remaining beam is extracted by resonant extraction to Swithyard. For a loss of 17 % in fixed target intensity the two types of operation are efficiently combined. The loss in stacking rate is about 50% when the long spill is needed but only about 20% when the short spill is used. The interleaving of single-use cycles is less efficient. For example, when a slow spill cycle is interleaved with an antiproton production cycle, the slow spill time is reduced by a third, and the antiproton production is reduced by two thirds. The expected number of protons per hour than can be delivered in the various modes are given in Table 2.2-1.

Table 2.2-1.
Protons Per Hour Under Various Modes of Operation

<u>Mode</u>	<u>Cycle Time</u>	<u>Protons/Hour</u>		
		<u>AP Target</u>	<u>Fast Spill</u>	<u>Slow Spill</u>
Antiproton Production	1.466 sec	1.2×10^{16}	-	-
Fast Spill	1.866	-	5.8×10^{16}	-
Slow Spill	2.866	-	-	3.8×10^{16}
Mixed - AP + Fast Spill	2.000	0.9×10^{16}	4.5×10^{16}	-
Mixed - AP + Slow Spill	3.000	0.6×10^{16}	-	3.0×10^{16}

Assumptions: 6×10^{10} protons per bunch, and additional time is required for bunch manipulations and turning off magnetic switch at F17 in mixed modes.

The Tevatron is filled for fixed target physics by two FMI injection cycles. Average feeder power sets a limit on the frequency of the injection cycles; they can not be repeated more than a few times per Tevatron cycle. The operating limits for the magnet power supply and the rf systems are discussed in Chapters 3.3 and 3.4 respectively.

The Tevatron collider injection cycle is a 4.0 second cycle with a 1.4 second flat top at 150 GeV for coalescing. Three Main Injector cycles are required to fill the Tevatron. Each Main Injector cycle requires the Booster to inject beam as follows. Each Booster cycle injects a small

number of bunches, typically 11 bunches; the remaining bunches from the Booster go to the Booster dump. Successive injections place the subsequent bunches 21 rf-buckets apart (center-to-center) for 36-on-36 operation in the Tevatron. Twelve Booster cycles are required to inject the proper number of proton bunches, which fill approximately one-half of the Main Injector circumference. The bunches are then accelerated to 150 GeV, coalesced, and injected into the Tevatron in a single turn. The cycle for injecting antiprotons into the Tevatron will have an identical power supply program. On each cycle, one transfer from the Antiproton Source injects four groups of 11 bunches, the groups being spaced 21 rf-buckets apart (center-to-center), which are accelerated to 150 GeV, coalesced, and injected into the Tevatron in a single turn. Nine Main Injector cycles are required to load the 36 antiproton bunches.

There are two accelerator physics concerns which could lead to changes in the details of the magnet ramps, especially the initial parabola. The first relates to the Main Ring experience that bunches are seriously disturbed if the synchrotron frequency approaches 720 Hz for even a few milliseconds. Although the FMI has improvements on the Main Ring magnet power supply, there is some possibility that the initial parabola might need to be slowed down to provide adequate bucket area without approaching this critical value for the synchrotron frequency. It is not anticipated that this will be a dominant concern because it will be possible to pass through the 720 Hz region quite fast from a higher value. On the other hand, it may be highly advantageous to speed up the initial parabola as much as the rf and power supplies will allow to pass the transition energy quickly. Figure 2.2-2 shows a ramp having an initial parabola with second derivative of 4500 GeV/c/s^2 which reaches 280 GeV/c/s before transition. The cycle time has also been reduced by one 15-Hz Booster cycle, to 1.400 s. For comparison, the ramps shown in Figure 2.2-1 reach 270 GeV/c/s at 39 GeV using a second derivative 1200 GeV/c/s^2 , and the ramp rate at transition is 168 GeV/c/s . The feasibility of this less conservative ramp is considered somewhat further in Chapters 3.3 and 3.4.

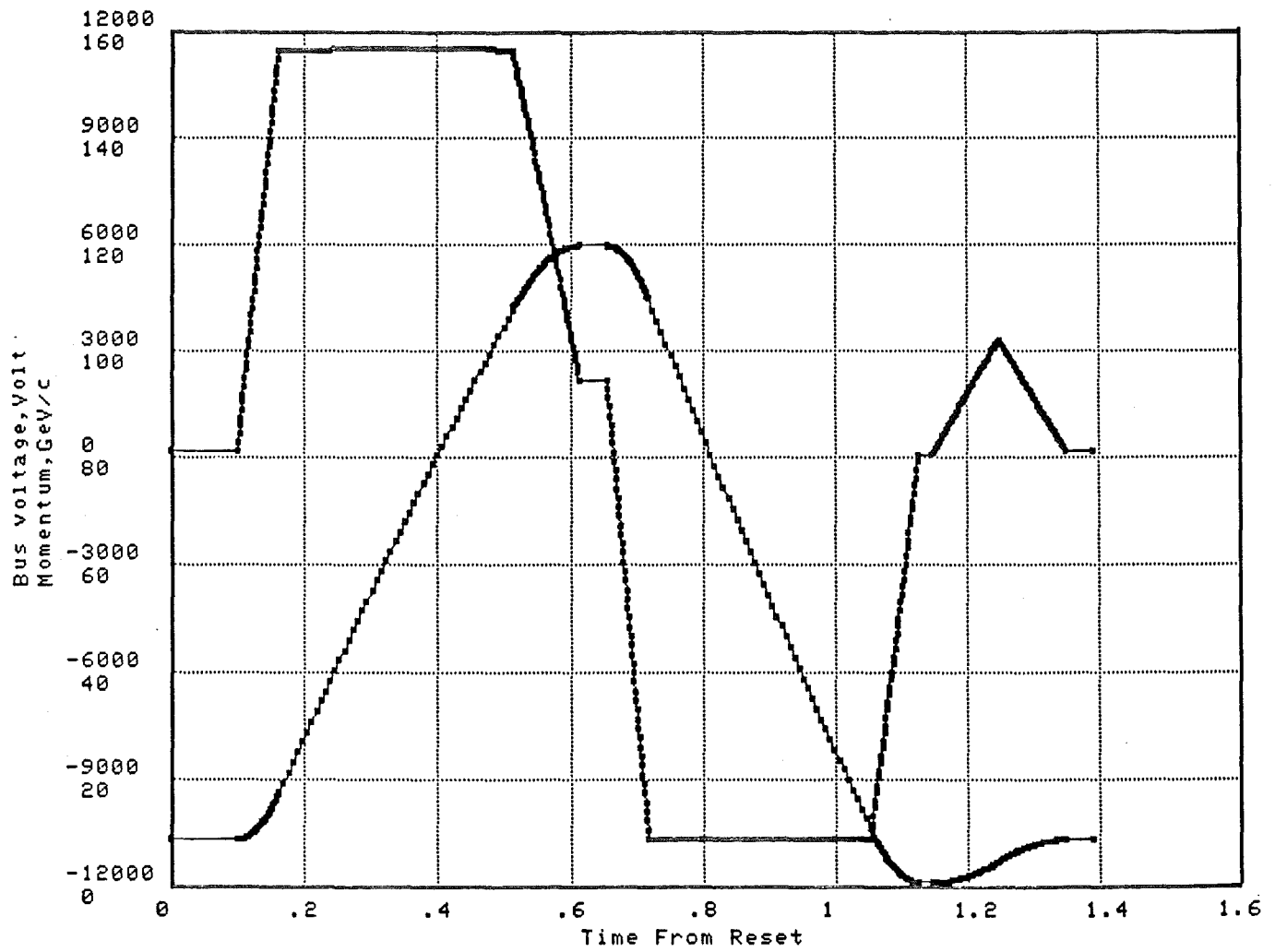


Figure 2.2-2. Faster 120 GeV Antiproton Production Acceleration Cycle

2.3. TRACKING STUDIES

This section describes the simulations to study the performance of the Main Injector at its two critical states, the injection energy of 8.9 GeV and the slow extraction energy of 120 GeV. These studies of the Main Injector lattice include closed orbit errors, betatron function errors, tune versus amplitude, dynamical aperture and correction schemes to improve the Main Injector performance. The description of the Main Injector lattice includes higher magnetic multipoles in dipoles, quadrupoles, and sextupoles, and both magnet and beam position monitor alignment errors. We also discuss correction schemes utilizing octupoles, trim quadrupoles and quadrupoles shuffling. These calculations were performed using a thin element tracking program TEAPOT [1].

Tracking Conditions And Errors

Recently we have built and measured ten FMI dipoles and completed the design of quadrupole, sextupole and dipole correctors. We use the information from the measurements of these new magnets in the calculations along with the previous measurements of the magnets that will be recycled from Main Ring magnets.

The Main Injector lattice has two different sizes dipole magnets with magnetic lengths of 6.096 m and 4.064 m at 120 GeV. The magnetic length of these dipoles varies with energy due to the saturation of ends, and at 8.9 GeV their length is 0.3 mm larger than the nominal length at 120 GeV, as shown in Figure 3.1-12 [2]. This change in length introduces a nonzero dipole multipole at each end of the magnet.

$$H_{\text{kick}} = 2\pi \times (\Delta L / 2L_{\text{ref}}) \times (904/3)^{-1} \text{ radians}$$

This additional bending of the particle is corrected by reducing the dipole excitation. The dipole body plus end multipoles, both normal and skew, are calculated by using the method described in [3]. In previous calculations [4], dipole systematic errors were calculated using the prototype dipoles and random errors were calculated using the Main Ring B2 dipoles. In those calculations we had used the design values of the higher order multipoles of the long quadrupoles. In calculations presented here we have used the data from ten R&D dipole measurements and initial measurements of new quadrupoles and sextupoles. The systematic and the random errors of the dipole multipoles are calculated by using the measurements of the ten R&D dipoles. The systematic errors of the long quadrupole are from new long quadrupole measurements, whereas the random errors are from the measurements of Main Ring 84" quadrupoles. Having built only two sextupoles, we don't have information on the random variation of the higher multipoles.

The values of the systematic and random errors of the 84" quadrupoles are calculated using the Main Ring (MR) quadrupole measurements. There are a very limited number of recent

measurements available for MR quadrupoles. The Main Ring quadrupoles have a large octupole component and a large random strength variation. Nominal multipoles are calculated by using the 195 A and 1575 A measurements, whereas the skew multipoles are calculated using the measurements at 1575 A. The variation of the octupole strength with current is about 25% between injection and slow extraction. All skew quadrupole field errors are turned off for the convenience of the simulation. Using a decoupling scheme any linear coupling effects due to the presence of skew quadrupole can be corrected. Tables 2.3-1 and 2.3-2 summarize all the multipoles used in the input file to TEAPOT. Details of the input to these tables can be found in reference [3,4]. Multipole field errors are quoted in units of 1.0×10^{-4} relative to the main field component and at a displacement of one inch. The misalignment of all the magnetic elements (dipoles, quadrupoles, sextupoles) and beam position monitors are included in these calculations. The rms of the alignment error with respect to the closed orbit is 0.25 mm in both horizontal and vertical directions. In addition dipole magnets have an rms roll angle of 0.5 mrad. Roll angles of other magnetic elements are not considered because their presence will dilute the effects we want to study. In principle the roll angles of all magnetic elements should be as small as possible, and they can be corrected by skew correction elements present in the ring. We have studied the effect of these random misalignments and systematic misalignment. These studies are summarized in reference [5].

Base tunes of $(Q_x, Q_y) = (26.425, 25.415)$ are used in all the simulations. These tunes are different from $(26.407, 25.409)$ which were used in earlier calculations of dynamic aperture. Particles are tracked with all magnetic and misalignment errors turned on, in the presence of synchrotron oscillations due to rf, and with chromaticity set to the desired value. In the lattice there are 18 rf cavities, each operating at a voltage $V_{rf} = 0.0218$ MV and 0.0555 MV at 8.9 and 120 GeV respectively. The rf frequency of 53 MHz corresponds to a harmonic number 588.

Tracking Results

Closed orbit Errors

In the Main Injector lattice there are 208 quadrupoles, of which 128 are recycled Main Ring quadrupoles, while the rest are newly fabricated. Located inside these quadrupoles are the beam position monitors. The vertical and horizontal beam positions are measured at the focusing and defocusing quadrupoles respectively. The vertical and horizontal displacements of the particles are corrected by applying corresponding kicks just after these position monitors.

A typical uncorrected closed orbit in both the horizontal and vertical plane is shown in Figure 2.3-1. The rms closed orbit deviation before correction is 5.10 mm horizontally and 5.56 mm vertically for the selected seed at 8.9 GeV. After three iterations of the orbit corrections

scheme the rms closed orbit deviation is reduced to 4.8×10^{-4} mm (H) and 1.0×10^{-8} mm (V). The correction scheme is based on a least square error minimization. We have studied the contribution of each magnetic error and the displacement error to the rms closed orbit deviation for one seed. The closed orbit error in the horizontal plane is due to 1) random quadrupole misalignment in the horizontal plane, 2) random errors in the dipole field and 3) systematic dipole strength variation (ΔL) at energies other than 120 GeV. The deviations in the vertical plane are mainly caused by 1) random quadrupole misalignment in the vertical plane and 2) the dipole roll. Details of the misalignment tolerances and corrector strength are described elsewhere[5]. Table 2.3-3 summarizes the contribution of different errors to the closed orbit error. Most of the horizontal closed orbit deviation is due to dipole random strength variations, misalignment errors and the change in the effective length of the dipole magnet. The vertical closed orbit error is mainly due to misalignment errors. Figures 2.3-2(a) and 2.3-2(b) show the distribution of uncorrected horizontal and vertical rms closed orbit errors for 20 different seeds at 8.9 and 120 GeV. The rms deviations of the distribution are 5.0 mm and 3.9 mm in the horizontal and vertical planes, respectively. The maximum corrector strength required to correct these orbit deviations are about 50 μ r in both planes at the two considered energies, as shown in Figure 2.3-3. In determining the maximum corrector strength we have considered the envelop of maximum corrector strength ignoring a few correctors which lie outside this envelop. In the Main Injector we plan to use newly built dipole correctors. At 8.9 GeV the Main Injector dipole correctors can provide 2000 μ r and 1300 μ r of horizontal and vertical corrections respectively.

Betatron Function Errors

The dipole and quadrupole random errors and magnet alignment errors change the β function around the FMI. The β function is different from that of the ideal lattice. A typical variation is shown in Figure 2.3-4. Figures 2.3-5(a) and 2.3-5(b) show the distribution of the maximum of horizontal and vertical $\delta\beta/\beta$ when all the errors are included at 8.9 GeV and 120 GeV. Most of these variations are due to the random errors in the strength of the magnetic elements. The average deviation is about 7%. Additional beta function errors at the level of a few percent (<2%) will also be present due to a mismatch between the length of the short and long quadrupoles.

Dynamical Aperture

We have studied the survival of particles launched at different amplitudes in the Main Injector at the injection energy. A single particle in FMI will circulate for 35000 turns at the injection energy of 8.9 GeV. This time is required for any operation that involves filling the ring with six batches coming from the Booster. At 120 GeV, during slow extraction of the proton beam, the beam will stay in the ring for 1.0 sec at flat-top, approximately 100,000 turns.

Synchrotron oscillations were included in the simulation by launching all particles with a momentum offset of $\delta_{\max} = (\Delta p/p)_{\max} = 2.0 \times 10^{-3}$ at 8.9 GeV and 0.33×10^{-3} at 120 GeV. The maximum beta function of the FMI lattice for a particular seed is less than 65 m, about 12% larger than the beta function with no errors. We have not found a random number seed that can produce a larger variation in beta function. Particles were launched with a maximum horizontal displacement "A" defined at a location where the horizontal beta function is at its maximum. We have conservatively assumed the maximum beta to be 70 meters. The maximum vertical displacement of the same particle is $0.4A$ ($x/y=2.5$), which approximates the available aperture of the beam pipe. Particles with amplitude varying from 15 mm to 35 mm were considered. Simulations were performed for five different seeds. Figures 2.3-6(a) and 2.3-6(b) are survival plots displaying how many turns a particle survives in the Main Injector at 8.9 and 120 GeV as a function of initial amplitude. If the dynamical aperture of the machine is defined as the smallest amplitude particle that did not survive the maximum number of turns, then the dynamical aperture for the Main Injector at the injection energy is predicted to be 30.6 ± 0.5 mm, corresponding to a normalized emittance of $127 \pm 4 \pi$ mm-mrad at 8.9 GeV.

In the FMI we have introduced local orbit distortions to move the beam away from the Lambertson magnet septum. Lambertson magnets are placed in the ring for injection and extraction of the beam. These local bumps, as shown in Figure 2.3-7, require the particles to be placed away from its nominal closed orbit and hence not in the best part of the magnetic field. We have measured the quadrupole magnet strength and higher order multipoles and have used these multipoles in our calculations at those locations. Figure 2.3-8 shows the quadrupole multipoles as a function of x in the magnet. We have studied the effect of the size of local bump at quadrupole locations Q618-Q622 on the FMI dynamical aperture at 8.9 GeV. Figure 2.3-9 shows the change in the dynamical aperture as a function of the size of the local bump at Q618-Q622. The size of the dynamical aperture starts to reduce for the bump sizes larger than 25 mm. We expect that a local bump of about 25 mm will be required to clear the Lambertson at these locations.

Detuning of Particles

We examined the variation of the horizontal and vertical tunes as a function of the particle's amplitude of motion. Figures 2.3-10(a) and 2.3-10(b) are the tune-tune plots at 8.9 and 120 GeV respectively. The numbers on the tune plot correspond to the initial amplitude "A" of a test particle, in millimeters. Points on the plots lie on a straight line up to an amplitude of 28 mm for 8.9 and 120 GeV. At both energies the change in tune is small for particles with small amplitude (less than 10 mm). It increases but remains uniform for large amplitude particles. This detuning is dominated by a combination of systematic octupole error in the recycled Main Ring

quadrupoles, and second order sextupole effects. Half of this detuning is due to the octupole multipole of the quadrupoles.

Correction Schemes

The FMI dynamical aperture is about twice its design aperture. Due to the multipurpose operations of the FMI we have studied possible ways to further increase the dynamical aperture. In the 120 GeV fixed target operation mode of the FMI, the 120 GeV proton beam will be slowly extracted from the FMI in 1 sec. The extraction process begins by changing the tune of the machine slowly from (.425,.415) to (.485,.415) using the main quadrupole power supplies. The trim quadrupoles and 0th-harmonics octupoles are used to slowly extract the beam as described in [6]. There is a significant loss (10 mm) of dynamical aperture due to change in tune. We have studied different correction schemes to increase the aperture at this tune setting.

In the FMI lattice there are 54 octupoles and 16 trim quadrupoles placed around the ring for extraction. At present there are 8 additional octupoles correctors in the ring. These octupole and trim quadrupoles can be used in a correction scheme to increase the dynamical aperture of the FMI. The Main Ring and newly constructed quadrupoles intentionally have a positive octupole component to facilitate slow extraction, but which is also one of the limiting factors in the dynamical aperture of the FMI. The extraction and corrector octupoles can be used to cancel the total effect of this octupole. The octupoles will have a bipolar power supply. This will enable us to use them as correctors at all the energies and to adjust the total octupole in the ring during slow extraction.

In the FMI, the focusing and defocusing quadrupoles are powered by two separate power supplies, so the currents in the two circuits can be different. This provides direct, separate control of the horizontal and vertical tunes. All the recycled Main Ring quadrupoles will be remeasured and reworked before they are placed in the FMI. Knowing the strength of each quadrupole will allow us to select which to place in the ring. Quadrupoles with larger deviations from the mean will be assigned to beamlines. The 128 quadrupoles selected for the FMI ring will be divided into two groups. One set will have quadrupoles strength higher than the mean value and the other set lower. This division will reduce the sigma of the quadrupole random error by creating two non-gaussian distributions. We have used a Monte Carlo simulation to generate a gaussian distribution of quadrupole strength. The sigma of this distribution was chosen to be the sigma derived from the available measurements of the Main Ring quadrupoles. The quadrupoles with strength larger than the mean value were placed on the focusing bus, whereas quadrupoles with lower strength were placed on the defocusing bus. By dividing the quadrupoles into two parts we have reduced the sigma of the quadrupole strength from 24 units to 7 units. This reduced the

$\Delta\beta/\beta$ around the ring by a few percent. Sorting of the quadrupoles by placing pairs of strong or weak quadrupoles exactly one FODO cell apart can further reduce this variation in beta function. The variation in $\delta\beta/\beta$ can be reduced even further by canceling the natural half-integer stop band of the FMI [6,7]. This is achieved by using the two families of 16 trim quadrupoles placed in the ring for slow extraction. These trim quadrupoles can be used as correctors at all the energies and as extraction elements for slow extraction. Figure 2.3-4 shows the $\delta\beta/\beta$ of the FMI before any correction is applied. Figure 2.3-11(a) is a similar plot after the quadrupole shuffling to reduce the random error at 8.9 GeV, whereas Figure 2.3-11(b) includes the quadrupole shuffling and half-integer stop band correction at the 120 GeV slow extraction setting. Figure 2.3-12 shows the detuning of the particle at 120 GeV after the quadrupole random error and octupole corrections. Detuning is very small for small amplitude particles. Detuning of large amplitude particle is reduced by about 30%.

We have studied the survival of particles for one seed only at the slow extraction tune of $(Q_x, Q_y) = (26.485, 25.425)$ with these corrections. Figure 2.3-14 is the survival plot before and after these corrections. The dynamical aperture increases by about 7 mm. This is mainly due to reduced $\delta\beta/\beta$ and smaller total octupole in the FMI.

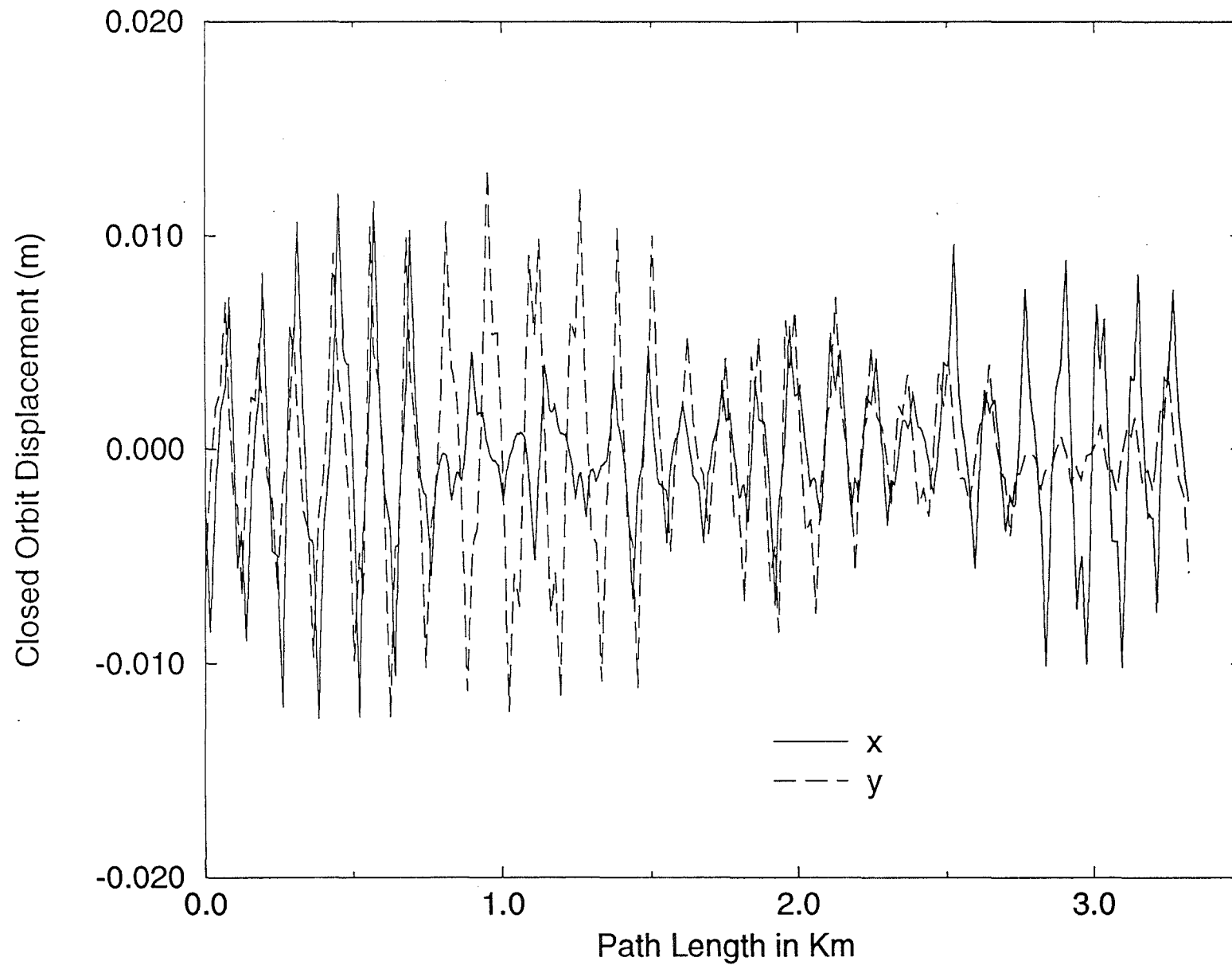


Figure 2.3-1. Typical Closed Orbit Errors Before Correction

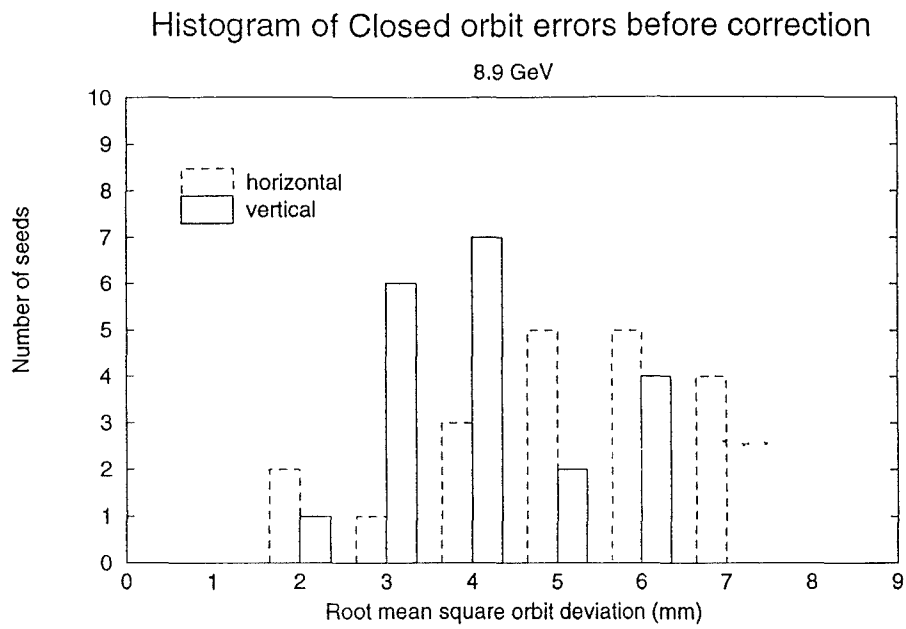


Figure 2.3-2(a). Histogram of Closed Orbit Errors Before Correction at 8.9 GeV

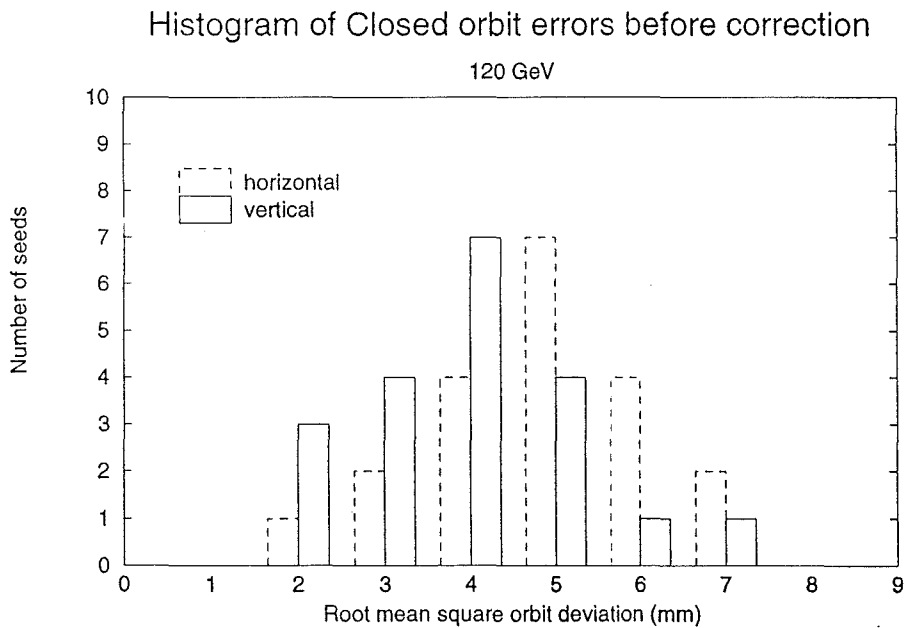


Figure 2.3-2(b). Histogram of Closed Orbit Errors Before Correction at 120 GeV

Corrector Strength at 8.9 GeV

Misalignment Sigma = 0.25 mm, Dipole Roll = 0.5 mrad, cut off at 3 sigma

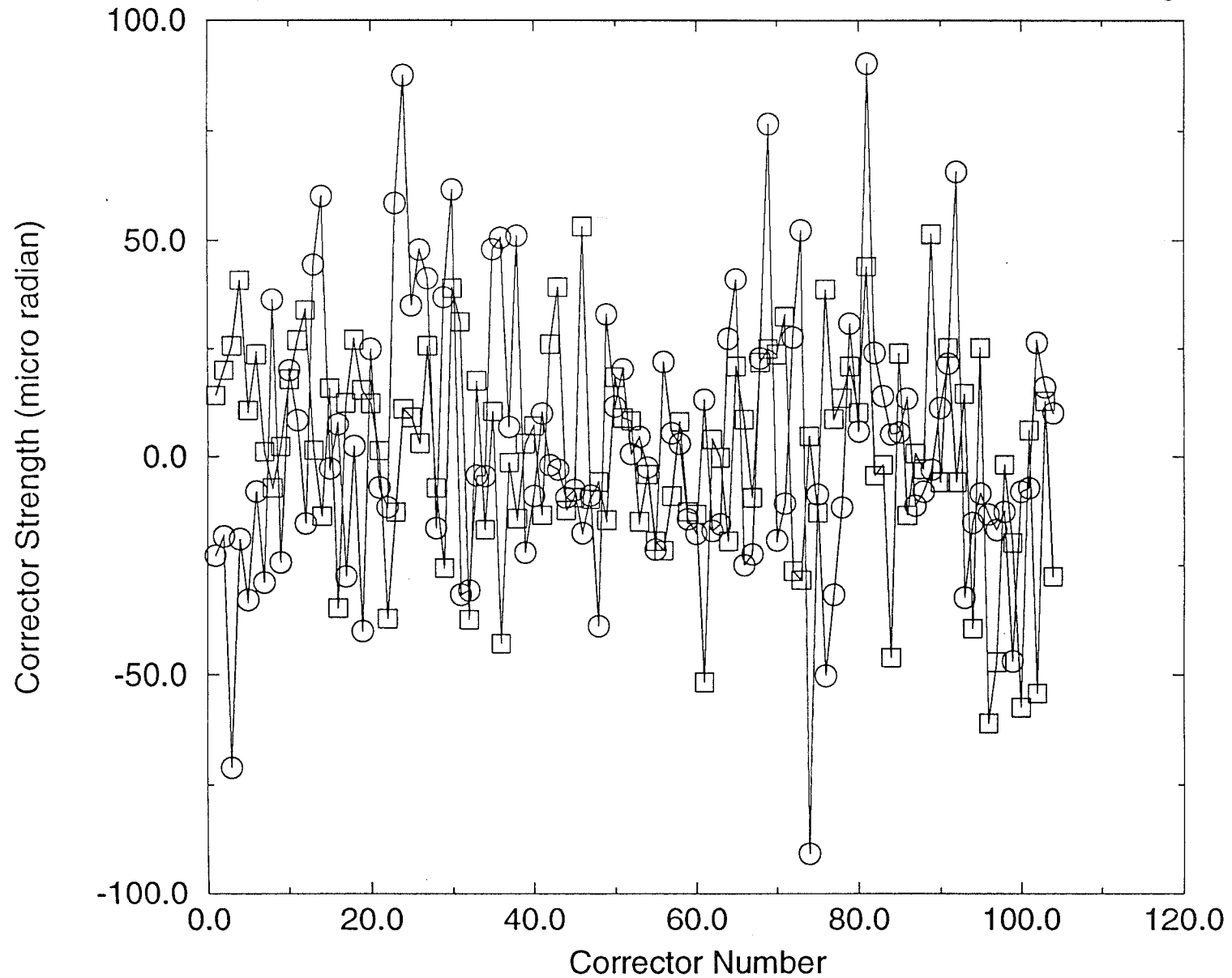


Figure 2.3-3 Corrector Strength at 8.9 GeV

Variation in Beta Function

At 8.9 GeV

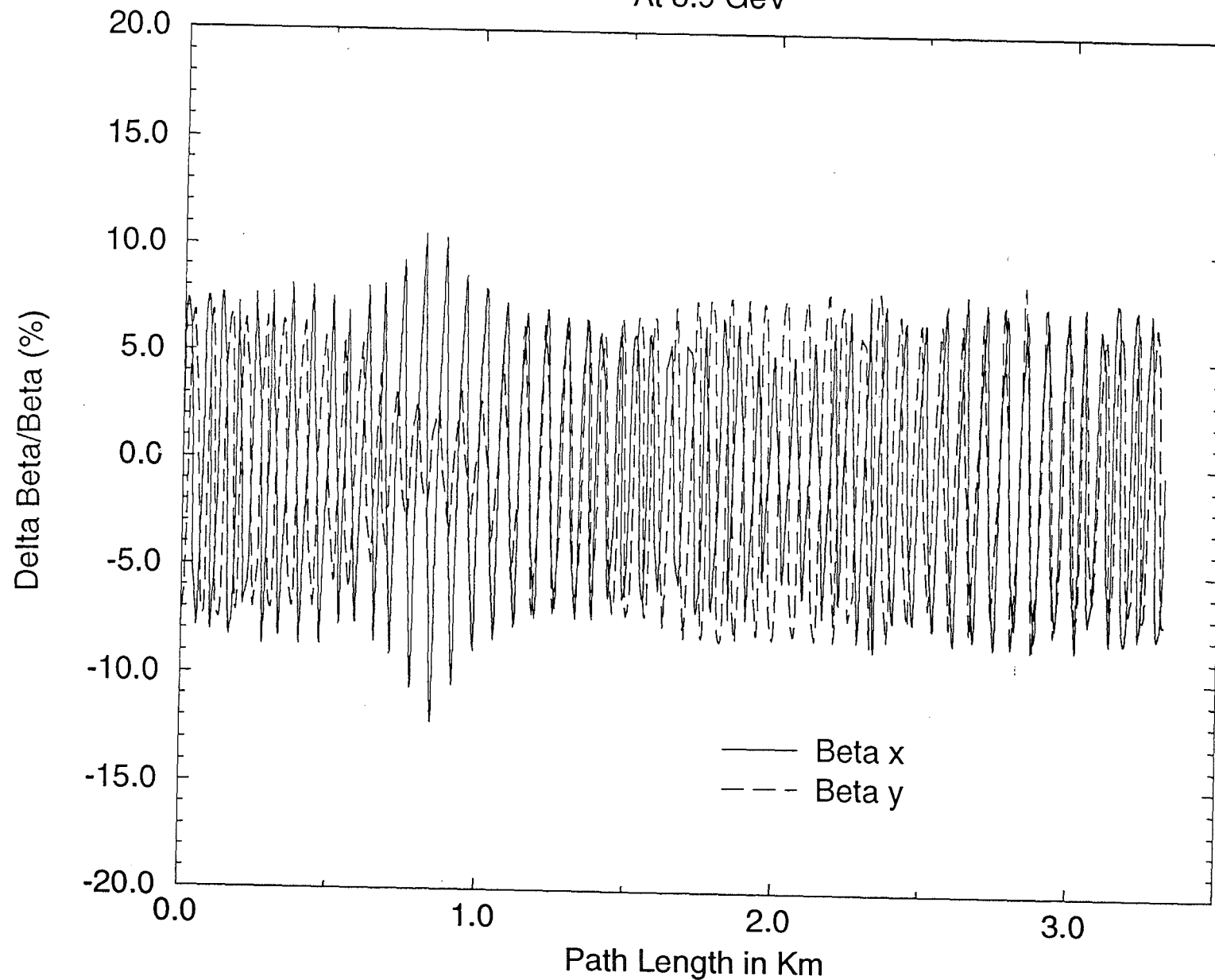


Figure 2.3-4. Typical Variation in Beta Function

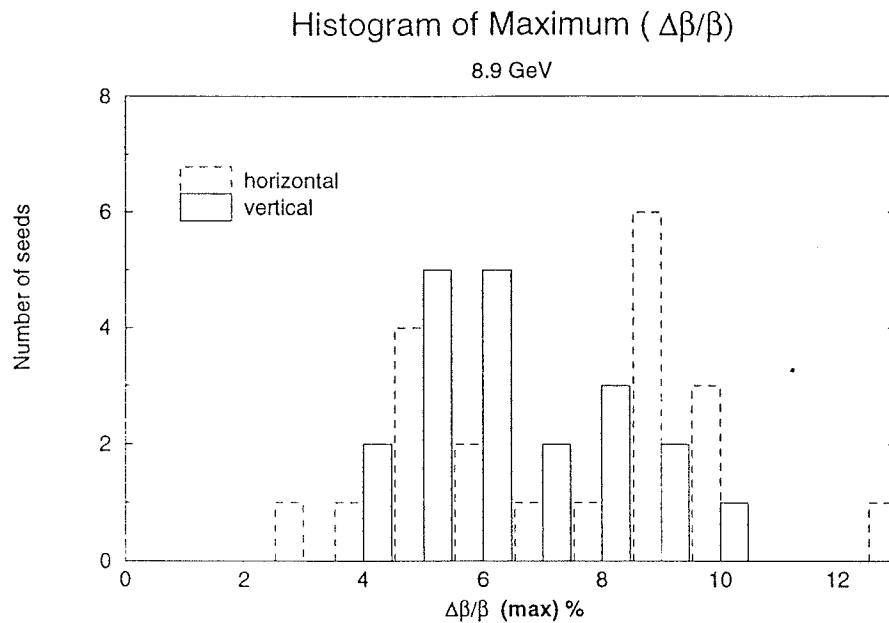


Figure 2.3-5(a). Histogram of ($\Delta\beta/\beta$) Errors at 8.9 GeV

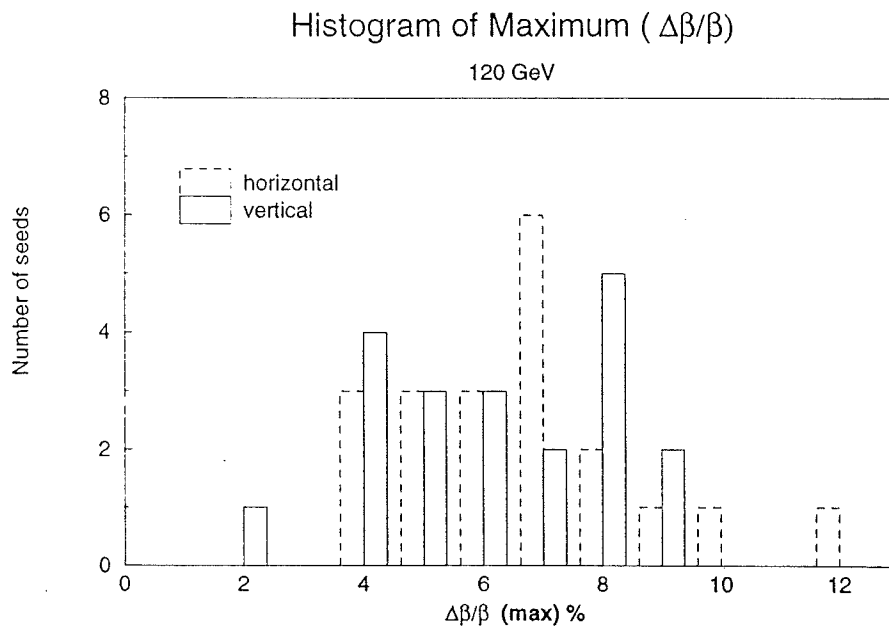


Figure 2.3-5(b). Histogram of ($\Delta\beta/\beta$) Errors at 120 GeV

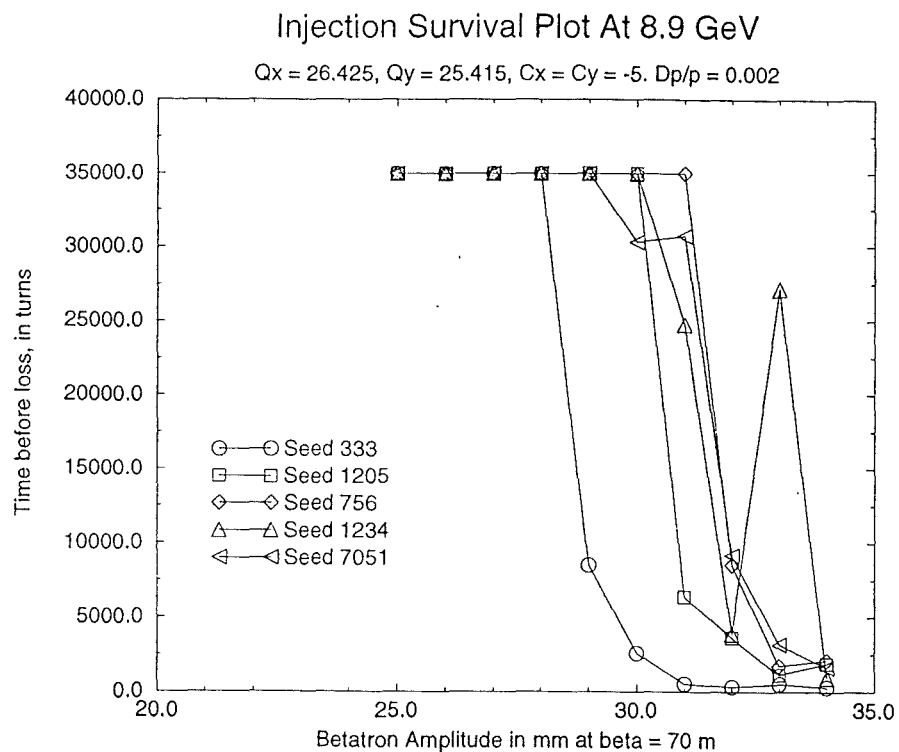


Figure 2.3-6(a). Survival Plot for Five Seeds at 8.9 GeV

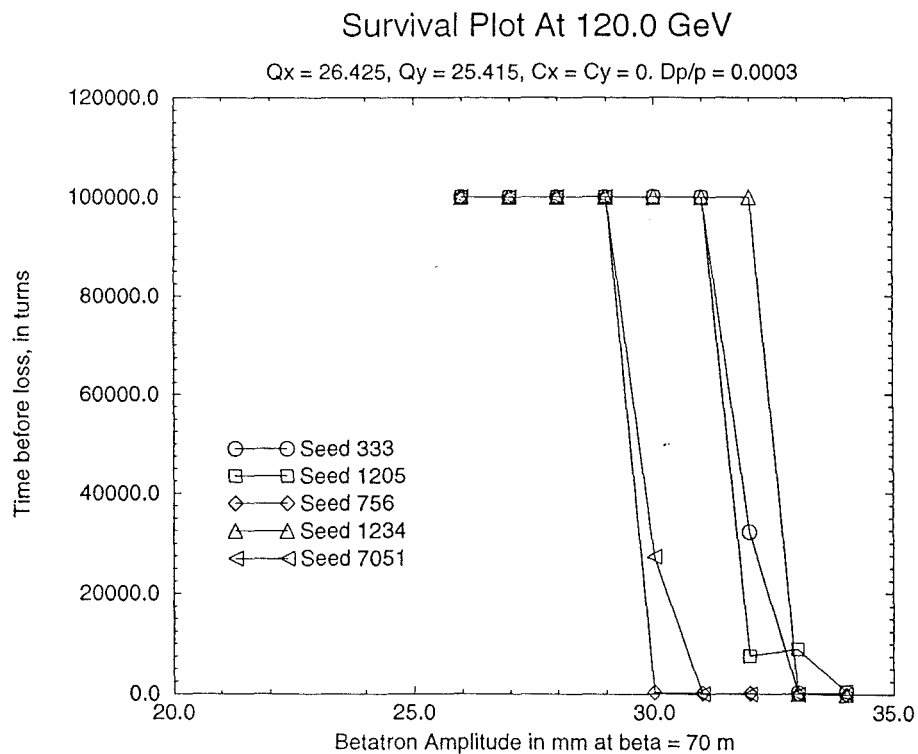


Figure 2.3-6(b). Survival Plot for Five Seeds at 120 GeV

Closed Orbit error with three local bumps

F Quad displaced at Q340-Q406, Q518-Q526, and Q618-Q622

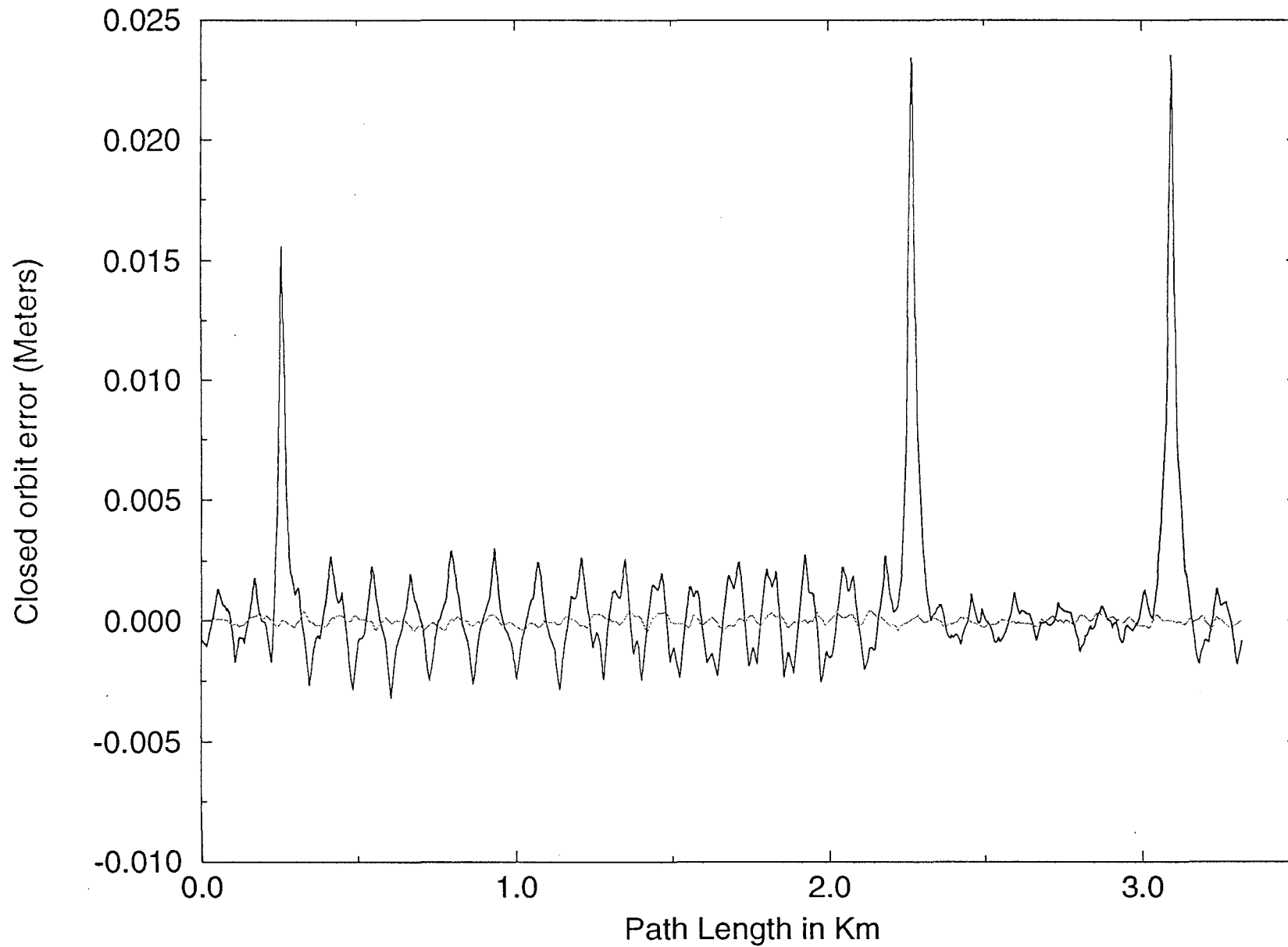


Figure 2.3-7. Closed Orbit Error with Three Local Bumps

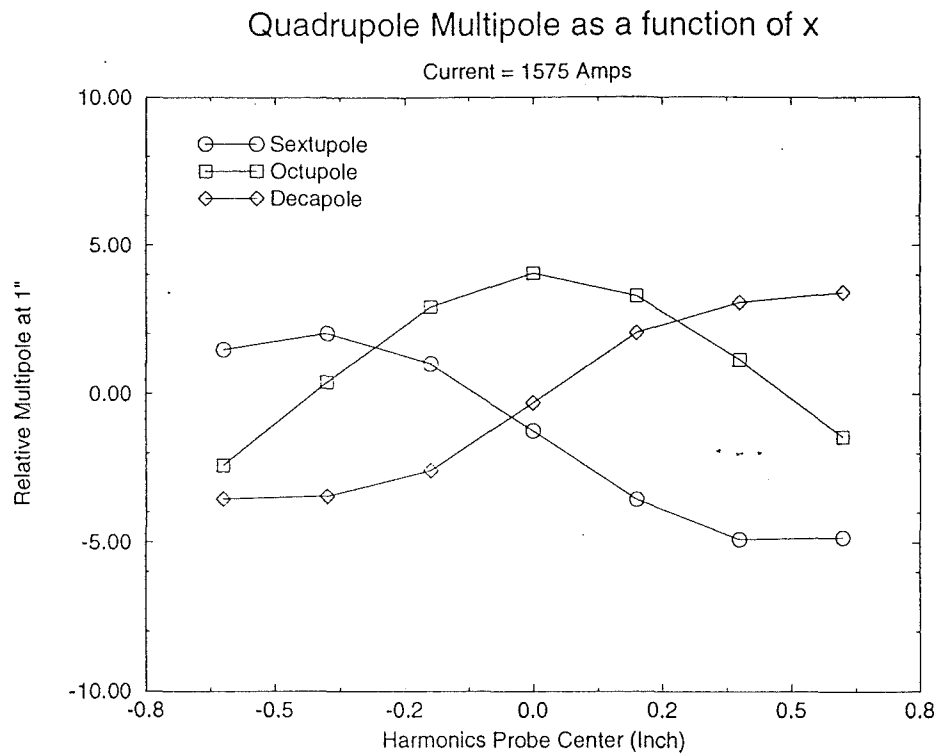


Figure 2.3-8. Quadrupole Multipoles as a Function of x

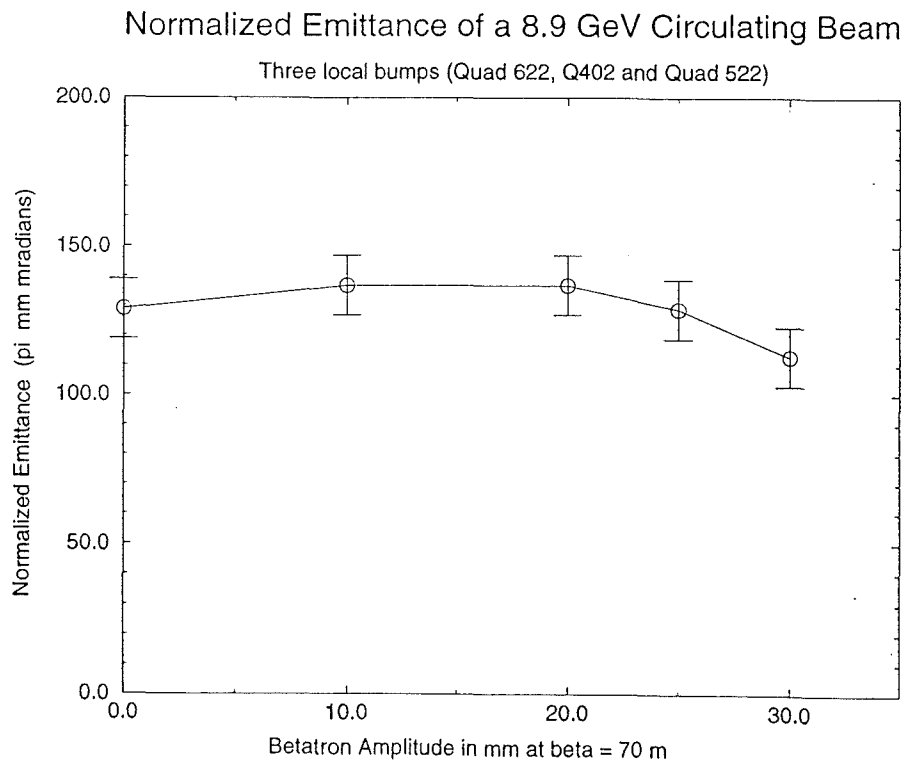


Figure 2.3-9. Dynamic Aperture as a Function of Bump Amplitude

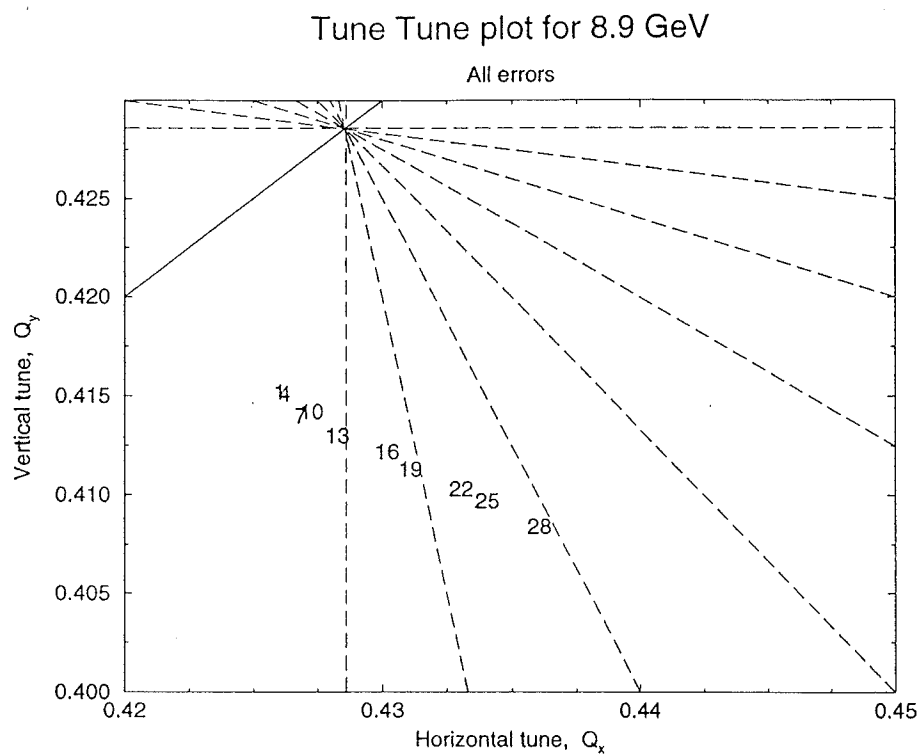


Figure 2.3-10(a). Tune-Tune Plot at 8.9 GeV

Numbers 1 to 28 are Initial Amplitude of the Launched Particle.

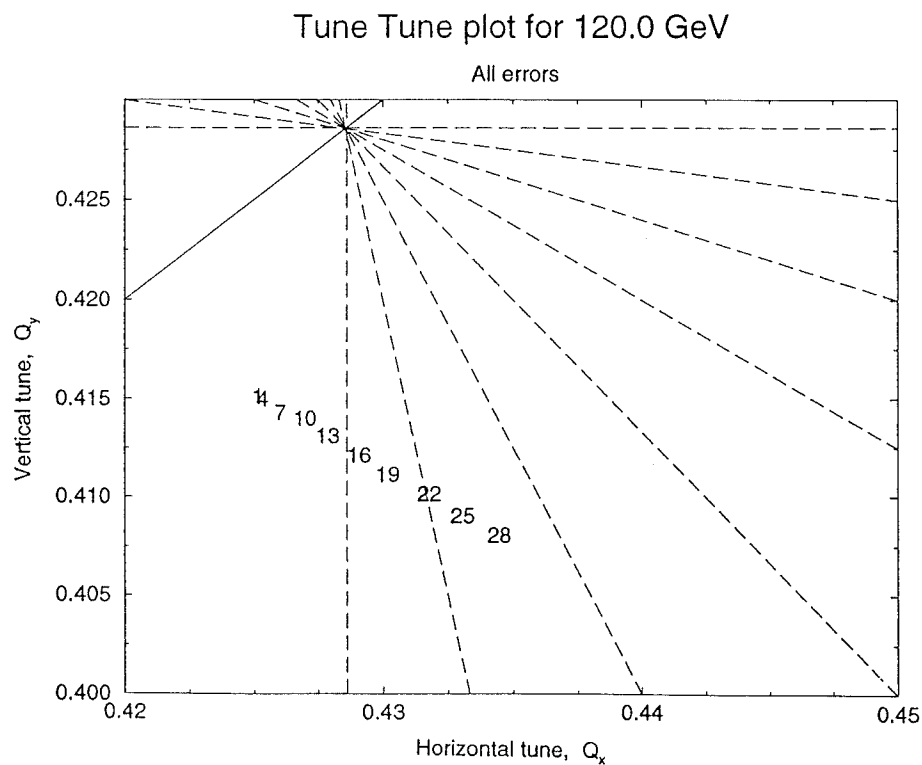


Figure 2.3-10(b). Tune-Tune Plot at 120 GeV

Numbers 1 to 28 are Initial Amplitude of the Launched Particle.

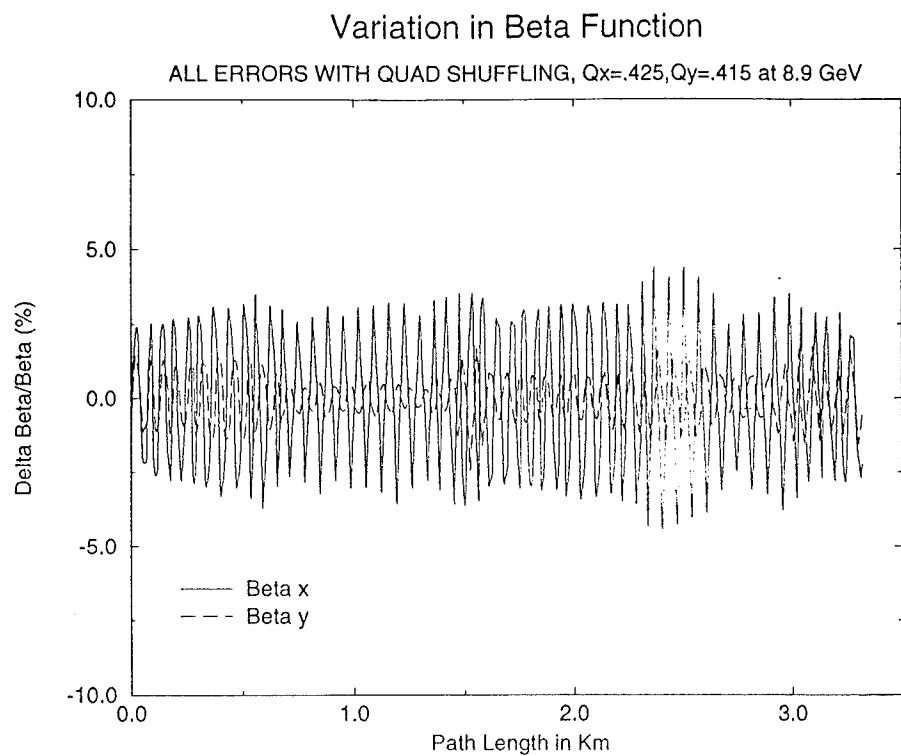
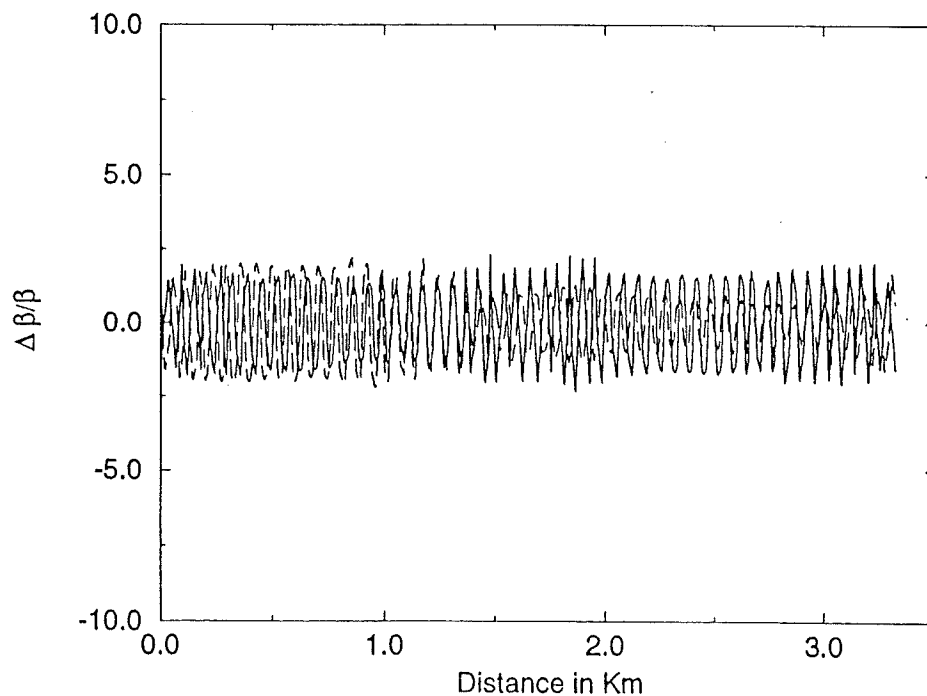


Figure 2.3-11(a) Beta Errors at 8.9 GeV After Quadrupole Shuffling



**Figure 2.3-11(b) Beta Errors at 120 GeV After Quadrupole Shuffling
and Half-Integer Stop Band Correction**

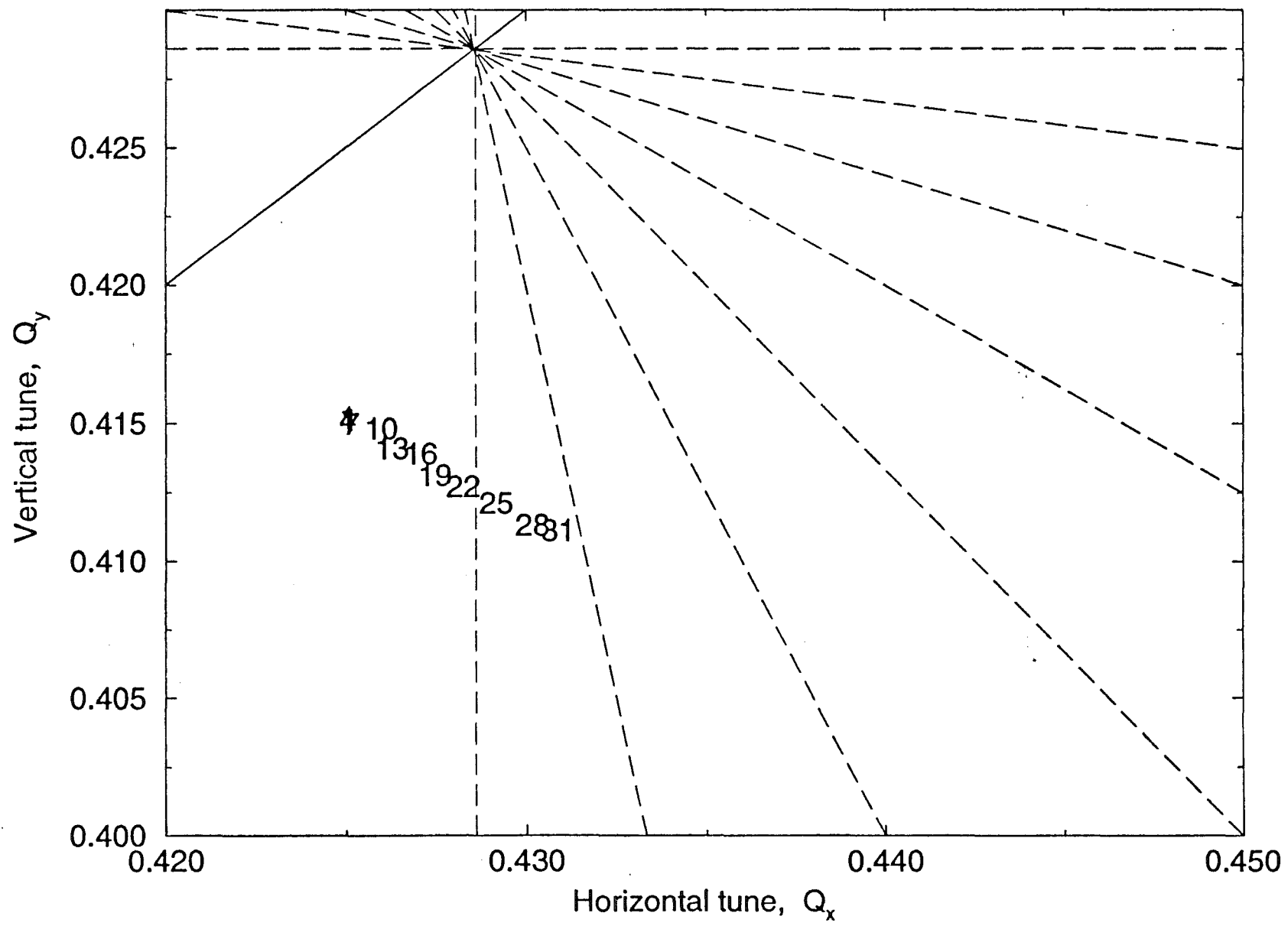


Figure 2.3-12. Detuning at 120 GeV After Correction

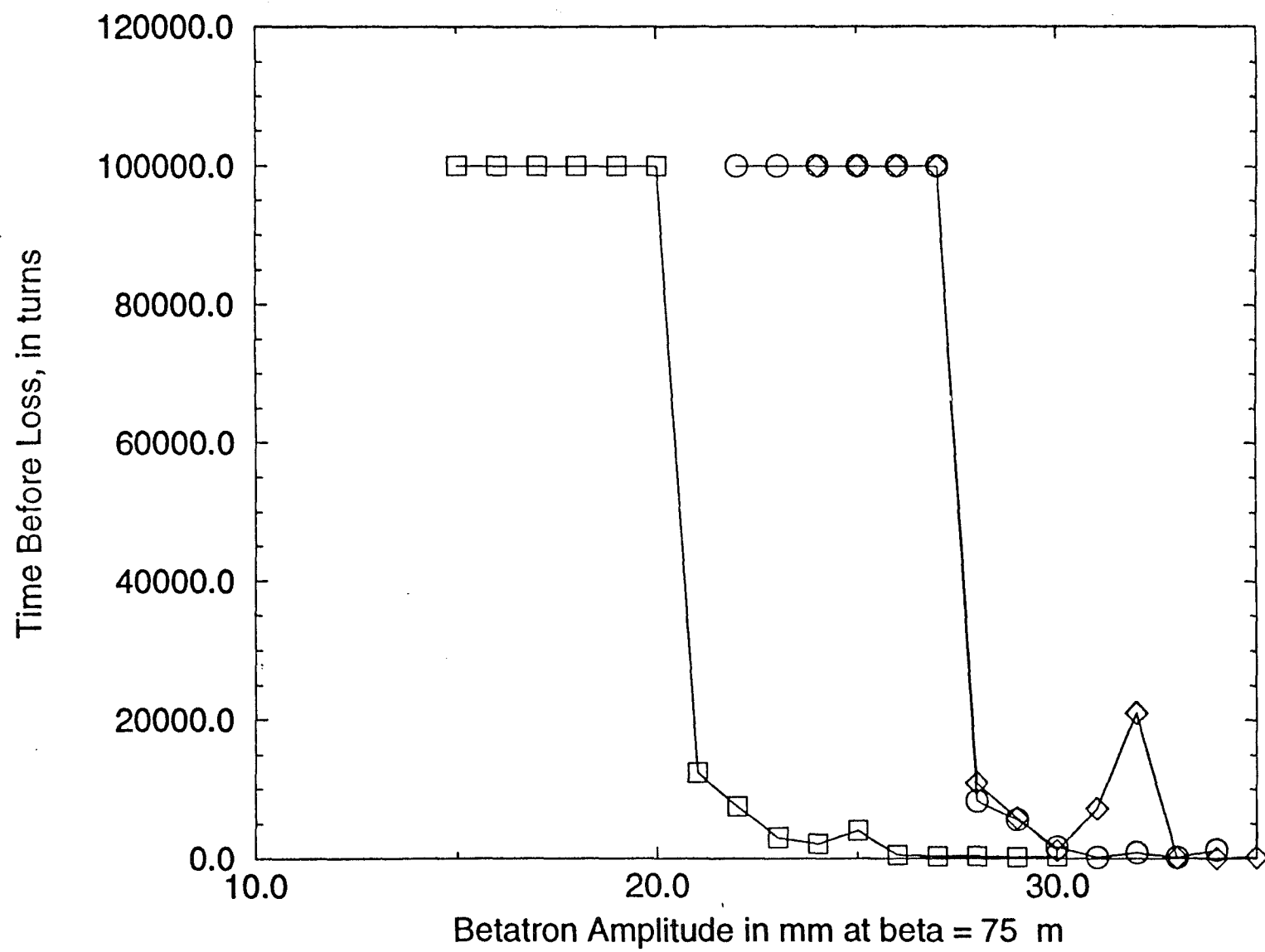


Figure 2.3-13. Survival Plot at 120 GeV and $\nu = .485$ Before and After Correction

Table 2.3-1 Magnetic errors used in the 8.9 GeV simulation.

	Multipole Order	Normal		Skew	
		$\langle b_n \rangle$	σ_{b_n}	$\langle a_n \rangle$	σ_{a_n}
Dipole	dipole	1.10	15.30	-	-
	quadrupole	0.06	0.80	-	-
	sextupole	-0.40	0.18	0.00	0.12
	8	0.04	0.06	0.03	0.03
	10	0.33	0.05	0.00	0.05
	12	-0.01	0.05	-0.03	0.04
	14	-0.03	0.05	0.00	0.05
Recycled Main Ring Quadrupoles (New Style)	quadrupole	-	24.00	-	-
	sextupole	0.50	2.73	0.12	1.85
	8	5.85	1.02	-1.16	2.38
	10	-0.10	1.12	0.42	0.47
	12	-1.82	0.63	0.40	0.70
	14	0.21	0.64	-0.55	0.44
	16	1.41	0.64	-	-
	18	-0.03	0.12	0.14	0.16
	20	-0.80	0.06	0.02	0.07
Newly Built MI Quadrupoles	quadrupole	-	24.00	-	-
	sextupole	-0.51	2.73	1.08	1.85
	8	3.41	1.02	-2.05	2.38
	10	0.03	1.12	-0.75	0.47
	12	-1.49	0.63	0.43	0.70
	14	0.21	0.64	-	0.44
	16	1.41	0.64	-	-
	18	-0.19	0.12	-0.07	0.16
	20	-0.77	0.06	-0.12	0.07

Table 2.3-2 Magnetic errors used in the 120 GeV simulation.

	Multipole Order	Normal		Skew	
		$\langle b_n \rangle$	σ_{b_n}	$\langle a_n \rangle$	σ_{a_n}
Dipole	dipole	0.00	5.50	-	-
	quadrupole	0.03	0.80	-	-
	sextupole	-2.04	0.15	0.00	0.14
	8	0.01	0.03	-0.01	0.05
	10	0.05	0.05	0.00	0.05
	12	-0.01	0.04	-0.02	0.05
	14	-0.07	0.04	0.01	0.05
Recycled Main Ring Quadrupoles (New Style)	quadrupole	-	24.00	-	-
	sextupole	1.69	2.29	-0.47	3.14
	8	5.29	1.29	0.68	0.43
	10	-0.72	0.90	0.41	0.34
	12	-1.71	0.16	-0.31	0.14
	14	0.25	0.92	-0.02	1.11
	16	1.37	0.92	-	-
	18	-0.22	0.92	0.06	0.25
	20	-0.82	0.33	-0.05	0.08
Newly Built MI Quadrupoles	quadrupole	-	24.00	-	-
	sextupole	-1.49	2.29	0.58	3.14
	8	4.10	1.29	-0.45	0.43
	10	-0.01	0.90	-0.29	0.34
	12	-1.86	0.16	0.02	0.14
	14	-0.22	0.92	-	1.11
	16	1.37	0.92	-	-
	18	-0.05	0.92	-0.01	0.25
	20	-0.79	0.33	-0.09	0.08
Chromaticity Sextupole*					
	dipole	358	-	2.6	-
	quadrupole	-	-	-	-
	octupole	0.6	-	2.6	-
	10	-78.9	-	1.3	-
	14	35.5	-	-1.3	-
	18	-9.4	-	0.4	-

* Chromaticity sextupole harmonics measured at 300 A and scaled to appropriate excitation for F and D loops at 120 GeV.

Table 2.3-3. Closed orbit errors at 8.8 GeV (in mm) for one seed.

Error(s)	H	V
All	5.93	4.37
Dipole Systematic (including ΔL)	1.05	0.00
Dipole Random	5.04	0.00
Quad Systematic and Random	0.00	0.00
Displacement and Rotational Error	2.62	4.09

Conclusion

Calculations presented in this section have shown that the Main Injector design exceeds the design specification of 40π mm mr admittance at injection. The larger octupole and the random variation of the quadrupole strengths are the limiting factor for the dynamical aperture at slow extraction. Using the correction schemes described, it is possible to reduce the effect of the quadrupole random error and octupole multipole. This correction scheme provides us with additional aperture at all energies.

References: Tracking Studies

1. L. Schachinger and R. Talman, Particle Accelerators 22, 1987.
2. C.S. Mishra et al., "Change in Effective Length of the Main Injector Dipole", MI Note-0118, 1994.
3. C.S. Mishra et al., "Summary of R&D Dipole Measurements", MI Note-0119, 1994.
4. C.S. Mishra and F.A. Harfoush, "Study of the Fermilab Main Injector Lattice", MI Note-0088, 1993.
5. C.S. Mishra, "Study of the Alignment Tolerance and the Corrector Strength in the FMI Lattice", MI Note-0109, 1994.
6. J.A. Johnstone, "A Simplified Analysis of Resonant Extraction at the Main Injector", MI Note-0091, 1993.
7. J.A. Johnstone, "A Numerical Simulation of Resonant Extraction", MI Note-0095, 1993.

2.4. BEAMLINES AND BEAM TRANSFERS

Five new beamlines with a combined length of about 1,425 m are required to integrate the FMI into the existing Fermilab accelerator complex. Lattice descriptions of each of these may be found in the Appendices.

1. A 760 m beamline for transporting the 8.9 GeV/c protons from Booster straight section L3 to the FMI injection point in straight section MI-10.
2. A 260 m beamline to transport 150 GeV/c antiprotons from the MI-62 straight section in the FMI to the Tevatron F0 straight section.
3. A 260 m Tevatron injection beamline which transports 150 GeV/c protons from the MI-52 straight section to the Tevatron F0 straight section.
4. A 15 m magnet section to match between the Tevatron injection Lambertsons and Main Ring station F11.

To connect the Main Injector complex with the Antiproton Source and Switchyard most of the existing magnets and power supplies in F-Sector(from F0 to A0) of the Main Ring and in the AP-1 beamline remain in place. The 150 GeV/c line from MI-52 also provides the link between the Injector and the F-Sector magnet string of the Main Ring. This dual functionality of the 150 GeV/c line is made possible by using the Tevatron injection Lambertsons as a magnetic switch for selecting either the Tevatron or Main Ring F-Sector. Figure 2.4-1 shows the geometry of the Tevatron F0 straight section.

The 120 GeV protons used for antiproton production are transferred at Main Ring station F17 into the existing AP-1 beamline. This section of beamline is also used to transfer 8.9 GeV/c antiprotons from the Antiproton Source to MI-52 for injection into the FMI. The 120 GeV/c protons used for test beams are transported through the entire F-Sector to A0 where the fifth beamline is installed.

5. A 130 m section which connects F49 to the upstream end of the Switchyard.

Finally, a sixth beamline is required to transport beam to the abort dump.

6. A 140 m beamline transport beam out of the FMI enclosure at the MI-40 straight section. The last 30 m are simply a drift from the enclosure to the dump itself. This beamline must be capable of transporting beam at any energy between 8 GeV and 150 GeV. The beamline, the enclosure and the beam dump itself have all been designed to allow this area to be used as a future

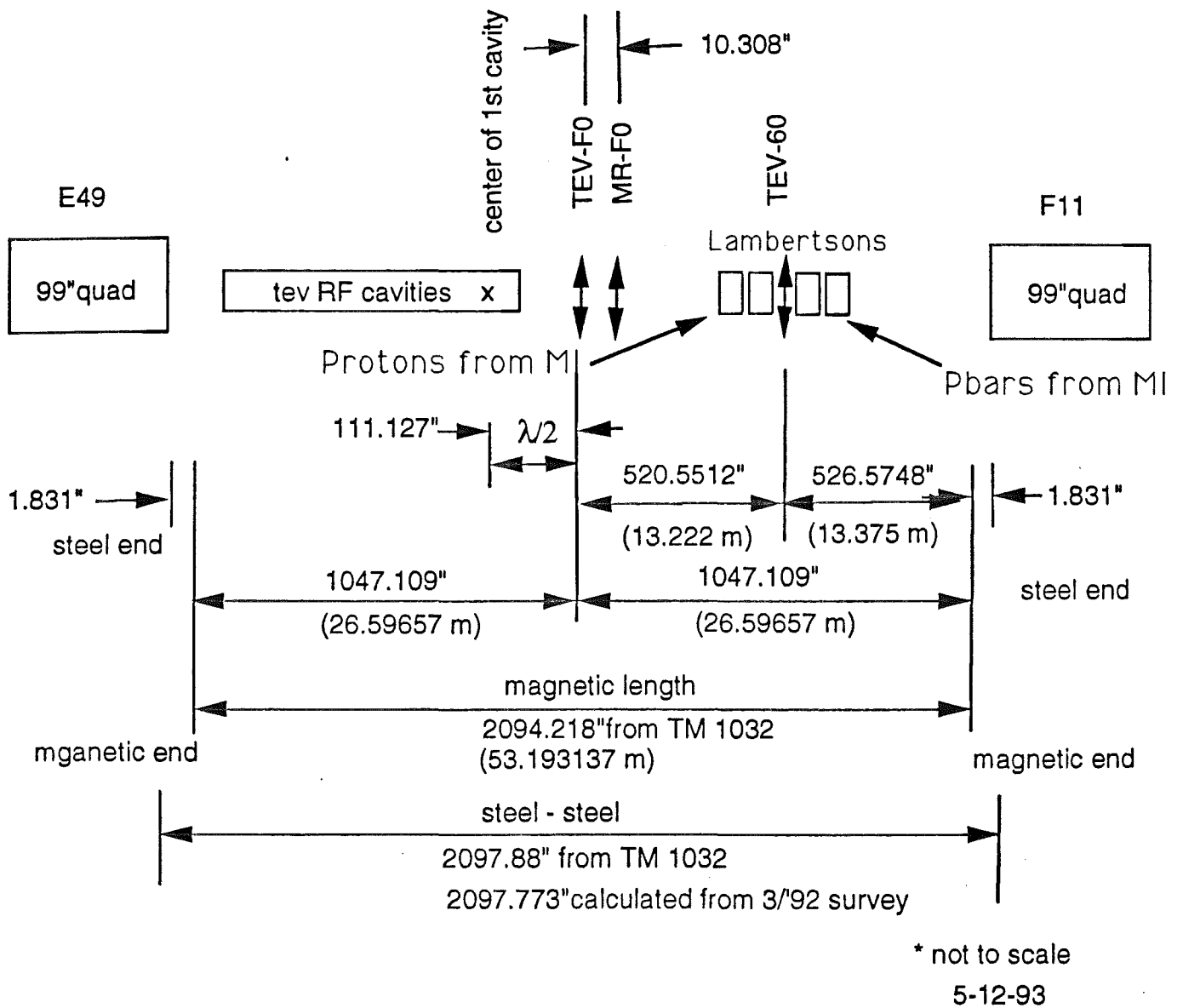


Figure 2.4-1. Geometry of the Tevatron F0 Straight Section.

120 GeV extracted beamline. With additional magnets installed in the MI-40 enclosure and in the abort dump enclosure, 120 GeV beam could be directed through a hole in the abort dump inner steel sections, refocussed and transported to a future downstream experimental area.

The layout of the beamlines and site coordinates of all beamline elements have been determined. Optical designs exist for the 8.9 GeV/c Booster to FMI line, the two 150 GeV/c FMI to Tevatron beamlines, and the FMI to Main Ring F11 beamlines. With a few exceptions, that are discussed in a subsequent section, all beamline dipoles and quadrupoles are recycled from the Main Ring and existing 8.9 GeV/c beamline between the Booster and the Main Ring. Every quadrupole focusing center has associated with it a beam position monitor and correction dipole recycled from the Main Ring.

2.4.1. The 8 GeV Line

Protons extracted from the Booster are transported 756 m for injection into the FMI. The 8 GeV transport line is comprised of three major sections: a matching section between the Booster and the main body of the beamline, which also incorporates the descent from the Booster to Main Injector elevation; a long section of periodic FODO cells; and a final section to match the optics between the beamline's FODO section and the FMI.

The 8 GeV line, as it is currently being installed, differs in concept so radically from the version described in the August 1994 release of the TDH that it can be regarded as a truly new design. The Booster and FMI matching sections exhibit some similarities with those described previously, in so far as tunable electromagnet quadrupoles are utilized to perform the optical matches. However, in the long arc of repetitive FODO structure all electromagnets have been eliminated and replaced with permanent dipoles, gradient magnets, and quadrupoles. The motivation for employing permanent magnets wherever possible in the line was primarily to acquire the manufacturing and operating experience necessary to ensure success of the future 8 GeV Recycler Ring. The permanent magnets to be used in the 8 GeV line are described in Chapter 3.1A. The conventional magnets are described in Chapter 3.1. The layout of the elements in the beamline are shown in Chapter 3.2, Figure 3.2-14, beginning from the Booster and ending at the Main Injector injection point, quad Q101.

The Booster extraction system and matching section geometry upstream of the dump are very different from those described in TDH(94). In early 1995 the Booster group realized that horizontal extraction was probably not feasible. Field leaking into the 'field-free' region of the Lambertson would unacceptably degrade the Booster beam at injection, possibly even prohibiting circulation. Protons will therefore be extracted using the existing vertical extraction system. A pulsed septum in straight section L3 extracts beam upwards at 2.77° . A vertically bending, 5' EPB dipole (VBC1) levels the trajectory 0.50 m above the Booster elevation. Centered downstream of VBC1 by 12.47 m, a 10' EPB provides 6.54° of horizontal bend, steering the beam away from the enclosure wall and onto a trajectory that avoids the dump. Immediately following the horizontal EPB is a vertical dogleg. The first EPB in the dogleg drops the beam at an angle of 6.54° . The second vertical EPB flattens the trajectory again at Booster elevation. The inclusion of this rather unnatural vertical dogleg was the least odious option studied that could accommodate the switch from horizontal to vertical Booster extraction without impacting civil construction downstream. An EPB centered 8.42 m after the vertical dogleg provides an additional 6.54° horizontally. Immediately following this last EPB two 3.556 m permanent dipoles provide 3.16° of vertical

bend, pitching the beam downwards for the next 59.28 m to obtain the 10'9" Booster-FMI elevation difference. Two more permanent dipoles then cancel the beam's vertical descent, marking the end of the Booster matching section.

One hundred and three degrees (103.45°) of bend are achieved in the next 644 m of the line exclusively via 45 permanent dipoles and 65 permanent gradient magnets, with each magnet providing 1.10° of horizontal bend. The first 8 dipoles have reverse bends relative to the remaining magnets in the series, which serves to keep the beam well clear of the existing roads around the Anti-Proton complex. The subsequent 37 dipoles and 65 gradient magnets take the trajectory of the line 10'9" below the existing AP2/AP3 enclosure, or 16'9" below the AP2/AP3 beamlines. The closest distance of approach of the 8 GeV line to the Tevatron is approximately 100'. The final 2.00° of horizontal bend from the recycled A0 8 GeV Lambertson places the protons on the horizontal closed orbit of the FMI. The 8 GeV proton line terminates at the defocusing quadrupole (Q101) situated 17 m upstream of the MI-10 straight section center.

Optics

Lattice functions for the 8 GeV line are illustrated in Figure 2.4-2(a). The corresponding 40π mm-mr beam envelopes and magnet apertures are shown in Figure 2.4-2(b). The apertures illustrated correspond to the 'effective' aperture seen by the beam, i.e.; the true interior beampipe dimensions reduced by the sagitta. The Booster matching section will use ten SQ series quadrupoles (designed for the Antiproton Source, and also used in the Booster-to-Main Ring 8 GeV line). However, until the present Booster-to-Main Ring injection line is decommissioned, there is a shortage of SQAs, and a spare SQC is being used at location 809. That will be replaced with an SQA later in order to increase the number of spare SQCs; the final configuration will employ 4 SQA, 4 SQC, and 2 SQF quads. Powered individually, they perform the optical match between lattice functions of the Booster and the standard values of the beamline's long FODO section. The quadrupole doublet downstream of the Booster extraction point merely constrains the amplitude of the extracted beam. The subsequent 8 quads perform the actual optical match to the FODO lattice, with the 6 quads in the vertical drop also producing $\sim 360^\circ$ of vertical betatron phase advance to ensure that the matching section is achromatic. Vertical dispersion does not exceed 1.20 m. The transverse beam size reaches its maximum in this matching section of the line. With $\beta \sim 68$ m, and a normalized transverse beam emittance of 40π mm-mr, the maximum beam size is ± 17 mm -- much less than the 3.5" pole-tip diameter of the SQ quadrupoles. However, it is the 4 EPB dipoles which form the aperture bottleneck of the 8 GeV line -- and the situation is nearly equally bad at each dipole. Typically, in the non-bend plane the 95% beam full-width is $\sim 1'' \rightarrow 1.25''$, compared to the 1.40" nominal interior beampipe dimension. In the bend plane, because of the

Permanent Magnet 8 GeV Proton Line

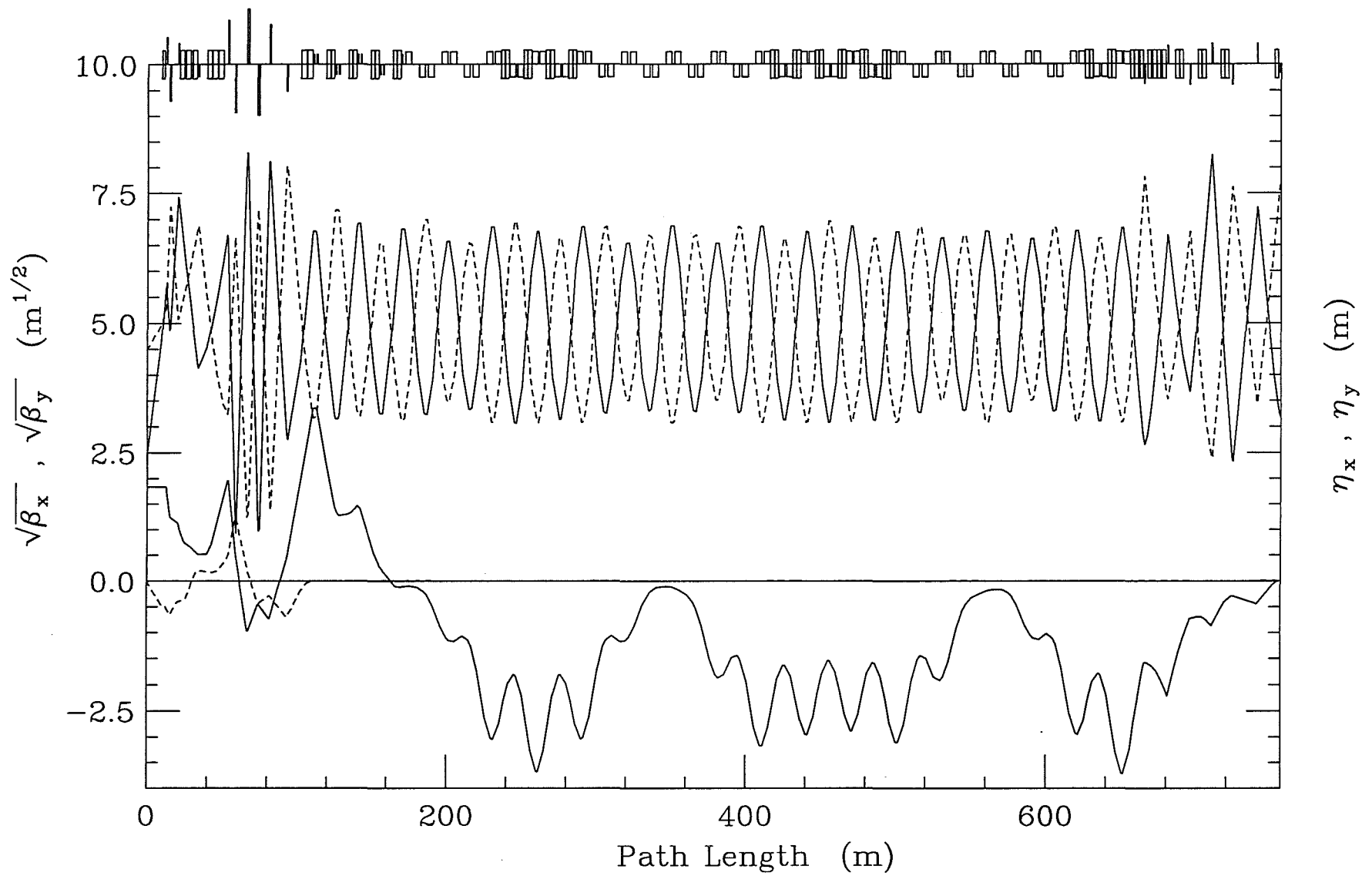


Figure 2.4-2(a). Lattice functions for the 8 GeV line.

8 GeV Beam Envelope & Magnet Apertures

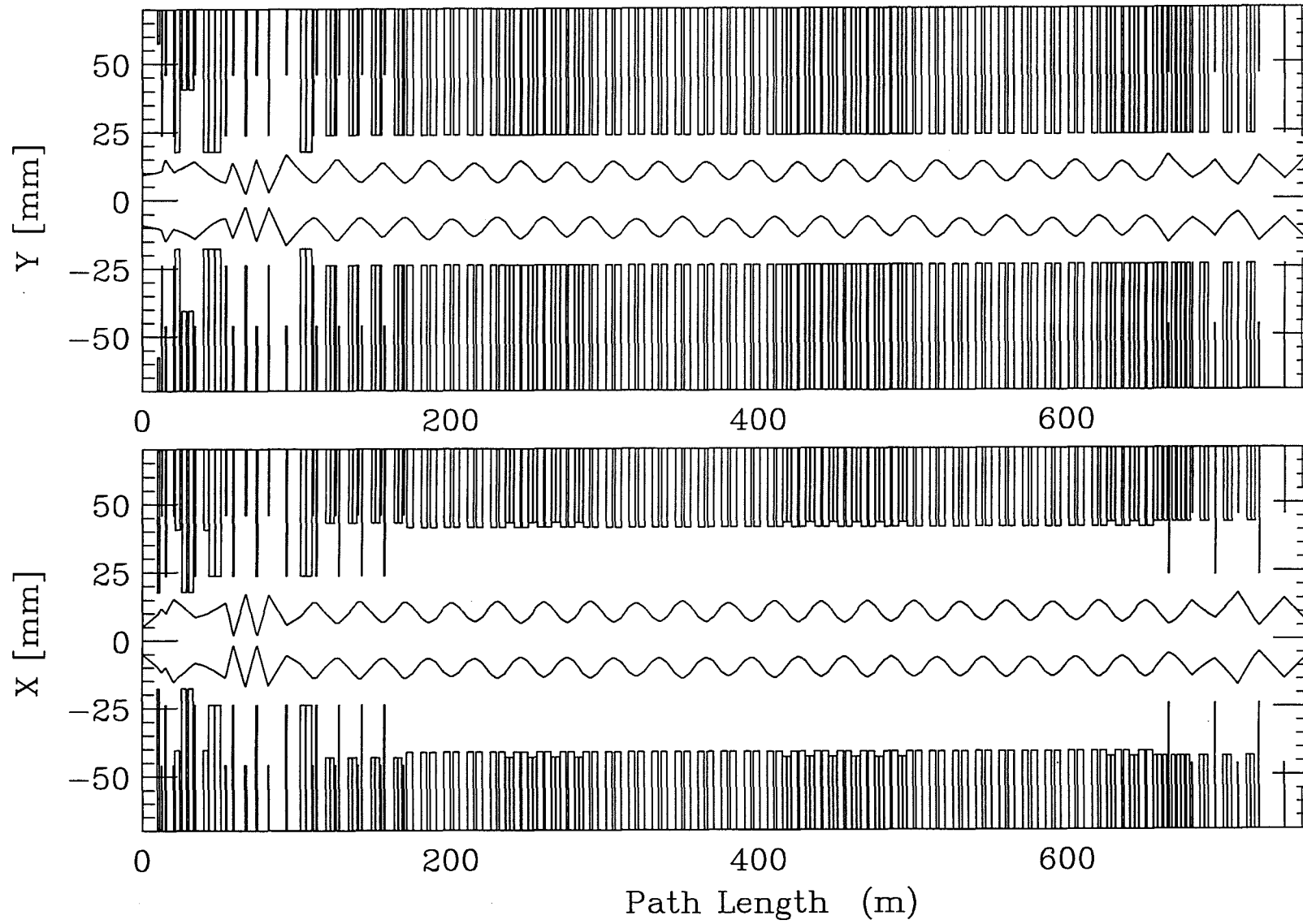


Figure 2.4-2(b). 40π mm-mr beam envelopes and magnet apertures.

large sagitta (1.71"), from 2.5"→3.0" of aperture are required, with 3" completely consuming the EPB good field region.

The 58.83 m following the Booster matching section (the 'reverse-bend' section) is comprised of two cells, each characterized by 4 permanent dipoles, 4 permanent quadrupoles, and 84° of betatron phase advance per cell. These cells represent a compromise between following as closely as possible the trajectory through the tunnel determined by previous electromagnet solutions and achieving a smooth optical match to the subsequent long arc of FODO cells.

The reverse-bend cells are followed by 495.46 m of repetitive FODO structure. This lattice section is constructed from two types of cells -- regular cells constructed from 4 permanent dipoles plus 4 gradient magnets per cell and dispersion suppressing cells with 4 gradient magnets per cell. Both types of cells have $\sim 90^\circ$ of phase advance but are not perfectly matched optically. The small mismatch is the consequence of intentionally creating additional space in the lattice to accommodate the possible insertion of diagnostics in the future. As a result, dispersion neither reaches precisely zero anywhere, nor is it optimally minimized through the arc. However, horizontal dispersion becomes as small as 0.12 m and does not exceed 3.71 m, which is acceptable. With a maximum $\beta = 47$ m and $\delta p/p = 0.2\%$ the transverse beam size is less than ± 16 mm for a 40π mm-mr emittance, which is compatible with the 48 mm (V) x 92 mm (H) aperture of the beampipe. With each dipole and gradient magnet producing 1.10° of bend, the sagitta is only 5.9 mm and 9.5 mm respectively. Again, this is compatible with the available aperture.

The matching section at the FMI end is very similar to that described in earlier versions, with the notable difference that each B2 has now been replaced by 2 permanent dipoles. Six individually powered SQA type quadrupoles perform the final optical match to the FMI.

Correction Elements

Every cell boundary in the 8 GeV cell has a BPM associated with it, with additional BPMs located in the regions of tight aperture around the EPBs at the Booster end. Every electric quadrupole in the line also has a recycled Main Ring correction dipole nearby. Additional correctors are located at the entrance and exit of the long arc, and one cell upstream of each beam profile monitor to provide centering capability on the monitor. For 8.9 GeV/c protons the angular correction produced by Main Ring horizontal (1.9"x5.4" aperture) and vertical (2.4"x4.2" aperture) dipoles is $\theta = 580 \mu\text{r}$ and $335 \mu\text{r}$, respectively, at 5 A. This provides the capability to correct central trajectory errors through both matching sections and also to provide position and angle adjustment of beam entering and exiting the long arc plus the injection trajectory at Q101 in the FMI. For vertical correction, rolled horizontal correctors will be used in the matching sections

to match the beam pipe which is oriented to give maximum vertical aperture; in the permanent magnet section, standard vertical correctors will be used.

The long permanent magnet section is almost completely devoid of correctors. Here, as will be the case in the Recycler Ring, any necessary trajectory corrections will be performed by moving gradient magnets. These magnets are designed, and installed, with the ability to 'float' transversely on the beam pipe by as much as ± 1 ". A 1 cm transverse displacement of the magnet translates into a bend angle change $\Delta\theta = 614 \mu\text{r}$, or $\sim 0.85\%$ of the nominal bend. Relatively modest magnet displacements therefore can produce steering capability equivalent to that of a Main Ring corrector.

The effect of dipole field errors on the trajectory through the long arc, and the consequent gradient magnet movements required for correction, have been investigated in simulations. Random field error compensation must be addressed by any beamline but, unlike electromagnet transfer lines, a systematic dipole field error (or, equivalently, a systematic beam momentum offset) becomes an important issue for permanent magnet lines.

Rather than using the true lattice configuration, trajectory error simulations were performed with a lattice constructed from 7 regular plus 12 dispersion suppressor cells to mimic the repetitive optics of the long arc. While results from the simulations should not be sensitive to this approximation, trajectory correction is simplified by being amenable to solution via the algorithms intrinsic to MAD. The optics of this approximate lattice are shown in Figure 2.4-3.

A systematic 1% dipole field error (much larger than any realistic error source imagined) was assigned to each of the 28 dipoles, 38 F-gradient, and 38 D-gradient magnets in the approximate lattice. Figure 2.4-4(a) shows the resulting trajectory and envelope of a 40π mm-mr beam with momentum spread $\delta p/p = 0.2\%$. Position and angle of the incoming beam are optimal for minimizing the rms transverse excursion. The resulting rms displacement of the orbit is $\Delta x(\text{rms}) = 18.5$ mm and, with maximum displacements of $\Delta x(\text{max}) = 31.0$ mm, the beam scrapes at all high dispersion locations. Figure 2.4-4(b) shows the beam trajectory and envelope after correction. Moving just the F-gradient magnets, 8 by 10 mm, 12 by 7.5 mm, and 18 by 5 mm, the excursion of the beam is significantly reduced, with $\Delta x(\text{rms}) = 1.7$ mm and $\Delta x(\text{max}) = 3.2$ mm, which is perfectly acceptable for the available aperture.

Random field errors are treated analogously to systematic field errors. Uniformly distributed, random dipole errors in the range $\pm 0.25\%$ were generated (compared to the anticipated range of better than $\pm 0.10\%$) and assigned to all 104 magnets in the approximate lattice. The beam trajectory resulting from 20 random generator seeds was calculated. The worst case had an orbit wobble characterized by $\Delta x(\text{rms}) = 3.7$ mm and $\Delta x(\text{max}) = 13.0$ mm. Figure 2.4-4(c) illustrates

Approximate Repetitive Cell Structure

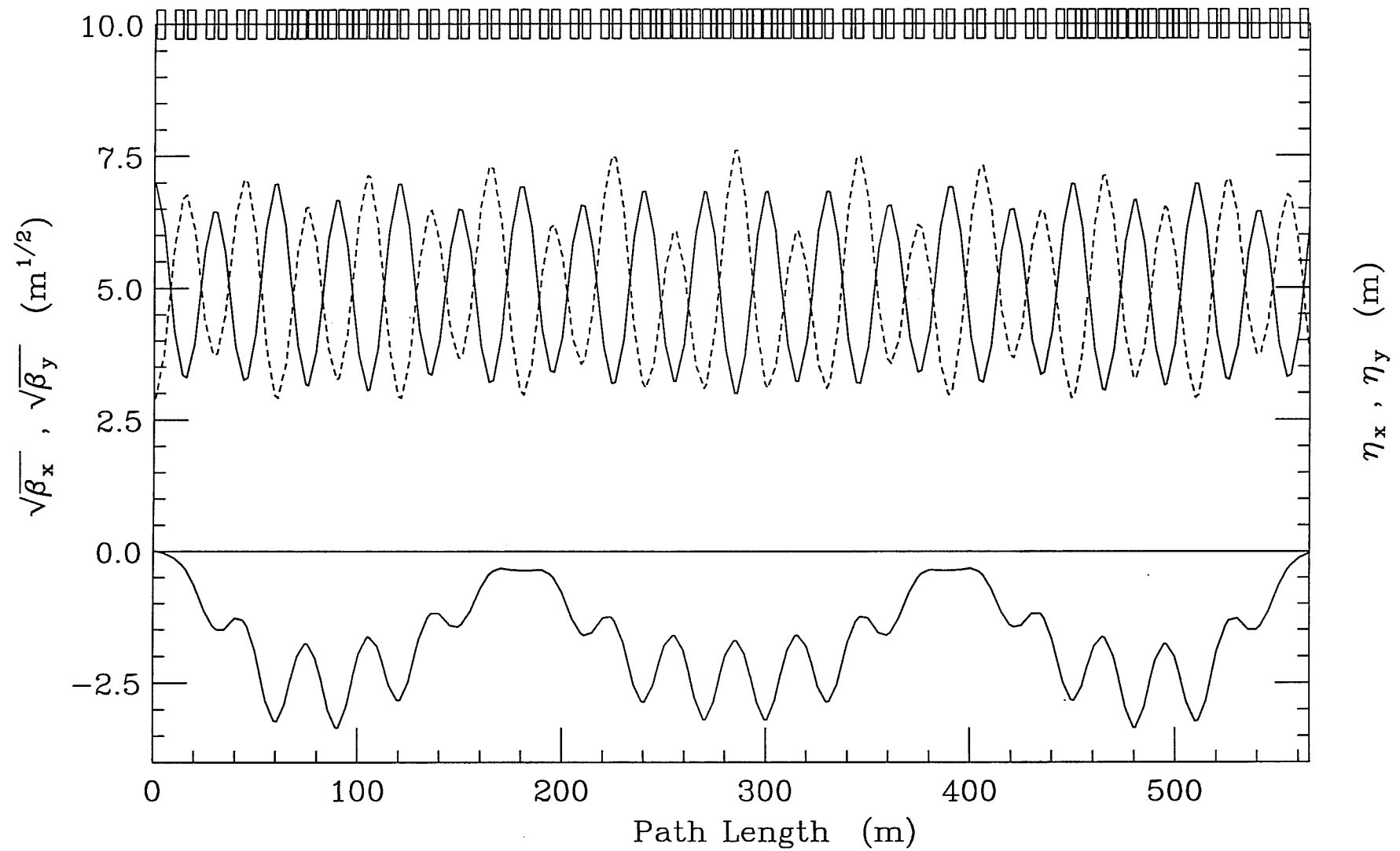


Figure 2.4-3. The optics of a ring lattice approximating the 8 GeV line.

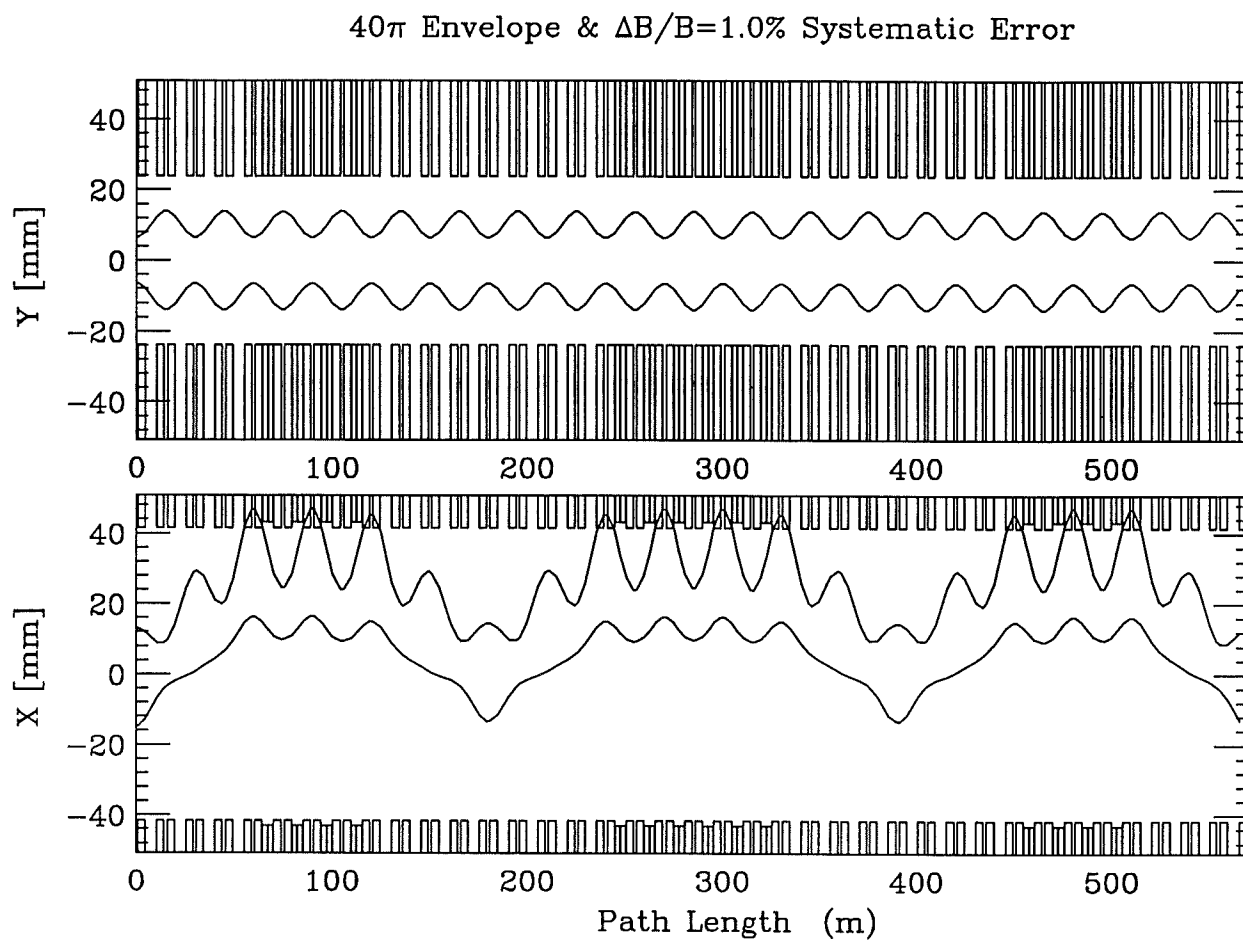


Figure 2.4-4(a). Trajectory and envelope with systematic field error of 1%.

δp Error Compensation by Moving Magnets

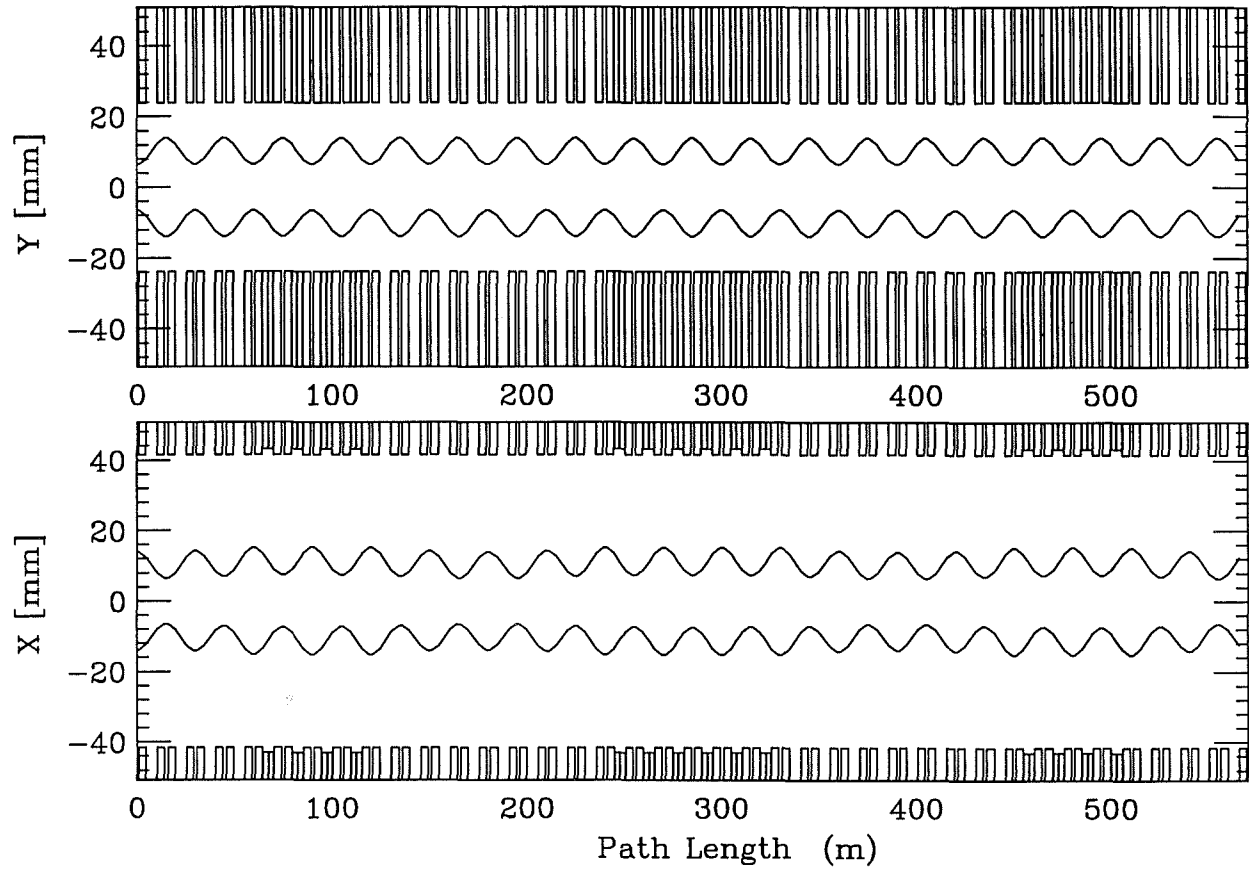


Figure 2.4-4(b). Beam trajectory and envelope after correction by moving magnets.

the uncorrected trajectory and beam envelope in this worst case for 40π mm-mr emittance and momentum spread $\delta p/p = 0.2\%$. It can be seen that no correction of the orbit is strictly necessary -- there is ample aperture for lossless beam transmission. However, with small adjustments to just 12 of the F-gradient magnets, moving 4 by 1.25 mm, 6 by 1.00 mm, and 2 by 0.5 mm, the trajectory deviation is reduced to the level achieved for the 1% systematic error. Figure 2.4-4(d) shows the corrected trajectory, where $\Delta x(\text{rms}) = 1.2$ mm and $\Delta x(\text{max}) = 3.0$ mm.

FMI Injection

Injection of 8.9 GeV/c protons is accomplished in the FMI straight section MI-10. The straight section is approximately 69 m long and has to accommodate the horizontal injection Lambertson and vertical kickers. The recycled A0 Lambertson is located at the FMI defocusing quad 17 m upstream of the straight section center; this quadrupole will be rotated by 90° to provide adequate vertical aperture for the injected beam. The beam trajectory in the horizontal plane approaches the FMI at an angle of approximately 35 mr in order for the beam pipe to clear the FMI quad Q100. At the entrance to the Lambertson the beam is displaced horizontally 39 mm from the Main Injector centerline. Vertically, the beam is 34 mm above the centerline; the circulating beam must be displaced 12 mm downwards at injection, but becomes centered at high field. The Lambertson is rolled through a small angle, on the order of 2.5° , to produce the vertical pitch necessary to cancel the off-axis dipole kick the beam receives from the downstream FMI quadrupole. The Lambertson removes the 35 mr angle to bring the beam onto the horizontal closed orbit of the FMI. Figure 2.4-5 shows the Lambertson magnet apertures and 40π mm-mr beam positions and profiles at 8 GeV and 150 GeV. The rolled quad has a good field region of ± 6 cm vertically, with a physical aperture slightly more than that. This is a full centimeter more than what the beam will see at injection, and two centimeters more than the edge of the circulating beam.

Three kicker modules located 90° downstream of the Lambertson, immediately upstream of Q103, provide the 1.03 mr of vertical kick necessary to cancel the vertical offset present at the Lambertson. This places the injected protons onto the vertical closed orbit of the Main Injector.

40π Envelope & $\Delta B/B=0.25\%$ Random Error

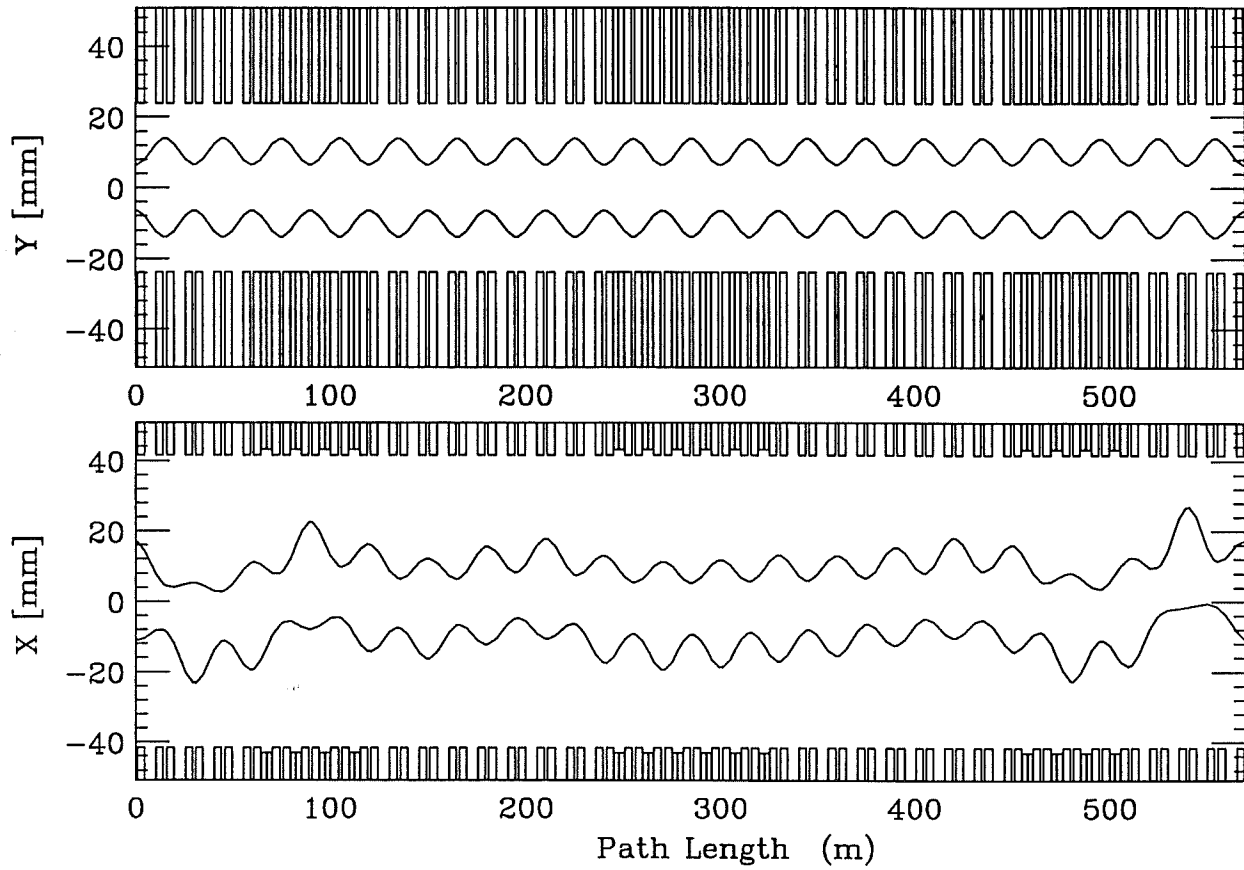


Figure 2.4-4(c).

Uncorrected trajectory and beam envelope for worst case random errors.

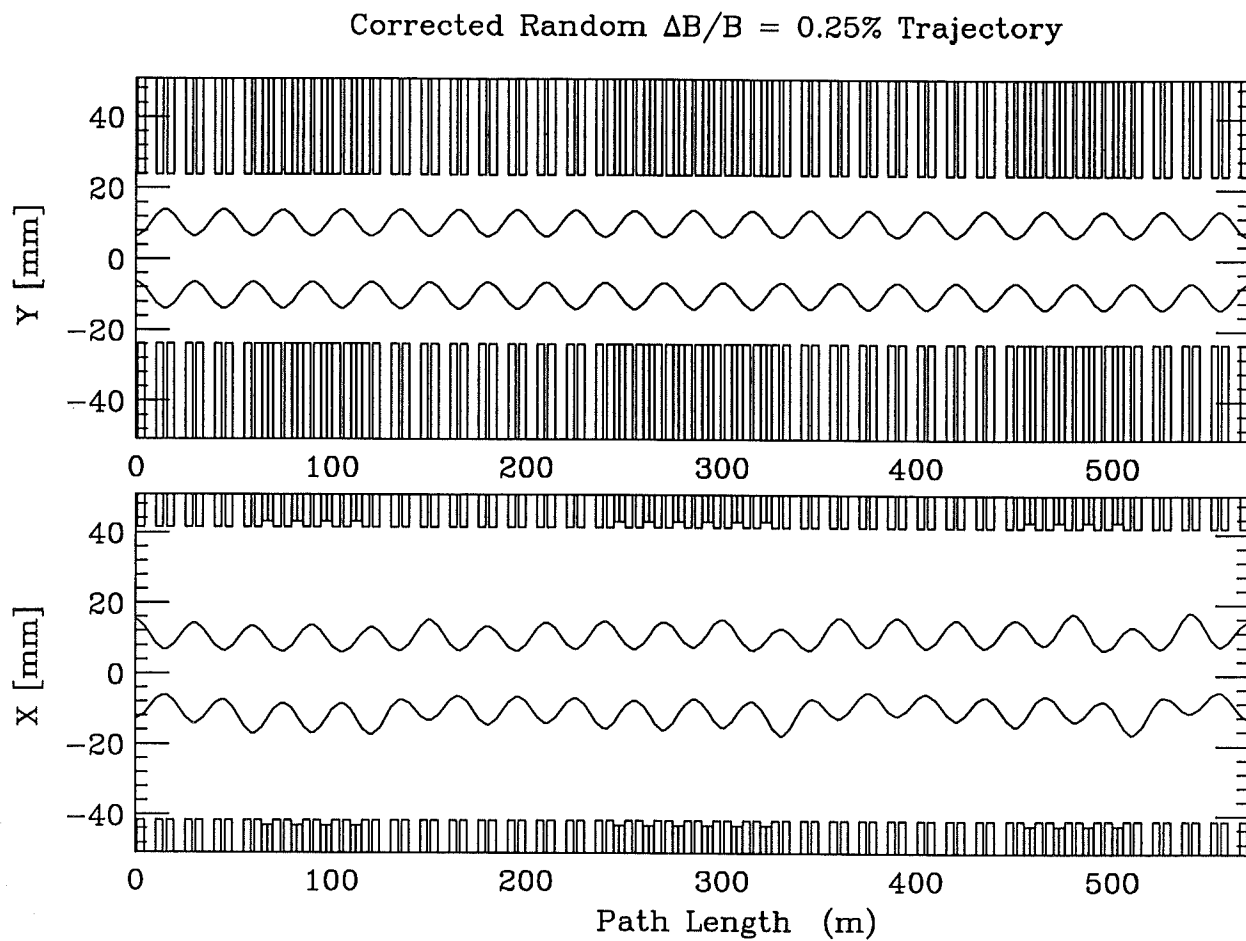


Figure 2.4-4(d). Beam trajectory and envelope after correction by moving magnets.

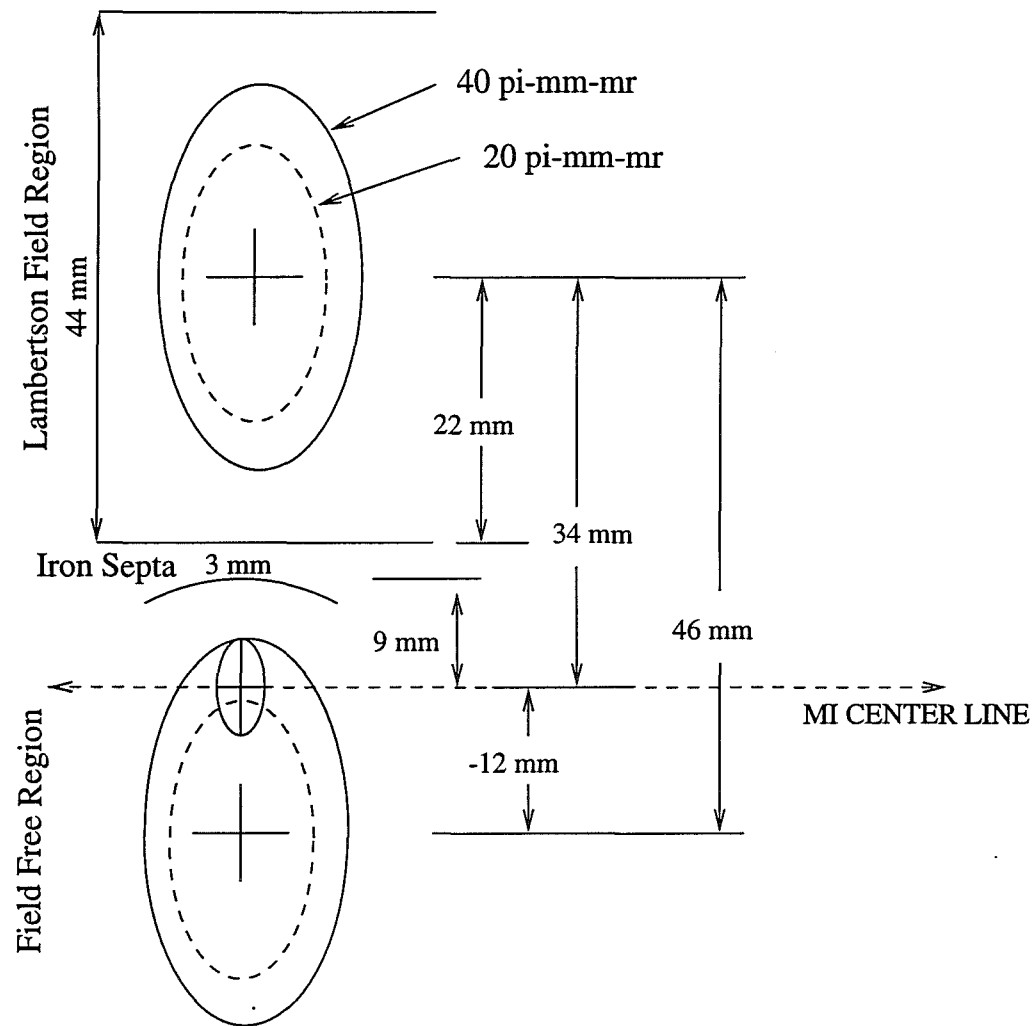


Figure 2.4-5. Lambertson magnet apertures.

2.4.2. The 150 GeV Lines

Two beamlines connect the FMI to the Tevatron. One of these transports the 150 GeV/c antiprotons. The other, in addition to its role of delivering 150 GeV/c protons to the Tevatron, is also required to transport 120 GeV/c protons destined for the antiproton production target or Switchyard, plus transport 8.9 GeV/c antiprotons to the FMI. In this section, only the two optically similar beamlines which transport 150 GeV/c particles from the FMI to the Tevatron are described. The supplementary transport commitments of the 150 GeV/c proton line are discussed in subsequent sections. Small differences exist between the proton and antiproton transfer lines, originating in the slight optical asymmetry of the Tevatron injection point with respect to the two species of particles.

The Main Injector lies 2.332 m lower in elevation than the Tevatron. Extraction of protons (antiprotons) is initiated by kicker magnets located at the extreme upstream end of MI-52 (MI-62) straight section. These provide the 525 μ r of kick necessary to deflect the beam across the septa of the vertically bending Lambertson magnets. The Lambertsons straddle the F quad located 90° in betatron phase downstream of the kickers. A C-magnet (current septum magnet) follows the third Lambertson. The Lambertsons and C-magnet deflect the beam upward by 24 mr; this is the minimum angle that provides clearance from the FMI quad at the downstream end of the straight section. Three vertical C-magnets then reduce the vertical pitch to 3 mr. The horizontal dipoles are rolled to produce the desired horizontal and vertical trajectory for vertical injection into the Tevatron.

The total length of each of the 150 GeV/c beamlines is 260 meters. Each line includes 15 recycled 6 m Main Ring B2 dipoles and 7 recycled Main Ring quads. A significant change since the Title I design report (Engineering Change Request #44) has been the replacement of ten recycled Main Ring quads (four 52" BQAs, and six 84" BQBs, also referred to as 3Q84s or 7000-series quadrupoles) with seven new 3Q120 and two new 3Q60 quadrupoles. The primary motivation for this change was to ease some of the tight clearances between elements in the beamlines and the Main Injector and Tevatron devices. A side benefit of the change comes from the fact that each of the new elements, which must be individually powered for lattice matching, runs at a much lower current than the Main Ring quads, resulting in a substantial cost savings in cables and power supplies, as well as a reduced operating cost. The five vertical C-magnets are identical in cross-section to the existing F-17 C-magnet, with the length increased from 118.4" to 132". The Lambertson magnets are a new design, discussed further in Chapter 3.1.

Optics

The lattice functions for the 150 GeV/c Tevatron injection lines for protons and antiprotons are shown in Figures 2.4-6 and 2.4-7. All eight lattice functions are well matched to the Tevatron optics. The two transport lines have essentially identical designs. Minor differences in the locations and gradients of the last four quadrupoles are necessary to accommodate the match into the optically asymmetric Tevatron F0 straight section. Basically, the lines continue the FMI lattice cell structure up to a pair of quadrupole doublets, which then achieve the final optical match to the Tevatron. Vertical dispersion generated by the FMI vertical extraction components is almost canceled by the Tevatron vertical injection magnets. To complete the cancellation, and satisfy the extremely tight geometric constraints, four families of rolled dipoles are utilized.

Correction Elements

Main Ring correction dipoles and BPMs are associated with each of the 14 quadrupole focusing centers in the 150 GeV/c lines. The operational mode in which 8.9 GeV/c antiprotons are transported dictates that fine trajectory control is essential for steering through the restricted aperture presented by the rolled dipoles. At 150 GeV/c steering tolerances through the line are not as stringent due to the smaller beam size.

Correction of central trajectory errors has been simulated with random magnet misalignments and dipole field errors assigned to the beamline elements. As discussed in connection with the 8 GeV proton line, suitable error values are: $\theta_x = \theta_y = 0.25$ mr, $\theta_{roll} = 0.5$ mr, and $\Delta B/B = 0.25\%$. Figure 2.4-8(a) illustrates deviations of the uncorrected central trajectory for 20 random error seeds. The consistently larger Δx values reflect the (approximate) absence of $\Delta B/B$ errors in the vertical plane. The maximum offsets at the end of the 260 m lines are $\Delta x \sim \pm 14$ mm and $\Delta y \sim \pm 6$ mm. Figure 2.4-8(b) shows the worst case trajectory, before and after correction. Maximum deviations in the line are reduced to ~ 1 mm, and the beam position and angle have been tuned at the injection point to $\Delta x = \Delta y = 0$ mm, and $\Delta x' = \Delta y' = 0$ mr. The maximum corrector strengths required are $\theta_H = 97$ μ r, and $\theta_V = 40$ μ r. At 150 GeV/c this horizontal strength is too large to be accommodated by the standard Main Ring correctors. Main Ring double-strength horizontal correctors are necessary to ensure correct beam position and angle matching at injection.

FMI Extraction

The requirements on the proton extraction Lambertson aperture are dictated not by the 150 GeV/c extraction but, rather, by its use as the injection Lambertson for 8.9 GeV/c antiprotons. Consequently, a new Lambertson magnet is being designed for use at MI-52, with a 2" wide by 14" high symmetric field region. With the reduced beta functions in the FMI straight section

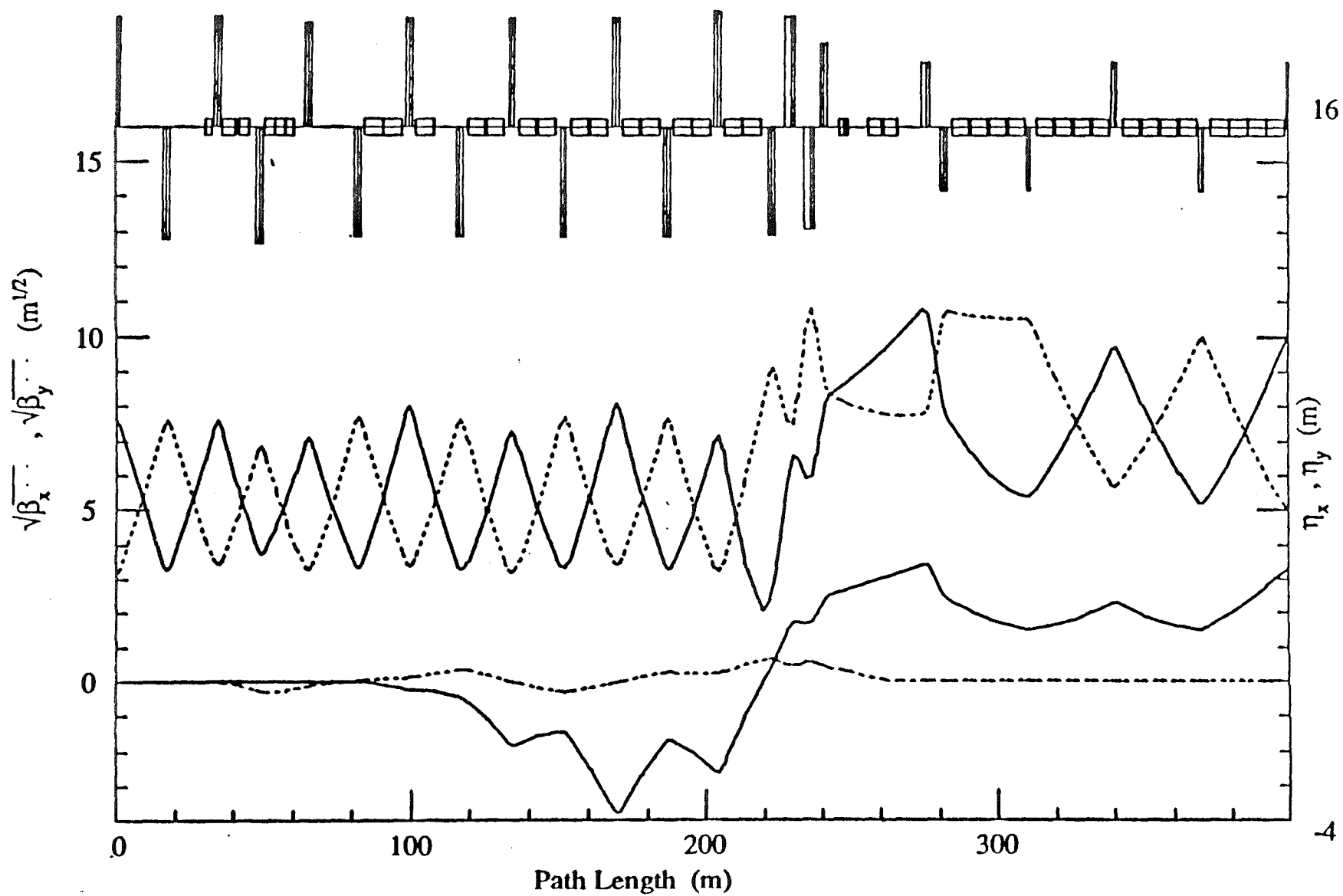


Figure 2.4-6. 150 GeV Proton Line Lattice Functions.

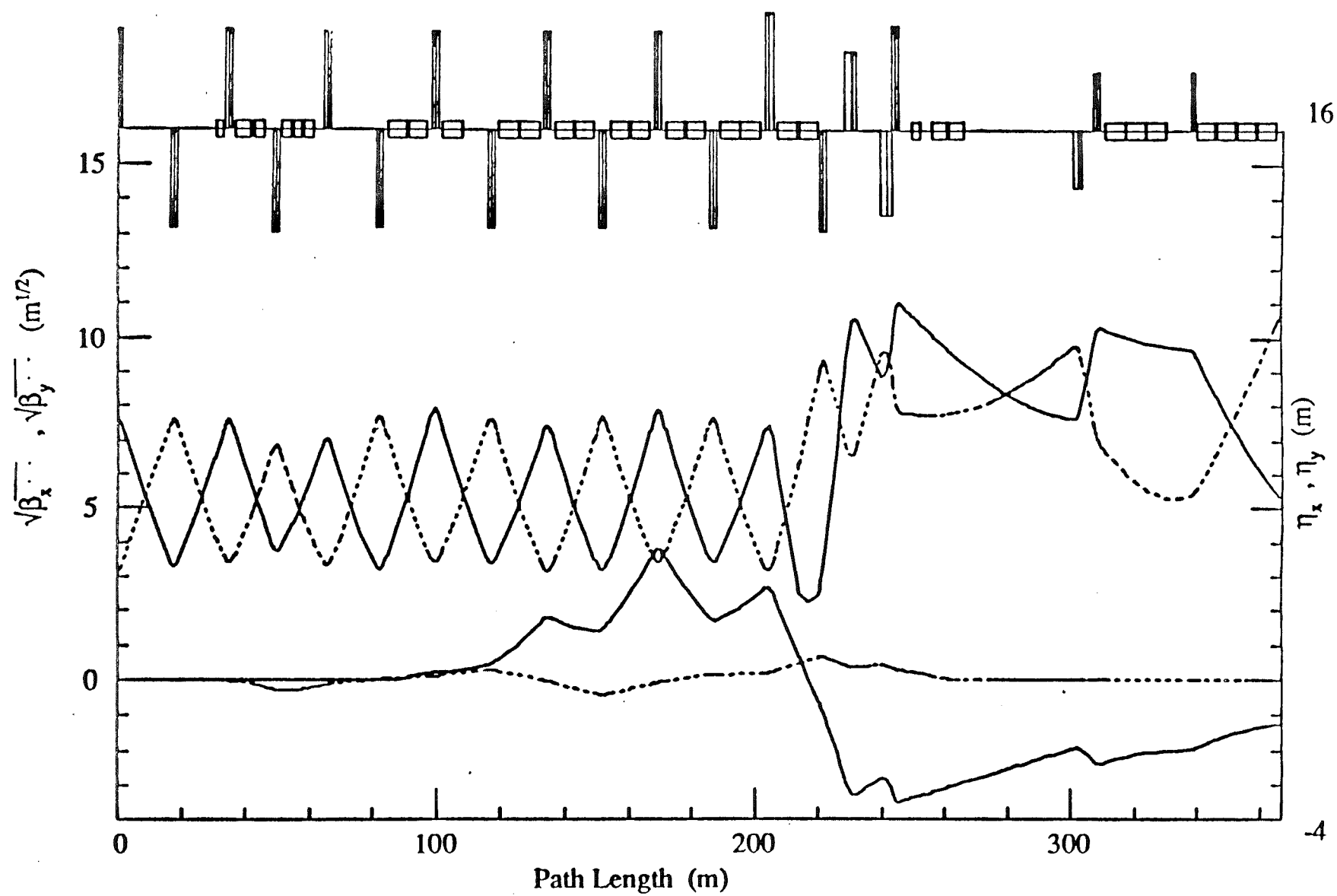


Figure 2.4-7. 150 GeV Antiproton Line Lattice Functions.

Errors: $\sigma(DX,DY) = 0.25 \text{ mm}$, $\sigma(\text{roll}) = 0.5 \text{ mr}$, $\Delta B/B = 25\text{E-}4$
 Central Trajectory Before Correction: 20 seeds

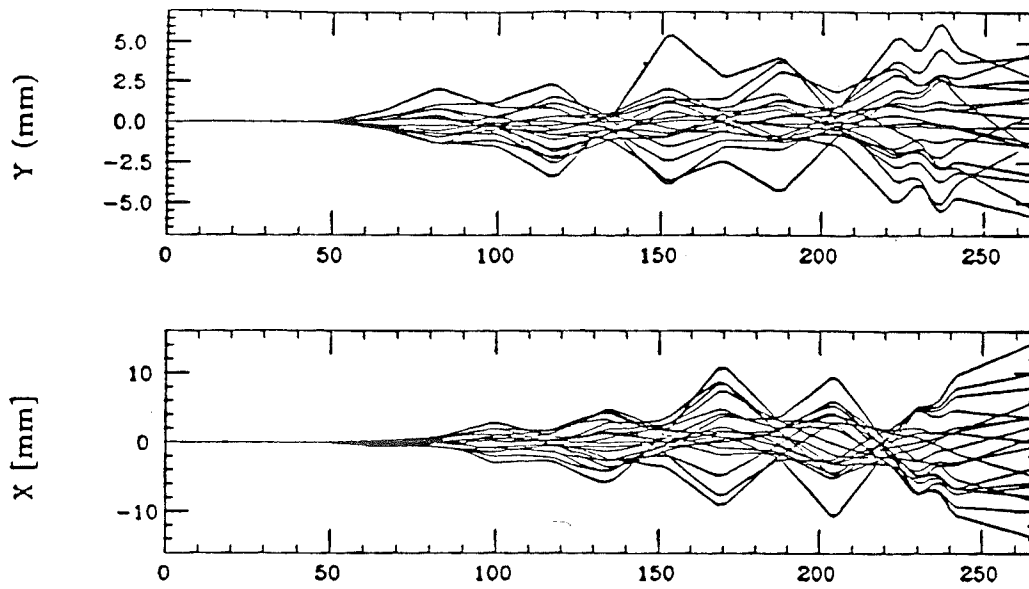


Figure 2.4-8(a). Uncorrected Orbit Errors in the 150 GeV Line.

Errors: $\sigma(DX,DY) = 0.25 \text{ mm}$, $\sigma(\text{roll}) = 0.5 \text{ mr}$, $\Delta B/B = 25\text{E-}4$
 Central Trajectory Before and After Correction: seed 1357
 $\theta_x(\text{rms}) = 62 \mu\text{r}$ $\theta_x(\text{max}) = 97 \mu\text{r}$ $\theta_y(\text{rms}) = 29 \mu\text{r}$ $\theta_y(\text{max}) = 40 \mu\text{r}$

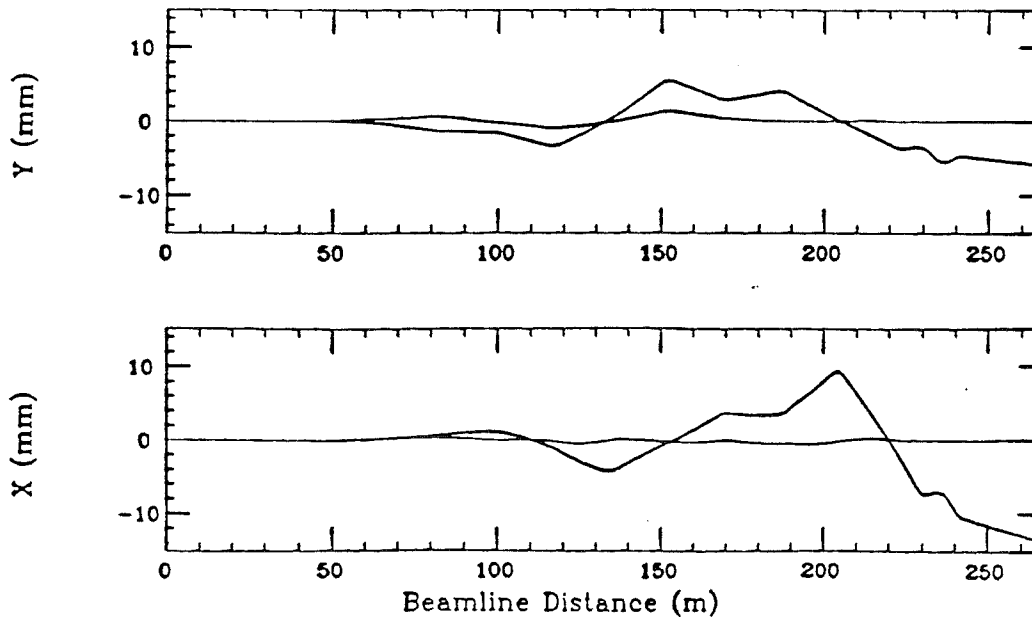


Figure 2.4-8(b). Worst-Case Uncorrected Orbit in the 150 GeV Line and Corrected Orbit.

compared to Main Ring, the Lambertson has sufficient aperture to accept 40π mm-mr antiproton beams from the Antiproton Source. The Lambertson magnets are the same type as those used for the abort in MI-40. The Lambertson and C-magnets are described in Chapter 3.1. Figure 2.4-9(a) shows the layout of the extraction devices in the MI-52 straight section. The MI-62 straight section for antiproton extraction is similar, but with no electrostatic septa required. Figure 2.4-9(b) shows the 8 GeV circulating beam closed orbit and the injected antiproton trajectory through the MI-52 region. Figure 2.4-9(c) shows the 120 GeV slow spill circulating beam closed orbit and extracted beam trajectory, while Figure 2.4-9(d) and Figure 2.4-9(e) show the 150 GeV closed orbit and extracted beam trajectories at MI-52 and MI-62, respectively. Figure 2.4-9(f) and Figure 2.4-9(g) show the beam profile and extraction element apertures through the MI-52 straight section for 8 GeV and for 150 GeV beams. The beam emittance indicated in all of these figures is 30π mm-mr. Generous clearance for the injected and circulating beams is afforded. Only the second and third Lambertson magnets are excited for 8.9 GeV/c beam transfers, so the beam passes through the quadrupole with no vertical offset.

Schematic of Extraction Straight Sections MI-40, MI-52, and MI-62

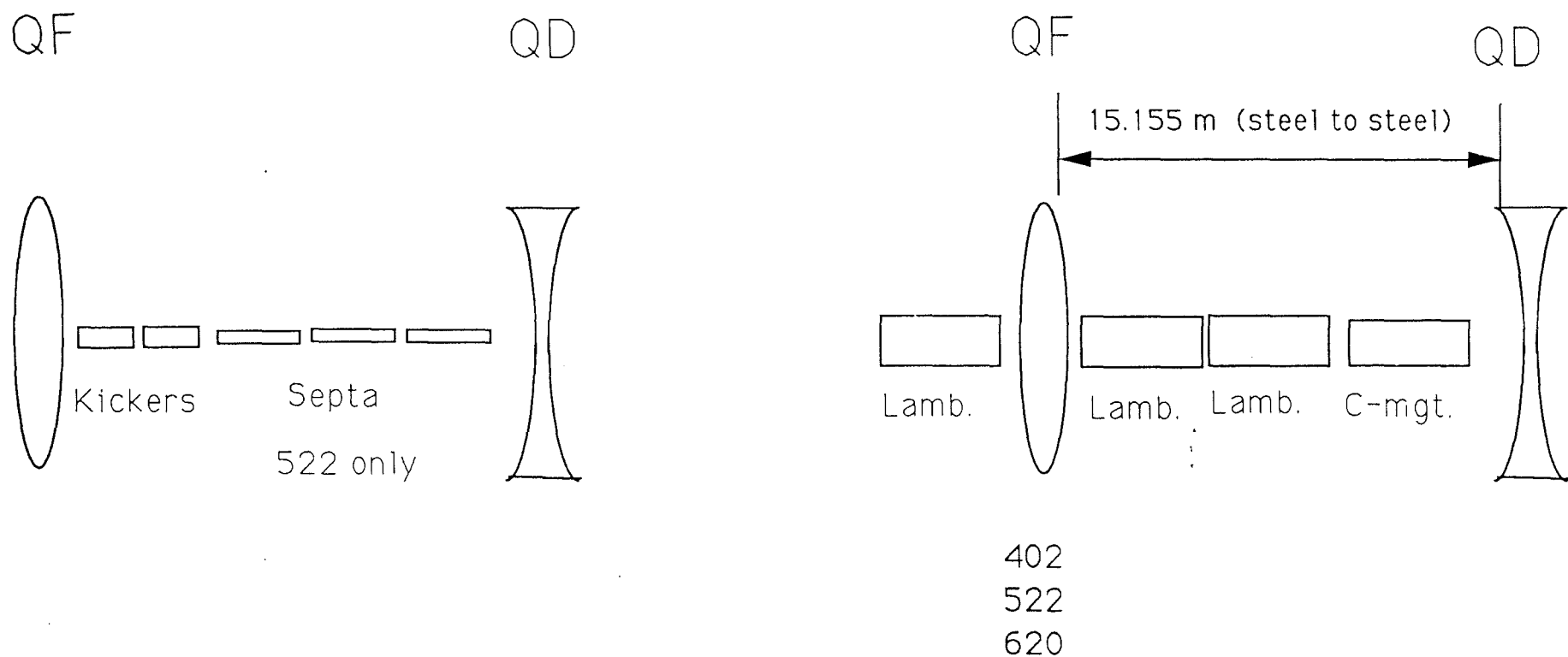


Figure 2.4-9(a). Layout of Extraction Elements in the MI-52 Straight Section

MI-52 PBAR INJECTION ORBIT

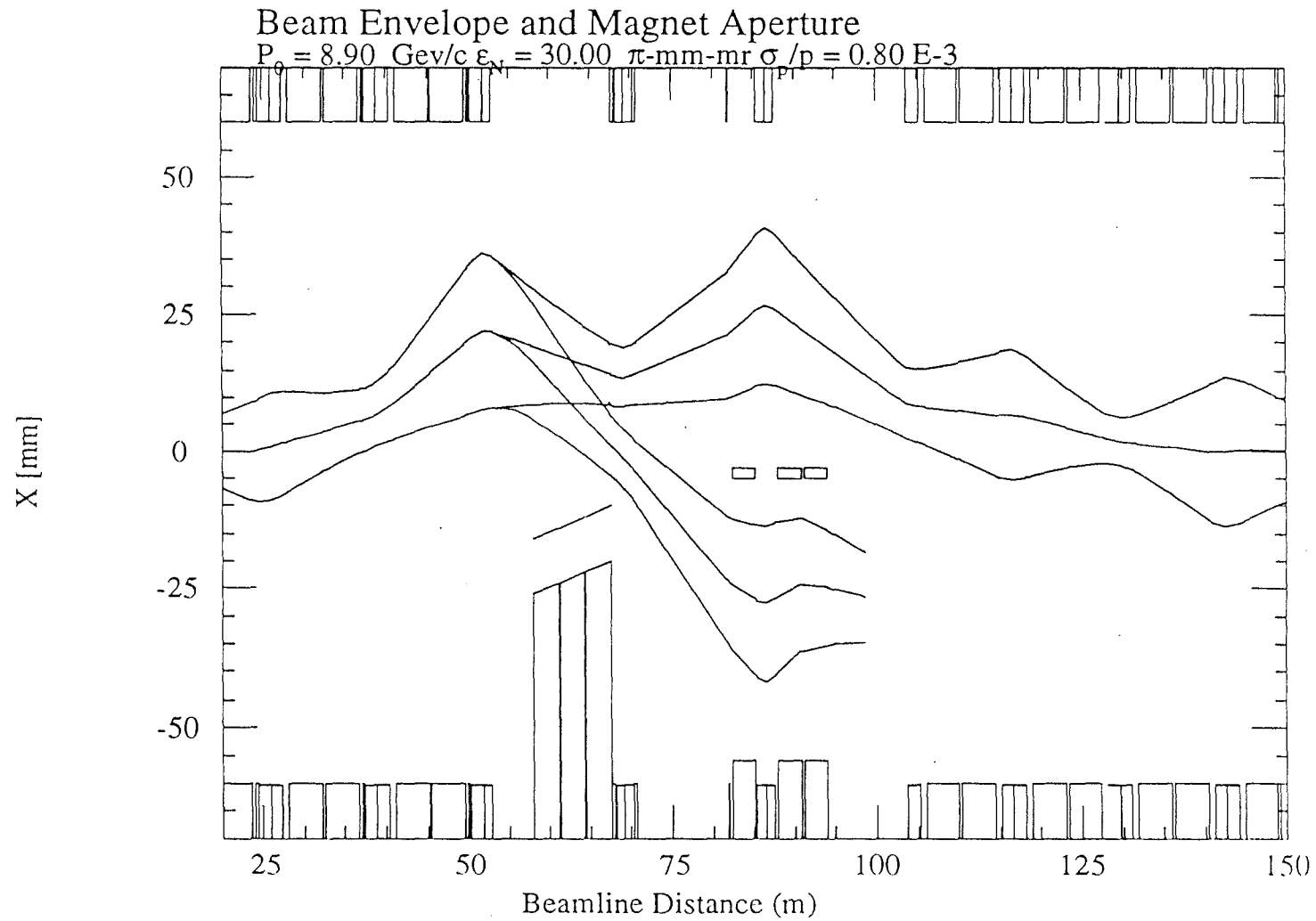


Figure 2.4-9(b). 8 GeV Antiproton Closed Orbit and Injected Beam Trajectories in the MI-52 Straight Section.

MI-52 PROTON EXTRACTION ORBIT

120 GeV/c Slow spill

Beamline Central Trajectory and Magnet Apert

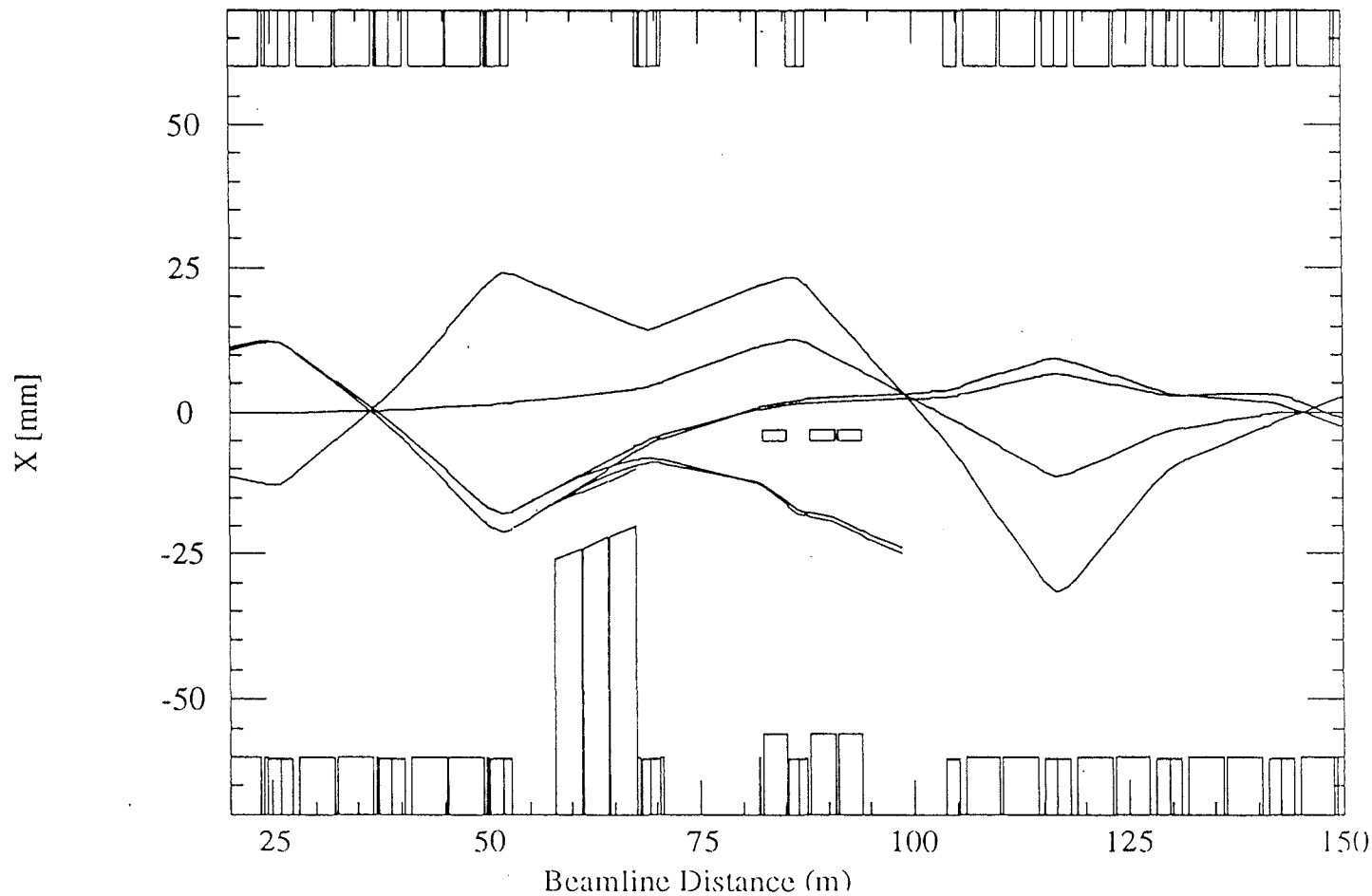


Figure 2.4-9(c). 120 GeV Slow Spill Closed Orbit and Extracted Beam Trajectories in the MI-52 Straight Section

MI-52 PROTON EXTRACTION ORBIT

120 GeV/c Pbar production

150 GeV/c Tevatron injection

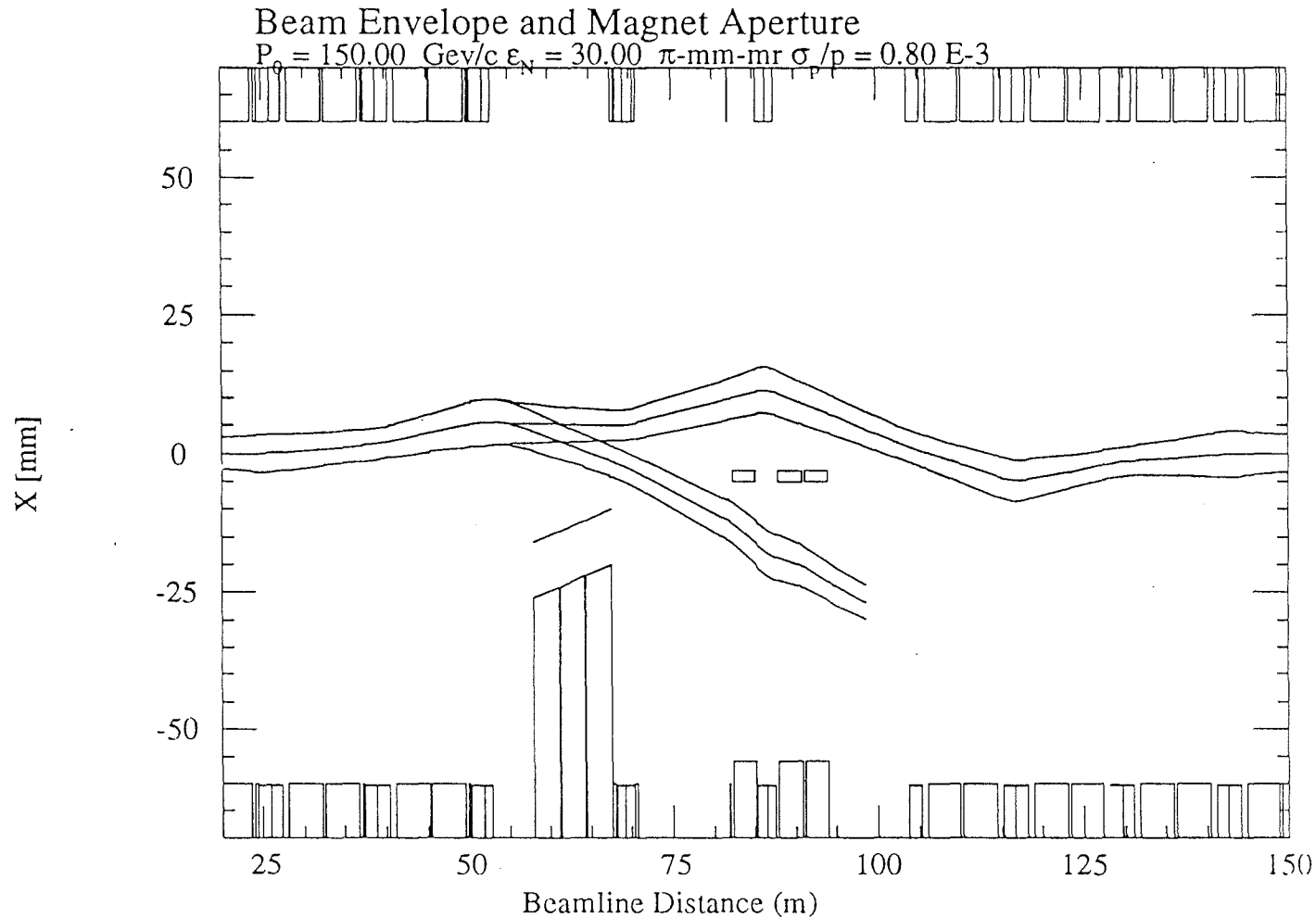


Figure 2.4-9(d). 150 GeV Closed Orbit and Extracted Beam Trajectories in the MI-52 Straight Section.

MI-62 PBAR EXTRACTION ORBIT

150 GeV/c Tevatron Injection

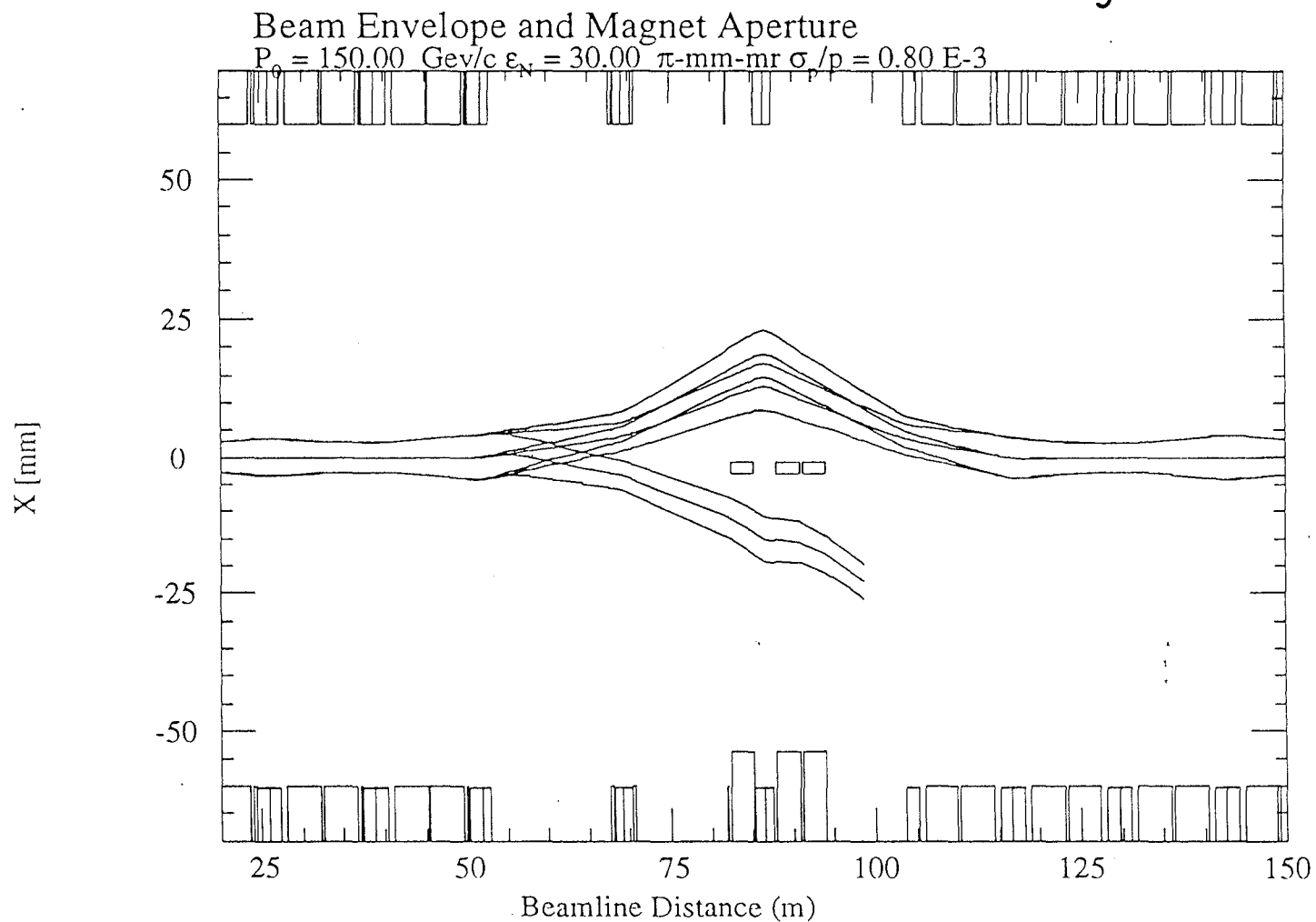


Figure 2.4-9(e). 150 GeV Closed Orbit and Extracted Beam Trajectories in the MI-62 Straight Section.

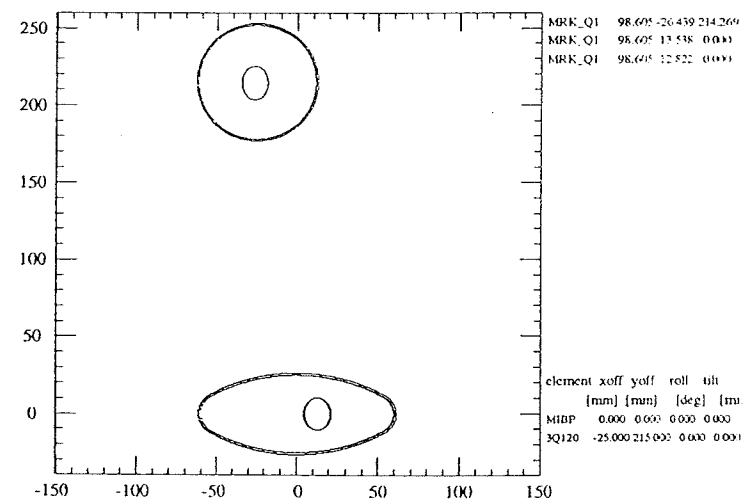
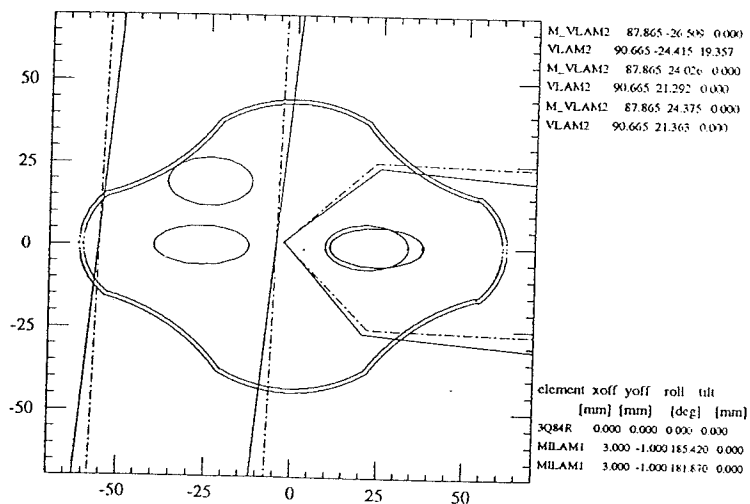
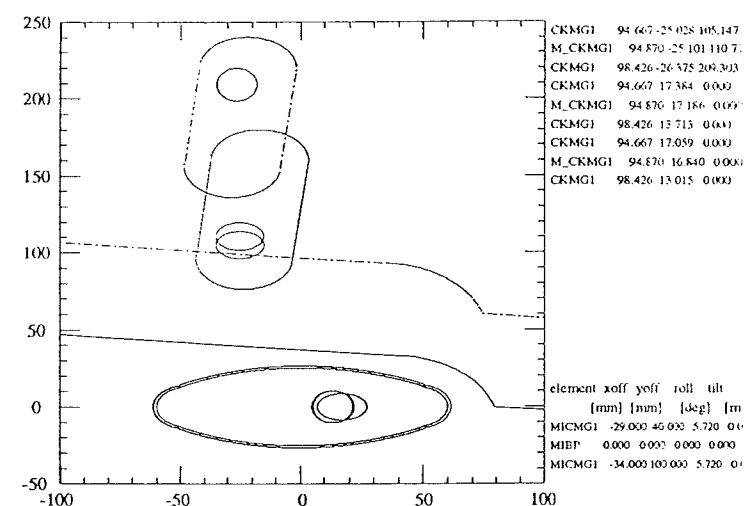
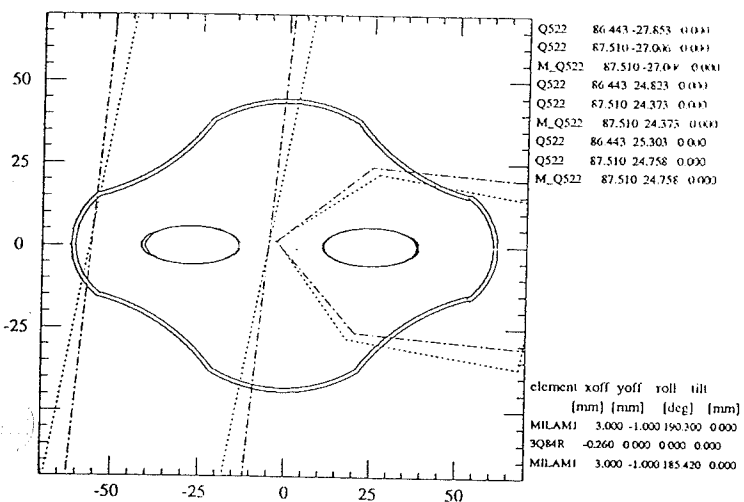
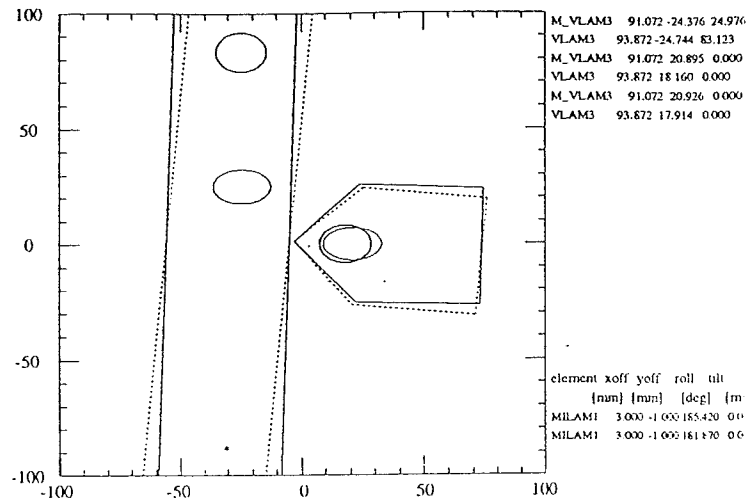
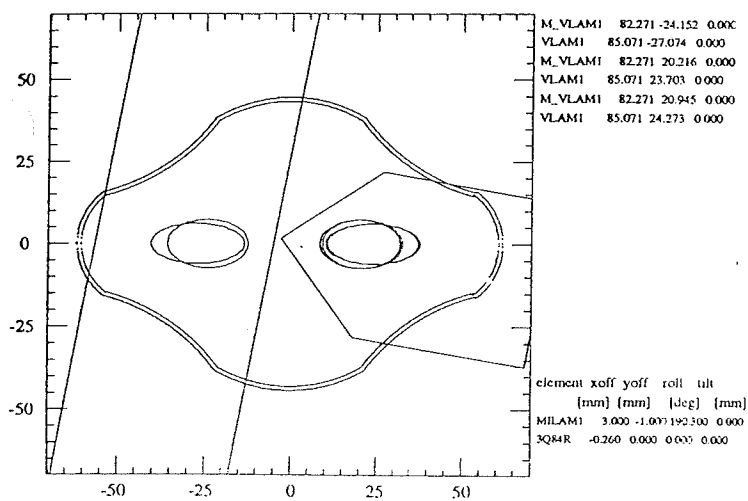


Figure 2.4-9(f). 8 GeV Beam Profiles and Magnet Apertures Through the MI-52 Straight Section

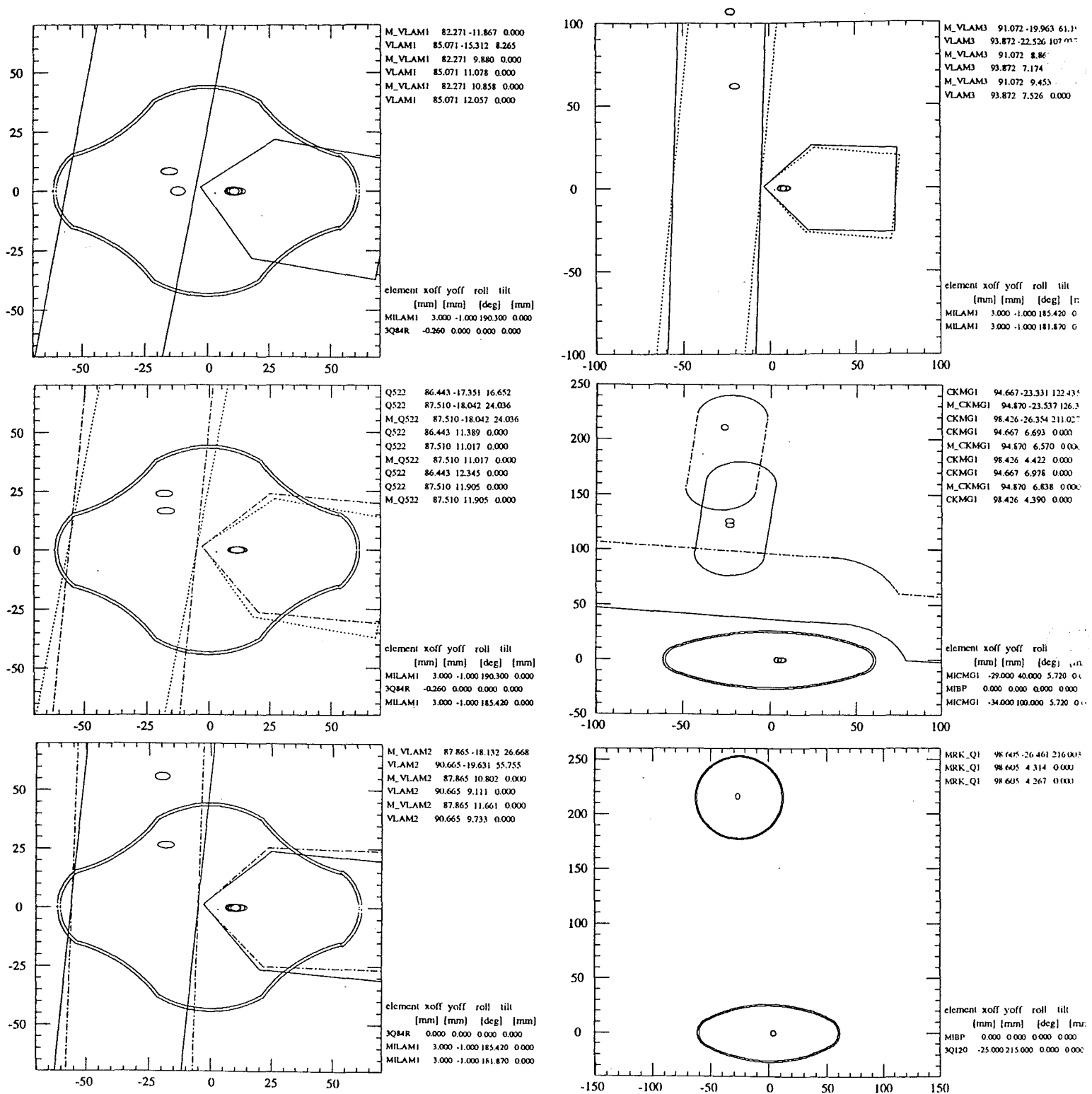


Figure 2.4-9(g). 150 GeV Beam Profiles and Magnet Apertures Through the MI-52 Straight Section

Tevatron Injection

Injection into the Tevatron is moved from its present location in the E0 straight section to the F0 straight section. This move leaves the E0 straight section completely free for possible use as an interaction region or for other purposes.

The F0 region continues to be used to accommodate the Tevatron rf systems. By rearranging the accelerating cavities in the upstream end (proton beam direction) of the straight section, as shown in Figure 2.4-1, the proton and antiproton injection lines converge toward a common set of injection septum magnets located at the downstream end of the straight section. This reduces the space requirements and the number of such elements needed for injection into the Tevatron, compared to that required in the current configuration at E0. The placement of the rf cavities is discussed in Chapter 3.4.

The incoming beam approaches the Tevatron vertically for injection, with the last vertical bend produced by four Lambertsons common to both proton and antiproton injection lines. These Lambertson magnets are identical in design to those at MI-52 and the other extraction points in the Main Injector, reducing costs for tooling and spares. Closure onto the horizontal orbit is accomplished by a kicker magnet downstream of the injection point. The nearest points on either side of the long straight section where kickers can be placed are the F17 medium straight section (for clockwise proton injection) and the E48 short straight section (for counterclockwise antiproton injection). The present Tevatron antiproton injection kicker will be recycled; a new proton kicker will be required.

Injection System Layout

The Tevatron rf system occupies roughly 26 m of the 52 m straight section. In the remaining 26 m, four Lambertson magnetic septa are placed symmetrically about a point 13.223 m upstream (proton direction) of the end of the straight section. Both the proton and antiproton beams pass through the field region of these magnets upon injection. With the Lambertson off, the 120 GeV/c proton and the 8.9 GeV/c antiprotons pass through the same field region (de-energized) to get to and from the Main Ring remnant. To accommodate the 120 GeV/c proton and 8.9 GeV/c antiproton trajectories, a Lambertson is being designed with a larger field region. The same Lambertson design is used for FMI extraction (proton, antiproton, and abort), as discussed previously. To provide more clearance at the ends of the free space, each of the injection lines incorporates one C-style magnet just in front of the Lambertsons. An elevation view of the the F0 region is shown in Figure 2.4-10.

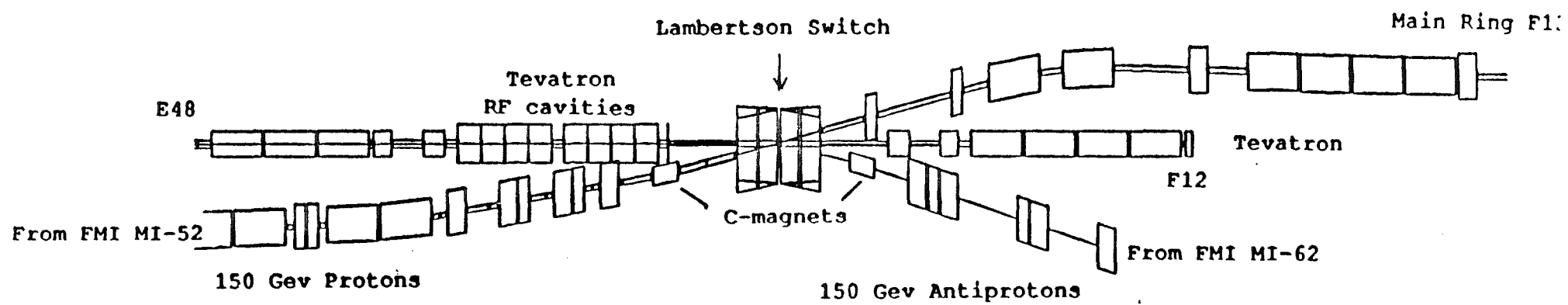


Figure 2.4-10. Elevation View of the F0 Region

2.4.3. 120 GeV Antiproton Production

The existing AP-1 beamline, which is used to target 120 GeV/c protons for antiproton production and transport 8.9 GeV/c antiprotons back to the Main Ring, remains intact. The Main Ring magnets used from F11 to F17 also remain in place, with only minor modifications to the bus and power supplies. The 120 GeV/c protons utilize the Tevatron proton injection line from the FMI (MI-52) to the Tevatron injection Lambertsons. With the Lambertsons off, the protons enter the Main Ring remnant at Main Ring station F11 for transport to Main Ring station F17. A vertically bending Main Ring B3 dipole, located immediately downstream of the Main Ring F17 quad, when energized, deflects the beam into the existing AP-1 beamline. De-energized, this magnet allows the 120 GeV/c slow spill to be transported to the Switchyard. Figure 2.4-11 shows the retune of the Tevatron proton injection line for matching into the Main Ring remnant.

Modifications to Main Ring F11 to F17 Magnet String

This section of magnets remains in its current location. Only minor modifications to the magnet bus are required to power the dipole and quadrupole circuits. The B1 magnets (1.5"x5" beam pipe) are replaced with B2 magnets (2"x4" beam pipe) to increase the acceptance for antiproton transfers. It may also be determined advantageous to replace the six B2 magnets at the locations of largest vertical β -function with B3 magnets (3"x5" beam pipe). The quadrupoles at F11 and F12 will be powered independently to facilitate matching into the Main Ring FODO lattice at Main Ring F13. The existing Main Ring quadrupoles at F11 (three BQAs and one BQB) will be replaced by two 3Q60s, and the BQA at F12 will be replaced by one 3Q60, each separately powered from F0. The rest of the quads (F13 to F17) will remain BQBs, powered in series from F1. The four Main Ring F11 dipoles are replaced by two B3 dipoles running at twice the field of a standard B2 dipole and rolled by about 40°. The Main Ring F12 dipoles are also rolled (with the first dipole being replaced by a B3 at twice the field) to produce the required horizontal and vertical trajectory for the present Main Ring trajectory at F13. A Main Ring power supply located at F1 powers the bending magnets in this section. The focusing and defocusing quadrupole busses are powered in series by a new supply. The dipole correction elements remain in this section for use in smoothing the orbit of 8.9 GeV/c antiprotons. Figure 2.4-12 shows the 8 GeV beam size and the magnet apertures in the beamline from MI-52 to F-17.

Connection with the Existing AP-1 Beamline

In the current Main Ring configuration, a kicker at E17 supplies the necessary orbit distortion to place the beam in the field region of the Lamberton magnet at F17. In the FMI era this Lamberton is replaced by a vertically bending B3 which deflects the beam upwards sufficiently to miss the first downstream Main Ring dipole and enter the AP-1 line. The match between the Main Ring F17 and the AP-1 line is not altered. Use of a B3 has the advantage that it

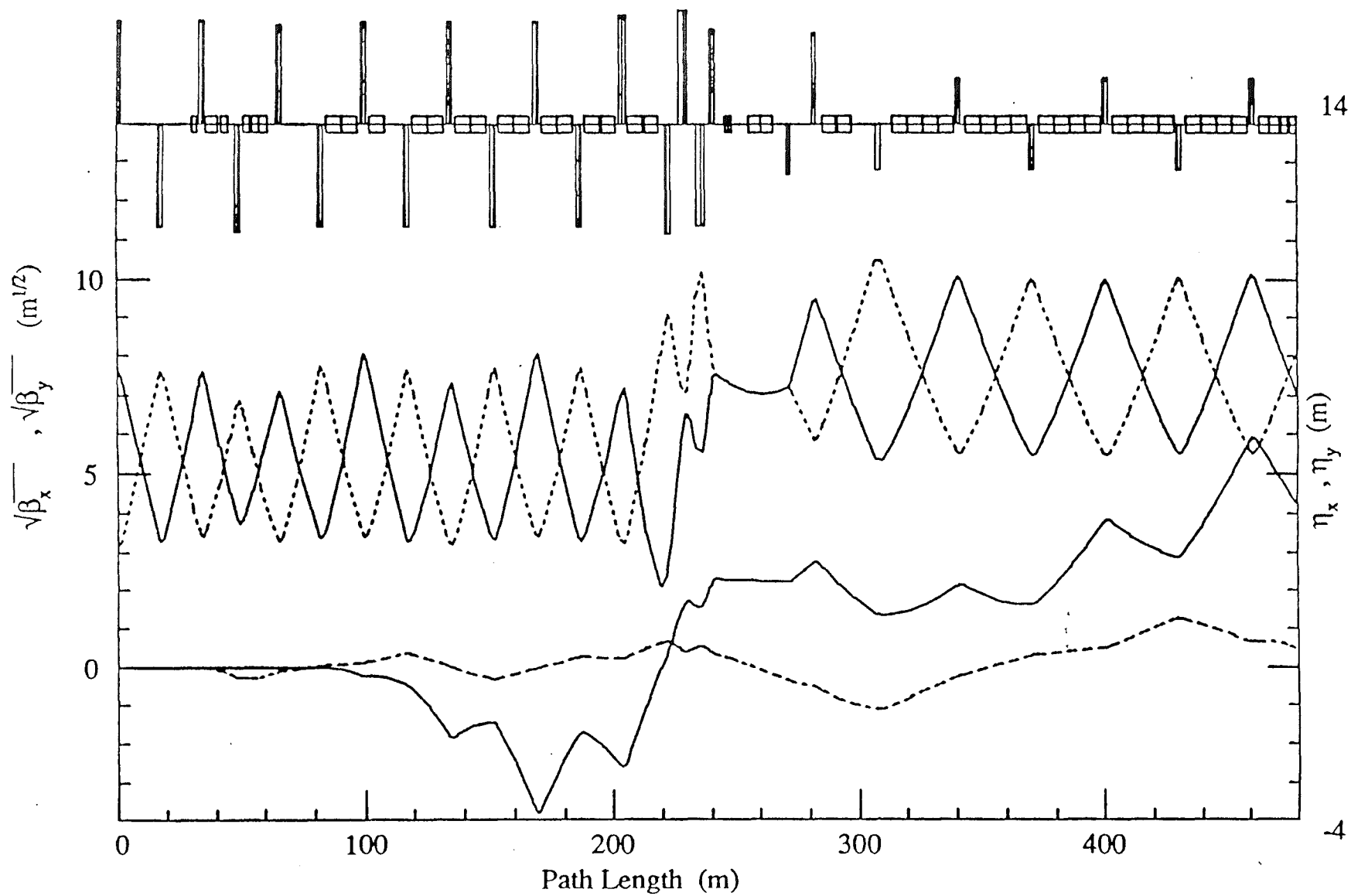


Figure 2.4-11. Lattice Functions for 8/120 GeV Transfers to Main Ring Remnant.

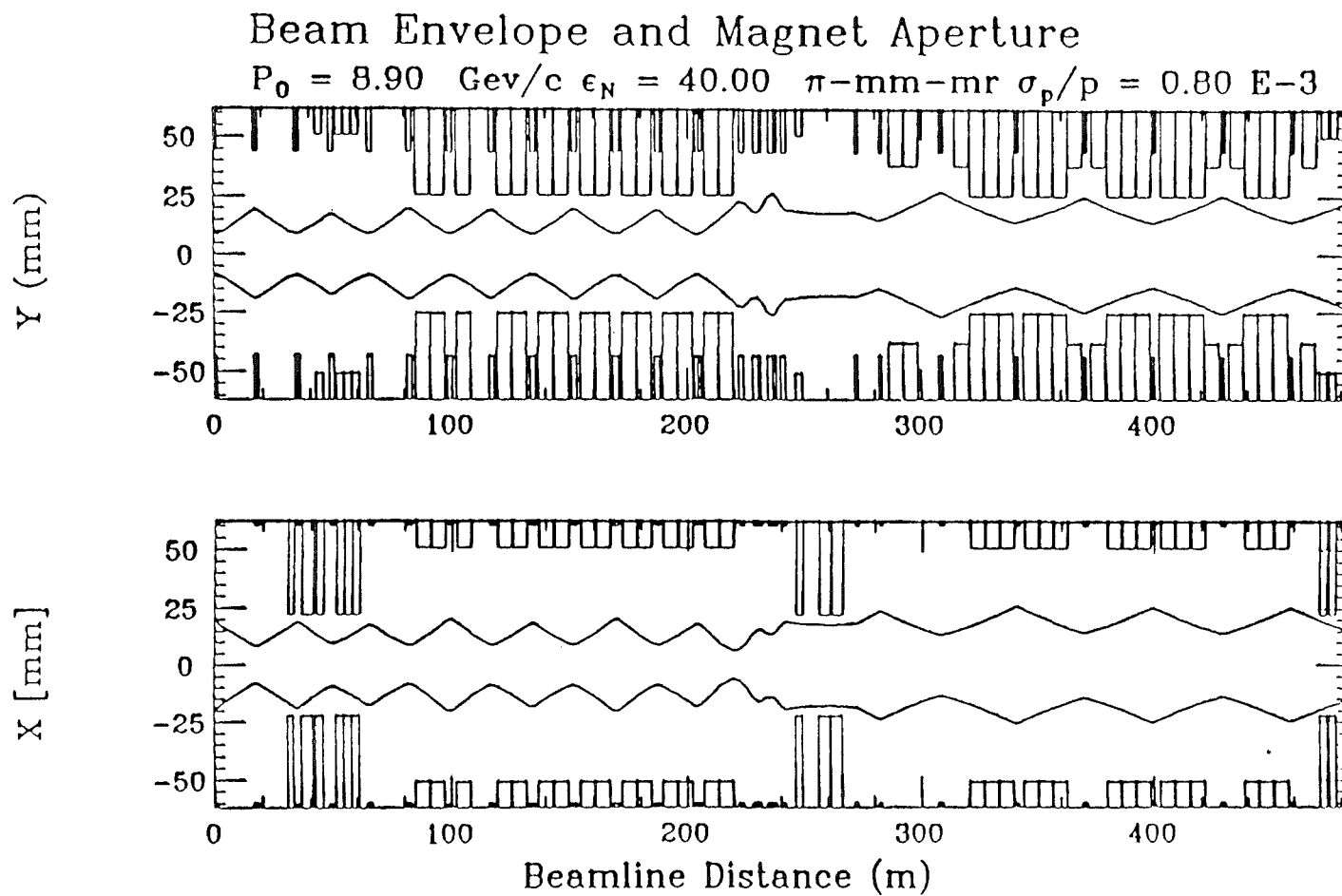


Figure 2.4-12. 8 GeV Antiproton Beam Envelope and Magnet Apertures.

provides a larger aperture for the 8.9 GeV/c antiprotons. The B3 is turned off during slow spill to Switchyard. Since the B3 is individually powered (in series with the two C-magnets at the beginning of the AP-1 line) this configuration is consistent with the FMI acceleration cycle in which antiproton production and slow spill are mixed on a common flattop.

2.4.4. The 120 GeV Slow Spill Line

The 120 GeV slow spill beamline transports both slow and fast extracted beam from the FMI to the experimental areas for a variety of purposes during collider and fixed-target runs. This beamline uses four beamline sections: MI-52 to F11; F11-F17 magnet string; F18-A0 magnet string, and the new section of beamline between F48 and Switchyard. The first two segments were described previously.

Modifications to F18-A0 Magnet String

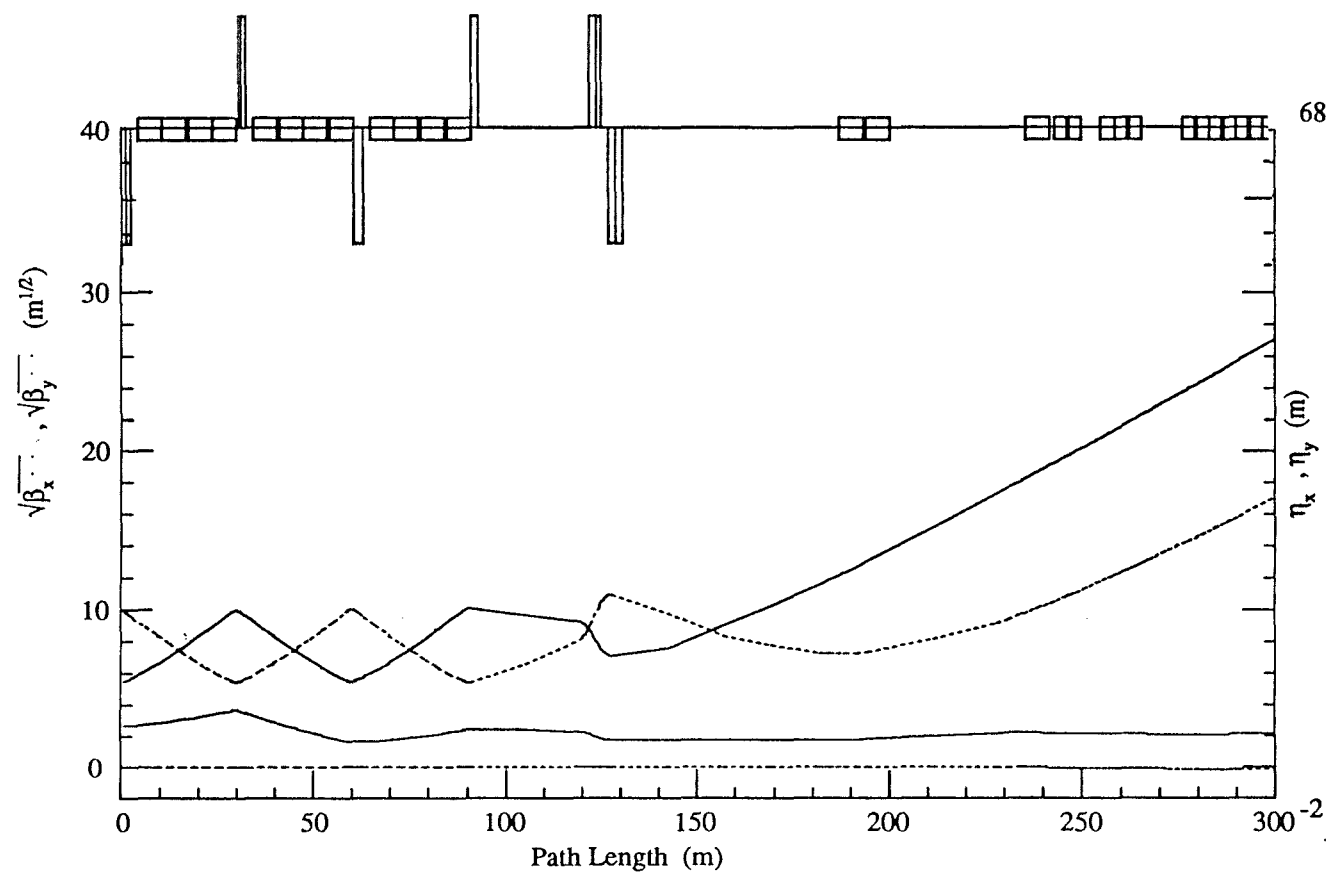
The magnet string remains in its current location. The fourth Main Ring F47 B2 dipole is replaced with a rolled ($\sim 4.4^\circ$) B3 dipole at twice the field, and the three Main Ring F48 dipoles are removed. These modifications produce a trajectory approximately 3' west of the entrance into the Switchyard with a downward pitch. Minor bus work is needed to connect the four power supplies required to ramp the bending magnets in this section. One Main Ring power supply at F3 is used to power two quad busses in series. The quadrupoles at F48 and F49 plus an additional recycled Main Ring quad are powered individually to produce the required optical match into the Switchyard. A savings in operating cost could be realized by replacing the B2 magnets in this section with B1 magnets, which have a lower impedance.

F49 to Switchyard

A pair of recycled Main Ring B2 horizontal bending dipoles located 60 m downstream of F49 are powered individually to produce a trajectory which intercepts the Switchyard beamline approximately 40 meters downstream of the present Switchyard channel. The final closure onto the horizontal and vertical Switchyard trajectory is produced by a rolled (17°) B3 dipole powered by the F-Sector bus. Figure 2.4-13 shows the lattice functions in this section. Plan and elevation views, in distorted scale, of the magnets in this section are shown in Figures 2.4-14(a) and 2.4-14(b).

Modifications to Switchyard

Minor modifications to the upstream end of the Switchyard are required. The first horizontal dipole and quad along with five of the seven proton electrostatic splitting septa modules (PSEPs) are moved upstream. The last two PSEP modules are shifted downstream to provide space for the rolled B3 magnet that provides the matching into Switchyard. The two PSEP modules downstream of the B3 are required to provide test beams to all areas.



TTITLE:
FILE: test_beam.trns

Wed Jul 15 15:36:35 1992

Figure 2.4-13. Lattice Functions for the 120 GeV Slow Spill Line Connection to Switchyard

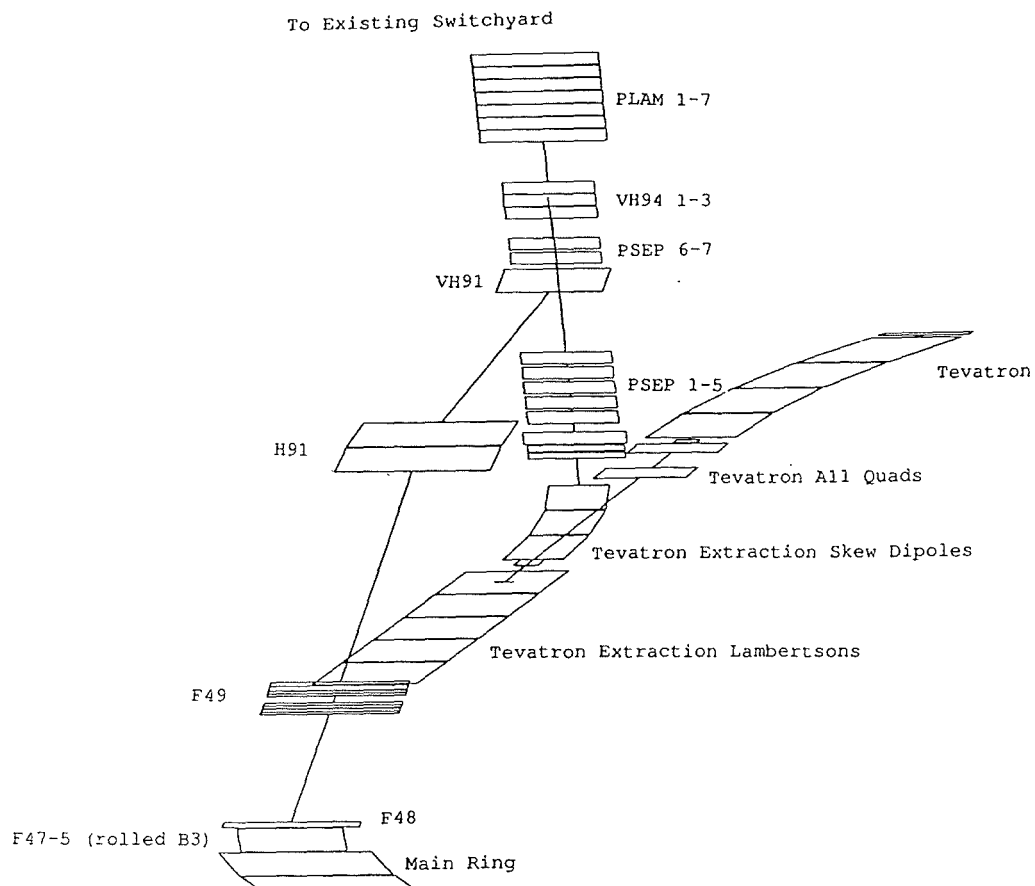


Figure 2.4-14(a). Plan View of 120 GeV Slow Spill Line Connection to Switchyard

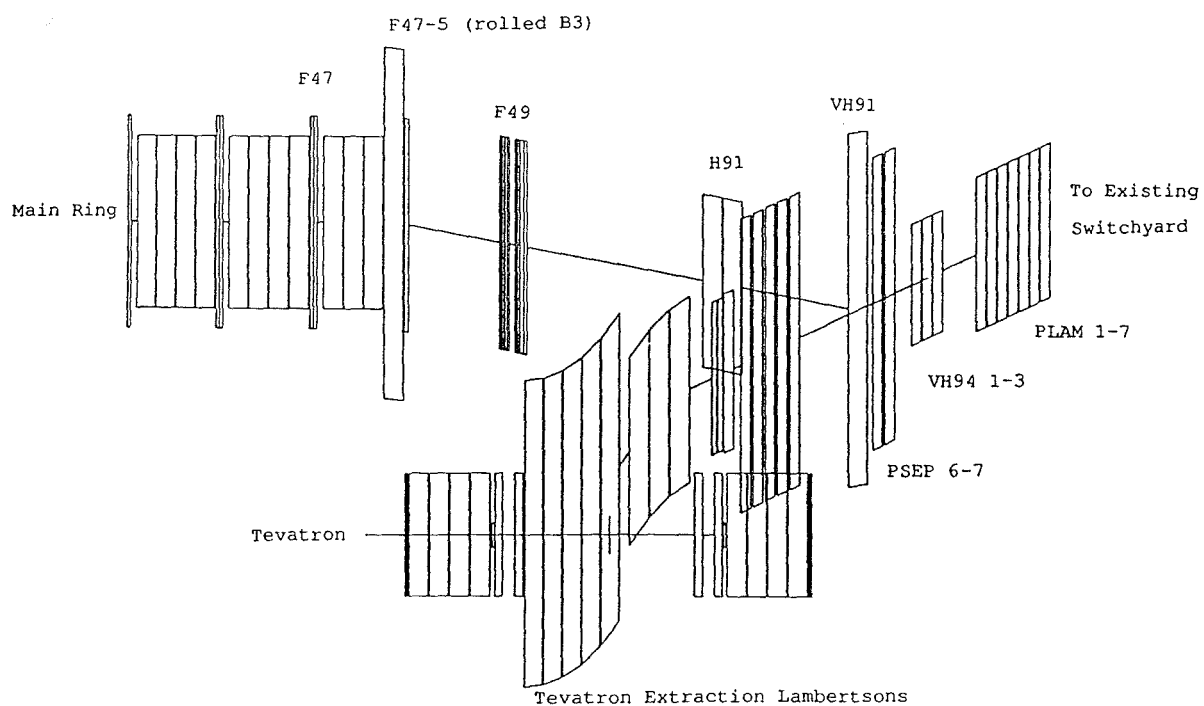
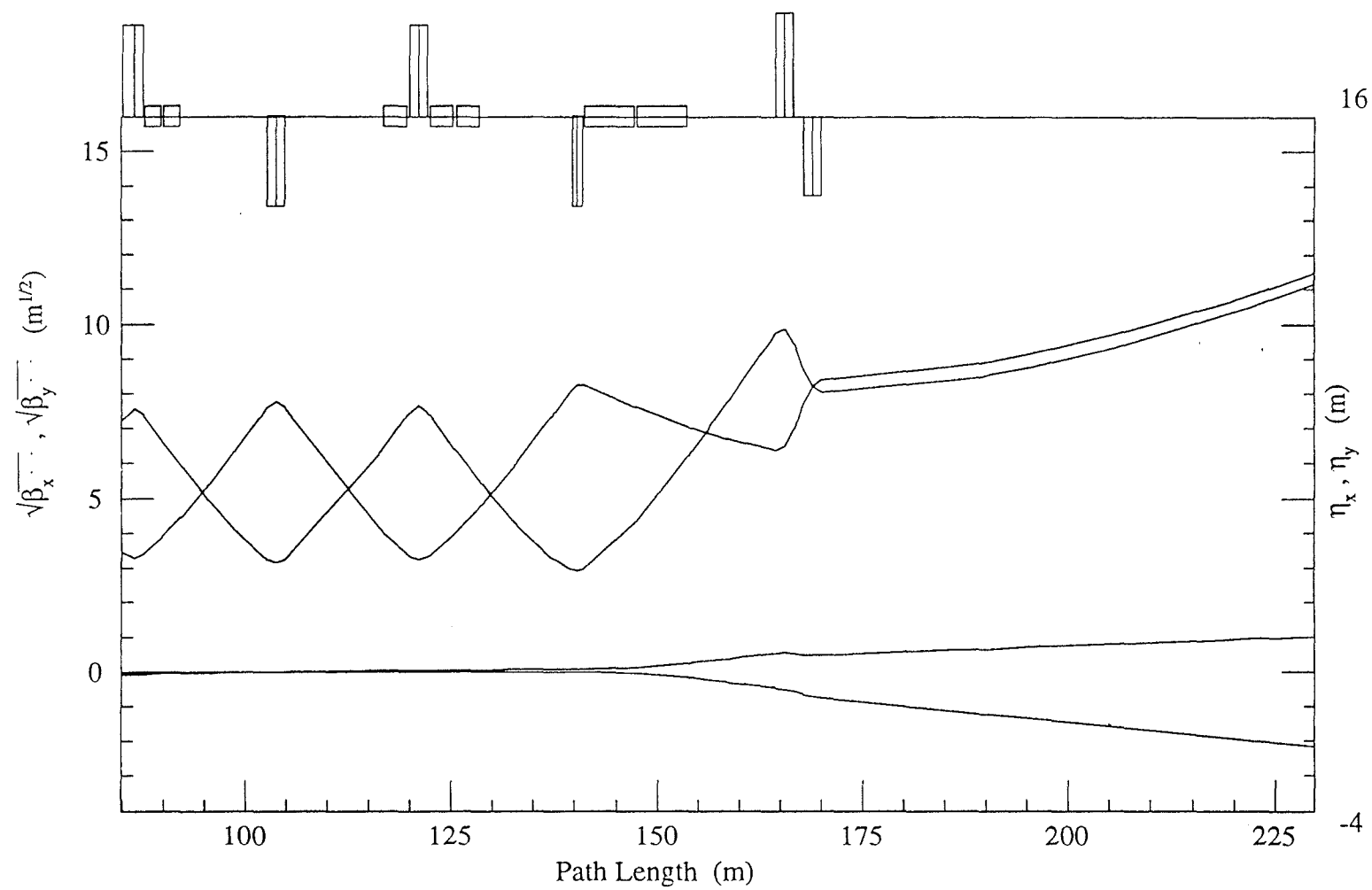


Figure 2.4-14(b). Elevation View of 120 GeV Slow Spill Line Connection to Switchyard

2.4.5. The Abort Line

Aborted beam is extracted from FMI straight section MI-40. Two kicker modules at the upstream end of the straight section provide sufficient displacement (38 mm at 8.9 GeV/c and 28 mm at 150 GeV/c) 90° in phase downstream for the beam to enter the extraction channel. Three vertically bending Lambertsons straddle the focusing quad situated at the straight section midpoint. The Lambertsons plus a C-magnet deflect the beam down by 24 mr to clear the next downstream FMI quad. The aborted beam is then leveled off and deflected outwards by two B2 dipole magnets rolled at a 50° angle. In addition, one BQA (52") and two BQB (84") quadrupoles are placed in the abort line to maintain a suitable beam size for transport to the beam dump. The optics of this line are designed such that the dipoles and quadrupoles are powered in series with the FMI quadrupole bus. Main Ring correctors are used for fine adjustment of the beam position at the dump. Sufficient free space exists in the downstream portion of the abort line for other magnetic elements which could be used to deflect 120 GeV beam around the beam dump to future experimental areas. Figure 2.4-15 shows the layout of the magnets in the abort line.



FILES: ml120.lat : tws_bend.prc

Fri Aug 19 14:15:21 1994

Figure 2.4-15. Abort Line Lattice Functions

2.4.6. Beamline Magnets and Power Supplies

Magnet Requirements

Magnet requirements for all beamlines are summarized in Table 2.4-1. Decommissioning the Main Ring and the 8 GeV line will provide a major source of magnets for the beamlines.

The new 8 GeV line utilizes 55 recycled Main Ring B2 magnets for all the required bends with a few exceptions in the upstream end of the beamline. The necessity for exceptions are due to tight spatial constraints (EPBs) and large apertures (Main Ring B3s). Of the 53 quadrupoles in the line, 16 are of the SQA type recycled from the current 8 GeV line and the remainder are BQAs recycled from Main Ring.

All dipole magnets required for the two Tevatron injection lines, the F0-F17 magnet string and the F18-SY magnet string are recycled from the Main Ring. The only new magnets required are the Lambertsons and C-magnets required at the FMI extraction and Tevatron injection straight sections.

Most quadrupoles in the beamlines are recycled BQBs (46) and BQAs (41) from the Main Ring, or SQAs (16) from the present 8 GeV line. The only new quadrupoles are 14 new 3Q120s, a copy of an existing Fermilab design, and 7 new 3Q60s, a shorter version of the 3Q120; these magnets are a low current, high inductance design. All of the 3Q120s and 3Q60s are used at locations requiring individual power supplies for matching lattice functions. The decision to build new quadrupole magnets for those locations was made in order to reduce the cost of power supplies and cabling/buswork. The new quads also have a smaller cross-section than Main Ring quads, and that is an additional benefit since they are being used in areas where the separation between beamlines is small. It also leaves more BQB and BQA quads as spares for the ring and beamlines.

Power Supply Requirements

The power supply requirements for all beamlines are discussed in Chapter 3.3. The power supplies will be located in the existing Booster Gallery, new MI-8 Service Building, new MI-10 Service Building, MI-40 Service Building, new extension to Main Ring F0, existing Main Ring F1 through F4, and the existing A0 Transfer Hall. All major dipole and quadrupole supplies for the 120 GeV and 150 GeV beamlines will be ramped to minimize the average power consumed. The 8 GeV line will run dc. Many of the major dipole and quadrupole supplies are reused from the present transfer lines. The kicker supplies will be located in the buildings at MI-10,-40,-52,-62, F0 (for E48), and F17.

Table 2.4-1: Beamline Magnet Requirements

	Number	Magnet Style	Status
<u>8 GeV</u>			
Dipoles	55	B2	Exist
	2	B3	Exist
	4	EPB	Exist
Quadrupoles	16	SQA	Exist
	37	BQA	Exist
Trims (H)	27	MR trim	Exist
Trims (V)	26	MR trim	Exist
Lambertson	1	A0	Exist
<u>150 GeV (both)</u>			
Lambertsons	10	New design	New
C-magnets	10	F17 style	New
Dipoles	30	B2	Exist
Quadrupoles	14	BQB	Exist
	14	3Q120	New
	4	3Q60	New
Trims (H)	12	MR trim	Exist
Trims (V)	12	MR trim	Exist
<u>F0/F17 Magnet String</u>			
Dipoles	14	B1/B2	Exist
	9	B3	Exist
Quadrupoles	5	BQB	Exist
	3	3Q60	New
Trims (H)	4	MR trim	Exist
Trims (V)	4	MR trim	Exist
<u>F18/SY Magnet String</u>			
Dipoles	101	B1/B2	Exist
	2	B3	Exist
	1	2xB2	Exist
Quadrupoles	27	BQB	Exist
	4	BQA	Exist
Trims (H)	14	MR trim	Exist
Trims (V)	14	MR trim	Exist
<u>Abort</u>			
Lambertsons	3	New design	New
C-magnet	1	F17 style	New
Dipoles	2	B2	Exist
Quadrupoles	1	BQA	Exist
	2	BQB	Exist
Trims (H)	2	MR trim	Exist
Trims (V)	2	MR trim	Exist

2.5 TRANSITION CROSSING

Like the Main Ring, the Main Injector crosses transition early in the magnet cycle. There are many years of experience on the problems of bunch dilution and beam loss associated with this part of the MR cycle, and accelerator studies have been undertaken with the specific intent of learning what to anticipate for the FMI. It is well established that bunches larger than about 0.2 eVs are significantly diluted and usually suffer some loss at transition. This behavior is understood in terms of the strong nonlinearity of the longitudinal motion and large momentum spread characteristic of 10 ms or so surrounding the transition crossing time. The Booster parameters used in the FMI conceptual design (Rev. 2.3 April 90) were based on extrapolation from operation with 200 MeV injection to expectations for 400 MeV injection. The assumed longitudinal emittance was 0.4 eVs coming from Booster in the Main Injector era. Not only are there now results from the Linac upgrade but also there is increased understanding of the beam behavior in the Booster and progress in controlling the most serious instabilities. This newer information indicates that the emittance at 6×10^{10} protons/bunch will be smaller in all three planes than previously assumed. Bunch intensity in the Booster has now reached the 5×10^{10} level and early results with new damper systems suggest that the longitudinal emittance is likely to be 0.2 eVs or less.

The ramps shown in Figure 2.2-1 represent a conservative extrapolation of Main Ring experience which leaves considerable margin between routine operating parameters and the design limits of the rf and magnet power supply systems. In Figure 2.5-1 is plotted the longitudinal emittance growth through the antiproton production cycle for a 0.2 eVs bunch of 6×10^{10} protons assuming a broadband longitudinal impedance of $Z_{||}/n = 5 \Omega$ but no other sources of wake field. Although there is no beam loss, there is significant emittance dilution. Because the simulation does not include other impedance sources and any non-ideal operating conditions, it is not likely that actual performance will be so good. On the other hand, by pushing closer to the limits on the rf systems and magnet power supply the transition energy region can be crossed almost twice as fast. Tests on the prototype dipole power supply show that it can sustain a ramp rate of nearly 300 GeV/c/s. If the curvature can be made high enough to achieve this rate at transition, the transition range will be passed nearly twice as fast as in the ramps of Figure 2.2-1 and nearly three times as fast as in Main Ring operation. The rf parameter curves of Figure 2.5-2 show that such a fast start does not exceed the available rf voltage, although it does require higher voltage early in the cycle. In Figure 2.5-3 is shown the emittance growth simulation for a 0.2 eVs bunch of 6×10^{10} protons on the fast antiproton production cycle. This cycle probably represents a practical limit for pushing up the early ramp rate, but steps taken in this direction will reduce

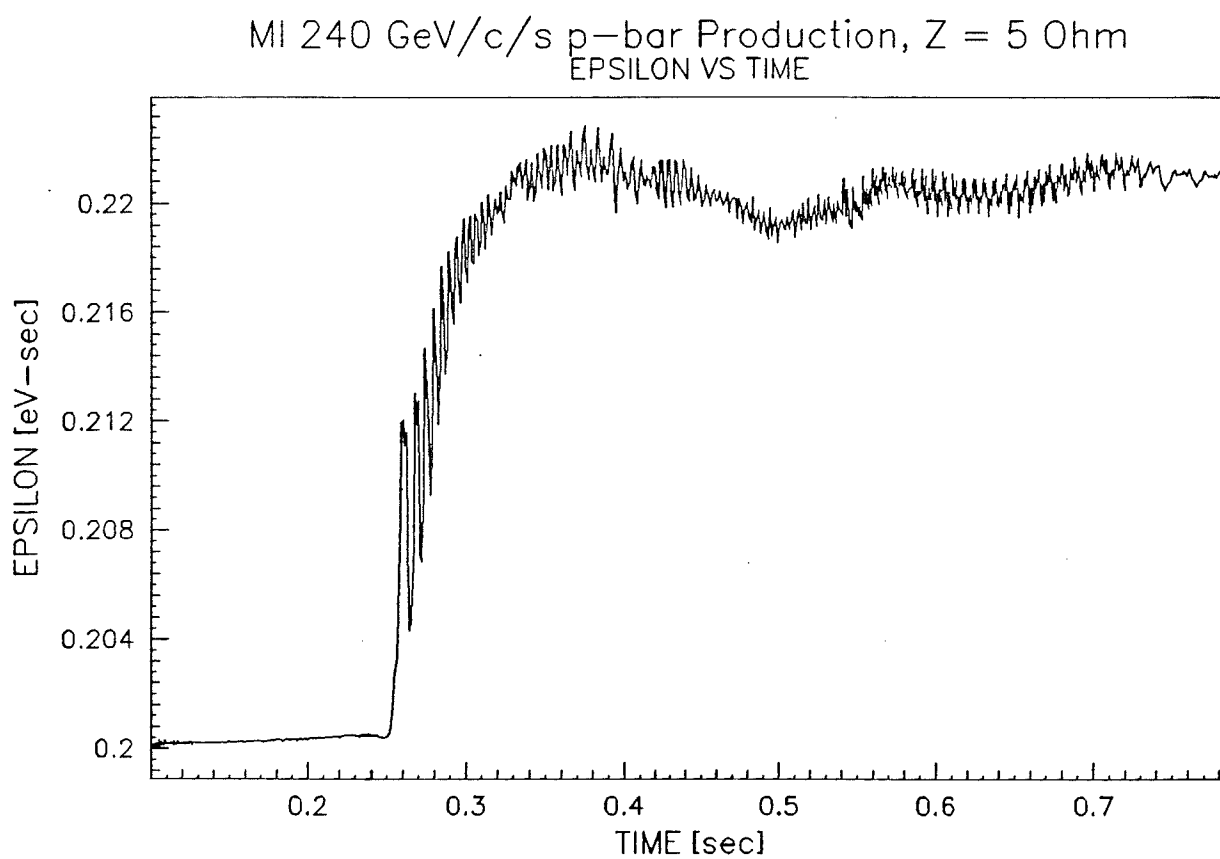


Figure 2.5-1. Longitudinal Emittance Growth for Normal Ramp Cycle

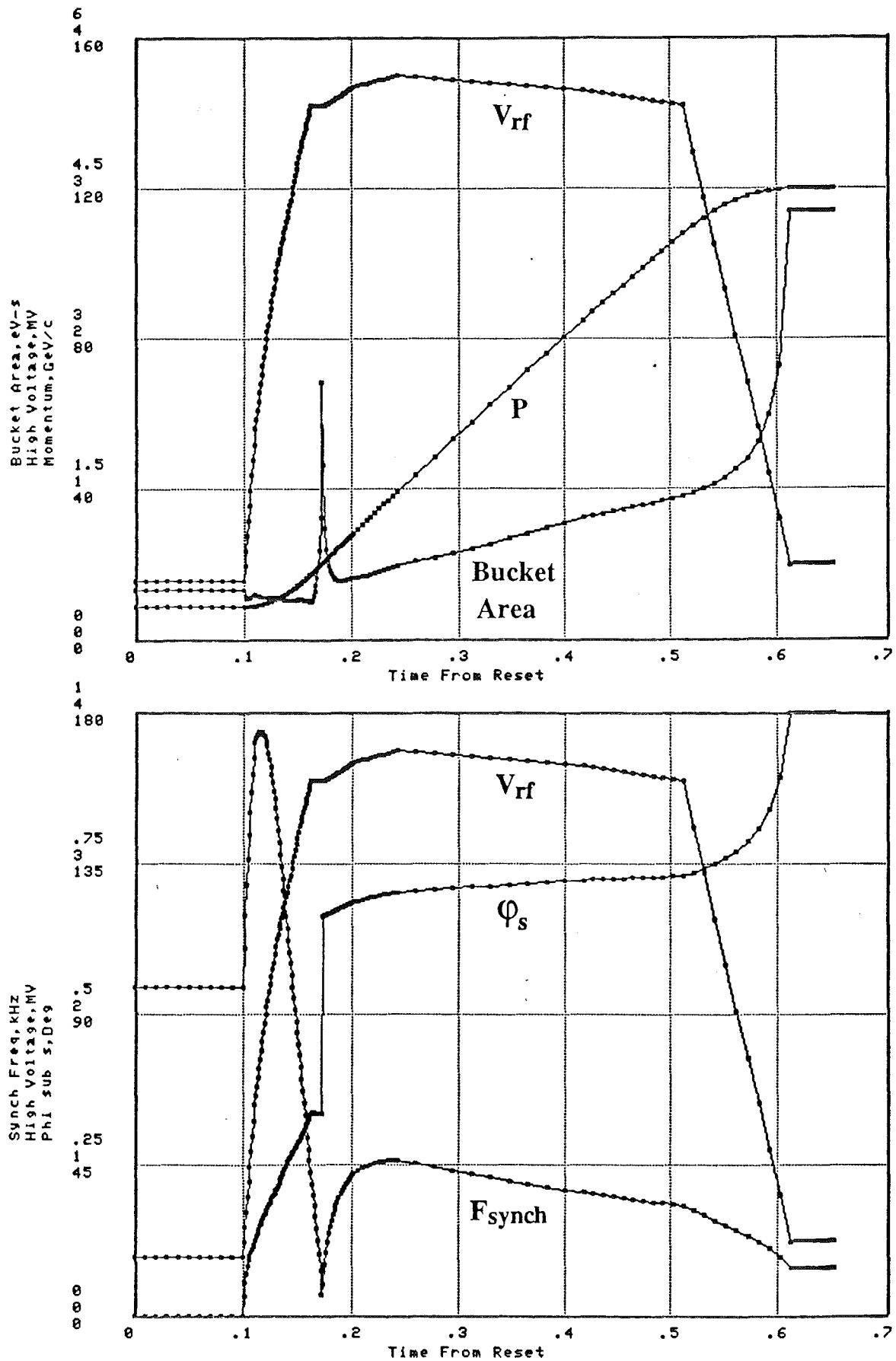


Figure 2.5-2. RF Parameter Curves for Faster Ramp Cycle

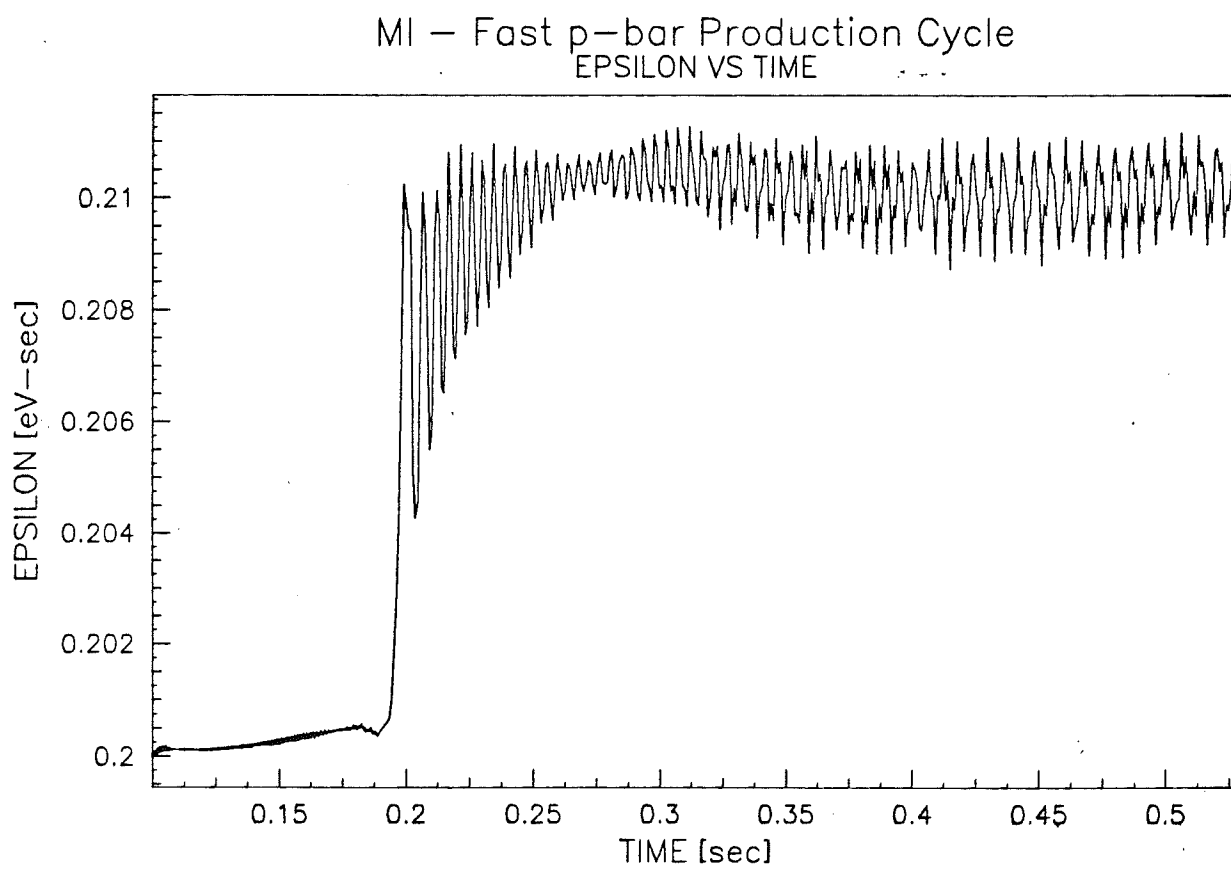


Figure 2.5-3. Longitudinal Emittance Growth for Faster Ramp Cycle

several of the hazards transition crossing, possibly avoiding a need for special systems to reduce emittance dilution or beam loss at transition.

When transition crossing is modeled excluding the effects of the beam current (i. e., collective effects), the 280 GeV/c/s ramp illustrated in Figure 2.2-2 results in a final emittance 0.206 eVs for an initial bunch of 0.2 eVs whereas the 240 GeV/c/s ramp shown in Figure 2.2-1 (with $dp/dt \sim 167$ GeV/c/s at transition) results in 0.23 eVs. This comparison exemplifies the sensitivity of the single-particle dynamics to ramp rate. However, when the bunch intensity is taken as the design value of 6×10^{10} protons and a broadband longitudinal impedance of $Z_{||}/n = 5 \Omega$ is included, the final emittances are 0.213 eVs and 0.221 eVs for the fast ramp and more conservative ramp respectively. The collective calculations use a simple impedance model, so the numbers just quoted are not quantitative predictions of FMI performance. However, the result that the difference in emittance growth for the fast and slower ramps is less pronounced when beam charge is taken into consideration supports an important qualitative observation, viz., for FMI parameters the single-particle pathologies of transition crossing are not the most important. The rather similar results for the two ramps are exhibiting predominantly the shape mismatch arising from the discontinuity of longitudinal focusing at transition; that is, the rf focusing has the same sign throughout, but the space charge term changes sign. It is not possible to compensate the discontinuity by raising the rf voltage higher after transition because for the intensities of interest there is not enough voltage available.

Two approaches have been considered for reducing longitudinal emittance dilution from transition crossing in the FMI, viz., a gamma-t jump to make the passage through the transition energy range extremely fast and a second harmonic rf scheme to eliminate both the nonlinear particle motion and the increased momentum spread characteristic of that energy range [1]. However, the basic FMI design has important advantages over the Main Ring which may make such refinements unnecessary or appropriate as a later enhancement. Most important is the faster magnet ramp which passes through the troublesome energy range two to three as fast, thereby reducing the time during which the nonlinear motion disrupts the bunches. The greater momentum aperture will accommodate substantially larger bunches without loss. Finally, the somewhat lower longitudinal impedance of the vacuum chamber will reduce the importance of microwave instability as a beam intensity limit. For emittances smaller than 0.2 eVs the intensity limit will most likely be set by negative mass instability; in this case a gamma-t jump system is the appropriate approach. If the longitudinal emittance from the Booster at high intensity proves much larger than now expected, the less costly addition of a second harmonic component to the rf to achieve what has been designated as a focus-free transition crossing scheme could be sufficient to meet operational needs. Because there is some uncertainty in how much more improvement

there will be in Booster performance and because the basic design of the FMI should give performance close to the original design criteria without any special measures for transition crossing, the decision on such measures is best made on the basis of operating experience. The design described in this Technical Design Handbook is intended to permit the implementation of either approach as needed.

A gamma-t jump changes the transition energy by modifying the lattice dispersion without changing the betatron tune by using a set of pulsed quadrupoles. It is possible to make a matched lattice change locally so that neither the dispersion function nor the beta function are affected over most of the ring. The pulsed quads must act to make a gamma-t change of order one unit in a time substantially shorter than that given by the main magnet ramp. The appropriate time scale is of order one tenth the duration of non-linear particle motion, that is about 1 ms for the FMI. This rate is an order of magnitude faster than the ramp. The design of a matched gamma-t jump for the FMI lattice has received recent attention, incorporating gradient changes in groups of three focussing quadrupoles separated by 180° in betatron phase [2], and producing only local dispersion and betatron waves. Alternative approaches using doublets rather than triplets have also been suggested for the Main Injector and for other machines [3,4]. There may be insufficient free beam pipe at the appropriate points on the lattice for installation of special pulsed quads. If the quad corrector coils (see Chapter 3.1) are inadequate, it may suffice to employ a less refined, unmatched gamma-t jump similar to that in the Booster. The modeling results quoted above which show similar emittance growth for two different ramp rates have some implication for the effectiveness of a gamma-t jump because it does not completely eliminate the focusing discontinuity. The jump does help because the bunches don't get quite so short, but some dilution is to be expected. Modeling of the gamma-t jump process is under way to estimate the performance gain at design intensity.

The focus-free rf approach to emittance preservation is directed toward correcting those problems arising from the special character of the single particle dynamics near transition energy. It is, therefore, a less general cure than a transition jump but is particularly appropriate to the situation where the emittance is large. That is, if the peak current is below threshold for microwave and negative mass instabilities but there is beam loss from momentum spread or dilution from bunch shape distortion, performance can be greatly improved by changing the rf waveform. The longitudinal focusing provided by the gradient of the rf waveform provides the phase stability which is fundamental to synchrotron operation throughout most of the acceleration cycle. For energy near transition, however, the focusing has two unfortunate consequences, both related to the fact that the frequency of longitudinal oscillation approaches zero. First, momentum spread is increased because particles receiving too large an energy increment do not exchange

position by synchrotron oscillation with those in the bunch receiving too little. Second, the motion is non-adiabatic because the equations of motion change rapidly compared to the time scale for the particle motion. The focusing can be eliminated during the time near transition by modifying the waveform with a second harmonic so that the peak is flattened. When the rf is phased so that the particles are accelerated on this flattened portion of the waveform, all receive just the acceleration needed to match the ramp. The absence of focusing means that the particles debunch slowly, but after transition the direction of debunching reverses and the bunch returns closely to its original shape. The absence of focusing also means that discontinuity in the image charge focusing is symmetric about transition and to some degree cancels out because the sense of the synchrotron oscillation reverses. Experiments have been carried out in the Main Ring which not only demonstrate the principles of the focus-free technique but also show some improvement under operational conditions. The significance of the studies for the FMI is that the longitudinal emittance provided by the Booster will determine whether focus-free rf will be helpful in preserving that emittance.

References: Chapter 2.5

1. J. MacLachlan, J. Griffin, C. Crawford, D. Wildman, C. Bhat and M. Martens, "Reducing Bunch Disruption in Transition Crossing by Modification of the RF Waveform", Proc. XVth Int'l. Conference on High Energy Accelerators, Int. J. Mod. Phys. A (Proc. Suppl.) 2B, 1993.
2. V. Visnjic, "Local Dispersion Insert, the γ_t Knob for Accelerators", Fermilab TM-1888, 1994.
3. A. Bogacz and K. Y. Ng, "Low Dispersion γ_t Jump Scheme for the Main Injector," MI Note-107.
4. S. Peggs, S. Tepikian and D. Trbojevic, "A First Order Matched Transition Jump at RHIC", Proc. of the IEEE Particle Accelerator Conf., 1993.

2.6 COALESCING

Coalescing Techniques

The luminosity goal for the Fermilab III program is $5 \times 10^{31} \text{ cm}^{-2} \text{ s}^{-1}$ to be obtained by colliding 36 bunches of 3×10^{11} protons with 36 bunches of 6×10^{10} antiprotons. Thus, the required proton bunches are five times as intense as specified in the FMI design parameters; it will be necessary to combine some number between five and thirteen bunches at 150 GeV into each proton bunch injected into the Tevatron. Bunches of 6×10^{11} antiprotons should have longitudinal emittance of about 0.4 eVs. Therefore, it might be practicable to accelerate such bunches in the FMI and eliminate the dilution from the coalescing step. However, there are at least two reasons why coalescing is desirable for the antiprotons also. The Accumulator does not have the necessary rf system to prepare isolated 53 MHz bunches. Furthermore, to get the large bunches through transition with acceptable dilution is likely to require special measures which may not be needed for any other operational mode.

There are three variants of the coalescing process relevant to collider operation. They have in common the debunching of short trains of 53 MHz ($h=588$) bunches, the rotation of those bunch trains in 2.5 MHz ($h=28$) buckets to the state of minimum phase extent, and recapture into a single 53 MHz bucket. They also have in common a fundamental limitation on the debunching given by the onset of microwave instability. They differ in how the initial debunching is obtained.

The process introduced for Tevatron I may be called adiabatic coalescing because the bunches are fully debunched from the 53 MHz buckets into a 2.5 MHz bucket by reduction of the 53 MHz voltage to less than one kV in the presence of 50 V or so of 2.5 MHz over a period of about one second. If the microwave instability threshold is not crossed, this technique is capable of producing coalesced bunches with emittance equal to the total emittance of the constituent bunches. However, Main Ring results for this mode fall considerably short of what can be expected from the microwave stability limitation. One problem has been the difficulty in precisely controlling a low 53 MHz voltage from high-Q, high voltage cavities. Another type of problem results from beam loading or wakefield reduction of the buckets for later bunches in the train. Because of this, beam begins to be lost from the later buckets before the leading bunches are fully debunched. To cope with these problems, other debunching techniques have replaced adiabatic debunching. The original scheme is of interest because the problems observed could be ameliorated for the FMI, and it is the ideal process by which alternatives are judged.

So-called slow coalescing is similar to the adiabatic process except that the debunching stops short of full 53 MHz buckets. The 53 MHz voltage is turned off and the 2.5 MHz rotating voltage is turned on when the 53 MHz voltage is a few kV and before beam starts to be

lost from trailing bunches in the train. Because there is empty phase space between the distinct bunches, there is dilution of the effective longitudinal emittance at least by the ratio of the empty space to the area of the matched 2.5 MHz bounding contour.

Because the proton beam used for the collider is more intense than the antiproton beam, the coalescing difficulties have been greater in this case and have led to another variant called snap coalescing which is now generally used for both protons and antiprotons. In this technique the 53 MHz voltage is suddenly reduced from its normal value on flattop, about 1 MV, to a voltage chosen so that the resulting bucket height is just slightly greater than the bunch height, perhaps 35 kV for 0.15 eVs bunches. After a quarter of a synchrotron oscillation the distribution has rotated to low momentum spread and extends over most of the bucket width. Good efficiency is obtained in this method by reducing the dependence of rotation period on synchrotron amplitude by addition of about 10 - 15 kV of 106 MHz rf. This linearization of the rotation makes it possible to obtain debunching to greater than ± 120 deg without producing the distorted bunch shape which leaves large amplitude particles where they will not be recaptured. Advantages in this approach are that the 53 MHz voltage is in an accessible range, the debunching time is only a few milliseconds, and the bunches spend the least possible time near their minimum momentum spread. Also, the total time for coalescing is reduced to about 100 ms. This scheme has been quite successful for proton coalescing and has been used for antiprotons with results nearly as good as the slow coalescing. The choice among the three debunching options is sensitive to several machine properties and will be reexamined as a part of FMI commissioning.

Coalescing Parameters

The rf parameters for the three variants of coalescing differ somewhat. The rf systems to be installed in the FMI will be suitable for any of them. Table 2.6-1 shows the parameters for a representative example of snap coalescing of protons, viz. of trains of nine bunches of 0.15 eVs each.

The process is illustrated by simulation results in Figures 2.6-1 through 2.6-4. Nine 53 MHz bunches, each with longitudinal emittance 0.15 eVs (95 % area), are coalesced into a single bunch of 2.8 eVs at the same frequency using the snap coalescing process. Figure 2.6-1 shows the three central bunches, the 1 MV rf waveform, and the bucket contour corresponding to the initial conditions on the 150 GeV flattop. Figure 2.6-2 represents the end of the rotation sixteen milliseconds later where the bunches have reached their minimum momentum spread in the linearized bucket produced by 35 kV of 53 MHz and 10 kV of 106 MHz rf. One sees here the result of an optimization which is emittance dependent, viz., the choice of the second rf harmonic to compensate the high amplitudes while over-compensating the lower amplitudes. The 106 MHz

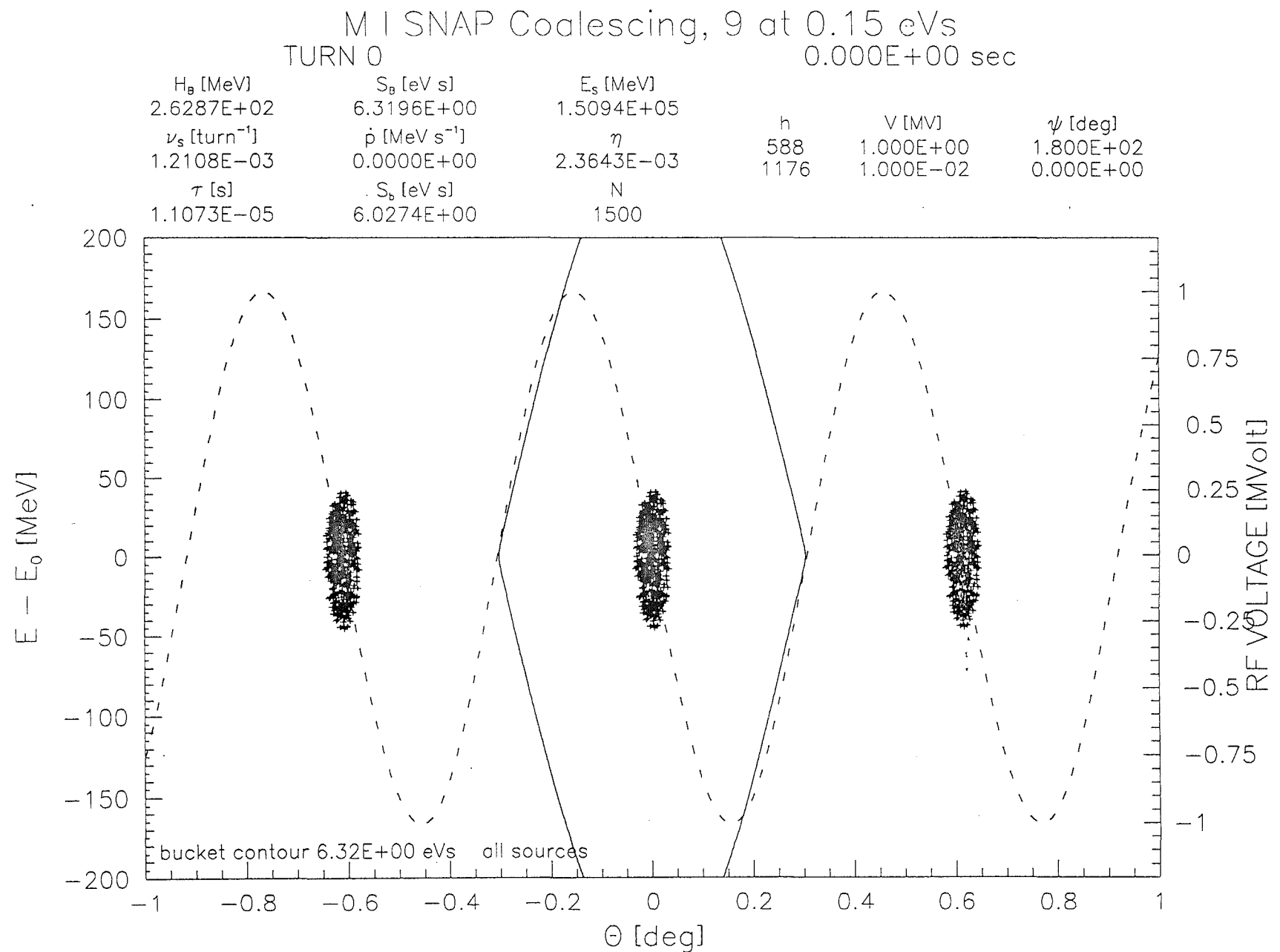


Figure 2.6-1. Snap Coalescing: Beginning of Process

M I SNAP Coalescing, 9 at 0.15 eVs TURN 1446 1.601E-02 sec

H_b [MeV]	S_b [eV s]	E_s [MeV]	h	V [MV]	ψ [deg]
4.9175E+01	1.2823E+00	1.5094E+05	588	3.500E-02	1.800E+02
ν_s [turn $^{-1}$]	\dot{p} [MeV s $^{-1}$]	η	1176	1.000E-02	0.000E+00
2.2651E-04	-1.3930E-13	2.3643E-03			
τ [s]	S_b [eV s]	N			
1.1073E-05	9.1142E-01	1505			

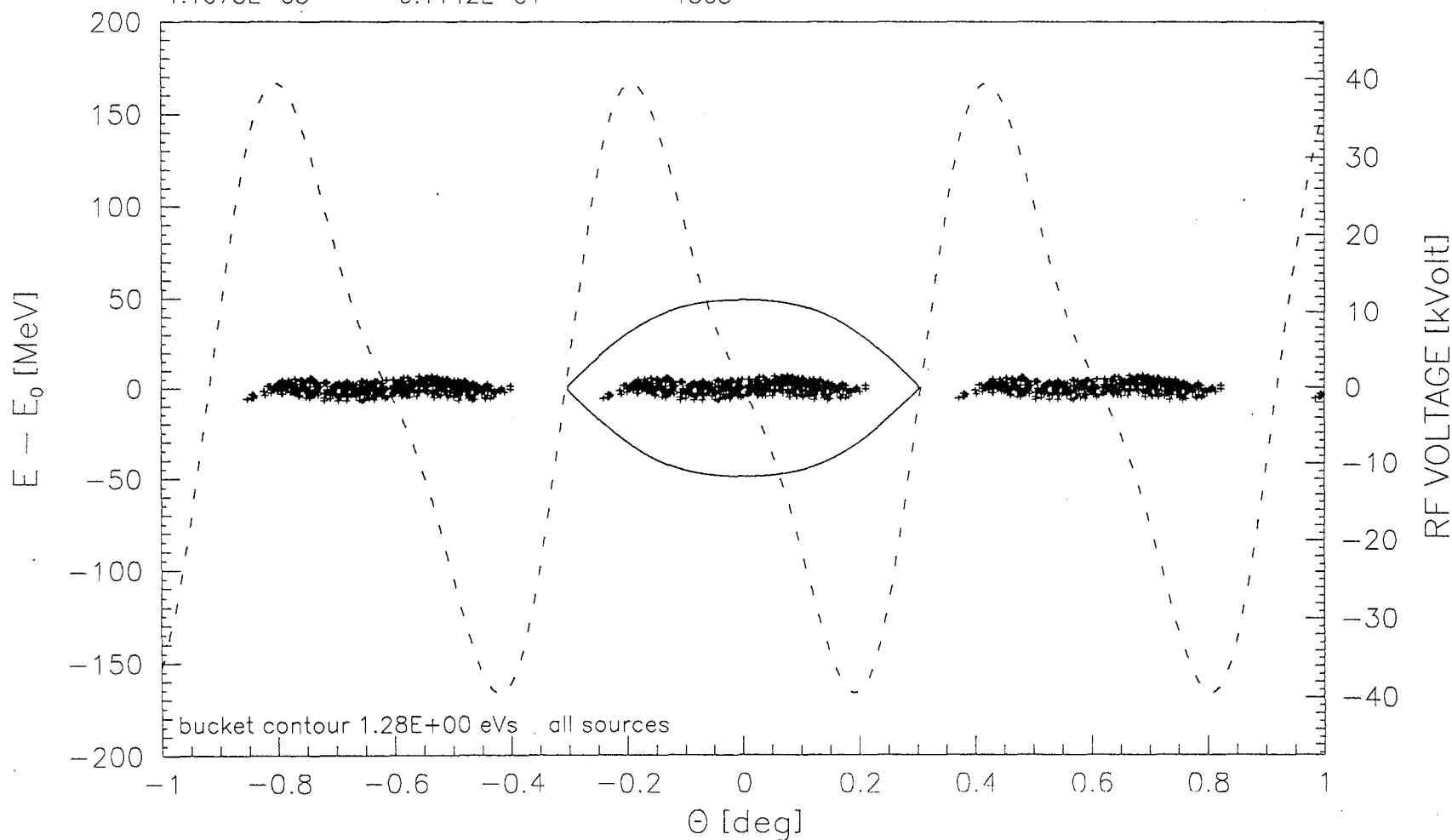


Figure 2.6-2. Snap Coalescing: End of Initial Rotation

M I SNAP Coalescing, 9 at 0.15 eVs TURN 5000 5.536E-02 sec

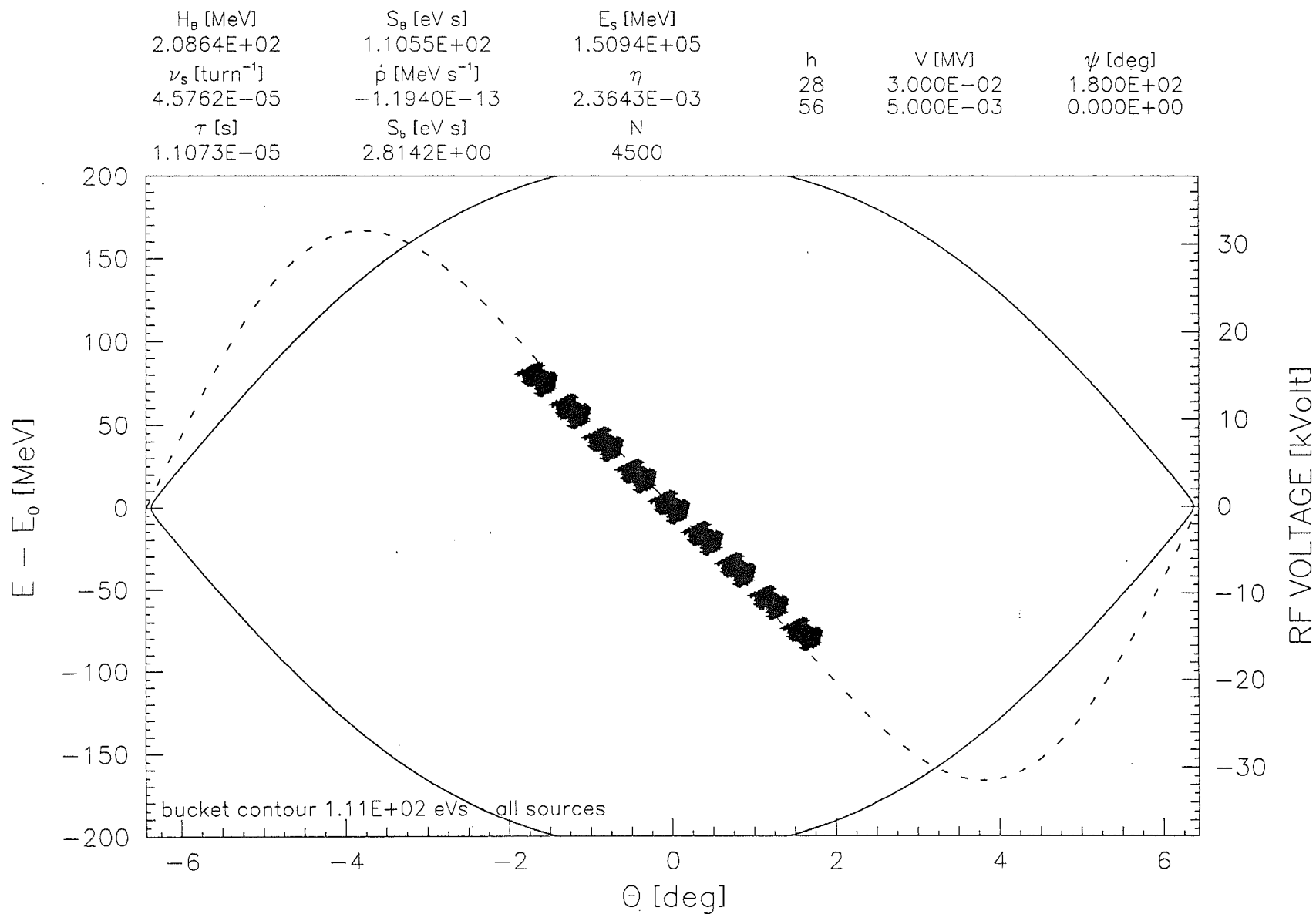


Figure 2.6-3. Snap Coalescing: Rotation in 2.5 MHz Bucket

M I SNAP Coalescing, 9 at 0.15 eVs TURN 8050 8.913E-02 sec

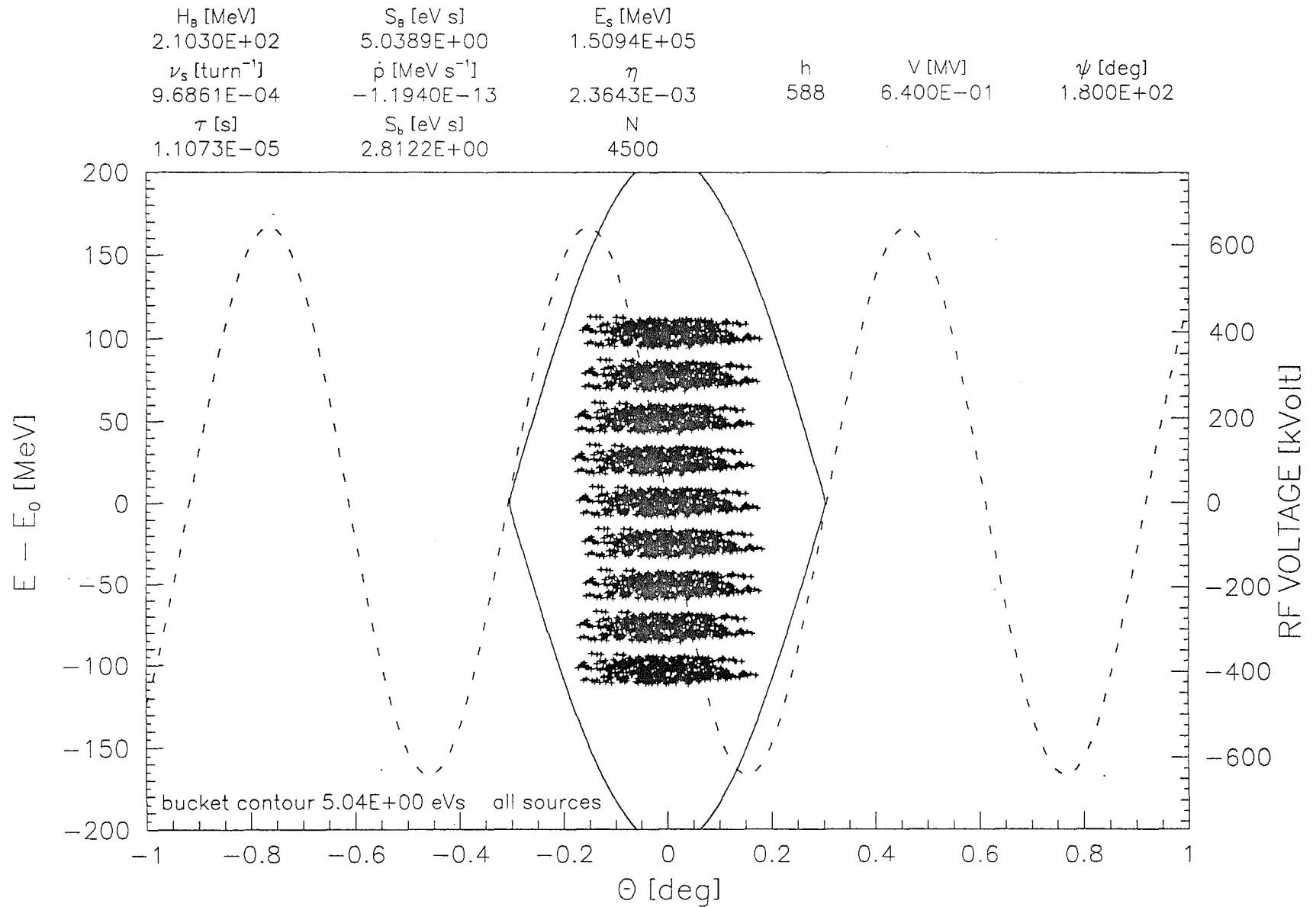


Figure 2.6-4. Snap Coalescing: Recapture in 53 MHz Bucket

M I SNAP Coalescing, 9 at 0.15 eVs TURN 17082 1.891E-01 sec

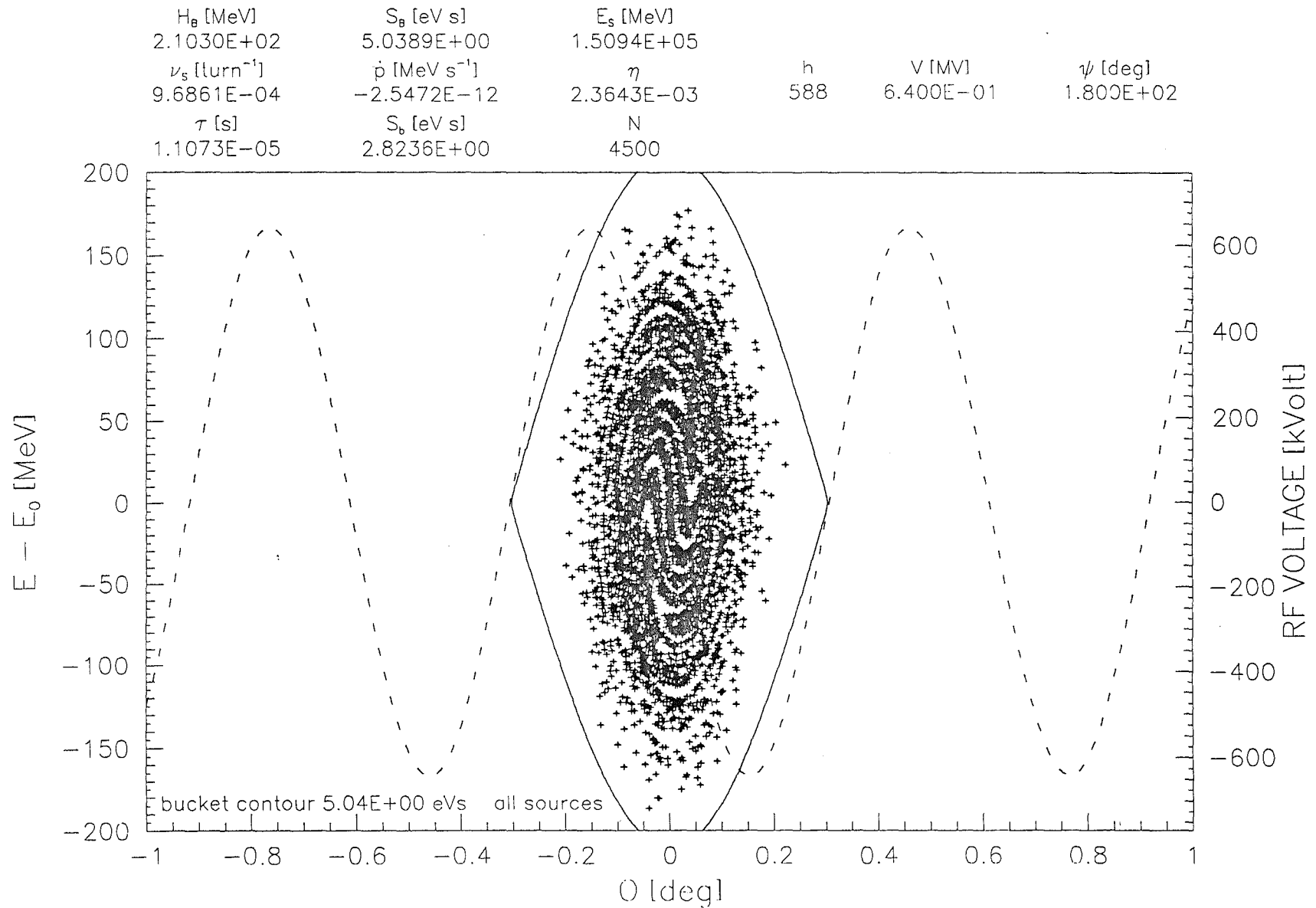


Figure 2.6-5. Snap Coalescing: 100 msec After Recapture

Table 2.6-1
Proton Bunch Coalescing at 150 GeV in the FMI

<hr/>		
53 MHz system, initial condition		
harmonic number (h)	588	
rf voltage (V_{588})	1	MV
synch. phase (ϕ_{588})	180	deg
initial bunches per final bunch	9	
initial bunch area	0.15	eVs
53 MHz system and 106 MHz system, bunch rotation		
V_{588}	0.035	MV
ϕ_{588}	180	deg
V_{1176}	0.010	MV
ϕ_{1176}	0	deg
time to minimum momentum spread	16	ms
2.5 MHz system and 5.0 MHz system, ensemble rotation		
harmonic number (h)	28	
V_{28}	0.03	MV
ϕ_{28}	180	deg
V_{56}	0.005	MV
ϕ_{56}	0	deg
time to minimum phase spread	73	ms
53 MHz system, ensemble recapture		
V_{588}	0.64	MV
ϕ_{588}	180	deg
final effective bunch area	2.8	eVs
<hr/>		

voltage is chosen to make the momentum spread the same for both. That is, the tails of the S-shaped bunch are equalized with the humps. The rotation of the ensemble of nine bunches in the 2.5 MHz bucket is shown in Figure 2.6-3. The bucket is produced by 30 kV of 2.5 MHz and linearized by 5 kV of 5.0 MHz rf. The fraction of second rf harmonic in this stage of the process is optimized somewhere in the range 15 - 30 % according to the number of bunches in the train. Figure 2.6-4 shows the ensemble rotated to its minimum phase spread and recaptured in a matched 53 MHz bucket produced by 640 kV. The effective emittance found by letting this distribution filament for several synchrotron periods is 2.8 eVs, Figure 2.6-5. The dilution of 100% with respect to the sum of the initial bunch areas is accounted for entirely by the incompleteness of the debunching; there is no significant contribution to the effective emittance from the coalescing rotation or filamentation of the coalesced distribution.

2.7 SLOW EXTRACTION

The Main Injector slow extraction system is designed to be capable of providing year-round, uniform spills of 120 GeV test beams with a 2.9 s cycle time and 1 s flattop. The following sections outline the principle of slow spill through excitation of the half-integer resonance [1], and summarize results from numerical simulation of extraction [2].

Half-Integer Resonant Extraction

The half-integer resonance is a linear resonance and can, therefore, be induced solely by a quadrupole field; the beam in this instance is either entirely stable or entirely unstable. With the addition of an octupole field, however, an amplitude-dependent tune spread is introduced into the beam ($\Delta\nu \sim x^2$). Particles with large betatron amplitudes have tunes closer to the half-integer than those of small amplitude. Consequently, the phase-space splits into stable and unstable regions, thereby providing a means for manipulating the extraction rate through control of the stable phase-space area. Recycled Main Ring octupoles distributed around the ring on the 0th-harmonic provide the non-linear tune shift, while two orthogonal families of Main Ring trim quads distributed on the 53rd-harmonic provide the half-integer driving term. One quadrupole family alone produces the desired phase-space for extraction, while both families are available for correcting the intrinsic half-integer stopband of the machine.

Slow extraction from the Main Injector proceeds basically as follows. The horizontal tune is raised towards the half-integer from $\nu_x = 26.425$ to 26.485 using the main quadrupole circuits. The desired orientation of the phase-space at the extraction septa is obtained by energizing the appropriate 53rd-harmonic quadrupole circuit plus the 0th-harmonic octupoles. The strengths of the harmonic elements are chosen such that the stable phase-space area equals the emittance of the circulating beam. The beam is just marginally stable, therefore, at the end of the initial ramp.

Extraction begins by further ramping the harmonic quadrupoles to increase the width of the half-integer stopband and start the stopband moving through the beam. Small amplitude particles (lower tune) remain stable, with their motion in phase-space oscillating between the 'fixed' points on successive turns. As the stable phase-space region shrinks, large amplitude particles enter the stopband and become unstable, with their amplitude then growing exponentially from turn to turn. The unstable particles stream out along the separatrices until they ultimately jump across (or hit) the wires of the electrostatic septa and enter the extraction channel. The kick supplied by the electrostatic septa provides sufficient separation between extracted and circulating beams that magnetic septa are used for the final extraction from the machine.

Extraction Elements

There are five major components of the resonant extraction system:

1. magnetic and electrostatic extraction septa;
2. one family of 0th-harmonic octupoles;
3. two families (cosine and sine) of 53rd-harmonic quadrupoles;
4. low frequency extraction regulation quadrupoles (QXR), and;
5. high frequency spill modulation regulation quadrupoles (Buckers).

The extraction septa are located in straight section MI-52. This region must accommodate extraction of 120 GeV/c slow-spill protons, single-turn extraction of 120 and 150 GeV/c protons, and 8.9 GeV/c antiproton injection. The Lambertson magnetic septa and C-magnets are common to all beam transfers. There is sufficient phase advance in the straight section that both the extraction kicker magnets and electrostatic septa can be placed at the upstream end of the straight section. Separation between extracted and circulating beams is provided by three electrostatic septum modules located immediately downstream of the kickers, and 70.1° in betatron phase upstream of the entrance to the first Lambertson. Each septum has a wire plane length of 3.048 m. The high voltage gap is 10 mm, with the anode consisting of 0.1 mm tungsten-rhenium wires. The septa are designed to produce 200 μ r of kick each at an applied voltage gradient of 79 kV/cm.

The 0th-harmonic octupole circuit is required to serve two functions. During resonant extraction it augments the (large) octupole component of the main quadrupoles to produce the appropriate stable and unstable phase-space regions. At injection, however, the octupole field generated by the main quads has a degrading effect on dynamic aperture. The harmonic octupoles in this case are used to cancel this detuning effect. The Main Injector has a single family of 54 octupoles - one at each focussing sextupole location. All octupoles are the same polarity, producing a 0th-harmonic contribution. The two-fold symmetry of the Injector ensures that half-integer driving terms cancel, and quarter-integer harmonics are found to be small.

The number of harmonic quads is determined by the strength required to raise the fractional horizontal tune from 0.485 to 0.500 at 120 GeV/c. With $\beta_x \sim 50$ m at the quadrupole locations, the total strength required is ~ 15 kG-m/m. For Main Ring trim quads this translates into 8 quadrupoles operating at ~ 7 A [3]. In the Main Injector 16 quadrupoles are utilized. These are distributed around the ring, separated into two orthogonal families (cosine and sine) of eight quads each. Within each family equal numbers of F and D quads ensures that 0th-harmonic

contributions cancel. The 53rd-harmonic is retained by separating opposite polarity quads by odd multiples of 90° in betatron phase. The orthogonality of the families provides the capability both to cancel the intrinsic half-integer stopband of the machine and to manipulate the orientation of the phase-space at the septa if necessary.

The purpose of slow extraction is to provide a constant spill rate over an extended time. This is achieved via two low frequency harmonic quads (dc to 4 Hz) as follows. The circulating beam intensity is sampled prior to extraction and subsequently at 720 Hz and compared with the ideal value. The resultant errors are saved, smoothed, and time-shifted to modify the extraction quadrupole current waveform on subsequent spills. The time-shifting is necessary because of the delayed response of the beam to quadrupole field changes. In the Injector, simulations have shown this delay to be ~ 40 turns, or 0.4 msec [4]. The quad current waveform is then the result of feedback and the modifications made to all previous spills. In this way repetitive errors are learned out. Current ripple in the main quad power supplies manifests itself as tune fluctuations. (Ripple contamination of 10^{-4} , for example, results in $\Delta v \sim \pm 0.003$). This appears in the spill structure as the beam is driven in and out of the half-integer stopband. Spill modulation is controlled primarily by real-time feedback with two high frequency 0th-harmonic Bucker quads (dc to 3 kHz). Extracted beam intensity is sampled at 5760 Hz. The time delay of 0.4 msec between beam response and a change in quadrupole field translates into an upper limit of a few hundred Hz for which feedback can effectively reduce spill modulation. Similar to the low frequency QXR system, repetitive high frequency components can be learned out.

Simulation of Resonant Extraction

Simulations of the extraction process from the Main Injector with ~ 1000 particles over a few thousand turns ($\sim 10 \mu\text{s}/\text{turn}$) can be performed in reasonable computer time. Within this framework the discussion that follows applies, strictly, to 'fast' resonant extraction, wherein the beam is fully extracted in a few milliseconds. The extension to extraction over periods on the order of 100,000 turns (~ 1 sec) is straightforward, however, and presents no additional physics issues. Simulations include the full complement of magnet harmonics plus random field and alignment errors [5]. The tracking module of the accelerator program MAD [6] is used to propagate the particles through the lattice via 2nd-order transfer matrices. Using MAD's intrinsic random number generator, random field and alignment errors are assigned to the machine elements to create a realistic lattice description.

The circulating beam during slow spill is very broad so large deviations from the design trajectory expose a significant portion of the beam to regions of poor magnetic field quality, thereby degrading the phase-space. Based on the BPM readings the Main Injector trim dipoles

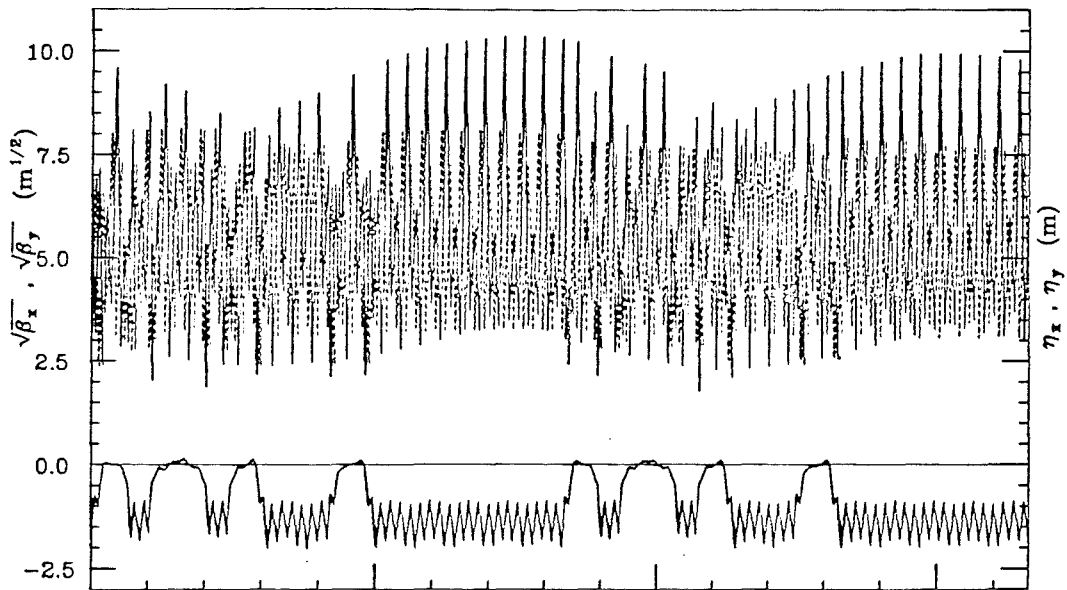
correct the central trajectory (in MAD through the MICADO algorithm). The maximum kick required to reduce $\langle x^2 \rangle^{1/2}$ from 6.2 mm to essentially zero is 98 μr - comfortably below the 150 μr available at 120 GeV/c.

Quadrupole errors in the ring propagate at twice the tune and contribute an additional (unwanted) half-integer driving term. The intrinsic half-integer stopband is measured by ramping the two orthogonal families independently through positive and negative current values to attain resonance. In the absence of dynamic non-linearities the four resonant current values lie on the circumference of a circle. The circle center defines the stopband width and phase and, therefore, the harmonic quad currents necessary to cancel it. The importance of stopband compensation is evident from Figure 2.7-1, which shows the Main Injector lattice functions before and after correction. The maximum $\Delta\beta/\beta$ is reduced from 76% to 6%, and the RMS deviation from 41% to just 3%. To a good approximation the design lattice is obtained.

The initial transverse co-ordinates of 1000 particles are randomly selected from a 30π mm-mr Gaussian-distributed phase-space. The particles are allowed to circulate unperturbed for 100 turns to establish 'steady-state' conditions. During the next 100 turns the harmonic extraction circuits are activated: one family of 53rd-harmonic quadrupoles are ramped to 5.5 A and the 0th-harmonic octupoles are energized. Extraction occurs over the subsequent 1000 turns. The quadrupoles are further ramped to 7.0 A, thereby increasing the width of the half-integer stopband. Gradually all the particles become unstable, stream out along the separatrices, and enter the extraction channel. The electrostatic septa provide a kick of 325 μr which, at the Lambertson, translates into 11 mm separation between circulating and extracted beams.

The phase-space at the septa entrance and exit is shown in Figure 2.7-2. The high density for $x < -16$ mm at the entrance ($x < -12$ mm at the exit) is the extracted particle phase-space accumulated over the entire cycle. The circulating beam phase-space is a snapshot taken half-way through extraction. The corresponding phase-space at the entrance to the Lambertson, and an enlargement of the extracted beam phase-space is shown in Figure 2.7-3. The smallest circle in phase-space that encompasses all the extracted particles corresponds to an emittance of $\epsilon = 0.235\pi$ mm-mr, or a normalized value of $\epsilon_N = 30\pi$ mm-mr.

$Q_x = .485, Q_y = .415$: Corrected Orbit



$Q_x = .485$: Corrected 1/2-Integer Stopband

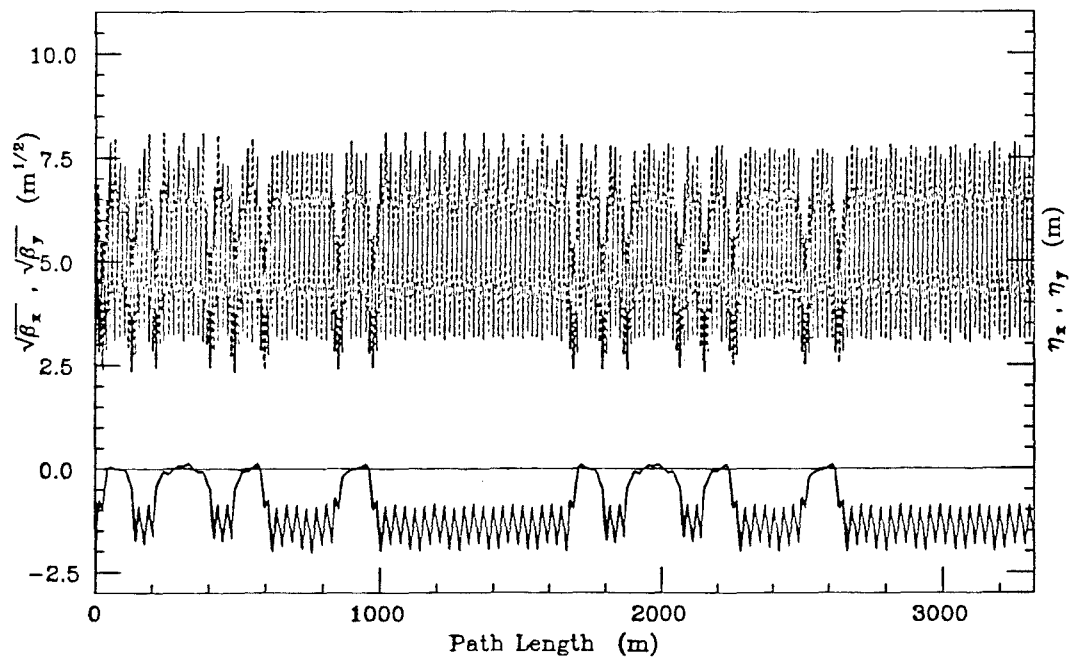


Fig.2.7-1: Main Injector lattice functions before and after stopband compensation.

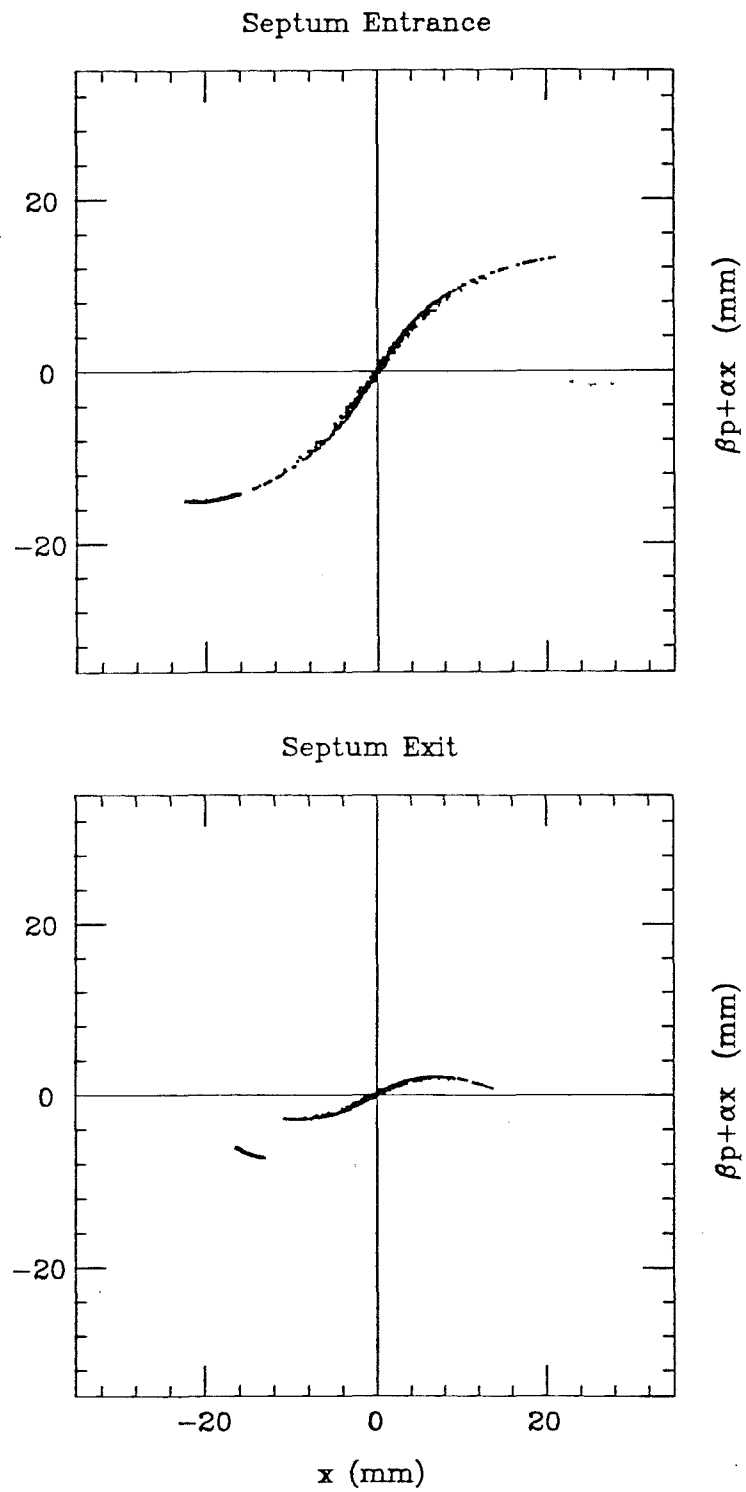


Fig.2.7-2: Circulating & extracted beam phase-space at the electrostatic septa.

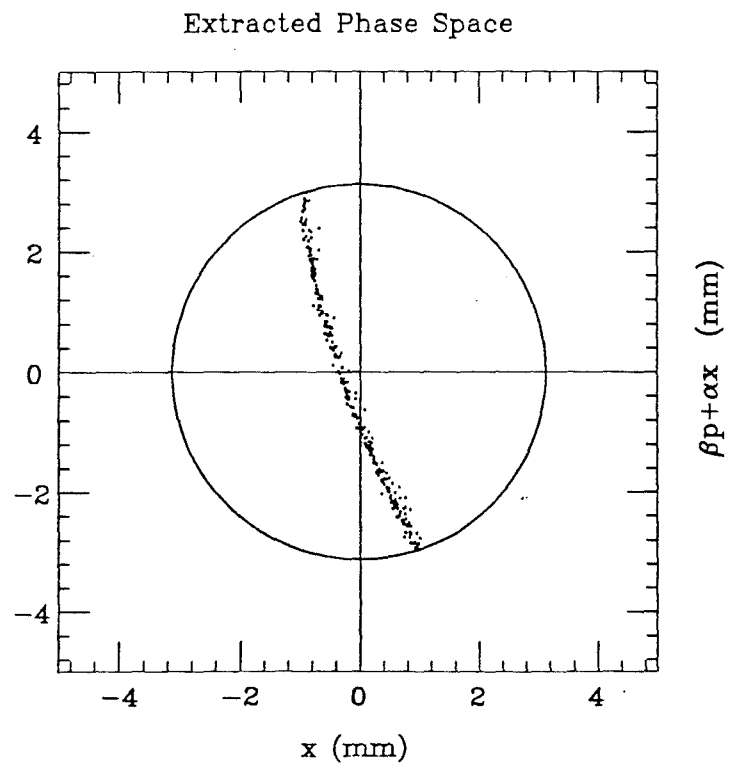
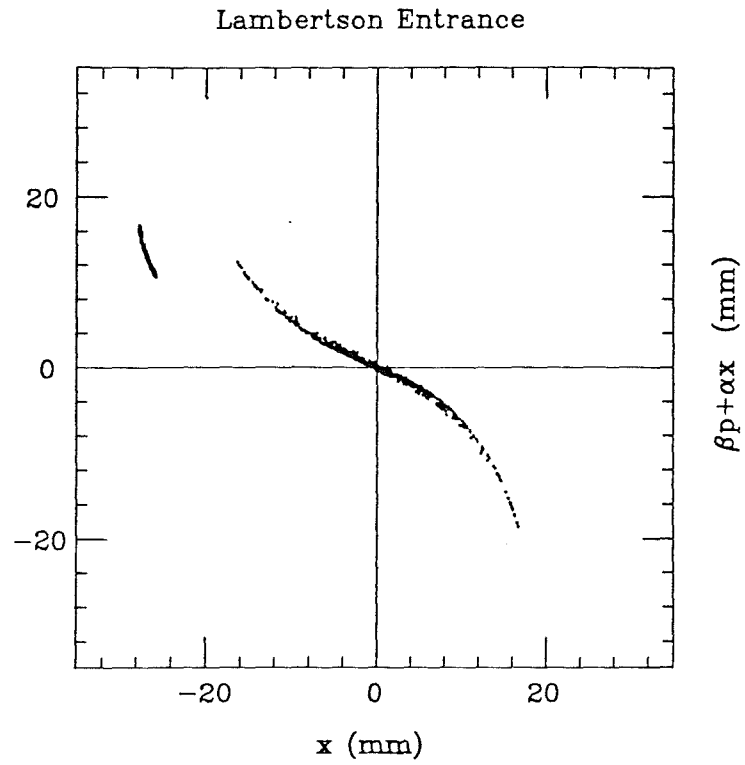


Fig.2.7-3: Circulating & extracted beam phase-space at the Lambertson.

References: Slow Extraction

1. J.A. Johnstone, "A Simplified Analysis of Resonant Extraction at the Main Injector", MI Note-0091, 1993.
2. J.A. Johnstone, "A Numerical Simulation of Resonant Extraction," MI-0101, 1993.
3. D. Trbojevic, "Magnetic Measurements of the Correction and Adjustment Magnets of the Main Ring", Fermilab TM-1412, 1986.
4. J.A. Johnstone, "Resonant Extraction", DOE Semi-Annual Review, 3/15/94.
5. F.A. Harfoush and S. Mishra, "Systematic & Random Errors for Main Injector Tracking:, MI Note-0066, 1993.
6. H. Grote, F.C. Iselin, "The MAD Program", CERN/SL/90-13(AP).

2.8 EMITTANCE GROWTH ISSUES

Dilution Requirements

For both antiproton production and injection into the Tevatron it is generally desirable to keep the beam emittances as small as practicable at extraction. Slow extraction is an exception; it is useful to increase the momentum spread at extraction by blowing up the longitudinal emittance. Because the experimenters usually want good duty factor on the rf time scale, the beam will be debunched as far as possible; the stability of the beam is improved by greater momentum spread. Furthermore, spill regulation becomes less critical. The priority for antiproton production is to minimize the longitudinal emittance to increase the effectiveness of the antiproton debunching operation. For the Tevatron collider or for Tevatron fixed target injection cycles smaller transverse emittance is more important.

The smallest final emittance is usually not to be obtained by seeking to eliminate all dilution at every stage of acceleration. Rather it is necessary to program dilution to avoid instabilities for which no other cures are available. Therefore, the proper program of emittance dilution will depend in part on the particular instabilities that prove most troublesome and the effectiveness of available dampers and feedback systems. (See following section, 2.9 Impedances and Instabilities.)

A comprehensive consideration of emittance growth management involves the entire injector chain. At certain stages of the acceleration process it is possible to increase either transverse or longitudinal brightness as needed with tolerable degradation of the other. However, if one takes the Booster beam emittances from Table 1.1 as fixed conditions, there are limited options, because the best opportunities for reducing emittance or trading off between longitudinal and transverse dimensions exist in or before Booster. The transverse emittance shown is less than originally expected in defining the FMI parameters (see Conceptual Design Report, Rev. 2.3, April 1990), and, in so far as possible, it should be preserved to reduce the intensity required for achieving design luminosity. This preservation will require primarily care in beam transfer and avoidance of transverse instabilities. The instability problems become simpler when the longitudinal emittance is larger.

The principal concern is that the expected longitudinal emittance is too small. Not only does it enter into transverse stability, but longitudinal instability at injection and transition and the spacecharge focusing discontinuity at transition are all severe. The Booster is limited in bucket area early in its cycle to about 0.08 eVs. Although more bucket area is available later, the cycle is so fast that there is limited opportunity for controlled dilution after transition. In fact, the value $\epsilon_l = 0.1$ eVs given in Table 1.1 may be a little optimistic. In current operation the bunches from

the Booster are about 0.06 eVs, although they often blow up at injection into the Main Ring. Whether the number in the time of the FMI is 0.06 or 0.1 eVs, there will be need to get the emittance up to about 0.2 eVs in a reproducible manner at least by transition. This is the emittance required to avoid negative mass instability immediately after transition. It is, however, small enough that it can be taken through transition with about ten to fifteen percent dilution.

Several approaches for getting the requisite dilution at injection into the Main Injector have been simulated. Most result in a peak current for the bunch which is not reduced quite in proportion to the increase in bunch length, because the resulting distributions tend to have a dense core and wide, thinly populated tails. Simply allowing a shape-mismatched bunch to filament, for example, produces almost no reduction in peak current. The most effective simple technique is to inject with a phase error about equal to the bunch half-width. Charge can be distributed more uniformly with a second rf harmonic, but this is an expensive remedy to be employed only if others are inadequate. If the 720 Hz ripple on the magnet power supply has a similar strength to that observed in the Main Ring, a brief excursion in the rf voltage to bring the synchrotron frequency close to that value might be used to assist in controlled dilution. Therefore, although the adjustment of the longitudinal emittance at injection will be important at the highest intensities in the FMI, it is probable that suitable operating techniques will serve without need for special purpose hardware.

Emittance Dilution Specifications for Beam Transfers

The maximum allowable transverse emittance dilution has been specified [1, 2] to be 1π mm-mr from lattice design errors and 2π mm-mr operationally, for the transfer of 20π mm-mr beams.

Intrabeam Scattering

Calculations have been done [3] of intrabeam scattering growth rates at injection for the nominal Main Injector beam parameters: 6×10^{10} protons per bunch, longitudinal emittance of 0.15 eVs, and transverse emittances of 20π mm-mr. Defining the growth time τ as

$$\frac{1}{\tau} = \frac{1}{\sigma} \frac{d\sigma}{dt}$$

the longitudinal growth time is 45 s, while the transverse dimensions are damped, although with damping times of 7800 s horizontally and 6300 s vertically.

Beam-Gas Scattering

The Main Injector vacuum has been specified to be $\sim 1 \times 10^{-8}$ Torr average pressure. This level of average pressure leads to an emittance growth rate [4,5] of 1% in 44 s for a 20π mm-mr beam. While such a small growth rate is not required for normal operations, it facilitates beam dynamics studies and makes it possible to consider unusual operations like stacking polarized protons or accelerating antiprotons in a low-harmonic rf system. The vacuum system to achieve this level is described in Chapter 3.2.

References: Chapter 2.8

- [1] S. Holmes, P. Martin and S. Peggs, "Physical Aperture and Beamline Matching Criteria for the Main Injector", Main Injector Note MI-44, 1990.
- [2] R. Gerig, "A Dispersion Mismatch Criteria for the Main Injector to Tevatron Transfer Line", Main Injector Note MI-01 1989.
- [3] W. Chou, SSCL, private communication.
- [4] J. MacLachlan, "Response to Recommendation from September, 1992, DOE Review", Main Injector Note MI-80, 1993.
- [5] M. Syphers, "Beam-Gas Scattering in the Fermilab Main Ring", Fermilab FN-484, 1988.

2.9 IMPEDANCE AND STABILITY ESTIMATIONS

One important consideration in the design of the Main Injector is the possibility of instabilities which lead to growth in beam emittances and/or the loss of beam. Therefore beam impedances and instability thresholds in the Main Injector have been estimated and are presented in this section. Impedance estimations were made for various components of the vacuum chamber including the RF cavities, beampipe resistive wall, beampipe bellows, vacuum valves, beam position monitors, and Lambertson magnets. Growth rates of the coupled bunch instabilities have been calculated and a microwave instability impedance budget established based on the beam parameters listed in Table 2.9-1. A more detailed report of the impedance and instability calculations can be found in [1].

Table 2.9-1.
Parameters used for instability threshold calculations.
Emittances are 95% normalized values.

<u>Main Injector</u>		
Number of particles per bunch	6 x 10 ¹⁰	
Number of bunches	498	
Number of particles total	3 x 10 ¹³	
Longitudinal emittance at 8.9 GeV	0.1	eVs
Longitudinal emittance at 150 GeV	0.25	eVs
Transverse emittance in x and y	20 π	mm-mrad
RF voltage at 8.9 Gev	400	kV
RF voltage at 150 Gev	400	kV
<u>Main Ring</u>		
Number of particles per bunch	3 x 10 ¹⁰	
Number of bunches	1008	
Number of particles total	3 x 10 ¹³	
Longitudinal emittance at 8.9 GeV	0.1	eVs
Longitudinal emittance at 150 GeV	0.25	eVs
RF voltage at 8.9 GeV	400	kV
RF voltage at 150 GeV	400	kV

Space Charge Impedance

The Main Injector beampipe, when installed in the Main Injector magnets and under vacuum, is approximately elliptical with a full height of 5.08 cm (2.00 inches) and a full width of 12.3 cm (4.84 inches). The elliptical beampipe shape makes calculation of the space charge impedance difficult so we make estimations using conformal mapping techniques [2] and a beampipe with rectangular cross section.

The space charge impedance is calculated at 8.9 GeV since it is largest at the lowest energy. Assuming a 95% normalized transverse emittance of 20π mm-mrad, we approximate the transverse beam distribution as a cylindrical beam with a radius of $a = 2.7$ mm in our calculations of the space charge impedances. The results of these calculations are shown in Table 2.9-2.

Table 2.9-2
Space charge impedance at 8.9 GeV for a rectangular beampipe.

$Z_{ }/n$	$-j\ 12.3\ \Omega$
$Z_{\perp x}$	$-j\ 317\ \text{M}\Omega/\text{m}$
$Z_{\perp y}$	$-j\ 303\ \text{M}\Omega/\text{m}$

As will be shown in the section on microwave instabilities, the longitudinal space charge impedance per harmonic is below the threshold of microwave instability, except in the region of transition. Near transition the Landau damping due to the revolution frequency spread becomes negligibly small implying that the impedance budget also becomes small. However, the growth rate at transition goes to zero, so the problem near transition must be handled another way. Simulations of longitudinal phase space during transition crossing have been done including space charge with a broadband longitudinal impedance of $Z_{||}/n = 5\Omega$. The results of these simulations are discussed in Chapter 2.5.

On the other hand, however, the transverse impedance due to space charge will not cause any microwave instability. There is always Landau damping due to tune spread although the revolution frequency spread become negligibly small.

Space Charge Tune Shifts

We are also interested in the coherent and incoherent tune shifts resulting from direct space charge forces, electric image charges, and magnetic image currents. These image charges

and image currents inside the vacuum chamber walls and magnet laminations create electromagnetic fields which alter the transverse focusing force on the particles thus changing their tune.

The total tune shift is the sum of the tune shifts from the various image fields. These include electric fields from charge induced on the vacuum chamber wall, magnetic fields from image currents induced in the magnets by DC beam current, and magnetic fields from image currents induced in the vacuum chamber walls by the AC beam current. The AC beam current is a result of both longitudinal bunching and coherent transverse betatron motion. The magnetic fields from the AC beam current do not penetrate the vacuum chamber while those from the DC beam current do penetrate the vacuum chamber walls and enter the magnet laminations.

Including all of the above contributions to the tune shift [3] the coherent and incoherent tune shifts have been calculated using an elliptical beampipe [4] and using the design beam intensity and emittance. The results are shown in Table 2.9-3.

Table 2.9-3
Coherent and incoherent tune shifts in the Main Injector at 8.9 GeV.

	Vertical	Vertical	Horizontal	Horizontal
	Coherent	Incoherent	Coherent	Incoherent
Electric Field	-0.180	-0.0595	-0.0010	+0.0572
DC Magnetic Field	-0.0111	-0.0111	+0.0107	+0.0107
Longitudinal AC Magnetic Field	+0.143	+0.0474	+0.0008	-0.0045
Betatron AC Magnetic	+0.0231		+0.013	
Direct Space Charge		-0.0630		-0.0630
Total Tune Shift	-0.0245	-0.0862	+0.0216	-0.0407

The coherent tune shifts were found to be less than -0.025 and are not expected to create any problems. The incoherent tune shifts on the other hand are calculated to be rather large, especially the vertical incoherent tune shift of $\Delta_{inc}^V = -0.086$. However, similar calculations for

the Main Ring also give $\Delta_{inc}^V = -0.095$ and $\Delta_{inc}^H = 0.085$. Therefore we don't expect the incoherent tune shifts to be a problem in the Main Injector.

RF Cavities and Coupled Bunch Instabilities

Higher order cavity modes in the RF accelerating cavities are often the cause of coupled bunch instabilities. In this section we estimate the growth times of these instabilities based on measurements of the longitudinal impedances of the cavities and calculations of the transverse impedances. We also compare the estimates for the Main Injector to estimates of growth times in the Main Ring.

The RF cavities to be used for the Main Injector are the 18 RF cavities presently installed and operating in the Main Ring. Stretched wire measurements of the longitudinal impedances of the cavities have been made [5] and the 6 modes with the largest impedances are listed in Table 2.9-4. The cavity mode at 128 MHz has limited the Main Ring performance in the past so a passive mode damper was designed and installed to reduce the shunt impedance of that particular mode [6] by a factor of 25 to the value of 6.3 k Ω /m listed in Table 2.9-4. This helped alleviate the problems with the coupled bunch instability.

In the Main Injector we find that the longitudinal coupled bunch growth times are shortest at 150 GeV. Therefore the growth times listed in Table 2.9-4 are at 150 GeV and use $M=498$ bunches with $N = 6 \times 10^{10}$ per bunch. As a comparison we also calculate the growth times in the Main Ring with $M = 1008$ bunches of $N = 3 \times 10^{10}$ particles per bunch and a longitudinal emittance of 0.25 eVs. The growth times for both machines are listed in Table 2.9-4.

The standard perturbation theory [9,10], which neglects Landau damping effects, predicts that about half of the coupled bunch modes will have a positive growth rate associated with each higher order cavity mode. Therefore it is important to make some estimations on the effectiveness of Landau damping in preventing instability. We do this by comparing calculated growth times in the Main Injector to the calculated growth times in the Main Ring. Since these cavities are presently used in the Main Ring, we can compare the calculated growth times to any observed instabilities.

Some of the calculated growth times for the Main Injector are short. It must be remembered however that these calculations do not include the Landau damping effect which may stabilize the beam and help prevent instability. The calculations are also worst case scenarios since it was assumed that the frequencies of the higher order modes in all 18 RF cavities are identical. In practice, the higher order modes are at slightly different frequencies in the individual

cavities. Although the growth times are short, they are not alarming when compared to the calculated Main Ring growth times which are also short.

Table 2.9-4
Calculated growth times for the longitudinal dipole and quadrupole coupled bunch instability in the Main Injector and Main Ring with 18 RF cavities.

Longitudinal Coupled Bunch Growth Times (msec)					
Freq of mode (MHz)	Z (kohm) per cavity	dipole		quadrupole	
		MI	MR	MI	MR
71.0	10.0	20.2	50.9	293	483
100.0	2.5	65.5	177	461	797
128.0	6.3	24.2	71.6	98.7	182
223.0	111.0	2.1	10.3	2.1	5.5
600.0	277.0	9.1	32.7	3.5	20.8
850.0	49.0	91.5	350	45	241

Experience with the Main Ring has shown that the 128 MHz mode can sometimes be a problem in fixed target operation with a full ring of bunches. Also of concern is the short growth time of the 223 MHz mode. As a result a set of passive mode dampers for the cavities was designed to reduce the shunt impedance of the 223 MHz mode and further damp the 128 MHz mode as well. With this mode damper installed the 223 MHz impedance is lowered to a value of about 10 k Ω reducing the calculated growth rate of the 223 MHz mode by a factor of about 10. If needed other RF cavity modes could be damped as well.

Also of concern is the coupled bunch instability with the short batches used in coalescing. Presently in the Main Ring there is evidence of an instability for short batches (about 11 consecutive bunches) with 3×10^{10} particles per bunch. Since this type of instability depends on R/Q and not on R, adding passive dampers does not remove the instability. The Main Injector calls for 6×10^{10} particles per bunch so there could be substantial difficulty with short batch operation. Dealing with this problem will probably require the development of an active feedback damping system.

Calculated growth times for the transverse coupled bunch instability modes are based on the same perturbation approach used in the longitudinal case [9] and use the transverse impedances shown in Table 2.9-5.

The growth times for both the Main Injector and the Main Ring are calculated at an energy of 8.9 GeV and are listed in Table 2.9-5. The calculated growth times in the Main Injector are about one half of those in the Main Ring. So far there has not been any evidence observed of transverse coupled bunch modes in the Main Ring driven by the transverse RF cavity modes.

The transverse modes of the RF cavities have been estimated previously using the computer code URMEL [7,8] and the cavity modes with the 5 largest transverse impedances are listed in Table 2.9-5.

Table 2.9-5
Calculated growth times for the transverse dipole and quadrupole coupled bunch modes
in the Main Injector and Main Ring with 18 RF cavities.

Transverse Coupled Bunch Growth Times (msec)					
Freq of mode (MHz)	Z_{\perp} (M Ω /m) per cavity	dipole		quadrupole	
		MI	MR	MI	MR
398	3.3	4.0	6.8	4.2	6.6
454	1.9	8.1	13	8.0	13.4
566	0.75	25.0	42	26	42
1270	1.7	25	41	25	48
1290	2.4	18.0	30	18.1	29.9

Resistive Wall

The elliptical shape of the beampipe makes an exact calculation of the resistive wall impedance difficult. Instead we make estimations using exact solutions for a beampipe with circular [11] and rectangular [2] cross sections. We use a circular beampipe with a radius of

$b=2.39$ cm and a rectangular beampipe with a height of 4.78 cm, a width of 12.0 cm, and a thickness of 1.5 mm.

Using the circular approximation to the Main Injector beampipe we get the results listed in Table 2.9-6. The results are expressed as a function of the revolution harmonic number n for both high and low frequencies.

Table 2.9-6

Resistive wall impedance as a function of revolution harmonic n for circular beampipe with radius $b=2.39$ cm and rectangular beampipe 4.78 cm by 12.0 cm. Results are given for frequencies where the skin depth is less (greater) than the thickness of the beampipe $n > n_c$ ($n < n_c$) where $n_c = 0.922$.

Circular Beampipe		
	$n < n_c$	$n > n_c$
$Z_{ }/n$	$10.9/n \ \Omega$	$(1+j)11.3/\sqrt{n} \ \Omega$
Z_{\perp}	$20.3/n \ \text{M}\Omega/\text{m}$	$(1+j)21.1/\sqrt{n} \ \text{M}\Omega/\text{m}$
Rectangular Beampipe		
	$n < n_c$	$n > n_c$
$Z_{ }/n$	$10.8/n \ \Omega$	$(1+j)11.2/\sqrt{n} \ \Omega$
$Z_{\perp x}$	$8.24/n \ \text{M}\Omega/\text{m}$	$(1+j)8.55/\sqrt{n} \ \text{M}\Omega/\text{m}$
$Z_{\perp y}$	$16.7/n \ \text{M}\Omega/\text{m}$	$(1+j)17.3/\sqrt{n} \ \text{M}\Omega/\text{m}$

In the interest of understanding the effect that the shape of the beam pipe has on the resistive wall instability, the beampipe cross section is also approximated by a rectangle. The results, shown in Table 2.9-6, indicate that the transverse impedance in the y direction in the rectangular case is not much less than that in the circular approximation. However, the transverse impedance in the x direction is only about one half of that in the y direction.

The most important effect of the resistive wall instability is the transverse coupled bunch mode at low frequencies and low energies. At low frequencies the resistive wall impedance is proportional to $\sqrt{\omega}$ and therefore sharply peaked at the origin. Since the vertical tune is 25.4 the

coupled bunch mode $s = -26$ has the largest growth rate. The lowest and most relevant frequency is only $-0.6 \omega_0/2\pi = 54$ kHz which is very small. Since the transverse impedance is so sharply peaked at the origin we consider only the impedance at 54 kHz in the calculation of the growth rate.

Using the low frequency estimates of the Lambertson magnets (discussed later) and the beampipe resistive wall impedance we calculate the corresponding growth time for mode $s = -26$. The resistive wall impedance of the beampipe is $\text{Re}\{Z_{\perp}(-0.6\omega_0)\} = -27.8 \text{ M}\Omega/\text{m}$ and the Lambertson impedance is $\text{Re}\{Z_{\perp}(-0.6\omega_0)\} = -35 \text{ M}\Omega/\text{m}$.

With these impedances the calculated growth time for the resistive wall instability, with zero chromaticity, is 0.35 ms at 8.9 GeV. Although this is a fast growth time, some observations of the Main Ring [12] lead us to believe that the resistive wall instability will not be a problem. Using an impedance of $-98 \text{ M}\Omega/\text{m}$ and intensity of 1.5×10^{13} in the Main Ring, the calculated growth time of the resistive wall instability is 0.65 ms. However at this intensity beam is stable in the Main Ring without providing any method of damping (transverse dampers turned off, chromaticity set to zero, and no octupole magnets used). At the higher intensity of 2×10^{13} beam is stable whenever any one of the following is true: 1) just the transverse dampers turned on, 2) just the chromaticity set between -30 to -40, and 3) just the octupole magnets turned on. The Main Injector, in addition to the transverse damper, has all three methods available to provide further damping. For instance, changing the chromaticity of the Main Injector at injection from zero to -20 increases the growth time from 0.35 ms to 2 msec. Thus we should not expect any problems with the transverse resistive wall instabilities in the Main Injector.

Beam Position Monitors

The Main Injector BPM consists of 4 stripline pickups which are cut out of the approximately elliptical beampipe. Two pickups are located on each of the top and bottom surfaces of the beampipe and are spaced 40 mm apart from center to center. Each stripline is about 1 cm wide, 40 cm long, and has a characteristic impedance of 50Ω . The downstream end of each stripline is shorted while the upstream end is connected in parallel with a 50Ω cable leading to the RF module.

As a bunch passes the BPM, a fraction of the image current traveling in the beampipe will enter the stripline at the upstream end and see the $Z_c = 50 \Omega$ cable and the shorted $Z_c = 50 \Omega$ stripline in parallel. Based on the impedance of the BPM stripline and an estimation of the fraction of image current that enters the stripline [1] the longitudinal impedance of all 208 BPMs can be estimated.

In the low frequency limit, the total longitudinal impedance of all 208 BPMs becomes $Z_{||}/n = j0.095 \Omega$ and the total transverse impedances becomes $Z_{\perp y} = j5.15 \text{ k}\Omega/\text{m}$ and $Z_{\perp x} = j2.66 \text{ k}\Omega/\text{m}$. These impedances are much lower than other components in the ring. This is mainly due to the relatively narrow width of the stripline pickups. Thus the BPMs are not expected to be a problem.

Bellows

The beampipe bellows will consist of approximately 10 to 17 convolutions extending over one inch. The inner dimensions of the bellows are an ellipse of similar size to the beampipe and the convolutions extend 1.28 cm (0.5 inches). To estimate the impedance the elliptical shape was approximated by a circular beampipe with radius 2.67 cm (1.05 inches). This was done for both 10 and 17 bellow convolutions using the program TBCI [13]. The calculated longitudinal impedance of the 10 and 17 bellow convolution models are very similar.

The longitudinal impedances of a single bellow can be characterized approximately as two resonators of the form

$$Z_{||}(\omega) = \frac{R_s}{1 + jQ(\omega / \omega_r - \omega_r / \omega)} \quad (2.9-1)$$

with values $R_s=40 \Omega$, $Q=5.3$, $\omega_r/2\pi = 4 \text{ GHz}$ and $R_s=120 \Omega$, $Q=4.3$, and $\omega_r/2\pi = 8.5 \text{ GHz}$.

In the Main Injector there are 516 bellows giving a total longitudinal impedance of $R_s/n = 0.47 \Omega$ or $R_s/Q = 3.9 \text{ k}\Omega$ at 4 GHz and $R_s/n = 0.658 \Omega$ or $R_s/Q = 14.4 \text{ k}\Omega$ at 8.5 GHz. The typical rms bunch length at 8.9 (150) GeV is 1.24 (0.69) ns corresponding to a rms spectral spread of 0.13 (0.23) GHz. On the other hand, the widths of the bellows impedance resonances are 0.75 GHz and 2.0 GHz at the resonance frequencies of 4 GHz and 8.5 GHz. Therefore these resonances should be treated as broadband and the impedance values should be compared with the microwave instability budget limits (as calculated in the section on microwave instabilities), which gives $|Z_{||}/n| < 36.9 \Omega$ at 8.9 GeV and $|Z_{||}/n| < 6.6 \Omega$ at 150 GeV.

The transverse impedance of the bellows can be approximated as a resonator of the form

$$Z_{\perp}(\omega) = \frac{1}{\omega} \frac{R_{\perp} \omega_r}{jQ(\omega / \omega_r - \omega_r / \omega)} \quad (2.9-2)$$

with values $R_{\perp} = 1.5 \text{ k}\Omega/\text{m}$, $Q=5.3$, and $\omega_r/2\pi = 8 \text{ GHz}$. With 516 bellows in the Main Injector the total transverse impedance is then $R_{\perp}/n = 8.74 \text{ k}\Omega/\text{m}$ and $R_{\perp}/Q = 146 \text{ k}\Omega/\text{m}$ at 8 GHz. Both of these values are well below the microwave instability limits at 8.9 GeV of $|Z_{\perp}/n| < 55 \text{ k}\Omega/\text{m}$

and $R_{\perp} < 71.6 \text{ M}\Omega/\text{m}$. Therefore the impedance of the bellows should not create any problems in the Main Injector.

Vacuum Valves

To estimate the impedance of the vacuum valves we consider the two different shapes shown in Figures 2.9-1 and 2.9-2. The difference between the two designs is the presence or absence of the cylindrical pillbox cavities on either side of the valve. Using these shapes the 3D computer code MAFIA [14] was used to calculate the longitudinal and transverse impedances. The beam pipe cross section is approximated by an ellipse with 5.12 cm by 12.3 cm diameters. The resistivity of

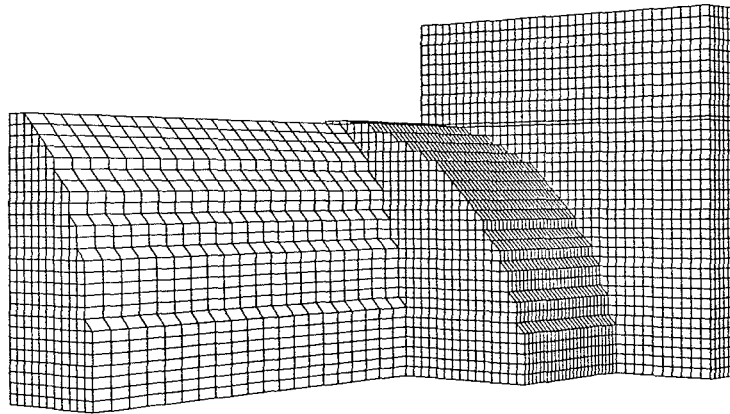


Figure 2.9-1.
Approximate geometry of Main Injector vacuum valve with pillbox cavities.

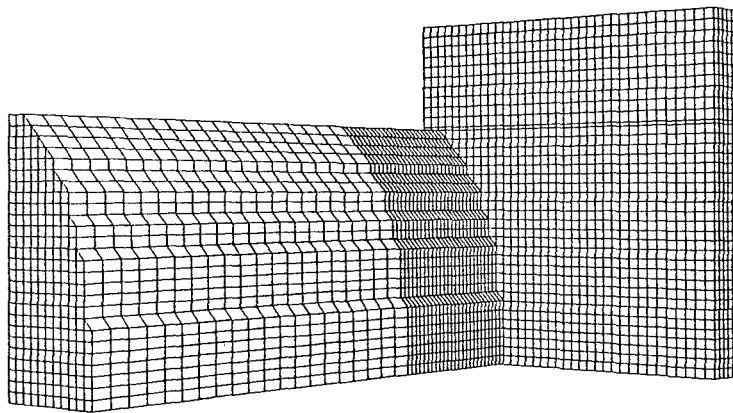


Figure 2.9-2.
Approximate geometry of Main Injector vacuum valve without pillbox cavities.

the vacuum valve is the same as the beam pipe, $\rho = 74 \mu\Omega\text{-cm}$, and the results from MAFIA are converted to match this assumption. The impedances of a single vacuum valve are shown in Table 2.9-7 and the net impedances of all 30 valves in the Main Injector are shown in Table 2.9-8.

Calculations for the coupled bunch growth rates show that the vacuum valve modes are benign. This is mainly due to the fact that the modes in the valves are at frequencies above the beam spectrum frequencies. All modes have a growth time of greater than 100 ms except for the quadrupole mode of the 2.46 GHz mode which has a growth rate of 62 ms.

Table 2.9-7.

Estimated frequency, impedance per vacuum valve, and Q value of longitudinal and transverse modes in two different Main Injector vacuum valve designs.

See Figures 2.9-1 and 2.9-2.

Vacuum valve with pillbox cavities		
Freq (GHz)	$Z_{ }$ (k Ω)	Q
1.511	76	2090
2.460	117	3800
Freq (GHz)	$Z_{\perp x}$ (M Ω /m)	Q
1.52	1.7	3000
3.11	0.071	4000
Freq (GHz)	$Z_{\perp xy}$ (M Ω /m)	Q
1.928	0.47	1980
3.154	0.21	3810
Vacuum valve without pillbox cavities		
Freq (GHz)	$Z_{ }$ (k Ω)	Q
1.30	52	1600
2.85	13.4	2700
Freq (GHz)	$Z_{\perp x}$ (M Ω /m)	Q
2.95	0.422	2500
Freq (GHz)	$Z_{\perp xy}$ (M Ω /m)	Q
3.10	0.032	2500

Table 2.9-8.
Estimated net impedances of 30 vacuum valves in the Main Injector.

Vacuum valve with pillbox cavities		
Freq (GHz)	$ Z_{ }/n (\Omega)$	$R_{ }/Q (\Omega)$
1.511	135	1090
2.460	129	924
Freq (GHz)	$ Z_{\perp x}/n (k\Omega/m)$	$R_{\perp x}/Q (k\Omega)$
1.52	3.0	17
3.11	0.06	0.53
Freq (GHz)	$ Z_{\perp y}/n (k\Omega/m)$	$R_{\perp y}/Q (k\Omega)$
1.928	.650	7.2
3.154	.178	1.6
Vacuum valve without pillbox cavities		
Freq (GHz)	$ Z_{ }/n (\Omega)$	$R_{ }/Q (\Omega)$
1.30	108	975
2.85	12.6	150
Freq (GHz)	$ Z_{\perp x}/n (k\Omega/m)$	$R_{\perp x}/Q (k\Omega)$
2.95	.387	5.04
Freq (GHz)	$ Z_{\perp y}/n (k\Omega/m)$	$R_{\perp y}/Q (k\Omega)$
3.10	0.028	0.384

Also of concern is the potential microwave instability due to the vacuum valves. Analysis of the microwave instabilities shows that the impedance of the resonator modes in the vacuum valve must have a longitudinal impedance $R_{||}/Q \leq 26.7 \Omega$ and their total transverse impedance $R_{\perp}/Q \leq 71.6 M\Omega/m$. The vacuum valve impedances are below these threshold values and therefore will present no problem.

Lambertsons

The main concern of the Lambertson magnets is the low frequency component created by the exposure of the bare magnet laminations to beam. A rough estimation of the Lambertson magnets is made by approximating the magnet as a series of annular laminations of 0.953 mm width. The inner radius is chosen to be $b = 2.54$ cm and the outer radius is chosen to be $d = 5.08$

cm. The low frequency current traveling through the magnet is assumed to flow in one lamination from the inner radius to the outer radius, cross over to the next lamination, and flow from the outer radius to the inner radius. Even though we are concerned about the low frequency impedance, the skin depth is less than the lamination thickness at the frequencies we are considering. The current is therefore constrained to one skin depth in the laminations. The impedance of the magnet is then calculated by adding up the resistance along the entire current path.

The lamination material has a resistivity of $\rho = 20 \mu\Omega\text{-cm}$ and a relative permeability of $\mu = 100$. With 25.8 meters of Lambertson magnets in the Main Injector the total estimated low frequency impedance is

$$Z_{\parallel} / n = (1 + j) \frac{16.4}{n} \text{M}\Omega \quad (2.9-3)$$

To estimate the transverse impedance we use the approximate relation

$$Z_{\perp} = \frac{2c}{b^2} \frac{Z_{\parallel}}{\omega} \quad (2.9-4)$$

and arrive at

$$Z_{\perp} = (1 + j) \frac{26.8}{\sqrt{n}} \text{M}\Omega / \text{m}. \quad (2.9-5)$$

It should be noted that the Lambertson magnet was assumed to have a circular geometry with inner radius of $b=2.54$ cm. The actual shape of the Lambertson is much different so this estimate can only be approximate. Using a slightly larger inner radius can change the impedance by a significant amount (i.e. if b is 10% larger the longitudinal impedance drops by 10% and the transverse impedance drops by 25%).

The impedance at higher frequencies was also calculated assuming the gap between the laminations acts as a radial waveguide. The material in the gap has a relative permittivity $\epsilon = 6$ and a small conductivity $\sigma = 0.01 \Omega^{-1}\text{m}^{-1}$. The results of this type of analysis are shown in Figures 2.9-3 and 2.9-4.

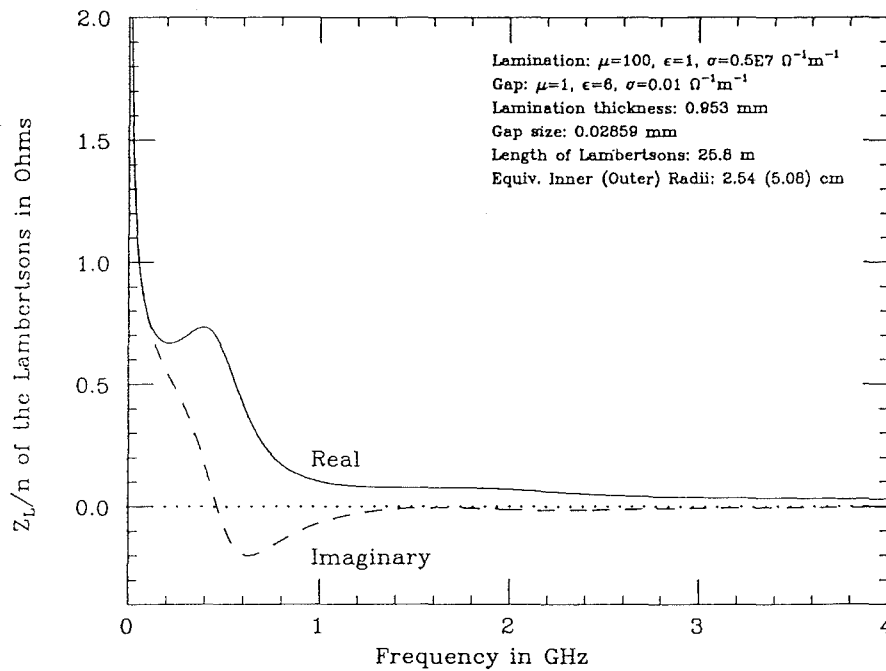


Figure 2.9-3.

Real and imaginary part of the longitudinal impedance for the Lambertson magnets.

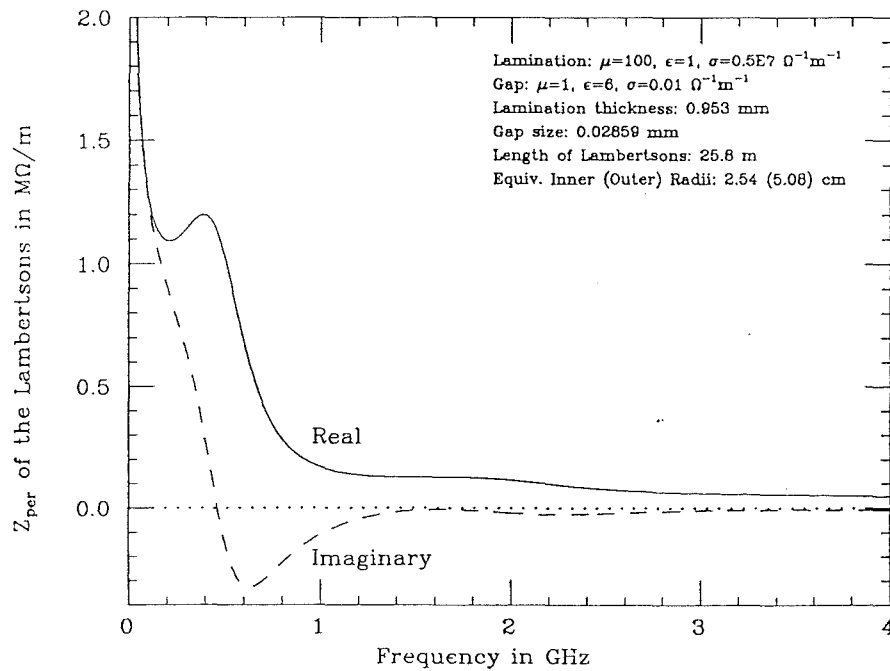


Figure 2.9-4.

Real and imaginary part of the transverse impedance for the Lambertson magnets.

Microwave Instabilities

The microwave stability limit for bunched beam with a Gaussian momentum distribution in the presence of a broadband resonator [15] depends on the rms momentum spread of a bunch σ_p/p and the peak current in the bunch I_p via the relation

$$\left| \frac{Z_{||}}{n} \right| = \frac{2\pi|\eta|(E/e)\beta^2}{I_p} \left(\frac{\sigma_p}{p} \right)^2 \quad (2.9-6)$$

Here $\eta = \gamma_t^{-2} - \gamma^{-2}$ is the frequency slip parameter where $\gamma_t = 21.8$ is the transition gamma.

Except for energies near transition, the microwave instability limit is most restrictive at 150 GeV where the momentum spread, σ_p/p , is the smallest. For a longitudinal emittance of 0.25 eVs the broadband impedance budget is $|Z_{||}/n| < 6.6 \Omega$.

For the case of sharp resonances, narrower than the bunch spectrum, the relevant quantity [16] is not $|Z_{||}/n|$ but $|R_{||}/Q|$ where $R_{||}$ is the shunt impedance of a high-Q resonator. The impedance budget in this narrowband case is

$$\frac{R_{||}}{Q} \leq \frac{4|\eta|\beta^2(E/e)}{I_b} \left(\frac{\sigma_p}{p} \right)^2 \quad (2.9-7)$$

where I_b is the average current in the bunch. As in the broadband case, the most restrictive limit is $R_{||}/Q < 27 \text{ k}\Omega$ at 150 GeV. The impedance budget at 8.9 and 150 GeV for longitudinal microwave instabilities is shown in Table 2.9-9. These values need to be compared with the estimated impedances of the Main Injector. In Figures 2.9-5 and 2.9-6 we show the impedance of the various components of the Main Injector at 8.9 GeV and at 150 GeV. These plots show that the space charge impedance is the dominant one at 8.9 GeV, while the vacuum valves are the largest contributor at 150 GeV. In both cases, the total impedance is below the budget. The contribution from the bellows shown in these figures is for the case of unshielded bellows. As discussed in Chapter 3.2, we have decided to shield the bellows, which will reduce that contribution by roughly a factor of two, providing additional margin.

In the transverse case the microwave instability limit for broadband resonances [16,17] written in terms of I_p and σ_p/p , is

$$|Z_{\perp}| \leq 4\sqrt{2\pi} \frac{Ev_\beta\beta\gamma}{eRI_p} |(n - v_\beta)\eta - \xi| \quad (2.9-8)$$

Main Injector Longitudinal Impedance at 8.9 GeV

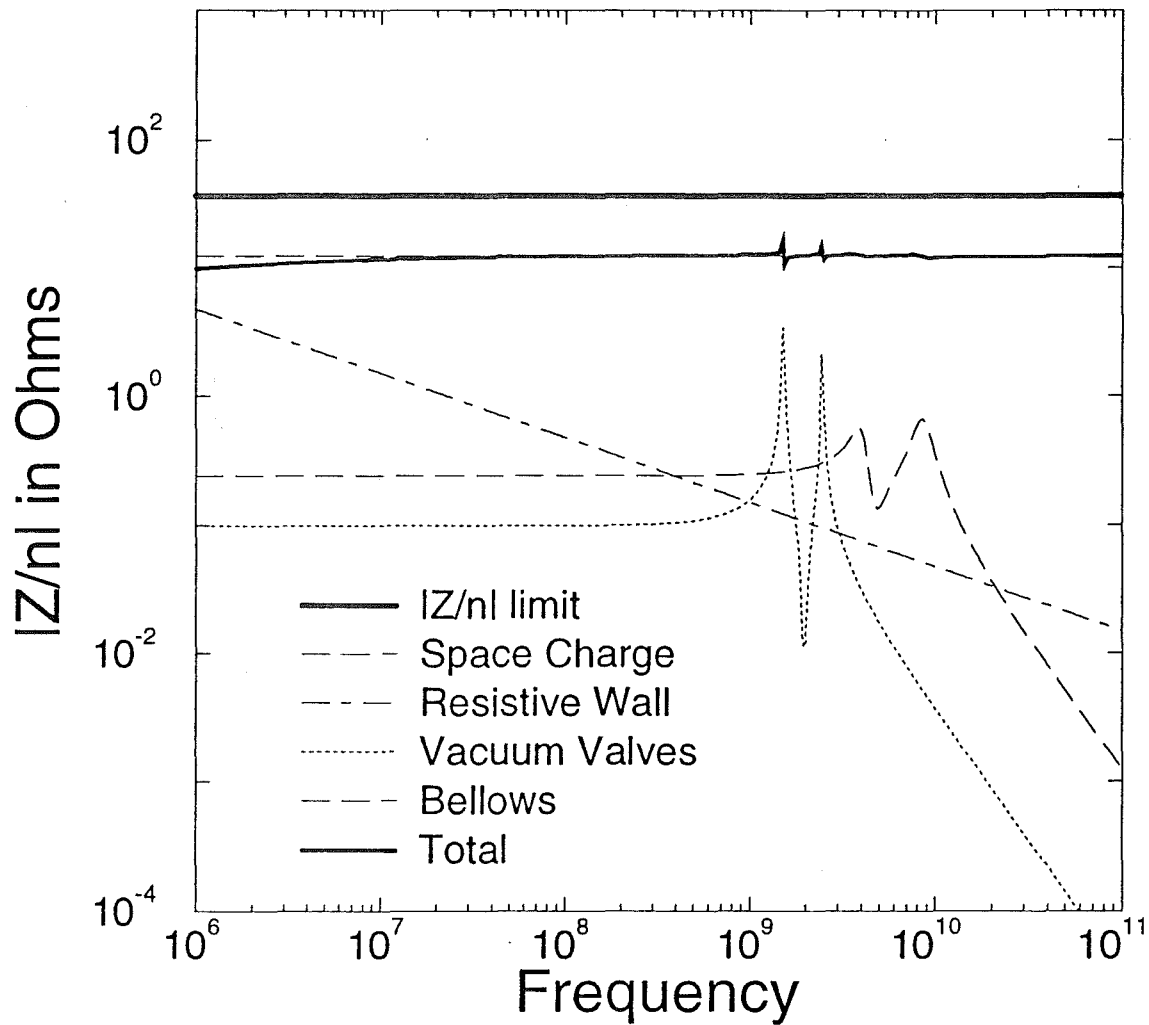


Figure 2.9-5. Longitudinal Impedance Contributions at 8.9 GeV

Main Injector Longitudinal Impedance at 150 GeV

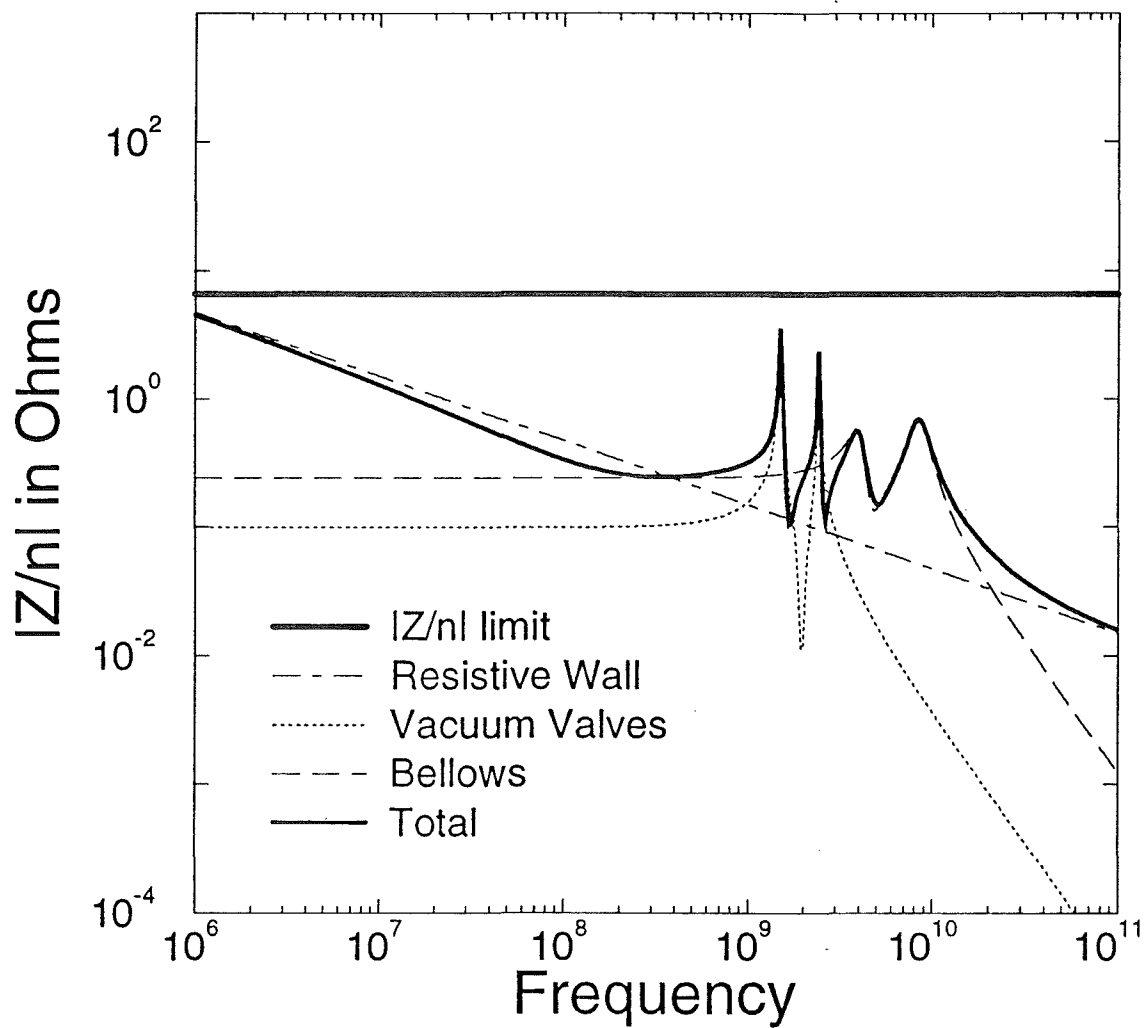


Figure 2.9-6. Longitudinal Impedance Contributions at 150 GeV.

where ξ is the chromaticity. The contribution to Landau damping from the revolution frequency spread and from the tune spread are included with the η and ξ terms respectively.

With the harmonic number n as a factor on the right side of Equation 2.9-8 the transverse impedance budget becomes more stringent at lower frequencies. However this equation applies only to microwave frequencies which have a wavelength λ smaller than the rms bunch length. In other words Equation 2.9-8 applies only for harmonic number $n > 2\pi/(\omega_0\sigma_t)$. Except near transition crossing where η is small, we have mostly $|(v-v_\beta)\eta| > |\xi|$, and the contribution of chromaticity can be neglected. Therefore we calculate the transverse impedance budget for the Main Injector using Equation 2.9-8 with $n = 2\pi/\omega_0\sigma_t$.

Unlike the longitudinal impedance budget which goes to zero at transition, the transverse impedance budget is still finite due to the contribution of chromaticity. As a result transverse microwave growth usually does not occur at transition.

For narrowband transverse impedances the impedance budget is given by

$$\frac{R_\perp}{Q} \leq \frac{8\sqrt{2}\beta\gamma Ev_\beta |\eta| \left(\frac{\sigma_p}{p} \right)}{e\pi R I_b} \quad (2.9-9)$$

Using the same parameters as in the longitudinal case the transverse microwave impedance budgets were calculated and are shown in Table 2.9-9.

Table 2.9-9.
Microwave instability impedance budget for broadband and narrowband impedances.

	8.9 GeV	150 GeV
$ Z n $	36.9 Ω	6.6 Ω
$R Q$	85.4 Ω	26.7 k Ω
$ Z_\perp /n $	0.055 M Ω /m	0.63 M Ω /m
$ Z_\perp $	500 M Ω /m	10.1 G Ω /m
@ Freq. [†]	0.81 GHz	1.44 GHz
R_\perp/Q	71.6 M Ω /m	1450 M Ω /m

[†]Transverse impedance budget $|Z_\perp|/n|$ applies only above microwave frequencies where the wavelength is smaller than the rms bunch length. Thus $|Z_\perp|$ is the relevant impedance budget.

References: Chapter 2.9

1. M. Martens and K.Y. Ng, "Impedance and Instability Threshold Estimates in the Main Injector", Fermilab Main Injector Note MI--0103, 1994.
2. K.Y. Ng, "Exact Solutions for the Longitudinal and Transverse Impedances of an Off-centered Beam in a Rectangular Beam Pipe", Particle Accelerators 16, 1984.
3. P.J. Bryant, "Betatron Frequency Shifts Due to Self and Image Fields", CERN Accelerator School, CERN 87-10, 1987.
4. B. Zotter, "The Q-Shift of Off-Center Particle Beams in Elliptic Vacuum Chambers", Nucl. Instrum. Methods 129, 1975.
5. R.A. Dehn and Q.A. Kerns and J.E. Griffin, "Mode Damping in NAL Main Ring Accelerating Cavities", IEEE Trans. Nucl. Sci. NS-18, 1971.
6. Q.A. Kerns and H.W. Miller, "Fermilab 500-GeV Main Accelerator RF Cavity 128-MHz Mode Damper", IEEE Trans. Nucl. Sci. NS-24, 1971.
- L.J. Laslett, "On Intensity Limitations Imposed by Transverse Space-Charge Effects in Circular Particle Accelerators", 1963 Summer Study on Storage Ring Accelerators and Experimentation at Super High Energies, BNL-753, 1963.
7. P. Colestock and S. Saritepe, "Transverse Instability Estimates in the Fermilab Booster and Main Ring", Proceedings of the Fermilab III Instabilities Workshop, 1990.
8. U. Laustroer, U. van Rienen and T. Weiland, "URMEL and URMEL-T User Guide", DESY M-87-03, 1987.
9. J.L. Laclare, "Bunched Beam Coherent Instabilities, CERN Accelerator School", CERN 87--03, 1985.
10. F.J. Sacherer, "A Longitudinal Stability Criterion for Bunched Beams", IEEE Trans. Nucl. Sci. NS-20, 1973.
11. B. Zotter and F. Sacherer, "Transverse Instabilities of Relativistic Particle Beams in Accelerators and Storage Ring", CERN 77-13, 1977.
12. S. Pruss, Fermilab, Private communication
13. R. Klatt and T. Weiland, "TBCI Short User Guide", DESY, 1988.
14. "MAFIA User Guide", DESY, LANL and KFA, 1989.
15. S. Krinsky and J.M. Wang, "Longitudinal Instabilities of Bunched Beams Subject to a Non-Harmonic RF Potential", Particle Accelerators 17, 1985.
16. K.Y. Ng, "Microwave Instability When Driven By Narrow Resonances," Proceedings of the 1986 Summer Study on the Physics of the Superconducting Super Collider, Snowmass, Colorado, 1986.
17. R.D. Ruth and J.M. Wang, "Vertical Fast Blow-up in a Single Bunch", IEEE Trans. Nucl. Sci. NS-28, 1981.

CHAPTER 3.1. MAGNETS

WBS 1.1.1.1 MAIN INJECTOR RING MAGNETS

- WBS 1.1.1.1.1. DIPOLES
- WBS 1.1.1.1.2. QUADRUPOLES
- WBS 1.1.1.1.3. HARMONIC CORRECTORS
- WBS 1.1.1.1.4. CORRECTION DIPOLES

WBS 1.1.1.2. 8 GEV LINE MAGNETS

- WBS 1.1.1.2.1. DIPOLES
- WBS 1.1.1.2.2. QUADRUPOLES
- WBS 1.1.1.2.4. CORRECTION DIPOLES
- WBS 1.1.1.2.5. INJECTION LAMBERTSON

WBS 1.1.1.3. 150 GEV PROTON MAGNETS

- WBS 1.1.1.3.1. DIPOLES
- WBS 1.1.1.3.2. QUADRUPOLES
- WBS 1.1.1.3.4. CORRECTION DIPOLES
- WBS 1.1.1.3.5. EXTRACTION MAGNETS

WBS 1.1.1.4 150 GEV ANTIPROTON MAGNETS

- WBS 1.1.1.4.1. DIPOLES
- WBS 1.1.1.4.2. QUADRUPOLES
- WBS 1.1.1.4.4. CORRECTION DIPOLES
- WBS 1.1.1.4.5. EXTRACTION MAGNETS

WBS 1.1.1.5 120 GEV (F0-F17) MAGNETS

- WBS 1.1.1.5.1. DIPOLES
- WBS 1.1.1.5.2. QUADRUPOLES
- WBS 1.1.1.5.4. CORRECTION DIPOLES

WBS 1.1.1.6 SLOW SPILL (F18-A0) MAGNETS

- WBS 1.1.1.6.1. DIPOLES
- WBS 1.1.1.6.2. QUADRUPOLES
- WBS 1.1.1.6.4. CORRECTION DIPOLES

WBS 1.1.1.8 ABORT MAGNETS

- WBS 1.1.1.8.1. DIPOLES
- WBS 1.1.1.8.2. QUADRUPOLES
- WBS 1.1.1.8.4. CORRECTION DIPOLES
- WBS 1.1.1.8.5. EXTRACTION MAGNETS

CHAPTER 3.1. MAGNETS

WBS 1.1.1. MAGNETS

WBS 1.1.1 includes all DC and ramped magnets. Pulsed magnets (kickers and septum magnets) are included in 1.1.6. The fourth level WBS under magnets indicates the area in which they are used. Table 3.1-1 lists these areas. The fifth level of the WBS indicates the class of magnet. The sixth level indicates the specific magnet design. Table 3.1-2 lists the classes and individual magnet designs. Gaps exist in the WBS numbers due to deletion or movement of items from previous versions. The total count of magnets of each type in each area is given in Table 3.1-3, including an approximate estimate of the number of spares of each type required. However, due to the varying configurations required, additional spares of some magnets will almost certainly be required. This is particular true for the BQB quadrupoles recycled from the Main Ring, which are used in a variety of locations, requiring different supports, beamtubes, etc.

The rapid cycle rate of the FMI dictates using conventional steel and copper magnets rather than superconducting magnets. Where possible existing magnets from the Main Ring are reused. Where reusing magnets is not practical, new magnets are built, either to existing designs or to new designs.

Table 3.1-1: Fermilab Main Injector Areas for Magnet WBS 1.1.1

-
-
- 1.1.1.1... FMI ring
 - 1.1.1.2... 8 GeV line from the Booster to the FMI ring
 - 1.1.1.3... 150 GeV proton line from the FMI ring to the Tevatron (also carries 120 GeV proton from the FMI ring to the Main Ring Remnant and 8 GeV anti-protons from the Remnant to the FMI ring)
 - 1.1.1.4... 150 GeV antiproton line from FMI ring to the Tevatron
 - 1.1.1.5... 120 GeV proton line, Main Ring Remnant from F0 to F17
 - 1.1.1.6... Slow spill line, 120 GeV protons in Main Ring Remnant from F17 to Switchyard
 - 1.1.1.8... Abort line
 - 1.1.1.10... Magnet tooling
-
-

Table 3.1-2: Fermilab Main Injector Magnets by Type

1.1.1.x.1 Main Dipoles

1.1.1.x.1.1	IDA dipole 240"	[new design]
1.1.1.x.1.2	IDB dipole 240"	[new design]
1.1.1.x.1.3	IDC dipole 160"	[new design]
1.1.1.x.1.4	IDC dipole 160"	[new design]
1.1.1.x.1.7	BDM (240" B2)	[rework old]
1.1.1.x.1.10	2XB2 (240")	[left in place]
1.1.1.x.1.12	EPB 5-1.5-120	[rework old]]
1.1.1.x.1.13	ODM (240" B3)	[rework old]
1.1.1.x.1.14	BDM (240" B1/B2)	[left in place]

1.1.1.x.2 Quadrupoles

1.1.1.x.2.3	IQC (100.13" MI)	[new design]
1.1.1.x.2.4	IQD (116.26" MI)	[new design]
1.1.1.x.2.5	BQB (84" MR)	[rework old]
1.1.1.x.2.6	BQA (52" MR)	[rework old]
1.1.1.x.2.7	SQA (17" P-Bar)	[rework old]
1.1.1.x.2.8	BQA (52" MR)	[rework old]
1.1.1.x.2.9	BQB, rolled	[rework old]
1.1.1.x.2.10	BQB (in place)	[left in place]
1.1.1.x.2.11	BQA (in place)	[left in place]
1.1.1.x.2.12	3Q120	[more existing]
1.1.1.x.2.13	3Q60	[more existing]

1.1.1.x.3 High Order Correction Elements

1.1.1.x.3.1	ISA (sextupoles)	[new design]
1.1.1.x.3.2	MR trim quads	[rework old]
1.1.1.x.3.3	MR skew quads	[rework old]
1.1.1.x.3.4	MR skew sext	[rework old]
1.1.1.x.3.5	MR trim sext	[rework old]
1.1.1.x.3.6	MR octupoles	[rework old]

1.1.1.x.4 Dipoles Trim Steering Magnets

1.1.1.x.4.1	HDC MR horz trim	[rework old]
1.1.1.x.4.2	IDH MI horz trim	[new design]
1.1.1.x.4.3	VDC MR vert trim	[rework old]
1.1.1.x.4.4	IDV MI vert trim	[new design]

1.1.1.x.5 Injection and Extraction Lambertson and C Magnets

1.1.1.x.5.1	Lambertson,A0	[rework old]
1.1.1.x.5.2	Lambertson,MI, 94"	[new design]
1.1.1.x.5.3	Lambertson,MI,189"	[new design]
1.1.1.x.5.5	C-magnet, MI, 118"	[new design]

WBS 1.1.1.1.

MAIN INJECTOR RING MAGNETS

WBS 1.1.1.1.1.

RING DIPOLES

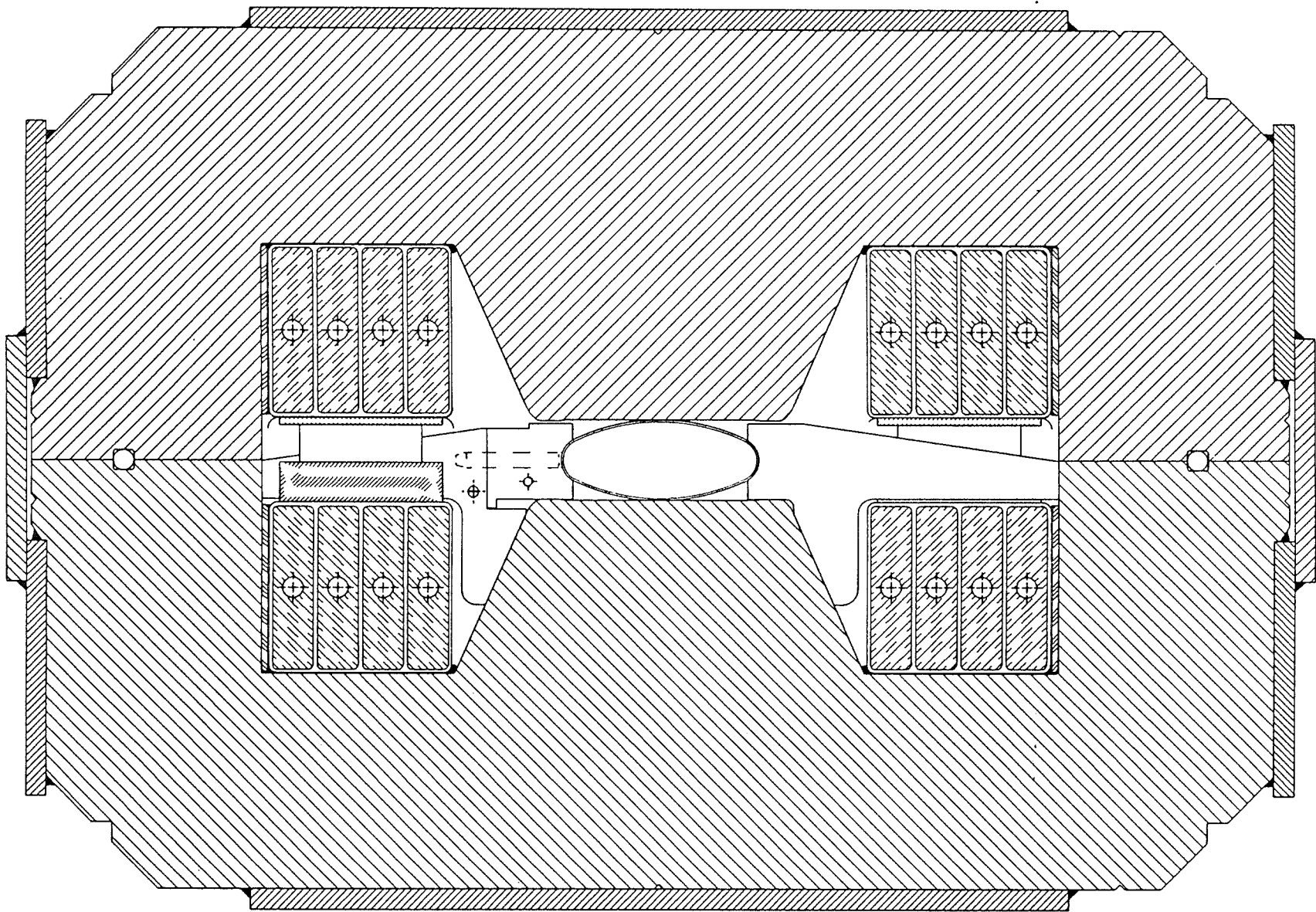
The FMI ring uses newly designed dipole magnets of two lengths, 6.096 meters and 4.064 meters, as described in Section 2.1. To facilitate the electrical connections in the tunnel, two styles of each length magnet are used, having the jumper between top and bottom coils at opposite ends of the magnet. The 6-m dipoles are designated type A and type B and are referred to as IDA and IDB magnets. The 4-m dipoles are types C and D and are referred to as IDC and IDD magnets. The configuration of two 6-m dipoles together in one half-cell is shown in Figure 3.1-1.

Dipole Design

A new dipole design for the FMI ring is needed for several reasons. First, the existing Main Ring magnets are straight. Reusing these magnets in the FMI would result in a loss of about 16 mm of aperture due to the sagitta of the beam path. This aperture is recovered by constructing curved magnets. Second, the existing magnets suffer from reliability problems. Most of the failures in the existing magnets occur at conductor joints within the coil. The number of such joints per magnet is reduced in the new magnet and the reliability of the joints is increased through improved construction techniques. Third, higher field quality can be achieved in a newly constructed magnet, so that the dynamic aperture is only limited by the magnet physical aperture - a situation not achieved in the existing Main Ring.

A cost optimization has been performed to minimize the sum of construction plus operating costs over five years. The result is a magnet with twice as much conductor and half as many turns as the existing Main Ring B2 magnet. The dipole magnet cross section is shown in Figure 3.1-2. The basic parameters of the dipoles are listed in Table 3.1-4. The core is constructed from 1.52 mm (0.0598") thick laminations which are split on the magnet midplane. The coil consists of four turns per pole of a 25.4 mm x 101.6 mm (1" x 4") copper conductor. Since no conductor is contained in the median plane of the magnet, the coil can be wound as two "pancakes" with no bends along the wide dimension of the conductor. This conductor is available in 6-m (20-ft) lengths, so each coil can be made with only eight internal joints. The water hole is 12.7 mm (0.5") in diameter. A single water circuit in each pancake (two circuits per magnet) provides sufficient cooling.

A four terminal design has been chosen for the dipole magnet. In a magnet of this design, the role of return bus is filled by one of the conductor turns within the magnet. This has the advantage of removing the need for approximately 3600 m (12,000 ft) of 2580 square mm (4 square inch) copper bus (@ \$130/m \$40/ft) in the FMI enclosure. The price paid for this benefit



FMI DIPOLE

TYPICAL CROSS SECTION

Figure 3.1-2. Cross-Section of the Main Injector Dipole Magnet.

**Table 3.1-3.
Main Injector Conventional Magnet Count**

		Ring	8 GeV	P150	A150	MR F0-F17	MR F17-SY	Abort	Total	Spares	NUMI
IDA dipole 240"	N	108	-	-	-	-	-	-	108	5	-
IDB dipole 240"	N	108	-	-	-	-	-	-	108	5	-
IDC dipole 160"	N	64	-	-	-	-	-	-	64	4	-
IDD dipole 160"	N	64	-	-	-	-	-	-	64	4	-
BDM (240" B1/B2)	E	-	-	15	15	15	101	2	148	6	4
DDM (240" 2XB2)	E	-	-	-	-	-	1	-	1	1	-
EPB 5-1.5-120	E	-	4	-	-	-	-	-	4	1	13
ODM (240" B3)	E	-	-	-	-	8	2	-	10	2	-
IQC (100.13" MI)	N	32	-	-	-	-	-	-	32	3	-
IQD (116.26" MI)	N	48	-	-	-	-	-	-	48	4	-
BQB (84" MR)	E	127	-	7	7	5	26	2	174	7	-
BQB, rolled	E	1	-	-	-	-	-	-	1	1	-
BQA (52" MR)	E	-	-	-	-	-	4	1	5	1	-
SQA (17" P-Bar)	E	-	10	-	-	-	-	-	10	2*	-
SQC (26" P-Bar)	E	-	4	-	-	-	-	-	4	2*	-
SQF (48" P-Bar)			2						2	1	
3Q120	N	-	-	7	7	1	-	-	15	2	3
3Q60	N	-	-	2	2	1	-	-	5	2	7
ISA (sextupoles)	N	108	-	-	-	-	-	-	108	5	-
MR trim quads	E	16	-	-	-	-	-	-	16	2	-
MR skew quads	E	16	-	-	-	-	-	-	16	2	-
MR octupoles	E	66	-	-	-	-	-	-	66	4	-
IDH MI horz trim	N	104	-	-	-	-	-	-	104	15	-
IDV MI vert trim	N	104	-	-	-	-	-	-	104	5	-
HDC MR horz trim	E	-	14	7	7	4	14	2	48	4	4
VDC MR vert trim	E	-	4	14	14	4	14	2	52	4	4
Rolled MR horz trim	N	-	7	-	-	-	-	-	7	2	-
Lambertson,A0	E	-	1	-	-	-	-	-	1	1	-
Lambertson,MI, 110"	N	-	-	5	5	-	-	3	13	3	3
C-magnet, MI, 131"	N	-	-	5	5	-	-	1	11	2	1
Totals:		966	46	62	62	38	162	13	1349	98	39

SPARES = INT(((SQRT(NUMBER))/2+.8) N = New Magnets E = Existing Magnets
 One additional Lambertson, one 3Q60, and 10 horizontal trim dipole spares provided
 * Spare SQA and SQC quadrupoles are shared with Antiproton Source Dept.
 Temporarily, we will use one of the spare SQCs, later to be replaced by an SQA
 NUMI magnets are not part of FMI project; provided for reference only

is the requirement that the insulation be sufficient to withstand 2,000 volts between conductors within the coil. The maximum voltage to ground, for either a two-terminal or a four-terminal design, is approximately 1,000 volts.

Development and procurement strategy

Development and construction of the dipoles is being done in three stages. First two prototype magnets were built, sequentially, and studied. Then ten preproduction "R&D" dipoles were built and studied. And finally full scale production of the dipoles began.

Prototype dipoles

After the initial design was complete, a development program proceeded. The first prototype dipole was built at Fermilab, with delivery to the Magnet Test Facility in September 1990. The end packs were removable to allow modifications during the studies. The coil was insulated with a B-stage epoxy tape, not the vacuum impregnation planned for production.

Table 3.1-4
Properties of Main Injector Ring Dipoles

	IDA/IDB	IDC/IDD
Length (meters)	6.096	4.064
Strength (Tesla)	1.72	1.72
Gap (mm)	50.8	50.8
Turns/pole	4	4
Conductor Dimensions (in x in)	1.00 x 4.00	1.00 x 4.00
Conductor Hole Diameter	0.500	0.500
Peak Current (A)	9375	9375
RMS Current (A)	4987	4987
Coil Resistance (mΩ)	0.8	0.6
Coil Inductance (mH)	2.0	1.3
Peak Power (kW)	69.8	53.0
RMS Power (kW)	19.8	15.0
Number Used	216	128
Weight (kG)	17000	12000
Sagitta (mm)	16	7

This first prototype magnet demonstrated that the design of the body field (determined by the lamination shape) had been met. The end field studies began. The sextupole and decapole fields induced by eddy currents in a beam pipe during ramping were measured.

With confidence in the lamination design, a second die was ordered to meet the anticipated production requirements. Fermilab built a second prototype dipole using these laminations. The end packs were again removable. Design refinements in the coil leads were incorporated. The coil was vacuum impregnated. The second prototype validated the second die and the fabrication techniques. End field studies intensified, culminating in January, 1993, with a design that meets the field requirements of the accelerator.

R&D dipoles

Ten dipoles were then built to the production design, including integrated end packs. Of these six were 6-meter and four were 4-meter. The first R&D dipole was completed in August, 1993. This phase of the project had four primary goals: to refine the fabrication process in preparation for production, to identify and qualify vendors for the major subassemblies, to give the vendors experience so that they could make accurate production cost proposals, and to accumulate some limited data about the magnet-to-magnet variations to expect in production. These goals have been met and the R&D project was declared complete at the end of January, 1994.

A secondary goal was to fabricate twelve dipoles ready for use in the ring. Ten of the magnets were built and tested. One of the coil insulation subcontractors was unable to complete its task, so the coils for the other two magnets were left ready to be insulated and assembled as part of the production run.

Production

Finally, with confidence in the design, the fabrication process, and the subcontractors, production of the balance of the dipoles for the project began. The total quantity to be built will include the number required for the Main Injector ring plus spares, reduced by the number (ten) built during the R&D phase. The first production dipole was assembled in August, 1994.

After an initial ramp up period, dipole production is planned to run at a steady rate of ten magnets per month. The rate and the starting date were determined primarily by the anticipated funding profile and the need for a uniform rate. The rate could be increased substantially if additional funds were available earlier.

Procurement strategy and experience

Fermilab proposed an Advanced Procurement Plan for the Main Injector dipoles in April, 1992. This was presented to a DOE Business Strategy Group (BSG) in May, 1992. Major sub-assemblies will be constructed by industrial subcontractors. Fermilab will do the final assembly of the components on-site. The BSG and DOE officials basically concurred with the proposal, while recommending some improvements. This plan, summarized here, is being followed.

The main change recommended by the BSG was to use the Source Evaluation Board (SEB) method for some critical subassemblies. In this procedure the offerors submit technical and cost proposals. These are evaluated independently against previously established and stated criteria. The SEB then recommends a vendor based on the best value to the project [1].

The key to the plan is that the major subassemblies of the magnets are being fabricated by industry but the final assembly is being done at Fermilab. The major subassemblies are the steel for the laminations, laminations themselves, the stacked half cores, the bare coils, the insulated coils, and the beam tubes. The subassemblies are being procured using fixed-price, build-to-print subcontracts. This plan maximizes the participation of industry, a DOE goal, while allowing Fermilab to keep tight control on the quality. This will minimize both risk and cost. The subcontractors will each perform tasks for which they are well-qualified.

The steel for the R&D dipoles was purchased through a competitive bid to which only one firm (Armco) responded. The low response was believed to be due to the tight magnetic requirements and the limited quantity of the order. For the production order Fermilab actively solicited additional vendors and received five bids. As part of the qualification process vendors were required to produce a full coil of steel meeting the magnetic requirements of the dipole. The steel supplier for the dipoles is LTV Steel, of Cleveland, Ohio.

The dipole lamination dies were procured with a competitive bid during the prototype phase. The stamping for the R&D dipoles was done by the vendor who built the dies, through the exercising of an option on the original order. The production subcontract was awarded in a competitive bid, with a technical score combined with the price to determine the selection. The lamination stamper is Electro-Metal Products of Skokie, Illinois.

The half core stacking is a process less familiar to industry, so a more elaborate selection procedure was used. Fermilab stacked three sets each of the 6-m and 4-m half cores. This gave us more experience with this geometry and let us identify some problems before the vendors did. Separate proposals were solicited from prospective offerors for three sets of 4-m cores and three sets of 6-m cores. Two vendors were selected using the SEB method, one for the 4-m cores and

one for the 6-m cores. These vendors fabricated the half cores for the remaining R&D dipoles. In the process they demonstrated to us that they were competent to do the job and they learned exactly what would be required to do the job. After the R&D subcontracts were completed, we held a limited competition between the two prequalified vendors for the production run. With great confidence in the two vendors and a well-tuned specification, we felt comfortable with a straight price competition. The vendors, with experience in fabricating the half cores, could submit bids that would assure themselves a fair profit without undue amounts for contingency to raise the price. SVF of Rock Falls, Illinois, is stacking the half cores.

The bare coil forming subcontract was also an SEB action. We used one solicitation, a base order for the coils needed in the R&D program with options for the production quantities. Everson Electric Company, of Bethlehem, Pennsylvania, is fabricating the bare coils. The bare coil vendor is responsible for the procurement of the copper bars and other parts required in the fabrication.

The insulation of the bare coils was deemed sufficiently risky that we used the SEB process to select three vendors to work on three R&D coils sets each (two coils per coil set). One of these made only three acceptable coils out of six and was dropped from the qualified list. Again a straight price limited competition was held between the two successful insulators. We felt that it would be advantageous to have two sources for coil insulation and agreed that we were willing to pay a premium over the price of having one vendor do the whole job. We asked for proposals on 1/3, 2/3, and the whole job. It turned out that dividing the job would cost more than the agreed premium, so the whole job has gone to one firm, Tesla Engineering of Storrington, Sussex, England.

We have also purchased bare beam tube from two firms, allowing them to develop the tooling and processes necessary to meet the Main Injector requirements. At an appropriate time a limited competition between the two vendors will lead to purchase of the bare beam tube material. The fabrication and attaching of the end components (bellows, flanges, pump-out ports) will be done by another vendor. The dipole magnets will be assembled without their beam tubes to facilitate magnetic measurements. The tubes will be inserted into the magnets and the last flange welded on shortly before the magnets are installed in the tunnel. The tubes will not be subject to damage or contamination during storage and handling until then. This has the added advantage of deferring the cost of the tubes. Further discussion of the beamtubes can be found in Chapter 3.2.

The quality of each of these components is critical and can be monitored, as discussed below. After they are assembled the monitoring is much more difficult. The final assembly of

these components into a complete dipole is estimated at 257 worker-hours. This comprises approximately 10% of the September, 1993 cost estimate for the dipoles.

The subassemblies will be received, inspected, stored, and assembled in Industrial Center Building. The building has adequate floor space, crane capacity, and vehicular access for staging the subassemblies and doing the final assembly. The complete magnets will be moved to the adjacent Magnet Test Facility (MTF) for final testing. Storage for complete, measured magnets will be available in the Main Injector service buildings and tunnels by the time that it is needed.

The procurement schedule is shown in Figure 3.1-3. The acquisition will require multi-year funding. This is being accomplished by writing contracts with options which can be exercised in the out years. The ability to exercise those options in a timely fashion is imperative.

Design issues - body field quality

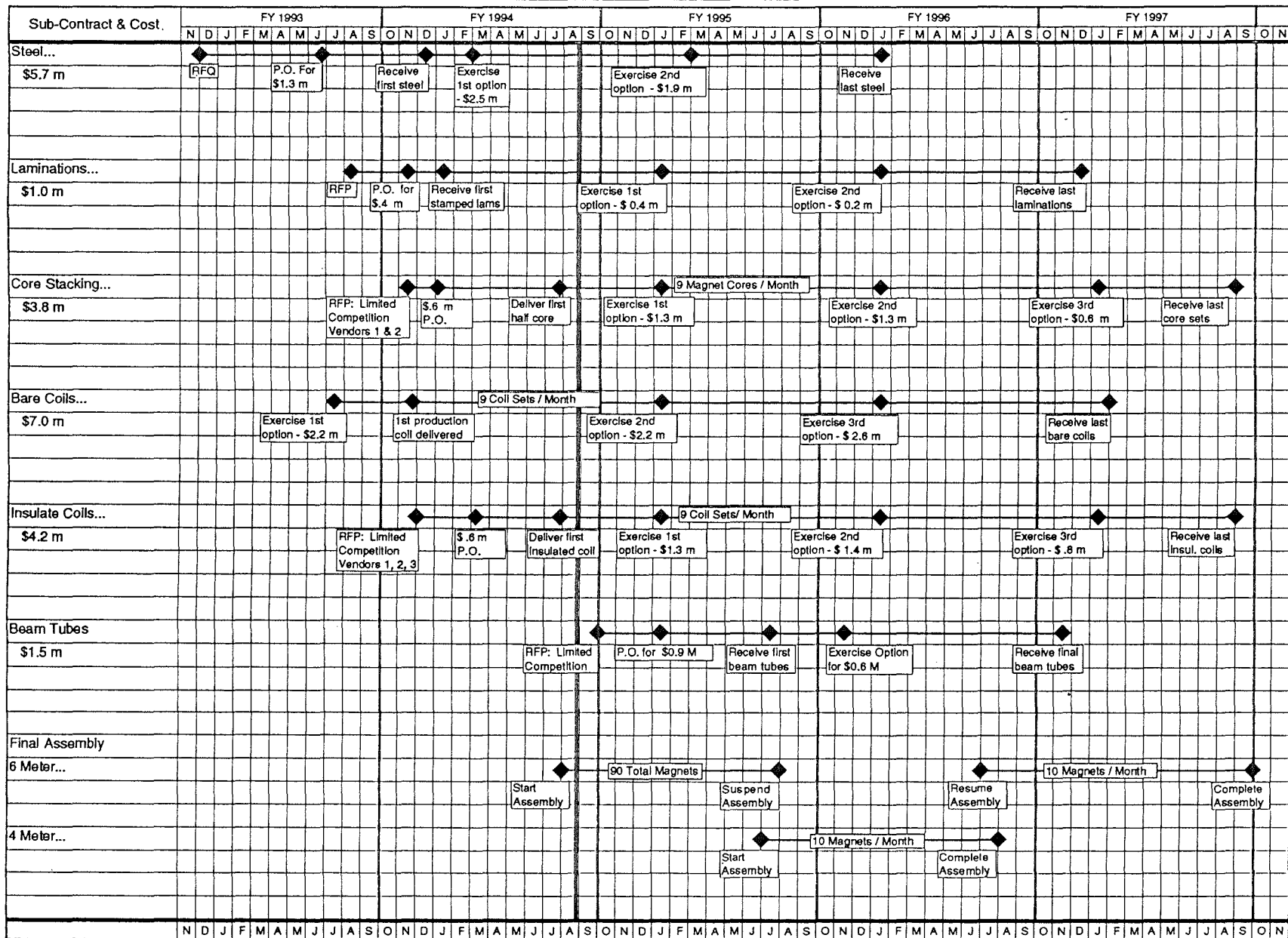
We ask that the integrated magnetic field be uniform to 1×10^{-4} over the region occupied by the beam. Any deviations should be predominantly a sextupole field. This means that the horizontal chromaticity-correcting sextupoles can completely correct for these deviations. The dipole field shape at four excitations, corresponding to injection, transition, 120 GeV, and 150 GeV, are shown in Figure 3.1-4. In Figure 3.1-4(a), the uncorrected data is shown. In Figure 3.1-4(b), the measured sextupole component and quadrupole (which results from feeddown from the sextupole due to probe misalignment) has been subtracted out from the two higher-energy data sets. We define the beam size to be the convolution of a transverse emittance of 40π mm-mr (95% normalized emittance), and a longitudinal emittance of 0.4 eVs. As discussed in Chapter 2, this is the largest beam envisioned for the Main Injector, and fully twice (both transverse and longitudinal) the emittances anticipated.

At injection energy the field shape is dominated by the lamination shape. The lamination shape is designed to provide a field at the injection energy which varies by no more than 1×10^{-4} over the range $-44 \text{ mm} < x < +44 \text{ mm}$. The beam will cover a region of $-17 \text{ mm} < x < +17 \text{ mm}$. The additional good field will allow steering to optimize the injection efficiency.

At transition the field shape from the magnet is still dominated by the lamination shape. Although the required good field region grows to $-19 \text{ mm} < x < +19 \text{ mm}$ at transition, the steel shape continues to provide a good field over $-43 \text{ mm} < x < +43 \text{ mm}$.

At the 120 GeV energy used for antiproton production and slow spill some saturation has started to set in on the edges of the pole face. The 1×10^{-4} tolerance still holds over the region $-37 \text{ mm} < x < +37 \text{ mm}$. Slow extraction requires approximately the same aperture as at injection,

Milestones for Main Injector Dipole Magnets



Nancy Theis August 22, 1994

Figure 3.1-3. Dipole Procurement Schedule

Costs shown in 1991 \$

Field Shape from Flatcoil Measurement

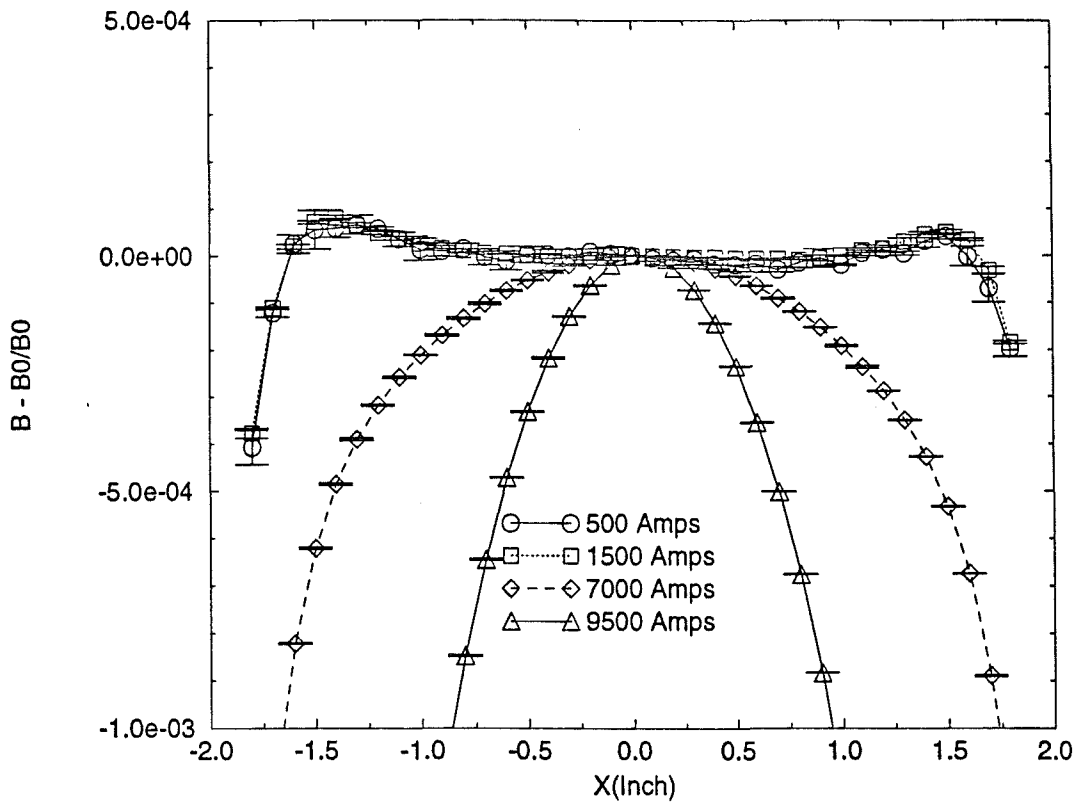


Figure 3.1-4(a). Measured Field Shape at Injection, Transition, 120 and 150 GeV. (Uncorrected Data.)

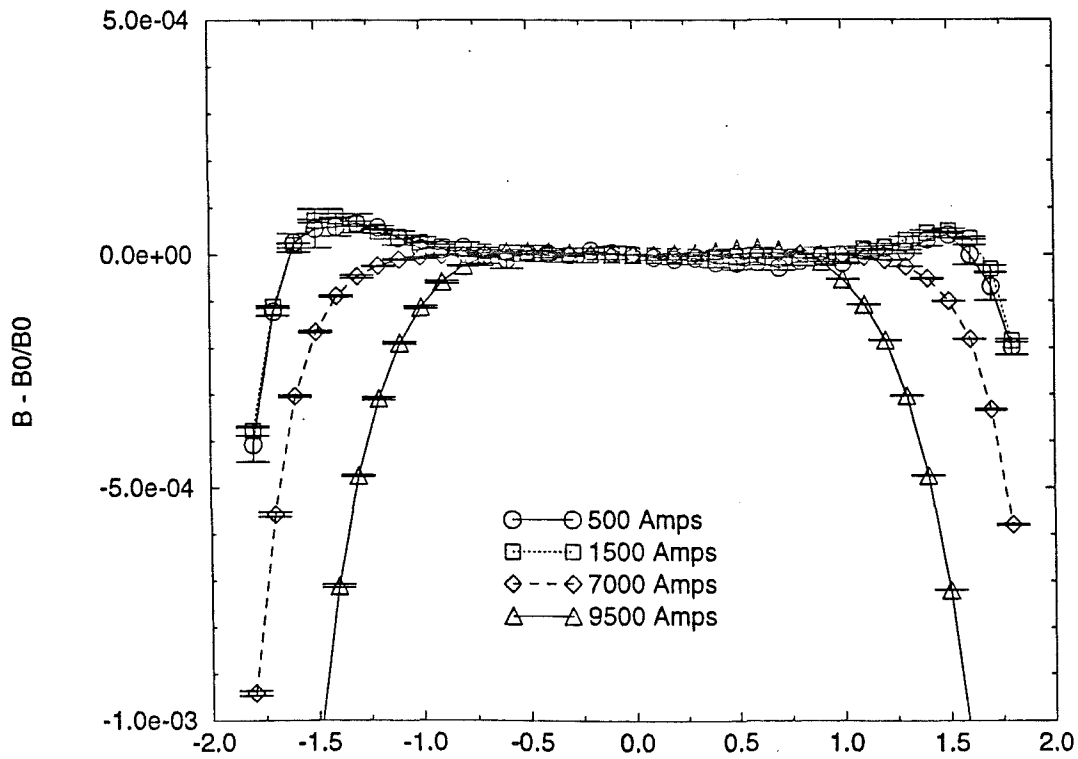


Figure 3.1-4(b). Field Shapes with Quadrupole and Sextupole Components Subtracted from 120 and 150 GeV Data.

-16 mm < x < +16 mm, while the single-turn extraction for antiproton production requires only -4 mm < x < +4 mm.

The beam size at 150 GeV has shrunk to 8 mm (95% full width), so the shrinkage of the 1×10^{-4} region to -25 mm < x < +25 mm is perfectly acceptable. If the sextupole term is not subtracted from the dipole field, the 1×10^{-4} region is only about ± 8 mm. The required strength of the sextupole corrector magnets is dominated by the the desire to control the chromaticity at full energy.

Table 3.1-5 summarizes the good field aperture acheived and required as a function of energy and for various assumptions of beam emittance. For 120 GeV slow spill, the aperture requirements are independent of the beam emittance.

Table 3.1-5
Good Field Aperture and Good Field Requirements (in mm)

	<u>Good Field Width</u>		<u>Good Field Requirement</u>			
	With Sext.	No Sext.	20 π , .2 eVs	20 π , .4 eVs	40 π , .2 eVs	40 π , .4 eVs
Injection	**	± 44	± 12	± 13	± 17	± 17
Transition	**	± 43	± 14	± 17	± 16	± 19
120 GeV	± 19	± 37	± 16	± 16	± 16	± 16
150 GeV	± 6	± 25	± 3	± 3	± 4	± 4

** At injection and transition, there is almost no sextupole term in the DC harmonics. At transition, however, the eddy currents dominate the field harmonics, with a large sextupole term contributing most. This will be corrected with the chromaticity-controlling sextupole magnets.

To achieve the desired uniformity of the field in the aperture while minimizing the total size of the pole face, the pole has been tapered to control saturation in the lamination [2]. We use low coercivity steel (<1 Oe) to reduce the remanent field.

The laminations are punched in a two-step process, first a rough hit to to remove most of the material, then a fine punch that determines the shape. Removing the bulk of the material first relieves stress in the steel before the final shape is punched.

The body field of the two prototype dipoles has been measured using four systems: a narrow loop moved across the aperture ("flat coil"); a rotating coil positioned at three locations

across the aperture; a Hall probe; and an NMR probe. From each measurement the field $B_y(x)$ has been reconstructed. The field has been modeled using the programs Poisson and PE2D. Figure 3.1-5 shows the relative variation from the central field of the first prototype at the injection energy as calculated by PE2D, as measured with flat coil, and as measured with the rotating coil. Agreement is quite good.

R&D measurements

The 10 R&D dipoles were measured at the Magnet Test Facility (MTF) soon after their construction. The purpose of these measurements was to confirm that the magnet production techniques reproduced the results obtained in the prototype dipoles, to explore the range of values that we could expect to find in production, and to develop techniques and analyses for the production measurements. The main measurement techniques are described under production measurements. As planned for production, the integrated field strength and shape were measured with complementary techniques to validate and cross-calibrate the systems.

The total integrated strength as a function of current was measured using the flatcoil and pointscan techniques. The flatcoil measurements are consistent with the pointscan results. Figure 3.1-6 shows the integrated strength for all magnets relative to the long (6 m) magnet average, as measured by pointscan. The short (4 m) magnet strengths have been multiplied by a factor of 1.50. The graph shows that the relative strength of the short magnets is about 8 units greater than the long magnet strength. This corresponds to the short magnets being too long by about 2 to 3 lamination thicknesses. The length of the production 4-m dipoles will be adjusted to correct for this small difference.

The variation in the field integral as a function of position was measured at several currents using the flatcoil and rotating coil harmonics systems. These shapes agree with the prototype measurements.

The harmonic components of the field were also determined from the rotating coil harmonics (normal and skew) and flatcoil (normal only) systems. Since the coil planned for the production measurements was not yet available, an existing probe was used to measure the harmonics coefficients. It is a 2-m long bucked tangential rotating coil that has been in use for a number of years at MTF and has produced reliable measurements. The total integrated harmonics were obtained by positioning the probe at three or four longitudinal positions (for 4-m and 6-m magnets, respectively).

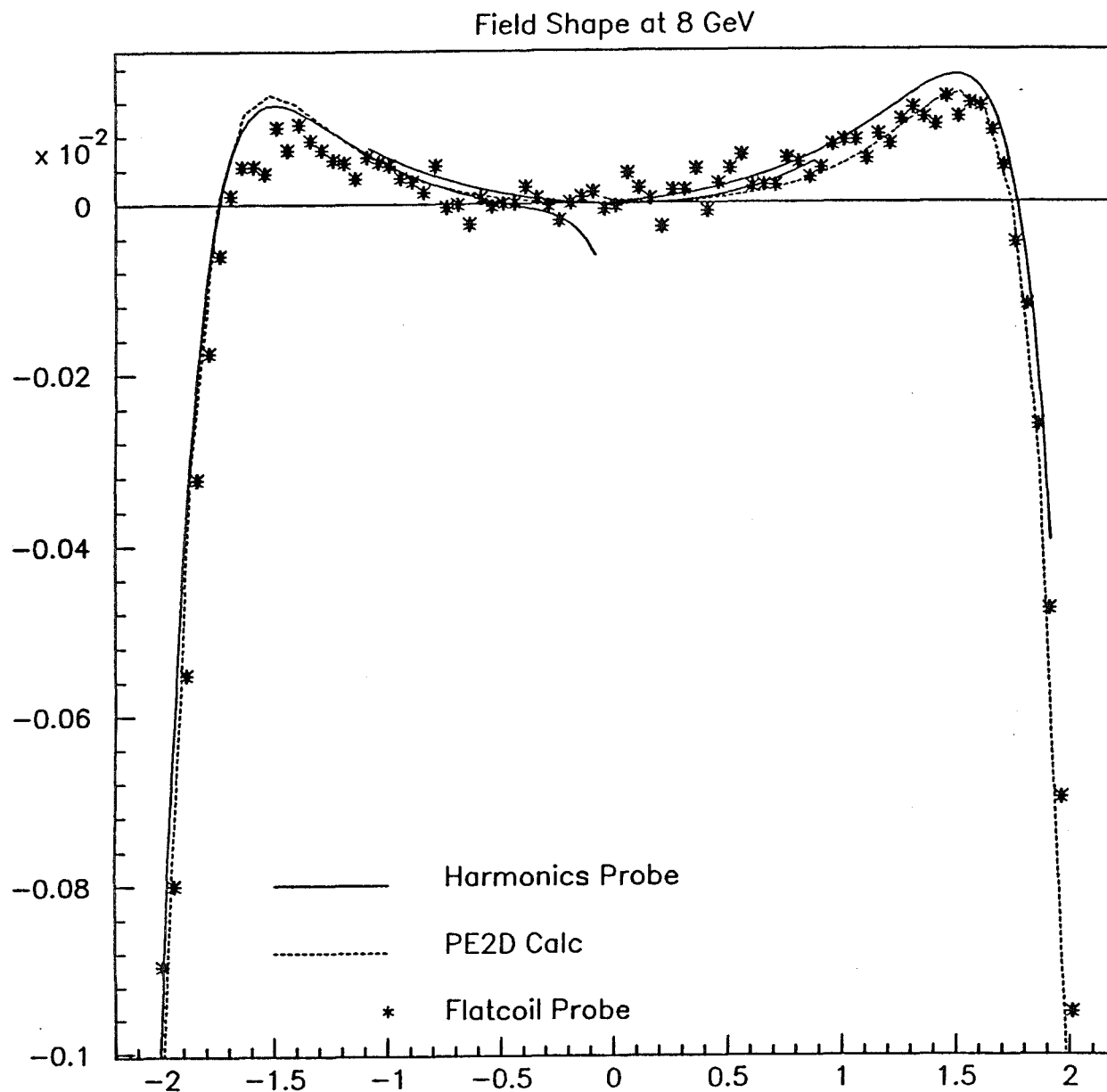


Figure 3.1-5. Comparison of Calculated and Measured Field Shape at Injection.

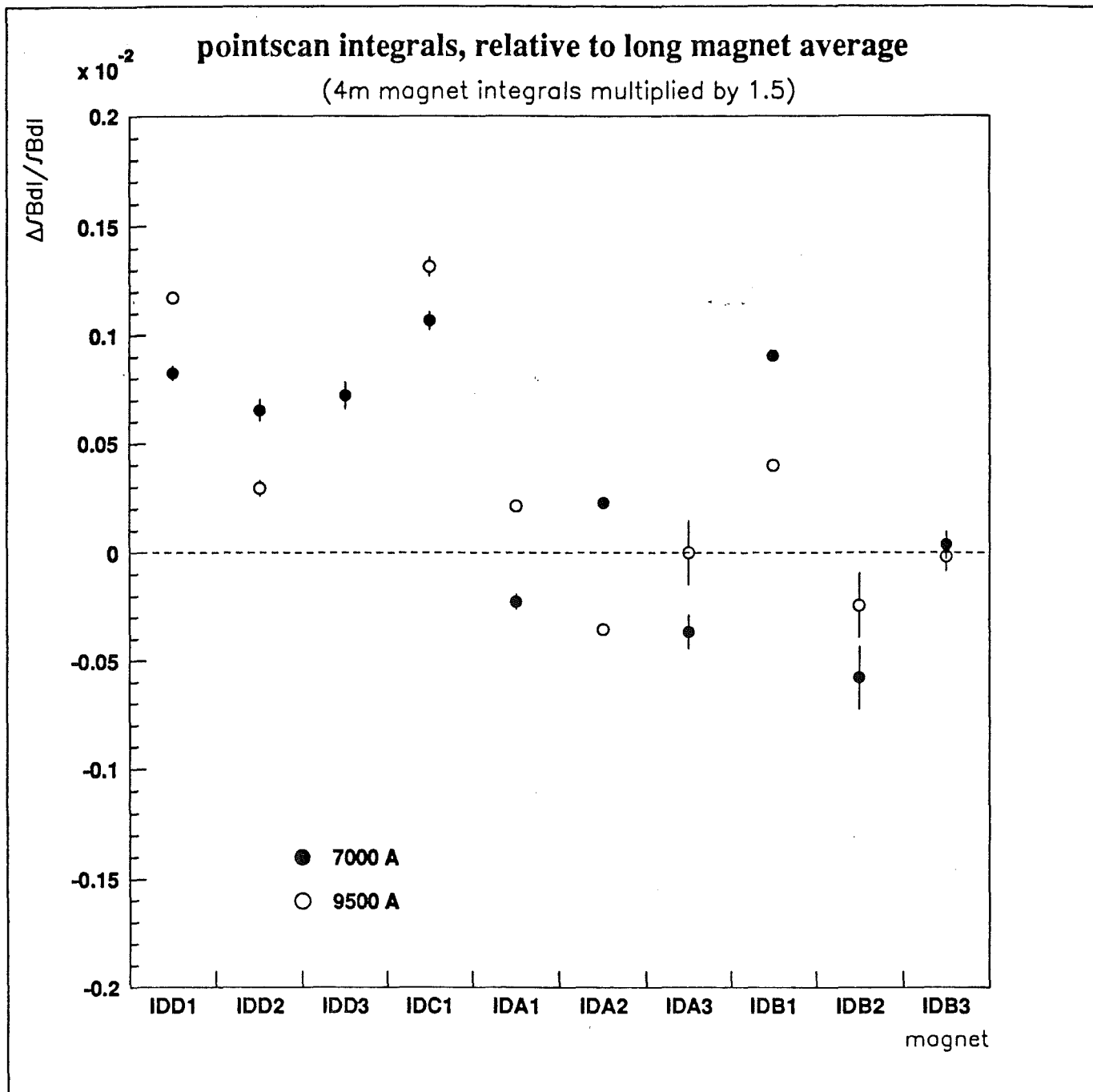


Figure 3.1-6. Point Scan Integrals for 10 R&D Dipoles

Figures 3.1-7(a) and 3.1-7(b) shows the variation of normal and skew quadrupole, sextupole, octupole, and decapole harmonic components in the R&D dipoles as a function of current. Figure 3.1-8 shows the distribution of the normal sextupole strength at three currents.

The longitudinal profile of the field was measured at several currents using the pointscan system. Figure 3.1-9 shows a typical body field longitudinal scan for one of the 6-m dipoles (IDB003) at 7000 A. The field shows excursions from the mean by as much as 20 units. Fourier analysis shows periodicities which have periods of about 16 inches, which may be correlated with manufacturing procedures in welding the half-cores together. However, none of this structure appears to have a significant impact on the performance of the magnets.

In addition to these three measurement systems, a small flatcoil probe was used for studying the endfields. This probe can be placed at various depths within the end of a dipole. Measurement of the flux as a function of probe depth allowed us to determine the contribution of the end to the effective length of the magnet, and also to measure the shape of the endfield compared to the body [3]. Only a limited sample of R&D dipoles (IDA003, IDB003, IDD001, IDD003) were subjected to endfield measurements. The endfield is discussed below.

Beam pipe eddy current sextupole

The ramping magnetic field induces eddy currents in the stainless steel beam pipe described in Chapter 3.2. These eddy currents produce magnetic fields that affect the beam. Symmetry allows only even terms in a multipole expansion: dipole, sextupole, decapole. The dipole term, predominantly from current flowing in the side walls of the beam pipe, merely requires a greater current to produce the desired magnetic field. The sextupole field, which is produced by infinite parallel plates, is significant but correctable. The decapole and higher fields are too small to be measurable or to have a significant effect.

The eddy current fields have been calculated for a simplified model of the Main Injector beam tube. The sextupole field has been measured for three ramp rates and two stainless steel alloys. Figure 3.1-10 shows the sextupole field as a function of time during a simplified, abbreviated ramp cycle for three conditions: no beam pipe, 330 beam pipe, and 316L beam pipe. The linear rise with current of the geometrical sextupole can be seen for the curve without beam pipe. The additional sextupole field, proportional to dB/dt , is seen adding to the geometrical term during the ramp for each of the cases with beam pipe. The eddy currents and the resulting field are smaller with the 330 stainless steel than with the 316L stainless due to the higher resistance of 330. The measurements and calculations agree to within 10%.

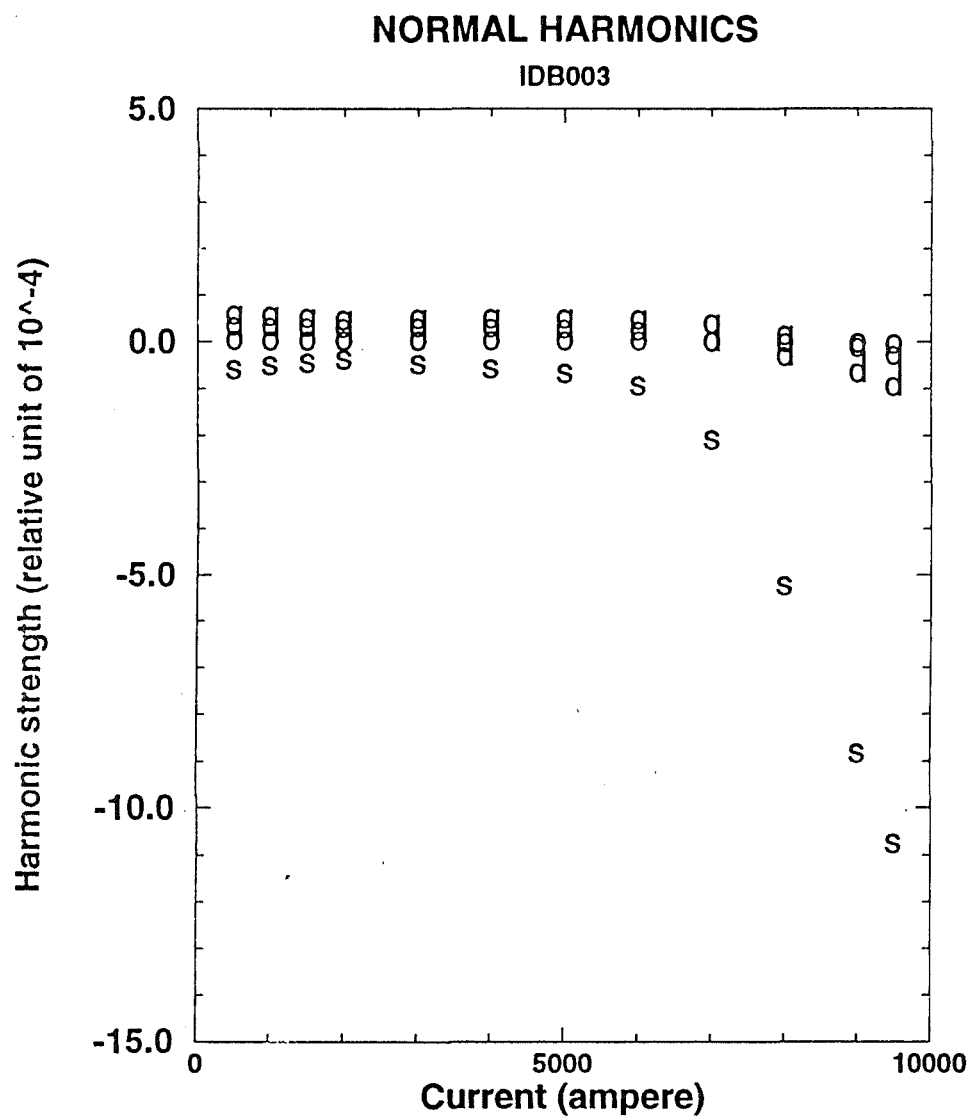


Figure 3.1-7(a). Variation of Normal Harmonic Components with Current

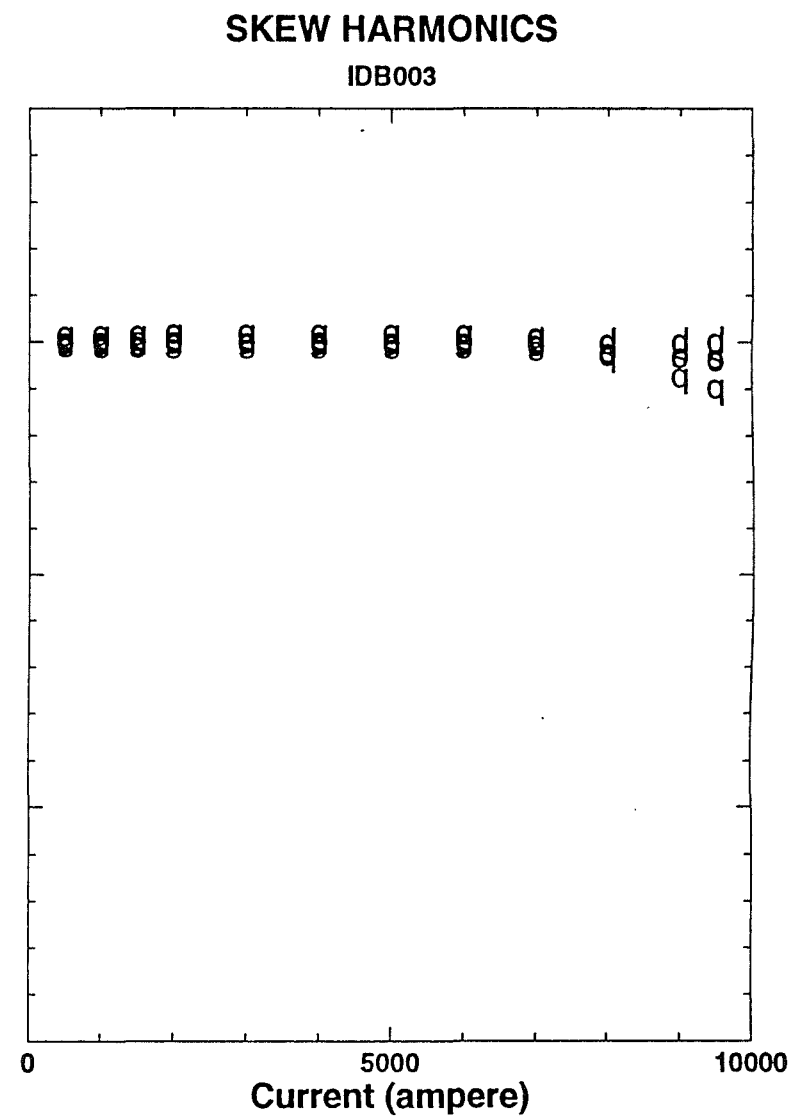


Figure 3.1-7(b). Variation of Skew Harmonic Components with Current

DISTRIBUTION OF SEXTUPOLE STRENGTH IN THE 10 RESEARCH DIPOLES

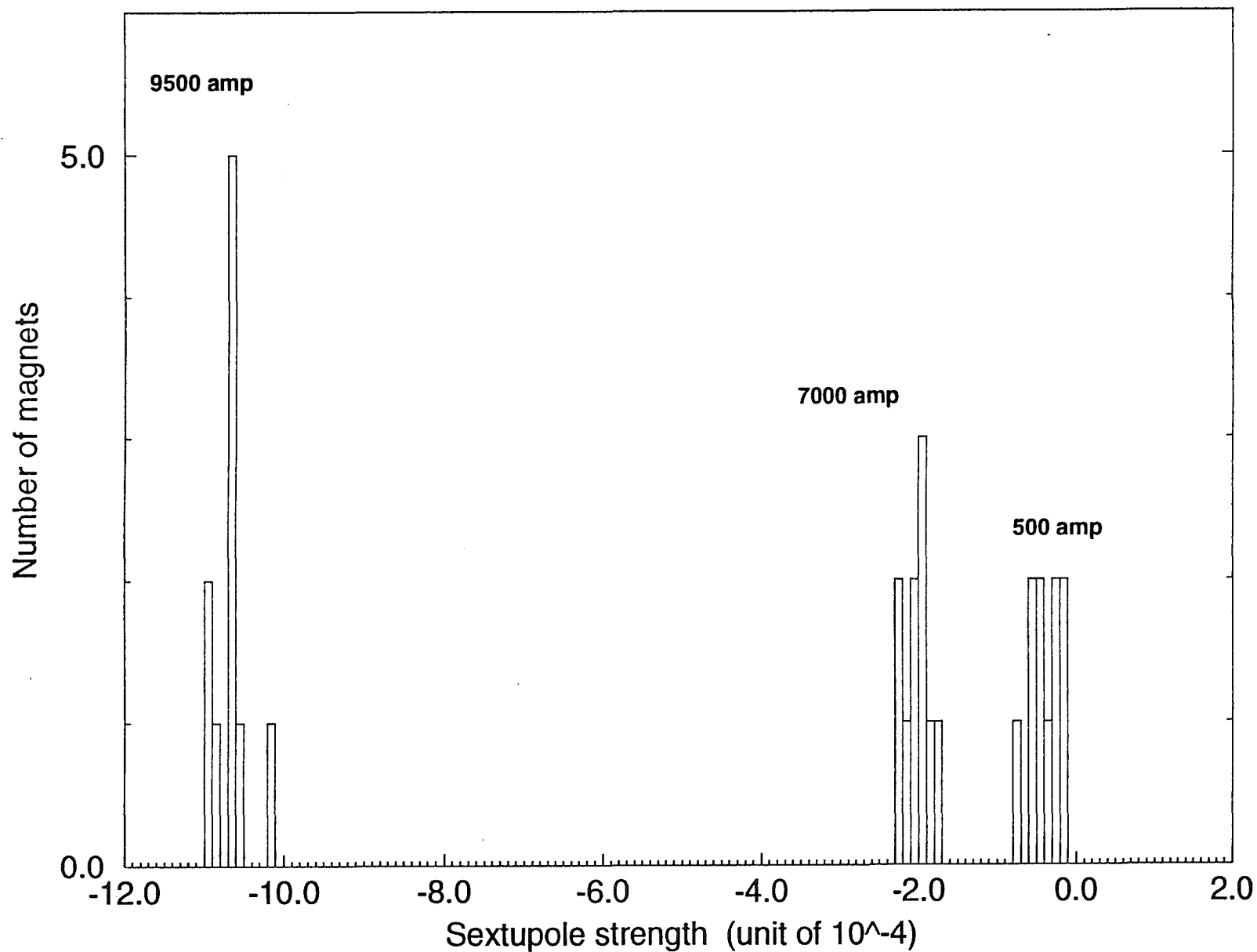


Figure 3.1-8. Distribution of Sextupole Strength at Three Currents for 10 R&D Dipoles

IDB003, longitudinal scan at 7000 A

body field scan $(B - \langle B \rangle) / \langle B \rangle$

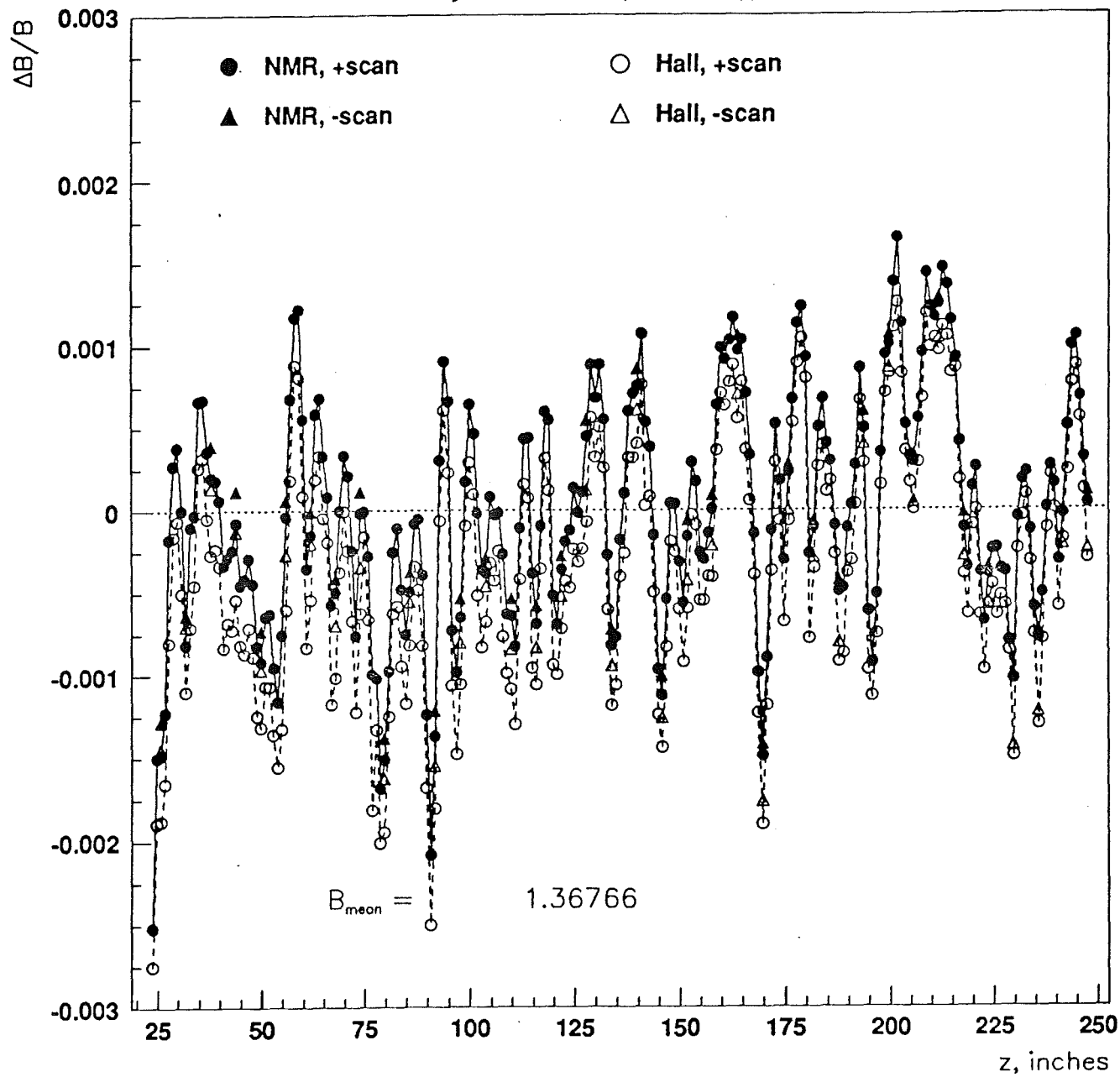


Figure 3.1-9. Body Field Scan at 7000 A.

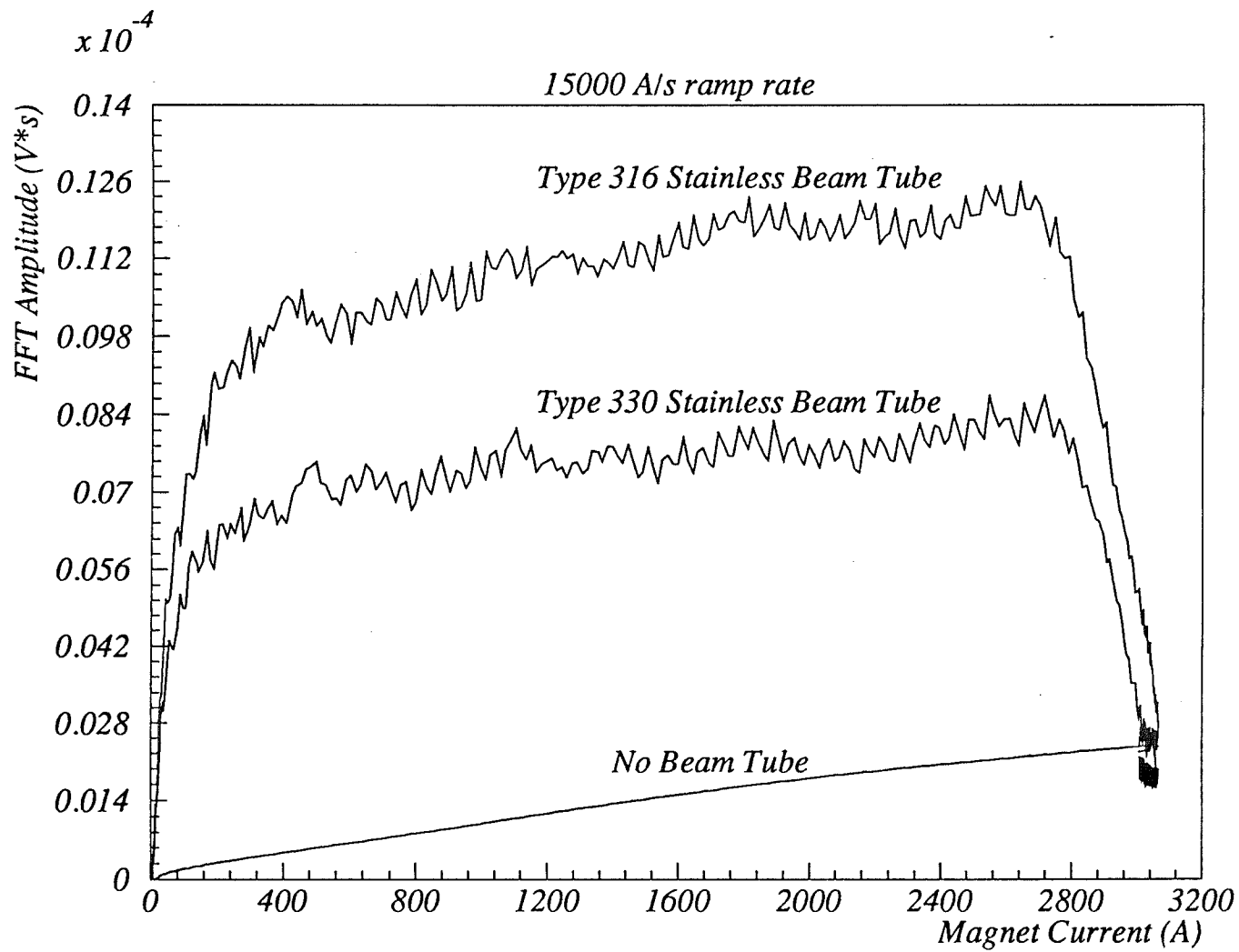


Figure 3.1-10. Sextupole Field for No Beam Pipe and for Beam Pipes made of 316L and 330 Stainless Steel.

The lower fields produced by the 330 stainless steel are attractive, but the higher cost, lesser availability, and worries about mating it to other vacuum components of a dissimilar stainless steel led to the choice of 316L for the beam pipe.

Insensitivity to copper location, defects, etc

In a steel and copper magnet the field is primarily determined by the steel geometry, not the copper. We have studied the effect of the transverse conductor placement in the dipole magnets [4] through computer modeling. Horizontal movement of the entire coil package by 0.75 mm and vertical movement of a single conductor by 5 mm produced calculable but trivial changes in the field strength and quality. Much greater motion would be required before there would be a concern. Setting the tolerances on positioning the coils in the half cores is thus purely a mechanical issue. We note also that a 10 mm deep cut in the top surface of one conductor would shift the center of the current distribution for the whole coil less than the 5 mm shift resulting from moving the whole conductor 5 mm. A variation in the resistance of the copper over a limited range would have a smaller effect.

Eddy currents in laminations

Halbach has discussed [5] a phenomenon which makes the field quality of a magnet dependent on the excitation ramping rate. Basically, eddy currents induced in the core render the magnetic field distribution spatially nonuniform. As a result, different portions of core are subjected to different excitation patterns; this affects the residual magnetization distribution and, consequently, the field uniformity at injection. An important observation made by Halbach is that particular attention should be paid to the down ramp since it is the eddy currents induced during the down ramp that determine the final magnetic state of different regions of the core. If the ramp rate is sufficiently high or if the eddy current decay time constant is large enough, a substantial fraction of core may be driven into the third quadrant of the B(H) curve by the eddy currents, causing the residual magnetization to be in the direction opposite to the expected one. Using a simple model, Halbach shows that the field distribution in the midplane of a H-magnet is approximately

$$B(\epsilon, t) = B(t) + \dot{B} \cdot \tau \cdot (3\epsilon^2 - 1) / 6$$

where ϵ is the normalized horizontal distance x/w , where w is the width of the backleg. The time constant τ depends on the conductivity of the steel σ and the lamination thickness t :

$$\tau = t^2 \sigma \mu_0 \mu / 4$$

For the Main Injector, using $\dot{B} = 1.8 \text{ T} / 0.4 \text{ s} = 4.5 \text{ T/s}$, $t = 1.5 \text{ mm}$ and $\mu/\mu_0 = 10000$, one gets $\tau \sim 0.05 \text{ s}$. The maximum deviation of the field with respect to its average (or DC) value is

$$\Delta B = \dot{B} \cdot \tau/3 = 0.06 \text{ T}$$

The utility of Halbach's model is to determine if the eddy currents can cause enough field non-uniformity to cause a degradation in field quality. For the Main Injector dipole magnets, the principal effect of residual magnetization is a small change in the field strength. Measurements have shown that the residual field is of the order of 10 Gauss. The effect described by Halbach might result in a small variation or even an inversion of the direction of this field. More troublesome is the possibility that the spatial nonuniformity caused by eddy currents might result in a degradation of the field homogeneity. In the first approximation, for an H-magnet such as the MI dipole magnet, this means the introduction of a residual (positive) sextupole component. Since this is a residual magnetization effect, the relative importance of this sextupole component is expected to be maximum at injection.

Since all magnets are on a common bus, residual magnetization effects are expected to be of a systematic nature. Systematic variations in field strength can easily be compensated by adjusting the excitation current. To the extent that the sextupole errors are not too large, they can be compensated using sextupole correctors. At this point, there is no reason to expect that eddy currents in the laminations would result in a sextupole component in the field at injection large enough that it could not be compensated. The Main Ring magnets, which are very similar to the MI magnets, have been operated in the past at ramp rates similar to those proposed for the Main Injector with no evidence of any particular problem. We intend to measure a magnet under realistic ramping conditions. It is also worth noting that in the unlikely case of a difficulty, it would be a straightforward matter to reduce the ramp rate at the end of the ramp in order to mitigate eddy current effects.

End field quality

End vs current

We characterize the integrated strength as being composed of a body component and an end component. The body component is equal to the central field times the length of the steel. The end component is the difference between the total and the body field. The effective length of the magnet of the magnet is the total integrated strength divided by the central field.

The FMI requires that the ratio of integrated strength of the 6-meter dipoles to the 4-meter dipoles be 3:2. Variation from the design strengths leads to closed orbit errors. The body field

varies with current in the same way in the 6-m and 4-m dipoles. The end field varies with current the same way in the 6-m and 4-m dipoles. But the body and end do not necessarily vary the same way. Therefore, since the total field is composed of different fractions of body and end in the two lengths of magnet, the total field integral varies differently with current. This leads to a change in the ratio of the integrated strengths of the two lengths and movement of the closed orbit.

The initial design of the ends led to variations in the closed orbit that could be corrected by the dipole trim magnets. That, however, would use up a significant fraction of the range of the trim dipoles which would be better kept available for other needs. After extensive calculations and trials, we have adopted an end design with an approximation of a Rogowski profile in the central region. The shape is shown in Figure 3.1-11. The variation of the effective length of the end with current is shown in Figure 3.1-12 [6].

End shape

The transverse profile of the end packs of the magnets has been designed to control the sextupole component at injection and transition. We have tailored the end contribution to the sextupole so that the total sextupole does not require a sign change in the chromaticity sextupole power supplies.

Current loop (solenoid)

The geometry of the coils at the ends of the dipole, including the connection between the upper and lower coils and the connections from one magnet to the next, were chosen primarily to conserve space and to facilitate installation in the tunnel. As an unintended side effect, we have created a loop at the lead end that carries an effective current of one half the current in the magnet. We have also created a loop where the non-lead ends of adjacent magnets meet that carries the full current. These loops produce solenoidal fields that couple the horizontal and vertical betatron oscillations.

We have calculated the strength of the solenoids and analyzed their effect on the beam [7]. We find that the coupling can be easily corrected using the skew quadrupoles already planned for the ring. These end fields will only require 1% of the available strength of the skew quads.

Effect of adjacent magnets

At the non-lead ends of the dipoles the magnet centers are only 0.355 m apart, suggesting a possible interaction of the magnetic fields of the dipoles. To assess the impact of this effect, we have measured the end field in the presence of a dipole half core located where the adjacent magnet will be in the tunnel [8]. The pointscan system was used to measure the field as a function of longitudinal position on axis.

Database: pole_tip

View : No stored View

Task: Object

Object: 1-WORK1, {END PACK, Bin1}

Units : IN

Display : No stored Option

Bin: 1-MAIN

Update Level: Full

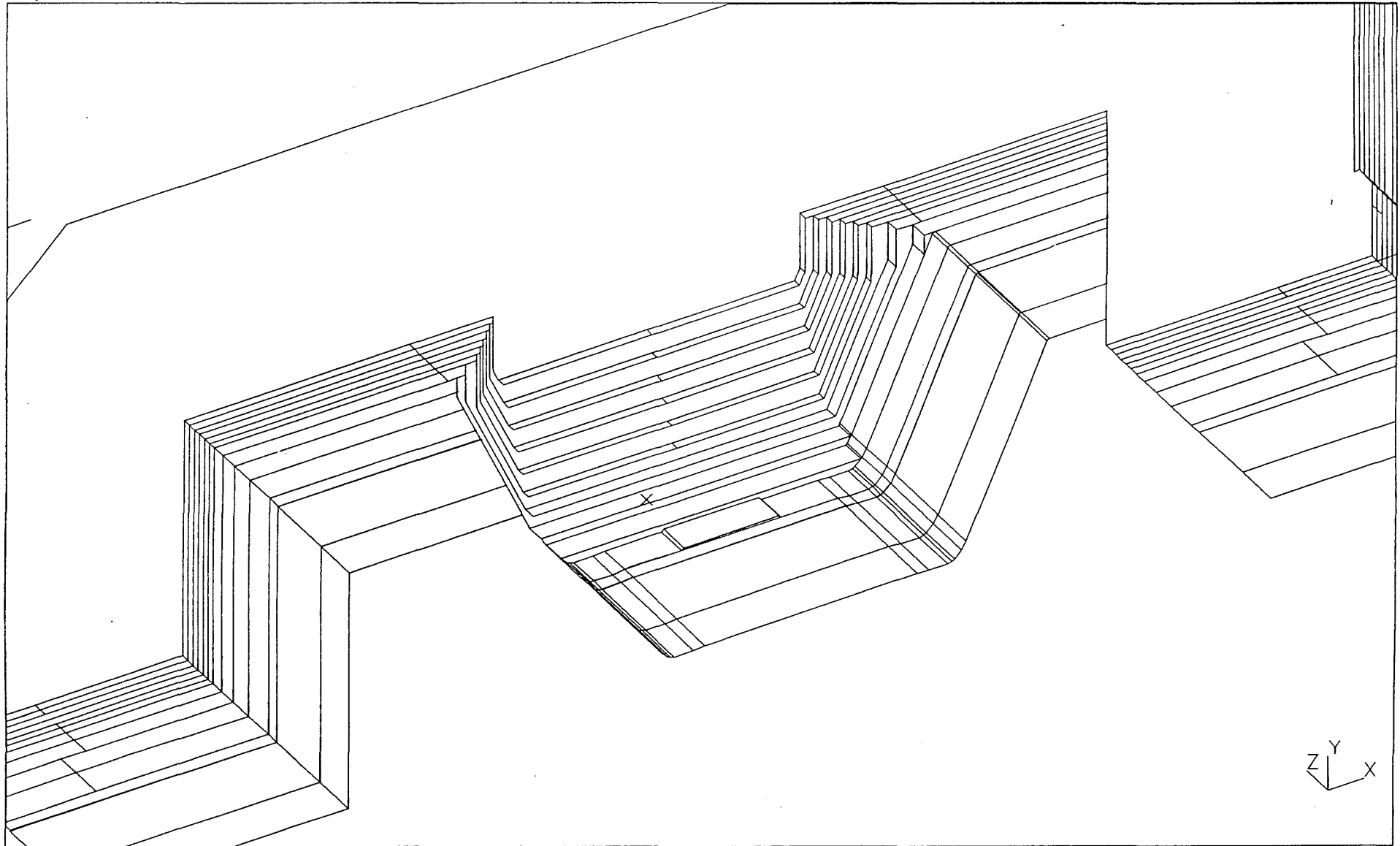


Figure 3.1-11. Dipole Endpack Shape

Change in Effective Length

IDB003

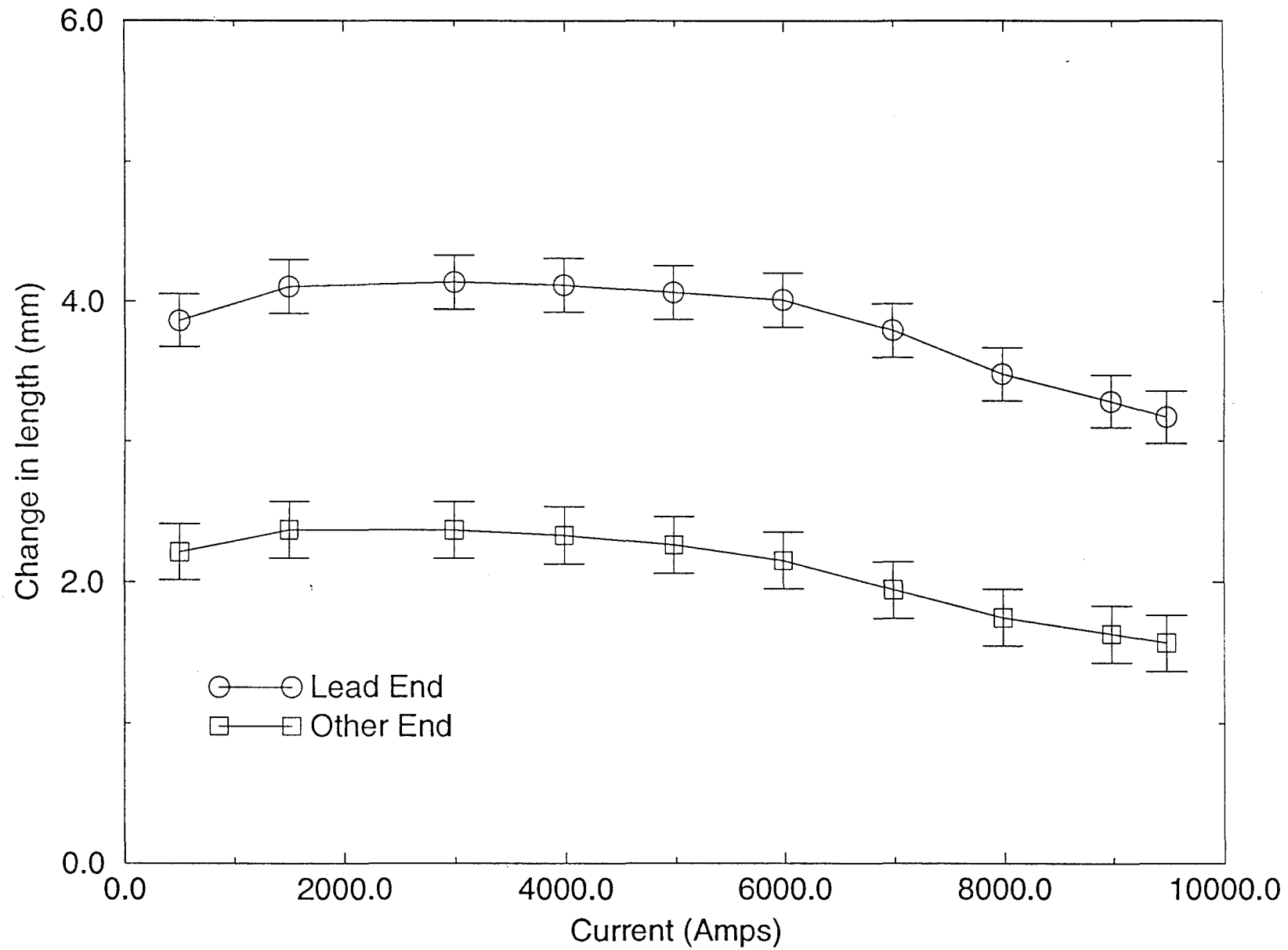


Figure 3.1-12. Variation with Current of Endpack Effective Length Relative to Physical Length.

Measurements were made with and without a dummy dipole core in place. For each configuration, data were taken with the magnet off and at full excitation (9500 A). The dummy core was not directly excited in any of the measurements. The dummy core had a square end profile, not the tapered shape of the dipole magnets.

Figure 3.1-13 shows the field at 9500 A as a function of position with and without the dummy core. The shielding effect of the unexcited dummy core can be seen clearly. With an excited magnet, we expect the flux lines to be less readily attracted into the adjacent steel. This measurement should represent the maximum effect that might occur.

We numerically integrate the field measurements from 0.20 m outside the dummy core to 0.25 m inside the dummy core, the region over which there is a visible difference in the fields. The results are listed in Table 3.1-6

Table 3.1-6
Study of Steel Adjacent to Dipole

Run	Configuration	Current	Integral
A	both magnets	9500 A	20.35×10^{-4} T-m
B	both magnets	0 A	-0.09×10^{-4} T-m
C	dipole only	9500 A	27.53×10^{-4} T-m
D	dipole only	0 A	0.24×10^{-4} T-m

From this we see that the difference between the integrals with and without the steel at full current is -7.18×10^{-4} T-m. The difference between the measurements at zero current gives the contribution of the remanant field of the dummy core steel, -0.33×10^{-4} T-m. The effect of the adjacent steel on the excitation field is thus -6.85×10^{-4} T-m.

For comparison, the field integral of a 6-m dipole at 9500 A is about 10.76 T-m. The maximum fractional change in the strength is therefore about 0.6 units (1 unit = 1×10^{-4}). This is a small uniform effect, so we do not anticipate any problems.

Strength matching - requirements & tolerances

We base our requirements for the magnet-to-magnet uniformity of the integrated field on our desire to control the closed orbit deviations with reasonable trim dipole correctors. As elsewhere, the most demanding conditions occur at 120 GeV/c during slow spill, when the beam is large and the momentum is high. The large beam makes us sensitive to aperture edges, both

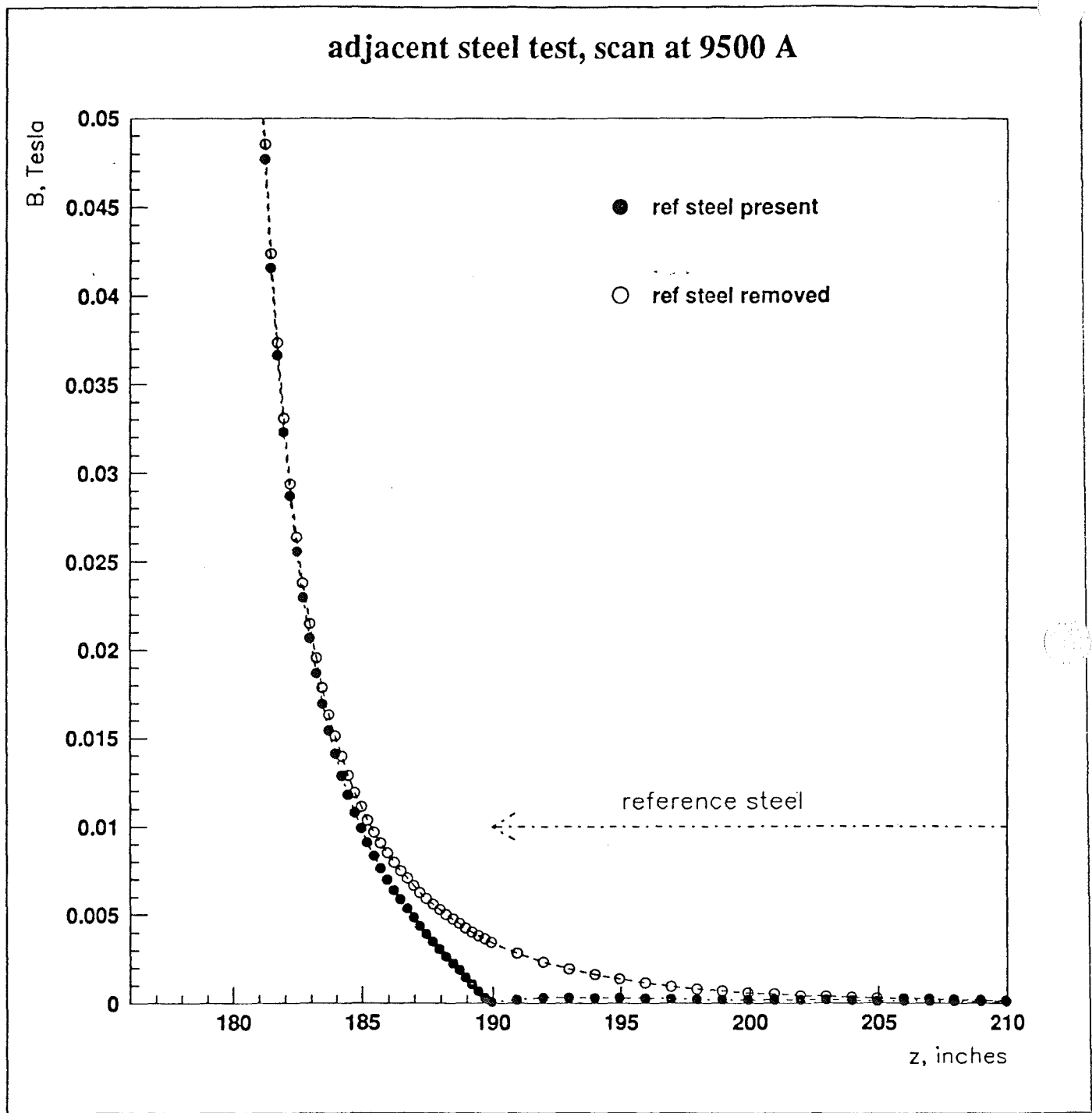


Figure 3.1-13. Effect of Adjacent Steel on End Field

mechanical and dynamic, and the high momentum reduces the relative strength of the correction elements.

We find that we can comfortably tolerate a systematic strength difference of about 5×10^{-4} from the ideal in the ratio of the 4-m dipoles to the 6-m dipoles. The design dipole correctors are capable of 0.030 T-m. This is sufficient to correct the closed orbit to 1 mm if we maintain the rms relative deviation of the dipole strengths to 10×10^{-4} . We will strive to maintain the total variation to 10×10^{-4} .

Recipe stacking

The integrated strength of a dipole depends on the average pole face gap, the coercivity of the steel, the permeability of the steel, the mechanical length of the magnet, and the packing factor of the laminations in the half core. It is not practical with current technology and a limited budget to require the tolerances on all of these parameters to be so tight that the cumulative tolerance is 10×10^{-4} .

The packing factor is fairly well controlled by requiring that the laminations be stacked in the half core at a pressure that we have determined to be sufficient to minimize variation. We have calculated that in the worst case (at 17 kG, corresponding to 150 GeV) a fractional variation in the packing factor of 15×10^{-4} leads to a variation in strength of 1×10^{-4} . At best, the physical length can only be controlled to within half a lamination thickness, or 1.25×10^{-4} (1.9×10^{-4} for the 4-m dipoles).

The variations in steel properties and lamination shape we experienced in the early production are discussed below. To reduce the variations in strength due to the variations in the laminations, we select the boxes of laminations to be used in each half core. We make a recipe for each half core that averages out the variations in the gap and permeability. We have planned the deliveries of the laminations to fall enough in advance of the stacking to give us a good selection of laminations to choose from at any time.

Assignment scheme

If our efforts to keep down the variation in integrated strength fall short of our goal, we can resort to assigning dipoles to locations in the ring on the basis of their strength. The 90 degree standard cells provide natural ways to accommodate matched pairs in local two-bumps. A pair of one strong and one weak dipole will fit 360 degrees in phase advance apart, or a matched pair of strong or weak dipoles will fit 180 degrees apart.

Production measurements and acceptance

Every dipole will be thoroughly and promptly tested after assembly at the Fermilab Magnet Test Facility (MTF). This will assure that every magnet installed meets the magnetic requirements of the project. Subtle manufacturing problems can be indentified early and corrected. Additional improvement of the accelerator performance can be achieved by assigning magnets to locations in the ring based on their magnetic properties. Finally, measurements on every magnet will allow improved accelerator modeling.

The integrated strength and the strength as a function of position will be measured by two methods each to provide continuous cross-calibration and some redundancy in the case of failures.

It is anticipated that a complete set of measurements will require two to three shifts per dipole. Keeping pace with the production rate of ten magnets per month will require one to one and one-half shifts per day, five days per week.

The measurement plan, the conditions, the raw data, the intermediate calculations, and the final results for every measurement will be stored in a database. This information will be readily accessible for further analysis and use by physicists and others in the Magnet Test Facility and the Accelerator Division.

Flatcoil

The primary measurement system will be a long, narrow, 16-turn coil of wire, rigidly formed to the trajectory of a particle through the magnet. Both strength and field shape can be measured. We call this a flatcoil. The probe is 7.32 m long, extending beyond the ends of dipole to integrate the total field seen by a particle traveling through the magnet.

-Strength

The field integral as a function of current is measured by placing the coil along the center line of the magnet and ramping the current. The voltage induced by the changing flux through the coil is integrated by scaling the output of a voltage-to-frequency converter. At selected currents we read the scaler, measuring the total change in flux from the initial state. This technique is quick and precise.

One limitation of the flatcoil for measuring relative strength is that the remanent field is not included and must be added as a correction. The remanent field is small, so even large fractional variations from the assumption of constancy will not significantly affect the final result.

To get a good absolute measure of the strength requires knowledge of the probe geometry to a precision that is difficult to achieve. Comparison with the NMR/Hall probe measurements provides an absolute calibration.

A probe with the same effective area as the test probe is placed in a short reference dipole excited in series with the magnet under test. Bucking this signal against the main probe allows more precise relative measurements of the dipole strengths. Measuring the response of this system with every magnet measurement provides a continuous monitor of the stability of the electronics.

-Scan

The variation of the field integral as a function of horizontal position is measured by moving the flatcoil transversely and recording the change in flux from the starting position. The coil is mounted on a baseplate which provides the drive mechanism for sweeping the coil horizontally across the magnet aperture. A stationary reference coil is placed in the center of the aperture. The bucked signal of moving coil minus reference coil provides a clean signal of field shape by cancelling variations in the excitation current. The development of the coil motion assembly and the use of a reference coil were done specifically for the R&D dipoles. Field shape measurements made with this coil show substantially better signal-to-noise than for the prototype dipoles, which used an earlier flatcoil model.

The flux changes are normalized to the strength in the center of the magnet, removing most systematic effects and providing a measure of the field uniformity far more precise than is required for the project. The field can be measured over a wider range of x than is available to the beam. The field as a function of x can be fit to a polynomial to determine the normal components of a harmonic decomposition of the field. This is a fairly quick measurement. It will be done at several currents.

-Pointscan

The pointscan system combines an NMR probe with a two-axis Hall probe. The NMR is precise and accurate, but is only sensitive in the range above approximately 1.0 Tesla. Also, because it is untuneable in regions with more than minimal field gradients, its utility is limited to the body of the dipoles. The ends and the low field excitations are measured with the Hall probes. Both the NMR and the Hall probes are mounted on a cart which rides on a curved rail and is pulled through the magnet in order to map out the longitudinal profile of the field. This system, including the capability for automated motion in z , was developed and first used with the R&D dipoles.

The probes will measure the field on a 25 mm grid along the center line. Numerically integrating this longitudinal profile gives the central field integral. This technique provides a measure of the remanent field and of the absolute strength integral, cross checking the flatcoil measurement. The profile is not significant for the performance of the accelerator, but it has the potential for being a useful monitor of the magnet assembly quality. It is very time consuming, so it will be performed at a very limited number of currents, and perhaps on a limited number of magnets.

-Harmonics

The alternate shape determination will be done with a rotating coil. A 6.6-m rotating tangential coil will extend through the entire magnet. The coil form will curve to follow the center line of the magnet. The form will be sufficiently flexible to allow it to rotate about its axis, even though it is held in a curved shape. The same voltage to frequency system used in the flatcoil system measures the change in flux through the coil as it rotates. This gives both the normal and skew components of the harmonic decomposition of the field integral. From this, field values can be reconstituted, if needed. Although the rotating coil gives a field integral, it is not expected to be sufficiently precise to replace either the flatcoil or pointscan measurements. The measurements are sufficiently quick to allow tests at multiple currents.

At the time of this writing the 6.6-m probe had not yet been fabricated and tested. If the plan does not work, the fallback position is to use the 2.0-m probe that was used in the prototype and R&D work. Harmonics for the full magnet can be determined by making multiple measurements with the probe placed at appropriate locations through the magnet. In that case, a reduced number of magnets will be fully measured with the system, or only a single body field measurement will be made on each magnet.

Magnetic acceptance criteria

All measurements will be analyzed immediately by the measuring technician. Important parameters will be compared to standard values stored in a database to evaluate the measurement and the magnet. These tests will monitor both the properties of the magnets and the behavior of the measurement system.

The measurements are checked for internal consistency. The results from redundant techniques are compared. The excitation curves are compared with the nominal values. The multipole strengths as a function of current are compared to nominal.

As noted above and discussed in the accelerator physics section, the Main Injector can tolerate a distribution of strengths and shapes, so a simple acceptance cut is not appropriate. A

tight cut with rejection of anything outside is too restrictive, unnecessarily rejecting usable magnets and raising the cost of the project. A loose cut with no other monitoring could lead to an unacceptably broad distribution. Every deviation from nominal results in some degradation of the accelerator performance. We seek to minimize those variations, but do not expect to eliminate them.

Instead of hard acceptance limits on field quality, we have specified a two-level test. Figure 3.1-14 shows a typical evaluation plot of the fractional deviation of one magnet from the nominal, along with the tight and loose limits. The tighter limit is initially set at twice the standard deviation (two sigma) of the distribution of the R&D dipoles. The looser limit is set at three sigma. The appropriateness of these limits is discussed below. The limits will be reviewed periodically.

If a magnet falls within the tighter limits, the measurement will be accepted. If the magnet falls outside the inner limit but inside the outer limit, it will be remeasured. A sample of magnets passing the inner limit will also be remeasured to monitor the repeatability of measurements and control for the regression to the mean tendency inherent in the remeasurement of deviant magnets. Magnets outside the outer limits will require assessment by physicists to determine the source of the problem and the disposition of the magnet.

The tracking studies have been done with an rms variation in the dipole strength of 10 units. The sigma for the six 6-m R&D dipoles was 4.5 units. Therefore, a magnet falling outside the outer limit (15 units), while quite likely usable in the accelerator, may indicate a problem in the fabrication process which needs attention.

Similarly, the tracking studies have used a variation of 0.5 units in sextupole component at 120 GeV/c. The observed variation in the R&D dipoles is ~0.15 units.

Fabrication

Bare coil fabrication

-Winding

The dipole coils are fabricated primarily from 25.4 mm x 101.6 mm copper bars with a 13 mm diameter water passage. The 6-m bars are brazed together end-to-end and then wound on a form to the desired shape. A hydraulic fixture assists in making the bend at each corner. Space constraints limit the number of bars of copper that can be brazed together before the winding process starts. During the winding, therefore, the brazing and bending operations alternate as a coil is fabricated.

Flatcoil Data Compared with R&D Dipole

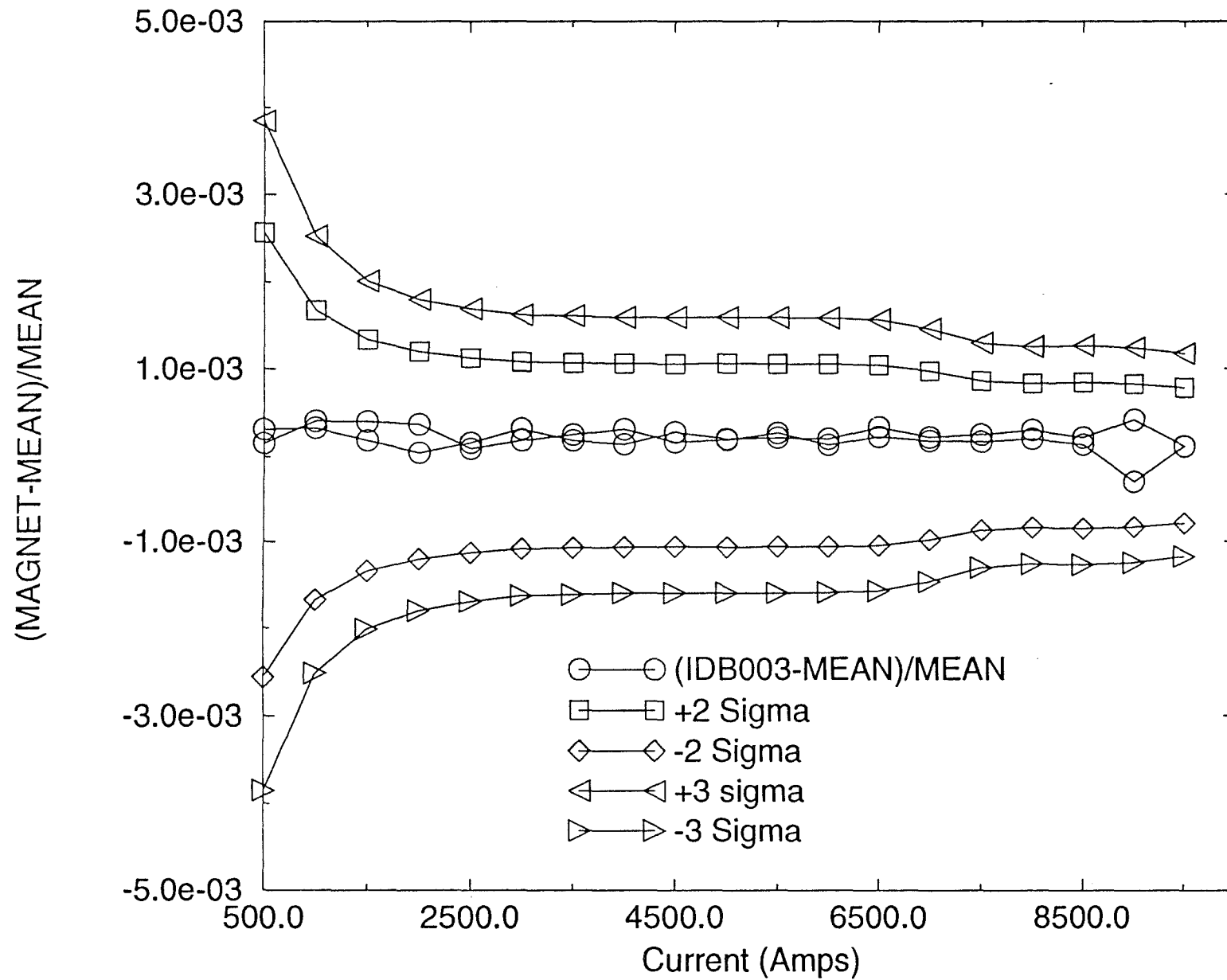


Figure 3.1-14. Magnetic Measurement Evaluation Plot.

-Induction brazing

The joints are of a type with demonstrated reliability in which conductors are faced-off, counterbored, and then brazed together with a ferrule inserted between the conductor water holes. Silfos rings and gaskets provide a consistent amount of brazing material. Induction brazing of the joint will assure uniformly high quality.

Fermilab purchased the induction brazing equipment and is furnishing it to the coil fabricator. We have taught the vendor to use the equipment, introducing the technology to this industry.

-Ultrasonic Joint Test

Each brazed joint is tested using ultrasonic testing equipment developed for Fermilab and provided to the coil fabricator. This system measures the ultrasonic energy reflected by the joint. A faulty braze joint appears as a discontinuity in the material and reflects energy. Both the conductor ends butted together and the copper to ferrule surfaces are tested. Before starting production the system was validated by making numerous joints with and without flaws intentionally introduced, measuring them, then sectioning the joint to compare the actual bond with the ultrasonic measurement. This measurement technology has also been transferred to the vendor, who is doing the tests on every joint with monitoring by Fermilab.

-Helium Leak Test

Every joint is subjected to a helium leak test, again using technology transferred to the vendor from the Fermilab experience. The vendor performs the tests and is monitored by the Fermilab inspector on site. A helium leak test is used rather than a hydrostatic leak test because the bare coils lack a full set of connectors suitable for high pressure use.

-Flow Test

Each coil must pass a water flow test at specified pressure drops characteristic of operation in the Main Injector tunnel. These tests assure us that the cooling passage is not obstructed. Required flows are based on calculations and verified by experience.

Coil insulation

Lessons from history

Over the course of 25 years Fermilab has built thousands of magnets. We experiment and we learn from our mistakes. Two recent studies have examined the Main Ring B2 and B3 dipoles with respect to reliability. The studies reported on design and operational problems and made recommendations for future magnets [9].

The studies clearly demonstrate that the choice of insulation is a major factor in the reliability of a magnet. A coil insulated with a full impregnation process is dramatically more reliable than one which merely uses B-stage epoxy tape. Over-heating of the coil can damage the epoxy insulation. Differential expansion of adjacent turns due to a poor choice of water flow patterns introduces stresses in the epoxy and can lead to failures. External water is also a clear enemy of insulation.

Choices

The Main Injector dipole coils have a very conservative insulation design, shown in Figure 3.1-15. The main insulation is provided by multiple layers of fiberglass tape, vacuum impregnated with epoxy. G-10 strips provide an additional barrier in the event of a crack in the epoxy.

The epoxy itself provides the insulation. The fiberglass tape serves as a matrix that prevents cracking. To avoid cracking we prohibit unsupported volumes of epoxy greater than 1.5 mm in their shortest dimension.

Different epoxy formulations and curing cycles result in products with different properties. We have chosen a relatively rigid final product which does not degrade significantly with exposure to radiation. Care must be taken in curing the epoxy to avoid rapid temperature changes that would introduce stresses and lead to cracking of the insulation.

Epoxy studies

Epoxy potting compounds used as electrical insulators have very good mechanical and electrical properties and are generally considered to be resistant to moderately intense ionizing radiation. These compounds would be even more desirable if they were less brittle. The epoxy resin, which is the basis of the potting compound, cannot vary a great deal because of the nature of its chemical make-up. The final properties of the cured epoxy are very dependent on the curing agent. The proper choice of a curing agent is very important in achieving the maximum desirable properties.

It is generally accepted that there are two groups of curing agents that are best for resisting ionizing radiation. They are aromatic amines and anhydrides. The aromatic amines are difficult to work with in large quantities because they present a health hazard that requires very strict controls in their handling and application. Their use frequently results in epoxy formulations that are high in viscosity and have a shorter pot life or working time. The anhydrides present a much lower health hazard, lower viscosity, and longer pot life but tend to be brittle.

FMI DIPOLE INSULATION SCHEME

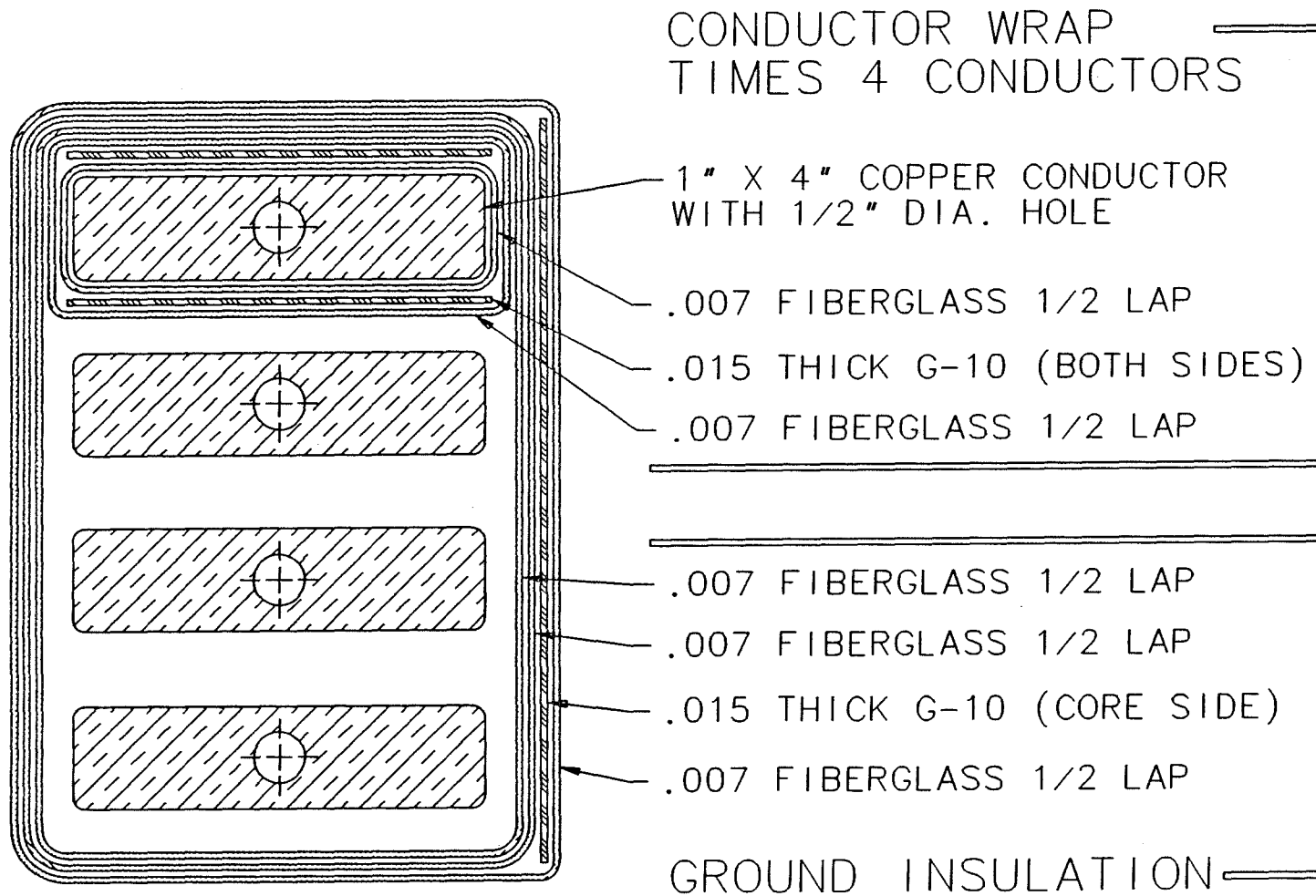


Figure 3.1-15. Dipole Coil Insulation Scheme.

It has been thought for some time that this brittleness could be reduced with the addition of flexibilizing, reactive diluents. These flexibilizers could also lead to a reduction in viscosity that would be desirable during processing. Two epoxy resins diluents which are known to be effective flexibilizers were chosen for evaluation. Samples were prepared with varying amounts of the flexibilizers added to the anhydride formulation and exposed to radiation of 100 megarads. Samples were then mechanically tested in tension and flexion. These tests gave values for tensile strength, flexural strength, elongation, and modules.

The results of these tests [10] on samples irradiated and not irradiated showed that the tensile strength was little affected by the radiation, but the difference in flexural strength and elongation all but disappeared. Any flexibility imparted to the epoxy by the flexibilizing resins was negated by the exposure to radiation. Therefore, the addition of the flexibilizer would only lead to a potential for error in weighing and mixing by introducing an unnecessary component into the potting formulation.

Additionally, it was found that the epoxy-anhydride formulation without the flexibilizer was resistant to an exposure of 100 megarads. A very small sampling of this formulation was exposed to one gigarad and showed a favorable retention of physical properties.

Thermal studies

Our concern about the stresses produced in the epoxy by the thermal expansion and contraction of the coils led us to study the expected behavior [11]. One of the dipole magnets was tested extensively at the Magnet Test Facility, both at the normal operating power of 18 kW (5000 A rms), and at a vastly elevated power level of 66 kW (corresponding to operation at 9500 A dc). Tests were performed with two different methods of cooling water connects: (i) with the water entering on the inside and exiting on the outside of the coil, and (ii) with water entering on the outside and exiting on the inside. In the first case, the copper is constrained only by the epoxy-insulation material, whereas in the second case, the hotter copper on the inside of the coil is trying to expand more than the cooler copper on the outside, putting the insulation layers in compression. The tests were under conditions similar to those anticipated in operation in the Main Injector ring, but not identical. For example, the water flow and input temperature were both slightly lower during the tests than they will be in operation, and the water supply could not be maintained at a constant temperature.

Measurements were made of both the thermal and dimensional changes in the coil. These are summarized in Table 3.1-7. No difference was seen between the two modes of cooling, indicating that the coil acts as a single body, with only elastic motion of the coil resulting from the

thermally-induced forces. The time for the coil to stabilize in temperature after changing the power level is fairly long, on the order of twenty minutes. Thus, these tests were aimed at measuring the effects resulting from the magnet ramp being turned on and off (changes in the average power), and not from individual ramp cycles (in which the instantaneous power varies dramatically over a time scale of less than 5 seconds.)

Table 3.1-7
Thermal Test Results

	<u>Calculated Values</u>		<u>Measured Values</u>	
	5000 A	9500 A	5000 A	9500 A
ΔT (°C)	8.8	31.7	8.2	28.0
Expansion (in)	0.0097	0.035	0.0094	0.040

(Expansion is the growth of one end of the coil, which is fixed to the steel in the center of the 20' dipole. The calculations are based upon a 10' piece of copper.)

Calculations were done of the stresses in the epoxy from the differential temperatures between adjacent turns of copper in the coil. Two different analyses were done. First, the compressional or tensile stresses on the ends were calculated, ignoring any bonding along the length of the coil. Second, shear stresses along the length were calculated by assuming the epoxy and insulation material in the ends deformed as a result of compression or tension, and then calculating the shear stress along the length due to that deformation. Both calculations show stresses below the allowable stresses, even for the 9500 A excitation. A finite element analysis to calculate the stresses is in progress. While no problems were observed during this rather brief test, questions of cyclic fatigue failure were raised. A detailed analysis (which includes the finite element analysis) may predict the long term effects and help in understanding the stress distribution. The analysis will be used in addressing the merits of doing a very lengthy life test on one or more magnets.

Steel

Specifications and monitoring

The steel for the dipoles is defined by a performance specification (Specification #8020-ES-186651, Rev. E.). The coercivity is required to be less than 1.0 Oersteds at $H_{\max}=100$ Oersteds, with a maximum variation of ± 0.2 Oe from the mean. The permeability is required to be between 176 and 181 Gauss/Oersted at 100 Oersteds. The vendor measures every batch of steel with an Epstein square and send the data to Fermilab. In addition, the vendor provides samples which Fermilab tests to monitor the vendor testing. The Rockwell hardness is specified to be between 20 and 50. The B-H curve for the steel is shown in Figure 3.1-16.

Experience

Figure 3.1-17(a) shows the variation of permeability from the first six months of steel production. Figure 3.1-17(b) shows a histogram of the coercivity over the same sample. These data are used in the formulation of the half core recipes.

The one pending concern at the time of this writing is that the production dipoles are being made from different steel than the R&D dipoles. The vendor and the process are different. The specifications are the same, but there is a lingering concern that there may be subtle differences that will surprise us. We eagerly await the measurements of production dipoles.

Laminations

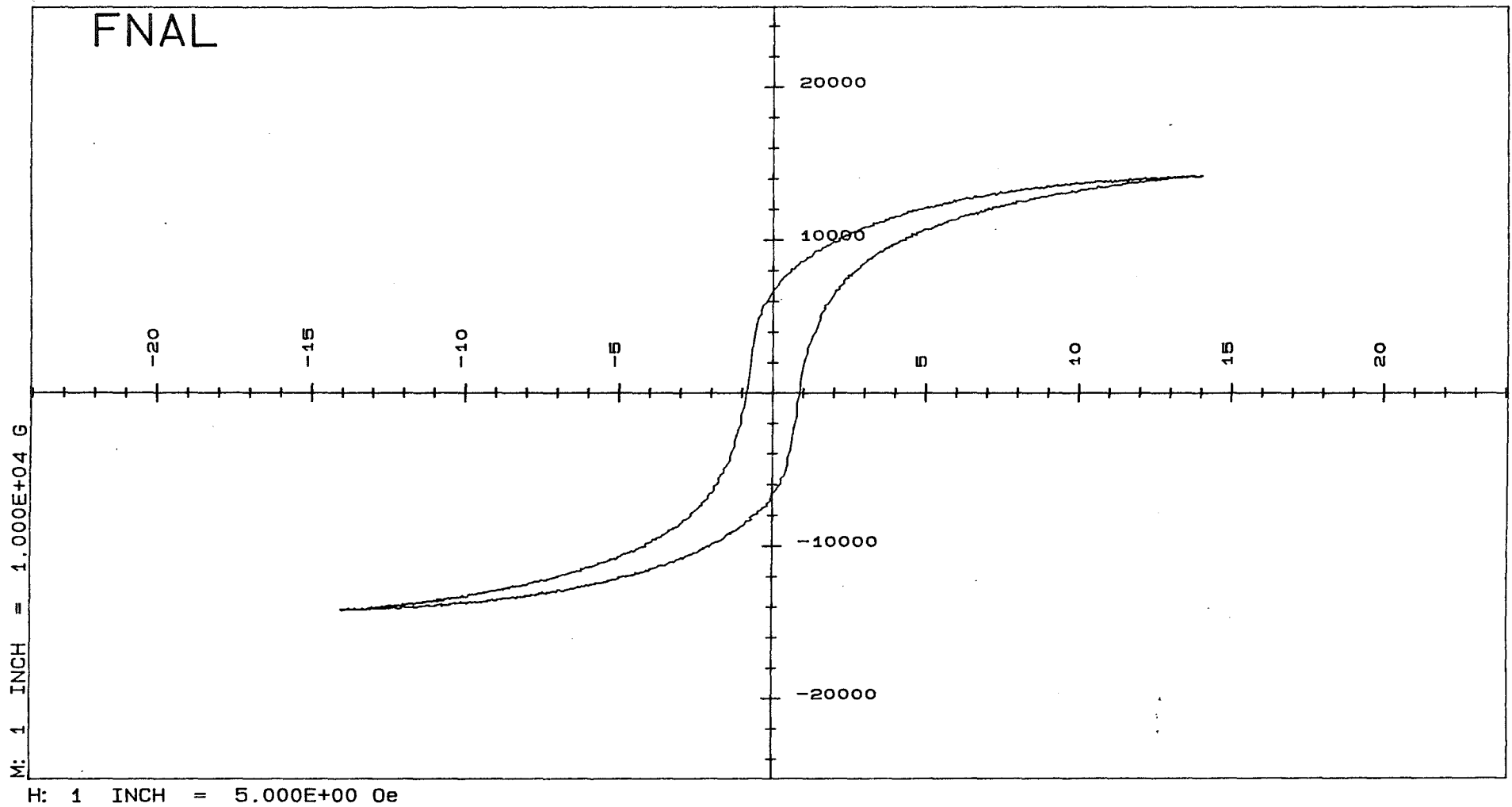
Cordax and gauges

Both the vendor and Fermilab measure in detail a sample of laminations, one from each slit of steel, using coordinate measuring machines with a precision of 0.0001". Each lamination that Fermilab measures is reviewed for conformance to the drawing tolerances. Trends are monitored informally, working with the vendor to identify drifts that could signal impending larger problems.

A Fermilab inspector at the stamping vendor's plant measures a larger sample of laminations in less detail. A set of three gauges measures the distance between the pole face and the parting plane at three positions and records the data electronically. Using this device the inspector can sample five laminations out of every 100 stamped. This data is transferred periodically to a database at Fermilab where it is used in the determination of recipes for stacking.

Experience

As with most properties that affect the magnetic field, we can tolerate a limited number of articles which fall outside the stated tolerances as long as the distribution is fairly tight. The



ID : LTV 3836499 tail
File Name: \LTV\38364##\h-99ta1
TRT 10 sec. AutoSweep: Enabled
Tested by LTV July/14/1994
Hmax : 14.019 Oe
Hc : 0.8772 Oe

Bmax : 14222 G
Br : 6690 G
LpArea: 5.536E+04 G-Oe
Date : 08-01-1994
Mu@Hm : 1014.423
T.Time: 128 sec

Figure 3.1-16. B-H Curve for LTV Steel

DISTRIBUTION OF STEEL MEASURED MAGNETIC PROPERTIES

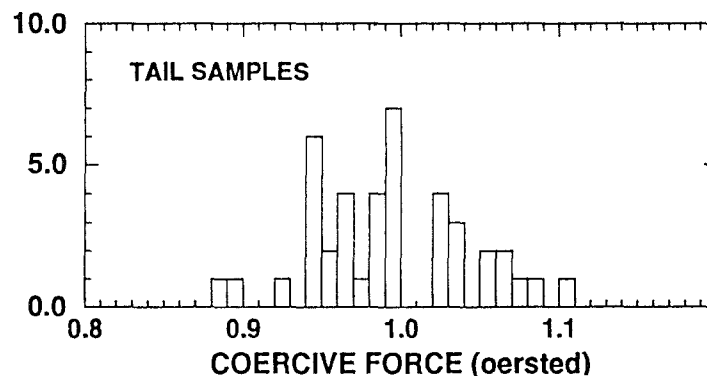
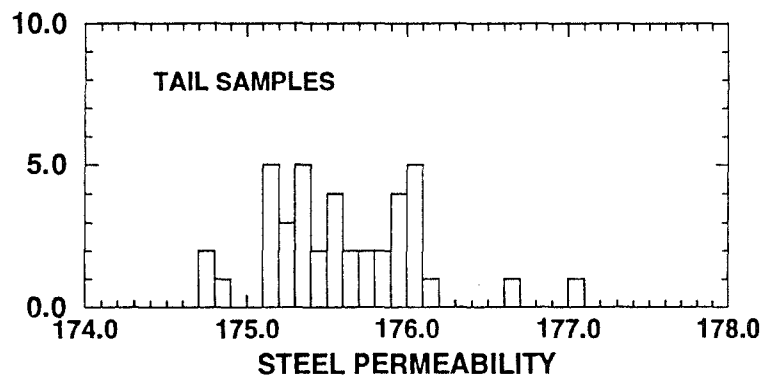
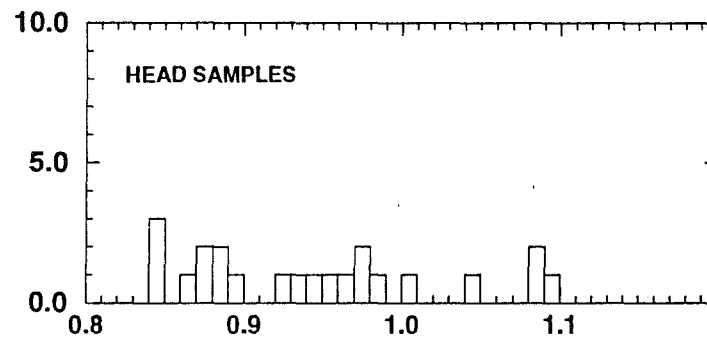
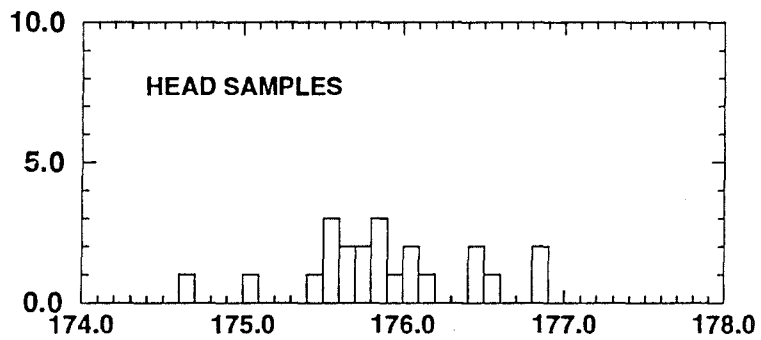
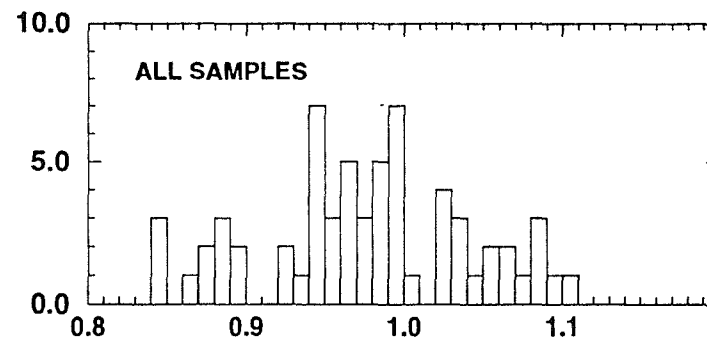
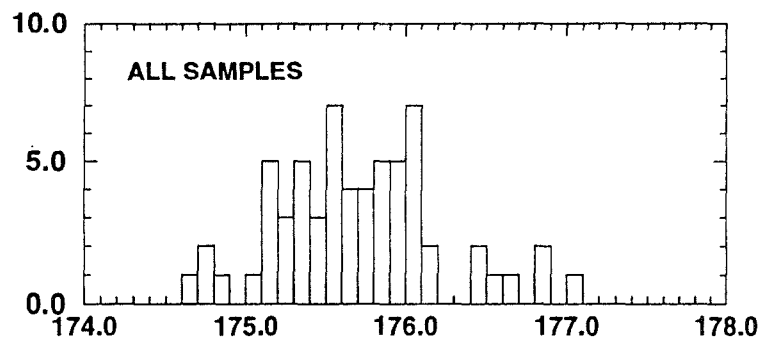


Figure 3.1-17.(a) Permeability of LTV Steel

Figure 3.1-17(b). Coercive Force of LTV Steel

lamination dimensions have that quality, with the added advantage that we can mix laminations to produce a uniform field from nonuniform laminations.

Figure 3.1-18 shows a typical report of the coordinate measuring machine. The deviation from the drawing dimensions is shown on an expanded scale relative to the nominal. Figure 3.1-19 shows the distribution of gap distances over the first 295,000 laminations. We anticipate no difficulty in making use of virtually all of the laminations.

Half cores

A half core is a stack of laminations sandwiched between two endpacks and held together by welded tie plates on each side and the top. The half cores will be built by a subcontractor using screw presses provided by Fermilab. A Fermilab inspector is present to monitor the performance of the subcontractor and to witness the inspections.

The end pack is composed of 51 laminations trimmed to form the end profile described above, followed by enough additional untrimmed laminations to make a thickness of 0.15 m (6 inches). These laminations are cleaned, coated with epoxy, stacked in a fixture, compressed, and cured in an oven.

An end pack is placed on the stacking press. Laminations are stacked against the endpack and against a side rail that controls the curvature of the half core. Every 75 mm (3 inches) the orientation of the laminations is reversed, so that any left-right (quadrupole) asymmetries of the dies are cancelled. As noted above, the stacking follows a recipe to produce a uniform product.

Every time an additional 0.6 meters (24 inches) has been added to the stack, the press squeezes the stack. A powered coil of wire provides a magnetic field that holds the laminations down against the stacking rail. The laminations are tapped to ensure that they are snug against the side stacking rail. Clamps then restrain the laminations, attempting to prevent relaxation of the compressed stack.

When the desired length approaches, an end pack is placed on the other end of the half core and the whole half core is compressed. Laminations are added or removed to bring the length within tolerance, within one-half of a lamination thickness (1.5 mm). Maintaining pressure, the intermediate clamps are removed. Tie plates are welded to the sides and the top of the half core to lock the half core in its compressed state. The half core can then be removed from the press for clean up, inspection, packing, and shipment to Fermilab.

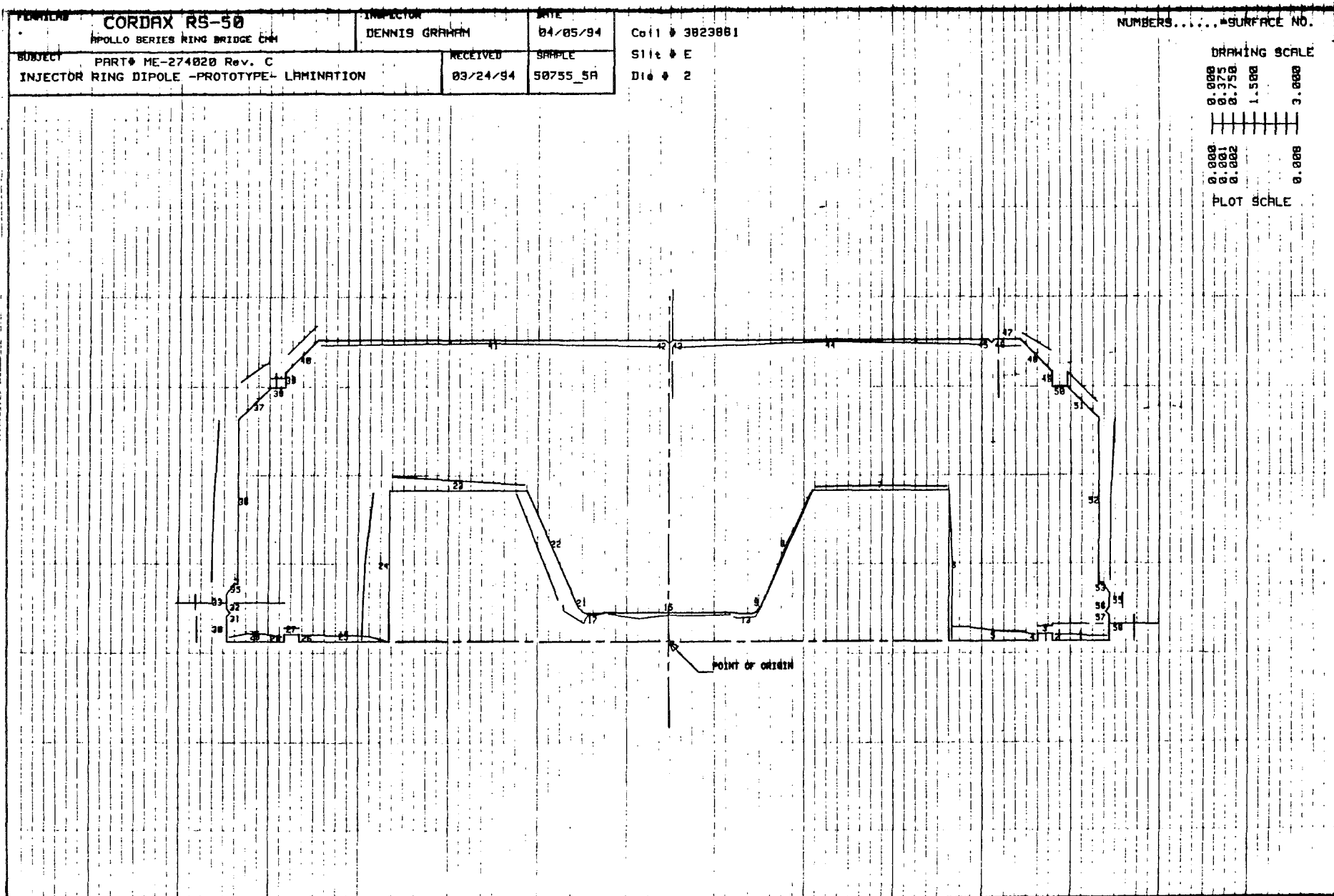


Figure 3.1-18. Typical Report from Coordinate Measuring Machine.

DISTRIBUTION OF POLETIP GAP IN THE LAMINATIONS

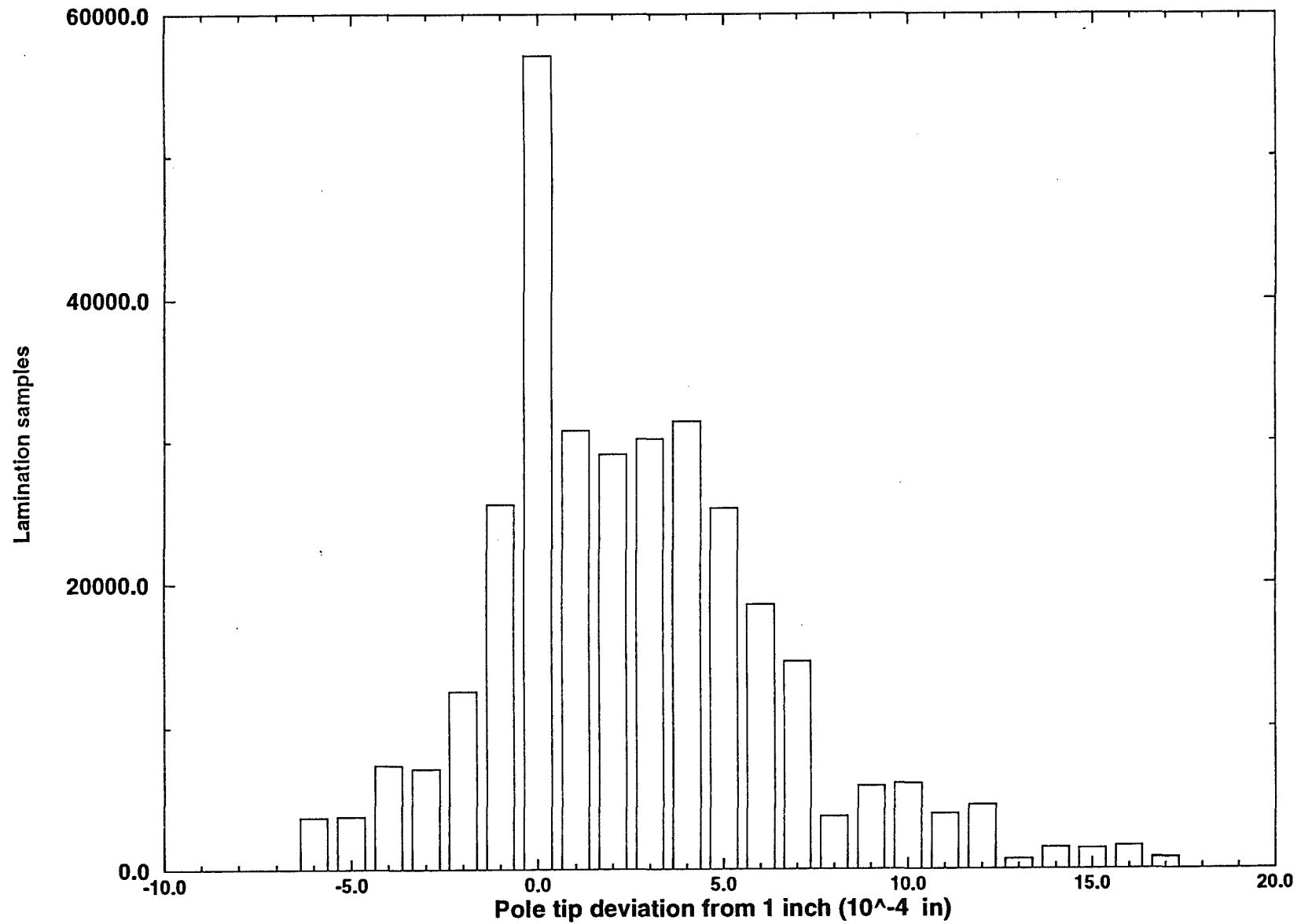


Figure 3.1-19. Distribution of Lamination Pole-Tip Gap

Parting plane flatness

To maintain the dipole field strength precisely, the gap in the back leg between the top and bottom half cores must be held to a minimum and kept uniform. The half cores are stacked on rails surveyed to be flat to 25 μm . The half cores are sufficiently flexible that the flatness is lost during handling, but during the final assembly the gap is drawn down to an average of less than 50 μm .

Packing factor

At high excitations the packing factor (the fraction of the length of the magnet occupied by steel) affects the field at which the magnet saturates and the slope of the excitation curve. We compress the stack of laminations to a constant pressure of 700 kG/m^2 (100 psi). Experiments have demonstrated that this pressure is sufficient to achieve a uniform packing factor (0.9860 ± 0.0008) insensitive to small variations in the pressure or laminations.

Some early production endpacks proved weaker than previous endpacks. An intense research effort was necessary to identify the problem. Initially various aspects of the epoxy bonding the laminations together was suspected. Eventually the primary problem seemed to be the thickness of the coating applied to all laminations as insulation against eddy currents within the cores. The steel supplier had already improved the surface finish of the steel to allow application of a thinner coat similar, comparable to the earlier laminations. End packs will be made with the thin-coated steel.

Final assembly

Fermilab will assemble the components into complete magnets in the Industrial Center Building. The job includes installing the coils into the half cores, welding the half cores together, brazing the coils together, and painting the magnet. Mechanical, electrical, and water flow measurements are performed at appropriate stages in the assembly. The assembly tooling is designed for a rate of ten dipoles per month working one shift per day. The capacity could be doubled with only a modest increase in tooling.

Sag

The dipole magnets will be supported utilizing the three-point support mechanism discussed in Chapter 3.10. Longitudinally, the supports are located near the quarter points of the cores, with a different spacing for the 6-m vs. the 4-m dipoles. Locating the supports at the quarter points reduces the sag of the dipole from approximately 0.11" (for end-supports) to about 0.02". The maximum allowable sag is 0.04".

Beamtubes and beamtube supports

The beamtube assemblies for the R&D dipoles were procured as a straight tubes, according to specification 1453-ES-305002. Two different vendors supplied the tubes, using significantly different techniques to fabricate the desired shape. A beamtube from one vendor was inserted into a fully-assembled dipole by sealing one end with a special fixture, and evacuating the tube from the flanged end. This procedure was done a number of times on different dipoles. The tubes from the other vendor are slightly stiffer and do not deform quite as much; a small change in finished dimensions will be required for the second vendor to supply tubes which can be inserted after magnetic measurements. Further details on the beamtubes and vacuum tests of the tubes can be found in Chapter 3.2.

Once inserted into the dipole, the beamtube will be formed to follow the beam trajectory by forcing it into shape and using three G-10 beamtube support pieces to hold it in the correct shape. One support piece is located in the center of the dipole on the inside radius of curvature. That support piece is placed in the dipole at the time of final assembly. Its surface has been cut to form an alignment surface to aid in probe positioning during magnetic measurements. The remaining two support pieces are placed into the dipole after the beamtube is inserted, on the outside radius of the dipole, a few inches from each end. The force required to bend the beamtube into the right curvature is quite modest. Following the final positioning of the tube, the vacuum flange is welded onto the tube.

End covers and ion pump support

The final components to be installed on the magnet are end covers on each end and an ion pump support bracket. The covers are intended to keep out metal chips and other debris and to reduce the exposure of the inner parts of the magnet in the event of a water leak in the tunnel. The ion pump support bracket is mounted on the downstream end only. It provides both the gravitational support for the ion pump, as well as a solid, 0.25" thick G-10 barrier between the beamtube and the magnet's electrical leads.

Storage

Completed dipoles will be stored in the MI-60 high-bay area until it becomes full. After that, they will need to be stored in the MI-60 enclosure. Beginning in early FY96, the MI tunnel should be complete, and, following survey monument work and utilities installation, the dipoles can begin to be placed into their final positions.

References: Main Injector Ring Dipoles

1. D.J. Harding et al., "Experience with the Source Evaluation Board Method of Procuring Technical Components for the Fermilab Main Injector", Proceedings of the 1993 Particle Accelerator Conference, 1993.
2. S. Snowdon, "Magnetic Design of the Main Injector Dipole", MI Note-0006, 1989.
3. H.D.Glass, "Techniques for Measurement of Dipole Endfields with a Rigid Integrating Probe", Proceedings of the 1993 Particle Accelerator Conference, 1993.
4. J-F. Ostiguy, "Eddy Current Induced Multipoles in the Main Injector", MI Note-0036, 1990.
5. K. Halbach, Nucl. Instr. & Methods 107, 1973; also, see J-F Ostiguy, "Effect of Eddy Cuurrents on Residual Magnetization", MI Note-0115, 1994
6. D. J. Harding, et al., "Design and Measurmeent of Prototype Fermilab Main Injector Dipole Endpacks", Proceedings of the 1993 Particle Accelerator Conference, 1993.
7. R. Baiod, "Evaluation of Beam Coupling Due to the Dipole Current Loop", MI Note-0113, 1994.
8. H.D.Glass, Field Modifications for Main Injector Dipoles due to Adjacent Magnet Iron, MTF-94-0050, 1994.
9. F.W.Markley, et al., 1989 Failure Committee Report, B3 Magnet Review, 1/4/89, private communication to the Fermilab Technical Support Section management; B.C. Brown, et al., An Analysis of Fermilab Main Ring B3 Dipole Failures, 12/30/93, MTF-93-0004; B C. Brown, et al., Report of the B2B3 Reliability Committee, 4/9/94, MTF-93-0009
10. J. Hoffman, MI Note-0120.
11. A. Lipski, "Summary Report on the MIR 20.0 Ft. Dipole Magnet Performance/Thermal Test", 1994, (unpublished.)

WBS 1.1.1.1.2 RING QUADRUPOLES

The majority of the quadrupoles magnets in the project are reused Main Ring quadrupoles. Since the beam travels straight through them, they do not suffer the trouble with sagitta that the dipoles do. They have been somewhat more reliable than the dipoles. To complement the existing quadrupoles, additional quadrupoles are built to essentially the same design but in different lengths. Figure 3.1-20 shows a cross-section of the quadrupole magnet.

The Main Ring quadrupoles that will be reused in the Main Injector ring have a nominal length of 84" and are sometimes referred to as BQBs, 3Q84s, or 7000-series quadrupoles. The Main Ring also uses a shorter version of the same design, 52" long, known as BQAs, 3Q52s, or 4000-series quadrupoles. The new quadrupoles, IQCs and IQDs, will be approximately 100" and 116" long, respectively.

WBS 1.1.1.1.2.3. AND 1.1.1.1.2.4. NEW MAIN INJECTOR QUADRUPOLES

The new and old quadrupoles will run on the same busses (one focussing, one defocussing), so it is imperative that their strengths track each other through the acceleration cycle, saturating in exactly the same way. Therefore we must use the same lamination for the new quadrupoles as the original Main Ring quadrupoles.

We took the opportunity of building these magnets to re-examine the insulation scheme for the quadrupoles. A new design for the insulation should improve reliability over the Main Ring insulation, already acceptably good. The turn-to-turn insulation thickness has been reduced slightly in order to accomodate an additional layer of coil-to-ground insulation. As before, the conductor insulation is a B-stage epoxy tape cured onto the coil in a mold before the magnet is assembled. The cured coil is wrapped with dry fiberglass tape and assembled into the half cores. The coil is then vacuum impregnated in the magnet. To allow adequate cooling water to flow through the longer coils, the hole in the conductor for cooling water has been expanded compared to the Main Ring quadrupole conductor. See Table 3.1-8 for the quadrupole parameters.

A 16-turn/pole trim coil has been added to the new quadrupoles, allowing adjustment of the gradient over a range of $\pm 1\%$ from the nominal full field. We do not plan to use these on a regular basis in operation, but, if necessary, this will allow more precise matching of the lattice between the arcs and the dispersionless straight sections. Independently adjustable quadrupoles also give valuable diagnostic opportunities for the accelerator. A trim coil is chosen rather than adding a comparable power supply to each quad in parallel. First, floating the power supplies significantly away from ground is more troublesome than not having to worry about it. Second, an independent coil allows bussing the trims of several quads together for grouped control.

FMI QUADRUPOLE MAGNET
CROSS SECTION VIEW

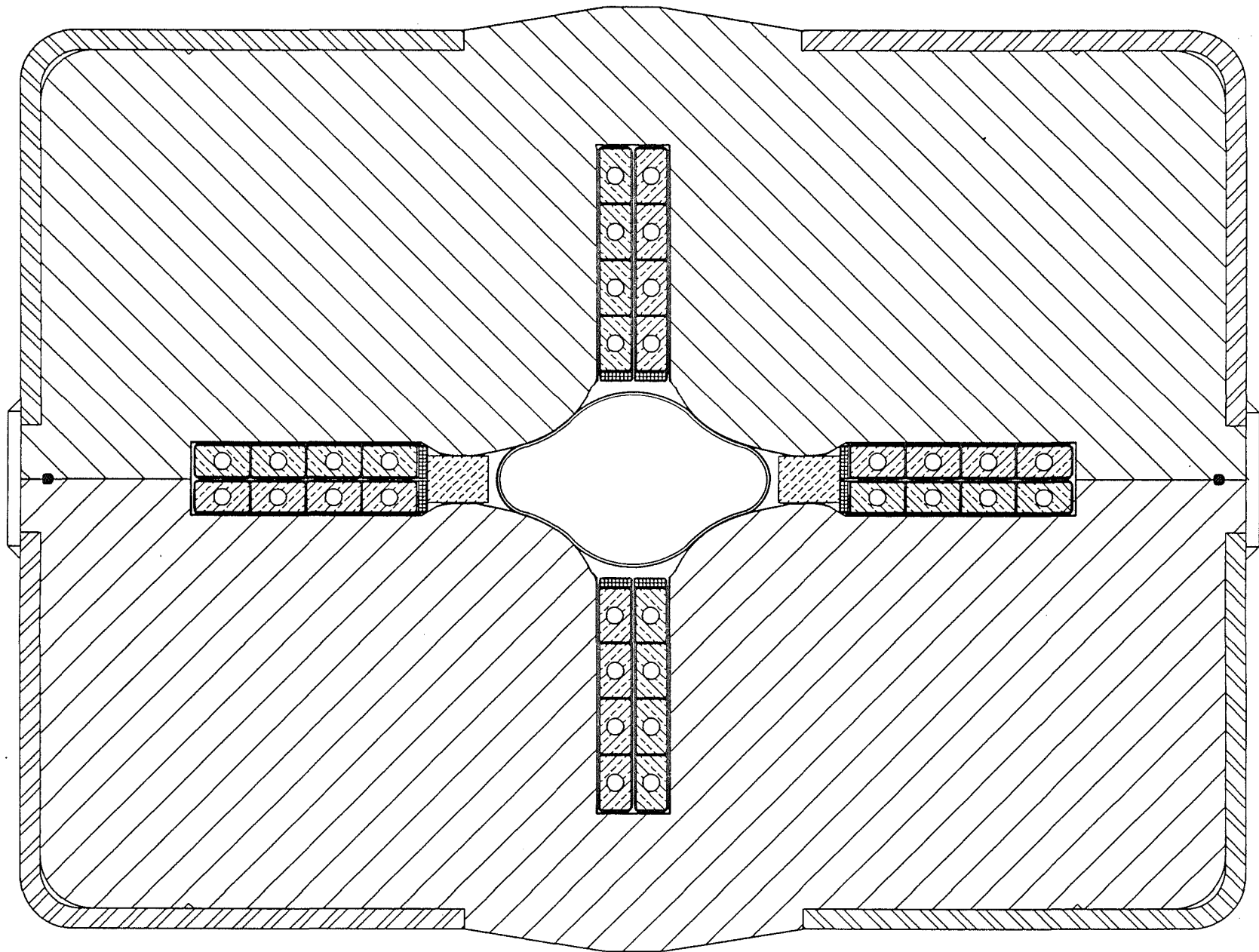


Figure 3.1-20. Cross-Section of Main Injector Quadrupole

However, the transformer coupling of the main and trim coils presents its own challenges for the power supply design. Figure 3.1-21 shows the lead end of a new quadrupoles, including the manifolding and routing of the main coil and of the trim coil conductor.

Table 3.1-8
Main Injector Ring Quadrupole Magnet Parameters

	IQD	IQC	BQB
Length (meters)	2.945	2.539	2.134
Strength (Tesla/m)	19.6	19.6	19.6
Int. strength (T-m/m)	57.79	49.83	41.87
Pole radius (in)	1.643	1.643	1.643
Pole radius (mm)	41.74	41.74	41.74
Turns/pole	4	4	4
Peak Current (A)	3630	3630	3630
RMS Current (A)	2000	2000	2000
Coil resistance (mΩ)	6.1	5.2	4.5
Coil inductance (mH)	1.8	1.5	1.3
Peak power (kW)	70	60	52
RMS power (kW)	24.4	20.8	18
Conductor Dim. (in x in)	.565 x 1.0	.565 x 1.0	.565 x 1.0
Cond. Hole Diameter (in)	.312	.312	.250
Number used	48	32	128*
Weight (kG)	5852	5046	4082
Trim Coil Turns/Pole	16	16	0

* One quadrupole, Q101, located adjacent to the injection Lambertson at MI-10, will be rolled 90° to provide adequate vertical aperture for the injected beam.

Lamination design

The original Main Ring quadrupole lamination was designed to be free from octupole contamination. Imperfections in the die led to a negative octupole component of the field. Most Main Ring quadrupoles were modified by milling 0.25 mm from the back legs of one half core, producing an octupole component of, typically, +5 units. A new die, of significantly inferior

technical quality, was built, incorporating a change of 0.25 mm in the back leg compared to the original design (not compared to the original die actually used).

For slow extraction at 120 GeV/c, the existing octupole correction elements require the assistance of at least +1 unit of octupole in the new quadrupoles. Accelerator tracking calculations indicate that beam stability is improved if the new quadrupoles have an octupole component of less than +3 units at all excitations. A larger octupole component can be corrected for with some effort. In the course of a long series of tests, we have modified the original Main Ring quadrupole die by removing about 0.12 mm from the back legs of the die. We now have an octupole component comparable to the Main Ring quadrupoles.

Lengths

The lattice design uses quadrupoles with integrated strengths in the ratio of 2.1336 m : 2.5433 m : 2.9530 m (84.00" : 100.13" : 116.26"). Lattice studies [1] indicate that there is no significant variation in the machine beta function and dispersion if the integrated strengths of the longer magnets systematically deviate by 10 parts in 10^4 . A systematic difference of 25 parts in 10^4 would be noticeable but tolerable.

The effective length of a quadrupole, the integral of the gradient through the magnet divided by the gradient in the center, is often not exactly equal to the length of the steel. To determine the steel length needed for the new quadrupoles, we must know the desired integrated strength, the central gradient, and the contribution of the ends. If we assume that the gradient of the new quadrupoles is the same as that of the old, then we need only know the desired effective length and the contribution of the ends.

To the extent that any of these numbers vary with current in a way other than linearly, we can only do our best at one current where which we match the strengths. We choose to try to match at 120 GeV/c, the slow extraction momentum, because everything is most sensitive there. This corresponds to a current of about 2900 A and a gradient of about 15.7 T/m.

The initial analysis [2] compared 84" and 52" Main Ring quadrupoles measured in 1986 and 1987, attributing the integrated strength to a body component proportional to the stacked lamination length and an end component independent of length associated with the end plate. The effective length of each end, measured from the last lamination, was 28 mm per end. This means that the effective length of the 84" quads (81" of laminations = 2.0574 m) is 2.1136 m. That is 20 mm shorter than the physical length of 2.1336 m.

FMI 100" IQC AND 116" IQD QUADRUPOLE
LEAD END VIEW

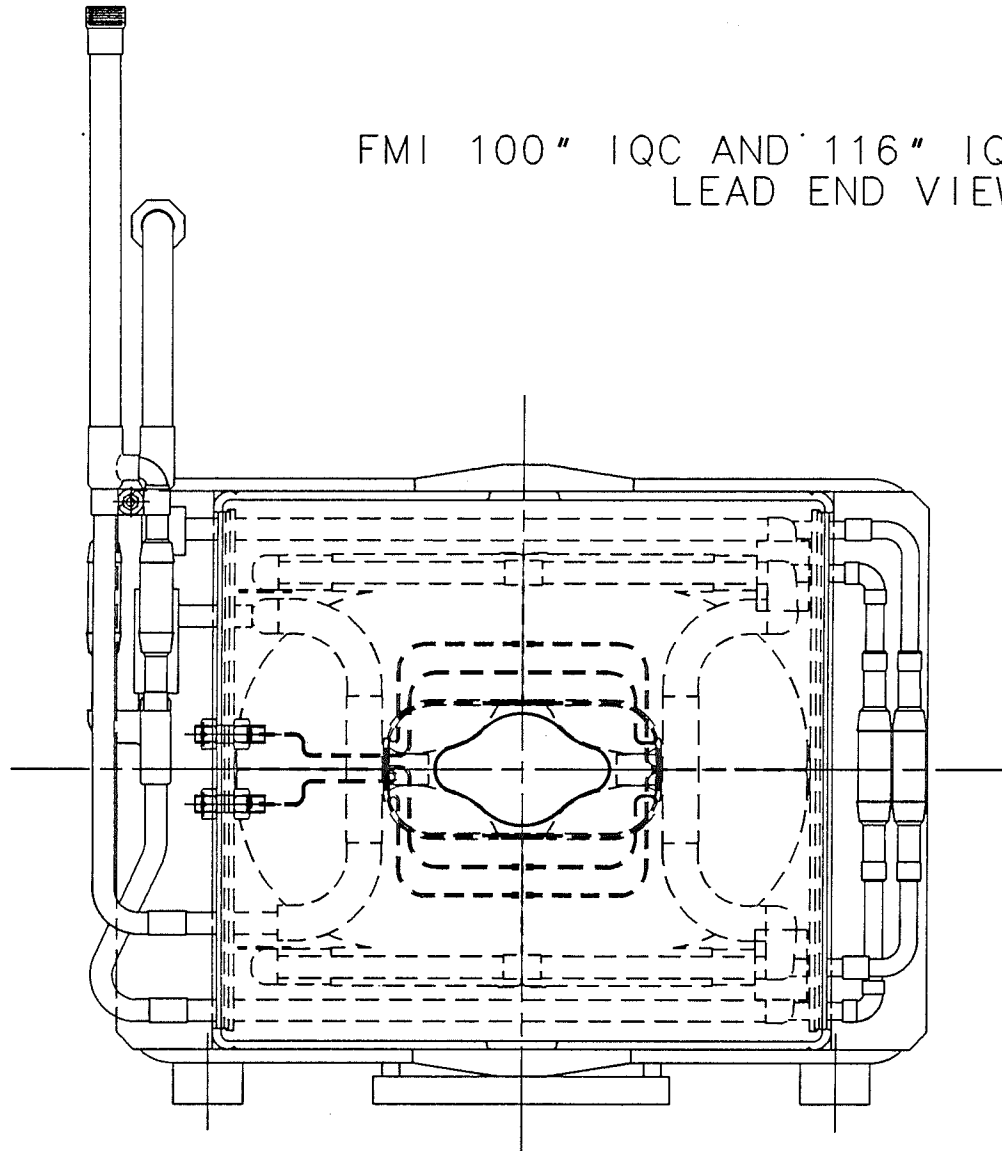


Figure 3.1-21. Lead-End View of Main Injector Quadrupole

FMI 116" IQD QUADRUPOLE
SIDE VIEW

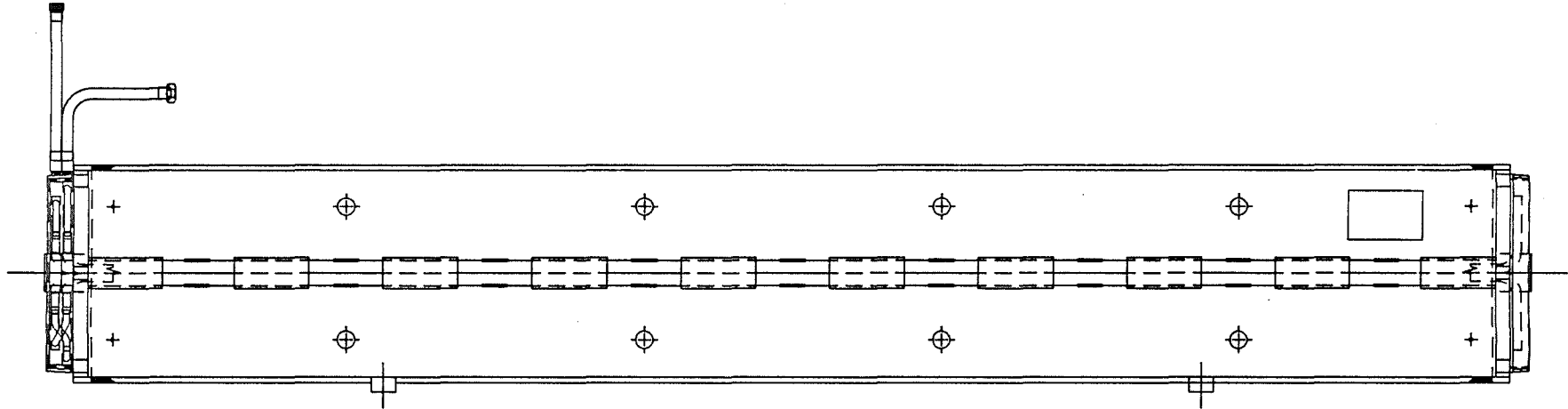


Figure 3.1-22. Side View of Main Injector 116"-Quadrupole

If the effective length of the BQB is 2.1136 m and if the gradient of the new quads is the same as that of the BQB, then from the strength ratios above, the effective length of the IQC should be 2.5313 m and the effective length of the IQD should be 2.9390 m. Adding the effective length of the ends leads to a steel length of 2.5394 m (99.976") and 2.9452 m (115.953") for the IQC and IQD. A side view of the the IQD quadrupole is shown in Figure 3.1-22.

Changing the lamination by reducing the back leg increases both the octupole and the gradient rather linearly over the range under consideration. In our effort to adjust the octupole, we have removed enough steel from the original die to match the Main Ring quadrupole closely. The gradient is therefore matched as well, and the calculation above stands.

Measurements of a sample of Main Ring quadrupoles were made in 1986 and 1987. These can be compared with measurements made on the early production IQCs [3]. To achieve the precision desired, it was necessary to remeasure two Main Ring quadrupoles to carry the current readout calibration from 1986 to 1994. From these measurements and analysis we concluded that the initial length determination was adequate. The tracking studies show that a satisfactory ring can be built from magnets with an RMS of 12 units in strength.

At the time of this writing, two IQC quadrupoles had been completed and measured. The strength and octupole component of the field are acceptable. The transfer function (integrated gradient divided by current) is shown in Figure 3.1-23. Note that saturation is beginning to set in above 3000 A. Plots of the normal and skew harmonic components of the field as a function of current are shown in Figure 3.1-24(a) and Figure 3.1-24(b). We note that the variation in the multipoles as a function of current below saturation is unexpected but does not degrade the accelerator performance.

We expect that in these steel and copper quadrupoles the magnetic center will be determined by the steel, lying in the geometric center of the core. Since the lamination edges are exposed in a sufficient variety of places, alignment of the magnet can be done relative to the laminations. Recent measurements of two Main Ring quadrupoles suggest that there may be a systematic deviation of the magnetic center from the geometric center of 0.25 mm [4]. We plan to measure the magnetic center of each of the first ten IQC quadrupoles to better understand the issue. If necessary, the offset between the magnetic and geometric centers will be measured for each quadrupole so that magnets can be properly placed in the tunnel. An efficient system for measuring centers is under development by Magnet Test Facility.

FMI Quadrupole Transfer Function

IQC010

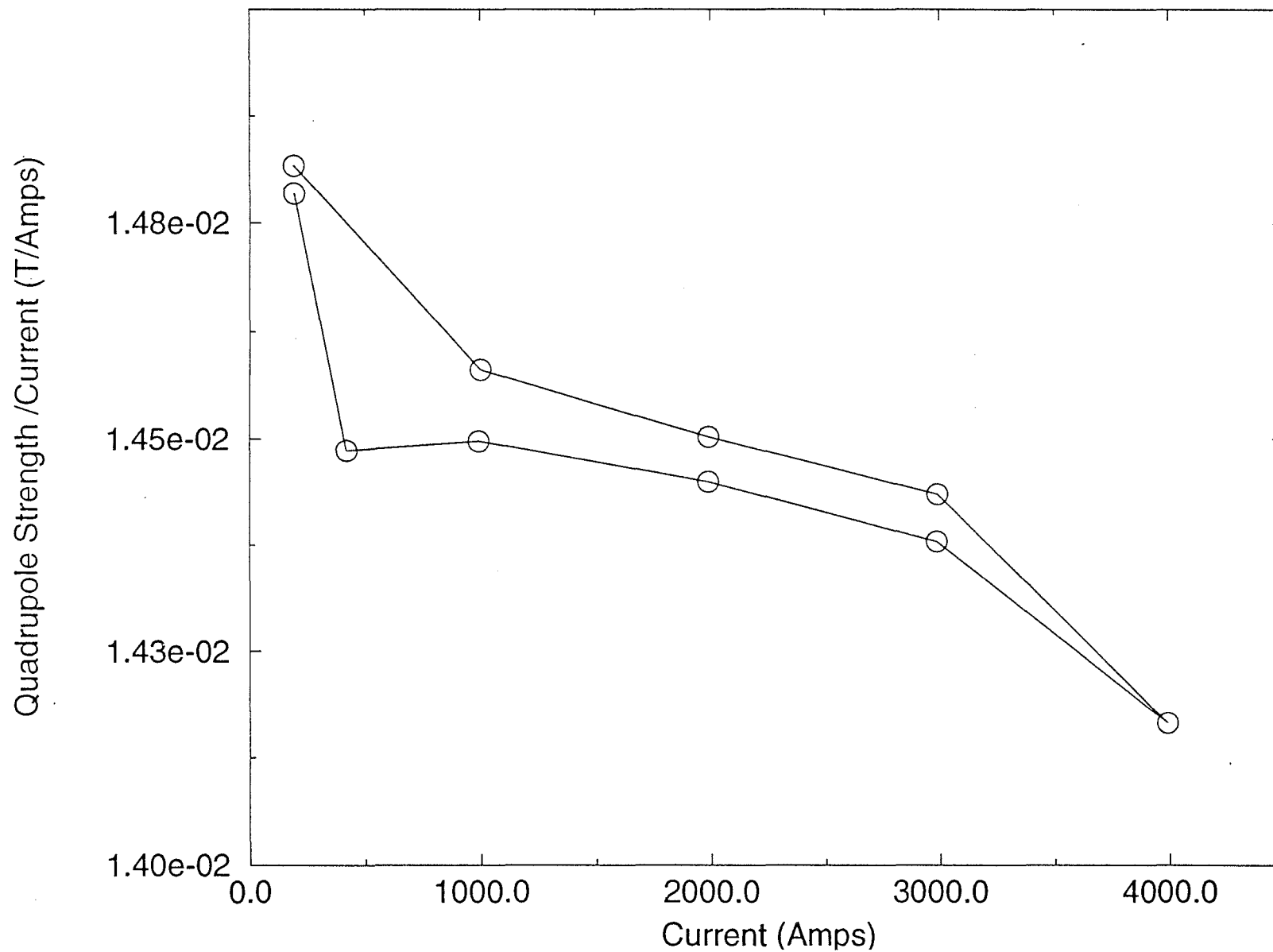


Figure 3.1-23. Transfer Function of Main Injector Quadrupole

FMI Quadrupole Normal Multipoles

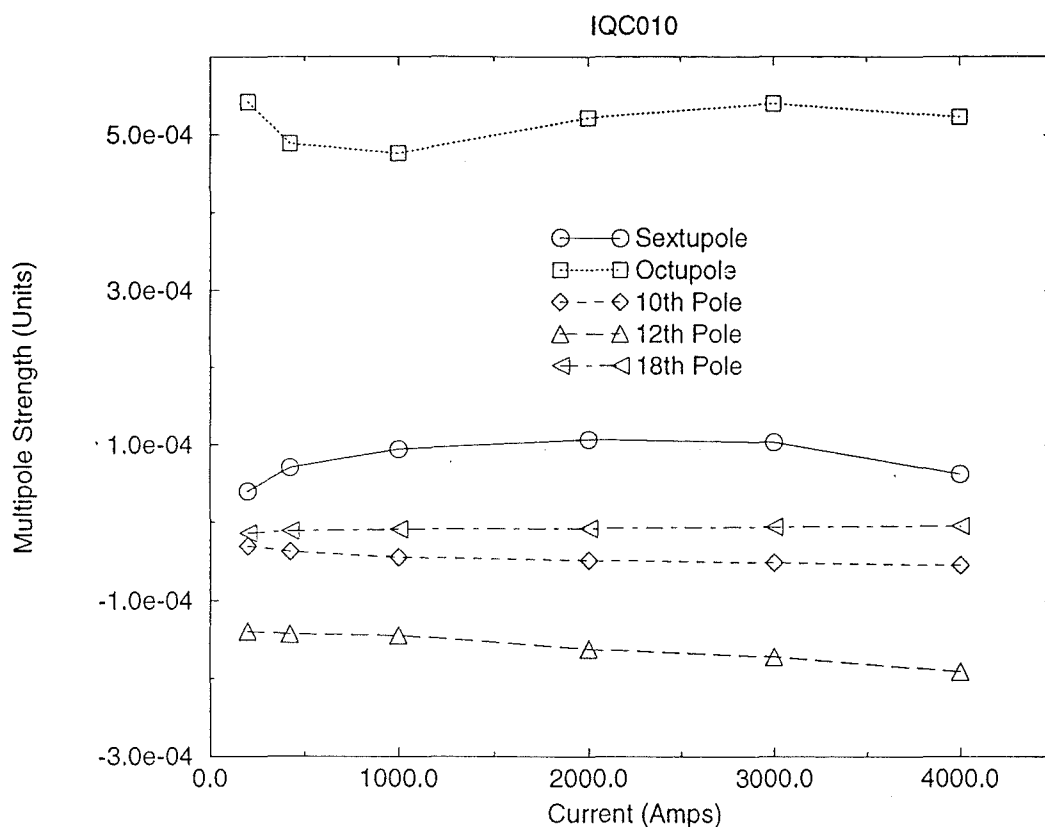


Figure 3.1-24(a). Current Variation of the Normal Harmonics of Main Injector Quadrupole

FMI Quadrupole Skew Multipoles

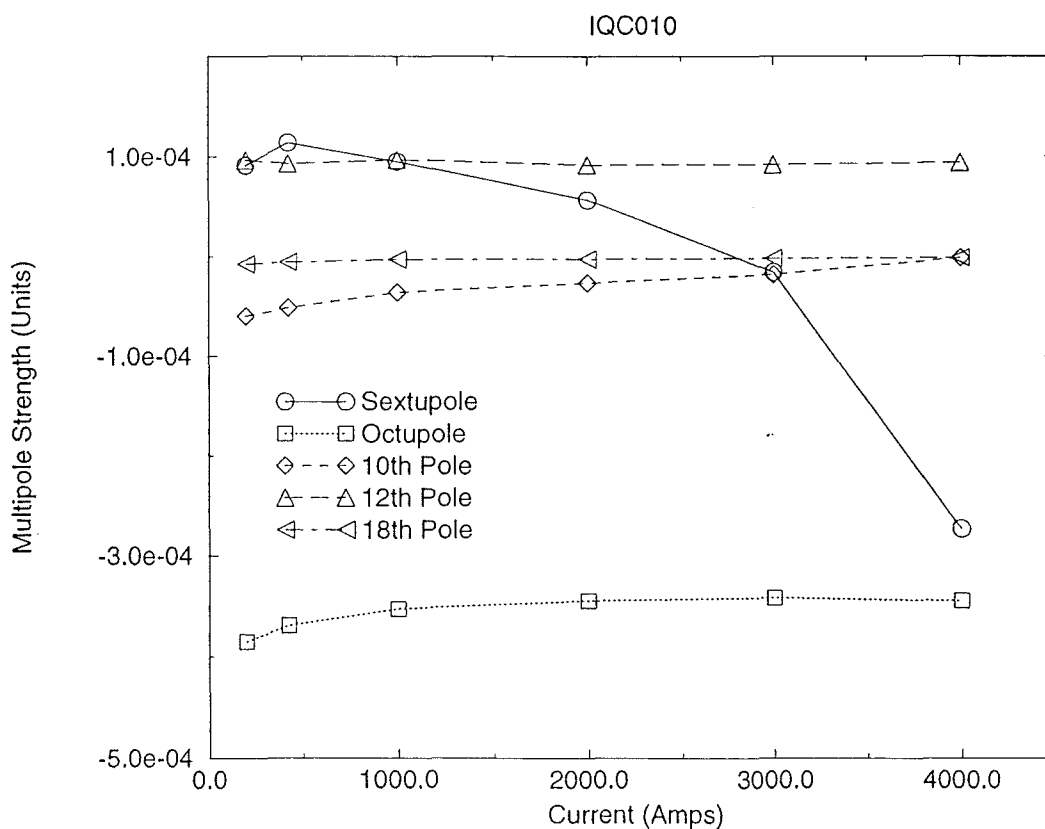


Figure 3.1-24(b). Current Variation of the Skew Harmonics of Main Injector Quadrupole

Schedule

We built one prototype of each length in late fiscal year 1993, using the original Main Ring die and some rather soft steel. Magnetic measurements led to a full appreciation of the impact of the imperfections in that die. Further accelerator calculations led to revision of the requirements to the current understanding. Additional studies on spare Main Ring quadrupoles and the first production Main Injector quadrupoles resulted in the current design.

Fermilab will build the quadrupoles on the schedule shown in Figure 3.1-25. In production the quadrupoles can be assembled at the rate of one every four days, working one shift. A partial second shift would increase the rate to one every three days. A small investment in additional tooling would allow production of one every two days. All new quadrupole construction will be complete and the magnets will be installed well before the shutdown.

Magnetic testing

Every quadrupole will be thoroughly tested promptly after assembly. This will assure that every magnet installed meets the magnetic requirements of the project. Subtle manufacturing problems can be indentified early and corrected. Additional improvement of the accelerator performance can be achieved by assigning magnets to locations in the ring based on their magnetic properties. Finally, measurements on every magnet will allow improved accelerator modeling.

As with the dipoles, the plan, the conditions, the raw data, the intermediate calculations, and the final results for every measurement will be stored in a database. This information will be readily accessible for further analysis and use by physicists and others in the Magnet Test Facility and the Accelerator Division.

A rotating Morgan coil will be the primary measurement tool. A full excitation curve will be taken from zero current, through the operating range, up to higher currents, and back to zero. The harmonic components of the field will be measured at all critical currents and at appropriate intermediate currents.

A second technique, involving movement of a stretched wire, will complement the rotating coil. The integrated gradient and the variation of the field with horizontal position (at least) will be measured with the second technique to provide continuous cross-calibration and redundancy in the measurements. This system will also address the possible need to determine the location of the magnetic center with respect to the laminations.

FMI INTEGRATED SCHEDULE Rev-none

T J Gardner

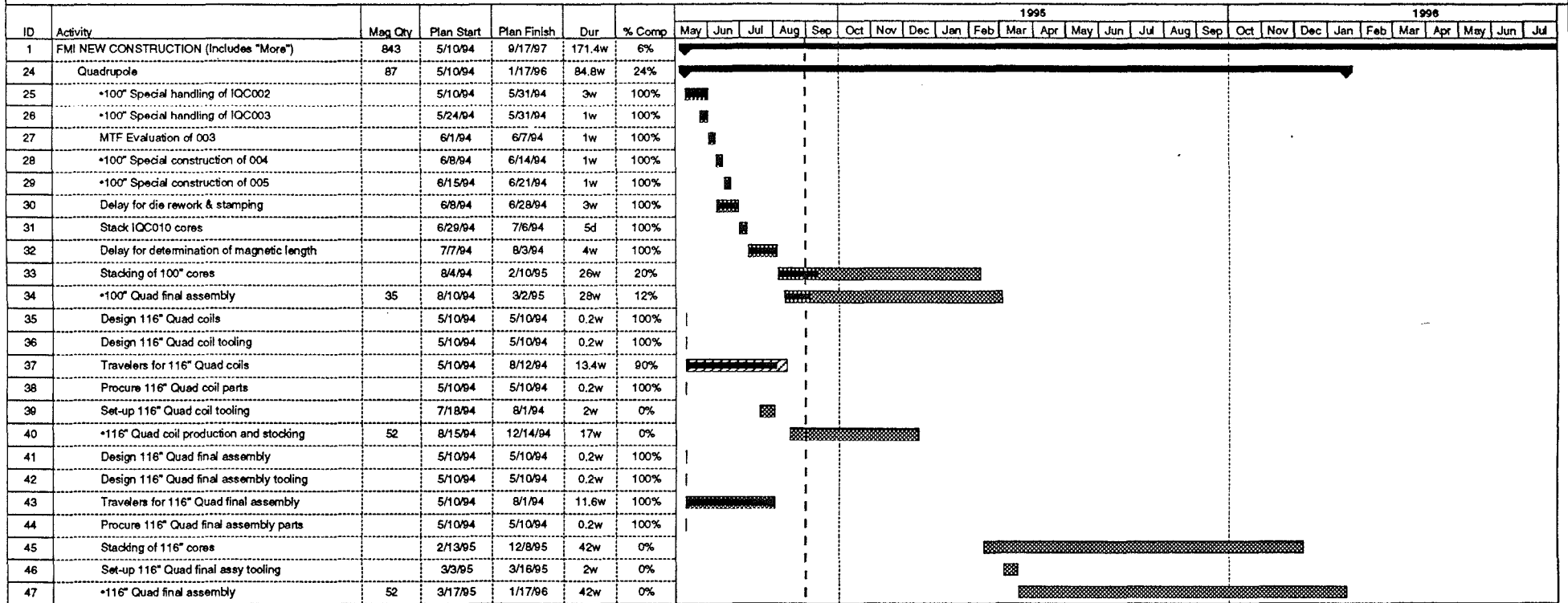


Figure 3.1-25. Schedule for Production of Main Injector Quadrupoles

Project: FMI INTEGRATED SCHE
Date: 8/30/94

Critical Noncritical Progress Milestone Summary Rolled Up

In production the measurements should take no more than a single shift. There should be no difficulty keeping up with the planned production rate of five quadrupoles per month.

Acceptance criteria

Dimensional, electrical, and water flow values are measured during production. Any values that are out of the tolerance range are reviewed by a project physicist to assess the impact of the deviation on the project and to determine the response. This will ensure that all magnets are acceptable.

As with the dipoles, all of the magnetic data will be analyzed while the magnet is on the test stand by the measurement technician. The integrated strength and harmonic components will be plotted as a function of current and compared to limits by the computer program. Measurements that fall outside of a tight normal range will be repeated, as will a sample of measurements within the range.

Measurements which fall outside of the nominal tolerances for the accelerator will be examined closely to determine the cause of the discrepancy. Each out of tolerance magnet will be assessed for the cost, schedule, and accelerator performance impact of accepting, reworking, or totally rejecting it.

WBS 1.1.1.1.2.5. 2.13-METER MAIN RING QUADRUPOLES

Most of the quadrupoles in the FMI ring arcs are reused 2.13-m (84-inch) Main Ring quadrupoles. The 2.13-m quads in the Main Ring are of two styles, "old" and "new". The old style has a small negative octupole component. The "new" style quads have about 0.25 mm milled from the backleg of the top half-core, resulting in an octupole component averaging +5 units. For the sake of uniformity and to help provide the octupole needed for resonant extraction, only new-style quads are reused in the FMI ring. The basic properties are shown in Table 3.1-8.

There are 180 new style quads and 12 old style quads in the Main Ring. 128 new style quads are needed for the Main Injector ring and 48 of either style for beam lines. This allows a selection of magnets for use in the ring based on magnetic, electrical, and mechanical properties.

Earlier analysis of old Main Ring quadrupole measurements suggested that the distribution of strengths in those magnets had a sigma of 24 parts in 10^4 , although a recent reanalysis of the data shows that the distribution width was probably inflated due to power supply calibration drifting. Tracking studies [5] show that a satisfactory ring can be built with magnets selected from the population of Main Ring magnets if they have this distribution. It will be necessary, however, to measure each magnet and select the middle two-thirds of the distribution for use in

the ring. The high half of these will go on one power supply bus and the low half on the other bus, further narrowing the distribution of strengths.

One of the quadrupoles will need to be mounted with an orientation rolled 90 degrees from usual to increase the vertical aperture for the beam just downstream of the injection Lamberton magnet. One magnet and one spare with this rolled configuration exist in the present Main Ring.

The Main Ring quadrupoles used in the FMI ring require two major modifications: The support structure and the vacuum system need to be changed. In the Main Ring the quadrupoles are supported by a long cradle welded to the magnet which holds the correction elements. For the FMI, these cradles are cut off and replaced by feet on the bottom which mate to a three-point support on a long cradle. The correction elements then mount on the same cradle. This is described in more detail in Chapter 3.10, Installation.

The vacuum system must also be modified to match the FMI system. The end connections are cut off flush and a new vacuum pipe is slid into the magnet. The new pipe is the same shape and dimensions as that used in the dipoles, reducing the impedance seen by the beam at shape transitions. The beampipe carries the beam position monitor pickups in the quadrupoles. (See Chapter 3.6) As discussed in the sections below on beam line magnets, those quadrupoles will not receive the same modifications. Therefore, it will be necessary to identify each magnet's destination before the reworking begins.

Additionally, the water and power manifolding will be carefully examined and replaced if necessary. This has been a frequent problem with quadrupoles removed from the Main Ring in less than ideal circumstances. We hope that with planning and care this damage can be minimized, but we have budgeted for reworking the manifolding on all quadrupoles.

Schedule

Removing, testing, modifying, retesting, and reinstalling these quadrupoles will be one of the major challenges of the installation period between shutting down the Main Ring and beginning to commission the FMI. The detailed schedule has not been fully worked out, but the following is a plausible outline. It is charted in Figure 3.1-26.

The removal of the quads can be done quite rapidly. They will not pose a limit on the schedule except during the first few weeks when all of the mechanical work will be focussed on preparing the F0 region for the civil construction. The quadrupoles will have been running immediately before the shutdown period and will thus be known to be in good shape electrically.

Each one will be tested electrically after being disconnected and will be visually inspected for potential problems before being moved.

Starting approximately three to four weeks after the shutdown begins, magnets ready for testing will arrive at the Magnet Test Facility. At MTF all of the quadrupoles will be tested quickly to identify their probable destination. The primary consideration will be the quadrupole strength at 120 GeV excitation, with octupole component secondary. An adequate set of measurements can be run in one hour. Allowing two hours for changeover, each measurement stand can easily measure three quads in two shifts per day. With two test stands running in parallel, we can measure six magnets a day, or 30 magnets/week. In fact, it is easy to imagine doubling the rate. At the lesser rate, all 180 "new-style" quadrupoles can be measured in six weeks.

We will accumulate as large a collection of measured quadrupoles as possible before starting the selection and rework process to establish the center and width of the strength distribution. Those magnets selected for the ring will be reworked at Industrial Building 2. The modifications detailed above for ring magnets are estimated to take 60 worker-hours/magnet. With 30 workers at 40 hours/week, we can rework 20 magnets/week. The 128 magnets required for the ring can be processed in seven weeks, starting three weeks after magnet testing begins.

After the reworking, the magnets selected for the ring will be retested at MTF, undergoing a slightly more extensive set of tests, starting as the first pass measurements are complete. Even if the testing rate drops to one shift per magnet, two testing stands allow us to keep up with the magnet reworking, lagging at most three weeks behind.

We may want to again accumulate a sample before starting to assign magnets to tunnel locations, although we will quickly know the correlation between the before and after strength measurements. If that delay is two weeks, then we can start installation twelve weeks after the start of the shutdown and finish nineteen weeks after the start of the shutdown.

Reworking the quadrupoles for the beamlines will either follow the ring quadrupoles or run in parallel. They will not require remeasurement after reworking.











ID	Name	cheduled Start	cheduled Finish	November 1997					December 1997					January 1998				February 1998				March 1998				
				26	2	9	16	23	30	7	14	21	28	4	11	18	25	1	8	15	22	1	8	15	22	
3	Clear F0	11/3/97	11/21/97																							
5	Remove new style quads from tunnel	11/24/97	1/1/98																							
6	Remove old style quads from tunnel	12/1/97	12/4/97																							
7	Clean up quads	11/25/97	1/2/98																							
9	First pass MTF measurement	11/27/97	1/6/98																							
11	Rework old style quads	12/4/97	12/12/97																							
12	Rework new style quads for ring	12/17/97	2/3/98																							
13	Rework new style quads for beamlines	2/3/98	2/10/98																							
15	MTF final measure ring quads	1/6/98	2/19/98																							
17	Install ring quads in MI tunnel	1/16/98	3/13/98																							

Figure 3.1-26. Schedule for Rework of Main Ring Quadrupoles

Project:
Date: 8/12/94

Critical



Noncritical



Progress



Milestone



Summary



Rolled Up



WBS 1.1.1.1.3. HARMONIC CORRECTORS

Wherever possible, existing components are reused from the Main Ring, with minimal modifications. The sextupoles require substantially more strength than is available from the Main Ring sextupoles, so a new design is required. The measured magnet strengths are summarized in Table 3.1-10.

WBS 1.1.1.1.3.1 CHROMATICITY SEXTUPOLES

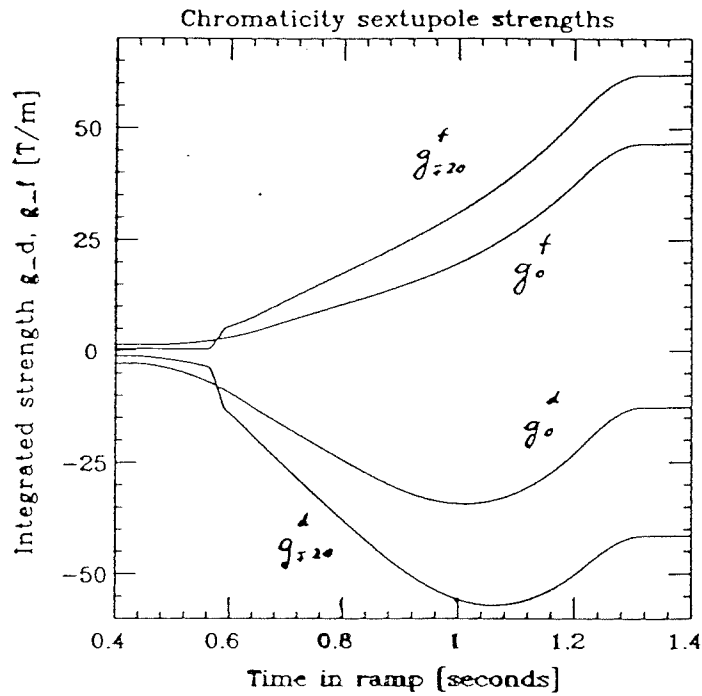
Requirements

The chromaticity sextupole magnets for the FMI are a new design, tailored to the geometrical, optical, and electrical requirements of the Main Injector. The natural chromaticities of the FMI are -33.65 horizontally and -32.87 vertically. The lattice has been designed to have low β and η (58 m and 1.9 m are the maximum values in the arcs). Thus, very strong sextupoles will be needed to cancel the natural chromaticity. The configuration chosen places an F(D) sextupole at each F(D) main quadrupole in the arcs where η is large. There are also large sextupole components in the dipole magnet induced by saturation of the steel as the beam energy approaches 150 GeV and by eddy currents in the beam pipe. These effects produce "natural" chromaticities of -77 horizontally (at 150 GeV) and -55 vertically (near 20 GeV). The correction sextupole magnets must be capable of compensating for all these effects.

Based on a requirement that the sextupoles be capable of producing a corrected chromaticity of +10 in each plane through the entire ramp, the sextupoles need to have a maximum field strength of 55 T-m/m² [6]. Geometric considerations lead to a steel length of 0.46 meters (18 inches), implying a field strength of 120 T/m², ignoring end effects. The desire to limit the power bus led to an attempt to keep the rms current under 200 A except for the short duration Tevatron injection cycles where it can peak at 300 A. The beam pipe size limits the dimensions of the pole faces. The magnet was designed for 120 T/m² at 300 A, assuming infinite permeability steel with the expectation that the end contribution would more than compensate. The integrated sextupole field has been measured as 59.3 T-m/m² at 293 A, or 0.202 T-m/m²/A. The anticipated ramp waveforms for the F and D circuits, which have been recalculated based upon the final dipole endpack geometry, are shown in Figure 3.1-27.

Design and Assembly

The cross section of the sextupole is shown in Figure 3.1-28. End and side views are shown in Figures 3.1-29(a) and 3.1-29(b). To reduce the resistance and inductance of the magnet the design is not six-fold symmetric, but rather matches the beam pipe with top and bottom poles



150 GeV Ramp

$\xi = -20$ below Transition

$\xi = +20$ above Transition

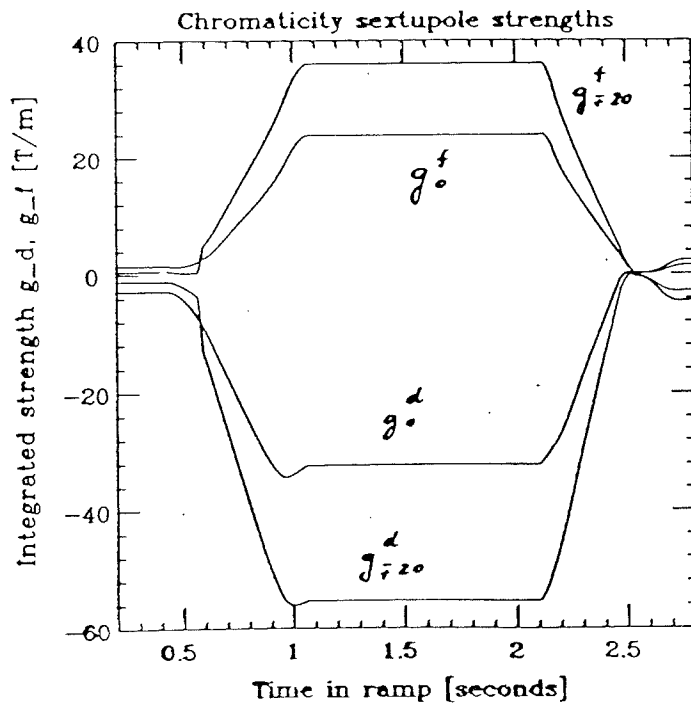
Max. $I_f = 331$ A

Max. $I_d = -304$ A

$\xi = 0$

Max. $I_f = 249$ A

Max. $I_d = -183$ A



120 GeV Ramp

$\xi = -20$ below Transition

$\xi = +20$ above Transition

RMS $I_f = 133$ A

RMS $I_d = 211$ A

$\xi = 0$

RMS $I_f = 87$ A

RMS $I_d = 125$ A

Figure 3.1-27. Excitation Curves for Main Injector Chromaticity Sextupoles

FMI SEXTUPOLE MAGNET
CROSS SECTION VIEW

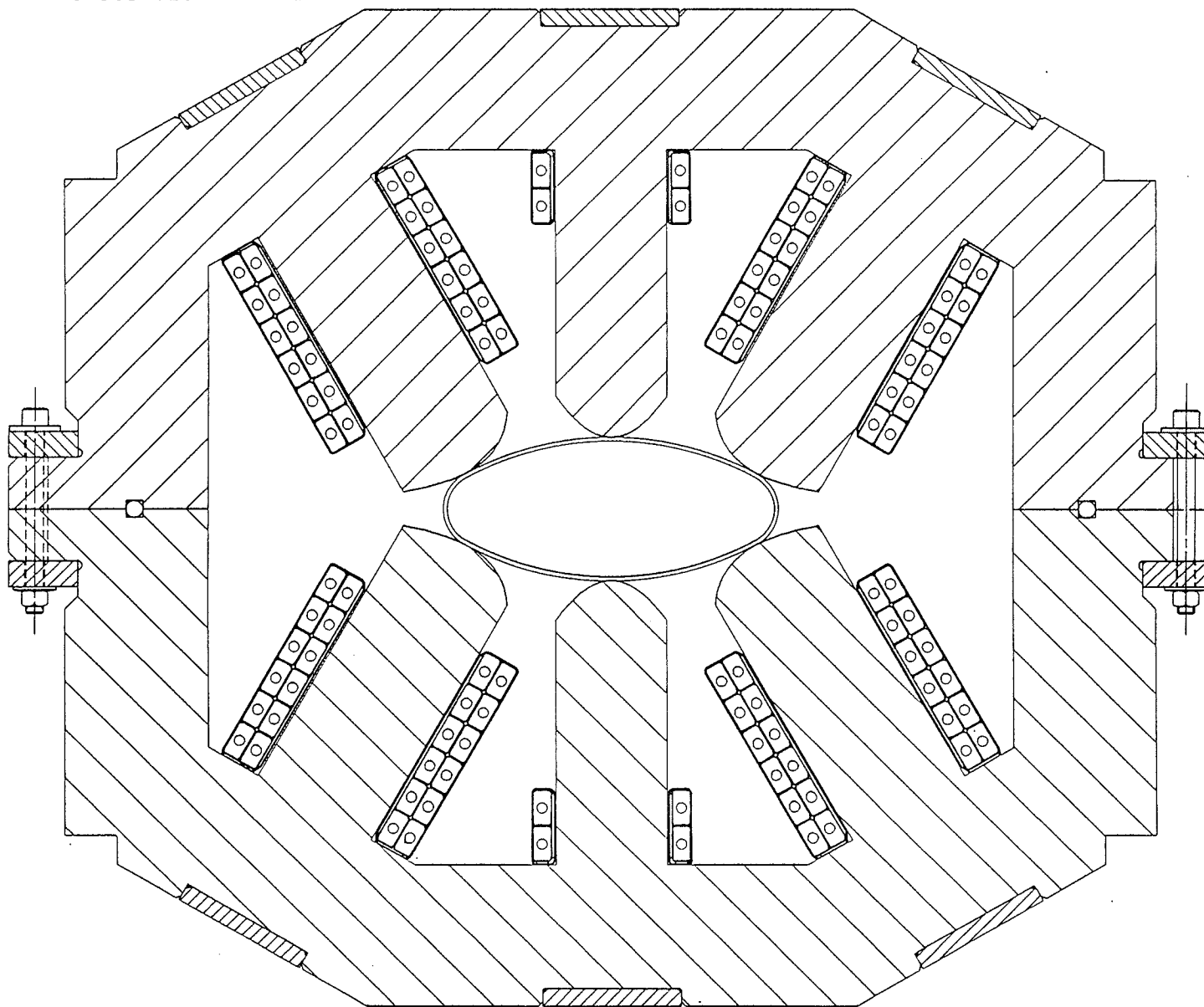


Figure 3.1-28. Cross-Section of Main Injector Sextupole

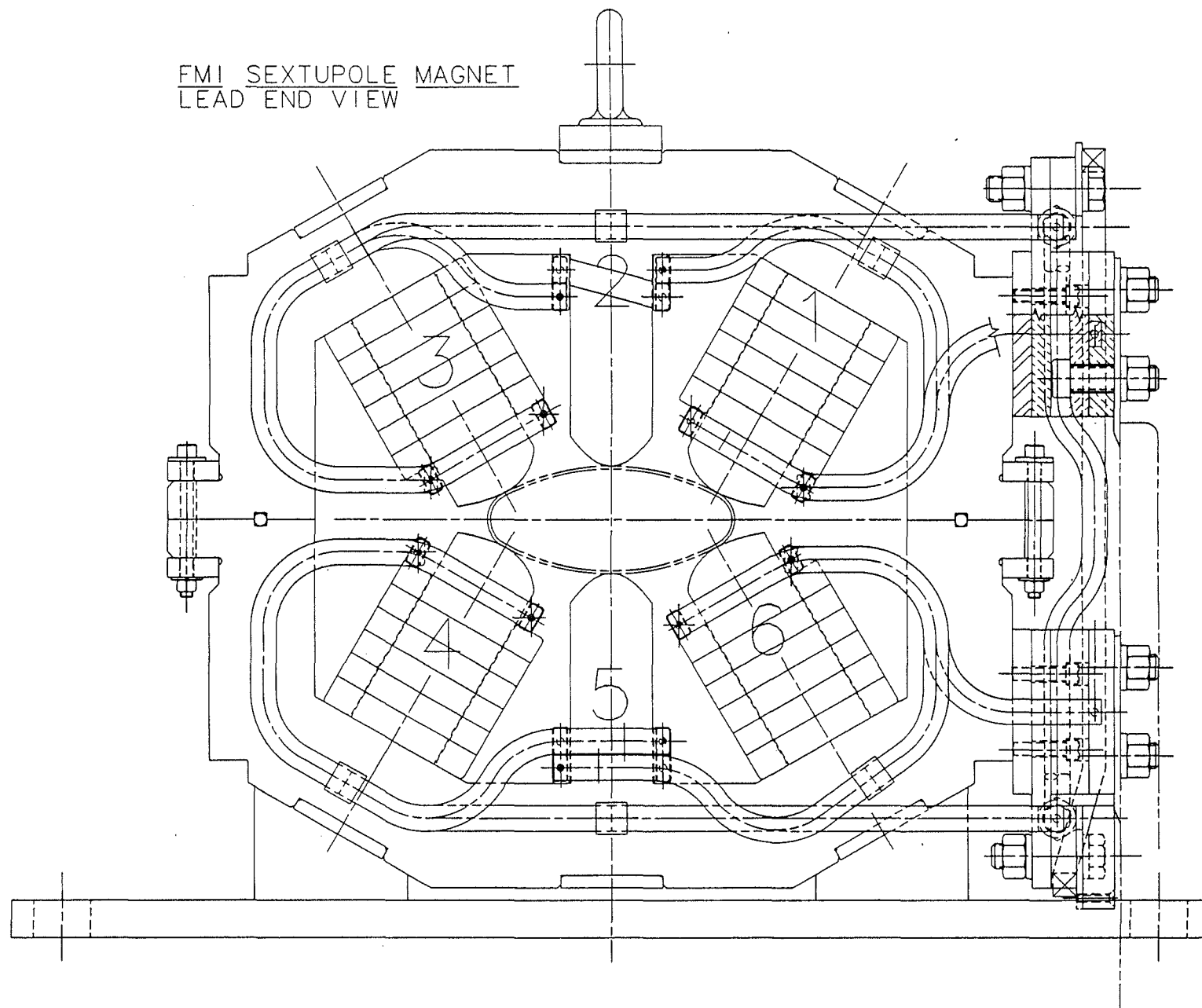


Figure 3.1-29(a). Lead-End View of Main Injector Sextupole

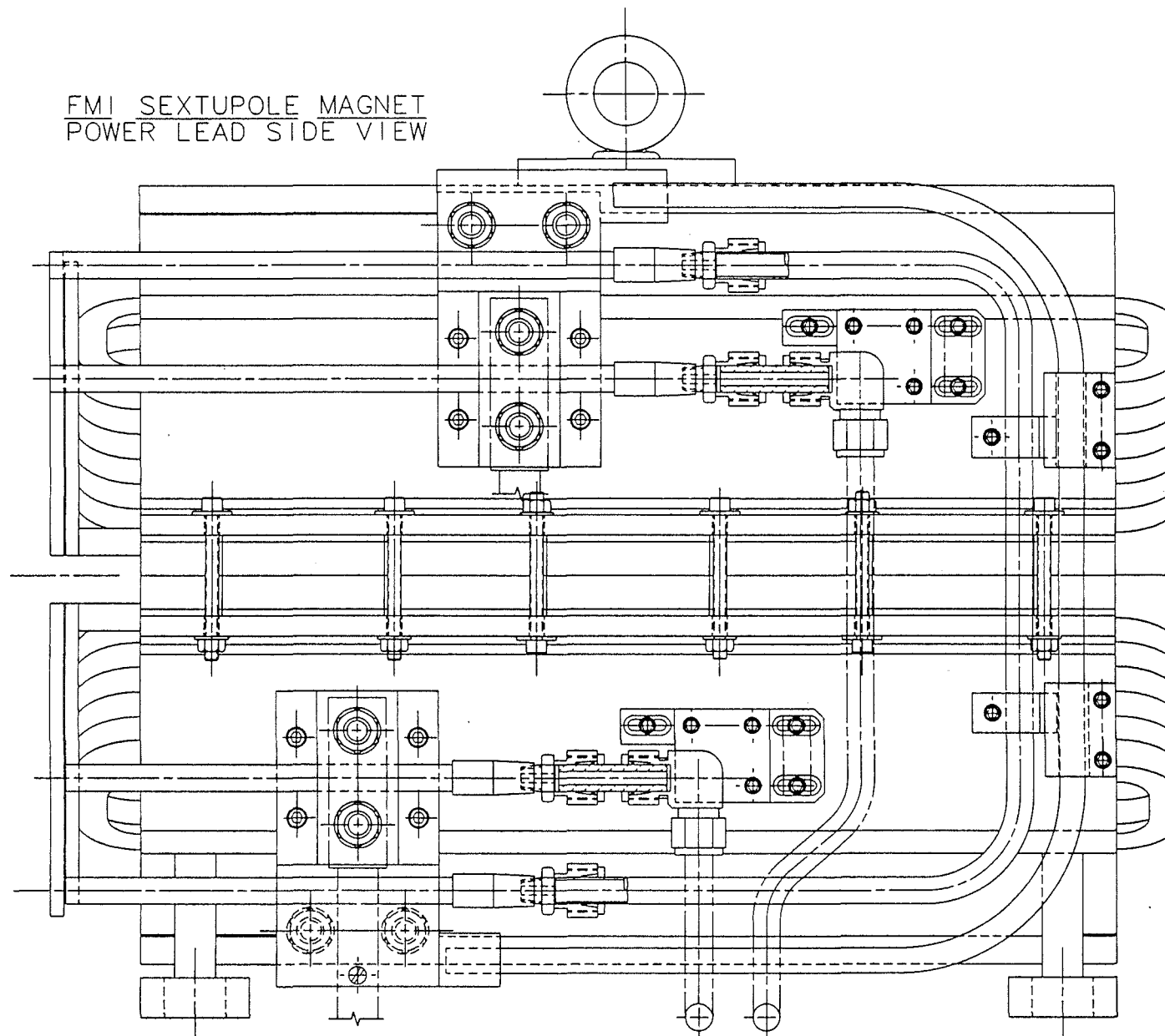


Figure 3.1-29(b). Side View of Main Injector Sextupole

that are closer to the axis than are the side poles. The number of turns on the top and bottom poles is correspondingly smaller. The properties are summarized in Table 3.1-9.

The sextupoles must be assembled around the beam tube after the beam tube is in place in the tunnel. The top and bottom halves of the magnets, therefore, are designed to be bolted together. The electrical and water connections from top to bottom are made with jumpers installed in the tunnel.

The half cores are stacked on a small hydraulic press. The outside edges are held together by welded tie bars. A 6 mm (0.25") carbon steel rod, threaded at each end, runs through a hole in each pole to maintain the compression at the poles. The conductor is insulated commercially before winding, first with a layer of Kapton, then with a layer of fused polyester tape. After the coils are wound, a ground layer of dry fiberglass tape is wrapped around them. The whole coil is then impregnated with epoxy and cured.

Table 3.1-9. Properties of the Main Injector Sextupoles

		Side poles	Top/bottom poles
Steel length (meters)	0.457		
Steel length (inches)	18.0		
Stength (T/m ²)	120		
Integrated strength (T-m/m ²)	55.0		
Physical length (including coils) (inches)	21.0		
Distance to pole (inch)		1.890	1.040
Distance to pole (mm)		48.0	26.4
Turns/pole		12	2
Weight (lb)	860		
Resistance (mΩ)	17		
Inductance(mH)	2.8		
Conductor dimensions (in x in)	0.25 x 0.50		
Conductor hole diameter (in)	0.150		
Current (A)	300		
Peak Power (kW)	1.4		
RMS Power (kW)	0.6		
Water Flow @ 100 psid (gpm)	0.2		
Number used	108		

FMI Sextupole Transfer Function

ISA002

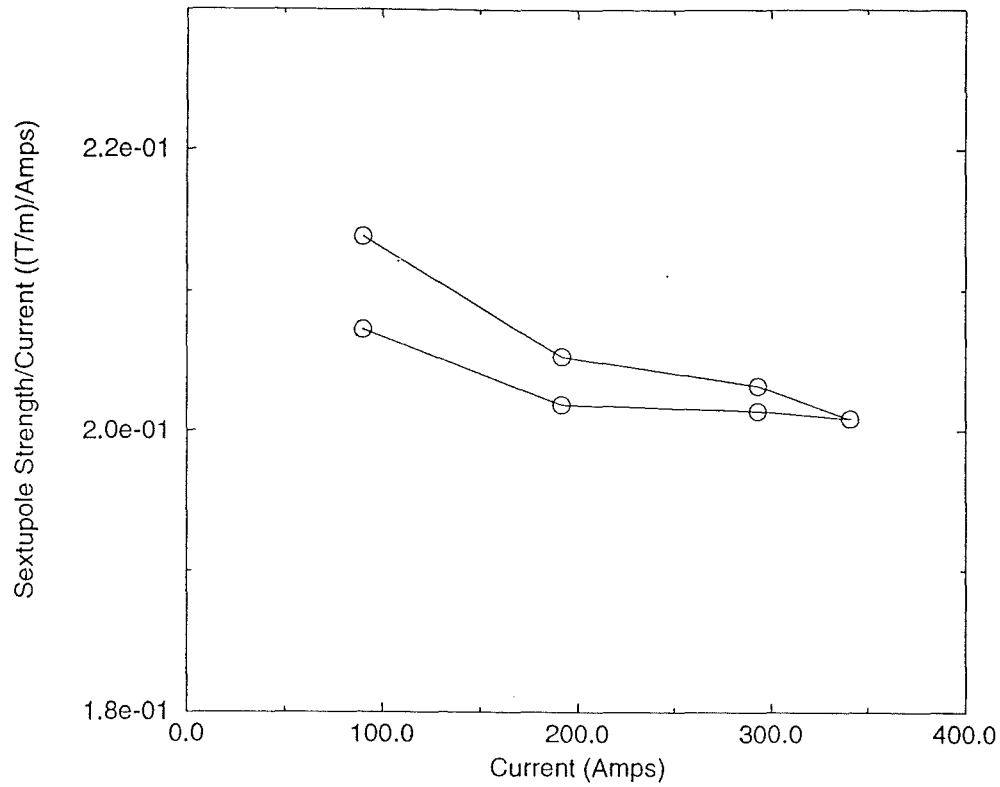


Figure 3.1-30(a). Transfer Function of Main Injector Sextupole

FMI Sextupole Multipole

ISA002

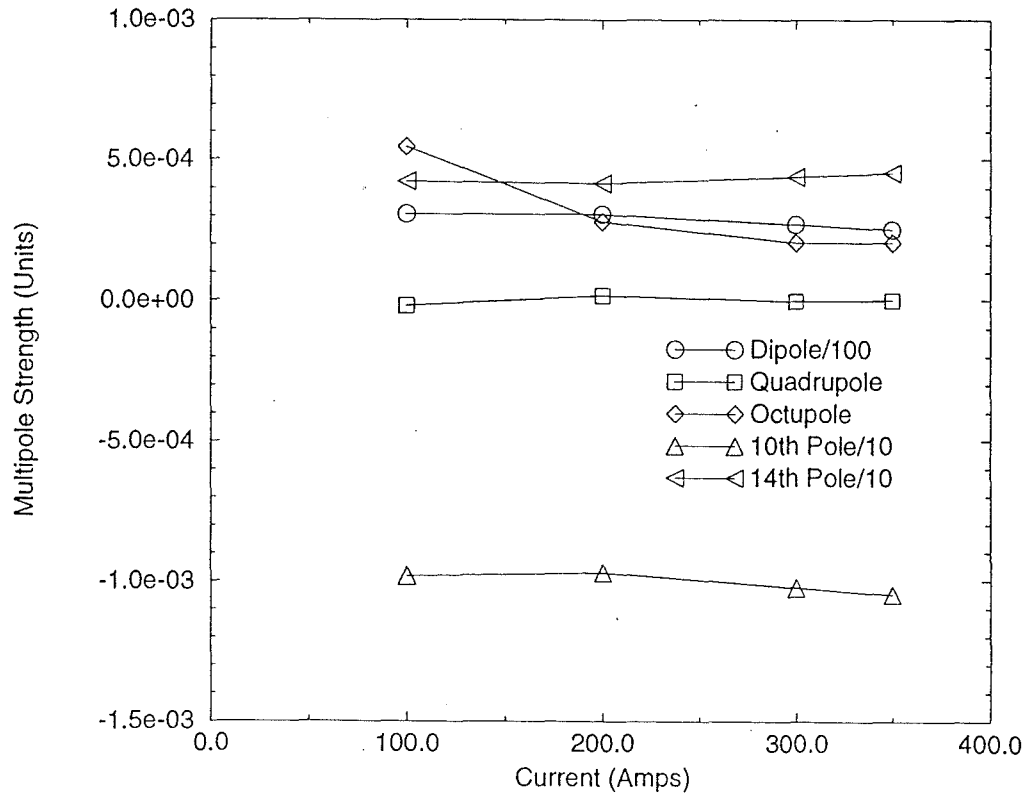


Figure 3.1-30(b). Current Variation of the Normal Harmonics of Main Injector Sextupole

The coils are installed on the poles and glued in place. The coils of one half magnet are brazed together in series and to the power leads. The top and bottom half cores are bolted together. The power and water leads for the top and bottom coils are connected together for testing. The water and power are jumpered independently.

The sextupoles will be built at Fermilab. They are a convenient size and quantity that their production can be used to level out manpower fluctuations as they arise in the production of the dipoles and quadrupoles. Their fabrication will be completed prior to the long shutdown. The strength of sextupole magnets will be measured as the final quality control check and to characterize the performance. At this time we believe that it is more cost efficient to make a limited set of measurements with existing standard MTF equipment and software than to develop a simpler measurement system. Measurement results from the second prototype sextupole are shown in Figure 3.1-30(a) and 3.1-30(b).

OTHER MULTIPOLE CORRECTORS

The main quadrupoles of the FMI will run on two separate busses and will be used for most operating tune adjustments. Trim quadrupoles are needed for harmonic generation or cancellation. A sufficient number of Main Ring trim quadrupoles will be installed around the ring to cancel half-integer stopbands, if they are significant. In addition, slow extraction will require trim quadrupoles for excitation of the half-integer resonance (see Chapters 2.7 and 3.5). Refurbished Main Ring trim quadrupoles (WBS 1.1.1.1.3.2) will be used for all of these purposes. The current plan calls for 16 of them to be refurbished and installed. Additional correction is possible with the trim windings on the new Main Injector quadrupoles, but the transformer coupling to the main coils presents a challenge for the power supplies. The parameters of the various correction elements are summarized in Table 3.1-10; the physical length, including the coils, of the Main Ring correctors, is 2-3" longer than the steel length.

Sixteen skew quads recovered from the Main Ring are necessary (WBS 1.1.1.1.3.3) to adjust the betatron coupling. Additionally, four quadrupoles from the old Fermilab Electron Cooling Ring (WBS 1.1.1.1.3.7) are available to be used as skew quads in the Main Injector, although they are not currently believed to be necessary. The Cooling Ring quads are attractive for their large aperture.

With the strong sextupoles required in this ring there was some concern that the dynamic aperture of the machine might be adversely affected. Tracking studies completed to date indicate that there is no loss of dynamic aperture due to the sextupole correction system. No additional sextupoles are planned. However, the Main Ring trim sextupoles (WBS 1.1.1.3.5) and the Main

Ring skew sextupoles (WBS 1.1.1.1.3.4) are available to be distributed and individually powered in the straight sections for control of third order resonant driving terms, should the need arise.

The Main Ring octupoles (WBS 1.1.1.1.3.6) are used to compensate for the octupole component in the Main Ring quads and to control the slow extraction. We plan to refurbish and install 62 octupoles. The strength is limited in operation by cooling considerations. With no additional cooling the octupoles can run at an RMS current of 10 A with the conductor rising to 70°C and the core to 56°C, corresponding to a peak current of 14 A in a slow spill cycle [7]. The need for additional strength and thus cooling remains under study. For example, a systematic one unit of octupole in the IQC and IQD quadrupoles can be compensated for by exciting the octupole correctors at 2.5 A. Adding some additional cooling to the core, if needed, appears to be effective and straightforward.

These magnets will have been running immediately before the shutdown period and will thus be known to be in good shape. Each one will be visually inspected for potential problems and electrically tested before being moved to its new location. Extensive reworking of these magnets is not expected.

Table 3-1.10. Multipole Corrector Parameters

Component	Steel Length	L (mH)	R (Ω)	Transfer Function
FMI Chromaticity Sextupoles ⁽²⁾	18"	0.95	0.016	0.202 T-m/m ² /A
MR trim quadrupoles ⁽¹⁾	12"	67	1.56	0.0255 T-m/m/A
MR skew quadrupoles ⁽¹⁾	6"			0.0075 T-m/m/A
CR quadrupoles ⁽⁴⁾	24"	1.75	0.013	0.0022 T-m/m/A
MR trim sextupoles ⁽¹⁾	6"			0.466 T-m/m ² /A
MR skew sextupoles ⁽¹⁾	6"			0.359 T-m/m ² /A
MR octupoles ⁽¹⁾⁽³⁾	6"	31	1.29	2.8 T-m/m ³ /A

(1) Dejan Trbojevic, Magnetic Measurements of the Correction and Adjustment Magnets of the Main Ring, TM-1412

(2) Hank Glass, Measurement Summary for MI Prototype Sextupoles ISA001 & ISA002", MTF-94-0058

(3) Hank Glass, Measurement Summary for Main Ring Octupole MOA001, to be published as MTF note.

(4) Cooling Ring Design Handbook.

WBS 1.1.1.1.4 RING CORRECTION DIPOLES

The steering dipoles correct the closed orbit. The primary sources of orbit distortion are quadrupole placement errors, dipole strength errors, and dipole rotations. These errors cause orbit distortions which, if uncorrected, would yield rms errors on the order of 6 mm. Although the present Main Ring trims have adequate strength for correcting these errors at low field, the effort of shimming and recentering them and engineering a new mounting scheme is nontrivial. Therefore, new trim dipoles for the FMI ring will be fabricated, with strengths a factor of two greater than the present Main Ring correctors, allowing correction of errors up to 4 mm horizontally (3 mm vertically) at 150 GeV. A horizontal (vertical) trim dipole will be placed next to every focussing (defocussing) quadrupole in the ring. Like the chromaticity sextupole magnets, the trim dipoles must be assembled in two pieces around the beampipe.

The Main Injector trim dipoles are a new design to provide the needed steering strength within the geometrical constraints. Parameters for the conceptual design of the horizontal (WBS 1.1.1.1.4.2) and vertical (WBS 1.1.1.1.4.4) trim dipoles are shown in Table 3.1-11. The conceptual lamination shapes are shown in Figures 3.1-31 and 3.1-32.

Table 3.1-11. Properties of Main Injector Trim Dipoles

	Horizontal	Vertical
Integrated strength (T-m)	0.060	0.030
Strength (T)	0.197	0.098
Steel length (m)	0.305	0.305
Steel length (in)	12.0	12.0
Maximum physical length (in)	17.0	17.0
Gap (in)	2.0	5.0
Number of turns	400	*
Maximum Current (A)	12	12

* to be determined

Maximum strength: 0.060 T-m at 10 Amps (normal corrector)
0.090 T-m at 15 Amps (straight section corr)

Maximum correction angle:

normal corrector: 120 μ r at 150 GeV/c

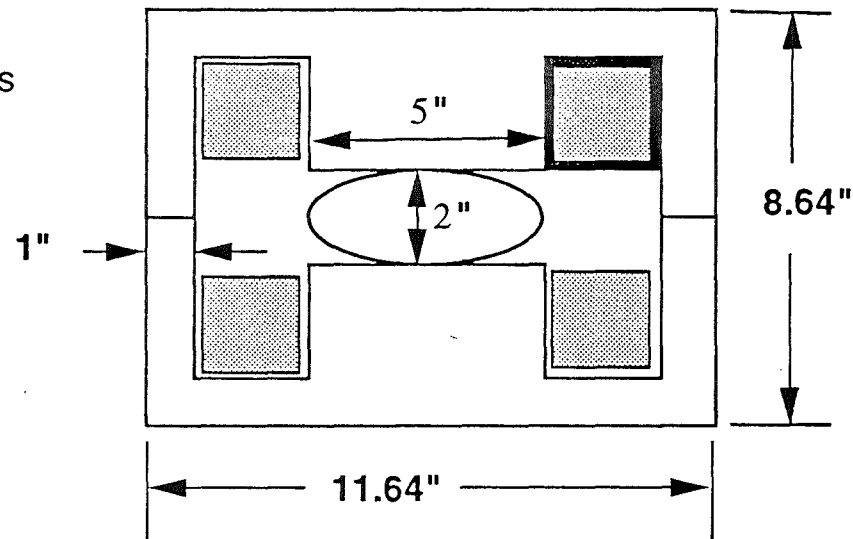
straight section corrector: 180 μ r at 150 GeV/c

Field quality at ± 1.5 inches: 0.5%

Steel length: 12 inches

Magnet length: 17 inches

Magnet weight: 321 lbs.



Coil: 400 turns #10 wire insulated (w&h) 2.32 inches

Resistance: 3.26 ohms Inductance: 0.89 H

External steel temperature: < 120 deg. F

Internal coil temperature: < 265 deg. F

Figure 3.1-31. Horizontal Trim Dipole Parameters and Dimensions

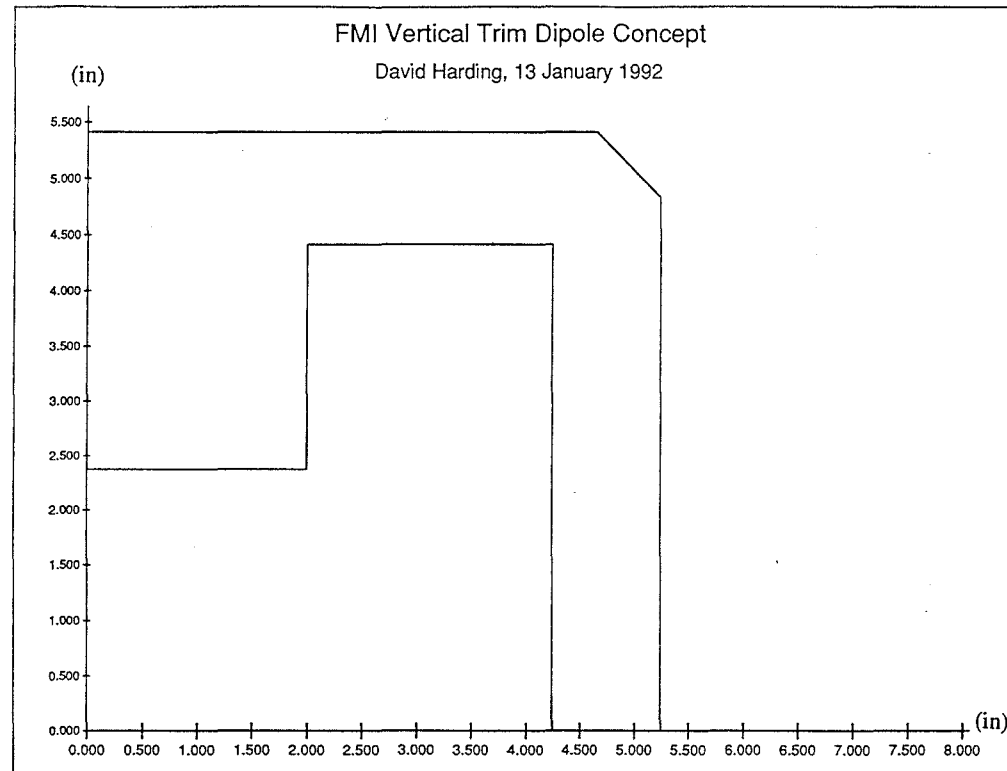


Figure 3.1-32. Vertical Trim Dipole Lamination Shape

WBS 1.1.1.2 8-GEV LINE MAGNETS

WBS 1.1.1.2.1 8-GEV LINE DIPOLES

The basic properties of all beamline dipoles are listed in Table 3.1-12.

Table 3.1-12. Properties of Beamline Dipoles in the Main Injector Project

	DDM (2XB2)	BDM (B2)	BDM (B2)	BDM (B2)	EPB 1.5-5-120	ODM (B3)	ODM (B3)
Where used	Slow	8 GeV	120 GeV	150 GeV	8 GeV	8 GeV	120 GeV
Length (meters)	6.071	6.071	6.071	6.071	3.048	6.071	6.071
Strength (Tesla)	1.08	0.20	.54	1.89	0.92	0.28	1.08
Gap (mm)	50.8	50.8	50.8	50.8	38.1	76.2	76.2
Conductor Dim. 1 (in)	0.900	1.096	1.096	1.096	0.636	0.793	0.793
Conductor Dim. 2 (in)	0.535	0.922	0.922	0.922	0.635	0.654	0.654
Cond. Hole Diam. (in)	0.250	0.455 ⁽¹⁾	0.455 ⁽¹⁾	0.455 ⁽¹⁾	0.250	0.163	0.163
Turns/pole	16	8	8	8	14	12	12
Peak Current (A)	1356	463	1356	4900	895	333	1356
RMS Current (A)	721	463	721	2600	895	333	721
Coil Resistance (mΩ)	30	7.2	7.2	7.2	17.5	45.6	45.6
Coil Inductance (mH)	32	8.0	8.0	8.0	30.0	60.1	60.1
Peak Power (kW)	55.2	1.5	13.2	172.9	14.0	3.2	83.8
RMS Power (kW)	15.6	1.5	3.7	48.6	14.0	3.2	23.7
Number Used	1	55	116	32	4	2	10 ⁽²⁾
Weight (kG)	11455	11455	11455	11455	2558	13454	13454
Sagitta (mm)	0	0	0	0	0	0	0

(1) Outer layer conductor has 0.455" hole; inner layer conductor has 0.340" hole.

(2) 3 B3 dipoles run at twice strength, with the parameters shown, and 7 run at single strength, or half the field and one-fourth the power.

WBS 1.1.1.2.1.7 REUSED MAIN RING B2 DIPOLES

The main horizontal bend of the 8 GeV line is composed of 55 B2 magnets recovered from the Main Ring. These magnets will have been running immediately before the shutdown period and will thus be known to be in good shape. Each one will be visually inspected for potential problems and electrically tested before being moved to its new location. There will be a surplus of B2s, so we can restrict ourselves to the better looking ones. Extensive reworking of

these magnets is not expected. However, an additional vacuum bellows will be welded to each B2 dipole to accommodate the larger angle between magnets.

WBS 1.1.1.2.1.12 EPB 5-1.5-120

The tight geometry of the existing Booster enclosure and the need for a wide aperture suggested the use of these dipoles. The design has been used in external beamlines for many years. These are reused beamline magnets. The magnets appear to have been built primarily by an outside vendor. No tooling, or even tooling drawings, seem to exist at Fermilab.

WBS 1.1.1.2.1.13 REUSED MAIN RING B3 DIPOLES

The vertical bends required to drop the beam 3.3 meters between Booster and the Main Injector ring heights are provided by two B3 magnets recovered from the Main Ring. The magnets are presently used as vertical bends for the Main Ring overpasses. Extensive reworking of these magnets is not expected. These magnets will have been running immediately before the shutdown period and will thus be known to be in good shape. Each one will be visually inspected for potential problems and electrically tested before being moved to its new location. B3 dipoles have had many failures in operation, but recent studies [8] have identified the primary problems as being improper handling, installation, and operation.

WBS 1.1.1.2.2 QUADRUPOLES

Beamline quadrupole magnets are for the most part, recycled from the Main Ring or the existing 8 GeV line. The exceptions are the 3Q120s, which are duplicates of an existing Fermilab design, and the 3Q60s, which are shorter versions of that design. They are used in locations in which there are tighter spatial constraints, and where the quadrupoles are being individually powered. The power supply and cabling costs associated with the lower current operation of the 3Q120s and 3Q60s more than offsets the magnet cost. The properties of all the beamline quadrupoles are listed in Table 3.1-13. Not all uses of quadrupoles are shown; the selection given represents either the most numerous use or the highest power use.

Table 3.1-13. Properties of Beamline Quadrupoles in the Main Injector Project

	SQA	BQA	BQA	BQB	BQB*	3Q120*	3Q60*
Where used	8 GeV	8 GeV	Abort	120 GeV	150 GeV	150 GeV	150 GeV
Steel length (in)	16.58	52	52	84	84	120	60
Max.Strength (T/m)	16.3	2.0	19.6	7.5	20.7	17.5	16.1
Conductor Dim. 1 (in)	0.750	1.000	1.000	1.000	1.000	0.410	0.410
Conductor Dim. 2 (in)	0.318	0.565	0.565	0.565	0.565	0.410	0.410
Cond. Hole Diameter (in)	0.188	0.250	0.250	0.250	0.250	0.229	0.229
Turns/pole	33	4	4	4	4	28	28
Peak Current (A)	388	372	3630	1356	3830	378	340
RMS Current (A)	388	372	2000	950	2150	210	190
Coil Resistance (mΩ)	32.3	2.6	2.6	4.5	4.5	161	82
Coil Inductance (mH)	43.0	0.8	0.8	1.3	1.3	60	30
Peak Power (kW)	4.9	0.4	34	8.3	66	23	9.5
RMS Power (kW)	4.9	0.4	13	4.1	21	7.1	3.0
Weight (kG)	1330	2722	2722	4082	4082	3200	1600
Number Used	16	37	1	31	7	7	2

* Quantities and rms currents refer to 150 GeV proton line. An equal number are used in the 150 GeV antiproton line at similar peak currents, but with low rms currents due to the low duty factor.

WBS 1.1.1.2.2.7 P-BAR SOURCE QUADRUPOLES - SQA

The SQA quadrupoles were designed for the Anti-Proton Source. SQAs were also used in 1986 when the 8 GeV beamline from Booster to Main Ring was rebuilt. Sixteen of the SQAs downstream of the dump in the old 8 GeV line are reused in the Booster to FMI 8 GeV line. The reused magnets do not require remeasurement, but a visual and electrical inspection will be conducted. There is a possibility that we will be able to use some of the SQC quads from the AP-4 line when it is decommissioned. These are a 26.18"-long version of the SQA, with resistance of 0.0416 Ω . A significant reduction in power consumption would result from their use in place of SQAs. The basic properties of the SQA quadrupoles are included in Table 3.1-13.

WBS 1.1.1.2.2.6 BQA - 52" MAIN RING QUADRUPOLES

Main Ring 1.32-m (52") quadrupoles comprise the balance of the quadrupoles in the 8 GeV beamline. Thirty-seven of these BQA quads are reused. These magnets will have been running immediately before the shutdown period and will thus be known to be in good shape. Each one will be visually inspected for potential problems and electrically tested before being moved to its new location. Magnetic measurements are not required, but will be considered if time permits.

WBS 1.1.1.2.4 DIPOLE CORRECTION MAGNETS

Main Ring correction dipoles will be used in the beamlines, providing either horizontal (1.1.1.2.4.1) or vertical (1.1.1.2.4.3) correction at every quadrupole. These magnets will have been running immediately before the shutdown period and will thus be known to be in good shape. Each one will be visually inspected for potential problems and electrically tested before being moved to its new location. No magnetic testing is required.

WBS 1.1.1.2.5.1 INJECTION LAMBERTSON MAGNET

The injection Lambertson for the 8 GeV line is the "A0 Lambertson" magnet from the old 8 GeV line. Only minor changes to the support structure and vacuum connections are required. As the shutdown approaches, we expect to seek permission to modify the spare A0 injection Lambertson for use in the Main Injector, then modify the old operational Lambertson as the Main Injector spare.

WBS 1.1.1.3 150 GEV PROTON LINE

In the 150 GeV Proton Line all of the dipoles, about half of the quadrupoles, and all of the trim dipoles are reused Main Ring magnets. The balance of the quadrupoles and the injection and extraction elements are new construction.

WBS 1.1.1.3.1.7 DIPOLES

The bending dipoles are B2s recovered from the Main Ring. Since they are all rolled to provide vertical as well as horizontal bends in the same magnet, they will require a change in their support structure. The vacuum connections should remain the same. Magnetic measurements are not necessary for these magnets. These magnets will have been running immediately before the shutdown period and will thus be known to be in good shape. Each one will be visually inspected for potential problems and electrically tested before being moved to its new location. There will be a surplus of B2s, so we can restrict ourselves to the better looking ones.

WBS 1.1.1.3.2 QUADRUPOLES

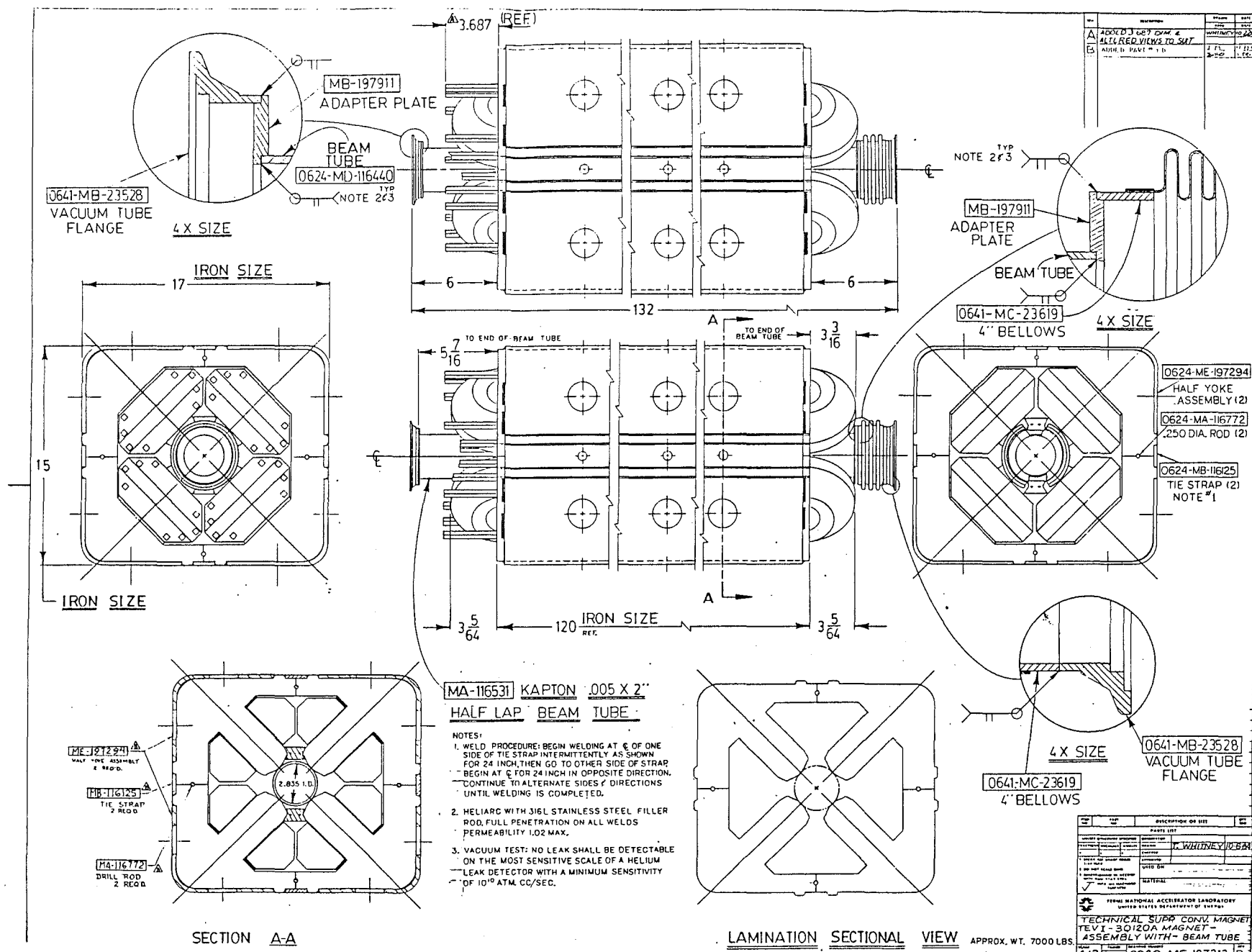
Seven quadrupoles are BQB 2.13-m (84") quads (1.1.1.3.2.5) reused from the Main Ring. These may require new support structures. The vacuum connections will not need to be changed. Any damaged manifolding will be repaired. We will choose these quads from those not selected for use in the ring. We will have made magnetic measurements on them as part of the selection process of quadrupoles to be used in the ring, as well as the usual electrical and mechanical checks.

Seven quadrupoles (1.1.1.3.2.12) are newly built 3Q120As. The properties are summarized in Table 3.1-13. Figure 3.1-33 shows several views of the 3Q120A magnet construction. These quadrupoles have smaller transverse dimensions than Main Ring quadrupoles, easing some installation difficulties in rather congested areas. They are also lower current, which reduces the cabling, power supply and power costs for these individually powered elements. Fermilab has built many of these quadrupoles for external beamlines in the past, refining the design with time to extend the performance. The magnetic behaviour of 3Q120s has been documented elsewhere [9]. The first magnet will be measured to verify its design and to provide documentation of its properties in the new measurement system. Only minimal measurements are needed on the balance of these magnets.

Two quadrupoles (1.1.1.3.2.13) are newly built 3Q60As. These are 1.524 m (60") long quadrupoles built to the same design as the 3Q120A. These have not been built before, but no trouble is expected in this modification. The first magnet will be measured to verify its design and to provide documentation of its properties in the new measurement system. Only minimal measurements are needed on the balance of these magnets.

WBS 1.1.1.3.4 TRIM DIPOLES

Trim dipoles will be recovered from the Main Ring. One strong horizontal trim (1.1.1.3.4.1) will be used at each focussing quadrupole. Two vertical trims (1.1.1.3.4.3) will run



in series at each defocussing quadrupole. These may also require a change in their support structure. Magnetic measurements are not necessary for these magnets.

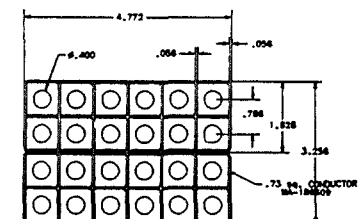
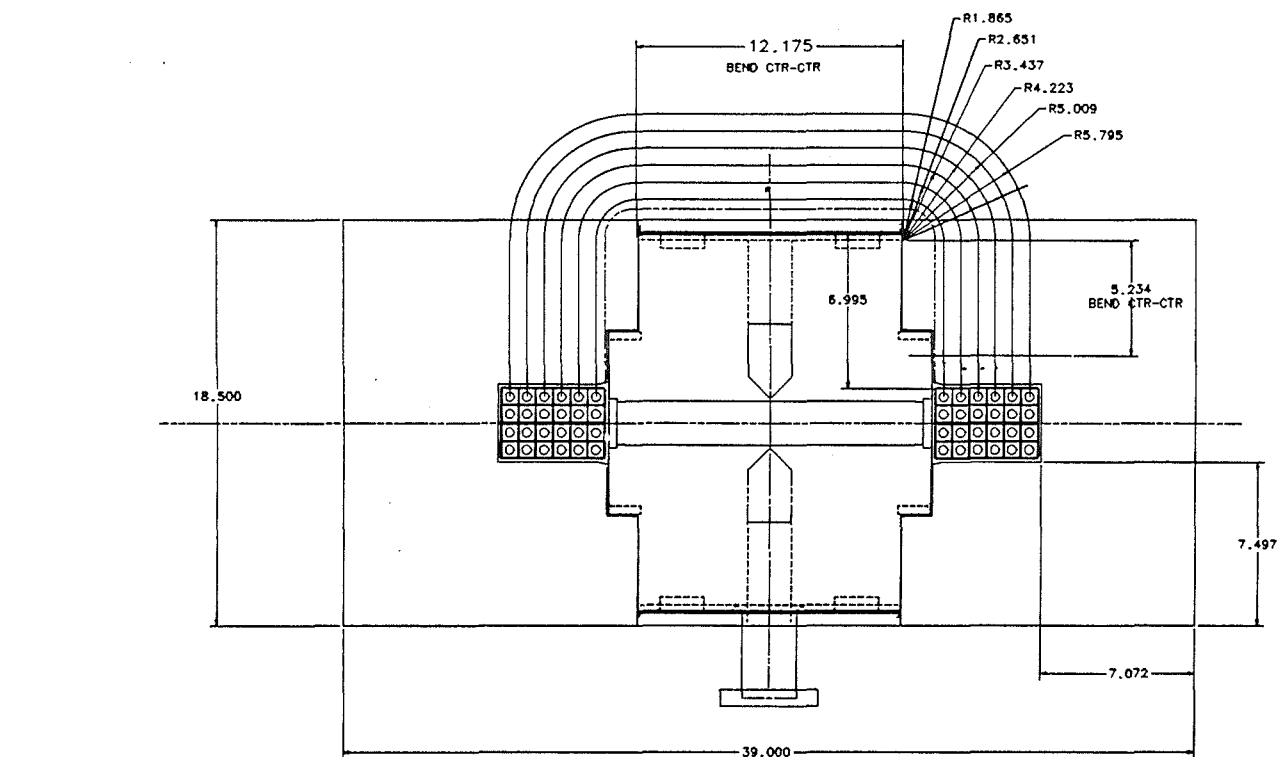
WBS 1.1.1.3.5 INJECTION AND EXTRACTION ELEMENTS

WBS 1.1.1.3.5.2 FMI LAMBERTSON MAGNETS

The combination of aperture and strength considerations require a new Lambertson design for extraction from the Main Injector Ring to the Tevatron, the antiproton production target, and Switchyard. A new design Lambertson is also required for injection into the Tevatron. These same magnets must also accommodate the transfer of antiprotons from the Accumulator back to the Main Injector. We find that we can satisfy all of the needs with a single design, saving on design and drafting effort, tooling, and spares. The design parameters are shown in Table 3.1-14. The combination of large gap height (2") and gap width (14") determine that the Lambertson magnet will have a large steel cross-section, as large as the MI dipole. Tight spatial constraints require a very compact end geometry. From the technical standpoint, the Lambertson magnet is probably the most challenging magnet required for the FMI project.

These Lambertson will be used at MI-40 (abort), MI-52 (proton extraction/antiproton injection), MI-62 (antiproton extraction) and TEV-60 (Tevatron injection). Additional Lambertson would be required in MI-60 for extractions for NUMI if that project is approved. Three Lambertsons are needed at each Main Injector extraction point, with a quadrupole situated between the first and the second Lambertsons. Four Lambertsons are needed for the Tevatron injection, with two being charged to each 150 GeV line in the WBS. By their very nature, Lambertson magnets require a magnetic septum close to the circulating beam. Especially in conjunction with slow extraction, they become a target for beam losses and are frequently high activated, making repair possible only after long cooldown periods. Consequently, additional spare magnets will be fabricated.

As of July, 1994, several conceptual designs were being evaluated, using different lamination and coil topologies. The four-lamination design has been selected as the one with the least technical risk. This design appears to have the advantage of easiest fabrication, assembly, and repair. A cross section and a side view of the preliminary design of the Lambertson are shown in Figure 3.1-34. It will feature saddle coils, with half the coils folding one direction, and half the other direction in order to shorten the ends of the magnet. While the field-free region is only required on one side, there are a number of advantages to placing it on both sides: (i) By providing complete symmetry, all stresses should balance and the assembled half-cores should be more naturally straight. (ii) It will allow placing ion pumps on both sides, improving the vacuum.



4-LAM W/ .73 SQ. CONDUCTOR

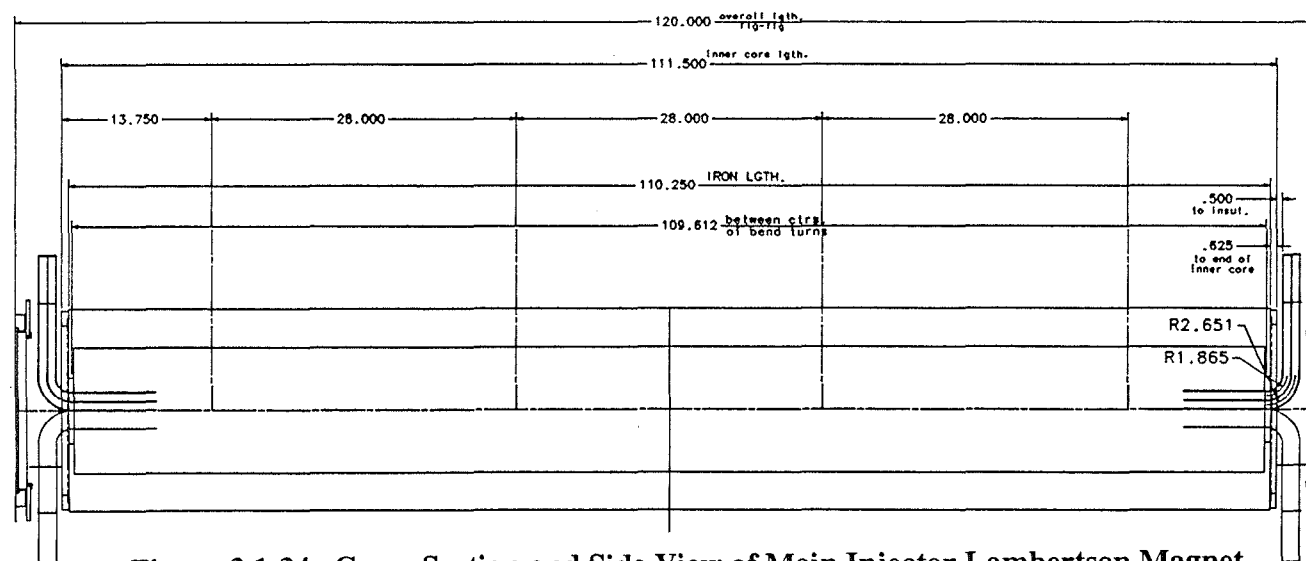


Figure 3.1-34. Cross-Section and Side View of Main Injector Lamberton Magnet

COIL LAYOUT

ITEM	PART NO.	DESCRIPTION OR SIZE	QTY.
PARTS LIST			
1.	4-LAM W/ .73 SQ. CONDUCTOR	COIL	
2.	4-LAM W/ .73 SQ. CONDUCTOR	COIL	
3.	4-LAM W/ .73 SQ. CONDUCTOR	COIL	
4.	4-LAM W/ .73 SQ. CONDUCTOR	COIL	
5.	4-LAM W/ .73 SQ. CONDUCTOR	COIL	
6.	4-LAM W/ .73 SQ. CONDUCTOR	COIL	
7.	4-LAM W/ .73 SQ. CONDUCTOR	COIL	
8.	4-LAM W/ .73 SQ. CONDUCTOR	COIL	
9.	4-LAM W/ .73 SQ. CONDUCTOR	COIL	
10.	4-LAM W/ .73 SQ. CONDUCTOR	COIL	
11.	4-LAM W/ .73 SQ. CONDUCTOR	COIL	
12.	4-LAM W/ .73 SQ. CONDUCTOR	COIL	
13.	4-LAM W/ .73 SQ. CONDUCTOR	COIL	
14.	4-LAM W/ .73 SQ. CONDUCTOR	COIL	
15.	4-LAM W/ .73 SQ. CONDUCTOR	COIL	
16.	4-LAM W/ .73 SQ. CONDUCTOR	COIL	
17.	4-LAM W/ .73 SQ. CONDUCTOR	COIL	
18.	4-LAM W/ .73 SQ. CONDUCTOR	COIL	
19.	4-LAM W/ .73 SQ. CONDUCTOR	COIL	
20.	4-LAM W/ .73 SQ. CONDUCTOR	COIL	
21.	4-LAM W/ .73 SQ. CONDUCTOR	COIL	
22.	4-LAM W/ .73 SQ. CONDUCTOR	COIL	
23.	4-LAM W/ .73 SQ. CONDUCTOR	COIL	
24.	4-LAM W/ .73 SQ. CONDUCTOR	COIL	
25.	4-LAM W/ .73 SQ. CONDUCTOR	COIL	
26.	4-LAM W/ .73 SQ. CONDUCTOR	COIL	
27.	4-LAM W/ .73 SQ. CONDUCTOR	COIL	
28.	4-LAM W/ .73 SQ. CONDUCTOR	COIL	
29.	4-LAM W/ .73 SQ. CONDUCTOR	COIL	
30.	4-LAM W/ .73 SQ. CONDUCTOR	COIL	
31.	4-LAM W/ .73 SQ. CONDUCTOR	COIL	
32.	4-LAM W/ .73 SQ. CONDUCTOR	COIL	
33.	4-LAM W/ .73 SQ. CONDUCTOR	COIL	
34.	4-LAM W/ .73 SQ. CONDUCTOR	COIL	
35.	4-LAM W/ .73 SQ. CONDUCTOR	COIL	
36.	4-LAM W/ .73 SQ. CONDUCTOR	COIL	
37.	4-LAM W/ .73 SQ. CONDUCTOR	COIL	
38.	4-LAM W/ .73 SQ. CONDUCTOR	COIL	
39.	4-LAM W/ .73 SQ. CONDUCTOR	COIL	
40.	4-LAM W/ .73 SQ. CONDUCTOR	COIL	
41.	4-LAM W/ .73 SQ. CONDUCTOR	COIL	
42.	4-LAM W/ .73 SQ. CONDUCTOR	COIL	
43.	4-LAM W/ .73 SQ. CONDUCTOR	COIL	
44.	4-LAM W/ .73 SQ. CONDUCTOR	COIL	
45.	4-LAM W/ .73 SQ. CONDUCTOR	COIL	
46.	4-LAM W/ .73 SQ. CONDUCTOR	COIL	
47.	4-LAM W/ .73 SQ. CONDUCTOR	COIL	
48.	4-LAM W/ .73 SQ. CONDUCTOR	COIL	
49.	4-LAM W/ .73 SQ. CONDUCTOR	COIL	
50.	4-LAM W/ .73 SQ. CONDUCTOR	COIL	
51.	4-LAM W/ .73 SQ. CONDUCTOR	COIL	
52.	4-LAM W/ .73 SQ. CONDUCTOR	COIL	
53.	4-LAM W/ .73 SQ. CONDUCTOR	COIL	
54.	4-LAM W/ .73 SQ. CONDUCTOR	COIL	
55.	4-LAM W/ .73 SQ. CONDUCTOR	COIL	
56.	4-LAM W/ .73 SQ. CONDUCTOR	COIL	
57.	4-LAM W/ .73 SQ. CONDUCTOR	COIL	
58.	4-LAM W/ .73 SQ. CONDUCTOR	COIL	
59.	4-LAM W/ .73 SQ. CONDUCTOR	COIL	
60.	4-LAM W/ .73 SQ. CONDUCTOR	COIL	
61.	4-LAM W/ .73 SQ. CONDUCTOR	COIL	
62.	4-LAM W/ .73 SQ. CONDUCTOR	COIL	
63.	4-LAM W/ .73 SQ. CONDUCTOR	COIL	
64.	4-LAM W/ .73 SQ. CONDUCTOR	COIL	
65.	4-LAM W/ .73 SQ. CONDUCTOR	COIL	
66.	4-LAM W/ .73 SQ. CONDUCTOR	COIL	
67.	4-LAM W/ .73 SQ. CONDUCTOR	COIL	
68.	4-LAM W/ .73 SQ. CONDUCTOR	COIL	
69.	4-LAM W/ .73 SQ. CONDUCTOR	COIL	
70.	4-LAM W/ .73 SQ. CONDUCTOR	COIL	
71.	4-LAM W/ .73 SQ. CONDUCTOR	COIL	
72.	4-LAM W/ .73 SQ. CONDUCTOR	COIL	
73.	4-LAM W/ .73 SQ. CONDUCTOR	COIL	
74.	4-LAM W/ .73 SQ. CONDUCTOR	COIL	
75.	4-LAM W/ .73 SQ. CONDUCTOR	COIL	
76.	4-LAM W/ .73 SQ. CONDUCTOR	COIL	
77.	4-LAM W/ .73 SQ. CONDUCTOR	COIL	
78.	4-LAM W/ .73 SQ. CONDUCTOR	COIL	
79.	4-LAM W/ .73 SQ. CONDUCTOR	COIL	
80.	4-LAM W/ .73 SQ. CONDUCTOR	COIL	
81.	4-LAM W/ .73 SQ. CONDUCTOR	COIL	
82.	4-LAM W/ .73 SQ. CONDUCTOR	COIL	
83.	4-LAM W/ .73 SQ. CONDUCTOR	COIL	
84.	4-LAM W/ .73 SQ. CONDUCTOR	COIL	
85.	4-LAM W/ .73 SQ. CONDUCTOR	COIL	
86.	4-LAM W/ .73 SQ. CONDUCTOR	COIL	
87.	4-LAM W/ .73 SQ. CONDUCTOR	COIL	
88.	4-LAM W/ .73 SQ. CONDUCTOR	COIL	
89.	4-LAM W/ .73 SQ. CONDUCTOR	COIL	
90.	4-LAM W/ .73 SQ. CONDUCTOR	COIL	
91.	4-LAM W/ .73 SQ. CONDUCTOR	COIL	
92.	4-LAM W/ .73 SQ. CONDUCTOR	COIL	
93.	4-LAM W/ .73 SQ. CONDUCTOR	COIL	
94.	4-LAM W/ .73 SQ. CONDUCTOR	COIL	
95.	4-LAM W/ .73 SQ. CONDUCTOR	COIL	
96.	4-LAM W/ .73 SQ. CONDUCTOR	COIL	
97.	4-LAM W/ .73 SQ. CONDUCTOR	COIL	
98.	4-LAM W/ .73 SQ. CONDUCTOR	COIL	
99.	4-LAM W/ .73 SQ. CONDUCTOR	COIL	
100.	4-LAM W/ .73 SQ. CONDUCTOR	COIL	

DATE: 10/11/84

CREATED WITH T-SKALVI USER: M. C. BERRY

(iii) With symmetric ends, there is hope that the end-field leakage into the field-free region will be reduced, perhaps eliminating the need for flux-catchers.

Table 3.1-14. Properties of Main Injector Lambertson Magnets

Integrated strength	3.00	T-m
Strength at 150 GeV	1.072	T
Steel length	2.80	m
Steel length	110.25	in
Maximum physical length	120	in
Gap Height	2.0	in
Gap Width	14.0	in
Straightness (over 110" length)	0.010	in
Number of turns	24	
Conductor Dimensions	0.730 x 0.730	in x in
Conductor Hole Diameter	0.400	in
Maximum Current	1806	A
Septum Thickness	4	mm
Septum Opening Angle	90	degrees
Field Uniformity (over $\pm 6"$ travel)	0.28	%
Leakage Field into Field-Free Region	10	G
Leakage Field Gradient into Field-Free Region	300	G/m
Achievable Vacuum Level	$< 1 \times 10^{-8}$	Torr
In-situ Bakeout Temperature	150	°C

The Lambertson magnets will require numerous additional steps in their fabrication, in comparison to other conventional magnets. Most notable is that there is no beampipe per se, rather, the inner core laminations are enclosed inside a 0.030" thick vacuum skin made from Type 321 stainless steel. All laminations must be washed to eliminate contaminants which could corrode the vacuum skin, and the inner core laminations must be vacuum baked at 750 °C. Following stacking, welding and vacuum skinning, the inner core assembly is vacuum-baked at 400 °C. The completed magnet may also have to be baked-out at 150 °C following installation in the tunnel. This in-situ bake-out will be required for the Lambertson installed at TEV-60; the magnets in the Main Injector may not need to be baked.

The first Lambertson will be constructed in FY95. It will be measured extensively to characterize its performance. Subsequent magnets are not expected to be measured due to the hazard of contaminating the vacuum surfaces and the insensitivity of the beam to small variations in the magnetic properties of these magnets.

WBS 1.1.1.3.5.6 FMI C-MAGNETS

C-magnets are required at each end to the beamline to complement the Lambertson magnets for injection and extraction. To achieve the bend strengths needed we build new magnets, all the same length. The basic design is the "F-17 C-magnet", designed for extraction from the Main Ring to the P-Bar production target. We will build 3.33-m long copies of these magnets. The C-magnet is shown in Figure 3.1-35. Parameters of the magnet are listed in Table 3.1-15.

The number of water circuits needs to be reviewed. Most C-magnets will be cooled by the higher pressure 150 GeV line LCW system; the cooling parameters for that usage are indicated in Table 3.1-15. For the C-magnet in the abort line, only 100 psid is available, and the temperature rise would be about 10 °C. This is at the upper end of the desired temperature rise. It may be sufficiently easy to provide four water circuits that this will be done for all C-magnets; in that case, the flow would be restricted external to the magnet to provide the appropriate flow for each particular location.

The first C-magnet will be measured extensively to characterize its performance. Subsequent magnets are not expected to be measured due to the insensitivity of the beam to small variations in the magnetic properties of these magnets.

WBS 1.1.1.4 150 GEV ANTIPROTON LINE

The 150 GeV Antiproton Line uses exactly the same combination of magnets as the 150 GeV Proton Line. Not having to deal with large 8 GeV beam relaxes the constraints on the line somewhat, but for the sake of uniformity the elements are kept identical. There are slight differences in the alignments and tunes of the two lines.

Rather than repeat everything from the previous section, the reader is referred to the descriptions for the 150 GeV Proton line.

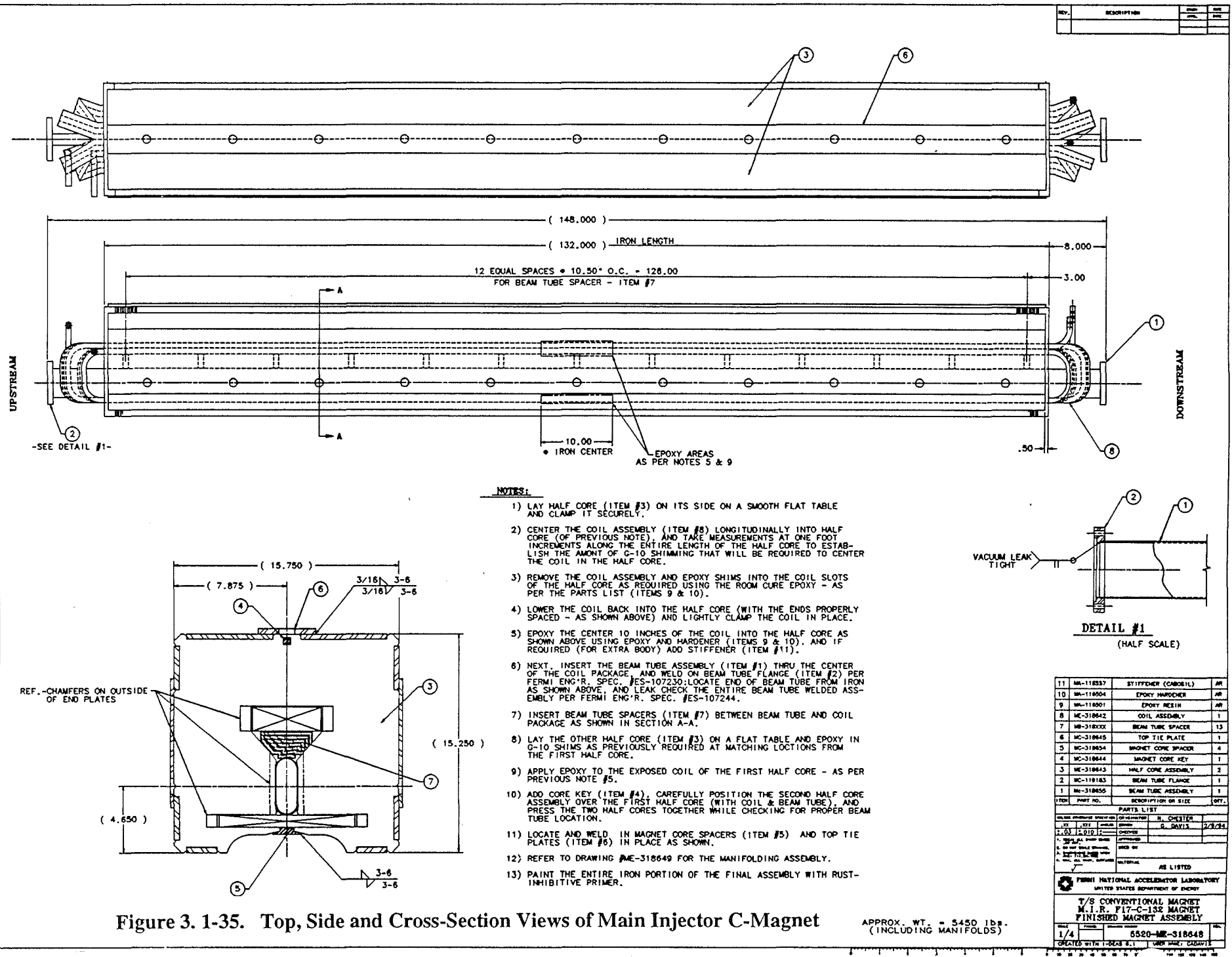


Figure 3. 1-35. Top, Side and Cross-Section Views of Main Injector C-Magnet

Table 3.1-15. Properties of Main Injector C-Magnets

Central field	1.260	T
Uniformity (across 2.0")	< 5	G
Gap height	1.600	in
Gap height	0.041	m
Gap width	4.000	in
Gap width	0.102	m
Maximum Power (@ 150 GeV)	75	kW
RMS Power	24	kW
Full current	3500	A
Full voltage	20.7	V
Resistance	6.1	mΩ
Inductance	2.4	mH
Number of water paths*	2	
Flow*	14	GPM
Delta P*	200	psid
Delta T (for rms power)*	6.5	°C
Conductor dimensions	0.730 x 0.730	in x in
Hole diameter	0.400	in
Total turns	12	
Average turn	296.2	in
Weight	8000	lb
Steel length	131.1	in
Steel length	3.330	m
Coils length	140.9	in
Flange-to-flange length	146.8	in

* See text for discussion of cooling considerations.

WBS 1.1.1.5 120 GEV PROTON LINE

The 120 GeV Line is composed mainly of the Main Ring remnant from F0 to F17. A new section joins the 150 Proton Line to the remnant. Also, the Lambertson magnets previously used to extract beam from the Main Ring to the AP1 line are replaced with B3 dipoles which need only be turned on or off to switch beam to AP1 or the slow spill line.

WBS 1.1.1.5.1.13 MAIN RING B3 DIPOLES

The larger aperture (compared to the B2) of the Main Ring B3 dipoles is desired in a few places. Each magnet will be visually inspected for potential problems before being moved to its new location. Extensive reworking of these magnets is not expected.

WBS 1.1.1.5.1.14 B1 AND B2 DIPOLES LEFT IN PLACE

The existing B1 and B2 dipoles that remain in place through the Main Ring remnant require no work except changes to the bussing and power supplies. They will be visually inspected for indications of problems.

WBS 1.1.1.5.2 MAIN RING QUADRUPOLES

The 2.13-m (84") Main Ring quadrupoles used in the Main Ring remnant will not require modification. We expect to remove all Main Ring 2.13-m quadrupoles from the tunnel, measure them, and choose the best matched ones for the Main Injector ring. The best of the rest will be used in the beam lines such as this one. Any manifold work or other necessary refurbishing will be done. At the present time, we anticipate filing an Engineering Change Request in the near future, calling for newly constructed 3Q60s (1.1.1.5.2.13) at the transition from the 150 GeV line, (F11 and F12 locations). Minimal magnetic measurements will be done on these magnets.

WBS 1.1.1.5.4 TRIM DIPOLES

The Main Ring trim dipoles will be reinstalled on the quadrupole cradles without modification except to repair or replace any problems detected during visual and electrical inspection.

WBS 1.1.1.6. SLOW SPILL (F18-A0) MAGNETS

Most of the Slow Spill Line is Main Ring remnant. The match to Switchyard requires a new configuration. Any magnets that do not simply remain in place will have been recovered from elsewhere in the Main Ring.

WBS 1.1.1.6.1 DIPOLES

The Slow Spill line will be composed primarily of B1 and B2 dipole magnets presently in place in the Main Ring. In addition, there is one B2 dipole modified to have twice as many turns as the standard B2, denoted as DDM or 2XB2. These magnets will remain in place with no modification unless a visual or electrical inspection reveals a potential problem. In that case, the magnet will be replaced with one from another part of the Main Ring.

WBS 1.1.1.6.2 QUADRUPOLES

Twenty-seven 2.13-m (84") Main Ring quadrupoles will be used in the Slow Spill line. These magnets will be used in essentially the same manner and at the same current levels as they are in the Main Ring. Most will have been removed and placed in the pool of Main Ring quadrupoles for the Main Injector ring. Those quadrupoles which are not selected, on the basis of magnetic testing, for the ring, will be available for the beamlines. No rework is planned except to repair significant deficiencies. Four 1.32-m (52") Main Ring quadrupoles will remain in place without any rework except to correct any problems detected during visual and electrical inspection.

WBS 1.1.1.6.4 TRIM DIPOLES

The Main Ring trim dipoles will be reinstalled on the quadrupole cradles without modification except to repair or replace any problems detected during visual and electrical inspection.

WBS 1.1.1.8 ABORT LINE

WBS 1.1.1.8.1 DIPOLES

The abort line bend elements are two reused B2 dipoles (1.1.1.8.1.7). These magnets are rolled at approximately 50 degrees to level off the aborted beam and deflect it away from the circulating beam to provide faster horizontal separation. Therefore, new mounting brackets may be required. Magnets from the Main Ring will be selected on the basis of visual and electrical inspection. No magnetic measurements will be required.

WBS 1.1.1.8.2 QUADRUPOLES

The Abort Line beam requires three quadrupoles, two 2.13-m (84") Main Ring quadrupoles (1.1.1.8.2.5) and one 1.32-m (52") Main Ring quadrupole (1.1.1.8.2.6). The 2.13-m quads will come from the pool of quadrupoles tested for inclusion in the Main Injector ring and

reworked appropriately. The 1.32-m quadrupole is not expected to require rework or magnetic measurements, although it will undergo a visual and electrical inspection for potential problems.

WBS 1.1.1.8.4 CORRECTION DIPOLES

Four Main Ring correction dipoles will be used in the Abort Line to allow adjustment of the angle and position of the beam in both planes as it enters the drift space before the abort dump. The correctors will be shimmed as needed to fit around the beam tube. New mounting brackets may be needed.

WBS 1.1.1.8.5 EXTRACTION MAGNETS

The abort extraction system follows the 150 GeV Proton and Antiproton beamline design. Three of the FMI Lambertsons (1.1.1.8.5.2) are followed by one C-magnet (1.1.1.8.5.6). These will be both be identical to the ones used in the 150 GeV extraction systems.

References: Quadrupoles and Beamline Magnets

1. C.S.Mishra, "Study of the Long and Short Quadrupoles Strength Match", MI Note-0110.
2. D.Harding, "Initial Determination of the Main Injector Quadrupole Strengths", MI Note-0117.
3. B.C.Brown, "Determination of the Stacking Length for IQC Quadrupoles", MTF-94-0044.
4. A. Mokhtarani, to be published as MTF note.
5. C.S.Mishra, "Study of the Main Injector Quadrupole Measurement Precision", MI Note-0108
6. A. Bogacz, "Main Injector Sextupole Strength - Reassessment", MI Note-0100.
7. G. Krafczyk and P. Prieto, MI Note-0121, 1994.
8. F.W.Markley, et al., 1989 Failure Committee Report, B3 Magnet Review, 1/4/89, private communication to the Fermilab Technical Support Section management; B.C. Brown, et al., An Analysis of Fermilab Main Ring B3 Dipole Failures, 12/30/93, MTF-93-0004; B.C. Brown, et al., Report of the B2B3 Reliability Committee, 4/9/94, MTF-93-0009
9. Alan Wehmann in "3Q120 Low Gradient Behaviour", PBar Note 430, October 1985; and "3Q120 Low Gradient Behaviour -- Companion Report", PBar Note 431, October 1985.

3.1A 8 GEV LINE PERMANENT MAGNETS

The 8 GeV line uses four types of permanent magnets: a gradient dipole (combined-function magnet) used in the normal arc cells, a short dipole used for horizontal bends in the arc cells, a vertical bend dipole used to pitch the beam down coming out of the Booster, and a normal quadrupole used in the “reverse bend” cells near the beginning of the line. The 8 GeV line optics are discussed in Chapter 2.4.1.

Table 3.1A-1. Types and numbers of permanent magnets for 8 GeV line.

Type	Description	L_{PHYS} (in.)	L_{MAG} (in.)	Integrated Strength	Number installed	Spares
PDD	Horizontal Bend Dipole	102	97	0.56953 T-m	45	1
PDV	Vertical Bend Dipole	145	140	0.8220 T-m	4	1
PGD	Gradient Dipole	161.5	157.5	0.56953 T-m + 1.851 T-m/m	65	6
PQP	Permanent Quadrupole	24.75	20	1.481 T-m/m	9	1

Only one polarity of each type is required, since the bend direction of dipole permanent magnets is reversed by installing them upside-down. The focusing action of gradient and quadrupole magnets is reversed by rotating them 180 degrees about a vertical axis (i.e. switching the upstream and downstream ends). By convention, the permanent magnets installed right side up bend protons to the right, and the horizontally defocussing configuration corresponds to protons entering the label end of quadrupole and gradient magnets.

Permanent Magnet Design

The designs are so-called “hybrid” permanent magnets in which the field is driven by permanent magnet material and the field shape is determined mainly by steel pole pieces. Strontium ferrite permanent magnet material is used for reasons of stability and cost. A representative assembly drawing (in this case the gradient dipole) is given in Fig. 3.1A-1. The permanent magnet bricks drive flux into the pole tips from the top and sides.

The pole tips are supported by an aluminum spacer which sets the magnetic gap. The entire assembly is enclosed in a flux return shell 0.75” thick. The magnets are straight and solid “bar stock” components are used throughout rather than laminations. The pole tip steel is 1008

low carbon steel and the flux return is construction grade (A36) steel. A temperature compensation alloy which cancels the temperature coefficient of the ferrite is interspersed with the permanent magnet material at the top and bottom. In the PDD and PDV dipoles, this compensator alloy is placed directly inside the magnet gap.

The end fields of the magnets are terminated by Flux Clamp/ End Plate assemblies which are magnetically connected to the flux return shell. See Fig. 3.1A-2. These prevent the stray flux from leaking out. An aluminum retainer plate immobilizes the beam tube and protects the magnetic pole tips from magnetic debris and curiosity seekers. The end plates are removable to allow access to the ends of the pole tips for shimming operations. The flux return extends 2" past the ends of the pole tips at each end and the end plates are 0.5" thick, so that the mechanical lengths of the 8 GeV line permanent magnets are 5" longer than their pole tip (magnetic) lengths.

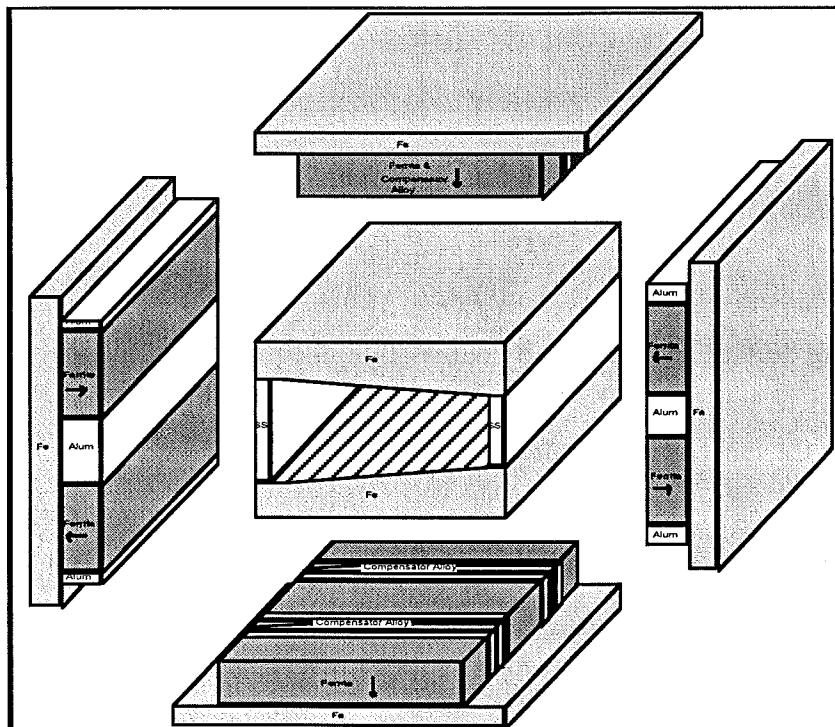


Figure 3.1A-1 - PGD permanent magnet assembly sequence.

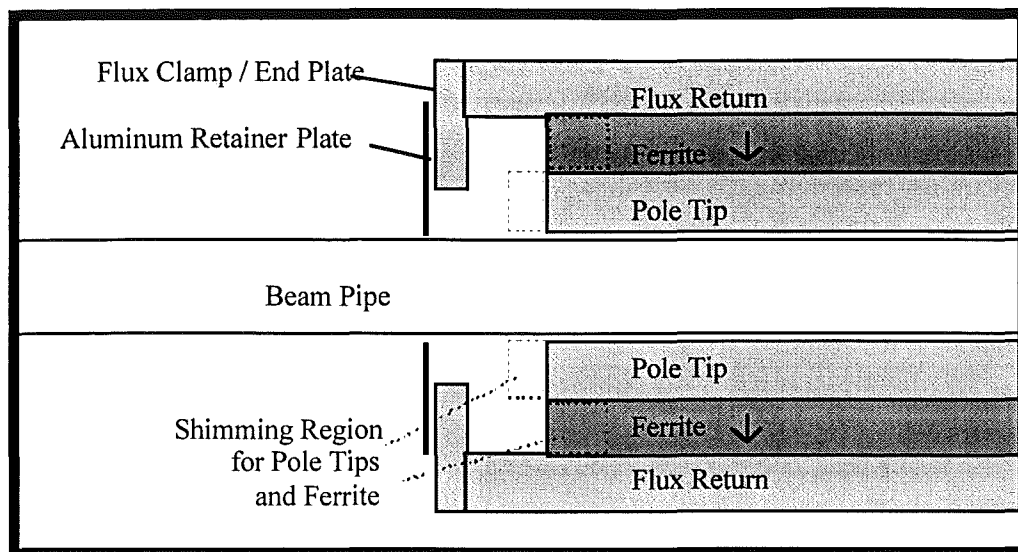


Figure 3.1A-2 - Side view of magnet, showing transition from naked beam pipe to magnet flux return. The beam pipe is held in place by an aluminum retainer plate with slotted holes which allow for $\pm 1\text{cm}$ transverse motion of the beam pipe. Also indicated are the regions at the ends of the pole tips which are available for shimming the field shape (not needed for the 8 GeV transfer line magnets), and the ends of the ferrite bricks which are used to trim the strength of the magnet by adjusting the total amount of magnetic material.

All magnets are designed to fit around an elliptical beam pipe with inner dimensions under vacuum of approximately 1.8" (v) x 3.9" (h). The beam pipe has the ability to move transversely $\pm 1\text{cm}$ inside the gradient magnets and quadrupoles, a feature which allows adjustment of the effective bend strength by $\pm 3\%$. A transition to a 4" round pipe has been provided on all magnets.

8 GeV Line Magnet Key Performance Specifications

Table 3.1A-2 contains the basic specifications for the 8 GeV line permanent magnets. Many of these are design guidelines rather than absolute performance specifications. These are discussed at exhaustive length in MI Note 150.

Table 3.1A-2. Key Design Parameters for Permanent Magnets in 8 GeV line.

Design Lifetime	30 years
Operating Temperature	20°C (68 °F) to 35°C (95 °F)
Storage Temperature	5°C (41 °F) to 50°C (120 °F).
Humidity	0% -100%
Corrosion Resistance	All parts resistant, plated, or painted.
Bakeout Compatibility	Not needed
Temperature Coefficient of Field	$\pm 0.01\%/^{\circ}\text{C}$
Time Stability	$\Delta B/B < 0.02\%/yr.$ after first month aging
Radiation Resistance	$\Delta B/B < 1\%$ for 1 GigaRad
Shock & Vibration	$\Delta B/B < 0.05\%$ from normal handling
Radiation Activation	Comparable to steel/copper magnets
Vertical Aperture (dipole & grad. mag.)	2.0" between the pole tips (at X=0)
Good-Field Aperture (dipole & grad.)	$\pm 1.0''$ at $ \delta B_y/B_0 < 0.1\%$ (100% tested) $\pm 1.75''$ at $ \delta B_y/B_0 < 0.2\%$ typ.(not tested)
Quadrupole Pole Tip Radius	1.650" (XY = 1.350 in ² , same as MI)
Magnet Sagitta	Zero (straight magnets)
Beam Sagitta Inside Dipole	~1cm (dipoles & grads), 1.5cm (vert)
Field Uniformity in Z	$\pm 5\%$ (systematic) $\pm 5\%$ (random)
Bend Center uncertainty	$\pm 3\text{cm}$ in Z (measured and surveyed)
Field Strength Modification	possible in range [+3%,-5%].
Field Shape Modification	+/- 5 units (modify end shims)
Magnetic Field in Flux Return	<1 Tesla
Termination of End Fields	via Flux Clamp / End Plate of Magnets
End Fields	<5 Gauss 2.5 cm past end of magnet
Beam Pipe Fixturing	allows $\pm 1\text{cm}$ horiz. range of motion (grads)
Survey Fiducials	8 "nests" at corners of magnets
Mechanical Rigidity (sag) of dipoles	< 0.010" for 25% , 75% support points

Permanent Magnet Material

Type 8 Strontium Ferrite [1] was chosen as the permanent magnet material because of its low cost and high stability over time, temperature, and radiation. Strontium ferrite is the material of choice in automotive applications and is available at low cost in standard grades and sizes from multiple vendors. It has documented stability in applications such as NMR magnets and is commonly used in ion pumps in accelerator applications. Material from the three major US vendors were evaluated and performed well in the R&D program.

We have studied the time stability (field strength vs. time) of a number of our model "stability test magnets" measured with an NMR probe over an 8-month period. This data is consistent with logarithmic aging at approximately 2×10^{-4} /decade. ("Logarithmic aging" means that one expects equal increments of aging from 1 year to 10 years, from 10 years to 100 years, etc.) This corresponds to 0.06% field change between 10 days and 30 years. Aging at this level, if it occurs, can be easily accommodated by occasional recentering of the gradient magnets over the lifetime of the 8 GeV line.

Magnet Assembly

The assembly sequence is as follows (see Fig. 3.1A-1). The pole tips are machined from solid bar stock. The pole tip spacing is set by bolting them down against aluminum pole tip supports at either edge. Magnetized bricks are then epoxied to the top flux return plates. Strips of compensator alloy are interspersed between the bricks above and below the pole tips, and aluminum spacer bars are used to separate the "side bricks". The flux return plates are then lowered (carefully!) onto the pole tip assembly using mechanical fixturing to control the magnetic forces. The magnet is measured using a flip-coil at the magnet factory and shimmed by adding magnetic material at the ends of the pole tips. A steel end plate which terminates the flux lines is then bolted onto each end of the magnet.

Details of the assembly procedures are given in the travelers for each type of magnet. Production drawings [2] of the four magnet types are stored in the Technical Division archives.

Magnetization and Strength Trimming

Ferrite bricks are shipped unmagnetized from the foundry and are magnetized immediately prior to assembly using a 2 Tesla dipole. The material is purchased in standard 1"x4"x6" bricks, with the 1" dimension ground to ± 0.005 " flatness and the 4"x6" dimensions as-fired ± 0.060 ". The dipole side bricks and quadrupole bricks are cut in half before magnetization. The magnetic strengths of the bricks are individually measured and they are

assembled into "kits" each of which contain a specified total magnetic strength. The magnet design is such that a magnet fully loaded with bricks of nominal strength is 3~5% stronger than required. Dummy bricks, fractional bricks and spacers are used to control the total strength of the "kits" to correct for brick-to-brick and lot-to-lot variations. A final strength trim is accomplished by adjusting the amount of ferrite at the ends of the magnet, which can take place by removing the cover plates at the ends of the magnets. This trimming operation was performed in the MP9 magnet factory using a dedicated flip coil system to measure the integrated magnetic strength. The acceptance tolerances on the strength measurements were 0.1%, 0.2% and 0.6% for the dipoles, gradient magnets, and quadrupoles respectively. The strength measurements on all magnets were independently verified with a harmonics probe after shipment to Fermilab's Magnet Test Facility (MTF).

The lot #, serial #, measured strength, and installed position of each ferrite brick was recorded in the travelers for all magnets in the 8 GeV production run. This was done to facilitate tracking of any strength or drift anomalies which might have been occurred in production due to nonuniformities or quality control problems in the ferrite. As of yet no such anomalies have been uncovered, and it is currently felt that this level of documentation is unnecessary for further (e.g. Recycler) production of these magnets.

Thermal Cycling (freezing) the magnets

The strontium ferrite material can be demagnetized by exposure to low temperatures, due to the shifting of the demagnetizing "knee" in the B-H curve to lower H values with decreasing temperature. This is a one-time loss which depends only on the lowest temperature to which the magnet has been exposed. Typical demagnetizations are in the range of 0.1% at 0°C and 10% at -20°C. The degree to which a magnet is demagnetized by a given temperature depends on the "load line" of the magnetic design, i.e. the position on the B-H curve that each region of ferrite is operating on. It also depends on the position of the knee (the coercivity H_c) of the magnetic material which exhibits significant ($\pm 10\%$) lot-to-lot variation from the manufacturer. For these reasons we decided to "freeze" each magnet to 0°C in a custom built refrigerator in the magnet factory prior to final trimming. The refrigerator could process up to 18 magnets overnight. Magnets were measured prior to freezing, at the end of freezing immediately after they were removed from the refrigerator, and after they had returned to room temperature. The strength losses from freezing in production were in the range of 0.1% as expected and no anomalous

strength losses were noted. Positive temperature excursions (up to 40°C) were observed to have no irreversible effects on the magnets.

Temperature Compensation

The intrinsic temperature coefficient of the Ferrite material ($-0.2\%/^{\circ}\text{C}$) is canceled[3] by interspersing a “compensator alloy”[4] between the ferrite bricks above and below the pole tips. The compensator is an iron-nickel alloy with a low Curie temperature and therefore a permeability which depends strongly on temperature. This shunts away flux in a temperature dependent manner which can be arranged to null out the temperature dependence of the ferrite. The degree of temperature compensation is linearly related to the amount of compensator material in the magnet. Thus the degree of compensation can be “fine tuned” to the required accuracy by adjusting the amount of compensator at the ends of the magnet in a manner similar to the strength trimming with the ferrite. For example, a 20-fold reduction of the temperature coefficient (from $0.2\%/^{\circ}\text{C}$ to $0.01\%/^{\circ}\text{C}$) requires that the amount of compensator in the magnet be adjusted correctly to 1 part in 20. This was our acceptance specification in production.

The temperature coefficient of all magnets was measured at the MP9 magnet factory during the warm-up period following the “freezing” of each magnet. In addition, the temperature coefficient of ~20% of the magnets was verified at MTF using a rotating coil and a positive temperature excursion produced by heating blankets and an insulating wrap.

The observed variation in the temperature coefficient of the compensator alloy received from the vendor in production was in the range of $\pm 10\%$. This made it necessary to iterate the temperature compensation in production in one of two ways. For the case of the straight dipoles, the compensator strips run longitudinally in the gap of the magnets and it proved possible to remove and replace these strips with the magnets fully assembled. Since the typical number of compensator strips required was ~13 on either side of the gap, it was straightforward to adjust the amount of compensator to within $\pm 5\%$ of nominal by adding or removing integer numbers of strips of compensator. This procedure was found to converge immediately, requiring in most cases only a single additional cooldown cycle to verify the compensation of the trimmed magnets.

The compensator situation in the gradient magnets was more complicated. In this design the compensator runs transversely between the bricks behind the pole tips and cannot be replaced after assembly of the magnets. The partial disassembly of the magnet necessary to retrim the compensation takes approximately two hours and was incompatible with the desired 2

magnets/day production rate. Thus we decided to pre-mix the compensator strips from a number of production lots into the kits for individual magnets. This made the compensator alloy a uniform and predictable product across a large number of magnets. After some false starts (apparently due to difficulties with the reproducibility of the magnet measurement apparatus) this procedure was successful at reducing the fraction of magnets which had to be reworked to less than 10% of the total production.

Nonlinearities of Temperature Compensation

The ultimate limit to the temperature range of the compensation technique is set by the nonlinearities of the opposing temperature coefficients. The ferrite material appears to be highly linear over the relevant temperature range; however, the compensator material tends to become weaker as it approaches its effective Curie temperature of $\sim 55^{\circ}\text{C}$. Fig. 3.1A-3 indicates the degree of compensation that we are able to achieve on a test magnet using ferrite and compensator materials from the production (low bidder) vendors.

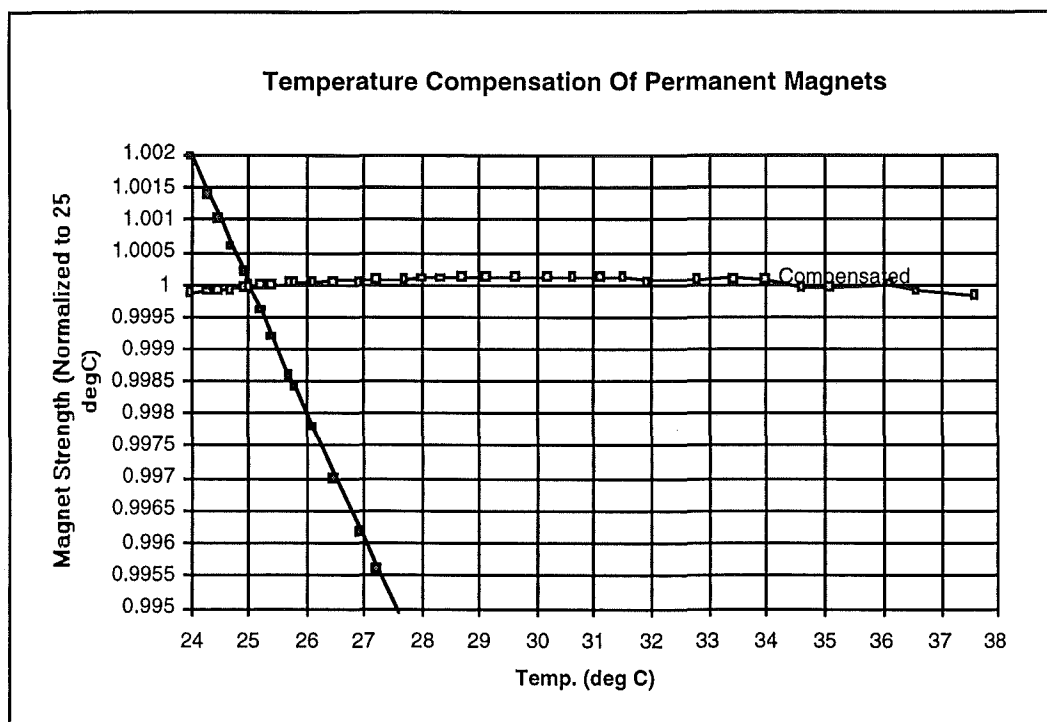


Figure 3.1A-3 - Field Strength vs. Temperature for a Stability Test Magnet using preproduction samples from the selected vendors for Compensator Alloy and Ferrite.

Magnet Sorting and Thermal Coefficients

In production, the amount of compensator was not fine-tuned to this accuracy and a maximum temperature coefficient of $\pm 0.01\%/^{\circ}\text{C}$ was tolerated. Following production, the measured thermal coefficients of individual magnets were used in the assignment of magnets to positions along the line. This procedure simultaneously optimized the closed-orbit distortion of the line at three different operating temperatures, and effectively used the betatron phase advance between magnets to cancel opposing temperature coefficients of the magnets. After sorting, the calculated horizontal closed-orbit distortion due to temperature changes of 10°C was less than 0.5mm RMS.

Transient Thermal Effects

A rapid thermal transient (such as can be produced by several hundred watts of heating tape, or condensation from exposure of a frozen magnet to a warm, humid environment) is observed to produce a large strength transient in the magnets[5]. This is believed to be due to a temporary temperature mismatch between the ferrite and compensator when the magnet is out of thermal equilibrium. The effect is most pronounced in the straight dipoles where the compensator is located in the magnet gap and the ferrite is located by the flux return, and can be as large as ~50 units. The thermal transients which produce these effects are substantially larger than one expects in the 8 GeV line tunnel, and it remains to be seen whether this is an operational difficulty.

Gradient Magnet (PGD) Design

The basic design of the PGD gradient magnet is shown in Fig. 3.1A-1. It is a 1.59 kG gradient (combined-function) dipole with a 2" gap and a 3.5" good-field aperture (5.5" physical aperture) in the bend direction. Overall dimensions are 7.5" high by 9.5" wide by 161.5" long. The weight is 2000 lb. The magnets are straight and the sagitta of the beam inside a magnet is 1 cm. A cross section of the magnet is shown in Fig. 3.1A-4, and a field map in Fig. 3.1A-5.

A significant design decision made in the 8 GeV line magnets was to include "side bricks" which drive flux into the pole tips from the sides. These provide a more magnetically efficient design than a design without side bricks, since the field strength drops by ~40% when they are removed. This allows a compact design to provide the 1.5kG average bend field needed to follow the 8 GeV line tunnel. The side bricks also provide useful field shaping at the edges of the aperture, which reduces the amount of end shimming necessary at the edges of the pole tips.

While the "side brick" design proved economical and more than adequate for meeting the 8 GeV line field quality requirements, a number of design and production issues arose which argue against the use of side bricks in higher-quality storage ring magnets e.g. for the Recycler. First, the amount of edge field shaping from the side bricks appeared to be underestimated in the POISSON model of the magnet. The first prototypes of each of the side brick designs showed an excess of field strength at the edges of the aperture. In order to obtain the optimal field shaping at the edges, the side bricks had to be moved upwards by inserting 3/16" shims on either side of

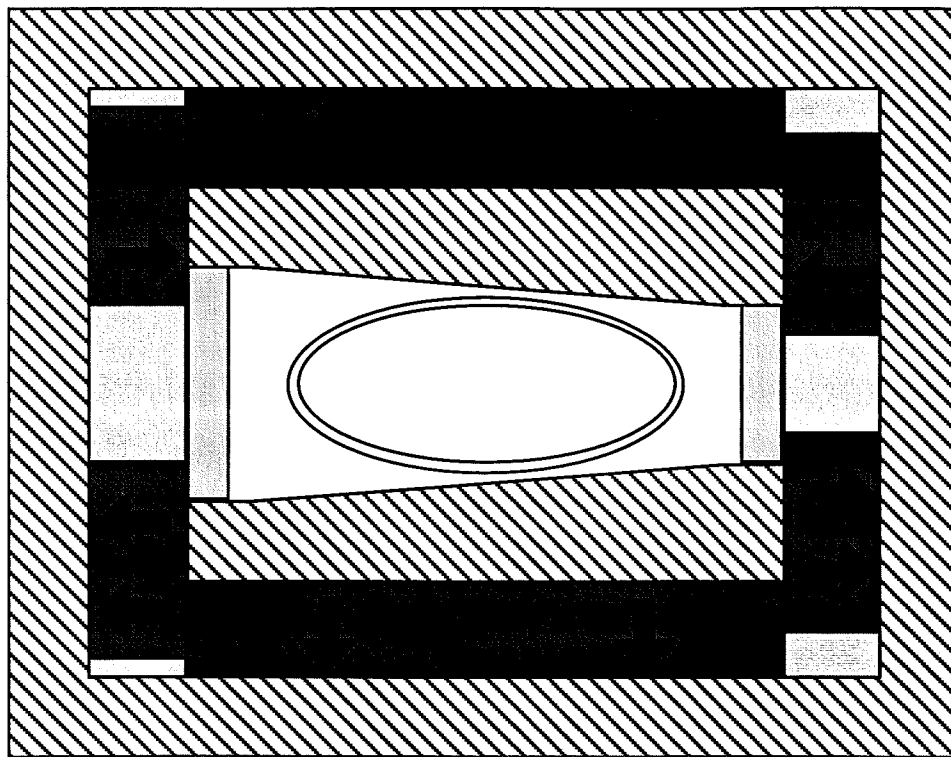


Figure 3.1A-4 - 8 GeV Line Gradient Dipole Permanent Magnet (PGD)

the midplane spacers. This reduced the strength of the magnet by a small amount ($<2\%$) which was well within the range of the strength trimming.

The second difficulty observed with of the side brick design was the magnet-to-magnet variation in the field shaping from the side bricks. These fluctuations were at the level of a few $\times 10^{-4}$ total field defect at 1" as described in the section on measurements. Presumably this was due to variations in the relative strength and installed position of the side and top bricks.

The final difficulty with the side brick design is that the observed multipoles exhibited some temperature dependence (a fraction of a unit per degree C) [6]. This is due to the compensator being interspersed with the top bricks but not the side bricks, with the result that the field shaping from the side bricks is temperature dependent.

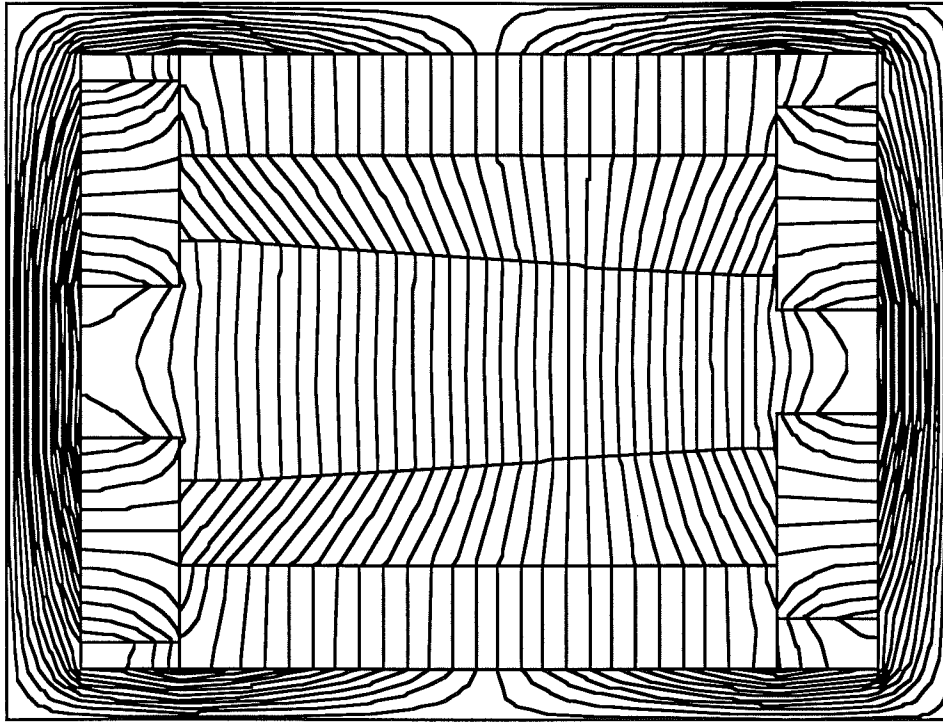


Figure 3.1A-5 - POISSON Field Map of PDG Gradient Dipole

Dipole Magnet (PDD and PDV) Design

The two straight dipoles PDD and PDV are identical in cross section and differ in length and integrated strength. A cross section of the magnet is shown in Fig. 3.1A-6, and a field map in Fig. 3.1A-7. The PDD (a.k.a. “Double-Double Dipole” or “Horizontal Bend Dipole”) provides the same 20mrad bend as the gradient magnet in a shorter package due to the higher 2.3 kG bend field. This higher strength is achieved by stacking the ferrite bricks two deep behind the poles and at the sides of the magnet. This shorter length provided a substantial amount of free space in the lattice to allow for the installation of additional correctors, instrumentation, etc. at a later date. The PDV magnets (a.k.a. “Vertical Bend Dipoles” or “PB2 Dipoles”) are longer versions of the PDD which are mounted on their sides to provide the bends in the vertical drop region of the 8 GeV line.

The PDD and PDV bend dipoles have a completely flat pole tip fabricated from a single piece of Blanchard-ground bar stock. No edge shims are needed on the pole face to provide adequate field quality because of the field shaping provided by the side bricks. This represented a significant cost savings over a custom ground pole profile.

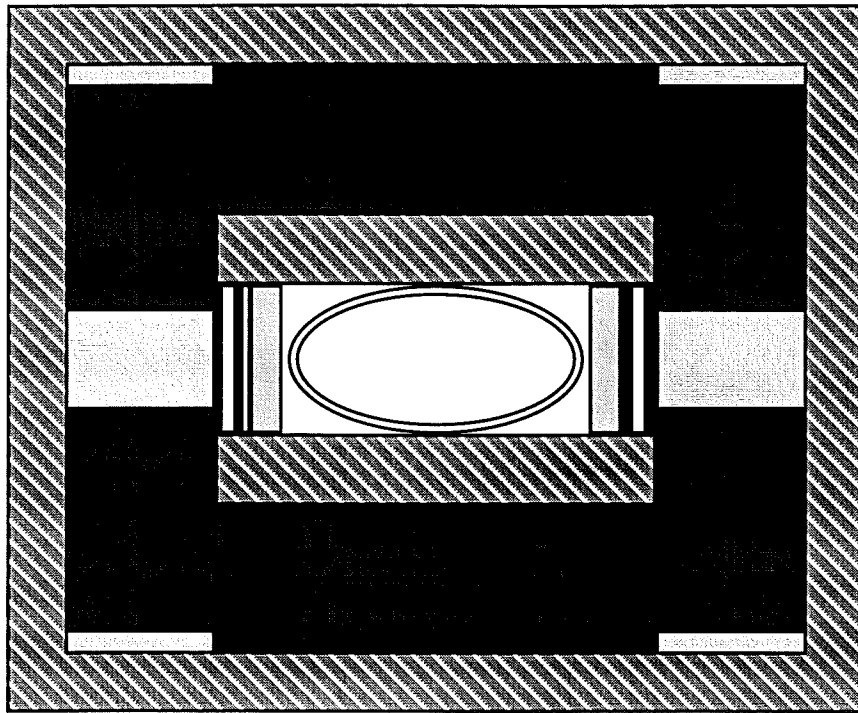


Figure 3.1A-6 - 8 GeV Line Dipole (PDD and PDV) Cross Section

A significant design choice for the PDD and PDV dipoles was the placement of the compensator material at the edges of the magnet gap region. (The compensator alloy is interspersed with the ferrite bricks behind the pole tips in the gradient magnet, as well as subsequent Recycler prototype magnets). The advantages of the gap compensator are 1) the design is more magnetically efficient since none of the ferrite space behind the pole tip is wasted, 2) less total compensator is used since it only spans the 1" half-gap of the magnet, and 3) the compensator strips run longitudinally and can be replaced and the compensation adjusted after assembly of the magnet. The disadvantage of the gap compensator is a slight sensitivity of the field shape to both compensator placement and temperature. Both effects are at the level of a few "units" in extreme cases, and thus are adequate for the 8 GeV transfer line magnets but undesirable for the Recycler storage ring magnets.

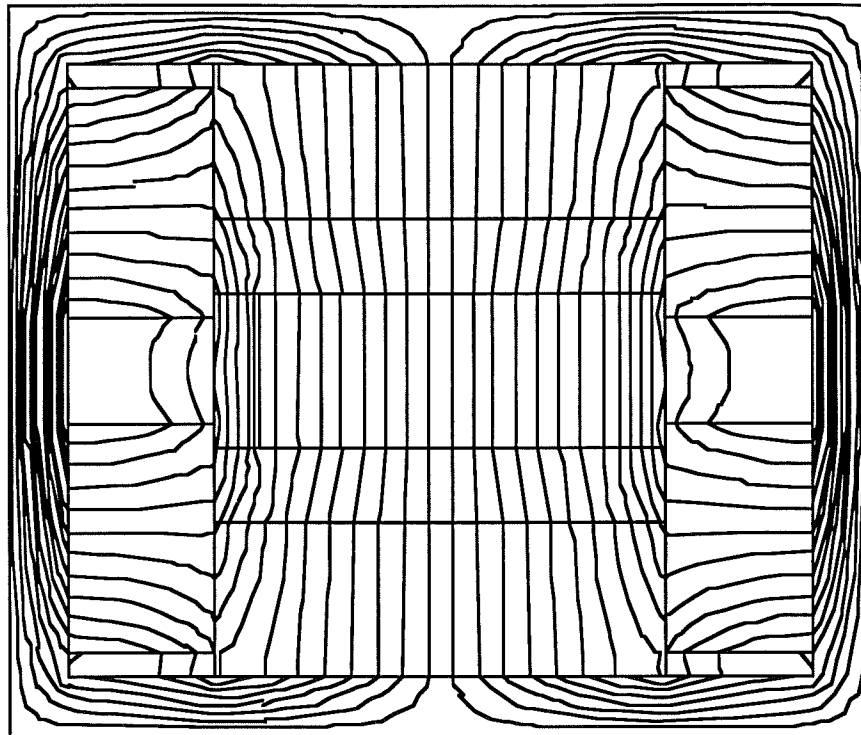


Figure 3.1A-7. POISSON Field Map of PDD and PDV Dipoles

Permanent Magnet Quadrupole Design

Nine permanent magnet quads are used in the FODO cells of the reverse bend section of the 8 GeV Line. The pole tip radius is 1.643", the same as the Main Ring/Main Injector quadrupoles. The magnetic (pole tip) length is 20" and the overall length (steel-to-steel including flux clamp end plates) is 24.5". The integrated gradient is [1.481 T-m/m].

The quadrupole (Fig. 3.1A-8) has a hybrid design analogous to the gradient dipole. The field shaping is provided by machined steel pole tips and the field is driven by strontium ferrite bricks. Temperature compensation of the ferrite is provided by interspersing strips of compensator alloy between the bricks along the length of the magnets. Solid "bar stock" construction is used throughout. The pole tips are supported at the ends by pinning and bolting into stainless steel support plate. A steel flux return shell surrounds the magnet, and "flux clamp" end plates are used to terminate the field at the ends of the magnet.

The magnetic strengths of the pole tips in the magnet are trimmed by placing variable number of steel washers in the corners of the magnet behind each pole tip. This trimming takes place using a "Rogowski Coil" to measure the magnetic potential of each pole tip. The field

shape (mainly the systematic 12-pole from the magnet ends) can then be trimmed out by adding steel washers to bolts at the ends of the pole tips.

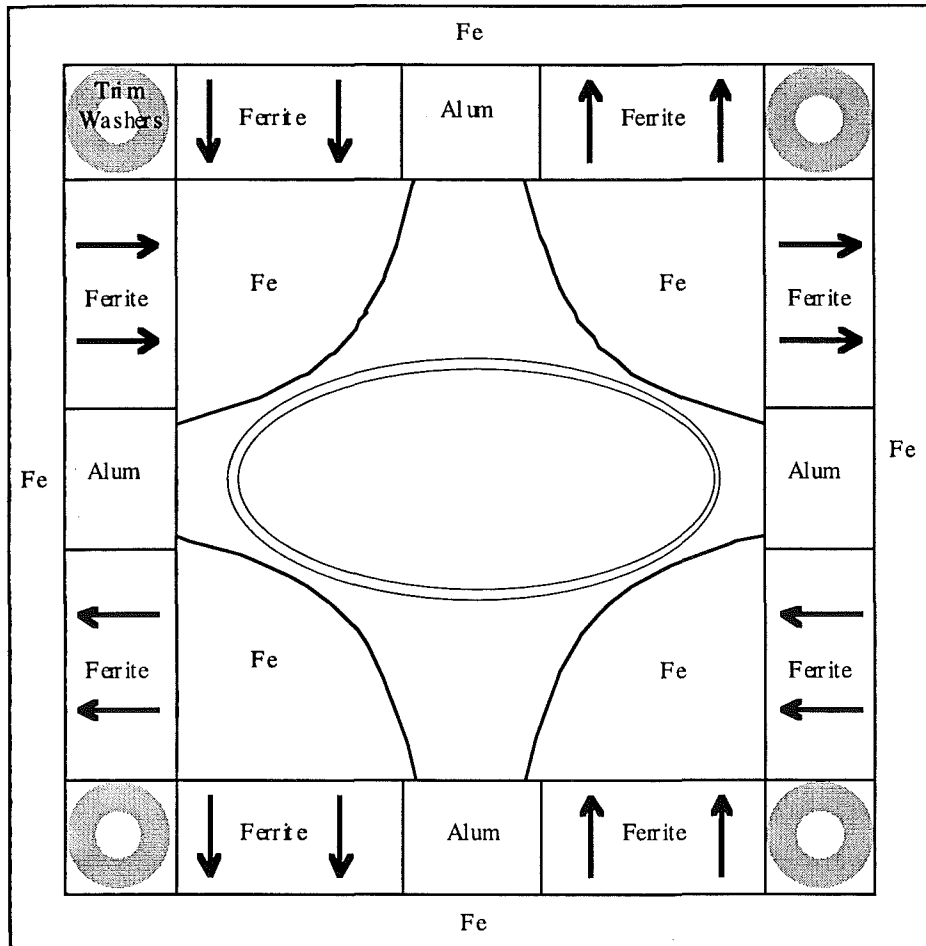


Figure 3.1A-8. Cross section of 8 GeV Quadrupole Magnet.

Magnetic Measurements - Field Strength

Several types of field strength measurements were performed on the 8 GeV line magnets. In the MP9 magnet factory the strength trim and temperature compensation trim were performed via a flip coil or Rogowski coil for the dipoles and quads respectively. A manual flip coil with non-precise positioning was used for the straight dipoles, and a motorized flip coil suspended from the survey fiducials was used for the gradient magnets. The magnets were then shipped to Fermilab's Magnet Test Facility (MTF) where the strength and field shape were measured using rotating coils and (for a limited subsample of production magnets) a stretched-wire system.

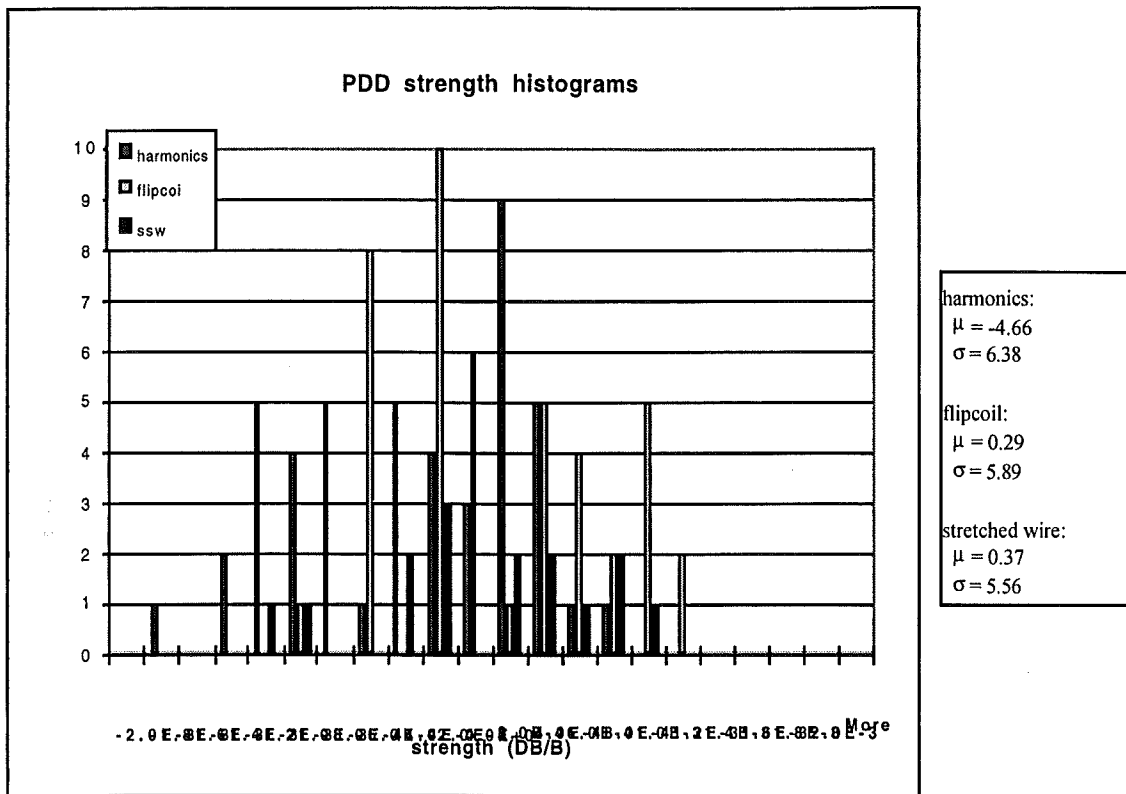


Figure 3.1A-9. Distribution of PDD strengths measured with the harmonics probe at MTF, the manual flip coil at the MP9 magnet factory, and the single stretched wire system at MTF.

A manually operated Rogowski coil was used to measure the strengths and temperature coefficients of the four independent pole tip potentials of the quadrupoles. These measurements were used to trim the strengths of each pole in the quad, by installing a variable number of washers on a threaded rod behind each pole tip.

Magnetic Measurements -Temperature Coefficients

Figures 3.1A-10 and 3.1A-11 show the distributions of temperature coefficients for the PDD and PGD magnets, respectively. Magnets outside the acceptance tolerances had the number of compensator strips changed, their strength re-trimmed, and the compensation remeasured.

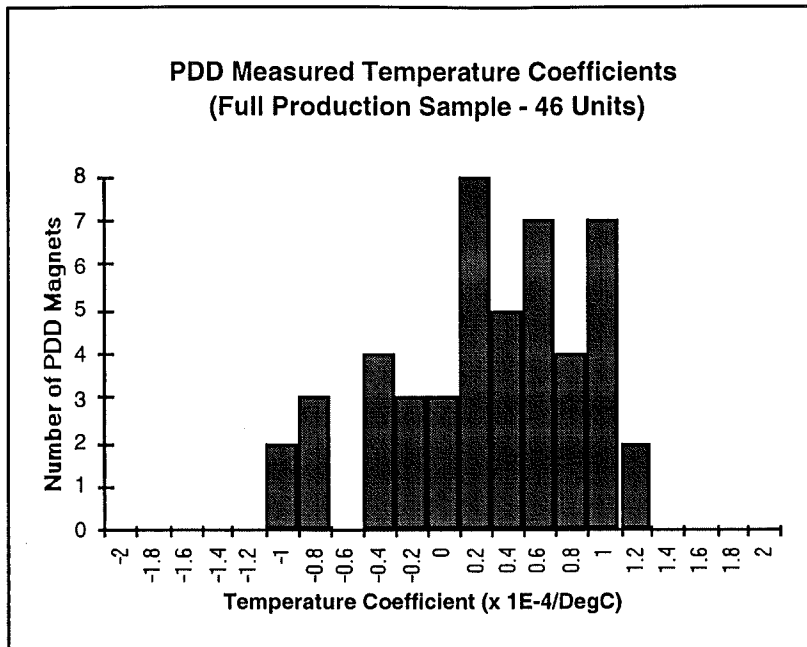


Figure 3.1A-10. Temperature Coefficients measured for the production run of PDD magnets. The mean is 0.15 units/°C, the standard deviation is 0.60 units/°C, and the acceptance tolerance was 1.2 units/°C.

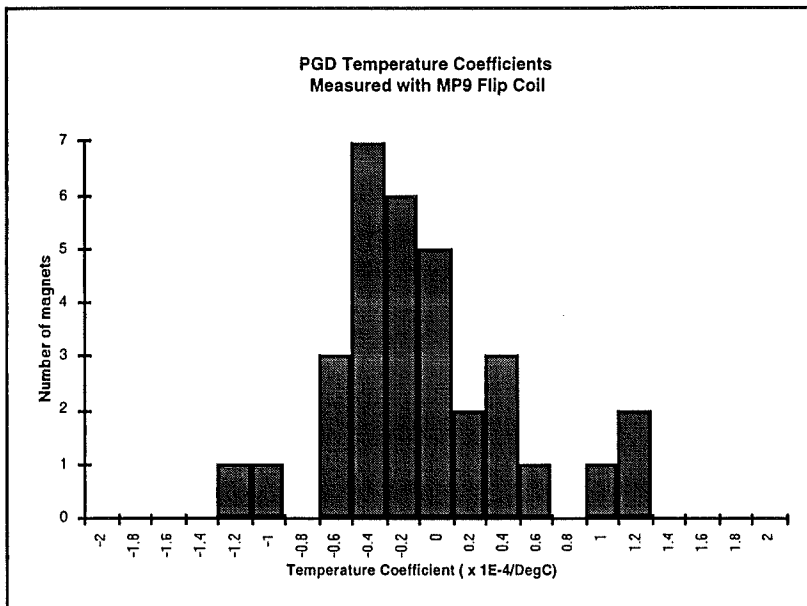


Figure 3.1A-11. Temperature Coefficients measured for the first 37 magnets of the production run of PGD magnets. The mean is 0.18 units/°C, the standard deviation is 0.55 units/°C, and the acceptance tolerance was 1.3 units/°C.

Magnetic Measurements - Field Quality

The field quality specification for acceptance of 8 GeV line dipoles and gradient magnets was set to 10 units of total field defect (By vs. X on the midplane) as measured at MTF by a single harmonics probe measurement at the center of the aperture. Since the observed field defect is dominantly a gradient error arising from non-parallelism of the pole tips, this scales roughly to $\delta B/B = 0.2\%$ over the design good-field aperture of 1.75"(v) x 3.5"(h). This specification represents a compromise between the minimum field quality required for adequate performance of a transfer line (where a field defect of $\sim 0.5\%$ would be adequate) and the Recycler permanent magnet field quality (which must be in the range of a $1-2 \times 10^{-4}$ over a 1" aperture).

The basic manufacturing strategy was to specify machining tolerances of typically ± 0.003 " for the iron pole tips of the magnets, which is sufficient to guarantee roughly 0.1% field defect over the aperture. Mechanical provisions were made for end shims on the ends of the pole tips which can be used to null out up to ~ 10 units of integrated field defect in the magnets. The end shims were not found to be necessary to meet the 8 GeV line field quality specifications. (This procedure was successfully used for the Recycler prototype magnets). The dominant source of field error arises from assembly tolerances in the parallelism of the pole tips, which produces a gradient error of roughly 1 unit per mil of mismatch between the side supports of the pole tips.

**Table 3.1A-3. Measured systematic and random multipoles (in Fermilab units @1")
for the production run of PDD dipoles.**

Pole	Normal		Skew	
	mean	std dev	mean	std dev
Quadrupole	-0.10	1.74	-2.65	3.66
Sextupole	-1.43	0.87	-0.24	2.75
Octupole	0.00	0.15	-1.09	1.34
10-pole	-0.73	0.56	-0.04	0.50
12-pole	-0.03	0.08	-0.10	0.14
14-pole	-0.12	0.18	0.00	0.08

Magnet Measurements - Quadrupoles

For the quadrupoles the field strength and shape specifications were driven by the requirement that the integrated field errors for a half-cell containing quadrupoles should be smaller than those of cells containing gradient magnets. As a result the field tolerances were considerably relaxed due to the 12x smaller normalization amplitude for the harmonics of the quads compared to the bend magnets. For example, a barely allowable 10-unit gradient error in the dipoles corresponds to a 120 unit strength error in the quadrupoles. The situation for higher multipoles is similar. In actual production the strength and multipole distributions [Fig.3.1A-12] were tighter than this. In addition, the assignment quadrupoles in the line paired one weak with one strong quadrupole, further attenuating any effects of quad strength variation.

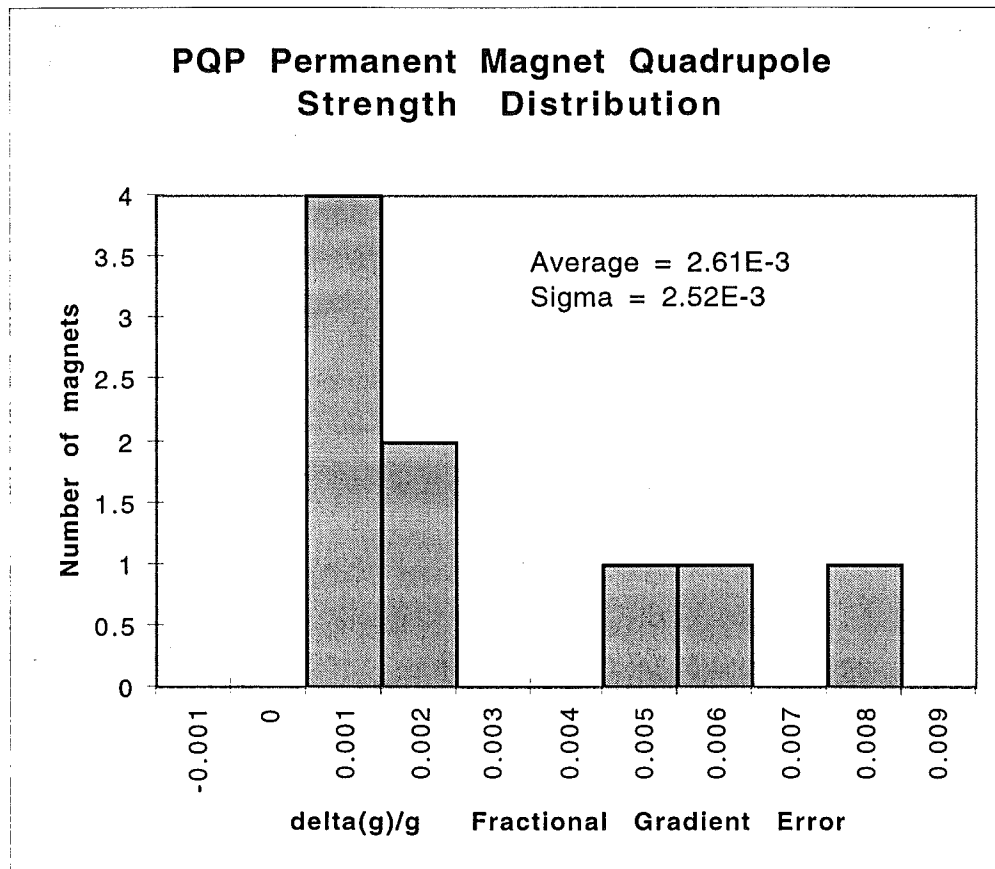


Figure 3.1A-12. Field strength distribution for 8 GeV line Quadrupoles.

REFERENCES

- ¹ Type 8 Strontium Ferrite data sheets & specs from Arnold, Crucible, Hitachi. Hitachi (Ardsmore, MI) was the low bidder on the ferrite for the 8 GeV line.
- ² The Technical Division assembly drawing package numbers for the 8 GeV line permanent magnets are: PGD (gradient magnet): ME-338124 , PDD (Horizontal dipole): ME-341007, PDV (vertical bend dipole) ME-341022, Quadrupole (PQP) : ME-341045.
- ³ Dallas 1995 PAC papers on permanent magnets by Bertsche & Ostiguy, Foster & Jackson.
- ⁴ Carpenter Technologies Compensator 30 type 4 data sheets from; Telecon data sheet, Eagle Alloys, Sumitomo Heavy metals.
- ⁵ Hank Glass, Presentation in the collected transparencies from the Main Injector Magnet Physics (MIMP) meetings.
- ⁶ Hank Glass, Presentation in the collected transparencies from the Main Injector Magnet Physics (MIMP) meetings.

CHAPTER 3.2 VACUUM

WBS 1.1.2. MAIN INJECTOR VACUUM

WBS 1.1.2.1. MAIN INJECTOR RING VACUUM

Main Injector Vacuum System WBS 1.1.2.1, 1.1.2.2, 1.1.2.3

The Main Injector vacuum system design incorporates the most useful features of both the Main Ring and the Tevatron. As shown in Figure 3.2-1, the ring is divided into 21 vacuum sections by 21 pneumatic, automatic (fail closed) sector valves. A typical sector valve assembly is shown in figure 3.2-2. There are two convectron gauges and one cold cathode gauge between each sector valve. The section gauges are connected to the vacuum system at the quadrupole vacuum chambers by means of a Conflat (copper gasket) flange. Spacing for the sector valves varies from 170 to 1000 ft. Additionally, each vacuum sector is fitted with hand valves which provide ample ports for pumpdown, letup and leak detection. Sector valves are used to isolate RF cavity groups from Main Injector magnetic components, enabling the cavities to remain under vacuum should maintenance be required within the Main Injector lattice. All permanently installed vacuum components are connected by metal seals, thereby limiting the Main Injector ring elastomers to the 21 gate seals, one per sector valve, and gate seals on rough valves and leak test valves. Sector rough down is accomplished by attaching a self protected turbomolecular pump to the system through a flex hose and a 2-1/2" "O"-ring hand valve roughing port. No permanently installed roughing stations are installed, thus permitting the 10 pumps to be utilized most effectively during initial installation and maintenance situations. Vacuum component specifications are incorporated in Table 3.2-1.

Main Injector sector valves are controlled electro-pneumatically using both the Pirani gauges and the ion pump currents as permitting parameters. Pneumatics are provided by at least 2 (for redundancy) 18 cfm, 125 psi screw type air compressors. Air leaving the compressor is cycled through an air cooled, refrigerated, auto-drain, air dryer before entering the receiving tank. The air is then regulated to 100 psi and delivered to the tunnel via a system of ball valves, check valves, and copper manifolding which allow for redirecting air in the event of a compressor failure. Each beam valve is provided with a ballast tank with sufficient volume to operate the valve once should the 110V solenoid power fail, thereby closing the valve.

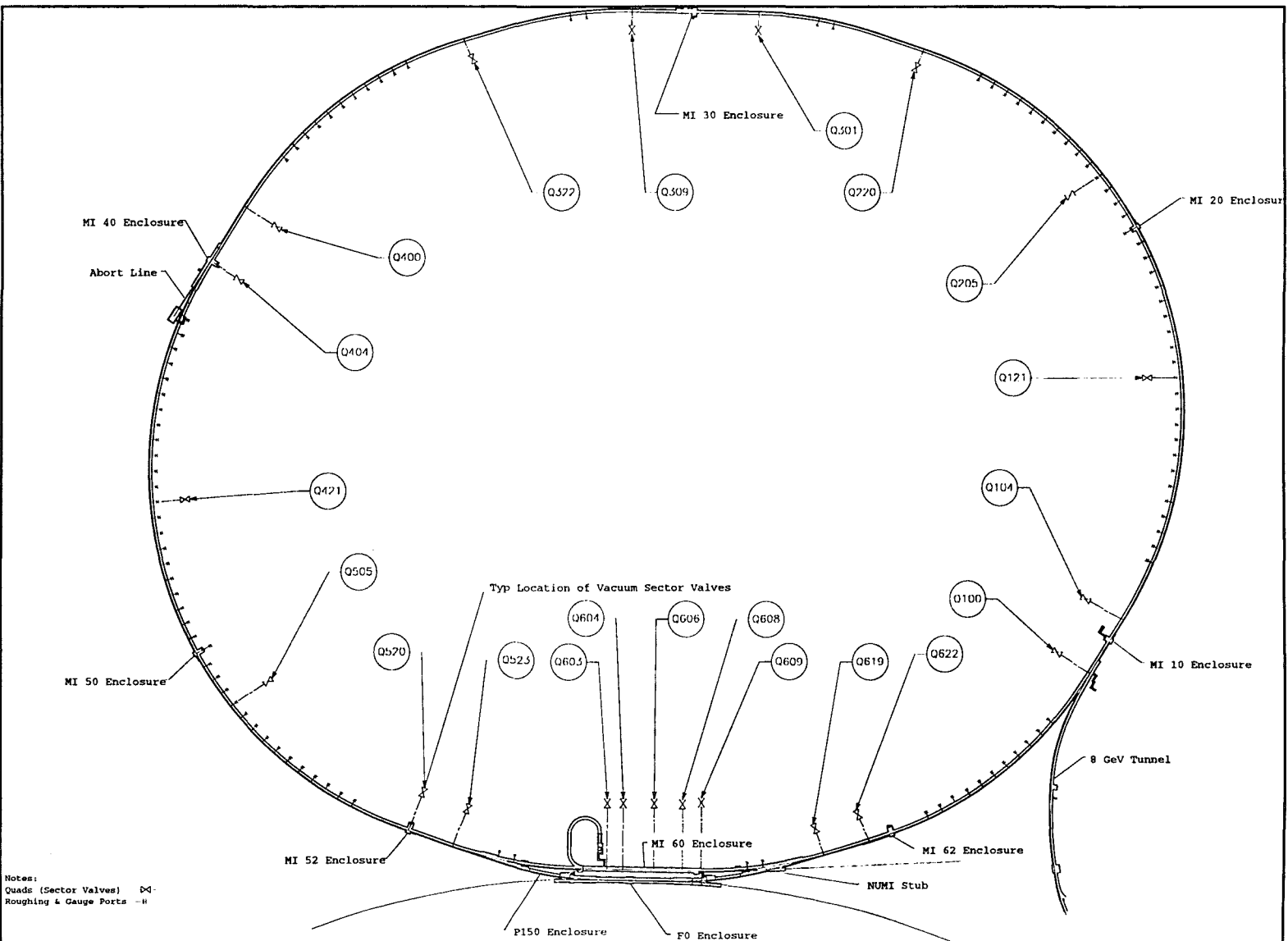


Figure 3.2-1 Main Injector Vacuum Valves and Instrumentation Layout.

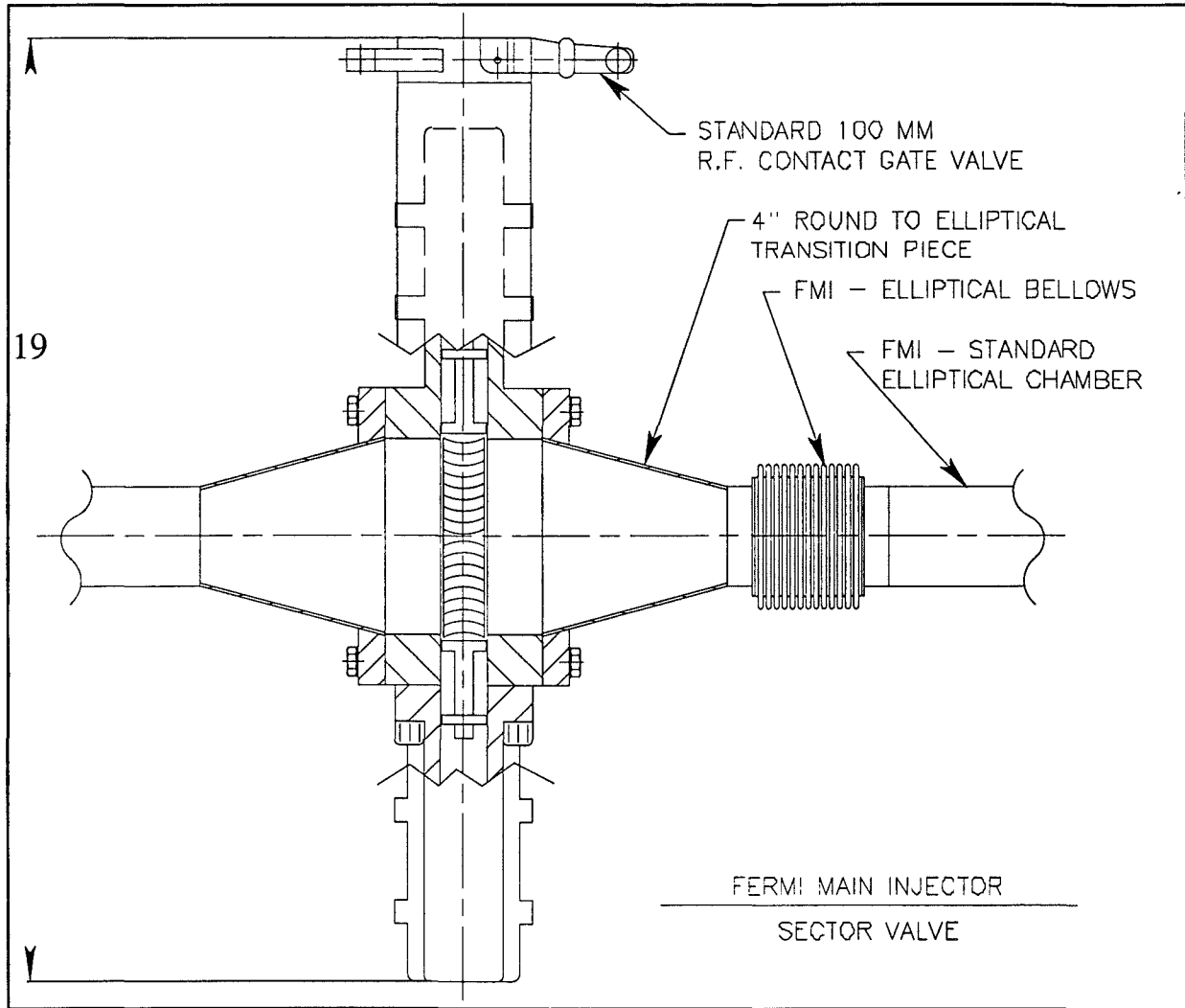


Figure 3.2-2 Main Injector Sector Valve.

Table 3.2-1

Component	Type	Quantity		
		MI	8GeV	150 GeV
Ion Pump	30 l/s diode	646	60	40
Ion Pump	600 l/s diode	25		
Sector Valve	4" pneumatic "O" ring gate R.F. shields	16	4	
Sector Valve	6" pneumatic "O" ring gate R.F. shields	5		
Sector Valve	6" pneumatic "O" ring gate			4
Rough Valve	2 1/2" hand "O" ring seal	48	8	
Rough Valve	4" hand "O" ring seal	4		
Utility Valve	1 1/2" hand "O" ring seal	50	8	12
Cold Cathode Gage	Penning	42		10
Pirani Gauge	Convectron	42	8	20

Main Injector dipole beam tubes are 16 gauge 316L stainless steel which is formed, seam welded, and chemically cleaned. The beam tube cross section is chosen such that it can be inserted through the existing Main Ring quadrupole tubes and be captured by the Main Injector dipole pole tips. Its section is shown in Figure 3.2-3. Attached to the tubes are access ports for gauging and ion pumps. Access ports are shown in figures 3.2-4 and 3.2-5. The access ports are provided with machined or laser cut slits which allow both pumping and conduction of the image current along the longitudinal direction of the tube.

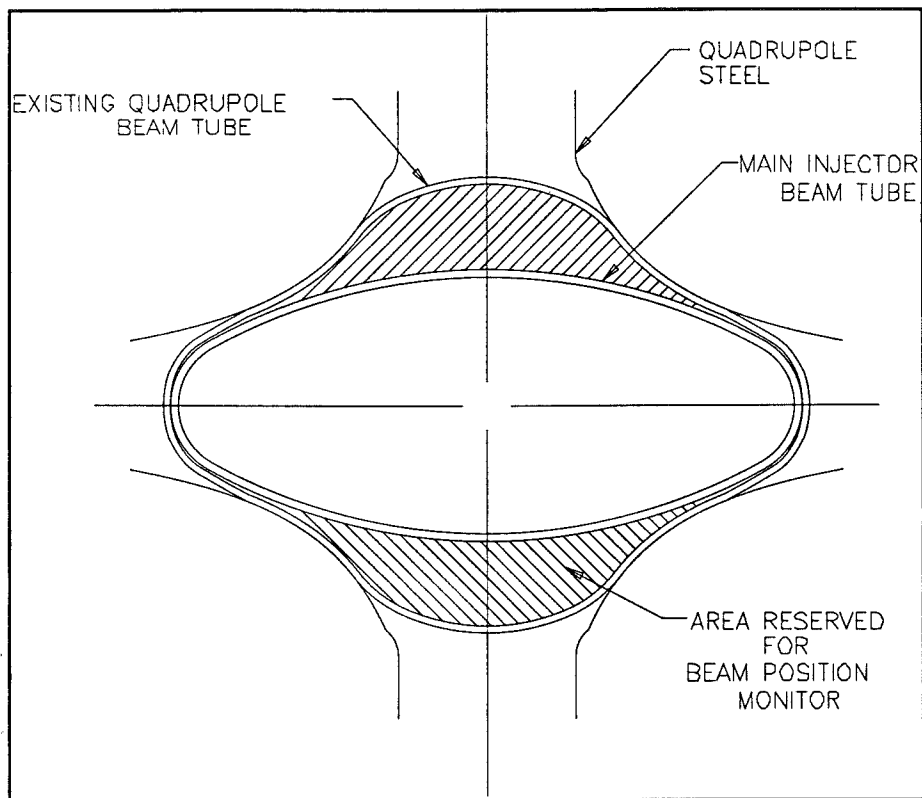


Figure 3.2-3 Beam Pipe Cross-Section
(Shown Inserted Inside Quadrupole “Star-Shaped” Beam Pipe).

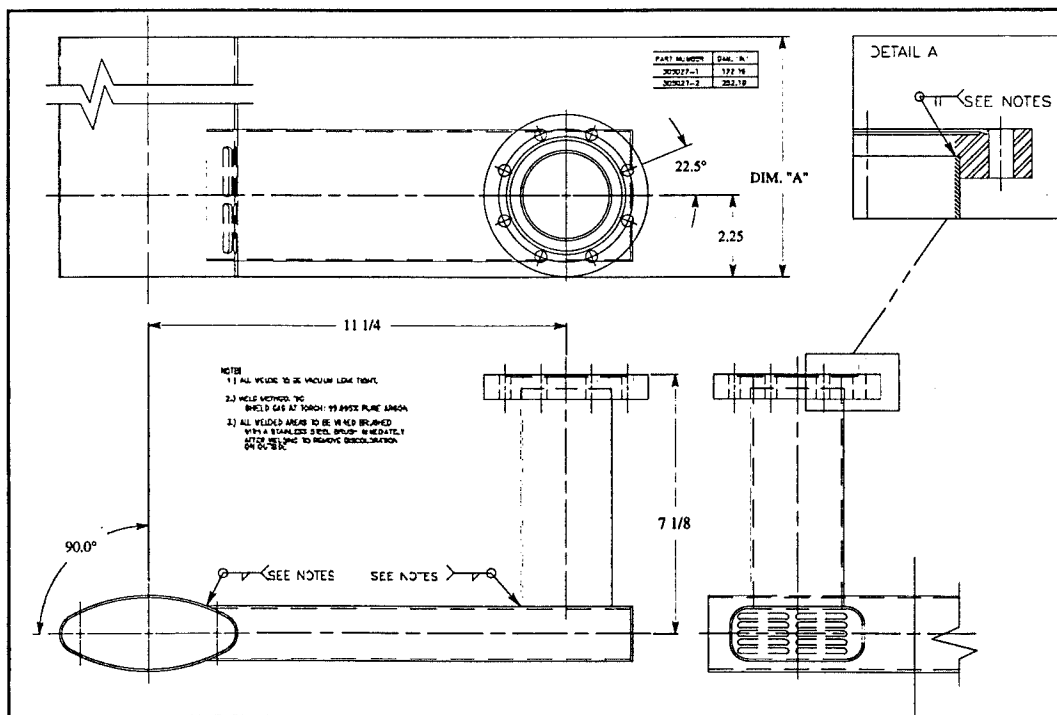


Figure 3.2-4 Ion Pump Port/Beam Tube Assembly.

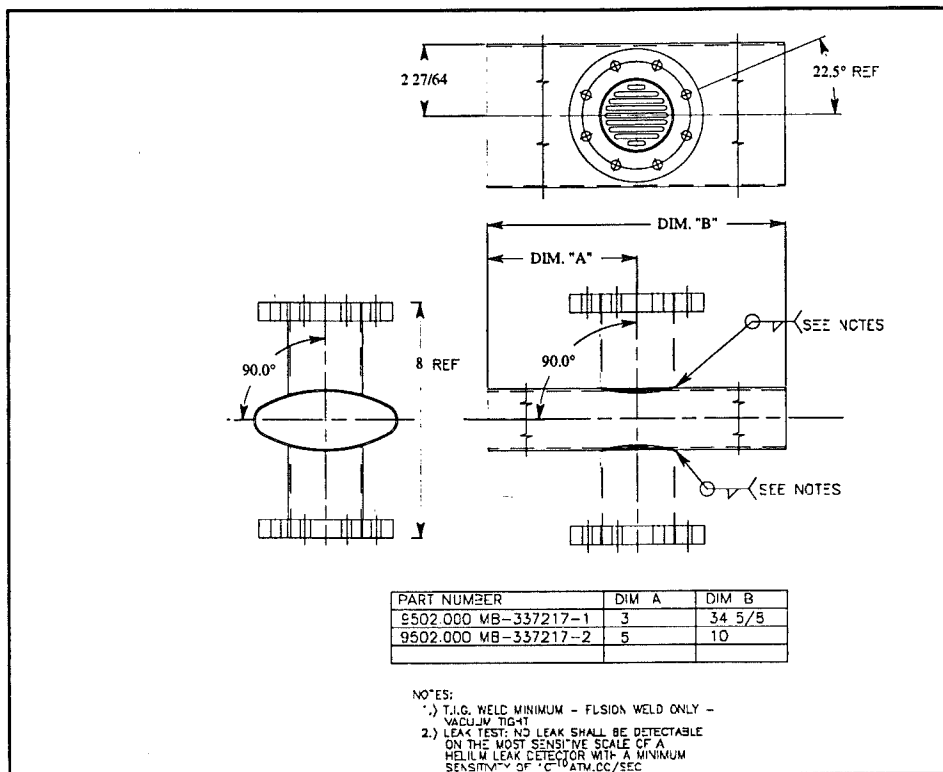


Figure 3.2-5 Dual Port Beam Tube Assembly.

Quadrupole vacuum chambers are constructed from the same material as the dipole chambers with the addition of a beam position monitor fabricated from 2 stainless steel half shells as shown in Figure 3.2-6 and assembled into a quadrupole chamber as shown in Figure 3.2-7. A typical quadrupole slot length including a valve is shown in Figure 3.2-8.

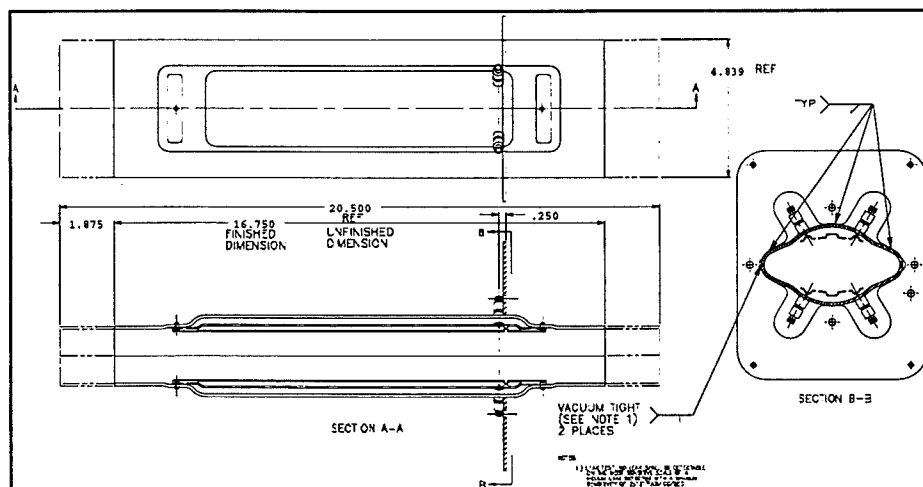


Figure 3.2-6 Main Injector BPM.

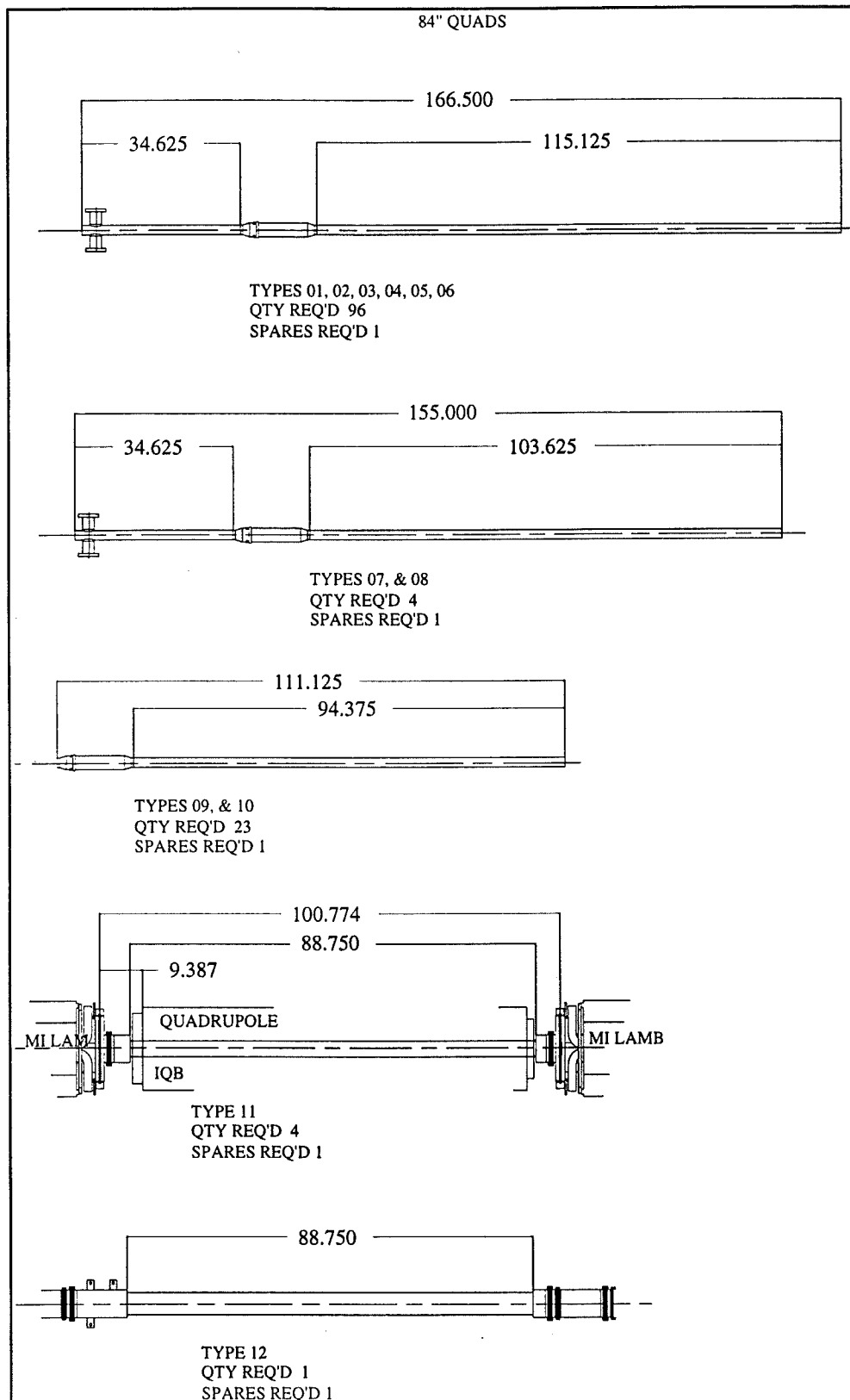


Figure 3.2-7 Quadrupole Beam Pipe Assembly.

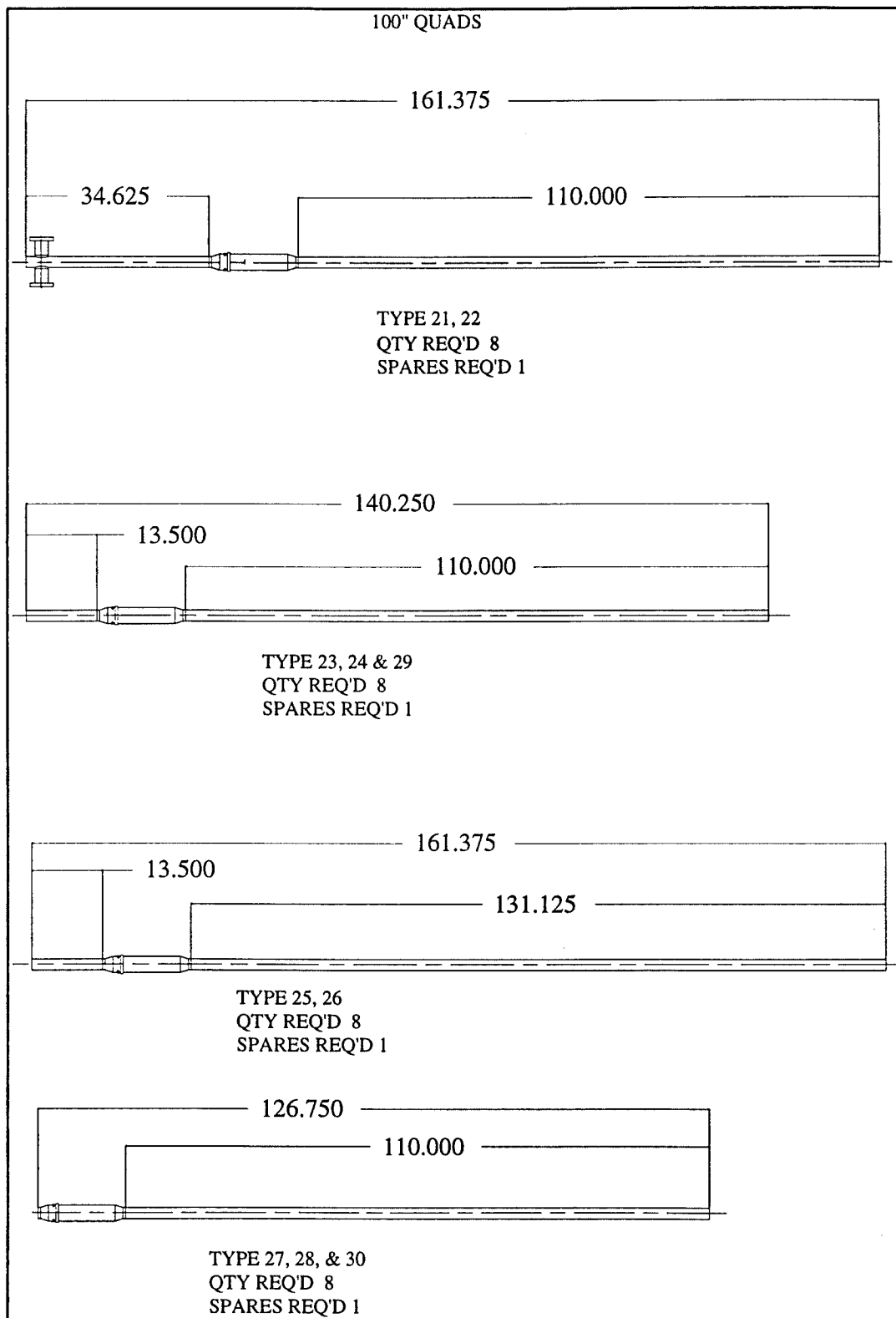


Figure 3.2-7 Quadrupole Beam Pipe Assembly (cont.).

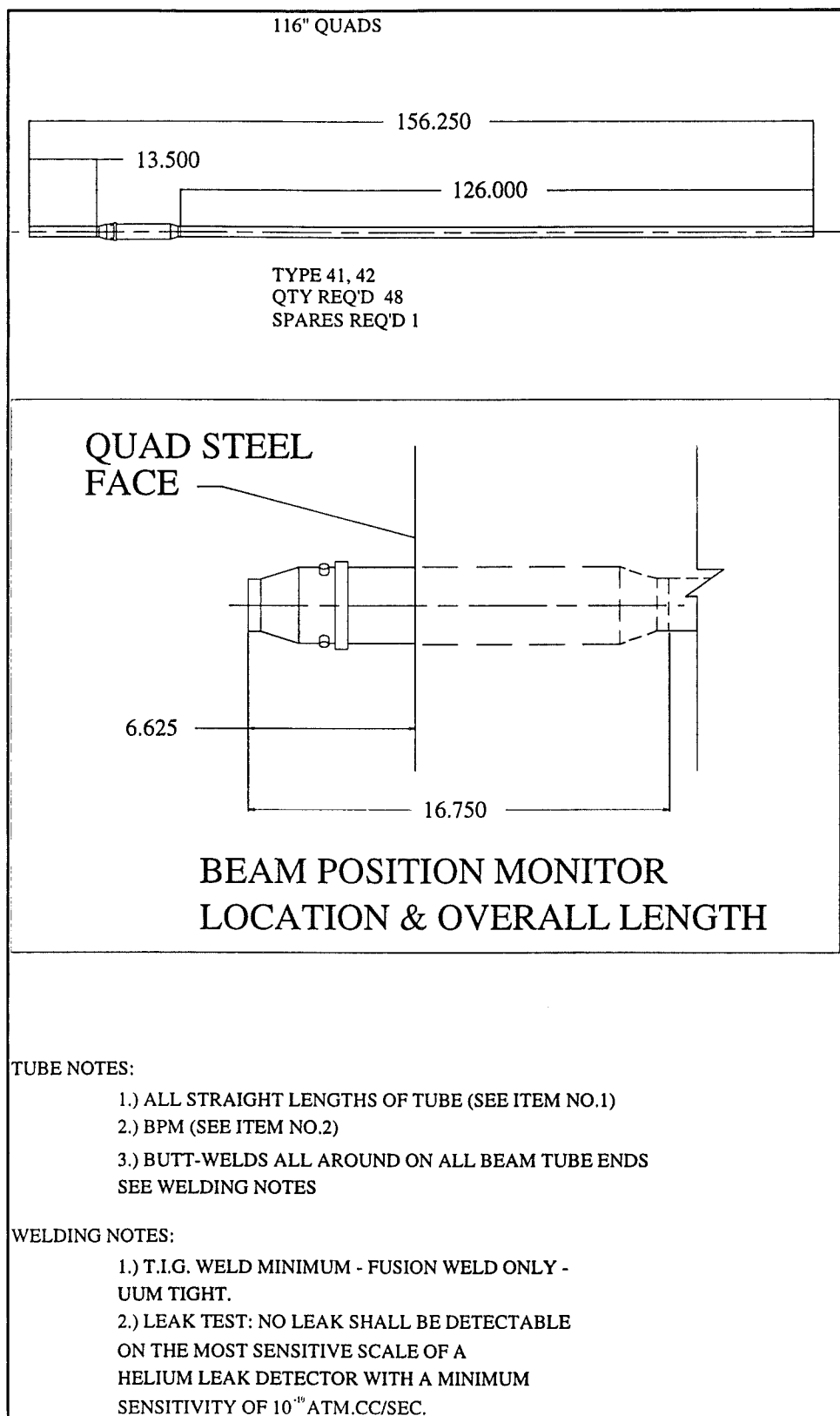


Figure 3.2-7 Quadrupole Beam Pipe Assembly (cont.).

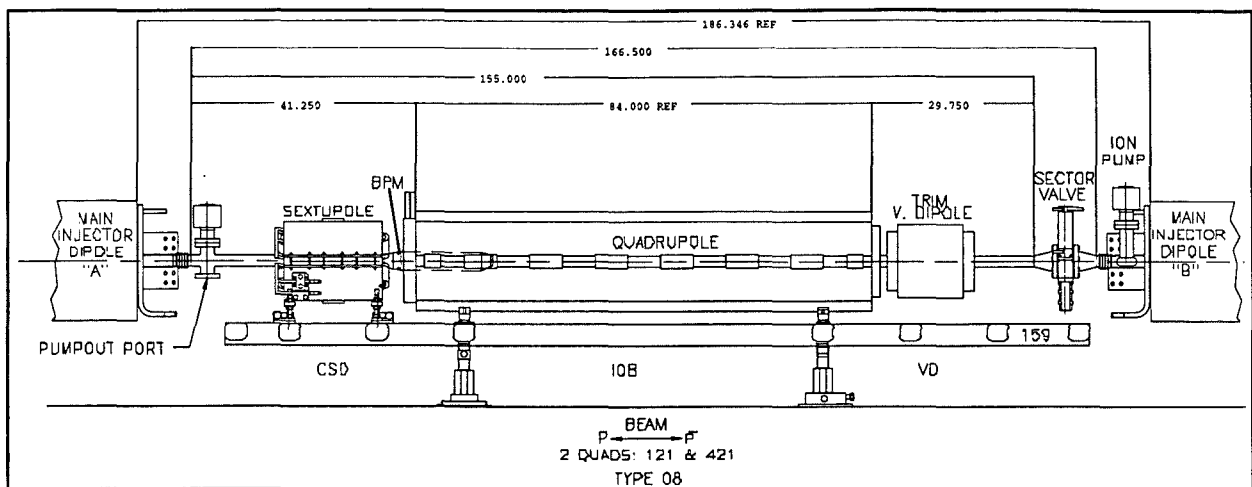


Figure 3.2-8 Typical Quadrupole Slot Length with Valve.

All vacuum chambers are connected by welded in place bellows assemblies. Bellows are elliptical formed convolutes made of 316L stainless steel. In order to minimize image current effects, special inserts and a moveable slide equipped with stainless steel spring fingers is provided as shown in Figure 3.2-9.

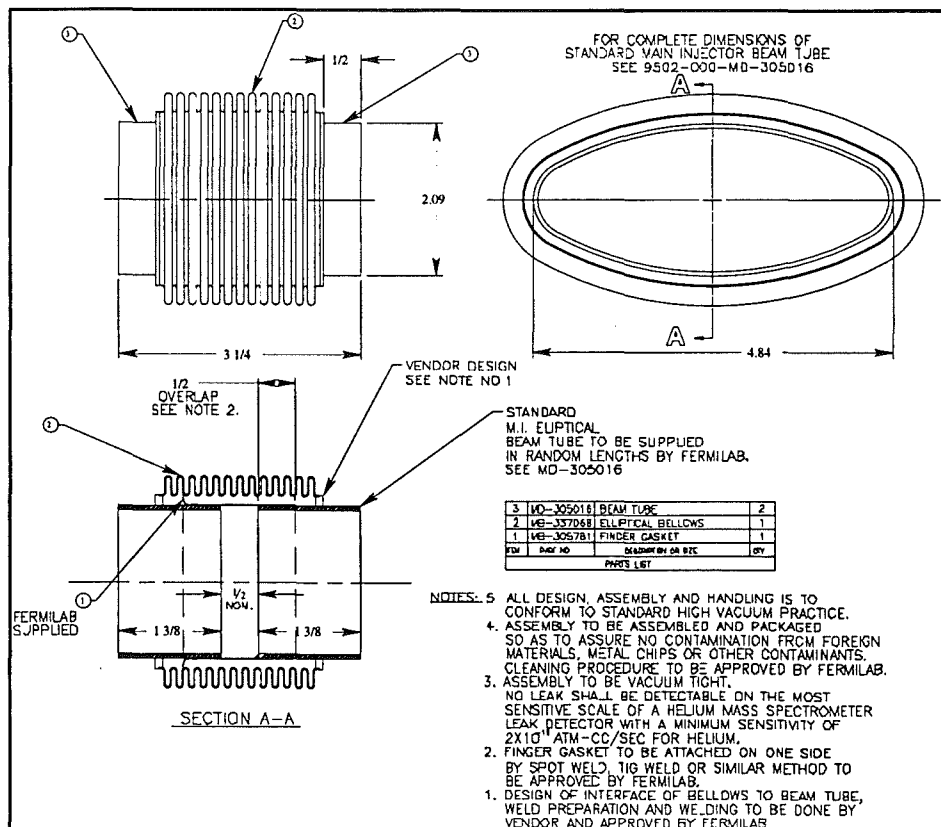


Figure 3.2-9 Bellows Assembly.

Vacuum controls are provided by new CIA crates located in each of 6 service buildings. The ion pump supplies are new. The instrumentation for the vacuum system consists of analog outputs from pirani gauges, cold cathode gauges, and ion pumps. The vacuum system is controlled from a CIA crate which provides all information remotely. The position of the sector valves is provided both locally and remotely. Sector valves have a special card for control and interface purposes and have interlocks tied to both pirani gauges and ion pumps. A permit from either one and the upstream house allows the valve to remain open. All valves are controlled locally and remotely.

The ion pump interface cards are designed to look at various different types of supplies. The card monitors digital status and an analog signal which is the output of a log amplifier. Therefore diode and triode supplies are interfaced to the CIA crate by the same card. This feature offers the flexibility in a system where different ion pump types are used. The bookkeeping requires programmer notification as to the type of supply on each channel in order to maintain proper calibration. Identical bookkeeping procedures apply in situations where more than one pump is powered by a single supply.

The beam tube configuration allows for three 30 l/s ion pumps per 17 meter half cell and two 30 l/s ion pumps per 12 meter half cell which equates to a pump density roughly 1.3 times that of the Main Ring. Combining the effects of increased pump density, careful beam tube processing, and minimization of elastomers the average pressure of the Main Injector ring is less than 2×10^{-8} Torr. Ion pumps are new 30 liter/second diode ion pumps and are attached to the ion pump access ports using Conflat seals. As confirmation of the attainable vacuum pressure, a single half cell of vacuum chamber has been constructed and extensively tested. Results of four tests are pictured in Figure 3.2-10.

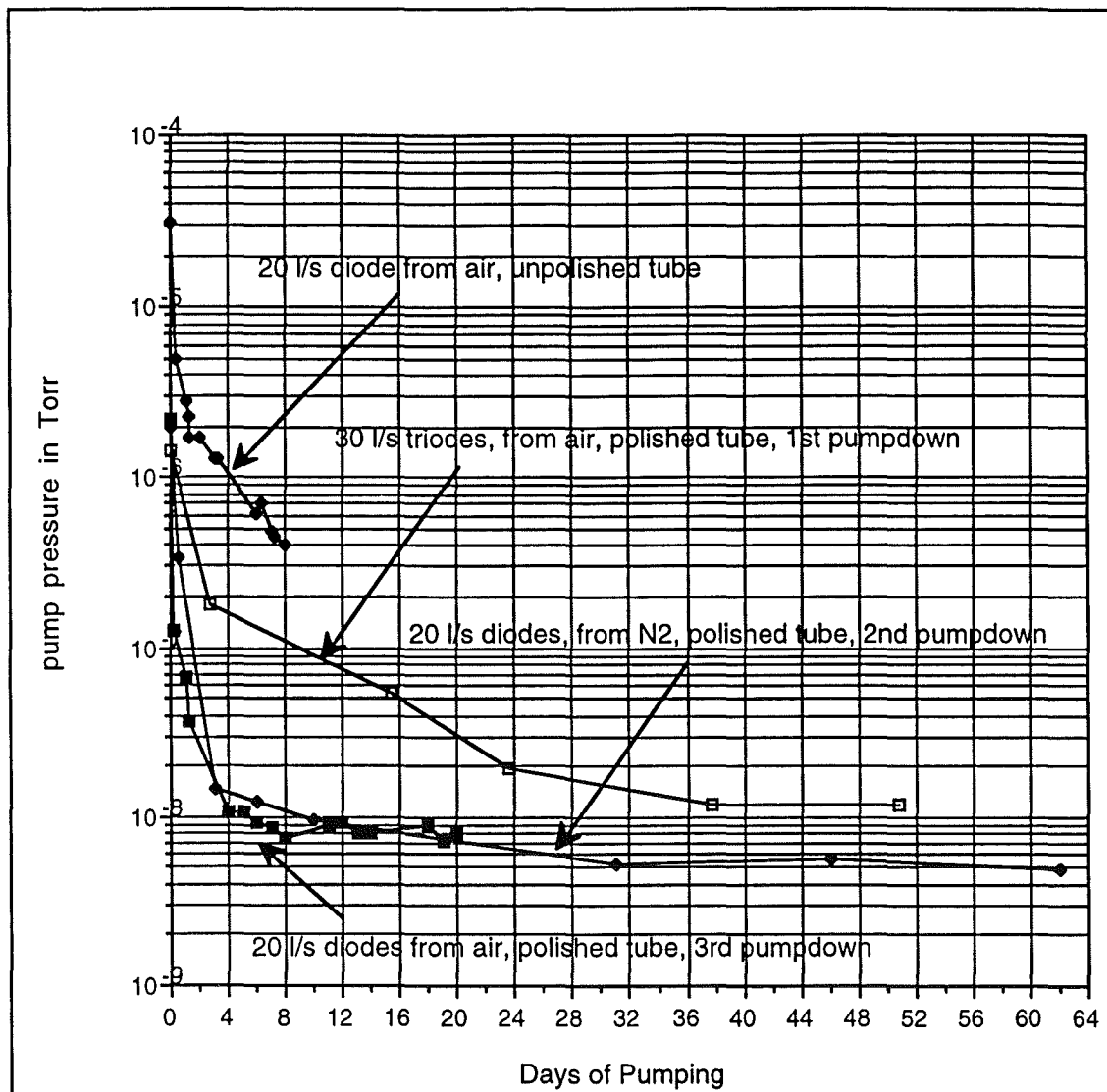


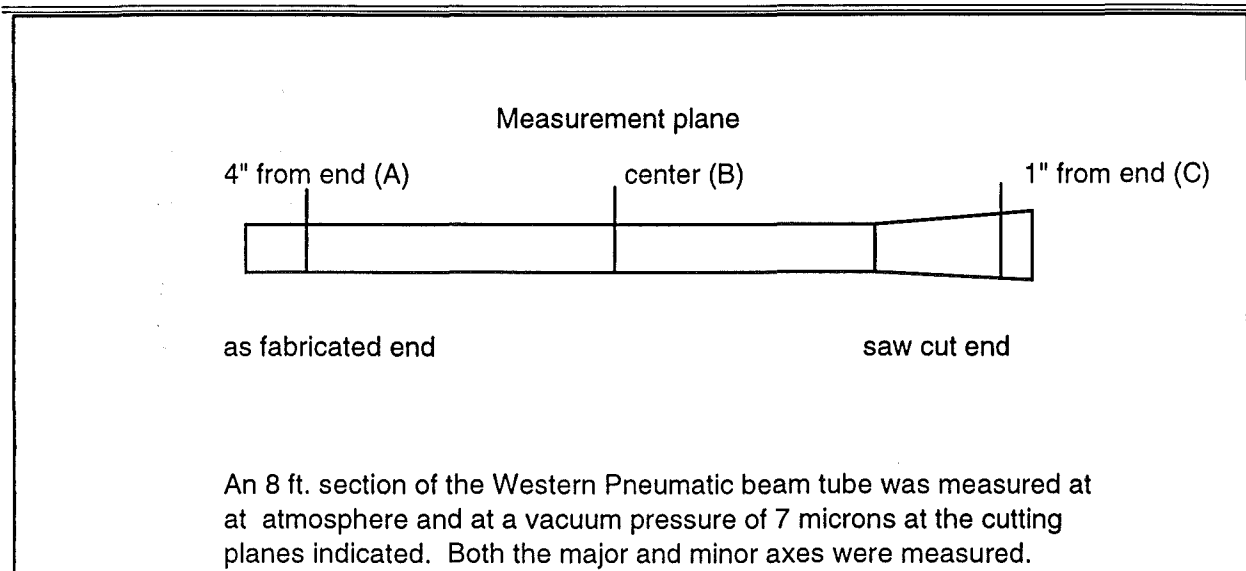
Figure 3.2-10 Beam Tube Pumpdown Results.

Some testing of the beam tube dimensional and structural stability has been performed. When prototype vacuum chambers were under construction, it was observed that whenever the tube was cut a local increase in the minor diameter of approximately .095 inch and a decrease in the major diameter of .030 inch resulted from the cut. This effect is due to the residual stresses resulting from the forming process and poses no fabrication problems once understood. A section of tube was measured at atmospheric pressure and under vacuum as shown below resulting in the data in Table 3.2-2.

Because a .115 inch deflection was noticed under vacuum, it was decided to put larger forces on the exterior of the tube (using hydraulics) to determine the safety margin and verify the

mathematical model. In this test the water pressure was increased incrementally from 0 to 30 psi on the outside of the tube while the inside was supported by 1 atmosphere. The notable result was that plastic deformation began at 22.5 psi. Consequently it is recommended that the tubes do not go through a stress relieving procedure during fabrication to reduce the flaring phenomenon discussed above.

Table 3.2-2
Beam Tube Deflection Measurements.



Measurement Location		A	B	C
Major Axis:	Atmosphere	4.835	4.825	4.795
	Vacuum	4.870	4.875	4.825
	Difference	0.035	0.050	0.030
Minor Axis:	Atmosphere	2.105	2.100	2.195
	Vacuum	1.990	1.985	2.095
	Difference	0.115	0.115	0.100

8 GeV Beamline Vacuum System

WBS 1.1.2.10.1.1, 1.1.2.10.2.1, 1.1.2.10.3.1, 1.1.13.2.3

The 8 GeV beamline vacuum system is divided into 4 vacuum sections by 4" automatic, beamline gate valves. The first one at 809 separates the 8 GeV line and Booster, from a vacuum control stand point. Control of all vacuum components upstream of 809 are through the Booster control system, all downstream components are controlled through MI-8. The other sector valves are located at 828, 846, and 852. The 852 location isolates the 8 GeV line from the Main Injector ring. Each section is provided with 2 Pirani gauges and 2 pump-out ports, incorporating a 2-1/2" hand valve. The hand valves provide access to the system for pump down and leak check functions. No permanently installed roughing stations are provided; portable roughing carts will be attached as needed. High vacuum pumping is provided by 30 l/s ion pumps, spaced approximately 50 ft. apart, along the length of the line. The system is designed to achieve an average pressure of 3×10^{-7} torr. The vacuum chamber will be all welded stainless steel, using a minimum of flanges, only for pumps, valves and gauges. The vacuum chamber geometry through the magnets is elliptical (Figure 3.2-11). All drift sections are 4" round tubing connected to the magnet chambers by 4" round bellows and a 4" round to elliptical transition piece (Figure 3.2-12). Drift sections between permanent magnet quad pairs and permanent magnet gradient pairs will be prefabricated multi-wire/ion pump/BPM or ion pump/BPM assemblies. These will have separate stands so that the beam diagnostic elements can be aligned independent of the magnets. Where possible drift sections or sub-components of drift sections will be pre-assembled prior to installation. Vacuum component specifications are included in Table 3.2-1 and Figures 3.2-13 and 3.2-14. Vacuum controls are identical to those described in the "Main Injector Vacuum System" and are housed in the MI-8 Building.

Figure 3.2-11 8 GeV Line Magnet Vacuum Chamber Section.

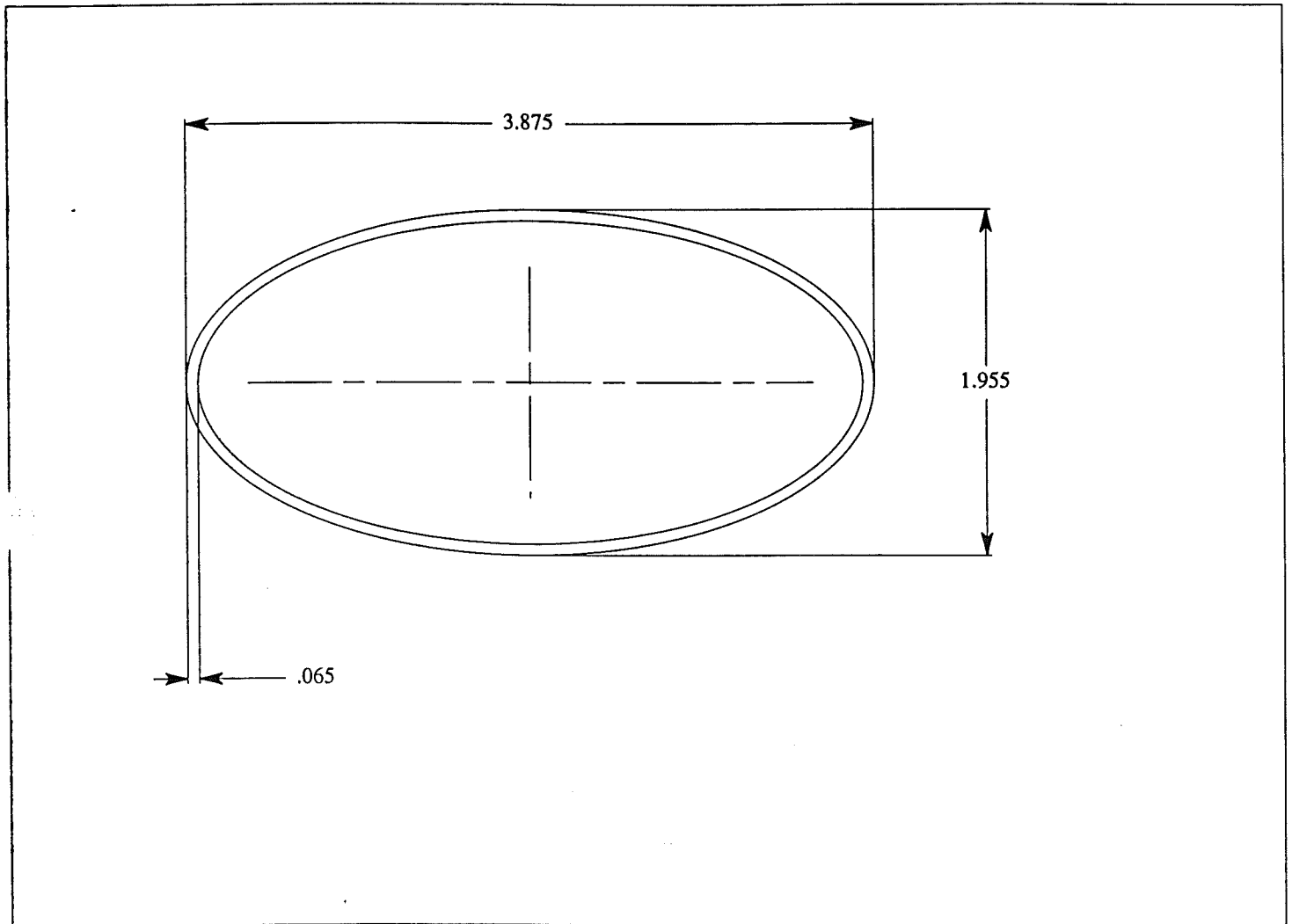
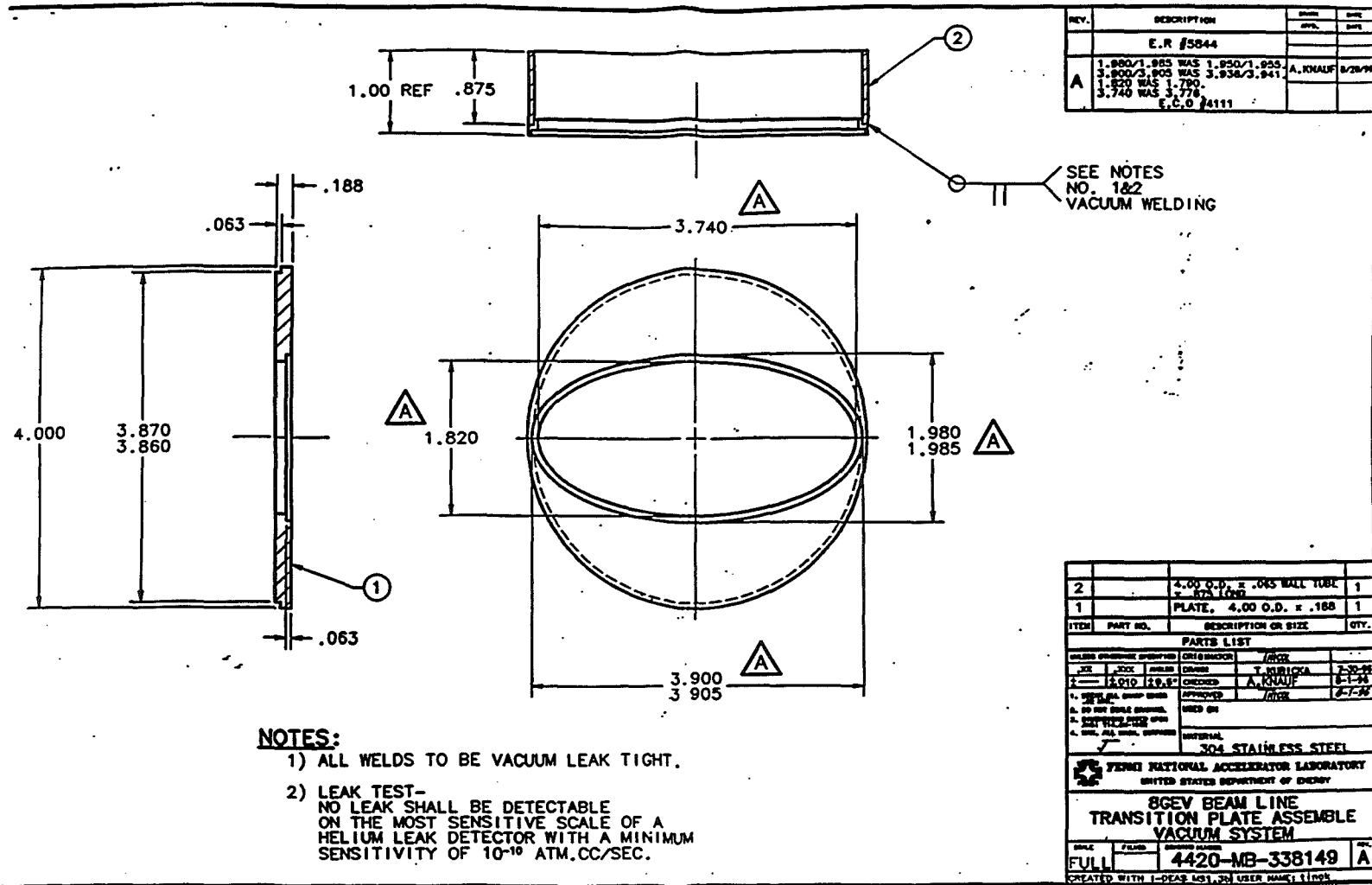


Figure 3.2-12 8 GeV Line Vacuum Chamber Transition Piece.



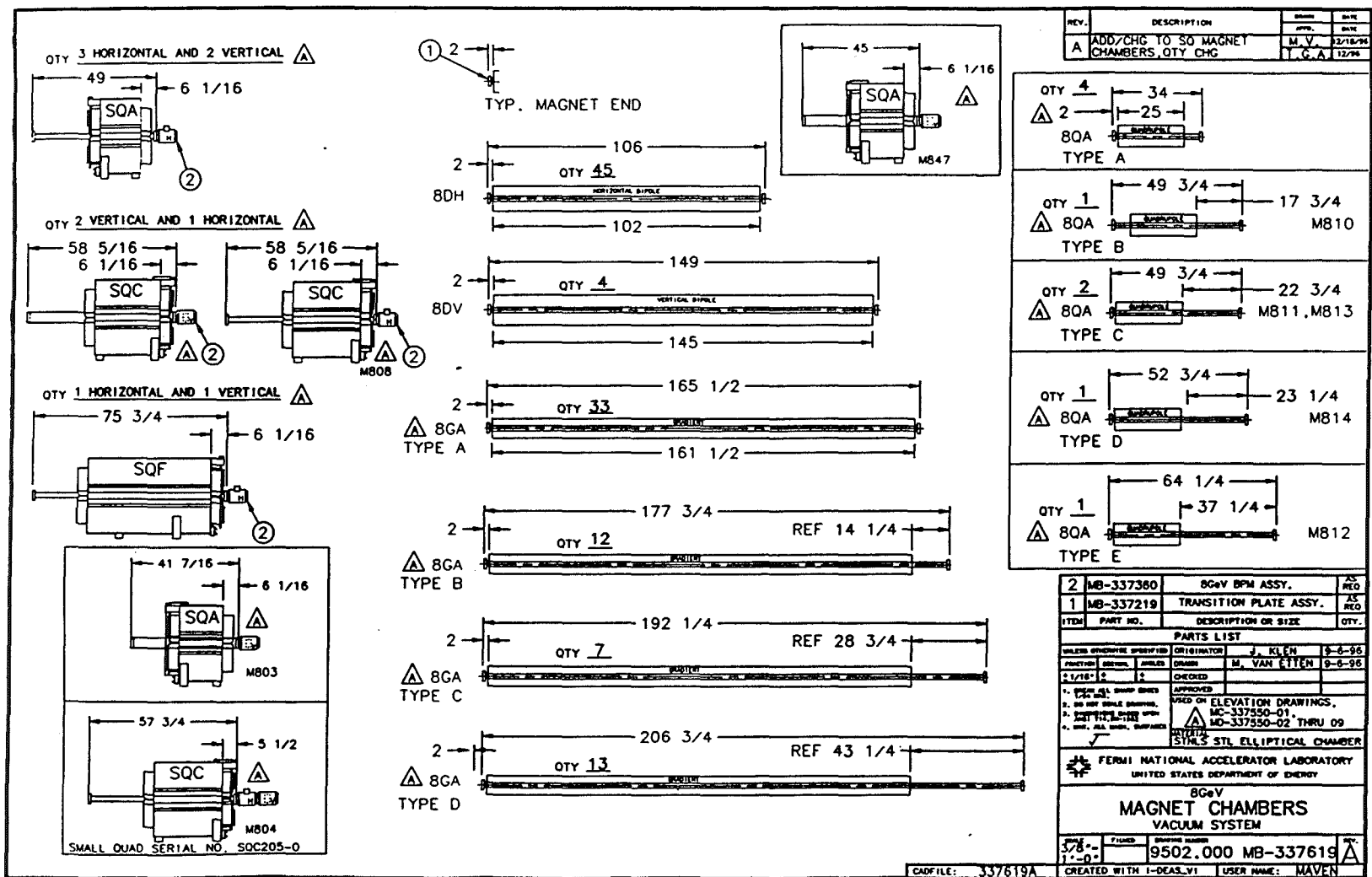
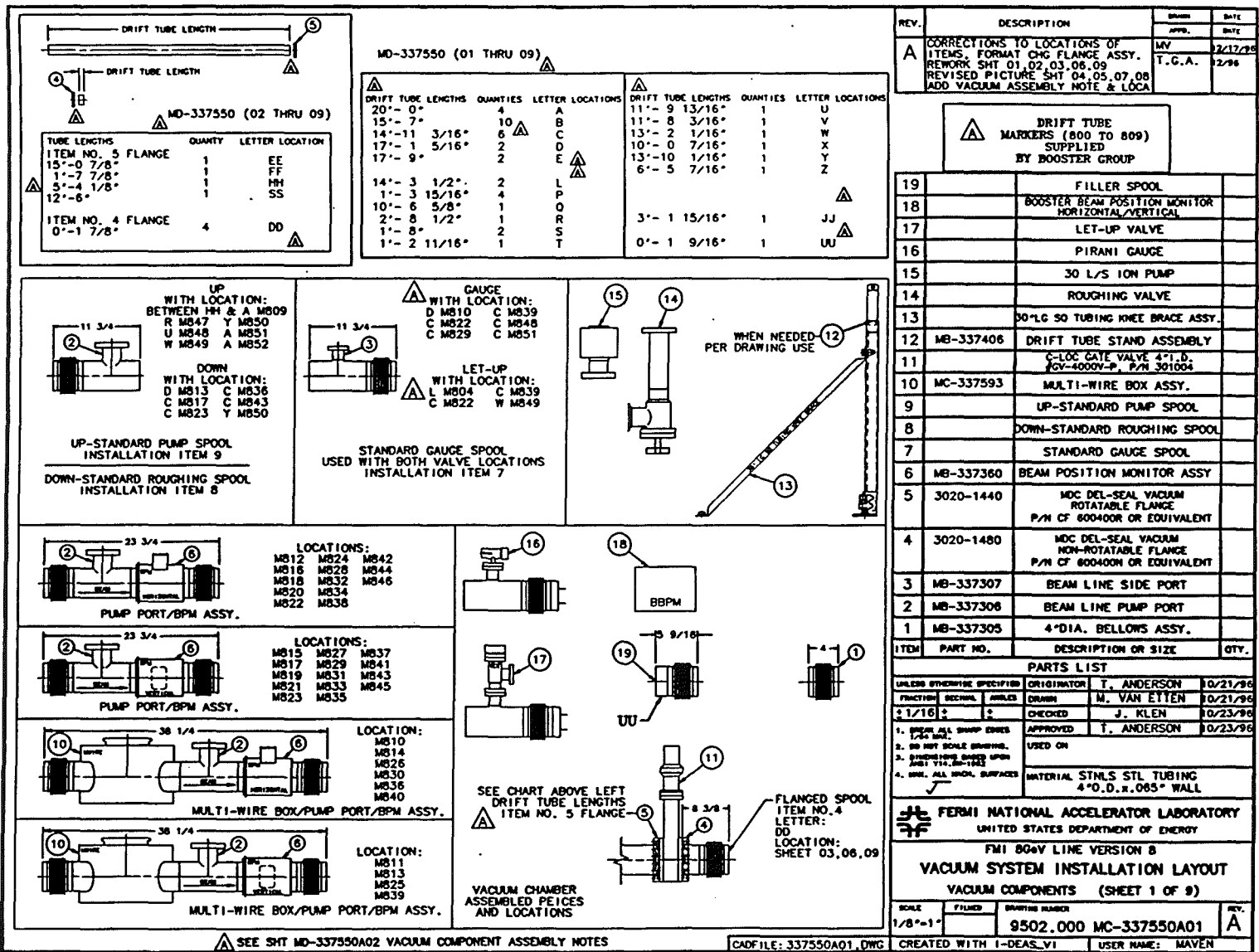


Figure 3.2-13 8 GeV Line Magnet Vacuum Chambers.

Figure 3.2-14 8 GeV Line Vacuum System Installation Layout.



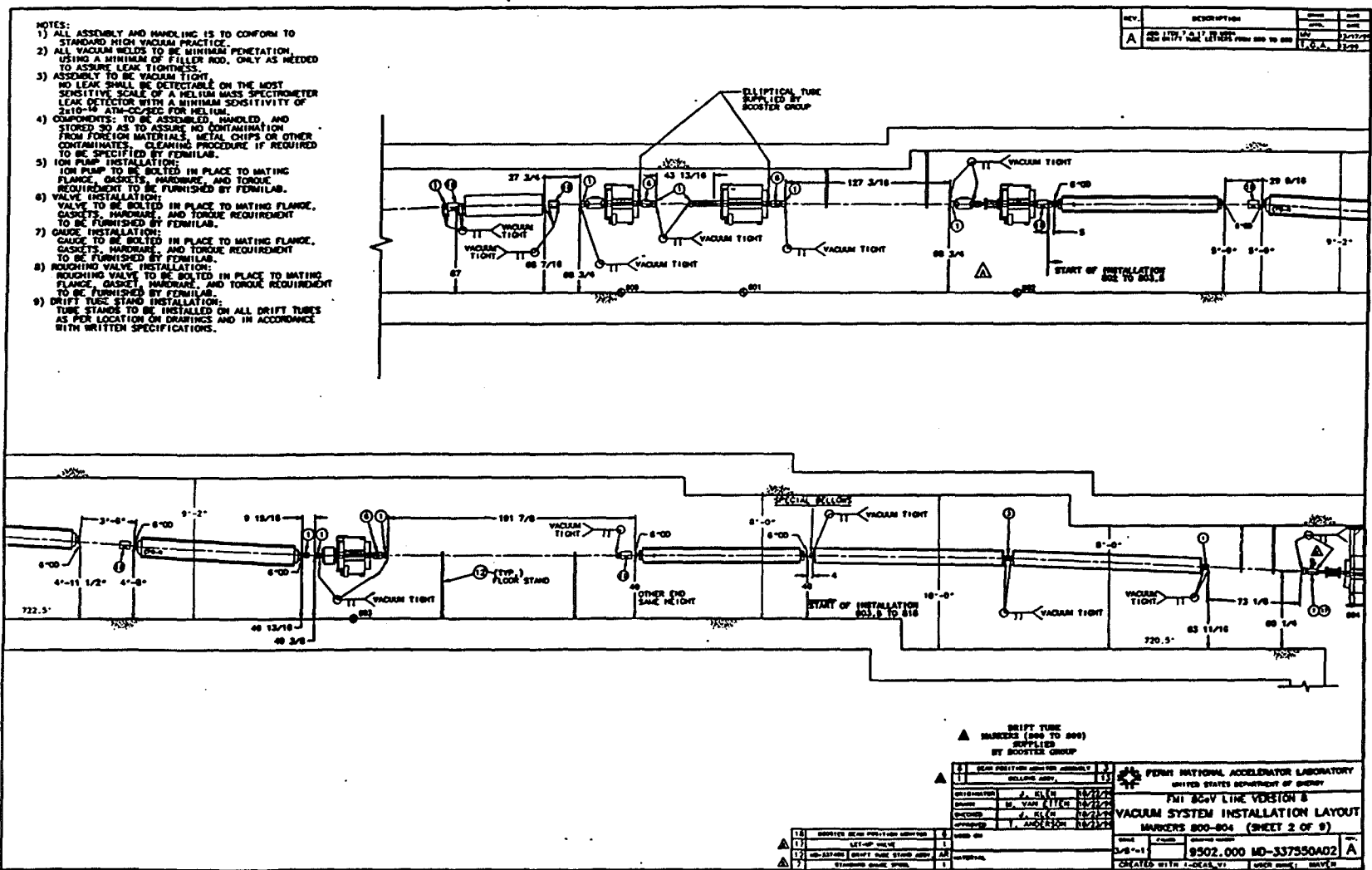


Figure 3.2-14 8 GeV Line Vacuum System Installation Layout continued.

Figure 3.2-14 8 GeV Line Vacuum System Installation Layout continued.

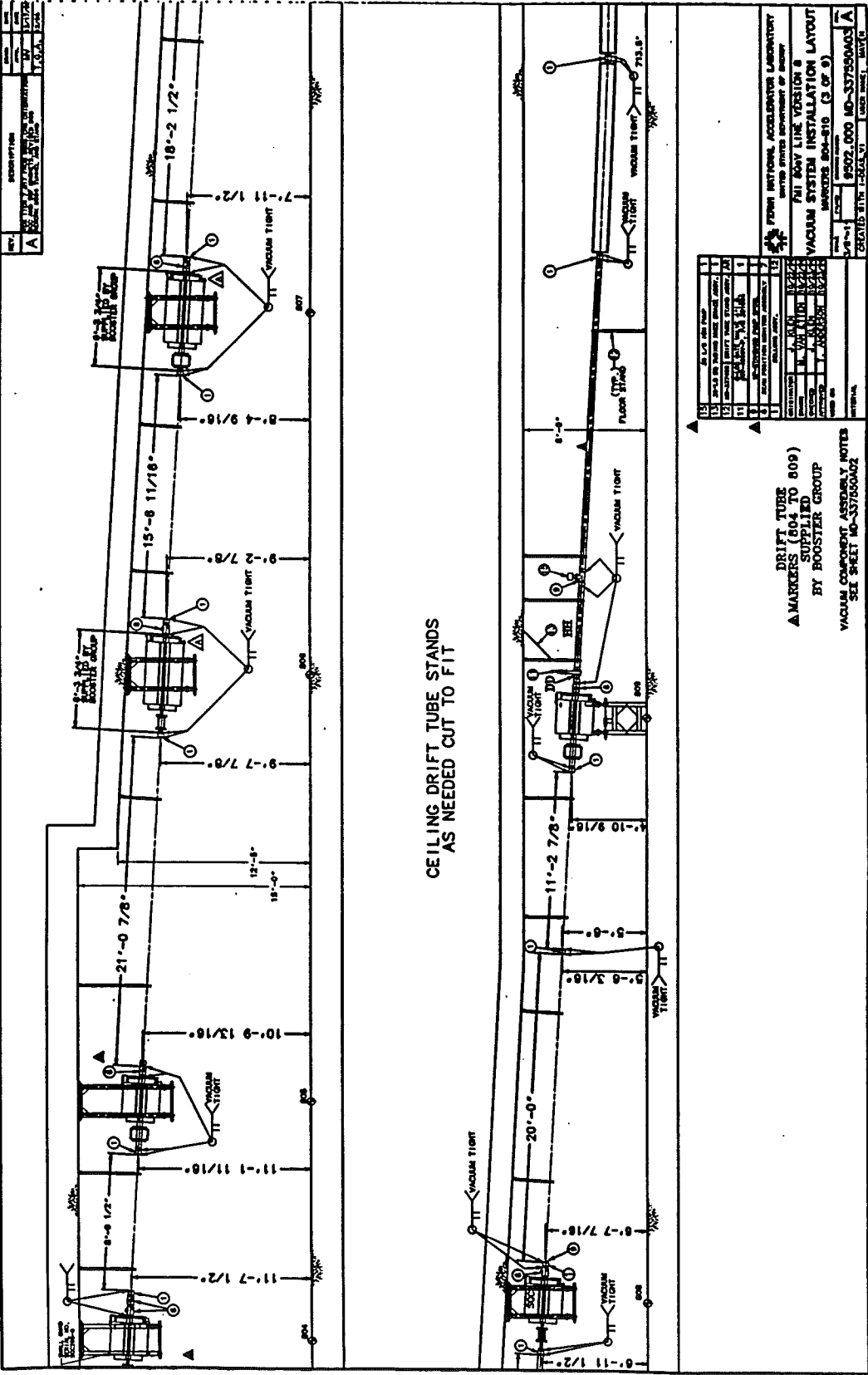


Figure 3.2-14 8 GeV Line Vacuum System Installation Layout continued.

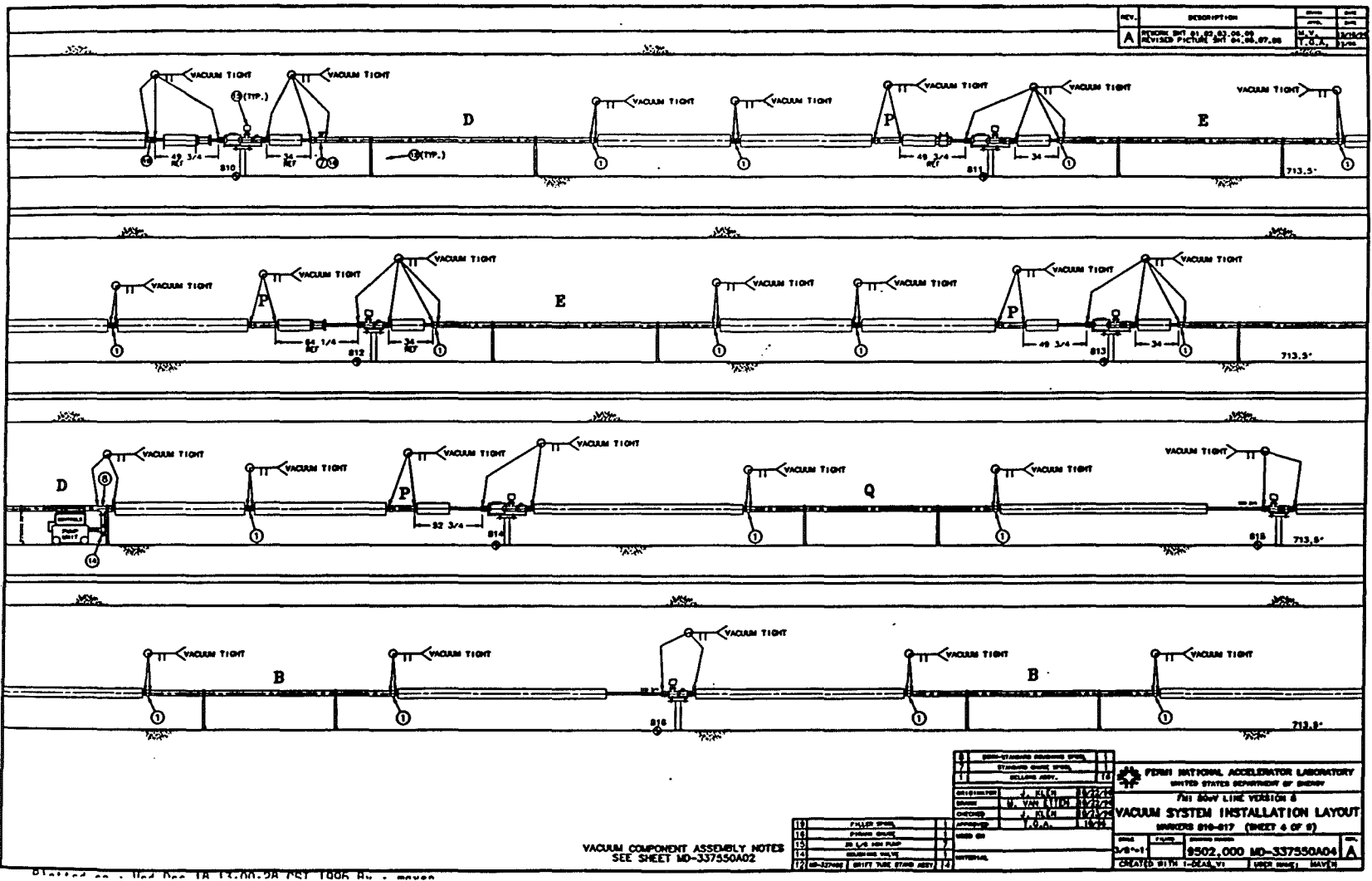


Figure 3.2-14 8 GeV Line Vacuum System Installation Layout continued.

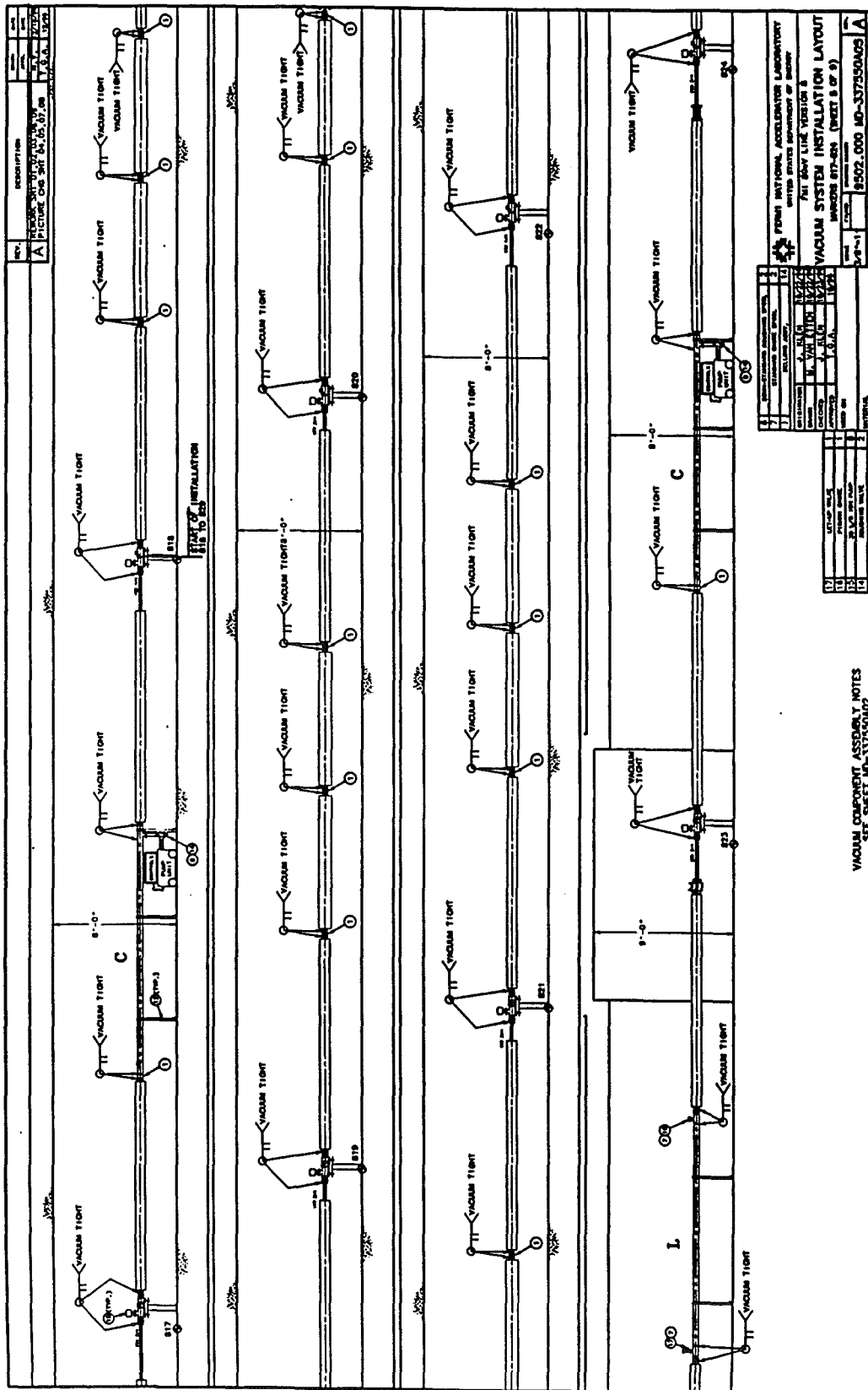




Figure 3.2-14 8 GeV Line Vacuum System Installation Layout continued.

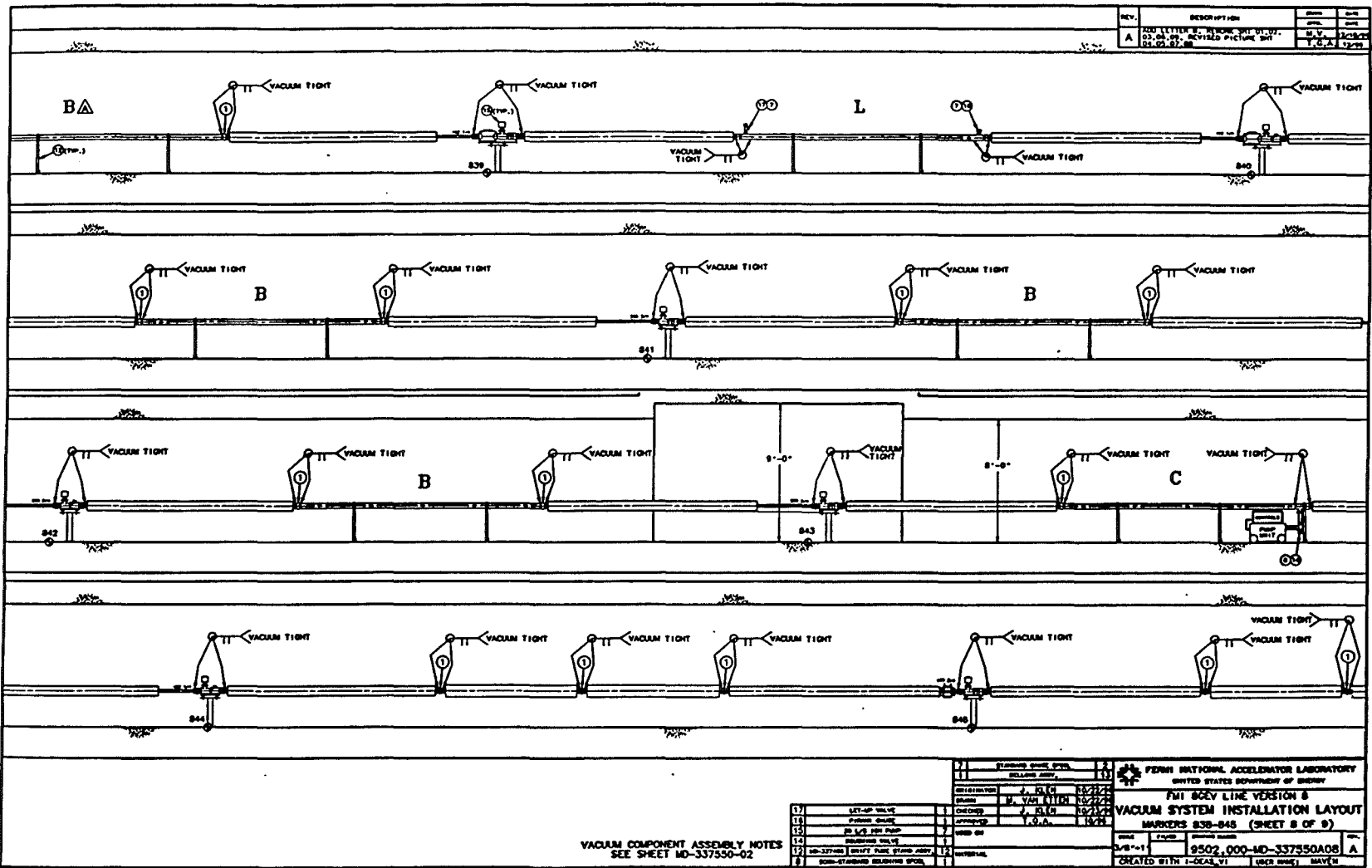
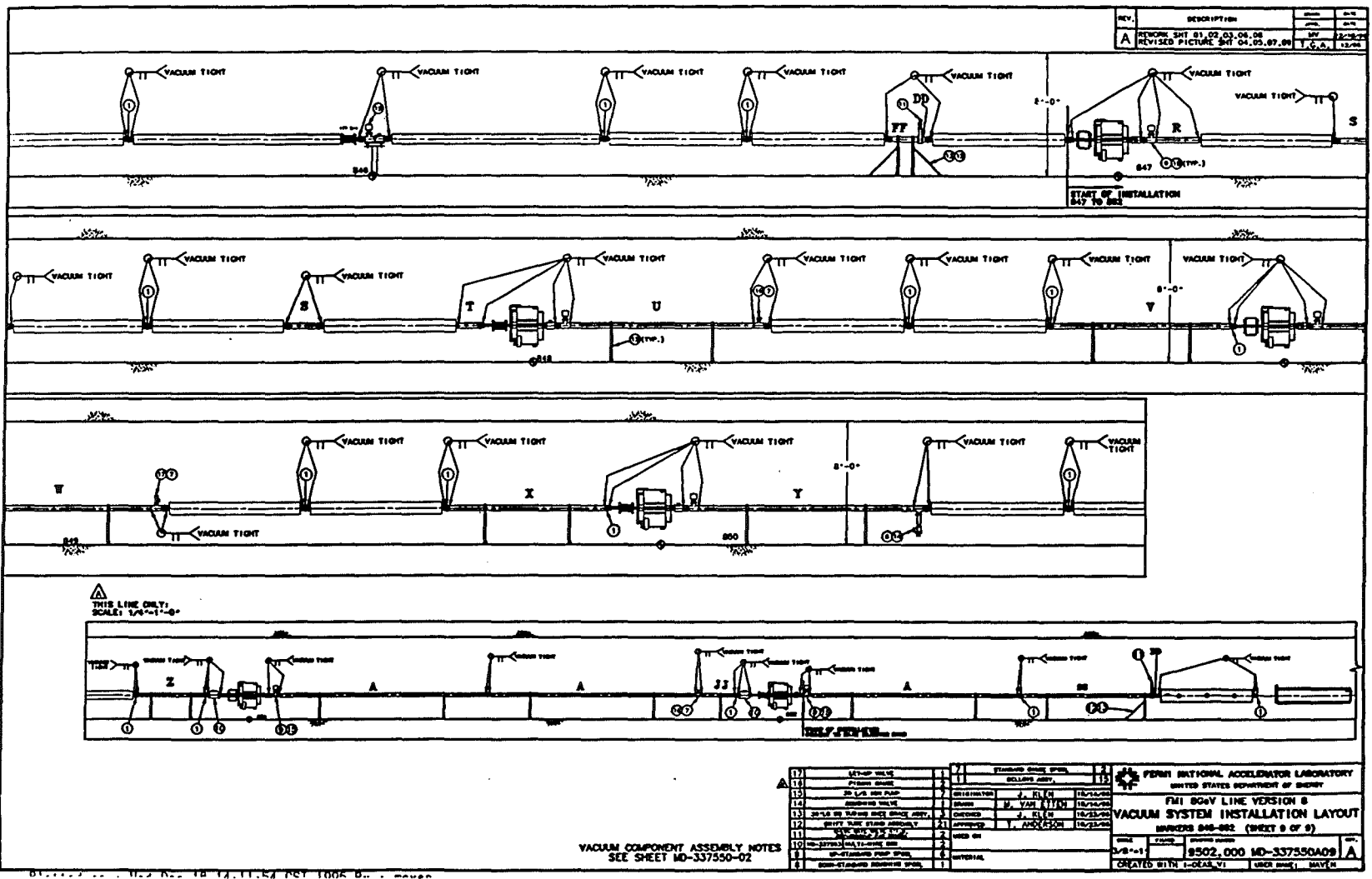


Figure 3.2-14 8 GeV Line Vacuum System Installation Layout continued.



150 GeV Beamline Vacuum System

WBS 1.1.2.10.1.2, 1.1.2.10.2.2, 1.1.2.10.3.2, 1.1.13.3.3

The 150 GeV beamline vacuum is isolated from the Tevatron vacuum system by 2 thin titanium windows centered about the MI-60 Lambertson magnets. Although the Main Injector circulating beam tube vacuum chamber and the 150 GeV vacuum chamber are, in practice, common at their intersections, effective isolation (in the operating mode) is maintained by differential pumping throughout the kicker and Lambertson areas. Each kicker is pumped by a pair of 60 l/s ion pumps, one at each end. All Lambertson magnets have distributed pumping in the form of 30 l/s ion pumps spaced 1 meter apart along the length. Additionally each Lambertson is provided with heating blankets and controls for in situ vacuum baking as necessary. The three Lambertson sets are situated between a pair of automatic, pneumatic gate valves. As shown in Figure 3.2-15, ample hand valves are installed for pump down and leak checking. Pump down is accomplished by the use of portable turbomolecular pumping stations as in the Main Injector. 30l/s ion pumps attached to recycled Main Ring dipoles provide permanent pumping capability along with additional pumps installed in the drift spaces between quads. The average spacing between ion pumps is approximately 8 meters, rendering the beamline virtually identical to the Main Ring. Therefore the attainable average pressure is 5×10^{-7} Torr. Vacuum controls are identical to those described in the "Main Injector Vacuum System" and are housed in the MI-60 Building. Vacuum components are described in Table 3.2-1.

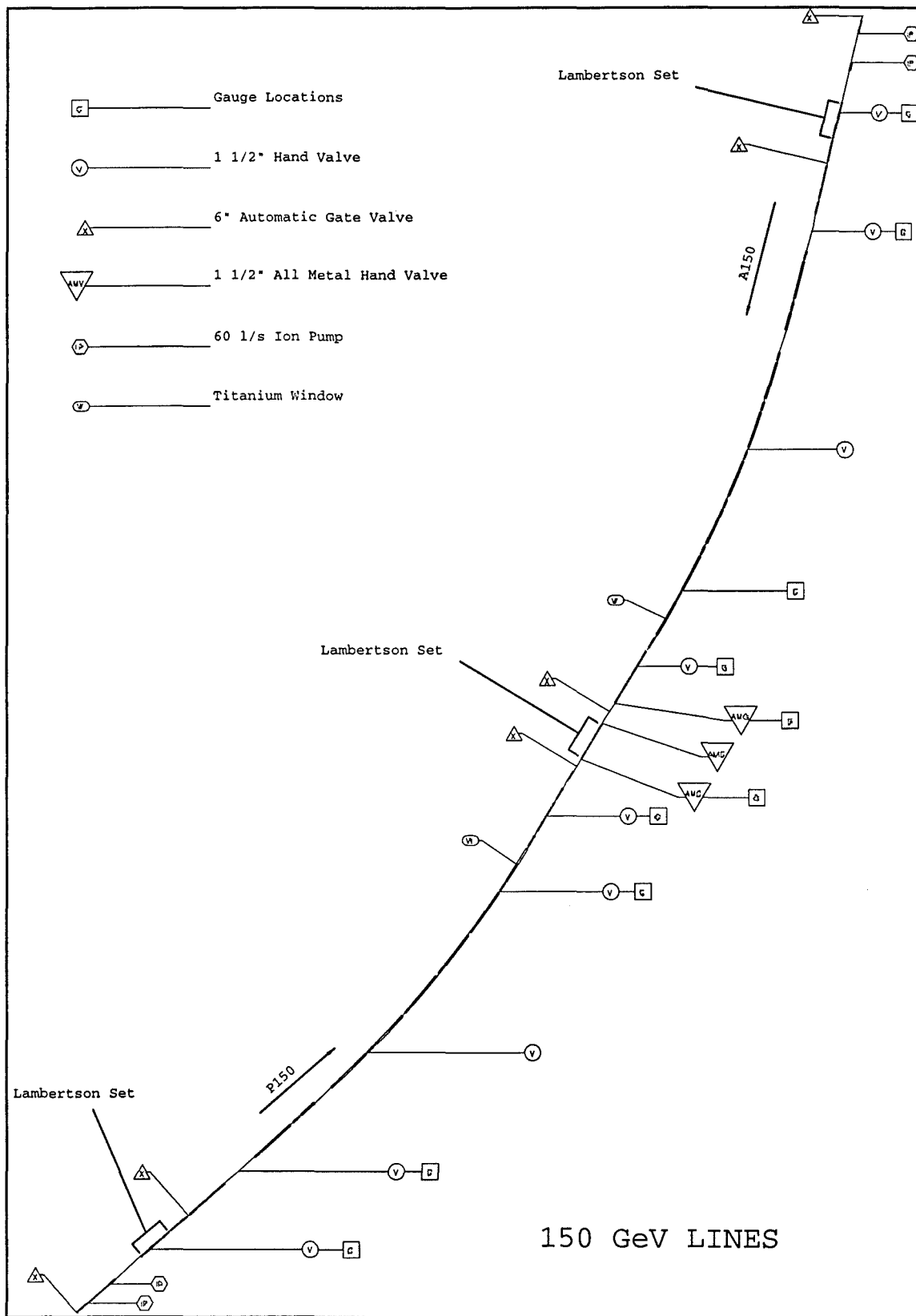


Figure 3.2-15 150 GeV Line Vacuum Valves and Instrumentation Layout.

Abort Vacuum System WBS 1.1.12.1.2.3

The Main Injector abort vacuum system is designed to achieve 1×10^{-8} Torr pressure in the portion common with the Main Injector and several microns in the remaining section. A pair of thin titanium windows downstream of the quadrupole pair separates MI vacuum from the rough vacuum leading to the dump. Located in the air gap between windows is the necessary instrumentation. Downstream of the windows a roughing pump can be connected through hand valve and pressure is monitored by a convectron. The Lambertson-quad-Lambertson trio can be isolated by a pair of 6" automatic gate valves. Lambertsons are provided with heating blankets and controls for in situ baking as required. They also support 30 l/s ion pumps spaced every meter along their length. A pair of all metal hand valves and a gauge tree are also located between the gate valves for pump down and pressure monitoring. Near MI quad 400, the kicker pair is permanently pumped by 3 60 l/s ion pumps equally spaced about the kickers. Roughing valves and vacuum instrumentation are provide by the MI vacuum system in the region between the kickers and the upstream Lambertson. An "o" ring hand valve and a convectron are located between the downstream Lambertson and the upstream window. No permanent roughing stations are provided in the high vacuum system, but a mechanical pump is provided for the system downstream of the air gap.

CHAPTER 3.3 POWER SUPPLIES

WBS 1.1.3.

POWER SUPPLIES

Introduction

The FMI power supply system has been designed to ramp the magnet system from an injection level of 8.9 GeV/c to an excitation level of 120 or 150 GeV/c at a repetition rate adequate to meet requirements for Antiproton Source stacking, Tevatron injection, and slow spill operations. The ring power system consists of 12 rectifier power supplies for the bend bus, 6 power supplies for the quadrupole busses, harmonic correction system, and the reuse of many smaller items from the present Main Ring. A new substation and 13.8 kV power feeder system are also required, provided under WBS 1.2. (civil construction). A summary of the FMI ring power supply requirements is shown in Table 3.3-1.

Table 3.3-1: Power Supply Summary for the FMI System

<u>Power Supplies</u>		<u>Maximum Voltage</u>	<u>Current</u>
Bend	12	1,000 V	9,375 A
Quad F	3 existing	850 V	3,630 A
Quad D	3 existing	850 V	3,630 A
Other Equipment Needed:			
Quad regulator	2	300 volts	500 A
Regulation			
Transducers	2		10,000 A
Transducers	2		5,000 A
Computer link	1		
Harmonic filters	2 (1 existing)		

Power supply spacing for minimum voltage-to-ground requires an equal impedance between power supplies. The system will use six service buildings each housing two dipole supplies and one quadrupole supply. The buildings are spaced so that there are 25 6 meter dipole magnets (or an equivalent mixture of 4 meter and 6 meter dipoles) between each supply, with the magnets on a folded bus loop. The third supply in each of the six buildings is configured such that three are in series with the focusing quadrupole magnet bus and three are similarly in series with the defocusing quadrupole bus.

Criteria for Ramps and Constraints on Power Supply Layout

The maximum ramp rate of rise will be set by the use of the existing, upgraded Main Ring RF system (see Chapter 3.4), which has at present an operational limit of approximately 300 GeV/sec. The maximum ramp repetition rate is set by the 40 MVA feeder current limit for each half of the ring; the dipole bus current is limited to $\sim 5,000$ A rms by the cooling water system.

The dipole configuration consists of two busses internal to the new magnets with a fold at MI-60, allowing for six upper bus supplies and six lower bus supplies. The inductance of the magnet load in the FMI dipole bus is estimated to be 0.67 H at low frequencies. Using 3.8 square-inch cross section copper for the magnets and power supply bus, the ring will have an estimated DC resistance of about 0.265Ω at 40°C . The required peak power supply voltage is ~ 12 kV.

The quadrupole configuration is two separate busses in continuous loops around the injector with current flowing in opposite directions, one focusing and one defocusing, each having three supplies for ramping and a transistor regulator supply for injection current regulation. Each quadrupole magnet loop inductance is 0.15 H, and with the use of 2.0 square-inch power distribution bus, will have a DC resistance of about 0.55Ω at 40°C . Thus the required peak power supply voltage is 2500 V for each quadrupole bus.

Dipole Magnet Details

The Main Injector dipole magnet is a five terminal device. It has two terminals for the coil bus, two terminals for the through bus, and a magnet core ground. The prototype dipole magnets have been measured in detail to develop an electrical model that can be used for dipole power supply system design [1]. The five-terminal dipole magnet device model consists of passive elements such as inductance, capacitance, and resistance. Figure 3.3-1 depicts the dipole magnet as a five-terminal linear network. Measuring the current I_j flowing into the j th terminal in response to voltage V_j , one may exploit superposition theory to develop an electrical model.

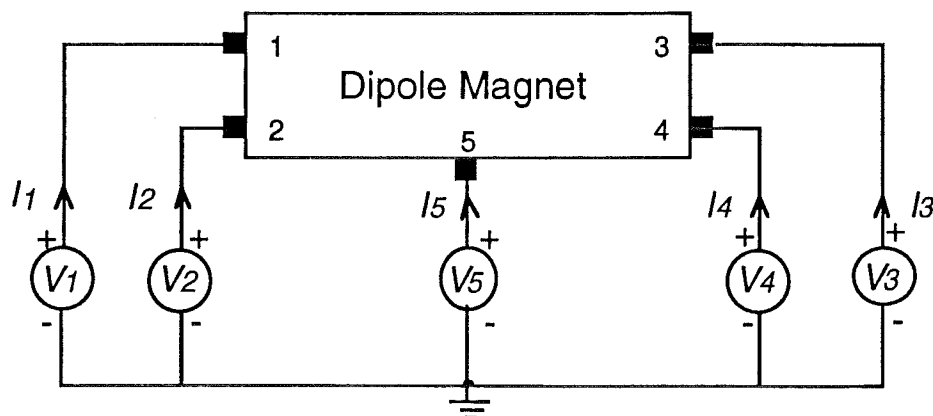


Figure 3.3-1. Five-Terminal Dipole Magnet Electrical Representation

The model developed from detailed testing of a prototype dipole magnet is used to construct an electrical model of the accelerator ring. Terminals one and three are the half turn through bus, two and four the seven and one-half turn coil bus and terminal five is the core ground connection to the magnets. Both the 6-meter and 4-meter magnets have been measured and show good agreement with the model to 10 kHz. Figure 3.3-2. shows the 6-m magnet electrical model. The magnet models are being used to help determine system parameters such as required peak power supply voltage, regulation bandwidth limits, and means of damping transmission line modes. As a cross check to the magnet measurements the models were used and compared to the measured values at the test string which has five 6-m and three 4-m magnets. The measured data and calculated values matched very well.

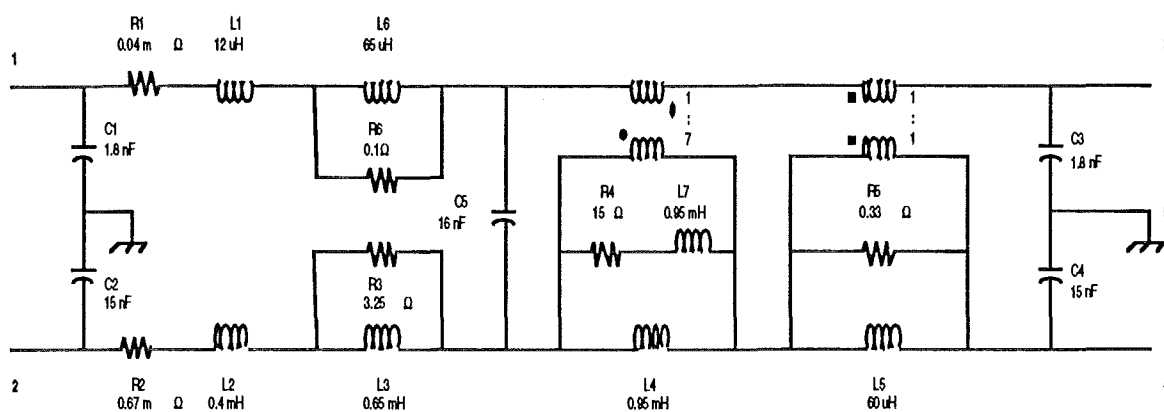


Figure 3.3-2. Injector 6 Meter Dipole Magnet Equivalent Circuit

Figure 3.3-3 shows the through bus measurements and calculated values (amplitudes) as a function of frequency out to 10 kHz, while Figure 3.3-4 shows the seven and one half turn coil bus measured values and model values.

An effort was made to simplify the model to remove cross coupling from the through-bus to the 7 1/2 turn bus. This effort had reasonable success up to about 1 kHz and will be used for ring wide calculations where the higher frequencies are not needed. This simplification allows the programs to run faster with no penalty for accuracy at the lower frequencies. The simplified model obtained is given in Figure 3.3-5.

The last step in model development was to characterize the inductance as a function of current with the goal of studying the effects of magnet saturation at higher currents. This has led to better understanding of the maximum required dipole power supply voltage.

Z11 MAGNITUDE PLOT

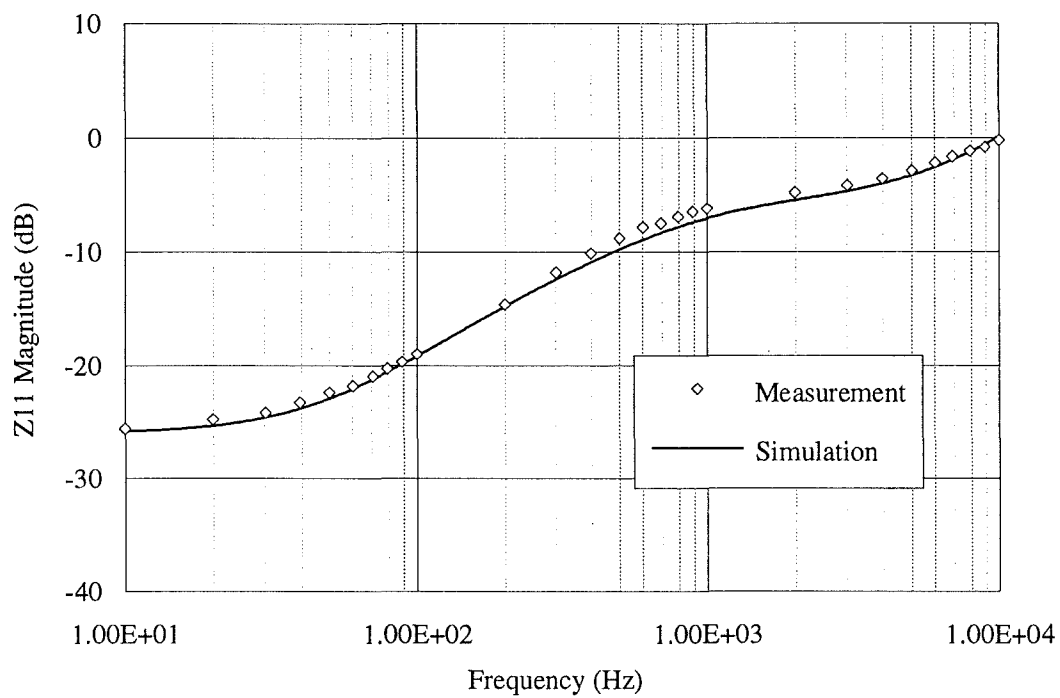


Figure 3.3-3. Through Bus Model and Measurement Data

Z22 MAGNITUDE PLOT

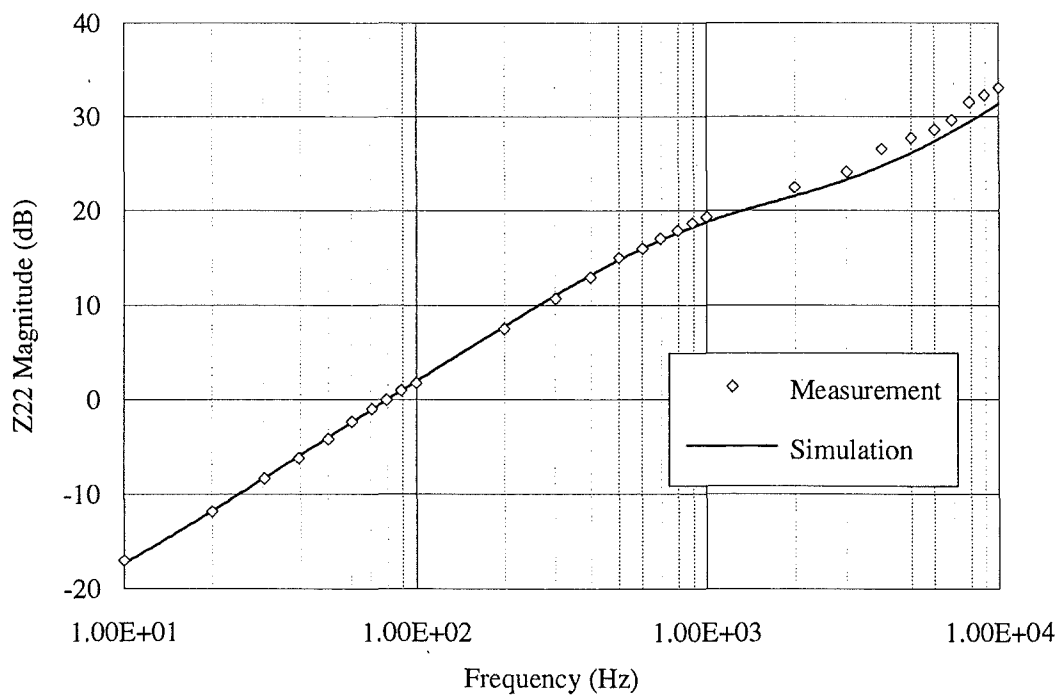


Figure 3.3-4. Coil Bus Model and Measurement Data

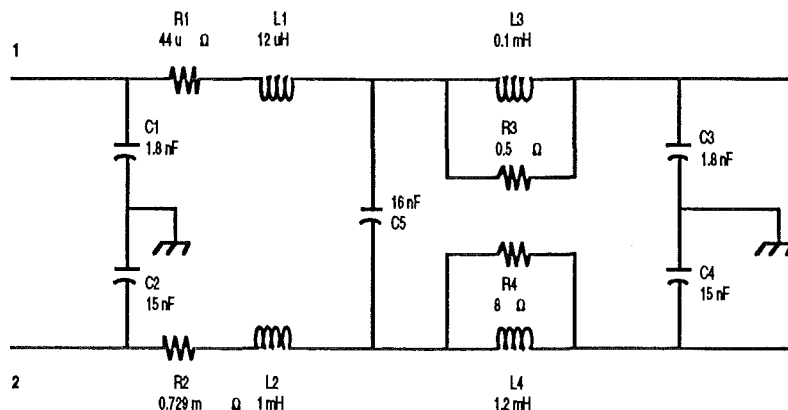


Figure 3.3-5. Simplified 6 Meter Magnet Model Used for Power Supply Development

Ramp Details

The ramp details are determined by a number of requirements and limitations which effect the overall form of the ramp: energy, flattop duration, RF voltage, power supply voltage, feeder currents, etc. Figure 2.2-1 and Table 3.3-2 give details on the five modes of operation. For antiproton stacking, the voltage and number of power supplies are chosen to provide a repetition rate of <1.5 seconds and a maximum rate of rise of 270 GeV/sec. The fixed target injection ramp requires a short flattop, run twice in succession, once a minute, with 120 GeV cycles the remainder of the time. The 120 GeV slow spill cycle (1 s flattop) has been used for calculations of rms power for the LCW systems, cable heating, etc.

With 12 kV maximum power supply voltage, the ramp rate will need to decrease from 270 GeV/sec (reached at ~40 GeV) to ~225 GeV/sec at 100 GeV. Feeder current and harmonic filter limitations on peak MVA loading require the ramp rate to decrease more dramatically above 100 GeV, to 120 GeV/sec at 144 GeV. This restriction limits the peak MVA load to 120 MVA.

To ensure reliable operation, the transformers for the FMI power supplies are being sized for a current which is an approximate average between the peak required and the rms demand. This requires two 345 kV, 40 MVA transformers located in the Kautz Road substation to provide 13.8 kV power.

Power Supply Control

The power supplies are controlled differently for different ramps. For the fast cycling 120 GeV cycles (with very short flattop) one power supply is used at 8 GeV, but as the ramp begins, the remaining power supplies are turned on aggregately. For the 150 GeV cycle, specific supplies are turned on and off as required by voltage demands, with either 1, 3, 6, 9 or 12 supplies on at once. For the 120 GeV slow spill cycle, 1, 3 or 12 supplies are energized. This sequential turn-

Table 3.3-2: Main Injector Ramp Parameters

Ramp	Fixed <u>Target</u>	Collider <u>Injection</u>	Antiproton <u>Production</u>	Slow <u>Spill</u>	Fast <u>Spill</u>	
Peak Energy	150	150	120	120	120	GeV
Cycle time	2.40	4.0	1.4667	2.8667	1.8667	sec
Time (Booster cycles)	36	60	22	43	28	
Injection Dwell	.441	.841	.100	.441	.441	sec
Flattop	.250	1.45	.040	1.04	.04	sec
DIPOLE BUS						
Max. Current	9375	9375	7100	7100	7100	A
RMS Current	5533	6691	3777	4992	3356	A
Power	8.2	11.9	3.8	6.6	3.0	MW
RMS Feeder Current	2061	1742	1850	1431	1639	A
Peak Feeder Volt-Amps	94	94	87	87	87	MVA
Average Feeder Volt-Amps	36	31	32	24	25	MVA
QUAD BUSSES						
Max. Current	3630	3630	2904	2904	2904	A
RMS Current	2142	2590	1545	2042	1373	A
The following numbers are the sum of both busses:						
Power	5.1	7.4	2.6	4.6	2.0	MW
RMS Feeder Current	431	551	264	330	235	A
Peak Feeder Volt-Amps	20	20	15	15	15	MVA
Average Feeder Volt-Amps	7	10	4	6	4	MVA

on is chosen to minimize voltage-to-ground distributions and RMS feeder currents. The ramping computer system presently under development for Main Ring operation will be relocated to the Main Injector and will only require minimal changes to operate the Main Injector. There are two ramping computer systems: the operational one and its spare. Temporary utilization of the spare system will allow operation of the Main Injector bend bus as soon as the magnets are installed in the tunnel. A new power supply control link for this computer will be installed and due to the higher current on both the quads and dipole bus, new transducers will be required.

Studies on the Main Ring supplies indicate that the regulation will not be degraded in going to a ramp rate of 300 GeV/sec, twice that of the Main Ring. Main Injector voltage demands do not require the power supplies to slew any faster than the present Main Ring supplies. The prototype dipole supply has been in extended operation with a 120 GeV ramp (7,100 A) in order to test the pulse loading effects on the hardware. The testing has included the supply, its controls and an 8 magnet string consisting of both 4-m and 6-m magnets. There are over 1 million pulses above 7100 A and more than 1,000 hours of operation logged on the test string.

Power Feeder Loading

The main 13.8 kV power feeders will consist of two 750 MCM aluminum cables to each of the 6 main service buildings. Two new 40 MVA power distribution transformers located at the new Kautz Master Substation (KSS) will be used in the new installation with a total operational limit set at 120 MVA peak and an rms load of 60 MVA. Each service building will source from a dedicated 1200 amp circuit breaker at the KSS. Each supply will have a circuit breaker and load break switch for maintenance and overcurrent protection. The power supply load break switch and circuit breaker will normally be closed. Energizing of the power system will be sequenced from the Main Control Room by closing the KSS service building breakers. This will allow for the use of the cable impedance to limit the voltage wave applied to the transformers and minimize turn-on transient voltages applied to the magnets. The turn-on sequence will close the harmonic filter breaker after all the feeders have been energized.

The use of rectifier power supplies on this system will produce significant amounts of harmonic current in the feeders. These currents interact with the feeder system impedance resulting in potentially harmful harmonic voltages. The present Main Ring has an harmonic filter to limit the peak voltages of higher frequencies superimposed on the 60 Hz line voltage. The FMI will run with 12 power supplies at 120 MVA peak versus 70 MVA for the Main Ring, requiring the filter to damp more harmonic power. Therefore, in the FMI a new filter is being designed to correct for the higher harmonic driving force of the system. The existing Main Ring filter will be relocated to the Main Injector and used in the most economical location of either one of the two on the main pulsed power feeder or on the beam line power supply feeder.

With the addition of the KSS, the Fermilab accelerator complex will be able to operate with either substation offline. However, operating in these modes will impose certain restrictions on machine cycle times in order to ensure that the back feed feeders will not be over heated [2]. In order to manage and control the power flow under back feed conditions a SCADA type system will be necessary.

WBS 1.1.3.1.**MAIN INJECTOR RING POWER SUPPLIES****WBS 1.1.3.1.1.****DIPOLE POWER SUPPLY**

The dipole bus requires twelve 1000 V, 5000 A RMS 12 pulse voltage regulated and filtered ramping supplies connected in series. There will be two dipole supplies in each of the six service buildings. The dipole magnet power supplies will power the 344 main bending magnets, which are configured in a folded-loop circuit, as shown in Figure 3.3-6. The fold is at the MI-60 straight section. The dipole supplies will be rated for continuous pulsed operation to 9400 A. Each power supply will consist of two 1000 V, 3 phase full wave bridges connected in parallel. The two bridges are shifted in phase by 30 degrees using one delta-delta and one delta-wye transformer. In order to improve the power factor on the 13.8 kV power lines, the output of the supply can be bypassed using an SCR switch, thus removing the transformer from the bus current. Each transformer is a 13.8 kV to 820 V, 3.6 MVA three phase source. The transformers are mineral oil filled exterior equipment. A vacuum circuit breaker (VCB) and manual disconnect are provided for isolating each supply from the 13.8 kV line. High current knife switches provide power supply isolation from the bus and magnets. All of the 13.8 kV switch gear is commercial medium voltage equipment, while the transformers are custom-built to Fermilab specifications.

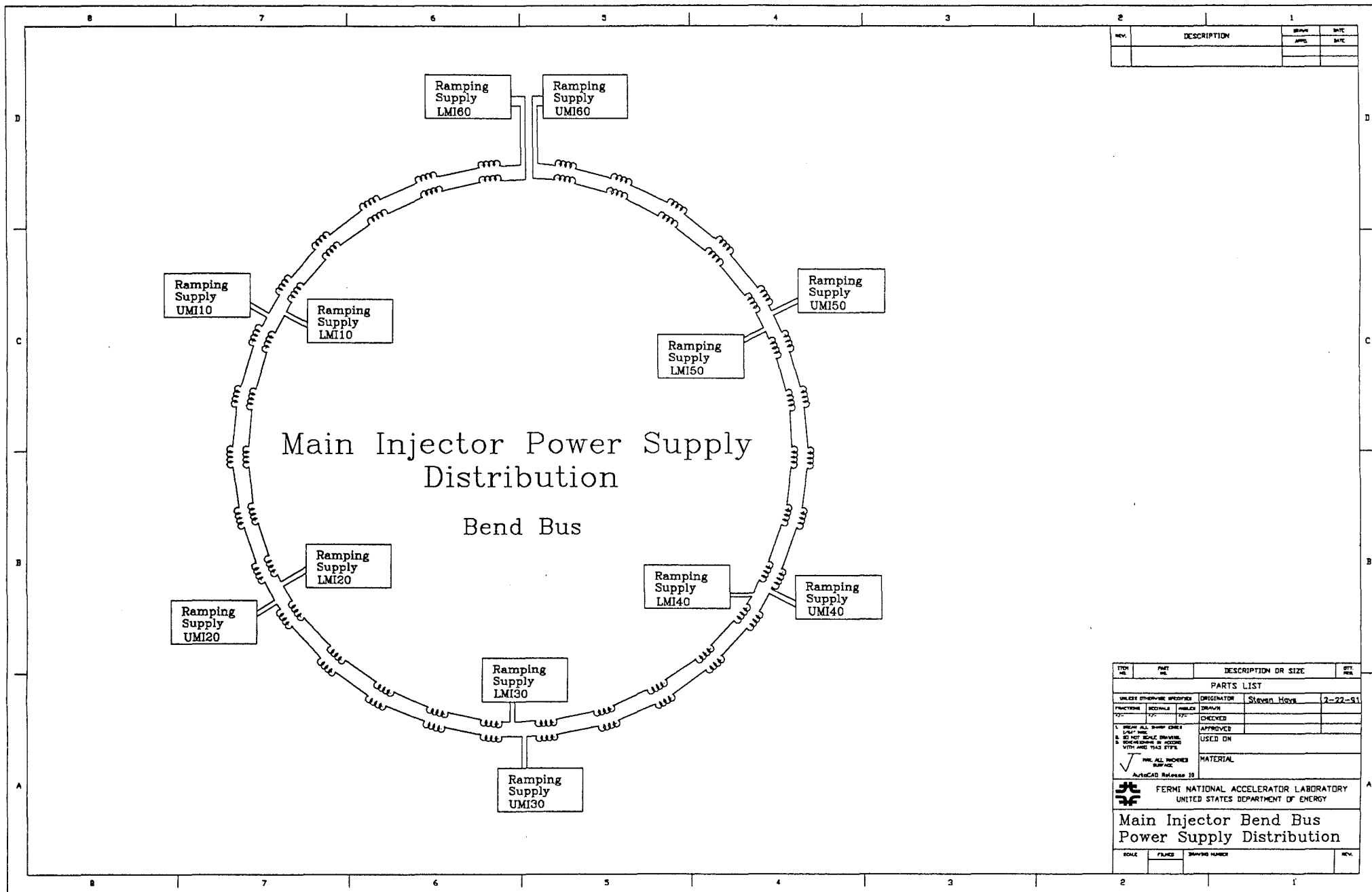


Figure 3.3-6. Main Injector Dipole Bus Configuration.

WBS 1.1.3.1.2.**QUADRUPOLE POWER SUPPLY**

The quadrupole magnets will be installed on two busses with the current flowing in opposite directions, as shown in Figure 3.3-7. Each power supply loop will require relocation of three Main Ring Power Supplies. Each power supply is a voltage regulated and filtered 12 pulse supply rated at 850 V and 2.8 MVA RMS. There are 16 decommissioned power supplies in the Main Ring which are available for the Main Injector. The full wave bridge, cabinet, VCB, filter choke and controls can be removed from Main Ring for relocation to the Main Injector once beneficial occupancy of the service buildings is granted. The relocation of transformers for these supplies will be deferred until the FMI installation shut down because the units are presently being used in the Main Ring. The transformers which will be moved are non-PCB type determined by independent lab testing. The following MR transformers will be relocated to the Main Injector ring: A4-1, A4-2, B2-1, D2-1, D2-2 and E3-2.

In addition to the six main ramping supplies there will be two new transistor regulated supplies (one on each bus). These supplies are used during injection and part way through the first parabola and have a higher bandwidth and lower ripple than the main supplies. Each supply will be rated for DC operation at 120 V and 120 A rms, but will need to continuously pulse to 350 V and 480 A.

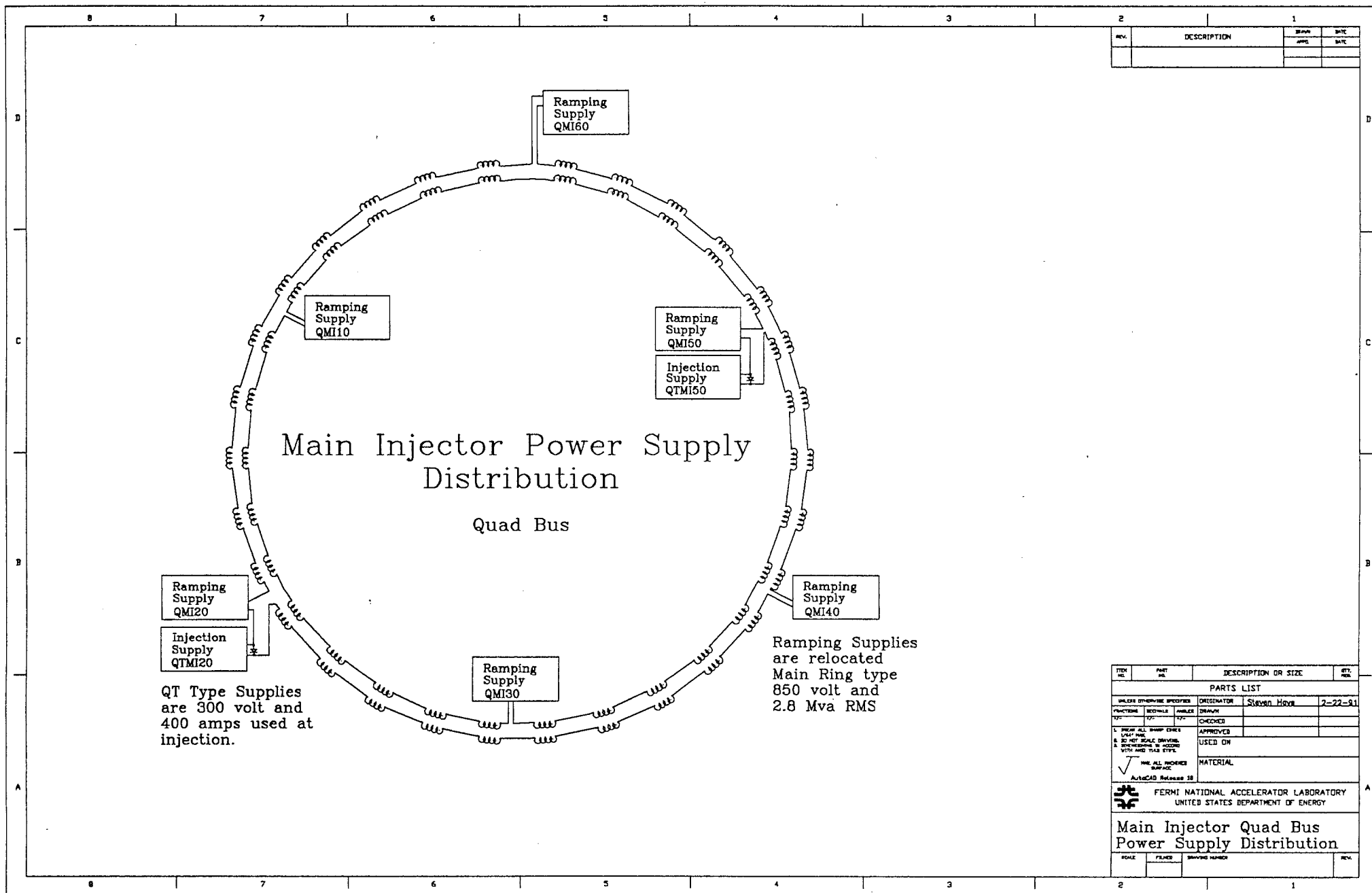


Figure 3.3-7. Main Injector Quadrupole Bus Configuration.

WBS 1.1.3.1.3.**SEXTUPOLE POWER SUPPLY**

The sextupole magnet load specification calls for two magnet loops with 54 elements in each loop. The inductance of each magnet is 2.8 mH and the DC resistance is 17 m Ω at 40° C [3]. Each load cable will be a folded loop ~21,600 feet long using 300 MCM cable (43 m Ω /1000 ft) with a total cable resistance of 0.93 Ω . Each loop will have a 750 V, 250 A RMS 3 phase SCR type power supply, rated for 350 A peak continuous pulse operation. In order to avoid overpowering the magnet or power supply, an RMS current trip device will be installed. Micro-controller devices developed for rms current monitoring, presently being used in the Main Ring sextupole loops, can be moved to the Main Injector.

Table 3.3-3 Sextupole P.S. Specifications

Number of loops	2	
Number of magnets per loop	54	
Magnet inductance	2.8	mH
Magnet DC resistance	17	m Ω
Cable DC resistance	0.93	Ω
Total load impedance	0.15	H
	1.85	Ω
Power Supply Voltage	750	V
Power Supply Current	350	A peak
	250	A RMS
Power Supply Rated Power	200	kW

WBS 1.1.3.1.4.**CORRECTION ELEMENT POWER SUPPLIES**

These supplies will be recycled from the Main Ring. Ring Correction Element Magnet Power Supply system consists of two 5 kW, ± 80 V bulk power supplies feeding power to 2 chassis each containing 6 power op-amp channels. Thus, twelve correction element channels form one MR correction power supply system. The Main Injector will require 36 channels per service building in five locations, and 48 channels in MI-60. The op-amps are water cooled so installation requires 95° F water connections. Each channel is designed to operate at ± 12 A with an rms current limit of 6 A and a bandwidth of 1 kHz. One channel per chassis can be configured for 160 V output voltage if needed for larger impedance magnets.

There are 24 sets of 12 channel correction power supplies which will be relocated to the Main Injector ring and beam lines. The C453 CAMAC control card will be relocated along with the supplies.

Table 3.3-4 Correction Element P.S. SpecificationsCorrection Element Power Supplies

Output Voltage Standard Channel	± 80 V
Output Voltage Dual	± 160 V
Output Current all channels	± 12 A peak
Average RMS over one minute	6 A rms
Ramping limits: Current to peak value	50 A/sec
Bandwidth	1 kHz
Total Bulk Power Supply Current	± 60 A

Note: The channels are grouped in sets of 12 per bulk supply. The total current draw must be less than the above number in any one direction.

Magnet Loads

	<u>L</u>	<u>R</u>
Horizontal Dipole	890 mH	3.3 Ω
Vertical Dipole (tentative)	390 mH	5.1 Ω
Main Ring Quadrupole	68 mH	1.6 Ω
Main Ring Octupole	31 mH	1.3 Ω
Main Ring Skew Quadrupole		

In order to control the power in the amplifiers the load resistance is set to 6 ohms for all standard channels and 12 ohms in the twice voltage channels. The resistance for each load is adjusted by installing resistors at the magnet. At the present time, we plan to install 104 horizontal trim dipoles, 104 vertical trim dipoles, 24 trim quadrupoles, 54 octupoles (powered in groups of one to four in series), and 16 skew quadrupoles.

WBS 1.1.3.1.6. MAIN BUS POWER SUPPLY CONTROLLERS

The current regulation of the dipole and quadrupole magnet bus system will be controlled by the existing Main Ring ramping computer. It consists of a VME based computer and a dedicated control link. New current monitoring equipment is required due to the higher bus current and will consist of 10 ppm DCCT type transducers. The link cards are CAMAC (C269) based and seven will be relocated to the Main Injector (two in MI-60, one in each of the remaining power supply service buildings). New voltage regulation controllers will be constructed for the dipole supplies and will be compatible with the existing power supply link interface.

WBS 1.1.3.2-1.1.3.6. BEAMLINE POWER SUPPLIES

WBS 1.1.3.2 8 GEV LINE POWER SUPPLIES

The 8 GeV line will be powered by recycled power supplies obtained from the existing 8 GeV line and the decommissioned AP-4 line. Table 3.3-5 gives the list of existing supplies for these two lines and their disposition after the Main Injector is installed.

Dipole Power Supplies:

The line is made up of two (2) electrically powered bend circuits, each powered by its own supply operated DC.

Bend Circuit #1 will consist of 4 EPB dipoles powered from the West Booster Gallery at a current of 1077 A. The supply will be a TRANSREX, Model ISR2220, 200 V/1,200 A supply reused from the present AP 4 line.

Bend Circuit #2 will be the Injection Lambertson in the MI-10 straight section and be powered from the MI-10 service building at 930 A. The supply will be a DYNAPOWER Type E, 25/40/60 V/1,200 A supply reused from the present 8 GeV line.

Quadrupole Power Supplies

The 8 GeV line quadrupoles will be powered by recycled power supplies. The line has three main sections, as discussed in Chapter 2.4. During the initial commissioning, the first part contains 3 SQAs, 5 SQCs and 2 SQFs, each running at a different current, and matches the Booster lattice to the 8 GeV line lattice. (The SQC at 809 will be replaced by an SQA later to improve the spares situation; the discussion below describes the initial configuration.) The second section part of the line will be made up of permanent magnet quadrupoles of combined function magnets and thus not use power supplies. The third section contains 6 SQAs, each running at a different current, and matches the 8 GeV line to the Main Injector lattice. Magnets requiring a similar current will be bussed in series with an individual shunt across each magnet. Quad currents are given in Table 3.3-5 below. Five quad circuits have been identified.

Quad Circuit #1 will consist of 1 SQA quad (Q800) and 2 SQC quads (Q804 and Q805) powered from the West Booster Gallery. The supply will be a DYNAPOWER Type D, 20/50/100 V/500 A supply reused from the present AP-4 line.

Quad Circuit #2 will consist of 2 SQC quads (Q801 and Q808) powered from the West Booster Gallery. The supply will be a DYNAPOWER Type D, 20/50/100 V/500 A supply reused from the present AP-4 line.

Quad Circuit #3 will consist of 1 SQA quad (Q802), 1 SQC quad (Q809) and 2 SQF quads powered from the West Booster Gallery. The supply will be a DYNAPOWER Type C, 25/40/70 V/200 A supply reused from the present AP-4 line.

Quad Circuit #4 will consist of SQA quad (Q803) powered from the West Booster Gallery. The supply will be a HEWLETT PACKARD - HP6453A, 15 V/200 A supply reused from the present 8 GeV line.

Quad Circuit #5 will consist of 6 SQA quads (Q847 through Q852) powered from the MI-8 Service Building. The supply will be a DYNAPOWER Type C, 25/40/70 V/200 A supply reused from the present AP-4 line.

Table 3.3-5. Quadrupole Currents

Quad #	Type	Nominal	Maximum	Minimum
800	SQA	213.7		
801	SQC	185.3		
802	SQA	163.9	+15.6	-16.8
803	SQA	95.7	+12.2	-13.8
804	SQC	225.1	+5.9	-6.5
805	SQC	245.6	+1.9	-2.3
806	SQF	159.4	+10.8	-7.2
807	SQF	145.9	+5.2	-4.7
808	SQC	203.1	+14.0	-11.3
809	SQC (SQA)	136.2 (207.5)	+3.6 (+5.5)	-3.2 (-5.0)
847	SQA	148.8	+7.3	-5.2
848	SQA	144.2	+2.0	-4.9
849	SQA	156.3	+15.8	-44.4
850	SQA	161.2	+3.1	-8.9
851	SQA	156.4	+4.2	-27.7
852	SQA	159.7	+5.6	-5.2

Diople/Quadrupole Transistor Shunts

The 19 shunts will be built around an existing design. These shunts will be placed across each magnet in a string of magnets to lower the individual magnet current as much as 75 A. In

Table 3.3-6. Beamline Power Supply Availability

Main Supplies in AP-4 Line							
Name	FNAL #	Manufacturer	Model	Power	Volts	Current	Supply
B:Q106	48185	DynaPower	Type B	1.5K	0-5/10/15	100	Available
B:Q110	48184	DynaPower	Type B	1.5K	0-5/10/15	100	Available
B:Q104	48265	DynaPower	Type C	14K	0-25/40/70	200	8 GeV Quad #6
B:Q108	48264	DynaPower	Type C	14K	0-25/40/70	200	Available
B:H101	48202	DynaPower	Type D	50K	0-20/50/100	500	8 GeV Quad #4
B:H110	48200	DynaPower	Type D	50K	0-20/50/100	500	8 GeV Quad #5
B:V110	48233	DynaPower	Type E	72K	0-25/40/60	1200	8 GeV Bend #2
B:V104	18969	TransREX	ISR2220	240K	0-200/400/600	1200/600/300	Available
Main Supplies in OLD 8 GeV Line							
Name	FNAL #	Manufacturer	Model	Power	Volts	Current	Supply Status
VTB1	SR #267	FNAL	Tev Corrector	750	15	50	150 GeV Quad #1
HTB1	SR #280	FNAL	Tev Corrector	750	15	50	150 GeV Quad #2
VTC2	SR #274	FNAL	Tev Corrector	750	15	50	150 GeV Quad #4
HTC5	SR #284	FNAL	Tev Corrector	750	15	50	150 GeV Quad #5
VTM4	SR #295	FNAL	Tev Corrector	750	15	50	150 GeV Quad #6
VTIN1	SR #263	FNAL	Tev Corrector	750	15	50	150 GeV Quad #7
Spare	None	FNAL	Tev Corrector	750	15	50	150 GeV Quad #8
QDB3	75378	Hewlett Packard	HP6260B	1.0K	10	100	Stay
Spare	18139	Hewlett Packard	HP6260B	1.0K	10	100	Available
VTC5	11298	Hewlett Packard	HP6269B	2.0K	40	50	Available
VTM1	77115	Hewlett Packard	HP6269B	2.0K	40	50	Available
Spare	32519	Hewlett Packard	HP6269B	2.0K	40	50	Available
Spare	36339	Hewlett Packard	HP6269B	2.0K	40	50	Available
VTIN2	29148	Hewlett Packard	HP6269B	2.0K	40	50	Available
QFB4	56224	Hewlett Packard	HP6453A	3.0K	15	200	Stay
QFM1	24553	Hewlett Packard	HP6453A	3.0K	15	200	8 GeV Quad #1
QDM2	24554	Hewlett Packard	HP6453A	3.0K	15	200	150 GeV Bend #4
QDM6	18138	Hewlett Packard	HP6453A	3.0K	15	200	150 GeV Bend #5
QDM8	18137	Hewlett Packard	HP6453A	3.0K	15	200	Available
Spare	56225	Hewlett Packard	HP6453A	3.0K	15	200	Available
QDB5	14635	Hewlett Packard	HP6466C	9.0K	18	500	Stay
QFB6	TE-420331	Hewlett Packard	HP6466C	9.0K	18	500	Stay
Spare	29149	Hewlett Packard	HP6466C	9.0K	18	500	150 GeV Bend #1
Spare	14635	Hewlett Packard	HP6466C	9.0K	18	500	150 GeV Bend #2
QFM5	31881	Hewlett Packard	HP6469C	10.8K	36	300	8 GeV Quad #3
QFM7	60591	Hewlett Packard	HP6469C	10.8K	36	300	150 GeV Bend #3
VBMP	31882	Hewlett Packard	HP6469C	10.8K	36	300	150 GeV Quad #3
VBMP	56247	Hewlett Packard	HP6469C	10.8K	36	300	Available
Spare		Hewlett Packard	HP6475C	11K	110	100	Available
Spare		Hewlett Packard	HP6475C	11K	110	100	Available
Spare	15161	Hewlett Packard	HP6475C	11K	110	100	Available
QDB1	56421	DynaPower	PPS-18-500	9K	18	500	Stay
QFB2	56424	DynaPower	PPS-18-500	9K	18	500	Stay
QFM3	56422	DynaPower	PPS-18-500	9K	18	500	Available
QDM4	60497	DynaPower	PPS-18-500	9K	18	500	Available
Spare	56423	DynaPower	PPS-18-500	9K	18	500	Available
QCELL	56426	DynaPower	PPS-65-350-F	22.75K	65	350	8 GeV Quad #2
Spare	56425	DynaPower	PPS-65-350-F	22.75K	65	350	Available
HB83	48232	DynaPower	Type E	72K	0-25/40/60	1200	8 GeV Bend #4
VB812	18978	TransREX	ISR2220	240K	0-200/400/600	1200/600/300	8 GeV Bend #3
HB812	18971	TransREX	ISR2220	240K	0-200/400/600	1200/600/300	Stay
LAMB	18962	TransREX	ISR2220	240K	0-200/400/600	1200/600/300	8 GeV Bend #1
Main Supplies in Main Ring to Tev Lines							
Name	FNAL #	Manufacturer	Model	Power	Volts	Current	Supply Status
ABTHOR	6799	TransREX	ISR2126-2A	500K	0-100/200/400		Available
ABTLM	6955	TransREX	ISR2126-2A	500K	0-100/200/400		Available
ILAM	6956	TransREX	ISR2126-2A	500K	0-100/200/400		Available
RIHTD	56602	DynaPower		19.5K	150	130	Available
Spare	56603	DynaPower		19.5K	150	130	Available

the case of the dipole string the current limit will be more like 35 A due to the increased voltage per magnet required.

Dipole Correction Element Power Supplies

The 8 GeV line dipole corrector magnets will be recycled Main Ring elements. The supplies will also be recycled Main Ring corrector supplies that will be moved. The corrector packages are built around a 12 channel group and the 8 GeV line will get 3 such packages for a total of 36 possible correctors.

WBS 1.1.3.3-1.1.3.4. 150 GEV PROTON/PBAR BEAM LINE POWER SUPPLIES

The 150 GeV Proton line and the 150 GeV Pbar line are very similar in design. The 150 GeV Proton line will serve three main functions:

- Transfer 150 GeV protons to the Tevatron,

- Transfer 120 GeV protons to the Main Ring remnant, and

- Transfer 8 GeV protons to and antiprotons from the Antiproton Source.

The 150 GeV Pbar line will serve one function:

- Transfer 150 GeV Pbars to and protons from the Tevatron.

The four very different functions require matching to lattice functions in each machine. Various magnets will be powered at different values for each function. A result of these requirements is that quadrupole magnets will in general be individually powered at each end of the beamlines.

The lines will use common supplies switched between equivalent magnet loads of the two lines. In all cases it will be advantageous to make the switch three pole such that when the main supply is driving the Pbar line the Proton line may be connected to a small auxiliary DC supply to allow 8 GeV proton or pbar transfers to or from the Antiproton Source. In general, lower RMS current rated cable will be used for the Antiproton line since its cycle time is much larger than the 120 GeV Pbar production cycle. In no case will the rating be less than 25% of the proton line rating, and in many cases the rating will be much closer to the proton line because of voltage constraints.

All main power supplies and auxiliary power supplies will contain passive filters in order for the magnet systems to meet the ripple specification for the field during slow spill. In the following circuit descriptions, the magnet nominal currents will be given in the order

150p/120p/8p/150pbar/[RMS] where the RMS current is calculated for the 120 GeV slow spill cycle. Since the supplies will be ramped both the peak current and the RMS current will be given for the proposed supply. All but two supplies will be located in F0 with both proton and pbar circuits having equal length cables. The first two supplies (extraction/injection lambertsons and C-magnets) will be located in the MI-52 service building with long cables of reduced RMS current capability driving current from MI-52 to the pbar magnets around MI-62.

Dipole Power Supplies

Six dipole magnet circuits have been identified

Bend Circuit #1 will consist of 3 MI extraction/injection lambertson magnets powered at nominal currents of 2011 A/1610 A/248 A /2011 A/[1119 A]. For this circuit the transfer switch between the proton and pbar line will be 3-pole with the first pole connected between the first and second magnets allowing you to power only the second and third magnet for 8 GeV operation. The main supply will be a TRANSREX, Model ISR2126, 200 V/2500 A peak/2500 A RMS supply reused from the MR to TEV transfer lines. The auxiliary supply will be a Hewlett Packard, Model HP 6466C, 18V/500 ADC supply reused from the old 8 GeV line (spare). This bend circuit is pictorially given in Figure 3.3-8.

Bend Circuit #2 will consist of 4 MI C-magnets powered at nominal currents of 3500 A/2853 A/211 A/3089 A/[1691 A]. As in the case of bend circuit #1 above the circuit will use a 3-pole transfer switch to allow bypassing the first C-magnet of the string for 8 GeV proton operation. The main supply will be a new, 150 V/4000 A peak/2700 A RMS power supply. The auxiliary supply will be a Hewlett Packard, Model HP 6466C, 18V/500 ADC supply reused from the old 8 GeV line (spare).

Bend Circuit #3 will consist of 14 B2 magnets powered at nominal currents of 4928 A/3941 A/292 A/4878 A/[2713 A]. The supply used to power the string will be one FNAL MR supply, 835 V/6800 A peak/3350 A RMS. The auxiliary supply will be a Hewlett Packard, Model HP 6469C, 36V/300 ADC supply reused from the old 8 GeV line (QFM7). This bend circuit is pictorially given in Figure 3.3-9.

Bend Circuit #4 will consist of 1 B2 magnet powered at currents of 1819 A/1452 A/108 A/1819 A/[1000 A]. The supply will be new, 50 V/2000 A peak/1300 A RMS. The auxiliary supply will be a Hewlett Packard, Model HP 6453A, 15 V/200 ADC supply reused from the old 8 GeV line (QDM2).

BEND CIRCUIT #1

150 Gev Proton/P-Bar Transfer

(wbs 1.1.3.3.1)

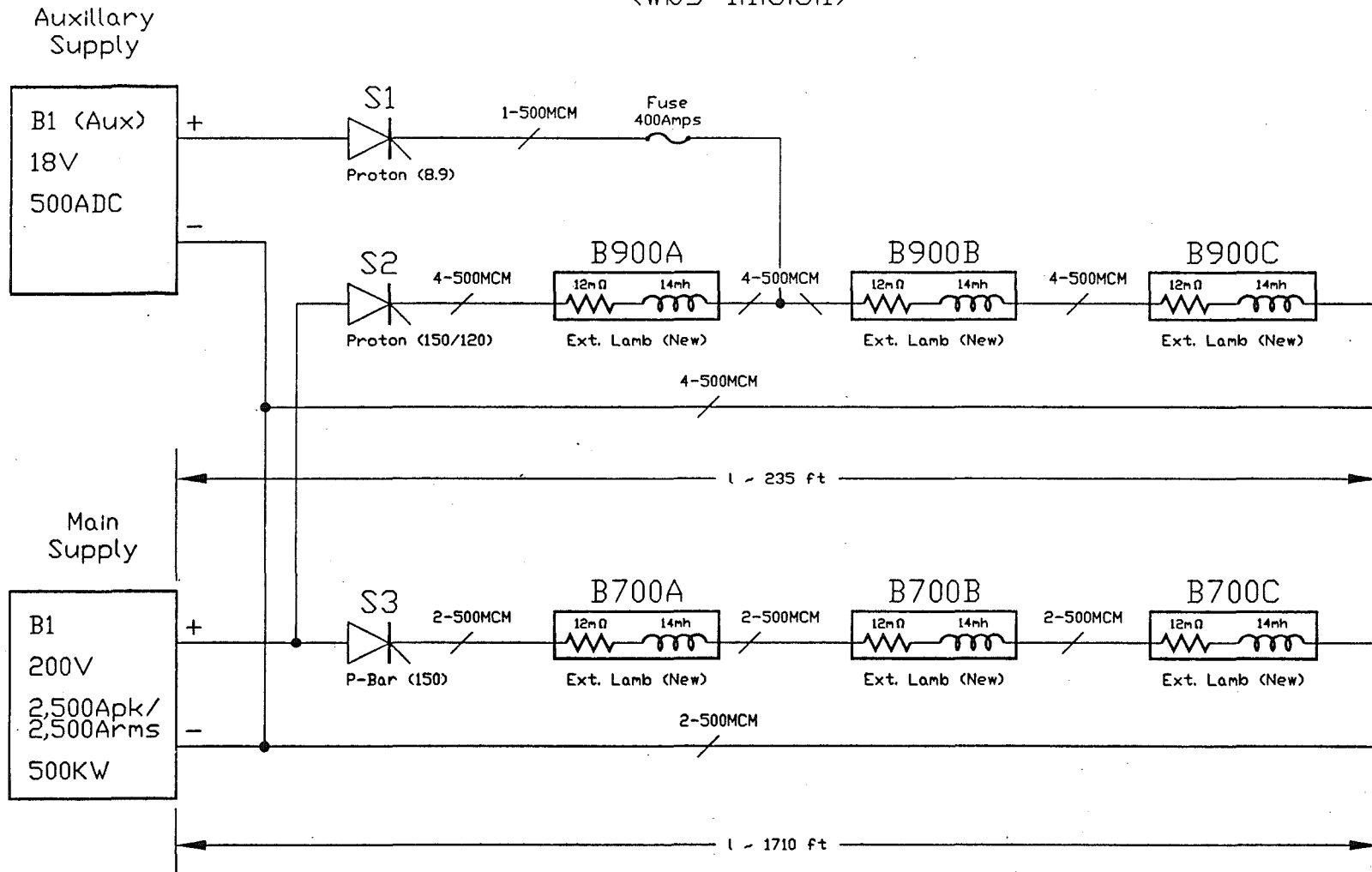
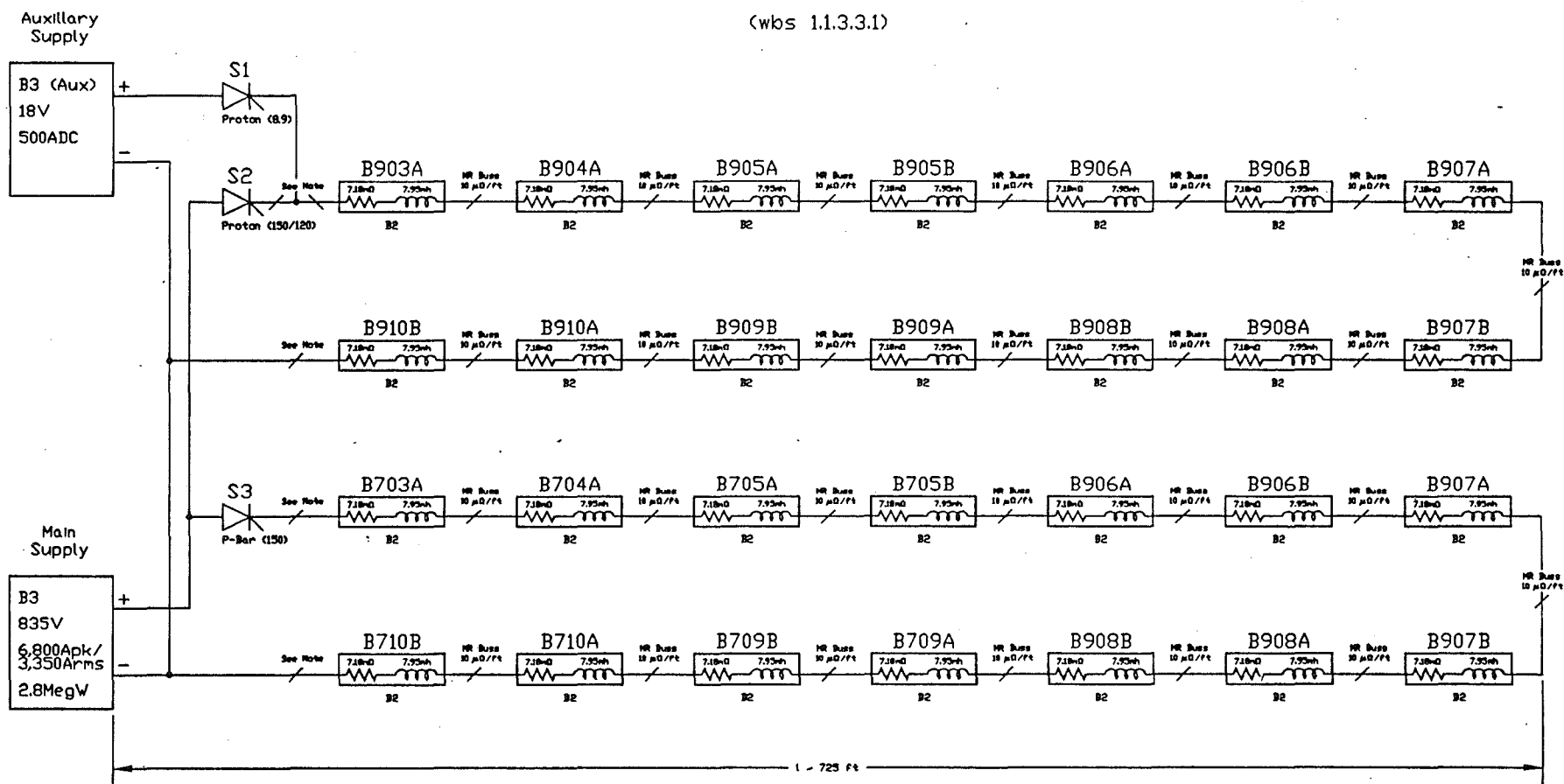


Figure 3.3-8. 150 GeV Line Lambertson Magnet Power Supply Configuration.

BEND CIRCUIT #3

150 GeV Proton/P-Bar Transfer

(wbs 1.1.3.3.1)



Note: In general $10\mu\Omega/\text{ft}$ Buss will be used. Flexible Cable of rated RMS current will be used through the cable penetrations.

Figure 3.3-9. 150 GeV Line Main Dipole Magnet Power Supply Configuration.

Bend Circuit #5 will consist of 1 C-magnet powered at currents of 3450 A/1386 A/103 A/2784 A/[899 A]. The supply will be new, 45 V/4000 A peak/2700 A RMS. The auxiliary supply will be a Hewlett Packard, Model HP 6453A, 15 V/200 ADC supply reused from the old 8 GeV line (QDM6).

Bend Circuit #6 will consist of 4 MI extraction/injection lambertson magnets powered at currents of 1979 A/0/0/1622 A/[303 A]. (In this special case the RMS current for the 150 GeV proton transfers to the Tevatron is given assuming two injection cycles per 60 seconds.) A transfer switch will not be used for this circuit since the magnets are common to both the 150 GeV proton and pbar lines. For 120 GeV or 8 GeV, the supply will be off allowing the beam to enter the MR remnant for transfer to or from the Antiproton Source or to transfer to the Switchyard. The supply will be a TRANSREX, Model ISR2126, 200 V/2500 A peak/2500 A RMS supply reused from the MR to TEV transfer lines.

Quadrupole Power Supplies

Quads at either end of the lines will be individually powered with the seven middle quads powered in series from a single supply. Eight magnet circuits have been identified. Again for each circuits nominal current will be given in the order 150p/120p/8p/150pbar/[RMS]. Peak and RMS supply currents will be given for each supply.

Quad Circuit #1 will consist of 1 3Q120 quad powered at currents of 332 A/266 A/19.7 A/311 A/[177 A]. The supply will be a new, 100 V/500 A peak/350 A RMS unit. The auxiliary supply will be a FNAL designed Tevatron correction element supply, 15 V/50 A, currently used in the old 8 GeV line (VTB1).

Quad Circuit #2 will consist of 1 3Q120 quad powered at currents of 296 A/237 A/17.6 A/293 A/[156 A]. The supply will be a new, 100 V/500 A peak/350 A RMS unit. The auxiliary supply will be a FNAL designed Tevatron correction element supply, 15 V/50 A, currently used in the old 8 GeV line (HTB1).

Quad Circuit #3 will consist of 7 3Q84 MR quads powered at currents of 3833 A/2607 A/194 A/3644 A/[1663 A]. The supply used to power the string will be a FNAL MR supply, 417 V/6800 A peak/3350 A RMS. This supply will be configured with the output bridges in parallel giving one-half the normal output voltage. The auxiliary supply will be a Hewlett Packard, Model HP 6469C, 36 V/300 ADC supply reused from the old 8 GeV line (VBMP).

Quad Circuit #4 will consist of 1 3Q120 quad powered at currents of 378 A/263 A/19.5 A/391 A/[174 A]. The supply will be a new, 100 V/500 A peak/350 A RMS. The auxiliary

supply will be a FNAL designed Tevatron correction element supply, 15 V/50 A, currently used in the old 8 GeV line (HTC2).

Quad Circuit #5 will consist of 1 3Q120 quad powered at currents of 290 A/137 A/10.2 A/259 A/[92 A]. The supply will be a new, 100 V/500 A peak/350 A RMS. The auxiliary supply will be a FNAL designed Tevatron correction element supply, 15 V/50 A, currently used in the old 8 GeV line (HTC5).

Quad Circuit #6 will consist of 1 3Q120 and 1 3Q60 quad powered at currents of 333 A/264 A/19.6 A/276 A/[182 A]. The supply will be a new, 100 V/500 A peak/350 A RMS. The auxiliary supply will be a FNAL designed Tevatron correction element supply, 15 V/50 A, currently used in the old 8 GeV line (HTM4).

Quad Circuit #7 will consist of 1 3Q120 and 1 3Q60 quad powered at currents of 341 A/349 A/25.9 A/359 A/[241 A]. The supply will be a new, 100 V/500 A peak/350 A RMS. The auxiliary supply will be a FNAL designed Tevatron correction element supply, 15 V/50 A, currently used in the old 8 GeV line (HTIN1).

Quad Circuit #8 will consist of 1 3Q120 quad powered at currents of 286 A/357 A/26.5 A/384 A/[238 A]. The supply will be a new, 100 V/500 A peak/350 A RMS. The auxiliary supply will be a FNAL designed Tevatron correction element supply, 15 V/50 A, currently used in the old 8 GeV line (HTIN2).

Correction Element Power Supplies

Dipole corrector magnets will be recycled Main Ring elements with new small dc supplies. Each of the lines will have 12 of these trim magnets generally located at each quad location. The supplies will be 60 V/10 A with an RMS current limit of 6 A.

Lambertson Power Supplies

The Lambertson magnet power supplies are discussed under the dipole power supplies.

WBS 1.1.3.5. 120 GEV (F0-F17) POWER SUPPLIES

The F0-to-A0 Beam line is generally referred to as the Main Ring remnant; the first section, F0-to-F17, will be used to perform three functions.

Transfer of 120 GeV protons to the AP-1 line and on to the target for antiproton production.

Transfer of 8 GeV pbars from the AP-3 line and on to the MI.

Transfer of 120 GeV protons to F18 and on to the rest of the MR remnants for delivery of slow spill beam to the switchyard.

Power supplies for this line will be ramped to minimize power consumption.

Dipole Power supplies

The dipoles that are included in this section will be a combination of B2s, B3s and the existing F17 C-magnets. Two bend circuits have been identified. Currents for each circuit will be given in the order 120p/8pbar.

Bend Circuit #1 will consist of 14 B2 magnets, 4 B3 magnets configured with their coils in parallel (such that when run with B2 current the B3 will have the same bend) and 4 B3 magnets configured with their coils in series (such that when run with B2 current the B3 will have twice the bend). This string will be run at currents of 1356 A/104 A. The supplies used to power the string will be two FNAL MR supplies, 835 V/6800 A peak/3350 A RMS. These two supplies will be located at F1 in their normal location. In normal operation a single supply will be used to power the line.

Bend Circuit #2 will consist of 1 B3 magnet configured with its coils in parallel and 2 F17-C magnets powered at currents of 2838 A/211 A. The supply will be a FNAL MR supply, 417 V/6800 A peak/3350 A RMS. This supply will be located at F2. The only change to this bend circuit from what is installed today is the substitution of the B3 for the extraction Lambertson.

Quadrupole Power Supplies

The quads at the front end of this line will be individually controlled to aid in the matching from the 150 GeV proton line lattice to the original Main Ring lattice. Four quad circuits have been identified for this line. The supplies for these four circuits will be located in the F0 service building.

Quad Circuit #1 will consist of 1 3Q60 magnet powered at a current of 286 A/21.2 A. The supply will be a new, 100 V/500 A peak/350 A RMS unit.

Quad Circuit #2 will consist of 1 3Q120 magnet powered at a current of 210 A/15.6 A. The supply will be a new, 100 V/500 A peak/350 A RMS unit.

Quad Circuit #3 will consist of 2 3Q60 magnet powered at a current of 235 A/17.5 A. The supply will be a new, 100 V/500 A peak/350 A RMS unit.

Quad Circuit #4 will consist of five 3Q84 magnets powered at a current of 1389 A/103 A. The supply will be a new, 75 V/1500 A peak/1070 A RMS unit.

Correction Element Power Supplies

Dipole corrector magnets will be recycled Main Ring elements with new small dc supplies. The line will have 8 of these trim magnets generally located at each quad location. The supplies will be 60 V/10 A with an RMS current limit of 6 A.

WBS 1.1.3.6. SLOW SPILL (F18-A0) POWER SUPPLIES

This line is the remainder of the MR remnant that will be used to transport 120 GeV protons to the Switchyard for delivery to the fixed target experimental areas. The line will in general remain unchanged from its operation at this time. Several dipole and quad magnet changes at A0 will be the only element changes. Quad currents will be different around the A0 section to facilitate matching into the Switchyard lattice.

Dipole Power Supplies

Two bend circuits have been identified for this line. The first will encompass most of the line and except for a few magnet changes will be what is installed at this time. The second will be new elements located at A0.

Bend Circuit #1 will consist of 49 B1s, 52 B2s, 1 2XB2 and 2 B3s configured with their coils in series powered at a current of 1356 A. This string of magnets will be powered from four FNAL MR supplies, 835 V/6800 A peak/3350 A RMS. These supplies will be located at F2 and F4 in normal slots for MR supplies.

Bend Circuit #2 will consist of two B2 magnets powered at a current of 650 A. The supply will be a new, 35 V/750 A peak/500 A RMS unit located in the A0 transfer hall.

Quadrupole Power Supplies

Five quad circuits have been identified for this line. The first will encompass most of the line. The last four will be used to match the Main Ring lattice into the present switchyard.

Quad Circuit #1 will consist of 25 3Q84 MR quads powered at a current of 1356 A. The supply will be a FNAL MR supply, 417 V/6800 A peak/3350 A RMS. The supply will be located at F3 in a normal location.

Quad Circuit #2 will consist of one 3Q52 MR quad powered at a current of 4000 A. The supply will be new, 45 V/4000 A peak/2856 A RMS. The supply will be located in the A0 transfer hall.

Quad Circuit #3 will consist of 2 3Q52 MR quads powered at a current of 4000 A. The supply will be new, 60 V/4000 A peak/2856 A RMS. The supply will be located in the A0 transfer hall.

Quad Circuit #4 will consist of 1 3Q52 and 1 3Q84 MR quads powered at a current of 4000 A. The supply will be new, 60 V/4000 A peak/2856 A RMS. The supply will be located in the A0 transfer hall.

Quad Circuit #5 will consist of 2 3Q52 MR quads powered at a current of 4000 A. The supply will be new, 60 V/4000 A peak/2856 A RMS. The supply will be located in the A0 transfer hall.

Correction Element Power Supplies

Dipole corrector magnets will be recycled Main Ring elements with new small dc supplies. The line will have 28 of these trim magnets generally located at each quad location. The supplies will be 60 V/10 A with an RMS current limit of 6 A.

References

1. S. Fang, to be published, 1994.
2. C. Jach, J. Ryk and D. Wolff, "MSS-KSS and KSS-MSS Backfeed Loading", MI Note-0122, 1994.
2. S. Fang, to be published, 1994.

CHAPTER 3.4 RF SYSTEMS

WBS 1.1.4.

RF SYSTEMS

WBS 1.1.4.1.1.

MAIN INJECTOR 53 MHZ RF SYSTEM

h=588 cavities

The 18 existing 53 MHz Main Ring rf cavities will be installed in straight section MI-60 and operated at harmonic number 588. The operating levels below transition are determined by an interplay between cycle time, bucket area, and synchrotron frequency. A bucket area of at least 0.2 eVs is required to accept beam out of the Booster. Historically, it has been necessary to keep the synchrotron frequency in the Main Ring below 720 Hz to avoid resonance with power supply ripple at the sixth harmonic of the line frequency. Figure 3.4-1 shows the rf voltage, bucket area, synchrotron frequency, and synchronous phase through the 120 GeV antiproton production cycle. A bucket area of 0.5 eVs is maintained, but with the synchrotron frequency rising above 720 Hz. The ramp would have to be slowed down to avoid this. The momentum spread in the beam, $\Delta p/p$ (95% half width), is $\pm 0.2\%$ at injection, increasing to about $\pm 0.8\%$ near transition, and decreasing to $\pm 0.1\%$ at extraction.

Since the FMI must accelerate antiprotons as well as protons, a degree of simplicity and system flexibility will be achieved by placing the cavities at spacings that are multiples of one-half the rf wavelength, Figure 3.4-2. Also shown are the six coalescing cavities and the second harmonic cavity used for "snap" coalescing. The 180° spacing of accelerating cavities will simplify the RF signal distribution (fan-out/fan-back) system as well as providing simpler choices for coalescing stations. Easier maintenance, better personnel understanding, and greater system reliability are expected as a result of the new spacing.

The rf system has the capability of generating enough voltage at injection to produce a 1.0 eVs bucket area at injection, where the limit of 150 kV per cavity is set by the tendency of the tuners to spark because they are close to parallel resonance. In this mode the synchrotron frequency lies well above 720 Hz at injection and descends rapidly, crossing 720 Hz when the beam energy is about 15 GeV. At the frequency for transition energy the cavities are capable of producing 240 kV each, so that 4.0 MV are available even with one cavity inoperative. If the rf system has more than a 50% duty factor it is not possible to maintain the 4 MV level all the way to top energy because of cavity heating. Operational experience will dictate the exact ramp scenario that is used.

One limitation of the existing Main Ring rf system is the power that it can deliver. The present requirements are 55 kW per cavity, which will grow to 70 kW after the Linac upgrade provides increased beam intensity. The FMI will require 112 kW for accelerating the full intensity

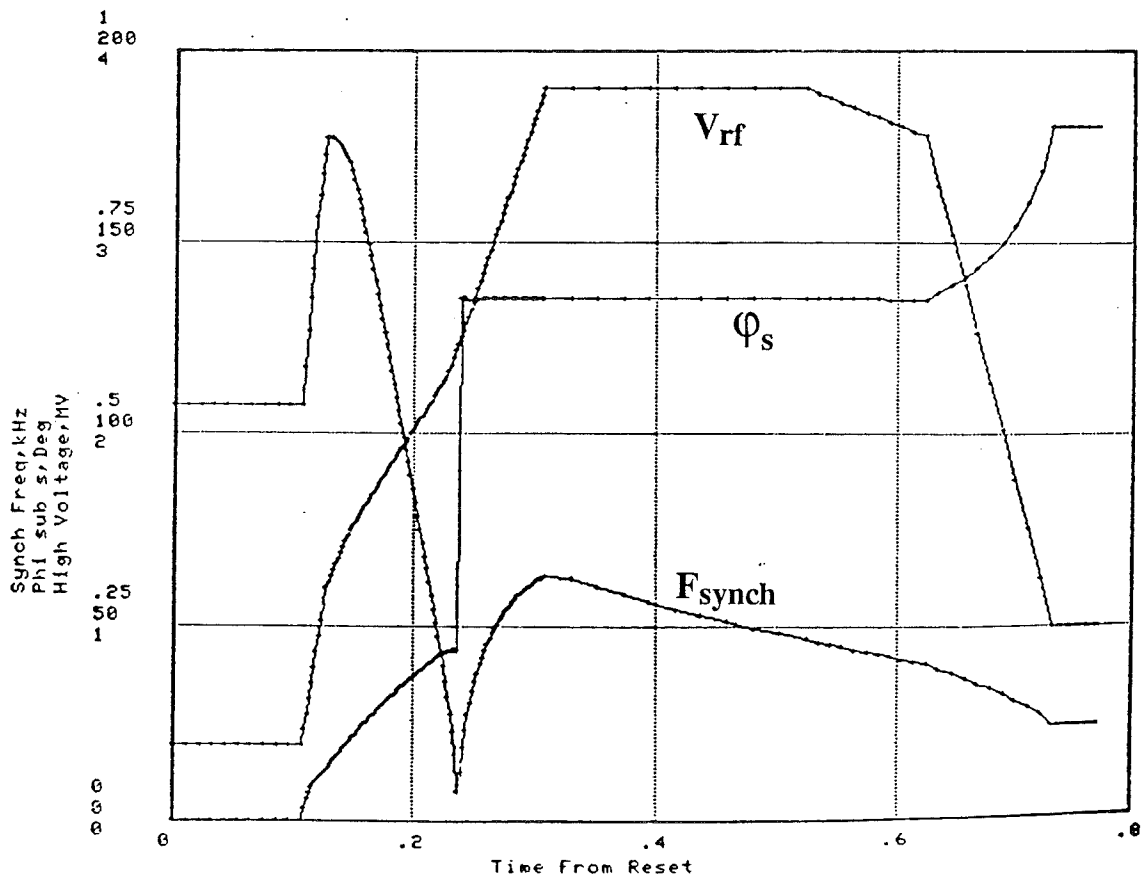
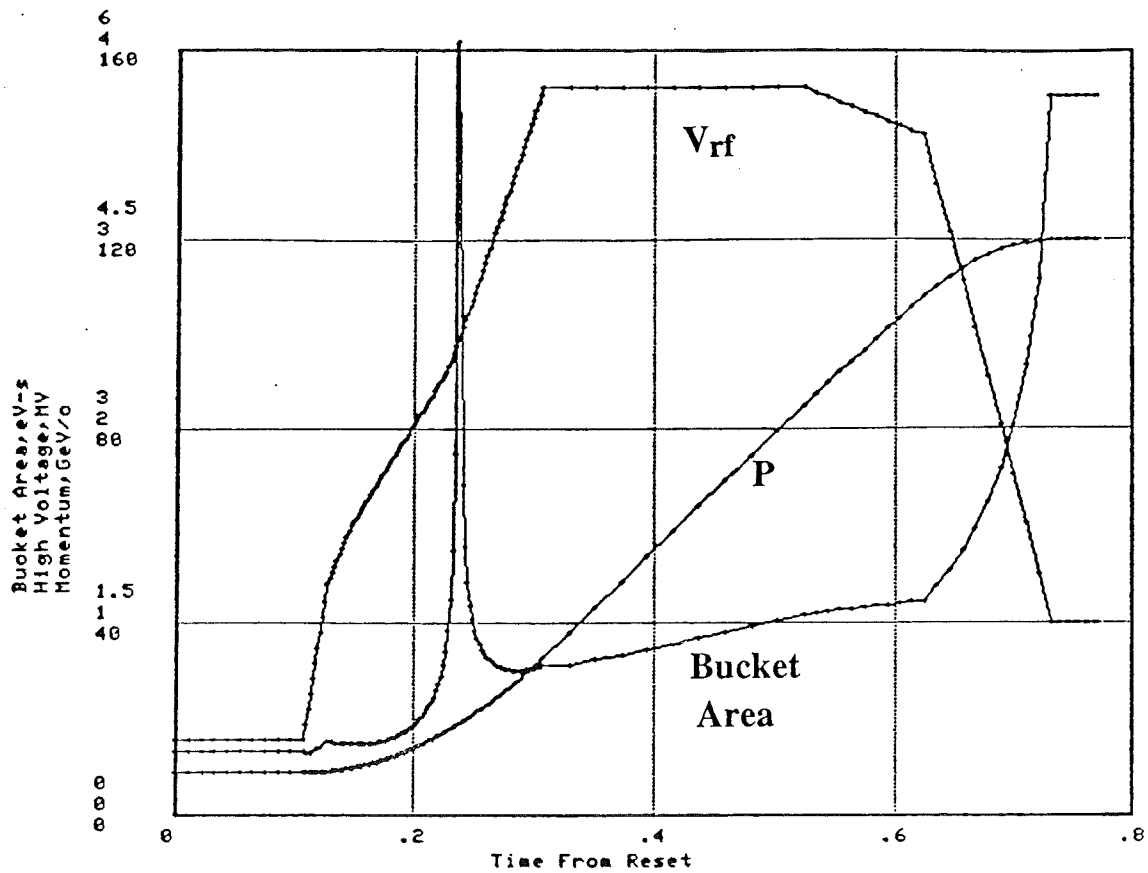


Figure 3.4-1. RF Parameters for the 120 GeV Antiproton Production Cycle with Bucket Area > 0.5 eVs

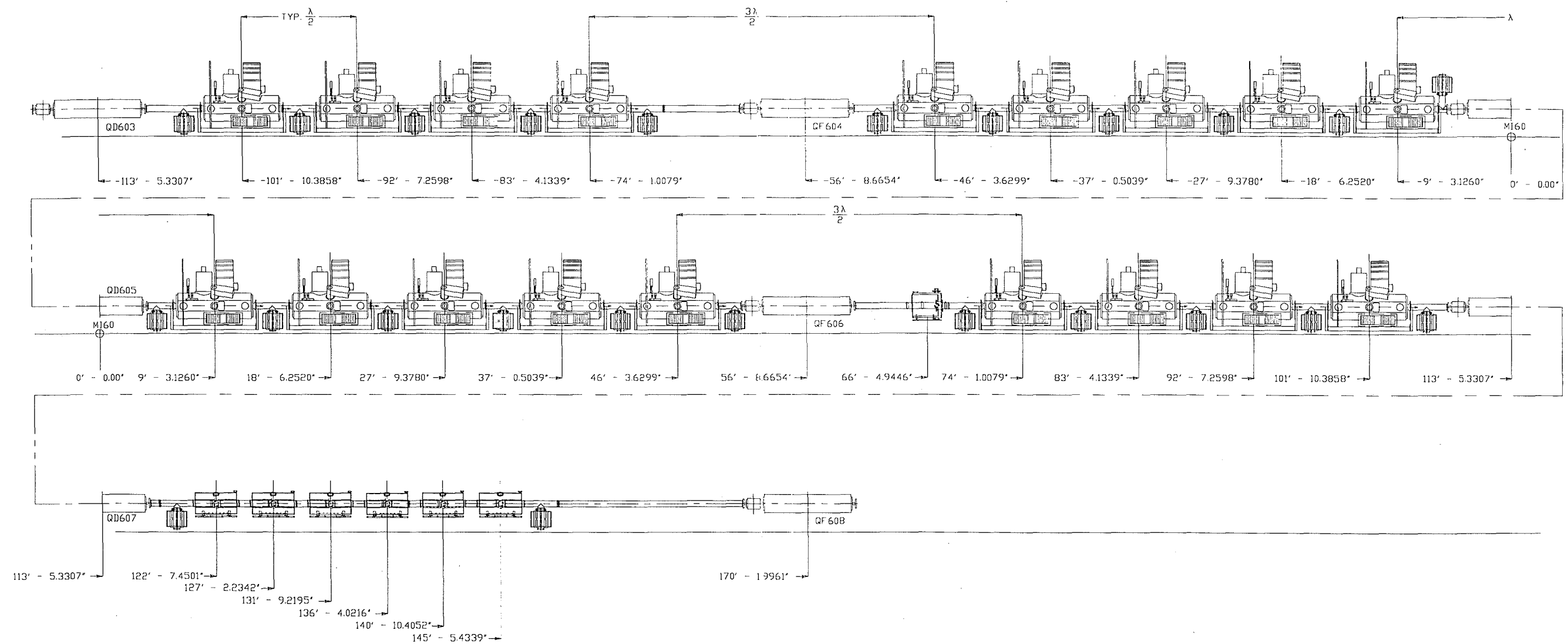


FIGURE 3.4-2. MI60 TUNNEL CAVITY ARRANGEMENT

at 240 GeV/sec, which is excessive for rf amplifier reliability using the present Main Ring rf system. Provision in the original cavity design allowed for a second amplifier to be installed on the cavity. This choice, while possible, places additional amplifier components in the enclosure thus increasing maintenance. To overcome this limitation, a new 200 kW power amplifier is placed in the tunnel with a 4 kW rf driver and 30 kV series tube modulator in the equipment gallery. A schematic of the rf cavity with the simplified amplifier is shown in Figure 3.4-3.

R&D development of a 200 kW RF power amplifier and a 4 kW driver has been completed. Three amplifier systems have been constructed and are being tested. Development work for three modulators is under way with the first prototype scheduled to be completed in FY94.

The new 200 kW amplifiers are cathode-driven, grounded-grid design with the operating point efficiently regulated with a dc grid bias voltage. The design retains much of the existing Main Ring final PA tube module. Figure 3.4-4 shows a cross section of the power amplifier. Only the Y-567B high power tetrode is in the enclosure.

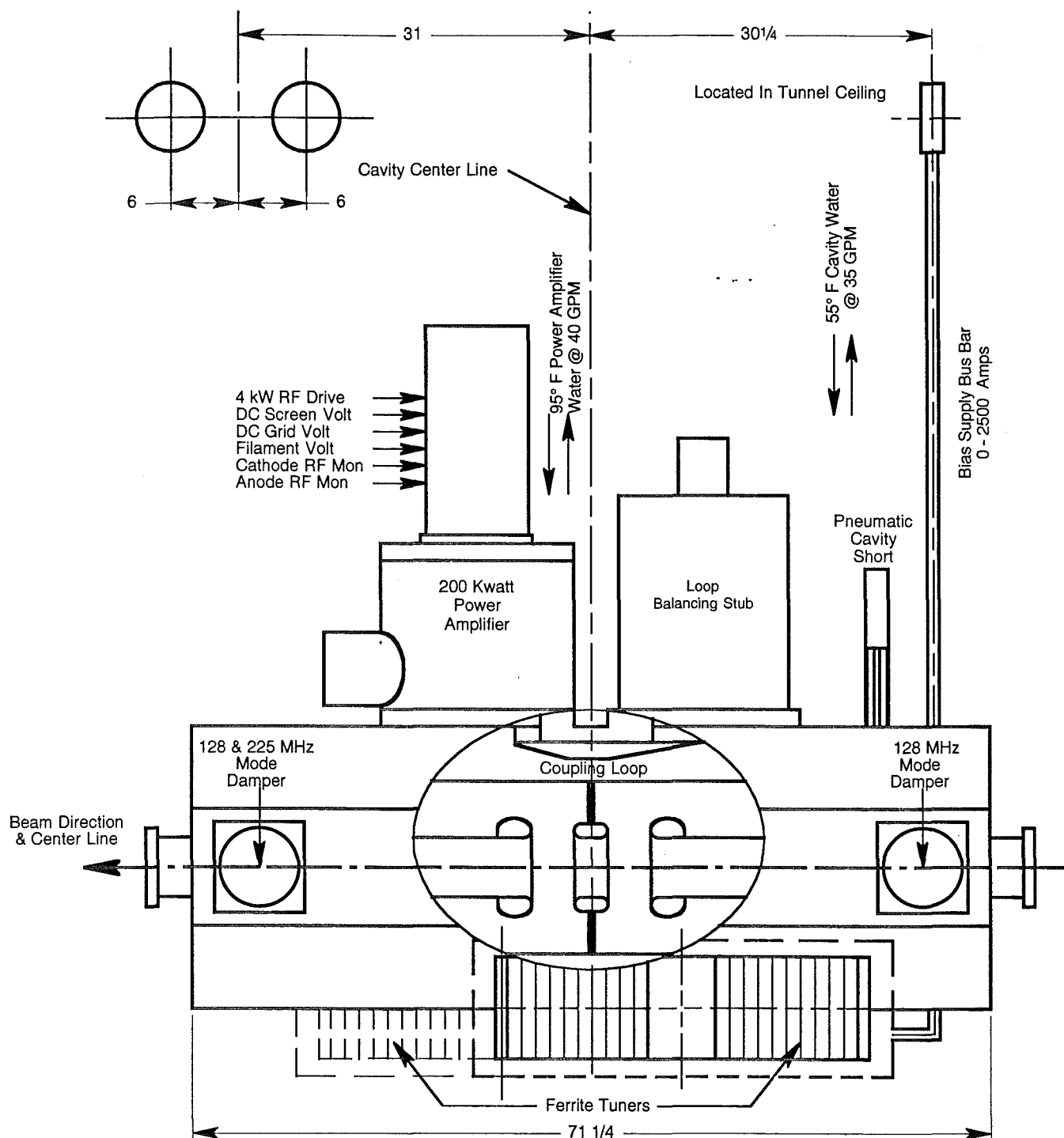
Tevatron style 500 volt programmable grid and screen supplies are used for dc biasing. RF drive is provided by a solid state 4 kW rf driver coupled to the final tube cathode.

More than 200 kW of output power has been achieved with the new amplifiers. Reliability testing is being made in a test station and in an active accelerating station in the Main Ring RF System. Operation in a Main Ring Station since May 15, 1994 without failure, although not yet a long term test, has given us encouragement that the design is sound.

The transient beam loading from 6×10^{10} protons per bunch will require about 1.25 amp delivered to the cavities, supplied by 15 A (12:1 cavity step-up ratio) of rf current generated by the power amplifier. A 200 kW rf power amplifier operated at a dc plate voltage of 20 kV will produce a peak rf current of approximately 21 A. The 40% surplus initial current capability will insure adequate operating lifetime as the power tube ages.

Low level beam signals will be monitored and processed with a one turn delay to provide the correct drive to the amplifier for transient beam loading compensation. An improved update of the presently used system will be developed and ready by the time the Main Injector is ready for operation.

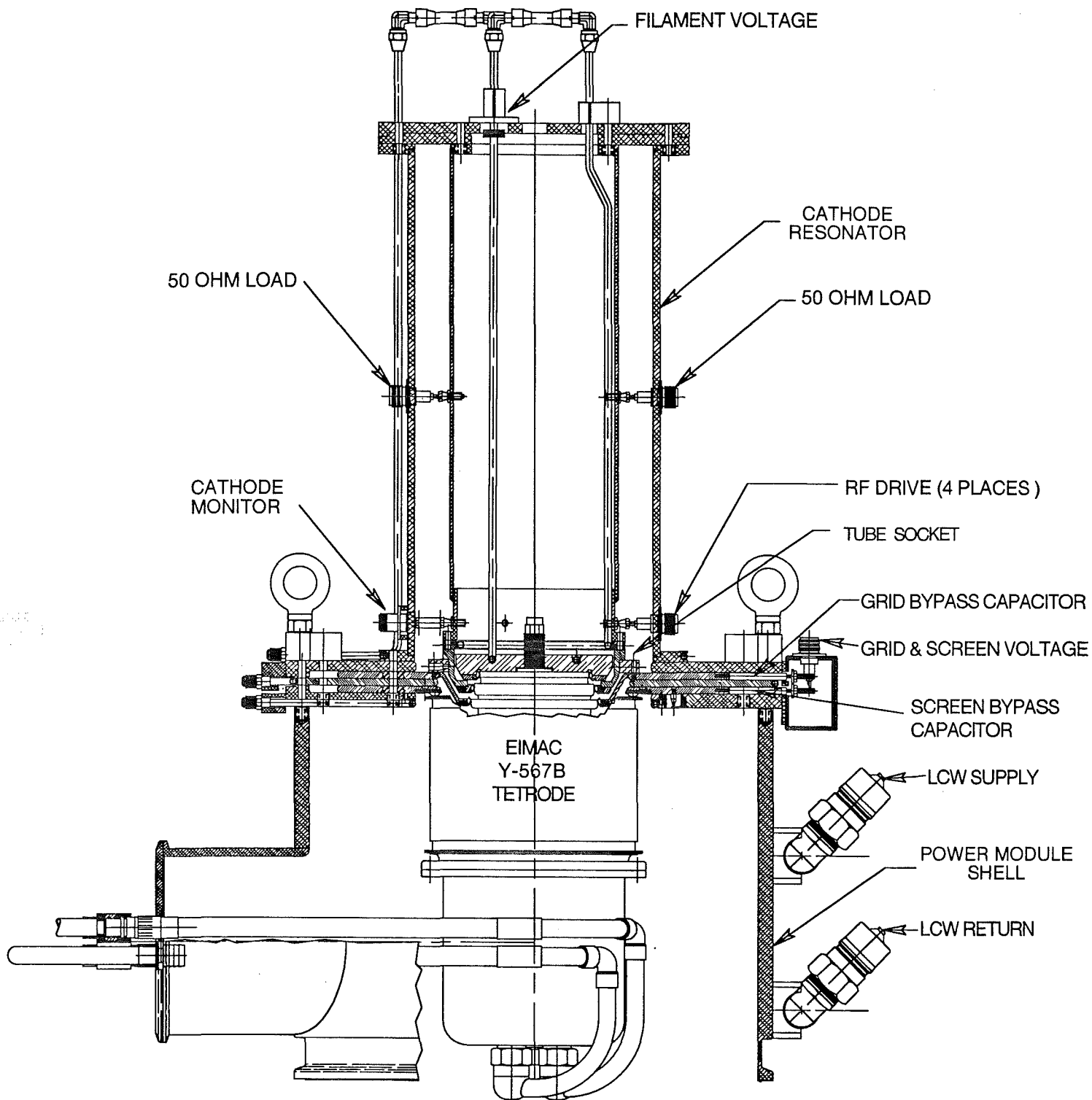
Figure 3.4-5 shows the equipment gallery layout proposed for MI-60. Cable tray, utilities and penetration designs have been completed and are ready to be installed.



As Viewed From Aisle Side

Cross Section of 53 MHz Main Injector Cavity

Figure 3.4-3



Cross Section of 200 Kwatt Power Amplifier

Figure 3.4-4

In the present Main Accelerator rf systems two 30 kV anode power supplies provide dc power to 18 rf stations. Nine stations are powered by each anode supply. Using 200 kW amplifiers only six stations can be powered by a MR anode supply. One additional anode supply will be provided. The two present MR anode supplies will be rebuilt at the MI-60 location when the present Main Ring is decommissioned. Design improvements proven to increase reliability in a similar supply used in the Tevatron rf systems will be implemented. This will make the Main Injector anode supplies similar to the Tevatron supply. Uniformity of the systems will improve both maintainability and provide consistent safety requirements in the two systems.

WBS 1.1.4.1.2. COALESCING RF SYSTEM

Coalescing Cavities

The FMI will use the 2.5 and 5.0 MHz coalescing cavities from the Main Ring to prepare intense bunches for collider loading; no significant modifications are required. The system consists of five 2.5 MHz ferrite loaded cavities producing 12 kV and one at 5.0 MHz producing 15 kV. These cavities are driven with solid state amplifiers which will be located in the MI-60 Service Building. Because the harmonic number for 2.5 MHz is 28 in the FMI compared to its Main Ring value of 53, the system will provide 1.4 times the bucket height available in the Main Ring. For longitudinal emittance of 0.15 eVs, about 30 kV of 2.5 MHz rf is required, so there is substantial reserve in this system. The FMI will also use a 15 kV, 106 MHz cavity from the Main Ring. It is used to linearize the 53 MHz bunch rotation in the procedure called snap coalescing, discussed in Chapter 2.6

WBS 1.1.4.1.1.3. MAIN INJECTOR LLRF

Requirements

The four operating modes of the Main Injector are listed below.

Energy	Mode	Beam	Extraction
120 GeV	Antiproton Production	1 batch	1 turn
120 GeV	Slow Spill	6 batch	1 sec
150 GeV	Fixed Target	6 batch	1 turn
150 GeV	Collider, 36 on 36	11 bunch	1 turn

Satisfying the 36 on 36 Collider mode requirements will also satisfy the Low Level RF, or LLRF, system requirements for the other modes.

In the 36 on 36 Collider mode, beam in the Tevatron will be distributed around the circumference in 1113 proton, and an equal number of counter rotating antiproton buckets, in a 3 fold symmetric pattern. Each group of 371 buckets will contain 12 bunches separated by 21 buckets and a 140 bucket gap.

The Main Injector will accept 12 Booster cycles of 11 bunches, each separated by 21 buckets. These will be accelerated, simultaneously coalesced into 12 bunches, phase locked to the Tevatron, transfer clogged, and injected into the correct Tevatron bucket. This process will be repeated 3 times.

A harmonic 4 rf system, to be developed for the Antiproton Source, will allow the simultaneous extraction of 4 groups of 11 harmonic 84 bunches separated by 21 buckets. These 4 bunches will be accelerated and injected into one of the 140 bucket gaps in the Tevatron. After filling the 3 gaps, the antiprotons will be collision clogged by 84 buckets to allow the injection of 3 more Main Injector cycles. The antiprotons will again be clogged by 84 buckets allowing 3 more Main Injector cycles. Final collision point clogging will complete the process.

In addition to controlling the beam energy and radial position through the acceleration cycle, the LLRF is required to perform the following functions.

1. Booster will phase lock to the Main Injector
2. Main Injector will phase lock to Antiproton Source
- 3 Main Injector will phase lock to Tevatron
4. Main Injector will transfer cog to Tevatron

Improvements to MR LLRF

With exception to differences in transfer clogging to the Tevatron, described in 1.9.1.1.1, all of the functionality of the Main Injector LLRF is currently implemented in the Main Ring LLRF system. In preparation for the Main Injector, the Main Ring LLRF system is being redesigned to exploit the features of Numerically Controlled Oscillators, or NCO's. The upgrade path has been broken into 4 major stages.

1) Replace the Voltage Controlled Oscillator, or VCO, with an NCO that is programmed with a digital signal processor, or DSP, used to calculate the frequency from the programmed bend bus current. The DSP will interpolate the frequency between the 720 Hz step rate of the program providing 180 Hz accuracy through the acceleration cycle. The DSP can also calculate the acceleration phase program from the measured cavity voltage and calculated beam energy.

The beam phase lock and radial position feedback loops will be applied to a ΔF module, designed for and used in the Tevatron. The ΔF module can accurately raise or lower the frequency of the NCO by small amounts according to the analog input.

2) Because the current VCO is only accurate to 25 kHz, it is necessary to phase lock to reference oscillators at injection and flat top. The accuracy of the NCO will allow the removal of these oscillators, their phase lock loops, and timing. The beam phase lock error signal will be digitally added to the NCO frequency program rather than the analog input of the ΔF module.

3) If the NCO is sufficiently accurate, phase and radial position feedback will not be required. Removal of these loops avoids problems associated with changes in closed orbit, sensitivity of position measurements on bunch intensity and shape, and makes running with debunched beam during coalescing much easier. The non-repeatability of the bend field may require feed back to reliably cross transition, however, the ability to run without feedback during injection and at flat top during coalescing will make the LLRF system simpler. Derivative phase feedback will be used to damp coherent synchrotron oscillations.

4) The rf cavities are divided into A and B groups which are counter phased to produce very low accelerating voltages during coalescing. The system can be simplified by using 3 NCOs, one each for the A and B cavities and one which remains in synch with the beam phase. With all 3 NCOs in synch, the phase offset ports can be used for phase control including acceleration phase, A and B counter phasing, transition phase jump, phase damping and, phase locking to booster and Tevatron.

The new LLRF system is being implemented within an VXI environment allowing the use of commercial hardware such as controllers and DSP modules. The Fermilab controls group has a VXI clock decoder allowing access to the various accelerator events, and clocks. This architecture was chosen to allow for future improvements or changes as more powerful hardware becomes available.

WBS 1.1.13.7.2.3.**TEV - RF INSTALLATION AT F0**

The existing 8 TEV RF stations will be removed from the present tunnel and service building at the start of the shutdown in order for civil construction to start. The TEV RF equipment will extend into a 25' addition constructed before the shutdown across the front of the existing RF building. The existing F0 LCW pump room will remain unchanged. The main equipment gallery water manifolds will be reused by rotating and modifying the present drops with longer pipes to the RF equipment. The two main power substations (RF #1 and RF #2) that supply 3-phase, 480 VAC, will be reused to power the building and the TEV RF equipment. As much as possible of the utilities and RF cabling will be installed or made prior to the shutdown.

The cavities will be reinstalled in the reconstructed F0 tunnel section. Due to radiation shielding requirements in the service building, the 9.188" copper transmission lines will be extended as shown in Figure 3.4-6. This is twice the electrical length we presently have for operation of the stations in the Tevatron. Hatch arrangements allow for initial installation and any subsequent servicing of the lines. Figure 3.4-7 is an elevation view of the TEV F0 section showing RF cavities, transmission lines, and proton injection line underneath the RF cavities. RF cavity spacing is set up for orthogonal phasing between pbar stations (stations 1-4) and the proton stations (stations 5-8). This produces a simple low level fan out and fan back cabling scheme. MI Note-0082 clarifies the geometry at TEV F0.

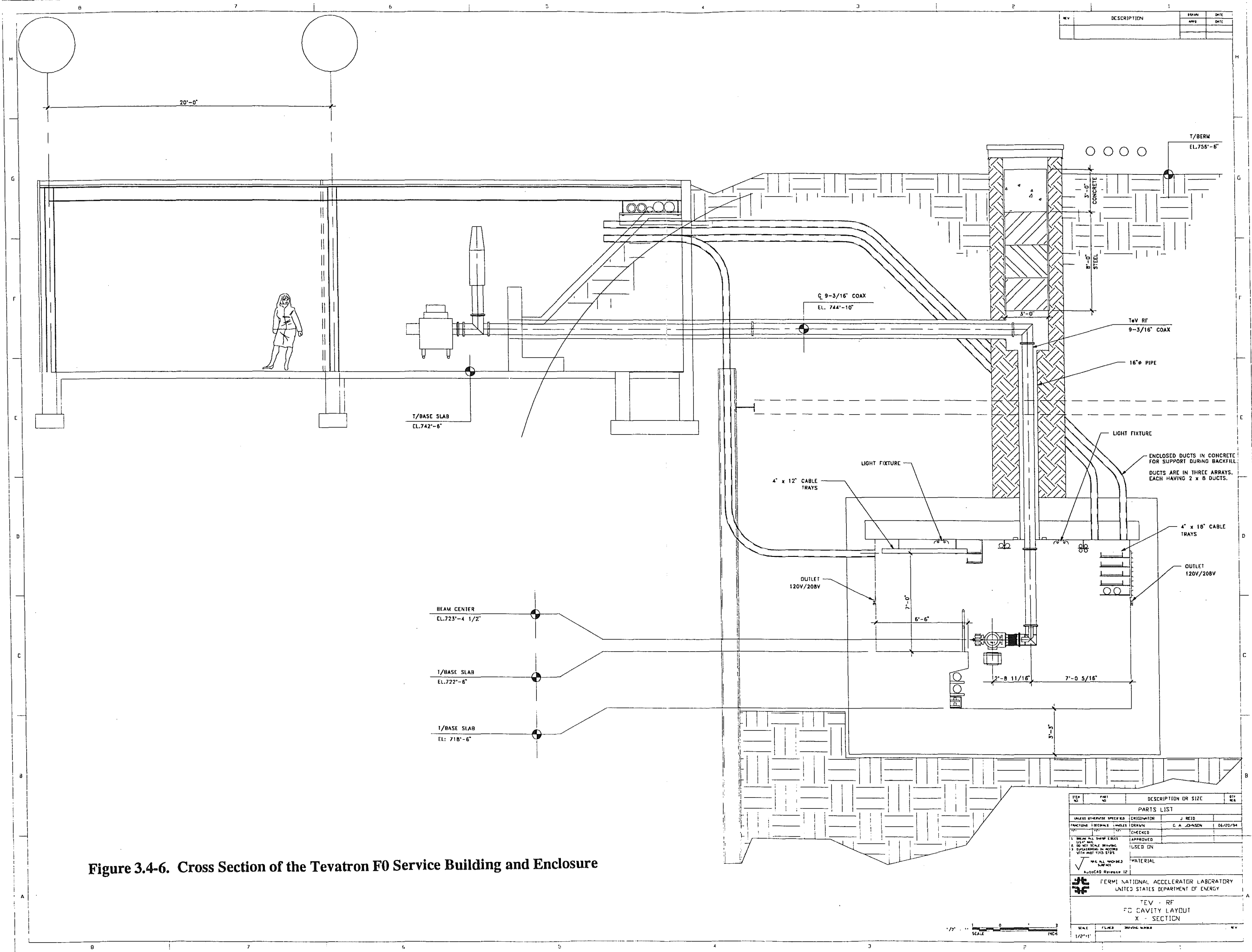
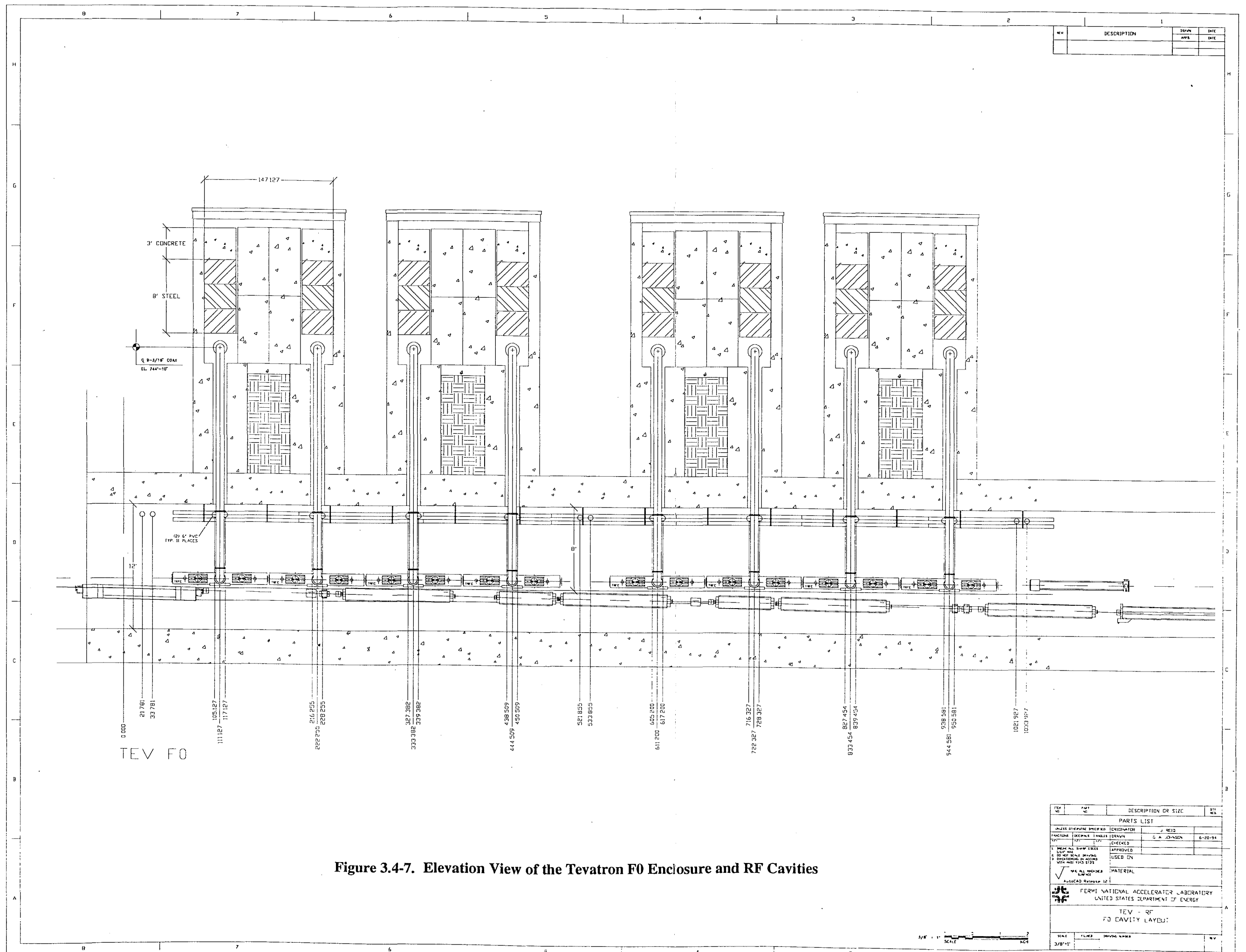


Figure 3.4-6. Cross Section of the Tevatron F0 Service Building and Enclosure



CHAPTER 3.5. KICKERS AND SLOW EXTRACTION

WBS 1.1.6.1.1

8 GEV PROTON INJECTION KICKER

Purpose:

This kicker functions to inject 6 batches of 8 GeV beam vertically into the FMI from the Booster. The trajectory of this beam must be bent 1.05 mr to place it onto the equilibrium orbit. Fast rise and fall times are required to insure that the circulating beam is not disturbed by the transition field at the beginning and end of the pulse. The anticipated operating modes of the Main Injector, i.e. for 120 GeV experimental programs and for Tevatron injection both for collider operation and for fixed target operation, together with concerns about transient beamloading, make the issues of rise and fall time of the injection kicker more complicated. Refer to Chapter 2.4 for a discussion of some of these issues.

Requirements:

Beam aperture	101.6 mm(H) x 50.8 mm(V)
Kick angle	1.05 mr vertical
$\int B \cdot dl$	0.309 kG-m
Field rise time (1% - 99%)	< 50 ns
Field fall time (99% - 5%)	< 150 ns
Field flattop	1.6 μ s
Field flatness ($\Delta B/B$)	$\pm 1\%$

Location:

Magnet	Q103 (upstream)
Power Supply	MI-10 Service Building

Magnet Parameters:

Peak current	1200 A
Field at peak current	0.136 kG
Impedance	25 Ω
Gap height	111.1 mm
Gap width	63.5 mm
Field rise time	22 ns
Number required	3

Power Supply:

Peak output voltage	30 kV
Peak output current	1200 A
Impedance	25 Ω

Power Supply (cont.):

Pulse length	1.6 μ s
Flatness	$\pm 1\%$
Repetition Rate	15 Hz
Number required	3

Design Approach:

Three separate power supplies will be required to drive the three magnets. The schematic is shown in Figure 3.5-1. The main switch tube will be a CX1671D, a 3-gap tube with a screen grid. This tube has been used successfully at SLAC, and has a voltage rating of 105 kV and a peak current rating of 3 kA. The absolute maximum ratings necessary to meet specifications are an output voltage of 33 kV and an output current of 1320 A; this corresponds to a maximum stress on the PFLs and thyatron of 66 kV. The screen grid will help prevent prefires as well as damage to the trigger circuitry. Each tube will be housed in a coaxial structure using 3M Fluorinert, FC-40, as a dielectric media for cooling and high voltage insulation. This configuration will reduce the system inductance and allow for a faster risetime compared to the existing proton injection kicker at MK90.

The magnets for this kicker will be ferrite loaded C-magnets impedance matched to form a 25 Ω transmission line. Modifications to the existing magnets will be necessary to meet the fast rise and fall time requirements. A cross section is shown in Figure 3.5-2.

The pulse length of the power supply is determined by the required flattop and the field rise time of the magnet itself. This 1.6 μ s pulse is generated by discharging the PFL (pulse forming line) through the thyatron into the magnet and attached resistive load. For this application, a modified, foil-wrapped version of RG-220 will be used. Each kicker magnet will require two ~500-foot lengths of cable. The 50 Ω cables will be connected to the thyatron at one end and the resonant charging supply at the other end to make a 25 Ω system with a 1.6 μ s effective pulse length.

Overall, the system will be an updated version of the present system currently used at MK90. In addition to the new coaxial housing for the switch tube, a resonant charging system will be added. This will further improve the rise time of the system by allowing operation of the tube at higher reservoir voltages without increasing the risk of prefires. The new foil-wrapped RG-220 will allow system operation at higher voltages. Frames for the new PFLs will be modeled after those used in the multibunch injection kicker system. Other aspects of the design not being used in the present MK90 system will be based on experience with the SLAC kicker and the multibunch injection kicker.

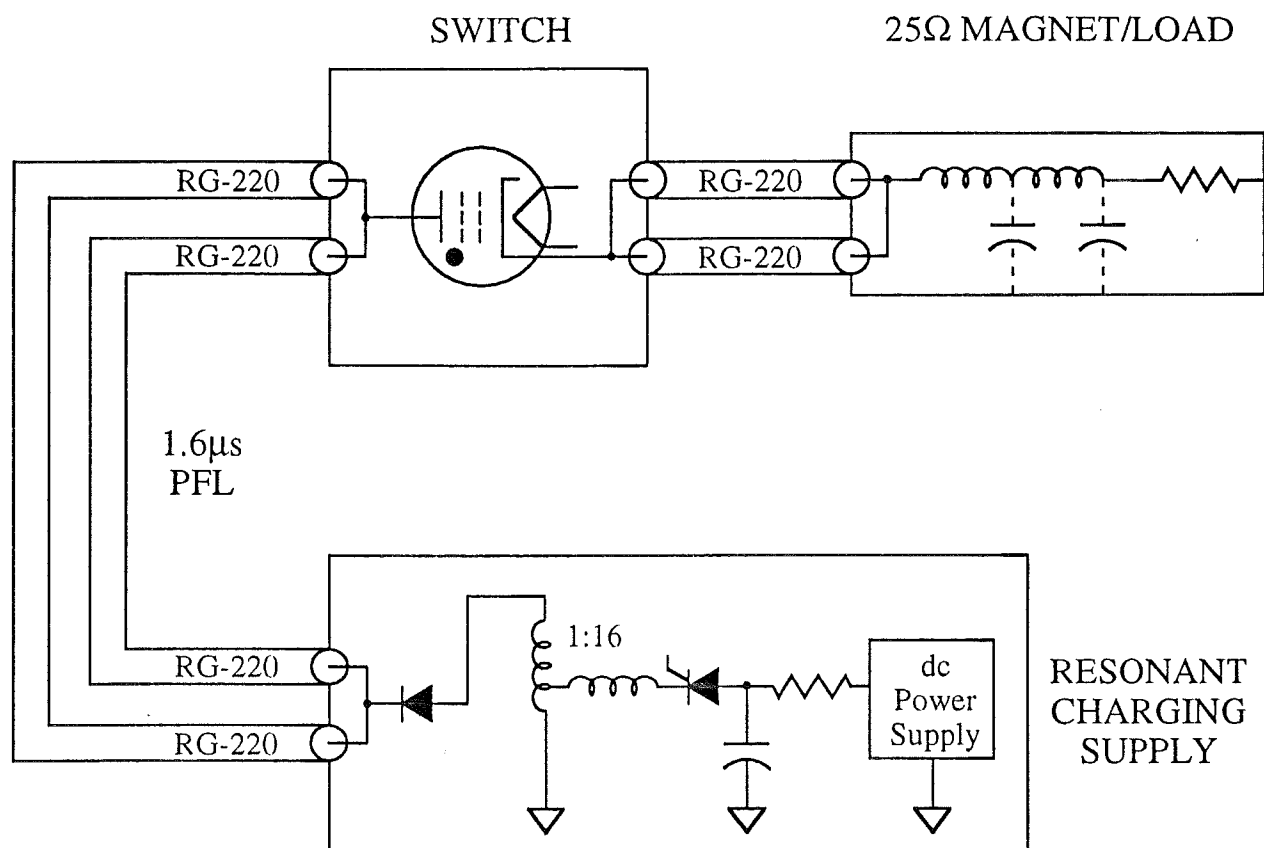


Figure 3.5-1
8 GEV Proton Injection Kicker Schematic

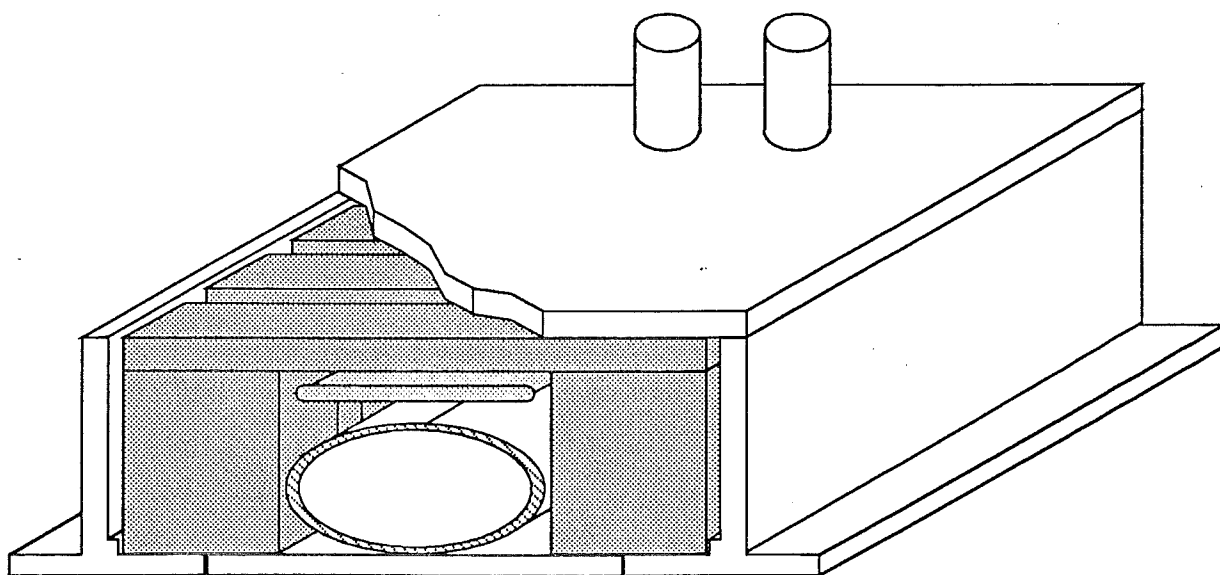


Figure 3.5-2
8 GEV Proton Injection Kicker Magnet Cross Section

WBS 1.1.6.1.2**P-BAR INJECTION/PROTON EXTRACTION KICKER**Purpose

This kicker functions for five different operating modes, any (and only) one of which might be required on a particular cycle. In Mixed Mode operation, 5 batches of Booster beam are injected tightly spaced with the sixth batch centered in the remaining gap. The sixth batch is extracted at 120 GeV using this kicker while the remaining 5 batches are extracted at 120 GeV using slow extraction techniques. In the Fixed Target mode, 6 batches of Booster beam are injected tightly spaced. They are all extracted at 150 GeV by this kicker. The Collider Mode requires 12 Booster cycles, each of which injects a group of eleven bunches. Consecutive groups are spaced at 21-bucket intervals; these are accelerated to 150 GeV, and then coalesced into 12 bunches and extracted by this kicker. The coalesced bunches span $11 \times 21 = 231$ buckets, or $4.4 \mu\text{s}$. The 8 GeV Extraction Mode is used to extract a single batch of Booster beam into the antiproton injection line for injection line tune-up. The 8 GeV Injection Mode simply kicks a single batch of antiprotons onto the FMI equilibrium orbit.

Requirements:

Beam aperture	85.7 mm (H) x 38.1 mm (V)
Field flatness ($\Delta B/B$)	$\pm 1\%$

Location:

Magnet	Q520 (downstream)
Power supply	MI-52 Service Building

Mode:		Mixed	Fixed Targ.	Collider	8 Gev Ext.	P-Bar Inj
Kick angle	[mr]	0.525 (H)	0.525 (H)	0.525 (H)	1.25 (H)	1.25 (H)
$\int B \cdot dl$	[kG-m]	2.10	2.625	2.625	0.37	0.37
Field rise	[μs]	<0.70	<1.48	<6.76	<9.6	NA
Field ftop	[μs]	1.6	9.8	>4.4	1.6	1.6
Field fall	[μs]	<0.70	NA	NA	NA	<9.6
Duty cycle	[s ⁻¹]	1/2.9	1/2.4	1/4	1/1	1/20

Magnet parameters:

	Nominal	Maximum
Peak current	2700 A	3000 A
Field at peak current	0.675 kG	0.742 kG
Impedance	10 Ω	
Gap height	50.8 mm	
Gap width	98 mm	
Magnetic length	1.95 m	
Physical length	2.24 m	
Field rise time	520 ns	
Number required	2	

Power supply:

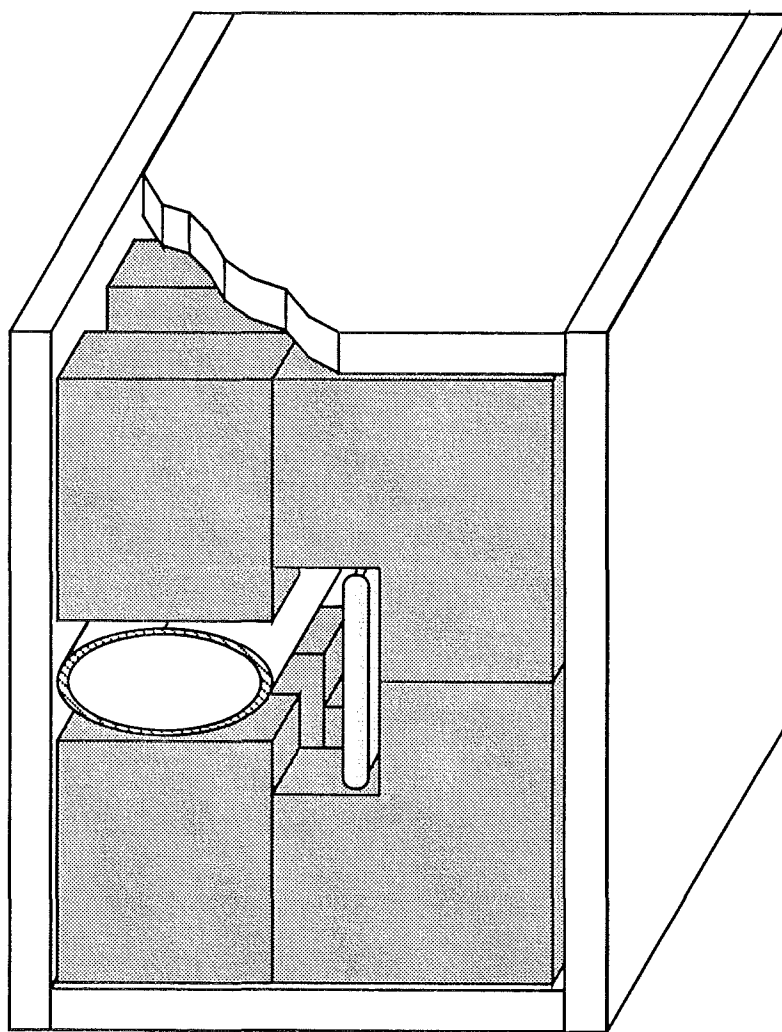
Impedance	5 Ω
Flatness	$\pm 1\%$
Number required	1

Design approach:

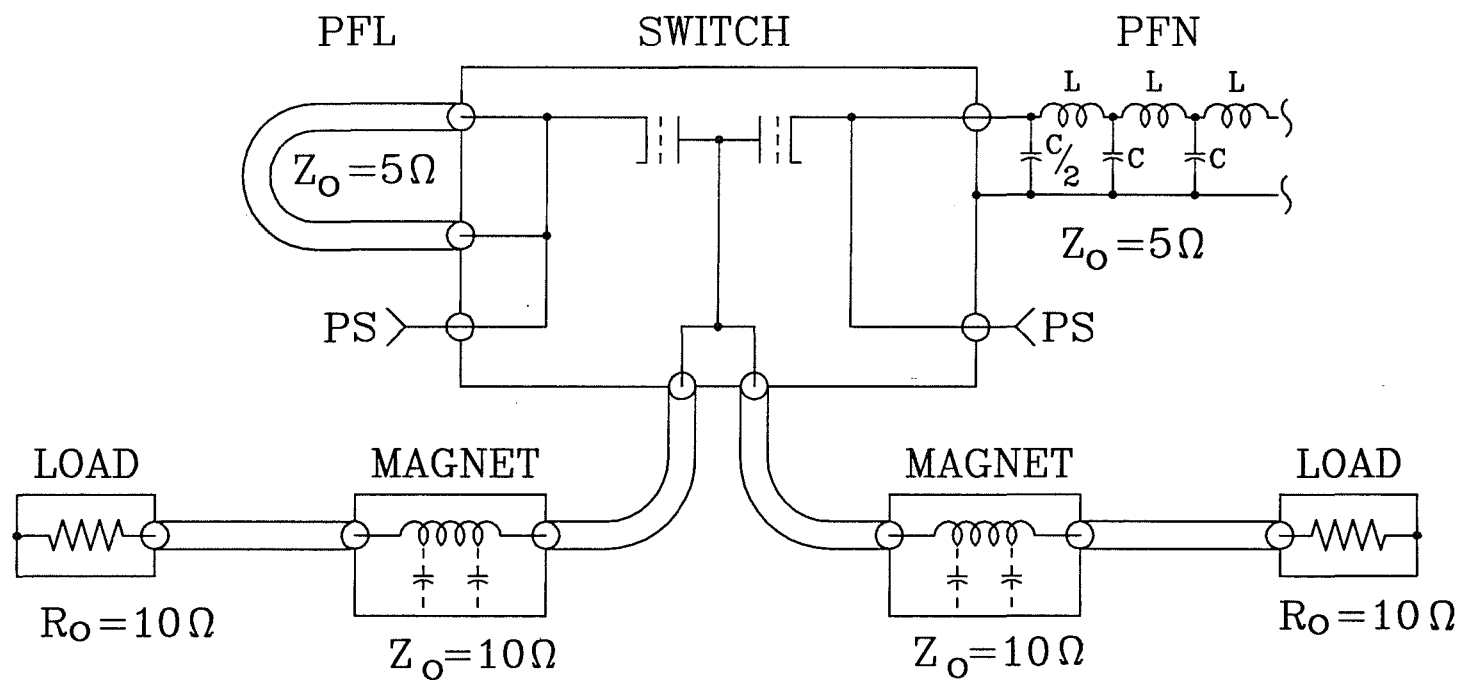
The magnets for this kicker will be ferrite loaded transmission line C-magnets, as shown in Figure 3.5-3. Each magnet will consist of 55 cells containing a ferrite pole piece and a 950 pF high voltage capacitor. The capacitors will be interleaved with the pole pieces. Cross coupling of the pole pieces will be used to minimize the inductance in the capacitor circuit. The termination resistors will become an integral part of the magnet.

Mode:		Mixed	Fixed Targ.	Collider	8 Gev Ext.	P-Bar Inj
Peak voltage	[kV]	21.8	27.0	27.0	3.85	3.85
Peak current	[kA]	4.36	5.4	5.4	0.77	0.77
Duty cycle	[s ⁻¹]	1/2.9	1/2.4	1/4	1/1	1/20
Pulse length	[μ s]	2.1	10.3	10.3	2.1	2.1

A single power supply drives two 10 Ω magnets in parallel. The power supply shown in Figure 3.5-4 consists of two separate pulsers tied to a common load. The thyatron switch tubes will be CX1592Ds which are a 3-gap hollow anode type. A screen grid is required to prevent prefires of the idle pulser when subjected to the full output voltage swing of the pulser. This tube is rated at 120 kV and has a peak current rating of 8 kA. Both switch tubes will be housed in a coaxial



P-Bar Injection / Proton Extraction Kicker
Figure 3.5 - 3



P-Bar Injection/Proton Extraction Kicker

Figure 3.5-4

structure. The dielectric fluid FC-40 will be circulated around the tubes for both cooling and insulating purposes.

The pulse length of the power supply is the sum of the magnet rise time and the required flattop. A 2.1 μs pulse is generated by discharging a pulse forming line (PFL) into the magnet load. This PFL consists of 10 - 720 ft. lengths of RG220 type cable made to Fermilab specifications. In similar fashion, a pulse forming network (PFN) is used to provide the 10.3 μs pulse. The ripple frequency period of the PFN is chosen to be equal to the field propagation time through the magnet to minimize its effect on $\int \mathbf{B} \cdot d\mathbf{l}$. This PFN is made up of 32 sections each consisting of a 33 nF capacitor and a nominal 1 μH inductor tapped at 20% to provide mutual coupling between cells. These inductors consist of 10 turns of .188 in copper tubing wound on a polycarbonate form the length of which may be readily changed to tune the inductor by $\pm 10\%$. The entire network can be contained in an aluminum housing 10 in x 15 in x 72 in. A mineral oil dielectric will be used for the PFN.

WBS CODE 1.1.6.1.4 150 GEV PBAR EXTRACTION KICKER

Purpose:

This kicker deflects a single pbar batch in a horizontal direction from the FMI equilibrium orbit at 150 GeV into the pbar extraction (A150) line.

Requirements:

Beam aperture	85.7 mm(H) x 38.1 mm(V)
Kick angle	0.525 mr horizontal
$\int B \cdot dl$	2.625 kG-m
Field rise time	<9.6 μ s
Field fall time	NA
Field flattop	1.6 μ s
Field flatness ($\Delta B/B$)	$\pm 1\%$

Location:

Magnet	Q622 (upstream)
Power Supply	MI-62 Service Building

Magnet Parameters (Nominal):

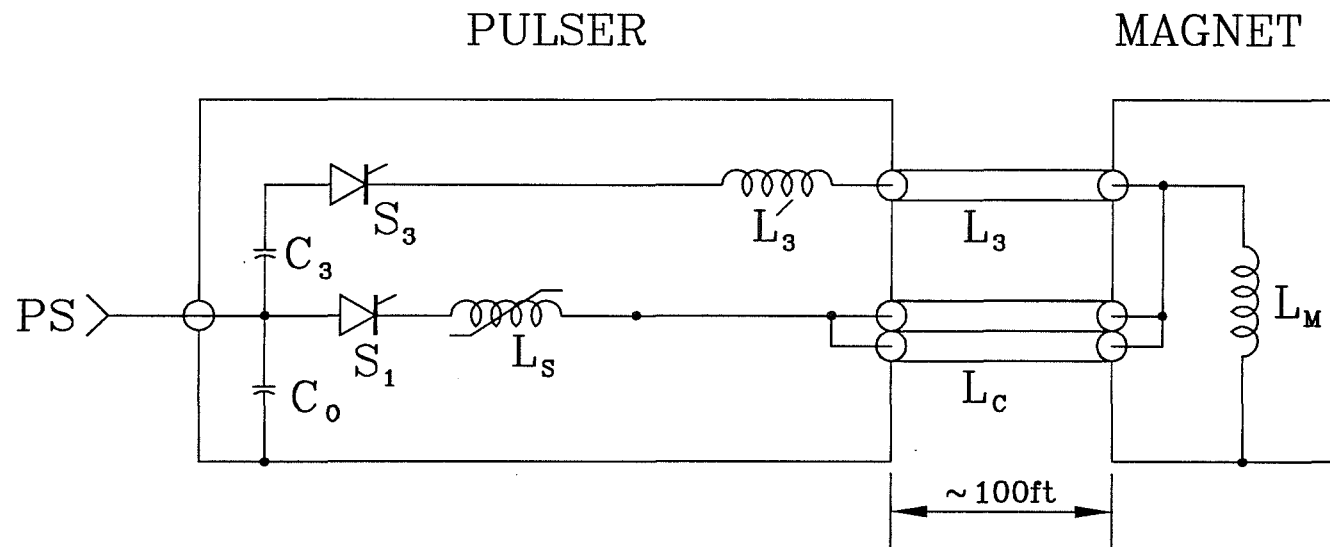
Peak current	2800A
Field at peak current	0.691kG
Inductance	5.05 μ H
Gap height	50.8 mm
Gap width	114.3 mm
Magnetic length	1.89 m
Physical length	2.20 m
Number required	2

Power Supply:

Peak output voltage	4750 V
Peak output current	5600 A
Current rise/fall time	9.6 μ s
Current flattop ($\pm 1\%$)	1.6 μ s
Number required	1

Design approach:

Two of the existing Main Ring abort kicker magnets will satisfy the requirements for this system. The power supply will be a half sine pulse with a small amount of third harmonic coupled in to flatten the peak of the fundamental as seen in Figure 3.5-5. The power supply will contain two pulse generator channels with a common dc power and timing source.



150 GEV P-Bar Extraction Kicker

Figure 3.5-5

WBS 1.1.6.1.5 PROTON ABORT KICKER

Purpose:

This kicker deflects the proton beam into a beam dump in the event of an anomaly in the FMI. This kicker is also operated after every extraction from the FMI to clean up any left residual beam. The kicker may operate any time there is beam in the FMI, however it is synchronized with a 700 ns gap in the circulating beam. The magnitude of the kicker field is proportional to the energy of the beam.

Requirements:

Beam aperture	85.7 mm(H) x 38.1 mm(V)	
Kick angle	@150GeV	0.50mr horizontal
	@8GeV	1.25mr horizontal
$\int B \cdot dl$	@150GeV	2.51 kG-m
	@8GeV	0.37 kG-m
Field rise time	(10-70%)	700 ns
	(10-90%)	1 μ s
Field fall time	NA	
Field flattop	>9.8 μ s	
Field flatness ($\Delta B/B$)	$\pm 10\%$	

Location:

Magnet	Q400 (downstream)
Power Supply	MI-40 Service Building

Magnet Parameters (Existing Main Ring Abort):

Peak current	2.7 kA
Field at peak current	0.66 kG
Magnetic length	1.89 m
Physical length	2.20 m
Gap height	50.8 mm
Gap width	108 mm
Beam Aperture (V)	35 mm
Beam Aperture (H)	82 mm
Inductance	5.05 μ H
Lamination Thickness	50 μ m
Number required	2

Power Supply:

Nominal output voltage	34 kV
Nominal output current	2.7 kA
Impedance	12.5 Ω
Pulse length	10 μ s
Flatness	± 10 %
Repetition Rate	1/1.5 s
Number required	2

Design Approach:

The abort system used at Fermilab in the Main Ring and the Tevatron is a resonant LC supply. A capacitor is discharged through the inductance of the abort magnet and cable. When the energy is transferred from the capacitor to the magnet and cable inductance, the current is allowed to free wheel by the use of an anti-parallel diode across this inductance. The result is a quarter sine rise and a long linear tail. This cable must be terminated with a series RC circuit in parallel with the magnet. A current ripple with a period equal to the round trip cable time would appear otherwise. The problem with this approach for MI is the long cable length between the power supply and the magnet. While the added inductance increases the capacitor voltage, this is not the limiting factor. Because the required rise time and the cable transit time are approximately the same, the magnet will be driven by the cable impedance during the rise time. However, during the flat top, the magnet will be driven by the impedance determined by the resonant capacitor and the cable and magnet inductance. The result is either a "rise time" or a "flat top" that exceeds specifications unless these two impedances are the same. The resonant LC approach thus shows the way to the alternative design.

A pulse forming network, a pulse transformer and a thyatron switch operating at modest voltage and current has been designed that will meet the design objectives, and can be done with the existing Main Ring abort magnets. With a pulse forming network modulator, a series resistive termination at the magnet is required. In addition, a RC cable termination is used at the modulator output to damp cable ringing. The pulse forming network will consist of identical LC sections. The high side of the primary of the pulse transformer is connected to the PFN and the low side of the primary to the thyatron, which has a grounded cathode (see Figure 3.5-6). The output is isolated resulting in lower ground currents, and the transformer reduces the operating voltage allowing operation in air instead of oil. The cable is four runs of improved RG/220 from Times Microwave. PFN, thyatron and pulse transformer nominal requirements are listed in Table 3.5-1.

Operation at 10% higher levels is possible indefinitely, and at 20% higher levels with reduced lifetime or reliability. A 10% increase in operating voltage for pulse capacitors reduces

lifetime by a factor of two. The prefire rate is also a strong function of voltage. Therefore the design stress for the capacitors is 37 kV (110%) with a design lifetime of 10^8 pulses; the design voltage for the thyatron is also 37 kV.

The PFN is built with Maxwell pulse discharge capacitors and Fermilab designed inductors. A standard charging power supply is available from three manufacturers, ALE, Converter Power and Maxwell.

The thyatron switch will be a Litton L4988 or an EEV CX1575C hydrogen thyatron. The design tube is currently the L4988. Should problems develop with this tube, the alternative could be substituted. This requires only a mechanical rework of the tube connections.

The pulse transformer is a 1:2 step up and will be potted with a silicone material. The DC voltage between primary and secondary suggests the use of a solid dielectric. An electrostatic shield may be required in the pulse transformer to meet lifetime requirements. The prototype design, from Stangenes Industries, does not have this shield.

Table 3.5-1: Main Injector Abort Kicker Power Supply Parameters

<u>PFN</u>			
Capacitance	0.14 μ F	Capacitor Voltage	37 kV
Inductance	1.4 μ H	Inductor Current	5.4 kA
Impedance	3.125 Ω	Number of Sections	14
Pulse Length	10 μ s	Rise Time	1 μ s
<u>Pulse Transformer</u>			
Primary Volt-seconds	0.21 V s	Leakage Inductance	1.4 μ H
Primary Current	5.4 kA	Primary Voltage	17 kV
Secondary Current	2.7 kA	Secondary Voltage	34 kV
<u>Thyatron</u>			
Hold Off Voltage	37 kV	Number of Gaps	2
Peak Current	5.4 kA	A-s per pulse	0.07 A-s

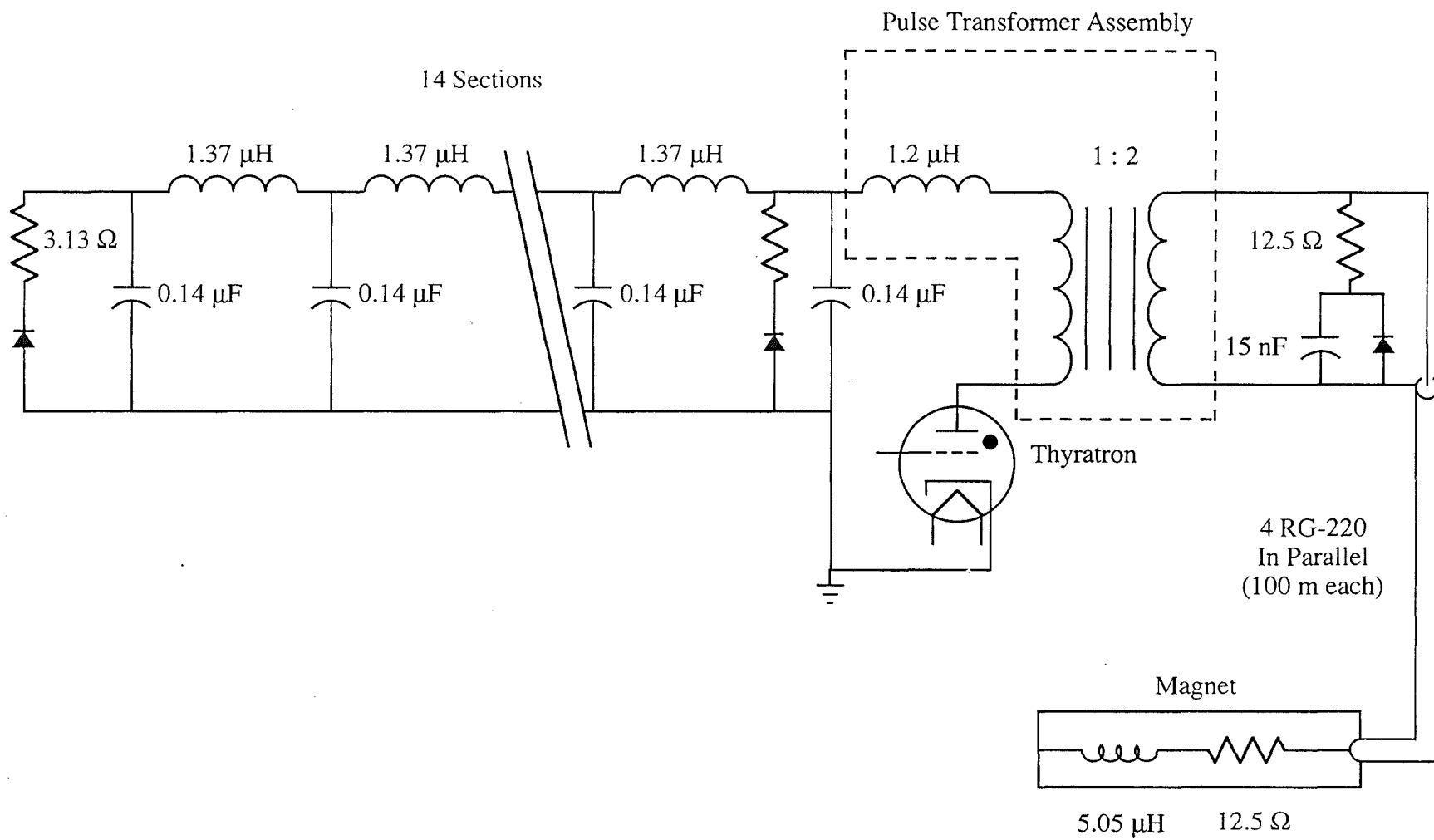


Figure 3.5-6. Proton Abort Kicker Schematic

The existing magnets were made with tape wound steel cores and are currently operating at ~ 8 kA. They will be modified to include a series resistance equal to the modulator output impedance. The new termination will also include an updated cable connection scheme using plugable connectors from Isolation Design.

The enclosure for the kicker will be a sealed and dust tight, semi-custom EMI/RFI shielded rack. The EMI/RFI shielding normally provided by the oil enclosure is necessary to allow reliable operation of low level logic in nearby racks. Controls and monitoring electronics will be compatible with other MI kickers as much as is reasonably possible.

WBS 1.1.6.3.1.**TEV PROTON INJECTION KICKER****Purpose**

This kicker will operate in two modes, each requiring .381 mr of kick to place the injected beam onto the Tevatron closed orbit. The Collider mode requires rise and fall times of 2.6 μ s with a flattop of 4.4 μ s to accommodate 12 coalesced bunches spaced by 21 buckets. The Fixed Target mode has a much more stringent rise and fall time requirement of < 800 ns each, with a flattop of 9.6 μ s. In this mode, two MI cycles of six batches each are required to load 12 batches into the Tevatron.

Requirements:

Beam aperture	85.7 mm (H) x 38.1 mm (V)
Kick angle	.381 mr
$\int B \cdot dl$	1.906 kG-m
Field rise time	< 800 ns
Field fall time	< 800 ns
Field flattop	4.4 or 9.8 μ s
Field flatness ($\Delta B/B$)	$\pm 1\%$

Location:

Magnet	TEV F17 Medium Straight Section
Power supply	F17 Kicker Buidling

Magnet parameters:

Peak current	1.93 kA
Field at peak current	.477 kG
Impedance	12.5 Ω
Gap height	50.8 mm
Gap width	108 mm
Magnetic length	2 m
Field rise time	< 550 ns
Number required	2

Power supply:

Peak output voltage	50 kV
Peak output current	4 kA
Impedance	6.25 Ω
Pulse length	10.35 μ s
Flatness	$\pm 1\%$
Repetition rate	1/2.4 s
Number required	1

Design approach:

Measurements on the present E17 kicker magnet indicate that its rise and fall times are far too long for the Fixed Target mode. The ferrite cores and perhaps the beam tube can be recycled into an upgraded design similar to the MI Pbar Injection/Proton Extraction magnet. The existing power supply would be moved to a new service building at F17. The present interlock and control hardware would be upgraded at this time.

WBS 1.1.6.3.2.**TEV PBAR INJECTION KICKER**Purpose

Four coalesced bunches spaced at 21 buckets (total of 1.6 μ s) will be injected horizontally into the Tevatron from the MI. A horizontal kick of 0.35 mr is required to place the beam on the proper horizontal trajectory. Fast rise and fall times are required to insure that the circulating beam is not disturbed by the transition field at the beginning and end of the pulse.

Requirements:

Beam aperture	85.7 mm (H) x 38.1 mm (V)
Kick angle	0.35 mr
$\int B dl$	1.75 kG-m
Field rise time	< 395 ns
Field fall time	< 395 ns
Field flattop	1.6 μ s
Field flatness ($\Delta B/B$)	$\pm 1\%$

Location:

Magnet	TEV E48 Short Straight Section
Power supply	F0 Service Building

Magnet parameters:

Peak current	3.3 kA
Field at peak current	0.724 kG
Impedance	6.25 Ω
Gap height	57.2 mm
Gap width	79.4 mm
Magnetic length	2.41 m
Field rise time	336 ns
Number required	1

Power supply:

Peak output current	3.3 kA
Peak output voltage	20.6 kV
Impedance	6.25 Ω
Pulse length	2.0 μ s
Flatness	$\pm 1\%$
Repetition rate	1/4 sec
Number required	1

Design approach

The existing two D48 kickers will be moved to E48. Since this is a new system, no upgrades are required.

WBS 1.1.6.2

MAIN INJECTOR SLOW EXTRACTION

The physics of the slow extraction process is described in Chapter 2.7. In this section we discuss the hardware required to implement resonant extraction. The future experimental program at Fermilab will likely require both fast (1 ms) and slow (1 s) spill on different Main Injector ramp cycles. It is also quite likely that the beam associated with the two modes will be extracted at different straight sections, so we indicate which devices can accommodate both modes, and which require duplication. For the purposes of this discussion, we will assume slow spill takes place from the MI-52 straight section and fast spill takes place from the MI-60 straight section.

Slow extraction parameters:

Number of bunches	498
N per bunch	6×10^{10}
Bunch spacing	18.83 ns or 5.66 m
Bunch sigma	5.0 ns
Repetition rate	1.8 - 2.9 s
Slow spill duration	0.001 - 1.0 s
Extracted N per bunch/turn	$10^4 < N < 6 \times 10^8$

Slow Extraction Elements

53rd Harmonic Quadrupoles

Sixteen quadrupoles in two families (sine and cosine) are formed from individually powered correction quadrupoles recycled from the Main Ring. These quadrupoles will be required to correct for lattice errors (see Chapters 2.3 and 2.7) prior to being used to control the half-integer stopband. Applications programs will provide the appropriate sine/cosine control of the sixteen elements listed below. The same elements are used for fast and slow spill; the currents in the two families determine the phase space orientation at each set of electrostatic septa, and hence the location at which extraction occurs. The current waveform will be programmed through console applications programs to provide the appropriate ramps for fast or slow spill. The location of these quadrupoles relative to the main quadrupoles is shown in figures in Chapter 3.10.

MI-10:	Q628,Q630,Q632,Q634
MI-20:	Q206,Q208,Q210,Q212
MI-40:	Q328,Q330,Q332,Q334
MI-50:	Q506,Q508,Q510,Q512

0th-Harmonic Octupoles

Correction octupole magnets, recycled from the Main Ring, are placed at 54 locations adjacent to focusing sextupoles, and powered in groups of one to four elements, as listed below. The same elements are used for both slow and fast resonant extraction. The location of the octupoles relative to the main quadrupoles is shown in figures in Chapter 3.10.

MI-10:	Q626,Q628,Q630 Q632,Q634,Q636 Q108,Q110,Q112	MI-40:	Q326,Q328,Q330 Q332,Q334,Q336 Q408,Q410,Q412
MI-20:	Q114,Q116,Q118 Q120,Q122,Q124 Q126,Q128,Q130,Q202 Q204,Q206,Q208 Q210,Q212,Q214	MI-50:	Q414,Q416,Q418 Q420,Q422,Q424 Q426,Q428,Q430,Q502 Q504,Q506,Q508 Q510,Q512,Q514
MI-30:	Q228 Q314	MI-60:	Q528 Q614

Electrostatic Septa

Three 10-foot long (3.048 m) electrostatic septa located between quads Q520 and Q521 provide the kick which places the extracted beam across the Lambertson magnetic septum. These devices are patterned after the existing Tevatron electrostatic septa; Figure 3.5-7 shows a cross-section of the septum magnet. An additional set of three modules will be required for fast spill at MI-60. The rf cavities occupy much of the straight section, and therefore the septa will be placed in the vicinity of Q602, approximately 270° in betatron phase upstream of the Lambertsons.

Lambertson Magnets and C-magnet

The Lambertson and C-magnets, while used for slow spill, are also required for transfers to the pbar production target and to the Tevatron. They are discussed in Chapters 2.4 and 3.1. For fast spill at the MI-60 straight section, an identical configuration of three Lambertsons and one C-magnet would be required at Q608.

Spill Regulation Elements

The spill regulation for extraction system can be divided functionally into two bandwidths.

1. A low bandwidth (dc to ~10 Hz) system, commonly called QXR, or quadrupole extraction regulation system, consists of two air-core quadrupoles, which may be configured either as a 0th-harmonic or as a 53rd-harmonic. Further analysis is being done to determine which mode

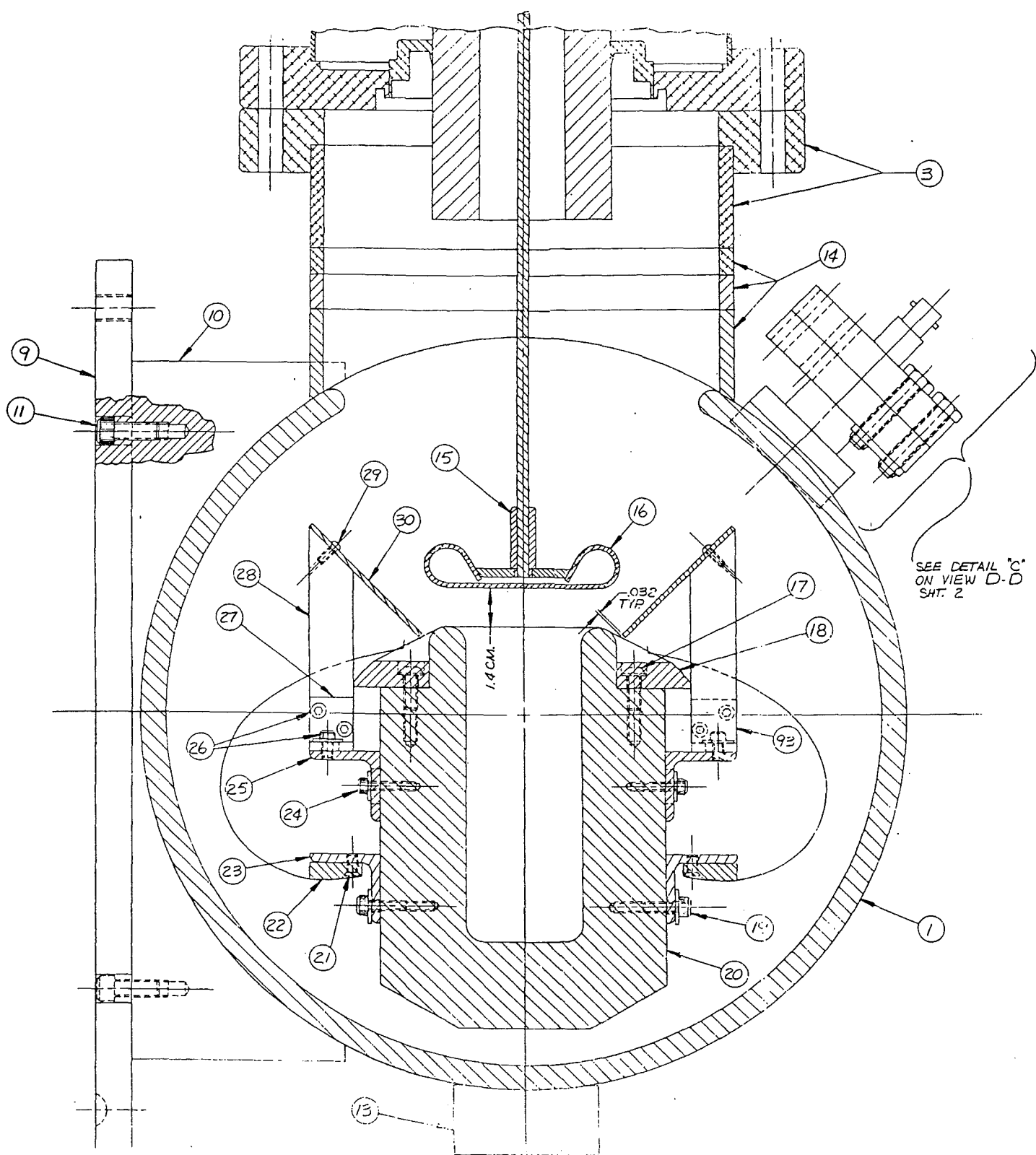


Figure 3.5-7. Cross Section of Tevatron Electrostatic Septum

is preferred. QXR is used to control the rate at which the beam is extracted. The system is regulated with feed-forward by monitoring the circulating beam intensity during slow extraction. On each machine cycle, the spill rate is sampled at 720 Hz, and compared to the desired spill rate. The error is saved, smoothed and time-shifted, and the current waveform for the next cycle is modified based on an average over many previous cycles. Figures 3.5-8(a) shows the spill rate that results from simply a linear ramp of the 53rd-harmonic quadrupoles; Figure 3.5-8(b) shows the spill rate when the current waveform is modified with feed-forward from five spill-cycles to produce a more uniform spill rate.

2. A higher bandwidth (0.1 Hz to 3 kHz) system consists of two air-core, 0th-harmonic quadrupoles powered in series, mounted on ceramic beam pipe. These are commonly referred to as Buckers. By sampling the extracted beam intensity at 5760 Hz and through feed-forward to the buckers, higher-frequency repetitive spill modulation is removed. Realtime feedback is also applied, limited in bandwidth to a few hundred Hz due to the time delay between a change in quadrupole current and the the beam response. Figures 3.5-9(a) shows the spill rate that results from 100 ppm ripple at 360 Hz in the main quadrupole bus, corresponding to tune modulation of $\Delta\nu \sim \pm 0.003$. Figure 3.5-9(b) shows the spill rate when the buckers are used with feedback and with feed-forward from five spill-cycles to produce a more uniform spill rate. Ripple in the main quadrupole bus could also be compensated by feeding back directly into the Bucker system.

The 12-year old Tevatron extraction regulation systems are presently being redesigned to bring them up to currently available technology. Much of this effort, especially in the area of software and controls, can be carried over directly to the Main Injector QXR system.

Magnet Power Supply Remote Control

Trim quadrupoles and octupoles ramping profiles will be downloaded to the local power supply controller (453 card) via the accelerator control system. The magnets are ramped by trigger events related to accelerator cycles. The power supply output current profile can be read back through an MADC channel.

The QXR and buckers will be ramped by the slow spill controls through a dedicated link and power supply controller, active during flattop and slow spill. A high D/A resolution (20 bits) will be used to drive the power supply controllers of these magnets.

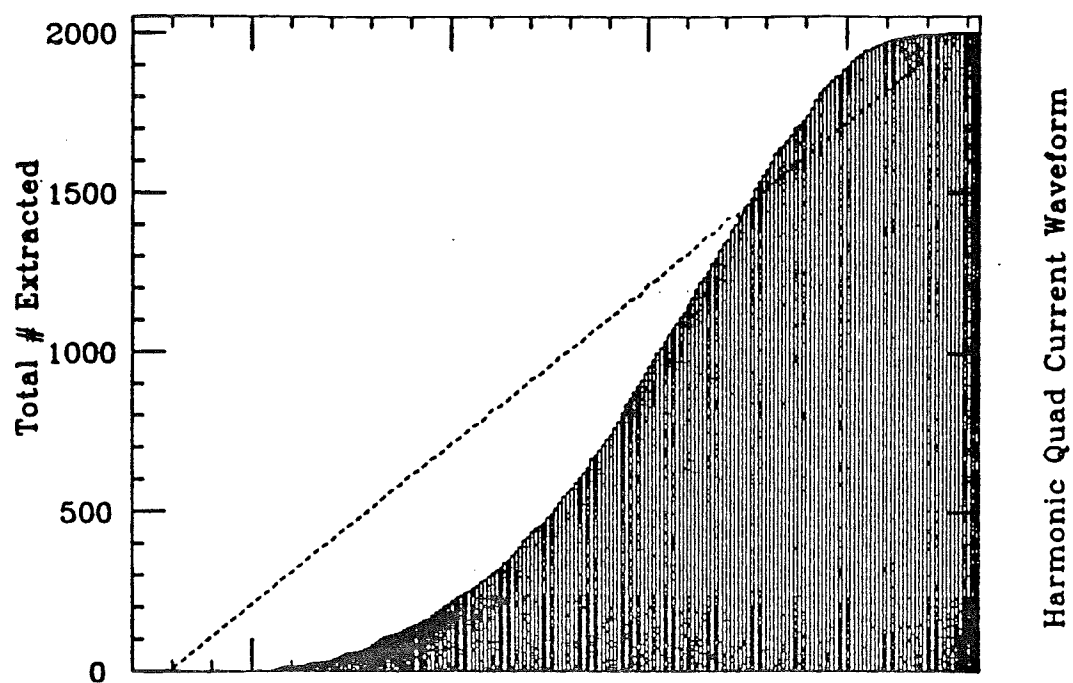


Figure 3.5-8(a). Spill Rate with Linear 53rd-Harmonic Quadrupole Ramp

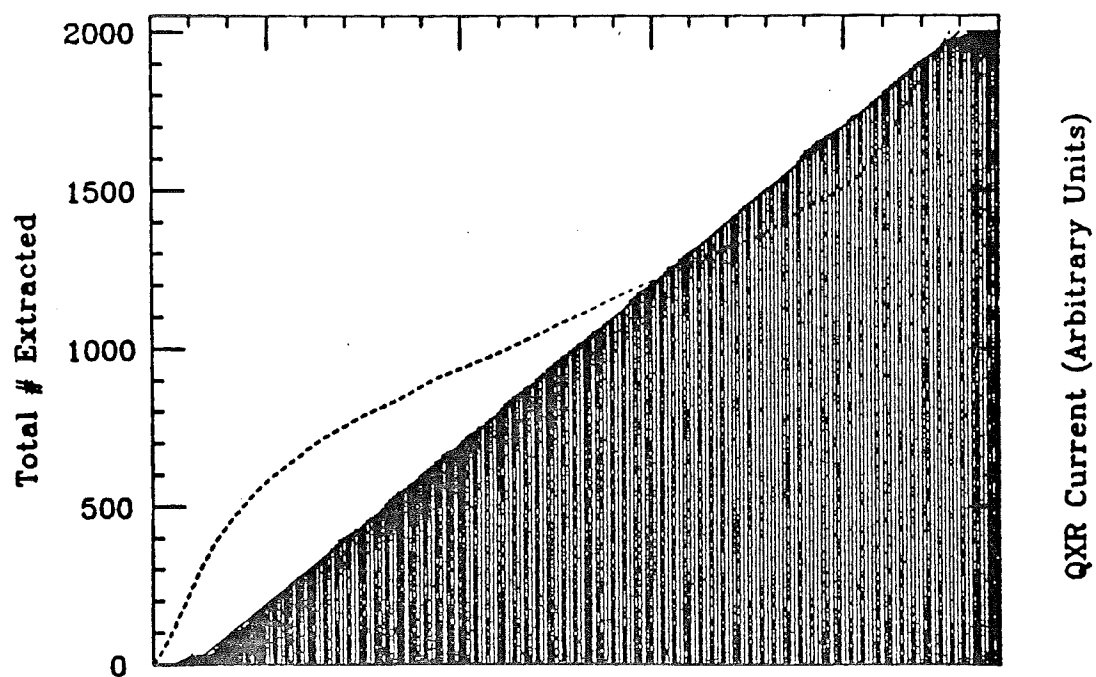


Figure 3.5-8(b). Spill Rate After Feed-Forward for 53rd-Harmonic QXR

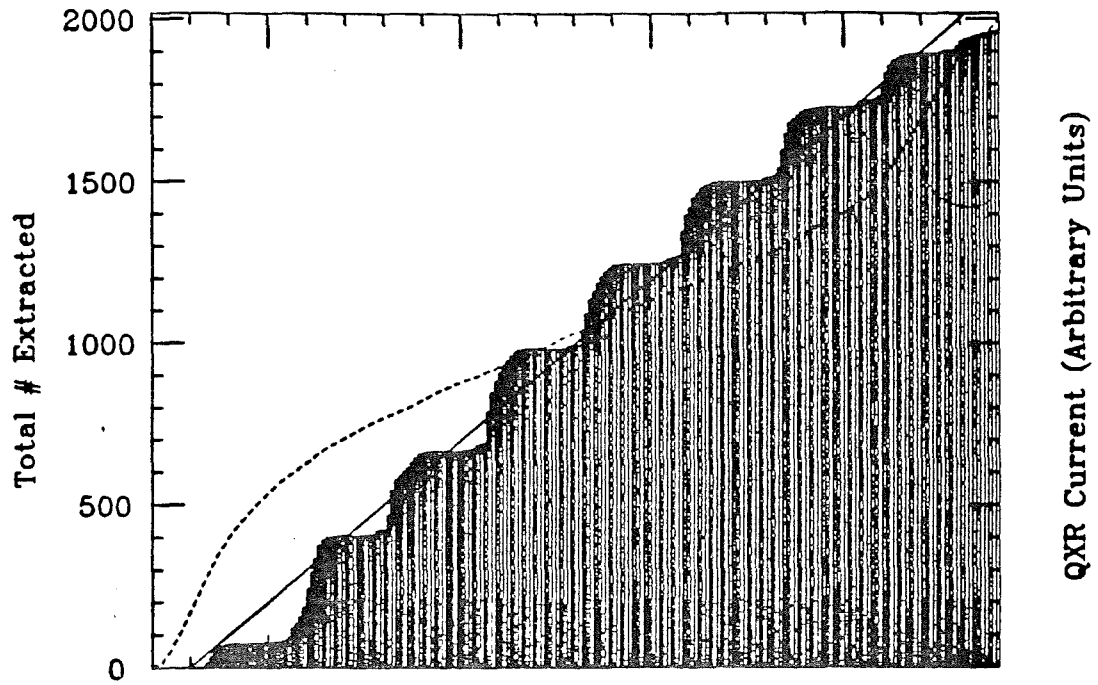


Figure 3.5-9(a). Spill Rate with Ripple on Main Quadrupole Bus

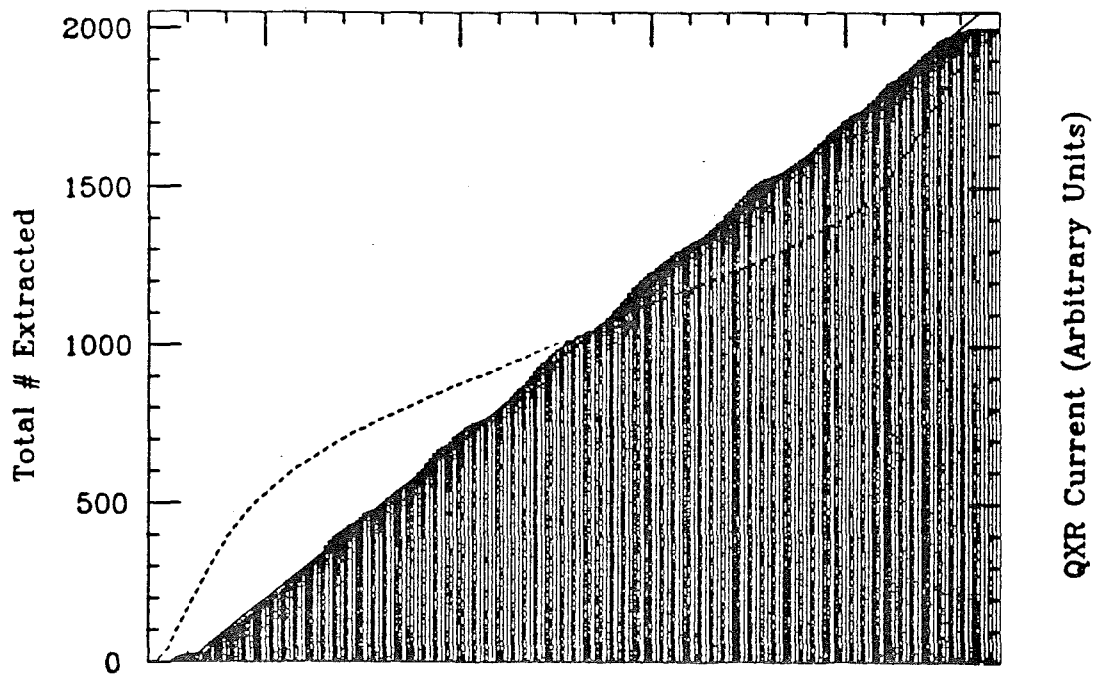


Figure 3.5-9(b). Spill Rate with Ripple on Main Quadrupole Bus
Using Buckers with Feedback and Feed-Forward

Beam Monitoring and Resolution

Slow spill regulation requires monitoring the circulating beam current in the FMI during extraction and the extracted beam current in the 120 GeV beam line.

The beam current before extraction is measured using a DCCT (Chapter 3.6) and used for feed-forward regulation of QXR. Extracted beam will be monitored in the 120 GeV line using rf spill monitors whose signal will be used by the bucker regulator. A spill beam intensity between $0.08 \mu\text{A}$ and $4.2 \mu\text{A}$ has to be detected with a resonant detector with a center frequency of 53 MHz, a Q of 140 and 100 kHz bandwidth. Such a cavity would have a resistance of $10.0 \text{ k}\Omega$, providing a 0.8 mV to 42 mV output for the $0.08 \mu\text{A}$ to $4.2 \mu\text{A}$ input.

The voltage at the input of the A/D converter is usually ± 5.0 volts, therefore a gain of 81.0 dB would be required to amplify the lowest of the intensity signals. A controller selectable attenuator will be needed to reduce the amplitude obtained during higher intensity extractions. QXR slow loop has operated at 720 Hz historically, today that could easily be made 1440 Hz without putting a large demand on memory on the system and not limited by bus cycle timing. Bucker loop was operated at 5760 Hz, which could be used. This requires further investigation. A/D of 18 bits can be used to sample beam intensity as well as extracted beam. This conversion resolution would provide a 110 dB dynamic range for both type of signals.

CHAPTER 3.6 INSTRUMENTATION

WBS 1.1.8. INSTRUMENTATION

WBS 1.1.8.1. MAIN INJECTOR RING INSTRUMENTATION

The Main Injector will use as much of the existing Main Ring diagnostics as possible. Reference 1 and 2 document the required instrumentation and tabulate the hardware available from Main Ring, summarized in Table 3.6.1. This paper presents details and specifications at the level known to date and is intended to be updated when appropriate. Specifications and References for existing equipment are provided where available.

Four of the tasks comprise about 70% of the instrumentation cost. They are the Ring BPMs, dampers, resonant position detectors for slow spill, and beam profile monitors. The others are simply moving modifying or duplicating existing Main Ring equipment.

Two items listed but not discussed are the Schottky detectors, which are currently being developed for the Main Ring, and the pinger. The pinger is currently residing in Main Ring. It is a few turn air core magnet on a ceramic beam tube driven by discharging capacitors with a few μ sec time constant through an SCR switch.

WBS 1.1.8.1.1. RING BPM SYSTEM

Detector

To conserve tunnel space, maintain the beam pipe shape, and reduce beam impedance, new detectors are being designed that fit inside the downstream end of every quadrupole, Figure 3.6-1. The 208 detectors will provide about 4 detectors per betatron wavelength in both the horizontal and vertical planes.

The four plates will be combined in the tunnel in pairs to measure either horizontal or vertical position at each quad. Measuring both planes improves the rms closed orbit distortion correction by only 10%, Reference 3. At twenty positions near beam transfer points, however, both planes will be measured. Five of these locations are adjacent to Lambertson magnets and require large aperture detectors mounted external to the quadrupole, Table 3.6-2. Current Booster BPMs have four 6" long plates, a 4.625" aperture, provide 0.52 db/mm, and will fit in the available space. For the 203 ring detectors and 5 large aperture detectors 228 rf modules will be required.

Table 3.6.1.

List of available and required instrumentation for the Main Injector.

Type/Location	Ring	Beamline	Available	Required
Position Monitors				
rf modules	228	121	260	89
Systems	19	11	26	4
New MI ring BPMs	203			203
Existing MR BPMs		104	216	
Large Aperture	5	17		22
Resonant detectors		11		11
Loss Monitors				
Ion Chambers	231	128	252	107
Integrating chassis	20	11	26	5
Intensity Monitors				
Resistive Wall	2		2	
Toroid		8	6	2
DCCT	1		1	
Spill Monitor		1	1	
Profile Monitors				
Flying Wire	3		3	
Multiwire	6	15	19	2
Ionization	2		3	
Dampers				
Hor and Ver	2			2
Scrapers				
Hor and Ver		2	4	
Schottky Detectors				
Hor and Ver	2		2	
Pinger				
Hor and Ver	1		1	

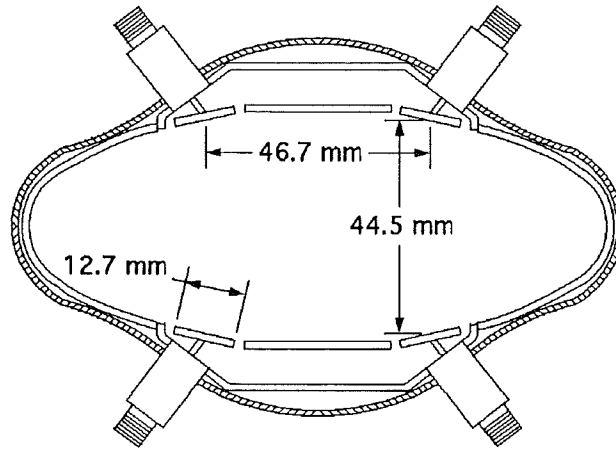


Figure 3.6-1.

Cross section of Main Injector BPM prototype II inside the quadrupole beam pipe.

Table 3.6-2.

Locations for wide aperture and dual plane detectors.

Location	type
Q101, 402, 522, 608, 620	wide aperture
Q101, 102, 103, 104	dual plane
Q400, 401, 402, 403	dual plane
Q520, 521, 522, 523	dual plane
Q606, 607, 608, 609	dual plane
Q619, 620, 621, 622	dual plane

The striplines in the Main Injector BPMs are connected to ground at one end to make them non-directional. The rf module input impedance is matched to 50 Ω only within a 5 MHz bandwidth centered at 53 MHz. To avoid resonances in the 150 to 1150 foot cables between the

detector and rf module, a diplexer circuit which terminates the detector output at other frequencies will be included in the plate combiner box located near the BPM.

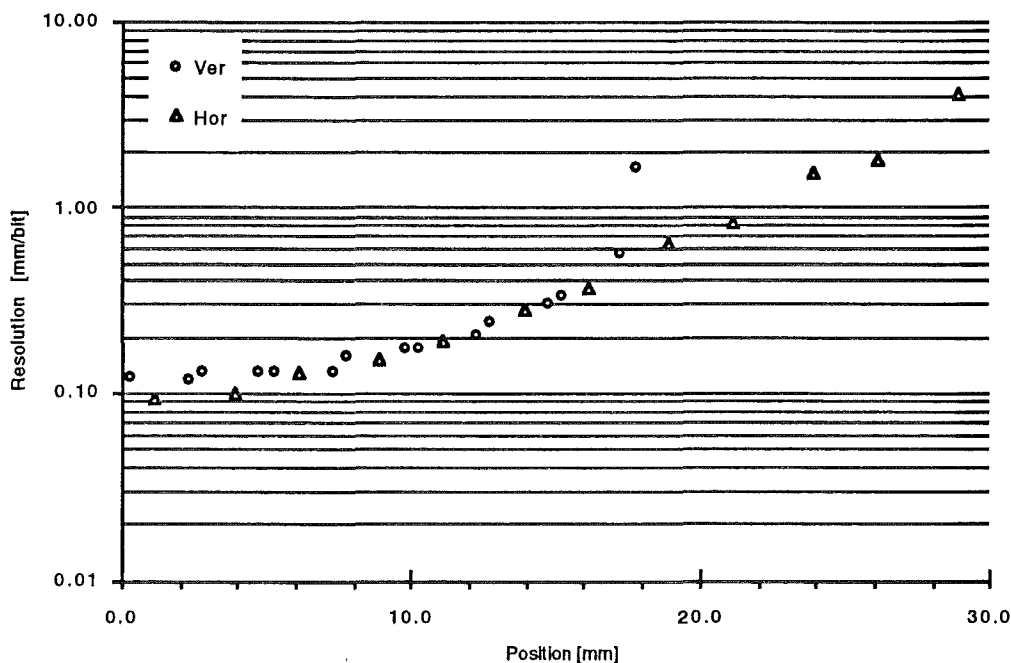


Figure 3.6-2. Resolution of the prototype Main Injector BPM using existing 8 bit Main Ring electronics.

The resolution, limited by the non linearity of the AM to PM detection and the 8 bit ADC used in the current Main Ring electronics, is shown in Figure 3.6-2. The measured position, corrected for rf module linearity, is shown in Figure 3.6-3 for wire positions spaced on a 5 mm grid. Measurements performed on a prototype detector are presented in Reference 4.

As tabulated in Table 3.6-3, the plate width and length of the BPM was selected for best linearity and match to Main Ring rf module. Both the Main Ring and Main Injector BPMs provide about 0.7 db/mm for the ratio of A to B. The plate length was also selected to be an odd multiple of $\lambda/4$ at 2 GHz. The SMA ceramic feedthroughs being considered for the detector have a low impedance resonance at this frequency.

Linearize on x,y = ± 5 mm

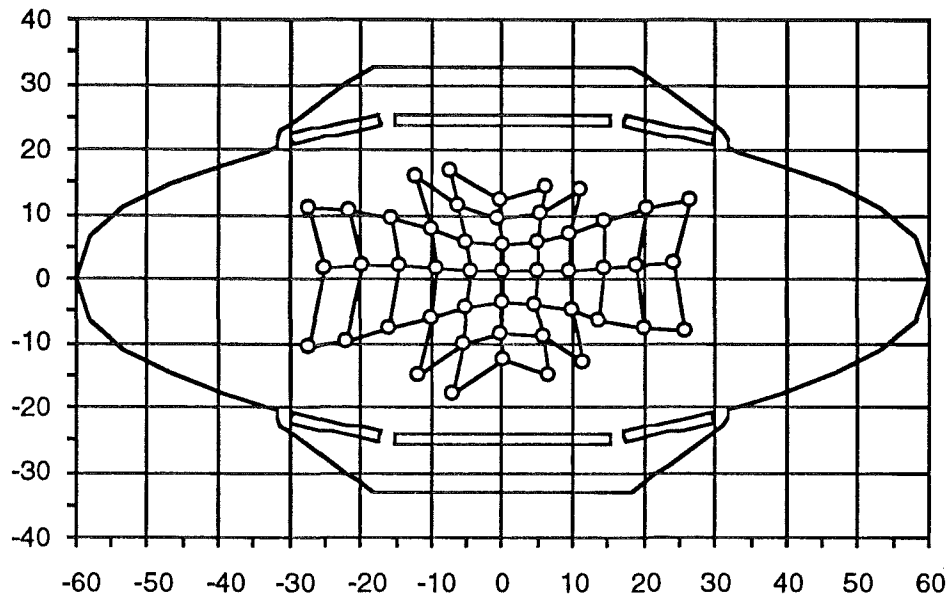


Figure 3.6-3. Two dimensional map of BPM using the rf module with linearity correction and 5 mm test wire spacing (Reference 5).

Table 3.6-3.

Power requirements for the rf modules, Reference 5.

Beam current ppb	$1 \times 10^9 - 6 \times 10^{10}$
Cable length, (RG8/U)	150-1150 feet
Position range	± 25 mm hor, ± 15 mm ver
Plate width	13 mm
Plate length	250 mm
Plate hor separation	47 mm
Detector output	-36 to +22 dBm
RF Module input range	-35 to +27 dBm

Replacing the computer interface with a VME contained system using 12 bit ADCs is being considered as an upgrade to the Main Ring. The upgrade would allow every BPM to collect turn by turn data and improve the resolution but not the accuracy of the measurement. This approach is being implemented in the Booster whose experience will be used to guide the decision. The cost of the core electronics is estimated at \$165K. This approach would require modification to the local software and existing application programs. There is no provision for loss monitor support in the Booster upgrade.

Alignment

The maximum random BPM alignment tolerance of 2.5 mm and systematic error of 1 mm is specified in Reference 6. For comparison, the Tev BPMs use a table of offsets to correct the BPM electrical center to the quadrupole magnetic center. The average of these offsets is 0.34 mm and the standard deviation is 0.60 mm. According to Reference 7, the electrical center is measured with an accuracy of ± 0.2 mm. The position measured from the up and down stream ends were required to agree within 0.13 mm. The magnetic center of two Main Ring quadrupoles was recently measured and found to be 0.26 and 0.47 mm from the lamination mechanical centers.

Accuracy

The following covers some of the phenomena which can contribute to a position measurement error or result in limited resolution. Many of these can be corrected or reduced with calibration.

The current 8 bit A/D converter provides 150 μm per bit resolution. The noise level of the rf module in batch mode ranges from 30 μm RMS at 3×10^{10} protons per bunch to 500 μm at 5×10^7 , Reference 8. One rf module measured 50 μm RMS or about 0.12 mm peak to peak. Including the effect of 1150 feet of RG8/U cable, KTB noise would be about 2.6 μm rms.

Because the A and B channels in the rf module are matched at a single frequency, the rf module output depends on the input frequency. The output of one rf module was measured to change by 0.4 $\mu\text{m}/\text{kHz}$ providing a 120 μm error through the 300 kHz Main Injector rf frequency program.

For a continuous bunch train, the frequency spectrum consists of narrow pulses spaced at rf frequency harmonics but the spectrum of a single bunch contains energy at all frequencies. The simultaneous presence of more than one frequency in the bandwidth of the rf module and the frequency dependence results in a complicated time dependent position output signal. This behavior is aggravated by using a delay cable to form the 90° phase shift for the AM to PM

detection scheme. Single bunch measurements using AM to PM conversion result in significant offsets and considerably more noise than batch mode. Single bunches are only expected in the Main Injector after coalescing at the very end of the cycle. The ability to accurately measure their position is not considered important.

The nonlinearity caused by the AM to PM conversion in the rf modules combined with the transverse size or distribution of the beam conspire to contribute a 1 mm error with 20π beam 10 mm off center at 8 GeV. The errors shown in Figure 3.6-4 were calculated by convolving the gaussian bunch shape with the measured transfer function of the BPM and rf module. These results are only approximate as the horizontal transfer function will also depend on vertical position and width. These effects will be reduced because the ratio of horizontal to vertical beta make the orthogonal beam size 2.4 times smaller.

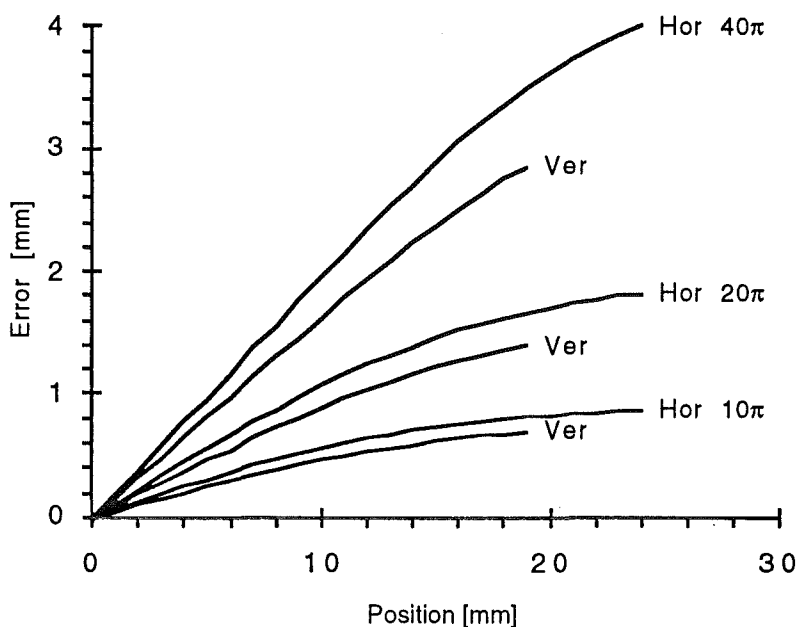


Figure 3.6-4.

Error caused by non linearity of the AM to PM detector and the beam size at 8 GeV.

The 150 to 1150 feet of cable required to transport the signal to the rf modules will effect accuracy and the range of signal amplitude. The dispersion of a single bunch signal is shown in Figure 3.6-5 for 3 types of cable. The cable response is found by convolving the stripline doublet signal with the cable impulse response, which assumes the cable losses are proportional to the square root of the frequency. As can be seen, the dispersion makes the doublet pulse

asymmetrical and spreads the shape out far enough to interfere with trailing bunches. The Main Injector bunch spacing is 18.8 nsec. The range of cable lengths will increase the dynamic range of the signal by 36 db at the rf module if RG58A/U is used. RG8/U would require 18 db and LDF4-50A only 5 db. About 300,000 feet of RG8/U cable will be used for the Main Injector BPMs.

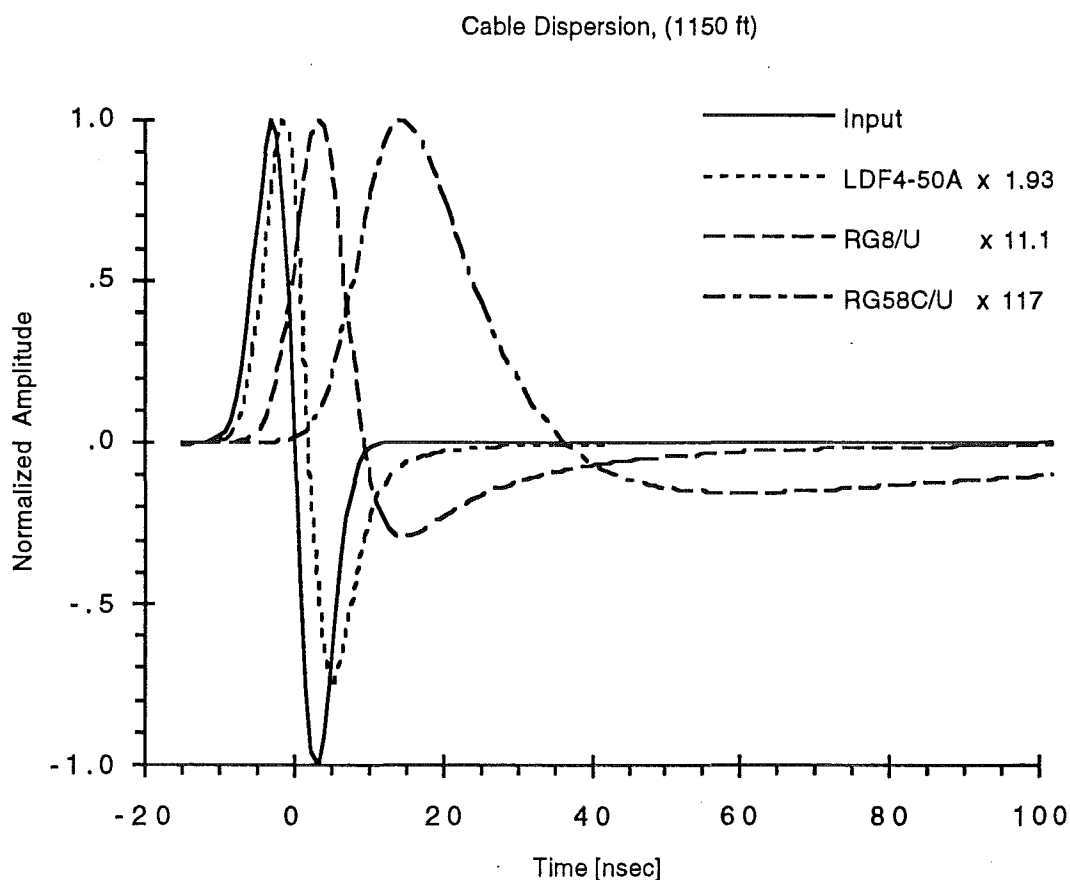


Figure 3.6-5. Calculated cable dispersion from a $\sigma_t = 3$ nsec bunch with an 18 cm stripline and 1150 feet of cable. The normalizing factors are indicated in the legend.

Differences between the A and B cables such as characteristic impedance, attenuation, or phase delay will cause errors in position measurement. Reference 8 indicates the Tevatron cables were phase matched to $\pm 3^\circ$ and balanced to ± 0.3 db. A phase error of 5° at 53 MHz will result in a position error less than 0.02 mm, Reference 9, and the attenuation imbalance would result in ± 0.4 mm, at 0.7db/mm. RG8/U cable has a characteristic impedance of $50 \pm 5 \Omega$. A difference of

5 ohms between the A and B cables would be interpreted as a 0.6 mm error. By pulling the A and B cables from the same reel, better matching could be obtained.

Connectors are another source of error. Kings type N connectors have a VSWR less than 1.3 which would cause a 1.5 mm error if applied to only one input. Because the rf modules use a limited bandwidth at 53 MHz the connector errors are expected to be much smaller.

The input impedance, or reflection coefficient, of the rf modules can cause an offset error which depends on frequency and the length of cable to the detector. Using the equation provided below and measurements from 57 Tev / Main Ring rf modules, the calculated distribution of position errors are shown in Figure 3.6-6.

$k_a, k_b = \text{reflection coefficient at port } a, b$

$$m = \text{mag}\left(\frac{1+k_b}{1+k_a}\right), \quad \phi = \text{ang}\left(\frac{1+k_b}{1+k_a}\right)$$

$$x = -\frac{mm}{db} 20 \log \left\{ \tan \left(\frac{1}{2} \left[\text{atan} \left(\frac{\cos \phi}{A/mB - \sin \phi} \right) + \text{atan} \left(\frac{\cos \phi}{A/mB + \sin \phi} \right) \right] \right) \right\}$$

for $\phi \ll A/mB$

$$x \approx \frac{mm}{db} 20 \log \left(\frac{A}{mB} \right)$$

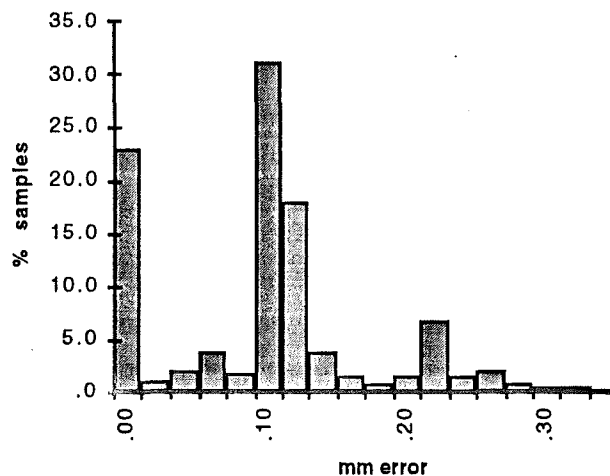


Figure 3.6-6. Distribution of position errors calculated from measured reflection coefficients for 57 Main Ring rf modules.

Table 3.6-4.

**Summary of possible position measurement errors, assuming 0.7 db/mm and 1×10^9 ppb.
Some errors can be corrected with calibration.**

μm	
1000	beam size at 8 GeV, 20π emittance, 10 mm offset
760	0.53 db cable attenuation match, from TeV experience
600	cable impedance match, 5 Ω difference
500	difference between geometric and magnetic center of quads
250	rf module reflection coefficient
200	A/D resolution and AM to PM non linearity at 10 mm offset
200	accuracy of measuring BPM electrical center, TeV experience
130	directionality, difference between p and pbar positions
120	measured peak to peak noise
120	Frequency sensitivity, 300 kHz frequency program
12	$\pm 3^\circ$ cable phase match
3	rms KTB noise for 1×10^9 ppb

Offsets in position measurement caused by cables, connectors, and impedance matching can be measured and corrected. A good method to measure these offsets would be to insert identical 53 MHz rf currents into the A and B cables in the tunnel and use the reported position as a new base line. These offsets could be combined with those which correct the reading for the difference between the BPM electrical center and the quadrupole magnetic center.

It is interesting to compare the rf module accuracy with a commercial network analyzer. With calibration, the HP 8753C, has 0.15 db uncertainty in amplitude measurement and changes by 0.01 db/ $^\circ\text{C}$. At 0.7 db/mm this becomes 210 μm and 14 $\mu\text{m}/^\circ\text{C}$. This represents the accuracy to which some of the BPM offsets can be measured and corrected.

Electronics

Currently the plan is to use existing Main Ring BPM electronics in the Main Injector. Each rack of equipment, shown in Figure 3.6-7, services 12 BPMs and 12 beam loss monitors, or BLMs. For 228 rf modules, 19 racks will be required for the Main Injector ring, 3 in each of the 6 service buildings with an additional one at MI-60. There are currently 26 racks used for the Main Ring. The test chassis can inject beam like signals into the rf modules and check that the BPM cables are terminated, or connected to the BPM. Each rf module has a sample and hold and 8 bit A/D card in the BPM analog chassis. The multibus chassis holds two Z80 microprocessor cards which run the system locally, Reference 8.

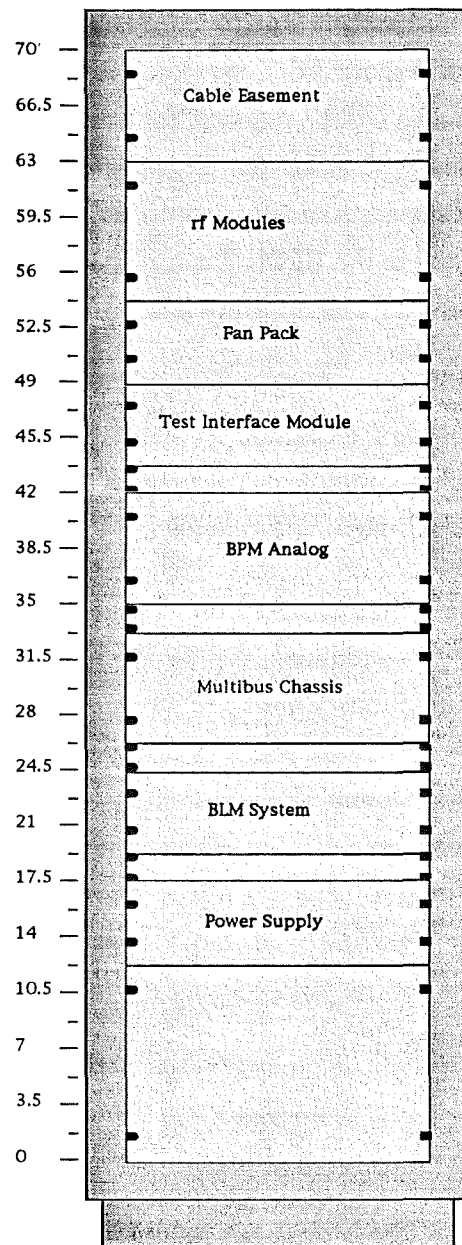
The position measurement is first armed by the controls system but triggered from the beam intensity signal from each rf module. The trigger threshold is adjustable by the host computer. The gate circuit looks for the 1.5 μ sec notch in the beam.

The basic running mode is called closed orbit. To smooth out the betatron oscillations the average from between 8 and 64 measurements, set by the host computer, is taken and recorded into memory. This mode runs continuously until a request for a flash is received. The flash event is designed to measure the same portion of beam as it travels around the accelerator. Only one position is measured for each detector and all measurements at the multibus chassis are placed in a 30 byte flash buffer. The response to a display request is to place the latest average position for each BPM in the 20 byte display buffer. There is also a 512 byte snapshot buffer which keeps the last 512 sets of averaged position data, the snapshot trigger freezes the buffer allowing the host computer to access the data. The profile buffer stores the average position each time the profile trigger is received, up to 128 times.

Two locations in the ring have additional electronics to store up to 1024 positions taken each turn for both the horizontal and vertical planes. Fourier transforms can be taken in the applications program to determine tune and coupling. Two MADC channels can be used at every building to time plot averaged positions.

Applications Programs

The main applications programs include page M37 which sets the BPM control parameters, M38 which performs hardware tests, M39 which displays the measured positions and intensities, and M42 for turn by turn displays. These are supplemented with M56, Orbit Jr., which can use the position data to calculate corrections. It is capable of reducing first turn oscillations, closing the orbit for the second turn, and calculating magnet changes to smooth the closed orbit.



**Figure 3.6-7. Standard BPM/BLM rack used in the Main Ring.
Each rack serves 12 BPMs and 12 BLMs.**

(MM) 04/18/94 0055:32

DISPLAY FRAME	.14		E	F	A	B	C	D
		VX11	.15	-1.53	2.75	2.82	-.76	.91
		VX12	.61	-3.37	1.53	1.87	1.53	-.15
TAKEN 04/18/94 0055:31	29	VX14	-1.37	.45	-.18	-.18	1.33	1.83
		VX16	-.76	-2.44	1.68	-.18	.76	.45
		VX18	1.83	.76	-1.22	-3.37	-.3	-.3
		VX21	3.82	.61	3.83	2.44	-.91	.3
		VX23	.15	-2.29	1.87	-.91	-.3	2.14
		VX25	-2.14	.45	1.87	-.45	1.83	.15
		VX27	0	2.6	.76	-1.99	1.87	1.83
		VX29	-1.83	1.87	-1.37	.45	-.18	.91
		VX33	4.14	-.76	2.91	1.87	.76	-1.37
		VX35	3.37	.61	1.99	-1.87	-.61	-2.44
		VX37	0	-.91	1.68	1.87	1.87	1.37
Injection BPM	(MM)	VX39	-1.87	2.14	-2.29	-2.14	1.87	-.61
DOWNSTREAM LAMB	10.45	VX43	.45	.91	-.61	2.29	.61	.91
END OF STRAIGHT	-4.48	VX45	2.29	3.83	-3.53	-.91	.61	-1.37
AB term angle	2 .1948 MF	VX47	.76	.61	-1.53	-.76	-3.53	.61
		VX49	-2.44	1.99	4.23	-1.68	6.18	3.86

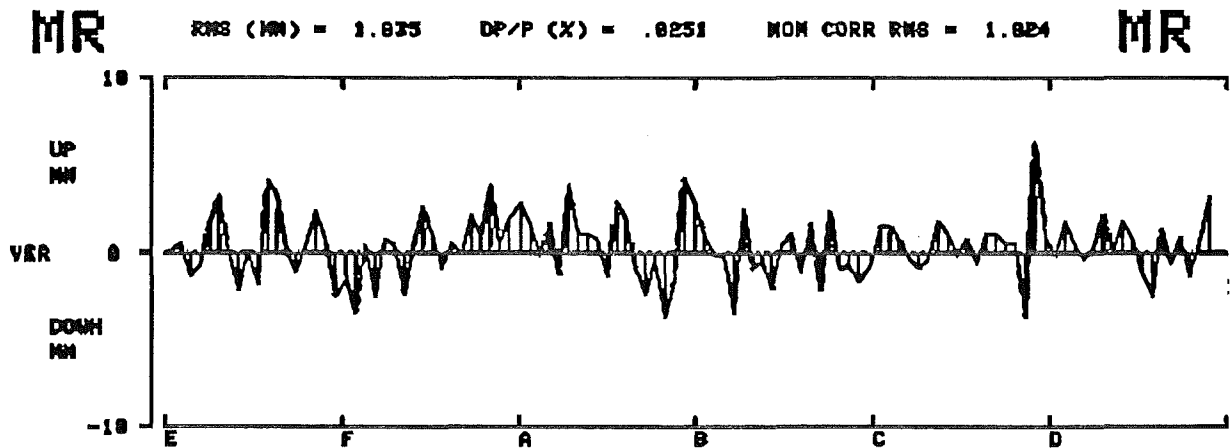


Figure 3.6-8.

Main Ring Display Frame from applications program M39 showing vertical orbit.

WBS 1.1.8.1.2.

Ring BLMs

WBS 1.1.8.10.2.

Beamline BLMS

Ion Chambers

The BLM detector consists of a sealed glass tube with 110 cc of argon at 1 atm pressure, Reference 10. With 2.5 kV of bias, the tube produces 7×10^{-8} coulombs per rad, is linear to 100 rads, and has a dynamic range of 10^6 . The leakage current is equivalent to 0.3 μ rad/sec. The detector is enclosed in a short section of PVC pipe and placed at every quadrupole. The bias voltage is adjustable from the host computer.

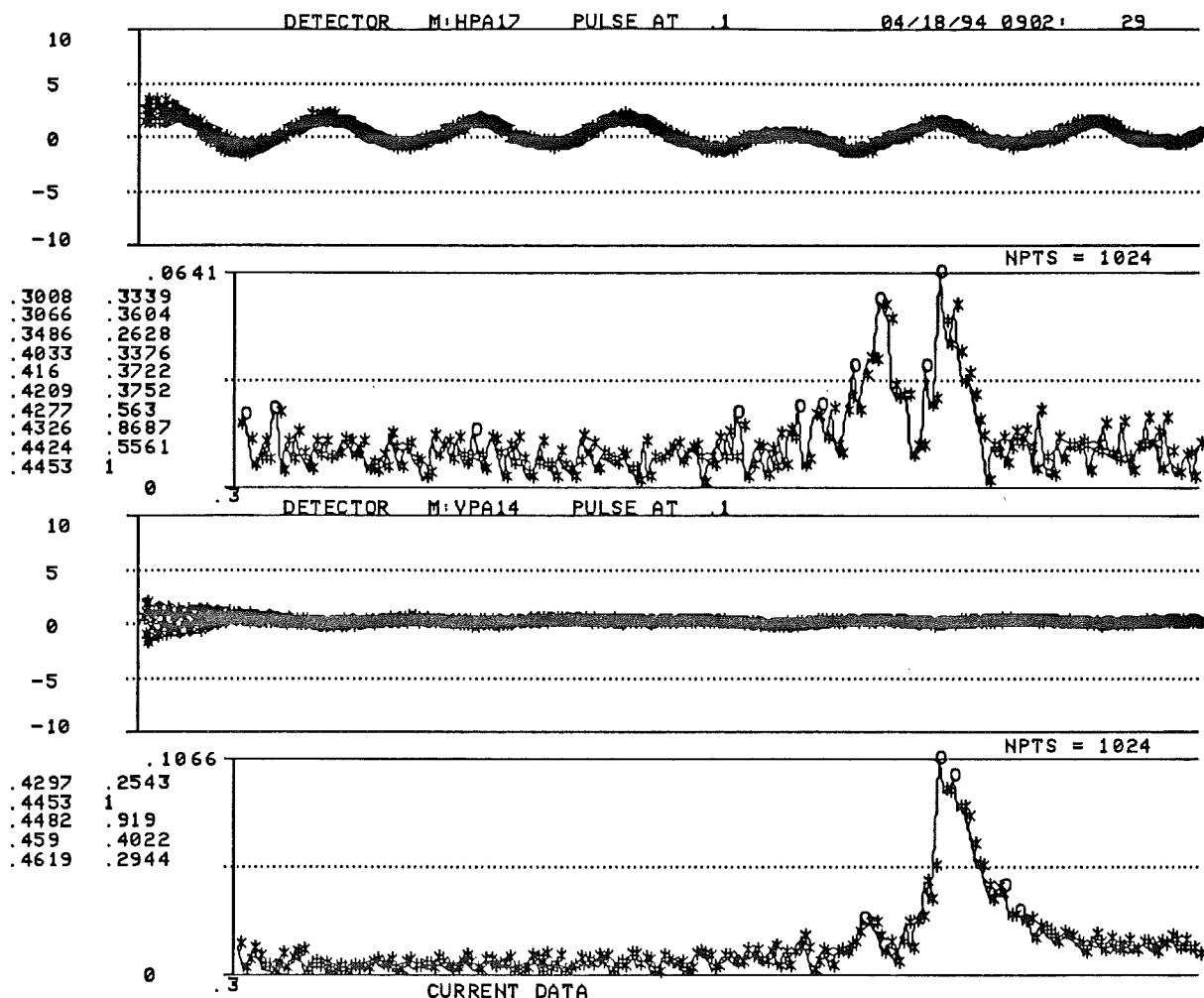


Figure 3.6-9. Main Ring turn by turn display at injection. FFT of horizontal and vertical positions indicates fractional tunes. Note the vertical tune in the horizontal display.

Electronics

Each detector has an amplifier, integrator, and sample and hold card. The integrator uses a .001 μf capacitor which provides 70 volts per rad. A four decade integrating logarithmic amplifier is used to increase the dynamic range.

The data collected for the loss monitors is similar to the data collected for the BLMs. The integrated loss is used for the following measurements. The flash event is designed to measure the same portion of beam as it travels around the accelerator. Each measurement of 12 BLMs is placed in a 30 byte flash buffer. The response to a display request is to place the latest integrated loss from each detector in a separate 20 byte buffer. There is also a snapshot buffer which stores the last 512 measurements of integrated loss data, the snapshot trigger freezes the buffer allowing

the host computer to access the data. The 128 byte profile buffer records the integrated loss each time the profile trigger is received. The BLM analog chassis supplies non integrated loss signals to 12 MADC channels to allow the time plotting of real time losses. There are two gain settings and a track and hold circuit.

MAIN RING BPM DISPLAY LOSSES

04/19/94 1642:13
2D Cycle
LOW Field limits

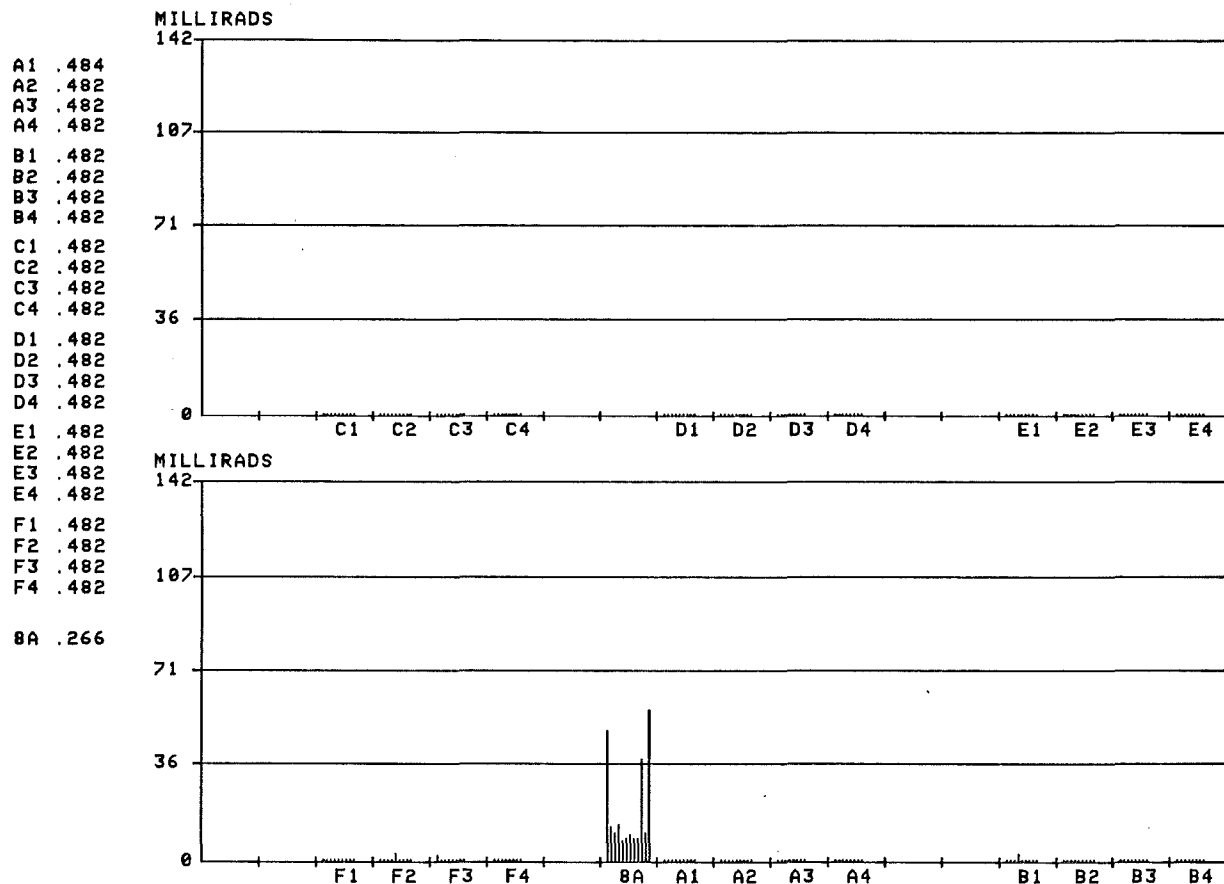


Figure 3.6-10. Typical Main Ring loss monitor display.

TLMs

In addition to the loss monitors at every quad, total loss monitors will be used along the tunnel at injection/extraction points. These are constructed from gas filled coaxial cables which run the length of the area of interest. High voltage is applied to the center conductor and the current indicates the amount of loss, Reference 10.

Design

One resistive wall longitudinal pickup will be adapted from the Main Ring for use in the Main Injector. The basic design is to insert a ceramic gap shunted with resistance in the vacuum tube and measure the voltage induced by the beam wall current, Reference 11. The ultimate bandwidth of such a detector is limited by the spreading of the electric field lines between the beam and the image charge on the inside wall by an angle approximated by $1/\gamma$ for relativistic beams. The length of the electric field lines at the surface of a round pipe of radius R is about $\lambda \approx R/\gamma$. Equating 2λ to the wavelength of the highest measurable frequency, the bandwidth becomes $f \approx c\gamma/2R$ where c is the speed of light. At injection to the Main Injector using a 3 cm radius pipe the bandwidth limit is 47 GHz. In practice the detector response is difficult to maintain above the microwave cutoff frequency of the beam tube, measured to be 1.5 GHz for the elliptical shaped Main Injector vacuum tube. The vacuum chamber impedance is in parallel with the gap impedance and above cutoff nearby devices such as bellows may effect the detector accuracy.

When the beam passes any discontinuity in the beam pipe around the circumference of the accelerator, electromagnetic energy is launched into the beam pipe. This energy can travel in either direction and typically travels slightly slower than the beam. The resistive wall monitor cannot differentiate between currents induced by beam and those induced by energy traveling along the wave guide, or vacuum tube. In the Fermilab Main Ring this spurious signal can approach 10% of the beam signal. To remove these signals, microwave absorber is placed inside the vacuum tube up and downstream of the resistive wall monitor.

If the charge density around the circumference of the gap is not uniform, Figure 3.6-11, and the impedance is, the voltage across the gap will vary around the circumference. The gap will act as an azimuthal transmission line transporting charge until the voltage equalizes. Position detectors have been made with a resistive gap by comparing the voltages induced at different points. To reduce this effect, several monitor points are placed around the detector and summed to form a single output. The elliptical shape of the Main Injector pipe would aggravate this problem.

To overcome these problems, the current round tube could be maintained through the resistive wall monitor with an abrupt transition to the elliptical Main Injector pipe at the microwave absorber. The absorber should terminate any modes traveling along the elliptical vacuum tube as well as damp any modes induced in the round tube. This should provide good signal at the gap and minimize any beam impedance which might contribute to instabilities.

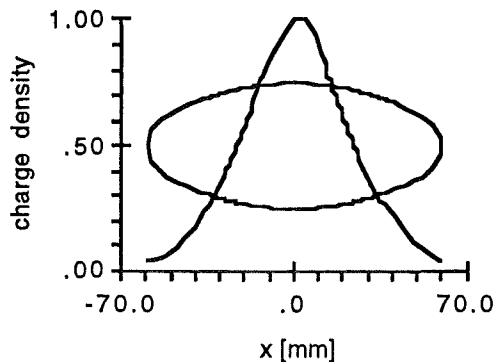


Figure 3.6-11. Cross section of beam tube and charge density induced by line charge at center versus horizontal position.

The current Main Ring resistive wall monitor has a 3.25" diameter round ceramic gap. The microwave absorber is placed inside 4" diameter pipe up and downstream of the gap in a way that preserves the 3.25" aperture. Cutoff in a 3.25" diameter pipe occurs at 2.1 GHz for the TE_{11} mode. The quality of the gap impedance was measured to 6 GHz by forming a 50 Ω transmission line with the appropriate diameter tube placed along the center of the detector. The response was flat to ± 1 db.

WBS 1.1.8.1.4. Transverse Wideband Pickups

Design

Standard striplines are planned for the horizontal and vertical planes. Feedthroughs at both ends will be used to observe both the proton and antiproton signals. The plate length of 55", $\lambda/4$ at the fundamental rf frequency of 53.1 MHz, will be used to maximize the doublet separation. In the time domain, this will allow observation of the bunch shape and changes in position within a bunch. In the frequency domain, zero's in transmission will occur at those frequencies where the plate is $\lambda/2$ long, or even multiples of the rf frequency.

With 50 Ω plates that intercept 1/6 of the wall current, the peak amplitude will be 10.6 volts for 6×10^{10} protons per bunch with a bunch length sigma of 3 nsec.

WBS 1.1.8.1.5. Dampers

Design

Horizontal and vertical dampers are planned to reduce the dilution caused by injecting off orbit and to damp instabilities.

For the Main Injector it is planned to use the digital filter scheme being designed for the Booster accelerator. The electronics consists of an 8 bit A/D converter and an 8K dual port memory. The difference from two memory locations drives a 10 bit D/A forming a single zero in the Z domain and a variable delay. Two cards are interleaved to relax speed requirements and their outputs are multiplexed to a single D/A to form a modal rather than a bunch by bunch damper. The cards are register based VXI cards and are currently being developed using Labview on an Apple computer through a National Instruments MXI interface.

By taking the difference between two memory locations separated by one turn, a repetitive filter can be formed that removes energy at every rotation harmonic and passes the betatron signal at $f = nf_{\text{rot}} \pm mv$. This filter will remove the effect of the closed orbit not being at the electrical center of the detector. The presence of noise, or undesired signal like the energy at the rotation harmonics, has the effect of limiting the gain of the system. For a given power capacity the gain must be limited to insure the amplifiers are not driven into saturation.

Injection Errors

Using the following equation, the 1/e damping rate in turns can be estimated, Reference 12.

$$N_D \approx \frac{2}{G \sqrt{\beta_k \beta_d} \sin \Delta \psi}$$

β_k, β_d at kicker, detector
 $\Delta \psi$ betatron phase advance

$$G = \frac{x'}{x} \quad \text{damper gain} \quad \left[\frac{\text{mRad}}{\text{mm}} \right]$$

For 500 V per mm of beam position, plate length of 48", and gap of 2", the damping rate would be 24 turns at injection. Most damper systems lack the power required to make them critically damped. Because the oscillation is not always measured at peak amplitude it is difficult to obtain better than 2 turns. This would require a gain of 5 kV/mm and to accommodate a reasonable range of amplitudes a peak deflection of 50 kV. For injection errors all that is required is that the oscillation is reduced before the phase space becomes diluted. The time required then depends on the tune spread of the beam. For a chromaticity of ξ the number of turns required to dilute the phase space is estimated below, Reference 12.

$$N \approx \frac{1}{\Delta v} \quad \Delta v = \xi \frac{\Delta P}{P}$$

For a chromaticity of 10 units and $\Delta p/p$ of .001 the number of turns becomes 100.

Instabilities

The current Main Ring damper system consists of horizontal and vertical slow dampers with 2 MHz bandwidth and a vertical bunch by bunch damper with 200 MHz bandwidth. The damper gains are typically 500 to 1000 V/mm. Using Reference 13 and an estimate of the Main Injector impedance, Reference 14, a gain of 470 V/mm is required for the resistive wall instability.

WBS 1.1.8.1.6.

Flying Wire Beam Profile Monitors

Design

Three flying wire systems will be modified and moved from Main Ring for use in the Main Injector, Reference 15, 16, 17. They will be positioned to provide measurements of transverse beam profiles and thus emittance. Two are required and one will be used as a "hot" spare.

The flying wire system rotates a 25 μm carbon fiber mounted on a 5" radius titanium fork through the beam at 5 meters per second. The beam density at the wire is determined with photomultiplier tubes measuring the flux of secondary particles passing through plastic scintillator placed a few feet away. Up and downstream photomultipliers allow the measurement of protons or antiprotons. The output of the photomultipliers is measured with a fast gated integrator which allows the simultaneous measurement of 6 proton and 6 antiproton bunches in the Tevatron. The angle of the shaft driving the fork is measured to 0.022° with an optical encoder providing a position resolution of 0.05 mm. The VME based μP acquires and analyzes the data as often as every 150 msec. Wire flies can be initiated by the "Colliding Beam Sequencer" to automatically record data at key times through the acceleration process.

The Flying wire systems are currently being upgraded to replace the VME μP with an Apple Macintosh running Labview. An example of the Labview output is shown in Figure 3.6-12.

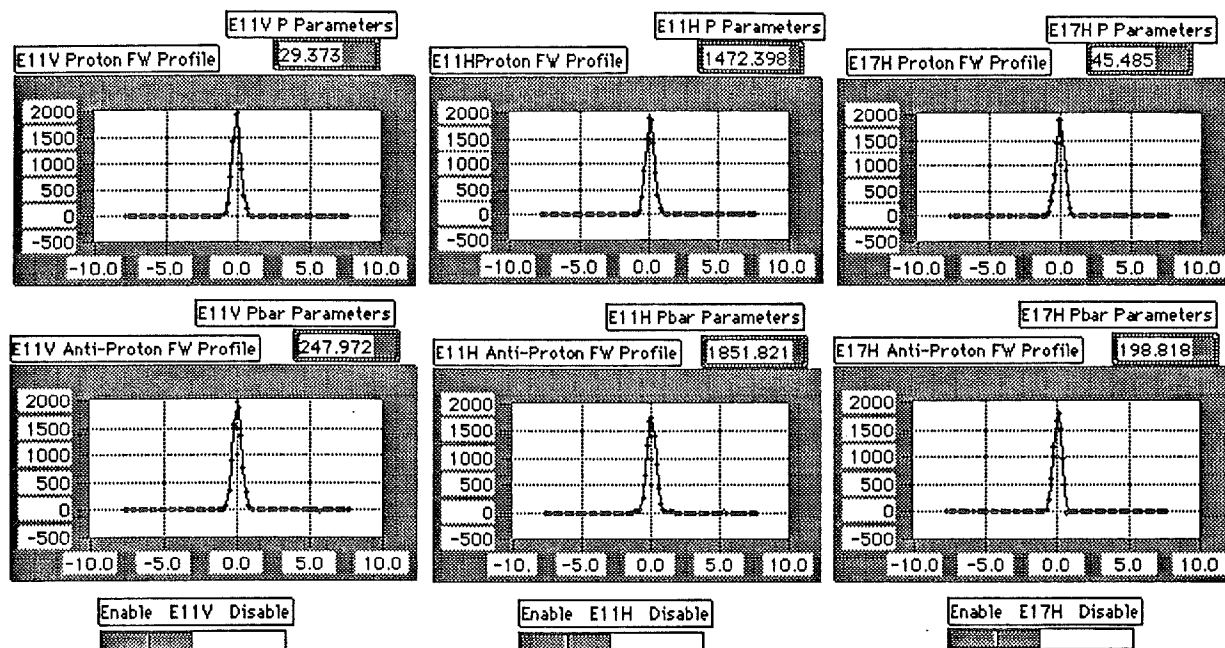


Figure 3.6-12. Typical set of data obtained from Tevatron Flying Wire.

WBS 1.1.8.1.7.

DCCT - Ring Intensity Monitor

Design

Currently it is planned to modify and move the Main Ring DCCT, or dc current transducer, to the Main Injector. Designed at Fermilab, the DCCT uses the second harmonic detection principal to measure the dc beam current in series with an ac transformer to extend the bandwidth, Reference 18. There are three output ports with gains of 5.24×10^{12} , 1×10^{12} , and 2×10^{10} /volt with bandwidths of 25, 12, and 8 kHz respectively. The DCCT also has a calibration winding to allow remote calibration from the service building. Identical DCCT's reside in the antiproton source and the Tevatron providing accurate comparison of beam intensities or transfer efficiencies.

The Main Ring DCCT is 42" long and the round vacuum tube has a 4.75" aperture. If the modification required is sufficient or the space in the accelerator limited, a commercial current monitor can be purchased from Bergoz. The Bergoz monitor is only about 4.25" long with several apertures available from 2" to almost 7" but does require a ceramic break be installed.

WBS 1.1.8.1.8.

Scrapers

Design

A pair of scrapers, horizontal and vertical, will be provided to limit the transverse emittance for machine studies. They will be placed in the P8 line leading from Booster to the Main Injector. Scrapers are not required in the ring as their usefulness is limited by the low dispersion of the Main Injector.

WBS 1.1.8.10.1.

Beamline BPMs

Resonant Detectors

In addition to reusing 104 Main Ring and 17 wide aperture pickups, which use ring style electronics, 11 tuned pickups are required. During slow spill, the beam will be extracted over a one second time period, or 100,000 turns, making the spill intensity 100 db smaller than the initial ring intensity. This is well below the capabilities of the ring BPM electronics. The signal to noise ratio of beam detectors is proportional to the square root of the impedance. The sensitivity of the detector can be improved by resonating the capacitance of the open ended plates with the appropriate inductance. The impedance will be increased and the bandwidth reduced by the factor Q. Resonant BPM's were designed for the Tevatron slow spill, Reference 19 and 20. The one meter long pickups resonate at the fundamental rf frequency of 53.1 MHz, have a loaded Q of 190, bandwidth of 200 kHz, time constant of 1 usec, and impedance of 9.5 k Ω . Beam position determination to 0.1 mm has been achieved for beam intensities as small as 1×10^3 protons per rf bucket. A shorter version 7" long was also developed.

Electronics

The electronics employs an AM to PM conversion scheme with low noise amplifiers that can be switched in to select slow or fast spill mode. The bandwidth can be limited at the output to 10, 100, or 1 kHz for slow spill and 3, 5, or 10 kHz for fast spill. Taking into account cable losses, ± 0.1 mm resolution with 10 Hz bandwidth can be obtained in slow spill mode.

WBS 1.1.8.10.7.

Toroid - Beamline Intensity Monitors

Design

The current toroid design uses Pearson Electronics, Inc. model number 3100 current monitors. The aperture is 3.5" and the output signal is 0.5 volts/amp into 50 Ω with a bandwidth of 40 Hz to 7 MHz. At the toroid output the signal is 85 mV for 10^{10} ppb. The toroid is electrically isolated from ground in the enclosure and good quality cable such as LDF4-50A is required to avoid noise problems. The toroid must be placed over a ceramic break in the vacuum tube. To reduce the rf energy radiated into the environment a ground connection is required across the break but external to the toroid.

The signal is transported to the service building where the electronics amplifies, limits the bandwidth, and integrates the signal to provide a voltage representing the total charge. The current design being used includes a baseline subtraction circuit, a fixed length integration window, and an A/D and D/A used to form a sample and infinite hold. The toroid integrator has a bandwidth of 100 Hz to 400 kHz and selectable gains of 2×10^{11} , 2×10^{10} , and 2×10^9 particles per volt.

The effect of the low frequency roll off can be compensated with a simple gain adjustment provided the signal width and its timing within the integration window stays constant. For a 100 Hz rolloff, the signal droop would cause a 1% error in 32 μ sec. If the integration window includes 32 μ sec of the undershoot trailing the signal, an additional 2% error would require compensation.

$$Error = 1 - \frac{\tau}{t_s} \left(e^{-\frac{t_w}{\tau}} - e^{-\frac{t_w + t_s}{\tau}} \right)$$

$$\tau = \frac{1}{2\pi BW}$$

$t_s = \text{length of signal}$

$t_w = \text{length of window after signal}$

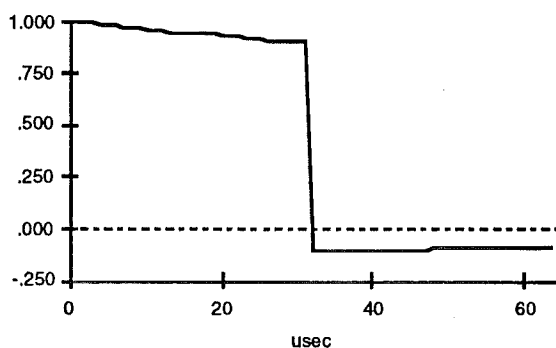


Figure 3.6-13. Response of 500 Hz high pass filter to step input demonstrating effect of droop and undershoot.

WBS 1.1.8.3.9.	150 GEV PROTON LINE PROFILE MONITORS
WBS 1.1.8.4.9.	150 GEV ANTIPROTON LINE PROFILE MONITORS
WBS 1.1.8.5.9.	120 GEV LINE PROFILE MONITORS
WBS 1.1.8.6.9.	SLOW SPILL LINE PROFILE MONITORS
WBS 1.1.8.10.	BEAMLINE INSTRUMENTATION

Beam Diagnostics in the 8 GeV beam line from Booster to MI

The purpose of the beam diagnostic system is twofold. First it should aid in the investigation of the problems associated with beam transport in the beam line and help establish the beam. For this a number of beam position and beam loss monitors will be installed in this beam line. Secondly, the beam diagnostic system should provide a reliable method for quick measurements of beam parameters like transverse emittances and emittance dilutions on batch by batch basis for the beam coming from the Booster. The multiwire systems of the type presently being used in 8 GeV beam line from Booster to Main Ring are adequate, but residual gas ionization monitors discussed below would provide monitoring of position changes through the batch. Each of the multiwire systems is capable of measuring both horizontal and vertical beam profiles at the same location in the lattice.

The emittance dilution in a beam line can arise from various types of errors like fluctuations and higher order components in field, misalignment- and/or roll-errors in the beam line elements. Calculations carried out using the program MAD shows that a 1% field error (random as well as systematic) in all beam line magnets (quadrupoles and bending magnets) gives a maximum of 10% emittance dilution from the amplitude functions and a maximum of 5% emittance dilution from the dispersion functions. But major contribution arises from the position errors which we correct by using correction dipoles downstream of each quadrupole.

To determine the beam emittances and establish matching of the beam during operation we will use six groups of profile monitors. The first set contains a pair of monitors close to the Booster end of the line, with one at large β_x , and the second at large β_y . There is little flexibility in selecting the magnitude of the horizontal dispersion in this section. A second pair will be located at the end of the Booster matching section, where the horizontal dispersion is zero. Three more pairs are located at the low dispersion points in the lattice, with the last set near the MI-matching section of the line. Finally, two more monitors are located at two high-dispersion points separated by 270° of phase advance. The two monitors at high-dispersion locations will allow a determination of the momentum spread of the beam, as shown in Figure 3.6-14. All locations have plenty of free space available for installation of the monitors. Tentative assignments of locations of profile monitors and the lattice functions at those locations are given in Table 3.6-5.

Table 3.6-5.
Locations of Beam Profile Monitors in the 8 GeV Beamline and MI-10 Straight Section

	Beta Function (m)		Dispersion Function (m)	
	x	y	x	y
<u>Booster end 1</u>				
Q801	29.5	68.2	-1.2	0.0
Q802	67.6	29.8	-1.9	0.0
<u>Booster end 2</u>				
Q813	8.9	50.6	-0.4	0.0
Q814	50.7	8.8	0.0	0.0
<u>Middle of line</u>				
Q825	8.9	50.6	-0.4	0.0
Q826	50.7	8.8	0.0	0.0
Q830	50.7	8.8	3.1	0.0
Q836	50.7	8.8	3.1	0.0
Q839	8.9	50.6	0.3	0.0
Q840	50.7	8.8	-0.0	0.0
<u>MI Matching Section</u>				
Q851	17.8	36.7	0.4	0.0
Q852	52.3	11.8	0.4	0.0
<u>MI Ring</u>				
Q101	~11	~55	~0.0	0.0
Q102	~55	~11	~0.0	0.0
Q103	~11	~55	~0.0	0.0
Q104	~55	~11	~0.0	0.0

(Beta and dispersion functions are quoted at center of quadrupole;
values at profile monitor will be slightly smaller.)

150 GeV Beamlines and Slow Spill Line

Beam position monitors and beam loss monitors will be provided at each quadrupole location. Multiwires will be placed at a few locations (to be determined) to provide profile information to assure that the lattice functions are matched between the beamlines and the Main Injector and Tevatron.

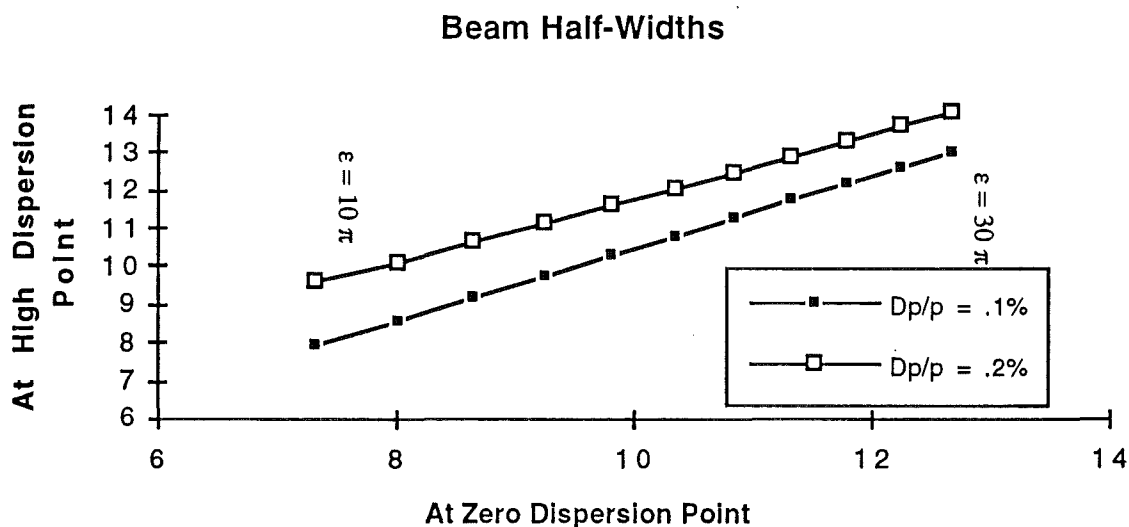


Figure 3.6-14. Beam Half-Widths in the 8 GeV Line

Requirements

The number of beam profile monitors required for the Main Injector is estimated to be 24. Although multiwire systems as used in the present 8 GeV line are adequate, we may choose to use either a residual gas ionization profile monitor or possibly phosphorescent flags with ccd cameras where appropriate. With a transverse emittance of 20π and β_{\max} of 57 m the 8 GeV beam width sigma is 4.5 mm and the 150 GeV sigma is 1.1 mm.

Multiwires

The current multiwire systems measure the integrated current induced when the beam knocks electrons from a grid of wires. A plot of the accumulated charge from each wire represents the beam profile. Twenty-four 2 mil nichrome wires are placed in a grid with 1 mm spacing, a few have 0.5 mm spacing. RG174 coaxial cable is used to transport the signal to the multiplexor located outside the enclosure where the wires are sequentially sampled over a period of a few milliseconds. The cable capacitance is used to integrate the 100 picocoulombs of charge typically accumulated. The capacitance of RG174 is 30.8 pf/ft which would result in 0.03 volts for 100 feet of cable. This signal is amplified and digitized.

Although two multiwires are typically left in the beam continuously in the 8 GeV line, the beam emittance is measurably increased. The wire grids are placed on paddles which can be rotated out of the beam path with an external motor coupled through a ferrofluidic vacuum seal. Horizontal and vertical grids are opposite each other from the paddle axis so either can be placed

in the beam with a $\pm 90^\circ$ rotation. Multiwires are also used in the accelerator to measure the first pass profiles but beam must be aborted in the first turn to allow time for sampling the charge.

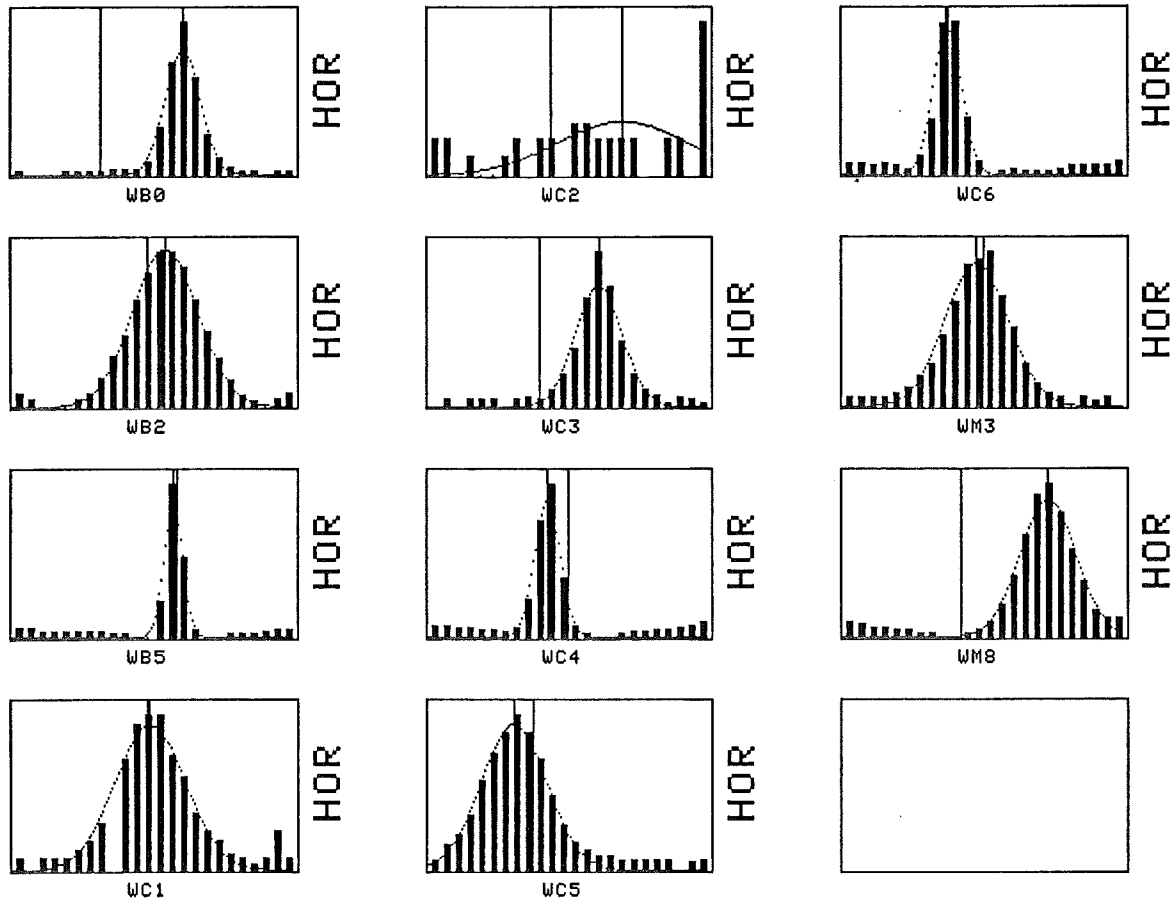


Figure 3.6-15. Horizontal beam profiles taken with multiwires in the 8 GeV beamline between Booster and Main Ring.

Ionization Profile Monitors

The IPM uses a micro channel plate to collect and amplify ions produced when the beam passes through residual gas in the detector, Reference 21 and 22. Two IPMs have been placed in the Booster and three are being developed for the Main Ring with the intention of moving them to the Main Injector. The Booster IPM is described here. The 8 kV clearing field sweeps the ions across the 10 cm aperture onto a micro channel plate which amplifies the current and deposits it onto a grid of 1.5 mm spaced conductors etched into a printed circuit card. The current induced in each conductor is amplified, digitized, and stored each turn. The amplifiers have a gain of

2.5 x 10⁶ volts per amp and 100 kHz bandwidth. The digitizers are commercial 4 channel 12 bit VME cards which have 64 Kwords of memory for each channel. A National Instruments MXI adapter is used to access the VME cards with an Apple computer using Labview software.

The IPMs being designed for the Main Ring will have a 30 kV clearing field across the 10 cm aperture with 0.5 mm conductor spacing on the collection grid. Provision is being made for stacking two microchannel plates to increase the gain to allow the amplifiers to be located outside the radiation enclosure.

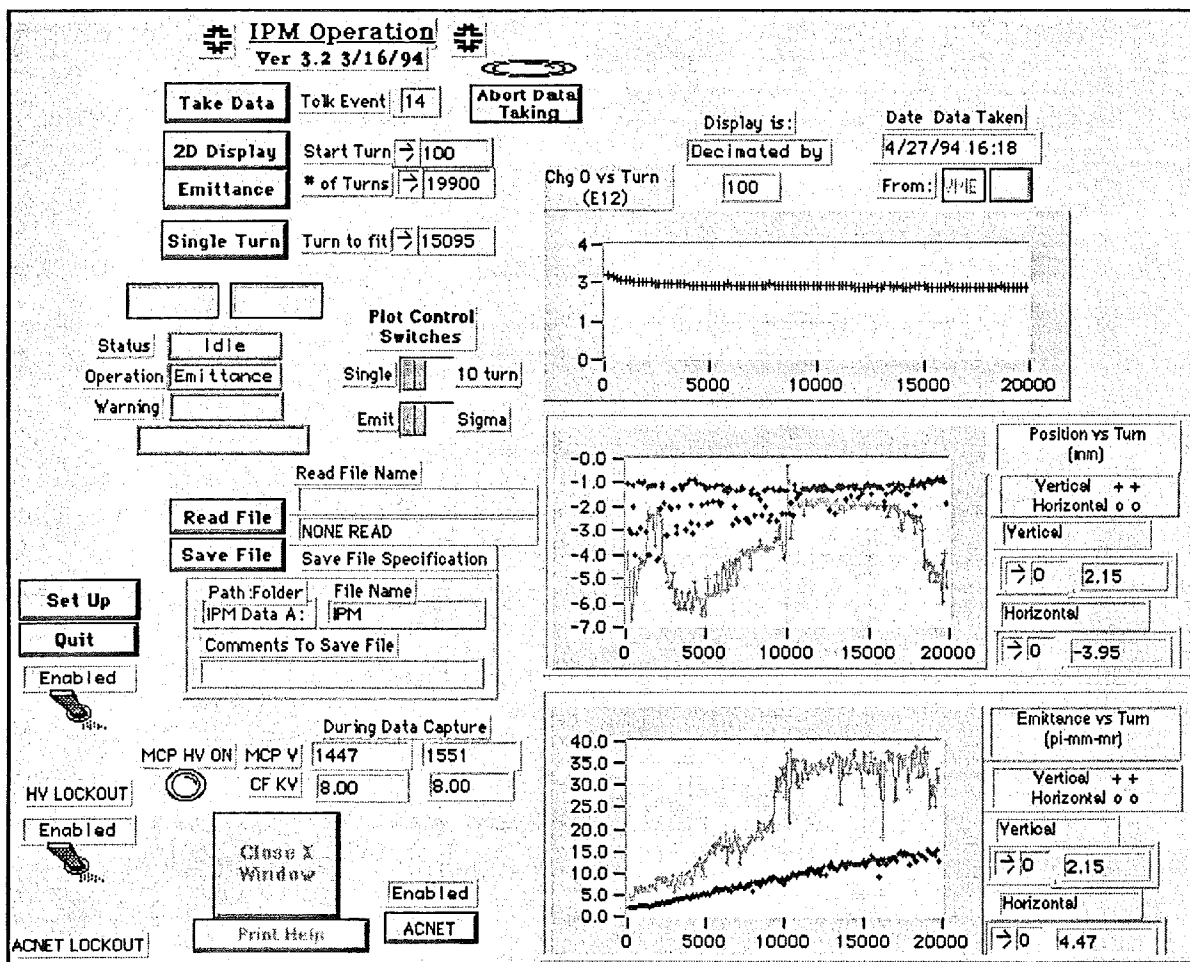


Figure 3.6-16. Front panel of the Labview program which controls the Booster IPMs. From the top down, beam charge, hor/ver position, and hor/ver emittance are shown.

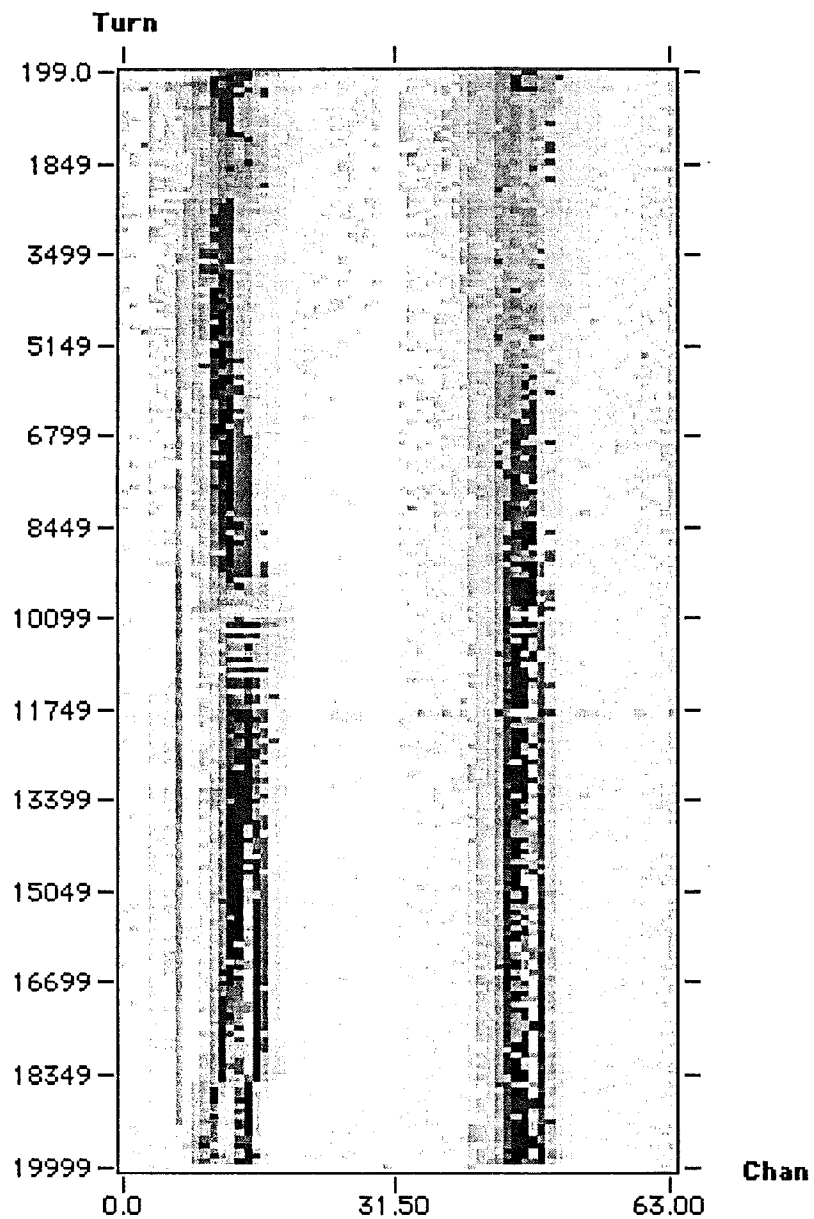


Figure 3.6-17.

**Beam intensity versus channel number and acceleration turn through the Booster cycle.
The horizontal profile uses channel 0 through 31 and vertical uses 32 through 63.**

References

- 1 Johnson, D., "Instrumentation Requirements for the Fermilab Main Injector", MI Note 76.
- 2 Bhat, C.M., Johnson, D., "Summary of the Existing MR Beam Diagnostics for use in Main Injector", MI Note 81, March 1993.
- 3 Harfoush, F.A. "Calculating Orbit Errors in Main Injector Using two or one BPM/Cell Correction Scheme", MI Note 75, December 1992.
- 4 Barsotti, Jr., Crisp, J., "Preliminary Design of the Beam Position Detectors for the Fermilab Main Injector", MI Note 96.
- 5 Ed Barsotti Jr., personal communication.
- 6 Martin, P.S., "BPM Alignment Tolerance Considerations", MI Note 102, January 1994.
- 7 Biallas, G.H. , Kerns, Q.A. , Turkot, F., Webber, R.C., Wehmann, A., "An R.F. Device for Precision Location of the Beam Position Detectors in the Energy Saver", IEEE Tran. Nuc. Sci, Vol. NS-30, No. 4, August 1983.
- 8 Baumbaugh, A.E., Gerig, R.E., Shafer, R.E., Wegner, C.R., "The Tevatron Beam Position and Beam Loss Monitoring Systems", BPM Design Note 20, 1983; also, Proc. 12th International Conf. on High Energy Accelerators, Fermi National Accelerator Laboratory, 609, 1983
- 9 Arthur, J., "Linac BPM Cable Phase Matching", TM-1852, August 1993.
- 10 Johnson, M., "Loss Monitors", AIP Acc. Inst. Conf. Proc. No. 212, 1989.
- 11 Webber, R.C., "Longitudinal Emittance an Introduction to the Concept and Survey of Measurement Techniques Including Designing of a Wall Current Monitor", AIP Acc. Inst. Conf. Proc. no. 212, 1989.
- 12 Chao, A.W., Morton, P.L., and Rees, J.R., "Single Feedback Systems for Simultaneous Damping of Horizontal and Longitudinal Coherent Oscillations", PEP Note-281, March 1979.
- 13 Ng, K.Y., "Transverse Coupled-Bunch Instability in the Fermilab Main Ring", FN-482, April 1988.
- 14 Martens, M.A., Ng, K.Y., "Impedance and Instability Threshold Estimates in the Main Injector I", MI Note 103.
- 15 Gannon, J., Crawford, C., Finley, D., Flora, R., Groves, T., MacPherson, M., "Flying Wires at Fermilab", IEEE PAC, 1989.
- 16 Zagel, J., Hahn, A., Jackson, G., Johnson, T., Martin, K., Misk, J. Wang, X., Ye, W., "Upgrades to the Fermilab Flying Wire Systems", IEEE PAC, 1991.
- 17 Wang, X.Q., Groves, T., Hahn, A.A., Jackson, G., Marriner, J., Martin, K., Misk, J., "Designing and Commissioning of Flying Wires in the Fermilab Accumulator", IEEE PAC, 1991.

- 18 Unser, K.B., "The Parametric Current Transformer, a beam current monitor developed for LEP", AIP Acc. Inst. Conf. Proc. No. 252, 1991.
- 19 Childress, S., Crawford, C., Kerns, Q., Fuja, R., Janes, R., "Tuned Beam Position Detector for the Fermilab Switchyard", IEEE Acc. Conf., CH2387-9, 1987.
- 20 Childress, S., Fuja, R., Janes, R., Lackey, S., Kerns, Q., "Electronics Design for the Fermilab Switchyard Beam Position Monitor System", IEEE Acc. Conf., CH2387-9, 1987.
- 21 Stillman, A., Thern, R., "Full Cycle Beam Diagnostics with an Ionization Profile Monitor", IEEE PAC, 1993.
- 22 Stillman, A., Thern, R., Witkover, R., "An Ultra-High Vacuum Beam Profile Monitor", Rev. Sci. Instrum. 63, 3412, 1992.

CHAPTER 3.7 CONTROLS

WBS 1.1.9. CONTROLS

Introduction

Since the creation of the original Title I document there have been some additions to the concept of the Main Injector control system, and a few details of that document have been expanded upon. As to changes, these are primarily coming about due to advancements in technology. The Main Injector will be part of the unified accelerator control system, and changes which are made, or contemplated, for the other machines must be encompassed in the MI design as well.

Networking

The major advance since the writing of the original Title I document involves computer networking in the control system. At that time, most real time connections were made via Token Ring, but in the interim it has been decided that Ethernet is a more appropriate choice. Although Token Ring is still utilized to advantage in locations in which it had already been installed or designed previous to the decision to change, nonetheless there are few new installations which use it. Thus if Main Injector were to be commissioned today Ethernet would be the primary network. However since that commissioning is still several years away, and Ethernet bandwidth utilization is already reaching saturation levels in accelerator operation, a different technology almost certainly will be used. The proposal which is in the process of slowly being implemented is installation of ATM (Asynchronous Transfer Mode) networks for controlling the present accelerators and, by implication, the Main Injector. ATM bandwidth can only be reached through use of fiber optic cable; this medium was indeed specified in the MI cost estimate.

Cabling

As in the original design, the major piece of new infrastructure required in the construction of MI controls involves cabling, primarily with fiber optics. Cabling represents that one hardware aspect of Main Ring controls which cannot be recycled into Main Injector. As the MI-60 service building was the first building ready for beneficial occupancy, it was decided to install enough cabling to make the control system available there at an early date. The first phase of this installation, completed in 1994, was to extend a link from the MAC Room in the X-Gallery basement to and through the Main Ring road duct bank to the F0 building, which is adjacent to MI-60. From F0 to MI-60, the cabling is carried by overhead lines on temporary poles.

General System Description

Structure

All of the Fermilab accelerators are operated through a uniform control system known as ACNET (Accelerator Controls Network); machines from the Linac to the Tevatron and Antiproton Source are connected through this system. The controls for the CDF detector and some of those for D-Zero are similarly included. A diagram of the computers and networks of this control system is presented in Figure 3.7-1. Since ACNET, as can be seen, is modular at the hardware level but generic at the user interface, it is a straightforward matter to attach a new major system such as FMI to it.

Front ends and alternatives

There are three major means in which accelerator hardware is connected to ACNET.

- Intelligent subsystems. These are the most modern interfaces. They consist of computer backplane bus crates with single board computers and direct connection to our backbone Token Ring network. At present, these systems are connected only to the Tevatron but not to the Main Ring. However by the time the FMI becomes operational, certain of its subsystems will be connected in this manner.

- CAMAC. The Tevatron control system was built utilizing this standard as a field bus, and in the period since the Tevatron's construction most of the older equipment has been reconfigured utilizing it. The most recent of these conversions has been that of the bulk of the equipment providing control and monitor of the Main Ring.

- Older equipment based on MAC computers. Before the construction of the Tevatron most connection to hardware was effected through Lockheed MAC-16 computers and Fermilab constructed MIUs (Module Interface Units). Main Ring (and Booster) RF is still controlled in this manner. Additionally the Main Ring guide field ramp is generated by two Digital Equipment Corporation PDP-11/55 computers which are made to look like MACs to the rest of the control system. All of this equipment will be replaced in Main Ring prior to completion of the Main Injector.

Host

The central Host system consists of a number of DEC-VAX computers. It is used for software development and archiving by programmers of the control system and for a variety of real time tasks. The most important single task is operation of database software. The ACNET database contains addressing and scaling information for all of the attached hardware. In addition the Host runs the software modules for central file sharing and alarm distribution. The control

TEVATRON CONTROL SYSTEM COMPUTERS AND NETWORKS

04-20-92

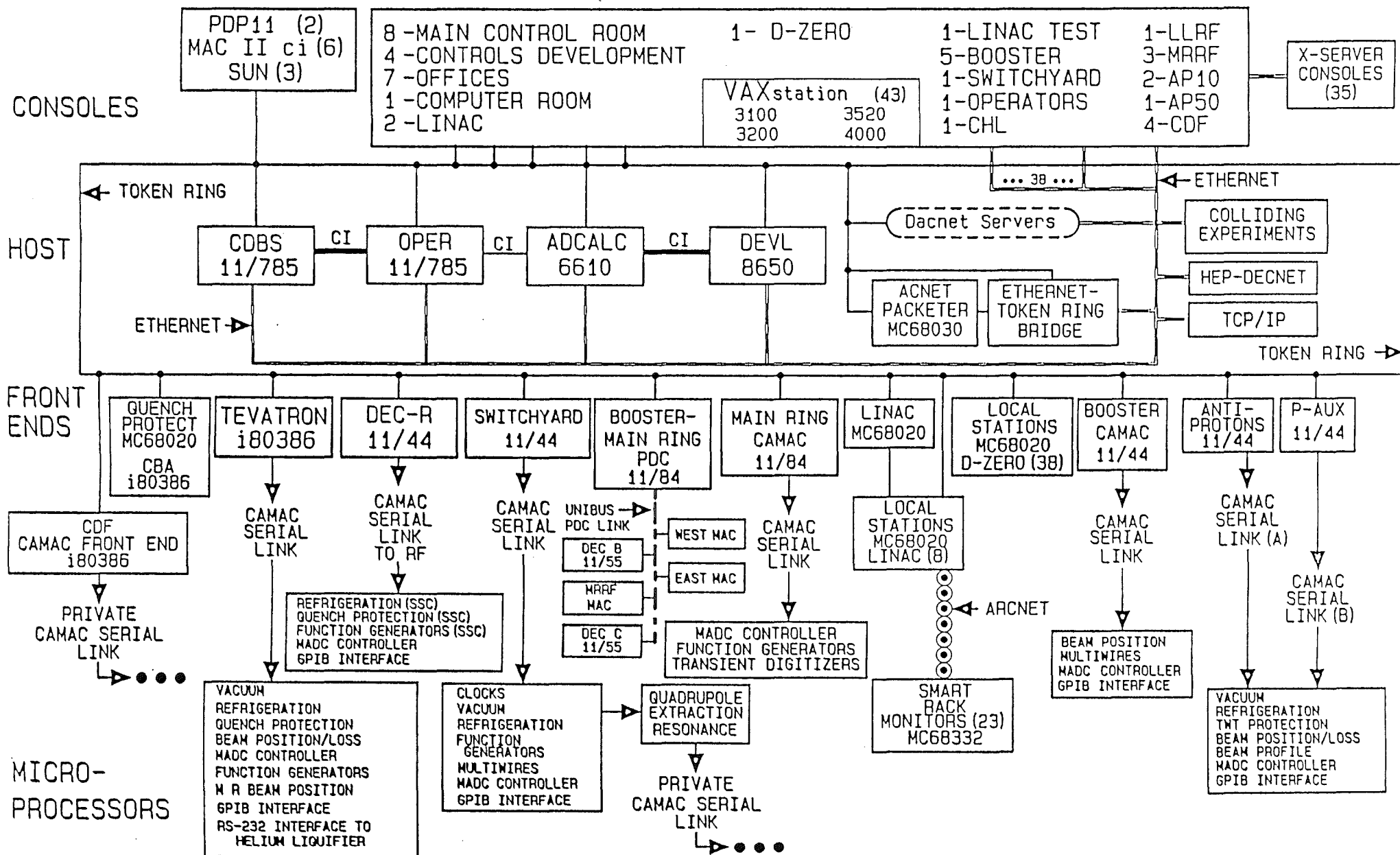


Figure 3.7-1. Schematic of Fermilab ACNET Computers and Control System

software will be made aware of the replacement of the Main Ring with the FMI by modifying this database appropriately.

Consoles

Most consoles are DEC VAXstations running the Motif windowing system, with X-terminals, Macintoshes, and a few UNIX workstations also utilized. As all consoles are either connected or bridged to the backbone network, each is able to monitor and control the operation of any of the accelerators. Furthermore, as the network is site-wide they may be placed at locations remote from any control room. In particular they will be made available at FMI service buildings to aid in commissioning.

Processor subsystems

The Title I document listed three processor systems which were to be installed and commissioned in Main Ring and then made available for Main Injector use. The first of these was the Main Ring front end computer (called NFE-M in Title I) which at the time of that writing was under construction, using parallel arrays of i80386 microprocessors housed in Multibus II and with direct Token Ring connection. Now the front end computers described earlier are mature devices in both hardware and software, controlling without incident a large fraction of the complex. The original specification was for a new front end to be constructed for Main Injector, to avoid disruption of remnant devices which would still have been connected to the original Main Ring link. This concept remains active, although the possibility of recycling the whole MR front end is still open.

The other two processor systems mentioned as to be constructed first for Main Ring were the MECAR main dipole ramp generator and a new system for control of MR HLRF. The first of these is nearly complete and has been given some preliminary tests with real MR power supplies. It is a VME-based microprocessor subsystem. Like other modern parts of the control system, this chassis will have a direct connection to the Ethernet backbone network. The MR HLRF system is in the process at this time of being specified in detail.

An idea which is slowly gaining acceptance is the construction of a generic VME "far front end." The control system as it exists consists primarily of CAMAC devices, with a certain number of remote microprocessor based subsystems. However almost all new development involves the latter concept. It appears that the cost effective way to move controls in this new direction is to make available VME (or under some circumstances VXI) crate space in service buildings, with appropriate timing, hardware, software, and networking interfaces. New developments will then be able to concentrate on the subsystem of interest and not be hindered by

infrastructure development. If such a system has become standard, or is indeed becoming a reality, by the time of Main Injector controls installation, then an ECR will be filed to include it. The timing of this development is such that it is unlikely such a system will ever be constructed for Main Ring. The testing of the concept will likely occur in the Tevatron or Booster.

WBS 1.1.9.1 CONTROLS FOR MAIN INJECTOR RING

Hardware work in Main Injector

As a general rule, the recycling of Main Ring equipment into the FMI works well for controls. As was discussed above, all of this hardware is either reasonably up to date, or is in the process of being modernized. The equipment to be recycled includes CAMAC crates and power supplies, a large number of CAMAC modules, multiplexed ADCs, the MECAR ramp generation system, and whatever is developed in the coming months for RF control. Detailed below are those pieces of hardware for which simple recycling is not appropriate.

WBS 1.9.1.1.1 COMPUTERS AND LINKS

Links and repeaters

The controls signals in the Main Ring/Tevatron complex are carried on a combination of copper Heliac and fiber optic cables. It is unrealistic that these be removed to a new location, and thus those currently serving Main Ring will be left in place to take care of future expansion of needs for Tevatron or the collider detectors. A trunk cable of 36 optic fibers will be installed, with half connected and the rest reserved for future expansion. The work involved is construction and installation of electro-optic repeaters, pulling of the cable, and termination of the fibers.

Clock systems

The present accelerator uses a number of clock systems to control devices and to time beam transfers. The primary accelerator time clock is a 10 MHz clock known as TCLK, onto which up to 256 events can be encoded. The TCLK system is widely distributed and utilized throughout the accelerator complex with transmitters and receivers in each service building and clock decoders embedded in a wide range of controls hardware equipment. A total of 174 TCLK events are presently defined and utilized. A TCLK event is realized by the transmission of 8 bits of data enveloped by a start and parity bit in the serial clock stream and is 1 microsecond in duration. TCLK events are designated by a two-character hexadecimal number preceded by a dollar sign and range from \$00 through \$FF. The events are generally allocated in groups to different parts of the accelerator with 23 currently associated with operation of the Main Ring. Clock events provide individual accelerator resets, initiation and monitor of magnet ramps, and initiation or notification of other sequences. For example, event \$29 is a reset for the Main Ring cycle assigned to antiproton production. Magnet power supplies, rf systems, diagnostics, etc. are

activated by the occurrence of \$29 to do specific things particular to antiproton production as distinguished from the other 6 types of Main Ring cycles.

Both the Main Ring and Tevatron also have clock systems which are locked to the rf frequency of the machines and are known as beam synchronous clocks, MRBS and TVBS. These are formed by dividing the rf frequency by 7 to produce a clock that is approximately 7.5 MHz in frequency. (Note that the Booster, Main Ring, Tevatron and Accumulator all have 53 MHz rf systems operating at harmonic numbers which are multiples of 7.) The beam sync clock systems are able to use the techniques, transmitters, receivers, and decoders identical to those used for TCLK. All beam transfers between the circular machines require this precise timing to initiate kicker firings which are synchronized to the gaps in the beam. Each of these beam sync clocks can have up to 256 events encoded, though event utilization is approximately an order of magnitude less than TCLK. An important aspect of each of these beam sync clocks is the presence of a revolution frequency event known as the "A" marker (\$AA) which in the Main Ring or Tevatron occurs every 21 μ s and to which injected and extracted beam is synchronized. Another example of a beam sync clock event is MRBS \$7C which initiates the transfer of a coalesced proton bunch from the Main Ring and the Tevatron. The actual beam transfer has a coarse timing reference to a TCLK event, a precise reference of \$7C to the \$AA Main Ring revolution event, and a final delay measured in multiples of 7 rf buckets from the \$7C event. When necessary, finer timing control is achieved with commercially available control cards.

Beam Transfer Control Issues

Transfer cogging refers to the operations necessary to place beam into a specific bucket(s) in the Tevatron from specific bucket(s) in the Main Ring. This operation arises from the need to inject beam on more than one injection cycle, either from the Main Ring now or from the Main Injector in the future. Transfer cogging involves the rf systems, instrumentation (which historically has provided low level rf control at Fermilab), and controls. In the Main Ring, which is the same circumference as the Tevatron, transfer cogging is done in a series of steps involving (i) phase-locking the Main Ring to the Tevatron; (ii) after phase-lock, measuring the offset, in rf buckets, between the "A" markers of the two machines; and (iii) executing a frequency program to bring the "A" markers into alignment (where "into alignment" can also mean with some offset specified in advance). For the Main Injector, with its circumference smaller than the Tevatron in the ratio of 28 to 53, transfer cogging will have to take a different course. One possible approach is discussed here; other techniques will also be considered.

As the Main Injector reaches the 150 GeV level, it is phased-locked to the Tevatron using a 21st subharmonic. To accomplish this, the rf signal for both the Main Injector and Tevatron is

divided by 21 in sync with each machine's revolution "A" marker, to produce clocks that are approximately 2.5 MHz in frequency. This developed clock of 2.5 MHz is an $h = 28$ clock for the Main Injector, and an $h = 53$ clock for the Tevatron. The phase-lock will align these 2.5 MHz clocks. After phase-lock has been accomplished, beam has been prepared for transfer (e.g. coalesced, if desired), and Lambertson power supplies have ramped to the proper level, a TCLK event or timing developed from TCLK can signal "prepare for transfer". Sometime during the next 53 revolution periods (or "turns") of the Main Injector, which is 28 turns of the Tevatron, there will be a singular coincidence between the Main Injector and Tevatron "A" markers. This coincidence, which occurs every 586 milliseconds, is simply a consequence of the fact that 28 and 53 have no common factors (in fact, 53 is a prime number). Beginning from this coincidence and while the Main Injector and Tevatron rf systems are in phase-lock, the relative positions of the two "A" markers and the Main Injector circulating beam are determinate and repetitive. From this coincidence, a Main Injector beam synchronous event may be easily developed to initiate and effect the successful transfer of Main Injector beam into particular Tevatron buckets. The MI extraction and Tevatron injection kicker firings will be referenced to this event with appropriate adjustment to account for kicker locations and rise times.

The general problem, albeit theoretical, of being able to transfer beam in any Main Injector bucket into any Tevatron bucket is not fully solved by the above outlined approach and will be explored to the extent necessary. Solutions include utilizing the existing capability to deliver Booster beam into any Main Ring rf bucket, or of offsetting the unique coincidence of Main Injector and Tevatron "A" markers by a specified number of rf cycles. The "Sequencer" program, which presently controls the beam transfers into the Tevatron, could be involved in setting parameters associated with Booster transfers or of controlling the "A" marker offset for each MI transfer cycle.

WBS 1.1.9.1.2 CRATES, CARDS , RELAY RACKS AND CABLING

Relay racks

The decision was made early in Main Injector planning that all relay racks would be the responsibility of Controls. As racks are typically shared among several groups, and serve several separate functions, it was found necessary to have a single person to whom all needs would be transmitted and who would be charged with assigning the appropriate space. The number of racks budgeted and the space for them allotted in service buildings is based on reasonable extrapolations of those needed to accomplish similar functions in the Main Ring. Detailed looks at the number of rack-inches required continue to show less budgeted excess than would be hoped at this stage in the project. Thus it is particularly important that needs be carefully monitored. Figures 3.7-1 to 3.7-4 indicate the positions and utilization of racks in both MI-60 and MI-10, the

latter having been chosen as a typical service building. Also shown are the proposed positions of controls and networking equipment in the racks at MI-10.

WBS 1.1.9.1.3 CATV SYSTEM

Until recently it was traditional at Fermilab to include television systems under accelerator controls, and that practice has been followed in the WBS. Several channels of CATV will be run around the ring and connected to the various control rooms. Some channels will convey beam diagnostic signals such as scope traces and fluorescent screens, and others will provide live observation of remote locations for security purposes.

WBS 1.1.9.1.4 FIRUS SYSTEM

The Facility Incident Reporting and Utility System (FIRUS) also falls under the province of controls. All new buildings and the new tunnel will have connection to the lab wide system for fire alarms and, where appropriate, for security alarms as well. There will also be one or more FIRUS display consoles installed in the new buildings.

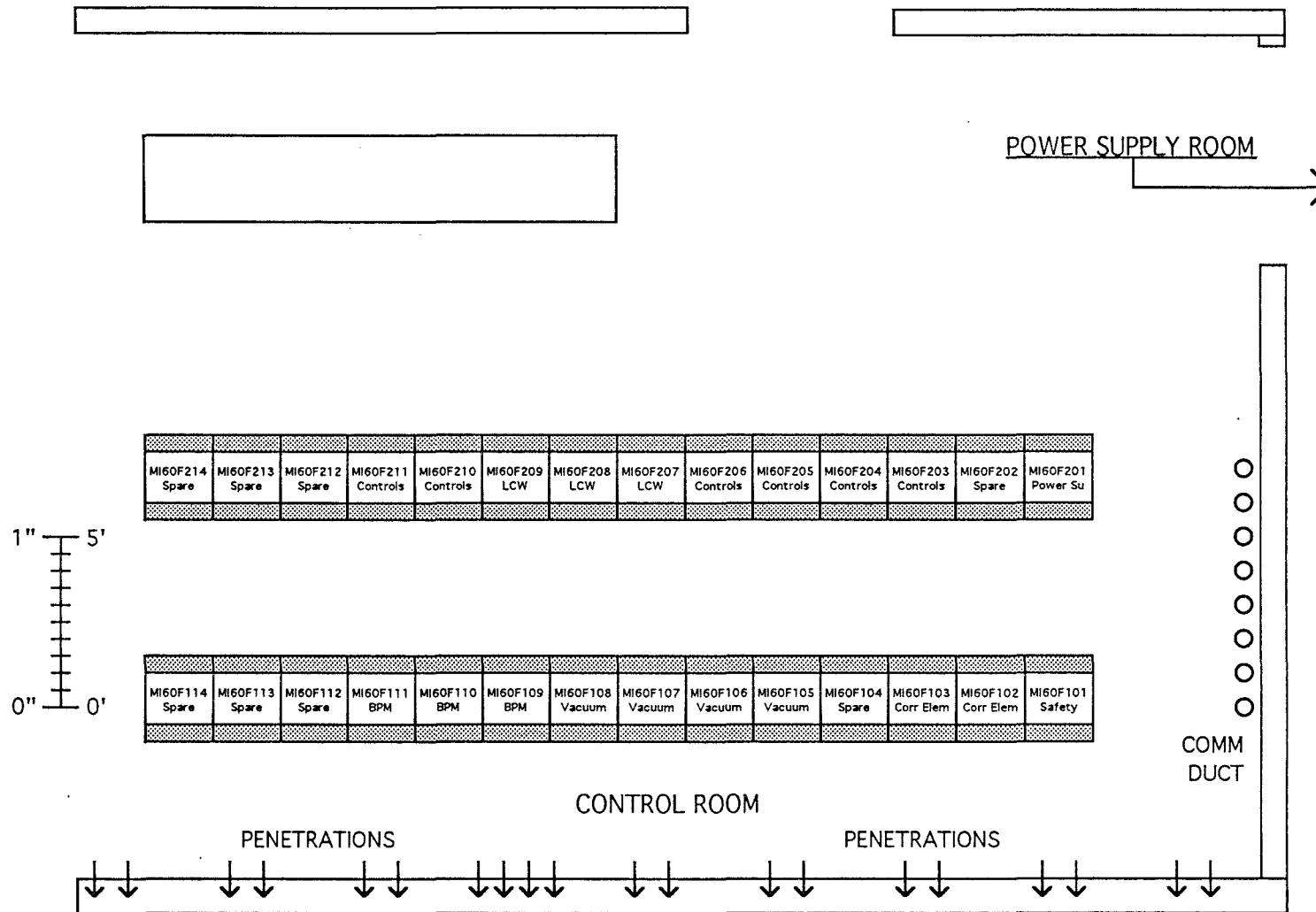
WBS 1.1.9.10 BEAMLINE CONTROLS

All of the topics which pertain to the hardware in the FMI ring pertain as well to the associated beamlines. However there is one major difference between the two, dealing with the fraction of CAMAC hardware which can be recycled. In the case of the ring, there is enough equipment of the proper types being decommissioned in Main Ring to cover virtually all the needs. However the new beamlines are longer and more complex than the current ones which they are replacing, and there is not sufficient controls equipment to service them. In particular a significant number of power supply and beam position monitor controllers will need to be constructed.

WBS 1.1.13.1.5 RING INSTALLATION

WBS 1.1.13.10.5 BEAMLINE INSTALLATION

The major installation task for the control system is the physical act of putting in place the various pieces of CAMAC equipment. As noted above, in the ring most of this equipment will be recycled, while in the beamlines a larger fraction will represent new construction. In both cases a relay rack must first be installed and powered; then CAMAC crates and MADC units put in place followed by CAMAC module insertion and cabling of the various system elements. In the case of the recycled components the above steps (with exception of the relay rack work) must first be undone in the old location. The other major installation efforts concern the optic cable and the reconfiguration of RF controls after completion of construction.

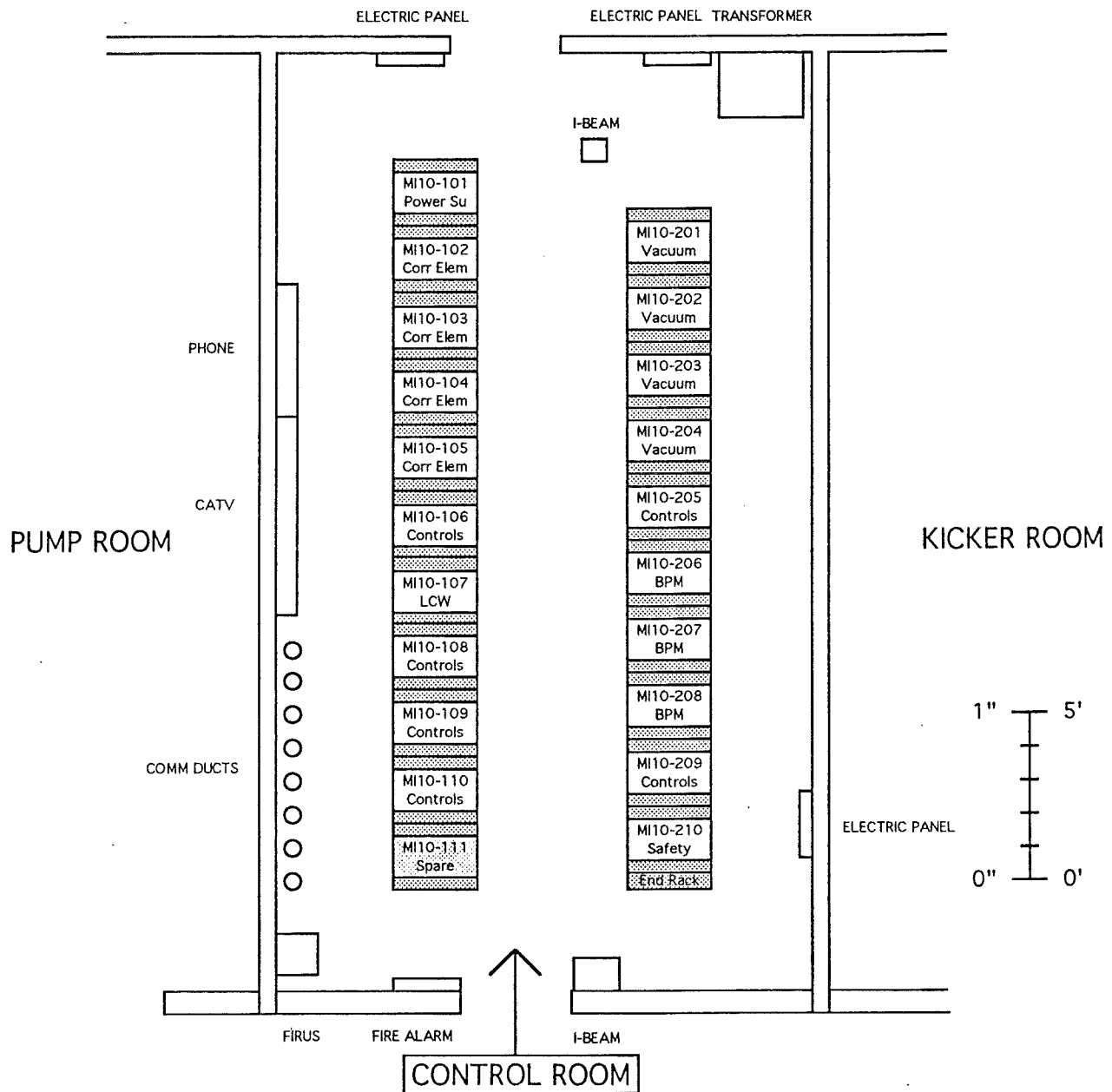


Rack Allocation for MI-60NW Control Room

Figure 3.7-2. Layout of Controls Racks in One End of the MI-60 Service Building

K. C. Seino, 11/24/92

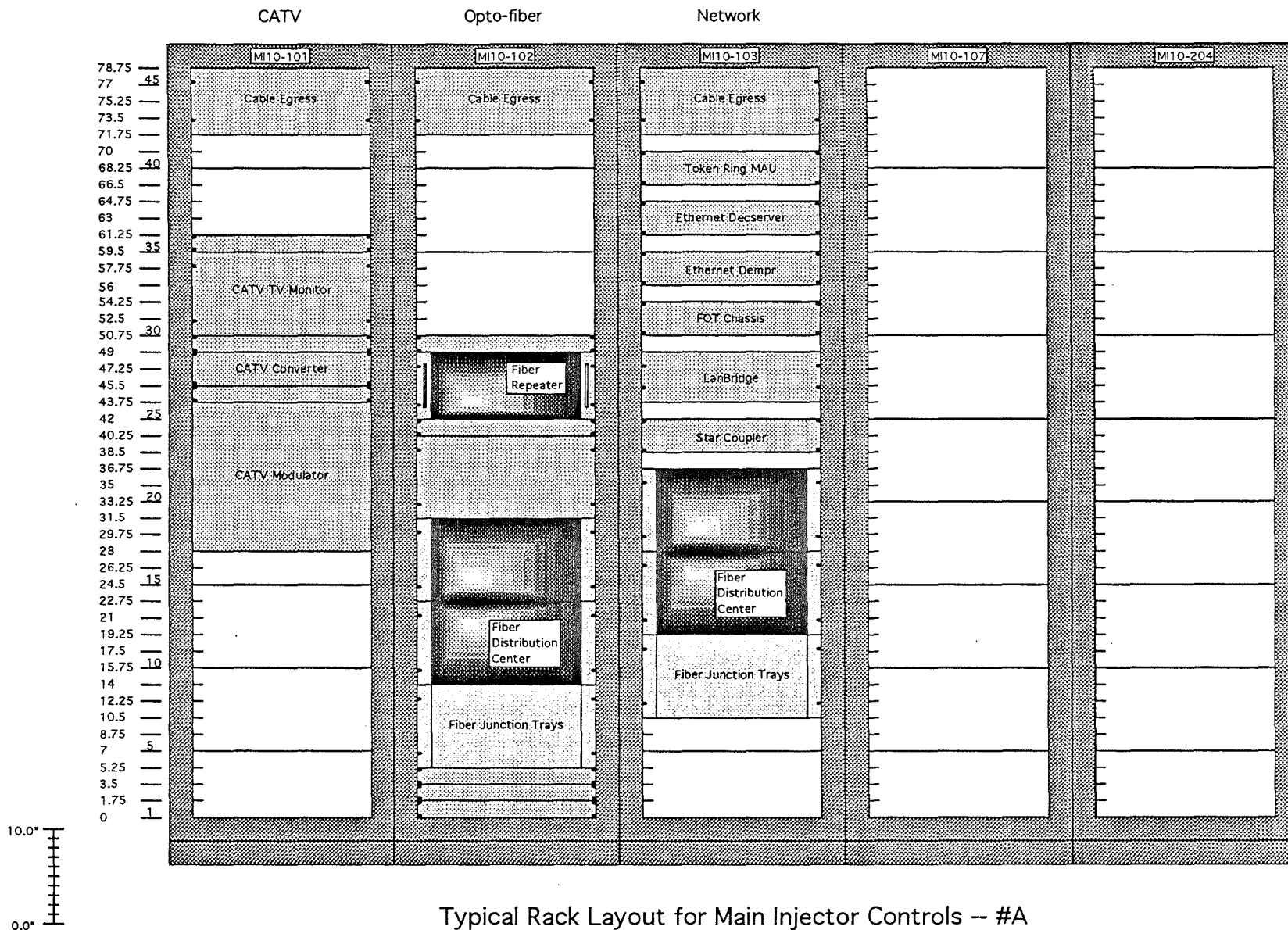
POWER SUPPLY ROOM



Rack Allocation for MI-10 (Typical) Control Room

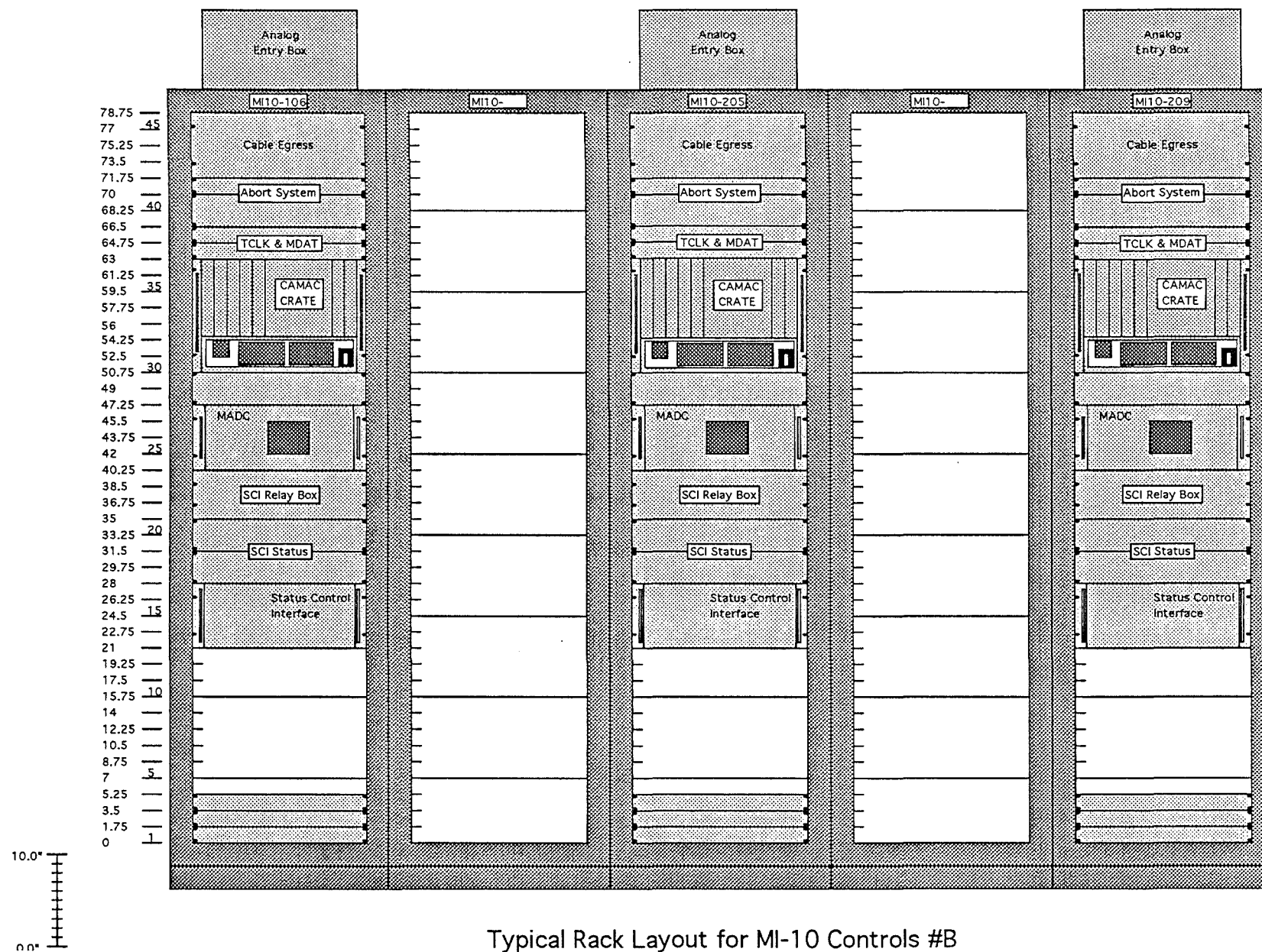
K. C. Seino, 11/ 5/93

Figure 3.7-3. Layout of Controls Racks in the MI-10 Service Building.



Typical Rack Layout for Main Injector Controls -- #A

Figure 3.7-4. Rack Layout for Controls Racks for CATV, Fiber Optics, and Ethernet



Typical Rack Layout for MI-10 Controls #B

Figure 3.7-5. Rack Layout for Controls Racks for Systems Control

WBS 4.1.8. SOFTWARE

The question of the amount of software effort required for this project has been the subject of serious discussion in the past. Since the controls hardware is precisely that of the Main Ring (or in the case of the beamlines copies of existing modules) new software support is by and large not required. A change in the database indicating the location of the module and the name of the hardware signal to which it is attached is generally sufficient. Described below are those areas where changes or additions are known to be required.

Far front ends

Those microprocessor crates which are attached directly to the backbone network, without benefit of an intervening front end computer, are sometimes referred to as far front ends. Those under construction for the Main Ring include the ramp generator and any intelligent RF controller which might emerge. Additionally a new universal BPM system is being proposed which will encompass the Main Ring and will utilize the far front end principle. Some changes of a significant nature will be required in the ramp generator, due to the higher ramp rate and different power supply configuration. However that software is being developed with such future changes in mind. Similarly some changes related to voltage levels and ramp rate are envisioned in a smart RF controller.

Front ends

The major functions of a CAMAC front end, such as that serving the Main Ring or FMI, are database driven. Since there has been no hardware proposed which does not already have support, a database change is in principle sufficient. In practice there are a number of tables required in a front end detailing the configuration of CAMAC crates, MADCs, and certain modules which are addressed in a "wild card" or ring-wide manner. Parameters arise in all accelerators which in practice can only be supported by a small piece of unique code in the front end. It is anticipated that this will happen for FMI as well.

Database

As has been frequently noted above, a database entry detailing the changes (in location, function, scale factors) pertaining to any particular piece of controls hardware is all that is required to have the system adapt. A systematic naming convention for FMI devices will have to be developed by the operations crew, and careful records kept by personnel who move the hardware. When these things are done the modification effort will be minimal.

An active project at this time is a change from our current in-house developed database to a commercial one. One of the features that such a system will be required to have is the ability to

prepare reports on entries satisfying a variety of conditions. Such a feature should be particularly valuable when large numbers of changes, such as those envisioned here, are being made.

Console applications

There are 99 application entries on the Main Ring index of ACNET software. Some of these programs will require significant changes, particularly those dealing with machine physics (WBS 1.3.2). Those which display all data from a particular subsystem in a ringwide fashion, or in general deal with global information, will require changes to the user interface and data acquisition to deal with the smaller ring. Many of the Main Ring programs are copies of the generic Parameter Page which is widely used for reading and setting any quantities in the database. Since certain combinations of parameters often need to be studied or set together, permanent subpages containing the lists are established and entered on the index as separate programs. Many of these pages will require reconfiguration; however no new software needs to be written for this to happen.

CHAPTER 3.8 SAFETY SYSTEM

WBS 1.1.10. SAFETY SYSTEM

3.8.1. Purpose

The purpose of safety systems is to prevent injury, death, or serious over exposure from beam-on radiation, X-Rays, or high voltage / high current power supplies.

3.8.2. Safety System Philosophy

The basic philosophy that determines all safety system designs is encompassed in the idea of providing the necessary hardware, procedures, and knowledge to insure the well being of personnel. To meet this goal, two systems have been developed to provide protection from the dangers of accelerator operations. Radiation systems are designed to protect personnel from exposure to particle beams. Electrical safety systems have been developed to provide protection from high voltage and/or high current devices.

Inherent in each of these systems is the concept of redundancy. All hardware shall be designed in such a way that no single failure will result in the loss of protection. To accomplish this, two separate circuits are used to detect specific conditions. For example, each door that is monitored uses two separate switches to detect the status of the door. Each of these switches in turn is connected to a separate control circuit. Thus if one switch were to fail, the other would still operate thereby providing the necessary protection. An extension of the redundancy concept is used in controlling radiation safety system critical devices. A critical device is one that prevents beam from entering an area. Two critical devices will be controlled by a radiation safety system. Thus when a possibility exists for personnel to be in an area, two devices are inhibited to provide protection.

Another key characteristic used in designing all safety systems, is the idea of "fail-safe" circuits. All circuits are designed in such a way that if a circuit fails, the failure would result in a safe condition. For example, if the cable that controls a device were cut, the device could not be enabled. In this way personnel are still safe.

Perhaps the most important part of the radiation and electrical safety systems is the searching and securing of an area. This is done to insure that the area is not occupied before beam or power supplies are enabled. The securing of an area requires that a minimum of two qualified persons thoroughly search an area in a predefined sequence.

The search sequence will be programmed into a Programmable Logic Controller for the Main Injector Radiation and Electrical safety systems. The order in which the interlocks are reset

has been designed to assure the area is searched in a logical order, thereby assuring personnel are not missed by the search team. Periodically dummies will be placed into an enclosure prior to being searched to verify the enclosure is being searched correctly.

Once an area has been searched and secured, status displays on the outside of each controlled access door and each section gate indicate to individuals that the area is interlocked and that access is forbidden to unauthorized personnel. Immediately before beam is brought into an area or power supplies are enabled, a prerecorded message consisting of a siren and verbal announcement will be played to allow personnel, which in the unlikely event of being missed on a search, time to push an emergency crash button and/or leave the area. In addition to the audible warning, strobe lights will flash giving a visual indication the area is transcending into a hazardous state while the audio message is played. Emergency crash buttons, audio warning speakers, and visual warning strobes will be located at approximately 125 foot increments. Pushing one of these buttons will inhibit beam and power supplies and require that the actuated switch be locally reset before the area can be enabled.

As a further means of assuring the proper operation of the safety systems, all systems shall be tested in accordance with the Fermilab Radiological Control Manual or the Fermilab Environmental, Safety, and Health Manual as applicable. During these tests, all circuits will be carefully checked and test results documented.

All doors to an area are locked and the keys to open these doors are interlocked and guarded in the Main Control Room or at MI-60 in a locked and interlocked remote key tree. Distribution of these keys is not taken lightly. Only authorized personnel are allowed access. The type of access determines the authorization level required for the individual.

3.8.3. Interlock Group Training

All new employees to the interlock group shall undergo job specific training on the Accelerator Division Interlock Systems prior to performing unsupervised maintenance or repair activities. This training begins with system walk-throughs and reading functional descriptions in the Accelerator Division Interlock Manual. After approximately one month of joining the interlock group, the technician will attend a series of lectures given by the Interlock Engineer or Senior Technicians on the internal workings of the interlock systems.

To further enhance employee knowledge, a training system has been developed. With this system, intentional system faults can be introduced to test and reinforce overall system knowledge. When the Interlock Engineer feels the technicians knowledge has progressed to the

point of allowing unsupervised work on the interlock systems, he will recommend the Accelerator Division Head authorize the technician to work on the interlock systems.

To insure the technicians maintain their system knowledge, monthly training lectures on subsystem components are given at one of the biweekly group meetings. This training shall be conducted and documented in accordance with Accelerator Division ES&H Departmental Procedure ADDP-SH-2007.

3.8.4. Working on the Safety System

Each of the Accelerator Division safety system interlock and junction boxes are locked and has the following label affixed to it:

This box to be opened only by persons authorized
by the Senior Radiation Safety Officer.

Any maintenance or repair work may only be made by personnel authorized in writing by the Accelerator Division Head. Those currently authorized to work on the safety system are listed in Appendix 1 of Accelerator Division ES&H Procedure ADDP-SH-2007. Appendix 1 is a memo signed by the Accelerator Division Head and is updated as necessary.

Prior to performing any work on the safety interlock system, adequate steps shall be taken to insure that beam can not enter or power supplies can not be energized in the area effected.

When repair or maintenance work is performed on a system, the open unit shall not be left unguarded.

3.8.5. Documentation and Modifications of Systems

All safety system related drawings, schematics, and procedures shall be clear, accurate, and up-to-date.

System documentation must contain a complete set of drawings detailing all system components and interconnections, a written functional description, and written, reviewed, and approved test procedures.

The initial Main Injector safety systems, or future modifications to these systems must be fully documented and approved for use by the ES&H Section Head **prior** to their use.

All modifications which increase the level of safety to an area must be fully documented and notification of the change sent to the ES&H Section Head. The placement of radiation detection devices and the trip level settings will be performed at the discretion of the Accelerator Division RSO. A list of all interlocked radiation detectors and associated trip levels will be maintained in the Accelerator ES&H interlock group area.

All work performed on the safety system shall be documented in the Interlock Group logbook. This includes normal maintenance, modifications, and repair of failures. This logbook shall be maintained in the interlock group area, and entries shall be made within 24 hours of the occurrence.

All failures will be completely documented with date, time, nature, and consequence of interlock failure (lost time, fail safe, fail unsafe, etc.). This reporting will also include unsafe failures of equipment utilized to provide part of the interlocks (at present radiation detectors and RF detectors). Fail safe failures of radiation detectors and replacement of radiation detectors due for calibration will be documented by the Accelerator Division Radiation Safety Officer or designee.

3.8.6. Safety System Keys

Within the Accelerator Division ES&H Department, only the ES&H Department Head and the ES&H Department Interlock Engineer are authorized to order safety system related keys. However, the Accelerator Division Head for AESH must also approve all requisitions before being sent to the Purchasing Department.

All uninterlocked keys shall be locked in cabinets. Control keys, power-on keys, and spare keys are located in a special cabinet. Only the AD ES&H Department Head, the AD ES&H Department Interlock Engineer, and the AD RSO have a key to these cabinets. When these keys are used, they must be logged "in" and "out" in the key logbook.

Uninterlocked radiation or electrical safety system keys are particularly important and their use requires additional precautionary measures. Prior to the actual use of the key, the Accelerator Division Head or designee will review the necessity of using the key, the manner of use, and any safety precautions required. If the usage of the key is to jumper or bypass portions of the radiation safety system, the ES&H Section Head will also be contacted for approval on these matters.

Once these approval(s) have been obtained, the manner in which the key is to be used will be recorded in the Main Control Room crew chief's logbook by a staff member of the Accelerator

ES&H Department. The expected length of use or period of time that the key will be used in this manner will also be recorded. At this point the key may be released from the VIK (Very Important Key) cabinet by either the ES&H Department Head, the ES&H Department Interlock Engineer, or the Accelerator Division RSO. At the conclusion of the special use period, the key will be returned to the VIK cabinet and noted in the crew chief's logbook. The Division Head and the ES&H Section Head as applicable will be informed that the key is again properly secured. The only exception to this is the use of spare interlocked safety system keys needed for safety system testing. These keys will be logged in and out of the VIK cabinet in the test procedure for the area being tested.

The spare interlocked keys to be maintained by the Accelerator Division will be area Enter keys, Search and Secure keys, and Kirk keys. Search and Secure and Kirk keys are not capable of allowing access into any enclosures. These keys will be maintained for replacement of broken keys and safety system testing only. All spare keys will be kept in the VIK cabinet and inventoried in conjunction with interlock tests for that area.

The loss of any interlocked key for an area will render the lock set compromised. All locks in the set will be replaced by a new or uncompromised lock set prior to use of the area. **Any deviation from this policy must be approved in advance, in writing by the Accelerator Division Head and the ES&H Section Head.**

3.8.7. Testing

In keeping with laboratory policy, the Accelerator Division safety systems shall be tested at least once every six months while operational or prior to startup of an area previously unused. A one month grace period is allowed for systems that are in use. All test procedures will be written and at a minimum include the precautions necessary to prevent the entrance of beam or the energizing of power supplies in the area(s) being tested, testing of each interlocked key, each door switch, each critical device, each radiation activated interlock, and an inventory of all spare uninterlocked keys and the area Control keys. At least once during interlock testing, the system shall be exercised from beginning to end, to insure an interlock violation causes the correct response.

After working on the safety system, the portion of the system affected by the work must be tested. In those cases where a definitive test is not practical, a preliminary check must be performed. At the earliest available time, a more complete test shall be performed when necessary. The Interlock Engineer shall review the adequacy of tests performed after repairs or maintenance.

The adequacy of all semi-annual interlock tests shall be reviewed by the ES&H Department Head, the ES&H Department Interlock Engineer, and the Accelerator Division RSO in accordance with Accelerator Division Procedure ADSH-10-0001. For additional information on safety system testing and approval requirements see the Accelerator Division ES&H Procedure ADDP-SH-2001.

3.8.8. Jumpering

Placing a jumper in a safety system shall be performed only as a last resort. When this jumper reduces the level of safety (i.e. jumpering one of two or more critical devices), authorization must be approved by the Accelerator Division Head, the Accelerator Division ES&H Department Head, and the ES&H Section Head.

In those cases where a jumper is placed in the system that does not reduce the level of safety, but is used merely as a means of permitting the normal operation of the machine (i.e., sequence loop jumper), authorization must be granted by the ES&H Department Head or the ES&H Department Interlock Engineer.

In those cases where a "jumper" (jumper is used here in its broadest sense) is necessary to investigate a problem, a written note must be made so as to preclude the possibility of leaving the jumper in place.

The placement of a jumper (usually a wire) shall be:

Given an identifying number.

If a wire, it should be colored red.

At least one foot in length.

Placed away from cable ducts and similar hardware so as not to give it the appearance of being an integral part of the system.

When requesting a power supply jumper, the requester must fill out an Accelerator Division Safety System Power Supply Jumper Request form for each power supply to be jumpered. This form is reproducible and is to be pink in color. Accompanying this form must be a written description of how long the jumper is needed, the additional safety precautions to be used to insure personnel safety, and who is authorized to energize the power supply while the jumper is in place. The form must then be approved by an Accelerator Division SSO and / or the Accelerator Division Interlock Engineer before the supply will be jumped by the Interlock Group.

When requesting a critical device jumper, the requester must fill out an Accelerator Division Safety System Critical Device Jumper Request form for each critical device to be jumpered. This form is reproducible and is to be yellow in color. Accompanying this form must be a written description of how long the jumper is needed, the additional safety precautions to be used to insure personnel safety, and who is authorized to energize the critical device while the jumper is in place. The form must then be approved by an Accelerator Division SSO and the Accelerator Division Head before the supply will be jumpered by the Interlock Group. If the jumper will decrease the level of safety for the area, the ES&H Section Head must also approve the request.

After approval of either a power supply jumper request or a critical device jumper request form, a copy of the completed form will be given to the Operations Department Crew Chief as notification of work in progress on a device. The original form will be maintained by the interlock group on the jumper status board until the jumper is removed and the safety system interlock is retested. Upon completion of testing, an additional copy of the form will be given to the Crew Chief, the original is to be maintained by the interlock group.

3.8.9. General Search and Secure Responsibilities and Procedures

It is the responsibility of the search team to insure that no one remains inside the searched enclosure after the search is complete. Searching an enclosure means looking above, under, behind, and inside spaces where a person could be. While searching, the team must move in a logical and coordinated manner. The sketches and text in this manual indicate more specifically the proper sequence for searching. The searching sequence has been designed to aid in preventing personnel from going undetected. However, a safety system is limited in its capability to enforce a proper search. The responsibility of searching an area must be taken very seriously. Should someone be left inside the enclosure, the number and types of dangers that exist make it likely that a serious accident would occur. As the searching proceeds, the team must insure that all doors lock properly and that the interlock boxes are functioning.

A problem arises when an area is not yet secure, but controlled access keys have been distributed to allow entry through a door, since personnel may not be on the authorized access list. To insure that only authorized personnel have controlled access keys, the search and secure team shall perform the following.

Before the Search and Secure Begins:

The key trees for the area must be checked to determine the number of keys out.

Every key for the area must be verified to be in the possession of a person on the authorized list. If any personnel not on the authorized list has a key, that key / person must be retrieved before the search and secure starts. All keys that are out, must be logged in the Controlled Access Logbook.

Bear in mind that although key accountability is important, it is not the most important function of the search team. The most important function is to insure that there is no possibility that personnel could be in an interlocked enclosure without having an interlocked key for that area. The search team is to insist that each individual encountered in the enclosure exit the enclosure ahead of the search team. In addition, the search team should also insure that individuals are keeping with the Accelerator Division policy of using the "buddy system".

3.8.10. Critical Device Interlock Interfacing

The number and types of critical devices makes it difficult to completely specify a standard for interfacing. However, the safety system must be able to control as well as monitor the device.

Control of the device will typically be to supply 24 Volts D.C. to the device directly. The control voltage will be enabled when the area has been determined to be safe.

Status of the device must be at a point in the circuit to completely indicate to the safety system that the device has functioned correctly. If a power supply is used, both the "ON" and "READY" status of the device are required. Contact closures will be used for this purpose. The safety system will supply the signal to detect the condition of the supply. Note that the safety system monitors critical devices in a fail-safe manner. Specifically, a surveillance current is constantly passed through the status contacts of the device. If the contact opens, or the cable is cut, the safety system will assume the worst case which is that beam is allowed.

If a power supply such as a pulsed power supply contains storage capacitors and therefore merely turning the supply off will not necessarily render the area safe, additional precautions such as a crowbar to discharge the capacitor bank should be used. Alternately, some circuit to monitor the state of the capacitors and supply that information to the safety system would serve equally well to determine the status of the device.

3.8.11. CARESS

Each of the Accelerator Division's radiation and electrical safety systems are connected to a central control module. Each of these modules are located in the Main Control Room in three relay racks. These racks have come to be called CARESS, the acronym for Central Accelerator Radiation and Electrical Safety Systems. The following describes the operation and use of each of the systems that make up CARESS.

Common Characteristics

The common characteristics for the Main Injector Radiation and Electrical safety systems include the hardwire loop, logic loop, emergency loop, ground fault detection, key tree, critical devices, and power supply permits. These represent inputs and outputs to the master control modules located in CARESS. The hardwire loop, logic loop, emergency loop, ground fault detection, and key tree are major inputs to any given master control module. The output of the module controls critical devices or power supplies for an area.

The **hardwire loop**, often called the "A" loop, consists of a group of switches hardwired in series. These switches are located on each access door to an enclosure. This loop becomes complete when all the doors to a particular enclosure are closed.

The **logic loop**, sometimes called the "B" loop, is used to augment the "A" loop and provide redundancy. This loop is connected to all the interlock boxes in an enclosure. The loop is hardwired through all the boxes and is not complete until all doors to the enclosure are closed and all the interlock boxes reset in their proper sequence. The sequence will be programmed into a programmable logic controller.

The **emergency loop**, consists of illuminated push button switches located within the enclosure. This system is provided to allow someone in the enclosure to disable the beam or power supplies in the unlikely event that he or she is trapped inside.

The **ground fault detector** is a circuit used to monitor for any ground connections on the hardware, logic, or emergency loops. This circuit will detect any cable faults with an impedance less than 680 ohms to ground. This circuit is used to detect cable faults, corrosion in junction boxes, and corrosion or water in interlock switches.

The **key tree** is also a major input to a system. The main key tree will be located in the Main Control Room and an additional key tree may be located at the MI-60 service building. The key tree contains keys to an enclosure and is provided to insure that only authorized persons are

allowed access. Persons needing enclosure access keys are logged in and out. Most important is that these keys are interlocked. This means that an area cannot be enabled if a key has been given to a person.

The **critical devices** for an area are those devices that the system controls to enable or disable beam to an enclosure. All input conditions mentioned above must be complete before the critical devices can be enabled. The Accelerator Division crew chief is the person responsible for resetting the master module. Resetting initiates a message consisting of a siren sound effect followed by a verbal announcement and ending with a siren sound effect again. The message lasts approximately 2 minutes. The strobe lights within the enclosure are also activated while the audio warning message is played. At the end of the announcement, the critical devices are given a permit and beam may be brought into the enclosure.

3.8.12. The Safety System Interlock Box

Each interlock box is connected to two switches. One is typically referred to as the "hardwire" switch and is a conventional lever actuated switch. The other switch referred to as the "logic" switch is a magnetic proximity switch. Status lights on the front of the interlock box are used to ascertain the condition of these switches as well as giving the search and secure team members information on the progress of the search.

All interlock boxes throughout the accelerator are identical. Refer to Figure 3.8-1 for an illustration of the box. The three indicators labeled: "DOOR - OPEN", "LOOP - OPEN", and "DOOR 1 - DOOR 2" are used to indicate the status of the interlock.

The "**DOOR 1 - DOOR 2**" indicator signifies the present status of the door(s). When the door is open, the DOOR 1 indicator will be lit red. When the door is closed, the indicator light will be off. The purpose of this indicator is to allow the search team to test the operation of the hardwire switch. To test the hardwire switch, the door should be opened and closed while the search team member notes the status of the indicator. In those cases where there is more than one door, the DOOR 2 indicator is connected to the outside door. Each door must be tested in this manner for proper operation.

The "**LOOP - OPEN**" indicator is used to insure that the area is searched in the proper sequence. This status light will be lit green only when the door is closed and the interlock is reset in the proper order. Should this indicator not reset during a search, either the search team is searching the area in the improper sequence, or an interlock has been broken "behind" the search team. In either case, the integrity of the search is destroyed. Therefore, the search team must return to the beginning (interlock 1) and start again.

The "**DOOR - OPEN**" indicator gives a history of the status of the door. This status light will be lit green when the door is closed and reset. The indicator will latch in this state whether or not the search is performed in the proper sequence. When the door is opened, this indicator will change to the "OPEN" status (red) and stay in that state until reset again. The purpose of this indicator is to allow the search team to test the operation of the logic switch. The search team should close the door, reset the interlock, and note that the indicator changes to the "DOOR" (green) state. When the door is opened, the indicator should be checked to make sure it changes states and remains in the "OPEN" (red) state even when the door is closed again. In other words, it must latch open.

The tests outlined above should be performed at each location except the emergency exit locations and the last interlock box in the sequence. To perform the tests as indicated above at emergency exits and the last interlock box would cause the area just searched to drop. This is because once the area is searched, it can no longer be tested without dropping the entire area. Therefore, at the emergency exits and the last interlock box to be reset, the search team tests as before with the additional requirement of keeping the reset key turned for the entire time the tests are performed. Keeping the reset key turned while testing tells the PLC not to drop the sequence loop to adjacent interlock boxes.

3.8.13 The Main Injector Safety System

3.8.13.1 Overview

The Main Injector accelerator accepts 8 GeV protons from the Booster or 8 GeV anti-protons from P-Bar and accelerates them to either 120 GeV or 150 GeV for extraction to the Tevatron or Experimental Areas. It is a synchrotron of approximately 2.1 miles in circumference. There is an 8 GeV injection line connecting the Main Injector to the Booster accelerator of approximately 0.4 miles.

3.8.13.2 The Electrical Safety System

The Main Injector Electrical Safety System is broken into two components, the MI Ring and the 8 GeV injection line. Each of these safety systems will interlock many power supplies. The electrical safety systems interlocks supplies by controlling several remote safety system interface units. The electrical safety system master module in CARESS will provide redundant permit signals to the first interface unit. The interface unit will repeat these signals to the next interface unit and so on. The interface unit is capable of interlocking 12 different power supplies or devices to the safety system. Each device connected is provided redundant relay contact closures to permit the device.

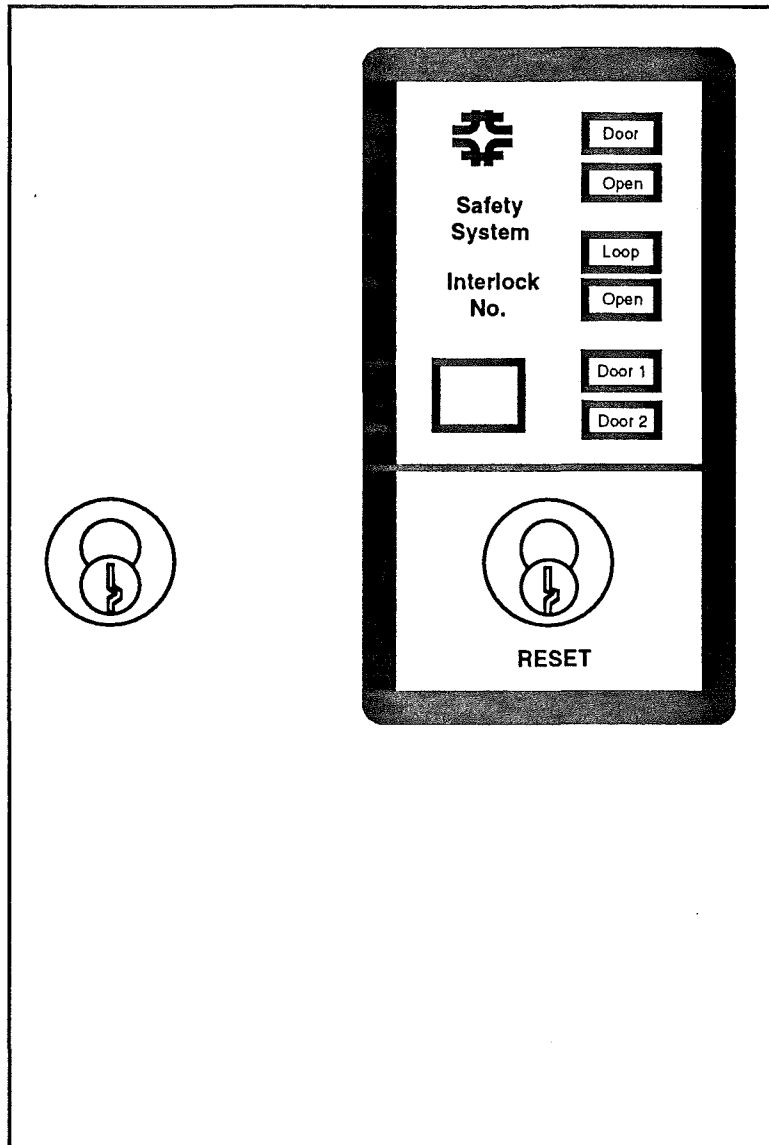
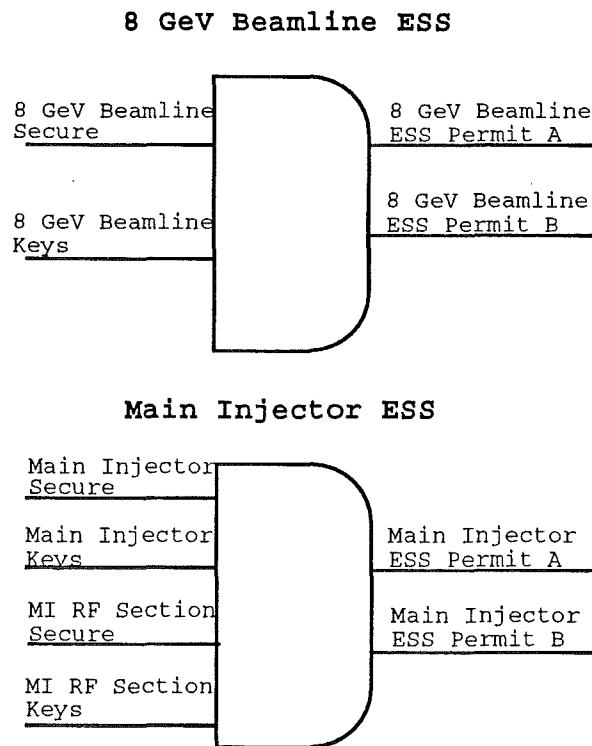


Figure 3.8-1
Safety System Interlock Box

Although all inputs and outputs to the electrical safety systems are redundant and fail safe, the interlock connections internal to the power supply are not. The electrical safety system functions as an electrical permit system and no credit for life safety is attempted or taken. Electrical safety is provided to personnel by the Fermilab Lock Out Tag Out system described in section 5120 of the Fermilab ES&H Manual and other applicable Division Policies.

Below is a logic diagram showing the major inputs and outputs for the 8 GeV Beamline and Main Injector Electrical safety systems.



Accelerator Division policy requires any device with steady state parameters exceeding 50 volts or the impulse energy content exceeding 1 Joule to be interlocked to the safety system (unless the device has no exposed conductors.) The following are the devices currently planned to be interlocked to the safety system.

8 GeV Interlocked Supplies

5 - Bend Buss 4 - Quad 4 - Correction Element Bulk

MI Ring Interlocked Supplies

12 - Bend Buss 6 - Quad 19 - Correction Element Bulk

Additional power supplies will be added to the above lists as they are identified.

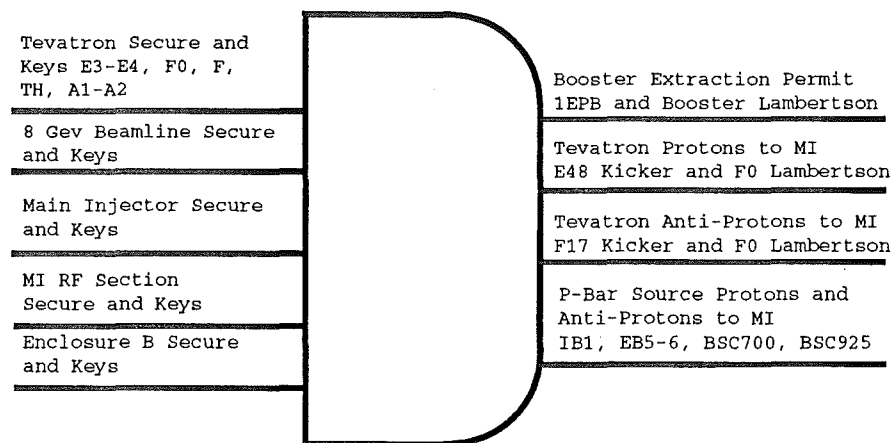
3.8.13.3

The Main Injector Radiation Safety System

The Main Injector radiation safety system controls nine critical devices, the IEPB power supply and the Booster Lambertson are the critical devices to insure beam is not extracted from the Booster into the 8 GeV line. To insure beam (anti-protons or protons) are not extracted from P-Bar to the Main Injector, IB1, EB5-6, BSC700, and BSC925 are the critical devices. To insure Tevatron beam (anti-protons or protons) can not enter the Main Injector, the E48 Kicker, F17 Kicker, and F0 Lambertson are the critical devices. Each critical device receives one of the two redundant permit signals from the radiation safety system. Each pair of critical devices receives different permit signals to maintain redundancy. For example, the E48 Kicker and the F0 Lambertson are a pair of critical devices to protection the MI Ring from protons. The E48 Kicker would receive a different permit signal than the F0 Lambertson.

Below is a logic diagram showing the major inputs and outputs for the Main Injector radiation safety system.

Main Injector RSS



8 GeV Critical Devices

IEPB The IEPB power supply drives a Booster extraction bend in the 8 GeV area of the Booster. This two-magnet string provides 10.23°. Inhibiting this supply prevents beam from entering the 8 GeV enclosure.

Booster Lambertson This is a ramped power supply used to steer protons into the 8 GeV line. With this supply off beam can not be extracted into the Main Injector.

Antiproton Source Critical Devices

The following devices are used to prevent beam from coming back from the Antiproton source. These devices are located in two different lines, AP-2 injection and AP-3 ejection. In some scenarios they insure that protons do not enter the Main Injector, and in others, that anti-protons do not enter the Main Injector.

IB1 (D:H704) This device is located in the AP-2 injection line of the Antiproton Source. With this supply off, it insures that beam cannot be extracted from the Accumulator / Debuncher Ring into the Main Injector.

EB 5/6 (D:H926) This device is located in the AP-3 ejection line of the Antiproton Source. Once again, with this supply off, it insures that beam will not enter the Main Injector.

AP0 Injection Line Beam Stop BSC700 This is a mechanical device that drops into the path of the beam. If this device is inserted into the AP-2 injection beam line, beam cannot enter the Main Injector. Therefore, it is a logical device to use to insure safety for the Main Injector.

AP0 Ejection Line Beam Stop BSC925 Once again, if this device is inserted in the AP-3 ejection beam line, we can be assured beam will not enter the Main Injector.

Tevatron Critical Devices

The following devices are used to prevent protons and anti-protons from being reverse extracted from the Tevatron to the Main Injector.

E48 Kicker This is a pulsed power supply used to kick anti-protons into the Tevatron orbit. With this supply off protons can not be reverse extracted into the Main Injector.

F17 Kicker This is a pulsed power supply used to kick protons into the Tevatron orbit. With this supply off anti-protons can not be reverse extracted into the Main Injector.

F0 Lambertson This is a ramped power supply used to steer protons and anti-protons into the Tevatron. With this supply off beam can not be extracted into the Main Injector.

3.8.13.4. Main Injector Search and Secure Procedures

The general search and secure procedures outlined in section 8 and the operation of the interlock box outlined in section 11 in conjunction with the following explanation should provide the necessary information to properly search the Main Injector Ring and the 8 GeV enclosure.

The Main Injector consist of 6 interlocked sections. The RF straight section, the remaining Main Injector ring, the 8 GeV enclosure, and a section of the existing Tevatron enclosure.

RF Straight Section

The RF straight section consists of two interlocked gates and a controlled access mini loop below the MI-60 service building. A two person search team begins at interlock 1 securing the enclosure in numerical order. After resetting interlock 1, one member remains at interlock 3 to insure no one enters the enclosure from behind while the other member resets interlock 2. At interlock 3 is a controlled access mini loop consisting of two doors and two interlock boxes. The team resets the first interlock of the mini loop and exits the enclosure resetting the second interlock of the mini loop. This concludes the searching of the RF straight section.

Main Injector Ring

The Main Injector ring consists of 8 gate interlocks, 18 emergency exit mini loops, 7 controlled access mini loops, and 1 beam dump access mini loop for a total of 34 interlocks. The ring is further subdivided into 3 major sections with section 1 beginning at cell 608 and ending at cell 221. Section 2 begins at cell 221 and ends at cell 401 and section 3 begins at cell 401 and ends at cell 602. The search sequence for the Main Injector ring is variable and controlled by the PLC. This has been done to allow the search team to skip emergency exits that have not been entered to minimize the time required to search and secure the enclosure. The first time the enclosure is secured, the search team proceeds starting at interlock 1 of each section and resets the interlocks in numerical order. At the emergency exits, one member of the team remains at the bottom of the stairwell while the other resets the interlock at the top of the stairs. Then the interlock at the bottom of the stairs may be reset and the search team proceeds to the next interlock. At the controlled access mini loops, one member remains at the bottom of the stairs while the other resets the two interlocks in the mini loop starting with the service building side. The team proceeds in this fashion until all interlocks in each section have been reset.

Once the emergency exit stairwell and controlled access mini loops have been secured, the search team on subsequent searches need only secure the tunnel side interlock box at the mini loops. If someone has entered the mini loop, the PLC will automatically require the interlock at the top of the stairs be reset again to insure a proper search and secure of the enclosure.

8 GeV Enclosure

The 8 GeV enclosure consists of 1 gate, 1 sequence start interlock, 4 emergency exits, and 1 controlled access mini loop for a total of 7 interlocks. The search sequence for the 8 GeV

enclosure is variable and controlled by the PLC. Again the search team starts at interlock 1 and proceeds in numerical order resetting each interlock in the same fashion as the Main Injector ring ending at interlock 7.

Tevatron Enclosure E3 to A2

The existing Tevatron enclosure is sectioned into 10 sectors, F, F0, E, E0, D, C, C0, B, A, and the Transfer Hall. The sectors F0, F, and TH must also be secured for the Main Injector radiation safety system. The search and secure procedures for these sectors is covered in the Main Ring search and secure procedures.

WBS 1.1.12. UTILITIES AND ABORT**WBS 1.1.12.1.1. MAIN INJECTOR RING WATER SYSTEM and****WBS 1.1.12.1.10. BEAMLINE WATER SYSTEM****FMI Low Conductivity Water System and Magnet Bus Connections**

The proposed system for connecting the power and water to the FMI is similar to the Main Ring. This is a system that requires minimum maintenance. Stainless steel headers supply low conductivity water (LCW) to local, secondary manifolds which regulate the flow to the dipole magnets and to the copper bus which conducts both power and cooling water to the quadrupole. A combination of ceramic feedthroughs and thermoplastic hoses insulate the piping electrically from the copper bus system.

The FMI components and associated utilities are grouped together at the outside wall of the tunnel leaving most of the enclosure space for servicing, as shown in Figure 3.9-1. All connections to the magnets are designed to be accessible from the inner space of the enclosure. Figure 3.9-2 shows a schematic representation of the cooling for a typical hydraulic cell in the Main Injector Ring. A group of magnets, consisting of two dipoles, one quadrupole and a sextupole, is cooled in parallel from a 2" water manifold. This manifold can be isolated from the main 6" header water pressure with one 1-1/2" ball valve and two check valves to prevent back-flow. The secondary manifold permits access to the magnet connections and minimizes the number of required electrical insulators. The smaller manifolds are electrically insulated from ground. With a second insulator at the magnets, each LCW connection to the bus has two insulators in series. In the Main Ring, this design has reduced the copper ion deposits inside the insulators. One inch thermoplastic hoses will be used for insulators farthest away from the beam line and where the thermal expansion of the pipes can be up to 3". Ceramic insulators will be used at the magnets and where restrictions are required to regulate the water flow. The supply water pressure around the ring enclosure is about 150 psi. The hydraulic cell is designed to give the correct flow to allow an average temperature rise of 8°C across each individual magnet.

The new dipole magnets have bolted electrical connections that incorporate flexible copper jumpers. Compression fittings are used for the water connections. Each magnet has two water circuits in parallel designed to minimize thermal stresses. The dipoles have a common water return at the connecting bus around the quadrupole location. This also reduces the number of electrical insulators. The quadrupoles connections are the same as in the Main Ring where the brazed copper joint carries both the water and the power to the magnet.

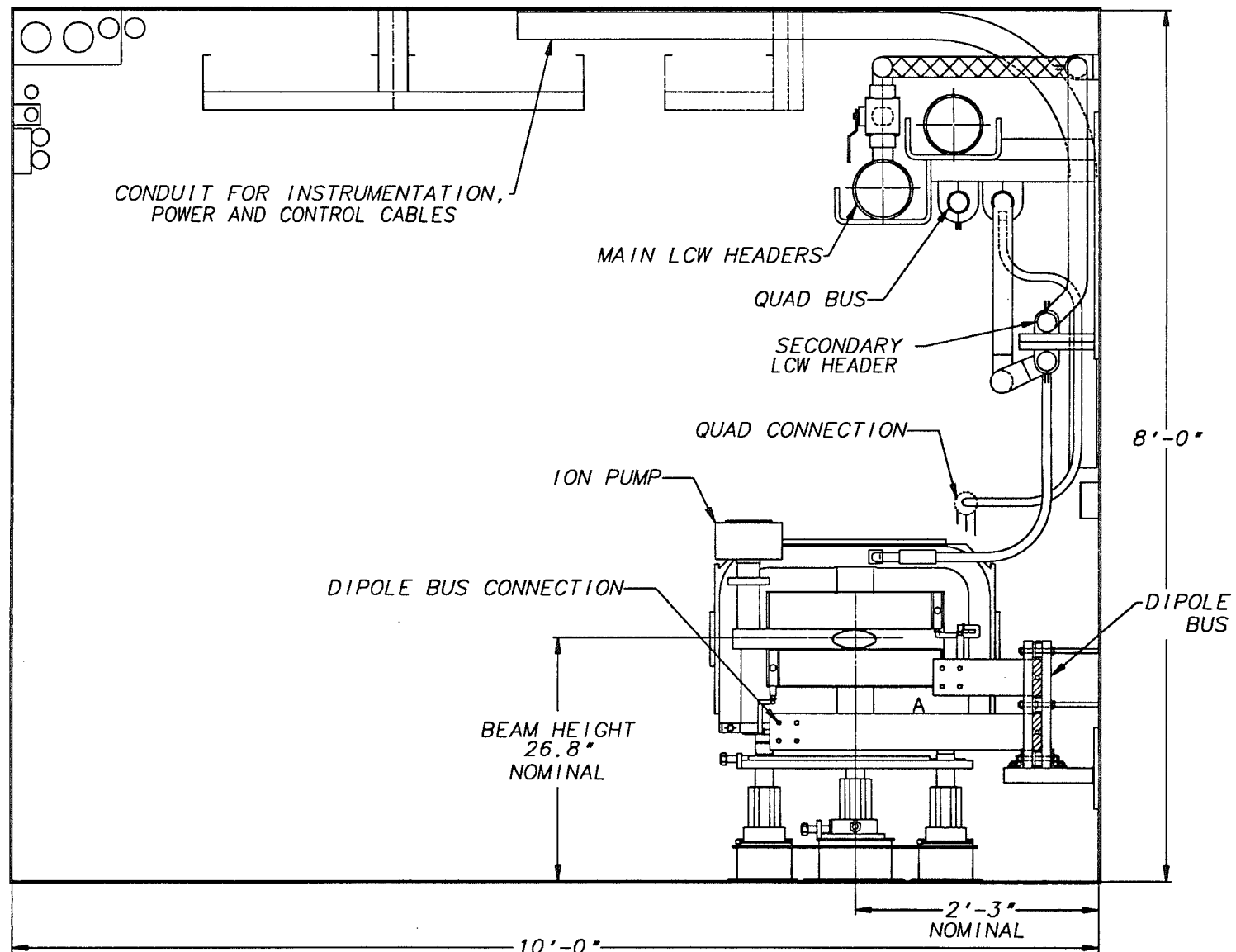


Figure 3.9-1. Cross Section of Main Injector Enclosure

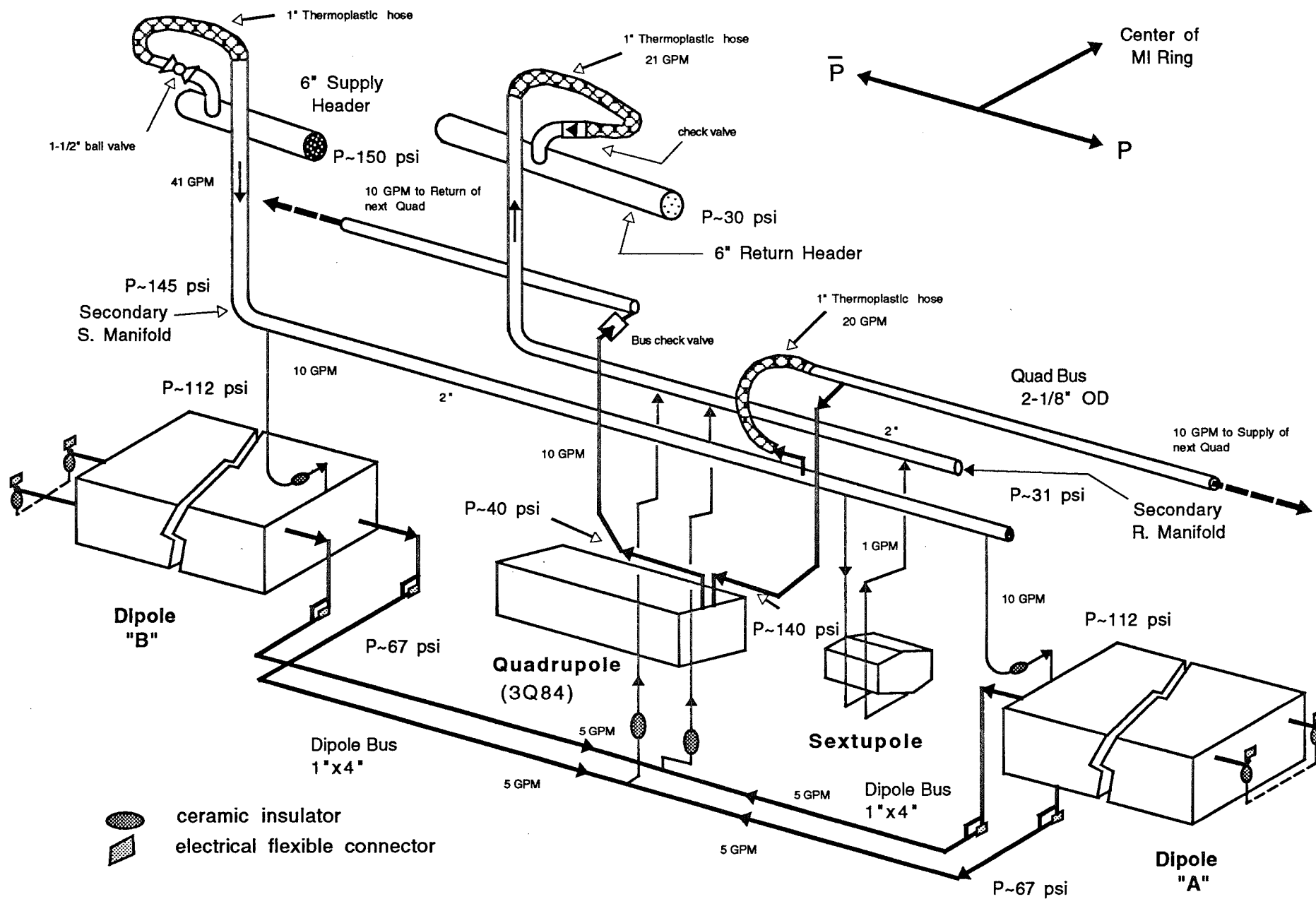


Figure 3.9-2. Typical MIR Hydraulic Cell Flow Schematic

There will be six utility buildings uniformly spaced along the perimeter of the FMI. These are labeled MI-10, -20, -30, -40, -50, and -60. Each utility building will supply power and cooling water to about 1,815 feet of circumference in the FMI. A total of 18 water pumps will be installed around the ring with 3 pumps per service building. Figure 3.9-3 shows a typical service building LCW schematic. Each pump has a 100 hp motor and delivers 550 GPM of LCW with a pressure head of 164 psi (380 TDH). This design, using new industrial ANSI pumps, is superior to recycling the Main Ring pumps and purchasing additional pumps of the same design. The cost of the two approaches is about the same and the new pumps have the advantage of being installed prior the Main Ring shutdown. Six and four inch stainless steel pipe headers will be installed above the magnets along the 10,891-foot circumference of the FMI. Eight inch headers will be used to connect the pumps from the service buildings to the manifolds in the enclosure. One heat exchanger per service building is required to transfer the LCW heat load to the pond water. The normal heat load removal capacity per building will be about 2.7 MW. Approximately 8,000 GPM of LCW will be required to cool magnets, bus, and power supplies in the Main Injector enclosure and service buildings. The 18 centrifugal pumps are capable of delivering approximately 9,900 GPM at the design head. The temperature of the water is regulated to 95° F by a 3 way control valve which diverts a portion of the water around the heat exchanger when less cooling is required. A constant flow of pond water is circulated in the tube side of the heat exchanger. The heat in the pond is removed by evaporation. In the MI design, the size of the ponds is the limiting factor in cooling the electrical components.

Figures 3.9-4 to 3.9-9 show the power and the required LCW flow from each service building in the Main Injector. All components are connected in parallel and, with the proper hydraulic impedance across each secondary manifold, the local water distribution will be balanced between service buildings. The centrifugal pumps, also connected in parallel with the magnets, will share the flow and will balance the pressure head to match the impedance across the LCW manifolds. This LCW system design has shown itself to work well in the Main Ring. The 150 GeV Antiproton Line has a relatively low RMS power cooling requirement and a branch from the enclosure served by the MI-60 building will be used to fill this cooling need. The abort line will be cooled by tapping into the LCW portion served by the MI-40 building. Figure 3.9-10 shows the power and the LCW required for 150 GeV Proton line. This line has a separate LCW system. Cooling for the B2 type dipole magnets requires a water pressure differential of 200 psi. The pumps and the heat exchangers will be installed in the MI-52 service building. This heat is also dissipated to the ponds. The power and cooling water required for the 8 GeV Line is shown in Figure 3.9-11. From the closest MI pond, water will be pumped to service building MI-8 where the 8 GeV Line LCW system will be located .

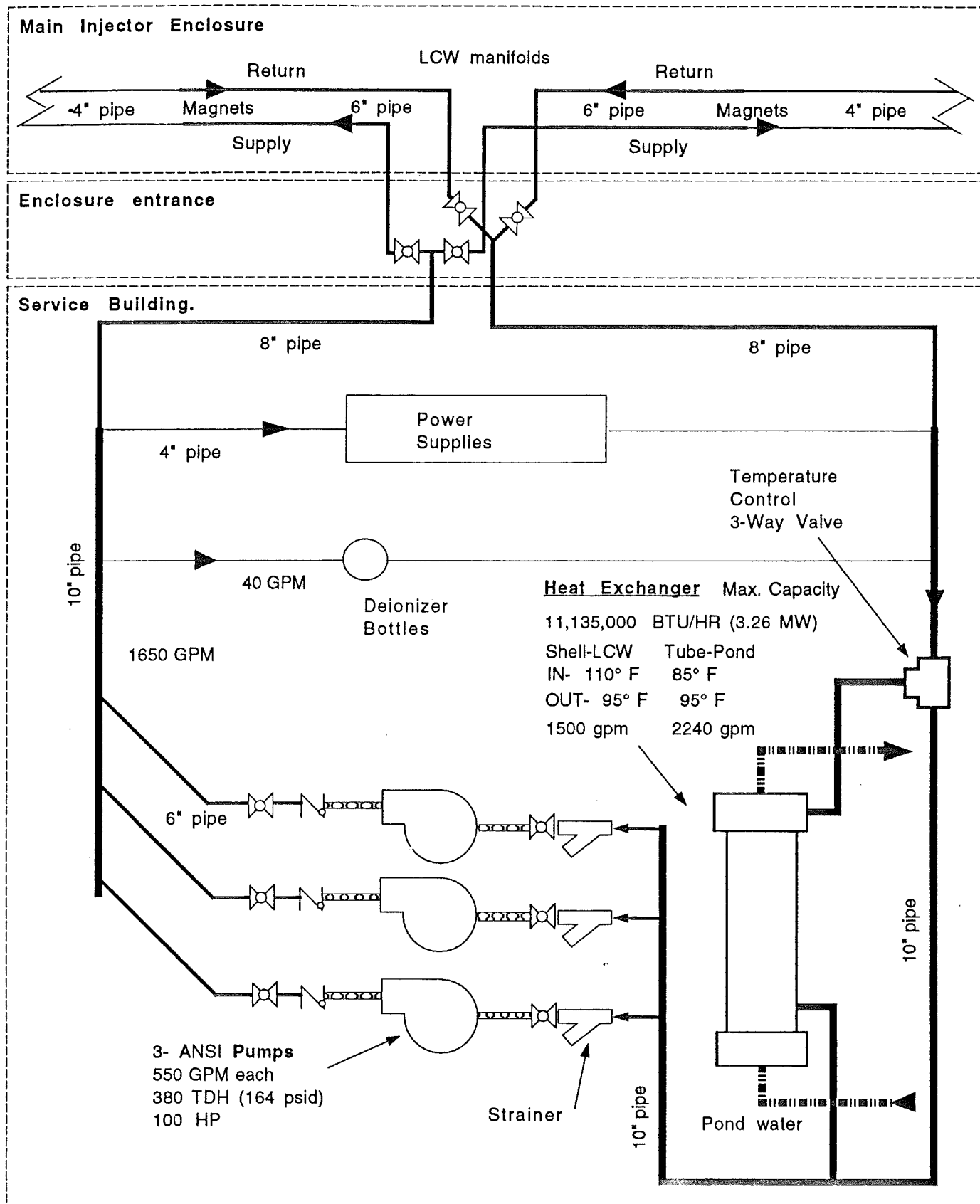
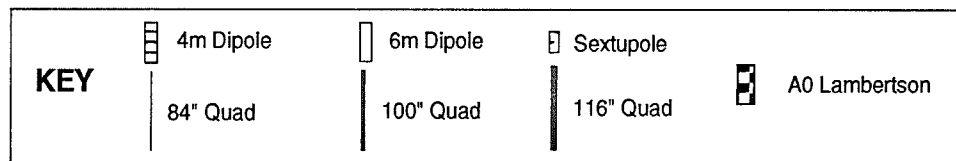
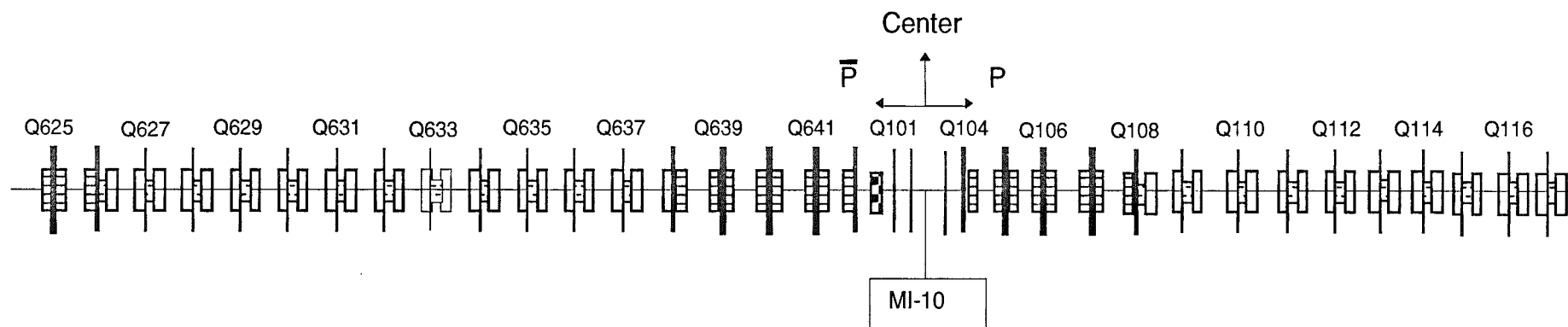


Figure 3.9-3. Typical M.I. Service Building LCW Schematic

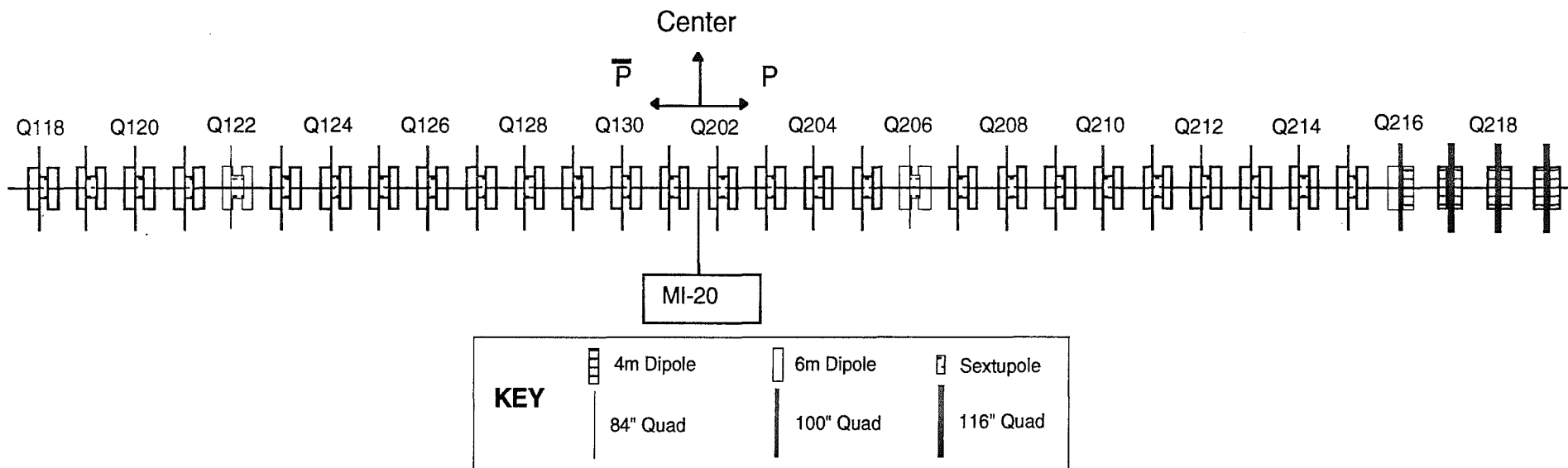


Quantity	Element Type	RMS Power (kW / Element)	Total Element RMS Power (kW)	Req'd Flow (GPM / Element)	ΔT of Water (°C)	Total Flow (GPM)
19	4m Dipole	14.4	273	8	7	152
43	6m Dipole	19.2	824	10	7	430
23	84" Quad	18.7	431	10	7	230
5	100" Quad	24.2	121	12	8	60
7	116" Quad	28.8	201	12	9	84
22	Sextupole	0.6	13	1	2	22
1	A0 Lamb.	20.2	22	10	8	10
1	Bus,Jumpers,etc.	217	217			
Service Building						
1	Power Supplies	290	290	200		200
3	Water Pump	75	225	35	8	105
1	LCW Polishing			40		40

Total RMS Power (kW) 2618
Average ΔT of Water (°C) 7

SUM 1333
Available Flow 1650
Extra GPM 317 19.21%

Figure 3.9-4. LCW Requirements for Service Building MI-10



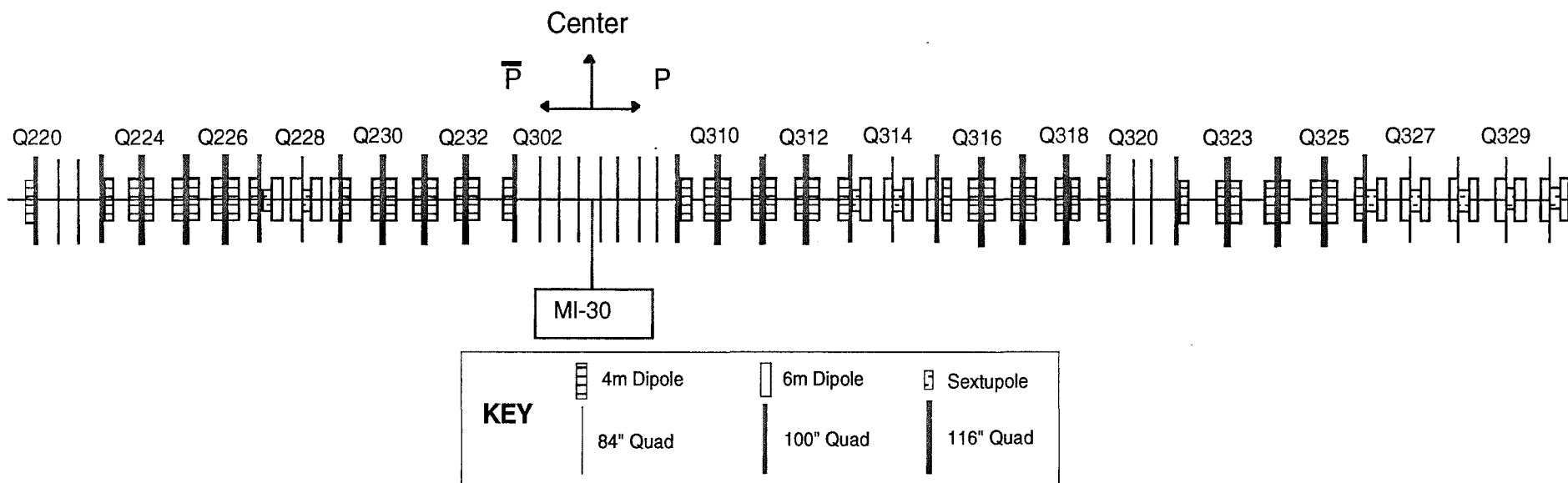
Quantity	Element Type	RMS Power (kW / Element)	Total Element RMS Power (kW)	Req'd Flow (GPM / Element)	ΔT of Water (°C)	Total Flow (GPM)
7	4m Dipole	14.4	101	8	7	56
57	6m Dipole	19.2	1093	10	7	570
28	84" Quad	18.7	524	10	7	280
1	100" Quad	24.2	24	12	8	12
3	116" Quad	28.8	86	12	9	36
28	Sextupole	0.6	17	1	2	28
1	Bus,Jumpers,etc.	194	194			
Service Building						
1	Power Supplies	290	290	200		200
3	Water Pump	75	225	35	8	105
1	LCW Polishing			40		40

Total RMS Power (kW) 2554

Average ΔT of Water (°C) 7

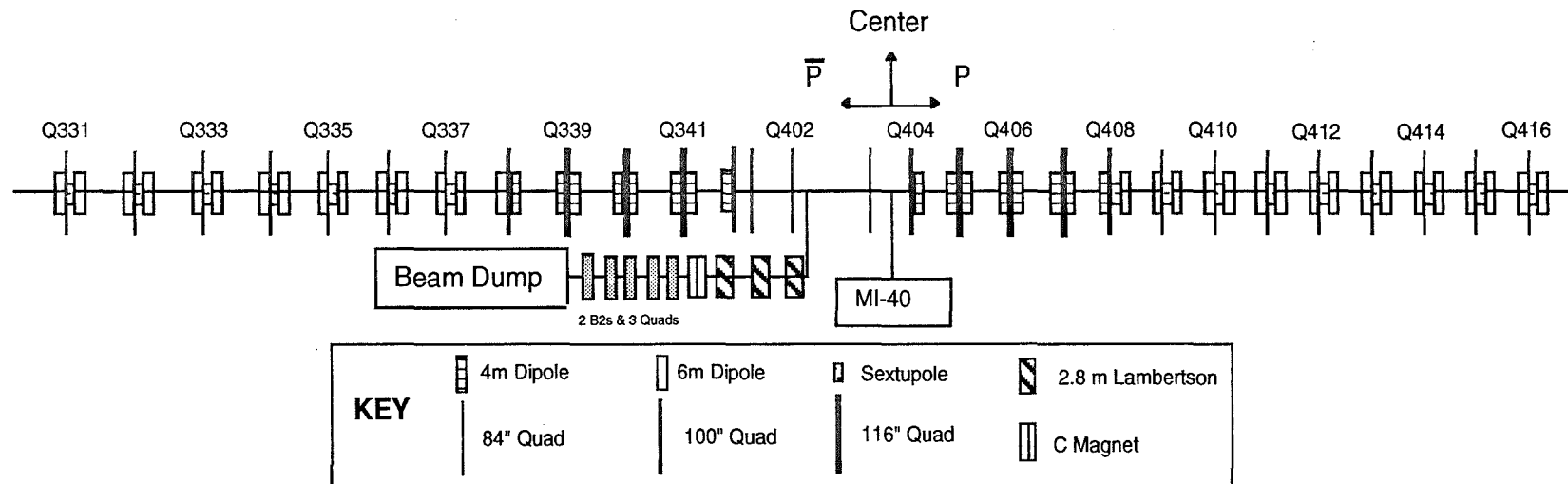
SUM	1327
Available Flow	1650
Extra GPM	323 19.58%

Figure 3.9-5. LCW Requirements for Service Building MI-20



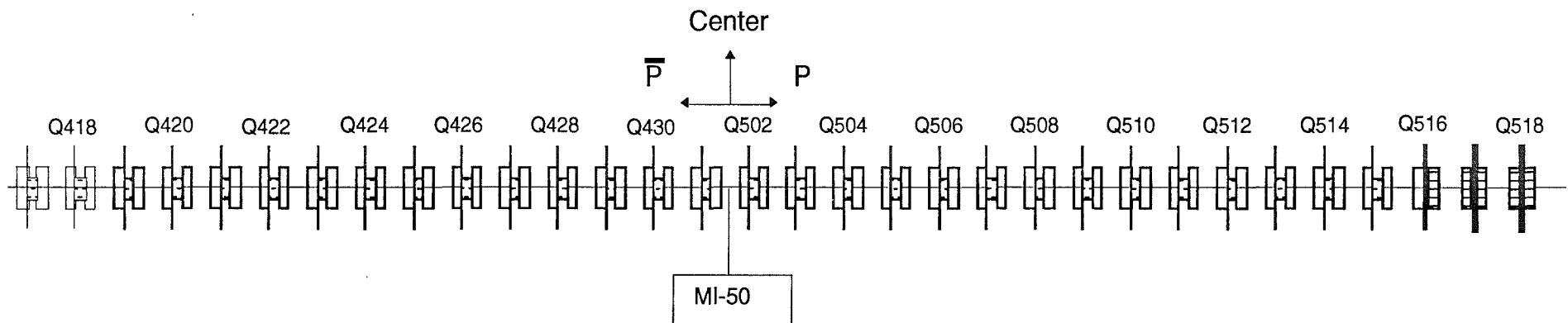
Quantity	Element Type	RMS Power (kW / Element)	Total Element RMS Power (kW)	Req'd Flow (GPM / Element)	ΔT of Water ($^{\circ}C$)	Total Flow (GPM)
41	4m Dipole	14.4	590	8	7	328
17	6m Dipole	19.2	326	10	7	170
17	84" Quad	18.7	318	10	7	170
11	100" Quad	24.2	266	12	8	132
15	116" Quad	28.8	431	12	9	180
9	Sextupole	0.6	5	1	2	9
1	Bus, Jumpers, etc.	287	287			
Service Building						
1	Power Supplies	266	266	185		185
3	Water Pump	75	225	35	8	105
1	LCW Polishing			40		40
Total RMS Power (kW)			2716		SUM	1319
Average ΔT of Water ($^{\circ}C$)			8		Available Flow	1650
						Extra GPM 331 20.06%

Figure 3.9-6. LCW Requirements for Service Building MI-30



Quantity	Element Type	RMS Power (kW / Element)	Total Element RMS Power (kW)	Req'd Flow (GPM / Element)	ΔT of Water ($^{\circ}C$)	Total Flow (GPM)
16	4m Dipole	14.4	230	8	7	128
32	6m Dipole	19.2	613	10	7	320
18	84" Quad	18.7	337	10	7	180
4	100" Quad	24.2	97	12	8	48
6	116" Quad	28.8	173	12	9	72
16	Sextupole	0.6	10	1	2	16
1	Bus, Jumpers, etc.	185	185			
	Abort Line					
3	2.8m Lamb.	20	60	10	8	30
1	C Magnet	20	20	10	8	10
1	2 B2s & 3 Quads	100	100	50	8	50
1	Beam Dump			150		150
	Service Building					
1	Power Supplies	290	290	210		210
3	Water Pump	75	225	35	8	105
1	LCW Polishing			40		40
Total RMS Power (kW)			2340		SUM	1359
Average ΔT of Water ($^{\circ}C$)			7		Available Flow	1650
					Extra GPM	291 17.64%

Figure 3.9-7. LCW Requirements for Service Building MI-40



KEY

	4m Dipole		6m Dipole		Sextupole
	84" Quad		100" Quad		116" Quad

Quantity	Element Type	RMS Power (kW / Element)	Total Element RMS Power (kW)	Req'd Flow (GPM / Element)	ΔT of Water ($^{\circ}C$)	Total Flow (GPM)
5	4m Dipole	14.4	72	8	7	40
59	6m Dipole	19.2	1131	10	7	590
29	84" Quad	18.7	543	10	7	290
1	100" Quad	24.2	24	12	8	12
2	116" Quad	28.8	58	12	9	24
29	Sextupole	0.6	18	1	2	29
1	Bus, Jumpers, etc.	193	193			
Service Building						
1	Power Supplies	290	290	200		200
3	Water Pump	75	225	35	8	105
1	LCW Polishing			40		40

Total RMS Power (kW) 2553

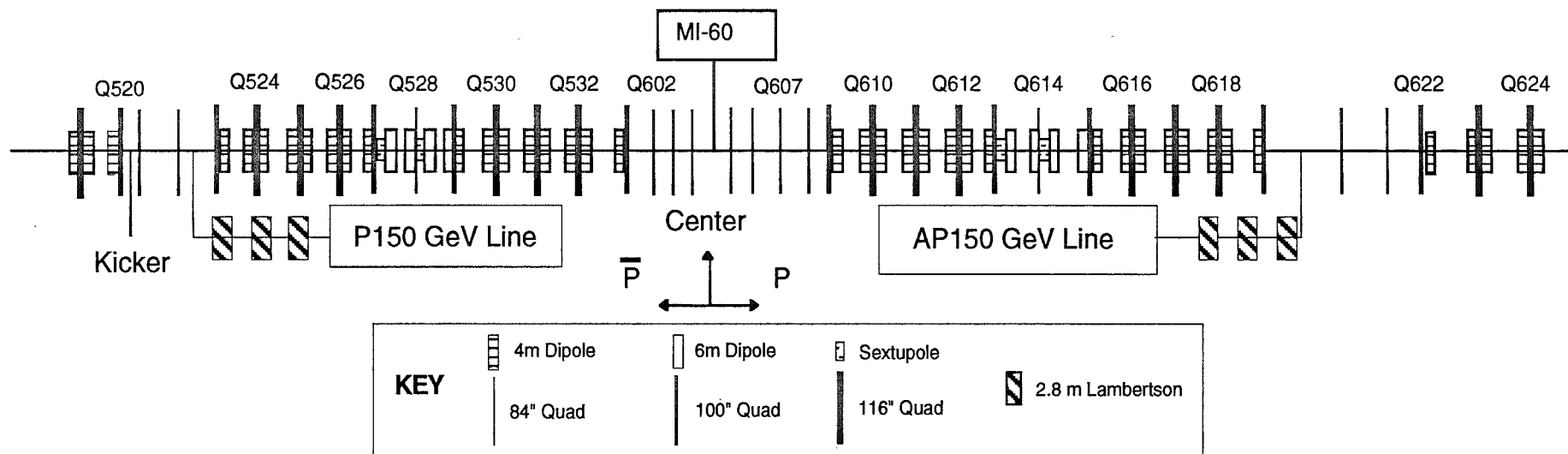
Average ΔT of Water ($^{\circ}C$) 7

SUM 1330

Available Flow 1650

Extra GPM 320 19.39%

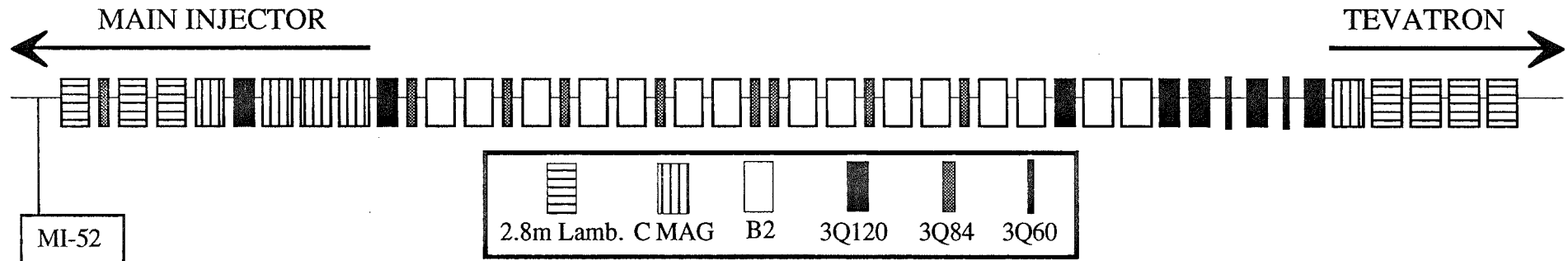
Figure 3.9-8. LCW Requirements for Service Building MI-50



Quantity	Element Type	RMS Power (kW / Element)	Total Element RMS Power (kW)	Req'd Flow (GPM / Element)	ΔT of Water ($^{\circ}C$)	Total Flow (GPM)
40	4m Dipole	14.4	576	8	7	320
8	6m Dipole	19.2	153	10	7	80
13	84" Quad	18.7	243	10	7	130
10	100" Quad	24.2	242	12	8	120
15	116" Quad	28.8	431	12	9	180
4	Sextupole	0.6	2	1	2	4
3	P150 2.8m Lamb.	20	60	10	8	30
1	AP150 GeV Line	57	57	54	4	54
1	Bus,Jumpers,etc.	256	256			
Service Building						
1	Power Supplies	266	266	185		185
3	Water Pump	75	225	35	8	105
1	LCW Polishing			40		40
Total RMS Power (kW)			2512	SUM		1248
Average ΔT of Water ($^{\circ}C$)			8	Available Flow		1650
						Extra GPM 402 24.36%

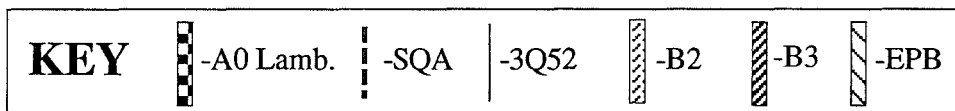
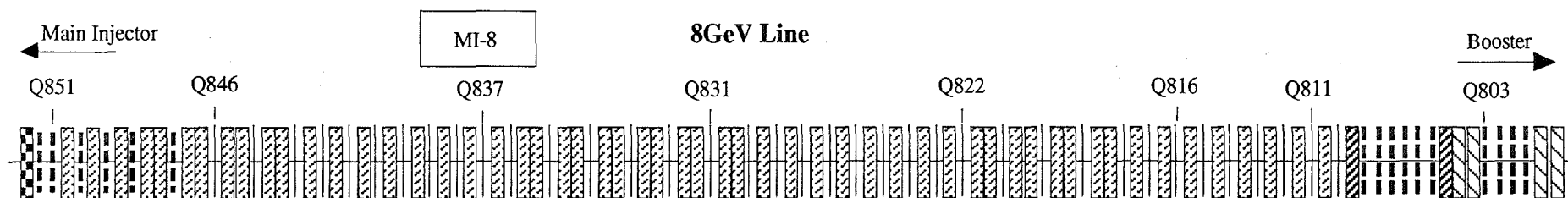
Figure 3.9-9. LCW Requirements for Service Building MI-60

150 GeV PROTON LINE



Circuit	Quantity	Magnet Type	Circuit Power (kW)	Mag. Power (kW/Magnet)	Req'd Flow (GPM/Magnet)	ΔT of Water (°C)	Total Flow (GPM)
B1	3	2.8m Lamb.	60.5	20	LCW from MI-60		
B2	4	C MAG	110.4	20	10	7.6	40
B3	14	B2	740.6	48.8	14	13.2	196
B4	1	B2	14.8	4.3	5	3.3	5
B5	1	C MAG	26.7	20	10	7.6	10
B6	4	2.8m Lamb.	53.5	13	10	4.9	40
Q1	1	3Q120	9.5	8.7	5	6.6	5
Q2	1	3Q120	9.8	8.7	5	6.6	5
Q3	7	3Q84	267.7	18.1	10	6.9	70
Q4	1	3Q120	10.1	8.7	5	6.6	5
Q5	1	3Q120	9.8	8.7	5	6.6	5
Q6	1,1	3Q120,3Q60	14.2	8.7,4.6	5,5	6.6,3.5	10
Q7	1,1	3Q120,3Q60	14.1	8.7,4.6	5,5	6.6,3.5	10
Q8	1	3Q120	9.4	8.7	5	6.6	5
Service Building MI-52					Magnet Total Flow (GPM)		406
2 Water Pump (125 hp = 93.3 kW/pump)					44.3 GPM/pump		89
Power Supplies							50
1 LCW Polishing							40
Total Power in Tunnel (kW)			1351.1	1096.3	Total LCW Req'd (GPM)		585
Losses from Bus, Cable, Filters (kW)				254.8			

Figure 3.9-10. LCW Requirements for Service Building MI-52



Circuit	Quantity	Element Type	Circuit Power (kW / Circuit)	Element RMS Power (kW / Element)	Req'd Flow (GPM / Element)	ΔT of Water ($^{\circ}C$)	Total Flow (GPM)
B1	2	EPB	27.3	12.4	5	9.4	10
B2	2	EPB	16.3	7.4	5	5.6	10
B3	2	B3	7.0	3.2	6	2.0	12
B4	55	B2	90.8	1.5	2	2.9	110
B5	1	A0 Lamb.	Power and LCW from MI-10				
Q1	4	SQA	4.8	1.1	2	2.1	8
Q2	6	SQA	24.4	3.7	2	7.0	12
Q3	37	3Q52	16.3	0.4	2	0.8	74
Q4	6	SQA	4.0	0.6	2	1.1	12
Bend	51	Trim	22.4	< 0.4	0		0
Quad	17	Trim	5.6	< 0.3	0		0
Service Building							
	8	Power Supply	40	5	5		40
	1	LCW Polishing			40		40
	1	Water Pump	74.6	74.6	36	8.0	36
TOTAL POWER			333.5	313.6		SUM	364
LOSSES FROM BUS AND FILTERS				19.9		Available Flow	550
						Extra GPM	186

33.8%

Figure 3.9-11. LCW Requirements for Service Building MI-8

At each utility entrance, as well as at locations half-way in-between, the enclosure will have a ceiling that is one foot higher than the standard tunnel. The purpose of this extra space is to provide space for the stainless steel pipe expansion joints. At this location, the enlarged enclosure allows the pipes to cross over the cable trays without obstructing the normal tunnel clearance for the magnet moving vehicle. At MI-52, the enclosure ceiling is also one foot higher. This space is required for the additional 150 GeV Proton Line LCW manifolds and its cable trays.

New, rectangular copper bus (1"x4") will be used for connecting the dipoles in the enclosure around the quadrupoles. The bus will be supported from the wall with insulating structural fiberglass material. The supports will have adjustments for alignment to the magnets. The flexible jumpers with bolted connections allow for thermal expansion of the coils and the bus. Pipe bus (4 square inches in cross section) will be used at the entrances going to the power supplies in the service buildings. The quadrupoles will have a pipe bus (2 square inches in cross section) with 2-1/8" outside diameter. This tube size will allow the use of standard water fittings for brazed connections. Porcelain clamps on channel supports will be used for all round bus.

Figure 3.9-12 shows a line representation of the Main Injector and 8 GeV Line LCW systems. The RF cooling in MI-60 and the 150 GeV Proton Line are separate LCW systems; however, they both use the MI LCW storage for water make up.

In each service building around the ring, portable, mixed-bed deionizer bottles will be installed. A continuous polishing flow of about 40 GPM per service building will be required to maintain low conductivity in the water. The bottles are only used for polishing action. Their use will guarantee that an average of 9 MΩ-cm resistivity of the LCW will be maintained in the ring. LCW fills will be done from the Central Utility Building (CUB) via the 8 GeV Line. The CUB has large industrial deionizer columns that meet the appropriate EPA guidelines for effluent discharge systems. The portable deionizer bottles will be regenerated in the CUB using its existing regeneration system. In service building MI-60, a 3,000 gallon combination storage and expansion tank will be installed for emergency LCW make-up for the MIR. A 1,500 gallon tank will be in MI-8 service building for the 8 GeV Line use. The FMI will require an estimated 37,000 gallons of LCW to fill the pipes, tanks, bus, and magnets.

As shown on Figure 3.9-13, a net clockwise flow in the ring will be accomplished with restricting orifices at each of the entrances. In addition to the local water circulation around each service building, about 100 GPM of circular flow will allow good mixing and deionizer processing at the Central Utility Building.

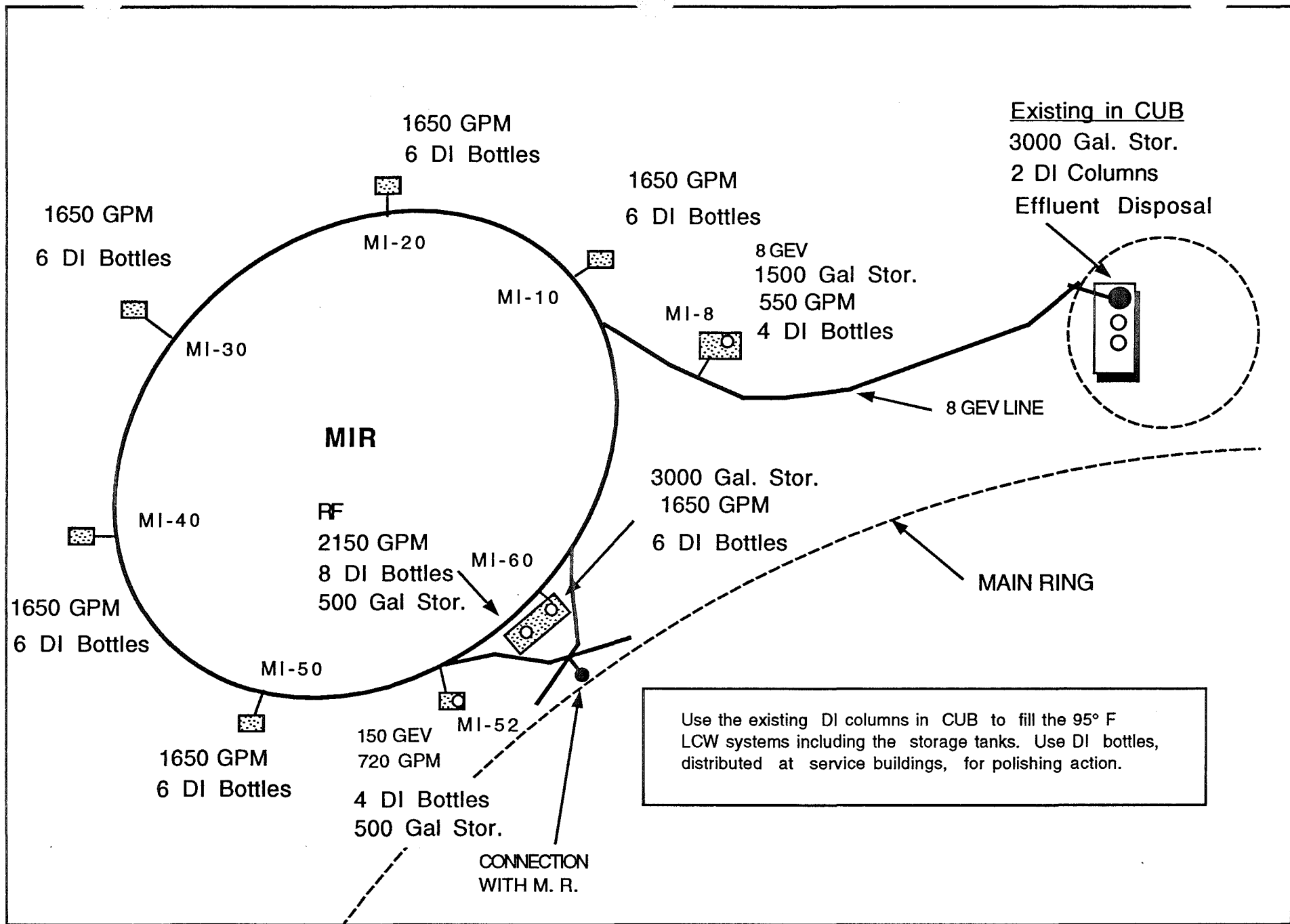


Figure 3.9-12. Main Injector and Beam Lines 95° F LCW System

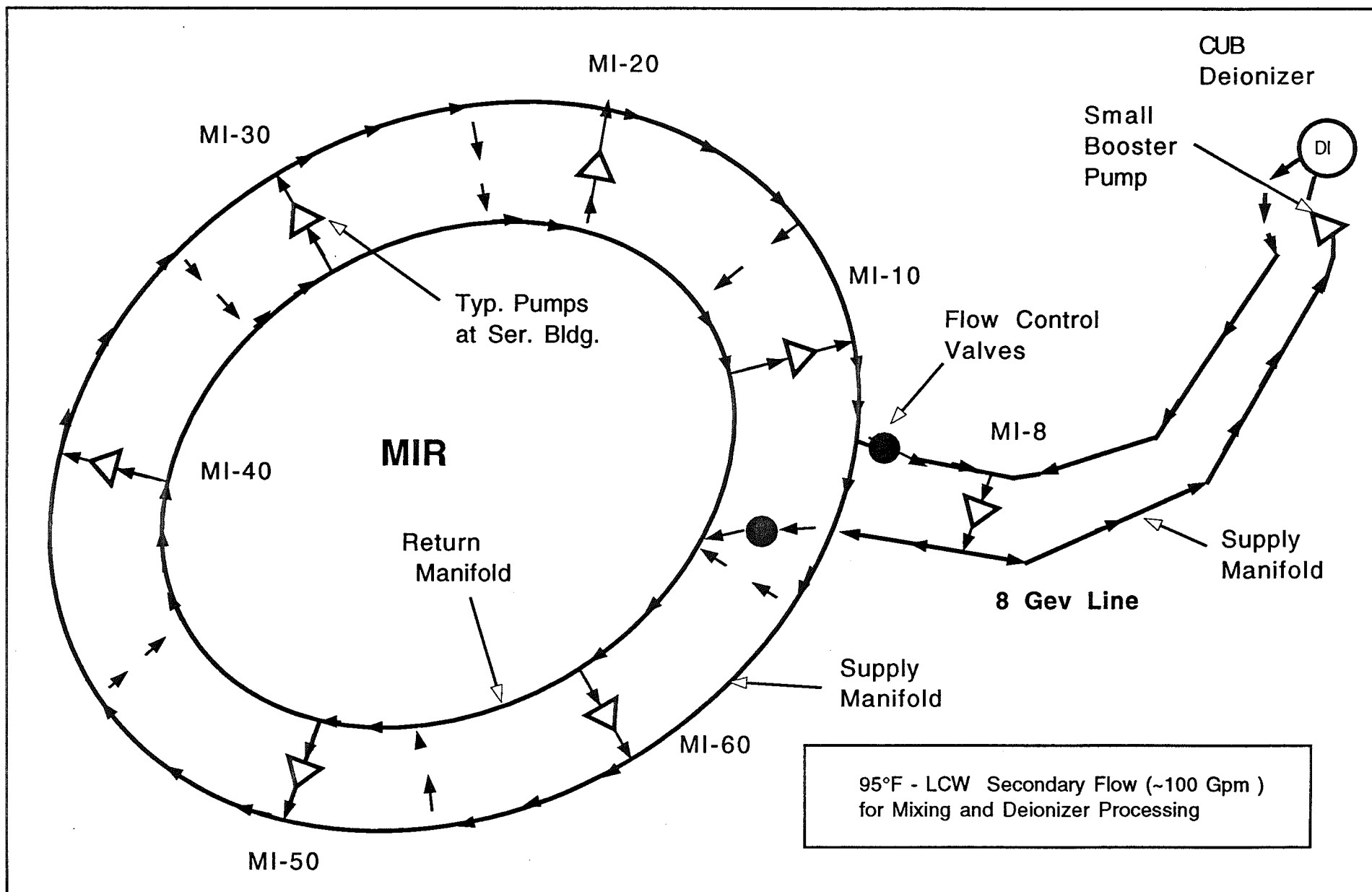


Figure 3.9-13. LCW Secondary Flow

WBS 1.1.12.1.2. CABLES AND CABLE TRAYS

Each of the 208 quadrupole locations in the Main Injector Ring has a variety of control devices. These include the diagnostic devices discussed in Chapter 3.8, and various individually- or series-powered correction magnetic elements discussed in Chapter 3.1. In addition, there are the vacuum pumps and gauges discussed in Chapter 3.2. All of these elements require cables running to/from the nearest service building. Two, 18" wide by 4" deep cable trays are provided for carrying these cables; one of these trays will in general be filled with coaxial signal cables. The other tray will be divided into two sections, one part for high voltage coaxial cables for the ion pumps, the other part for cables for powering the magnetic elements, either #10 or 250 MCM cable.

Table 3.9-1.
Cable Count for Typical Service Building

Item	Number Cables	Cable Type	Total Area (sq. in.)	Total Weight (lb./ft.)
"Signal" Tray				
BPMs:	72	RG-8	12	12
BLMs:	36	RG-58	2	2
Safety System	4	Multicon.	1	1
Misc.	16	Various	4	4
<i>Total</i>			19	19
<i>Total x .56</i>			11	11
"Power" Tray				
Dipole CE:	72	#10	2	2
Misc. & other CE:	16	#10	2	2
Ion Pumps:	96	RG-58	4	4
ξ Sext.	4	250 MCM	1	3
<i>Total</i>			9	11
<i>Total x .56</i>			5	6
Cable properties: (R at 35°C. Area & weight = copper only for non-coax)				
Cable Type	Diameter	Area	R/1000'	#/1000'
250 MCM	.500 in	.196 sq in	.044 Ω	755 lbs.
#10	.102	.030	1.06	31
RG-8	.405	.129	-	120
RG-58	.195	.030	-	29
Multiconductor	.530	.221	-	220

Each service building must provide control for up to 36 channels of beam position monitors and beam loss monitors, 36 dipole correctors, 16 other correction elements, and 96 vacuum ion pumps. The service buildings are placed according to the dipole bus requirements to reduce voltage to ground stress on the magnets. Consequently, the "servicing" of quadrupole locations by a particular service building is not necessarily evenly distributed upstream and downstream of the building. In the worst situation, 56% of the cables run one direction, and 44% run the other direction. Table 3.9-1. lists the various cable types and quantities that are anticipated. These quantities will only fill about one fourth of the tray depth at the location nearest the service building, with the amount of cables dropping off as one moves away from the building.

WBS 1.1.12.1.3. ABORT SYSTEM

The proposed proton abort system for the new FMI relies heavily on the technology and design utilized in the existing Main Ring abort system commissioned in 1983. This system has successfully provided clean single-turn abort capability for all subsequent Main Ring proton beam operation. Because of the low intensities transported, no pbar abort is required. The kicker system which deflects the circulating beam into the extraction channel is discussed in Chapter 3.5. The elements and optics of the extraction line are discussed in Chapter 2.4, while vacuum aspects of the abort line are covered in Chapter 3.2. In this section, we discuss only the abort core box, its cooling system, and the shielding surrounding the core box.

The abort dump consists of a graphite absorber, encased in a water-cooled aluminum box. This assembly is surrounded by steel and concrete. There are a number of new features incorporated in the design of the new beam dump which are intended to enhance the serviceability and reliability of the system. At the same time, an effort has been made to be as conservative as possible with regards to groundwater activation and surface radiation levels. The primary differences in the two designs, Main Injector vs. Main Ring are as follows:

1. The present Main Ring abort dump is shared with the Tevatron. This sharing results in a rectangular core box, with two stacks of 6" x 6" graphite blocks. The Main Injector only needs one stack. The higher Tevatron beam energy requires a 4.4-m long graphite absorber. The Main Injector absorber will only need to be 2.4 m long to reduce the energy density of the shower, as it enters the steel, to a safe level.
2. The present Main Ring/Tevatron beam dump is direct buried. No direct inspection is possible, and careful monitoring of groundwater is required. In the event of a failure (and fortunately, there has not been one!) repair will be difficult and time-consuming. Radiation

exposure of personnel will pose a problem. The Main Injector abort dump will be in its own enclosure, accessible from the Main Injector tunnel for inspection and, if necessary, repair. By providing direct access, the time required for repair or replacement is minimized, resulting in shorter downtime and less exposure of personnel to the activated components.

3. The Main Ring/Tevatron abort dump is cooled by the same LCW system as the magnets in the Main Ring tunnel. Short-lived isotopes produced while the water is passing through the abort pose a problem. In spite of a delay imposed by passing through a storage tank in the Main Ring tunnel, the LCW returns to the nearest service building with rather high levels of activation. The Main Injector abort dump core box will be cooled by a closed loop system. A heat exchanger located in the rear of the abort dump enclosure will transfer the heat to the magnet LCW system.

4. Because of the higher intensity and shorter cycle time for the Main Injector, the thickness of steel will be increased to reduce the levels of groundwater activation and surface radiation. The calculations using the computer modeling program CASIM [1] of the expected levels resulting from the Main Injector beam abort have been discussed in a separate document [2]. Using the annual aborted beam intensity listed in the PSAR [3], the groundwater activation levels are below the limits allowed by the Single Resident Well model [4], and by the more recent Concentration Model [5,6].

5. One final design difference is the incorporation in the Main Injector abort dump of a beampipe which would be used for 120 GeV extracted beams to some future experimental area. This 3" diameter pipe will be placed in the steel shielding, just outside the aluminum box. The beampipe will be plugged with steel until the need for extracted beams arises.

The beam dump will be constructed with a graphite core of length 2.4 m, enclosed and steel and concrete, as shown in Figures 3.9-14, 3.9-15 and 3.9-16, to avoid groundwater contamination and to reduce radiation levels at the surface to levels which permit unlimited occupancy. The entire assembly is constructed in an enclosure, as shown in Figures 3.9-17 and 3.9-18. Underdrains on each side of the dump connect to sumps in the Main Injector enclosure, while the sampling underdrain connects to a standpipe in the Main Injector enclosure, from which samples can be drawn for analysis. The steel plates and the large concrete blocks will be installed at the same time the enclosure is being constructed. The core box and the hand stacked blocks in front of it will be installed at a later date. The hand stacked blocks are quite useful in reducing the soft backward-scattered components in the beam shower, and account for a sizable reduction in the groundwater activation. Figure 3.9-19 shows the isodose contours (per 150 GeV incident

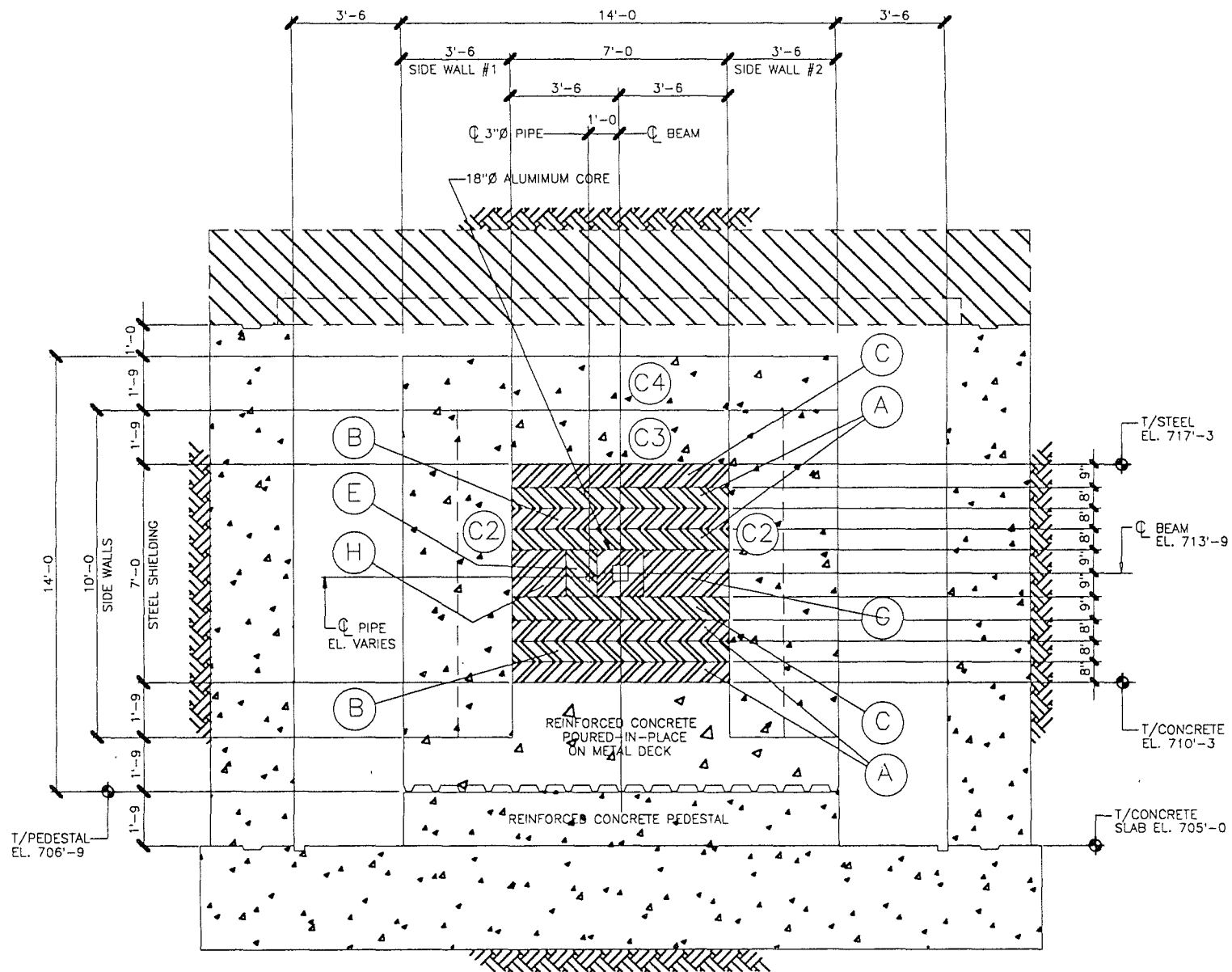


Figure 3.9-15. Cross Section of Main Injector Abort Dump

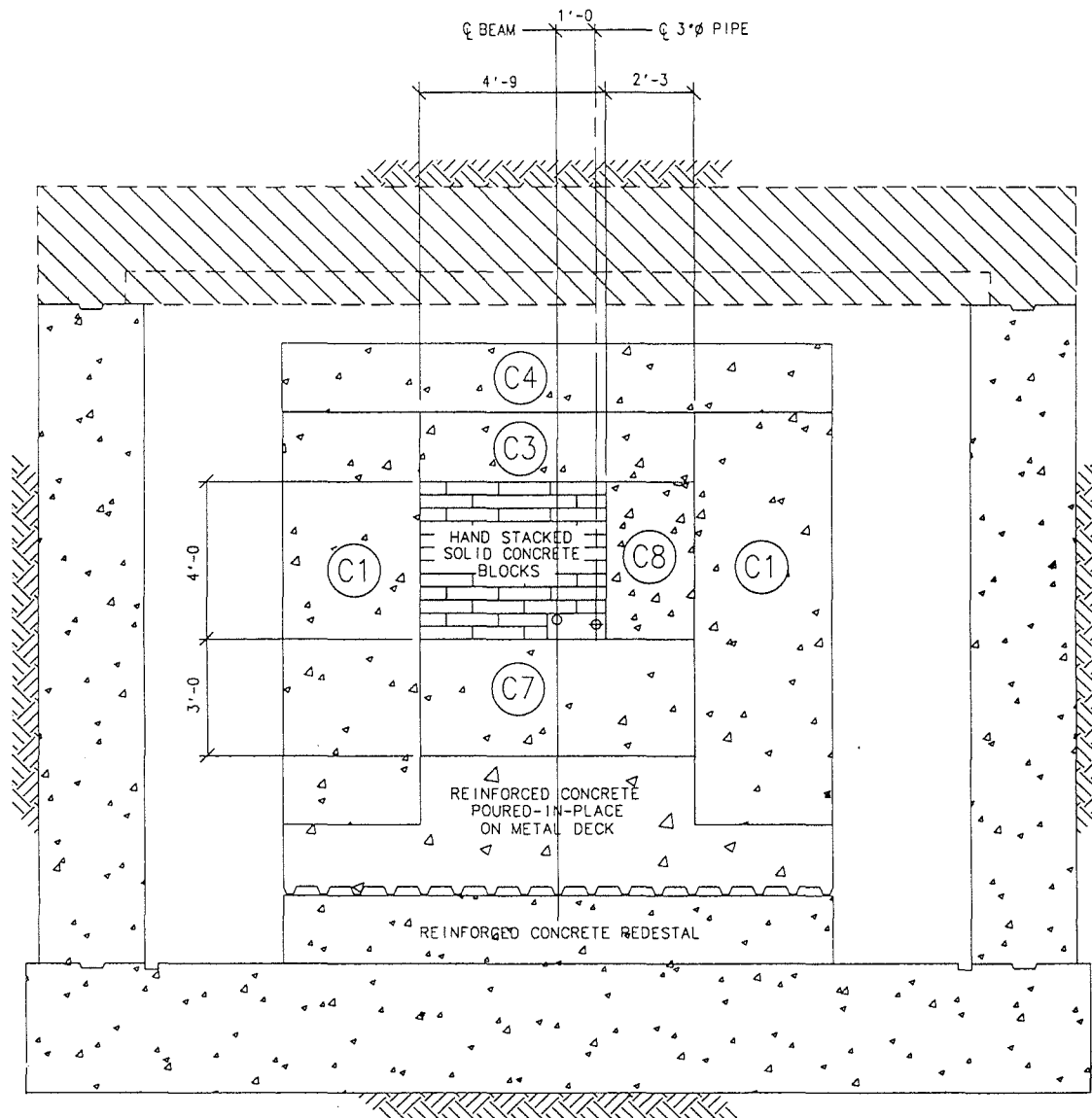


Figure 3.9-16. Front View of Main Injector Abort Dump

Main Injector Beam Dump Plan View

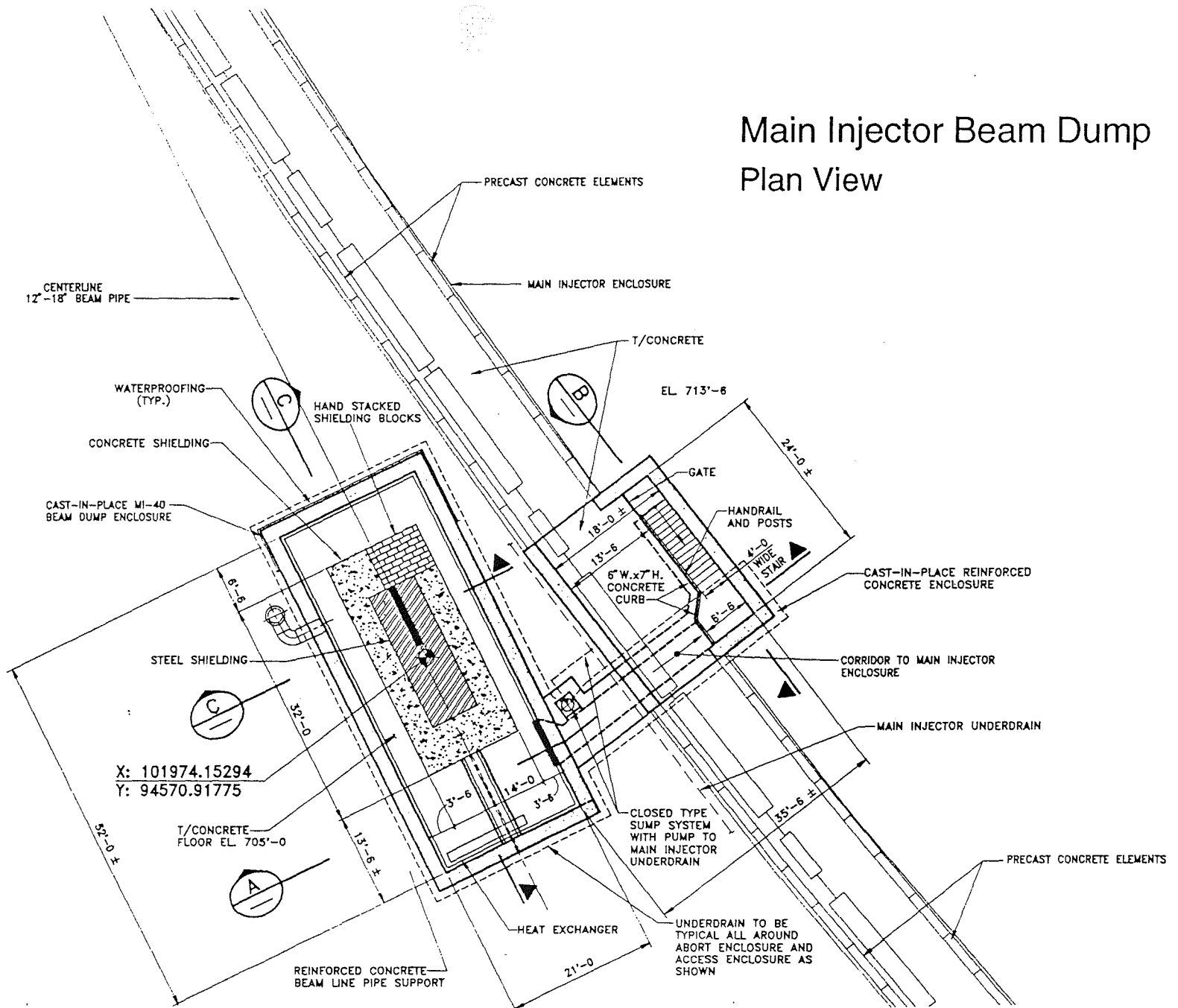
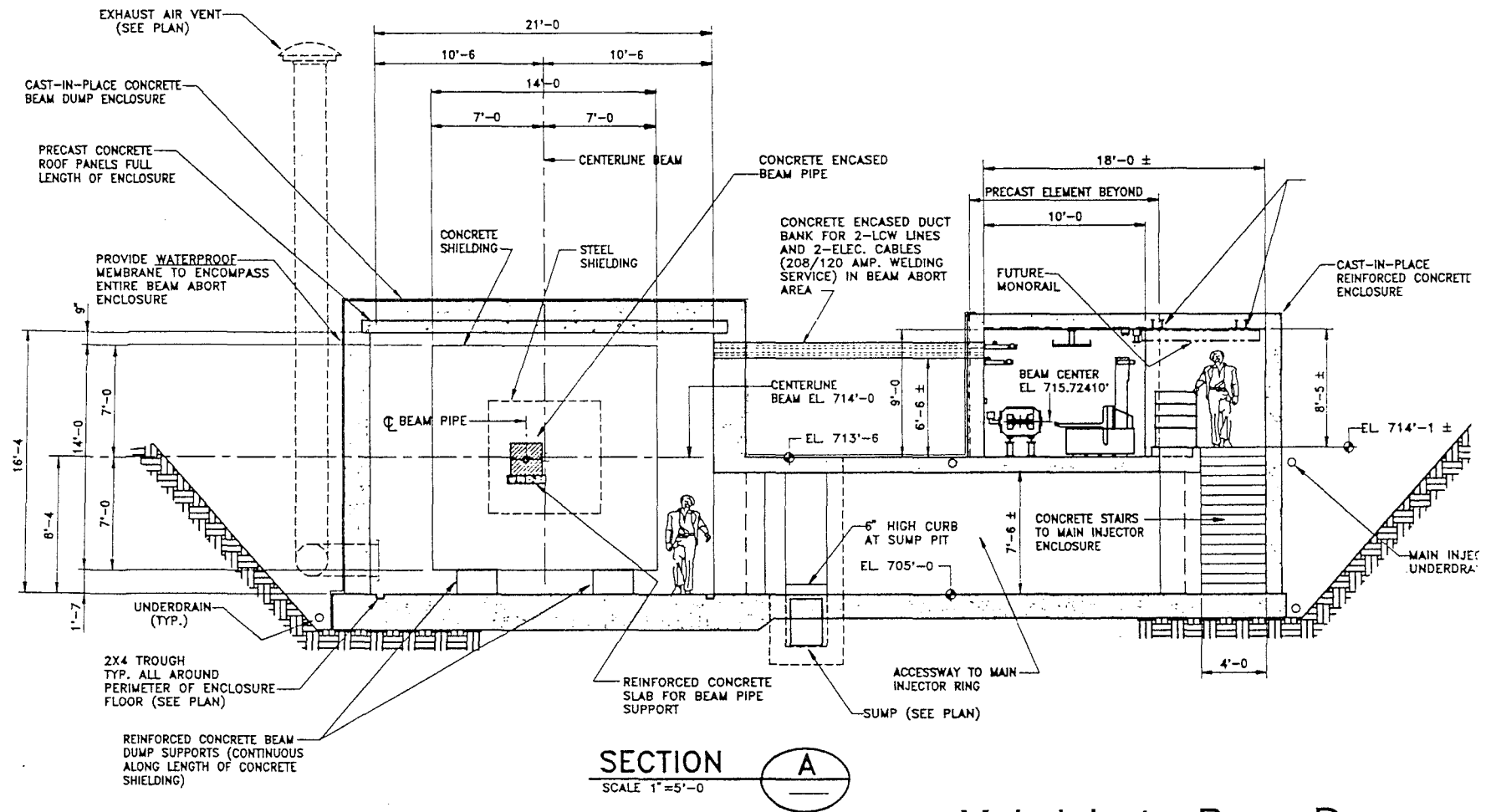


Figure 3.9-17. Plan View of Main Injector Abort Dump Enclosure



Main Injector Beam Dump
Elevation View

Figure 3.9-18. Elevation View of Main Injector Abort Dump Enclosure

ISODOSE CONTOURS DUE TO HADRONS IN THE MI BEAM DUMP
(VERTICAL PLANE)

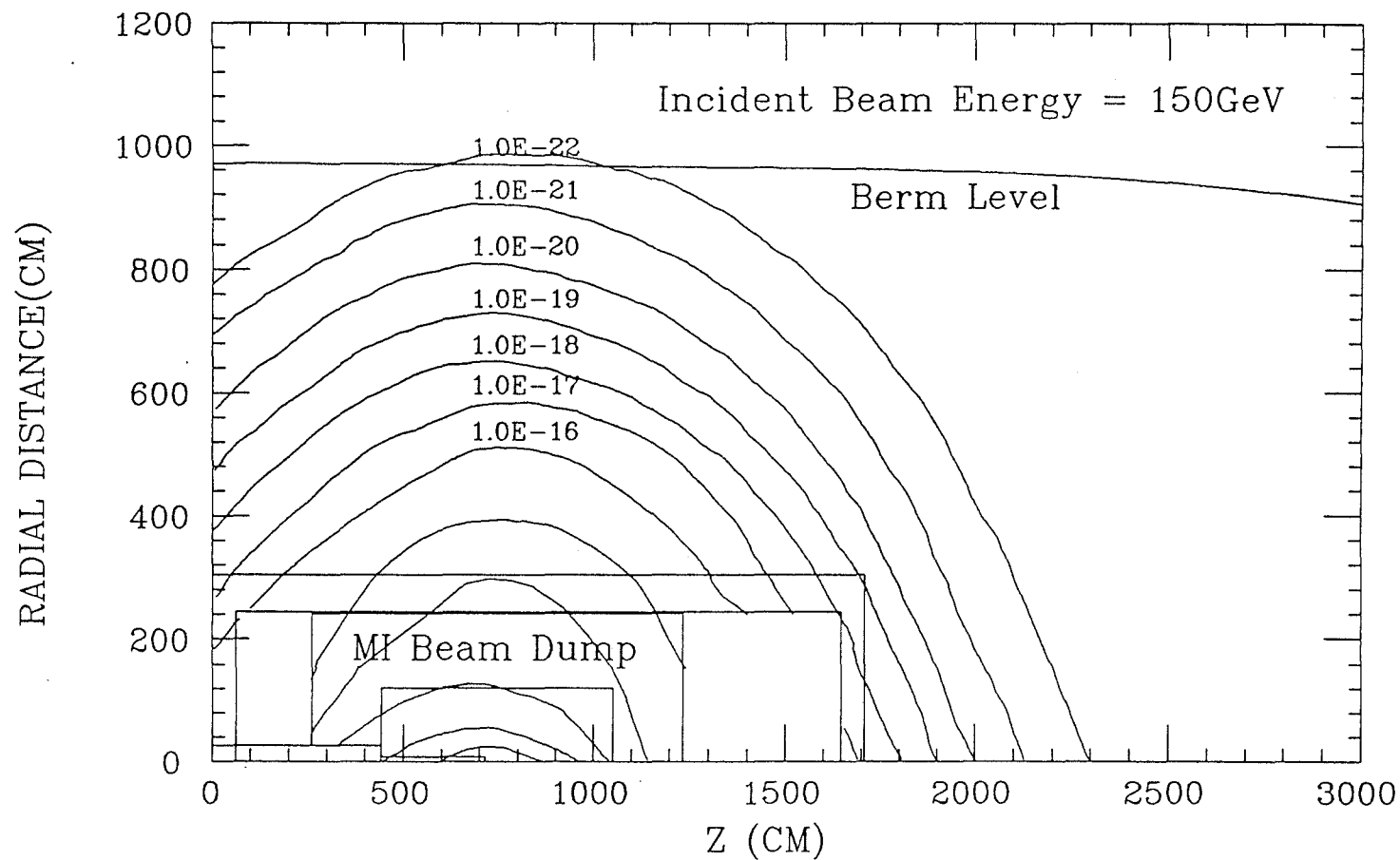


Figure 3.9-19. Isodose Contours Around the Main Injector Abort Dump Due to Hadron Showers

proton) due to hadrons for the proposed abort dump geometry; similarly, Figure 3.9-20 shows the dose at the surface due to muons.

The abort dump enclosure will almost certainly be a confined space, with documented procedures for personnel making accesses including minimum beam-off times prior to access. Manually activated ventilation fans will provide fresh air drawn from the Main Injector enclosure. A vent line will be provided for automatically venting any hydrogen buildup in the heat exchanger system. Any water found inside the enclosure will have to be analyzed prior to disposal to determine its origin: groundwater leaking in, water from the closed loop system, or water from the LCW system.

The beam dump will be instrumented with a variety of sensors, e.g. beam profile monitors, redundant temperature sensors, monitor and control for the cooling system. The graphite core box will be immersed in an oxygen-free environment such as argon to prevent oxidation of the graphite.

Abort Cooling Water System

The aluminum case that surrounds the graphite core will be cooled by a closed loop water system. This equipment will be located in the abort enclosure and consists of a heat exchanger, pumps, an expansion tank, and appropriate filters, instrumentation, and safety devices. The expansion tank is cushioned by nitrogen gas and has sensors that will detect potential hydrogen accumulations. A standby pump will facilitate normal maintenance and repairs, allowing that work to be done in a minimum amount of time. The heat exchanger will be the tube and shell type and its all-welded construction avoids potentially leaky seals, an obvious advantage in a radioactive environment. The designs of both the expansion tank and the heat exchanger will be in accordance with the ASME Boiler and Pressure Vessel Code and both will be certified with ASME Code stamps. A portion of the 95° F LCW that is circulating in the Main Injector ring is diverted to the abort enclosure and passes through the shell side of the heat exchanger. The flow of the coolant is maintained by the pressure differential between the supply and return headers in the MI enclosure. The flow rate is regulated by a temperature controlled valve. The process fluid on the tube side of the heat exchanger will initially be filled with LCW. Since the fluids in the exchanger derive from LCW, fouling is a minimal concern. With the exception of the aluminum core box, most of the cooling elements, including the heat exchanger, will be constructed of stainless steel. Other materials that will be used, such as the mechanical pump seals, consist of ceramic and graphite. To make the valves as radiation resistant as possible, they will have metal seats in combination with the best available stem seals. All components that have the potential to

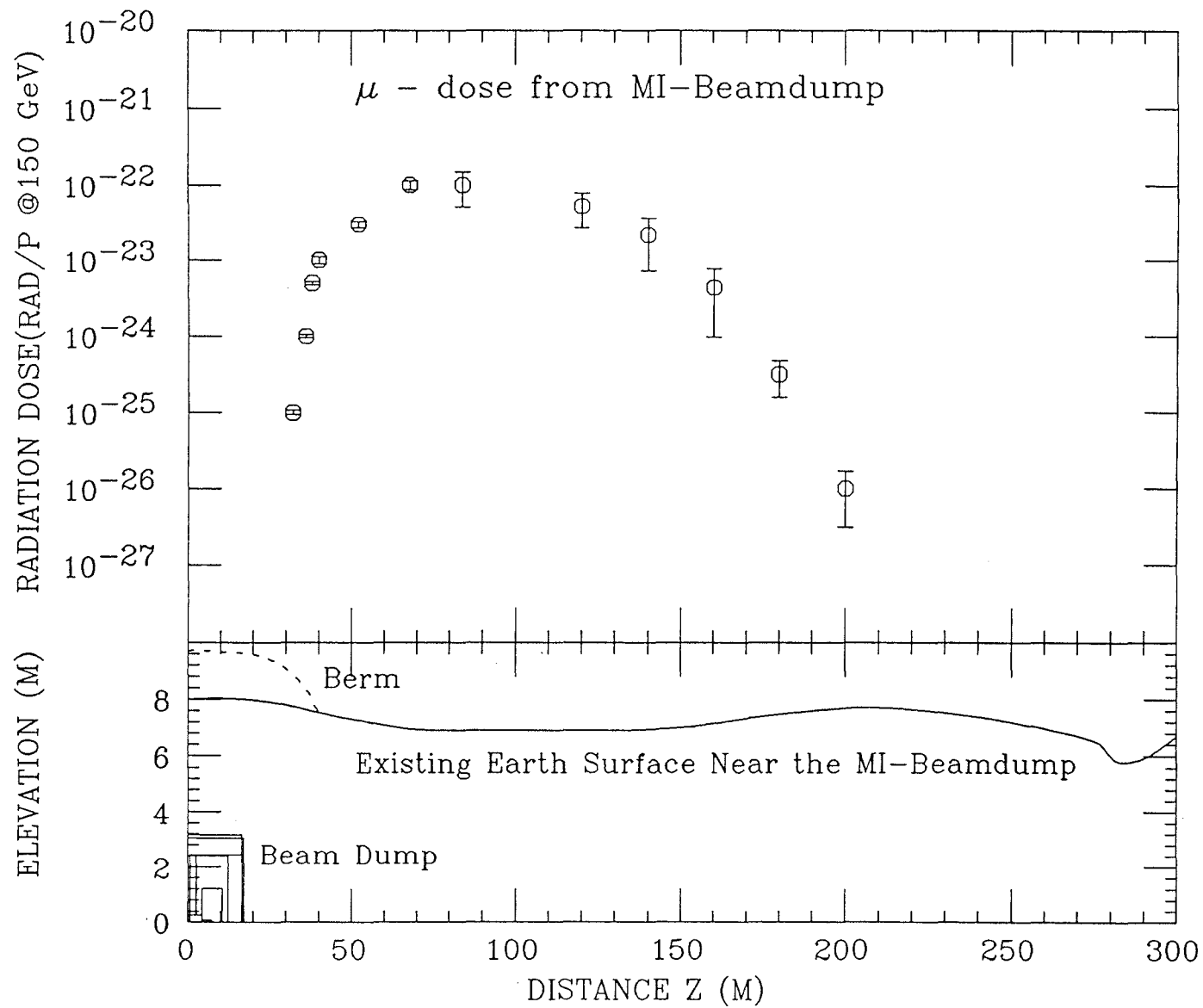


Figure 3.9-20. Dose at the Surface Near the Main Injector Abort Dump Due to Muons

leak will be grouped together and surrounded with a retainer that will collect any accidental water spills.

The cooling system is designed to remove an estimated heat load of 300 kW (1,024,500 BTU/Hr) from the aluminum core box. The use of a centrifugal pump with a capacity of approximately 80 gallons per minute is consistent with a temperature rise of 15° C in the process water. A flow of 115 gallons per minute on the coolant side of the heat exchanger will raise the LCW temperature by 10° C.

References

1. A. VanGinneken, "CASIM-Program to Simulate Transport of Hadronic Cascades in Bulk Matter", Fermilab FN-272, 1975.
2. C. Bhat, "A Design Study of the MI-40 Beam Abort Dump", MI Note-0086, 1993.
3. S.D. Holmes, D. Bogert and A.L. Read, "Fermilab Main Injector Preliminary Safety Analysis Report", 1992.
4. A.M. Jonckheere, "Aquifer Dilution Factors of Ground Water Activity Produced Around Fermilab Targets and Dumps", Fermilab TM-838, 1978.
5. A.J. Malensek, et al., Groundwater Migration of Radionuclides at Fermilab, 1993 (to be published).

CHAPTER 3.10 INSTALLATION

WBS 1.1.13. INSTALLATION

The installation WBS covers a large number of diverse tasks and requires careful coordination of the various tasks and tradesmen. Much thought has gone into the planning of these activities, how to sequence them around each other, and integrate them with the Main Ring and Tevatron shutdowns. The vast majority of the equipment and systems that will be installed as part of this WBS will have been designed and fabricated under different WBSs and are consequently described elsewhere in this report. Supports and positioning hardware for dipole, quadrupole, correction magnets, specialty devices, and utilities will be described in this section.

In the overall scheme, certain tasks need to follow a sensible sequence. Before receiving full or partial beneficial occupancy of the enclosures, lighting will have to be installed. Alignment crews will establish reference points in finished portions of the enclosures which will guide the installation of all components that do not require very precise location. The physical support for devices other than those that lie in the beam path will come from Unistrut rails that have been strategically imbedded in the ceiling and outer wall of the enclosure. At this point, installation of LCW piping, magnet busses, and cable trays will begin. The LCW piping will start first, followed by cable tray installation, then bypass buss installation, magnet stands, and finally magnets. Approximately a month will elapse between the start of each activity allowing adequate tunnel space for each installation group. After approximately 50% of the dipoles have been installed, cable installation will commence in the half tunnel vacated by all other personnel.

Over the years, several schemes have been used for adjusting and supporting magnets in the existing Main and Tevatron rings, the Pbar rings, and various beam lines. The Main Injector magnets will be supported by adjusters and supports that have performed best in the past. These designs use thrust bearings so that heavy magnets (dipoles weigh over 40,000 lbs) can be adjusted up and down requiring a reasonable amount of torque; thin inserts that have a low coefficient of friction are placed between sliding steel surfaces, and bronze bearing material is used in conjunction with steel actuators to reduce friction where large forces need to be applied.

With magnets that have sufficient rigidity, a three point support scheme is used; a four point scheme is used wherever conditions make it necessary. Dipoles and quadrupoles have three axis adjustment: ± 0.75 " in the transverse and longitudinal directions and ± 2.00 " in the vertical direction. The large vertical travel is readily built into the stands and requires less installation time compared to other techniques, such as using shims or selectively inserting segments that have variable height. The need for the large vertical travel comes about because of the combination of three circumstances: the anticipated deviation of the tunnel floor from its nominal

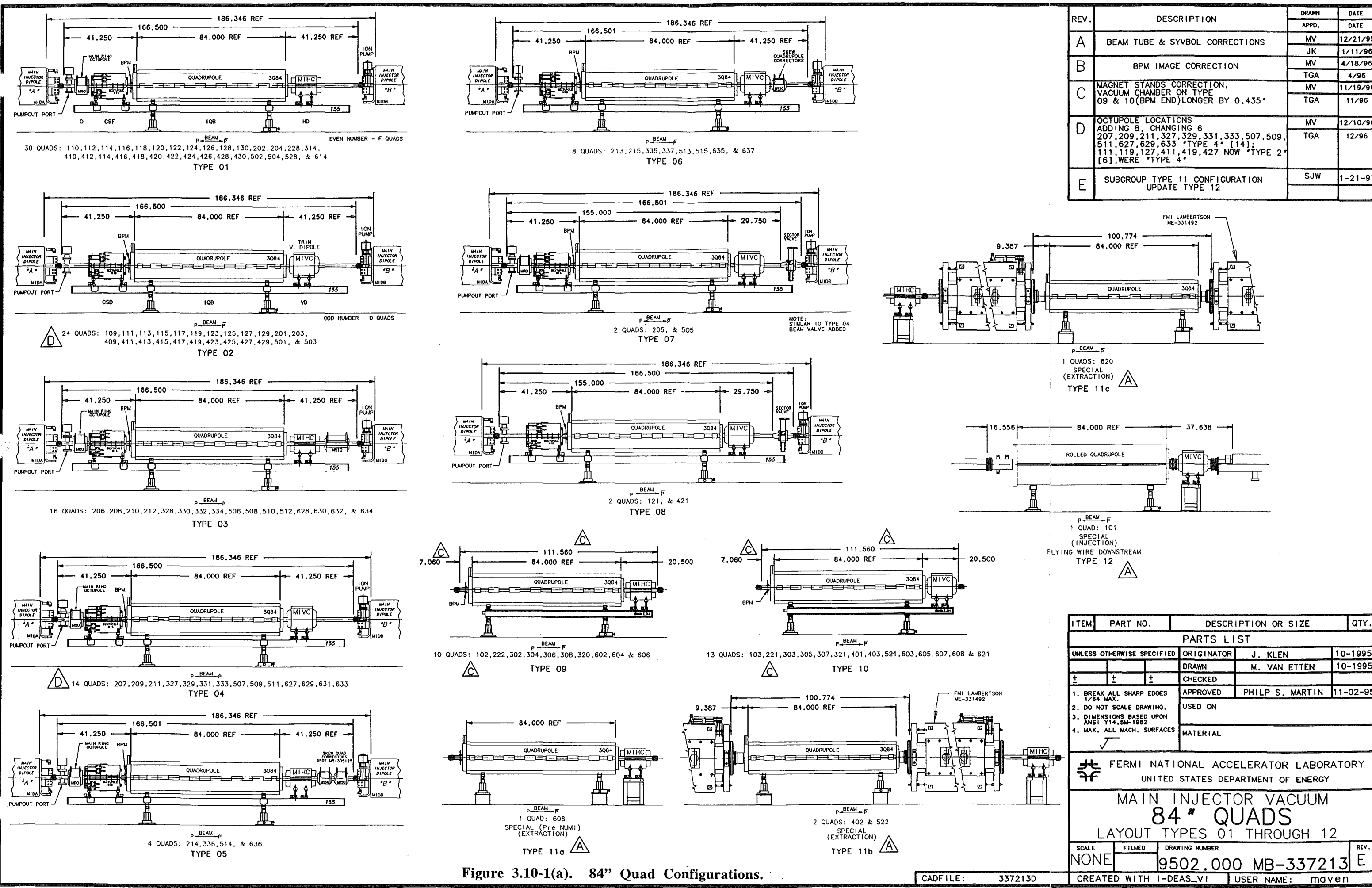
elevation resulting from normal construction tolerances, the eccentricity of the MI ring, and the 3.5 μ r tilt of the plane of the MI ring discussed in Chapter 2.1. Figure 3.10-1(a) shows the twelve anticipated combinations of the 84" (IQB) quadrupoles, together with the correction elements, and vacuum valves. Similarly, Figure 3.10-1(b) shows the 100" (IQC) quad configurations, and Figure 3.10-1(c) shows the 116" (IQD) quad configurations.

Installation of the dipole magnet stands was done after the LCW piping had been installed, progressing around the ring one task behind the other. The cable tray installation was initiated shortly thereafter. Once the entire ring enclosure is available, the alignment crews will return for a second survey. The crews will establish specific reference marks on the enclosure floor for the magnet stand locations. Using these marks, an installation crew, with the aid of custom templates, will locate and install mounting hardware in the floor to which the appropriate magnet stands will be bolted. When the installation of magnet stands of a common type is completed, the stands will be coarsely adjusted using a light weight, custom fixture that represents the actual magnet. It is expected that this additional step will position the magnets to within 1/4 inch of their specified locations. Figure 3.10-2 shows in some detail the dipole support design.

The intent of these procedures is to substitute, wherever possible, low cost labor for highly skilled labor. Magnet stands will be installed by relatively inexpensive labor. By pre-adjusting the stands, again using unskilled labor, the amount of time needed by rigging crews to set the magnets will be minimized. An additional benefit should be the reduced time that an alignment crew will need to make final adjustments.

Transporting and positioning the magnets to their locations in the enclosure will again be patterned after procedures that have evolved at the Laboratory over several years. Several compact magnet moving carts will transport magnets from their staging area in the enclosure to their designated locations as shown in Figure 3.10-3. At that point, a compact, hydraulically operated device will shift the magnet from the transporter to its permanent support, as shown in Figure 3.10-4. These devices were custom designed and fabricated for the specific magnets used in the Main Injector. This particular technique was successfully employed during the Pbar ring magnet installation.

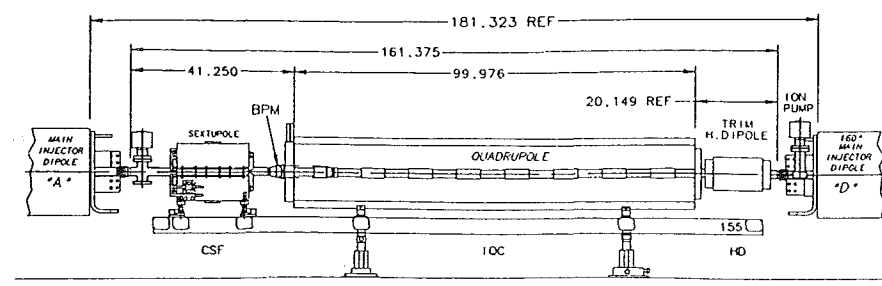
Since the dipoles for the Main Injector ring will be newly constructed, they will be installed during the early phases of the installation cycle. As of the date of this revision, 240 dipoles have been installed. The remainder will be installed as they become available in groups of approximately thirty. This will require an installation period of about one week every three months. The majority of the quadrupoles will be recycled from the existing Main Ring. During



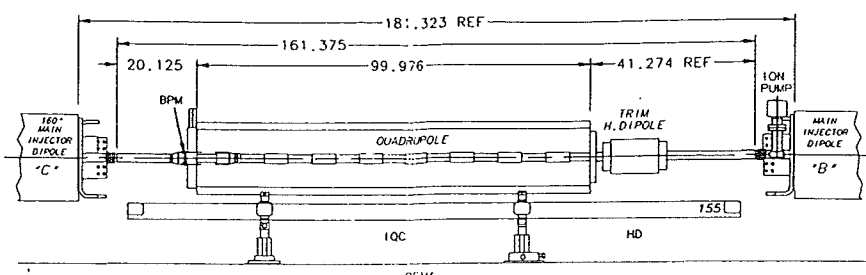
REV.	DESCRIPTION	DRAWN	DATE
A	BEAM TUBE & SYMBOL CORRECTIONS	MV	12/21/95
B	BPM IMAGE CORRECTION	JK	1/11/96
C	MAGNET STANDS CORRECTION, VACUUM CHAMBER ON TYPE 09 & 10(BPM END) LONGER BY 0.435'	MV	11/19/96
D	OCTUPOLE LOCATIONS ADDING 8, CHANGING 6 207, 209, 211, 327, 329, 331, 333, 507, 509, 511, 627, 629, 633 TYPE 4 [14]; 111, 119, 127, 411, 419, 427 NOW TYPE 2 [6], WERE TYPE 4	TGA	12/96
E	SUBGROUP TYPE 11 CONFIGURATION UPDATE TYPE 12	SJW	1-21-97

ITEM	PART NO.	DESCRIPTION OR SIZE	QTY.
PARTS LIST			
UNLESS OTHERWISE SPECIFIED		ORIGINATOR	J. KLEN
		DATE	10-1995
		DRAWN	M. VAN ETEN
		DATE	10-1995
		CHECKED	
		APPROVED	PHILP S. MARTIN
		DATE	11-02-95
		USED ON	
		MATERIAL	
1. BREAK ALL SHARP EDGES 1/64 MAX. 2. DO NOT SCALE DRAWING. 3. DIMENSIONS BASED UPON ANSI Y14.5M-1982 4. MAX. ALL MACH. SURFACES			
FERMILAB FERMILAB NATIONAL ACCELERATOR LABORATORY UNITED STATES DEPARTMENT OF ENERGY MAIN INJECTOR VACUUM 84" QUADS LAYOUT TYPES 01 THROUGH 12			
SCALE	FILMED	DRAWING NUMBER	REV.
NONE		9502.000 MB-337213	E
CADFILE: 337213D		CREATED WITH I-DEAS_V1 USER NAME: maven	

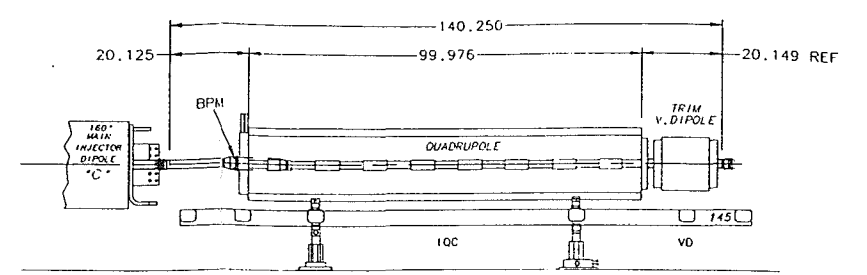
Figure 3.10-1(a). 84" Quad Configurations.



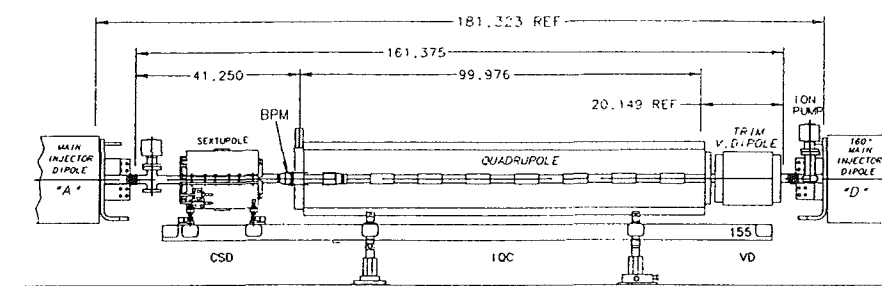
4 QUADS: 108, 326, 408, & 626
TYPE 21



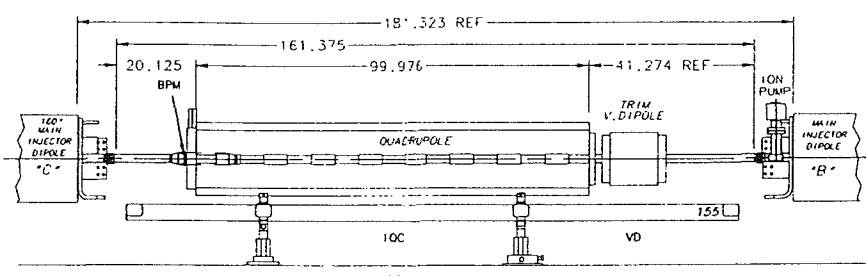
4 QUADS: 216, 338, 516, & 638
TYPE 25



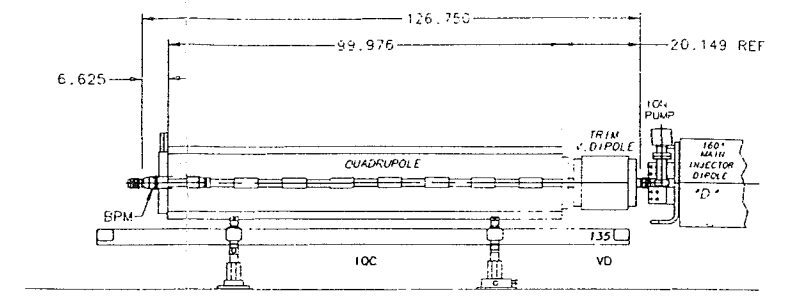
1 QUAD: 223
TYPE 29
NOTE: SIMILAR TO TYPE 24 WITHOUT THE BEAM VALVE



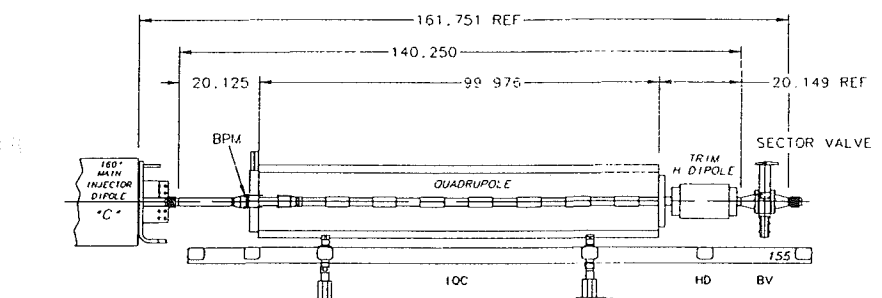
4 QUADS: 227, 313, 527, & 613
TYPE 22



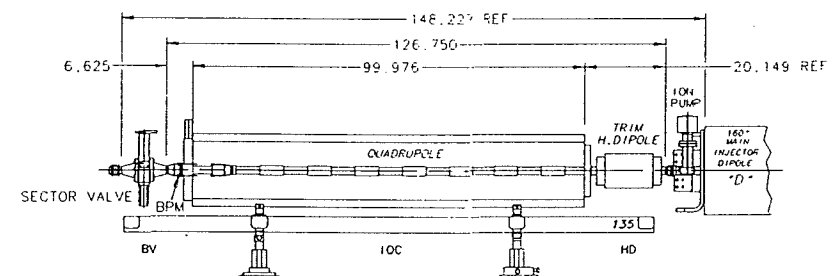
4 QUADS: 228, 315, 529, & 615
TYPE 26



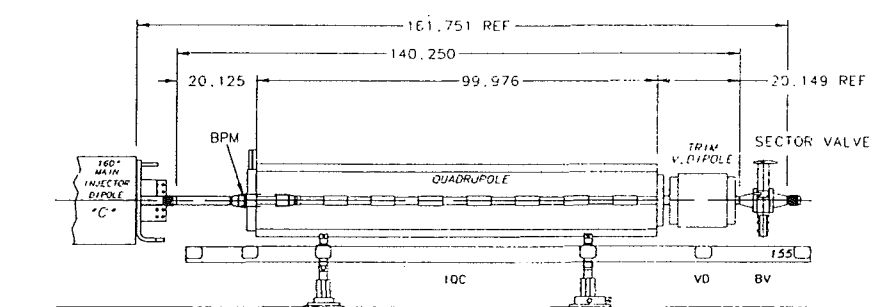
2 QUADS: 319, & 601
TYPE 30
NOTE: SIMILAR TO TYPE 27 WITHOUT THE BEAM VALVE



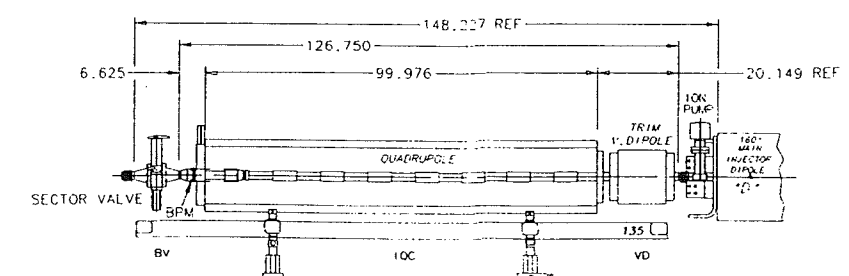
4 QUADS: 104, 322, 404, & 622
TYPE 23



4 QUADS: 100, 220, 400, & 520
TYPE 27



3 QUADS: 302, 523, & 609
TYPE 24
* VALVE ROTATED

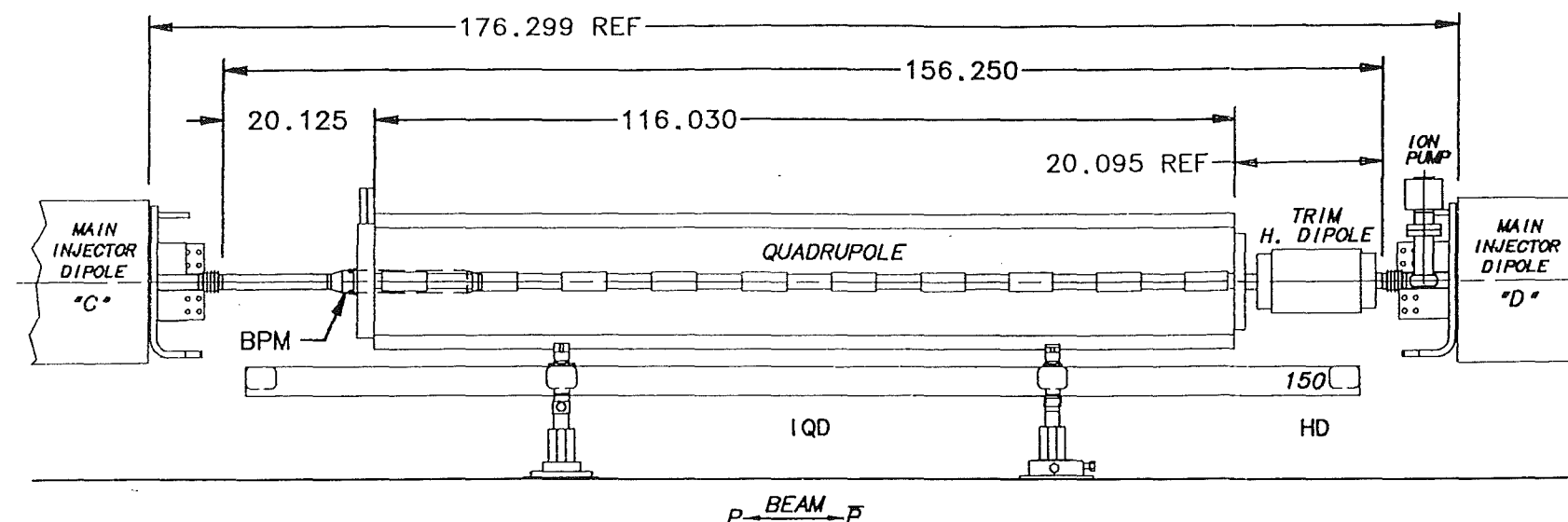


2 QUADS: 301, & 619
TYPE 28
* VALVE ROTATED

REV.	DESCRIPTION	DRAWN	DATE
APPD.			DATE

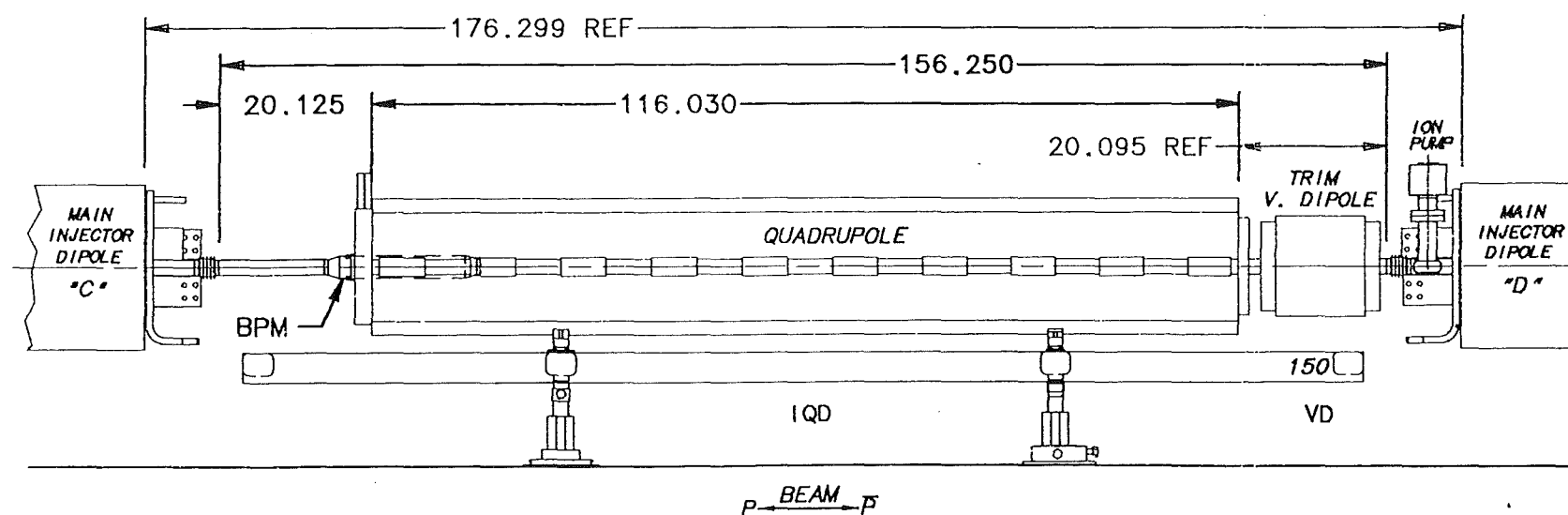
ITEM	PART NO.	DESCRIPTION OR SIZE	QTY.
PARTS LIST			
UNLESS OTHERWISE SPECIFIED		ORIGINATOR	J. KLEN
		DRAWN	M. VAN ETEN
		CHECKED	
1. BREAK ALL SHARP EDGES 1/64 MAX.		APPROVED	Philip S. Math 11/2/95
2. DO NOT SCALE DRAWING.		USED ON	
3. DIMENSIONS BASED UPON ANSI Y14.5M-1982		MATERIAL	
4. MAX. ALL MACH. SURFACES			
FERMI NATIONAL ACCELERATOR LABORATORY UNITED STATES DEPARTMENT OF ENERGY			
MAIN INJECTOR VACUUM 100" QUADS LAYOUT TYPE 21 THROUGH 30			
SCALE	FILMED	DRAWING NUMBER	REV.
		9502.000 MB-337214	
CADFILE: 337214		CREATED WITH I-DEAS_VI	USER NAME: maven

Figure 3.10-1(b). 100" Quad Configurations.



24 QUADS: 106, 218, 224, 226, 230, 232, 310, 312, 316, 318, 324, 340,
406, 518, 524, 526, 530, 532, 610, 612, 616, 618, 624, & 640


TYPE 41



24 QUADS: 105, 107, 217, 219, 225, 231, 311, 317, 323, 325, 339, 341, 405,
407, 517, 519, 525, 531, 611, 617, 623, 625, 639, & 641

TYPE 42

Figure 3.10-1(c). 116" Quad Configurations.

ITEM	PART NO.	DESCRIPTION OR SIZE	QTY.
PARTS LIST			
UNLESS OTHERWISE SPECIFIED		ORIGINATOR	J. KLEN
		DATE	10-1995
		DRAWN	M. VAN ETEN
		DATE	10-1995
		CHECKED	
		APPROVED	Philip S. maven
		DATE	11/2/15
		USED ON	
		MATERIAL	
<div>  FERMI NATIONAL ACCELERATOR LABORATORY UNITED STATES DEPARTMENT OF ENERGY </div>			
MAIN INJECTOR VACUUM 116" QUADS LAYOUT TYPE 41 & 42			
SCALE	FILMED	DRAWING NUMBER	REV.
1/2IN-1FT		9502.000 MB-337215	
CADFILE: 337215		CREATED WITH I-DEAS_VI	USER NAME: maven

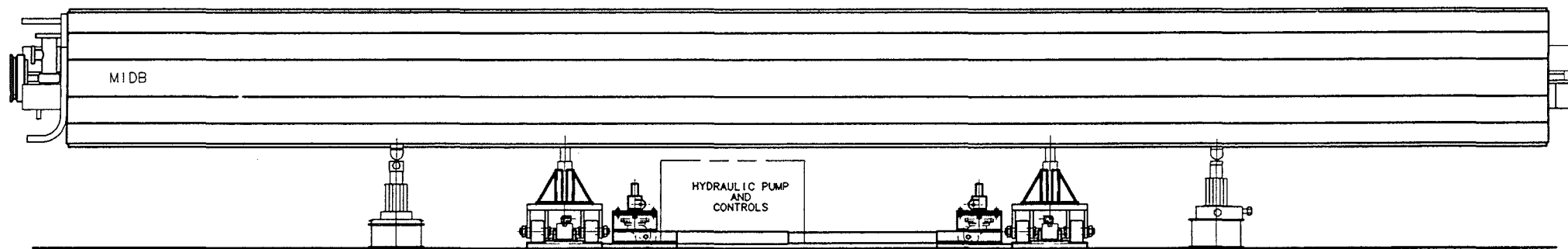


Figure 3.10-4(d). Magnet Installation Equipment Installing 6-m Dipole.

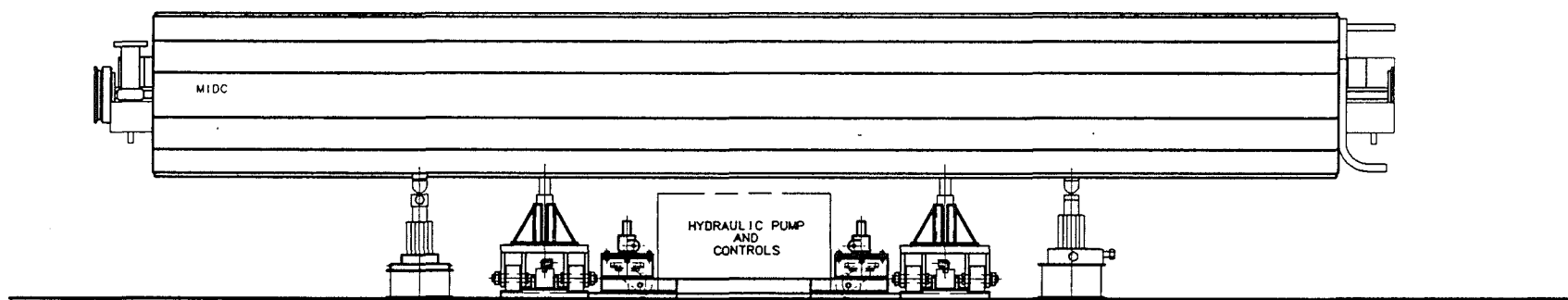


Figure 3.10-4(c). Magnet Installation Equipment Installing 4-m Dipole.

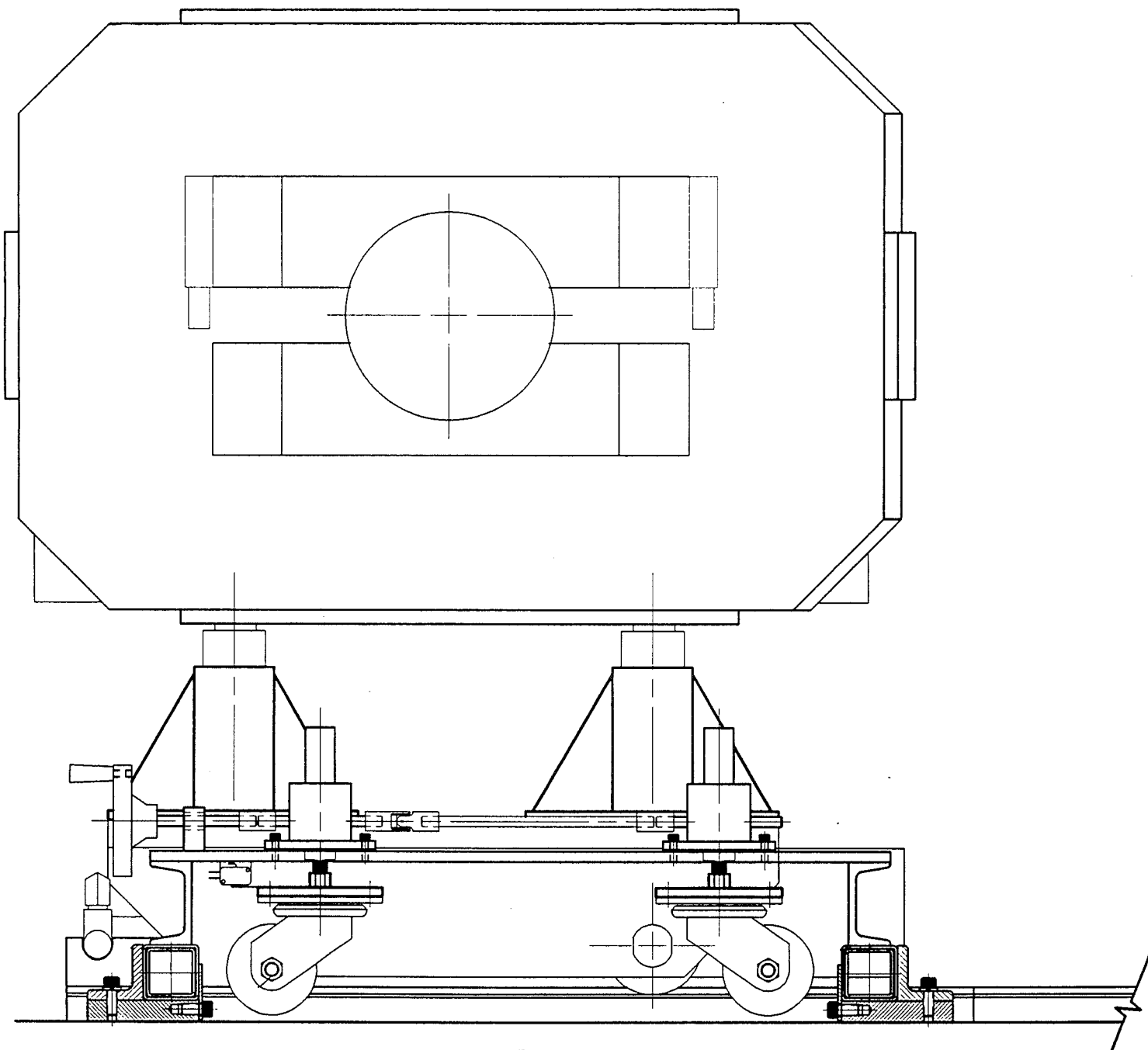


Figure 3.10-4(b). Section of Magnetic Installation Equipment with Dipole.

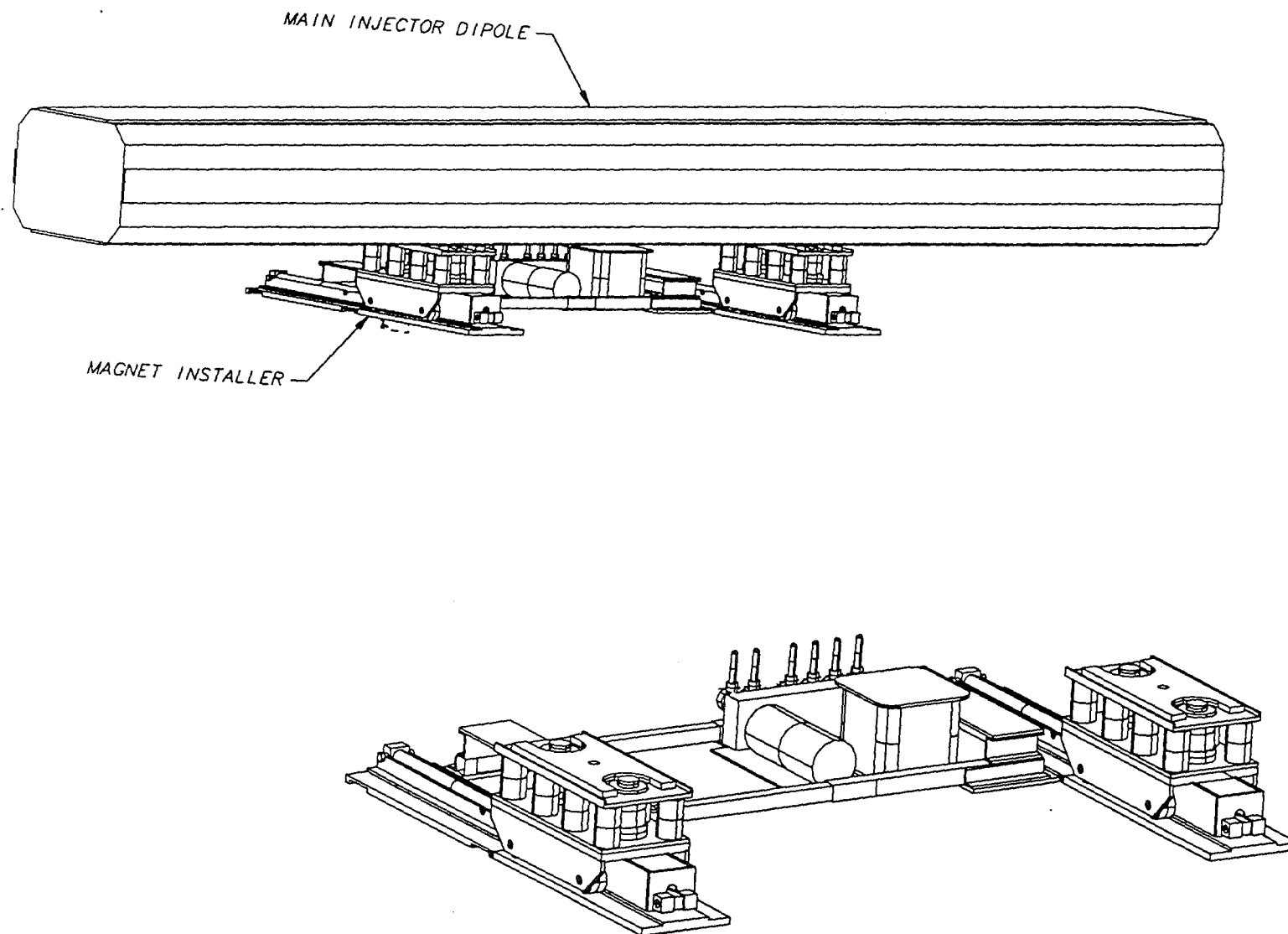


Figure 3.10-4(a). Magnet Installation Equipment.

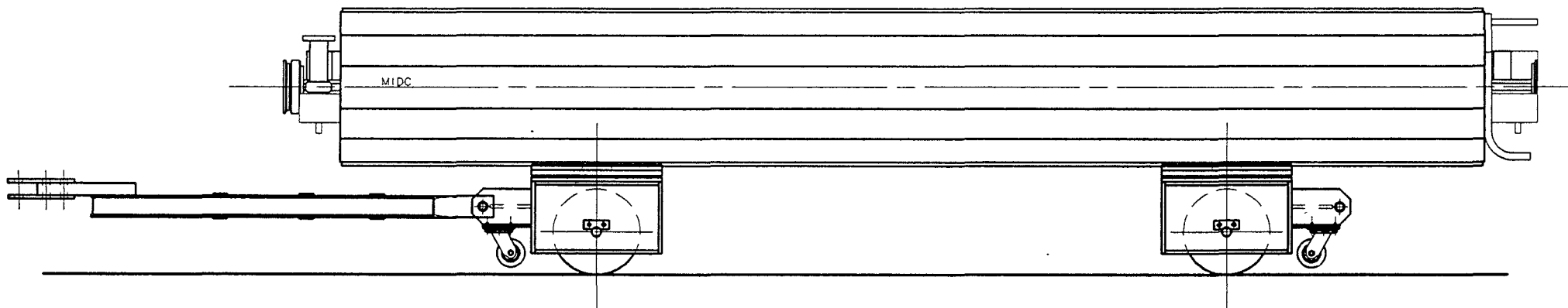


Figure 3.10-3. Magnet Transportation Equipment.

the shut down period marking the end of Main Ring operation, they will be removed from the Main Ring and will undergo modifications at the magnet factory. A major operation will be the insertion of a new beam tube into the existing quadrupole tube. Another key modification will be the addition of internal beam position monitors. Once refurbished, they will be transported to the Main Injector enclosure and installed using techniques similar to those used for the dipole magnet installation. Their support stands will be new and will have been installed as described above.

The rolled magnets in the abort line and specialty devices, such as Lambertson magnets, kicker magnets, etc., follow mounting schemes that are patterned after those described earlier. Their installation, however, will be done by rigging crews using the existing Main Ring magnet mover and installer.

Many details, especially at the magnet interfaces, are complex and congested. Several full scale mockups will be used during the final design stages to verify the feasibility of the designs. One mockup, which includes a segment of the tunnel enclosure as well as replicas of magnets and other major component, was fabricated in 1993. It has been enormously useful in refining designs and arrangement of the various utilities, and has been reconfigured as the designs evolve. Subsequently a 3 dipole 2 quadrupole magnet string and associated LCW system has been installed in the actual tunnel just upstream of the RF straight section.

Magnets that have been mounted, can be surveyed and aligned. When groups of dipoles and quadrupoles have been aligned, cooling water and bus connections (Chapter 3.9) will be made and vacuum components (Chapter 3.2) will be installed.

Small correction magnets, (Chapter 3.1), some of which will be recycled from the Main Ring, will be mounted on either side of the quadrupoles. The beam pipe that runs through each quadrupole is, in most cases, one continuous piece which connects directly to the dipoles on either end. Therefore, the correction magnets need to split into halves in order to install them. With the exception of the sextupole magnet, these small magnets halves can be lifted by hand and put into their proper positions. Because of their heavier weight, a fixture will be necessary to support the sextupole halves while they are being positioned around the beam pipe. Again, the techniques used for these installations will make use of templates and mechanical aids that will permit the use of low cost labor.

As far as instrumentation is concerned, the most prevalent devices will be the beam position monitors and the beam loss monitors. Many of the beam position monitors will be incorporated into the spaces that remain when the new beam tubes are inserted into the old beam tubes of the quadrupoles as shown in Figure 3.2-4. The beam position monitors will be installed

as part of the Main Ring quadrupole rework program. The beam loss monitors are the same type as the Tevatron system and will be installed at each quadrupole.

Laying out the cabling for a complex machine with a large number of diverse devices needs careful planning to prevent clutter and disorder. Wiring for the smaller devices will be brought through a conduit that runs from the cable tray to the individual devices. The conduit is mounted transversely along the ceiling and runs vertically down on the wall nearest the beam line. (See Figure 3.9-1) A generous bend radius will make wire pulling easier. With the use of a conduit at each quadrupole, wiring will be neatly collected at the cable tray and at the other end the wires will be fanned out to their respective components.

Power lines for devices requiring 120 VAC and 208 VAC will be provided via outlets on the wall closest to the beam line. Four 20 A, 120 VAC outlets will be located at each quadrupole, along with two 20 A, 3-phase 208 VAC outlets. However, the 208 VAC outlets at two adjacent quadrupole locations can be powered from the same circuit breaker. This provides adequate coverage for the pump-out ports and where leak checking equipment and turbopumps will be connected.

The various magnets (dipoles, quadrupoles, trim magnets, C-magnets, Lambertsons, etc.), the vacuum components, the cable trays, the LCW piping, the power bus, and the instrumentation represent most of the major physical components that will be installed in the enclosures. There are additional groups of devices and systems that will complete the installation of the key elements of the Main Injector. These are the power supplies (Chapter 3.3), the RF systems (Chapter 3.4), the control system (Chapter 3.7), the safety system (Chapter 3.8), and the abort system (Chapter 3.9). Their installation will be staggered with respect to the other installations. With careful coordination, different activities can take place simultaneously in different sections of the Main Injector complex.

The revised 8 GeV beam line consists primarily of permanent magnets with a mix of 45 pure dipoles, 65 combined function (gradient magnets), and 9 quadrupoles. To supply supplemental steering and adequate focusing functions, Main Ring style trim magnets and p-bar style quadrupoles are installed at both the Booster end and the Main Injector intersection. Additionally there are 4 powered dipoles (EPBs) to provide sufficient bending both vertically and horizontally at the upstream end of the beam line. 8 GeV conventional wall power is formatted almost identically to the power provided for the Main Injector Ring as described earlier.

The magnet stands for the permanent magnets are a simple 3 point support design and have been installed. This design will be used as a test bed for the upcoming Recycler installation.

Powered quads and dipoles are supported by a wide range of p-bar style stands and hangers which are complicated by the sloped ceiling at the upstream end of the beam line. The 9 permanent quadrupoles are supported in a fashion similar to the other permanent magnets. Trim magnets are supported independently from the adjacent quad allowing independent alignment and simple replacement in the event of failure. Special consideration was given to the stand or hanger design at the upstream end of the beam line in order to provide access to replace a powered magnet if necessary. As of this writing, 43 dipoles, 37 gradient magnets, and 3 powered quads have been installed. The permanent magnets were installed using special, but simple, dollies for transport and a pallet mover. The 3 powered quads were rigged into position by jacks and cribbing. Ceiling hung quads will be maneuvered into position by a fork truck capable of reaching the high, sloped ceiling. The EPBs are to be transported through Booster on high capacity die tables and lifted up to their hangers.

CHAPTER 4. CIVIL CONSTRUCTION

1. OVERVIEW

The civil construction for the Fermilab Main Injector (FMI) includes all below-grade beamline enclosures with connections to the existing Booster and Tevatron enclosures; passive earth, concrete and steel shielding; equipment, utility and personnel access structures; above ground service buildings; a major electrical power substation and 345 kV power transmission line and site work such as wetland mitigation, compensatory floodplain storage, storm drainage, roads, parking, survey monuments, cooling ponds and cooling water system, utilities and services to accommodate the equipment for, and operation of, the FMI.

The below-grade enclosures include the FMI ring enclosure and the various beam transport enclosures which provide for the following beam transport lines:

1. 8 GeV protons from the Booster to the FMI,
2. 150 GeV protons from the FMI to the Tevatron,
3. 150 GeV antiprotons from the FMI to the Tevatron,
4. 120 GeV protons from the FMI to the Antiproton Source,
5. 8 GeV antiprotons from the Antiproton Source to the FMI, and
6. 120 GeV protons from the FMI, via the Main Ring remnant in the F-sector, to the beam extraction lines for the fixed target areas.

The conventional construction has been planned to permit completion of the entire MI (Main Injector) enclosure, the majority of the 8 GeV enclosure, all the new service buildings and access structures and a functional utility system concurrent with the full and uninterrupted operation of the existing Fermilab accelerator complex and the experimental areas. Early construction has been sequenced to permit early occupancy of the MI-60 Enclosure and the MI-60 Service Building to accommodate R&D and testing work for power supplies and controls as well as to provide equipment access to the MI enclosure for magnet delivery and storage. The last phase of the conventional construction, consisting of the 150 GeV enclosure and the F0 (pronounced F-Zero) enclosure connecting the MI to the Tevatron, the 8 GeV enclosure link at the Antiproton crossing, and the modifications to the F0 Service Building, will be accomplished during a minimum seven month shutdown of the accelerator complex. The relocation of existing Main Ring technical and control components, heat exchangers, harmonic filters and other

equipment will also be accomplished during this shutdown. Hence, the civil work will be completed in a sequence which corresponds to the needs of the technical development, assembly, installation and testing of the MI with minimal interruptions to the Fermilab operations.

The FMI conventional design is very similar to previously utilized and proven structural systems and construction methods developed for other Fermilab projects. The industrial, utilitarian architectural style of the above-ground buildings reflects, and is harmonious with, existing nearby buildings. Existing wetlands, topography, vegetation, natural habitat, road system and site boundaries have been carefully observed in the planning of the new construction. All these aspects have been thoroughly addressed in the Environmental Assessment (EA) for the FMI which resulted in the issuance of a Finding of No Significant Impact (FONSI) by DOE on July 6, 1992.

Safety provisions for radiation, fire protection, and conventional life safety are included in this Design Handbook and further detailed in the Preliminary Safety Analysis Report (PSAR) for the FMI.

In the following text, references to drawing numbers should be interpreted as referring to the Title 1 drawings which are included in the appendix. In addition to the Title 1 drawings, the appendix also contains a selection of drawings from the bid sets for the various construction packages, which contain much additional information.

2. SITE CHARACTERISTICS

The FMI ring enclosure encompasses 440 acres of the southwest corner of the Fermilab site and is located approximately 245 feet from the site boundary. This southwest boundary parallels an abandoned railroad embankment which has been converted to the Illinois Prairie Path. The majority of this area is open cropland, one-third of which has been in recent cultivation with the remainder lying fallow for more than ten years. Indian Creek and small tributary ditches meander through the site from the north to the southwest following the general topography which slopes from elevation 747' to 731' within the ring limits. Indian Creek, with its headwaters located on site, drains approximately 1,480 Fermilab acres before leaving the site via a double box culvert under the Prairie Path on a seven mile journey south and west to the Fox River.

The FMI site crosses through the limits of the 100 year floodplain of Indian Creek at two locations (see Drawing C1) where shielding berms, road embankments and cooling ponds will displace 29 acre-feet of storage. The required compensatory storage can be readily accommodated in the FMI infield and has been combined with the wetland mitigation area to provide a total of 40.9 acre-feet as shown on Drawings C2 and C7. The FMI storm drainage system will be

designed not to exceed a discharge at the site boundary of 618 c.f.s. or a maximum flood elevation of 734' which represent the historic 100 year flood conditions. Discharge from the site will be controlled by impounding storm water within the FMI infield and designing the culverts through the berm at the southwest quadrant to limit flows for all storms with less than a ten year frequency. A 100 year storm will result in a maximum impoundment of 340 acre-feet and a water level in the infield which will peak at approximately elevation 735.5'. The FMI berm has been designed as a Class III dam in accordance with the Illinois Department of Transportation (IDOT) standards, and relocated Kautz Road as well as the emergency exit stairways on the infield side of the berm will all be located well above the maximum impoundment elevation. All service buildings, except MI-60, are located along the outer perimeter of the berm while service building MI-60 is separated from the infield by relocated Kautz Road. All building floors and almost all road elevations are above 100 year flood levels. The section of Indian Creek Road located between box culverts 3 and 5 has been designed as a broad-crested weir to allow 100 year storm runoff from the northwest to overtop the road for a few hours during the hydrographic peak. This feature prevents the flooding of upstream areas near the Antiproton Source. Any storm flow greater than the 100 year flood will be diverted into the perimeter cooling ponds via rip-rap lined spillways and carried outside the FMI ring to the Prairie Path culvert.

A wetland survey by Envirodyne Engineers, Inc. in the spring of 1990 identified nine different classifications of wetlands covering a total of 100.4 acres within the environs of the FMI ring which are subject to regulation by Section 404 of the Clean Water Act. By careful design modification, the FMI will only require permanent filling of 5.7 acres of these wetlands. These modifications included altered cooling pond configuration, road alignment changes, relocation of service building MI-40, and minimal construction limits through the major wetland area as demonstrated by cross sections shown on Drawing C-6. A wetland mitigation area of 10.3 acres has been constructed in the infield area east of and adjacent to Indian Creek exceeding the required 1.5 to 1.0 ratio for the mitigation area. Hydric soils from the existing wetland have been transferred to the mitigation area which is divided into a central sedge meadow with a perimeter forested zone. All work, including erosion control and the five year monitoring plan, is in accordance with a U.S. Army Corps of Engineers (COE) 404 permit. In addition, Fermilab has relocated a number of trees and shrubs from the existing wetland to augment the new plantings in the mitigation area.

During the site work construction of the perimeter of Indian Creek Road and underground utilities in the fall of 1993, an existing, active 12-inch diameter clay tile drain was discovered on the west side of the FMI ring near road station 50+25. It was learned that this tile was the main drain for a farm tile network located on the Roth farm extending 4800 feet west of the Fermilab

site boundary. The tile field, constructed by Roth's grandfather in the early 1900s, drains farm land still under active cultivation. Since the 12-inch tile extended to Indian Creek, future construction of the cooling pond and the FMI ring enclosure would interfere with the tile drain. It was decided to intercept this tile at the Fermilab property line with a 12-inch PVC pipe and extend the new piping approximately 975 LF. along the west shoulder of Indian Creek Road to an outfall at Indian Creek before it passes under the Prairie Path. Mr. Roth accepted the diversion and immediately noted an improved drainage of those fields abutting the Fermilab boundary.

A three acre great blue heron rookery was located in a stand of dead maple trees within the southern quadrant of the FMI infield. However, in the spring of 1991, the herons abandoned this nesting site in favor of an area located in the center of the Main Ring infield almost one mile to the northeast. Should the herons return, construction activities within a 200 meter radius would be limited during the nesting season. However, it has been demonstrated that construction can be scheduled around the nesting season without delaying the project completion. Fermilab has employed an ornithologist to observe the movements of the herons and to make recommendations to ensure the birds are protected under the Federal Migratory Bird Treaty Act. Very limited access to the FMI infield after completion of construction will actually provide a higher degree of protection to the rookery site than presently exists.

Three archaeological sites have been identified within the region of the FMI (see Drawing C-2), but all have been classified as not eligible for the National Register of Historic Places. The Lorenz site, located adjacent to the wetland mitigation area in the infield, as well as the Pioneer and Tadpole sites, have been fenced and will be left undisturbed but accessible. More definitive and extensive information regarding these and other environmental aspects of the FMI site have been addressed in the EA document. The EA was the basis for a FONSI by U.S. Department of Energy (DOE) as published in the Federal Register on July 6, 1992.

The sub-surface characteristics of the FMI site have been thoroughly investigated and conditions are generally consistent with the remainder of the Fermilab site. Seven existing soil borings have been augmented with an additional 32 new borings (see Drawing C-1) around the MI perimeter plus an additional 8 borings at the Kautz Road Substation and along the 345 kV transmission line. Typically, the site is overlain with several feet of topsoil, then either a layer of weathered till or an alluvial deposit followed by the unweathered glacial till. This brown-gray clay with traces of sand and gravel has proven to be an excellent foundation strata. The unweathered till is found at depths between 4' and 22' on the FMI site and, hence, the entire ring enclosure will be founded on this strata. The glacial till has unconfined compressive strengths ranging from 2.5 to 5.0 tons per square foot which will be adequate for superimposed enclosure

and shielding berm loads. Moisture contents range up to 30% near the surface to 18% in the till. Predicted long-term settlements for the enclosure base slab are in the range of 0.1 inches to 0.2 inches with the majority occurring soon after construction. Permeability ranges from 10^{-4} to 10^{-6} cm/sec above the till and 10^{-7} to 10^{-8} cm/sec in the glacial till. Construction dewatering will be required to protect initial cut slopes with ditches, benches and pumped sumps at the excavation base. However, construction experience at the nearby Antiproton Source indicated much of the groundwater was perched and presented no significant problems after initial pumping because of the slow recharge rate. All completed underground enclosures will be protected by perimeter underdrains and membrane waterproofing.

3. SITE PREPARATION AND UTILITIES

Site drainage will be controlled by ditches and culverts while preserving the existing watershed characteristics both during construction and subsequent operation. The cooling pond system will generally follow the ground elevations with pumping stations utilized to circulate the water. Culverts passing through the shielding berm over the FMI enclosure will be designed to attenuate radiation by limiting culvert diameter, spacing multiple culverts approximately two diameters on center and adding steel shielding above the enclosure roof to provide the equivalent passive protection afforded by the typical berm.

An early subcontract, MI site work, included installation of a 30' wide crushed stone road base along the Indian Creek Road alignment to serve as a construction access road. Since the principle power and communication duct bank is sited below the road, its construction along with the manholes was included in this scope and preceded the installation of the base course. The manhole frames and covers as well as one or more rings of the manhole access have been temporarily omitted to avoid severe loading caused by earthmoving equipment. The openings are temporarily covered with steel plate and buried under the road base. This stone base will be maintained throughout the construction period for access requirements including hauling and earthwork activities, delivery of construction material and early installation of technical components. At the completion of major construction work, the manhole access, frames and covers will be installed. The base will then be cleaned, new stone added where required, recompact and paved with two 1 1/2-inch courses of bituminous aggregate. The final paved width will be 22' with 4 foot aggregate shoulders. The road profile will be designed with a maximum grade of 3%.

The same subcontract has provided a temporary overhead power line at 13.8 kV. The power source will be an existing 34.5 kV Commonwealth Edison pole line along Giese Road located approximately 1,000 feet northwest of the FMI ring. A transformer with a capacity of 7.5

MVA has been located at Giese Road, temporary poles installed along Indian Creek and Kautz Roads (except through the wetland borrow area) and drops terminating with fused disconnects provided at future service building sites for the subcontractor's use. (See Drawing E-3.) There will be sufficient temporary power available to operate pumping stations, subcontractor's equipment, and the initial power requirements for the early occupancy of the MI-60 service building.

Underground utility systems include ICW, domestic water (DWS), sanitary sewer, chilled water supply (CHWS) and chilled water return (CHWR), all extensions of existing site-wide systems (see Drawing C-5). An ICW loop consisting of 12-inch ductile iron pipe has been installed along the majority of Indian Creek Road and relocated Kautz Road as part of the initial site work package. The remaining ICW work is included with the MI Enclosure subcontract. When completed, the ICW loop will be connected to the existing site system at three locations to provide the water source for the fire protection system at all service buildings including interior wet sprinklers and pairs of exterior hydrants. Post indicator valves located at each service building between the two hydrants provide isolation of segments between service buildings while still maintaining fire protection.

Domestic water and sanitary sewer services are required for toilet facilities located at the MI-8 (formerly designated the North Hatch) and MI-60 Service Buildings. The DWS has been extended from the Antiproton Target Hall (AP-0) to the MI-60 Service Building under the initial site work subcontract. This package also included construction of the sanitary sewer from the MI-60 Service Building to an existing force main in the Antiproton area near Well Pond Road. The sewer extension is a combination gravity line and force main and includes two lift stations. Later subcontracts will extend the DWS to Service Building MI-8 and provide a sanitary sewer connection to the nearest lift station.

Chilled water service is limited to RF systems and environmental cooling requirements at the MI-60 Service Building. The service building construction subcontract included one 150 ton air-cooled chiller with provisions for a future second unit of the same capacity. However, in anticipation of planned improvements at the Central Utility Building (CUB), underground chilled water supply and return piping will be installed as part of several subcontracts to eventually connect the MI-60 Service Building with the CUB. When the chiller upgrades are completed at the CUB, the MI-60 Service Building requirements can be supplied by the more reliable central system and the air-cooled chiller will become a standby source. Chilled water service to the existing F0 Service Building, presently supplied by 6 inch underground supply and return piping from the CUB routed along the Main Ring Road, will also be switched over to the new piping allowing the abandonment of the old and unreliable existing piping.

4. RING ENCLOSURE

The MI ring enclosure (WBS 1.2.2.1 and 1.2.2.2) is an oval-shaped, below-grade structure approximately 10,890' in length, with a rectangular cross-section typically 10'-0" wide by 8'-0" high. At utility alcoves opposite the seven typical service buildings the enclosure height is increased to 9'-0" and widths are increased to accommodate utility penetrations, sump pumps, dehumidifiers, electrical panels, dry-type transformers, LCW expansion loops and services crossing the enclosure width along the ceiling. Four additional utility alcoves will be provided midway between service buildings MI-10 through MI-50 as illustrated on Drawing AS-3. Alcove lengths are nominally 16' but the total length of this CIP concrete varies to match the placing pattern of the adjacent precast concrete elements typical for the majority of the ring enclosure. The enclosure plan and sections are shown on Drawings AS-2 through AS-8. The floor of the ring enclosure is at a constant (locally defined) elevation of 713'-6" or between 18' and 33' below existing grade. The MI technical components for the circulating beam are in a true plane nominally centered at elevation 715'-9" (or more precisely at 715.724'), approximately 2'-3" above the enclosure floor and nominally positioned 2'-3" from the inside face of the outer enclosure wall. The stationing of the MI Enclosure is based on the machine lattice defined by Cell Boundaries (CB). In general the geometries shown on Drawing AS-1 are derived from the three typical cells of the machine—dispersion, normal and straight (normal cells without dipoles).

The base for the FMI ring enclosure will be a CIP concrete slab over a 3" thick lean concrete "mud slab" located on undisturbed glacial till. The mud slab is placed immediately after the excavation is completed to minimize disturbance of the bearing strata and to provide an all-weather work surface for placing the base slab. The majority (approximately 8,387 l.f.) of the walls and roof of the ring enclosure with a typical cross-section 10'-0" wide by 8'-0" high will consist of precast reinforced concrete inverted U-shaped elements averaging approximately 7' in length. These precast elements will be cast off site under a separate subcontract and delivered to the site for installation by the erecting subcontractor. The elements, weighing up to 18.3 tons, are lowered onto the base slab and held in place by welded anchors in four locations. The joints between units are made watertight with sealant applied over a backer rod. This underground enclosure construction system is a proven procedure at Fermilab with nearly 26,000 feet of this general type of precast element placed during the last 20 years. Drawing AS-8 illustrates the typical precast element details and placing plan while the typical precast section for the MI enclosure is shown on Drawing AS-7. Segments of the ring enclosure requiring varying widths or special configurations, such as the injection or extraction regions, the alcoves, the abort region, intersections of the ring enclosure with access labyrinth or exit stairs, regions requiring a ceiling height greater than 8' or the MI-60 region with a larger cross-section will be constructed of CIP

walls and roof as illustrated on Drawings AS-4, AS-18 and AS-19. the width at the 8 GeV injection area, shown on Drawing AS-14, varies from 17' to 26'. At the proton abort region, which may also be utilized as an extraction point for future experimental areas, the enclosure width varies from 16' to 25' while the base slab is stepped with the outer region (extracted beam area) at elevation 712'-0" as illustrated on Drawing AS-4. The MI-60 region, which houses the MI rf accelerating and coalescing cavities, will be approximately 460' long with a cross section 15'-0" wide by 9'-0" high. The 150 GeV transition regions for the proton and antiproton injection, which intersect the MI ring enclosure approximately 680' to either side of CB-605 (MI-60), will generally be 10'-0" high enclosures with widths varying from the typical 10' to a maximum of 27'. The 150 GeV proton extraction begins with a 10' wide by 9' high enclosure upstream of CB-521 adjacent to the alcove for the MI-52 Service Building. Just upstream (proton direction) of CB-523, the ceiling height becomes 10' and the enclosure width begins to increase to a maximum of approximately 22' downstream of CB-527. At this point the enclosure branches into two enclosures. The ring enclosure continues as a 10' wide by 10' high enclosure to a point midway between CB-528 and 529 where the ceiling drops down to the typical 8'-0". The 150 GeV transport enclosure continues toward F0 with a cross-section 10' wide by 10' high. The stair near CB-529 provides separate exits from both the ring enclosure and the 150 GeV enclosure to a common labyrinth and stair to the exit at grade since the MI beam line components separate the two aisles. The extraction region includes a 3' deep by 60' long pocket or niche along the inner ring wall near CB-526 designed as a temporary storage location for translated beam line components to permit access from the MI aisle to the 150 GeV aisle for equipment installation.

The 150 GeV antiproton extraction is generally symmetrical to the proton extraction. A 10' wide by 9' high enclosure extends clockwise from a point adjacent to the alcove for the MI-62 Service Building midway between CB-621 and 622. Just downstream (proton direction) of CB-619, the ceiling height becomes 10' and the enclosure width begins to increase approximately 18' at a point roughly 15' downstream of CB-615, mirroring the proton transition and including the 3' x 60' temporary storage niche along the inner ring wall. The next region, however, is significantly different from the proton counterpart because it must accommodate a future experimental proton beam extraction in the counterclockwise direction as well as the clockwise 150 GeV antiproton transition. Hence, the plan of the next 95' of enclosure resembles a railroad cross-over with the CIP enclosure width varying from approximately 23' to 31' while the height remains at 10'. The future extracted proton beam enclosure ends opposite a point between CB-615 and 616 as a 10' wide by 10' high stub with provisions for later extension. The 150 GeV antiproton enclosure proceeds clockwise as a separate 10' high enclosure of varying width until a point opposite CB-613 where the enclosure assumes the nominal 10' wide by 10' high geometry

of the 150 GeV transport. The exit stair separates and serves both the 150 GeV enclosure and the adjacent MI ring enclosure. The ring enclosure ceiling height drops to 9'-0" at this region but the width varies from approximately 12' at CB-613 to the standard 10' at the juncture with the MI-60 enclosure at CB-611 to accommodate the extraction of the experimental proton beam.

The MI ring enclosure was divided into two principle regions—the MI-60 enclosure (WBS 1.2.2.1) and the remainder of the ring originally designated as the ring enclosure between MI-62 and MI-52 (WBS 1.2.2.2). The ultimate limits of the subcontract packages were revised to define the "MI-60 Enclosure" as located roughly between CB-531 and CB-611 or approximately 625 LF while the "Main Injector Enclosure" includes the remainder of the ring or 10,265 LF. The MI-60 Enclosure was planned as the first major construction effort for several reasons. Most importantly, the MI-60 enclosure plus the adjacent MI-60 service building will be the hub of FMI functions and activities during both installation and operation phases. All magnets and beamline equipment will be installed into the MI enclosure via an elevator or crane-covered vertical shaft extending from the high bay space of the MI-60 service building to the MI-60 enclosure. The MI-60 enclosure houses atypical functional components such as the rf accelerating and coalescing cavities and, at regions to either side of MI-60, the extraction systems for the 150 GeV beamlines which will require more time to install and test. There are over 200 utility penetrations between the MI-60 enclosure and its service building including waveguides, power bus or cables, controls, diagnostics, and three LCW systems. The MI-60 service building, which immediately followed the MI-60 enclosure construction, houses assembly areas and will be utilized for initial installation and testing of power supplies, rf components and controls. The MI-60 enclosure and service building can be used to temporarily store delivered magnets and equipment prior to final testing and installation. Hence, the early occupancy of the MI-60 enclosure and service building are critical to the project schedule.

There was also a basic construction scheduling logic for starting the enclosure work at MI-60. The majority of the MI enclosure (exclusive of the MI-60 region) will be constructed using precast concrete inverted U-shaped elements for the walls and roof. Use of these elements makes the below grade work more independent of weather conditions, provides a drier enclosure with a better interior surface finish and minimizes the construction schedule by eliminating form work and concrete curing time. However, because 1,181 of these elements are required and because steel forms must be fabricated first, some lead time was necessary before these elements were available for installation. Consequently, the CIP MI-60 enclosure with its larger atypical cross section was the logical initial on-site construction project while a separate concurrent procurement of the elements was initiated at an off-site concrete precasting plant.

One of the basic design parameters of the FMI was to place the new facility as close to the existing Main Ring enclosure as possible to minimize the length of the transfer beamlines between the FMI and the Tevatron, as well as maximizing the distance to the site boundary at the opposite side of the new machine. Since the construction was planned to proceed while the existing accelerator remained operational, the minimum distance between the old and new ring enclosures was determined by radiation shielding requirements. Hence, the MI-60 enclosure work area has been separated from the existing F0 enclosure by a minimum of 21' of earth shielding. It is also an economical and functional expedient to locate grade-level service buildings as close to their associated underground enclosures as feasible without actually placing the service building directly above the enclosure. This latter procedure restricts the ability to increase the shielding between the two structures should regulations become more conservative and new penetrations, enclosure improvements, and construction on backfill with the probability of increased settlements all pose potential future problems. In order to place the MI-60 enclosure close to the Tevatron and, later, construct the MI-60 service building with minimal penetration and access lengths, two parallel lines of steel sheet piling with walers and crosslot bracing were utilized to form an earth retention system both southwest and northeast of the MI-60 enclosure. This procedure provided the required 21' of earth shielding to the existing F0 region of the Tevatron, located the MI beamline only 38'-9" from the parallel Tevatron beamline and placed the near wall along column line A of the MI-60 service building slightly more than 28' horizontally from the MI beamline while still providing 26' of shielding. The retention wall configuration is shown in plan on Drawing AS-3 while Drawings AS-25 and AS-26 show several transverse cross sections. The final relationship of the MI-60 enclosure and service building in plan view as well as a tabulation of the utility penetrations is shown on Drawing AS-22. A detailed cross-section of the MI-60 enclosure is shown on Drawing AS-7.

Earth berms over the FMI ring enclosure typically provide the required 24'-6" earth equivalent radiation shielding for unlimited occupancy resulting in a normal top of berm elevation of 747'-0". The extraction regions are shielded with 25'-0" of earth equivalent. Areas where future accessibility for increasing the shielding will be restricted, such as between the MI-60 and F0 service buildings or directly behind typical service buildings at the service corridor, will be shielded with 26'-0" of earth. Shielding throughout the project will be augmented by the use of steel plate where physical limitations preclude "all earth" berms. A foot of steel nominally replaces 2.89 feet of earth. Steel will be added at culvert crossings over the enclosure (see Section through Indian Creek Outfall on Drawing C-6) or where the passageway between the MI-60 and F0 service buildings and exit stairways pass over the MI enclosure (Section A on Drawing AS-25).

The exterior walls and roof of the entire ring enclosure and all underground extensions such as stairways and labyrinths will be waterproofed and backfilled with free-draining compacted crushed stone fill for 1' above the enclosures and 2' from the walls. A continuous underdrain system along each side of the base slab composed of a 6" perforated corrugated metal pipe surrounded by crushed stone filter media and a geotextile filter fabric will eliminate any hydrostatic head against the enclosure. The underdrains lead to a total of 13 sumps located at the service building and intermediate alcoves where 125 gpm duplex pumps will discharge the underdrain water to ditches or the cooling ponds. In selected areas where the soil borings indicate deep deposits of alluvial soils or unusually wet soils such as through the mitigated wetland area, the backfilled enclosure will be overlain with a layer of compacted impervious clay to minimize groundwater infiltration.

Equipment access to the FMI ring enclosure is provided at the MI-60 region via the adjacent MI-60 service building. An 8' x 30' floor hatch and shaft connect the service building high bay area with a 10' wide by 8' high curved labyrinth illustrated on Drawing AS-3. The high bay is serviced by a 30 ton overhead bridge crane capable of handling all anticipated magnet configurations. A 6,000 pound capacity hydraulic elevator also provides equipment access via the same labyrinth. Hence, all major equipment for the FMI ring enclosure, including magnets, magnet stands, cable, beam pipe, vacuum pumps and LCW piping, will be delivered to the MI-60 service building and installed via crane through the hatch or via elevator connected by labyrinth to the MI-60 region of the enclosure. When not in use, the magnet moving vehicle and the electric carts will be stored in the equipment labyrinth beyond a fire-rated door separating them from the open hatchway. Electric power will be supplied for battery charging and a small explosion-proof ventilation fan will exhaust the area.

Personnel access from the seven typical service buildings plus the MI-60 service building is provided by CIP concrete stairs and labyrinths with interlocked doors at the head of the stairway. By including a direct outside egress at grade level at each of these eight stair/labyrinths, they also serve as emergency exits from the FMI ring enclosure. Exiting is also provided at an additional 18 intermediate stair/labyrinths insuring that the maximum distance to an exit is no more than 300' in accordance with the classification of the enclosure as a Special Industrial Occupancy under the NFPA 101 Life Safety Code. All stair labyrinths will include a rated door at the ring enclosure with a direct outside exit at grade level. The 24 designated exit stairs will discharge on the infield side of the berm and there will be no exterior door hardware so they will function solely as emergency exits. The location of access and egress stairs is indicated as part of the enclosure criteria shown on Drawing AS-2.

Survey access to the ring enclosure is provided by 10 survey riser pipes extending periodically from the top of the enclosure over the aisle way. These pipes will initially extend 4'-6" above the top of the berm and provide a minimum 8" diameter vertical aperture for alignment. Prior to commencement of beam operation, the upper pipe segment will be removed to a point 3'-6" below grade, an 8' long solid steel shielding plug will be inserted, a pipe flange added and a concrete block placed above the pipe. The survey risers can be uncovered and reassembled as needed during future shutdown periods.

Cable trays, power bus, LCW piping, lighting, convenience power and other services are ceiling- or wall-mounted facilitated by channel inserts embedded in the enclosure walls and ceilings at regular intervals. Numerous penetrations located at the alcoves or the atypical enclosure segments connect to the above-ground service buildings. Most penetrations are designed to eliminate any "line-of-sight" configurations between the technical components and the service buildings above to maximize radiation protection. Some penetrations, such as those for hard bus or water piping, must be straight-line; these will be situated so as not to point directly at the peamline, and the annular region around the bus or pipe will be filled with radiation-absorbing material.

Ventilation for the FMI enclosure is provided by above-ground pad-mounted air-handling units connected via buried 2' diameter steel ducts. Supply units with electric heating coils will be located at service buildings MI-10,20,30,40,50 and 60. Exhaust fans will be located between the supply units at service buildings MI-52 and 62, as well as the intermediate alcoves at CB-118, 218, 327 and 418. Seven dehumidifier units will be ceiling mounted at service building alcoves around the FMI enclosure. Condensate drains will be directed to nearby sump pump basins.

The MI abort is located near service building MI-40. The divergence of the abort line from the MI beamline requires a CIP enclosure extending 106' beyond the MI-40 alcove with a width varying from 18' to almost 23'. Since the abort line is extracted vertically downward, the enclosure floor is stepped 1'-6" down to accommodate the abort line components. A separate stair labyrinth (not included in the earlier exit summary) provides a grade level exit from the downstream end of the abort line enclosure. The beam dump is located in a separate enclosure centered approximately 112' from the downstream end of the abort enclosure connected by a buried 24" diameter steel beam pipe with centerline located at elevation 713'-9" provided with cathodic protection. The central feature of the dump is a graphite core surrounded by aluminum with cooling channels in a "box" measuring approximately 1'-6" square by 9' long. The core box will be fabricated by Fermilab and furnished to the construction subcontractor for installation in the dump. The core box is surrounded by steel shielding with a 7' square cross-section and 20'

length. The steel is encased in concrete shielding with approximate overall dimensions of 14' wide by 14' high by 32' long. The upstream end of the shielding is composed of hand-stacked solid concrete bricks measuring 4" x 8" x 16" to afford access to the core box. The steel and concrete shielding, each totaling approximately 475,000 pounds will be procured by Fermilab and furnished to the construction subcontractor in designated sizes with a maximum unit weight of approximately 18 tons.

The dump assembly is housed in a waterproofed CIP dump enclosure centered 23' outside the ring enclosure opposite CB-409. This enclosure has inside dimensions measuring 21' wide by 52' long by 16'-9" with a floor elevation at 705'-0" or 8'-6" below the ring enclosure floor. The roof of the enclosure utilizes 12 precast concrete slabs as forms to support the weight and act compositely with CIP roof slab concrete. This design eliminates the need for forms and shoring which would be difficult to remove from the enclosure. The dump enclosure is connected to a CIP concrete alcove along the ring enclosure by a 4' wide by 7'-6" high labyrinth crossing under the ring to the aisle side with a stairway to a landing at elevation 713'-9" or 3" above the ring enclosure floor. The landing plus a curb around the stair opening provide a barrier to insure that any spillage in the ring enclosure cannot migrate to the dump enclosure. The floor of the ring enclosure above the connecting labyrinth consists of a removable slab measuring 7'-6" by 5'-0" to afford equipment access to the dump. The joints around this removable slab are sealed to prevent water infiltration. The labyrinth includes a niche with a small sump and 10 gpm pump. The pump is separated from the labyrinth floor by a raised curb so that any water on the floor of the dump enclosure will not drain into the sump. A separate 6" diameter metal underdrain system around the dump enclosure with an invert elevation of 704'-0" drains into this sump and the pump discharges into the adjacent ring enclosure underdrain. A monitoring connection will be provided. The dump enclosure is connected to the ring enclosure by eight 5" diameter conduits for piping or power and signal wiring, and a 2" stainless steel hydrogen vent pipe leads from the dump enclosure to an above-grade discharge. The dump enclosure contains adequate space for a small heat exchanger and circulating pump to be installed by Fermilab to isolate the dump LCW cooling circuit from the drain injector LCW system.

The dump box and surrounding shielding is supported in the dump enclosure by a CIP concrete base pad 3'-6" in total thickness which, in turn, is supported 1'-9" above the enclosure floor by transverse concrete beams at 5'-2" spacing. This arrangement provides access below the dump box to permit radiation monitoring on all sides. The lower elevation of the dump enclosure insures no spillage will reach the ring enclosure. Perimeter gutters will be provided to collect any water leaks.

The abort beamline will be designed to accommodate an extracted proton beam for future experiments including short or long baseline neutrino oscillation studies. Space will be provided downstream of the abort dump for the required additional magnets and equipment. The buried beam pipe upstream of the abort dump will be large enough to accommodate two separate beam alignments and a bypass will be provided through the dump itself.

5. BEAM TRANSPORT ENCLOSURES

Although there are six functionally different beam transport lines (listed earlier in the Overview), only three distinct new beam enclosures are required due to the use of shared beam elements and common enclosures. The civil work therefore includes the 8 GeV beam enclosure and the two 150 GeV transport enclosures. Drawing AS-1 illustrates the various beamlines, their direction and a general geometric layout.

The 8 GeV beam enclosure, connecting the existing Booster enclosure with the FMI ring enclosure, requires the construction of a 2,132' long below-grade structure with a majority of its length composed of a 10'-0" wide by 8'-0" high cross-section identical to the MI ring enclosure (see Drawing AS-14). The 8 GeV enclosure has been conceived as four separate segments because some construction will be restricted by on-going accelerator operations. The segment which connects to the Booster enclosure (WBS 1.2.3.2) and the segment which passes below the antiproton transport enclosure housing beamlines AP2 and AP3 (WBS 1.2.3.3) must be constructed during accelerator shutdown periods. The other two segments, totaling approximately 1,865 l.f., (WBS 1.2.2.7), will be constructed while the present accelerator is operational.

The completion of the Title II design has demonstrated that the antiproton crossing is far less complicated than the Booster connection. It has also been demonstrated that the "seven month" shutdown will involve several major simultaneous efforts including the F0 enclosure and the removal and reinstallation of Main Ring components and equipment. It would be a distinct advantage if some shutdown work that can be moved forward in the schedule to be accomplished during an earlier routine maintenance shutdown. Therefore the 8 GeV construction will be divided into two subcontracts. The first will consist of three phases, including the antiproton crossing, and the two adjacent segments which can be constructed during accelerator operations. This package will extend the 8 GeV enclosure from CB-848, its connection with the injector ring enclosure, to CB-810 just southeast of Well Pond Road. This 1,870 LF. segment includes the equipment access labyrinth, elevator shaft and concrete foundations for the MI-8 Service Building, a temporary vertical drop hatch at CB-817 and three exit stairs to grade. The antiproton crossing, scoped as one phase of this package, will be awarded in a manner to permit all critical material to be ordered and available. Once the maintenance shutdown period has been firmly established,

notice to proceed will be issued and the work prosecuted under an accelerated schedule. The temporary drop hatch provides for equipment access to the 8 GeV enclosure north of the antiproton crossing, while the MI-8 Service Building provides the same function for the south phase. If the maintenance shutdown occurs early in the product schedule, the three phases will be continuous and the temporary drop hatch can be deleted from the subcontract.

At the completion of the construction of the 8 GeV enclosure segment near Well Pond Road, a separate project for the relocation of the South Booster Road will be initiated. This GPP project, designed by Fermilab, will eliminate the present South Booster Road location while still preserving access to the Tevatron Ring Road and to the Booster and CUB area. The relocation of the South Booster Road will simplify the 8 GeV enclosure connection to the Booster, which is the second construction subcontract and will be scheduled to be completed during the "seven month" shutdown. This work includes the physical connection of the 8 GeV enclosure with the existing Booster enclosure, the demolition of 111' of an existing enclosure for the AP-4 beamline (which will be abandoned), the shoring of a portion of the Southwest Booster Tower to provide access for the new construction, the removal and reinstallation of shielding steel, and the re-routing, temporary support and protection of several underground utilities. The enclosure, measuring approximately 262' in length, will primarily be constructed of CIP concrete of various cross-sections, 10 precast concrete elements and a single exit stair labyrinth.

The 8 GeV beamline slopes downward from elevation 726.552' at the Booster to elevation 715.724' at the FMI so the 8 GeV enclosure will be constructed in stepped segments with level base slabs. The new enclosure abutting the Booster enclosure will be 11' wide by 8' high with a floor slab at elevation 720'-6" or 2'-0" below the Booster enclosure floor slab. Approximately 75' downstream, the 8 GeV enclosure meets the alcove at CB-804 and the base slab drops 7'-0" to elevation 713'-6" to match the Main Injector ring enclosure more than 2,050' to the south. The underside of the roof slab remains at elevation 728'-6" forming an enclosure 11' wide by 15' high which extends 30'-6" downstream. At this point the enclosure width reduces to the typical 10' and the underside of the roof slab steps down to elevation 725'-11" or a clear height of 12'-5". Over the succeeding 80' length of enclosure the roof slopes downward 4'-5" to match the descending beamline so that approximately 7'-7" downstream of CB-808 the 8 GeV enclosure assumes its typical cross-section of 10' wide by 8' high—identical to the ring enclosure. Returning to the alcove at CB-804, a stair will be provided for access between the 713'-6" and 720'-6" elevations which will also connect to an exit stair labyrinth leading to an exterior exit. A 60' long trolley beam mounted to the ceiling will support two monorail trolleys with 10 ton hoists to move equipment between the 713'-6" and 720'-6" elevations. The alcove will house a duplex sump pump, power panels and the intake for the supply fan mounted above grade.

As noted earlier, the 8 GeV enclosure Booster connection must be constructed during the "seven month" shutdown. This portion of the 8 GeV enclosure traverses an area with several active underground utilities including domestic water, sanitary force main, natural gas, two sets of chilled water supply and return, industrial cold water, power and communication ducts, storm sewer, pump discharge and a cooling water return pipe to the Booster bond. The enclosure also passes below Well Pond Road, the parking lot for the Southwest Booster Lab office building and a portion of the building itself. Because the 8 GeV enclosure at this location is at a relatively shallow depth (to accommodate the extracted beam at the Booster elevation), the shielding equivalent of 24'-6" of earth will require significant quantities of steel shielding to maintain roads at existing elevations and to minimize interference with existing facilities. In addition, sheet piling, steel H-piles with timber lagging, underpinning techniques and retaining walls will be required to protect existing utilities and structures. Approximately 111 LF. of the existing Booster extension enclosure will be demolished and reconstructed to support the heavier shielding load. Portions of the existing Booster enclosure will be reinforced with additional concrete or straddled with a separate support structure to carry the added shielding weight. A limited area of the Southwest Booster Lab office building will require modifications including underpinning, replacing windows with a concrete retaining wall and small quantities of interior shielding.

With the exception of the antiproton AP2/AP3 line crossing, the remaining portion of the 8 GeV enclosure will be constructed using identical methods described for the MI ring enclosure. A total of 211 precast concrete enclosure elements 10' wide by 8' high (including two new types) will be used for a total length of approximately 1,500 LF. Two intermediate alcoves at CB-823 and 843 will be CIP concrete measuring 24' wide (offset to the west) by 16' long by 9' high to accommodate duplex sump pumps, LCW expansion loops, electrical power panels, dehumidifiers and intake grills for supply air. Segments with atypical geometry at the connection to the MI ring enclosure and the area downstream of the antiproton crossing will also be CIP concrete. Three exit stair labyrinths at CB-818, 828 and 842 will intersect the 8 GeV enclosure with CIP concrete sections. A temporary CIP concrete drop hatch located at CB-817 over the enclosure aisle provides a clear opening 7'-0" wide by 24'-2" long. The hatch extends 1'-0" above the berm to elevation 747'-0" and is designed to be filled with standard sized concrete shielding blocks with a lockable steel cover installed over the hatch. A crushed stone hardstand around the hatch and a short access drive connecting to Indian Creek Road will be provided.

The principal equipment access as well as the power and cooling water source for the 8 GeV enclosure will be provided by the MI-8 Service Building (formerly designated the North Hatch Building). Utility connections from this service building will be accommodated by a large CIP concrete alcove along the 8 GeV enclosure at CB-837 measuring 24'-3" wide by 28' long by

9' high. Utilities including two 8" diameter steel pipes (LCW carrier pipes) and twenty-four 6" diameter PVC penetrations will extend from the alcove toward the MI-8 service building terminating at elevation 743'-0". At CB-835 a 10' wide by 8' high CIP concrete curving equipment access enclosure will intersect the 8 GeV enclosure and extend westward in a 180 degree arc to meet the equipment access hatch located within the footprint of the MI-8 service building. The construction subcontract for the 8 GeV enclosure will provide the 10' wide x 30' long vertical access shaft, the pit and shaft for a 6,000 pound capacity freight elevator, a stair labyrinth to grade, a sump enclosure, the lower level enclosure between the access labyrinth, elevator and the stair and four caissons necessary to support columns for the future service building. The stair, elevator shaft and equipment shaft openings will be covered at grade with temporary timber closures.

The two places of the 8 GeV enclosure constructed while the existing accelerator is operational may be required to be terminated with a sheetpiling earth retention system at the interface with the third phase for the 8 GeV crossing of the antiproton depending upon the schedule of the maintenance shutdown. A sheetpiling retention wall will be required at the downstream end of the 8 GeV enclosure to prevent unbalanced lateral earth pressure acting upon the adjacent MI ring enclosure. Portions of the 8 GeV enclosure will require the removal of an abandoned 4' diameter concrete sewer pipe at invert elevation 727'-0". This work also includes a run-around and relocation of Kautz Road, temporary support and reconstruction of protective covers at the helium line crossing and the installation of segments of new utilities including pump discharge piping, culverts, chilled water supply and return and power and communications ducts. Three portakamps located east of Indian Creek Road will be relocated by Fermilab prior to the start of this project.

The 8 GeV enclosure crossing under the AP2 and AP3 beamline enclosure during a maintenance shutdown will require Fermilab removal of beamline equipment and utilities from an approximately 100' long segment of the existing enclosure. This material and equipment will be stored within the enclosure to either side of the area to be demolished with temporary timber partitions erected to isolate the construction zone. Eleven identical existing precast concrete inverted "U"-shaped elements will then be carefully removed from the base slab and stored nearby for later reinstallation. Approximately 88 LF of the AP enclosure base slab will be demolished to permit completion of the excavation to elevation 711'-6" for the 8 GeV enclosure segment. Both the base slab at elevation 713'-6" and the 8 GeV enclosure with typical dimensions of 10' wide by 8' high will be CIP concrete for the connecting length of approximately 160 LF. Typical precast concrete elements cannot be used for this segment because of the heavier loads imposed by the shielding. If the adjacent 8 GeV enclosure segment has been completed to a sheet

pile retaining wall, the connection will involve cutting an opening through the steel piling to accomplish the connections. Waterproofing, underdrains and backfilling will be identical to the previously described procedures with special care for adequate compaction of fill below the AP enclosure. Steel shielding will be required between the 8 GeV enclosure roof and the underside of the base slab of the rebuilt AP enclosure. A new CIP base slab will be constructed for the AP enclosure, the precast elements will be replaced, welded in place, caulked, waterproofed and repainted. A shielded sight riser which accesses both enclosures will be installed extending to a point 4'-6" above the final berm elevation of 747'-0". Backfill around the AP enclosure will include reconnection of the underdrains and another layer of steel shielding over the AP enclosure. Fermilab will reinstall the AP2 and AP3 beamline components and related equipment.

The stair connected to the equipment access enclosure at the MI-8 Service Building, the three exit stairs along the 8 GeV enclosure of Phase 1, the exit stair from the alcove at CB-805 at the Booster connection under Phase 2 and the stair constructed at the 8 GeV connection to the injector ring under the MI enclosure project insure no "dead-end" longer than 50' and no exit distance greater than 300'. As noted earlier, the primary equipment access for the entire 8 GeV enclosure will be via the equipment hatch at the MI-8 Service Building. If the maintenance shutdown schedule permits early construction of the 8 GeV enclosure crossing of the AP2 and AP3 enclosure, the major segments of the 8 GeV enclosure will be connected and the temporary access hatch at CB-815 can be eliminated.

The other two beam transport enclosures are the nearly symmetrical structures connecting the MI and Tevatron enclosures. Identified by their major functions as the 150 GeV proton injection (P-150 GeV) and 150 GeV antiproton injection (A-150 GeV) enclosures, the plan is shown on Drawing AS-3 with longitudinal sections on Drawings AS-5 and AS-6, and the transverse section on Drawing AS-7. In addition to the 150 GeV proton injection beamline, the southeastern enclosure also houses another magnet string for both the 120 GeV proton beam from the FMI to the antiproton production target and the 120 GeV extracted proton test beam to the fixed target areas. These beams travel to the Tevatron enclosure at F0 where both beams are injected into a beamline arc composed of the former Main Ring accelerator components as far as either F-17 in the case of the antiproton production, or the A0 Transfer Hall and the start of the Switchyard for fixed target beams in the case of the test beam. The 8 GeV antiprotons are transported to the FMI following the 120 GeV antiproton production line in reverse from F-17 to F0 and back to the FMI. While the injector beam lines are approximately 900' in length, a significant portion of their components are housed in widened portions of the Injector enclosure and the F0 sector of the Tevatron enclosure leaving only 116' long segments as 10'-0" wide by 10'-0" high enclosures with a floor elevation at 713'-6". Because the 150 GeV enclosures

physically connect the early Phase 2 MI enclosure work with the Phase 3 shutdown work at the F0 enclosure, they must necessarily be constructed in two phases. Drawing AS-3 shows the interface between these construction phases as a line of sheet piling transverse to the 150 GeV enclosures and clearly demonstrates why a portion of each enclosure is part of the injector enclosure between MI-62 and MI-52 (WBS 1.2.2.2) with the remaining segments are included with the F0 enclosure (WBS 1.2.3.1). The Phase 2 enclosure will be CIP concrete but the majority of the Phase 3 portion of the 150 GeV enclosure will incorporate precast concrete roof planks which serve as a form and become composite with the CIP concrete roof topping while still providing continuity at the roof-wall joint. This procedure saves the time and cost involved in forming and shoring the roof slab and eliminates the problem of installing and removing material from an area with limited outside access. A similar procedure will be utilized for the F0 enclosure.

The transfer beams must transition from the MI beamline at elevation 715'-9" to meet either the Tevatron or remnant Main Ring at elevations 723'-4 1/2" and 725'-6" respectively. Provisions must also be made to install (or later replace) magnets and other equipment along these several beamlines. With the floor of the MI enclosure at 713'-6" or 9'-0" below the Main Ring enclosure floor elevation of 722'-6", one possible solution was holding the transition enclosures and one side of the F0 enclosure at the MI floor elevation of 713'-6". This configuration would have allowed the magnet mover a level access floor throughout but requires mounting magnets 12' above the floor. It also requires the MI side of the F0 enclosure to be 17'-0" high - a very large expensive structure. The final solution is a compromise providing a 5'-0" vertical step from the 150 GeV enclosures to the F0 enclosure with a floor elevation of 718'-6". The majority of the transfer line magnets can be installed from elevation 713'-6" with the magnet mover but hoists and rigging are required to install equipment for the MI components in the F0 enclosure. Longitudinal sections of the two 150 GeV enclosures shown on Drawings AS-5 and AS-6 show the beamlines in relation to the enclosure elevation.

The plan of the enclosures and beamlines in the area of CB-526 and CB-616, shown on Drawing AS-3, indicates that a 60' long segment of Main Injector components must be moved laterally toward a pocket along the inside wall to provide access for the magnet mover to travel from the MI aisle to the 150 GeV enclosure. Provisions for a one ton jib crane have been furnished at the bifurcation of the two enclosures so that smaller components can be moved over the MI beamline into the 150 GeV enclosure without moving magnets. Note also an exit stair from the 150 GeV enclosure near the jib crane location. This stair labyrinth passes over the beam enclosures to connect with the exit stair from the MI enclosure. Hence access between the MI enclosure and the 150 GeV enclosure, as well as exiting, is provided without crossing under or over beamlines. The ceiling of a portion of the 150 GeV transition enclosure will be provided

with two lines of embedded steel plates centered on the beamline for the support of elevated beam components. These 90' long continuous plates extend downstream of CB-523 and upstream of CB-619.

6. F0 ENCLOSURE

The F0 Enclosure (WBS 1.2.3.1) construction as shown on Drawing AS-3, encompasses a region slightly longer than the long straight section of the existing Tevatron enclosure and connects with the 150 GeV transition enclosures. This region will house the rf accelerating cavities reinstalled from the existing Tevatron, the remnant Main Ring elements and components of the several transport beamlines. Functionally, these are elements of the 150 GeV proton injection line, the 150 GeV antiproton injection line, the 120 GeV antiproton production line, the 8 GeV antiproton accumulator to the FMI, and the 120 GeV extracted test beam line. As noted above, some of these lines share common elements or share common enclosures. But the existing F0 long straight section has insufficient space for the new transport beams to be included in addition to space required for the existing Tevatron rf cavities and beamline components. Hence, except for the equipment access labyrinth at the south end, 626' of the existing Tevatron enclosure, including all of the F0 long straight section, must be demolished and a new larger enclosure rebuilt with all work to be accomplished during the "seven month" Phase 3 shutdown. The sequence of construction in the F0/MI-60 area is illustrated by several cross-sections shown on Drawing AS-26. Stages 1 and 2 show the completion of the MI-60 Enclosure, MI-60 Service Building and the North Addition to the F0 Service Building - all completed while the Tevatron remains in operation. Note that the two initial lines of sheet piling remain in place. The southwestern line has been used to support utility penetrations and allow an early start of the MI-60 Service Building construction. The second or middle line of piling remains in place to be used again during the Phase 3 work.

Once the shutdown of the Tevatron operation commences, equipment will be relocated (by Fermilab) from the southwest portion of the existing F0 Service Building to the North Addition and demolition will begin from the southeast. Fortunately, the section of the service building to be demolished is actually a former building addition and the demarcation line is a full-height concrete wall which will function well in the remodeled configuration. Concurrently with the removal of equipment from the service building, beamline components will be removed from the underground F0 enclosure by Fermilab. Equipment, such as the Tevatron rf cavities which must be reinstalled later, will be stored in the E-sector of the Tevatron enclosure. Removal will be sequenced to provide early access to the 200' long CIP concrete section between stations E-49 and F-11 so that transverse saw cutting of the concrete can commence from inside the enclosure. The majority of the remaining enclosure to be demolished consists of precast concrete hoop-shaped

elements on a CIP base slab. After the above-grade service building is removed along with the helium transfer lines and the upper portion of the waveguide and utility penetrations, the third (northeast) retention wall will be constructed between the remaining section of the F0 Service Building and the northeast side of the underground Tevatron enclosure. The retention wall will be designed by a specialty sub-subcontractor and will probably consist of a combination of braced sheetpiling or soldier piles and timber sheeting with drilled and grouted tie-backs to laterally brace the piles and eliminate cross bracing. Approximately 680' of a retention system will be required extending roughly between points opposite Tevatron stations E47 to F14. Two 100' long segments of sheetpiling must also be driven between the 150 GeV enclosures and the southwest side of the Tevatron enclosure near E47 and F14 because the new enclosure is 9' below the existing Tevatron floor slab. The retention wall system is depicted as Stage 3 on Drawing AS-26. The retention wall system, like the service building demolition will move from the southeast toward the northwest. Interior saw cutting will be similarly sequenced so no piling is driven above occupied areas of the F0 Enclosure. Excavation between the new extension wall and the existing middle line of piling will follow the piling operation with walers and crosslot bracing installed as the excavation proceeds.

As the existing Tevatron enclosure is exposed by the excavation work, demolition will proceed in earnest. There are three types of demolition or removal operations planned. The central 200' of F0 Enclosure walls and roof are CIP concrete approximately 20" thick. This area will be sawcut transversely at approximately 6' intervals and then sawcut horizontally at the base of the walls to free the inverted U-shapes in 25 ton units. The 31 units will then be removed from the excavation and hauled to the railhead storage area on the Fermilab site for future use. The majority of the remaining F0 Enclosure is composed of 12' diameter (176') and 10' diameter (194') hoop-shaped precast concrete elements each approximately 10' long. Experience has shown that these elements, with a maximum weight of 16 tons, are readily broken free of the base slab and easily removed to be stored at the railhead. An additional three precast hoops will be removed for access to the work and later reinstalled. The 34' long CIP concrete enclosure at the equipment access, two transitional enclosure sections between the 12' and 10' diameter hoops and the entire 626' long CIP concrete base slab, with a maximum thickness of 18", will be sawcut into manageable pieces, removed and deposited in the excavation along the middle line of sheet piling as shown in Stage 4, Section A on Drawing AS-26.

Beginning just upstream of the Tevatron station E48 and continuing for 496' the reconstructed F0 enclosure will have a floor slab at two different elevations. The southwest or MI portion of the floor will be at elevation 718'-6" while the northeast side will match the Tevatron enclosure floor at elevation 722'-6" as shown in Section D on Drawing AS-7. The beamline

components will be mounted on stands fixed to the lower floor but both levels will include an aisle space to permit magnets and equipment to be moved longitudinally along both sides of the enclosure. In particular, the upper level at elevation 722'-6" will allow the magnet mover to travel through the F0 enclosure providing continuous access around the Tevatron ring. The enclosure width will vary in steps from the typical 18'-0" minimum to a maximum of 24'-0" to meet the requirements of the diverging beamlines as indicated on Drawing AS-3. The ceiling elevation of 730'-6" provides a minimum clear height of 8'-0" on the Tevatron side and 12'-0" on the MI side. The F0 enclosure will be a CIP concrete enclosure except for precast concrete roof beams. These roof beams will be utilized as a composite roof element to speed the construction by eliminating the need for interior shoring. The precast beams will be designed to carry the weight of the CIP roof concrete with provision to tie the two elements structurally so that the composite roof can support the full shielding loads. Centered at a point approximately 22'-9" upstream of Tevatron station E49 or directly below the passageway between the MI-60 and F0 service buildings, a 22' long section of the F0 enclosure roof will be constructed of three layers of steel totaling 2'-6" topped with 6" of concrete. The steel structure provides required shielding below the passageway whose floor elevation of 742'-6" is only 12' above the F0 enclosure ceiling. Another atypical section occurs just downstream of Tevatron station F0, where the enclosure widens to 22'-6" for a length of 23'-0" and the ceiling height increases to elevation 735'-4". This alcove will house an underhung bridge crane with two 10-ton hoists for the purpose of transferring magnets or equipment transversely between the Tevatron and the MI sides of the enclosure. This hoist area is located at beamline segments without magnets to provide maximum vertical clearance for material handling. The existing curved access labyrinth leading to the stair and hydraulic freight elevator at the F0 Service Building will be reconnected to the new F0 enclosure.

Eight waveguides serving the Tevatron RF cavities must be reinstalled between the F0 enclosure and the F0 service building, as discussed in Chapter 3.4. Located at 9'-3 1/8" centers beginning downstream of Tevatron station E49, the waveguide penetrations will extend horizontally from the southwest retaining wall of the F0 service building as 16" diameter steel pipes centered at elevation 744'-10" or 2'-4" above the floor of the service building. Each of the four pairs of horizontal pipes will intersect a vertical rectangular CIP concrete shaft which extends from the roof slab of the F0 enclosure to elevation 757'-6" or one foot above the berm. The inside of the shaft measures a nominal 3'-0" wide (transverse to the enclosure) by 12'-0" long down to elevation 743'-0". The 16" diameter horizontal penetrations intersect the shaft 1'-10" above this level. The structure below elevation 743'-0" is a solid CIP concrete prism with outside dimensions matching those of the shaft above and penetrated by two 16" diameter pipe alcoves down through the F0 roof slab. The open 3'x12' shaft provides ample work space to install and connect the

vertical and horizontal components of the pair of waveguides. After assembly, the shaft will be filled with a combination of steel shielding and standard sized precast concrete shield blocks to affect a total shielding above elevation 743'-0" equivalent to the typical 26' earth berm. The shaft will be covered with a 6" thick concrete slab and sealed weather tight. Rare maintenance access can be achieved during shutdowns by removing the shielding.

A similar shielded shaft located downstream of station E49 will provide access from grade to the F0 enclosure for 10" diameter carrier pipes for helium supply and return and 6" diameter carrier pipes for nitrogen supply and return. The carrier pipes will exit the shaft enclosure at 45 degrees and terminate 1'-0" above grade with blind flanges. Fermilab will install the cryogenic piping after completion of the construction.

The F0 enclosure is connected to the adjacent service buildings by several other types of utility penetrations. Control conduits for the 150 GeV beamlines consisting of two groups of eight 6" diameter PVC ducts will extend from the MI-60 Service Building to the top of the southwest F0 enclosure wall at locations 172' upstream and 223' downstream of Tevatron station F0. A pair of 6" diameter PVC "S"-shaped conduits centered at each waveguide location will extend from the back wall of the F0 service building at elevation 751'-11" to the northeast wall of the F0 enclosure. Three groups of fifteen 6" diameter PVC conduits each will extend from the rear wall of the F0 service building centered at elevation 751'-11" to penetrations through the roof slab on the southwest side of the F0 enclosure. These conduits, designated for beamline power, will be located upstream and downstream of the crane alcove near station F0 and opposite the pump room in the F0 service building. Other groups of 6", 3", and 2" diameter conduits will connect the F0 service building and the F0 enclosure.

The 4' step between the 722'-6" and 718'-6" floor levels in the F0 enclosure will be formed with a 1'-4" corbel or projection at the upper level producing a minimum floor width of 6'-6" on the Tevatron side. The corbel will be designed to support equipment loads while the protected area below will be the location of cryogenic bypass piping. A removable pipe handrail located 1'-6" from the edge of the corbel will run the length of the enclosure. At four locations along the wall on the Tevatron side of the enclosure, a 6" diameter stainless steel pipe with a capped exterior end will be cast into the wall 6'-6" above the floor providing a 4' long sleeve to house components for the Tevatron quench protection system. A series of transverse steel plates will be embedded in the F0 enclosure ceiling 4'-11" on center for 132'-9" length beginning 9' downstream of F11. These plates will provide a future anchorage for 120 GeV beamline components to be supported from above.

The F0 enclosure connection to the 150 GeV enclosures at each end will have nearly symmetrical features. The 150 GeV enclosure floor elevation at 713'-6" will meet the F0 enclosure floor at 718'-6" at a single 5'-0" step approximately 205' upstream and 291' downstream from station F0. A combined stairway will be located at this step providing personnel access from both levels of the 150 GeV enclosure and also from the adjacent MI-60 enclosure to a common exit stair labyrinth leading to grade level. A physical barrier with an air-tight door will be required beyond the stairways at both 150 GeV enclosures to isolate the Oxygen Deficiency Hazard potential of the Tevatron enclosure from the MI enclosure. The step area is also the location of a ceiling mounted monorail with two 10 ton hoists which provide a means of transferring beamline equipment between the 713'-6" level and the 718'-6" level of the F0 enclosure. The hoist area includes a shallow alcove area for storing rigging equipment and locating power panels. The hoist enclosure will be 17'-0" high, a maximum of 18'-0" wide and extend 30'-0" beyond the step to meet the 10'-0" wide by 10'-0" high 150 GeV enclosure. The hoist area is shown in plan view on Drawing AS-3 and as longitudinal sections on Drawings AS-5 and AS-6.

Other features of the F0 enclosure are identical to the beamline enclosures described earlier including channel inserts at walls and ceiling, underdrains, waterproofing and backfilling procedures. Underdrains for the F0 area will connect with the existing Tevatron system and the adjacent MI-60 enclosure underdrains. Since the F0 enclosure is generally higher in elevation, the added hydrostatic head will insure good drainage. Granular backfill between the F0 enclosure and the retention wall systems to either side will be specified to an elevation 1' above the structure to speed the backfilling process and to insure construction can proceed during subfreezing weather.

Shielding for the F0 enclosure has been established at 26' primarily because the ground level area between the MI-60 and F0 service building will be difficult to access in the future. As shown on the cross-section on Drawing AS-26, the final berm over the F0 enclosure will be at elevation 756'-6" or 8'-0" higher than the adjacent berm over the MI-60 enclosure. The F0 enclosure will require steel shielding above the bridge crane alcove with its raised ceiling, below the passageway connecting the F0 and MI-60 service buildings (in addition to the steel used for the enclosure roof construction) and along the top of the northeast wall for a distance of 325' to provide sufficient shielding for the adjacent F0 service building. This construction subcontract will also place shielding steel below the aforementioned passageway at its crossing of the MI-60 enclosure.

Once the majority of the backfill between the MI-60 and F0 service buildings is complete, an 8'-0" wide by 8'-0" high connecting passageway of CIP concrete will be constructed between the buildings for personnel and control cabling access. The floor elevation of 742'-6" matches

both buildings. This construction subcontract will include modifications to the remaining portion of the F0 service building. The existing utility trench extruding 253' along the southwest wall of the F0 service building will be abandoned and filled with concrete to provide the necessary 26' of radiation shielding to the building interior. A new 1'-0" thick CIP concrete retaining wall will be constructed 2'-0" beyond the existing 8" thick CIP concrete southwest building wall for a distance of 400'. Reinforcing steel will be doveled into the existing wall, reinforcing steel will be placed in the 2' space between the walls and the void filled with lean concrete. The resulting 3'-8" thick wall structure will be capable of retaining the lateral load of the earth shielding berm. The existing roofing and insulation over the remaining portion of the F0 service building will be removed and replaced with new material to meet the roofing of the North Addition to the F0 service building constructed earlier under a separate MI subcontract. A combination gutter and drain tile will be constructed along the top of the aforementioned concrete wall to carry the roof drainage out to either end of the building. The pump room at the north end and most existing interior masonry partitions will remain. One new partition between column lines 8 and 9 will be constructed and the existing metal siding, door and windows separating the North Addition from the existing building will be removed. Mechanical work will include roof-top ventilators and exhaust fans, cabinet heaters and fan coil units connected to the existing chilled water system. Sprinkler piping will be extended from the North Addition as well as the fire detection/alarm system and the central system. Electrical work will include new power panels, power distribution, convenience power, grounding and lighting. At the completion of these modifications the existing portion of the F0 service building and the North Addition will function as a single 13,250 S.F. service building.

7. SERVICE BUILDINGS

Eleven above-grade service buildings in five configurations will house equipment, services and utilities for the FMI and beam transport lines. The locations of the eleven service buildings are shown on the site plan, Drawing C3, and the site criteria plan, Drawing C4.

Five typical service buildings, MI-10, 20, 30, 40 and 50 (WBS 1.2.2.3) are identical in size, construction and function. Floor elevations vary so the buildings are slightly above the local terrain and nearby roads to insure positive drainage away from the buildings. These buildings are located outside the FMI shielding berm approximately 1,800' apart. Since the buildings contain the magnet power supplies, their locations correspond to equal strings of magnets or approximately one-sixth of the dipoles in the beam enclosure below. A secondary consideration for MI-10 and 40 is the desire to locate the building adjacent to the kickers to minimize cable lengths. The narrow construction limits through the wetland mitigation area, however, will force MI-40 to be offset from the kicker it serves. The buildings also contain control racks, cable trays,

LCW pumps, heat exchangers, deionizing bottles and controls for the LCW system and power distribution equipment. At two buildings, MI-10 and MI-40, power supplies and controls for kicker magnets (8 GeV injection and 150 GeV proton abort respectively) are also housed in a separate room with a depressed floor to retain oil spills. Each typical service building provides a direct personnel access via a CIP concrete service corridor over the berm to a stair and labyrinth connecting to an alcove area of the injector enclosure below. The stair and labyrinth contain no utilities, cable trays or ventilation air for the enclosure. Supply or return air to the FMI enclosure alcove below is directed via a vertical duct to an outdoor air handling unit. A rated door at the base of the stairs and an outside door at the top of the berm provide an emergency exit from the FMI enclosure at each typical service building. The service corridor between the back of the service building and the interlocked doors at the head of the stairway provide three functions other than personnel access to the FMI enclosure. The 6'-0" width permits a 2'-6" wide utility aisle for dc bus in a protective enclosure, sprinkler piping and LCW piping to extend from the building to penetrations which connect with the alcove below. The penetrations consist of steel tubes or carrier pipes which extend vertically to the ceiling of the alcove or enclosure structure below. A door to the outside just before reaching the interlocked door provides a second exit from the service building. Since the corridor is constructed of reinforced concrete and the aforementioned outside door will be protected against flying projectiles by a concrete retaining wall, the service corridor also serves as a tornado shelter.

These five typical service buildings are nominally 50'-0" square in plan with a clear interior height of 11'-0" at the front wall and 12'-0" at the rear wall abutting the shielding berm. The foundations consist of concrete spread footings and a retaining wall at the rear wall with concrete floor slabs. The access corridor with its labyrinth and stairs will be supported by three concrete piers extending down to the enclosure roof. The buildings will be framed in steel columns and roof beams with metal deck, rigid insulation and built-up roofing. The exterior walls will consist of insulated metal siding over an insulated, reinforced 8" concrete masonry wall. The concrete masonry units (CMU) will provide lateral stiffness, a fire rated wall opposite the substation area and a sturdy mounting surface for equipment. These typical buildings are subdivided into a power supply room, pump room, control room and a kicker room. Equipment access is provided by a 10'-0" wide by 8'-0" high roll-up door at the power supply room, a 6'-0" wide by 9'-0" high roll-up door at the pump room and a double door to the kicker room. The structural steel roof beam over the kicker room will be sized to support a future 1-ton monorail hoist. Kicker room floors will be depressed 3" below the general service building floor elevation to retain any potential oil spills from the kicker supplies. A transformer yard will typically be located immediately outside the power supply room of each building. Outdoor equipment will

include pad-mounted transformers for the dipole and quadrupole power supplies, a conventional power transformer, vacuum circuit breakers and switchgear. Below grade concrete retaining walls filled with stone will be provided around the perimeter of all equipment using oil coolants to serve as a secondary containment basin. Because the proximity of the transformers to the power supplies significantly reduces power costs, the distance will be minimized and the service building will be protected by an 8" concrete block fire-rated wall adjacent to the transformer yard. Elevated bus ducts will penetrate this wall to connect transformers and power supplies with proper fire stops. All interior partitions will be concrete masonry units (CMU) with hollow metal doors and frames.

Service buildings will typically be located 25'-6" from the FMI beam centerline except for MI-40 which, because of its location opposite the abort extraction, will be 31'-0" from the beamline. This siting arrangement provides a minimum of 26' equivalent earth shielding between the service building and the FMI enclosure. Utility penetrations, consisting of 6" PVC ducts and shaped in a reverse curve to avoid line-of-sight radiation leaks, will extend from the top of the rear wall of the enclosure to the top of the concrete retaining wall at the rear of the building. Typically three sets of four conduits will service the kicker room and a total of 20 conduits will extend from the enclosure alcove to service both the power supply and kicker rooms. The retaining wall will permit earth fill behind the building to extend above the horizontal run of these conduits to provide radiation shielding.

The MI-52 and 62 service buildings (WBS 1.2.2.4) have the same dimensions and typical features except for the following variations. Because of site limitations, the floor plan and substation of MI-62 will be opposite hand of the other buildings. MI-52 will not include a control room. The pump room and kicker room will be expanded. MI-62 will not include a pump room although stub-up piping for pond water supply and return will be provided. The power supply room will occupy three-quarters of the floor area with the kicker room occupying the remainder. The transformer yard will be laid out in a similar pattern to the typical buildings, but will initially contain few transformers and isolated containment basins.

All buildings will include underground power and communication duct bank connections to manholes located along the service roads. The building will be provided with underground piping connections for pond water supply and return. Concrete aprons will be added at all doors and a hardstand area for vehicular parking will be provided on the side of the building opposite the transformer yard.

Kicker Service Building F17 (WBS 1.2.3.1) is located adjacent to the Main Ring berm between existing service buildings F1 and F2. The power supplies and controls in this building are required by the kicker magnets to be installed in the existing Main Ring enclosure to inject the 150 GeV protons into the Tevatron. The complementary function for the 150 GeV antiproton insertion at E48 will be powered from a room in the remodeled F0 building above Tevatron location E48. No new kicker building is required at that location. The F17 kicker building, shown on Drawing AS-21, is nominally 20' wide by 35' long with a 10'-3" inside clear height. The foundation and walls of this building will be CIP concrete primarily because it is set into the Main Ring shielding berm. The side walls and front of the building will be faced with insulated metal panels. Two double doors on the front wall provide access to the building. The roof structure will consist of steel beams, metal roof deck, rigid insulation and built-up roofing. Provisions typical for kicker rooms such as a depressed floor and future monorail supports will be provided. Three sets of 3-6" diameter PVC utility penetrations will be constructed between the Tevatron enclosure and the floor of the service building during an accelerator shutdown since the work requires removal of the shielding berm, core drilling of the enclosure hoops and temporary support of the helium lines on the berm. A hardstand and driveway will provide access to the existing ring roads.

The MI-8 service building (WBS 1.2.2.8), formerly designated as the North Hatch, is sited along the 8 GeV beamline near the intersection of Kautz and Indian Creek Roads. The MI-8 building nominally measures 90' by 75' and consists of a 75' x 40' high bay approximately 30' high and a 50' x 75' low bay with a 13' high clearance. Functionally the low bay mimics the typical service building functions of a pump room, power supply space and control room area. No kicker room is required but the MI-8 building will have toilet facilities and a janitor's closet. The stair and labyrinth access to the 8 GeV enclosure is also of a different configuration but serves the same functions of an exit from the below grade enclosure to a direct outside egress, tornado shelter and second exit from the service building. Power supplies, controls, LCW cooling equipment, and penetrations service the dipole and quadrupole magnets of the 8 GeV beam line.

The high bay of the North Hatch building primarily provides equipment access to the same 8 GeV beam enclosure. A 10' x 30' hatch is located at one end of the high bay connecting directly with a semi-circular 10' wide by 8' high labyrinth at elevation 713'-6". The hatch will be covered with 1'-6" thick precast concrete blocks as additional shielding whenever the 8 GeV beamline is operational. A 12' wide by 13' high roll-up door provides truck access to the high bay which is serviced by a 30-ton bridge crane. The high bay will also serve as a magnet storage and staging area for the 8 GeV beam line. Other features, including utility penetrations to an enclosure alcove, earth shielding parameters, transformer yard, hardstand and all construction features, are similar to those described for the typical service building.

The largest of the new service buildings, completed in FY94, is located parallel to and southwest of the MI-60 segment of the FMI enclosure directly across the berm from the existing F0 service building. The MI-60 Service Building (WBS 1.2.2.8) as shown in plan view on Drawing AS-22 and AS-23 with elevations shown on Drawing AS-24 and sections illustrated on Drawing AS-26, houses a number of functions, including two power supply areas at opposite ends of the building for dipole and quadrupole magnets, all power supply and control requirements for the FMI rf cavities, a pump room and deionizing facility for LCW, technician space, rf development and assembly spaces, magnet test area, the FMI control room, and toilet facilities all located in a 22,500 sq ft low bay area. An adjacent 5,000 sq ft high bay features an open 8'-0" by 30'-0" long hatch connecting directly with a curving 10' wide by 8' high labyrinth at elevation 713'-6" which is the equipment access for the entire FMI ring enclosure as well as the 150 GeV FMI enclosures. A 12' wide by 13' high roll-up door provides truck access to the high bay which is serviced by a 30-ton bridge crane. A 6,000 pound capacity hydraulic freight elevator and a stairway located immediately adjacent to the high bay area provide additional access to the FMI enclosure below. The stair and adjoining labyrinth provide a rated exit for the MI-60 enclosure and the lower elevator lobby and hatch area serve as a tornado shelter. The high bay space will also serve as a staging and storage area for the FMI magnets and other beam line components.

The MI-60 Service Building is 450' long with a low bay width of 50' while the high bay measures 50' by 100'. As indicated on the building sections shown on Drawing AS-25, the floor elevation of the MI-60 Service Building is set at elevation 742'-6" to match the existing F0 service building floor and the clear interior heights are 12' for the low bay and approximately 28' for the high bay. The majority of the low bay area is provided with a continuous floor trench located along the northeast wall for routing of the ac power for the rf systems. The northeast wall also has numerous utility penetrations leading to the MI-60 Enclosure. The MI-60 Service Building is positioned far enough from the MI-60 Enclosure to provide 26' of equivalent earth shielding to the lower outer corner of the aforementioned cable trench.

Transformer yards are located at either end of the MI-60 Service Building as well as directly southwest of the LCW pump room. Anode power transformers will be housed in special enclosures connecting to the rf gallery and because the entire service building is air conditioned, two 150-ton pad-mounted chillers will also be located southwest of the building. One chiller is presently installed; the second one will be required once all the rf equipment becomes operational. In addition to the high bay area, equipment access via roll-up doors will be provided at the pump room and at each beamline power supply room at the ends of the building. Construction features generally are identical with those outlined for the typical service buildings. Some departures include CMU walls at the anode power supply enclosures, horizontal strip windows at occupied

areas such as the high bay, tech area and rf development lab and a continuous, full height CIP concrete wall adjacent to the berm.

The existing F0(RF) Service Building will undergo several modifications as part of the FMI project. These changes are required because the underground F0 Enclosure, which lies directly below the southwest half of the F0 Service Building must be demolished and reconstructed to accommodate the expanded beamline functions. Consequently, the overlying portion of the service building must be vacated of equipment and demolished. These steps take place during the Phase 3 shutdown and will be described in the following section of this report. They are mentioned here to explain the ultimate need to replace space in the F0 (RF) Service Building.

Since equipment must be relocated before demolition can commence, the substitute space will be created before the shutdown. The scope of Service Building F0 North Addition (WBS 1.2.2.6) accomplishes this work. Conceived as a concurrent project with other service building construction, the north addition will be constructed without disturbing the ongoing functions within the F0 Service Building. Drawing AS-22 shows the plan view of the addition while the section is shown as Stage 2, Section A on Drawing AS-26. Construction will first require the relocation of approximately 650' of the Main Ring Road away from the present F0 service building to the far side of the transformers. Some relocation of underground utilities will also be required involving short duration shutdowns for reconnection. The 25'-0" wide addition will consist of the same structural and architectural details as the typical MI service buildings. The existing northeast wall of the F0 Service Building will remain in place except for small cut-outs required to connect new roof beams to existing columns. The existing foundation wall has been shown to have adequate strength and bearing to support its share of the new addition. The North Addition will be approximately 228' long and enclose an added floor area of 5,720 sq ft. After the shutdown commences, Tevatron rf power supplies and controls, beamline power supplies and the control room will be relocated into the addition. Exterior transformers, anode power transformers and chillers will be provided to augment existing equipment.

8. KAUTZ ROAD MASTER SUBSTATION AND POWER DISTRIBUTIONS

Power for the FMI project will be provided via a new 345 kV overhead transmission line, a new 345 kV substation and a 13.8 kV secondary distribution system in underground ductbanks to various substations for three FMI power systems: the pulsed power system, the conventional power system and the beamline power system.

A new 345 kV switching station will be installed at the southeast corner of the Fermilab site along the Commonwealth Edison Co. transmission line corridor paralleling the EJ&E railroad tracks as indicated on Drawing C-1. Two manually operated 1,600 amp, 345 kV switches will connect the new transmission line to Commonwealth Edison transmission lines No. 11119 and No. 11120.

A new overhead transmission line, approximately 13,200' long will be installed parallel to the southern boundary within the Fermilab site, at least 500' from Illinois Highway 56, Butterfield Road. The line will bend northward and terminate at the new Kautz Road Master Substation (KMS). Double arm steel poles at an average span of 760' will carry a single 345 kV circuit with static shield wires above.

The new KMS will be located east of Kautz Road approximately 900' from the nearest arc of the FMI, 0.5 miles from the south site boundary and 1.6 miles from the existing Master Substation (MSS) at the intersection of Roads A-1 and B. The new substation area is well drained and lies east of the wooded areas that abut the Tevatron ring between service buildings E-3 and E-4.

The new KMS will consist of an 194,000 sq. ft. rock base enclosed within a security fence with an access gate to Kautz Road. Within this area will be the 345 kV dead-end structures, aluminum tubular bus and insulators, motor operated 345 kV switches, SF6 main circuit breaker, four transformers, three harmonic filters and a walk-in switchgear building for secondary equipment. Foundation pads and vaults, oil containment sumps, lightning and ground grids are also included.

Two new transformers and two existing transformers from the present MSS will be installed in the new KMS. Refer to Drawing E-1. The new transformers will be 40 MVA capacity (40/53/66.6 MVA-OA/FA/FOA), 345/13.8 kV, 3-phase, 60 Hz, oil filled, and will be used for the FMI pulsed power supply and beamline power systems. An existing 60 MVA transformer 82B, that will be retired from Main Ring pulsed power supply service, will be used for the FMI conventional power system. Another existing 40 MVA transformer 84A, currently an MSS on-line spare, will be moved and reinstalled in the new KMS.

The secondary sides of the four transformers will be connected by 3,000 A, 13.8 kV non-segregated outdoor bus to 13.8 kV, SF-6 type main and feeder breaker with sufficient interrupting capacity for the available short circuit currents. These breakers, together with metering, relaying and communication equipment are all housed in an enclosed metal walk-in switchgear building.

Underground concrete-encased ductbanks with precast concrete manholes will route the 13.8 kV feeders from vaults under the switchgear equipment at the new KMS to the various FMI power systems. Refer to Drawings E-1 and E-2. Other ductbanks will connect back to the existing Main Ring ductbank between service buildings E-2 and E-3. With these connections and the use of existing but unused or retired Main Ring feeders, approximately 40 MVA of primary power may be back-fed to the MSS to provide emergency and maintenance power in either direction between the KRS and MSS.

The pulsed power supply system will be fed from the two new 40 MVA transformers in the KMS through a modified primary selective distribution system with parallel feeders to each service building. The FMI ring will use two feeders per service building carried through an underground ductbank, the ends of which connect through switchgear at the KMS and at each service building. At each service building, there will be a disconnect switch to supply power to the power supplies. This routing is shown in Drawing F-2. This switch can also be used for feeder isolation for maintenance purposes. The power for the beamlines will also require a modified primary selective distribution system for two 1,500 kVA substations at MI-60 and one 1,500 kVA substation at the MI-8 service building.

The Conventional Power System will be fed from the relocated transformer 82B and will consist of one 13.8 kV feeder around the FMI ring, with two 1,500 kVA transformers at MI-60 service building, a 750 kVA transformer at each of the principal ring service buildings and a 750 kVA at the MI-8 service building. The conventional power will be used for building power, lights, pumps, heating and air conditioning. At each service building there will be a disconnect switch with a ductbank connection to the conventional power transformer. Conventional power will be connected to power distribution panelboards in each service building. Power for the water pumps, heating and ventilating equipment, control racks and service outlets will be provided by 480/277 V, 3-phase branch circuits. Step-down transformers and panelboards provide 208/120 V power for lighting and outlets. Separate panelboards for isolating beam equipment at 480/277 V and 208/120 V are provided. Drawing E-4 summarizes the criteria used for determining general lighting levels and convenience power distribution.

9. PRIMARY COOLING AND MECHANICAL SYSTEMS

The primary heat rejection medium for the 21.9 MW water-cooled load generated by the FMI is cooling pond water (PW). Drawings M-3 and M-4 show the eight new interconnected cooling ponds (A through H) that roughly follow the MI ring perimeter and provide 18.8 acres of cooling surface. The ponds total 11,900' in length, range from 60' to 90' in width and generally have a depth range of from 4'-6" to 7'-0". A transverse concrete dam near service building MI-30 permits a change in water level between ponds D and E. Generally, the pond water levels vary from elevation 741' to 737' following the general site topography with ponds A, B, G and H at elevation 739' to match the Main Ring pond elevations at the F0 area. Transfer piping between the FMI ponds and the existing Main Ring ponds allow for make-up and temperature control.

As described in Chapter 3.9, the LCW system consists of parallel supply and return loops exchanging heat from the FMI beamline magnets, rf components and power supplies to the pond water. Primary deionized water will be supplied to the FMI LCW system along piping in the 8 GeV enclosure from existing Main Ring columns at the Central Utility Building. This building will also be fitted with 3,000 gallons of LCW tanked storage for make-up use in the FMI similar to the existing Main Ring system. An additional 3,000 gallon storage tank will be located at the MI-60 service building. Continuous slip-stream deionizing bottles will be located at the six typical FMI service buildings, the MI-60 and the MI-8 service buildings.

The civil construction scope (WBS 1.2.1.2) includes the pond excavation and berm construction, dams between ponds, interconnecting underground piping, pond liners, rip-rap slope protection, and pond overflow structures. The pond water system included as WBS 1.2.1.11 includes the pond water intake and discharge pipes, pump vaults, pond water pumps, level control system and supply and return piping to the service building as shown schematically on Drawing M-3. The installation of heat exchangers, LCW pumps, LCW piping and related work is included in the technical scope of work.

Service building MI-60 includes a new 150 ton air-cooled chiller with provisions for a future second unit. Underground 12" diameter chilled water supply and return piping will be extended from the MI-60 service building to the Central Utility Plant with taps for the AP Target Hall and future experimental area loads near the MI-8 service building. It is anticipated that a chilled water system retrofit will provide ample CHW for the MI-60 environmental as well as RF cooling loads prior to commissioning of the FMI service from the central plant will negate the need for the second air-cooled unit and permit abandoning the leaky CHW piping along the Ring Road.

An existing chilled water (CW) system at the F0 service building, which originates at the Central Utility Building, will be retained and extended to the pump room of the new MI-60 service building to cool the LCW for the MI rf system. The new combined loads on the CW system will be comparable to the present loads.

An underdrain system, typically consisting of 6" perforated pipe surrounded by a granular filter media and covered by a geotextile fabric, will be installed along both sides of the base slab for all underground enclosures. Similar underdrain systems are typically used for all Fermilab beam enclosures. Sump basins with alternating duplex pumps will be located in alcoves along the enclosures to collect the underdrain flow and discharge it into surface ditches or cooling ponds as indicated on Drawing M-3. Based upon the Main Ring experience, the average MI ring underdrain flow is anticipated to be 200 gpm.

A slurry wall or similar barrier will be constructed on either side of the MI enclosure as it passes through the wetland area along Indian Creek at the south quadrant of the ring. The cutoff wall will extend through the alluvial soil and 5' into the glacial till to seal off any wetland groundwater flow into the underdrain system. A cross-section of the proposed slurry (cutoff) wall is shown on Drawing C-6.

Moderate ventilation rates with dehumidification will be used in the FMI enclosures. Drawing M-1 presents a general layout of this arrangement. Ventilation supply fans with filters and electric heat are located at each service building with exhaust fans at intermediate points between, all connected by underground ducts to alcove areas of the FMI enclosures. Two air changes per hour will be provided when needed during non-operating periods. Dehumidification units will be located periodically along the beam enclosures at the ceiling in alcoves or opposite exit stairways where sump basins are available to receive condensate. Small fans in the units will afford some circulation as a further aid in controlling humidity. Both the ventilation and dehumidification systems are patterned after the existing Main Ring systems.

The FMI service buildings are equipped with a variety of HVAC systems to accommodate the required occupancy, as outlined on Drawings M-1 and M-2. Local exterior wall-mounted air conditioning units with electric heat will provide temperature control in all kicker rooms and control rooms in the typical service buildings. Electric unit heaters and filtered ventilative cooling supply fans with interlocked relief louvers will serve pump rooms, power supply rooms and magnet staging and storage areas in these same buildings. Temperature control at the F0/MI-60 service building will be provided by a combination of fan coil units and HVAC units with electric

heat and fed from local central air-cooled chillers totaling about 425 tons capacity. All of the above buildings will be equipped with required ventilation provisions.

10. FIRE PROTECTION AND LIFE SAFETY

All FMI structures will be provided with fire protection systems as scoped on Drawing M-1. Automatic sprinkler systems will be supplied from a direct buried 12" diameter ICW loop encircling the FMI and tied into the existing site ICW fire protection system in two places, just north of the F0 area and just south of the existing Antiproton Target Hall. All service buildings including F0 and F-17 will be fully sprinklered with a wet system design hydraulically for ordinary hazard, group 1 with a water density of 0.14 gpm per sq. ft. over a minimum area of 2,000 sq. ft. In addition, the enclosure alcoves at the typical FMI service building will be served by a 4" standpipe with hose connection and a wet sprinkler system within the immediate alcove area. Two hydrants will be provided at every service building with an intermediate PIV to provide limited fire protection even when one leg of the 12" loop between adjacent buildings is out of service. The FMI and beamline enclosures will be protected with a continuous line-type heat detection system. Alarms and manual pull stations will be used throughout with smoke and heat detectors supplied in above grade structures including detection in HVAC and fan units. All systems will be integrated with the site-wide FIRUS system.

The ten service buildings range in area from 700 sq. ft. at the F17 Kicker building to 27,500 sq. ft. at the MI-60 service building. All service buildings are Type II (000) construction consisting primarily of insulated metal siding and built-up roofing on steel frames. Where transformers are in close proximity to a service building, the adjacent wall will include two-hour fire rated masonry construction with a metal siding facing. All exit enclosures including stair labyrinths will include 1 1/2-hour rated door assemblies. Penetrations between enclosures and service buildings for cabling and other services will be sealed with fire stopping materials. Exits will be provided in accordance with the criteria of NFPA 101, the Life Safety Code. For this purpose, DOE-CH has classified the underground beamline enclosures as a "Special Purpose Industrial Occupancy" under Subsection 28-2.6.3 which requires the maximum travel distance for emergency egress not to exceed 300 feet. The addition of the exit stair labyrinths combined with access stairs at the service buildings results in intervals between exits at less than 600' at all locations. Additionally, where beamline components present a barrier to an aisle, such as diverging beams at the abort, 8 GeV injection or the 150 GeV extraction regions, exits are provided on both sides of the beamline. Wherever possible, dead end enclosures have been limited to 50' and stairways between enclosure levels are enclosed. Handrails, railings around equipment hatches, stair configurations, aisle widths and vertical headroom have been designed in accordance with recognized standards - most notably OSHA standards. Emergency lighting is

provided throughout the FMI facility and all electrical work will be in conformance with the National Electric Code and Underwriters Laboratory. Emergency power for the beamline enclosures will be provided by 480 V uninterruptible power supplies (UPS) located in the service buildings to eliminate battery power sources in radioactive environments. Refer to the FMI Preliminary Safety Analysis Report for details of the fire protection and life safety provisions.

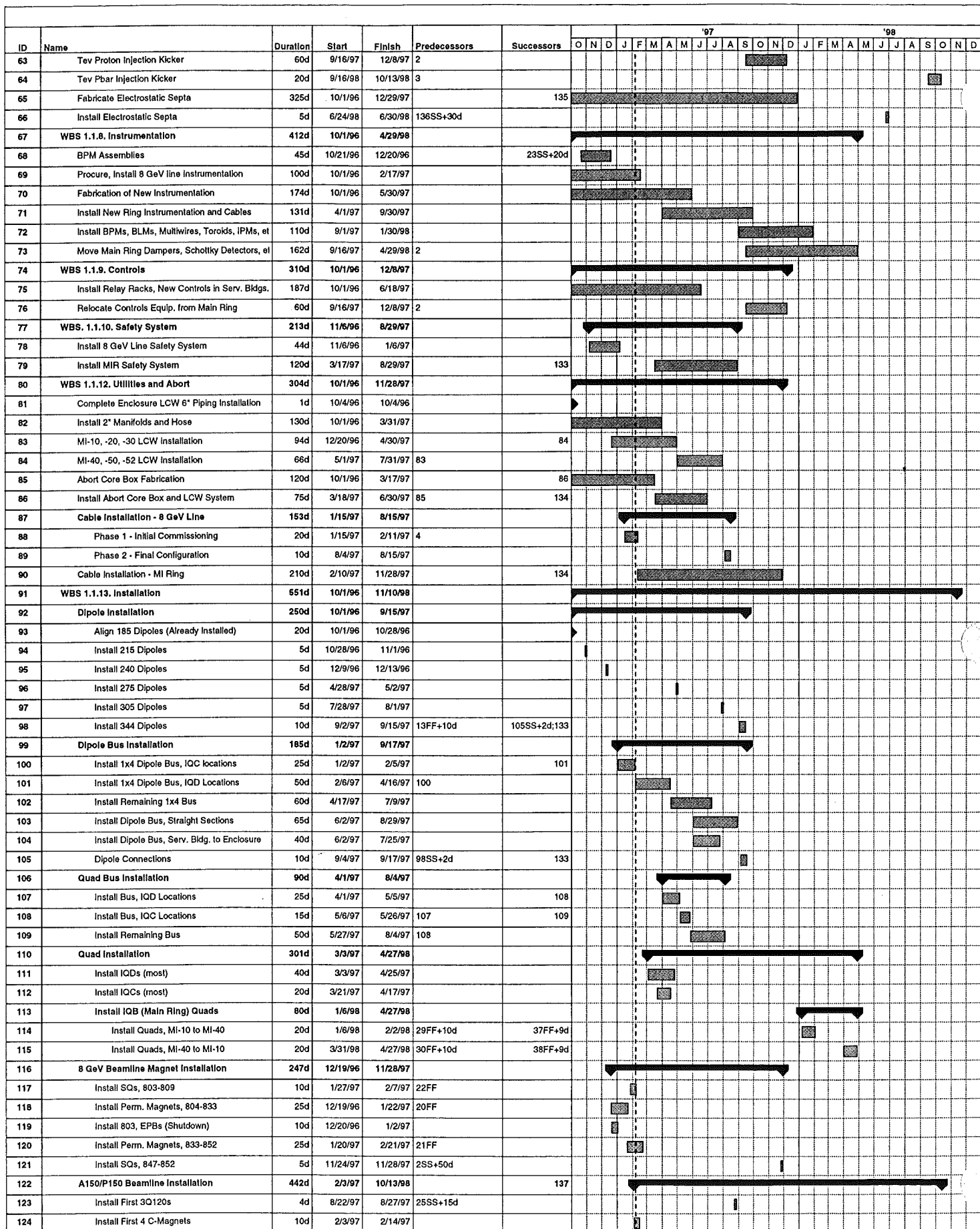
11. ENVIRONMENTAL CONCERNS AND ACTIONS

Detailed and specific definitions of the wetland areas, floodplain and storm water management, archaeological concerns and ecological resources have been identified by environmental consultants resulting in the preparation, submittal and approval of a Floodplain/Wetland Assessment Report and an EA. As a result of these efforts, the following approvals/permits have been obtained:

<u>AGENCY</u>	<u>ACTION REQUESTED</u>	<u>ISSUED</u>
Division of Air Pollution Control Illinois Environmental Protection Agency Springfield, Illinois	Application for Permit to Construct Il. Adm. Code 201.142 NESHAP ID #0438 07AA1	April 1, 1991
U.S. Environmental Protection Agency Region V (SAC-26) Chicago, Illinois	Application for Permit to Construct 40 CFR Part 61.07 Radionuclides National Emission Standards for Hazardous Air Pollutions (NESHAP) REF: 5AT-26	May 9, 1991
Division of Water Pollution Control Illinois Environmental Protection Agency Springfield, Illinois	Clean Water Act Section 401, Water Quality Certification	June 4, 1991
Department of the Army Chicago District U.S. Corps of Engineers Chicago, Illinois	Clean Water Act Section 404, Nationwide 26 Permit Application No. 3499102	June 26, 1991
U.S. Department of Agriculture Soil Conservation Service Champaign, Illinois	Farmland Conversion Impact Rating	Sept. 18, 1991
U.S. Department of Energy	Finding of No Significant Impact (FONSI)	July 6, 1992

In addition, other environmental agencies have been consulted resulting in the following accords:

<u>AGENCY</u>	<u>CONSULTATION REQUESTED</u>	<u>ISSUED</u>
U.S. Fish & Wildlife Service Rock Island, Illinois	Consultation in Accordance With Fish & Wildlife Coordination Act 48 Stat. 401 16 U.S.C. 661 Endangered Species Act	April 30, 1991
Illinois Department of Conservation Springfield, Illinois	Consultation in Accordance with Fish & Wildlife Coordination Act	June 20, 1991
State Historical Preservation Officer Illinois Historic Preservation Agency Springfield, Illinois	106 Determination of No Effect 36 CFR 800	July 22, 1991



ID	Name	Duration	Start	Finish	Predecessors	Successors	'97												'98															
							O	N	D	J	F	M	A	M	J	J	A	S	O	N	D	J	F	M	A	M	J	J	A	S	O	N	D	
125	Install First B2s, 84" Quads	15d	12/8/97	12/28/97	2SS+60d																													
126	LCW, Cabling	10d	9/16/98	9/29/98	3	127																												
127	Install Remaining Magnets	10d	9/30/98	10/13/98	126																													
128	Tevatron	40d	9/16/98	11/10/98		137																												
129	Restore Cables, Bus, etc.	10d	9/16/98	9/29/98	3																													
130	Install Cryogenic Devices, Leak Check, Cook	40d	9/16/98	11/10/98	3																													
131	Install RF cavities	10d	9/16/98	9/29/98	3																													
132																																		
133	DIPOLE POWER TEST	1d	10/31/97	10/31/97	5;6;79;98;105																													
134	PHASE 1 COMMISSIONING (BEAM TO MI-40)	1d	2/16/98	2/16/98	37;42;44;86;90																													
135	PHASE 2 COMMISSIONING (COASTING BEAM)	1d	5/11/98	5/11/98	38;45;59;60;65	136SS+2d																												
136	PHASE 3 COMMISSIONING (ACCELERATE)	1d	5/13/98	5/13/98	135SS+2d;7;48	137;66SS+30d																												
137	PHASE 4 COMMISSIONING (BEAM TRANSFERS)	1d	11/11/98	11/11/98	122;128;136																													

APPENDICES

SCHEDULE 44

SUMMARY SCHEDULES

LATTICE FILES

1. Main Injector Ring Lattice Description (MI_19)
and Main Injector Ring Site Coordinates (MI_19)
2. 8 GeV Line Lattice Description
and 8 GeV Line Site Coordinates
3. 150 GeV Line Lattice Description
and 150 GeV Line Site Coordinates
4. 120 GeV Line Lattice Description
and 120 GeV Line Site Coordinates

CIVIL DRAWINGS

1. Title I Drawings
2. Selected Drawings from Bid Sets

FERMILAB
FY 1996 BUDGET REQUEST
CONSTRUCTION PROJECT DATA SHEET
GENERAL SCIENCE AND RESEARCH - PLANT AND CAPITAL EQUIPMENT
HIGH ENERGY PHYSICS
(Tabular dollars in thousands. Narrative material in whole dollars)

CHICAGO OPERATIONS

Field Office

FERMI NATIONAL ACCELERATOR

1. Title and Location of Project:
Fermilab Main Injector
Fermi National Accelerator Laboratory, Batavia, Illinois

2. Project No. 92-G-302

3. Date A-E work initiated: 3rd Quarter FY 1992

5. Previous Cost Estimate
Total Estimated Cost: \$229,600
Total Project Cost: \$259,300

3a. Date physical construction starts: 3rd Quarter FY 1992

6. Current Cost Estimate
Total Estimated Cost: \$229,600
Total Project Cost: \$259,300

Date: January, 1994

4. Date construction ends: 4th Quarter FY 1998

7. Financial Schedule:	<u>Fiscal Year</u>	<u>Appropriation</u>	<u>Obligation</u>	<u>Cost</u>
	1992	\$11,650	\$11,650	\$1,000
	1993	15,000	15,000	10,000
	1994	25,000	25,000	35,500
	1995	43,000	43,000	43,700
	1996	70,000	70,000	60,900
	1997	64,950	50,000	49,100
	1998	-----	14,950	29,400
Total		\$229,600	\$229,600	\$229,600

8. Brief Physical Description of Project

This project provides for the construction of a new accelerator, called the Fermilab Main Injector, which will replace the aging Fermilab Main Ring accelerator in all its functions. This accelerator will provide particles for injection into the existing Fermilab superconducting Tevatron accelerator and for direct delivery to the existing fixed target

CONSTRUCTION PROJECT DATA SHEET

1. Title and location of Project:

Fermilab Main Injector

Fermi National Accelerator Laboratory, Batavia, Illinois

2. Project No. 92-G-302

experimental and test beam areas. The accelerator is 3.3 km in circumference and is capable of accelerating protons and antiprotons to 150 GeV. It is constructed using conventional iron core magnets. Also provided are five new beamlines which tie the Main Injector into the existing accelerator complex, transport 120 GeV proton beams to the fixed target experimental areas, and provide particle beams for the testing and calibration of detector components and subsystems.

The Fermilab Main Injector accelerator will recycle many technical components from the existing Main Ring, including quadrupole magnets, some power supplies and correction magnets, radio frequency systems, some controls components, and diagnostic devices.

The Main Injector will be located on the southwest side of the Fermilab site, tangent to the existing Tevatron at the F-zero straight section.

Specifically provided for in the scope of the project are:

- a. Construction of a 3.3 km ring enclosure with service buildings and utilities, and the fabrication of new technical components including dipole magnets, high current power supplies, and vacuum systems.
- b. Construction of beamline enclosures, service buildings, utilities, and technical components required to implement the 8 GeV Booster-to-Main Injector beamline, the 150 GeV proton and antiproton Main Injector-to-Tevatron transfer lines, and the 120 GeV Main Injector-to-Antiproton Production Target beamline.
- c. Construction of technical components required to implement the delivery of 120 GeV beam from the Main Injector to the A-zero Transfer Hall, from which distribution to the existing experimental areas is possible.
- d. Construction of a new sub-station and 345 kV power lines for delivery of electrical power to the Main Injector location.
- e. Modifications to the Tevatron ring tunnel at the F-zero straight section for installation of the 150 GeV proton and antiproton transfer lines.
- f. Refurbishment and reinstallation in the Main Injector ring enclosure of those technical components which will be recycled from the old Main Ring.

CONSTRUCTION PROJECT DATA SHEET

1. Title and location of Project:

Fermilab Main Injector

Fermi National Accelerator Laboratory, Batavia, Illinois

2. Project No. 92-G-302

9. Purpose, Justification of Need for, and Scope of Project

The primary purpose of this project is to greatly increase the luminosity which the Tevatron proton-antiproton collider can deliver to the two existing collider detector facilities at Fermilab. Fermilab is the only operational high energy physics facility in the world with sufficiently high energy to produce the top quark, the last unobserved fundamental building block forming the basis of our current understanding of the structure of matter. Increasing the luminosity available at the Fermilab Proton-Antiproton Collider to $5 \times 10^{31} \text{ cm}^{-2} \text{ sec}^{-1}$ will nearly assure discovery and determination of the properties of the Top quark if it lies within the range indicated by all present experimental data. The project will also increase significantly the number of protons which can be delivered to the Tevatron for acceleration and delivery to the fixed target experimental areas. Other important purposes are to provide a new capability for 120 GeV beams for fixed target physics research, and to provide year-round beams for the testing and calibration of detector components and subsystems simultaneously with Tevatron collider operations for physics research.

Increasing the collider luminosity requires increasing both the number of protons and antiprotons injected into the Tevatron. The substantial improvement in injection intensities results from the large effective aperture of the Main Injector ring, and from its rapid repetition rate capability. These are achieved through tighter focusing, improved field quality, and the elimination of overpasses which were installed in the Main Ring to accommodate the collider detector facilities. The Main Injector will be capable of accelerating an intense beam of protons to 120 GeV every 1.5 seconds for antiproton production, as compared to a 2.4 second cycle for the present Main Ring. The beam intensity injected into the Tevatron by the Main Injector will approach 6×10^{13} protons per 60 second cycle, which is about two times as great as could be achieved with the Main Ring. The Tevatron proton-antiproton colliding beam luminosity will be increased to at least $5 \times 10^{31} \text{ cm}^{-2} \text{ sec}^{-1}$, which is five times greater than could be achieved using the Main Ring. These performance goals are expected to be reached after some months of operational experience with the upgraded facilities.

10. Details of Cost Estimate*

	<u>Item Cost</u>	<u>Total Cost</u>
a. EDI&A at 16.9% of construction costs		\$28,200
b. Main Injector construction costs		\$166,800
1. Conventional construction	\$77,500	
2. Special facilities	\$89,300	
c. Contingency at 17.7% of above cost		<u>\$34,600</u>
Total		\$229,600

CONSTRUCTION PROJECT DATA SHEET

1. Title and location of Project:
Fermilab Main Injector
Fermi National Accelerator Laboratory, Batavia, Illinois

2. Project No. 92-G-302

* The annual escalation rates assumed for FY1992 through FY1998 are 3.1, 2.6, 3.4, 4.0, 3.9, 3.8, and 3.6 percent respectively.

11. Method of Performance

Design of facilities will be by the operating contractor and subcontractors as appropriate. To the extent feasible construction and procurement will be accomplished by fixed-price contracts awarded on the basis of competitive bids.

12. Schedule of Project Funding and Other Related Funding Requirements

[illegible]

CONSTRUCTION PROJECT DATA SHEET

1. Title and location of Project:
Fermilab Main Injector
Fermi National Accelerator Laboratory, Batavia, Illinois

2. Project No. 92-G-302

13. Narrative Explanation of Total Project Funding and Other Related Funding Requirements

a. Total project costs

1. Total facility cost

(a) Construction line item - explained in items 8, 9, 10.

2. Other project costs

(a) Direct R&D operating costs - This provides for project conceptual design activities, for design and development of new components, and for the fabrication and testing of prototypes. R&D on all elements of the project to optimize performance and minimize costs will continue through early stages of the project. Specifically included are development of the high current dipole magnet, the associated power supply system, a new sextupole magnet, and new rf power amplifiers. A small number of these components will be fabricated and tested using R&D operating funds.

(b) Pre-operating costs - Includes personnel costs for a several month commissioning period.

(c) Capital equipment - Includes test instruments, electronics, and other general equipment to support 12.a.1 and 2.

(d) Inventories and Spares - Provides for special process spares for the major technical components, primarily magnets and power supplies, and for an increase in common use inventories for Main Injector related items.

b. Total incremental funding requirements - It is assumed that the Fermilab Tevatron complex will continue to operate both the fixed target and collider programs, with each running about 40% of the time. The Main Injector replaces the existing Main Ring in all its functional roles and it is designed to require nearly the same amount of power to operate for those purposes. The new Main Injector capability for test beam operations simultaneous with Tevatron operations for physics research will require an average increase in power plus other operating cost of about \$6.6M annually. The increase in operating costs in 12.b.1 and 2 reflects solely the incremental demands of delivering 120 GeV protons to the fixed target experimental areas during Tevatron collider operations.

14. Incorporation of Fallout Shelters in Future Federal Buildings

Not specifically incorporated into this project as sufficient space is available at other locations on the site.

15. Incorporation of Measures for the Prevention, Control, and Abatement of Air and Water Pollution at Federal Facilities.

CONSTRUCTION PROJECT DATA SHEET

1. Title and location of Project:

Fermilab Main Injector
Fermi National Accelerator Laboratory, Batavia, Illinois

2. Project No. 92-G-302

The total estimated cost of this project includes the cost of those measures necessary to assure the facility will comply with Executive Order 12088. A Section 404 permit from the Army Corps of Engineers has been issued for this construction.

16. Evaluation of Flood Hazard

This project will be partially located in the flood plain of Indian Creek, which originates on the Fermilab site. An active drainage system will allow the control of water levels within the region encompassed by the Main Injector ring. Measures will be taken to insure that the water retention capacity of the Indian Creek drainage basin is maintained both during the construction and operational phases of the project. Components installed in the underground Main Injector ring and beamline enclosures will be protected by pumps, as are all existing underground enclosures on the Fermilab site. Service buildings and enclosure access points will be located well above the floodplain. Construction will be in accordance with Executive Order 11988. An Army Corps of Engineers permit has been issued for this construction.

17. Environmental Impact

Environmental documentation has been prepared for this project and a Finding of No Significant Impact (FONSI) issued. Any wetlands that will be disturbed during the course of the project will be restored as closely as possible to their original condition. Mitigation plans for any disturbance and/or loss of wetlands have been finalized after consultation with the Corps of Engineers. Compensatory wetlands will be created in the vicinity of the disturbed wetlands in a ratio of 1-1/2 to 1 of existing wetlands impacted by construction of the Main Injector site. The project will be in compliance with the National Environmental Policy Act.

18. Accessibility to the Handicapped


All tunnel enclosures and service buildings are occupied only temporarily. They do not provide permanent working space, and are considered hazardous areas with restricted access under laboratory policy. As such, no special measures for accessibility to the handicapped will be provided in these areas.

SCHEDULES

THE FOLLOWING SCHEDULES WERE PRODUCED FROM THE PROJECT CONTROL SYSTEM'S MICROSOFT PROJECT® FILES. THESE FILES WERE CREATED BY AND ARE UPDATED MONTHLY BY THE WBS LEVEL 3 MANAGERS. THE GANTT CHARTS HAVE BEEN CONDENSED FIRST BY REMOVING EDI&A, AND THEN FORMATTING THE FILES TO SHOW ONLY THE "SUMMARY TASKS", WHICH SPAN THE DURATION OF THE SUBORDINATE TASKS. THE CALENDAR SHOWS FISCAL YEAR QUARTERS.

Name	Duration	start	finish	1994	1995	1996	1997	1998	19
Magnets	1263d	10/1/93	8/4/98						
Dipole	1055d	10/1/93	10/16/97						
IDA	1055d	10/1/93	10/16/97						
IDB	1055d	10/1/93	10/16/97						
IDC	849d	7/18/94	10/16/97						
IDD	1055d	10/1/93	10/16/97						
QUADS	529d	12/8/93	12/18/95						
IQC	323d	12/8/93	3/3/95						
IQD	416d	5/16/94	12/18/95						
Reworked 84" Quads	817d	4/17/95	6/2/98						
BQB Magnets	424d	10/17/96	6/2/98						
BQA Magnets	393d	4/17/95	10/16/96						
New Small Magnets	973d	2/1/94	10/23/97						
Sextupole Magnets	973d	2/1/94	10/23/97						
Horizontal Trim Magnets	262d	5/15/95	5/14/96						
Vertical Trim Magnets	272d	9/11/95	9/24/96						
New Beam Magnets	628d	1/30/95	6/25/97						
132" C-magnet	361d	1/30/95	6/17/96						
3Q120A Magnets	343d	10/31/95	2/20/97						
3Q160 Magnets	379d	10/31/95	4/11/97						
110" Lambertsons (5 total)	593d	3/20/95	6/25/97						
Reworked Other Magnets	470d	10/16/96	8/4/98						
TRIM QUADS	350d	10/16/96	2/17/98						
SKEW QUADS	352d	10/16/96	2/19/98						
OCTUPOLES	360d	10/16/96	3/3/98						
CR SKEW QUADS	146d	10/16/96	5/7/97						
B2's (BDM)	398d	10/16/96	4/24/98						
EPB DIPOLES	405d	10/16/96	5/5/98						
B3's (ODM)	351d	10/16/96	2/18/98						
SQA Magnets	353d	10/16/96	2/20/98						
HORIZ AND VERT TRIMS, REWORK Magnets	470d	10/16/96	8/4/98						

Project:
Date: 9/19/94


Critical 

Noncritical 

Progress 

Milestone 

Summary 

Rolled Up 

WBS	Name	Duration	start	finish	1993	1994	1995	1996	1997	1998
	FMI Vacuum System	1524.51d	10/1/92	8/5/98						
	Ring Vacuum System Design	1255.09d	10/1/92	7/24/97						
1.1.2.1.1	MIR VAC CHAMBERS/BELLOWS	875d	3/3/94	7/10/97						
1.1.2.1.1	VACUUM CHAMBER /SPECS COMPLE	0w	3/3/94	3/3/94						
1.1.2.1.1	TECHNICAL COMPONENTS REV 1 COI	0w	3/31/94	3/31/94						
1.1.2.1.2	MIR VACUUM PUMPS	459.38d	10/19/95	7/24/97						
1.1.2.1.3	MIR VACUUM GAUGES	458.59d	10/12/95	7/16/97						
	8 GEV Vacuum System Design	872.78d	4/7/94	8/12/97						
1.1.2.10.1.1	8 GEV VAC BELLOWS/CHAMBERS	213.04d	10/17/96	8/12/97						
1.1.2.10.2.1	8 GEV VACUUM PUMPS	227.5d	9/26/96	8/12/97						
1.1.2.10.3.1	8 GEV VACUUM GAUGES	212.5d	10/3/96	7/29/97						
	150 GEV Vacuum System Design	567.5d	4/6/95	6/10/97						
1.1.2.10.1.2	150 GEV VAC CHAMBERS/BELLOWS	327.5d	3/7/96	6/10/97						
1.1.2.10.2.2	150 GEV VACUUM PUMPS	325d	3/7/96	6/5/97						
1.1.2.10.3.2	150 GEV VACUUM GAUGES	325d	3/7/96	6/5/97						
1.1.2.10.1.3	REMNANT VACUUM	847d	5/8/95	8/4/98						
1.1.12.1.3.2	ABORT VACUUM	469.79d	10/3/96	7/22/98						
1.1.13.1.3	MIR VACUUM INSTALLATION	610d	3/21/96	7/23/98						
1.1.13.2.3	8 GEV VACUUM INSTALLATION	195d	11/3/97	7/31/98						
1.1.13.3.3	150 GEV VACUUM INSTALLATION	195d	11/5/97	8/4/98						
1.1.13.6.3	REMNANT VACUUM INSTALLATION	195.51d	11/5/97	8/5/98						
1.1.13.7.1	TEV E-0 VACUUM	424.82d	9/26/96	5/14/98						
1.1.13.7.2.2	TEV F-0 VACUUM	350.79d	12/24/96	4/28/98						
1.1.2.14	1.1.2.14 EDI&A	1255.09d	10/1/92	7/24/97						
1.1.12.14	1.1.12.14 EDI&A (vacuum portion only)	254.31d	4/4/96	3/27/97						
1.1.13.14	1.1.13.14 ED&IA (vacuum portion only)	614.9d	3/21/96	7/30/98						

Project: FORECAST/wbs 1.1.2 Vc
Date: 9/19/94

Critical 
Noncritical 

Progress 
Milestone 

Summary 
Rolled Up 

WBS	Name	Duration	start	finish	1992	1993	1994	1995	1996	1997	1998	1999
1.1.3.1.1.1	MIR /Dipole Power Supplies	1094.59d	10/1/93	12/11/97								
1.1.3.1.1.1	Transformers	140d	7/10/95	1/19/96								
1.1.3.1.1.1	VCB/Switch Gear	140d	7/10/95	1/19/96								
1.1.3.1.1.1	Transformers	140d	11/13/95	5/24/96								
1.1.3.1.1.1	VCB/Switch Gear	140d	7/10/95	1/19/96								
1.1.3.1.1.2	MIR/Dipole Power Supplies	916.31d	10/1/93	4/7/97								
1.1.3.1.1.2	Total Labor (T2)	916.31d	10/1/93	4/7/97								
1.1.3.1.1.2	Total Budget Labor (T2) to Date	521d	10/1/93	9/29/95								
1.1.3.1.2	MIR/Quadrupole Power Supplies	145d	10/1/96	4/21/97								
1.1.3.1.3	MIR/Sextupole Power Supplies	324d	4/1/96	6/26/97								
1.1.3.1.4	MIR/Corr Elem Power Supplies	80d	1/2/98	4/23/98								
1.1.3.1.6	MIR Injector Regulation System	330d	3/7/96	6/12/97								
1.1.3.1.7	MIR Regulation System	250d	10/1/96	9/15/97								
1.1.3.1.8	MIR Abort Power Supplies	205d	10/1/96	7/14/97								
1.1.3.2.1	8 GEV Line/Dipole Power Supplies	572d	3/6/96	5/14/98								
1.1.3.2.2	8 GEV Line/Quadrupole Power Supplies	585.13d	3/6/96	6/3/98								
1.1.3.2.3	8 GEV Line/Corr Elem Power Supplies	611.75d	4/1/96	8/4/98								
1.1.3.2.4	8 GEV Line/Inj Lamb Power Supply	613.75d	4/1/96	8/6/98								
1.1.3.3.1	150 GEV Proton Line/Dipole P S	621.25d	4/1/96	8/18/98								
1.1.3.3.2	150 GEV Proton Line/Quadrupole P S	647.5d	4/1/96	9/23/98								
1.1.3.3.3	150 GEV Proton Line/Corr Elem P S	651.5d	4/1/96	9/29/98								
1.1.3.4.3	150 GEV P-Bar Line/Corr Elem P S	655.5d	4/1/96	10/5/98								
1.1.3.5.2	P-Bar Prod Line (F11-F17)/Quad Supplies	665.5d	4/1/96	10/19/98								
1.1.3.5.3	P-Bar Prod Line (F11-F17)/Corr Elem Supplies	666.5d	4/1/96	10/20/98								
1.1.3.6.1	Slow Spill Line/Dipole Power Supplies	683.38d	4/1/96	11/12/98								
1.1.3.6.2	Slow Spill Line/Quadrupole P S	703.38d	4/1/96	12/10/98								
1.1.3.7	Beam Line Power Supply Controllers	490d	10/2/95	8/15/97								
1.1.3.14	Power Supplies ED&A	1293.62d	10/1/92	9/16/97								
1.1.3.14	Total ED&I Budget To Date	782d	10/1/92	9/29/95								
1.1.3.14	Labor FY '93	234.38d	10/1/92	8/25/93								
1.1.3.14	Labor FY '94	260.55d	10/1/93	9/30/94								
1.1.3.14	Labor FY '95	260d	10/3/94	9/29/95								
1.1.3.14	Labor Out Years	511.62d	10/2/95	9/16/97								
	Power Supplies Milestones TO FMI 1.0	427.38d	4/21/97	12/10/98								
	Main Injector Ring Power Supplies Milestones	263d	4/21/97	4/23/98								
	8 GEV Line/Power Supplies Milestones	57.75d	5/14/98	8/4/98								
	150 GEV Proton Line/Power Supplies Milestones	30.25d	8/18/98	9/29/98								
	150 GEV P-Bar Line/Power Supplies Milestones	0d	10/5/98	10/5/98								
	P-Bar Production Line (F11 to F17)/PS Milestones	1d	10/19/98	10/20/98								
	Slow Spill Line/Power Supplies Milestone	20d	11/12/98	12/10/98								
	Power Supplies Milestones FROM FMI 1.0	0d	3/1/92	3/1/92								
	Civil Milestones	757d	9/16/94	8/12/97								
	Level 0 Milestones	1771d	5/1/92	2/12/99								
	Level 1 Milestones	1790d	3/1/92	1/8/99								
	Level 2 Milestones	1815d	3/1/92	2/12/99								

Project: FORECAST/wbs 1.1.3 Pc
Date: 9/19/94

Critical 
Noncritical 

Progress 
Milestone 

Summary 
Rolled Up 

WBS	Name	Duration	start	finish	1992	1993	1994	1995	1996	1997	1998	19
1.1.4.1.1.1.1	MIR rf 53 mhz/200kw POWER AMPLIFIER	920d	10/7/93	4/16/97								
1.1.4.1.1.1.1	Start 200 KW PA-.1.1.1.1	0d	12/1/93	12/1/93								
1.1.4.1.1.1.1	Order PA Components	210d	1/2/95	10/20/95								
1.1.4.1.1.1.1	Fabricate PA Sub-Assemblies	175d	9/8/95	5/9/96								
1.1.4.1.1.1.1	Final PA Assembly	230d	2/15/96	1/1/97								
1.1.4.1.1.1.1	PA's Ready to Install	0d	4/16/97	4/16/97								
1.1.4.1.1.1.2	MIR rf 53 mhz/4KW SOLID STATE DRIVER	911d	10/7/93	4/3/97								
1.1.4.1.1.1.2	Start 4KW Driver -.1.1.1.2	0d	12/1/93	12/1/93								
1.1.4.1.1.1.2	4KW Drivers Installed	0d	4/3/97	4/3/97								
1.1.4.1.1.2.1	MIR rf 53 mhz/ANODE SUPPLIES	845d	10/1/94	12/26/97								
1.1.4.1.1.2.1	Start Anode Supplies-.1.1.2.1	0d	10/1/94	10/1/94								
1.1.4.1.1.2.1	Spec. & Order Components	106d	11/1/94	3/28/95								
1.1.4.1.1.2.1	Fabricate APS Sub-Assemblies	126d	12/1/94	5/25/95								
1.1.4.1.1.2.1	Install APS Sub-Assemblies	100d	5/26/95	10/12/95								
1.1.4.1.1.2.1	13.8KV Vacuum Contactors Install	273d	9/6/95	9/20/96								
1.1.4.1.1.2.1	RECEIVE VC-1	0d	9/6/95	9/6/95								
1.1.4.1.1.2.1	RECEIVE VC-2	0d	3/3/96	3/3/96								
1.1.4.1.1.2.1	RECEIVE VC-3	0d	9/8/96	9/8/96								
1.1.4.1.1.2.1	13.8 KV Transformer	260d	11/17/96	11/17/97								
1.1.4.1.1.2.1	Order 13.8 KV Transformer	0d	11/17/96	11/17/96								
1.1.4.1.1.2.1	Receive 13.8KV Transformer	0d	11/17/97	11/17/97								
1.1.4.1.1.2.1	Transformers Installed	565d	10/1/95	11/28/97								
1.1.4.1.1.2.1	Test APS	576d	10/13/95	12/26/97								
1.1.4.1.1.2.1	Complete Anode Supplies-.1.1.2.1	0d	12/26/97	12/26/97								
1.1.4.1.1.2.2	MIR rf 53 mhz/MODULATORS	1000d	12/1/93	10/1/97								
1.1.4.1.1.2.2	Start Modulator-.1.1.2.2	0d	10/1/94	10/1/94								
1.1.4.1.1.2.2	Modulators Installed	0d	10/1/97	10/1/97								
1.1.4.1.1.3	MIR rf 53 mhz/LOW LEVEL	375.5d	9/2/95	2/10/97								
1.1.4.1.1.3	Start LLRF -.1.1.3	0d	9/2/95	9/2/95								
1.1.4.1.1.3	Complete LLRF	0d	2/10/97	2/10/97								
1.1.4.1.1.4	MIR rf 53 mhz/TRANSMISSION LINE	1096d	10/15/93	12/26/97								
1.1.4.1.1.4	Start Transmission Lines -.1.1.4	0d	10/15/93	10/15/93								
1.1.4.1.1.4	Bus Bars Installed In Penetrations	0d	11/23/93	11/23/93								
1.1.4.1.1.4	Transmission Lines Installed	0d	12/26/97	12/26/97								
1.1.4.1.1.6	MIR rf 53 mhz/H=588 CAVITIES	417d	6/15/96	1/20/98								
1.1.4.1.1.6	Start H=588 Cavities -.1.1.6	0d	6/15/96	6/15/96								
1.1.4.1.1.6	H=588 Cavities Complete	0d	1/20/98	1/20/98								
1.1.4.1.2.1	COALESCING SYSTEM/rf CAVITIES, TRSM LINE	342d	8/10/96	12/2/97								
1.1.4.1.2.1	Start CoalCav -.1.2.1&-.1.2.4	0d	8/10/96	8/10/96								
1.1.4.1.2.1	Coal Cav Ready For Move	0d	1/8/97	1/8/97								
1.1.4.1.4	rf SYSTEMS EDI&A	1106d	10/1/93	12/26/97								

Project: FORECAST/wbs 1.1.4 rf:
Date: 9/19/94

Critical 
Noncritical 

Progress 
Milestone 



Summary 
Rolled Up 

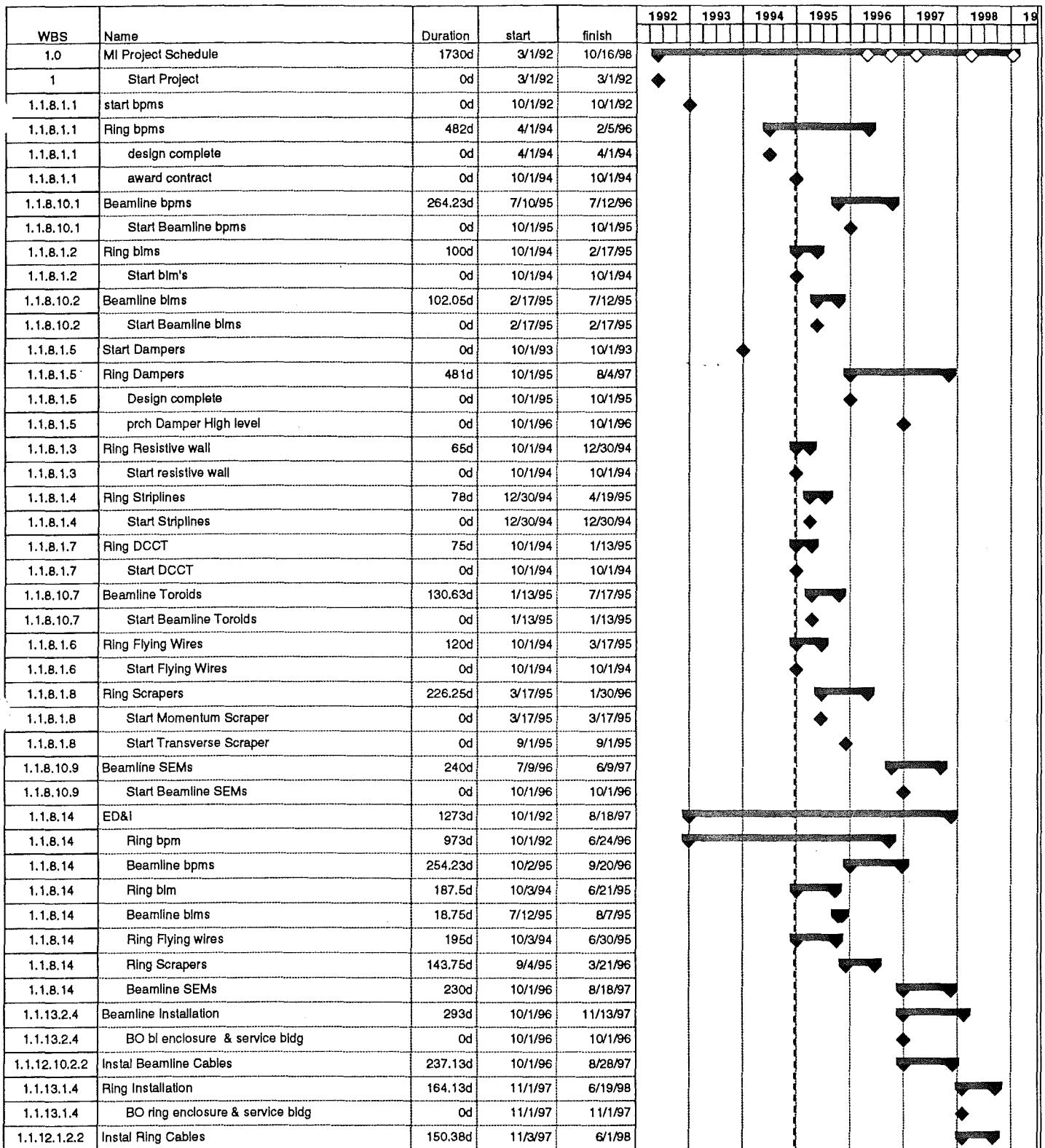
WBS	Name	Duration	start	finish	1992	1993	1994	1995	1996	1997	1998	1999
1.1.6.1.1.1	8 GeV Proton Inj/Kicker Magnet	1032d	9/1/94	8/14/98								
1.1.6.1.1.1	Magnet #1	160d	1/19/95	8/30/95								
1.1.6.1.1.1	Mechanical & Assembly (Magnet #1)	160d	1/19/95	8/30/95								
1.1.6.1.1.1	Magnet #2 and #3	160d	1/5/98	8/14/98								
1.1.6.1.1.1	Mechanical & Assembly (Magnet #2 and #3)	130d	2/16/98	8/14/98								
1.1.6.1.1.2	8 GeV Proton Inj/Kicker Power Supply	944d	1/27/94	9/9/97								
1.1.6.1.1.2	Pulser #1	659d	1/27/94	8/6/96								
1.1.6.1.1.2	Thyratron Pulser	331d	1/27/94	5/4/95								
1.1.6.1.1.2	Resonant Charging Supply	170d	12/13/95	8/6/96								
1.1.6.1.1.2	PFL	95d	12/9/94	4/20/95								
1.1.6.1.1.2	Load Resistor	65d	12/30/94	3/30/95								
1.1.6.1.1.2	Pulser #2 and #3	180d	1/1/97	9/9/97								
1.1.6.1.1.2	Initiate Procurement	0d	1/1/97	1/1/97								
1.1.6.1.1.2	Thyratron Pulser	81d	1/1/97	4/23/97								
1.1.6.1.1.2	Resonant Charging Supply	140d	1/1/97	7/15/97								
1.1.6.1.1.2	PFL	170d	1/1/97	8/26/97								
1.1.6.1.1.2	Load Resistor	180d	1/1/97	9/9/97								
1.1.6.1.1.2	Installation	63.75d	10/21/96	1/16/97								
1.1.6.1.2.1	8 GeV Pbar Inj/Kicker Magnet (Multi-mode)	320d	7/3/95	9/20/96								
1.1.6.1.2.2	Thyratron Pulser	816.5d	1/1/94	2/18/97								
1.1.6.1.2.2	PFN	504d	1/1/94	12/7/95								
1.1.6.1.2.2	Load Resistor	150d	4/7/95	11/2/95								
1.1.6.1.2.2	Installation	75d	10/21/96	1/31/97								
1.1.6.1.4.1	150 GeV Pbar Extraction/Kicker Magnet	60d	3/25/96	6/14/96								
1.1.6.1.4.2	150 GeV Pbar Extraction/Kicker P S	345d	1/1/96	4/25/97								
1.1.6.1.4.2	Pulser Construction	285d	3/25/96	4/25/97								
1.1.6.1.4.2	Pulser Installation	65d	7/5/96	10/3/96								
1.1.6.1.5.1	Proton Abort Kicker Magnet	70d	4/15/96	7/19/96								
1.1.6.1.5.1	Magnet Rework	70d	4/15/96	7/19/96								
1.1.6.1.5.2	Proton Abort Kicker Power Supply	813.9d	10/1/93	11/13/96								
1.1.6.1.5.2	Charging Supply	111d	11/1/95	4/3/96								
1.1.6.1.5.2	Pulser	737.9d	1/15/94	11/13/96								
1.1.6.1.5.2	Pulser #1	505d	1/15/94	12/22/95								
1.1.6.1.5.2	Pulser #2	270.9d	11/1/95	11/13/96								
1.1.6.1.5.2	Installation	65d	11/20/95	2/16/96								
1.1.6.2.1	MIR Slow Extraction/Electrostatic Septum	37.88d	1/1/96	2/21/96								
1.1.6.2.2	MIR Slow Extraction/Spec Magnetic Elem	62.5d	1/1/96	3/27/96								
1.1.6.2.3	Start QXR System	0d	1/1/97	1/1/97								
1.1.6.2.3	Microprocessor	153.75d	3/12/97	10/13/97								
1.1.6.3.1.1	TEV 150 GeV Proton Inj Kicker Magnet	150d	1/1/97	7/29/97								
1.1.6.3.1.2	Controls Rework	168.75d	6/1/95	1/23/96								
1.1.6.3.1.2	Cable Installation	115d	1/1/97	6/10/97								
1.1.6.3.2.1	TEV 150 GeV Pbar Inj Kicker Magnet	10d	2/2/98	2/13/98								
1.1.6.3.2.2	Controls Rework	168.75d	6/1/95	1/23/96								
1.1.6.3.2.2	Cable Installation	369d	10/1/96	2/27/98								
1.1.6.14	Kickers & Slow Extraction EDI&A	1363.45d	10/1/92	12/23/97								
1.1.6.14	Labor ED&I Budget to Date	782d	10/1/92	9/29/95								
1.1.6.14	Labor FY93	235.85d	10/1/92	8/26/93								
1.1.6.14	Labor FY94	261d	10/1/93	9/30/94								
1.1.6.14	Labor FY '95	260d	10/3/94	9/29/95								
1.1.6.14	Labor Out Years	581.45d	10/2/95	12/23/97								

Project: FORECAST/wbs 1.1.6 Kik
Date: 9/19/94

Critical 
Noncritical 

Progress 
Milestone 

Summary 
Rolled Up 



Project: FORECAST/wbs 1.1.8 IN
Date: 9/19/94



Critical
Noncritical

Progress
Milestone

Summary
Rolled Up

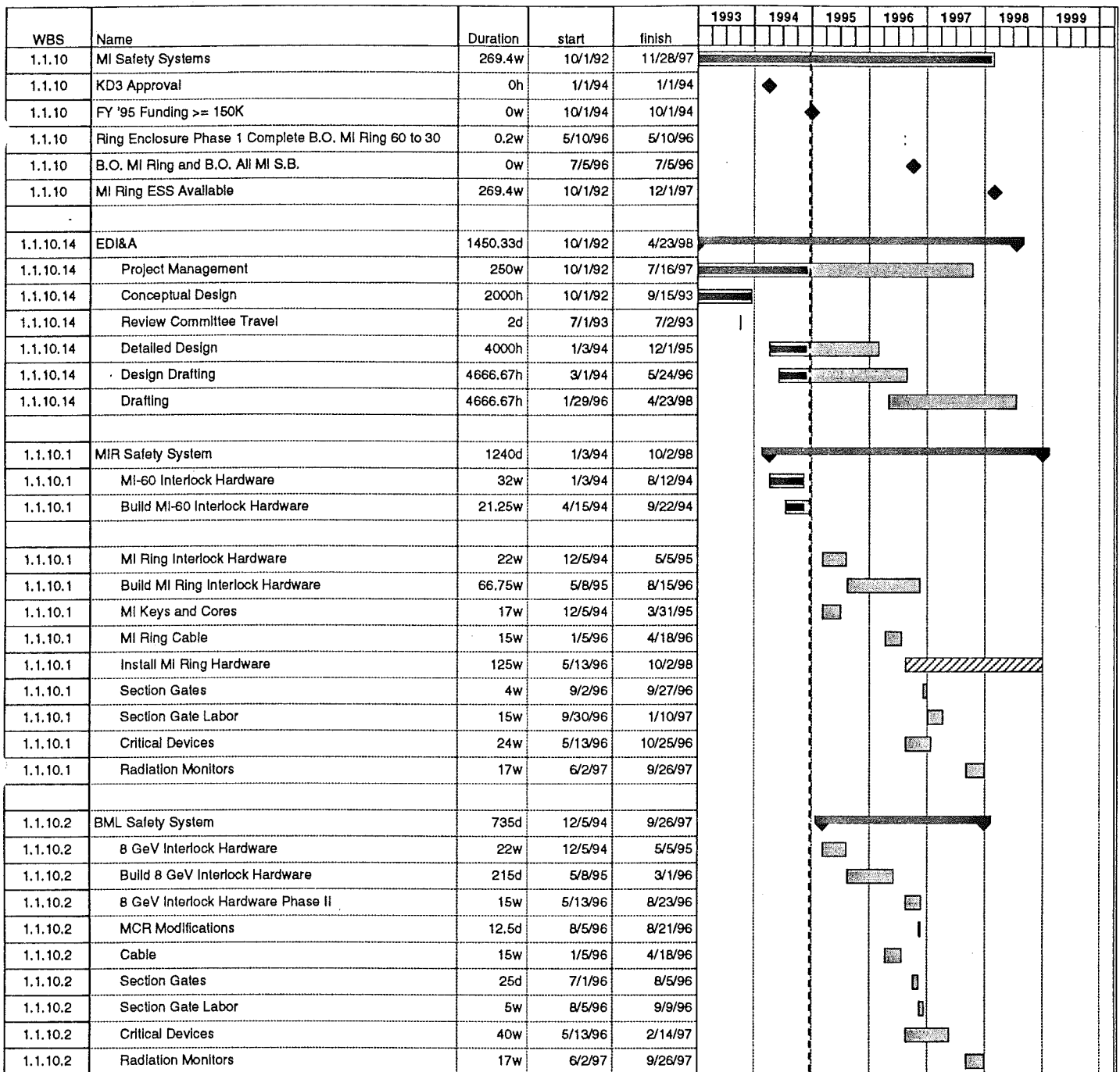
WBS	Name	Duration	start	finish	1992	1993	1994	1995	1996	1997	1998
1.1.9	MI20 b/o	0d	4/25/96	4/25/96					◆		
1.1.9	MI30 b/o	0d	5/9/96	5/9/96					◆		
1.1.9	MI40 b/o	0d	5/23/96	5/23/96					◆		
1.1.9	MI50 b/o	0d	6/6/96	6/6/96					◆		
1.1.9	Total controls	1540d	12/11/92	11/5/98							
1.1.9.1	Total controls (MIR)	1102d	3/2/94	5/21/98							
1.1.9.1.1	Computer, Links (incl install'n)	1014d	7/4/94	5/21/98							
1.1.9.1.2	Crates, Cards, etc (incl install'n)	892d	12/1/94	5/1/98							
1.1.9.1.3	CATV (incl install'n)	370d	5/29/95	10/25/96							
1.1.9.1.4	FIRUS (incl install'n)	613d	3/2/94	7/5/96							
1.1.9.1.5	Ethernet (incl install'n)	631d	8/1/94	12/30/96							
1.1.9.1.5	Present firm networking plan, w/cost est	0d	8/1/94	8/1/94							
1.1.9.10	Total Controls (BeamLines)	727d	10/24/95	8/5/98							
1.1.9.10.1	BML Computer, Links (incl install'n)	1d	1/26/96	1/26/96							
1.1.9.10.2	BML Crates, Racks, etc (incl install'n)	727d	10/24/95	8/5/98							
1.1.9.14	Controls EDI&A	1540d	12/11/92	11/5/98							
1.1.13.1.5	WBS 1.1.13.1.5 not included above	40d	2/1/98	3/27/98							
1.1.9	TOTAL CONTROLS OBLIGATIONS	1540d	12/11/92	11/5/98							
1.1.9.1	Total controls obligations/MIR	1123d	2/1/94	5/21/98							
1.1.9.1.1	Computer, Links (incl install'n) Oblig	1123d	2/1/94	5/21/98							
1.1.9.1.2	Crates, Cards, etc (incl install'n) Oblig	914d	11/1/94	5/1/98							
1.1.9.1.3	CATV (incl install'n) Oblig	370d	5/29/95	10/25/96							
1.1.9.1.4	FIRUS (incl install'n) Oblig	613d	3/2/94	7/5/96							
1.1.9.1.5	Ethernet (incl install'n) Oblig	631d	8/1/94	12/30/96							
1.1.9.1.5	Present firm networking plan, w/cost est, oblig	0d	8/1/94	8/1/94							
1.1.9.10	TOTAL CONTROLS OBLIGATIONS (BEAMLINES)	727d	10/24/95	8/5/98							
1.1.9.10.1	BML Computer, Links (incl install'n) Oblig	1d	1/26/96	1/26/96							
1.1.9.10.2	BML Crates, Racks, etc (incl install'n) Oblig	727d	10/24/95	8/5/98							
1.1.9.14	Controls EDI&A Oblig	1540d	12/11/92	11/5/98							
1.1.13.1.5	1.1.13.1.5 not included above obligations	40d	2/1/98	3/27/98							

Project: FORECAST/wbs 1.1.9 C
Date: 9/19/94

Critical 
Noncritical 

Progress 
Milestone 

Summary 
Rolled Up 

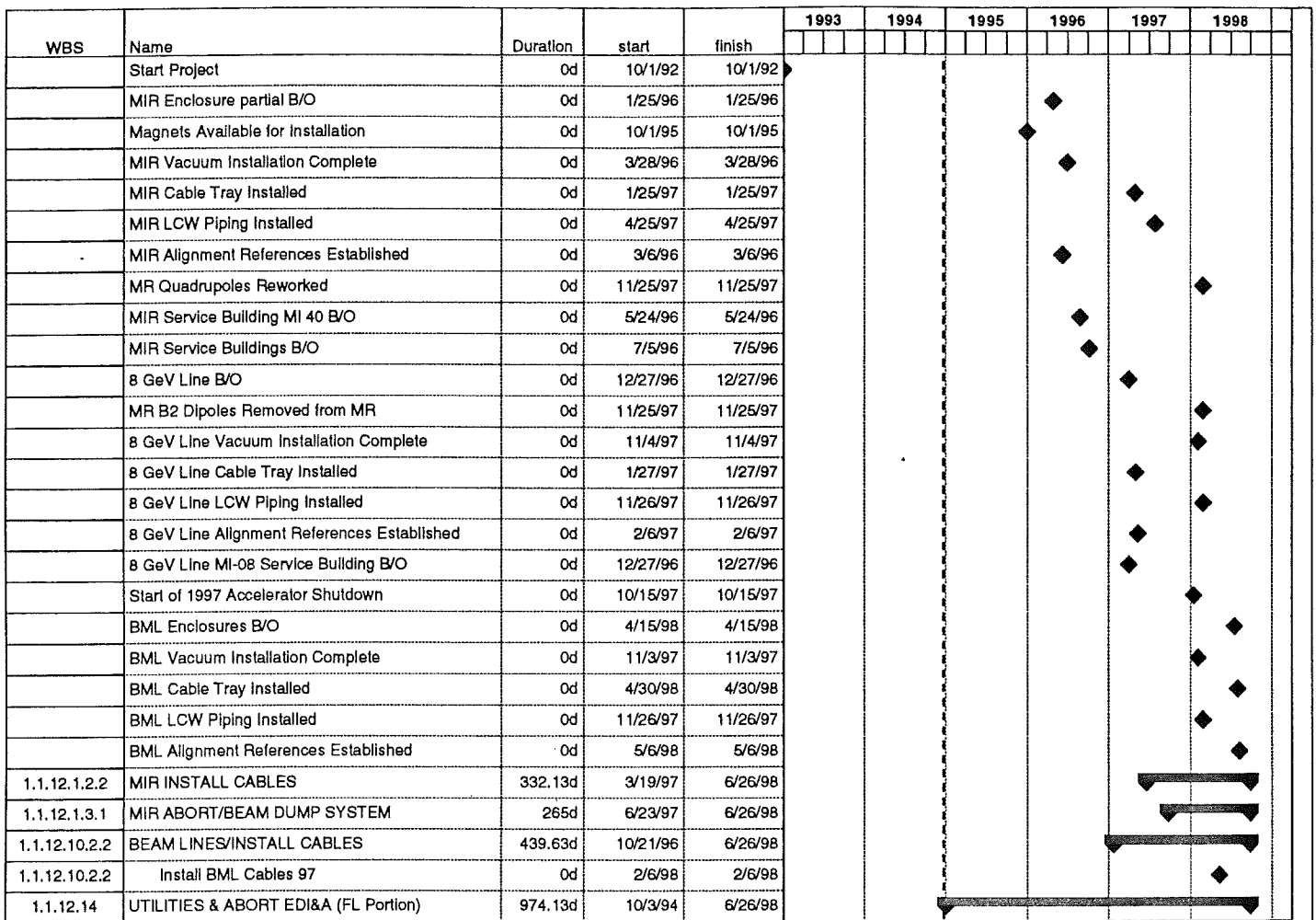


Project: FORECAST/wbs 1.1.10 E
Date: 9/19/94

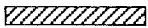

Critical 
Noncritical 

Progress 
Milestone 

Summary 
Rolled Up 



Project: FORECAST/wbs 1.1.12 L
Date: 9/19/94

Critical 
Noncritical 

Progress 
Milestone 

Summary 
Rolled Up 

WBS	Name	Duration	start	finish	1993	1994	1995	1996	1997	1998
1.1.12.1.1.2	MIR-HEAT EXCHANGER	869.55d	8/29/94	12/29/97						
1.1.12.1.1.2	MI-60 Beneficial Occupancy	0d	8/29/94	8/29/94						
1.1.12.1.1.2	Funding-10/1/96	0d	10/1/96	10/1/96						
1.1.12.1.1.2	Partial Occupancy Ser. Bldgs. 10 to 50	0d	8/19/96	8/19/96						
1.1.12.1.1.3	MIR LCW PROCESSING	683.5d	10/17/94	5/29/97						
1.1.12.1.1.3	Funding-10/1/95	0d	10/1/95	10/1/95						
1.1.12.1.1.3	Funding-10/1/96	0d	10/1/96	10/1/96						
1.1.12.1.1.4	MIR-LCW PUMP SYSTEM	649d	12/13/94	6/6/97						
1.1.12.1.1.4	Funding-10/1/96	0d	10/1/96	10/1/96						
1.1.12.1.1.5	MIR-LCW PIPING	769.83d	10/3/94	9/12/97						
1.1.12.1.1.5	MI-10-20-30 Enclosure Partial Occup.	0d	3/30/95	3/30/95						
1.1.12.1.1.5	Funding-10/1/95	0d	10/1/95	10/1/95						
1.1.12.1.1.5	MI 40-50 Enclosure Partial Occup.	0d	7/27/95	7/27/95						
1.1.12.1.1.5	MI 10-20-30-40-50 S. B. Partial Occup.	0d	6/7/96	6/7/96						
1.1.12.1.1.6	RF95- HEAT EXCHANGER/PUMP	840.75d	10/1/94	12/22/97						
1.1.12.1.1.6	Main Ring Shutdown	0d	11/1/97	11/1/97						
1.1.12.1.1.6	Funding-10/1/94	0d	10/1/94	10/1/94						
1.1.12.1.1.7	RF95-PROCESSING	116.88d	10/3/94	3/14/95						
1.1.12.1.1.8	RF95-LCW PIPING	513.5d	10/1/93	9/20/95						
1.1.12.1.1.8	Funding- 10/1/93	0d	10/1/93	10/1/93						
1.1.12.1.1.8	Funding-10/1/94	0d	10/1/94	10/1/94						
1.1.12.1.1.9	RF55-LCW PROCESSING	155.38d	10/3/94	5/8/95						
1.1.12.1.1.10	RF55-HEAT EXCHANGER/PUMP	819.42d	10/3/94	11/21/97						
1.1.12.1.1.10	Procure Ht. Exch. Fittings/Pipe	0d	6/23/97	6/23/97						
1.1.12.1.1.11	RF55-LCW PIPING	1129.83d	10/1/93	1/29/98						
1.1.12.1.1.11	Funding-10/1/93	0d	10/1/93	10/1/93						
1.1.12.1.1.11	Funding-10/1/96	0d	10/1/96	10/1/96						
1.1.12.1.1.11	Install RF Cavities	0d	12/22/97	12/22/97						
1.1.12.10.1.2	BML-HEAT EXCHANGER	334.38d	9/3/96	12/15/97						
1.1.12.10.1.2	North Hatch Bldg. Beneficial Occupancy	0d	12/25/96	12/25/96						
1.1.12.10.1.3	BML-LCW PROCESSING	235.88d	10/1/96	8/26/97						
1.1.12.10.1.3	Funding-10/1/96	0d	10/1/96	10/1/96						
1.1.12.10.1.4	BML-LCW PUMP	202d	10/1/96	7/9/97						
1.1.12.10.1.5	BML-LCW PIPING	452.63d	3/1/96	11/26/97						
1.1.12.10.1.5	8 Gev-150 Gev Encl. Initial Occupancy	0d	3/1/96	3/1/96						
1.1.12.14	UTILITIES & ABORT EDI&A (Satli)	1325.64d	10/1/92	10/30/97						

Project: FORECAST/wbs 1.1.12 L
Date: 9/19/94

Critical 
Noncritical 

Progress 
Milestone 

Summary 
Rolled Up 

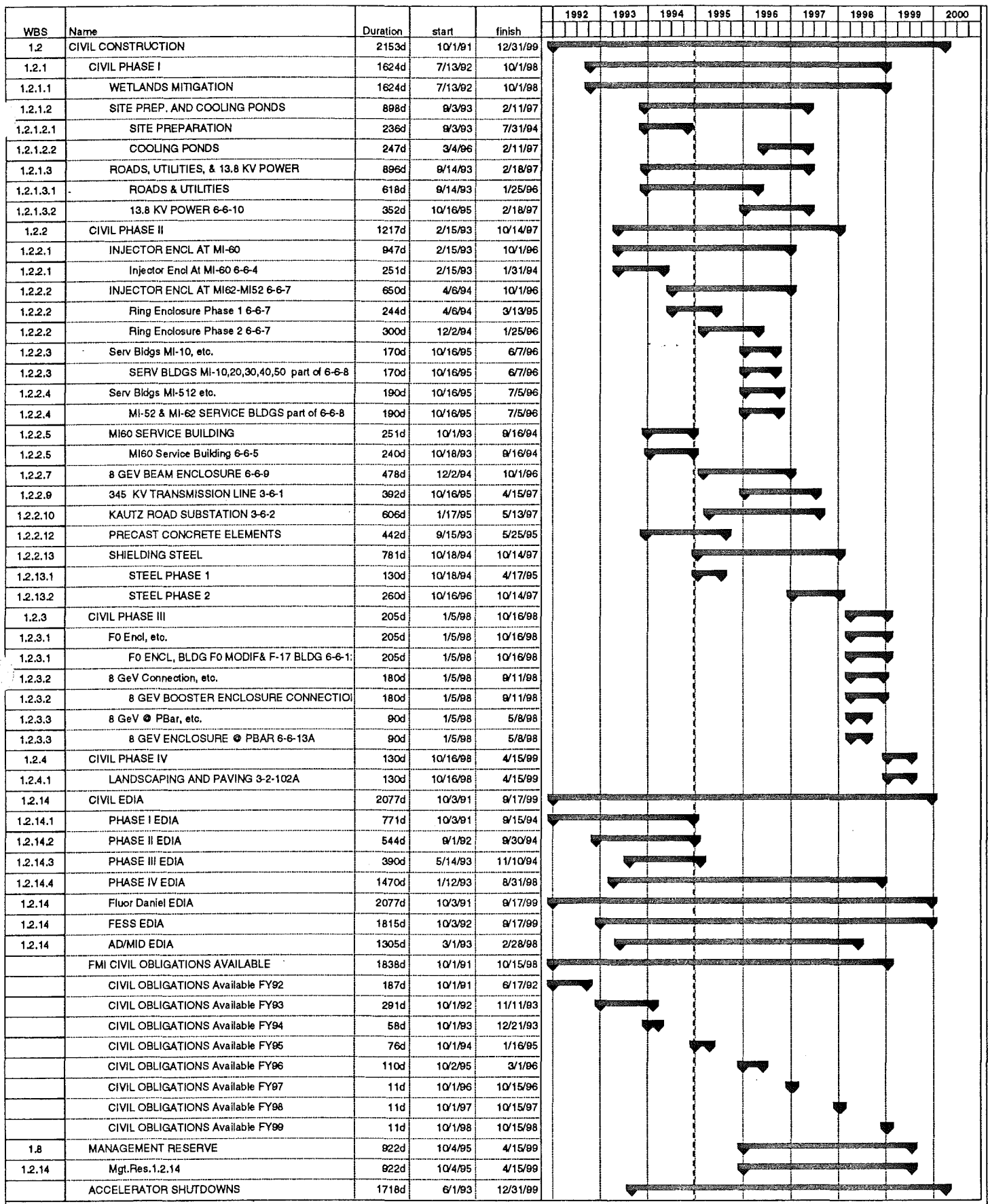
WBS	Name	Duration	start	finish	1993	1994	1995	1996	1997	1998	19
	Total \$	1559.5d	10/1/92	9/23/98							
1.1.13.1.1.1	INST MIR MAGNET STANDS	585.69d	11/10/94	2/6/97							
1.1.13.1.1.2	INSTALL MIR MAGNETS	983.72d	11/17/94	8/25/98							
1.1.13.1.1.3	ALIGN MIR MAGNETS	560d	1/19/95	3/12/97							
1.1.13.1.1.4	OLD MR MAGNET REMOVAL	659.96d	9/29/95	4/9/98							
1.1.13.1.2.1	MIR POWER SUPPLIES	311.13d	4/11/97	6/22/98							
1.1.13.1.2.2	MIR MAGNET BUS INSTALLATION	740d	1/5/95	11/6/97							
1.1.13.1.2.3	MIR HARMONIC FILTER	355.5d	1/19/96	5/30/97							
1.1.13.1.4	MIR INSTRUMENTATION INSTALL'N	424.38d	7/8/96	2/20/98							
1.1.13.1.6.1	ABORT STAND INSTALLATION	251.88d	7/10/95	6/25/96							
1.1.13.1.6.2	ABORT MAGNET INSTALLATION	263.75d	9/30/96	10/2/97							
1.1.13.1.8	MIR SAFETY SYSTEM INSTALL'N	611.67d	1/26/96	6/1/98							
1.1.13.2.1.1	8 GeV LINE MAG STAND INSTALL'N	343.66d	10/26/95	2/18/97							
1.1.13.2.1.2	8 GeV LINE MAGNET INSTALL'N	97.5d	2/20/98	7/7/98							
1.1.13.2.1.3	8 GeV LINE ALIGNMENT	693.33d	9/29/95	5/27/98							
1.1.13.2.4	8 GeV LINE INSTR INSTALL'N	54.72d	4/17/98	7/2/98							
1.1.13.3.1.1	150 GeV LINE MAG STAND INSTALL'N	425d	1/9/97	8/26/98							
1.1.13.3.1.2	150 GeV LINE MAG INSTALL'N	19.5d	8/27/98	9/23/98							
1.1.13.6.1.1	SLOW SPILL MAGNET STANDS	265.75d	3/17/97	3/23/98							
1.1.13.6.1.2	SLOW SPILL MAGNET INSTALL'N	43.39d	2/20/98	4/22/98							
1.1.13.7.2.1	F0 COMPONENT REMOVAL	151.67d	1/30/98	8/31/98							
1.1.13.7.2.3	F0 TEV REINSTALLATION	568.38d	7/8/96	9/10/98							
1.1.13.10.2.1	BML POWER SUPPLY INSTALL'N	570.56d	7/8/96	9/14/98							
1.1.13.10.2.2	BML MAGNET BUS INSTALL'N	423.79d	1/3/97	8/20/98							
1.1.13.10.8	BML SAFETY SYSTEM INSTALL'N	571.08d	5/14/96	7/22/98							
	Dummy Entries	1d	10/1/92	10/1/92							
	Dummy_Sauer-13.1.3	1d	10/1/92	10/1/92							
	Dummy_Sauer-13.2.3	1d	10/1/92	10/1/92							
	Dummy_Sauer-13.3.3	1d	10/1/92	10/1/92							
	Dummy_Sauer-13.6.3	1d	10/1/92	10/1/92							
	Dummy_Sauer-13.7.1	1d	10/1/92	10/1/92							
	Dummy_Sauer-13.7.2.2	1d	10/1/92	10/1/92							
1.1.13.14	INSTALLATION EDI&A (FL Portion)	1498.72d	10/1/92	6/30/98							

Project: FORECAST/wbs 1.1.13.14
Date: 9/19/94

Critical 
Noncritical 

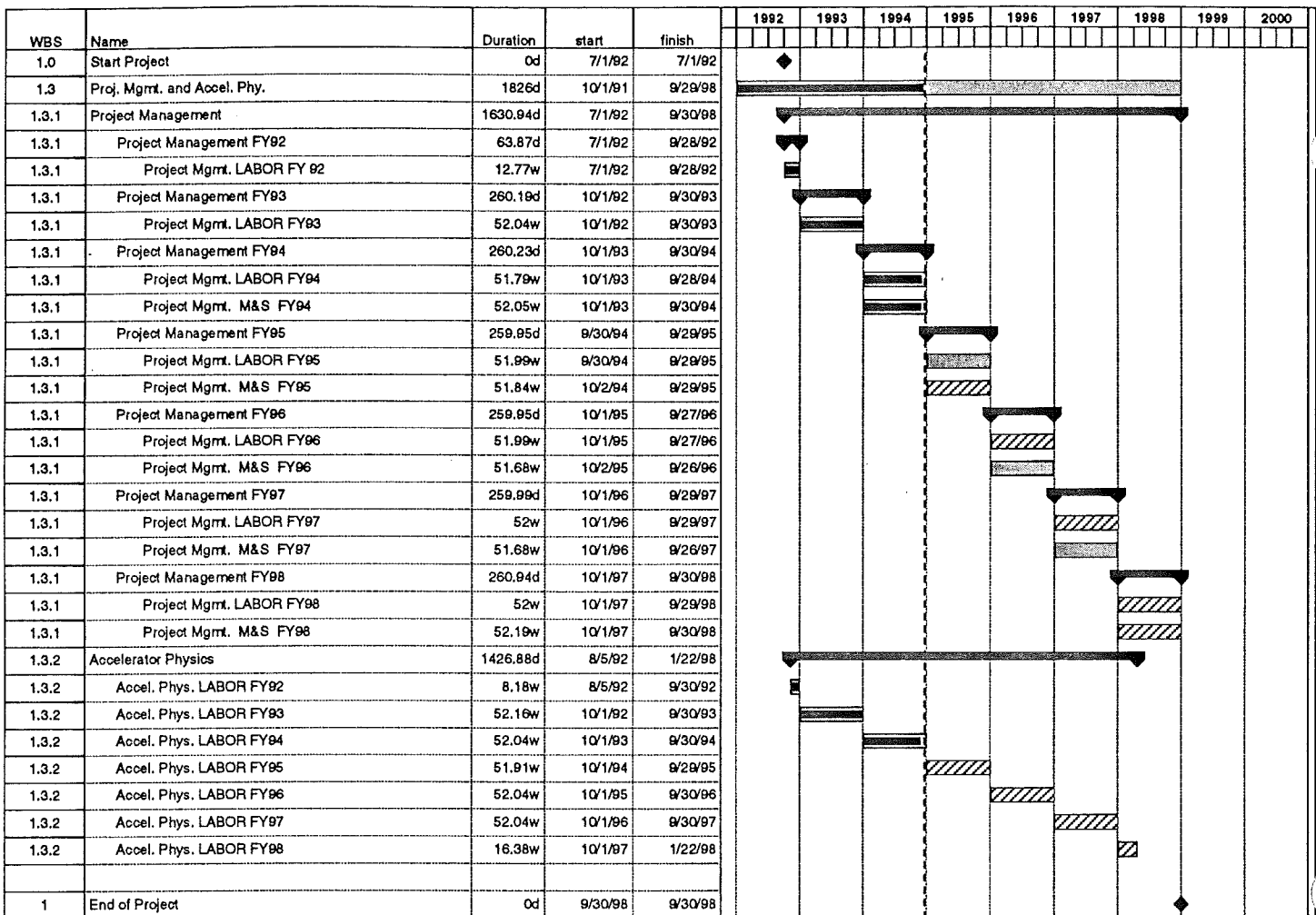
Progress 
Milestone 

Summary 
Rolled Up 



Project: FORECAST/wbs 1.2 CIVI
Date: 9/19/94

Critical Progress Summary
Noncritical Milestone Rolled Up



Project: FORECAST/wbs 1.3 Proj
Date: 9/19/94

Critical  Progress  Summary 
 Noncritical  Milestone  Rolled Up 

LATTICE FILES

1

Linear lattice functions for beam line: MI_19
 delta(p)/p = 0.000000 symm = F

"MAD" Version: 8.17

Run: 09/09/94 15.47.38

Range: #S/#E

page 1

ELEMENT SEQUENCE			H O R I Z O N T A L								V E R T I C A L								
pos.	element	occ.	dist I	betax	alfax	mux	x(co)	px(co)	Dx	Dpx	I	betay	alfay	muy	y(co)	py(co)	Dy	Dpy	
no.	name	no.	[m]	I	[m]	[1]	[2pi]	[mm]	[.001]	[m]	[1]	I	[m]	[1]	[2pi]	[mm]	[.001]	[m]	[1]
begin	MI_19	1	0.000		9.783	0.027	0.000	0.000	0.000	0.054	0.000		62.329	0.040	0.000	0.000	0.000	0.000	
11	CAV	1	3.728		13.855	-0.833	0.053	0.000	0.000	0.061	0.002		46.743	2.228	0.011	0.000	0.000	0.000	
19	CAV	2	6.550		19.531	-1.178	0.080	0.000	0.000	0.067	0.002		35.180	1.868	0.022	0.000	0.000	0.000	
27	CAV	3	9.373		27.156	-1.523	0.100	0.000	0.000	0.073	0.002		25.650	1.508	0.037	0.000	0.000	0.000	
35	CAV	4	12.195		36.729	-1.868	0.114	0.000	0.000	0.079	0.002		18.155	1.148	0.058	0.000	0.000	0.000	
43	CAV	5	15.018		48.249	-2.213	0.125	0.000	0.000	0.086	0.002		12.693	0.787	0.088	0.000	0.000	0.000	
52	HC606	1	16.076		53.068	-2.343	0.128	0.000	0.000	0.088	0.002		11.170	0.652	0.102	0.000	0.000	0.000	
57	M_606	1	17.289		56.344	-0.029	0.132	0.000	0.000	0.088-0.002		10.248	0.065	0.120	0.000	0.000	0.000	0.000	
68	CAV	6	23.486		33.278	1.706	0.154	0.000	0.000	0.057-0.005		18.798	-1.087	0.195	0.000	0.000	0.000	0.000	
76	CAV	7	26.309		24.585	1.374	0.170	0.000	0.000	0.042-0.005		25.861	-1.415	0.216	0.000	0.000	0.000	0.000	
84	CAV	8	29.131		17.764	1.043	0.191	0.000	0.000	0.027-0.005		34.775	-1.743	0.231	0.000	0.000	0.000	0.000	
92	CAV	9	31.954		12.814	0.711	0.221	0.000	0.000	0.011-0.005		45.538	-2.070	0.242	0.000	0.000	0.000	0.000	
101	VC607	1	33.364		11.042	0.545	0.240	0.000	0.000	0.004-0.005		51.611	-2.234	0.247	0.000	0.000	0.000	0.000	
106	M_607	1	34.577		10.357	-0.025	0.258	0.000	0.000	-0.003-0.005		54.742	-0.035	0.250	0.000	0.000	0.000	0.000	
115	HC608	1	36.192		11.674	-0.650	0.282	0.000	0.000	-0.012-0.006		50.045	2.127	0.255	0.000	0.000	0.000	0.000	
123	M_608	1	51.866		59.288	0.030	0.381	0.000	0.000	-0.098-0.001		10.987	-0.067	0.375	0.000	0.000	0.000	0.000	
136	VC609	1	67.954		10.524	0.579	0.490	0.000	0.000	-0.056	0.003		59.260	-2.500	0.486	0.000	0.000	0.000	
141	M_609	1	69.155		9.756	0.023	0.509	0.000	0.000	-0.054	0.000		62.618	0.034	0.489	0.000	0.000	0.000	
152	DIPOLE_C	1	75.458		21.197	-1.424	0.584	0.000	0.000	-0.097-0.017		29.253	2.364	0.512	0.000	0.000	0.000	0.000	
164	DIPOLE_D	1	79.881		36.588	-2.056	0.609	0.000	0.000	-0.199-0.031		12.744	1.368	0.549	0.000	0.000	0.000	0.000	
176	HC610	1	80.528		39.304	-2.148	0.612	0.000	0.000	-0.219-0.031		11.069	1.223	0.557	0.000	0.000	0.000	0.000	
181	M_610	1	82.121		42.741	0.243	0.618	0.000	0.000	-0.257-0.016		8.524	0.379	0.584	0.000	0.000	0.000	0.000	
192	DIPOLE_C	2	88.424		18.269	1.615	0.653	0.000	0.000	-0.299-0.014		14.332	-0.925	0.685	0.000	0.000	0.000	0.000	
204	DIPOLE_D	2	92.848		7.848	0.741	0.713	0.000	0.000	-0.391-0.028		25.050	-1.497	0.722	0.000	0.000	0.000	0.000	
216	VC611	1	93.494		6.972	0.614	0.727	0.000	0.000	-0.409-0.028		27.040	-1.581	0.726	0.000	0.000	0.000	0.000	
221	M_611	1	95.087		6.033	-0.035	0.767	0.000	0.000	-0.472-0.054		29.844	0.000	0.735	0.000	0.000	0.000	0.000	
232	DIPOLE_C	3	101.391		18.348	-1.668	0.874	0.000	0.000	-1.007-0.098		15.021	0.972	0.781	0.000	0.000	0.000	0.000	
244	DIPOLE_D	3	105.814		37.132	-2.579	0.901	0.000	0.000	-1.468-0.112		8.955	0.400	0.844	0.000	0.000	0.000	0.000	
256	HC612	1	106.461		40.552	-2.712	0.904	0.000	0.000	-1.540-0.112		8.493	0.316	0.855	0.000	0.000	0.000	0.000	
261	M_612	1	108.054		45.728	-0.241	0.909	0.000	0.000	-1.648-0.016		8.531	-0.379	0.886	0.000	0.000	0.000	0.000	
272	DIPOLE_C	4	114.357		23.518	1.603	0.939	0.000	0.000	-1.232	0.068		27.592	-2.283	0.956	0.000	0.000	0.000	
284	DIPOLE_D	4	118.781		12.305	0.932	0.981	0.000	0.000	-0.960	0.054		52.184	-3.276	0.975	0.000	0.000	0.000	
296	VC613	1	119.427		11.165	0.834	0.990	0.000	0.000	-0.925	0.054		56.513	-3.421	0.976	0.000	0.000	0.000	
301	M_613	1	121.020		9.732	0.047	1.014	0.000	0.000	-0.877	0.002		62.621	-0.033	0.981	0.000	0.000	0.000	
311	S613	1	122.783		10.927	-0.570	1.042	0.000	0.000	-0.919-0.035		56.486	2.432	0.985	0.000	0.000	0.000	0.000	
320	DIPOLE_A	1	129.485		24.009	-1.382	1.110	0.000	0.000	-1.219-0.056		29.365	1.614	1.012	0.000	0.000	0.000	0.000	
332	DIPOLE_B	1	135.940		46.906	-2.165	1.141	0.000	0.000	-1.644-0.077		13.637	0.822	1.064	0.000	0.000	0.000	0.000	
344	HC614	1	137.077		51.984	-2.303	1.144	0.000	0.000	-1.731-0.077		11.927	0.683	1.078	0.000	0.000	0.000	0.000	
349	M_614	1	138.309		55.302	-0.035	1.148	0.000	0.000	-1.785-0.001		10.936	0.069	1.095	0.000	0.000	0.000	0.000	
355	S614	1	139.976		50.220	2.189	1.153	0.000	0.000	-1.700	0.076		12.054	-0.577	1.119	0.000	0.000	0.000	
359	O614	1	140.218		49.167	2.161	1.154	0.000	0.000	-1.681	0.076		12.340	-0.604	1.122	0.000	0.000	0.000	
369	DIPOLE_A	2	146.773		25.790	1.405	1.183	0.000	0.000	-1.249	0.055		25.006	-1.328	1.183	0.000	0.000	0.000	
381	DIPOLE_B	2	153.229		12.454	0.661	1.242	0.000	0.000	-0.958	0.034		46.735	-2.038	1.213	0.000	0.000	0.000	
396	VC615	1	154.397		11.067	0.526	1.258	0.000	0.000	-0.918	0.034		51.646	-2.166	1.217	0.000	0.000	0.000	

401 M_615	1	155.597	10.439	-0.045	1.276	0.000	0.000	-0.898-0.004	54.548	0.037	1.221	0.000	0.000	0.000	0.000
412 DIPOLE_C	5	161.901	23.304	-1.553	1.345	0.000	0.000	-1.248-0.071	25.586	2.036	1.247	0.000	0.000	0.000	0.000
424 DIPOLE_D	5	166.324	39.911	-2.201	1.368	0.000	0.000	-1.591-0.085	11.507	1.147	1.288	0.000	0.000	0.000	0.000

1
Linear lattice functions for beam line: MI_19
delta(p)/p = 0.000000 symm = F

"MAD" Version: 8.17 Run: 09/09/94 15.47.38
Range: #S/#E

page 2

ELEMENT SEQUENCE			H O R I Z O N T A L								V E R T I C A L								
pos.	element	occ.	dist I	betax	alfax	mux	x(co)	px(co)	Dx	Dpx	I	betay	alfay	muy	y(co)	py(co)	Dy	Dpy	
no.	name	no.	[m]	I	[m]	[1]	[2pi]	[mm]	[.001]	[m]	[1]	I	[m]	[1]	[2pi]	[mm]	[.001]	[m]	[1]
436	HC616	1	166.970		42.817	-2.296	1.370	0.000	0.000	-1.646-0.085	10.109	1.017	1.298	0.000	0.000	0.000	0.000	0.000	
441	M_616	1	168.563		46.406	0.314	1.376	0.000	0.000	-1.707 0.016	8.110	0.235	1.326	0.000	0.000	0.000	0.000	0.000	
452	DIPOLE_C	6	174.867		19.304	1.786	1.408	0.000	0.000	-1.080 0.102	15.939	-1.122	1.424	0.000	0.000	0.000	0.000	0.000	
464	DIPOLE_D	6	179.290		7.749	0.826	1.467	0.000	0.000	-0.659 0.088	28.640	-1.748	1.457	0.000	0.000	0.000	0.000	0.000	
476	VC617	1	179.937		6.772	0.686	1.481	0.000	0.000	-0.603 0.088	30.959	-1.840	1.460	0.000	0.000	0.000	0.000	0.000	
481	M_617	1	181.530		5.623	0.030	1.524	0.000	0.000	-0.487 0.056	34.244	-0.015	1.468	0.000	0.000	0.000	0.000	0.000	
492	DIPOLE_C	7	187.833		17.014	-1.603	1.640	0.000	0.000	-0.306 0.016	17.016	1.164	1.509	0.000	0.000	0.000	0.000	0.000	
504	DIPOLE_D	7	192.257		35.295	-2.530	1.669	0.000	0.000	-0.263 0.002	9.423	0.552	1.565	0.000	0.000	0.000	0.000	0.000	
516	HC618	1	192.903		38.653	-2.666	1.672	0.000	0.000	-0.262 0.002	8.767	0.463	1.577	0.000	0.000	0.000	0.000	0.000	
521	M_618	1	194.496		43.862	-0.316	1.678	0.000	0.000	-0.247 0.018	8.356	-0.236	1.607	0.000	0.000	0.000	0.000	0.000	
532	DIPOLE_C	8	200.800		23.351	1.497	1.708	0.000	0.000	-0.088 0.017	24.448	-1.960	1.683	0.000	0.000	0.000	0.000	0.000	
544	DIPOLE_D	8	205.223		12.824	0.883	1.749	0.000	0.000	-0.039 0.003	45.653	-2.833	1.704	0.000	0.000	0.000	0.000	0.000	
556	VC619	1	205.869		11.741	0.793	1.758	0.000	0.000	-0.037 0.003	49.398	-2.961	1.706	0.000	0.000	0.000	0.000	0.000	
561	M_619	1	207.463		10.460	-0.015	1.781	0.000	0.000	-0.033 0.001	54.651	-0.007	1.711	0.000	0.000	0.000	0.000	0.000	
572	HC620	1	209.177		11.877	-0.654	1.806	0.000	0.000	-0.032 0.000	49.444	2.140	1.716	0.000	0.000	0.000	0.000	0.000	
580	M_620	1	224.751		58.697	0.040	1.904	0.000	0.000	-0.031 0.001	10.645	-0.067	1.838	0.000	0.000	0.000	0.000	0.000	
592	VC621	1	240.827		10.414	0.566	2.014	0.000	0.000	0.012 0.003	59.019	-2.523	1.952	0.000	0.000	0.000	0.000	0.000	
597	M_621	1	242.040		9.662	0.013	2.033	0.000	0.000	0.015 0.003	62.512	-0.002	1.955	0.000	0.000	0.000	0.000	0.000	
610	HC622	1	258.128		53.874	-2.389	2.161	0.000	0.000	0.079 0.004	11.611	0.668	2.054	0.000	0.000	0.000	0.000	0.000	
615	M_622	1	259.329		57.160	-0.037	2.165	0.000	0.000	0.082 0.000	10.682	0.066	2.072	0.000	0.000	0.000	0.000	0.000	
626	DIPOLE_C	9	265.632		26.838	2.145	2.189	0.000	0.000	0.030-0.018	21.922	-1.384	2.142	0.000	0.000	0.000	0.000	0.000	
638	DIPOLE_D	9	270.056		11.946	1.222	2.229	0.000	0.000	-0.079-0.032	36.765	-1.971	2.167	0.000	0.000	0.000	0.000	0.000	
650	VC623	1	270.702		10.454	1.087	2.238	0.000	0.000	-0.100-0.032	39.368	-2.057	2.169	0.000	0.000	0.000	0.000	0.000	
655	M_623	1	272.295		8.252	0.295	2.266	0.000	0.000	-0.156-0.040	42.581	0.283	2.176	0.000	0.000	0.000	0.000	0.000	
666	DIPOLE_C	10	278.599		15.075	-1.024	2.366	0.000	0.000	-0.495-0.065	18.262	1.602	2.210	0.000	0.000	0.000	0.000	0.000	
678	DIPOLE_D	10	283.022		26.789	-1.624	2.401	0.000	0.000	-0.809-0.078	7.907	0.738	2.270	0.000	0.000	0.000	0.000	0.000	
690	HC624	1	283.668		28.945	-1.712	2.405	0.000	0.000	-0.860-0.078	7.034	0.612	2.284	0.000	0.000	0.000	0.000	0.000	
695	M_624	1	285.261		31.942	0.027	2.413	0.000	0.000	-0.945-0.024	6.111	-0.045	2.324	0.000	0.000	0.000	0.000	0.000	
706	DIPOLE_C	11	291.565		15.389	1.088	2.457	0.000	0.000	-0.809 0.019	18.709	-1.693	2.429	0.000	0.000	0.000	0.000	0.000	
718	DIPOLE_D	11	295.988		8.541	0.460	2.520	0.000	0.000	-0.755 0.005	37.729	-2.606	2.455	0.000	0.000	0.000	0.000	0.000	
730	VC625	1	296.635		8.006	0.369	2.533	0.000	0.000	-0.752 0.005	41.183	-2.739	2.458	0.000	0.000	0.000	0.000	0.000	
735	M_625	1	298.228		7.840	-0.296	2.565	0.000	0.000	-0.777-0.039	46.473	-0.286	2.464	0.000	0.000	0.000	0.000	0.000	
746	DIPOLE_C	12	304.531		24.916	-2.088	2.643	0.000	0.000	-1.319-0.101	24.684	1.595	2.492	0.000	0.000	0.000	0.000	0.000	
758	DIPOLE_D	12	308.955		47.591	-3.039	2.663	0.000	0.000	-1.794-0.115	13.378	0.961	2.532	0.000	0.000	0.000	0.000	0.000	
770	HC626	1	309.601		51.608	-3.178	2.665	0.000	0.000	-1.868-0.115	12.196	0.868	2.540	0.000	0.000	0.000	0.000	0.000	
775	M_626	1	311.194		57.265	-0.017	2.670	0.000	0.000	-1.967 0.000	10.738	0.023	2.562	0.000	0.000	0.000	0.000	0.000	
785	S626	1	312.938		51.585	2.280	2.675	0.000	0.000	-1.864 0.085	12.100	-0.633	2.587	0.000	0.000	0.000	0.000	0.000	
789	O626	1	313.180		50.488	2.251	2.676	0.000	0.000	-1.843 0.085	12.413	-0.661	2.590	0.000	0.000	0.000	0.000	0.000	
798	DIPOLE_A	3	319.659		26.366	1.472	2.704	0.000	0.000	-1.359 0.064	25.825	-1.409	2.649	0.000	0.000	0.000	0.000	0.000	
810	DIPOLE_B	3	326.114		12.363	0.697	2.762	0.000	0.000	-1.010 0.043	48.816	-2.152	2.678	0.000	0.000	0.000	0.000	0.000	
822	VC627	1	327.251		10.935	0.560	2.778	0.000	0.000	-0.962 0.043	53.857	-2.283	2.682	0.000	0.000	0.000	0.000	0.000	

827	M_627	1	328.483	10.194	-0.009	2.797	0.000	0.000	-0.930	0.003	57.089	0.016	2.685	0.000	0.000	0.000	0.000
833	S627	1	330.150	11.511	-0.634	2.822	0.000	0.000	-0.969	-0.036	51.790	2.260	2.690	0.000	0.000	0.000	0.000
843	DIPOLE_A	4	336.947	25.747	-1.461	2.886	0.000	0.000	-1.277	-0.057	26.503	1.460	2.719	0.000	0.000	0.000	0.000
855	DIPOLE_B	4	343.403	49.682	-2.247	2.915	0.000	0.000	-1.708	-0.078	12.569	0.698	2.777	0.000	0.000	0.000	0.000
867	QC628	1	344.123	52.984	-2.335	2.917	0.000	0.000	-1.764	-0.078	11.624	0.613	2.786	0.000	0.000	0.000	0.000
871	HC628	1	344.539	54.947	-2.385	2.919	0.000	0.000	-1.796	-0.078	11.135	0.563	2.792	0.000	0.000	0.000	0.000

1

Linear lattice functions for beam line: MI_19

delta(p)/p = 0.000000 symm = F

"MAD" Version: 8.17

Run: 09/09/94 15.47.38

Range: #S/#E

page

3

ELEMENT SEQUENCE			H O R I Z O N T A L										V E R T I C A L						
pos.	element	occ.	dist	I	betax	alfax	mux	x(co)	px(co)	Dx	Dpx	I	betay	alfay	muy	y(co)	py(co)	Dy	Dpy
no.	name	no.	[m]	I	[m]	[1]	[2pi]	[mm]	[.001]	[m]	[1]	I	[m]	[1]	[2pi]	[mm]	[.001]	[m]	[1]
876	M_628	1	345.771		58.329	0.014	2.922	0.000	0.000	-1.850	0.001		10.403	-0.022	2.811	0.000	0.000	0.000	0.000
882	S628	1	347.439		52.804	2.356	2.927	0.000	0.000	-1.758	0.080		11.802	-0.665	2.835	0.000	0.000	0.000	0.000
886	O628	1	347.681		51.671	2.326	2.927	0.000	0.000	-1.738	0.080		12.131	-0.694	2.838	0.000	0.000	0.000	0.000
896	DIPOLE_A	5	354.236		26.509	1.513	2.956	0.000	0.000	-1.275	0.060		26.475	-1.493	2.898	0.000	0.000	0.000	0.000
908	DIPOLE_B	5	360.691		12.147	0.712	3.014	0.000	0.000	-0.954	0.039		50.824	-2.278	2.926	0.000	0.000	0.000	0.000
920	VC629	1	361.828		10.689	0.571	3.030	0.000	0.000	-0.910	0.039		56.158	-2.416	2.929	0.000	0.000	0.000	0.000
925	M_629	1	363.060		9.916	0.008	3.050	0.000	0.000	-0.883	0.001		59.616	-0.017	2.933	0.000	0.000	0.000	0.000
931	S629	1	364.727		11.151	-0.606	3.075	0.000	0.000	-0.923	-0.036		54.184	2.333	2.937	0.000	0.000	0.000	0.000
941	DIPOLE_A	6	371.524		25.048	-1.439	3.142	0.000	0.000	-1.233	-0.057		27.945	1.527	2.965	0.000	0.000	0.000	0.000
953	DIPOLE_B	6	377.979		48.734	-2.230	3.171	0.000	0.000	-1.665	-0.078		13.193	0.758	3.020	0.000	0.000	0.000	0.000
965	QC630	1	378.700		52.013	-2.319	3.174	0.000	0.000	-1.721	-0.078		12.162	0.672	3.029	0.000	0.000	0.000	0.000
969	HC630	1	379.116		53.963	-2.370	3.175	0.000	0.000	-1.754	-0.078		11.624	0.622	3.034	0.000	0.000	0.000	0.000
974	M_630	1	380.348		57.353	-0.014	3.178	0.000	0.000	-1.809	-0.001		10.767	0.021	3.052	0.000	0.000	0.000	0.000
980	S630	1	382.016		52.010	2.292	3.183	0.000	0.000	-1.722	0.077		12.043	-0.627	3.076	0.000	0.000	0.000	0.000
984	O630	1	382.258		50.908	2.263	3.184	0.000	0.000	-1.704	0.077		12.354	-0.655	3.079	0.000	0.000	0.000	0.000
994	DIPOLE_A	7	388.812		26.411	1.475	3.213	0.000	0.000	-1.265	0.056		25.907	-1.412	3.139	0.000	0.000	0.000	0.000
1006	DIPOLE_B	7	395.268		12.381	0.699	3.271	0.000	0.000	-0.968	0.035		48.937	-2.155	3.168	0.000	0.000	0.000	0.000
1023	VC631	1	396.424		10.926	0.560	3.287	0.000	0.000	-0.928	0.035		54.071	-2.288	3.171	0.000	0.000	0.000	0.000
1028	M_631	1	397.636		10.203	-0.008	3.305	0.000	0.000	-0.906	-0.003		57.217	0.019	3.175	0.000	0.000	0.000	0.000
1037	S631	1	399.401		11.639	-0.644	3.331	0.000	0.000	-0.959	-0.042		51.458	2.256	3.180	0.000	0.000	0.000	0.000
1047	DIPOLE_A	8	406.101		25.722	-1.458	3.395	0.000	0.000	-1.304	-0.063		26.527	1.465	3.209	0.000	0.000	0.000	0.000
1059	DIPOLE_B	8	412.556		49.611	-2.243	3.423	0.000	0.000	-1.773	-0.084		12.550	0.700	3.266	0.000	0.000	0.000	0.000
1071	QC632	1	413.277		52.907	-2.330	3.426	0.000	0.000	-1.834	-0.084		11.602	0.614	3.276	0.000	0.000	0.000	0.000
1075	HC632	1	413.693		54.867	-2.381	3.427	0.000	0.000	-1.869	-0.084		11.112	0.565	3.282	0.000	0.000	0.000	0.000
1080	M_632	1	414.925		58.242	0.015	3.430	0.000	0.000	-1.928	-0.001		10.376	-0.019	3.300	0.000	0.000	0.000	0.000
1086	S632	1	416.592		52.723	2.353	3.435	0.000	0.000	-1.837	0.081		11.764	-0.661	3.325	0.000	0.000	0.000	0.000
1090	O632	1	416.835		51.591	2.323	3.436	0.000	0.000	-1.817	0.081		12.092	-0.691	3.328	0.000	0.000	0.000	0.000
1100	DIPOLE_A	9	423.389		26.464	1.510	3.464	0.000	0.000	-1.349	0.060		26.390	-1.490	3.388	0.000	0.000	0.000	0.000
1112	DIPOLE_B	9	429.845		12.130	0.710	3.523	0.000	0.000	-1.024	0.039		50.695	-2.274	3.416	0.000	0.000	0.000	0.000
1124	VC633	1	430.981		10.677	0.569	3.539	0.000	0.000	-0.979	0.039		56.022	-2.413	3.419	0.000	0.000	0.000	0.000
1129	M_633	1	432.213		9.908	0.007	3.558	0.000	0.000	-0.952	-0.001		59.479	-0.020	3.423	0.000	0.000	0.000	0.000
1135	S633	1	433.881		11.147	-0.607	3.584	0.000	0.000	-0.999	-0.041		54.067	2.325	3.427	0.000	0.000	0.000	0.000
1145	DIPOLE_A	10	440.678		25.075	-1.442	3.650	0.000	0.000	-1.345	-0.062		27.914	1.522	3.455	0.000	0.000	0.000	0.000
1157	DIPOLE_B	10	447.133		48.807	-2.235	3.680	0.000	0.000	-1.810	-0.083		13.209	0.756	3.510	0.000	0.000	0.000	0.000
1169	QC634	1	447.854		52.092	-2.323	3.682	0.000	0.000	-1.870	-0.083		12.182	0.670	3.519	0.000	0.000	0.000	0.000
1173	HC634	1	448.270		54.046	-2.374	3.683	0.000	0.000	-1.905	-0.083		11.645	0.621	3.525	0.000	0.000	0.000	0.000
1178	M_634	1	449.502		57.443	-0.015	3.687	0.000	0.000	-1.963	0.001		10.793	0.018	3.542	0.000	0.000	0.000	0.000
1184	S634	1	451.169		52.094	2.295	3.692	0.000	0.000	-1.866	0.085		12.080	-0.631	3.566	0.000	0.000	0.000	0.000

1188	O634	1	451.411	50.990	2.266	3.692	0.000	0.000	-1.846	0.085	12.392	-0.659	3.569	0.000	0.000	0.000	0.000
1198	DIPOLE_A	11	457.966	26.457	1.477	3.721	0.000	0.000	-1.355	0.064	25.994	-1.416	3.629	0.000	0.000	0.000	0.000
1210	DIPOLE_B	11	464.422	12.397	0.701	3.779	0.000	0.000	-1.007	0.043	49.072	-2.158	3.657	0.000	0.000	0.000	0.000
1222	SQ635	1	465.139	11.454	0.615	3.789	0.000	0.000	-0.976	0.043	52.229	-2.241	3.660	0.000	0.000	0.000	0.000
1226	VC635	1	465.558	10.960	0.564	3.795	0.000	0.000	-0.958	0.043	54.128	-2.289	3.661	0.000	0.000	0.000	0.000
1231	M_635	1	466.790	10.211	-0.006	3.813	0.000	0.000	-0.926	0.004	57.364	0.021	3.664	0.000	0.000	0.000	0.000
1237	S635	1	468.458	11.517	-0.631	3.838	0.000	0.000	-0.965	-0.036	52.023	2.275	3.669	0.000	0.000	0.000	0.000
1247	DIPOLE_A	12	475.255	25.693	-1.455	3.903	0.000	0.000	-1.271	-0.057	26.563	1.470	3.699	0.000	0.000	0.000	0.000
1259	DIPOLE_B	12	481.710	49.536	-2.239	3.932	0.000	0.000	-1.700	-0.077	12.536	0.703	3.756	0.000	0.000	0.000	0.000

1

Linear lattice functions for beam line: MI_19

delta(p)/p = 0.000000 symm = F

"MAD" Version: 8.17

Run: 09/09/94 15.47.38

Range: #S/#E

page 4

ELEMENT SEQUENCE			H O R I Z O N T A L										V E R T I C A L					
pos.	element	occ.	dist I	betax	alfax	mux	x(co)	px(co)	Dx	Dpx	I	betay	alfay	muy	y(co)	py(co)	Dy	Dpy
no.	name	no.	[m]	[m]	[1]	[2pi]	[mm]	[.001]	[m]	[1]	I	[m]	[1]	[2pi]	[mm]	[.001]	[m]	[1]
1271	SQ636	1	482.199	51.754	-2.298	3.933	0.000	0.000	-1.738	-0.077	11.877	0.644	3.762	0.000	0.000	0.000	0.000	
1275	SQ636	2	482.427	52.811	-2.326	3.934	0.000	0.000	-1.756	-0.077	11.589	0.617	3.766	0.000	0.000	0.000	0.000	
1279	HC636	1	482.847	54.782	-2.376	3.935	0.000	0.000	-1.788	-0.077	11.093	0.567	3.771	0.000	0.000	0.000	0.000	
1284	M_636	1	484.078	58.149	0.015	3.939	0.000	0.000	-1.842	0.001	10.351	-0.017	3.790	0.000	0.000	0.000	0.000	
1290	S636	1	485.746	52.637	2.350	3.943	0.000	0.000	-1.750	0.080	11.729	-0.658	3.814	0.000	0.000	0.000	0.000	
1294	O636	1	485.988	51.507	2.320	3.944	0.000	0.000	-1.731	0.080	12.054	-0.687	3.818	0.000	0.000	0.000	0.000	
1304	DIPOLE_A	13	492.543	26.418	1.508	3.973	0.000	0.000	-1.270	0.059	26.302	-1.486	3.878	0.000	0.000	0.000	0.000	
1316	DIPOLE_B	13	498.998	12.115	0.708	4.031	0.000	0.000	-0.952	0.038	50.553	-2.270	3.906	0.000	0.000	0.000	0.000	
1328	SQ637	1	499.716	11.163	0.619	4.041	0.000	0.000	-0.925	0.038	53.873	-2.357	3.908	0.000	0.000	0.000	0.000	
1332	VC637	1	500.135	10.666	0.567	4.047	0.000	0.000	-0.909	0.038	55.871	-2.408	3.909	0.000	0.000	0.000	0.000	
1337	M_637	1	501.367	9.902	0.005	4.067	0.000	0.000	-0.882	0.001	59.323	-0.022	3.913	0.000	0.000	0.000	0.000	
1343	S637	1	503.035	11.146	-0.609	4.092	0.000	0.000	-0.923	-0.037	53.933	2.317	3.917	0.000	0.000	0.000	0.000	
1353	DIPOLE_A	14	509.831	25.105	-1.445	4.159	0.000	0.000	-1.235	-0.057	27.873	1.516	3.945	0.000	0.000	0.000	0.000	
1365	DIPOLE_B	14	516.287	48.884	-2.239	4.188	0.000	0.000	-1.669	-0.078	13.220	0.753	4.000	0.000	0.000	0.000	0.000	
1380	HC638	1	517.455	54.284	-2.383	4.192	0.000	0.000	-1.761	-0.078	11.623	0.615	4.015	0.000	0.000	0.000	0.000	
1385	M_638	1	518.655	57.534	-0.012	4.195	0.000	0.000	-1.813	-0.001	10.816	0.015	4.032	0.000	0.000	0.000	0.000	
1396	DIPOLE_C	13	524.959	26.800	2.168	4.220	0.000	0.000	-1.253	0.092	23.000	-1.477	4.100	0.000	0.000	0.000	0.000	
1408	DIPOLE_D	13	529.382	11.785	1.227	4.260	0.000	0.000	-0.875	0.078	38.768	-2.087	4.124	0.000	0.000	0.000	0.000	
1420	VC639	1	530.028	10.287	1.090	4.270	0.000	0.000	-0.825	0.078	41.524	-2.176	4.127	0.000	0.000	0.000	0.000	
1425	M_639	1	531.622	8.072	0.302	4.298	0.000	0.000	-0.734	0.033	44.928	0.296	4.132	0.000	0.000	0.000	0.000	
1436	DIPOLE_C	14	537.925	14.787	-1.021	4.400	0.000	0.000	-0.788	-0.023	19.199	1.705	4.165	0.000	0.000	0.000	0.000	
1448	DIPOLE_D	14	542.349	26.521	-1.632	4.436	0.000	0.000	-0.917	-0.037	8.097	0.805	4.223	0.000	0.000	0.000	0.000	
1460	HC640	1	542.995	28.688	-1.721	4.440	0.000	0.000	-0.941	-0.037	7.141	0.673	4.237	0.000	0.000	0.000	0.000	
1465	M_640	1	544.588	31.739	0.002	4.448	0.000	0.000	-0.958	0.020	6.042	0.008	4.276	0.000	0.000	0.000	0.000	
1476	DIPOLE_C	15	550.892	15.508	1.072	4.492	0.000	0.000	-0.549	0.062	17.731	-1.604	4.385	0.000	0.000	0.000	0.000	
1488	DIPOLE_D	15	555.315	8.739	0.459	4.554	0.000	0.000	-0.303	0.048	35.858	-2.494	4.413	0.000	0.000	0.000	0.000	
1500	VC641	1	555.961	8.203	0.369	4.566	0.000	0.000	-0.272	0.048	39.165	-2.624	4.416	0.000	0.000	0.000	0.000	
1505	M_641	1	557.555	8.044	-0.302	4.598	0.000	0.000	-0.206	0.034	44.263	-0.295	4.422	0.000	0.000	0.000	0.000	
1516	DIPOLE_C	16	563.858	25.242	-2.092	4.674	0.000	0.000	-0.079	0.010	23.781	1.499	4.452	0.000	0.000	0.000	0.000	
1528	DIPOLE_D	16	568.281	47.921	-3.035	4.694	0.000	0.000	-0.065	-0.004	13.189	0.896	4.492	0.000	0.000	0.000	0.000	
1540	HC100	1	568.928	51.932	-3.173	4.696	0.000	0.000	-0.067	-0.004	12.088	0.807	4.500	0.000	0.000	0.000	0.000	
1545	M_100	1	570.521	57.541	0.008	4.701	0.000	0.000	-0.071	0.000	10.807	-0.030	4.523	0.000	0.000	0.000	0.000	
1556	VC101	1	572.235	51.886	2.316	4.706	0.000	0.000	-0.068	0.003	12.331	-0.693	4.547	0.000	0.000	0.000	0.000	
1564	M_101	1	587.810	9.937	-0.005	4.829	0.000	0.000	-0.023	0.002	60.319	0.016	4.641	0.000	0.000	0.000	0.000	
1576	HC101	1	603.885	54.796	-2.402	4.954	0.000	0.000	-0.006	0.001	11.305	0.622	4.744	0.000	0.000	0.000	0.000	

1581	M_102	1	605.098	58.136	-0.012	4.957	0.000	0.000	-0.005	0.001	10.457	0.032	4.762	0.000	0.000	0.000	0.000
1593	VC103	1	621.174	10.927	0.574	5.064	0.000	0.000	0.018	0.001	53.403	-2.291	4.885	0.000	0.000	0.000	0.000
1598	M_103	1	622.387	10.172	0.006	5.083	0.000	0.000	0.020	0.002	56.590	-0.014	4.888	0.000	0.000	0.000	0.000
1611	HC104	1	638.475	54.285	-2.356	5.206	0.000	0.000	0.069	0.003	11.441	0.559	4.994	0.000	0.000	0.000	0.000
1616	M_104	1	639.676	57.469	0.015	5.209	0.000	0.000	0.072	0.000	10.758	-0.034	5.012	0.000	0.000	0.000	0.000
1627	DIPOLE_C	17	645.979	26.551	2.173	5.234	0.000	0.000	0.020	-0.018	23.765	-1.563	5.079	0.000	0.000	0.000	0.000
1639	DIPOLE_D	17	650.402	11.546	1.220	5.275	0.000	0.000	-0.088	-0.032	40.419	-2.202	5.102	0.000	0.000	0.000	0.000
1651	VC105	1	651.049	10.059	1.080	5.284	0.000	0.000	-0.109	-0.032	43.325	-2.295	5.104	0.000	0.000	0.000	0.000
1656	M_105	1	652.642	7.862	0.300	5.314	0.000	0.000	-0.165	-0.040	46.951	0.288	5.110	0.000	0.000	0.000	0.000
1667	DIPOLE_C	18	658.945	14.595	-1.031	5.418	0.000	0.000	-0.509	-0.065	20.156	1.788	5.141	0.000	0.000	0.000	0.000
1679	DIPOLE_D	18	663.369	26.484	-1.657	5.454	0.000	0.000	-0.826	-0.079	8.410	0.867	5.196	0.000	0.000	0.000	0.000
1691	HC106	1	664.015	28.684	-1.748	5.458	0.000	0.000	-0.878	-0.079	7.376	0.733	5.209	0.000	0.000	0.000	0.000

1

Linear lattice functions for beam line: MI_19

delta(p)/p = 0.000000 symm = F

"MAD" Version: 8.17

Run: 09/09/94 15.47.38

Range: #S/#E

page 5

ELEMENT SEQUENCE			I			H O R I Z O N T A L					I			V E R T I C A L					
pos.	element	occ.	dist	I	betax	alfax	mux	x(co)	px(co)	Dx	Dpx	I	betay	alfay	muy	y(co)	py(co)	Dy	Dpy
no.	name	no.	[m]	I	[m]	[1]	[2pi]	[mm]	[.001]	[m]	[1]	I	[m]	[1]	[2pi]	[mm]	[.001]	[m]	[1]
1696	M_106	1	665.608		31.824	-0.025	5.466	0.000	0.000	-0.964	-0.024		6.110	0.055	5.248	0.000	0.000	0.000	0.000
1707	DIPOLE_C	19	671.912		15.764	1.068	5.510	0.000	0.000	-0.820	0.020		16.961	-1.515	5.359	0.000	0.000	0.000	0.000
1719	DIPOLE_D	19	676.335		8.975	0.467	5.570	0.000	0.000	-0.760	0.006		34.158	-2.372	5.389	0.000	0.000	0.000	0.000
1731	VC107	1	676.982		8.428	0.379	5.582	0.000	0.000	-0.756	0.006		37.305	-2.498	5.392	0.000	0.000	0.000	0.000
1736	M_107	1	678.575		8.247	-0.299	5.613	0.000	0.000	-0.779	-0.038		42.163	-0.283	5.398	0.000	0.000	0.000	0.000
1747	DIPOLE_C	20	684.878		25.397	-2.079	5.688	0.000	0.000	-1.314	-0.100		22.755	1.414	5.429	0.000	0.000	0.000	0.000
1759	DIPOLE_D	20	689.302		47.887	-3.006	5.708	0.000	0.000	-1.785	-0.114		12.821	0.832	5.471	0.000	0.000	0.000	0.000
1771	HC108	1	689.948		51.859	-3.141	5.710	0.000	0.000	-1.858	-0.114		11.801	0.746	5.479	0.000	0.000	0.000	0.000
1776	M_108	1	691.541		57.371	0.035	5.715	0.000	0.000	-1.956	0.001		10.688	-0.077	5.502	0.000	0.000	0.000	0.000
1786	S108	1	693.285		51.511	2.329	5.720	0.000	0.000	-1.853	0.085		12.419	-0.748	5.527	0.000	0.000	0.000	0.000
1790	O108	1	693.527		50.390	2.299	5.721	0.000	0.000	-1.832	0.085		12.789	-0.778	5.530	0.000	0.000	0.000	0.000
1799	DIPOLE_A	15	700.006		25.841	1.491	5.749	0.000	0.000	-1.348	0.064		28.133	-1.590	5.585	0.000	0.000	0.000	0.000
1811	DIPOLE_B	15	706.461		11.791	0.686	5.810	0.000	0.000	-1.000	0.043		53.863	-2.395	5.612	0.000	0.000	0.000	0.000
1823	VC109	1	707.598		10.393	0.544	5.826	0.000	0.000	-0.951	0.043		59.470	-2.537	5.615	0.000	0.000	0.000	0.000
1828	M_109	1	708.830		9.677	-0.009	5.846	0.000	0.000	-0.919	0.004		63.076	0.005	5.618	0.000	0.000	0.000	0.000
1834	S109	1	710.497		10.958	-0.620	5.872	0.000	0.000	-0.957	-0.035		57.249	2.492	5.623	0.000	0.000	0.000	0.000
1844	DIPOLE_A	16	717.294		25.218	-1.478	5.939	0.000	0.000	-1.260	-0.056		29.177	1.638	5.649	0.000	0.000	0.000	0.000
1856	DIPOLE_B	16	723.749		49.567	-2.294	5.968	0.000	0.000	-1.685	-0.077		13.283	0.824	5.702	0.000	0.000	0.000	0.000
1868	HC110	1	724.886		54.944	-2.437	5.972	0.000	0.000	-1.772	-0.077		11.573	0.680	5.717	0.000	0.000	0.000	0.000
1873	M_110	1	726.118		58.457	-0.038	5.975	0.000	0.000	-1.825	0.001		10.577	0.078	5.735	0.000	0.000	0.000	0.000
1879	S110	1	727.786		53.084	2.317	5.980	0.000	0.000	-1.735	0.079		11.638	-0.557	5.759	0.000	0.000	0.000	0.000
1883	O110	1	728.028		51.969	2.288	5.981	0.000	0.000	-1.716	0.079		11.914	-0.584	5.763	0.000	0.000	0.000	0.000
1893	DIPOLE_A	17	734.583		27.135	1.501	6.008	0.000	0.000	-1.260	0.058		24.398	-1.320	5.825	0.000	0.000	0.000	0.000
1905	DIPOLE_B	17	741.038		12.749	0.727	6.065	0.000	0.000	-0.948	0.037		46.113	-2.043	5.856	0.000	0.000	0.000	0.000
1917	VC111	1	742.175		11.250	0.591	6.080	0.000	0.000	-0.905	0.037		50.901	-2.170	5.860	0.000	0.000	0.000	0.000
1922	M_111	1	743.406		10.446	0.011	6.098	0.000	0.000	-0.879	0.000		53.992	0.000	5.864	0.000	0.000	0.000	0.000
1928	S111	1	745.074		11.708	-0.617	6.123	0.000	0.000	-0.921	-0.037		49.033	2.121	5.869	0.000	0.000	0.000	0.000
1932	O111	1	745.316		12.013	-0.646	6.126	0.000	0.000	-0.930	-0.037		48.012	2.094	5.870	0.000	0.000	0.000	0.000
1942	DIPOLE_A	18	751.871		25.545	-1.419	6.187	0.000	0.000	-1.237	-0.058		25.367	1.360	5.900	0.000	0.000	0.000	0.000
1954	DIPOLE_B	18	758.326		48.777	-2.180	6.216	0.000	0.000	-1.675	-0.079		12.479	0.636	5.959	0.000	0.000	0.000	0.000
1966	HC112	1	759.463		53.886	-2.314	6.220	0.000	0.000	-1.765	-0.079		11.179	0.508	5.974	0.000	0.000	0.000	0.000
1971	M_112	1	760.695		57.141	0.038	6.223	0.000	0.000	-1.821	-0.001		10.582	-0.078	5.992	0.000	0.000	0.000	0.000

1977	S112	1	762.362	51.655	2.328	6.228	0.000	0.000	-1.734	0.077	12.195	-0.735	6.016	0.000	0.000	0.000	0.000
1981	O112	1	762.605	50.536	2.298	6.229	0.000	0.000	-1.716	0.077	12.559	-0.766	6.019	0.000	0.000	0.000	0.000
1991	DIPOLE_A	19	769.159	25.755	1.483	6.258	0.000	0.000	-1.276	0.056	28.022	-1.592	6.076	0.000	0.000	0.000	0.000
2003	DIPOLE_B	19	775.615	11.784	0.681	6.318	0.000	0.000	-0.979	0.035	53.822	-2.403	6.103	0.000	0.000	0.000	0.000
2020	VC113	1	776.770	10.375	0.538	6.335	0.000	0.000	-0.938	0.035	59.545	-2.549	6.106	0.000	0.000	0.000	0.000
2025	M_113	1	777.983	9.689	-0.013	6.354	0.000	0.000	-0.917	-0.004	63.078	-0.005	6.109	0.000	0.000	0.000	0.000
2034	S113	1	779.748	11.107	-0.637	6.382	0.000	0.000	-0.971	-0.043	56.801	2.471	6.114	0.000	0.000	0.000	0.000
2044	DIPOLE_A	20	786.448	25.324	-1.485	6.447	0.000	0.000	-1.322	-0.064	29.288	1.635	6.140	0.000	0.000	0.000	0.000
2056	DIPOLE_B	20	792.903	49.768	-2.302	6.477	0.000	0.000	-1.796	-0.084	13.398	0.826	6.193	0.000	0.000	0.000	0.000
2068	HC114	1	794.040	55.164	-2.446	6.480	0.000	0.000	-1.892	-0.084	11.682	0.683	6.207	0.000	0.000	0.000	0.000
2073	M_114	1	795.272	58.688	-0.037	6.483	0.000	0.000	-1.952	-0.001	10.682	0.078	6.225	0.000	0.000	0.000	0.000
2079	S114	1	796.939	53.288	2.327	6.488	0.000	0.000	-1.859	0.082	11.752	-0.560	6.249	0.000	0.000	0.000	0.000
2083	O114	1	797.181	52.169	2.298	6.489	0.000	0.000	-1.839	0.082	12.030	-0.587	6.252	0.000	0.000	0.000	0.000
2093	DIPOLE_A	21	803.736	27.217	1.509	6.517	0.000	0.000	-1.363	0.061	24.525	-1.318	6.314	0.000	0.000	0.000	0.000
2105	DIPOLE_B	21	810.192	12.754	0.732	6.573	0.000	0.000	-1.030	0.041	46.185	-2.036	6.345	0.000	0.000	0.000	0.000

1
Linear lattice functions for beam line: MI_19
delta(p)/p = 0.000000 symm = F

"MAD" Version: 8.17 Run: 09/09/94 15.47.38
Range: #S/#E

page 6

ELEMENT SEQUENCE			I			H O R I Z O N T A L						I			V E R T I C A L					
pos.	element	occ.	dist	I	betax	alfax	mux	x(co)	px(co)	Dx	Dpx	I	betay	alfay	muy	y(co)	py(co)	Dy	Dpy	
no.	name	no.	[m]	I	[m]	[1]	[2pi]	[mm]	[.001]	[m]	[1]	I	[m]	[1]	[2pi]	[mm]	[.001]	[m]	[1]	
2117	VC115	1	811.328		11.246	0.595	6.588	0.000	0.000	-0.983	0.041		50.958	-2.163	6.349	0.000	0.000	0.000	0.000	
2122	M_115	1	812.560		10.432	0.015	6.606	0.000	0.000	-0.955	0.000		54.027	0.010	6.353	0.000	0.000	0.000	0.000	
2128	S115	1	814.228		11.678	-0.612	6.631	0.000	0.000	-1.001	-0.040		49.033	2.131	6.358	0.000	0.000	0.000	0.000	
2138	DIPOLE_A	22	821.025		25.439	-1.412	6.695	0.000	0.000	-1.339	-0.061		25.272	1.365	6.389	0.000	0.000	0.000	0.000	
2150	DIPOLE_B	22	827.480		48.579	-2.172	6.725	0.000	0.000	-1.799	-0.082		12.367	0.634	6.448	0.000	0.000	0.000	0.000	
2162	HC116	1	828.617		53.669	-2.306	6.728	0.000	0.000	-1.892	-0.082		11.072	0.505	6.464	0.000	0.000	0.000	0.000	
2167	M_116	1	829.849		56.915	0.036	6.732	0.000	0.000	-1.949	0.001		10.478	-0.077	6.482	0.000	0.000	0.000	0.000	
2173	S116	1	831.516		51.455	2.317	6.737	0.000	0.000	-1.853	0.084		12.079	-0.731	6.506	0.000	0.000	0.000	0.000	
2177	O116	1	831.758		50.341	2.287	6.737	0.000	0.000	-1.832	0.084		12.441	-0.762	6.509	0.000	0.000	0.000	0.000	
2187	DIPOLE_A	23	838.313		25.678	1.476	6.767	0.000	0.000	-1.342	0.064		27.881	-1.593	6.566	0.000	0.000	0.000	0.000	
2199	DIPOLE_B	23	844.768		11.782	0.677	6.827	0.000	0.000	-0.996	0.043		53.718	-2.408	6.593	0.000	0.000	0.000	0.000	
2211	VC117	1	845.905		10.403	0.536	6.843	0.000	0.000	-0.947	0.043		59.356	-2.552	6.596	0.000	0.000	0.000	0.000	
2216	M_117	1	847.137		9.705	-0.017	6.863	0.000	0.000	-0.915	0.004		63.005	-0.015	6.599	0.000	0.000	0.000	0.000	
2222	S117	1	848.805		11.016	-0.630	6.889	0.000	0.000	-0.953	-0.035		57.248	2.472	6.604	0.000	0.000	0.000	0.000	
2232	DIPOLE_A	24	855.601		25.430	-1.491	6.956	0.000	0.000	-1.254	-0.056		29.366	1.630	6.630	0.000	0.000	0.000	0.000	
2244	DIPOLE_B	24	862.057		49.963	-2.309	6.985	0.000	0.000	-1.678	-0.077		13.506	0.827	6.683	0.000	0.000	0.000	0.000	
2256	HC118	1	863.193		55.377	-2.454	6.988	0.000	0.000	-1.765	-0.077		11.787	0.685	6.697	0.000	0.000	0.000	0.000	
2261	M_118	1	864.425		58.909	-0.035	6.992	0.000	0.000	-1.818	0.001		10.786	0.076	6.715	0.000	0.000	0.000	0.000	
2267	S118	1	866.093		53.483	2.338	6.996	0.000	0.000	-1.728	0.079		11.869	-0.565	6.739	0.000	0.000	0.000	0.000	
2271	O118	1	866.335		52.358	2.308	6.997	0.000	0.000	-1.709	0.079		12.149	-0.592	6.742	0.000	0.000	0.000	0.000	
2281	DIPOLE_A	25	872.890		27.290	1.516	7.025	0.000	0.000	-1.257	0.058		24.679	-1.319	6.804	0.000	0.000	0.000	0.000	
2293	DIPOLE_B	25	879.345		12.753	0.736	7.081	0.000	0.000	-0.947	0.037		46.320	-2.033	6.834	0.000	0.000	0.000	0.000	
2305	VC119	1	880.482		11.236	0.599	7.096	0.000	0.000	-0.905	0.037		51.083	-2.158	6.838	0.000	0.000	0.000	0.000	
2310	M_119	1	881.714		10.414	0.019	7.115	0.000	0.000	-0.879	0.000		54.136	0.019	6.842	0.000	0.000	0.000	0.000	
2316	S119	1	883.381		11.645	-0.607	7.139	0.000	0.000	-0.922	-0.038		49.101	2.144	6.847	0.000	0.000	0.000	0.000	
2320	O119	1	883.624		11.946	-0.636	7.142	0.000	0.000	-0.931	-0.038		48.070	2.116	6.848	0.000	0.000	0.000	0.000	
2330	DIPOLE_A	26	890.178		25.333	-1.406	7.204	0.000	0.000	-1.241	-0.058		25.210	1.371	6.878	0.000	0.000	0.000	0.000	
2342	DIPOLE_B	26	896.634		48.388	-2.165	7.233	0.000	0.000	-1.682	-0.079		12.264	0.634	6.938	0.000	0.000	0.000	0.000	
2354	HC120	1	897.770		53.462	-2.299	7.237	0.000	0.000	-1.772	-0.079		10.970	0.504	6.953	0.000	0.000	0.000	0.000	

2359	M_120	1	899.002	56.699	0.034	7.240	0.000	0.000	-1.828-0.001	10.375	-0.075	6.972	0.000	0.000	0.000	0.000
2365	S120	1	900.670	51.266	2.306	7.245	0.000	0.000	-1.741 0.077	11.961	-0.726	6.996	0.000	0.000	0.000	0.000
2369	O120	1	900.912	50.157	2.277	7.246	0.000	0.000	-1.723 0.077	12.320	-0.757	6.999	0.000	0.000	0.000	0.000
2379	DIPOLE_A	27	907.467	25.609	1.469	7.275	0.000	0.000	-1.282 0.056	27.714	-1.591	7.057	0.000	0.000	0.000	0.000
2391	DIPOLE_B	27	913.922	11.785	0.673	7.336	0.000	0.000	-0.983 0.035	53.554	-2.410	7.084	0.000	0.000	0.000	0.000
2408	VC121	1	915.078	10.395	0.530	7.352	0.000	0.000	-0.943 0.035	59.295	-2.557	7.087	0.000	0.000	0.000	0.000
2413	M_121	1	916.291	9.726	-0.021	7.372	0.000	0.000	-0.921-0.004	62.861	-0.024	7.090	0.000	0.000	0.000	0.000
2422	S121	1	918.055	11.175	-0.647	7.399	0.000	0.000	-0.976-0.043	56.670	2.446	7.095	0.000	0.000	0.000	0.000
2432	DIPOLE_A	28	924.755	25.536	-1.497	7.464	0.000	0.000	-1.327-0.064	29.411	1.622	7.121	0.000	0.000	0.000	0.000
2444	DIPOLE_B	28	931.211	50.150	-2.316	7.493	0.000	0.000	-1.802-0.085	13.604	0.826	7.173	0.000	0.000	0.000	0.000
2456	HC122	1	932.347	55.579	-2.460	7.497	0.000	0.000	-1.898-0.085	11.886	0.685	7.187	0.000	0.000	0.000	0.000
2461	M_122	1	933.579	59.119	-0.033	7.500	0.000	0.000	-1.958-0.001	10.887	0.073	7.205	0.000	0.000	0.000	0.000
2467	S122	1	935.247	53.666	2.348	7.505	0.000	0.000	-1.865 0.083	11.987	-0.571	7.229	0.000	0.000	0.000	0.000
2471	O122	1	935.489	52.536	2.319	7.505	0.000	0.000	-1.845 0.083	12.270	-0.598	7.232	0.000	0.000	0.000	0.000
2481	DIPOLE_A	29	942.044	27.354	1.523	7.533	0.000	0.000	-1.366 0.062	24.858	-1.322	7.293	0.000	0.000	0.000	0.000
2493	DIPOLE_B	29	948.499	12.747	0.740	7.589	0.000	0.000	-1.030 0.041	46.514	-2.032	7.323	0.000	0.000	0.000	0.000
2505	VC123	1	949.636	11.222	0.602	7.604	0.000	0.000	-0.984 0.041	51.276	-2.157	7.327	0.000	0.000	0.000	0.000
2510	M_123	1	950.867	10.391	0.023	7.623	0.000	0.000	-0.955 0.000	54.316	0.029	7.331	0.000	0.000	0.000	0.000

1
Linear lattice functions for beam line: MI_19
delta(p)/p = 0.000000 symm = F

"MAD" Version: 8.17 Run: 09/09/94 15.47.38
Range: #S/#E

page 7

E L E M E N T S E Q U E N C E						H O R I Z O N T A L						V E R T I C A L						
pos.	element	occ.	dist I	betax	alfax	mux	x(co)	px(co)	Dx	Dpx	I	betay	alfay	muy	y(co)	py(co)	Dy	Dpy
no.	name	no.	[m]	[m]	[1]	[2pi]	[mm]	[.001]	[m]	[1]	I	[m]	[1]	[2pi]	[mm]	[.001]	[m]	[1]
2516	S123	1	952.535	11.609	-0.603	7.647	0.000	0.000	-1.000-0.040	49.235	2.159	7.336	0.000	0.000	0.000	0.000	0.000	
2526	DIPOLE_A	30	959.332	25.227	-1.401	7.712	0.000	0.000	-1.336-0.061	25.182	1.379	7.367	0.000	0.000	0.000	0.000	0.000	
2538	DIPOLE_B	30	965.787	48.206	-2.159	7.742	0.000	0.000	-1.792-0.082	12.172	0.636	7.427	0.000	0.000	0.000	0.000	0.000	
2550	HC124	1	966.924	53.266	-2.292	7.745	0.000	0.000	-1.885-0.082	10.875	0.505	7.443	0.000	0.000	0.000	0.000	0.000	
2555	M_124	1	968.156	56.496	0.032	7.749	0.000	0.000	-1.942 0.001	10.276	-0.071	7.461	0.000	0.000	0.000	0.000	0.000	
2561	S124	1	969.824	51.090	2.296	7.754	0.000	0.000	-1.845 0.084	11.843	-0.719	7.486	0.000	0.000	0.000	0.000	0.000	
2565	O124	1	970.066	49.986	2.266	7.755	0.000	0.000	-1.825 0.084	12.199	-0.750	7.489	0.000	0.000	0.000	0.000	0.000	
2575	DIPOLE_A	31	976.620	25.550	1.462	7.784	0.000	0.000	-1.337 0.063	27.523	-1.587	7.547	0.000	0.000	0.000	0.000	0.000	
2587	DIPOLE_B	31	983.076	11.794	0.669	7.845	0.000	0.000	-0.991 0.043	53.331	-2.409	7.574	0.000	0.000	0.000	0.000	0.000	
2599	VC125	1	984.212	10.431	0.530	7.861	0.000	0.000	-0.943 0.043	58.973	-2.554	7.577	0.000	0.000	0.000	0.000	0.000	
2604	M_125	1	985.444	9.750	-0.024	7.881	0.000	0.000	-0.911 0.004	62.645	-0.033	7.581	0.000	0.000	0.000	0.000	0.000	
2610	S125	1	987.112	11.089	-0.639	7.907	0.000	0.000	-0.949-0.035	56.981	2.441	7.585	0.000	0.000	0.000	0.000	0.000	
2620	DIPOLE_A	32	993.909	25.641	-1.502	7.973	0.000	0.000	-1.249-0.056	29.422	1.613	7.612	0.000	0.000	0.000	0.000	0.000	
2632	DIPOLE_B	32	1000.364	50.326	-2.322	8.001	0.000	0.000	-1.672-0.077	13.690	0.824	7.664	0.000	0.000	0.000	0.000	0.000	
2644	HC126	1	1001.501	55.769	-2.466	8.005	0.000	0.000	-1.759-0.077	11.976	0.684	7.678	0.000	0.000	0.000	0.000	0.000	
2649	M_126	1	1002.733	59.314	-0.031	8.008	0.000	0.000	-1.812 0.001	10.983	0.069	7.695	0.000	0.000	0.000	0.000	0.000	
2655	S126	1	1004.400	53.835	2.358	8.013	0.000	0.000	-1.723 0.078	12.105	-0.579	7.719	0.000	0.000	0.000	0.000	0.000	
2659	O126	1	1004.642	52.700	2.329	8.014	0.000	0.000	-1.704 0.078	12.392	-0.605	7.722	0.000	0.000	0.000	0.000	0.000	
2669	DIPOLE_A	33	1011.197	27.408	1.530	8.041	0.000	0.000	-1.254 0.058	25.060	-1.327	7.782	0.000	0.000	0.000	0.000	0.000	
2681	DIPOLE_B	33	1017.653	12.735	0.743	8.097	0.000	0.000	-0.946 0.037	46.764	-2.035	7.813	0.000	0.000	0.000	0.000	0.000	
2693	VC127	1	1018.789	11.203	0.605	8.112	0.000	0.000	-0.905 0.037	51.531	-2.159	7.816	0.000	0.000	0.000	0.000	0.000	
2698	M_127	1	1020.021	10.365	0.026	8.131	0.000	0.000	-0.879-0.001	54.565	0.038	7.820	0.000	0.000	0.000	0.000	0.000	
2704	S127	1	1021.689	11.569	-0.598	8.155	0.000	0.000	-0.923-0.038	49.433	2.177	7.825	0.000	0.000	0.000	0.000	0.000	
2708	O127	1	1021.931	11.866	-0.627	8.159	0.000	0.000	-0.932-0.038	48.386	2.149	7.826	0.000	0.000	0.000	0.000	0.000	
2718	DIPOLE_A	34	1028.486	25.123	-1.396	8.221	0.000	0.000	-1.245-0.059	25.189	1.389	7.856	0.000	0.000	0.000	0.000	0.000	
2730	DIPOLE_B	34	1034.941	48.036	-2.154	8.251	0.000	0.000	-1.689-0.080	12.091	0.639	7.916	0.000	0.000	0.000	0.000	0.000	

2742	HC128	1	1036.078	53.083	-2.287	8.254	0.000	0.000	-1.779-0.080	10.789	0.507	7.932	0.000	0.000	0.000	0.000
2747	M_128	1	1037.310	56.309	0.029	8.258	0.000	0.000	-1.836-0.001	10.183	-0.067	7.951	0.000	0.000	0.000	0.000
2753	S128	1	1038.977	50.929	2.286	8.263	0.000	0.000	-1.749 0.077	11.727	-0.711	7.976	0.000	0.000	0.000	0.000
2757	O128	1	1039.219	49.829	2.257	8.263	0.000	0.000	-1.730 0.077	12.078	-0.742	7.979	0.000	0.000	0.000	0.000
2767	DIPOLE_A	35	1045.774	25.501	1.455	8.293	0.000	0.000	-1.288 0.056	27.311	-1.581	8.038	0.000	0.000	0.000	0.000
2779	DIPOLE_B	35	1052.229	11.808	0.666	8.353	0.000	0.000	-0.988 0.035	53.054	-2.405	8.065	0.000	0.000	0.000	0.000
2791	VC129	1	1053.366	10.452	0.527	8.370	0.000	0.000	-0.947 0.035	58.687	-2.551	8.068	0.000	0.000	0.000	0.000
2796	M_129	1	1054.598	9.778	-0.028	8.389	0.000	0.000	-0.925-0.004	62.364	-0.042	8.071	0.000	0.000	0.000	0.000
2802	S129	1	1056.266	11.130	-0.643	8.415	0.000	0.000	-0.975-0.043	56.752	2.422	8.076	0.000	0.000	0.000	0.000
2812	DIPOLE_A	36	1063.062	25.744	-1.507	8.481	0.000	0.000	-1.332-0.064	29.398	1.602	8.102	0.000	0.000	0.000	0.000
2824	DIPOLE_B	36	1069.518	50.490	-2.327	8.510	0.000	0.000	-1.808-0.085	13.764	0.820	8.154	0.000	0.000	0.000	0.000
2836	HC130	1	1070.654	55.944	-2.471	8.513	0.000	0.000	-1.904-0.085	12.058	0.682	8.168	0.000	0.000	0.000	0.000
2841	M_130	1	1071.886	59.493	-0.028	8.516	0.000	0.000	-1.964-0.001	11.074	0.064	8.185	0.000	0.000	0.000	0.000
2847	S130	1	1073.554	53.988	2.368	8.521	0.000	0.000	-1.870 0.083	12.220	-0.587	8.209	0.000	0.000	0.000	0.000
2851	O130	1	1073.796	52.849	2.339	8.522	0.000	0.000	-1.850 0.083	12.511	-0.614	8.212	0.000	0.000	0.000	0.000
2861	DIPOLE_A	37	1080.351	27.452	1.536	8.549	0.000	0.000	-1.369 0.062	25.281	-1.334	8.272	0.000	0.000	0.000	0.000
2873	DIPOLE_B	37	1086.806	12.718	0.746	8.605	0.000	0.000	-1.030 0.041	47.067	-2.040	8.302	0.000	0.000	0.000	0.000
2890	VC201	1	1087.962	11.157	0.605	8.621	0.000	0.000	-0.983 0.041	51.929	-2.167	8.305	0.000	0.000	0.000	0.000
2895	M_201	1	1089.175	10.336	0.029	8.639	0.000	0.000	-0.954 0.001	54.879	0.046	8.309	0.000	0.000	0.000	0.000
2904	S201	1	1090.940	11.644	-0.605	8.665	0.000	0.000	-1.002-0.040	49.265	2.185	8.314	0.000	0.000	0.000	0.000
2914	DIPOLE_A	38	1097.639	25.022	-1.392	8.729	0.000	0.000	-1.331-0.060	25.230	1.402	8.345	0.000	0.000	0.000	0.000

1
Linear lattice functions for beam line: MI_19
delta(p)/p = 0.000000 symm = F

"MAD" Version: 8.17 Run: 09/09/94 15.47.38
Range: #S/#E

page 8

ELEMENT SEQUENCE			H O R I Z O N T A L									V E R T I C A L							
pos.	element	occ.	dist	I	betax	alfax	mux	x(co)	px(co)	Dx	Dpx	I	betay	alfay	muy	y(co)	py(co)	Dy	Dpy
no.	name	no.	[m]	I	[m]	[1]	[2pi]	[mm]	[.001]	[m]	[1]	I	[m]	[1]	[2pi]	[mm]	[.001]	[m]	[1]
2926	DIPOLE_B	38	1104.095		47.879	-2.149	8.759	0.000	0.000	-1.785-0.081			12.024	0.644	8.405	0.000	0.000	0.000	0.000
2938	HC202	1	1105.231		52.916	-2.283	8.763	0.000	0.000	-1.878-0.081			10.713	0.510	8.421	0.000	0.000	0.000	0.000
2943	M_202	1	1106.463		56.139	0.026	8.766	0.000	0.000	-1.934 0.001			10.096	-0.061	8.440	0.000	0.000	0.000	0.000
2949	S202	1	1108.131		50.785	2.277	8.771	0.000	0.000	-1.838 0.084			11.614	-0.702	8.465	0.000	0.000	0.000	0.000
2953	O202	1	1108.373		49.689	2.247	8.772	0.000	0.000	-1.817 0.084			11.961	-0.733	8.468	0.000	0.000	0.000	0.000
2963	DIPOLE_A	39	1114.928		25.463	1.449	8.801	0.000	0.000	-1.330 0.063			27.081	-1.573	8.528	0.000	0.000	0.000	0.000
2975	DIPOLE_B	39	1121.383		11.828	0.663	8.862	0.000	0.000	-0.987 0.042			52.726	-2.398	8.555	0.000	0.000	0.000	0.000
2987	VC203	1	1122.520		10.477	0.525	8.878	0.000	0.000	-0.939 0.042			58.344	-2.544	8.558	0.000	0.000	0.000	0.000
2992	M_203	1	1123.752		9.808	-0.030	8.898	0.000	0.000	-0.907 0.004			62.019	-0.050	8.562	0.000	0.000	0.000	0.000
2998	S203	1	1125.419		11.173	-0.648	8.924	0.000	0.000	-0.945-0.035			56.465	2.402	8.566	0.000	0.000	0.000	0.000
3008	DIPOLE_A	40	1132.216		25.842	-1.511	8.989	0.000	0.000	-1.245-0.056			29.340	1.589	8.593	0.000	0.000	0.000	0.000
3020	DIPOLE_B	40	1138.672		50.640	-2.331	9.018	0.000	0.000	-1.667-0.076			13.824	0.814	8.645	0.000	0.000	0.000	0.000
3032	HC204	1	1139.808		56.102	-2.475	9.021	0.000	0.000	-1.754-0.076			12.128	0.677	8.659	0.000	0.000	0.000	0.000
3037	M_204	1	1141.040		59.654	-0.025	9.025	0.000	0.000	-1.807 0.001			11.156	0.058	8.676	0.000	0.000	0.000	0.000
3043	S204	1	1142.708		54.123	2.377	9.029	0.000	0.000	-1.718 0.078			12.330	-0.597	8.699	0.000	0.000	0.000	0.000
3047	O204	1	1142.950		52.979	2.348	9.030	0.000	0.000	-1.699 0.078			12.626	-0.624	8.702	0.000	0.000	0.000	0.000
3057	DIPOLE_A	41	1149.505		27.484	1.542	9.057	0.000	0.000	-1.252 0.057			25.518	-1.343	8.761	0.000	0.000	0.000	0.000
3069	DIPOLE_B	41	1155.960		12.697	0.749	9.114	0.000	0.000	-0.946 0.036			47.418	-2.049	8.791	0.000	0.000	0.000	0.000
3081	VC205	1	1157.097		11.153	0.609	9.129	0.000	0.000	-0.905 0.036			52.216	-2.173	8.795	0.000	0.000	0.000	0.000
3086	M_205	1	1158.328		10.304	0.032	9.147	0.000	0.000	-0.880-0.001			55.252	0.054	8.798	0.000	0.000	0.000	0.000
3092	S205	1	1159.996		11.483	-0.590	9.172	0.000	0.000	-0.925-0.038			50.005	2.218	8.803	0.000	0.000	0.000	0.000
3096	O205	1	1160.238		11.775	-0.618	9.175	0.000	0.000	-0.934-0.038			48.938	2.190	8.804	0.000	0.000	0.000	0.000
3106	DIPOL	42	1166.793		24.926	-1.388	9.238	0.000	0.000	-1.250-0.059			25.305	1.415	8.834	0.000	0.000	0.000	0.000

3118	DIPOLE_B	42	1173.248	47.737	-2.146	9.268	0.000	0.000	-1.696-0.080	11.972	0.650	8.894	0.000	0.000	0.000	0.000
3130	QC206	1	1173.969	50.891	-2.230	9.270	0.000	0.000	-1.754-0.080	11.097	0.564	8.904	0.000	0.000	0.000	0.000
3134	HC206	1	1174.385	52.766	-2.279	9.271	0.000	0.000	-1.787-0.080	10.648	0.515	8.910	0.000	0.000	0.000	0.000
3139	M_206	1	1175.617	55.988	0.023	9.275	0.000	0.000	-1.844-0.001	10.018	-0.055	8.930	0.000	0.000	0.000	0.000
3145	S206	1	1177.285	50.658	2.268	9.280	0.000	0.000	-1.757 0.077	11.506	-0.692	8.955	0.000	0.000	0.000	0.000
3149	O206	1	1177.527	49.568	2.238	9.281	0.000	0.000	-1.738 0.077	11.848	-0.723	8.958	0.000	0.000	0.000	0.000
3159	DIPOLE_A	43	1184.081	25.437	1.444	9.310	0.000	0.000	-1.294 0.057	26.838	-1.563	9.018	0.000	0.000	0.000	0.000
3171	DIPOLE_B	43	1190.537	11.852	0.661	9.371	0.000	0.000	-0.992 0.036	52.355	-2.388	9.045	0.000	0.000	0.000	0.000
3183	VC207	1	1191.673	10.506	0.523	9.387	0.000	0.000	-0.952 0.036	57.949	-2.534	9.049	0.000	0.000	0.000	0.000
3188	M_207	1	1192.905	9.842	-0.033	9.407	0.000	0.000	-0.929-0.004	61.619	-0.057	9.052	0.000	0.000	0.000	0.000
3194	S207	1	1194.573	11.218	-0.651	9.432	0.000	0.000	-0.979-0.043	56.125	2.379	9.056	0.000	0.000	0.000	0.000
3204	DIPOLE_A	44	1201.370	25.936	-1.514	9.498	0.000	0.000	-1.336-0.064	29.248	1.574	9.083	0.000	0.000	0.000	0.000
3216	DIPOLE_B	44	1207.825	50.774	-2.334	9.526	0.000	0.000	-1.812-0.085	13.869	0.807	9.135	0.000	0.000	0.000	0.000
3228	QC208	1	1208.546	54.203	-2.425	9.528	0.000	0.000	-1.874-0.085	12.767	0.722	9.144	0.000	0.000	0.000	0.000
3232	HC208	1	1208.962	56.242	-2.478	9.529	0.000	0.000	-1.909-0.085	12.187	0.672	9.149	0.000	0.000	0.000	0.000
3237	M_208	1	1210.194	59.795	-0.021	9.533	0.000	0.000	-1.969-0.001	11.230	0.051	9.166	0.000	0.000	0.000	0.000
3243	S208	1	1211.861	54.240	2.386	9.537	0.000	0.000	-1.874 0.083	12.435	-0.607	9.189	0.000	0.000	0.000	0.000
3247	O208	1	1212.103	53.092	2.356	9.538	0.000	0.000	-1.854 0.083	12.735	-0.634	9.192	0.000	0.000	0.000	0.000
3257	DIPOLE_A	45	1218.658	27.505	1.547	9.565	0.000	0.000	-1.371 0.063	25.767	-1.354	9.251	0.000	0.000	0.000	0.000
3269	DIPOLE_B	45	1225.114	12.670	0.751	9.622	0.000	0.000	-1.030 0.042	47.809	-2.060	9.280	0.000	0.000	0.000	0.000
3281	VC209	1	1226.250	11.123	0.611	9.637	0.000	0.000	-0.983 0.042	52.634	-2.185	9.284	0.000	0.000	0.000	0.000
3286	M_209	1	1227.482	10.268	0.034	9.656	0.000	0.000	-0.953 0.001	55.679	0.061	9.288	0.000	0.000	0.000	0.000
3292	S209	1	1229.150	11.437	-0.586	9.680	0.000	0.000	-0.997-0.039	50.371	2.241	9.293	0.000	0.000	0.000	0.000
3302	DIPOLE_A	46	1235.947	24.835	-1.385	9.746	0.000	0.000	-1.326-0.060	25.412	1.430	9.323	0.000	0.000	0.000	0.000

```

1
Linear lattice functions for beam line: MI_19
delta(p)/p =      0.000000      symm = F

```

"MAD" Version: 8.17 Run: 09/09/94 15.47.38
Range: #S/#E

page 9

ELEMENT SEQUENCE			H O R I Z O N T A L										V E R T I C A L						
pos.	element	occ.	dist	I	betax	alfax	mux	x(co)	px(co)	Dx	Dpx	I	betay	alfay	muy	y(co)	py(co)	Dy	Dpy
no.	name	no.	[m]	I	[m]	[1]	[2pi]	[mm]	[.001]	[m]	[1]	I	[m]	[1]	[2pi]	[mm]	[.001]	[m]	[1]
3314	DIPOLE_B	46	1242.402		47.611	-2.143	9.777	0.000	0.000	-1.777	-0.081		11.934	0.657	9.383	0.000	0.000	0.000	0.000
3326	QC210	1	1243.123		50.762	-2.228	9.779	0.000	0.000	-1.836	-0.081		11.049	0.571	9.393	0.000	0.000	0.000	0.000
3330	HC210	1	1243.539		52.636	-2.277	9.780	0.000	0.000	-1.869	-0.081		10.595	0.521	9.399	0.000	0.000	0.000	0.000
3335	M_210	1	1244.771		55.858	0.019	9.784	0.000	0.000	-1.925	0.001		9.949	-0.047	9.419	0.000	0.000	0.000	0.000
3341	S210	1	1246.438		50.552	2.259	9.789	0.000	0.000	-1.829	0.084		11.406	-0.681	9.444	0.000	0.000	0.000	0.000
3345	O210	1	1246.680		49.465	2.230	9.789	0.000	0.000	-1.809	0.084		11.743	-0.712	9.447	0.000	0.000	0.000	0.000
3355	DIPOLE_A	47	1253.235		25.421	1.439	9.819	0.000	0.000	-1.324	0.063		26.585	-1.552	9.508	0.000	0.000	0.000	0.000
3367	DIPOLE_B	47	1259.690		11.881	0.659	9.880	0.000	0.000	-0.982	0.042		51.944	-2.376	9.536	0.000	0.000	0.000	0.000
3384	VC211	1	1260.846		10.519	0.520	9.896	0.000	0.000	-0.934	0.042		57.606	-2.523	9.539	0.000	0.000	0.000	0.000
3389	M_211	1	1262.059		9.879	-0.035	9.915	0.000	0.000	-0.903	0.004		61.168	-0.064	9.542	0.000	0.000	0.000	0.000
3398	S211	1	1263.824		11.393	-0.667	9.942	0.000	0.000	-0.944	-0.035		55.279	2.344	9.547	0.000	0.000	0.000	0.000
3408	DIPOLE_A	48	1270.523		26.024	-1.517	10.006	0.000	0.000	-1.240	-0.056		29.126	1.559	9.574	0.000	0.000	0.000	0.000
3420	DIPOLE_B	48	1276.979		50.890	-2.335	10.034	0.000	0.000	-1.663	-0.076		13.899	0.799	9.626	0.000	0.000	0.000	0.000
3432	QC212	1	1277.700		54.322	-2.427	10.036	0.000	0.000	-1.718	-0.076		12.807	0.714	9.634	0.000	0.000	0.000	0.000
3436	HC212	1	1278.115		56.363	-2.480	10.038	0.000	0.000	-1.750	-0.076		12.234	0.665	9.640	0.000	0.000	0.000	0.000
3441	M_212	1	1279.347		59.913	-0.018	10.041	0.000	0.000	-1.803	0.001		11.293	0.043	9.657	0.000	0.000	0.000	0.000
3447	S212	1	1281.015		54.336	2.394	10.045	0.000	0.000	-1.714	0.078		12.531	-0.618	9.679	0.000	0.000	0.000	0.000
3451	O212	1	1281.257		53.184	2.364	10.046	0.000	0.000	-1.696	0.078		12.837	-0.645	9.682	0.000	0.000	0.000	0.000
3461	DIPOLE_A	49	1287.812		27.514	1.552	10.074	0.000	0.000	-1.250	0.057		26.023	-1.366	9.741	0.000	0.000	0.000	0.000
3473	DIPOLE_B	49	1294.267		12.639	0.752	10.130	0.000	0.000	-0.947	0.036		48.237	-2.074	9.770	0.000	0.000	0.000	0.000

3485	SQ213	1	1294.985	11.623	0.663	10.139	0.000	0.000	-0.921	0.036	51.270	-2.153	9.772	0.000	0.000	0.000	0.000
3489	VC213	1	1295.404	11.089	0.612	10.145	0.000	0.000	-0.906	0.036	53.093	-2.199	9.773	0.000	0.000	0.000	0.000
3494	M_213	1	1296.636	10.231	0.036	10.164	0.000	0.000	-0.882	-0.001	56.152	0.066	9.777	0.000	0.000	0.000	0.000
3500	S213	1	1298.303	11.390	-0.583	10.189	0.000	0.000	-0.927	-0.039	50.782	2.265	9.782	0.000	0.000	0.000	0.000
3510	DIPOLE_A	50	1305.100	24.751	-1.383	10.255	0.000	0.000	-1.255	-0.060	25.550	1.446	9.812	0.000	0.000	0.000	0.000
3522	DIPOLE_B	50	1311.556	47.504	-2.142	10.285	0.000	0.000	-1.704	-0.081	11.913	0.666	9.872	0.000	0.000	0.000	0.000
3534	SQ214	1	1312.045	49.627	-2.200	10.287	0.000	0.000	-1.743	-0.081	11.291	0.607	9.879	0.000	0.000	0.000	0.000
3538	SQ214	2	1312.273	50.639	-2.227	10.288	0.000	0.000	-1.762	-0.081	11.020	0.579	9.882	0.000	0.000	0.000	0.000
3542	HC214	1	1312.692	52.526	-2.276	10.289	0.000	0.000	-1.796	-0.081	10.556	0.528	9.889	0.000	0.000	0.000	0.000
3547	M_214	1	1313.924	55.751	0.016	10.292	0.000	0.000	-1.853	-0.001	9.891	-0.039	9.908	0.000	0.000	0.000	0.000
3553	S214	1	1315.592	50.467	2.251	10.297	0.000	0.000	-1.765	0.078	11.314	-0.670	9.934	0.000	0.000	0.000	0.000
3557	O214	1	1315.834	49.384	2.222	10.298	0.000	0.000	-1.746	0.078	11.646	-0.701	9.937	0.000	0.000	0.000	0.000
3567	DIPOLE_A	51	1322.389	25.418	1.434	10.328	0.000	0.000	-1.300	0.057	26.327	-1.538	9.998	0.000	0.000	0.000	0.000
3579	DIPOLE_B	51	1328.844	11.914	0.658	10.388	0.000	0.000	-0.997	0.036	51.502	-2.360	10.026	0.000	0.000	0.000	0.000
3591	SQ215	1	1329.562	11.032	0.572	10.398	0.000	0.000	-0.971	0.036	54.955	-2.452	10.028	0.000	0.000	0.000	0.000
3595	VC215	1	1329.981	10.574	0.521	10.404	0.000	0.000	-0.956	0.036	57.032	-2.505	10.029	0.000	0.000	0.000	0.000
3600	M_215	1	1331.213	9.917	-0.037	10.424	0.000	0.000	-0.932	-0.003	60.674	-0.069	10.033	0.000	0.000	0.000	0.000
3606	S215	1	1332.880	11.312	-0.658	10.449	0.000	0.000	-0.983	-0.043	55.304	2.331	10.037	0.000	0.000	0.000	0.000
3616	DIPOLE_A	52	1339.677	26.104	-1.519	10.514	0.000	0.000	-1.340	-0.064	28.973	1.542	10.064	0.000	0.000	0.000	0.000
3628	DIPOLE_B	52	1346.133	50.988	-2.336	10.542	0.000	0.000	-1.816	-0.085	13.912	0.790	10.116	0.000	0.000	0.000	0.000
3643	HC216	1	1347.301	56.620	-2.484	10.546	0.000	0.000	-1.915	-0.085	12.225	0.654	10.131	0.000	0.000	0.000	0.000
3648	M_216	1	1348.501	60.005	-0.010	10.549	0.000	0.000	-1.972	0.000	11.346	0.034	10.147	0.000	0.000	0.000	0.000
3659	DIPOLE_C	21	1354.805	27.876	2.270	10.573	0.000	0.000	-1.358	0.101	23.434	-1.457	10.213	0.000	0.000	0.000	0.000
3671	DIPOLE_D	21	1359.228	12.113	1.294	10.611	0.000	0.000	-0.938	0.088	38.924	-2.045	10.236	0.000	0.000	0.000	0.000
3683	VC217	1	1359.874	10.533	1.151	10.621	0.000	0.000	-0.881	0.088	41.623	-2.131	10.239	0.000	0.000	0.000	0.000
3688	M_217	1	1361.467	8.153	0.346	10.648	0.000	0.000	-0.778	0.040	44.869	0.346	10.244	0.000	0.000	0.000	0.000
3699	DIPOLE_C	22	1367.771	14.256	-0.964	10.752	0.000	0.000	-0.802	-0.018	18.781	1.713	10.278	0.000	0.000	0.000	0.000

"MAD" Version: 8.17

Run: 09/09/94 15.47.38

1
Linear lattice functions for beam line: MI_19

delta(p)/p = 0.000000 symm = F

Range: #S/#E

page 10

ELEMENT SEQUENCE			H O R I Z O N T A L										V E R T I C A L						
pos.	element	occ.	dist	I	betax	alfax	mux	x(co)	px(co)	Dx	Dpx	I	betay	alfay	muy	y(co)	py(co)	Dy	Dpy
no.	name	no.	[m]	I	[m]	[1]	[2pi]	[mm]	[.001]	[m]	[1]	I	[m]	[1]	[2pi]	[mm]	[.001]	[m]	[1]
3711	DIPOLE_D	22	1372.194		25.428	-1.562	10.789	0.000	0.000	-0.912-0.032			7.723	0.787	10.338	0.000	0.000	0.000	0.000
3723	HC218	1	1372.841		27.504	-1.650	10.793	0.000	0.000	-0.932-0.032			6.794	0.651	10.352	0.000	0.000	0.000	0.000
3728	M_218	1	1374.434		30.435	-0.002	10.802	0.000	0.000	-0.942 0.024			5.754	-0.007	10.394	0.000	0.000	0.000	0.000
3739	DIPOLE_C	23	1380.737		15.001	1.011	10.848	0.000	0.000	-0.516 0.065			17.833	-1.664	10.505	0.000	0.000	0.000	0.000
3751	DIPOLE_D	23	1385.161		8.694	0.415	10.911	0.000	0.000	-0.259 0.051			36.686	-2.597	10.533	0.000	0.000	0.000	0.000
3763	VC219	1	1385.807		8.214	0.328	10.923	0.000	0.000	-0.226 0.051			40.131	-2.734	10.536	0.000	0.000	0.000	0.000
3768	M_219	1	1387.400		8.186	-0.346	10.955	0.000	0.000	-0.154 0.040			45.503	-0.347	10.542	0.000	0.000	0.000	0.000
3779	DIPOLE_C	24	1393.704		26.305	-2.189	11.028	0.000	0.000	0.027 0.018			24.783	1.531	10.571	0.000	0.000	0.000	0.000
3791	DIPOLE_D	24	1398.127		49.981	-3.163	11.048	0.000	0.000	0.081 0.005			13.873	0.935	10.609	0.000	0.000	0.000	0.000
3803	HC220	1	1398.773		54.161	-3.306	11.050	0.000	0.000	0.084 0.005			12.721	0.848	10.617	0.000	0.000	0.000	0.000
3808	M_220	1	1400.367		59.997	0.014	11.054	0.000	0.000	0.087-0.001			11.355	-0.019	10.638	0.000	0.000	0.000	0.000
3822	VC221	1	1416.442		10.693	0.598	11.161	0.000	0.000	0.021-0.004			56.704	-2.354	10.750	0.000	0.000	0.000	0.000
3827	M_221	1	1417.655		9.873	0.036	11.180	0.000	0.000	0.016-0.004			59.889	0.067	10.754	0.000	0.000	0.000	0.000
3839	HC222	1	1433.731		52.567	-2.312	11.308	0.000	0.000	-0.031-0.003			10.746	0.597	10.860	0.000	0.000	0.000	0.000
3844	M_222	1	1434.944		55.790	-0.020	11.311	0.000	0.000	-0.034-0.001			9.941	0.025	10.879	0.000	0.000	0.000	0.000
3857	VC223	1	1451.032		10.916	0.530	11.421	0.000	0.000	-0.035 0.000			53.751	-2.356	11.005	0.000	0.000	0.000	0.000
3862	M_223	1	1452.233		10.274	-0.036	11.440	0.000	0.000	-0.036-0.001			57.018	-0.061	11.008	0.000	0.000	0.000	0.000

3873	DIPOLE_C	25	1458.536	22.924	-1.535	11.510	0.000	0.000	-0.085-0.018	27.511	2.107	11.033	0.000	0.000	0.000	0.000
3885	DIPOLE_D	25	1462.960	39.366	-2.182	11.533	0.000	0.000	-0.191-0.031	12.737	1.233	11.071	0.000	0.000	0.000	0.000
3897	HC224	1	1463.606	42.248	-2.277	11.536	0.000	0.000	-0.212-0.031	11.226	1.105	11.079	0.000	0.000	0.000	0.000
3902	M_224	1	1465.199	45.829	0.298	11.541	0.000	0.000	-0.252-0.017	9.021	0.276	11.105	0.000	0.000	0.000	0.000
3913	DIPOLE_C	26	1471.503	19.181	1.758	11.574	0.000	0.000	-0.303-0.016	16.391	-1.049	11.196	0.000	0.000	0.000	0.000
3925	DIPOLE_D	26	1475.926	7.800	0.815	11.633	0.000	0.000	-0.402-0.030	28.177	-1.615	11.229	0.000	0.000	0.000	0.000
3937	VC225	1	1476.572	6.836	0.677	11.647	0.000	0.000	-0.421-0.030	30.318	-1.698	11.232	0.000	0.000	0.000	0.000
3942	M_225	1	1478.165	5.713	0.022	11.689	0.000	0.000	-0.487-0.056	33.196	0.086	11.240	0.000	0.000	0.000	0.000
3953	DIPOLE_C	27	1484.469	17.188	-1.604	11.804	0.000	0.000	-1.042-0.101	15.736	1.147	11.283	0.000	0.000	0.000	0.000
3965	DIPOLE_D	27	1488.892	35.449	-2.524	11.832	0.000	0.000	-1.518-0.115	8.464	0.496	11.345	0.000	0.000	0.000	0.000
3977	HC226	1	1489.539	38.798	-2.658	11.835	0.000	0.000	-1.592-0.115	7.884	0.401	11.358	0.000	0.000	0.000	0.000
3982	M_226	1	1491.132	43.967	-0.299	11.841	0.000	0.000	-1.703-0.016	7.625	-0.269	11.391	0.000	0.000	0.000	0.000
3993	DIPOLE_C	28	1497.435	23.249	1.508	11.871	0.000	0.000	-1.270 0.071	24.325	-2.057	11.471	0.000	0.000	0.000	0.000
4005	DIPOLE_D	28	1501.859	12.666	0.885	11.913	0.000	0.000	-0.984 0.057	46.723	-3.006	11.492	0.000	0.000	0.000	0.000
4017	VC227	1	1502.505	11.581	0.794	11.921	0.000	0.000	-0.947 0.057	50.697	-3.145	11.494	0.000	0.000	0.000	0.000
4022	M_227	1	1504.098	10.289	-0.007	11.945	0.000	0.000	-0.895 0.004	56.435	-0.111	11.499	0.000	0.000	0.000	0.000
4032	S227	1	1505.861	11.729	-0.647	11.971	0.000	0.000	-0.934-0.034	51.184	2.117	11.504	0.000	0.000	0.000	0.000
4041	DIPOLE_A	53	1512.563	25.825	-1.457	12.034	0.000	0.000	-1.225-0.055	27.604	1.401	11.533	0.000	0.000	0.000	0.000
4053	DIPOLE_B	53	1519.018	49.668	-2.237	12.063	0.000	0.000	-1.642-0.076	13.980	0.709	11.586	0.000	0.000	0.000	0.000
4065	HC228	1	1520.155	54.910	-2.374	12.066	0.000	0.000	-1.728-0.076	12.508	0.587	11.600	0.000	0.000	0.000	0.000
4070	M_228	1	1521.387	58.266	0.023	12.070	0.000	0.000	-1.780 0.001	11.764	-0.043	11.616	0.000	0.000	0.000	0.000
4076	S228	1	1523.054	52.719	2.361	12.074	0.000	0.000	-1.693 0.077	13.343	-0.732	11.637	0.000	0.000	0.000	0.000
4080	O228	1	1523.296	51.583	2.331	12.075	0.000	0.000	-1.674 0.077	13.705	-0.760	11.640	0.000	0.000	0.000	0.000
4090	DIPOLE_A	54	1529.851	26.383	1.514	12.104	0.000	0.000	-1.236 0.056	28.602	-1.512	11.694	0.000	0.000	0.000	0.000
4102	DIPOLE_B	54	1536.307	12.040	0.708	12.163	0.000	0.000	-0.940 0.035	52.901	-2.251	11.720	0.000	0.000	0.000	0.000
4117	VC229	1	1537.475	10.555	0.563	12.179	0.000	0.000	-0.899 0.035	58.317	-2.385	11.724	0.000	0.000	0.000	0.000
4122	M_229	1	1538.675	9.827	0.006	12.198	0.000	0.000	-0.877-0.002	61.437	0.109	11.727	0.000	0.000	0.000	0.000
4133	DIPOLE_C	29	1544.979	21.582	-1.454	12.272	0.000	0.000	-1.209-0.068	28.109	2.337	11.750	0.000	0.000	0.000	0.000
4145	DIPOLE_D	29	1549.402	37.269	-2.092	12.297	0.000	0.000	-1.539-0.082	11.927	1.321	11.789	0.000	0.000	0.000	0.000
4157	HC230	1	1550.048	40.033	-2.186	12.300	0.000	0.000	-1.592-0.082	10.316	1.172	11.798	0.000	0.000	0.000	0.000

1
Linear lattice functions for beam line: MI_19
delta(p)/p = 0.000000 symm = F

"MAD" Version: 8.17 Run: 09/09/94 15.47.38
Range: #S/#E

page 11

ELEMENT SEQUENCE			I		H O R I Z O N T A L						I		V E R T I C A L						
pos.	element	occ.	dist	I	betax	alfax	mux	x(co)	px(co)	Dx	Dpx	I	betay	alfay	muy	y(co)	py(co)	Dy	Dpy
no.	name	no.	[m]	I	[m]	[1]	[2pi]	[mm]	[.001]	[m]	[1]	I	[m]	[1]	[2pi]	[mm]	[.001]	[m]	[1]
4162	M_230	1	1551.642		43.524	0.251	12.306	0.000	0.000	-1.651	0.016		7.886	0.358	11.827	0.000	0.000	0.000	0.000
4173	DIPOLE_C	30	1557.945		18.544	1.650	12.340	0.000	0.000	-1.044	0.098		13.939	-0.972	11.934	0.000	0.000	0.000	0.000
4185	DIPOLE_D	30	1562.368		7.876	0.762	12.400	0.000	0.000	-0.639	0.084		25.266	-1.588	11.972	0.000	0.000	0.000	0.000
4197	VC231	1	1563.015		6.975	0.632	12.414	0.000	0.000	-0.585	0.084		27.377	-1.678	11.976	0.000	0.000	0.000	0.000
4202	M_231	1	1564.608		5.980	-0.018	12.454	0.000	0.000	-0.474	0.054		30.470	-0.077	11.985	0.000	0.000	0.000	0.000
4213	DIPOLE_C	31	1570.911		18.024	-1.643	12.562	0.000	0.000	-0.307	0.014		15.921	0.976	12.029	0.000	0.000	0.000	0.000
4225	DIPOLE_D	31	1575.335		36.574	-2.551	12.590	0.000	0.000	-0.274	0.000		9.683	0.434	12.087	0.000	0.000	0.000	0.000
4237	HC232	1	1575.981		39.957	-2.684	12.592	0.000	0.000	-0.273	0.000		9.174	0.355	12.098	0.000	0.000	0.000	0.000
4242	M_232	1	1577.574		45.097	-0.250	12.598	0.000	0.000	-0.261	0.016		9.125	-0.364	12.127	0.000	0.000	0.000	0.000
4253	DIPOLE_C	32	1583.878		23.319	1.573	12.628	0.000	0.000	-0.105	0.017		27.965	-2.236	12.194	0.000	0.000	0.000	0.000
4265	DIPOLE_D	32	1588.301		12.317	0.914	12.670	0.000	0.000	-0.059	0.003		51.938	-3.183	12.212	0.000	0.000	0.000	0.000
4277	VC301	1	1588.948		11.198	0.818	12.679	0.000	0.000	-0.057	0.003		56.142	-3.321	12.214	0.000	0.000	0.000	0.000
4282	M_301	1	1590.541		9.814	0.030	12.704	0.000	0.000	-0.054	0.000		61.954	0.044	12.218	0.000	0.000	0.000	0.000
4296	HC302	1	1606.617		52.918	-2.333	12.832	0.000	0.000	-0.093-0.002			11.055	0.643	12.321	0.000	0.000	0.000	0.000

4301	M_302	1	1607.829	56.176	-0.026	12.835	0.000	0.000	-0.093	0.002	10.153	0.059	12.339	0.000	0.000	0.000	0.000
4313	VC303	1	1623.905	11.005	0.541	12.944	0.000	0.000	-0.007	0.006	51.903	-2.256	12.466	0.000	0.000	0.000	0.000
4318	M_303	1	1625.118	10.328	-0.028	12.963	0.000	0.000	0.000	0.005	55.074	-0.044	12.470	0.000	0.000	0.000	0.000
4330	HC304	1	1641.194	56.138	-2.423	13.082	0.000	0.000	0.089	0.006	11.727	0.540	12.576	0.000	0.000	0.000	0.000
4335	M_304	1	1642.407	59.464	0.027	13.085	0.000	0.000	0.093	0.002	11.086	-0.062	12.593	0.000	0.000	0.000	0.000
4347	VC305	1	1658.482	10.575	0.585	13.193	0.000	0.000	0.056	-0.002	58.942	-2.478	12.704	0.000	0.000	0.000	0.000
4352	M_305	1	1659.695	9.783	0.027	13.213	0.000	0.000	0.054	0.000	62.329	0.040	12.707	0.000	0.000	0.000	0.000
4364	HC306	1	1675.771	53.068	-2.343	13.341	0.000	0.000	0.088	0.002	11.170	0.652	12.809	0.000	0.000	0.000	0.000
4369	M_306	1	1676.984	56.344	-0.029	13.344	0.000	0.000	0.088	-0.002	10.248	0.065	12.827	0.000	0.000	0.000	0.000
4381	VC307	1	1693.060	11.042	0.545	13.453	0.000	0.000	0.004	-0.005	51.611	-2.234	12.954	0.000	0.000	0.000	0.000
4386	M_307	1	1694.273	10.357	-0.025	13.471	0.000	0.000	-0.003	-0.005	54.742	-0.035	12.958	0.000	0.000	0.000	0.000
4398	HC308	1	1710.348	55.979	-2.413	13.590	0.000	0.000	-0.093	-0.006	11.610	0.531	13.065	0.000	0.000	0.000	0.000
4403	M_308	1	1711.561	59.288	0.030	13.594	0.000	0.000	-0.098	-0.001	10.987	-0.067	13.082	0.000	0.000	0.000	0.000
4416	VC309	1	1727.650	10.524	0.579	13.702	0.000	0.000	-0.056	0.003	59.260	-2.500	13.194	0.000	0.000	0.000	0.000
4421	M_309	1	1728.850	9.756	0.023	13.721	0.000	0.000	-0.054	0.000	62.618	0.034	13.197	0.000	0.000	0.000	0.000
4432	DIPOLE_C	33	1735.153	21.197	-1.424	13.796	0.000	0.000	-0.097	-0.017	29.253	2.364	13.219	0.000	0.000	0.000	0.000
4444	DIPOLE_D	33	1739.577	36.588	-2.056	13.822	0.000	0.000	-0.199	-0.031	12.744	1.368	13.256	0.000	0.000	0.000	0.000
4456	HC310	1	1740.223	39.304	-2.148	13.824	0.000	0.000	-0.219	-0.031	11.069	1.223	13.265	0.000	0.000	0.000	0.000
4461	M_310	1	1741.816	42.741	0.243	13.830	0.000	0.000	-0.257	-0.016	8.524	0.379	13.292	0.000	0.000	0.000	0.000
4472	DIPOLE_C	34	1748.120	18.269	1.615	13.865	0.000	0.000	-0.299	-0.014	14.332	-0.925	13.392	0.000	0.000	0.000	0.000
4484	DIPOLE_D	34	1752.543	7.848	0.741	13.926	0.000	0.000	-0.391	-0.028	25.050	-1.497	13.430	0.000	0.000	0.000	0.000
4496	VC311	1	1753.189	6.972	0.614	13.939	0.000	0.000	-0.409	-0.028	27.040	-1.581	13.434	0.000	0.000	0.000	0.000
4501	M_311	1	1754.783	6.033	-0.035	13.980	0.000	0.000	-0.472	-0.054	29.844	0.000	13.443	0.000	0.000	0.000	0.000
4512	DIPOLE_C	35	1761.086	18.348	-1.668	14.086	0.000	0.000	-1.007	-0.098	15.021	0.972	13.489	0.000	0.000	0.000	0.000
4524	DIPOLE_D	35	1765.510	37.132	-2.579	14.113	0.000	0.000	-1.468	-0.112	8.955	0.400	13.551	0.000	0.000	0.000	0.000
4536	HC312	1	1766.156	40.552	-2.712	14.116	0.000	0.000	-1.540	-0.112	8.493	0.316	13.563	0.000	0.000	0.000	0.000
4541	M_312	1	1767.749	45.728	-0.241	14.122	0.000	0.000	-1.648	-0.016	8.531	-0.379	13.593	0.000	0.000	0.000	0.000
4552	DIPOLE_C	36	1774.053	23.518	1.603	14.151	0.000	0.000	-1.232	0.068	27.592	-2.283	13.664	0.000	0.000	0.000	0.000
4564	DIPOLE_D	36	1778.476	12.305	0.932	14.193	0.000	0.000	-0.960	0.054	52.184	-3.276	13.682	0.000	0.000	0.000	0.000
4576	VC313	1	1779.122	11.165	0.834	14.202	0.000	0.000	-0.925	0.054	56.513	-3.421	13.684	0.000	0.000	0.000	0.000
4581	M_313	1	1780.716	9.732	0.047	14.227	0.000	0.000	-0.877	0.002	62.621	-0.033	13.688	0.000	0.000	0.000	0.000
4591	S313	1	1782.478	10.927	-0.570	14.255	0.000	0.000	-0.919	-0.035	56.486	2.432	13.693	0.000	0.000	0.000	0.000
4600	DIPOLE_A	55	1789.180	24.009	-1.382	14.323	0.000	0.000	-1.219	-0.056	29.365	1.614	13.719	0.000	0.000	0.000	0.000

"MAD" Version: 8.17 Run: 09/09/94 15.47.38

Range: #S/#E

1 Linear lattice functions for beam line: MI_19

delta(p)/p = 0.000000 symm = F

page 12

ELEMENT SEQUENCE				H O R I Z O N T A L								V E R T I C A L							
pos.	element	occ.	dist	I	betax	alfax	mux	x(co)	px(co)	Dx	Dpx	I	betay	alfay	muy	y(co)	py(co)	Dy	Dpy
no.	name	no.	[m]	I	[m]	[1]	[2pi]	[mm]	[.001]	[m]	[1]	I	[m]	[1]	[2pi]	[mm]	[.001]	[m]	[1]
4612	DIPOLE_B	55	1795.635		46.906	-2.165	14.353	0.000	0.000	-1.644	-0.077		13.637	0.822	13.771	0.000	0.000	0.000	0.000
4624	HC314	1	1796.772		51.984	-2.303	14.357	0.000	0.000	-1.731	-0.077		11.927	0.683	13.786	0.000	0.000	0.000	0.000
4629	M_314	1	1798.004		55.302	-0.035	14.361	0.000	0.000	-1.785	-0.001		10.936	0.069	13.803	0.000	0.000	0.000	0.000
4635	S314	1	1799.672		50.220	2.189	14.366	0.000	0.000	-1.700	0.076		12.054	-0.577	13.827	0.000	0.000	0.000	0.000
4639	O314	1	1799.914		49.167	2.161	14.366	0.000	0.000	-1.681	0.076		12.340	-0.604	13.830	0.000	0.000	0.000	0.000
4649	DIPOLE_A	56	1806.468		25.790	1.405	14.396	0.000	0.000	-1.249	0.055		25.006	-1.328	13.891	0.000	0.000	0.000	0.000
4661	DIPOLE_B	56	1812.924		12.454	0.661	14.454	0.000	0.000	-0.958	0.034		46.735	-2.038	13.921	0.000	0.000	0.000	0.000
4676	VC315	1	1814.092		11.067	0.526	14.470	0.000	0.000	-0.918	0.034		51.646	-2.166	13.925	0.000	0.000	0.000	0.000
4681	M_315	1	1815.292		10.439	-0.045	14.488	0.000	0.000	-0.898	-0.004		54.548	0.037	13.928	0.000	0.000	0.000	0.000
4692	DIPOLE_C	37	1821.596		23.304	-1.553	14.557	0.000	0.000	-1.248	-0.071		25.586	2.036	13.954	0.000	0.000	0.000	0.000
4704	DIPCOND	37	1826.019		39.911	-2.201	14.580	0.000	0.000	-1.591	-0.085		11.507	1.147	13.996	0.000	0.000	0.000	0.000

4716	HC316	1	1826.666	42.817	-2.296	14.583	0.000	0.000	-1.646-0.085	10.109	1.017	14.005	0.000	0.000	0.000	0.000
4721	M_316	1	1828.259	46.406	0.314	14.588	0.000	0.000	-1.707 0.016	8.110	0.235	14.034	0.000	0.000	0.000	0.000
4732	DIPOLE_C	38	1834.562	19.304	1.786	14.621	0.000	0.000	-1.080 0.102	15.939	-1.122	14.131	0.000	0.000	0.000	0.000
4744	DIPOLE_D	38	1838.986	7.749	0.826	14.680	0.000	0.000	-0.659 0.088	28.640	-1.748	14.164	0.000	0.000	0.000	0.000
4756	VC317	1	1839.632	6.772	0.686	14.694	0.000	0.000	-0.603 0.088	30.959	-1.840	14.168	0.000	0.000	0.000	0.000
4761	M_317	1	1841.225	5.623	0.030	14.736	0.000	0.000	-0.487 0.056	34.244	-0.015	14.176	0.000	0.000	0.000	0.000
4772	DIPOLE_C	39	1847.529	17.014	-1.603	14.853	0.000	0.000	-0.306 0.016	17.016	1.164	14.216	0.000	0.000	0.000	0.000
4784	DIPOLE_D	39	1851.952	35.295	-2.530	14.882	0.000	0.000	-0.263 0.002	9.423	0.552	14.273	0.000	0.000	0.000	0.000
4796	HC318	1	1852.598	38.653	-2.666	14.884	0.000	0.000	-0.262 0.002	8.767	0.463	14.284	0.000	0.000	0.000	0.000
4801	M_318	1	1854.192	43.862	-0.316	14.890	0.000	0.000	-0.247 0.018	8.356	-0.236	14.315	0.000	0.000	0.000	0.000
4812	DIPOLE_C	40	1860.495	23.351	1.497	14.921	0.000	0.000	-0.088 0.017	24.448	-1.960	14.390	0.000	0.000	0.000	0.000
4824	DIPOLE_D	40	1864.919	12.824	0.883	14.962	0.000	0.000	-0.039 0.003	45.653	-2.833	14.411	0.000	0.000	0.000	0.000
4836	VC319	1	1865.565	11.741	0.793	14.970	0.000	0.000	-0.037 0.003	49.398	-2.961	14.413	0.000	0.000	0.000	0.000
4841	M_319	1	1867.158	10.460	-0.015	14.994	0.000	0.000	-0.033 0.001	54.651	-0.007	14.418	0.000	0.000	0.000	0.000
4855	HC320	1	1883.234	55.445	-2.380	15.113	0.000	0.000	-0.031 0.000	11.252	0.519	14.528	0.000	0.000	0.000	0.000
4860	M_320	1	1884.447	58.697	0.040	15.116	0.000	0.000	-0.031 0.001	10.645	-0.067	14.545	0.000	0.000	0.000	0.000
4872	VC321	1	1900.522	10.414	0.566	15.226	0.000	0.000	0.012 0.003	59.019	-2.523	14.659	0.000	0.000	0.000	0.000
4877	M_321	1	1901.735	9.662	0.013	15.246	0.000	0.000	0.015 0.003	62.512	-0.002	14.662	0.000	0.000	0.000	0.000
4890	HC322	1	1917.824	53.874	-2.389	15.374	0.000	0.000	0.079 0.004	11.611	0.668	14.762	0.000	0.000	0.000	0.000
4895	M_322	1	1919.024	57.160	-0.037	15.377	0.000	0.000	0.082 0.000	10.682	0.066	14.779	0.000	0.000	0.000	0.000
4906	DIPOLE_C	41	1925.327	26.838	2.145	15.402	0.000	0.000	0.030-0.018	21.922	-1.384	14.849	0.000	0.000	0.000	0.000
4918	DIPOLE_D	41	1929.751	11.946	1.222	15.442	0.000	0.000	-0.079-0.032	36.765	-1.971	14.874	0.000	0.000	0.000	0.000
4930	VC323	1	1930.397	10.454	1.087	15.451	0.000	0.000	-0.100-0.032	39.368	-2.057	14.877	0.000	0.000	0.000	0.000
4935	M_323	1	1931.990	8.252	0.295	15.479	0.000	0.000	-0.156-0.040	42.581	0.283	14.883	0.000	0.000	0.000	0.000
4946	DIPOLE_C	42	1938.294	15.075	-1.024	15.578	0.000	0.000	-0.495-0.065	18.262	1.602	14.918	0.000	0.000	0.000	0.000
4958	DIPOLE_D	42	1942.717	26.789	-1.624	15.614	0.000	0.000	-0.809-0.078	7.907	0.738	14.978	0.000	0.000	0.000	0.000
4970	HC324	1	1943.364	28.945	-1.712	15.617	0.000	0.000	-0.860-0.078	7.034	0.612	14.992	0.000	0.000	0.000	0.000
4975	M_324	1	1944.957	31.942	0.027	15.625	0.000	0.000	-0.945-0.024	6.111	-0.045	15.032	0.000	0.000	0.000	0.000
4986	DIPOLE_C	43	1951.260	15.389	1.088	15.670	0.000	0.000	-0.809 0.019	18.709	-1.693	15.136	0.000	0.000	0.000	0.000
4998	DIPOLE_D	43	1955.684	8.541	0.460	15.733	0.000	0.000	-0.755 0.005	37.729	-2.606	15.163	0.000	0.000	0.000	0.000
5010	VC325	1	1956.330	8.006	0.369	15.745	0.000	0.000	-0.752 0.005	41.183	-2.739	15.165	0.000	0.000	0.000	0.000
5015	M_325	1	1957.923	7.840	-0.296	15.778	0.000	0.000	-0.777-0.039	46.473	-0.286	15.171	0.000	0.000	0.000	0.000
5026	DIPOLE_C	44	1964.227	24.916	-2.088	15.855	0.000	0.000	-1.319-0.101	24.684	1.595	15.200	0.000	0.000	0.000	0.000
5038	DIPOLE_D	44	1968.650	47.591	-3.039	15.876	0.000	0.000	-1.794-0.115	13.378	0.961	15.239	0.000	0.000	0.000	0.000
5050	HC326	1	1969.296	51.608	-3.178	15.878	0.000	0.000	-1.868-0.115	12.196	0.868	15.247	0.000	0.000	0.000	0.000
5055	M_326	1	1970.890	57.265	-0.017	15.882	0.000	0.000	-1.967 0.000	10.738	0.023	15.270	0.000	0.000	0.000	0.000

1
Linear lattice functions for beam line: MI_19
delta(p)/p = 0.000000 symm = F

"MAD" Version: 8.17 Run: 09/09/94 15.47.38
Range: #S/#E

page 13

ELEMENT SEQUENCE			H O R I Z O N T A L										V E R T I C A L						
pos.	element	occ.	dist	I	betax	alfax	mux	x(co)	px(co)	Dx	Dpx	I	betay	alfay	muy	y(co)	py(co)	Dy	Dpy
no.	name	no.	[m]	I	[m]	[1]	[2pi]	[mm]	[.001]	[m]	[1]	I	[m]	[1]	[2pi]	[mm]	[.001]	[m]	[1]
5065	S326	1	1972.633		51.585	2.280	15.887	0.000	0.000	-1.864	0.085		12.100	-0.633	15.294	0.000	0.000	0.000	0.000
5069	O326	1	1972.875		50.488	2.251	15.888	0.000	0.000	-1.843	0.085		12.413	-0.661	15.298	0.000	0.000	0.000	0.000
5078	DIPOLE_A	57	1979.354		26.366	1.472	15.917	0.000	0.000	-1.359	0.064		25.825	-1.409	15.357	0.000	0.000	0.000	0.000
5090	DIPOLE_B	57	1985.810		12.363	0.697	15.975	0.000	0.000	-1.010	0.043		48.816	-2.152	15.386	0.000	0.000	0.000	0.000
5102	VC327	1	1986.946		10.935	0.560	15.990	0.000	0.000	-0.962	0.043		53.857	-2.283	15.389	0.000	0.000	0.000	0.000
5107	M_327	1	1988.178		10.194	-0.009	16.009	0.000	0.000	-0.930	0.003		57.089	0.016	15.393	0.000	0.000	0.000	0.000
5113	S327	1	1989.846		11.511	-0.634	16.034	0.000	0.000	-0.969	-0.036		51.790	2.260	15.397	0.000	0.000	0.000	0.000
5123	DIPOLE_A	58	1996.643		25.747	-1.461	16.099	0.000	0.000	-1.277	-0.057		26.503	1.460	15.427	0.000	0.000	0.000	0.000

5135	DIPOLE_B	58	2003.098	49.682	-2.247	16.128	0.000	0.000	-1.708-0.078	12.569	0.698	15.484	0.000	0.000	0.000	0.000
5147	QC328	1	2003.819	52.984	-2.335	16.130	0.000	0.000	-1.764-0.078	11.624	0.613	15.494	0.000	0.000	0.000	0.000
5151	HC328	1	2004.235	54.947	-2.385	16.131	0.000	0.000	-1.796-0.078	11.135	0.563	15.500	0.000	0.000	0.000	0.000
5156	M_328	1	2005.466	58.329	0.014	16.134	0.000	0.000	-1.850 0.001	10.403	-0.022	15.518	0.000	0.000	0.000	0.000
5162	S328	1	2007.134	52.804	2.356	16.139	0.000	0.000	-1.758 0.080	11.802	-0.665	15.543	0.000	0.000	0.000	0.000
5166	O328	1	2007.376	51.671	2.326	16.140	0.000	0.000	-1.738 0.080	12.131	-0.694	15.546	0.000	0.000	0.000	0.000
5176	DIPOLE_A	59	2013.931	26.509	1.513	16.168	0.000	0.000	-1.275 0.060	26.475	-1.493	15.605	0.000	0.000	0.000	0.000
5188	DIPOLE_B	59	2020.386	12.147	0.712	16.227	0.000	0.000	-0.954 0.039	50.824	-2.278	15.633	0.000	0.000	0.000	0.000
5200	VC329	1	2021.523	10.689	0.571	16.243	0.000	0.000	-0.910 0.039	56.158	-2.416	15.637	0.000	0.000	0.000	0.000
5205	M_329	1	2022.755	9.916	0.008	16.262	0.000	0.000	-0.883 0.001	59.616	-0.017	15.640	0.000	0.000	0.000	0.000
5211	S329	1	2024.423	11.151	-0.606	16.288	0.000	0.000	-0.923-0.036	54.184	2.333	15.645	0.000	0.000	0.000	0.000
5221	DIPOLE_A	60	2031.219	25.048	-1.439	16.354	0.000	0.000	-1.233-0.057	27.945	1.527	15.673	0.000	0.000	0.000	0.000
5233	DIPOLE_B	60	2037.675	48.734	-2.230	16.384	0.000	0.000	-1.665-0.078	13.193	0.758	15.727	0.000	0.000	0.000	0.000
5245	QC330	1	2038.395	52.013	-2.319	16.386	0.000	0.000	-1.721-0.078	12.162	0.672	15.736	0.000	0.000	0.000	0.000
5249	HC330	1	2038.811	53.963	-2.370	16.387	0.000	0.000	-1.754-0.078	11.624	0.622	15.742	0.000	0.000	0.000	0.000
5254	M_330	1	2040.043	57.353	-0.014	16.391	0.000	0.000	-1.809-0.001	10.767	0.021	15.760	0.000	0.000	0.000	0.000
5260	S330	1	2041.711	52.010	2.292	16.396	0.000	0.000	-1.722 0.077	12.043	-0.627	15.783	0.000	0.000	0.000	0.000
5264	O330	1	2041.953	50.908	2.263	16.396	0.000	0.000	-1.704 0.077	12.354	-0.655	15.787	0.000	0.000	0.000	0.000
5274	DIPOLE_A	61	2048.508	26.411	1.475	16.425	0.000	0.000	-1.265 0.056	25.907	-1.412	15.846	0.000	0.000	0.000	0.000
5286	DIPOLE_B	61	2054.963	12.381	0.699	16.483	0.000	0.000	-0.968 0.035	48.937	-2.155	15.875	0.000	0.000	0.000	0.000
5303	VC331	1	2056.119	10.926	0.560	16.499	0.000	0.000	-0.928 0.035	54.071	-2.288	15.879	0.000	0.000	0.000	0.000
5308	M_331	1	2057.332	10.203	-0.008	16.518	0.000	0.000	-0.906-0.003	57.217	0.019	15.882	0.000	0.000	0.000	0.000
5317	S331	1	2059.097	11.639	-0.644	16.544	0.000	0.000	-0.959-0.042	51.458	2.256	15.887	0.000	0.000	0.000	0.000
5327	DIPOLE_A	62	2065.796	25.722	-1.458	16.607	0.000	0.000	-1.304-0.063	26.527	1.465	15.916	0.000	0.000	0.000	0.000
5339	DIPOLE_B	62	2072.252	49.611	-2.243	16.636	0.000	0.000	-1.773-0.084	12.550	0.700	15.974	0.000	0.000	0.000	0.000
5351	QC332	1	2072.972	52.907	-2.330	16.638	0.000	0.000	-1.834-0.084	11.602	0.614	15.983	0.000	0.000	0.000	0.000
5355	HC332	1	2073.388	54.867	-2.381	16.639	0.000	0.000	-1.869-0.084	11.112	0.565	15.989	0.000	0.000	0.000	0.000
5360	M_332	1	2074.620	58.242	0.015	16.643	0.000	0.000	-1.928-0.001	10.376	-0.019	16.008	0.000	0.000	0.000	0.000
5366	S332	1	2076.288	52.723	2.353	16.648	0.000	0.000	-1.837 0.081	11.764	-0.661	16.032	0.000	0.000	0.000	0.000
5370	O332	1	2076.530	51.591	2.323	16.648	0.000	0.000	-1.817 0.081	12.092	-0.691	16.035	0.000	0.000	0.000	0.000
5380	DIPOLE_A	63	2083.085	26.464	1.510	16.677	0.000	0.000	-1.349 0.060	26.390	-1.490	16.095	0.000	0.000	0.000	0.000
5392	DIPOLE_B	63	2089.540	12.130	0.710	16.735	0.000	0.000	-1.024 0.039	50.695	-2.274	16.124	0.000	0.000	0.000	0.000
5404	VC333	1	2090.677	10.677	0.569	16.751	0.000	0.000	-0.979 0.039	56.022	-2.413	16.127	0.000	0.000	0.000	0.000
5409	M_333	1	2091.909	9.908	0.007	16.771	0.000	0.000	-0.952-0.001	59.479	-0.020	16.130	0.000	0.000	0.000	0.000
5415	S333	1	2093.576	11.147	-0.607	16.796	0.000	0.000	-0.999-0.041	54.067	2.325	16.135	0.000	0.000	0.000	0.000
5425	DIPOLE_A	64	2100.373	25.075	-1.442	16.863	0.000	0.000	-1.345-0.062	27.914	1.522	16.163	0.000	0.000	0.000	0.000
5437	DIPOLE_B	64	2106.828	48.807	-2.235	16.892	0.000	0.000	-1.810-0.083	13.209	0.756	16.217	0.000	0.000	0.000	0.000
5449	QC334	1	2107.549	52.092	-2.323	16.895	0.000	0.000	-1.870-0.083	12.182	0.670	16.226	0.000	0.000	0.000	0.000
5453	HC334	1	2107.965	54.046	-2.374	16.896	0.000	0.000	-1.905-0.083	11.645	0.621	16.232	0.000	0.000	0.000	0.000

1
Linear lattice functions for beam line: MI_19

delta(p)/p = 0.000000 symm = F

"MAD" Version: 8.17 Run: 09/09/94 15.47.38

Range: #S/#E

page 14

ELEMENT SEQUENCE				H O R I Z O N T A L								V E R T I C A L							
pos.	element	occ.	dist	I	betax	alfax	mux	x(co)	px(co)	Dx	Dpx	I	betay	alfay	muy	y(co)	py(co)	Dy	Dpy
no.	name	no.	[m]	I	[m]	[1]	[2pi]	[mm]	[.001]	[m]	[1]	I	[m]	[1]	[2pi]	[mm]	[.001]	[m]	[1]
5458	M_334	1	2109.197		57.443	-0.015	16.899	0.000	0.000	-1.963	0.001		10.793	0.018	16.250	0.000	0.000	0.000	0.000
5464	S334	1	2110.865		52.094	2.295	16.904	0.000	0.000	-1.866	0.085		12.080	-0.631	16.273	0.000	0.000	0.000	0.000
5468	O334	1	2111.107		50.990	2.266	16.905	0.000	0.000	-1.846	0.085		12.392	-0.659	16.277	0.000	0.000	0.000	0.000
5478	DIPOLE_A	65	2117.661		26.457	1.477	16.934	0.000	0.000	-1.355	0.064		25.994	-1.416	16.336	0.000	0.000	0.000	0.000
5490	DIPOLE_B	65	2124.117		12.397	0.701	16.992	0.000	0.000	-1.207	0.043		49.072	-2.158	16.365	0.000	0.000	0.000	0.000

5502	SQ335	1	2124.834	11.454	0.615	17.001	0.000	0.000	-0.976	0.043	52.229	-2.241	16.367	0.000	0.000	0.000	0.000
5506	VC335	1	2125.253	10.960	0.564	17.007	0.000	0.000	-0.958	0.043	54.128	-2.289	16.368	0.000	0.000	0.000	0.000
5511	M_335	1	2126.485	10.211	-0.006	17.026	0.000	0.000	-0.926	0.004	57.364	0.021	16.372	0.000	0.000	0.000	0.000
5517	S335	1	2128.153	11.517	-0.631	17.051	0.000	0.000	-0.965	-0.036	52.023	2.275	16.377	0.000	0.000	0.000	0.000
5527	DIPOLE_A	66	2134.950	25.693	-1.455	17.115	0.000	0.000	-1.271	-0.057	26.563	1.470	16.406	0.000	0.000	0.000	0.000
5539	DIPOLE_B	66	2141.405	49.536	-2.239	17.144	0.000	0.000	-1.700	-0.077	12.536	0.703	16.464	0.000	0.000	0.000	0.000
5551	SQ336	1	2141.894	51.754	-2.298	17.146	0.000	0.000	-1.738	-0.077	11.877	0.644	16.470	0.000	0.000	0.000	0.000
5555	SQ336	2	2142.123	52.811	-2.326	17.147	0.000	0.000	-1.756	-0.077	11.589	0.617	16.473	0.000	0.000	0.000	0.000
5559	HC336	1	2142.542	54.782	-2.376	17.148	0.000	0.000	-1.788	-0.077	11.093	0.567	16.479	0.000	0.000	0.000	0.000
5564	M_336	1	2143.774	58.149	0.015	17.151	0.000	0.000	-1.842	0.001	10.351	-0.017	16.497	0.000	0.000	0.000	0.000
5570	S336	1	2145.441	52.637	2.350	17.156	0.000	0.000	-1.750	0.080	11.729	-0.658	16.522	0.000	0.000	0.000	0.000
5574	O336	1	2145.684	51.507	2.320	17.157	0.000	0.000	-1.731	0.080	12.054	-0.687	16.525	0.000	0.000	0.000	0.000
5584	DIPOLE_A	67	2152.238	26.418	1.508	17.185	0.000	0.000	-1.270	0.059	26.302	-1.486	16.585	0.000	0.000	0.000	0.000
5596	DIPOLE_B	67	2158.694	12.115	0.708	17.244	0.000	0.000	-0.952	0.038	50.553	-2.270	16.614	0.000	0.000	0.000	0.000
5608	SQ337	1	2159.411	11.163	0.619	17.254	0.000	0.000	-0.925	0.038	53.873	-2.357	16.616	0.000	0.000	0.000	0.000
5612	VC337	1	2159.830	10.666	0.567	17.260	0.000	0.000	-0.909	0.038	55.871	-2.408	16.617	0.000	0.000	0.000	0.000
5617	M_337	1	2161.062	9.902	0.005	17.279	0.000	0.000	-0.882	0.001	59.323	-0.022	16.620	0.000	0.000	0.000	0.000
5623	S337	1	2162.730	11.146	-0.609	17.305	0.000	0.000	-0.923	-0.037	53.933	2.317	16.625	0.000	0.000	0.000	0.000
5633	DIPOLE_A	68	2169.527	25.105	-1.445	17.371	0.000	0.000	-1.235	-0.057	27.873	1.516	16.653	0.000	0.000	0.000	0.000
5645	DIPOLE_B	68	2175.982	48.884	-2.239	17.401	0.000	0.000	-1.669	-0.078	13.220	0.753	16.708	0.000	0.000	0.000	0.000
5660	HC338	1	2177.150	54.284	-2.383	17.405	0.000	0.000	-1.761	-0.078	11.623	0.615	16.723	0.000	0.000	0.000	0.000
5665	M_338	1	2178.351	57.534	-0.012	17.408	0.000	0.000	-1.813	-0.001	10.816	0.015	16.740	0.000	0.000	0.000	0.000
5676	DIPOLE_C	45	2184.654	26.800	2.168	17.433	0.000	0.000	-1.253	0.092	23.000	-1.477	16.808	0.000	0.000	0.000	0.000
5688	DIPOLE_D	45	2189.078	11.785	1.227	17.473	0.000	0.000	-0.875	0.078	38.768	-2.087	16.831	0.000	0.000	0.000	0.000
5700	VC339	1	2189.724	10.287	1.090	17.482	0.000	0.000	-0.825	0.078	41.524	-2.176	16.834	0.000	0.000	0.000	0.000
5705	M_339	1	2191.317	8.072	0.302	17.510	0.000	0.000	-0.734	0.033	44.928	0.296	16.840	0.000	0.000	0.000	0.000
5716	DIPOLE_C	46	2197.621	14.787	-1.021	17.612	0.000	0.000	-0.788	-0.023	19.199	1.705	16.873	0.000	0.000	0.000	0.000
5728	DIPOLE_D	46	2202.044	26.521	-1.632	17.648	0.000	0.000	-0.917	-0.037	8.097	0.805	16.931	0.000	0.000	0.000	0.000
5740	HC340	1	2202.690	28.688	-1.721	17.652	0.000	0.000	-0.941	-0.037	7.141	0.673	16.944	0.000	0.000	0.000	0.000
5745	M_340	1	2204.283	31.739	0.002	17.660	0.000	0.000	-0.958	0.020	6.042	0.008	16.984	0.000	0.000	0.000	0.000
5756	DIPOLE_C	47	2210.587	15.508	1.072	17.704	0.000	0.000	-0.549	0.062	17.731	-1.604	17.093	0.000	0.000	0.000	0.000
5768	DIPOLE_D	47	2215.010	8.739	0.459	17.766	0.000	0.000	-0.303	0.048	35.858	-2.494	17.121	0.000	0.000	0.000	0.000
5780	VC341	1	2215.657	8.203	0.369	17.779	0.000	0.000	-0.272	0.048	39.165	-2.624	17.124	0.000	0.000	0.000	0.000
5785	M_341	1	2217.250	8.044	-0.302	17.811	0.000	0.000	-0.206	0.034	44.263	-0.295	17.130	0.000	0.000	0.000	0.000
5796	DIPOLE_C	48	2223.553	25.242	-2.092	17.886	0.000	0.000	-0.079	0.010	23.781	1.499	17.160	0.000	0.000	0.000	0.000
5808	DIPOLE_D	48	2227.977	47.921	-3.035	17.907	0.000	0.000	-0.065	-0.004	13.189	0.896	17.200	0.000	0.000	0.000	0.000
5820	HC400	1	2228.623	51.932	-3.173	17.909	0.000	0.000	-0.067	-0.004	12.088	0.807	17.208	0.000	0.000	0.000	0.000
5825	M_400	1	2230.216	57.541	0.008	17.913	0.000	0.000	-0.071	0.000	10.807	-0.030	17.231	0.000	0.000	0.000	0.000
5839	VC401	1	2246.292	10.655	0.554	18.023	0.000	0.000	-0.026	0.003	56.992	-2.417	17.346	0.000	0.000	0.000	0.000
5844	M_401	1	2247.505	9.937	-0.005	18.042	0.000	0.000	-0.023	0.002	60.319	0.016	17.349	0.000	0.000	0.000	0.000
5853	HC402	1	2249.120	11.156	-0.615	18.067	0.000	0.000	-0.021	0.001	54.968	2.397	17.353	0.000	0.000	0.000	0.000
5861	M_402	1	2264.794	58.136	-0.012	18.169	0.000	0.000	-0.005	0.001	10.457	0.032	17.470	0.000	0.000	0.000	0.000

1
Linear lattice functions for beam line: MI_19

delta(p)/p = 0.000000 symm = F

"MAD" Version: 8.17 Run: 09/09/94 15.47.38

Range: #S/#E

page 15

ELEMENT SEQUENCE				H O R I Z O N T A L										V E R T I C A L					
pos.	element	occ.	dist	I	betax	alfax	mux	x(co)	px(co)	Dx	Dpx	I	betay	alfay	muy	y(co)	py(co)	Dy	Dpy
no.	name	no.	[m]	I	[m]	[1]	[2pi]	[mm]	[.001]	[m]	[1]	I	[m]	[1]	[2pi]	[mm]	[.001]	[m]	[1]
5873	VC403	1	2280.869		10.927	0.574	18.277	0.000	0.000	0.018	0.001		53.403	-2.291	17.592	0.000	0.000	0.000	0.000
5878	M_403	1	2282.082		10.172	0.006	18.295	0.000	0.000	0.020	0.002		56.590	-0.014	17.596	0.000	0.000	0.000	0.000

5891	HC404	1	2298.171	54.285	-2.356	18.418	0.000	0.000	0.069	0.003	11.441	0.559	17.702	0.000	0.000	0.000	0.000
5896	M_404	1	2299.371	57.469	0.015	18.422	0.000	0.000	0.072	0.000	10.758	-0.034	17.719	0.000	0.000	0.000	0.000
5907	DIPOLE_C	49	2305.674	26.551	2.173	18.447	0.000	0.000	0.020	-0.018	23.765	-1.563	17.786	0.000	0.000	0.000	0.000
5919	DIPOLE_D	49	2310.098	11.546	1.220	18.487	0.000	0.000	-0.088	-0.032	40.419	-2.202	17.809	0.000	0.000	0.000	0.000
5931	VC405	1	2310.744	10.059	1.080	18.497	0.000	0.000	-0.109	-0.032	43.325	-2.295	17.812	0.000	0.000	0.000	0.000
5936	M_405	1	2312.337	7.862	0.300	18.526	0.000	0.000	-0.165	-0.040	46.951	0.288	17.817	0.000	0.000	0.000	0.000
5947	DIPOLE_C	50	2318.641	14.595	-1.031	18.630	0.000	0.000	-0.509	-0.065	20.156	1.788	17.849	0.000	0.000	0.000	0.000
5959	DIPOLE_D	50	2323.064	26.484	-1.657	18.667	0.000	0.000	-0.826	-0.079	8.410	0.867	17.904	0.000	0.000	0.000	0.000
5971	HC406	1	2323.710	28.684	-1.748	18.670	0.000	0.000	-0.878	-0.079	7.376	0.733	17.917	0.000	0.000	0.000	0.000
5976	M_406	1	2325.304	31.824	-0.025	18.679	0.000	0.000	-0.964	-0.024	6.110	0.055	17.956	0.000	0.000	0.000	0.000
5987	DIPOLE_C	51	2331.607	15.764	1.068	18.722	0.000	0.000	-0.820	0.020	16.961	-1.515	18.067	0.000	0.000	0.000	0.000
5999	DIPOLE_D	51	2336.031	8.975	0.467	18.783	0.000	0.000	-0.760	0.006	34.158	-2.372	18.096	0.000	0.000	0.000	0.000
6011	VC407	1	2336.677	8.428	0.379	18.795	0.000	0.000	-0.756	0.006	37.305	-2.498	18.099	0.000	0.000	0.000	0.000
6016	M_407	1	2338.270	8.247	-0.299	18.826	0.000	0.000	-0.779	-0.038	42.163	-0.283	18.105	0.000	0.000	0.000	0.000
6027	DIPOLE_C	52	2344.574	25.397	-2.079	18.900	0.000	0.000	-1.314	-0.100	22.755	1.414	18.137	0.000	0.000	0.000	0.000
6039	DIPOLE_D	52	2348.997	47.887	-3.006	18.921	0.000	0.000	-1.785	-0.114	12.821	0.832	18.178	0.000	0.000	0.000	0.000
6051	HC408	1	2349.643	51.859	-3.141	18.923	0.000	0.000	-1.858	-0.114	11.801	0.746	18.187	0.000	0.000	0.000	0.000
6056	M_408	1	2351.236	57.371	0.035	18.927	0.000	0.000	-1.956	0.001	10.688	-0.077	18.210	0.000	0.000	0.000	0.000
6066	S408	1	2352.980	51.511	2.329	18.932	0.000	0.000	-1.853	0.085	12.419	-0.748	18.234	0.000	0.000	0.000	0.000
6070	O408	1	2353.222	50.390	2.299	18.933	0.000	0.000	-1.832	0.085	12.789	-0.778	18.237	0.000	0.000	0.000	0.000
6079	DIPOLE_A	69	2359.701	25.841	1.491	18.962	0.000	0.000	-1.348	0.064	28.133	-1.590	18.293	0.000	0.000	0.000	0.000
6091	DIPOLE_B	69	2366.156	11.791	0.686	19.022	0.000	0.000	-1.000	0.043	53.863	-2.395	18.319	0.000	0.000	0.000	0.000
6103	VC409	1	2367.293	10.393	0.544	19.038	0.000	0.000	-0.951	0.043	59.470	-2.537	18.323	0.000	0.000	0.000	0.000
6108	M_409	1	2368.525	9.677	-0.009	19.058	0.000	0.000	-0.919	0.004	63.076	0.005	18.326	0.000	0.000	0.000	0.000
6114	S409	1	2370.193	10.958	-0.620	19.084	0.000	0.000	-0.957	-0.035	57.249	2.492	18.330	0.000	0.000	0.000	0.000
6124	DIPOLE_A	70	2376.989	25.218	-1.478	19.151	0.000	0.000	-1.260	-0.056	29.177	1.638	18.357	0.000	0.000	0.000	0.000
6136	DIPOLE_B	70	2383.445	49.567	-2.294	19.181	0.000	0.000	-1.685	-0.077	13.263	0.824	18.410	0.000	0.000	0.000	0.000
6148	HC410	1	2384.581	54.944	-2.437	19.184	0.000	0.000	-1.772	-0.077	11.573	0.680	18.425	0.000	0.000	0.000	0.000
6153	M_410	1	2385.813	58.457	-0.038	19.188	0.000	0.000	-1.825	0.001	10.577	0.078	18.442	0.000	0.000	0.000	0.000
6159	S410	1	2387.481	53.084	2.317	19.192	0.000	0.000	-1.735	0.079	11.638	-0.557	18.467	0.000	0.000	0.000	0.000
6163	O410	1	2387.723	51.969	2.288	19.193	0.000	0.000	-1.716	0.079	11.914	-0.584	18.470	0.000	0.000	0.000	0.000
6173	DIPOLE_A	71	2394.278	27.135	1.501	19.221	0.000	0.000	-1.260	0.058	24.398	-1.320	18.533	0.000	0.000	0.000	0.000
6185	DIPOLE_B	71	2400.733	12.749	0.727	19.277	0.000	0.000	-0.948	0.037	46.113	-2.043	18.564	0.000	0.000	0.000	0.000
6197	VC411	1	2401.870	11.250	0.591	19.292	0.000	0.000	-0.905	0.037	50.901	-2.170	18.567	0.000	0.000	0.000	0.000
6202	M_411	1	2403.102	10.446	0.011	19.311	0.000	0.000	-0.879	0.000	53.992	0.000	18.571	0.000	0.000	0.000	0.000
6208	S411	1	2404.769	11.708	-0.617	19.335	0.000	0.000	-0.921	-0.037	49.033	2.121	18.576	0.000	0.000	0.000	0.000
6212	O411	1	2405.011	12.013	-0.646	19.338	0.000	0.000	-0.930	-0.037	48.012	2.094	18.577	0.000	0.000	0.000	0.000
6222	DIPOLE_A	72	2411.566	25.545	-1.419	19.399	0.000	0.000	-1.237	-0.058	25.367	1.360	18.607	0.000	0.000	0.000	0.000
6234	DIPOLE_B	72	2418.022	48.777	-2.180	19.429	0.000	0.000	-1.675	-0.079	12.479	0.636	18.666	0.000	0.000	0.000	0.000
6246	HC412	1	2419.158	53.886	-2.314	19.432	0.000	0.000	-1.765	-0.079	11.179	0.508	18.682	0.000	0.000	0.000	0.000
6251	M_412	1	2420.390	57.141	0.038	19.436	0.000	0.000	-1.821	-0.001	10.582	-0.078	18.700	0.000	0.000	0.000	0.000
6257	S412	1	2422.058	51.655	2.328	19.441	0.000	0.000	-1.734	0.077	12.195	-0.735	18.724	0.000	0.000	0.000	0.000
6261	O412	1	2422.300	50.536	2.298	19.441	0.000	0.000	-1.716	0.077	12.559	-0.766	18.727	0.000	0.000	0.000	0.000
6271	DIPOLE_A	73	2428.855	25.755	1.483	19.470	0.000	0.000	-1.276	0.056	28.022	-1.592	18.783	0.000	0.000	0.000	0.000
6283	DIPOLE_B	73	2435.310	11.784	0.681	19.531	0.000	0.000	-0.979	0.035	53.822	-2.403	18.810	0.000	0.000	0.000	0.000

1

Linear lattice functions for beam line: MI_19

delta(p)/p = 0.000000 symm = F

"MAD" Version: 8.17 Run: 09/09/94 15.47.38

Range: #S/#E

page 16

ELEMENT SEQUENCE			H O R I Z O N T A L								V E R T I C A L							
pos.	element	occ.	dist I	betax	alfax	mux	x(co)	px(co)	Dx	Dpx	I	betay	alfay	muy	y(co)	py(co)	Dy	Dpy
no.	name	no.	[m]	[m]	[1]	[2pi]	[mm]	[.001]	[m]	[1]	I	[m]	[1]	[2pi]	[mm]	[.001]	[m]	[1]

6300	VC413	1	2436.466	10.375	0.538	19.547	0.000	0.000	-0.938	0.035	59.545	-2.549	18.813	0.000	0.000	0.000	0.000
6305	M_413	1	2437.679	9.689	-0.013	19.567	0.000	0.000	-0.917	-0.004	63.078	-0.005	18.816	0.000	0.000	0.000	0.000
6314	S413	1	2439.443	11.107	-0.637	19.595	0.000	0.000	-0.971	-0.043	56.801	2.471	18.821	0.000	0.000	0.000	0.000
6324	DIPOLE_A	74	2446.143	25.324	-1.485	19.660	0.000	0.000	-1.322	-0.064	29.288	1.635	18.847	0.000	0.000	0.000	0.000
6336	DIPOLE_B	74	2452.598	49.768	-2.302	19.689	0.000	0.000	-1.796	-0.084	13.398	0.826	18.900	0.000	0.000	0.000	0.000
6348	HC414	1	2453.735	55.164	-2.446	19.692	0.000	0.000	-1.892	-0.084	11.682	0.683	18.915	0.000	0.000	0.000	0.000
6353	M_414	1	2454.967	58.688	-0.037	19.696	0.000	0.000	-1.952	-0.001	10.682	0.078	18.932	0.000	0.000	0.000	0.000
6359	S414	1	2456.635	53.288	2.327	19.701	0.000	0.000	-1.859	0.082	11.752	-0.560	18.956	0.000	0.000	0.000	0.000
6363	O414	1	2456.877	52.169	2.298	19.701	0.000	0.000	-1.839	0.082	12.030	-0.587	18.960	0.000	0.000	0.000	0.000
6373	DIPOLE_A	75	2463.431	27.217	1.509	19.729	0.000	0.000	-1.363	0.061	24.525	-1.318	19.022	0.000	0.000	0.000	0.000
6385	DIPOLE_B	75	2469.887	12.754	0.732	19.785	0.000	0.000	-1.030	0.041	46.185	-2.036	19.053	0.000	0.000	0.000	0.000
6397	VC415	1	2471.024	11.246	0.595	19.801	0.000	0.000	-0.983	0.041	50.958	-2.163	19.056	0.000	0.000	0.000	0.000
6402	M_415	1	2472.255	10.432	0.015	19.819	0.000	0.000	-0.955	0.000	54.027	0.010	19.060	0.000	0.000	0.000	0.000
6408	S415	1	2473.923	11.678	-0.612	19.843	0.000	0.000	-1.001	-0.040	49.033	2.131	19.065	0.000	0.000	0.000	0.000
6418	DIPOLE_A	76	2480.720	25.439	-1.412	19.908	0.000	0.000	-1.339	-0.061	25.272	1.365	19.096	0.000	0.000	0.000	0.000
6430	DIPOLE_B	76	2487.175	48.579	-2.172	19.937	0.000	0.000	-1.799	-0.082	12.367	0.634	19.156	0.000	0.000	0.000	0.000
6442	HC416	1	2488.312	53.669	-2.306	19.941	0.000	0.000	-1.892	-0.082	11.072	0.505	19.171	0.000	0.000	0.000	0.000
6447	M_416	1	2489.544	56.915	0.036	19.944	0.000	0.000	-1.949	0.001	10.478	-0.077	19.190	0.000	0.000	0.000	0.000
6453	S416	1	2491.211	51.455	2.317	19.949	0.000	0.000	-1.853	0.084	12.079	-0.731	19.214	0.000	0.000	0.000	0.000
6457	O416	1	2491.454	50.341	2.287	19.950	0.000	0.000	-1.832	0.084	12.441	-0.762	19.217	0.000	0.000	0.000	0.000
6467	DIPOLE_A	77	2498.008	25.678	1.476	19.979	0.000	0.000	-1.342	0.064	27.881	-1.593	19.274	0.000	0.000	0.000	0.000
6479	DIPOLE_B	77	2504.464	11.782	0.677	20.040	0.000	0.000	-0.996	0.043	53.718	-2.408	19.301	0.000	0.000	0.000	0.000
6491	VC417	1	2505.600	10.403	0.536	20.056	0.000	0.000	-0.947	0.043	59.356	-2.552	19.304	0.000	0.000	0.000	0.000
6496	M_417	1	2506.832	9.705	-0.017	20.076	0.000	0.000	-0.915	0.004	63.005	-0.015	19.307	0.000	0.000	0.000	0.000
6502	S417	1	2508.500	11.016	-0.630	20.102	0.000	0.000	-0.953	-0.035	57.248	2.472	19.311	0.000	0.000	0.000	0.000
6512	DIPOLE_A	78	2515.297	25.430	-1.491	20.168	0.000	0.000	-1.254	-0.056	29.366	1.630	19.338	0.000	0.000	0.000	0.000
6524	DIPOLE_B	78	2521.752	49.963	-2.309	20.197	0.000	0.000	-1.678	-0.077	13.506	0.827	19.390	0.000	0.000	0.000	0.000
6536	HC418	1	2522.889	55.377	-2.454	20.201	0.000	0.000	-1.765	-0.077	11.787	0.685	19.405	0.000	0.000	0.000	0.000
6541	M_418	1	2524.121	58.909	-0.035	20.204	0.000	0.000	-1.818	0.001	10.786	0.076	19.422	0.000	0.000	0.000	0.000
6547	S418	1	2525.788	53.483	2.338	20.209	0.000	0.000	-1.728	0.079	11.869	-0.565	19.446	0.000	0.000	0.000	0.000
6551	O418	1	2526.030	52.358	2.308	20.210	0.000	0.000	-1.709	0.079	12.149	-0.592	19.449	0.000	0.000	0.000	0.000
6561	DIPOLE_A	79	2532.585	27.290	1.516	20.237	0.000	0.000	-1.257	0.058	24.679	-1.319	19.511	0.000	0.000	0.000	0.000
6573	DIPOLE_B	79	2539.041	12.753	0.736	20.294	0.000	0.000	-0.947	0.037	46.320	-2.033	19.542	0.000	0.000	0.000	0.000
6585	VC419	1	2540.177	11.236	0.599	20.309	0.000	0.000	-0.905	0.037	51.083	-2.158	19.545	0.000	0.000	0.000	0.000
6590	M_419	1	2541.409	10.414	0.019	20.327	0.000	0.000	-0.879	0.000	54.136	0.019	19.549	0.000	0.000	0.000	0.000
6596	S419	1	2543.077	11.645	-0.607	20.352	0.000	0.000	-0.922	-0.038	49.101	2.144	19.554	0.000	0.000	0.000	0.000
6600	O419	1	2543.319	11.946	-0.636	20.355	0.000	0.000	-0.931	-0.038	48.070	2.116	19.555	0.000	0.000	0.000	0.000
6610	DIPOLE_A	80	2549.874	25.333	-1.406	20.416	0.000	0.000	-1.241	-0.058	25.210	1.371	19.585	0.000	0.000	0.000	0.000
6622	DIPOLE_B	80	2556.329	48.388	-2.165	20.446	0.000	0.000	-1.682	-0.079	12.264	0.634	19.645	0.000	0.000	0.000	0.000
6634	HC420	1	2557.466	53.462	-2.299	20.449	0.000	0.000	-1.772	-0.079	10.970	0.504	19.661	0.000	0.000	0.000	0.000
6639	M_420	1	2558.697	56.699	0.034	20.453	0.000	0.000	-1.828	-0.001	10.375	-0.075	19.679	0.000	0.000	0.000	0.000
6645	S420	1	2560.365	51.266	2.306	20.458	0.000	0.000	-1.741	0.077	11.961	-0.726	19.703	0.000	0.000	0.000	0.000
6649	O420	1	2560.607	50.157	2.277	20.458	0.000	0.000	-1.723	0.077	12.320	-0.757	19.707	0.000	0.000	0.000	0.000
6659	DIPOLE_A	81	2567.162	25.609	1.469	20.488	0.000	0.000	-1.282	0.056	27.714	-1.591	19.764	0.000	0.000	0.000	0.000
6671	DIPOLE_B	81	2573.617	11.785	0.673	20.548	0.000	0.000	-0.983	0.035	53.554	-2.410	19.791	0.000	0.000	0.000	0.000
6688	VC421	1	2574.773	10.395	0.530	20.565	0.000	0.000	-0.943	0.035	59.295	-2.557	19.794	0.000	0.000	0.000	0.000
6693	M_421	1	2575.986	9.726	-0.021	20.584	0.000	0.000	-0.921	-0.004	62.861	-0.024	19.798	0.000	0.000	0.000	0.000

1
Linear lattice functions for beam line: MI_19
delta(p)/p = 0.000000 symm = F

"MAD" Version: 8.17 Run: 09/09/94 15.47.38
Range: #S/#E

ELEMENT SEQUENCE			I			H O R I Z O N T A L						I			V E R T I C A L					
pos.	element	occ.	dist	I	betax	alfax	mux	x(co)	px(co)	Dx	Dpx	I	betay	alfay	muy	y(co)	py(co)	Dy	Dpy	
no.	name	no.	[m]	I	[m]	[1]	[2pi]	[mm]	[.001]	[m]	[1]	I	[m]	[1]	[2pi]	[mm]	[.001]	[m]	[1]	
6702	S421	1	2577.751		11.175	-0.647	20.612	0.000	0.000	-0.976-0.043			56.670	2.446	19.802	0.000	0.000	0.000	0.000	
6712	DIPOLE_A	82	2584.450		25.536	-1.497	20.677	0.000	0.000	-1.327-0.064			29.411	1.622	19.828	0.000	0.000	0.000	0.000	
6724	DIPOLE_B	82	2590.906		50.150	-2.316	20.706	0.000	0.000	-1.802-0.085			13.604	0.826	19.881	0.000	0.000	0.000	0.000	
6736	HC422	1	2592.042		55.579	-2.460	20.709	0.000	0.000	-1.898-0.085			11.886	0.685	19.895	0.000	0.000	0.000	0.000	
6741	M_422	1	2593.274		59.119	-0.033	20.712	0.000	0.000	-1.958-0.001			10.887	0.073	19.912	0.000	0.000	0.000	0.000	
6747	S422	1	2594.942		53.666	2.348	20.717	0.000	0.000	-1.865 0.083			11.987	-0.571	19.936	0.000	0.000	0.000	0.000	
6751	O422	1	2595.184		52.536	2.319	20.718	0.000	0.000	-1.845 0.083			12.270	-0.598	19.939	0.000	0.000	0.000	0.000	
6761	DIPOLE_A	83	2601.739		27.354	1.523	20.745	0.000	0.000	-1.366 0.062			24.858	-1.322	20.000	0.000	0.000	0.000	0.000	
6773	DIPOLE_B	83	2608.194		12.747	0.740	20.802	0.000	0.000	-1.030 0.041			46.514	-2.032	20.031	0.000	0.000	0.000	0.000	
6785	VC423	1	2609.331		11.222	0.602	20.817	0.000	0.000	-0.984 0.041			51.276	-2.157	20.035	0.000	0.000	0.000	0.000	
6790	M_423	1	2610.563		10.391	0.023	20.835	0.000	0.000	-0.955 0.000			54.316	0.029	20.038	0.000	0.000	0.000	0.000	
6796	S423	1	2612.230		11.609	-0.603	20.860	0.000	0.000	-1.000-0.040			49.235	2.159	20.043	0.000	0.000	0.000	0.000	
6806	DIPOLE_A	84	2619.027		25.227	-1.401	20.925	0.000	0.000	-1.336-0.061			25.182	1.379	20.074	0.000	0.000	0.000	0.000	
6818	DIPOLE_B	84	2625.483		48.206	-2.159	20.954	0.000	0.000	-1.792-0.082			12.172	0.636	20.134	0.000	0.000	0.000	0.000	
6830	HC424	1	2626.619		53.266	-2.292	20.958	0.000	0.000	-1.885-0.082			10.875	0.505	20.150	0.000	0.000	0.000	0.000	
6835	M_424	1	2627.851		56.496	0.032	20.961	0.000	0.000	-1.942 0.001			10.276	-0.071	20.169	0.000	0.000	0.000	0.000	
6841	S424	1	2629.519		51.090	2.296	20.966	0.000	0.000	-1.845 0.084			11.843	-0.719	20.193	0.000	0.000	0.000	0.000	
6845	O424	1	2629.761		49.986	2.266	20.967	0.000	0.000	-1.825 0.084			12.199	-0.750	20.197	0.000	0.000	0.000	0.000	
6855	DIPOLE_A	85	2636.316		25.550	1.462	20.996	0.000	0.000	-1.337 0.063			27.523	-1.587	20.255	0.000	0.000	0.000	0.000	
6867	DIPOLE_B	85	2642.771		11.794	0.669	21.057	0.000	0.000	-0.991 0.043			53.331	-2.409	20.282	0.000	0.000	0.000	0.000	
6879	VC425	1	2643.908		10.431	0.530	21.073	0.000	0.000	-0.943 0.043			58.973	-2.554	20.285	0.000	0.000	0.000	0.000	
6884	M_425	1	2645.140		9.750	-0.024	21.093	0.000	0.000	-0.911 0.004			62.645	-0.033	20.288	0.000	0.000	0.000	0.000	
6890	S425	1	2646.807		11.089	-0.639	21.119	0.000	0.000	-0.949-0.035			56.981	2.441	20.292	0.000	0.000	0.000	0.000	
6900	DIPOLE_A	86	2653.604		25.641	-1.502	21.185	0.000	0.000	-1.249-0.056			29.422	1.613	20.319	0.000	0.000	0.000	0.000	
6912	DIPOLE_B	86	2660.060		50.326	-2.322	21.214	0.000	0.000	-1.672-0.077			13.690	0.824	20.371	0.000	0.000	0.000	0.000	
6924	HC426	1	2661.196		55.769	-2.466	21.217	0.000	0.000	-1.759-0.077			11.976	0.684	20.385	0.000	0.000	0.000	0.000	
6929	M_426	1	2662.428		59.314	-0.031	21.221	0.000	0.000	-1.812 0.001			10.983	0.069	20.403	0.000	0.000	0.000	0.000	
6935	S426	1	2664.096		53.835	2.358	21.225	0.000	0.000	-1.723 0.078			12.105	-0.579	20.426	0.000	0.000	0.000	0.000	
6939	O426	1	2664.338		52.700	2.329	21.226	0.000	0.000	-1.704 0.078			12.392	-0.605	20.429	0.000	0.000	0.000	0.000	
6949	DIPOLE_A	87	2670.893		27.408	1.530	21.254	0.000	0.000	-1.254 0.058			25.060	-1.327	20.490	0.000	0.000	0.000	0.000	
6961	DIPOLE_B	87	2677.348		12.735	0.743	21.310	0.000	0.000	-0.946 0.037			46.764	-2.035	20.520	0.000	0.000	0.000	0.000	
6973	VC427	1	2678.485		11.203	0.605	21.325	0.000	0.000	-0.905 0.037			51.531	-2.159	20.524	0.000	0.000	0.000	0.000	
6978	M_427	1	2679.716		10.365	0.026	21.343	0.000	0.000	-0.879-0.001			54.565	0.038	20.527	0.000	0.000	0.000	0.000	
6984	S427	1	2681.384		11.569	-0.598	21.368	0.000	0.000	-0.923-0.038			49.433	2.177	20.532	0.000	0.000	0.000	0.000	
6988	O427	1	2681.626		11.866	-0.627	21.371	0.000	0.000	-0.932-0.038			48.386	2.149	20.533	0.000	0.000	0.000	0.000	
6998	DIPOLE_A	88	2688.181		25.123	-1.396	21.433	0.000	0.000	-1.245-0.059			25.189	1.389	20.563	0.000	0.000	0.000	0.000	
7010	DIPOLE_B	88	2694.636		48.036	-2.154	21.463	0.000	0.000	-1.689-0.080			12.091	0.639	20.624	0.000	0.000	0.000	0.000	
7022	HC428	1	2695.773		53.083	-2.287	21.467	0.000	0.000	-1.779-0.080			10.789	0.507	20.639	0.000	0.000	0.000	0.000	
7027	M_428	1	2697.005		56.309	0.029	21.470	0.000	0.000	-1.836-0.001			10.183	-0.067	20.658	0.000	0.000	0.000	0.000	
7033	S428	1	2698.673		50.929	2.286	21.475	0.000	0.000	-1.749 0.077			11.727	-0.711	20.683	0.000	0.000	0.000	0.000	
7037	O428	1	2698.915		49.829	2.257	21.476	0.000	0.000	-1.730 0.077			12.078	-0.742	20.686	0.000	0.000	0.000	0.000	
7047	DIPOLE_A	89	2705.469		25.501	1.455	21.505	0.000	0.000	-1.288 0.056			27.311	-1.581	20.745	0.000	0.000	0.000	0.000	
7059	DIPOLE_B	89	2711.925		11.808	0.666	21.566	0.000	0.000	-0.988 0.035			53.054	-2.405	20.772	0.000	0.000	0.000	0.000	
7071	VC429	1	2713.061		10.452	0.527	21.582	0.000	0.000	-0.947 0.035			58.687	-2.551	20.775	0.000	0.000	0.000	0.000	
7076	M_429	1	2714.293		9.778	-0.028	21.602	0.000	0.000	-0.925-0.004			62.364	-0.042	20.779	0.000	0.000	0.000	0.000	
7082	S429	1	2715.961		11.130	-0.643	21.628	0.000	0.000	-0.975-0.043			56.752	2.422	20.783	0.000	0.000	0.000	0.000	
7092	DIPOLE_A	90	2722.758		25.744	-1.507	21.693	0.000	0.000	-1.332-0.064			29.398	1.602	20.810	0.000	0.000	0.000	0.000	

Linear lattice functions for beam line: MI_19
 delta(p)/p = 0.000000 symm = F

Range: #S/#E

page 18

ELEMENT SEQUENCE			H O R I Z O N T A L								V E R T I C A L							
pos.	element	occ.	dist I	betax	alfax	mux	x(co)	px(co)	Dx	Dpx	I	betay	alfay	muy	y(co)	py(co)	Dy	Dpy
no.	name	no.	[m]	[m]	[1]	[2pi]	[mm]	[.001]	[m]	[1]	I	[m]	[1]	[2pi]	[mm]	[.001]	[m]	[1]
7104	DIPOLE_B	90	2729.213	50.490	-2.327	21.722	0.000	0.000	-1.808-0.085			13.764	0.820	20.862	0.000	0.000	0.000	0.000
7116	HC430	1	2730.350	55.944	-2.471	21.726	0.000	0.000	-1.904-0.085			12.058	0.682	20.876	0.000	0.000	0.000	0.000
7121	M_430	1	2731.582	59.493	-0.028	21.729	0.000	0.000	-1.964-0.001			11.074	0.064	20.893	0.000	0.000	0.000	0.000
7127	S430	1	2733.249	53.988	2.368	21.734	0.000	0.000	-1.870 0.083			12.220	-0.587	20.916	0.000	0.000	0.000	0.000
7131	O430	1	2733.491	52.849	2.339	21.734	0.000	0.000	-1.850 0.083			12.511	-0.614	20.919	0.000	0.000	0.000	0.000
7141	DIPOLE_A	91	2740.046	27.452	1.536	21.762	0.000	0.000	-1.369 0.062			25.281	-1.334	20.979	0.000	0.000	0.000	0.000
7153	DIPOLE_B	91	2746.502	12.718	0.746	21.818	0.000	0.000	-1.030 0.041			47.067	-2.040	21.009	0.000	0.000	0.000	0.000
7170	VC501	1	2747.657	11.157	0.605	21.833	0.000	0.000	-0.983 0.041			51.929	-2.167	21.013	0.000	0.000	0.000	0.000
7175	M_501	1	2748.870	10.336	0.029	21.852	0.000	0.000	-0.954 0.001			54.879	0.046	21.017	0.000	0.000	0.000	0.000
7184	S501	1	2750.635	11.644	-0.605	21.878	0.000	0.000	-1.002-0.040			49.265	2.185	21.022	0.000	0.000	0.000	0.000
7194	DIPOLE_A	92	2757.335	25.022	-1.392	21.942	0.000	0.000	-1.331-0.060			25.230	1.402	21.052	0.000	0.000	0.000	0.000
7206	DIPOLE_B	92	2763.790	47.879	-2.149	21.972	0.000	0.000	-1.785-0.081			12.024	0.644	21.113	0.000	0.000	0.000	0.000
7218	HC502	1	2764.927	52.916	-2.283	21.975	0.000	0.000	-1.878-0.081			10.713	0.510	21.129	0.000	0.000	0.000	0.000
7223	M_502	1	2766.159	56.139	0.026	21.979	0.000	0.000	-1.934 0.001			10.096	-0.061	21.148	0.000	0.000	0.000	0.000
7229	S502	1	2767.826	50.785	2.277	21.984	0.000	0.000	-1.838 0.084			11.614	-0.702	21.173	0.000	0.000	0.000	0.000
7233	O502	1	2768.068	49.689	2.247	21.984	0.000	0.000	-1.817 0.084			11.961	-0.733	21.176	0.000	0.000	0.000	0.000
7243	DIPOLE_A	93	2774.623	25.463	1.449	22.014	0.000	0.000	-1.330 0.063			27.081	-1.573	21.235	0.000	0.000	0.000	0.000
7255	DIPOLE_B	93	2781.078	11.828	0.663	22.075	0.000	0.000	-0.987 0.042			52.726	-2.398	21.263	0.000	0.000	0.000	0.000
7267	VC503	1	2782.215	10.477	0.525	22.091	0.000	0.000	-0.939 0.042			58.344	-2.544	21.266	0.000	0.000	0.000	0.000
7272	M_503	1	2783.447	9.808	-0.030	22.110	0.000	0.000	-0.907 0.004			62.019	-0.050	21.269	0.000	0.000	0.000	0.000
7278	S503	1	2785.115	11.173	-0.648	22.136	0.000	0.000	-0.945-0.035			56.465	2.402	21.274	0.000	0.000	0.000	0.000
7288	DIPOLE_A	94	2791.911	25.842	-1.511	22.202	0.000	0.000	-1.245-0.056			29.340	1.589	21.300	0.000	0.000	0.000	0.000
7300	DIPOLE_B	94	2798.367	50.640	-2.331	22.230	0.000	0.000	-1.667-0.076			13.824	0.814	21.352	0.000	0.000	0.000	0.000
7312	HC504	1	2799.503	56.102	-2.475	22.234	0.000	0.000	-1.754-0.076			12.128	0.677	21.366	0.000	0.000	0.000	0.000
7317	M_504	1	2800.735	59.654	-0.025	22.237	0.000	0.000	-1.807 0.001			11.156	0.058	21.383	0.000	0.000	0.000	0.000
7323	S504	1	2802.403	54.123	2.377	22.242	0.000	0.000	-1.718 0.078			12.330	-0.597	21.406	0.000	0.000	0.000	0.000
7327	O504	1	2802.645	52.979	2.348	22.242	0.000	0.000	-1.699 0.078			12.626	-0.624	21.409	0.000	0.000	0.000	0.000
7337	DIPOLE_A	95	2809.200	27.484	1.542	22.270	0.000	0.000	-1.252 0.057			25.518	-1.343	21.469	0.000	0.000	0.000	0.000
7349	DIPOLE_B	95	2815.655	12.697	0.749	22.326	0.000	0.000	-0.946 0.036			47.418	-2.049	21.498	0.000	0.000	0.000	0.000
7361	VC505	1	2816.792	11.153	0.609	22.341	0.000	0.000	-0.905 0.036			52.216	-2.173	21.502	0.000	0.000	0.000	0.000
7366	M_505	1	2818.024	10.304	0.032	22.360	0.000	0.000	-0.880-0.001			55.252	0.054	21.506	0.000	0.000	0.000	0.000
7372	S505	1	2819.691	11.483	-0.590	22.385	0.000	0.000	-0.925-0.038			50.005	2.218	21.511	0.000	0.000	0.000	0.000
7376	O505	1	2819.934	11.775	-0.618	22.388	0.000	0.000	-0.934-0.038			48.938	2.190	21.512	0.000	0.000	0.000	0.000
7386	DIPOLE_A	96	2826.488	24.926	-1.388	22.450	0.000	0.000	-1.250-0.059			25.305	1.415	21.541	0.000	0.000	0.000	0.000
7398	DIPOLE_B	96	2832.944	47.737	-2.146	22.480	0.000	0.000	-1.696-0.080			11.972	0.650	21.602	0.000	0.000	0.000	0.000
7410	QC506	1	2833.664	50.891	-2.230	22.483	0.000	0.000	-1.754-0.080			11.097	0.564	21.612	0.000	0.000	0.000	0.000
7414	HC506	1	2834.080	52.766	-2.279	22.484	0.000	0.000	-1.787-0.080			10.648	0.515	21.618	0.000	0.000	0.000	0.000
7419	M_506	1	2835.312	55.988	0.023	22.488	0.000	0.000	-1.844-0.001			10.018	-0.055	21.637	0.000	0.000	0.000	0.000
7425	S506	1	2836.980	50.658	2.268	22.492	0.000	0.000	-1.757 0.077			11.506	-0.692	21.662	0.000	0.000	0.000	0.000
7429	O506	1	2837.222	49.568	2.238	22.493	0.000	0.000	-1.738 0.077			11.848	-0.723	21.666	0.000	0.000	0.000	0.000
7439	DIPOLE_A	97	2843.777	25.437	1.444	22.523	0.000	0.000	-1.294 0.057			26.838	-1.563	21.725	0.000	0.000	0.000	0.000
7451	DIPOLE_B	97	2850.232	11.852	0.661	22.583	0.000	0.000	-0.992 0.036			52.355	-2.388	21.753	0.000	0.000	0.000	0.000
7463	VC507	1	2851.369	10.506	0.523	22.600	0.000	0.000	-0.952 0.036			57.949	-2.534	21.756	0.000	0.000	0.000	0.000
7468	M_507	1	2852.601	9.842	-0.033	22.619	0.000	0.000	-0.929-0.004			61.619	-0.057	21.760	0.000	0.000	0.000	0.000
7474	S507	1	2854.268	11.218	-0.651	22.645	0.000	0.000	-0.979-0.043			56.125	2.379	21.764	0.000	0.000	0.000	0.000

7484 DIPOLE_A 98 2861.065 25.936 -1.514 22.710 0.000 0.000 -1.336-0.064
 7496 DIPOLE_B 98 2867.521 50.774 -2.334 22.739 0.000 0.000 -1.812-0.085

29.248 1.574 21.791 0.000 0.000 0.000 0.000
 13.869 0.807 21.843 0.000 0.000 0.000 0.000

1

"MAD" Version: 8.17 Run: 09/09/94 15.47.38

Linear lattice functions for beam line: MI_19

delta(p)/p = 0.000000 symm = F

Range: #S/#E

page 19

ELEMENT SEQUENCE			H O R I Z O N T A L										V E R T I C A L					
pos.	element	occ.	dist I	betax	alfax	mux	x(co)	px(co)	Dx	Dpx	I	betay	alfay	muy	y(co)	py(co)	Dy	Dpy
no.	name	no.	[m]	[m]	[1]	[2pi]	[mm]	[.001]	[m]	[1]	I	[m]	[1]	[2pi]	[mm]	[.001]	[m]	[1]
7508	QC508	1	2868.241	54.203	-2.425	22.741	0.000	0.000	-1.874-0.085			12.767	0.722	21.851	0.000	0.000	0.000	0.000
7512	HC508	1	2868.657	56.242	-2.478	22.742	0.000	0.000	-1.909-0.085			12.187	0.672	21.857	0.000	0.000	0.000	0.000
7517	M_508	1	2869.889	59.795	-0.021	22.745	0.000	0.000	-1.969-0.001			11.230	0.051	21.874	0.000	0.000	0.000	0.000
7523	S508	1	2871.557	54.240	2.386	22.750	0.000	0.000	-1.874 0.083			12.435	-0.607	21.896	0.000	0.000	0.000	0.000
7527	O508	1	2871.799	53.092	2.356	22.751	0.000	0.000	-1.854 0.083			12.735	-0.634	21.900	0.000	0.000	0.000	0.000
7537	DIPOLE_A	99	2878.354	27.505	1.547	22.778	0.000	0.000	-1.371 0.063			25.767	-1.354	21.958	0.000	0.000	0.000	0.000
7549	DIPOLE_B	99	2884.809	12.670	0.751	22.834	0.000	0.000	-1.030 0.042			47.809	-2.060	21.988	0.000	0.000	0.000	0.000
7561	VC509	1	2885.946	11.123	0.611	22.849	0.000	0.000	-0.983 0.042			52.634	-2.185	21.991	0.000	0.000	0.000	0.000
7566	M_509	1	2887.177	10.268	0.034	22.868	0.000	0.000	-0.953 0.001			55.679	0.061	21.995	0.000	0.000	0.000	0.000
7572	S509	1	2888.845	11.437	-0.586	22.893	0.000	0.000	-0.997-0.039			50.371	2.241	22.000	0.000	0.000	0.000	0.000
7582	DIPOLE_A	100	2895.642	24.835	-1.385	22.959	0.000	0.000	-1.326-0.060			25.412	1.430	22.030	0.000	0.000	0.000	0.000
7594	DIPOLE_B	100	2902.097	47.611	-2.143	22.989	0.000	0.000	-1.777-0.081			11.934	0.657	22.091	0.000	0.000	0.000	0.000
7606	QC510	1	2902.818	50.762	-2.228	22.991	0.000	0.000	-1.836-0.081			11.049	0.571	22.101	0.000	0.000	0.000	0.000
7610	HC510	1	2903.234	52.636	-2.277	22.993	0.000	0.000	-1.869-0.081			10.595	0.521	22.107	0.000	0.000	0.000	0.000
7615	M_510	1	2904.466	55.858	0.019	22.996	0.000	0.000	-1.925 0.001			9.949	-0.047	22.126	0.000	0.000	0.000	0.000
7621	S510	1	2906.134	50.552	2.259	23.001	0.000	0.000	-1.829 0.084			11.406	-0.681	22.152	0.000	0.000	0.000	0.000
7625	O510	1	2906.376	49.465	2.230	23.002	0.000	0.000	-1.809 0.084			11.743	-0.712	22.155	0.000	0.000	0.000	0.000
7635	DIPOLE_A	101	2912.930	25.421	1.439	23.032	0.000	0.000	-1.324 0.063			26.585	-1.552	22.215	0.000	0.000	0.000	0.000
7647	DIPOLE_B	101	2919.386	11.881	0.659	23.092	0.000	0.000	-0.982 0.042			51.944	-2.376	22.243	0.000	0.000	0.000	0.000
7664	VC511	1	2920.541	10.519	0.520	23.109	0.000	0.000	-0.934 0.042			57.606	-2.523	22.247	0.000	0.000	0.000	0.000
7669	M_511	1	2921.754	9.879	-0.035	23.128	0.000	0.000	-0.903 0.004			61.168	-0.064	22.250	0.000	0.000	0.000	0.000
7678	S511	1	2923.519	11.393	-0.667	23.155	0.000	0.000	-0.944-0.035			55.279	2.344	22.255	0.000	0.000	0.000	0.000
7688	DIPOLE_A	102	2930.219	26.024	-1.517	23.218	0.000	0.000	-1.240-0.056			29.126	1.559	22.281	0.000	0.000	0.000	0.000
7700	DIPOLE_B	102	2936.674	50.890	-2.335	23.247	0.000	0.000	-1.663-0.076			13.899	0.799	22.333	0.000	0.000	0.000	0.000
7712	QC512	1	2937.395	54.322	-2.427	23.249	0.000	0.000	-1.718-0.076			12.807	0.714	22.342	0.000	0.000	0.000	0.000
7716	HC512	1	2937.811	56.363	-2.480	23.250	0.000	0.000	-1.750-0.076			12.234	0.665	22.347	0.000	0.000	0.000	0.000
7721	M_512	1	2939.043	59.913	-0.018	23.253	0.000	0.000	-1.803 0.001			11.293	0.043	22.364	0.000	0.000	0.000	0.000
7727	S512	1	2940.710	54.336	2.394	23.258	0.000	0.000	-1.714 0.078			12.531	-0.618	22.387	0.000	0.000	0.000	0.000
7731	O512	1	2940.952	53.184	2.364	23.259	0.000	0.000	-1.696 0.078			12.837	-0.645	22.390	0.000	0.000	0.000	0.000
7741	DIPOLE_A	103	2947.507	27.514	1.552	23.286	0.000	0.000	-1.250 0.057			26.023	-1.366	22.448	0.000	0.000	0.000	0.000
7753	DIPOLE_B	103	2953.963	12.639	0.752	23.342	0.000	0.000	-0.947 0.036			48.237	-2.074	22.477	0.000	0.000	0.000	0.000
7765	SQ513	1	2954.680	11.623	0.663	23.352	0.000	0.000	-0.921 0.036			51.270	-2.153	22.480	0.000	0.000	0.000	0.000
7769	VC513	1	2955.099	11.089	0.612	23.358	0.000	0.000	-0.906 0.036			53.093	-2.199	22.481	0.000	0.000	0.000	0.000
7774	M_513	1	2956.331	10.231	0.036	23.376	0.000	0.000	-0.882-0.001			56.152	0.066	22.484	0.000	0.000	0.000	0.000
7780	S513	1	2957.999	11.390	-0.583	23.401	0.000	0.000	-0.927-0.039			50.782	2.265	22.489	0.000	0.000	0.000	0.000
7790	DIPOLE_A	104	2964.796	24.751	-1.383	23.468	0.000	0.000	-1.255-0.060			25.550	1.446	22.520	0.000	0.000	0.000	0.000
7802	DIPOLE_B	104	2971.251	47.504	-2.142	23.498	0.000	0.000	-1.704-0.081			11.913	0.666	22.580	0.000	0.000	0.000	0.000
7814	SQ514	1	2971.740	49.627	-2.200	23.499	0.000	0.000	-1.743-0.081			11.291	0.607	22.587	0.000	0.000	0.000	0.000
7818	SQ514	2	2971.969	50.639	-2.227	23.500	0.000	0.000	-1.762-0.081			11.020	0.579	22.590	0.000	0.000	0.000	0.000
7822	HC514	1	2972.388	52.526	-2.276	23.501	0.000	0.000	-1.796-0.081			10.556	0.528	22.596	0.000	0.000	0.000	0.000
7827	M_514	1	2973.620	55.751	0.016	23.505	0.000	0.000	-1.853-0.001			9.891	-0.039	22.615	0.000	0.000	0.000	0.000
7833	S514	1	2975.287	50.467	2.251	23.510	0.000	0.000	-1.765 0.078			11.314	-0.670	22.641	0.000	0.000	0.000	0.000

7837	O514	1	2975.529	49.384	2.222	23.511	0.000	0.000	-1.746	0.078	11.646	-0.701	22.644	0.000	0.000	0.000	0.000
7847	DIPOLE_A	105	2982.084	25.418	1.434	23.540	0.000	0.000	-1.300	0.057	26.327	-1.538	22.705	0.000	0.000	0.000	0.000
7859	DIPOLE_B	105	2988.539	11.914	0.658	23.601	0.000	0.000	-0.997	0.036	51.502	-2.360	22.733	0.000	0.000	0.000	0.000
7871	SQ515	1	2989.257	11.032	0.572	23.611	0.000	0.000	-0.971	0.036	54.955	-2.452	22.736	0.000	0.000	0.000	0.000
7875	VC515	1	2989.676	10.574	0.521	23.617	0.000	0.000	-0.956	0.036	57.032	-2.505	22.737	0.000	0.000	0.000	0.000

1

Linear lattice functions for beam line: MI_19

delta(p)/p = 0.000000 symm = F

"MAD" Version: 8.17 Run: 09/09/94 15.47.38
Range: #S/#E

page 20

ELEMENT SEQUENCE			H O R I Z O N T A L										V E R T I C A L					
pos.	element	occ.	dist I	betax	alfax	mux	x(co)	px(co)	Dx	Dpx	I	betay	alfay	muy	y(co)	py(co)	Dy	Dpy
no.	name	no.	[m]	[m]	[1]	[2pi]	[mm]	[.001]	[m]	[1]	I	[m]	[1]	[2pi]	[mm]	[.001]	[m]	[1]
7880	M_515	1	2990.908	9.917	-0.037	23.636	0.000	0.000	-0.932-0.003			60.674	-0.069	22.740	0.000	0.000	0.000	0.000
7886	S515	1	2992.576	11.312	-0.658	23.662	0.000	0.000	-0.983-0.043			55.304	2.331	22.745	0.000	0.000	0.000	0.000
7896	DIPOLE_A	106	2999.372	26.104	-1.519	23.726	0.000	0.000	-1.340-0.064			28.973	1.542	22.772	0.000	0.000	0.000	0.000
7903	DIPOLE_B	106	3005.828	50.988	-2.336	23.755	0.000	0.000	-1.816-0.085			13.912	0.790	22.824	0.000	0.000	0.000	0.000
7923	HC516	1	3006.996	56.620	-2.484	23.758	0.000	0.000	-1.915-0.085			12.225	0.654	22.838	0.000	0.000	0.000	0.000
7928	M_516	1	3008.196	60.005	-0.010	23.762	0.000	0.000	-1.972 0.000			11.346	0.034	22.855	0.000	0.000	0.000	0.000
7939	DIPOLE_C	53	3014.500	27.876	2.270	23.785	0.000	0.000	-1.358 0.101			23.424	-1.457	22.920	0.000	0.000	0.000	0.000
7951	DIPOLE_D	53	3018.923	12.113	1.294	23.824	0.000	0.000	-0.938 0.088			38.924	-2.045	22.944	0.000	0.000	0.000	0.000
7963	VC517	1	3019.570	10.533	1.151	23.833	0.000	0.000	-0.881 0.088			41.623	-2.131	22.946	0.000	0.000	0.000	0.000
7968	M_517	1	3021.163	8.153	0.346	23.861	0.000	0.000	-0.778 0.040			44.869	0.346	22.952	0.000	0.000	0.000	0.000
7979	DIPOLE_C	54	3027.466	14.256	-0.964	23.965	0.000	0.000	-0.802-0.018			18.781	1.713	22.986	0.000	0.000	0.000	0.000
7991	DIPOLE_D	54	3031.890	25.428	-1.562	24.002	0.000	0.000	-0.912-0.032			7.723	0.787	23.045	0.000	0.000	0.000	0.000
8003	HC518	1	3032.536	27.504	-1.650	24.006	0.000	0.000	-0.932-0.032			6.794	0.651	23.060	0.000	0.000	0.000	0.000
8008	M_518	1	3034.129	30.435	-0.002	24.014	0.000	0.000	-0.942 0.024			5.754	-0.007	23.101	0.000	0.000	0.000	0.000
8019	DIPOLE_C	55	3040.433	15.001	1.011	24.060	0.000	0.000	-0.516 0.065			17.833	-1.664	23.213	0.000	0.000	0.000	0.000
8031	DIPOLE_D	55	3044.856	8.694	0.415	24.124	0.000	0.000	-0.259 0.051			36.686	-2.597	23.241	0.000	0.000	0.000	0.000
8043	VC519	1	3045.502	8.214	0.328	24.136	0.000	0.000	-0.226 0.051			40.131	-2.734	23.243	0.000	0.000	0.000	0.000
8048	M_519	1	3047.096	8.186	-0.346	24.167	0.000	0.000	-0.154 0.040			45.503	-0.347	23.249	0.000	0.000	0.000	0.000
8059	DIPOLE_C	56	3053.399	26.305	-2.189	24.241	0.000	0.000	0.027 0.018			24.783	1.531	23.278	0.000	0.000	0.000	0.000
8071	DIPOLE_D	56	3057.823	49.981	-3.163	24.260	0.000	0.000	0.081 0.005			13.873	0.935	23.316	0.000	0.000	0.000	0.000
8083	HC520	1	3058.469	54.161	-3.306	24.262	0.000	0.000	0.084 0.005			12.721	0.848	23.324	0.000	0.000	0.000	0.000
8088	M_520	1	3060.062	59.997	0.014	24.267	0.000	0.000	0.087-0.001			11.355	-0.019	23.346	0.000	0.000	0.000	0.000
8102	VC521	1	3076.138	10.693	0.598	24.373	0.000	0.000	0.021-0.004			56.704	-2.354	23.458	0.000	0.000	0.000	0.000
8107	M_521	1	3077.351	9.873	0.036	24.392	0.000	0.000	0.016-0.004			59.889	0.067	23.461	0.000	0.000	0.000	0.000
8116	HC522	1	3078.965	10.946	-0.567	24.417	0.000	0.000	0.011-0.003			54.424	2.423	23.466	0.000	0.000	0.000	0.000
8124	M_522	1	3094.639	55.790	-0.020	24.524	0.000	0.000	-0.034-0.001			9.941	0.025	23.586	0.000	0.000	0.000	0.000
8137	VC523	1	3110.728	10.916	0.530	24.634	0.000	0.000	-0.035 0.000			53.751	-2.356	23.712	0.000	0.000	0.000	0.000
8142	M_523	1	3111.928	10.274	-0.036	24.652	0.000	0.000	-0.036-0.001			57.018	-0.061	23.716	0.000	0.000	0.000	0.000
8153	DIPOLE_C	57	3118.231	22.924	-1.535	24.722	0.000	0.000	-0.085-0.018			27.511	2.107	23.740	0.000	0.000	0.000	0.000
8165	DIPOLE_D	57	3122.655	39.366	-2.182	24.746	0.000	0.000	-0.191-0.031			12.737	1.233	23.778	0.000	0.000	0.000	0.000
8177	HC524	1	3123.301	42.248	-2.277	24.748	0.000	0.000	-0.212-0.031			11.226	1.105	23.787	0.000	0.000	0.000	0.000
8182	M_524	1	3124.894	45.829	0.298	24.754	0.000	0.000	-0.252-0.017			9.021	0.276	23.813	0.000	0.000	0.000	0.000
8193	DIPOLE_C	58	3131.198	19.181	1.758	24.787	0.000	0.000	-0.303-0.016			16.391	-1.049	23.903	0.000	0.000	0.000	0.000
8205	DIPOLE_D	58	3135.621	7.800	0.815	24.846	0.000	0.000	-0.402-0.030			28.177	-1.615	23.936	0.000	0.000	0.000	0.000
8217	VC525	1	3136.268	6.836	0.677	24.860	0.000	0.000	-0.421-0.030			30.318	-1.698	23.940	0.000	0.000	0.000	0.000
8222	M_525	1	3137.861	5.713	0.022	24.901	0.000	0.000	-0.487-0.056			33.196	0.086	23.947	0.000	0.000	0.000	0.000
8233	DIPOLE_C	59	3144.164	17.188	-1.604	25.016	0.000	0.000	-1.042-0.101			15.736	1.147	23.990	0.000	0.000	0.000	0.000
8245	DIPOLE_D	59	3148.588	35.449	-2.524	25.045	0.000	0.000	-1.518-0.115			8.464	0.496	24.053	0.000	0.000	0.000	0.000
8257	HC526	1	3149.234	38.798	-2.658	25.047	0.000	0.000	-1.592-0.115			7.884	0.401	24.065	0.000	0.000	0.000	0.000

8262	M_526	1	3150.827	43.967	-0.299	25.054	0.000	0.000	-1.703-0.016	7.625	-0.269	24.099	0.000	0.000	0.000	0.000
8273	DIPOLE_C	60	3157.131	23.249	1.508	25.084	0.000	0.000	-1.270 0.071	24.325	-2.057	24.179	0.000	0.000	0.000	0.000
8285	DIPOLE_D	60	3161.554	12.666	0.885	25.125	0.000	0.000	-0.984 0.057	46.723	-3.006	24.200	0.000	0.000	0.000	0.000
8297	VC527	1	3162.200	11.581	0.794	25.134	0.000	0.000	-0.947 0.057	50.697	-3.145	24.202	0.000	0.000	0.000	0.000
8302	M_527	1	3163.794	10.289	-0.007	25.158	0.000	0.000	-0.895 0.004	56.435	-0.111	24.206	0.000	0.000	0.000	0.000
8312	S527	1	3165.556	11.729	-0.647	25.184	0.000	0.000	-0.934-0.034	51.184	2.117	24.212	0.000	0.000	0.000	0.000
8321	DIPOLE_A	107	3172.258	25.825	-1.457	25.247	0.000	0.000	-1.225-0.055	27.604	1.401	24.240	0.000	0.000	0.000	0.000
8333	DIPOLE_B	107	3178.714	49.668	-2.237	25.275	0.000	0.000	-1.642-0.076	13.980	0.709	24.293	0.000	0.000	0.000	0.000

```
"MAD" Version: 8.17      Run: 09/09/94  15.47.38
Range: #S/#E
```

```

1
Linear lattice functions for beam line: MI_19
delta(p)/p =      0.000000      symm = F

```

page 21

ELEMENT SEQUENCE			H O R I Z O N T A L									V E R T I C A L						
pos.	element	occ.	dist I	betax	alfax	mux	x(co)	px(co)	Dx	Dpx	I	betay	alfay	muy	y(co)	py(co)	Dy	Dpy
no.	name	no.	[m]	I	[m]	[1]	[mm]	[.001]	[m]	[1]	I	[m]	[1]	[2pi]	[mm]	[.001]	[m]	[1]
8345	HC528	1	3179.850		54.910	-2.374	25.279	0.000	0.000	-1.728	-0.076	12.508	0.587	24.307	0.000	0.000	0.000	0.000
8350	M_528	1	3181.082		58.266	0.023	25.282	0.000	0.000	-1.780	0.001	11.764	-0.043	24.323	0.000	0.000	0.000	0.000
8356	S528	1	3182.750		52.719	2.361	25.287	0.000	0.000	-1.693	0.077	13.343	-0.732	24.345	0.000	0.000	0.000	0.000
8360	O528	1	3182.992		51.583	2.331	25.288	0.000	0.000	-1.674	0.077	13.705	-0.760	24.348	0.000	0.000	0.000	0.000
8370	DIPOLE_A	108	3189.547		26.383	1.514	25.316	0.000	0.000	-1.236	0.056	28.602	-1.512	24.401	0.000	0.000	0.000	0.000
8382	DIPOLE_B	108	3196.002		12.040	0.708	25.375	0.000	0.000	-0.940	0.035	52.901	-2.251	24.428	0.000	0.000	0.000	0.000
8397	VC529	1	3197.170		10.555	0.563	25.392	0.000	0.000	-0.899	0.035	58.317	-2.385	24.431	0.000	0.000	0.000	0.000
8402	M_529	1	3198.370		9.827	0.006	25.411	0.000	0.000	-0.877	-0.002	61.437	0.109	24.434	0.000	0.000	0.000	0.000
8413	DIPOLE_C	61	3204.674		21.582	-1.454	25.485	0.000	0.000	-1.209	-0.068	28.109	2.337	24.458	0.000	0.000	0.000	0.000
8425	DIPOLE_D	61	3209.097		37.269	-2.092	25.510	0.000	0.000	-1.539	-0.082	11.927	1.321	24.497	0.000	0.000	0.000	0.000
8437	HC530	1	3209.744		40.033	-2.186	25.512	0.000	0.000	-1.592	-0.082	10.316	1.172	24.506	0.000	0.000	0.000	0.000
8442	M_530	1	3211.337		43.524	0.251	25.518	0.000	0.000	-1.651	0.016	7.886	0.358	24.535	0.000	0.000	0.000	0.000
8453	DIPOLE_C	62	3217.640		18.544	1.650	25.553	0.000	0.000	-1.044	0.098	13.939	-0.972	24.642	0.000	0.000	0.000	0.000
8465	DIPOLE_D	62	3222.064		7.876	0.762	25.612	0.000	0.000	-0.639	0.084	25.266	-1.588	24.680	0.000	0.000	0.000	0.000
8477	VC531	1	3222.710		6.975	0.632	25.626	0.000	0.000	-0.585	0.084	27.377	-1.678	24.684	0.000	0.000	0.000	0.000
8482	M_531	1	3224.303		5.980	-0.018	25.666	0.000	0.000	-0.474	0.054	30.470	-0.077	24.692	0.000	0.000	0.000	0.000
8493	DIPOLE_C	63	3230.607		18.024	-1.643	25.775	0.000	0.000	-0.307	0.014	15.921	0.976	24.737	0.000	0.000	0.000	0.000
8505	DIPOLE_D	63	3235.030		36.574	-2.551	25.802	0.000	0.000	-0.274	0.000	9.683	0.434	24.795	0.000	0.000	0.000	0.000
8517	HC532	1	3235.676		39.957	-2.684	25.805	0.000	0.000	-0.273	0.000	9.174	0.355	24.806	0.000	0.000	0.000	0.000
8522	M_532	1	3237.270		45.097	-0.250	25.811	0.000	0.000	-0.261	0.016	9.125	-0.364	24.834	0.000	0.000	0.000	0.000
8533	DIPOLE_C	64	3243.573		23.319	1.573	25.841	0.000	0.000	-0.105	0.017	27.965	-2.236	24.901	0.000	0.000	0.000	0.000
8545	DIPOLE_D	64	3247.997		12.317	0.914	25.883	0.000	0.000	-0.059	0.003	51.938	-3.183	24.920	0.000	0.000	0.000	0.000
8557	VC601	1	3248.643		11.198	0.818	25.892	0.000	0.000	-0.057	0.003	56.142	-3.321	24.922	0.000	0.000	0.000	0.000
8562	M_601	1	3250.236		9.814	0.030	25.916	0.000	0.000	-0.054	0.000	61.954	0.044	24.926	0.000	0.000	0.000	0.000
8576	HC602	1	3266.312		52.918	-2.333	26.044	0.000	0.000	-0.093	-0.002	11.055	0.643	25.028	0.000	0.000	0.000	0.000
8581	M_602	1	3267.525		56.176	-0.026	26.048	0.000	0.000	-0.093	0.002	10.153	0.059	25.047	0.000	0.000	0.000	0.000
8593	VC603	1	3283.601		11.005	0.541	26.157	0.000	0.000	-0.007	0.006	51.903	-2.256	25.174	0.000	0.000	0.000	0.000
8598	M_603	1	3284.813		10.328	-0.028	26.175	0.000	0.000	0.000	0.005	55.074	-0.044	25.177	0.000	0.000	0.000	0.000
8609	CAV	10	3289.247		16.307	-0.998	26.232	0.000	0.000	0.024	0.006	39.230	1.822	25.192	0.000	0.000	0.000	0.000
8617	CAV	11	3292.069		22.916	-1.344	26.255	0.000	0.000	0.040	0.006	29.820	1.511	25.205	0.000	0.000	0.000	0.000
8625	CAV	12	3294.892		31.476	-1.689	26.272	0.000	0.000	0.055	0.006	22.165	1.201	25.223	0.000	0.000	0.000	0.000
8633	CAV	13	3297.714		41.986	-2.035	26.284	0.000	0.000	0.071	0.006	16.266	0.890	25.247	0.000	0.000	0.000	0.000
8642	HC604	1	3300.889		56.138	-2.423	26.295	0.000	0.000	0.089	0.006	11.727	0.540	25.284	0.000	0.000	0.000	0.000
8647	M_604	1	3302.102		59.464	0.027	26.298	0.000	0.000	0.093	0.002	11.086	-0.062	25.301	0.000	0.000	0.000	0.000
8658	CAV	14	3306.182		42.879	2.108	26.311	0.000	0.000	0.085	-0.002	16.921	-1.025	25.350	0.000	0.000	0.000	0.000
8666	CAV	15	3309.005		31.991	1.750	26.323	0.000	0.000	0.078	-0.002	23.672	-1.367	25.372	0.000	0.000	0.000	0.000

8674 CAV	16	3311.828	23.125	1.391	26.339	0.000	0.000	0.072-0.002	32.353	-1.709	25.389	0.000	0.000	0.000	0.000
8682 CAV	17	3314.650	16.283	1.033	26.362	0.000	0.000	0.065-0.002	42.965	-2.051	25.401	0.000	0.000	0.000	0.000
8690 CAV	18	3317.473	11.463	0.675	26.396	0.000	0.000	0.058-0.002	55.508	-2.393	25.410	0.000	0.000	0.000	0.000
8699 VC605	1	3318.178	10.575	0.585	26.406	0.000	0.000	0.056-0.002	58.942	-2.478	25.412	0.000	0.000	0.000	0.000
8704 M_605	1	3319.391	9.783	0.027	26.425	0.000	0.000	0.054 0.000	62.329	0.040	25.415	0.000	0.000	0.000	0.000
end MI_19	1	3319.391	9.783	0.027	26.425	0.000	0.000	0.054 0.000	62.329	0.040	25.415	0.000	0.000	0.000	0.000

1
Linear lattice functions for beam line: MI_19
delta(p)/p = 0.000000 symm = F

"MAD" Version: 8.17 Run: 09/09/94 15.47.38
Range: #S/#E

page 22

total length =	3319.390644	Qx	=	26.425002	Qy	=	25.414999
delta(s) =	0.000000 mm	Qx'	=	-33.680129	Qy'	=	-32.868866
alfa =	0.214335E-02	betax(max)	=	60.004873	betay(max)	=	63.077526
gamma(tr) =	21.599969	Dx(max)	=	1.972394	Dy(max)	=	0.000000
		Dx(r.m.s.)	=	1.203958	Dy(r.m.s.)	=	0.000000
		xco(max)	=	0.000000	yco(max)	=	0.000000
		xco(r.m.s.)	=	0.000000	yco(r.m.s.)	=	0.000000

1

Survey of beam line: MI_19

"MAD" Version: 8.17

Run: 09/09/94 16.01.53

range: #S/#E

page 1

E L E M E N T			S E Q U E N C E		P O S I T I O N S			A N G L E S		
pos.	element	occ.	sum(L)	arc	x	y	z	theta	phi	psi
no.	name	no.	[m]	[m]	[m]	[m]	[m]	[rad]	[rad]	[rad]
begin	MI_19	1	0.000000	0.000000	29606.625709	218.153141	30942.395446	2.596497	0.000000	0.000000
57	M_606	1	17.288639	17.288639	29615.589860	218.153141	30927.612312	2.596497	0.000000	0.000000
106	M_607	1	34.577278	34.577278	29624.554010	218.153141	30912.829179	2.596497	0.000000	0.000000
123	M_608	1	51.865917	51.865917	29633.518161	218.153141	30898.046045	2.596497	0.000000	0.000000
141	M_609	1	69.154556	69.154556	29642.482312	218.153141	30883.262911	2.596497	0.000000	0.000000
181	M_610	1	82.120970	82.121035	29649.050305	218.153141	30872.083777	2.624299	0.000000	0.000000
221	M_611	1	95.087384	95.087515	29655.305001	218.153141	30860.726385	2.652101	0.000000	0.000000
261	M_612	1	108.053798	108.053994	29661.241565	218.153141	30849.199513	2.679903	0.000000	0.000000
301	M_613	1	121.020212	121.020474	29666.855411	218.153141	30837.512070	2.707704	0.000000	0.000000
349	M_614	1	138.308630	138.309113	29673.794179	218.153141	30821.679054	2.749407	0.000000	0.000000
401	M_615	1	155.597048	155.597752	29680.066829	218.153141	30805.570524	2.791109	0.000000	0.000000
441	M_616	1	168.563462	168.564231	29684.348951	218.153141	30793.332264	2.818911	0.000000	0.000000
481	M_617	1	181.529876	181.530710	29688.289217	218.153141	30780.979698	2.846713	0.000000	0.000000
521	M_618	1	194.496290	194.497190	29691.884583	218.153141	30768.522374	2.874514	0.000000	0.000000
561	M_619	1	207.462704	207.463669	29695.132268	218.153141	30755.969919	2.902316	0.000000	0.000000
580	M_620	1	224.751343	224.752308	29699.229672	218.153141	30739.173839	2.902316	0.000000	0.000000
597	M_621	1	242.039982	242.040947	29703.327075	218.153141	30722.377758	2.902316	0.000000	0.000000
615	M_622	1	259.328621	259.329586	29707.424478	218.153141	30705.581677	2.902316	0.000000	0.000000
655	M_623	1	272.295035	272.296066	29710.321974	218.153141	30692.943794	2.930118	0.000000	0.000000
695	M_624	1	285.261449	285.262545	29712.867041	218.153141	30680.230250	2.957920	0.000000	0.000000
735	M_625	1	298.227863	298.229025	29715.057712	218.153141	30667.450970	2.985721	0.000000	0.000000
775	M_626	1	311.194277	311.195504	29716.892293	218.153141	30654.615533	3.013523	0.000000	0.000000
827	M_627	1	328.482695	328.484143	29718.742198	218.153141	30637.428074	3.055226	0.000000	0.000000
876	M_628	1	345.771113	345.772782	29719.873942	218.153141	30620.178435	3.096928	0.000000	0.000000
925	M_629	1	363.059531	363.061421	29720.285556	218.153141	30602.896611	3.138631	0.000000	0.000000
974	M_630	1	380.347949	380.350060	29719.976324	218.153141	30585.612651	3.180333	0.000000	0.000000
1028	M_631	1	397.636367	397.638698	29718.946786	218.153141	30568.356610	3.222036	0.000000	0.000000
1080	M_632	1	414.924785	414.927337	29717.198730	218.153141	30551.158495	3.263738	0.000000	0.000000
1129	M_633	1	432.213203	432.215976	29714.735196	218.153141	30534.048209	3.305441	0.000000	0.000000
1178	M_634	1	449.501621	449.504615	29711.560468	218.153141	30517.055505	3.347143	0.000000	0.000000
1231	M_635	1	466.790039	466.793254	29707.680066	218.153141	30500.209931	3.388846	0.000000	0.000000
1284	M_636	1	484.078457	484.081893	29703.100738	218.153141	30483.540778	3.430549	0.000000	0.000000
1337	M_637	1	501.366875	501.370532	29697.830447	218.153141	30467.077033	3.472251	0.000000	0.000000
1385	M_638	1	518.655293	518.659170	29691.878357	218.153141	30450.847322	3.513954	0.000000	0.000000
1425	M_639	1	531.621707	531.625650	29686.993778	218.153141	30438.836807	3.541755	0.000000	0.000000
1465	M_640	1	544.588121	544.592129	29681.777217	218.153141	30426.966716	3.569557	0.000000	0.000000
1505	M_641	1	557.554535	557.558609	29676.232705	218.153141	30415.246222	3.597359	0.000000	0.000000
1545	M_100	1	570.520949	570.525088	29670.364528	218.153141	30403.684385	3.625161	0.000000	0.000000
1564	M_101	1	587.809588	587.813727	29662.326333	218.153141	30388.378032	3.625161	0.000000	0.000000
1581	M_102	1	605.098227	605.102366	29654.288137	218.153141	30373.071679	3.625161	0.000000	0.000000
1598	M_103	1	622.386866	622.391005	29646.249942	218.153141	30357.765325	3.625161	0.000000	0.000000
1616	M_104	1	639.675505	639.679644	29638.211746	218.153141	30342.458972	3.625161	0.000000	0.000000
1656	M_105	1	652.641919	652.646124	29632.024440	218.153141	30331.064727	3.652962	0.000000	0.000000
1696	M_106	1	665.608333	665.612603	29625.522786	218.153141	30319.846881	3.680764	0.000000	0.000000
1736	M_107	1	678.574747	678.579083	29618.711809	218.153141	30308.814103	3.708566	0.000000	0.000000

1776 M_108	1	691.541161	691.545562	29611.596774	218.153141	30297.974922	3.736367	0.000000	0.000000
1828 M_109	1	708.829579	708.834201	29601.614214	218.153141	30283.861829	3.778070	0.000000	0.000000
1873 M_110	1	726.117997	726.122840	29591.051952	218.153141	30270.177185	3.819772	0.000000	0.000000

1
Survey of beam line: MI_19

"MAD" Version: 8.17 Run: 09/09/94 16.01.53
range: #S/#E page 2

E L E M E N T			S E Q U E N C E		P O S I T I O N S				A N G L E S			
pos. no.	element name	occ. no.	sum(L) [m]	arc [m]	I I I	x [m]	y [m]	z [m]	I I I	theta [rad]	phi [rad]	psi [rad]
1922	M_111	1	743.406415	743.411479		29579.928353	218.153141	30256.944784		3.861475	0.000000	0.000000
1971	M_112	1	760.694833	760.700117		29568.262761	218.153141	30244.187635		3.903178	0.000000	0.000000
2025	M_113	1	777.983251	777.988756		29556.075459	218.153141	30231.927922		3.944880	0.000000	0.000000
2073	M_114	1	795.271669	795.277395		29543.387640	218.153141	30220.186962		3.986583	0.000000	0.000000
2122	M_115	1	812.560087	812.566034		29530.221366	218.153141	30208.985172		4.028285	0.000000	0.000000
2167	M_116	1	829.848505	829.854673		29516.599531	218.153141	30198.342028		4.069988	0.000000	0.000000
2216	M_117	1	847.136923	847.143312		29502.545822	218.153141	30188.276039		4.111690	0.000000	0.000000
2261	M_118	1	864.425341	864.431951		29488.084676	218.153141	30178.804707		4.153393	0.000000	0.000000
2310	M_119	1	881.713759	881.720590		29473.241238	218.153141	30169.944502		4.195095	0.000000	0.000000
2359	M_120	1	899.002177	899.009228		29458.041319	218.153141	30161.710830		4.236798	0.000000	0.000000
2413	M_121	1	916.290595	916.297867		29442.511350	218.153141	30154.118008		4.278501	0.000000	0.000000
2461	M_122	1	933.579013	933.586506		29426.678335	218.153141	30147.179239		4.320203	0.000000	0.000000
2510	M_123	1	950.867431	950.875145		29410.569804	218.153141	30140.906589		4.361906	0.000000	0.000000
2555	M_124	1	968.155849	968.163784		29394.213770	218.153141	30135.310965		4.403608	0.000000	0.000000
2604	M_125	1	985.444267	985.452423		29377.638671	218.153141	30130.402096		4.445311	0.000000	0.000000
2649	M_126	1	1002.732685	1002.741062		29360.873330	218.153141	30126.188519		4.487013	0.000000	0.000000
2698	M_127	1	1020.021103	1020.029701		29343.946900	218.153141	30122.677561		4.528716	0.000000	0.000000
2747	M_128	1	1037.309521	1037.318339		29326.888812	218.153141	30119.875326		4.570418	0.000000	0.000000
2796	M_129	1	1054.597939	1054.606978		29309.728728	218.153141	30117.786687		4.612121	0.000000	0.000000
2841	M_130	1	1071.886357	1071.895617		29292.496487	218.153141	30116.415275		4.653824	0.000000	0.000000
2895	M_201	1	1089.174775	1089.184256		29275.222054	218.153141	30115.763477		4.695526	0.000000	0.000000
2943	M_202	1	1106.463193	1106.472895		29257.935466	218.153141	30115.832424		4.737229	0.000000	0.000000
2992	M_203	1	1123.751611	1123.761534		29240.666782	218.153141	30116.621997		4.778931	0.000000	0.000000
3037	M_204	1	1141.040029	1141.050173		29223.446029	218.153141	30118.130824		4.820634	0.000000	0.000000
3086	M_205	1	1158.328447	1158.338811		29206.303152	218.153141	30120.356279		4.862336	0.000000	0.000000
3139	M_206	1	1175.616865	1175.627450		29189.267960	218.153141	30123.294495		4.904039	0.000000	0.000000
3188	M_207	1	1192.905283	1192.916089		29172.370074	218.153141	30126.940361		4.945742	0.000000	0.000000
3237	M_208	1	1210.193701	1210.204728		29155.638877	218.153141	30131.287538		4.987444	0.000000	0.000000
3286	M_209	1	1227.482119	1227.493367		29139.103463	218.153141	30136.328468		5.029147	0.000000	0.000000
3335	M_210	1	1244.770537	1244.782006		29122.792584	218.153141	30142.054383		5.070849	0.000000	0.000000
3389	M_211	1	1262.058955	1262.070645		29106.734603	218.153141	30148.455329		5.112552	0.000000	0.000000
3441	M_212	1	1279.347373	1279.359284		29090.957440	218.153141	30155.520174		5.154254	0.000000	0.000000
3494	M_213	1	1296.635791	1296.647922		29075.488532	218.153141	30163.236634		5.195957	0.000000	0.000000
3547	M_214	1	1313.924209	1313.936561		29060.354776	218.153141	30171.591292		5.237659	0.000000	0.000000
3600	M_215	1	1331.212627	1331.225200		29045.582486	218.153141	30180.569619		5.279362	0.000000	0.000000
3648	M_216	1	1348.501045	1348.513839		29031.197351	218.153141	30190.156004		5.321065	0.000000	0.000000
3688	M_217	1	1361.467459	1361.480318		29020.664223	218.153141	30197.716743		5.348866	0.000000	0.000000
3728	M_218	1	1374.433873	1374.446798		29010.345339	218.153141	30205.567362		5.376668	0.000000	0.000000
3768	M_219	1	1387.400287	1387.413277		29000.248675	218.153141	30213.701793		5.404470	0.000000	0.000000
3808	M_220	1	1400.366701	1400.379757		28990.382035	218.153141	30222.113748		5.432271	0.000000	0.000000
3827	M_221	1	1417.655340	1417.668396		28977.382997	218.153141	30233.512083		5.432271	0.000000	0.000000
3844	M_222	1	1434.943979	1434.957035		28964.383958	218.153141	30244.910417		5.432271	0.000000	0.000000

3862 M_223	1	1452.232618	1452.245674	28951.384919	218.153141	30256.308752	5.432271	0.000000	0.000000
3902 M_224	1	1465.199032	1465.212153	28941.755928	218.153141	30264.991730	5.460073	0.000000	0.000000
3942 M_225	1	1478.165446	1478.178633	28932.372030	218.153141	30273.939022	5.487875	0.000000	0.000000
3982 M_226	1	1491.131860	1491.145112	28923.240475	218.153141	30283.143710	5.515676	0.000000	0.000000
4022 M_227	1	1504.098274	1504.111592	28914.368322	218.153141	30292.598681	5.543478	0.000000	0.000000
4070 M_228	1	1521.386692	1521.400230	28902.984597	218.153141	30305.607974	5.585181	0.000000	0.000000

1

"MAD" Version: 8.17

Run: 09/09/94 16.01.53

Survey of beam line: MI_19

range: #S/#E

page 3

E L E M E N T			S E Q U E N C E		P O S I T I O N S			A N G L E S				
pos.	element	occ.	sum(L)	arc	I	x	y	z	I	theta	phi	psi
no.	name	no.	[m]	[m]	I	[m]	[m]	[m]	I	[rad]	[rad]	[rad]
4122	M_229	1	1538.675110	1538.688869	28892.153133	218.153141	30319.080548	5.626883	0.000000	0.000000	0.000000	0.000000
4162	M_230	1	1551.641524	1551.655349	28884.385076	218.153141	30329.461727	5.654685	0.000000	0.000000	0.000000	0.000000
4202	M_231	1	1564.607938	1564.621828	28876.908598	218.153141	30340.054831	5.682487	0.000000	0.000000	0.000000	0.000000
4242	M_232	1	1577.574352	1577.588308	28869.729477	218.153141	30350.851674	5.710288	0.000000	0.000000	0.000000	0.000000
4282	M_301	1	1590.540766	1590.554787	28862.853263	218.153141	30361.843910	5.738090	0.000000	0.000000	0.000000	0.000000
4301	M_302	1	1607.829405	1607.843426	28853.889113	218.153141	30376.627044	5.738090	0.000000	0.000000	0.000000	0.000000
4318	M_303	1	1625.118044	1625.132065	28844.924962	218.153141	30391.410177	5.738090	0.000000	0.000000	0.000000	0.000000
4335	M_304	1	1642.406683	1642.420704	28835.960811	218.153141	30406.193311	5.738090	0.000000	0.000000	0.000000	0.000000
4352	M_305	1	1659.695322	1659.709343	28826.996660	218.153141	30420.976444	5.738090	0.000000	0.000000	0.000000	0.000000
4369	M_306	1	1676.983961	1676.997982	28818.032509	218.153141	30435.759578	5.738090	0.000000	0.000000	0.000000	0.000000
4386	M_307	1	1694.272600	1694.286621	28809.068358	218.153141	30450.542712	5.738090	0.000000	0.000000	0.000000	0.000000
4403	M_308	1	1711.561239	1711.575260	28800.104208	218.153141	30465.325845	5.738090	0.000000	0.000000	0.000000	0.000000
4421	M_309	1	1728.849878	1728.863899	28791.140057	218.153141	30480.108979	5.738090	0.000000	0.000000	0.000000	0.000000
4461	M_310	1	1741.816292	1741.830379	28784.572064	218.153141	30491.288113	5.765892	0.000000	0.000000	0.000000	0.000000
4501	M_311	1	1754.782706	1754.796858	28778.317367	218.153141	30502.645505	5.793694	0.000000	0.000000	0.000000	0.000000
4541	M_312	1	1767.749120	1767.763337	28772.380803	218.153141	30514.172377	5.821495	0.000000	0.000000	0.000000	0.000000
4581	M_313	1	1780.715534	1780.729817	28766.766957	218.153141	30525.859820	5.849297	0.000000	0.000000	0.000000	0.000000
4629	M_314	1	1798.003952	1798.018456	28759.828189	218.153141	30541.692835	5.890999	0.000000	0.000000	0.000000	0.000000
4681	M_315	1	1815.292370	1815.307095	28753.555538	218.153141	30557.801365	5.932702	0.000000	0.000000	0.000000	0.000000
4721	M_316	1	1828.258784	1828.273574	28749.273417	218.153141	30570.039626	5.960504	0.000000	0.000000	0.000000	0.000000
4761	M_317	1	1841.225198	1841.240053	28745.333150	218.153141	30582.392191	5.988305	0.000000	0.000000	0.000000	0.000000
4801	M_318	1	1854.191612	1854.206533	28741.737785	218.153141	30594.849515	6.016107	0.000000	0.000000	0.000000	0.000000
4841	M_319	1	1867.158026	1867.173012	28738.490099	218.153141	30607.401970	6.043909	0.000000	0.000000	0.000000	0.000000
4860	M_320	1	1884.446665	1884.461651	28734.392695	218.153141	30624.198051	6.043909	0.000000	0.000000	0.000000	0.000000
4877	M_321	1	1901.735304	1901.750290	28730.295292	218.153141	30640.994131	6.043909	0.000000	0.000000	0.000000	0.000000
4895	M_322	1	1919.023943	1919.038929	28726.197889	218.153141	30657.790212	6.043909	0.000000	0.000000	0.000000	0.000000
4935	M_323	1	1931.990357	1932.005409	28723.300392	218.153141	30670.428095	6.071711	0.000000	0.000000	0.000000	0.000000
4975	M_324	1	1944.956771	1944.971888	28720.755325	218.153141	30683.141640	6.099512	0.000000	0.000000	0.000000	0.000000
5015	M_325	1	1957.923185	1957.938368	28718.564654	218.153141	30695.921019	6.127314	0.000000	0.000000	0.000000	0.000000
5055	M_326	1	1970.889599	1970.904847	28716.730073	218.153141	30708.756357	6.155116	0.000000	0.000000	0.000000	0.000000
5107	M_327	1	1988.178017	1988.193486	28714.880168	218.153141	30725.943815	6.196818	0.000000	0.000000	0.000000	0.000000
5156	M_328	1	2005.466435	2005.482125	28713.748424	218.153141	30743.193454	6.238521	0.000000	0.000000	0.000000	0.000000
5205	M_329	1	2022.754853	2022.770764	28713.336810	218.153141	30760.475279	6.280223	0.000000	0.000000	0.000000	0.000000
5254	M_330	1	2040.043271	2040.059403	28713.646041	218.153141	30777.759238	6.321926	0.000000	0.000000	0.000000	0.000000
5308	M_331	1	2057.331689	2057.348041	28714.675579	218.153141	30795.015279	6.363628	0.000000	0.000000	0.000000	0.000000
5360	M_332	1	2074.620107	2074.636680	28716.423635	218.153141	30812.213394	6.405331	0.000000	0.000000	0.000000	0.000000
5409	M_333	1	2091.908525	2091.925319	28718.887169	218.153141	30829.323680	6.447034	0.000000	0.000000	0.000000	0.000000
5458	M_334	1	2109.196943	2109.213958	28722.061897	218.153141	30846.316384	6.488736	0.000000	0.000000	0.000000	0.000000
5511	M_335	1	2126.485361	2126.502597	28725.942298	218.153141	30863.161959	6.530439	0.000000	0.000000	0.000000	0.000000

5564	M_336	1	2143.773779	2143.791236	28730.521626	218.153141	30879.831111	6.572141	0.000000	0.000000
5617	M_337	1	2161.062197	2161.079875	28735.791916	218.153141	30896.294857	6.613844	0.000000	0.000000
5665	M_338	1	2178.350615	2178.368514	28741.744007	218.153141	30912.524567	6.655546	0.000000	0.000000
5705	M_339	1	2191.317029	2191.334993	28746.628586	218.153141	30924.535082	6.683348	0.000000	0.000000
5745	M_340	1	2204.283443	2204.301472	28751.845147	218.153141	30936.405174	6.711150	0.000000	0.000000
5785	M_341	1	2217.249857	2217.267952	28757.389658	218.153141	30948.125667	6.738951	0.000000	0.000000
5825	M_400	1	2230.216271	2230.234431	28763.257835	218.153141	30959.687505	6.766753	0.000000	0.000000
5844	M_401	1	2247.504910	2247.523070	28771.296030	218.153141	30974.993858	6.766753	0.000000	0.000000
5861	M_402	1	2264.793549	2264.811709	28779.334226	218.153141	30990.300211	6.766753	0.000000	0.000000

1

"MAD" Version: 8.17

Run: 09/09/94 16.01.53

Survey of beam line: MI_19

range: #S/#E

page 4

pos. no.	E L E M E N T element name	occ. no.	S E Q U E N C E sum(L) [m]	arc [m]	I I I	P O S I T I O N S x [m]	y [m]	z [m]	I I I	A N G L E S theta [rad]	phi [rad]	psi [rad]
5878	M_403	1	2282.082188	2282.100348	28787.372421	218.153141	31005.606565	6.766753	0.000000	0.000000	0.000000	
5896	M_404	1	2299.370827	2299.388987	28795.410616	218.153141	31020.912918	6.766753	0.000000	0.000000	0.000000	
5936	M_405	1	2312.337241	2312.355467	28801.597923	218.153141	31032.307163	6.794555	0.000000	0.000000	0.000000	
5976	M_406	1	2325.303655	2325.321946	28808.099576	218.153141	31043.525009	6.822357	0.000000	0.000000	0.000000	
6016	M_407	1	2338.270069	2338.288426	28814.910553	218.153141	31054.557787	6.850158	0.000000	0.000000	0.000000	
6056	M_408	1	2351.236483	2351.254905	28822.025588	218.153141	31065.396969	6.877960	0.000000	0.000000	0.000000	
6108	M_409	1	2368.524901	2368.543544	28832.008148	218.153141	31079.510061	6.919663	0.000000	0.000000	0.000000	
6153	M_410	1	2385.813319	2385.832183	28842.570410	218.153141	31093.194706	6.961365	0.000000	0.000000	0.000000	
6202	M_411	1	2403.101737	2403.120822	28853.694008	218.153141	31106.427107	7.003068	0.000000	0.000000	0.000000	
6251	M_412	1	2420.390155	2420.409461	28865.359601	218.153141	31119.184256	7.044770	0.000000	0.000000	0.000000	
6305	M_413	1	2437.678573	2437.698099	28877.546902	218.153141	31131.443969	7.086473	0.000000	0.000000	0.000000	
6353	M_414	1	2454.966991	2454.986738	28890.234721	218.153141	31143.184929	7.128175	0.000000	0.000000	0.000000	
6402	M_415	1	2472.255409	2472.275377	28903.400995	218.153141	31154.386719	7.169878	0.000000	0.000000	0.000000	
6447	M_416	1	2489.543827	2489.564016	28917.022829	218.153141	31165.029863	7.211580	0.000000	0.000000	0.000000	
6496	M_417	1	2506.832245	2506.852655	28931.076539	218.153141	31175.095853	7.253283	0.000000	0.000000	0.000000	
6541	M_418	1	2524.120663	2524.141294	28945.537685	218.153141	31184.567185	7.294986	0.000000	0.000000	0.000000	
6590	M_419	1	2541.409081	2541.429933	28960.381123	218.153141	31193.427390	7.336688	0.000000	0.000000	0.000000	
6639	M_420	1	2558.697499	2558.718572	28975.581041	218.153141	31201.661062	7.378391	0.000000	0.000000	0.000000	
6693	M_421	1	2575.985917	2576.007210	28991.111010	218.153141	31209.253884	7.420093	0.000000	0.000000	0.000000	
6741	M_422	1	2593.274335	2593.295849	29006.944025	218.153141	31216.192653	7.461796	0.000000	0.000000	0.000000	
6790	M_423	1	2610.562753	2610.584488	29023.052556	218.153141	31222.465303	7.503498	0.000000	0.000000	0.000000	
6835	M_424	1	2627.851171	2627.873127	29039.408590	218.153141	31228.060928	7.545201	0.000000	0.000000	0.000000	
6884	M_425	1	2645.139589	2645.161766	29055.983689	218.153141	31232.969797	7.586903	0.000000	0.000000	0.000000	
6929	M_426	1	2662.428007	2662.450405	29072.749030	218.153141	31237.183374	7.628606	0.000000	0.000000	0.000000	
6978	M_427	1	2679.716425	2679.739044	29089.675460	218.153141	31240.694332	7.670309	0.000000	0.000000	0.000000	
7027	M_428	1	2697.004843	2697.027682	29106.733548	218.153141	31243.496568	7.712011	0.000000	0.000000	0.000000	
7076	M_429	1	2714.293261	2714.316321	29123.893632	218.153141	31245.585207	7.753714	0.000000	0.000000	0.000000	
7121	M_430	1	2731.581679	2731.604960	29141.125872	218.153141	31246.956619	7.795416	0.000000	0.000000	0.000000	
7175	M_501	1	2748.870097	2748.893599	29158.400306	218.153141	31247.608418	7.837119	0.000000	0.000000	0.000000	
7223	M_502	1	2766.158515	2766.182238	29175.686894	218.153141	31247.539470	7.878821	0.000000	0.000000	0.000000	
7272	M_503	1	2783.446933	2783.470877	29192.955578	218.153141	31246.749897	7.920524	0.000000	0.000000	0.000000	
7317	M_504	1	2800.735351	2800.759516	29210.176331	218.153141	31245.241071	7.962226	0.000000	0.000000	0.000000	
7366	M_505	1	2818.023769	2818.048155	29227.319208	218.153141	31243.015615	8.003929	0.000000	0.000000	0.000000	
7419	M_506	1	2835.312187	2835.336793	29244.354400	218.153141	31240.077400	8.045632	0.000000	0.000000	0.000000	
7468	M_507	1	2852.600605	2852.625432	29261.252286	218.153141	31236.431534	8.087334	0.000000	0.000000	0.000000	
7517	M_508	1	2869.889023	2869.914071	29277.983483	218.153141	31232.084357	8.129037	0.000000	0.000000	0.000000	

7566 M_509	1	2887.177441	2887.202710	29294.518897	218.153141	31227.043428	8.170739	0.000000	0.000000
7615 M_510	1	2904.465859	2904.491349	29310.829776	218.153141	31221.317512	8.212442	0.000000	0.000000
7669 M_511	1	2921.754277	2921.779988	29326.887758	218.153141	31214.916567	8.254144	0.000000	0.000000
7721 M_512	1	2939.042695	2939.068627	29342.664920	218.153141	31207.851722	8.295847	0.000000	0.000000
7774 M_513	1	2956.331113	2956.357265	29358.133828	218.153141	31200.135262	8.337549	0.000000	0.000000
7827 M_514	1	2973.619531	2973.645904	29373.267585	218.153141	31191.780605	8.379252	0.000000	0.000000
7880 M_515	1	2990.907949	2990.934543	29388.039874	218.153141	31182.802278	8.420955	0.000000	0.000000
7928 M_516	1	3008.196367	3008.223182	29402.425009	218.153141	31173.215893	8.462657	0.000000	0.000000
7968 M_517	1	3021.162781	3021.189662	29412.958138	218.153141	31165.655154	8.490459	0.000000	0.000000
8008 M_518	1	3034.129195	3034.156141	29423.277022	218.153141	31157.804535	8.518261	0.000000	0.000000
8048 M_519	1	3047.095609	3047.122620	29433.373686	218.153141	31149.670104	8.546062	0.000000	0.000000
8088 M_520	1	3060.062023	3060.089100	29443.240326	218.153141	31141.258149	8.573864	0.000000	0.000000

1

"MAD" Version: 8.17

Run: 09/09/94 16.01.53

Survey of beam line: MI_19

range: #S/#E

page 5

E L E M E N T		S E Q U E N C E		P O S I T I O N S				A N G L E S				
pos.	element	occ.	sum(L)	arc	I	x	y	z	I	theta	phi	psi
no.	name	no.	[m]	[m]	I	[m]	[m]	[m]	I	[rad]	[rad]	[rad]
8107 M_521	1	3077.350662	3077.377739	29456.239365	218.153141	31129.859815	8.573864	0.000000	0.000000			
8124 M_522	1	3094.639301	3094.666378	29469.238404	218.153141	31118.461480	8.573864	0.000000	0.000000			
8142 M_523	1	3111.927940	3111.955017	29482.237443	218.153141	31107.063146	8.573864	0.000000	0.000000			
8182 M_524	1	3124.894354	3124.921496	29491.866433	218.153141	31098.380167	8.601666	0.000000	0.000000			
8222 M_525	1	3137.860768	3137.887976	29501.250332	218.153141	31089.432876	8.629467	0.000000	0.000000			
8262 M_526	1	3150.827182	3150.854455	29510.381887	218.153141	31080.228188	8.657269	0.000000	0.000000			
8302 M_527	1	3163.793596	3163.820935	29519.254040	218.153141	31070.773217	8.685071	0.000000	0.000000			
8350 M_528	1	3181.082014	3181.109574	29530.637765	218.153141	31057.763925	8.726773	0.000000	0.000000			
8402 M_529	1	3198.370432	3198.398212	29541.469229	218.153141	31044.291350	8.768476	0.000000	0.000000			
8442 M_530	1	3211.336846	3211.364692	29549.237287	218.153141	31033.910172	8.796278	0.000000	0.000000			
8482 M_531	1	3224.303260	3224.331171	29556.713765	218.153141	31023.317067	8.824079	0.000000	0.000000			
8522 M_532	1	3237.269674	3237.297651	29563.892885	218.153141	31012.520225	8.851881	0.000000	0.000000			
8562 M_601	1	3250.236088	3250.264130	29570.769099	218.153141	31001.527989	8.879683	0.000000	0.000000			
8581 M_602	1	3267.524727	3267.552769	29579.733250	218.153141	30986.744855	8.879683	0.000000	0.000000			
8598 M_603	1	3284.813366	3284.841408	29588.697401	218.153141	30971.961722	8.879683	0.000000	0.000000			
8647 M_604	1	3302.102005	3302.130047	29597.661552	218.153141	30957.178588	8.879683	0.000000	0.000000			
8704 M_605	1	3319.390644	3319.418686	29606.625703	218.153141	30942.395455	8.879683	0.000000	0.000000			
end MI_19	1	3319.390644	3319.418686	29606.625703	218.153141	30942.395455	8.879683	0.000000	0.000000			

total length =	3319.390644	arc length =	3319.418686		
error(x) =	-0.583462E-05	error(y) =	0.000000E+00	error(z) =	0.872414E-05
error(theta) =	-0.223796E-07	error(phi) =	0.000000E+00	error(psi) =	0.000000E+00

LINEAR LATTICE FUNCTIONS OF THE PROTON 8 GEV BEAM LINE

"MAD" Version: 8.17

Run: 13/05/94 15.09.04

Range: #S/#E

ELEMENT SEQUENCE		H O R I Z O N T A L										V E R T I C A L					
element name	quad type	dist [m]	betax [m]	alfax [1]	mux [2pi]	x(co) [mm]	px(co) [0.001]	Dx [m]	Dpx [1]	I	betay [m]	alfay [1]	muy [2pi]	y(co) [mm]	py(co) [0.001]	Dy [m]	Dpy [1]
BOOSTER		0.000	6.270	0.174	0.000	0.000	0.000	-1.841	0.087		20.060	0.050	0.000	0.000	0.000	0.000	0.000
EPB	us	7.077	12.038	-0.989	0.152	0.000	0.000	-1.228	0.087		21.855	-0.304	0.055	0.000	0.000	0.000	0.000
	ds	10.125	19.578	-1.489	0.183	0.000	0.000	-1.100	-0.003		23.989	-0.394	0.076	0.000	0.000	0.000	0.000
EPB	us	10.582	20.974	-1.564	0.187	0.000	0.000	-1.101	-0.003		24.359	-0.416	0.079	0.000	0.000	0.000	0.000
	ds	13.630	32.019	-2.064	0.206	0.000	0.000	-1.245	-0.092		27.137	-0.492	0.098	0.000	0.000	0.000	0.000
Q800	SQA	15.212	38.597	-0.579	0.213	0.000	0.000	-1.383	-0.030		29.082	-1.871	0.107	0.000	0.000	0.000	0.000
Q801	SQA	20.129	29.468	-1.560	0.236	0.000	0.000	-1.240	-0.070		68.181	0.612	0.125	0.000	0.000	0.000	0.000
Q802	SQA	24.005	67.648	-1.555	0.250	0.000	0.000	-1.888	-0.044		29.806	1.977	0.138	0.000	0.000	0.000	0.000
Q803	SQA	34.816	19.318	0.955	0.298	0.000	0.000	-0.967	0.063		34.765	0.413	0.193	0.000	0.000	0.000	0.000
EPB	us	37.160	17.313	0.331	0.319	0.000	0.000	-0.873	0.039		29.404	1.094	0.205	0.000	0.000	0.000	0.000
	ds	40.208	15.890	0.136	0.348	0.000	0.000	-0.859	-0.030		23.304	0.902	0.223	0.000	0.000	0.000	0.000
EPB	us	40.666	15.779	0.107	0.353	0.000	0.000	-0.872	-0.030		22.496	0.867	0.226	0.000	0.000	0.000	0.000
	ds	43.714	15.724	-0.089	0.384	0.000	0.000	-1.068	-0.099		17.841	0.657	0.251	0.000	0.000	0.000	0.000
B3	us	44.171	15.818	-0.118	0.388	0.000	0.000	-1.113	-0.099		17.258	0.620	0.255	0.000	0.000	0.000	0.000
	ds	50.241	19.560	-0.498	0.444	0.000	0.000	-1.711	-0.098		12.687	0.133	0.322	0.000	0.000	0.167	0.055
Q804	SQA	55.786	26.462	1.885	0.483	0.000	0.000	-2.230	0.132		13.972	-1.736	0.391	0.000	0.000	0.479	0.103
Q805	SQA	60.627	1.712	0.433	0.611	0.000	0.000	-0.526	0.297		61.650	-0.254	0.418	0.000	0.000	1.204	0.023
Q806	SQA	70.497	57.144	0.710	0.873	0.000	0.000	1.852	0.028		1.617	-0.496	0.691	0.000	0.000	0.149	-0.090
Q807	SQA	77.928	1.161	0.160	1.056	0.000	0.000	-0.486	-0.128		61.492	-0.236	0.825	0.000	0.000	-0.396	-0.027
Q808	SQA	85.360	48.571	-1.801	1.286	0.000	0.000	-0.055	-0.067		2.563	0.782	0.925	0.000	0.000	-0.256	-0.005
Q809	SQA	96.088	9.064	0.182	1.371	0.000	0.000	-0.719	-0.114		49.003	-1.261	1.222	0.000	0.000	-0.570	0.013
B3	us	103.449	23.790	-1.521	1.455	0.000	0.000	-1.963	-0.169		21.487	1.405	1.258	0.000	0.000	-0.167	0.055
	ds	109.520	47.295	-2.345	1.484	0.000	0.000	-2.988	-0.168		9.530	0.565	1.328	0.000	0.000	0.000	0.000
Q810	3Q52	110.561	50.703	0.000	1.488	0.000	0.000	-3.114	-0.018		8.784	0.000	1.346	0.000	0.000	0.000	0.000
B2	us	118.537	21.383	1.392	1.526	0.000	0.000	-2.105	0.133		24.027	-1.525	1.440	0.000	0.000	0.000	0.000
	ds	124.608	9.547	0.558	1.596	0.000	0.000	-1.417	0.094		47.601	-2.355	1.469	0.000	0.000	0.000	0.000
Q811	3Q52	125.573	8.882	0.000	1.613	0.000	0.000	-1.347	0.028		50.653	-0.002	1.472	0.000	0.000	0.000	0.000
B2	us	133.548	24.133	-1.522	1.706	0.000	0.000	-1.623	-0.037		21.389	1.390	1.510	0.000	0.000	0.000	0.000
	ds	139.619	47.669	-2.356	1.734	0.000	0.000	-1.966	-0.076		9.547	0.559	1.580	0.000	0.000	0.000	0.000
Q812	3Q52	140.584	50.720	0.000	1.738	0.000	0.000	-2.007	0.022		8.880	0.001	1.597	0.000	0.000	0.000	0.000
B2	us	148.560	21.390	1.393	1.776	0.000	0.000	-1.096	0.118		24.104	-1.520	1.690	0.000	0.000	0.000	0.000
	ds	154.630	9.548	0.559	1.846	0.000	0.000	-0.496	0.080		47.569	-2.343	1.719	0.000	0.000	0.000	0.000
Q813	3Q52	155.596	8.882	0.000	1.863	0.000	0.000	-0.426	0.058		50.597	0.008	1.722	0.000	0.000	0.000	0.000
B2	us	163.571	24.126	-1.521	1.956	0.000	0.000	-0.115	0.038		21.261	1.391	1.761	0.000	0.000	0.000	0.000
	ds	169.642	47.653	-2.355	1.984	0.000	0.000	0.000	0.000		9.444	0.555	1.831	0.000	0.000	0.000	0.000
Q814	3Q52	170.607	50.703	0.000	1.988	0.000	0.000	0.000	0.000		8.784	0.000	1.848	0.000	0.000	0.000	0.000
B2	us	175.354	31.806	1.836	2.006	0.000	0.000	-0.001	0.000		15.622	-1.079	1.916	0.000	0.000	0.000	0.000
	ds	181.424	14.584	1.002	2.052	0.000	0.000	0.114	0.038		33.787	-1.912	1.958	0.000	0.000	0.000	0.000
Q815	3Q52	185.618	8.882	0.000	2.113	0.000	0.000	0.278	0.051		50.823	-0.005	1.974	0.000	0.000	0.000	0.000
B2	us	190.365	15.737	-1.078	2.179	0.000	0.000	0.584	0.065		31.797	1.829	1.993	0.000	0.000	0.000	0.000
	ds	196.436	33.887	-1.912	2.222	0.000	0.000	1.097	0.104		14.593	1.003	2.038	0.000	0.000	0.000	0.000
Q816	3Q52	200.630	50.720	0.000	2.238	0.000	0.000	1.508	0.031		8.885	0.000	2.099	0.000	0.000	0.000	0.000
B2	us	205.376	31.816	1.836	2.256	0.000	0.000	1.334	-0.042		15.736	-1.078	2.166	0.000	0.000	0.000	0.000
	ds	211.447	14.588	1.002	2.302	0.000	0.000	1.195	-0.004		33.847	-1.904	2.208	0.000	0.000	0.000	0.000
Q817	3Q52	215.641	8.882	0.000	2.363	0.000	0.000	1.200	0.054		50.598	0.006	2.224	0.000	0.000	0.000	0.000
B2	us	220.388	15.733	-1.078	2.429	0.000	0.000	1.719	0.114		31.698	1.835	2.243	0.000	0.000	0.000	0.000
	ds	226.458	33.876	-1.912	2.472	0.000	0.000	2.526	0.152		14.468	1.001	2.289	0.000	0.000	0.000	0.000

LINEAR LATTICE FUNCTIONS OF THE PROTON 8 GEV BEAM LINE

"MAD" Version: 8.17

Run: 13/05/94 15.09.04

Range: #S/#E

ELEMENT SEQUENCE		H O R I Z O N T A L										V E R T I C A L						
element name	quad type	dist [m]	I [m]	betax [m]	alfax [1]	mux [2pi]	x(co) [mm]	px(co) [.001]	Dx [m]	Dpx [1]	I [m]	betay [m]	alfay [1]	muy [2pi]	y(co) [mm]	py(co) [.001]	Dy [m]	Dpy [1]
Q818	3Q52	230.653	50.703	0.000	2.488	0.000	0.000	0.000	3.114	0.002	8.784	0.000	0.000	2.350	0.000	0.000	0.000	0.000
B2		us	232.170	45.093	2.279	2.493	0.000	0.000	2.938	-0.149	10.101	-0.632	2.376	0.000	0.000	0.000	0.000	0.000
	3Q52	238.241	22.487	1.445	2.523	0.000	0.000	0.000	2.151	-0.110	22.852	-1.467	2.442	0.000	0.000	0.000	0.000	0.000
B2		us	238.628	21.388	1.392	2.526	0.000	0.000	0.000	2.109	-0.110	24.009	-1.521	2.444	0.000	0.000	0.000	0.000
	3Q52	244.699	9.549	0.558	2.596	0.000	0.000	0.000	1.556	-0.072	47.509	-2.347	2.473	0.000	0.000	0.000	0.000	0.000
Q819		us	245.664	8.883	0.000	2.613	0.000	0.000	0.000	1.511	0.002	50.549	0.000	2.478	0.000	0.000	0.000	0.000
B2	us	247.182	10.208	-0.634	2.638	0.000	0.000	0.000	1.601	0.076	44.955	2.273	2.481	0.000	0.000	0.000	0.000	0.000
	3Q52	253.252	22.969	-1.468	2.703	0.000	0.000	0.000	2.176	0.114	22.370	1.445	2.512	0.000	0.000	0.000	0.000	0.000
B2		us	253.640	24.127	-1.521	2.706	0.000	0.000	0.000	2.220	0.114	21.272	1.391	2.515	0.000	0.000	0.000	0.000
	3Q52	259.710	47.656	-2.355	2.734	0.000	0.000	0.000	3.029	0.152	9.445	0.555	2.585	0.000	0.000	0.000	0.000	0.000
Q820		us	260.675	50.706	0.000	2.738	0.000	0.000	0.000	3.126	0.001	8.784	0.000	2.602	0.000	0.000	0.000	0.000
B2	us	262.193	45.095	2.279	2.743	0.000	0.000	0.000	2.949	-0.150	10.098	-0.631	2.628	0.000	0.000	0.000	0.000	0.000
	3Q52	268.264	22.488	1.446	2.773	0.000	0.000	0.000	2.158	-0.111	22.837	-1.466	2.694	0.000	0.000	0.000	0.000	0.000
B2		us	268.651	21.389	1.392	2.776	0.000	0.000	0.000	2.115	-0.111	23.993	-1.520	2.696	0.000	0.000	0.000	0.000
	3Q52	274.722	9.549	0.559	2.846	0.000	0.000	0.000	1.557	-0.073	47.475	-2.346	2.725	0.000	0.000	0.000	0.000	0.000
Q821		us	275.687	8.883	0.000	2.863	0.000	0.000	0.000	1.511	0.001	50.513	0.000	2.728	0.000	0.000	0.000	0.000
B2	us	277.204	10.208	-0.634	2.888	0.000	0.000	0.000	1.600	0.075	44.923	2.271	2.733	0.000	0.000	0.000	0.000	0.000
	3Q52	283.275	22.968	-1.468	2.953	0.000	0.000	0.000	2.170	0.113	22.356	1.444	2.764	0.000	0.000	0.000	0.000	0.000
B2		us	283.662	24.126	-1.521	2.956	0.000	0.000	0.000	2.214	0.113	21.258	1.390	2.767	0.000	0.000	0.000	0.000
	3Q52	289.733	47.653	-2.355	2.984	0.000	0.000	0.000	3.018	0.152	9.444	0.554	2.837	0.000	0.000	0.000	0.000	0.000
Q822		us	290.698	50.703	0.000	2.988	0.000	0.000	0.000	3.115	0.001	8.784	0.000	2.854	0.000	0.000	0.000	0.000
B2	us	295.445	31.806	1.836	3.006	0.000	0.000	0.000	2.456	-0.149	15.623	-1.079	2.922	0.000	0.000	0.000	0.000	0.000
	3Q52	301.515	14.584	1.002	3.052	0.000	0.000	0.000	1.666	-0.111	33.792	-1.912	2.964	0.000	0.000	0.000	0.000	0.000
Q823		us	305.710	8.882	0.000	3.113	0.000	0.000	0.000	1.222	-0.050	50.630	-0.005	2.980	0.000	0.000	0.000	0.000
B2	us	310.456	15.737	-1.078	3.179	0.000	0.000	0.000	1.242	0.008	31.801	1.830	2.999	0.000	0.000	0.000	0.000	0.000
	3Q52	316.527	33.887	-1.912	3.222	0.000	0.000	0.000	1.410	0.047	14.594	1.003	3.044	0.000	0.000	0.000	0.000	0.000
Q824		us	320.721	50.720	0.000	3.238	0.000	0.000	0.000	1.581	-0.030	8.885	0.000	3.105	0.000	0.000	0.000	0.000
B2	us	325.468	31.816	1.836	3.256	0.000	0.000	0.000	1.104	-0.106	15.734	-1.077	3.172	0.000	0.000	0.000	0.000	0.000
	3Q52	331.538	14.588	1.002	3.302	0.000	0.000	0.000	0.578	-0.067	33.842	-1.903	3.214	0.000	0.000	0.000	0.000	0.000
Q825		us	335.732	8.882	0.000	3.363	0.000	0.000	0.000	0.300	-0.052	50.591	0.006	3.230	0.000	0.000	0.000	0.000
B2	us	340.479	15.733	-1.078	3.429	0.000	0.000	0.000	0.114	-0.038	31.694	1.834	3.249	0.000	0.000	0.000	0.000	0.000
	3Q52	346.550	33.876	-1.912	3.472	0.000	0.000	0.000	-0.001	0.000	14.467	1.001	3.295	0.000	0.000	0.000	0.000	0.000
Q826		us	350.744	50.703	0.000	3.488	0.000	0.000	0.000	-0.001	0.000	8.784	0.000	3.356	0.000	0.000	0.000	0.000
B2	us	355.490	31.806	1.836	3.506	0.000	0.000	0.000	0.001	0.000	15.625	-1.079	3.424	0.000	0.000	0.000	0.000	0.000
	3Q52	361.561	14.584	1.002	3.552	0.000	0.000	0.000	0.119	0.039	33.796	-1.912	3.466	0.000	0.000	0.000	0.000	0.000
Q827		us	365.755	8.882	0.000	3.613	0.000	0.000	0.000	0.285	0.052	50.637	-0.005	3.482	0.000	0.000	0.000	0.000
B2	us	370.502	15.737	-1.078	3.679	0.000	0.000	0.000	0.596	0.067	31.806	1.830	3.501	0.000	0.000	0.000	0.000	0.000
	3Q52	376.572	33.887	-1.912	3.722	0.000	0.000	0.000	1.117	0.105	14.595	1.003	3.546	0.000	0.000	0.000	0.000	0.000
Q828		us	380.767	50.720	0.000	3.738	0.000	0.000	0.000	1.533	0.031	8.885	0.001	3.607	0.000	0.000	0.000	0.000
B2	us	385.513	31.816	1.836	3.756	0.000	0.000	0.000	1.353	-0.043	15.732	-1.077	3.674	0.000	0.000	0.000	0.000	0.000
	3Q52	391.584	14.588	1.002	3.802	0.000	0.000	0.000	1.208	-0.005	33.837	-1.903	3.716	0.000	0.000	0.000	0.000	0.000
Q829		us	395.778	8.882	0.000	3.863	0.000	0.000	0.000	1.207	0.053	50.584	0.006	3.732	0.000	0.000	0.000	0.000
B2	us	400.525	15.733	-1.078	3.929	0.000	0.000	0.000	1.725	0.113	31.690	1.834	3.751	0.000	0.000	0.000	0.000	0.000
	3Q52	406.595	33.876	-1.912	3.972	0.000	0.000	0.000	2.528	0.152	14.466	1.001	3.797	0.000	0.000	0.000	0.000	0.000
Q830		us	410.789	50.703	0.000	3.988	0.000	0.000	0.000	3.115	0.001	8.785	-0.001	3.858	0.000	0.000	0.000	0.000
B2	us	412.307	45.093	2.279	3.993	0.000	0.000	0.000	2.938	-0.149	10.102	-0.632	3.884	0.000	0.000	0.000	0.000	0.000
	ds	418.378	22.487	1.445	4.023	0.000	0.000	0.000	2.148	-0.111	22.858	-1.468	3.950	0.000	0.000	0.000	0.000	0.000

LINEAR LATTICE FUNCTIONS OF THE PROTON 8 GEV BEAM LINE

"MAD" Version: 8.17

Run: 13/05/94 15.09:04

Range: #S/#E

ELEMENT SEQUENCE			H O R I Z O N T A L										V E R T I C A L					
element name	quad type	dist [m]	I I	betax [m]	alfax [1]	mux [2pi]	x(co) [mm]	px(co) [.001]	Dx [m]	Dpx [1]	I I	betay [m]	alfay [1]	muy [2pi]	y(co) [mm]	py(co) [.001]	Dy [m]	Dpy [1]
B2	us	418.765		21.388	1.392	4.026	0.000	0.000	2.105-0.111			24.016	-1.521	3.952	0.000	0.000	0.000	0.000
	ds	424.836		9.549	0.558	4.096	0.000	0.000	1.549-0.072			47.522	-2.348	3.981	0.000	0.000	0.000	0.000
Q831	3Q52	425.801		8.883	0.000	4.113	0.000	0.000	1.504 0.001			50.563	0.001	3.984	0.000	0.000	0.000	0.000
B2	us	427.318		10.208	-0.634	4.138	0.000	0.000	1.592 0.074			44.967	2.273	3.989	0.000	0.000	0.000	0.000
	ds	433.389		22.969	-1.468	4.203	0.000	0.000	2.160 0.113			22.375	1.445	4.020	0.000	0.000	0.000	0.000
B2	us	433.776		24.127	-1.521	4.206	0.000	0.000	2.204 0.113			21.276	1.392	4.023	0.000	0.000	0.000	0.000
	ds	439.847		47.656	-2.355	4.234	0.000	0.000	3.005 0.151			9.445	0.555	4.093	0.000	0.000	0.000	0.000
Q832	3Q52	440.812		50.706	0.000	4.238	0.000	0.000	3.102 0.001			8.784	0.001	4.110	0.000	0.000	0.000	0.000
B2	us	442.330		45.095	2.279	4.243	0.000	0.000	2.926-0.148			10.097	-0.630	4.136	0.000	0.000	0.000	0.000
	ds	448.400		22.488	1.446	4.273	0.000	0.000	2.142-0.110			22.830	-1.466	4.202	0.000	0.000	0.000	0.000
B2	us	448.788		21.389	1.392	4.276	0.000	0.000	2.099-0.110			23.987	-1.519	4.204	0.000	0.000	0.000	0.000
	ds	454.858		9.549	0.559	4.346	0.000	0.000	1.548-0.072			47.462	-2.345	4.233	0.000	0.000	0.000	0.000
Q833	3Q52	455.824		8.883	0.000	4.363	0.000	0.000	1.503 0.002			50.499	0.000	4.236	0.000	0.000	0.000	0.000
B2	us	457.341		10.208	-0.634	4.388	0.000	0.000	1.593 0.075			44.911	2.270	4.241	0.000	0.000	0.000	0.000
	ds	463.412		22.968	-1.468	4.453	0.000	0.000	2.166 0.114			22.351	1.443	4.272	0.000	0.000	0.000	0.000
B2	us	463.799		24.126	-1.521	4.456	0.000	0.000	2.210 0.114			21.254	1.390	4.275	0.000	0.000	0.000	0.000
	ds	469.870		47.653	-2.355	4.484	0.000	0.000	3.017 0.152			9.444	0.554	4.345	0.000	0.000	0.000	0.000
Q834	3Q52	470.835		50.703	0.000	4.488	0.000	0.000	3.114 0.002			8.785	-0.001	4.362	0.000	0.000	0.000	0.000
B2	us	472.353		45.093	2.279	4.493	0.000	0.000	2.938-0.149			10.102	-0.632	4.388	0.000	0.000	0.000	0.000
	ds	478.423		22.487	1.445	4.523	0.000	0.000	2.152-0.110			22.858	-1.468	4.454	0.000	0.000	0.000	0.000
B2	us	478.811		21.388	1.392	4.526	0.000	0.000	2.109-0.110			24.016	-1.521	4.456	0.000	0.000	0.000	0.000
	ds	484.881		9.549	0.558	4.596	0.000	0.000	1.558-0.072			47.522	-2.348	4.485	0.000	0.000	0.000	0.000
Q835	3Q52	485.846		8.883	0.000	4.613	0.000	0.000	1.511 0.002			50.563	0.001	4.488	0.000	0.000	0.000	0.000
B2	us	487.364		10.208	-0.634	4.638	0.000	0.000	1.601 0.076			44.967	2.273	4.493	0.000	0.000	0.000	0.000
	ds	493.435		22.969	-1.468	4.703	0.000	0.000	2.176 0.114			22.375	1.445	4.524	0.000	0.000	0.000	0.000
B2	us	493.822		24.127	-1.521	4.706	0.000	0.000	2.221 0.114			21.276	1.392	4.527	0.000	0.000	0.000	0.000
	ds	499.893		47.656	-2.355	4.734	0.000	0.000	3.029 0.152			9.445	0.555	4.597	0.000	0.000	0.000	0.000
Q836	3Q52	500.858		50.706	0.000	4.738	0.000	0.000	3.127 0.001			8.783	0.001	4.614	0.000	0.000	0.000	0.000
B2	us	505.604		31.807	1.836	4.756	0.000	0.000	2.466-0.150			15.611	-1.077	4.682	0.000	0.000	0.000	0.000
	ds	511.675		14.585	1.002	4.802	0.000	0.000	1.675-0.111			33.758	-1.910	4.724	0.000	0.000	0.000	0.000
Q837	3Q52	515.869		8.882	0.000	4.863	0.000	0.000	1.229-0.050			50.581	-0.006	4.740	0.000	0.000	0.000	0.000
B2	us	520.616		15.737	-1.078	4.929	0.000	0.000	1.251 0.009			31.772	1.828	4.759	0.000	0.000	0.000	0.000
	ds	526.686		33.885	-1.912	4.972	0.000	0.000	1.421 0.047			14.585	1.001	4.804	0.000	0.000	0.000	0.000
Q838	3Q52	530.881		50.717	0.000	4.988	0.000	0.000	1.594-0.030			8.886	-0.001	4.865	0.000	0.000	0.000	0.000
B2	us	535.627		31.814	1.836	5.006	0.000	0.000	1.112-0.107			15.746	-1.079	4.932	0.000	0.000	0.000	0.000
	ds	541.698		14.587	1.002	5.052	0.000	0.000	0.581-0.068			33.876	-1.905	4.974	0.000	0.000	0.000	0.000
Q839	3Q52	545.892		8.882	0.000	5.113	0.000	0.000	0.300-0.053			50.641	0.006	4.990	0.000	0.000	0.000	0.000
B2	us	550.639		15.734	-1.078	5.179	0.000	0.000	0.110-0.039			31.723	1.836	5.009	0.000	0.000	0.000	0.000
	ds	556.709		33.878	-1.912	5.222	0.000	0.000	-0.010-0.001			14.475	1.003	5.054	0.000	0.000	0.000	0.000
Q840	3Q52	560.903		50.706	0.000	5.238	0.000	0.000	-0.013 0.000			8.783	0.001	5.116	0.000	0.000	0.000	0.000
B2	us	565.650		31.807	1.836	5.256	0.000	0.000	-0.010 0.001			15.612	-1.078	5.183	0.000	0.000	0.000	0.000
	ds	571.721		14.585	1.002	5.302	0.000	0.000	0.110 0.039			33.763	-1.910	5.228	0.000	0.000	0.000	0.000
Q841	3Q52	575.915		8.882	0.000	5.363	0.000	0.000	0.278 0.052			50.588	-0.006	5.242	0.000	0.000	0.000	0.000
B2	us	580.661		15.737	-1.078	5.429	0.000	0.000	0.587 0.066			31.776	1.828	5.261	0.000	0.000	0.000	0.000
	ds	586.732		33.885	-1.912	5.472	0.000	0.000	1.106 0.105			14.587	1.002	5.306	0.000	0.000	0.000	0.000
Q842	3Q52	590.926		50.717	0.000	5.488	0.000	0.000	1.521 0.032			8.886	0.000	5.367	0.000	0.000	0.000	0.000

LINEAR LATTICE FUNCTIONS OF THE PROTON 8 GEV BEAM LINE

"MAD" Version: 8.17

Run: 13/05/94 15.09.04

Range: #S/#E

ELEMENT SEQUENCE		H O R I Z O N T A L																V E R T I C A L			
element name	quad type	dist [m]	I	betax [m]	alfax [1]	mux [2pi]	x(co) [mm]	px(co) [0.001]	Dx [m]	Dpx [1]	I	betay [m]	alfay [1]	muy [2pi]	y(co) [mm]	py(co) [0.001]	Dy [m]	Dpy [1]			
B2	us	595.673		31.814	1.836	5.506	0.000	0.000	1.344-0.042			15.745	-1.079	5.434	0.000	0.000	0.000	0.000			
	ds	601.743		14.587	1.002	5.552	0.000	0.000	1.204-0.004			33.871	-1.905	5.476	0.000	0.000	0.000	0.000			
Q843	3Q52	605.938		8.882	0.000	5.613	0.000	0.000	1.207 0.054			50.634	0.006	5.492	0.000	0.000	0.000	0.000			
B2	us	610.684		15.734	-1.078	5.679	0.000	0.000	1.729 0.114			31.719	1.836	5.511	0.000	0.000	0.000	0.000			
	ds	616.755		33.878	-1.912	5.722	0.000	0.000	2.537 0.152			14.474	1.002	5.556	0.000	0.000	0.000	0.000			
Q844	3Q52	620.949		50.706	0.000	5.738	0.000	0.000	3.127 0.001			8.783	0.000	5.618	0.000	0.000	0.000	0.000			
B2	us	622.467		45.095	2.279	5.743	0.000	0.000	2.949-0.150			10.097	-0.631	5.644	0.000	0.000	0.000	0.000			
	ds	628.537		22.488	1.446	5.773	0.000	0.000	2.158-0.111			22.836	-1.466	5.709	0.000	0.000	0.000	0.000			
B2	us	628.925		21.389	1.392	5.776	0.000	0.000	2.115-0.111			23.992	-1.520	5.712	0.000	0.000	0.000	0.000			
	ds	634.995		9.549	0.559	5.846	0.000	0.000	1.557-0.073			47.476	-2.346	5.741	0.000	0.000	0.000	0.000			
Q845	3Q52	635.960		8.883	0.000	5.863	0.000	0.000	1.511 0.001			50.514	0.000	5.744	0.000	0.000	0.000	0.000			
B2	us	637.478		10.208	-0.634	5.888	0.000	0.000	1.600 0.075			44.924	2.271	5.749	0.000	0.000	0.000	0.000			
	ds	643.549		22.968	-1.468	5.953	0.000	0.000	2.170 0.113			22.358	1.444	5.780	0.000	0.000	0.000	0.000			
B2	us	643.936		24.126	-1.521	5.956	0.000	0.000	2.214 0.113			21.260	1.390	5.783	0.000	0.000	0.000	0.000			
	ds	650.007		47.653	-2.355	5.984	0.000	0.000	3.017 0.152			9.445	0.554	5.853	0.000	0.000	0.000	0.000			
Q846	3Q52	650.972		50.703	0.000	5.988	0.000	0.000	3.114 0.001			8.785	0.000	5.870	0.000	0.000	0.000	0.000			
B2	us	652.489		45.093	2.279	5.993	0.000	0.000	2.937-0.149			10.102	-0.632	5.896	0.000	0.000	0.000	0.000			
	ds	658.560		22.487	1.445	6.023	0.000	0.000	2.148-0.111			22.853	-1.467	5.962	0.000	0.000	0.000	0.000			
B2	us	658.947		21.388	1.392	6.026	0.000	0.000	2.105-0.111			24.010	-1.521	5.964	0.000	0.000	0.000	0.000			
	ds	665.018		9.549	0.558	6.096	0.000	0.000	1.549-0.072			47.509	-2.347	5.993	0.000	0.000	0.000	0.000			
Q847	SQA	665.983		8.685	0.017	6.113	0.000	0.000	1.487-0.002			51.653	-0.029	5.996	0.000	0.000	0.000	0.000			
B2	us	667.501		10.099	-0.596	6.139	0.000	0.000	1.583 0.068			45.122	2.221	6.001	0.000	0.000	0.000	0.000			
	ds	673.571		22.280	-1.411	6.205	0.000	0.000	2.115 0.107			22.953	1.428	6.031	0.000	0.000	0.000	0.000			
B2	us	673.959		23.393	-1.463	6.208	0.000	0.000	2.156 0.107			21.866	1.377	6.034	0.000	0.000	0.000	0.000			
	ds	680.029		46.093	-2.277	6.237	0.000	0.000	2.921 0.145			10.012	0.575	6.101	0.000	0.000	0.000	0.000			
Q848	SQA	680.563		48.092	-0.114	6.239	0.000	0.000	2.984 0.007			9.529	0.064	6.110	0.000	0.000	0.000	0.000			
B2	us	685.741		29.625	1.535	6.261	0.000	0.000	2.321-0.131			16.576	-1.003	6.178	0.000	0.000	0.000	0.000			
	ds	691.812		15.166	0.847	6.307	0.000	0.000	1.644-0.092			33.172	-1.729	6.220	0.000	0.000	0.000	0.000			
Q849	SQA	698.829		8.931	-0.327	6.411	0.000	0.000	1.000-0.049			62.799	0.111	6.244	0.000	0.000	0.000	0.000			
B2	us	700.753		12.195	-1.032	6.440	0.000	0.000	0.982-0.007			53.121	2.528	6.249	0.000	0.000	0.000	0.000			
	ds	706.823		30.962	-2.060	6.491	0.000	0.000	1.056 0.031			27.501	1.689	6.275	0.000	0.000	0.000	0.000			
Q850	SQA	712.087		56.826	-0.484	6.511	0.000	0.000	1.216-0.021			13.724	0.359	6.319	0.000	0.000	0.000	0.000			
B2	us	715.764		43.922	1.667	6.522	0.000	0.000	0.951-0.074			16.360	-0.518	6.358	0.000	0.000	0.000	0.000			
	ds	721.835		26.855	1.145	6.551	0.000	0.000	0.620-0.035			25.476	-0.983	6.406	0.000	0.000	0.000	0.000			
Q851	SQA	726.744		17.835	0.019	6.587	0.000	0.000	0.448-0.017			36.679	0.094	6.432	0.000	0.000	0.000	0.000			
Q852	SQA	740.632		52.284	0.250	6.662	0.000	0.000	0.448-0.018			11.789	-0.195	6.548	0.000	0.000	0.000	0.000			
A0	us	752.019		15.387	0.941	6.727	0.000	0.000	0.047-0.035			42.778	-2.067	6.633	0.000	0.000	0.000	0.000			
	ds	754.305		11.724	0.661	6.755	0.000	0.000	0.006 0.000			52.812	-2.320	6.641	0.000	0.000	0.000	0.000			
P8_GEV		756.328		10.000	0.000	6.785	0.000	0.000	0.005 0.000			59.997	0.000	6.647	0.000	0.000	0.000	0.000			
total length =		756.327823		mux		=		6.785014		muy		=		6.646503							
delta(s) =		0.000000 mm		dmux		=		-8.441496		dmuy		=		-10.415721							
				betax(max)		=		67.648191		betay(max)		=		68.180677							
				Dx(max)		=		3.126693		Dy(max)		=		1.203951							
				Dx(r.m.s.)		=		1.737252		Dy(r.m.s.)		=		0.176398							

ELEMENT	SEQUENCE	I	POSITIONS			I	ANGLES		
element name	sum(L) [ft]	arc [ft]	x [ft]	y [ft]	z [ft]	I I	theta [rad]	phi [rad]	psi [rad]
P8_GEV	0.00000	0.00000	99511.38281	99309.84375	726.58203		-1.13370	0.00000	0.00000
EPB	23.21700	23.21700	99521.21094	99288.80469	726.58203		-1.13370	0.00000	0.00000
	33.21698	33.22030	99525.84375	99279.94531	726.58203		-1.04446	0.00000	0.00000
EPB	34.71698	34.72030	99526.80156	99278.64844	726.58203		-1.04446	0.00000	0.00000
	44.71696	44.72360	99532.00000	99270.24219	726.58203		-0.95523	0.00000	0.00000
M800 (SQA)	49.90789	49.91453	99535.00000	99265.99219	726.58203		-0.95523	0.00000	0.00000
M801 (SQA)	66.03976	66.04639	99544.32031	99252.82031	726.58203		-0.95523	0.00000	0.00000
M802 (SQA)	78.75495	78.76159	99551.65625	99242.44531	726.58203		-0.95523	0.00000	0.00000
M803 (SQA)	114.22593	114.23257	99572.14844	99213.47656	726.58203		-0.95523	0.00000	0.00000
EPB	121.91686	121.92349	99576.58594	99207.19531	726.58203		-0.95523	0.00000	0.00000
	131.91685	131.92546	99582.63281	99199.24219	726.58203		-0.88634	0.00000	0.00000
EPB	133.41684	133.42545	99583.58594	99198.08594	726.58203		-0.88634	0.00000	0.00000
	143.41682	143.42741	99590.16406	99190.55469	726.58203		-0.81744	0.00000	0.00000
B3	144.91681	144.92741	99591.18750	99189.46094	726.58203		-0.81744	0.00000	0.00000
	164.83345	164.84657	99604.81250	99174.93750	726.03253		-0.81744	-0.05518	0.00000
M804 (SQA)	183.02435	183.03746	99617.24219	99161.68750	725.02930		-0.81744	-0.05518	0.00000
M805 (SQA)	198.90620	198.91933	99628.09375	99150.12500	724.15338		-0.81744	-0.05518	0.00000
M806 (SQA)	231.28802	231.30115	99650.19531	99126.53906	722.36743		-0.81744	-0.05518	0.00000
M807 (SQA)	255.66988	255.68300	99666.85156	99108.78125	721.02271		-0.81744	-0.05518	0.00000
M808 (SQA)	280.05170	280.06485	99683.50781	99091.02344	719.67798		-0.81744	-0.05518	0.00000
M809 (SQA)	315.18353	315.19666	99707.50781	99065.43750	717.74030		-0.81744	-0.05518	0.00000
B3	339.40021	339.41336	99724.05469	99047.80469	716.40479		-0.81744	-0.05518	0.00000
	359.31886	359.33249	99737.66406	99033.28125	715.85529		-0.81744	0.00000	0.00000
M810 (3Q52)	362.73352	362.74915	99740.00781	99030.78906	715.85529		-0.81744	0.00000	0.00000
B2	388.90012	388.91577	99757.90625	99011.69531	715.85529		-0.81744	0.00000	0.00000
	408.81674	408.83362	99771.81250	98997.43750	715.85529		-0.77902	0.00000	0.00000
M811 (3Q52)	411.98340	412.00027	99774.06250	98995.21875	715.85529		-0.77902	0.00000	0.00000
B2	438.15002	438.16690	99792.67969	98976.83594	715.85529		-0.77902	0.00000	0.00000
	458.06665	458.08475	99807.12500	98963.11719	715.85529		-0.74061	0.00000	0.00000
M812 (3Q52)	461.23331	461.25137	99809.46094	98960.97656	715.85529		-0.74061	0.00000	0.00000
B2	487.39993	487.41800	99828.77344	98943.32031	715.85529		-0.74061	0.00000	0.00000
	507.31658	507.33591	99843.72656	98930.16406	715.85529		-0.70219	0.00000	0.00000
M813 (3Q52)	510.48318	510.50253	99846.14844	98928.12500	715.85529		-0.70219	0.00000	0.00000
B2	536.84984	536.86913	99866.12500	98911.21875	715.85529		-0.70219	0.00000	0.00000
	556.56647	556.58698	99881.57031	98898.65625	715.85529		-0.66377	0.00000	0.00000
M814 (3Q52)	559.73309	559.75366	99884.06250	98896.69531	715.85529		-0.66377	0.00000	0.00000
B2	575.30597	575.32654	99896.33594	98887.10156	715.85529		-0.66377	0.00000	0.00000
	595.22260	595.24438	99911.78125	98874.53125	715.85529		-0.70219	0.00000	0.00000
M815 (3Q52)	608.98297	609.00476	99922.28906	98865.64844	715.85529		-0.70219	0.00000	0.00000
B2	624.55591	624.57770	99934.17969	98855.59375	715.85529		-0.70219	0.00000	0.00000
	644.47253	644.49548	99949.12500	98842.43750	715.85529		-0.74061	0.00000	0.00000
M816 (3Q52)	658.23285	658.25592	99959.28906	98833.15625	715.85529		-0.74061	0.00000	0.00000
B2	673.80579	673.82880	99970.77344	98822.64844	715.85529		-0.74061	0.00000	0.00000
	693.72241	693.74664	99985.21875	98808.92969	715.85529		-0.77902	0.00000	0.00000
M817 (3Q52)	707.48285	707.50702	99995.00781	98799.25781	715.85529		-0.77902	0.00000	0.00000
B2	723.05566	723.07990	100006.09375	98788.31250	715.85529		-0.77902	0.00000	0.00000
	742.97235	742.99774	100020.00000	98774.05469	715.85529		-0.81744	0.00000	0.00000
M818 (3Q52)	756.73273	756.75812	100029.40625	98764.02344	715.85529		-0.81744	0.00000	0.00000

ELEMENT		SEQUENCE		POSITIONS			ANGLES		
element name		sum(L) [ft]	arc [ft]	x [ft]	y [ft]	z [ft]	theta [rad]	phi [rad]	psi [rad]
B2		761.71185	761.73730	100032.81250	98760.38281	715.85529	-0.81744	0.00000	0.00000
		781.62848	781.65521	100046.15625	98745.60156	715.85529	-0.85586	0.00000	0.00000
B2		782.89935	782.92596	100046.99219	98744.64844	715.85529	-0.85586	0.00000	0.00000
		802.81592	802.84381	100059.75781	98729.35156	715.85529	-0.89427	0.00000	0.00000
M819 (3Q52)		805.98260	806.01050	100061.74219	98726.88281	715.85529	-0.89427	0.00000	0.00000
B2		810.96173	810.98969	100064.85156	98723.00000	715.85529	-0.89427	0.00000	0.00000
		830.87842	830.90753	100077.02344	98707.22656	715.85529	-0.93269	0.00000	0.00000
B2		832.14923	832.17828	100077.78125	98706.21094	715.85529	-0.93269	0.00000	0.00000
		852.06586	852.09619	100089.33594	98690.00000	715.85529	-0.97111	0.00000	0.00000
M820 (3Q52)		855.23248	855.26294	100091.12500	98687.38281	715.85529	-0.97111	0.00000	0.00000
B2		860.21167	860.24200	100093.92969	98683.27344	715.85529	-0.97111	0.00000	0.00000
		880.12823	880.15991	100104.85156	98666.61719	715.85529	-1.00952	0.00000	0.00000
B2		881.39917	881.43066	100105.53125	98665.53125	715.85529	-1.00952	0.00000	0.00000
		901.31573	901.34857	100115.80469	98648.47656	715.85529	-1.04794	0.00000	0.00000
M821 (3Q52)		904.48242	904.51520	100117.38281	98645.72656	715.85529	-1.04794	0.00000	0.00000
B2		909.46149	909.49438	100119.87500	98641.41406	715.85529	-1.04794	0.00000	0.00000
		929.37823	929.41229	100129.49219	98623.97656	715.85529	-1.08636	0.00000	0.00000
B2		930.64899	930.68304	100130.07031	98622.85156	715.85529	-1.08636	0.00000	0.00000
		950.56567	950.60089	100139.00781	98605.05469	715.85529	-1.12477	0.00000	0.00000
M822 (3Q52)		953.73236	953.76758	100140.37500	98602.19531	715.85529	-1.12477	0.00000	0.00000
B2		969.30518	969.34039	100147.09375	98588.14844	715.85529	-1.12477	0.00000	0.00000
		989.22174	989.25830	100155.34375	98570.00781	715.85529	-1.16319	0.00000	0.00000
M823 (3Q52)		1002.98218	1003.01862	100160.78906	98557.38281	715.85529	-1.16319	0.00000	0.00000
B2		1018.55518	1018.59155	100166.96875	98543.08594	715.85529	-1.16319	0.00000	0.00000
		1038.47180	1038.50940	100174.50781	98524.65825	715.85529	-1.20161	0.00000	0.00000
M824 (3Q52)		1052.23218	1052.26978	100179.47656	98511.81250	715.85529	-1.20161	0.00000	0.00000
B2		1067.80505	1067.84277	100185.10156	98497.30469	715.85529	-1.20161	0.00000	0.00000
		1087.72156	1087.76050	100191.92969	98478.58594	715.85529	-1.24002	0.00000	0.00000
M825 (3Q52)		1101.48206	1101.52087	100196.39844	98465.57031	715.85529	-1.24002	0.00000	0.00000
B2		1117.05493	1117.09375	100201.46094	98450.84375	715.85529	-1.24002	0.00000	0.00000
		1136.97156	1137.01160	100207.56250	98431.88281	715.85529	-1.27844	0.00000	0.00000
M826 (3Q52)		1150.73193	1150.77209	100211.53125	98418.71094	715.85529	-1.27844	0.00000	0.00000
B2		1166.30481	1166.34485	100216.00781	98403.78906	715.85529	-1.27844	0.00000	0.00000
		1186.22144	1186.26282	100221.38281	98384.61719	715.85529	-1.31686	0.00000	0.00000
M827 (3Q52)		1199.98181	1200.02307	100224.84375	98371.30469	715.85529	-1.31686	0.00000	0.00000
B2		1215.55469	1215.59607	100228.75781	98356.22656	715.85529	-1.31686	0.00000	0.00000
		1235.47131	1235.51404	100233.38281	98336.85156	715.85529	-1.35527	0.00000	0.00000
M828 (3Q52)		1249.23169	1249.27429	100236.33594	98323.41406	715.85529	-1.35527	0.00000	0.00000
B2		1264.80457	1264.84729	100239.65625	98308.19531	715.85529	-1.35527	0.00000	0.00000
		1284.72131	1284.76501	100243.53906	98288.66406	715.85529	-1.39369	0.00000	0.00000
M829 (3Q52)		1298.48157	1298.52539	100245.96875	98275.12500	715.85529	-1.39369	0.00000	0.00000
B2		1314.05457	1314.09827	100248.71094	98259.78906	715.85529	-1.39369	0.00000	0.00000
		1333.97107	1334.01611	100251.84375	98240.12500	715.85529	-1.43211	0.00000	0.00000
M830 (3Q52)		1347.73157	1347.77649	100253.75000	98226.49219	715.85529	-1.43211	0.00000	0.00000
B2		1352.71057	1352.75574	100254.43750	98221.56250	715.85529	-1.43211	0.00000	0.00000
		1372.62732	1372.67346	100256.81250	98201.78125	715.85529	-1.47052	0.00000	0.00000
B2		1373.89807	1373.94446	100256.93750	98200.52344	715.85529	-1.47052	0.00000	0.00000
		1393.81482	1393.86230	100258.55469	98180.66406	715.85529	-1.50894	0.00000	0.00000

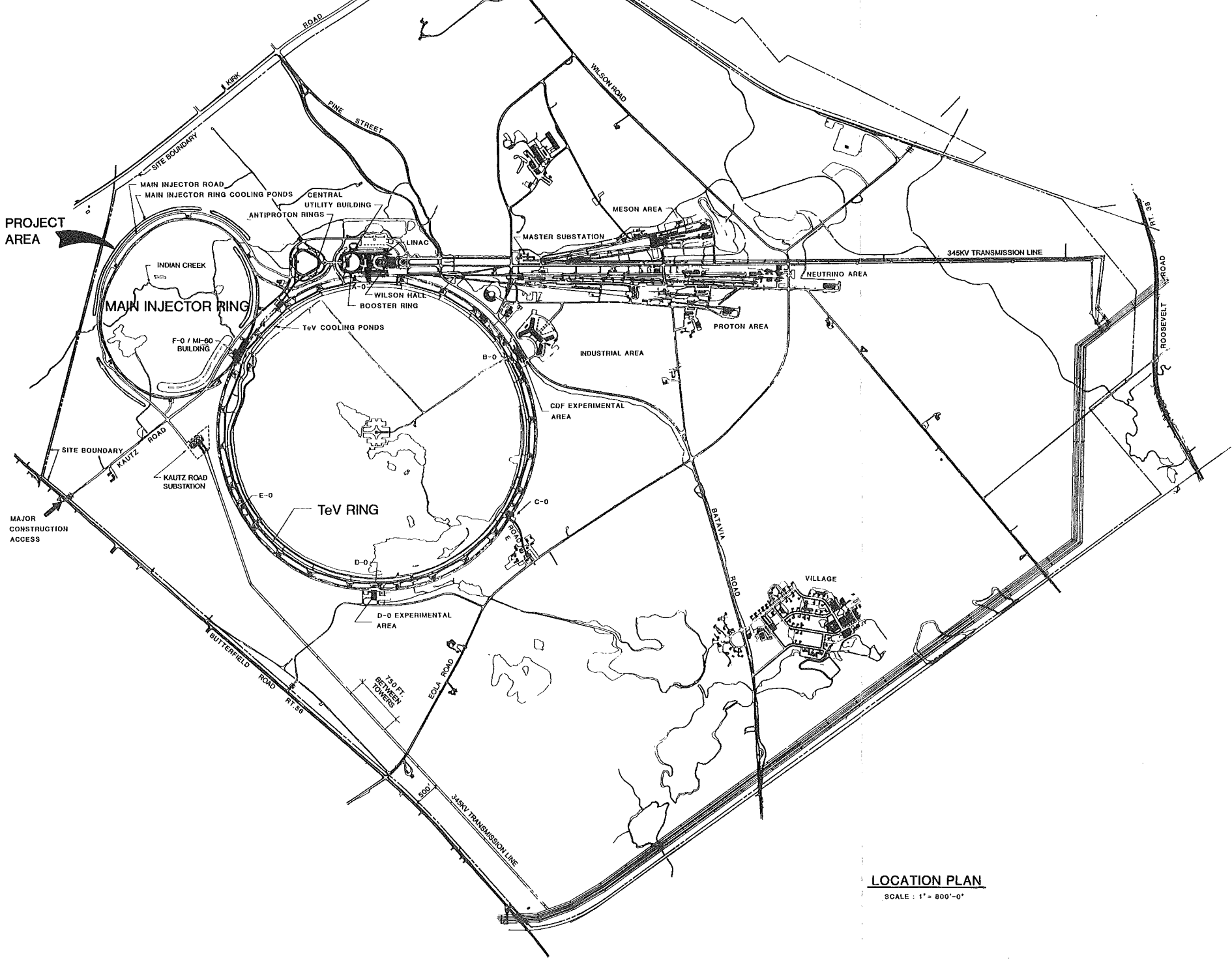
ELEMENT		SEQUENCE		POSITIONS			I		ANGLES		
element		sum(L)	arc	x	y	z	I		theta	phi	psi
name		[ft]	[ft]	[ft]	[ft]	[ft]	I		[rad]	[rad]	[rad]
M831	(3Q52)	1396.98145	1397.02893	100258.75000	98177.50781	715.85529			-1.50894	0.00000	0.00000
B2		1401.96057	1402.00793	100259.05469	98172.53906	715.85529			-1.50894	0.00000	0.00000
		1421.87708	1421.92590	100259.89844	98152.64844	715.85529			-1.54736	0.00000	0.00000
B2		1423.14795	1423.19678	100259.92969	98151.37500	715.85529			-1.54736	0.00000	0.00000
		1443.06458	1443.11462	100260.00781	98131.46094	715.85529			-1.58577	0.00000	0.00000
M832	(3Q52)	1446.23132	1446.28125	100259.96875	98128.28906	715.85529			-1.58577	0.00000	0.00000
B2		1451.21045	1451.26038	100259.89844	98123.31250	715.85529			-1.58577	0.00000	0.00000
		1471.12708	1471.17822	100259.21875	98103.40625	715.85529			-1.62419	0.00000	0.00000
B2		1472.39795	1472.44910	100259.14844	98102.13281	715.85529			-1.62419	0.00000	0.00000
		1492.31458	1492.36682	100257.69531	98082.27344	715.85529			-1.66261	0.00000	0.00000
M833	(3Q52)	1495.48132	1495.53369	100257.41406	98079.11719	715.85529			-1.66261	0.00000	0.00000
B2		1500.46045	1500.51270	100256.94531	98074.15625	715.85529			-1.66261	0.00000	0.00000
		1520.37695	1520.43066	100254.75000	98054.36719	715.85529			-1.70102	0.00000	0.00000
B2		1521.64783	1521.70154	100254.58594	98053.11719	715.85529			-1.70102	0.00000	0.00000
		1541.56445	1541.61926	100251.61719	98033.41406	715.85529			-1.73944	0.00000	0.00000
M834	(3Q52)	1544.73108	1544.78601	100251.09375	98030.28906	715.85529			-1.73944	0.00000	0.00000
B2		1549.71033	1549.76514	100250.25000	98025.38281	715.85529			-1.73944	0.00000	0.00000
		1569.62695	1569.68298	100246.53125	98005.82031	715.85529			-1.77786	0.00000	0.00000
B2		1570.89783	1570.95374	100246.27344	98004.57031	715.85529			-1.77786	0.00000	0.00000
		1590.81433	1590.87158	100241.80469	97985.16406	715.85529			-1.81627	0.00000	0.00000
M835	(3Q52)	1593.98096	1594.03821	100241.03125	97982.09375	715.85529			-1.81627	0.00000	0.00000
B2		1598.96008	1599.01746	100239.82031	97977.25781	715.85529			-1.81627	0.00000	0.00000
		1618.87683	1618.93542	100234.61719	97958.03906	715.85529			-1.85469	0.00000	0.00000
B2		1620.14758	1620.20618	100234.25000	97956.82031	715.85529			-1.85469	0.00000	0.00000
		1640.06433	1640.12402	100228.31250	97937.81250	715.85529			-1.89311	0.00000	0.00000
M836	(3Q52)	1643.23096	1643.29065	100227.31250	97934.81250	715.85529			-1.89311	0.00000	0.00000
B2		1658.80383	1658.86340	100222.37500	97920.03906	715.85529			-1.89311	0.00000	0.00000
		1678.72034	1678.78137	100215.71094	97901.27344	715.85529			-1.93152	0.00000	0.00000
M837	(3Q52)	1692.48083	1692.54163	100210.84375	97888.39844	715.85529			-1.93152	0.00000	0.00000
B2		1708.05371	1708.11462	100205.35156	97873.82031	715.85529			-1.93152	0.00000	0.00000
		1727.97021	1728.03259	100197.96875	97855.33594	715.85529			-1.96994	0.00000	0.00000
M838	(3Q52)	1741.73083	1741.79285	100192.61719	97842.64844	715.85529			-1.96994	0.00000	0.00000
B2		1757.30359	1757.36572	100186.56250	97828.30469	715.85529			-1.96994	0.00000	0.00000
		1777.22021	1777.28369	100178.47656	97810.10156	715.85529			-2.00836	0.00000	0.00000
M839	(3Q52)	1790.98047	1791.04395	100172.64844	97797.63281	715.85529			-2.00836	0.00000	0.00000
B2		1806.55334	1806.61682	100166.03906	97783.53125	715.85529			-2.00836	0.00000	0.00000
		1826.47021	1826.53479	100157.25781	97765.65625	715.85529			-2.04677	0.00000	0.00000
M840	(3Q52)	1840.23047	1840.29504	100150.94531	97753.42969	715.85529			-2.04677	0.00000	0.00000
B2		1855.80334	1855.86816	100143.82031	97739.58594	715.85529			-2.04677	0.00000	0.00000
		1875.72009	1875.78601	100134.35156	97722.06250	715.85529			-2.08519	0.00000	0.00000
M841	(3Q52)	1889.48047	1889.54626	100127.58594	97710.08594	715.85529			-2.08519	0.00000	0.00000
B2		1905.05334	1905.11926	100119.91406	97696.52344	715.85529			-2.08519	0.00000	0.00000
		1924.96985	1925.03699	100109.78906	97679.37500	715.85529			-2.12361	0.00000	0.00000
M842	(3Q52)	1938.73035	1938.79736	100102.56250	97667.66406	715.85529			-2.12361	0.00000	0.00000
B2		1954.30322	1954.37048	100094.38281	97654.41406	715.85529			-2.12361	0.00000	0.00000
		1974.21973	1974.28809	100083.60156	97637.66406	715.85529			-2.16202	0.00000	0.00000
M843	(3Q52)	1987.98035	1988.04846	100075.93750	97626.24219	715.85529			-2.16202	0.00000	0.00000
B2		2003.55310	2003.62122	100067.25781	97613.31250	715.85529			-2.16202	0.00000	0.00000

ELEMENT		SEQUENCE		POSITIONS			ANGLES				
element name		sum(L) [ft]	arc [ft]	I I I	x [ft]	y [ft]	z [ft]	I I I	theta [rad]	phi [rad]	psi [rad]
M844 (3Q52) B2		2023.46973	2023.53918	100055.84375	97596.99219	715.85529	-2.20044		0.00000		0.00000
		2037.22998	2037.29980	100047.74219	97585.86719	715.85529	-2.20044		0.00000		0.00000
		2042.20935	2042.27881	100044.80469	97581.84375	715.85529	-2.20044		0.00000		0.00000
B2		2062.12573	2062.19678	100032.77344	97565.97656	715.85529	-2.23886		0.00000		0.00000
		2063.39673	2063.46753	100031.97656	97564.97656	715.85529	-2.23886		0.00000		0.00000
		2083.31323	2083.38550	100019.34375	97549.58594	715.85529	-2.27727		0.00000		0.00000
M845 (3Q52) B2		2086.47998	2086.55200	100017.28906	97547.17969	715.85529	-2.27727		0.00000		0.00000
		2091.45923	2091.53125	100014.06250	97543.38281	715.85529	-2.27727		0.00000		0.00000
		2111.37573	2111.44897	100000.84375	97528.49219	715.85529	-2.31569		0.00000		0.00000
B2		2112.64648	2112.71997	99999.97656	97527.55469	715.85529	-2.31569		0.00000		0.00000
		2132.56323	2132.63770	99986.19531	97513.17969	715.85529	-2.35411		0.00000		0.00000
		2135.72998	2135.80444	99983.96875	97510.93750	715.85529	-2.35411		0.00000		0.00000
M846 (3Q52) B2		2140.70898	2140.78345	99980.44531	97507.40625	715.85529	-2.35411		0.00000		0.00000
		2160.62573	2160.70142	99966.13281	97493.56250	715.85529	-2.39252		0.00000		0.00000
		2161.89648	2161.97217	99965.19531	97492.69531	715.85529	-2.39252		0.00000		0.00000
M847 (SQA) B2		2181.81323	2181.89014	99950.36719	97479.41406	715.85529	-2.43094		0.00000		0.00000
		2184.97974	2185.05688	99947.96094	97477.35156	715.85529	-2.43094		0.00000		0.00000
		2189.95898	2190.03589	99944.18750	97474.10156	715.85529	-2.43094		0.00000		0.00000
B2		2209.87573	2209.95386	99928.84375	97461.40625	715.85529	-2.46936		0.00000		0.00000
		2211.14648	2211.22461	99927.85156	97460.61719	715.85529	-2.46936		0.00000		0.00000
		2231.06323	2231.14233	99912.03125	97448.50781	715.85529	-2.50777		0.00000		0.00000
M848 (SQA) B2		2232.81323	2232.89233	99910.61719	97447.47656	715.85529	-2.50777		0.00000		0.00000
		2249.80249	2249.88184	99896.92969	97437.41406	715.85529	-2.50777		0.00000		0.00000
		2269.71924	2269.79980	99880.65625	97425.92969	715.85529	-2.54619		0.00000		0.00000
M849 (SQA) B2		2292.73999	2292.82056	99861.59375	97413.02344	715.85529	-2.54619		0.00000		0.00000
		2299.05249	2299.13306	99856.36719	97409.47656	715.85529	-2.54619		0.00000		0.00000
		2318.96924	2319.05103	99839.66406	97398.62500	715.85529	-2.58461		0.00000		0.00000
M850 (SQA) B2		2336.23999	2336.32178	99825.00781	97389.50000	715.85529	-2.58461		0.00000		0.00000
		2348.30249	2348.38403	99814.77344	97383.12500	715.85529	-2.58461		0.00000		0.00000
		2368.21899	2368.30200	99797.66406	97372.91406	715.85529	-2.62302		0.00000		0.00000
M851 (SQA)		2384.32666	2384.40991	99783.67969	97364.93750	715.85529	-2.62302		0.00000		0.00000
M852 (SQA)		2429.88916	2429.97241	99744.10156	97342.35156	715.85529	-2.62302		0.00000		0.00000
A0		2467.24829	2467.33130	99711.65625	97323.83594	715.85529	-2.62302		0.00000		0.00000
		2474.74829	2474.83179	99705.08594	97320.24219	715.85529	-2.65802		0.00000		0.00000
P8_GEV		2481.38550	2481.46899	99699.21094	97317.14844	715.85529	-2.65802		0.00000		0.00000

THE 150 GEV LINE AND 120 GEV LINE LATTICE FILE
DESCRIPTIONS ARE PRESENTLY BEING UPDATED TO
PROVIDE MORE INFORMATION AND CELL NOMENCLATURE.
THE DATA SHEETS WILL BE DISTRIBUTED AT A LATER DATE.

FERMILAB MAIN INJECTOR

6-6-2



LIST OF DRAWINGS

- G-1 LOCATION PLAN
- G-2 AERIAL PERSPECTIVE
- C-1 EXISTING CONDITIONS
- C-2 MITIGATION PLAN
- C-3 SITE PLAN
- C-4 SITE CRITERIA PLAN
- C-5 UTILITY PLAN
- C-6 EXCAVATION SECTIONS
- C-7 MITIGATION AREA PLAN & PROFILES
- AS-1 BEAMLINE GEOMETRICS
- AS-2 ENCLOSURE CRITERIA PLAN
- AS-3 F-0/MI-60 ENCLOSURE PLAN
- AS-4 MAIN INJECTOR ABORT PLAN & SECTION
- AS-5 P-150 GeV ENCLOSURE LONG. SECTION
- AS-6 A-150 GeV ENCLOSURE LONG. SECTION
- AS-7 INJECTOR ENCLOSURE SECTIONS
- AS-8 PRECAST ENCLOSURE DETAILS
- AS-9 8GeV BEAMLINE SHT. 1
- AS-10 8GeV BEAMLINE SHT. 2
- AS-11 8GeV BEAMLINE SHT. 3
- AS-12 8GeV BEAMLINE SHT. 4
- AS-13 8GeV BEAMLINE SHT. 5
- AS-14 8GeV BEAMLINE SHT. 6
- AS-15 8GeV SECTION SHT. 1
- AS-16 8GeV SECTIONS SHT. 2
- AS-17 TYPICAL SERVICE BUILDING PLAN
- AS-18 ALCOVE PLANS
- AS-19 SERVICE BUILDING SECTION
- AS-20 KICKER SERVICE BUILDING MI-52 AND MI-62
- AS-21 KICKER SERVICE BUILDING F-17
- AS-22 F-0 / MI-60 PLAN
- AS-23 MI-60 FLOOR PLAN
- AS-24 MI-60 BUILDING ELEVATIONS
- AS-25 MI-60 BUILDING SECTIONS
- AS-26 MI-60 CONSTRUCTION SECTIONS
- AS-27 NORTH HATCH BUILDING PLAN
- AS-28 NORTH HATCH BUILDING SECTIONS
- M-1 HVAC AND FIRE PROTECTION CRITERIA
- M-2 HVAC PLANS
- M-3 PROCESS SYSTEMS CRITERIA
- M-4 PROCESS SYSTEMS FLOW DIAGRAM
- E-1 345-13.8KV SINGLE LINE DIAGRAM
- E-2 SINGLE LINE POWER DISTRIBUTION
- E-3 POWER & COMMUNICATION DUCT PLAN
- E-4 ELECTRICAL CRITERIA

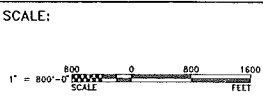
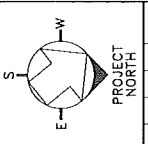
LOCATION PLAN

SCALE : 1" = 800'-0"

REV.	DATE	DESCRIPTIONS

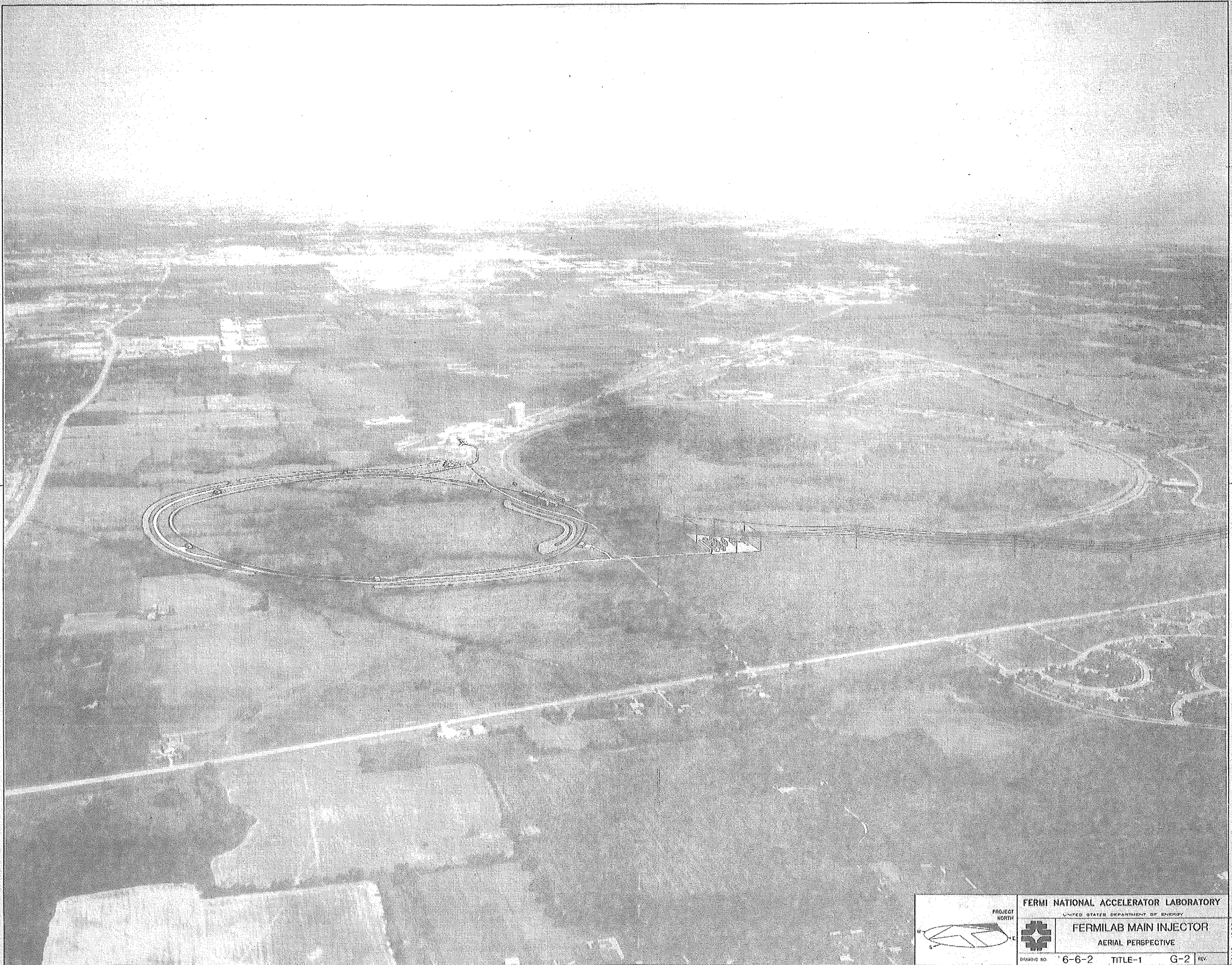
FLUOR DANIEL		
PROJECT NO. - 21842300		
NAME	DATE	
DESIGNED R. JEDZINIAK	JULY, 1992	
DRAWN RAY DELA CRUZ	JULY, 1992	
CHECKED A. VASONIS	JULY, 1992	
APPROVED		

NAME	DATE
DESIGNED C. FEDEROWICZ	
DRAWN C. FEDEROWICZ	
CHECKED	
APPROVED	
SUBMITTED	

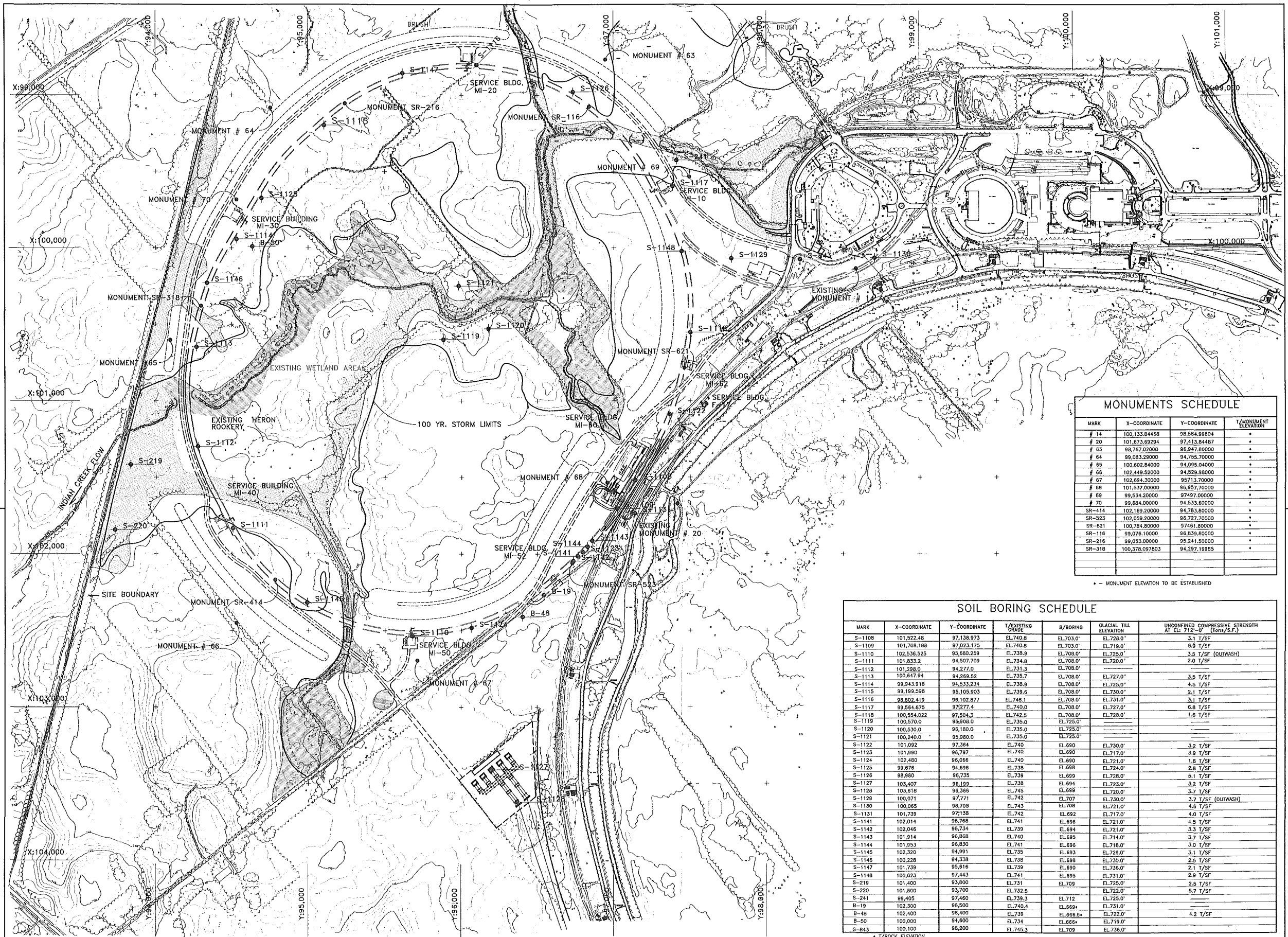


FERMI NATIONAL ACCELERATOR LABORATORY	
UNITED STATES DEPARTMENT OF ENERGY	
FERMILAB MAIN INJECTOR	
LOCATION PLAN	
DRAWING NO. 6-6-2 TITLE-1	G-1 REV.

AUG. 1992



	PROJECT NORTH					
	FERMI NATIONAL ACCELERATOR LABORATORY UNITED STATES DEPARTMENT OF ENERGY					
	FERMILAB MAIN INJECTOR AERIAL PERSPECTIVE					
DRAWING NO. 6-6-2		TITLE-1		G-2	REV.	AUG. 1992



MONUMENTS SCHEDULE			
MARK	X-COORDINATE	Y-COORDINATE	T/MONUMENT ELEVATION
# 14	100,133.84468	98,584.99804	*
# 20	101,573.69284	97,413.84467	*
# 63	98,767.02000	96,947.80000	*
# 64	99,083.28000	94,756.70000	*
# 65	100,602.84000	94,095.04000	*
# 66	102,449.52000	94,529.98000	*
# 67	102,694.30000	95,713.70000	*
# 68	101,537.00000	96,957.70000	*
# 69	99,534.20000	97,497.00000	*
# 70	99,684.00000	94,533.60000	*
SR-414	100,69,20000	94,783.80000	*
SR-523	102,059.20000	96,727.70000	*
SR-621	100,784.80000	97,461.80000	*
SR-116	99,076.10000	96,839.60000	*
SR-216	99,053.00000	95,241.50000	*
SR-318	100,378.097803	94,297.19855	*

* - MONUMENT ELEVATION TO BE ESTABLISHED

SOIL BORING SCHEDULE						
MARK	X-COORDINATE	Y-COORDINATE	T/EXISTING ELEVATION	B/BORING	GLACIAL TILL ELEVATION	UNCONFINED COMPRESSIVE STRENGTH AT EL. 712'-0" (tons/sq. ft.)
S-1108	101,522.48	97,138.973	EL.740.8	EL.703.0'	EL.728.0'	3.1 T/SF
S-1109	101,708.188	97,023.175	EL.740.8	EL.703.0'	EL.719.0'	6.9 T/SF
S-1110	102,536.525	95,680.259	EL.738.9	EL.708.0'	EL.725.0'	3.5 T/SF (OUTWASH)
S-1111	101,833.2	94,507.709	EL.734.8	EL.708.0'	EL.720.0'	2.0 T/SF
S-1112	101,288.0	94,277.0	EL.731.3	EL.708.0'	---	---
S-1113	100,647.94	94,269.52	EL.735.7	EL.708.0'	EL.727.0'	3.5 T/SF
S-1114	99,943.918	94,533.234	EL.738.9	EL.708.0'	EL.725.0'	4.5 T/SF
S-1115	99,199.598	95,105.803	EL.738.0'	EL.708.0'	EL.730.0'	2.1 T/SF
S-1116	98,802.419	95,102.877	EL.746.1	EL.708.0'	EL.731.0'	3.1 T/SF
S-1117	99,554.675	97,727.4	EL.740.0	EL.708.0'	EL.727.0'	6.8 T/SF
S-1118	100,554.022	97,504.3	EL.742.5	EL.708.0'	EL.728.0'	1.6 T/SF
S-1119	100,570.0	95,908.0	EL.735.0	EL.725.0'	---	---
S-1120	100,530.0	96,180.0	EL.735.0	EL.725.0'	---	---
S-1121	100,240.0	95,980.0	EL.735.0	EL.725.0'	---	---
S-1122	101,092	97,364	EL.740	EL.690	EL.730.0'	3.2 T/SF
S-1123	101,990	96,797	EL.740	EL.690	EL.717.0'	3.8 T/SF
S-1124	102,480	96,066	EL.740	EL.690	EL.721.0'	1.8 T/SF
S-1125	99,676	94,695	EL.738	EL.695	EL.724.0'	2.8 T/SF
S-1126	98,980	96,735	EL.739	EL.699	EL.728.0'	5.1 T/SF
S-1127	103,407	96,189	EL.738	EL.694	EL.723.0'	3.2 T/SF
S-1128	103,618	96,365	EL.745	EL.699	EL.720.0'	3.7 T/SF
S-1129	100,071	97,771	EL.742	EL.707	EL.730.0'	3.7 T/SF (OUTWASH)
S-1130	100,065	98,708	EL.743	EL.708	EL.721.0'	4.6 T/SF
S-1131	101,739	97,158	EL.742	EL.692	EL.717.0'	4.0 T/SF
S-1141	102,014	96,768	EL.741	EL.695	EL.721.0'	4.5 T/SF
S-1142	102,046	96,734	EL.739	EL.694	EL.721.0'	3.3 T/SF
S-1143	101,914	96,868	EL.740	EL.695	EL.714.0'	3.7 T/SF
S-1144	101,953	96,830	EL.741	EL.696	EL.718.0'	3.0 T/SF
S-1145	102,320	94,991	EL.735	EL.693	EL.728.0'	3.1 T/SF
S-1146	100,228	94,338	EL.738	EL.698	EL.730.0'	2.5 T/SF
S-1147	101,739	95,616	EL.739	EL.690	EL.736.0'	2.1 T/SF
S-1148	100,023	97,443	EL.741	EL.695	EL.731.0'	2.9 T/SF
S-219	101,400	93,600	EL.731	EL.709	EL.725.0'	2.5 T/SF
S-220	101,600	93,700	EL.732.5	---	EL.722.0'	3.7 T/SF
S-241	99,405	97,460	EL.738.3	EL.712	EL.725.0'	---
B-19	102,300	96,500	EL.740.4	EL.699+	EL.731.0'	---
B-48	102,400	96,400	EL.739	EL.695+	EL.722.0'	4.2 T/SF
B-50	100,000	94,600	EL.734	EL.695+	EL.719.0'	---
S-843	100,100	98,200	EL.745.3	EL.709	EL.736.0'	---

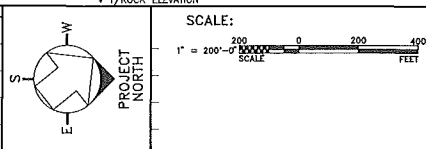
* T/ROCK ELEVATION

REV.		DATE	DESCRIPTIONS

FLUOR DANIEL	
PROJECT NO. - 21842300	
DESIGNED	D. ABRAHAM
DRAWN	I. MASIS
CHECKED	A. VASONIS
APPROVED	

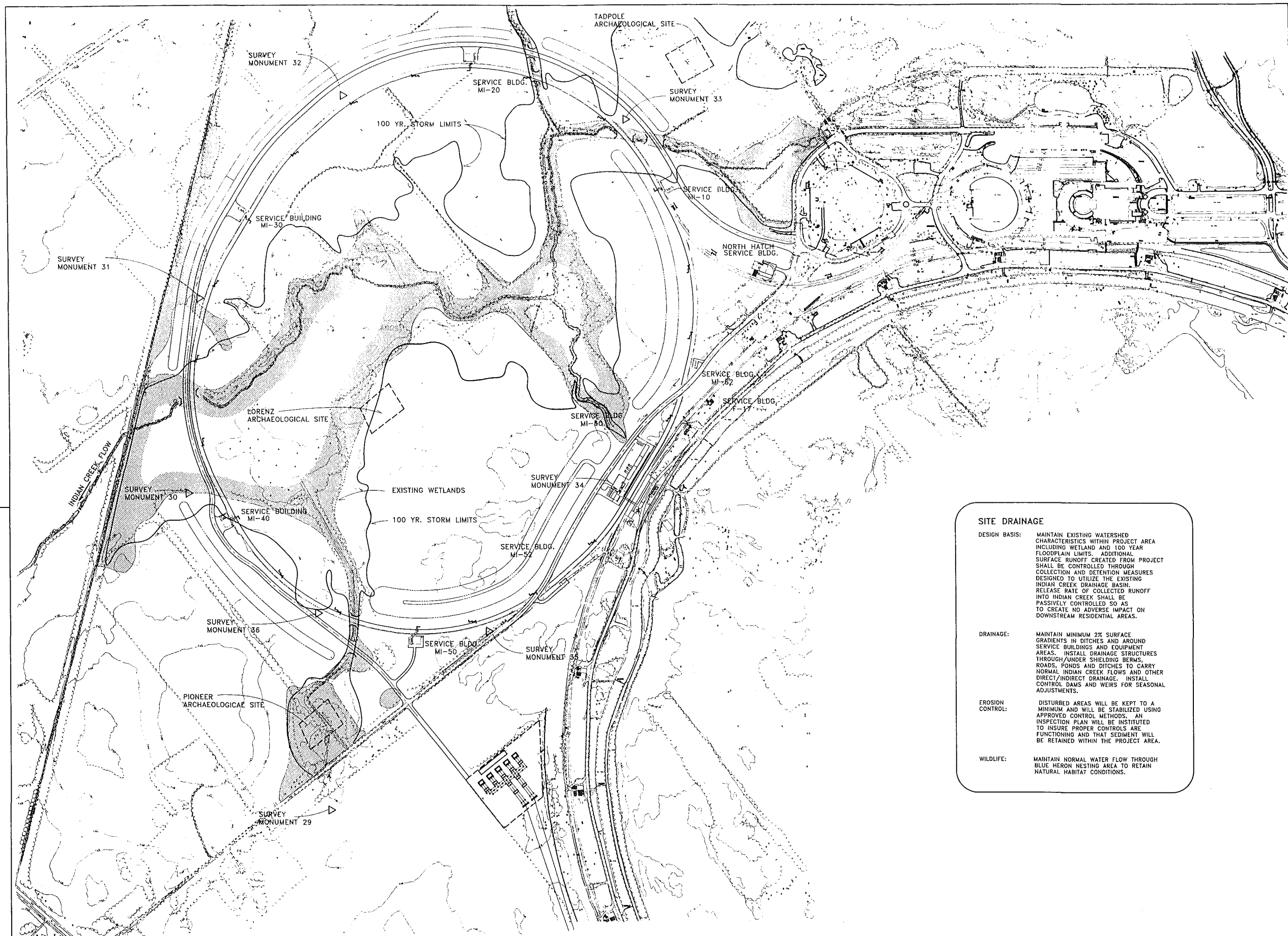
DATE	JULY, 1992
DATE	JULY, 1992
DATE	JULY, 1992

DESIGNED	C. FEDEROWICZ	DATE	
DRAWN	C. FEDEROWICZ		
CHECKED			
APPROVED			
SUBMITTED			



FERMI NATIONAL ACCELERATOR LABORATORY	
UNITED STATES DEPARTMENT OF ENERGY	
FERMILAB MAIN INJECTOR	
EXISTING CONDITIONS	
DRAWING NO.	6-6-2 TITLE-1 C-1

AUG. 1992



SITE DRAINAGE

DESIGN BASIS: MAINTAIN EXISTING WATERSHED CHARACTERISTICS WITHIN PROJECT AREA INCLUDING WETLAND AND 100 YEAR FLOODPLAIN LIMITS. ADDITIONAL SURFACE RUNOFF CREATED FROM PROJECT SHALL BE CONTROLLED THROUGH COLLECTION AND DETENTION MEASURES DESIGNED TO UTILIZE THE EXISTING INDIAN CREEK DRAINAGE BASIN. RELEASE RATE OF COLLECTED RUNOFF INTO INDIAN CREEK SHALL BE PASSIVELY CONTROLLED SO AS TO CREATE NO ADVERSE IMPACT ON DOWNSTREAM RESIDENTIAL AREAS.

DRAINAGE: MAINTAIN MINIMUM 2% SURFACE GRADIENTS IN DITCHES AND AROUND SERVICE BUILDINGS AND EQUIPMENT AREAS. INSTALL DRAINAGE STRUCTURES THROUGH/UNDER SHIELDING BERMS, ROADS, PONDS AND DITCHES TO CARRY NORMAL INDIAN CREEK FLOWS AND OTHER DIRECT/INDIRECT DRAINAGE. INSTALL CONTROL DAMS AND WEIRS FOR SEASONAL ADJUSTMENTS.

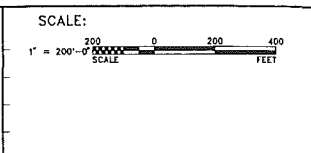
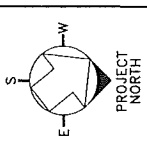
EROSION CONTROL: DISTURBED AREAS WILL BE KEPT TO A MINIMUM AND WILL BE STABILIZED USING APPROVED CONTROL METHODS. AN INSPECTION PLAN WILL BE INSTITUTED TO INSURE PROPER CONTROLS ARE FUNCTIONING AND THAT SEDIMENT WILL BE RETAINED WITHIN THE PROJECT AREA.

WILDLIFE: MAINTAIN NORMAL WATER FLOW THROUGH BLUE HERON NESTING AREA TO RETAIN NATURAL HABITAT CONDITIONS.

REV.	DATE	DESCRIPTIONS

FLUOR DANIEL		
PROJECT NO. - 21842300		
DESIGNED	R. JEDZINIAK	JULY, 1992
DRAWN	I. MASIS	JULY, 1992
CHECKED	A. VASONIS	JULY, 1992
APPROVED		

NAME	DATE
DESIGNED	C. FEDEROWICZ
DRAWN	C. FEDEROWICZ
CHECKED	
APPROVED	
SUBMITTED	



FERMI NATIONAL ACCELERATOR LABORATORY

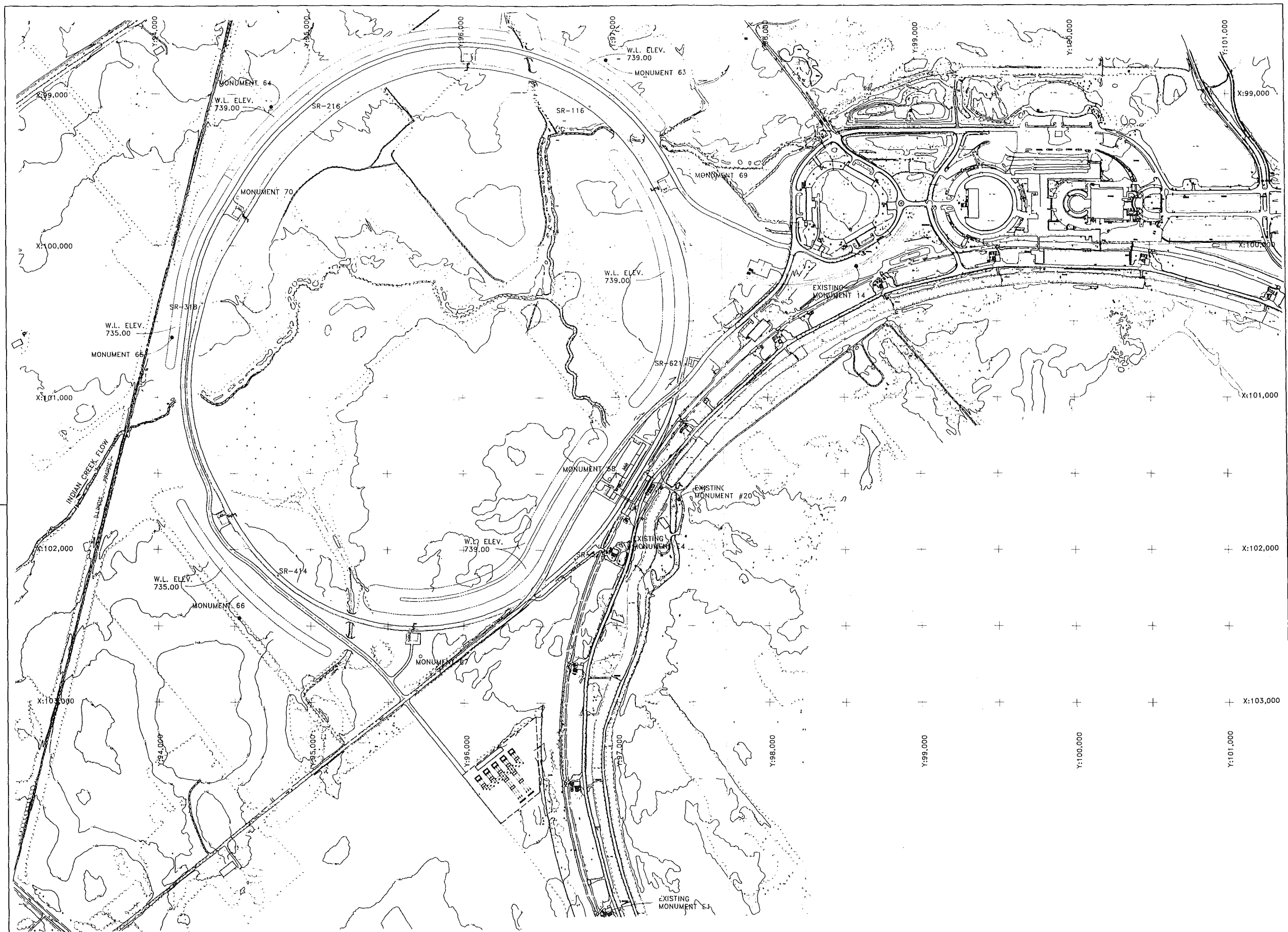
UNITED STATES DEPARTMENT OF ENERGY

FERMILAB MAIN INJECTOR

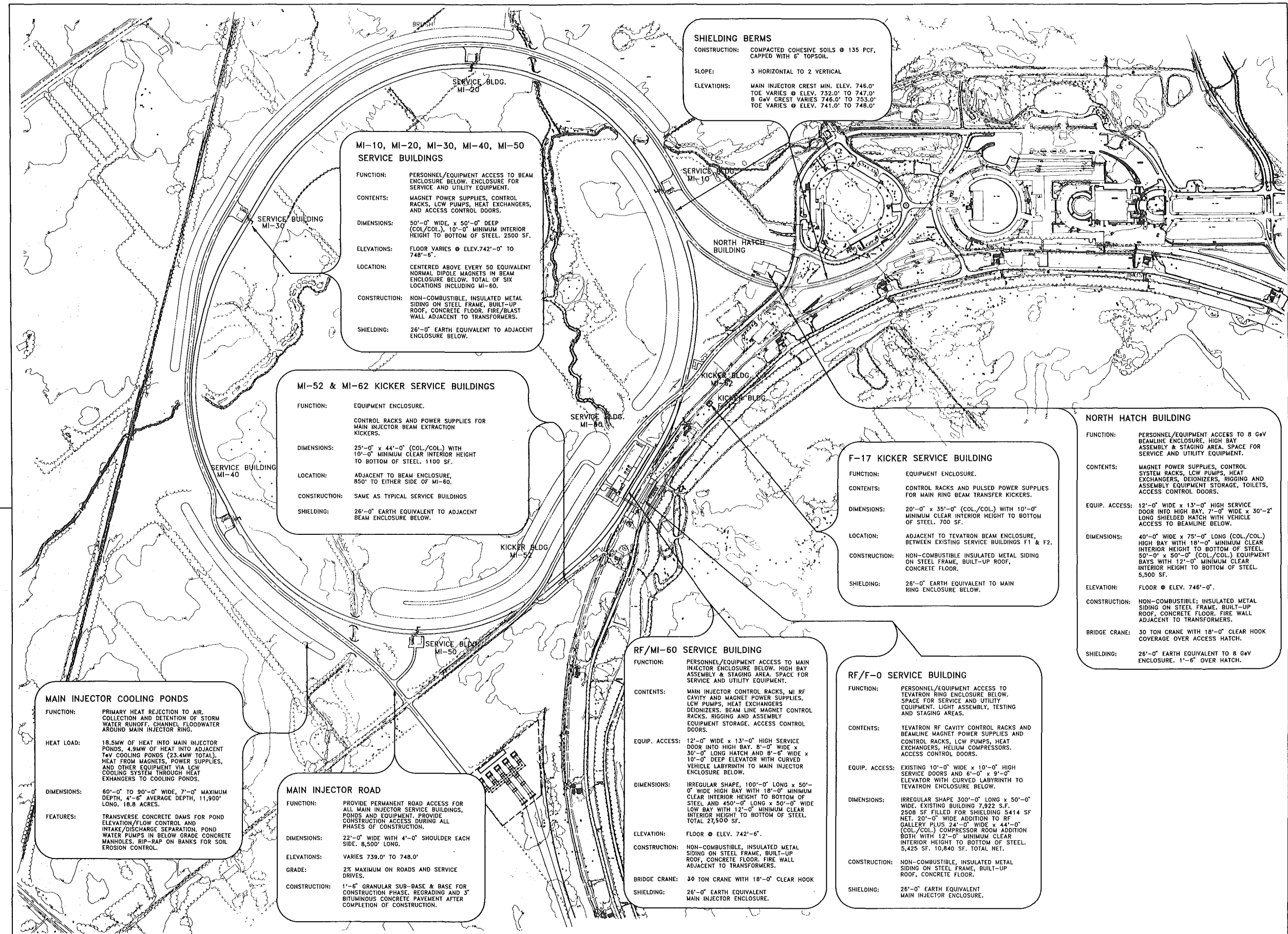
MITIGATION PLAN

DRAWING NO. 6-6-2 TITLE-1 C-2 REV.

AUG. 1992



<table border="1" style="width: 100%; border-collapse: collapse;"> <tr> <th style="width: 10%;">REV.</th> <th style="width: 10%;">DATE</th> <th style="width: 80%;">DESCRIPTIONS</th> </tr> <tr><td> </td><td> </td><td> </td></tr> <tr><td> </td><td> </td><td> </td></tr> <tr><td> </td><td> </td><td> </td></tr> <tr><td> </td><td> </td><td> </td></tr> <tr><td> </td><td> </td><td> </td></tr> <tr><td> </td><td> </td><td> </td></tr> <tr><td> </td><td> </td><td> </td></tr> <tr><td> </td><td> </td><td> </td></tr> <tr><td> </td><td> </td><td> </td></tr> </table>		REV.	DATE	DESCRIPTIONS																												<table border="1" style="width: 100%; border-collapse: collapse;"> <tr> <th style="width: 10%;">DESIGNED</th> <th style="width: 10%;">NAME</th> <th style="width: 10%;">DATE</th> </tr> <tr> <td> </td> <td>C. FEDROWICZ</td> <td> </td> </tr> <tr> <td> </td> <td>C. FEDROWICZ</td> <td> </td> </tr> <tr> <td> </td> <td> </td> <td> </td> </tr> <tr> <td> </td> <td> </td> <td> </td> </tr> <tr> <td> </td> <td> </td> <td> </td> </tr> <tr> <td> </td> <td> </td> <td> </td> </tr> </table>		DESIGNED	NAME	DATE		C. FEDROWICZ			C. FEDROWICZ														<table border="1" style="width: 100%; border-collapse: collapse;"> <tr> <th style="width: 10%;">DRAWN</th> <th style="width: 10%;">NAME</th> <th style="width: 10%;">DATE</th> </tr> <tr> <td> </td> <td>C. FEDROWICZ</td> <td> </td> </tr> <tr> <td> </td> <td> </td> <td> </td> </tr> <tr> <td> </td> <td> </td> <td> </td> </tr> <tr> <td> </td> <td> </td> <td> </td> </tr> <tr> <td> </td> <td> </td> <td> </td> </tr> <tr> <td> </td> <td> </td> <td> </td> </tr> </table>		DRAWN	NAME	DATE		C. FEDROWICZ																	<table border="1" style="width: 100%; border-collapse: collapse;"> <tr> <th style="width: 10%;">CHECKED</th> <th style="width: 10%;">NAME</th> <th style="width: 10%;">DATE</th> </tr> <tr> <td> </td> <td> </td> <td> </td> </tr> <tr> <td> </td> <td> </td> <td> </td> </tr> <tr> <td> </td> <td> </td> <td> </td> </tr> <tr> <td> </td> <td> </td> <td> </td> </tr> <tr> <td> </td> <td> </td> <td> </td> </tr> <tr> <td> </td> <td> </td> <td> </td> </tr> </table>		CHECKED	NAME	DATE																			<table border="1" style="width: 100%; border-collapse: collapse;"> <tr> <th style="width: 10%;">APPROVED</th> <th style="width: 10%;">NAME</th> <th style="width: 10%;">DATE</th> </tr> <tr> <td> </td> <td> </td> <td> </td> </tr> <tr> <td> </td> <td> </td> <td> </td> </tr> <tr> <td> </td> <td> </td> <td> </td> </tr> <tr> <td> </td> <td> </td> <td> </td> </tr> <tr> <td> </td> <td> </td> <td> </td> </tr> <tr> <td> </td> <td> </td> <td> </td> </tr> </table>		APPROVED	NAME	DATE																			<table border="1" style="width: 100%; border-collapse: collapse;"> <tr> <th style="width: 10%;">SUBMITTED</th> <th style="width: 10%;">NAME</th> <th style="width: 10%;">DATE</th> </tr> <tr> <td> </td> <td> </td> <td> </td> </tr> <tr> <td> </td> <td> </td> <td> </td> </tr> <tr> <td> </td> <td> </td> <td> </td> </tr> <tr> <td> </td> <td> </td> <td> </td> </tr> <tr> <td> </td> <td> </td> <td> </td> </tr> <tr> <td> </td> <td> </td> <td> </td> </tr> </table>		SUBMITTED	NAME	DATE																			<div style="text-align: center;"> <p>PROJECT NORTH</p> </div> <div style="text-align: center;"> <p>SCALE:</p> <p>1" = 200'-0"</p> <p>0 200 400</p> <p>FEET</p> </div> <div style="text-align: center;"> <p>FERMI NATIONAL ACCELERATOR LABORATORY</p> <p>UNITED STATES DEPARTMENT OF ENERGY</p> <p>FERMILAB MAIN INJECTOR</p> <p>SITE PLAN</p> <p>DRAWING NO. 6-6-2 TITLE-1 C-3 REV.</p> </div>	
REV.	DATE	DESCRIPTIONS																																																																																																																																																		
DESIGNED	NAME	DATE																																																																																																																																																		
	C. FEDROWICZ																																																																																																																																																			
	C. FEDROWICZ																																																																																																																																																			
DRAWN	NAME	DATE																																																																																																																																																		
	C. FEDROWICZ																																																																																																																																																			
CHECKED	NAME	DATE																																																																																																																																																		
APPROVED	NAME	DATE																																																																																																																																																		
SUBMITTED	NAME	DATE																																																																																																																																																		



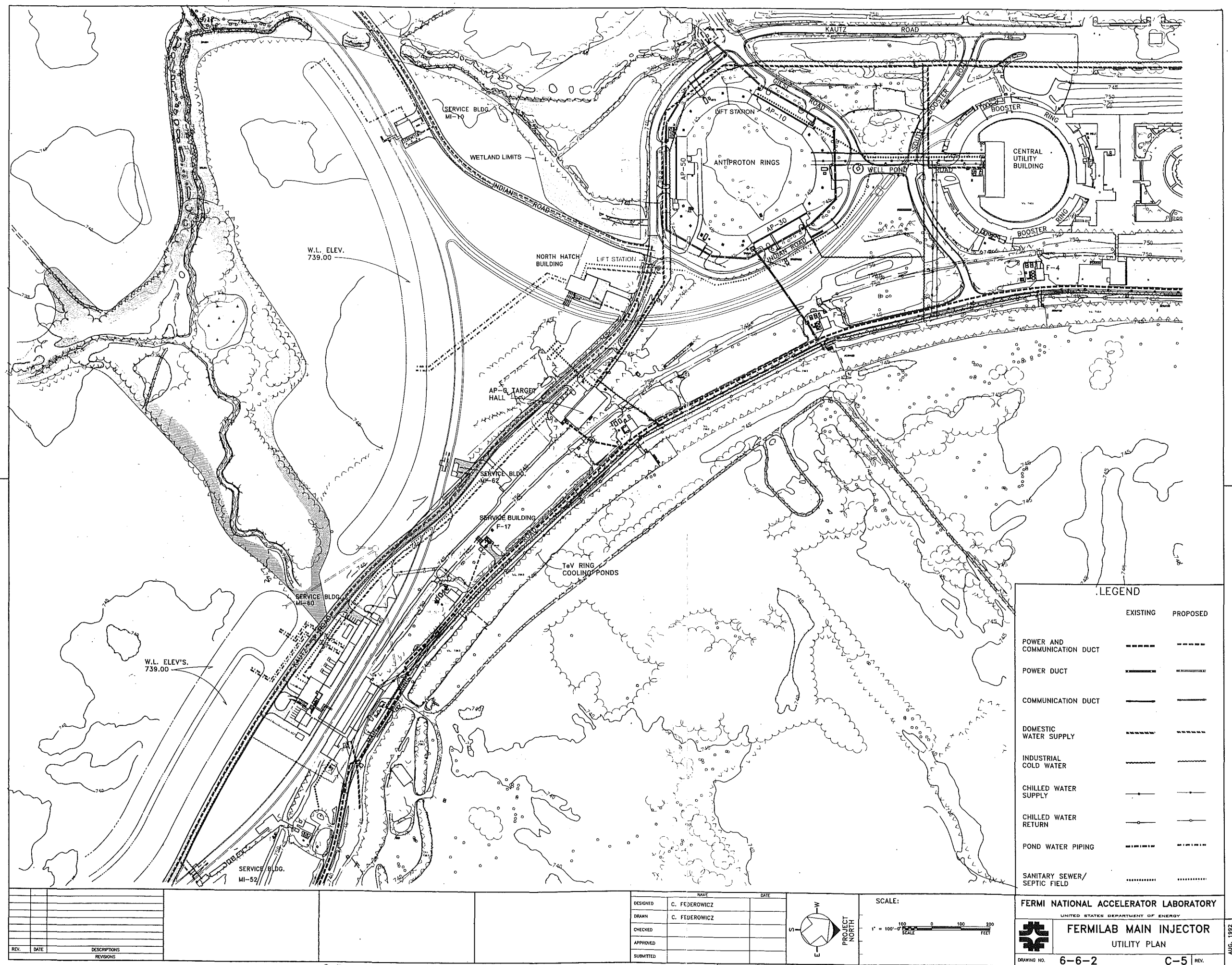
DESIGNED		C. FEDEROWICZ		DATE			
DRAWN		C. FEDEROWICZ					
CHECKED							
APPROVED							
SUBMITTED							

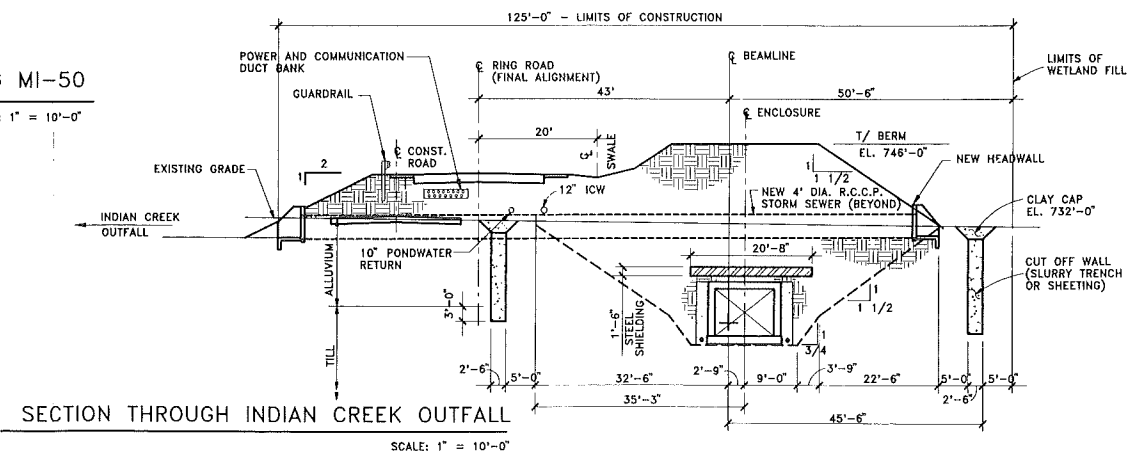
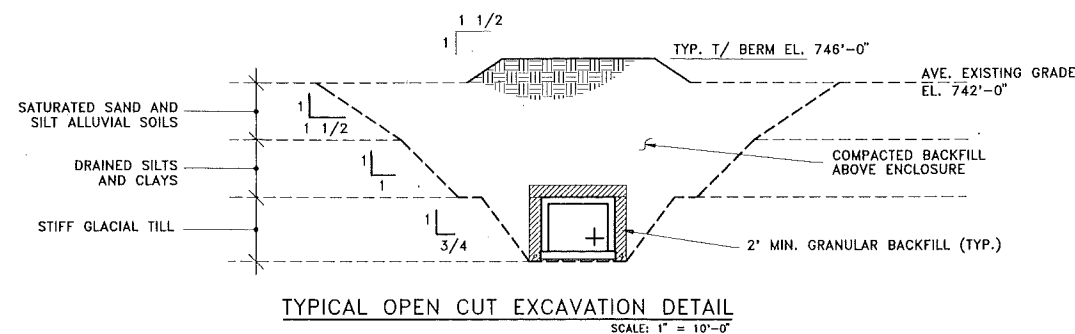
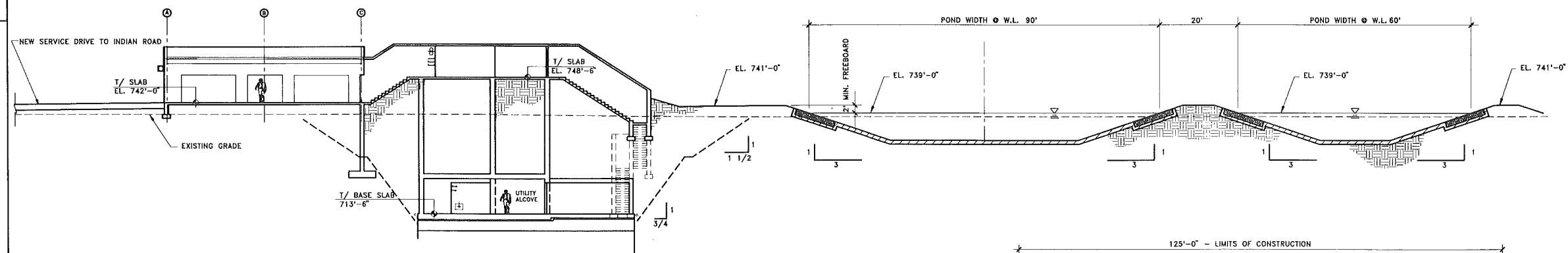
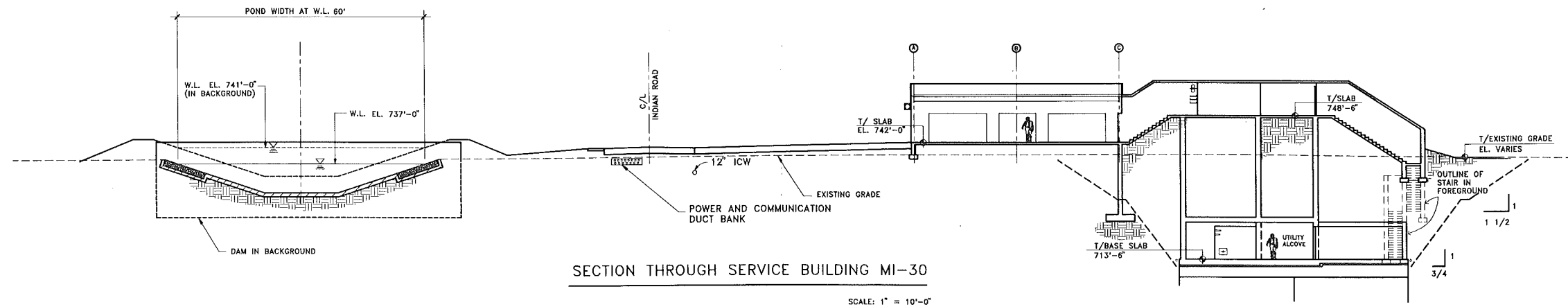
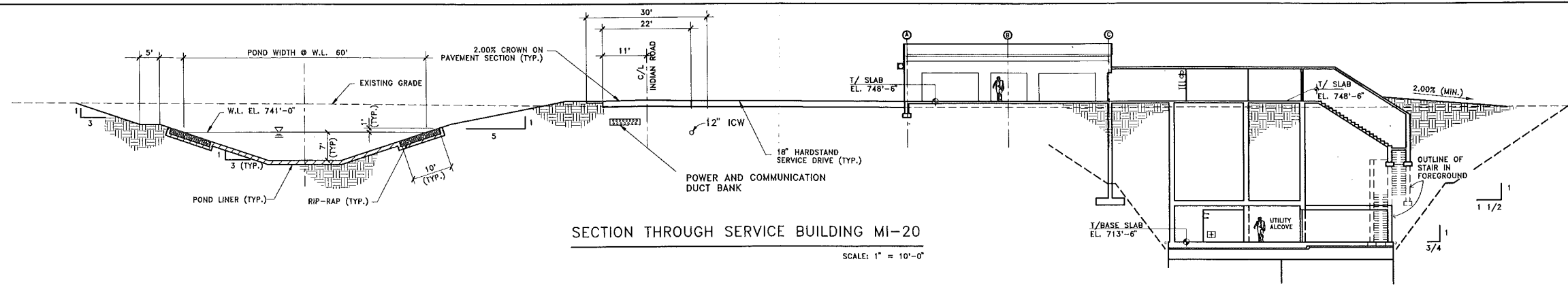
DESIGNED		R. JEDZINIAK		DATE		JULY, 1992	
DRAWN		REY DELA CRUZ				JULY, 1992	
CHECKED		A. VASONIS				JULY, 1992	
APPROVED							

REV.		DATE		DESCRIPTIONS		REVISIONS	

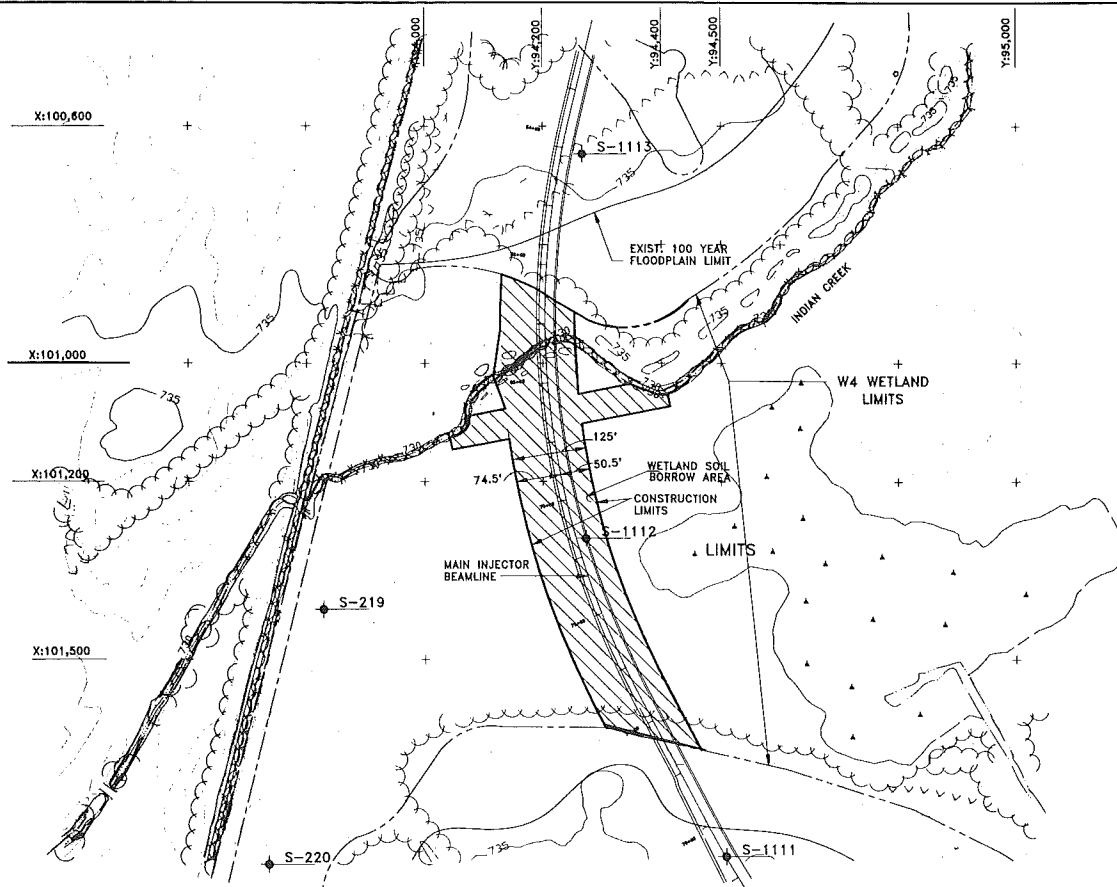
FLUOR DANIEL		PROJECT NO. - 21842300	
NAME		DATE	
DESIGNED		JULY, 1992	
DRAWN		JULY, 1992	
CHECKED		JULY, 1992	
APPROVED			

Fermilab Main Injector		SITE CRITERIA PLAN	
DRAWING NO.		6-6-2 TITLE-1 C-4	



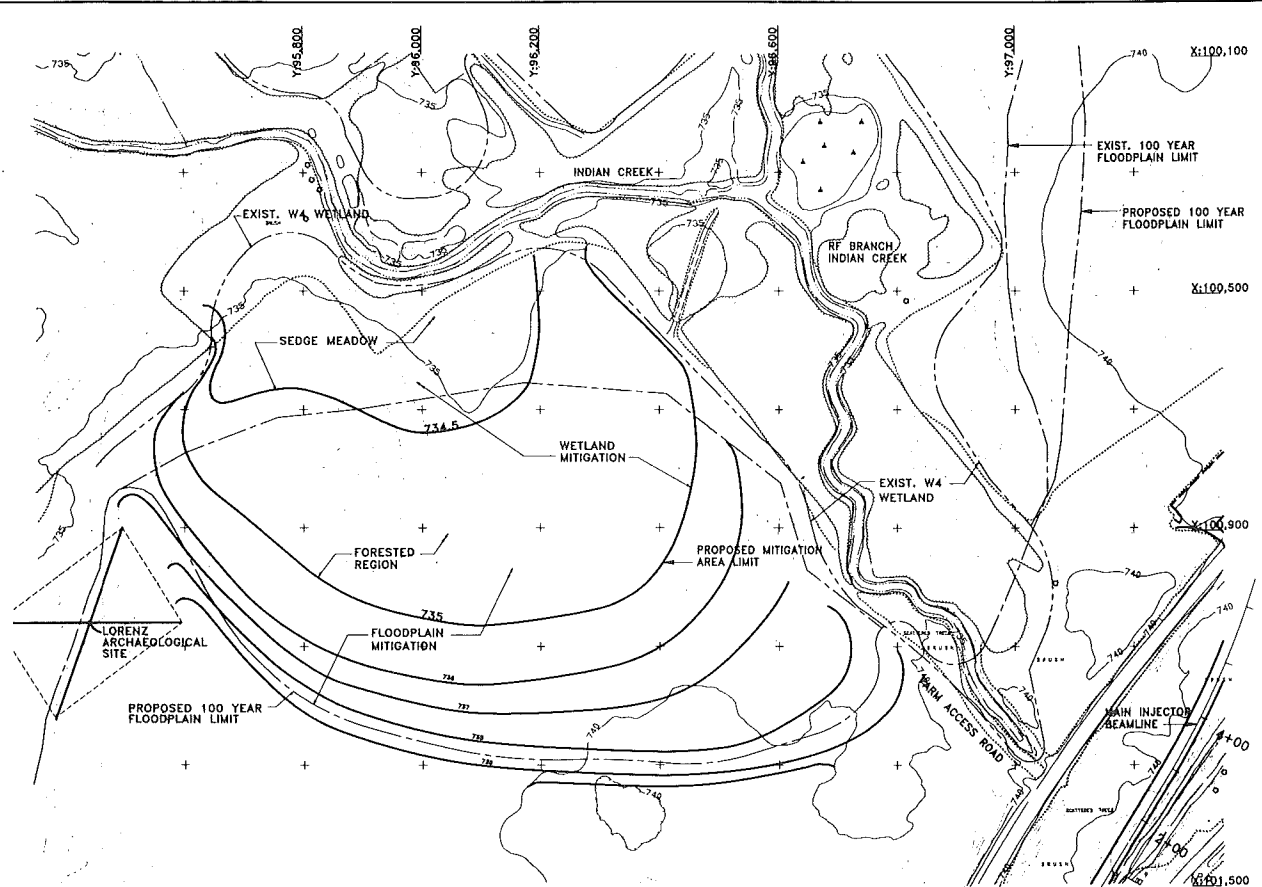


REV. DATE DESCRIPTIONS 1 1/2 1 3/4	FLUOR DANIEL PROJECT NO. - 21842300		NAME DATE DESIGNED C. FEDEROWICZ DRAWN C. FEDEROWICZ CHECKED APPROVED SUBMITTED		SCALE: 1" = 10'-0" 10 20 FEET	FERMILAB MAIN INJECTOR EXCAVATION SECTIONS DRAWING NO. 6-6-2 TITLE-1 C-6 REV.
	DESIGNED	D. ABRAHAM	JULY, 92			
	DRAWN	R. JEDZINIAK	JULY, 92			
	CHECKED	A. VASONIS	JULY, 92			
	APPROVED					



PLAN AT SOUTHWEST IMPACT AREA

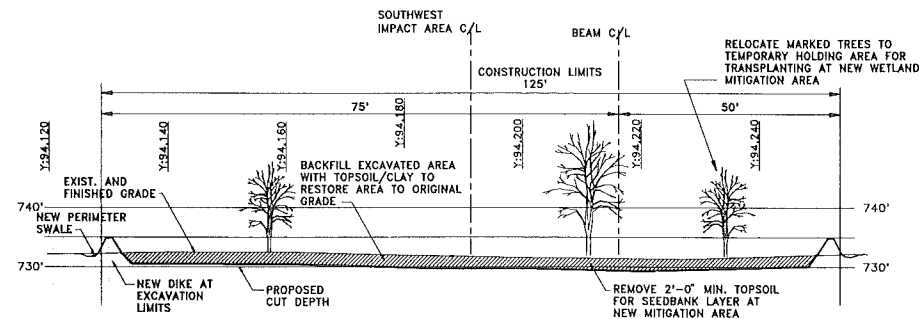
SCALE: 1" = 100'-0"



PLAN AT MITIGATION AREA

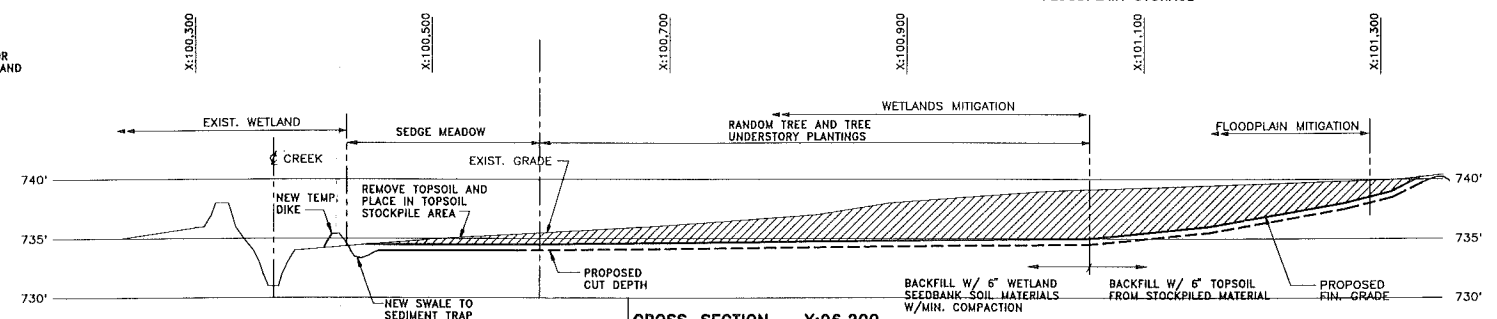
SCALE: 1" = 100'-0"

PROVIDED COMPENSATORY AREAS
10.3 ACRES COMPENSATORY WETLANDS
40.9 ACRE-FEET OF COMPENSATORY
FLOODPLAIN STORAGE



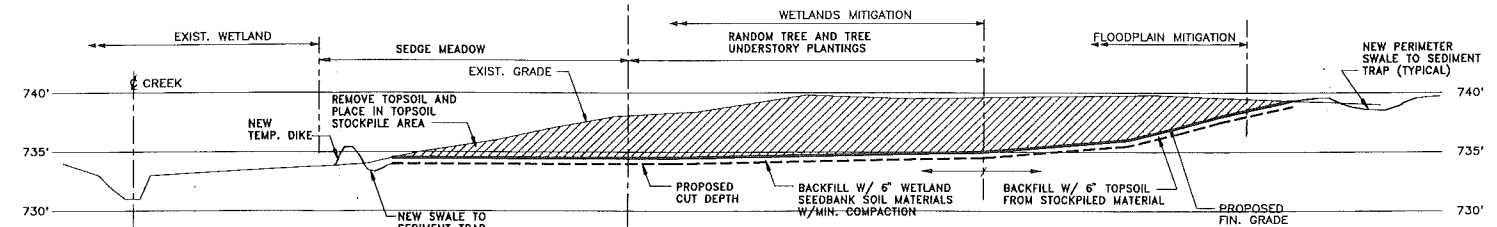
CROSS-SECTION - X:101.120

SCALE: 1" = 10'-0" (LOOKING WEST)



CROSS-SECTION - Y:96.200

SCALE: HOR. 1" = 50'-0" (LOOKING NORTH)
VERT. 1" = 5'-0"



CROSS-SECTION - Y:95.800

SCALE: HOR. 1" = 50'-0" (LOOKING NORTH)
VERT. 1" = 5'-0"

ENVIRONMENTAL APPROVAL ACTIONS

PERMITS

AGENCY	ACTION REQUESTED	ISSUED
DEPARTMENT OF THE ARMY CHICAGO DISTRICT, U.S. CORPS OF ENGINEERS CHICAGO, ILLINOIS	CLEAN WATER ACT SECTION 404, NATIONWIDE 28 PERMIT APPLICATION NO. 3499102	JUNE 26, 1991
DIVISION OF WATER POLLUTION CONTROL ILLINOIS ENVIRONMENTAL PROTECTION AGENCY SPRINGFIELD, ILLINOIS	CLEAN WATER ACT SECTION 401, WATER QUALITY CERTIFICATION	JUNE 4, 1991
ILLINOIS DAM SAFETY SECTION ILLINOIS DEPT. OF TRANSPORTATION DIVISION OF WATER RESOURCES SPRINGFIELD, ILLINOIS	SECTION 70 (FLOOD CONTROL) AND SECTION 70A (CONSTRUCTION OF CLASS III DAM) (RIVERS, LAKES AND STREAMS ACT)	
U.S. ENVIRONMENTAL PROTECTION AGENCY REGION V (SAC-26) CHICAGO, ILLINOIS	APPLICATION FOR PERMIT TO CONSTRUCT 40 CFR PART 61.07 RADIONUCLIDES NATIONAL EMISSION STANDARDS FOR HAZARDOUS AIR POLLUTANTS (NESHAP) REF: SAT-28	MAY 9, 1991
DIVISION OF AIR POLLUTION CONTROL ILLINOIS ENVIRONMENTAL PROTECTION AGENCY SPRINGFIELD, ILLINOIS	APPLICATION FOR PERMIT TO CONSTRUCT IL ADM. CODE 201.142 NESHAP ID# 0438 07A1	APRIL 1, 1991
U.S. DEPT. OF AGRICULTURE SOIL CONSERVATION SERVICE CHAMPAIGN, ILLINOIS	FARMLAND CONVERSION IMPACT RATING	SEPT. 18, 1991
U.S. DEPT. OF ENERGY	FINDING OF NO SIGNIFICANT IMPACT (FONSI)	JULY 6, 1992

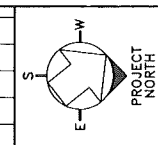
CONSULTATIONS

AGENCY	CONSULTATION REQUESTED	DATE
U.S. FISH & WILDLIFE SERVICE ROCK ISLAND, ILLINOIS	CONSULTATION IN ACCORDANCE WITH FISH & WILDLIFE COORDINATION ACT 48 STAT. 401 16 U.S.C. 661 ENDANGERED SPECIES ACT	APRIL 30, 1991
ILLINOIS DEPT. OF CONSERVATION SPRINGFIELD, ILLINOIS	CONSULTATION IN ACCORDANCE WITH FISH AND WILDLIFE COORDINATION ACT	JUNE 20, 1991
STATE HISTORICAL PRESERVATION OFFICER ILLINOIS HISTORIC PRESERVATION AGENCY SPRINGFIELD, ILLINOIS	106 DETERMINATION OF NO EFFECT 35 CFR 800	JULY 22, 1991

REV.	DATE	DESCRIPTIONS	REVISIONS

FLUOR DANIEL	
PROJECT NO. - 21842300	
DESIGNED	R. JEDZINIAK
DRAWN	REY DELA CRUZ
CHECKED	A. VASONIS
DATE	JULY, 1992
DATE	JULY, 1992
DATE	JULY, 1992

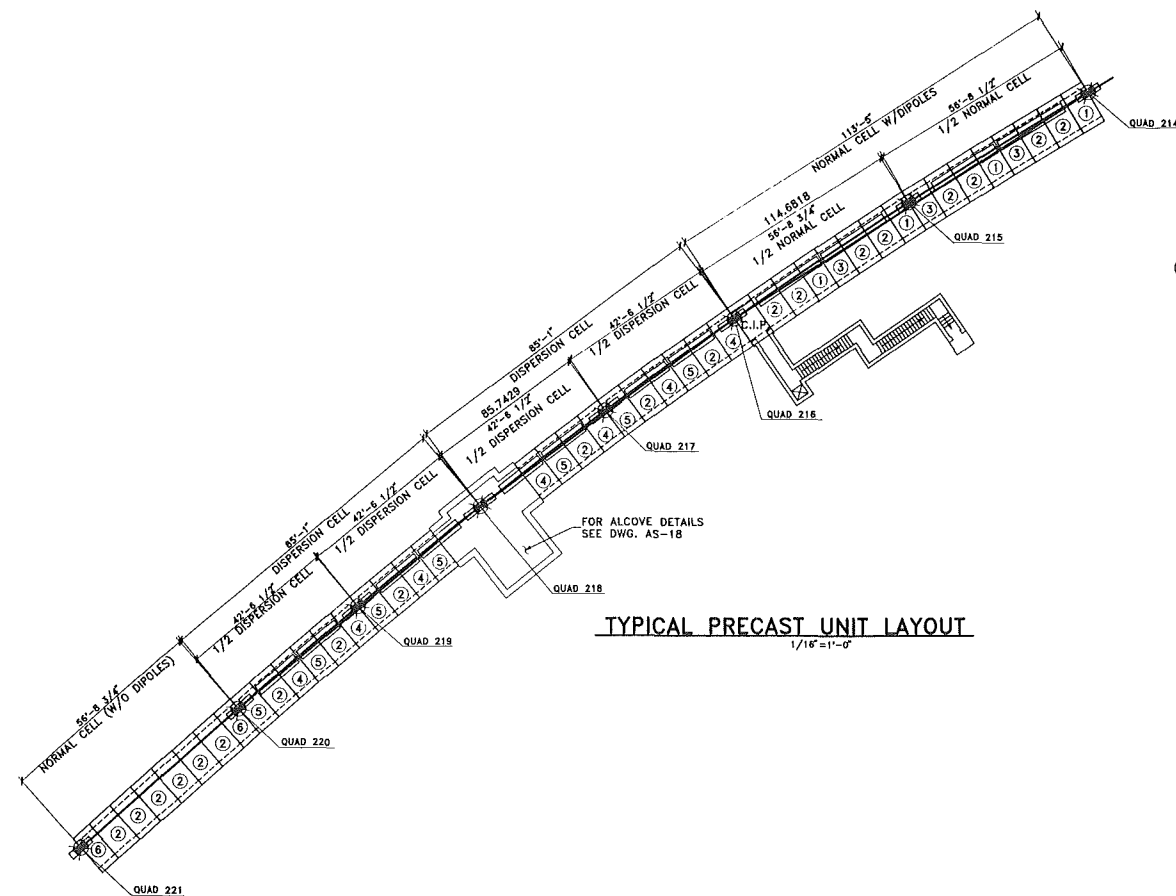
NAME	DATE
DESIGNED	FLUOR DANIEL, L. EVEN
DRAWN	FLUOR DANIEL, L. EVEN
CHECKED	
APPROVED	
SUBMITTED	



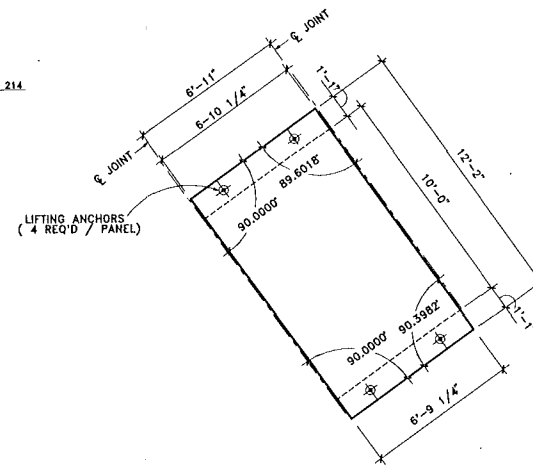
SCALE:	1" = 100'-0"
HORIZONTAL	1" = 50'-0"
VERTICAL	1" = 5'-0"
SCALE	1" = 10'-0"

FERMI NATIONAL ACCELERATOR LABORATORY	
UNITED STATES DEPARTMENT OF ENERGY	
FERMILAB MAIN INJECTOR	
MITIGATION AREA PLAN AND PROFILES	
DRAWING NO.	6-6-2 TITLE-1 C-7
REV.	

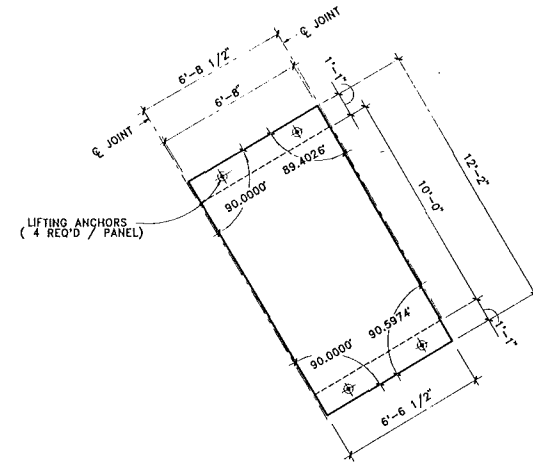
AUG. 1992



TYPICAL PRECAST UNIT LAYOUT
1/16"=1'-0"



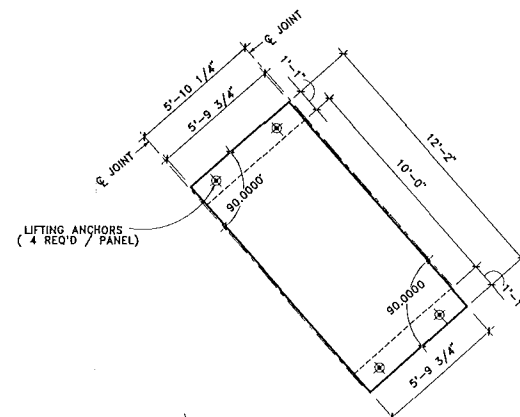
PRECAST UNIT TYPE "4"
3/8"=1'-0"



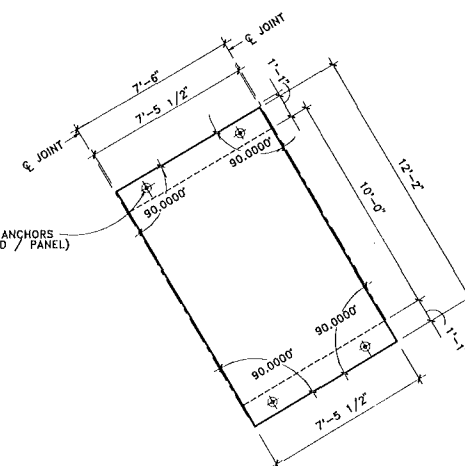
PRECAST UNIT TYPE "1"
3/8"=1'-0"

PRECAST UNIT TYPE "5" (OPPOSITE HAND)
3/8"=1'-0"

PRECAST UNIT TYPE "3" (OPPOSITE HAND)
3/8"=1'-0"



PRECAST UNIT TYPE "6"
3/8"=1'-0"

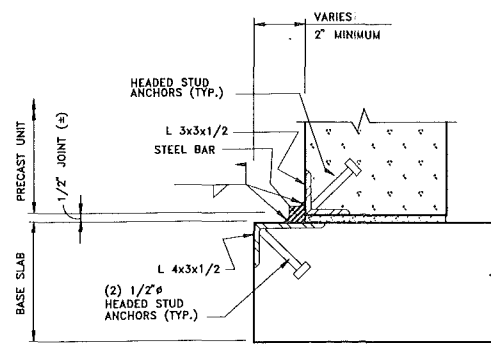


PRECAST UNIT TYPE "2"
3/8"=1'-0"

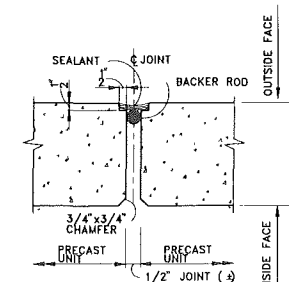
TYP. NORMAL CELL (W/O DIPOLES) PRECAST PLACING SCHED.			
ENCLOSURE SEGMENT	WORK POINT #	DISTANCE FROM STATION POINT TO WORK POINT ON REFERENCE LINE	PERPENDICULAR OFFSET FROM REFERENCE LINE TO WORK POINT
QUAD 220 THROUGH 221	220 + 0	0'-0"	2'-5"
	220 + 1	5'-10 1/4"	2'-5"
	220 + 2	13'-4 1/4"	2'-5"
	220 + 3	20'-10 1/4"	2'-5"
	220 + 4	28'-4 1/4"	2'-5"
	220 + 5	35'-10 1/4"	2'-5"
	220 + 6	43'-4 1/4"	2'-5"
	220 + 7	50'-10 1/4"	2'-5"
	221 + 0	58'-8 3/4"	2'-5"

TYP. NORMAL CELL (W/DIPOLES) PRECAST PLACING SCHED.			
ENCLOSURE SEGMENT	WORK POINT #	DISTANCE FROM STATION POINT TO WORK POINT ON REFERENCE LINE	PERPENDICULAR OFFSET FROM REFERENCE LINE TO WORK POINT
QUAD 214 THROUGH 216	214 + 0	0'-0"	2'-5"
	214 + 4	28'-4 1/4"	3'-1 3/4"
	215 + 0	56'-8 1/2"	3'-5 1/4"
	215 + 4	85'-0 3/4"	3'-1 3/4"
	216 + 0	113'-5"	2'-5"

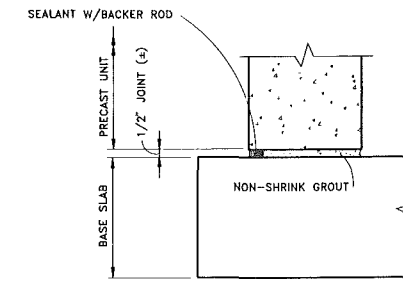
TYP. DISPERSION CELL PRECAST PLACING SCHED.			
ENCLOSURE SEGMENT	WORK POINT #	DISTANCE FROM STATION POINT TO WORK POINT ON REFERENCE LINE	PERPENDICULAR OFFSET FROM REFERENCE LINE TO WORK POINT
QUAD 218 THROUGH 220	218 + 0	0'-0"	2'-5"
	218 + 3	21'-3 1/4"	2'-8 1/4"
	219 + 0	42'-6 1/2"	2'-10"
	219 + 3	63'-9 3/4"	2'-8 1/4"
	220 + 0	85'-1"	2'-5"



TYPICAL PRECAST ANCHOR DETAIL
NO SCALE



TYPICAL PRECAST JOINT DETAIL
NO SCALE

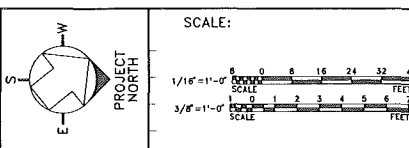


TYPICAL PRECAST BASE DETAIL
NO SCALE

REV.	DATE	DESCRIPTIONS

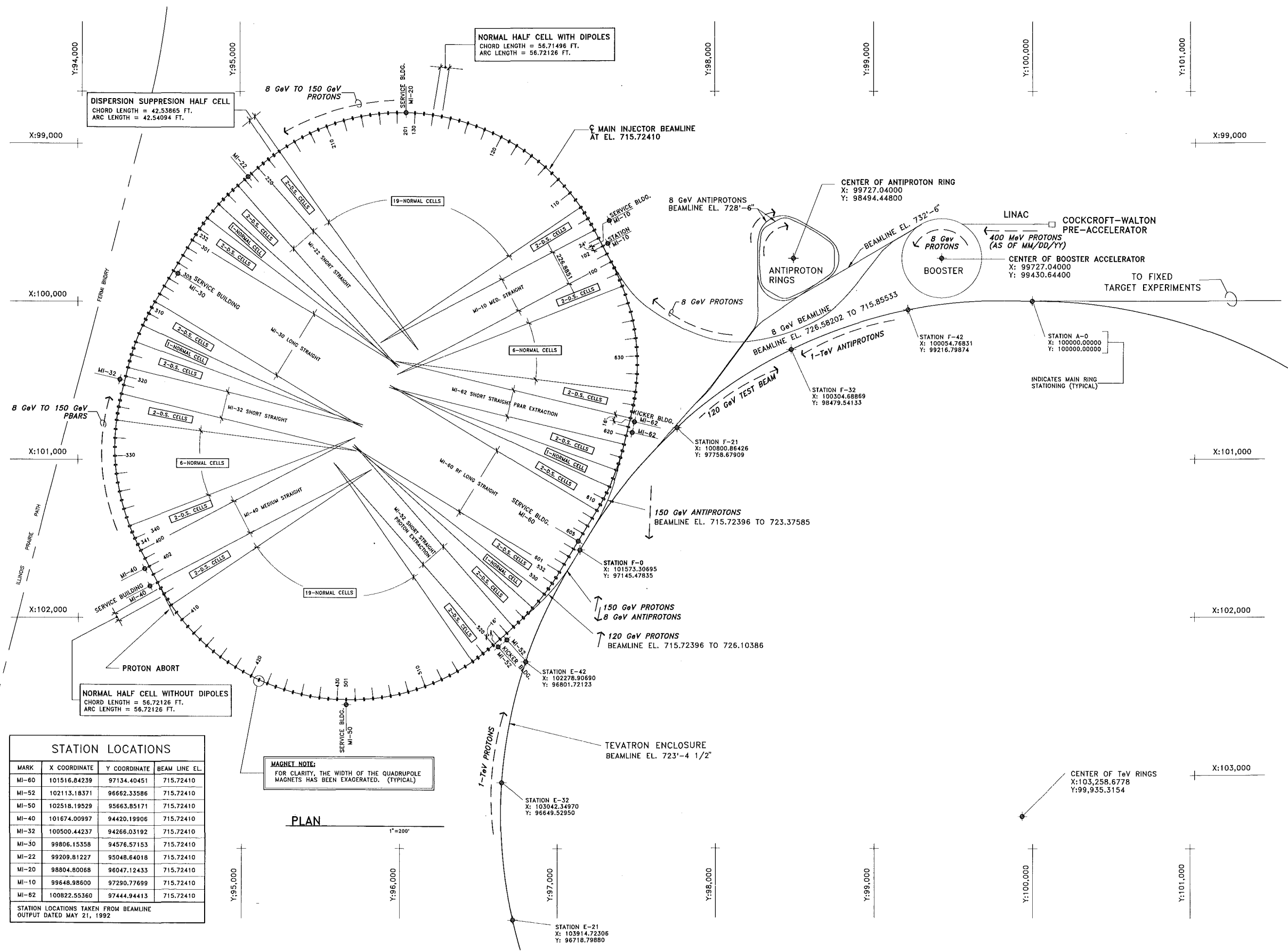
FLUOR DANIEL		
PROJECT NO. - 21842300		
DESIGNED	R. JEDZINIAK	DATE JULY, 1992
DRAWN	A. SKUZA	JULY, 1992
CHECKED	A. VASONIS	JULY, 1992
APPROVED		

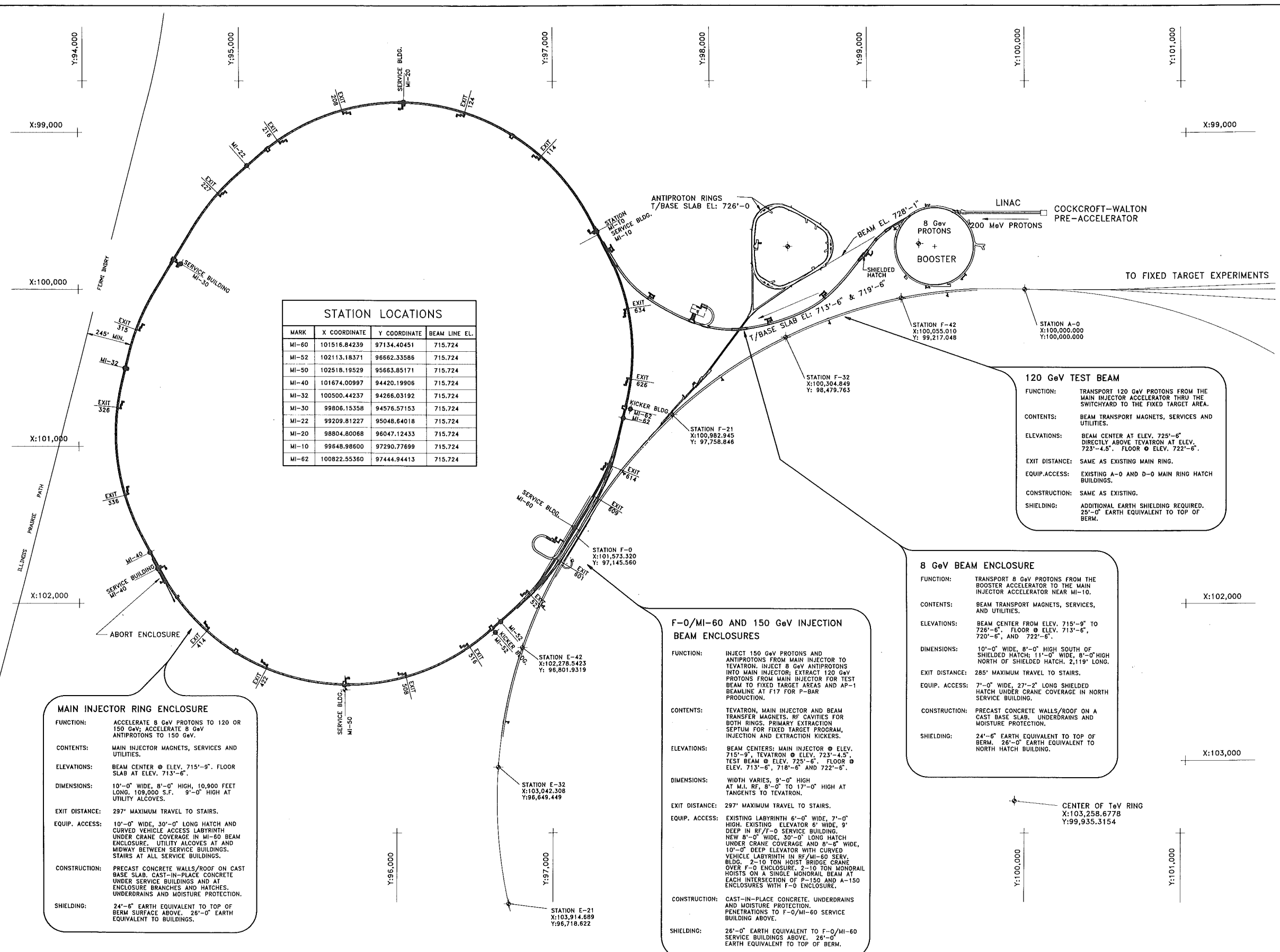
DESIGNED	NAME	DATE
	TOMSKI, MIKE GRIMSON	
DRAWN	MIKE GRIMSON	
CHECKED		
APPROVED		
SUBMITTED		



FERMI NATIONAL ACCELERATOR LABORATORY		
UNITED STATES DEPARTMENT OF ENERGY		
FERMILAB MAIN INJECTOR		
PRECAST ENCLOSURE DETAILS		
DRAWING NO.	6-6-2 TITLE-1	AS-8
REV.		

AUG. 1992





STATION LOCATIONS			
MARK	X COORDINATE	Y COORDINATE	BEAM LINE EL.
MI-60	101516.84239	97134.40451	715.724
MI-52	102113.18371	96662.33586	715.724
MI-50	102518.19529	95663.85171	715.724
MI-40	101674.00997	94420.19906	715.724
MI-32	100500.44237	94266.03192	715.724
MI-30	99806.15358	94576.57153	715.724
MI-22	99209.81227	95048.64018	715.724
MI-20	98804.80068	96047.12433	715.724
MI-10	98648.98600	97290.77699	715.724
MI-62	100822.55360	97444.94413	715.724

MAIN INJECTOR RING ENCLOSURE

FUNCTION: ACCELERATE 8 GeV PROTONS TO 120 OR 150 GeV; ACCELERATE 8 GeV ANTIPROTONS TO 150 GeV.

CONTENTS: MAIN INJECTOR MAGNETS, SERVICES AND UTILITIES.

ELEVATIONS: BEAM CENTER @ ELEV. 715'-9". FLOOR SLAB AT ELEV. 713'-6".

DIMENSIONS: 10'-0" WIDE, 8'-0" HIGH, 10,900 FEET LONG, 109,000 S.F. 9'-0" HIGH AT UTILITY ALCOVES.

EXIT DISTANCE: 297' MAXIMUM TRAVEL TO STAIRS.

EQUIP. ACCESS: 10'-0" WIDE, 30'-0" LONG HATCH AND CURVED VEHICLE ACCESS LABYRINTH UNDER CRANE COVERAGE IN MI-60 BEAM ENCLOSURE. UTILITY ALCOVES AT AND MIDWAY BETWEEN SERVICE BUILDINGS. STAIRS AT ALL SERVICE BUILDINGS.

CONSTRUCTION: PRECAST CONCRETE WALLS/ROOF ON CAST BASE SLAB. CAST-IN-PLACE CONCRETE UNDER SERVICE BUILDINGS AND AT ENCLOSURE BRANCHES AND HATCHES. UNDERDRAINS AND MOISTURE PROTECTION.

SHIELDING: 24'-6" EARTH EQUIVALENT TO TOP OF BERM SURFACE ABOVE. 26'-0" EARTH EQUIVALENT TO BUILDINGS.

F-0/MI-60 AND 150 GeV INJECTION BEAM ENCLOSURES

FUNCTION: INJECT 150 GeV PROTONS AND ANTIPROTONS FROM MAIN INJECTOR TO TEVATRON. INJECT 8 GeV ANTIPROTONS INTO MAIN INJECTOR; EXTRACT 120 GeV PROTONS FROM MAIN INJECTOR FOR TEST BEAM TO FIXED TARGET AREAS AND AP-1 BEAMLINE AT F17 FOR P-BAR PRODUCTION.

CONTENTS: TEVATRON, MAIN INJECTOR AND BEAM TRANSFER MAGNETS, RF CAVITIES FOR BOTH RINGS. PRIMARY EXTRACTION SEPTUM FOR FIXED TARGET PROGRAM, INJECTION AND EXTRACTION KICKERS.

ELEVATIONS: BEAM CENTERS: MAIN INJECTOR @ ELEV. 715'-9", TEVATRON @ ELEV. 723'-4.5". TEST BEAM @ ELEV. 725'-6". FLOOR @ ELEV. 713'-6", 718'-6" AND 722'-6".

DIMENSIONS: WIDTH VARIES, 9'-0" HIGH AT M.I. RF, 8'-0" TO 17'-0" HIGH AT TANGENTS TO TEVATRON.

EXIT DISTANCE: 297' MAXIMUM TRAVEL TO STAIRS.

EQUIP. ACCESS: EXISTING LABYRINTH 6'-0" WIDE, 7'-0" HIGH. EXISTING ELEVATOR 6' WIDE, 9' DEEP IN RF/F-0 SERVICE BUILDING; NEW 8'-0" WIDE, 30'-0" LONG HATCH UNDER CRANE COVERAGE AND 8'-6" WIDE, 10'-0" DEEP ELEVATOR WITH CURVED VEHICLE LABYRINTH IN RF/MI-60 SERV. BLDG. 2-10 TON HOIST BRIDGE CRANE OVER F-0 ENCLOSURE. 2-10 TON MONORAIL HOISTS ON A SINGLE MONORAIL BEAM AT EACH INTERSECTION OF F-150 AND A-150 ENCLOSURES WITH F-0 ENCLOSURE.

CONSTRUCTION: CAST-IN-PLACE CONCRETE, UNDERDRAINS AND MOISTURE PROTECTION. PENETRATIONS TO F-0/MI-60 SERVICE BUILDING ABOVE.

SHIELDING: 26'-0" EARTH EQUIVALENT TO F-0/MI-60 SERVICE BUILDINGS ABOVE. 26'-0" EARTH EQUIVALENT TO TOP OF BERM.

8 GeV BEAM ENCLOSURE

FUNCTION: TRANSPORT 8 GeV PROTONS FROM THE BOOSTER ACCELERATOR TO THE MAIN INJECTOR ACCELERATOR NEAR MI-10.

CONTENTS: BEAM TRANSPORT MAGNETS, SERVICES, AND UTILITIES.

ELEVATIONS: BEAM CENTER FROM ELEV. 715'-9" TO 726'-6". FLOOR @ ELEV. 713'-6", 720'-6", AND 722'-6".

DIMENSIONS: 10'-0" WIDE, 8'-0" HIGH SOUTH OF SHIELDED HATCH; 11'-0" WIDE, 8'-0" HIGH NORTH OF SHIELDED HATCH, 2,119' LONG.

EXIT DISTANCE: 285' MAXIMUM TRAVEL TO STAIRS.

EQUIP. ACCESS: 7'-0" WIDE, 27'-2" LONG SHIELDED HATCH UNDER CRANE COVERAGE IN NORTH SERVICE BUILDING.

CONSTRUCTION: PRECAST CONCRETE WALLS/ROOF ON A CAST BASE SLAB. UNDERDRAINS AND MOISTURE PROTECTION.

SHIELDING: 24'-6" EARTH EQUIVALENT TO TOP OF BERM. 26'-0" EARTH EQUIVALENT TO NORTH HATCH BUILDING.

120 GeV TEST BEAM

FUNCTION: TRANSPORT 120 GeV PROTONS FROM THE MAIN INJECTOR ACCELERATOR THRU THE SWITCHYARD TO THE FIXED TARGET AREA.

CONTENTS: BEAM TRANSPORT MAGNETS, SERVICES AND UTILITIES.

ELEVATIONS: BEAM CENTER AT ELEV. 725'-6" DIRECTLY ABOVE TEVATRON AT ELEV. 723'-4.5". FLOOR @ ELEV. 722'-6".

EXIT DISTANCE: SAME AS EXISTING MAIN RING.

EQUIP. ACCESS: EXISTING A-0 AND D-0 MAIN RING HATCH BUILDINGS.

CONSTRUCTION: SAME AS EXISTING.

SHIELDING: ADDITIONAL EARTH SHIELDING REQUIRED. 25'-0" EARTH EQUIVALENT TO TOP OF BERM.

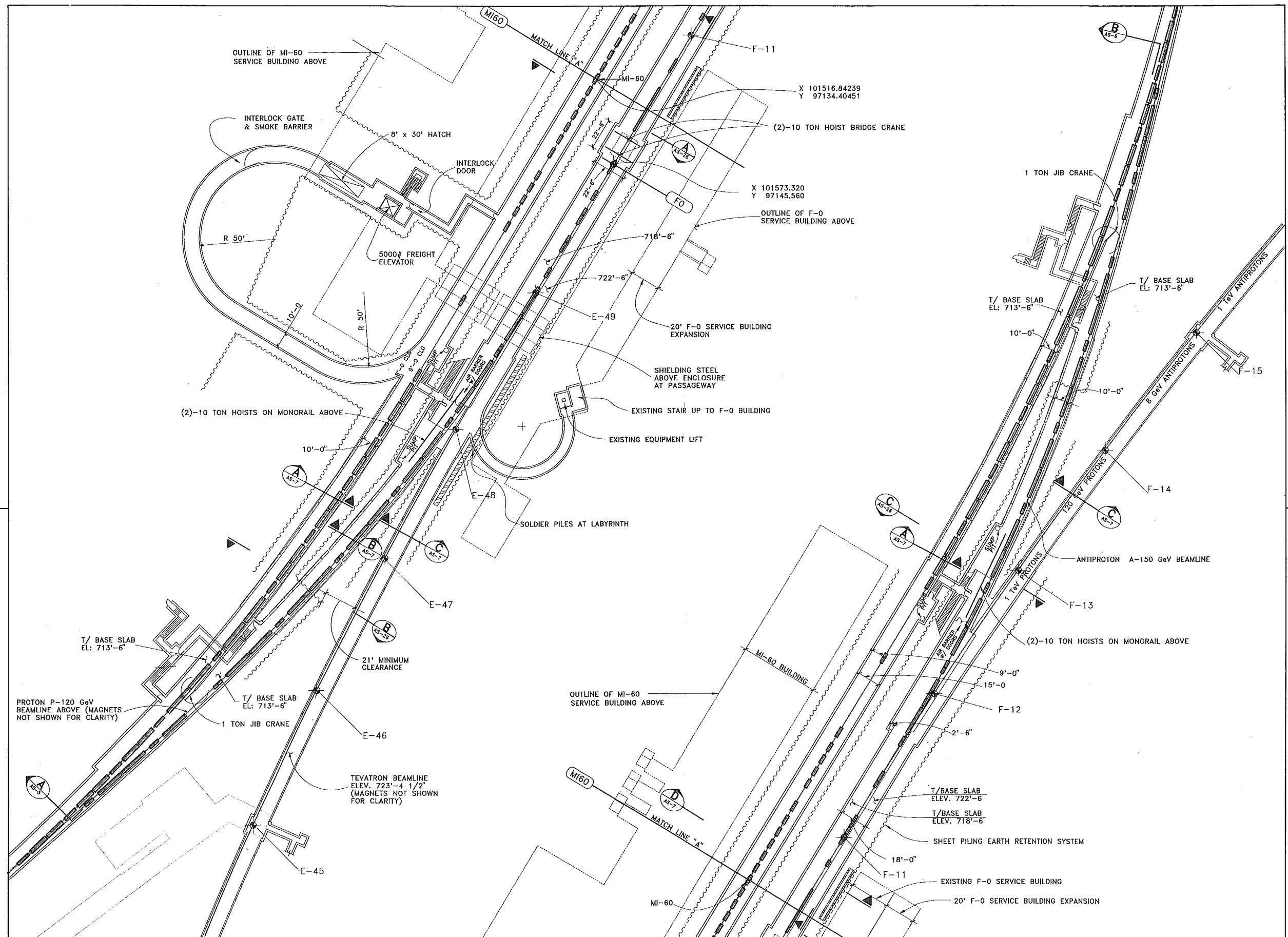
DESIGNED T. LACKOWSKI		DATE	
DRAWN T. LACKOWSKI			
CHECKED			
APPROVED			
SUBMITTED			

NAME		DATE	
T. LACKOWSKI			
T. LACKOWSKI			

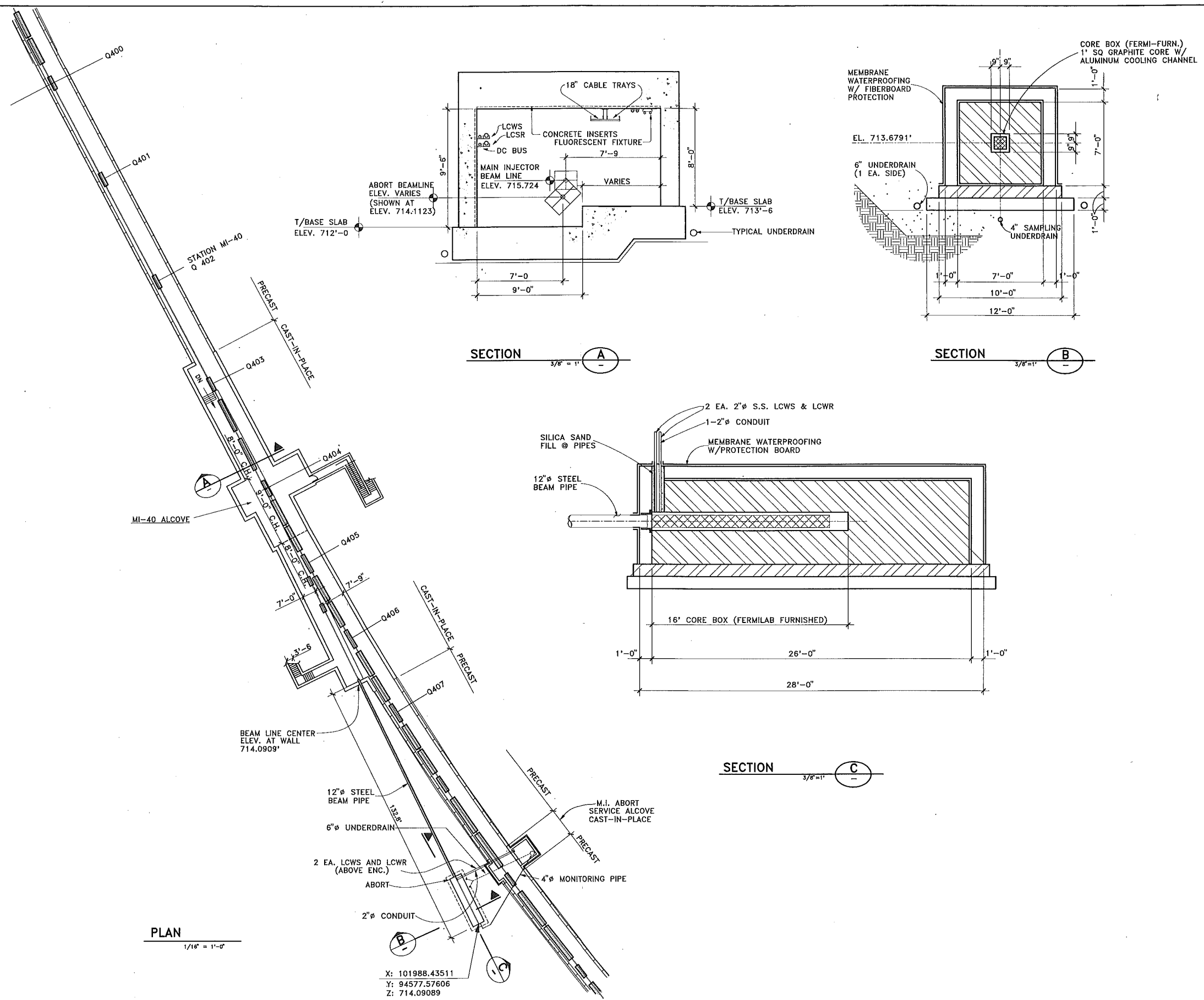
SCALE: 1" = 200'-0" SCALE		FERMI NATIONAL ACCELERATOR LABORATORY	
		UNITED STATES DEPARTMENT OF ENERGY	
		FERMILAB MAIN INJECTOR	
		ENCLOSURE CRITERIA PLAN	
		DRAWING NO. 6-6-2 TITLE-1 AS-2 REV.	

FLUOR DANIEL		AUG. 1992	
CHICAGO ILLINOIS			
PROJECT NO. - 21842300			
NAME		DATE	
T. LAREN		JULY, 92	
I. MASIS		JULY, 92	
A. VASONIS		JULY, 92	

REV.	DATE	DESCRIPTIONS

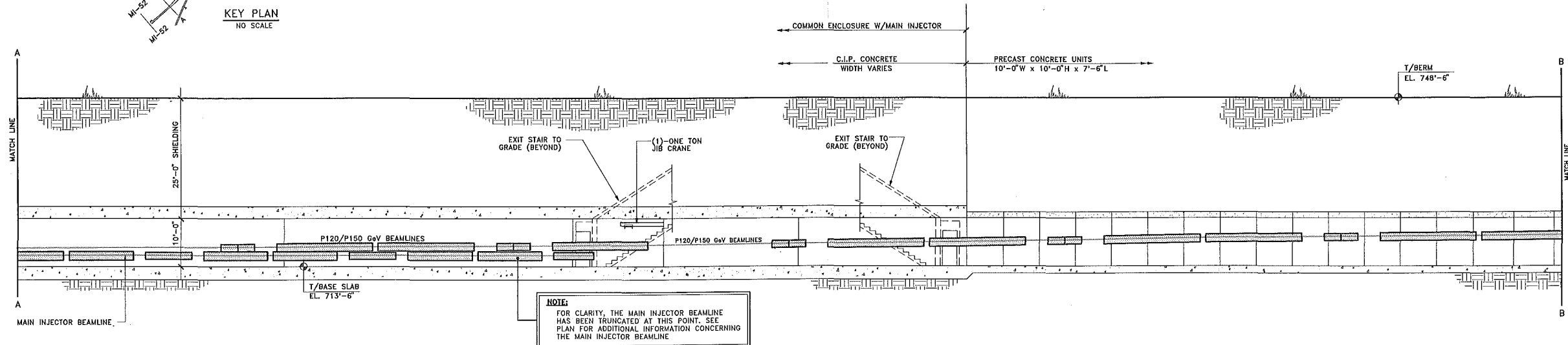
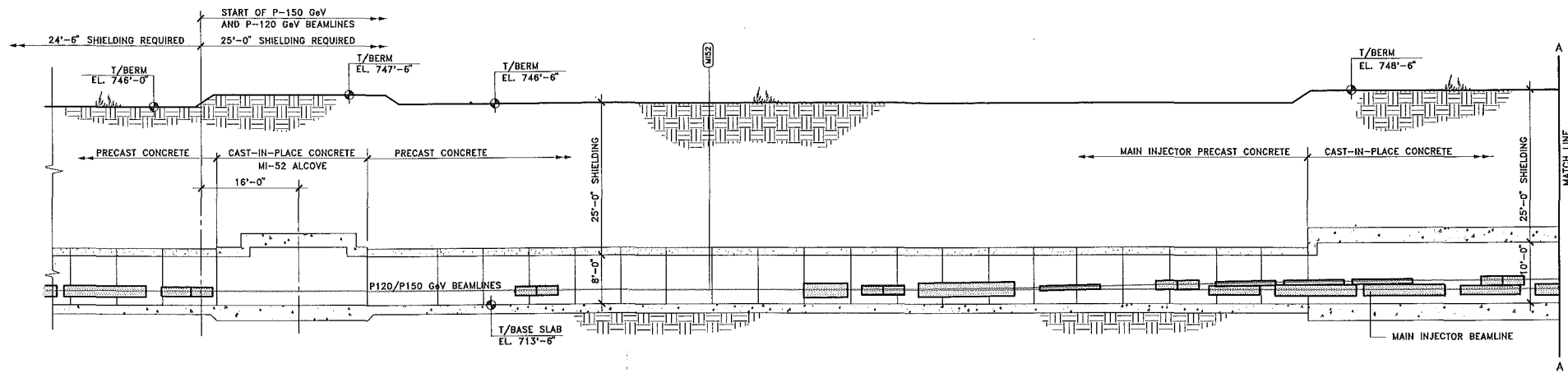
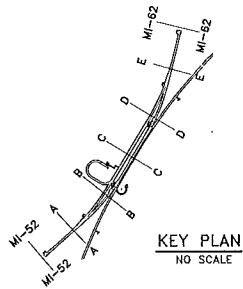


REV.		DATE	DESCRIPTIONS	FLUOR DANIEL PROJECT NO. - 21842300 NAME DATE DESIGNED R. JEDZINIAK JULY, 1992 DRAWN R. JEDZINIAK JULY, 1992 CHECKED A. VASONIS JULY, 1992 APPROVED		DESIGNED T. LACKOWSKI DRAWN T. LACKOWSKI / T. BURKE CHECKED APPROVED SUBMITTED	SCALE: 1" = 20'-0" SCALE	FERMILAB MAIN INJECTOR F-0 / MI-60 ENCLOSURE PLAN DRAWING NO. 6-6-2 TITLE-1 AS-3	AUG. 1992
------	--	------	--------------	--	--	--	--------------------------------	--	-----------

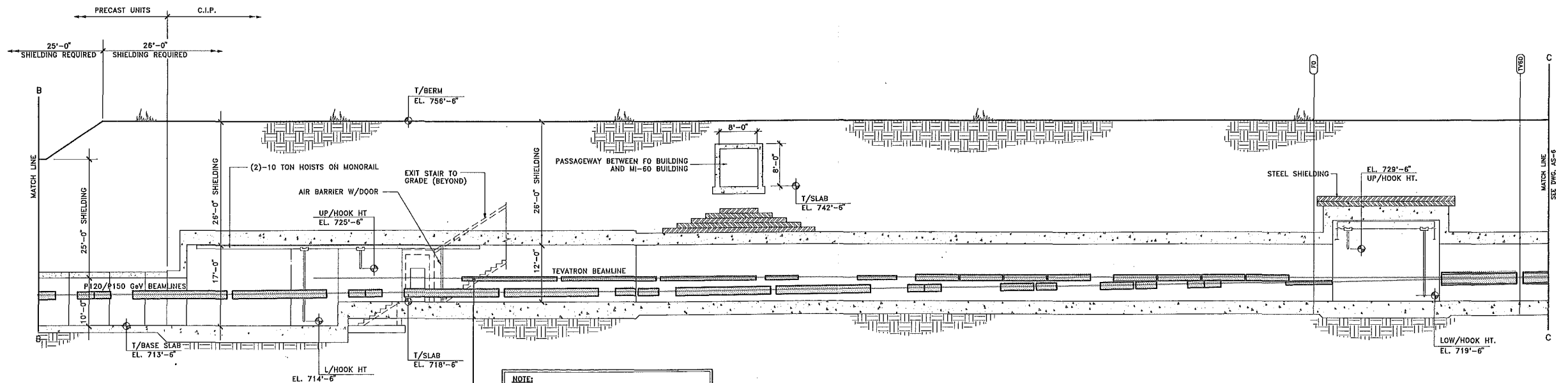


FLUOR DANIEL PROJECT NO. 21842300 NAME: R. JEDZINIAK DATE: JULY, 1992 DRAWN: A. SKUZA JULY, 1992 CHECKED: A. VASONIS JULY, 1992 APPROVED:		DESIGNED: T. LACKOWSKI DATE:		DRAWN: T. LACKOWSKI/T. BURKE		CHECKED:		APPROVED:		SUBMITTED:	
REV. DATE DESCRIPTIONS REVISIONS		X: 101988.43511 Y: 94577.57606 Z: 714.09089		SCALE: 1/16" = 1'-0" 3/8" = 1'-0"		FERMILAB MAIN INJECTOR ABORT PLAN AND SECTION		FERMILAB MAIN INJECTOR ABORT PLAN AND SECTION		FERMILAB MAIN INJECTOR ABORT PLAN AND SECTION	

DIMENSION NOTE:
THE HORIZONTAL DIMENSIONS ON THIS DRAWING HAVE BEEN DISTORTED IN ORDER TO PROVIDE AN IDEALIZED PROJECTION OF THE VARIOUS BEAMLINES. ALL HORIZONTAL DIMENSIONS SHOULD BE TAKEN FROM THE PLAN VIEW OF THE ENCLOSURE.



NOTE:
FOR CLARITY, THE MAIN INJECTOR BEAMLINE HAS BEEN TRUNCATED AT THIS POINT. SEE PLAN FOR ADDITIONAL INFORMATION CONCERNING THE MAIN INJECTOR BEAMLINE.



NOTE:
FOR CLARITY, THE TEVATRON BEAMLINE HAS BEEN TRUNCATED AT THIS POINT. SEE PLAN FOR ADDITIONAL INFORMATION CONCERNING THE TEVATRON BEAMLINE.

SECTION
(LOOKING SOUTHWEST) 1/8"=1'-0" AS-3

REV.	DATE	DESCRIPTIONS

FLUOR DANIEL		
PROJECT NO. - 21842300		
DESIGNED	R. JEDZINIAK	JULY, 1992
DRAWN	A. SKUZA	JULY, 1992
CHECKED	A. VASONIS	JULY, 1992
APPROVED		

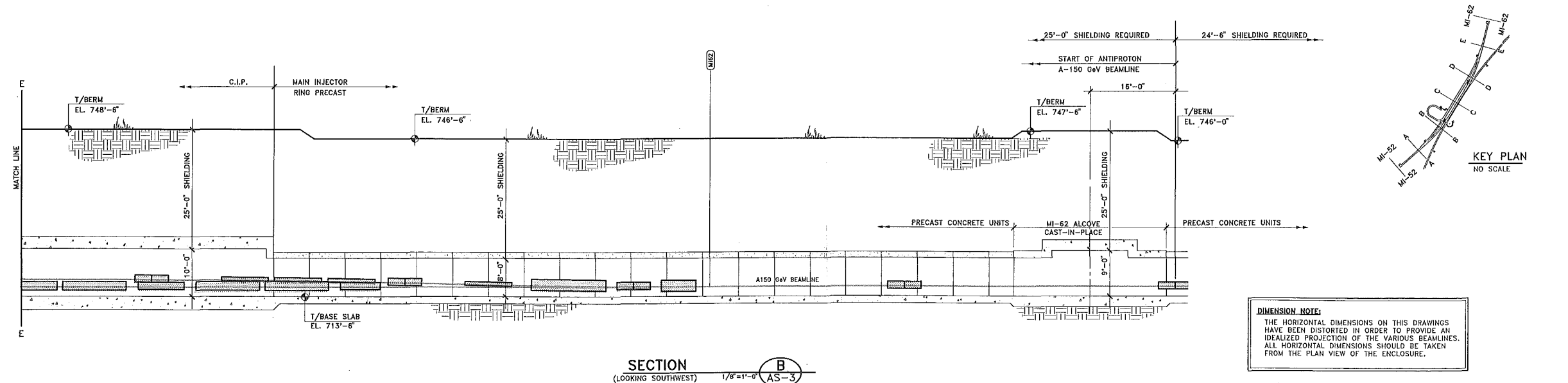
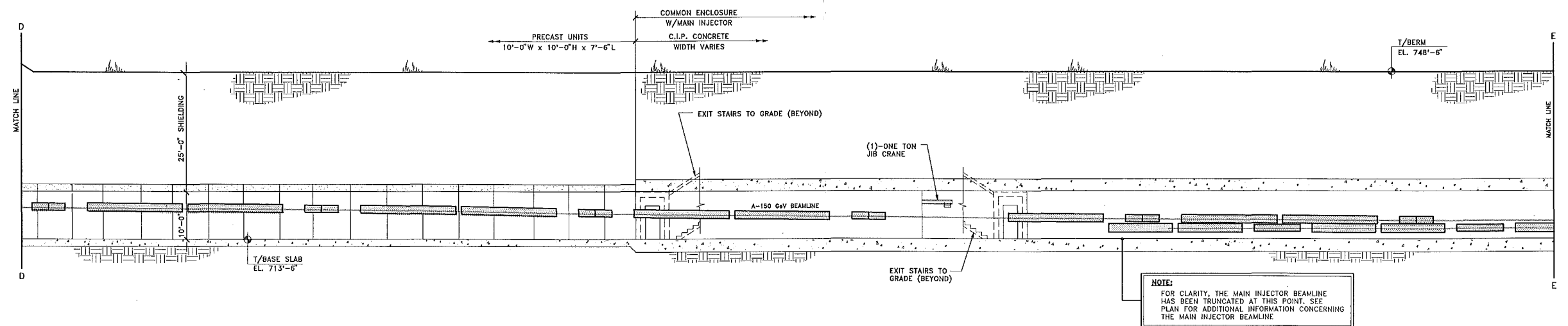
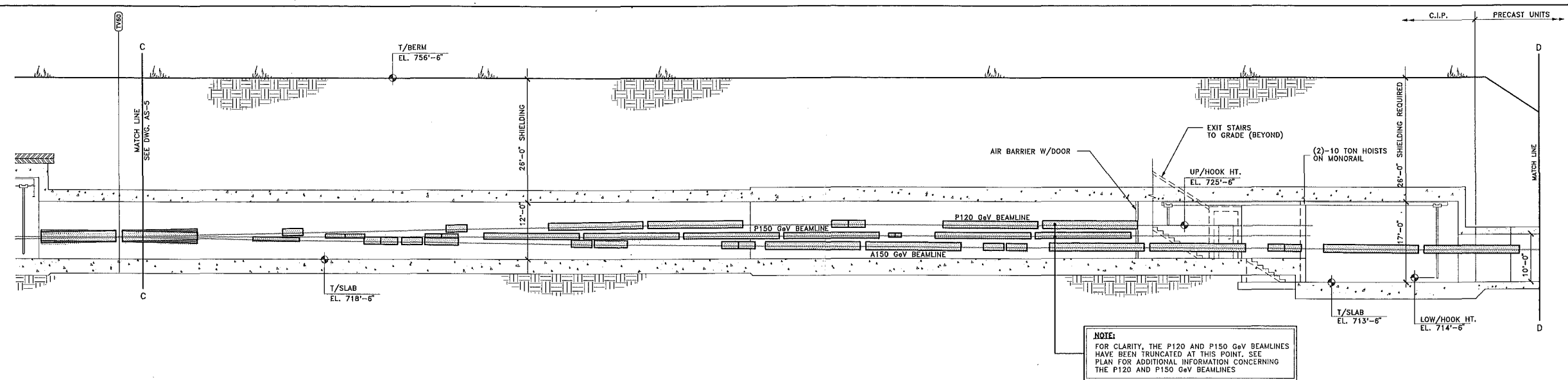
DESIGNED	T. LACKOWSKI	DATE
DRAWN	S. DIXON	
CHECKED		
APPROVED		
SUBMITTER		



FERMI NATIONAL ACCELERATOR LABORATORY	
UNITED STATES DEPARTMENT OF ENERGY	
FERMILAB MAIN INJECTOR	
P-150 GeV ENCLOSURE LONG. SECTION	
DRAWING NO.	6-6-2 TITLE-1 AS-5
REV.	

AUG. 1992

AS-5



REV.	DATE	DESCRIPTIONS	REVISIONS

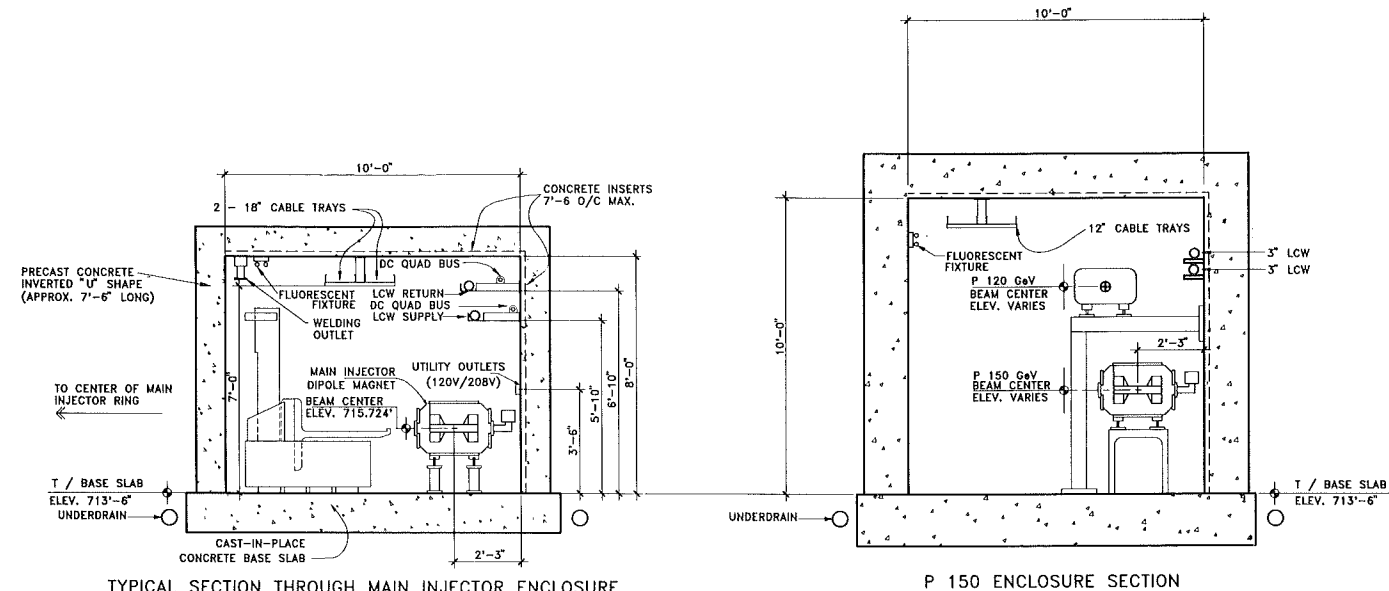
FLUOR DANIEL		
PROJECT NO. - 21842300		
DESIGNED	R. JEDZINIAK	JULY, 1992
DRAWN	A. SKUZA	JULY, 1992
CHECKED	A. VASONIS	JULY, 1992
APPROVED		

DESIGNED	T. LACKOWSKI	
DRAWN	S. DIXON	
CHECKED		
APPROVED		
SUBMITTED		

SCALE:	1/8"=1'-0"	0 4 8 12 16 20 FEET
--------	------------	---------------------

FERMI NATIONAL ACCELERATOR LABORATORY		
UNITED STATES DEPARTMENT OF ENERGY		
FERMILAB MAIN INJECTOR		
A-150 GeV ENCLOSURE LONG. SECTION		
DRAWING NO.	6-6-2 TITLE-1	AS-6
REV.		

AS-6

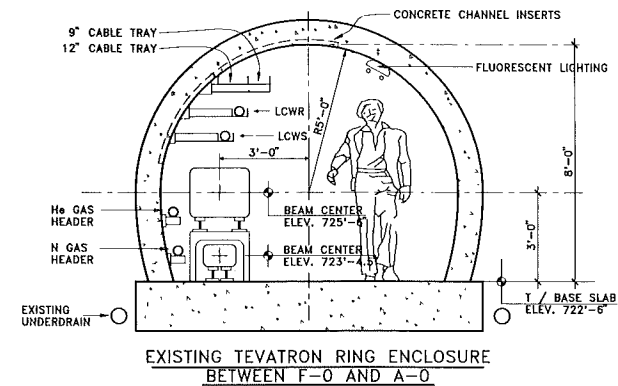


TYPICAL SECTION THROUGH MAIN INJECTOR ENCLOSURE

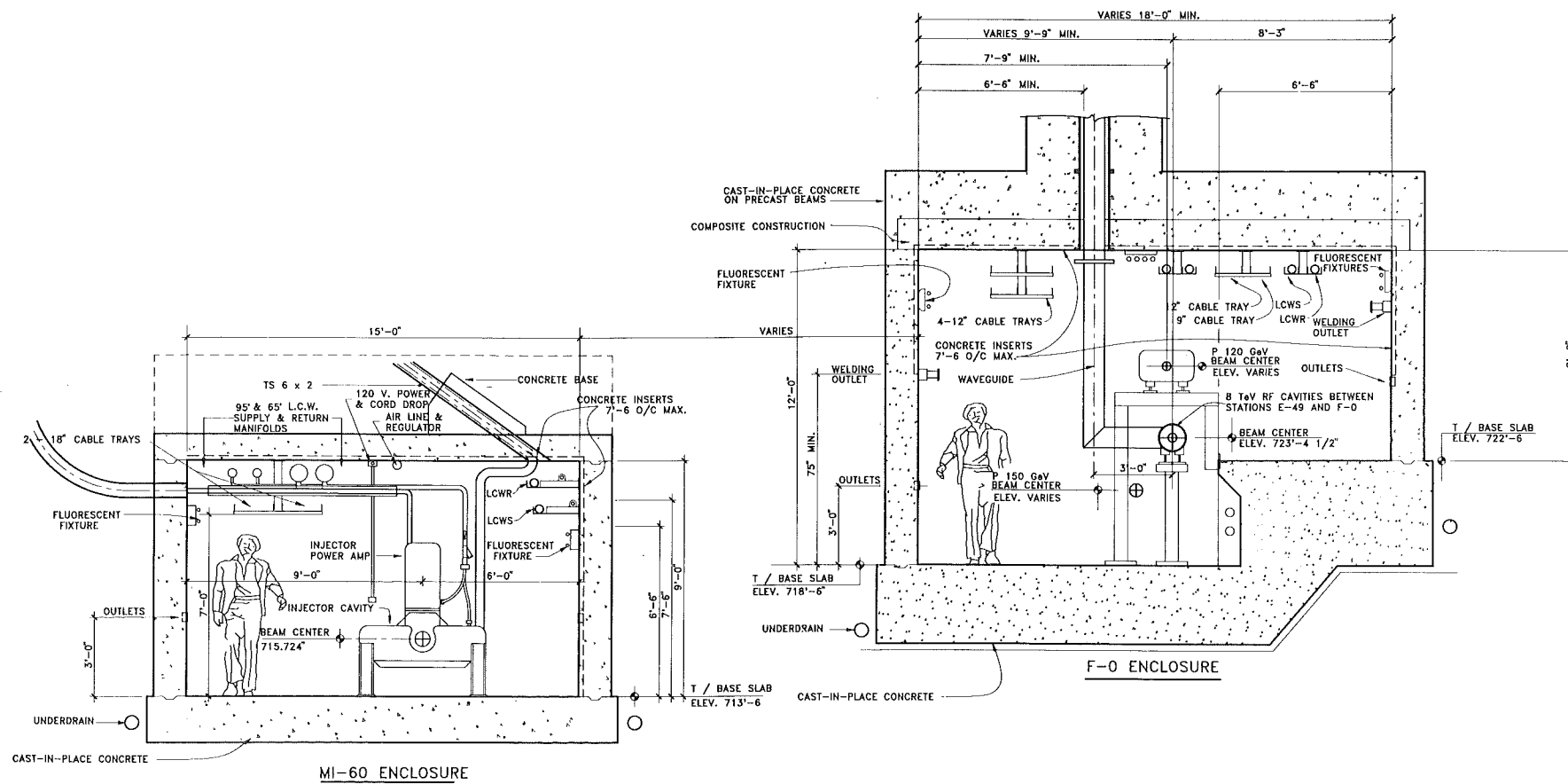
P 150 ENCLOSURE SECTION

SECTION
1/2"=1'-0"
AS-3

SECTION
1/2"=1'-0"
AS-3



SECTION
1/2"=1'-0"
AS-3



MI-60 ENCLOSURE

F-0 ENCLOSURE

SECTION
1/2"=1'-0"
AS-3

REV.	DATE	DESCRIPTIONS	REVISIONS

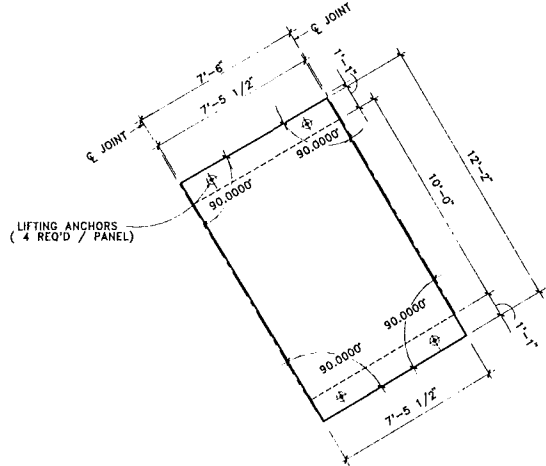
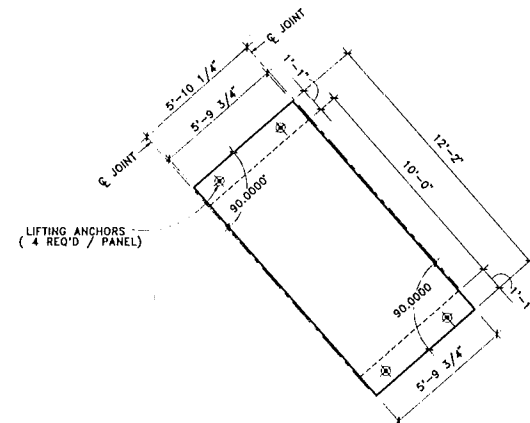
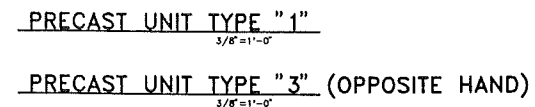
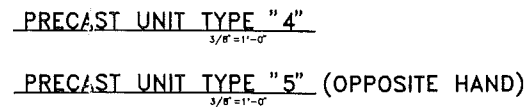
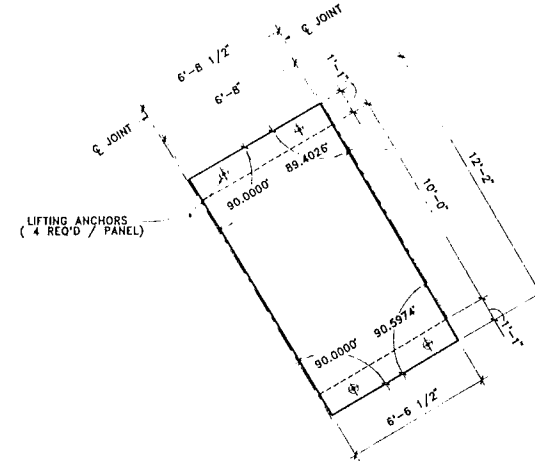
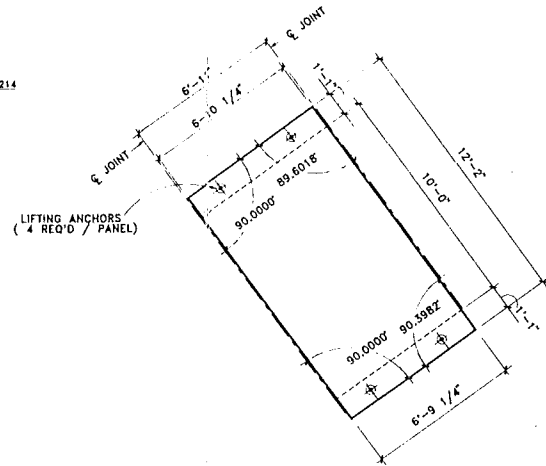
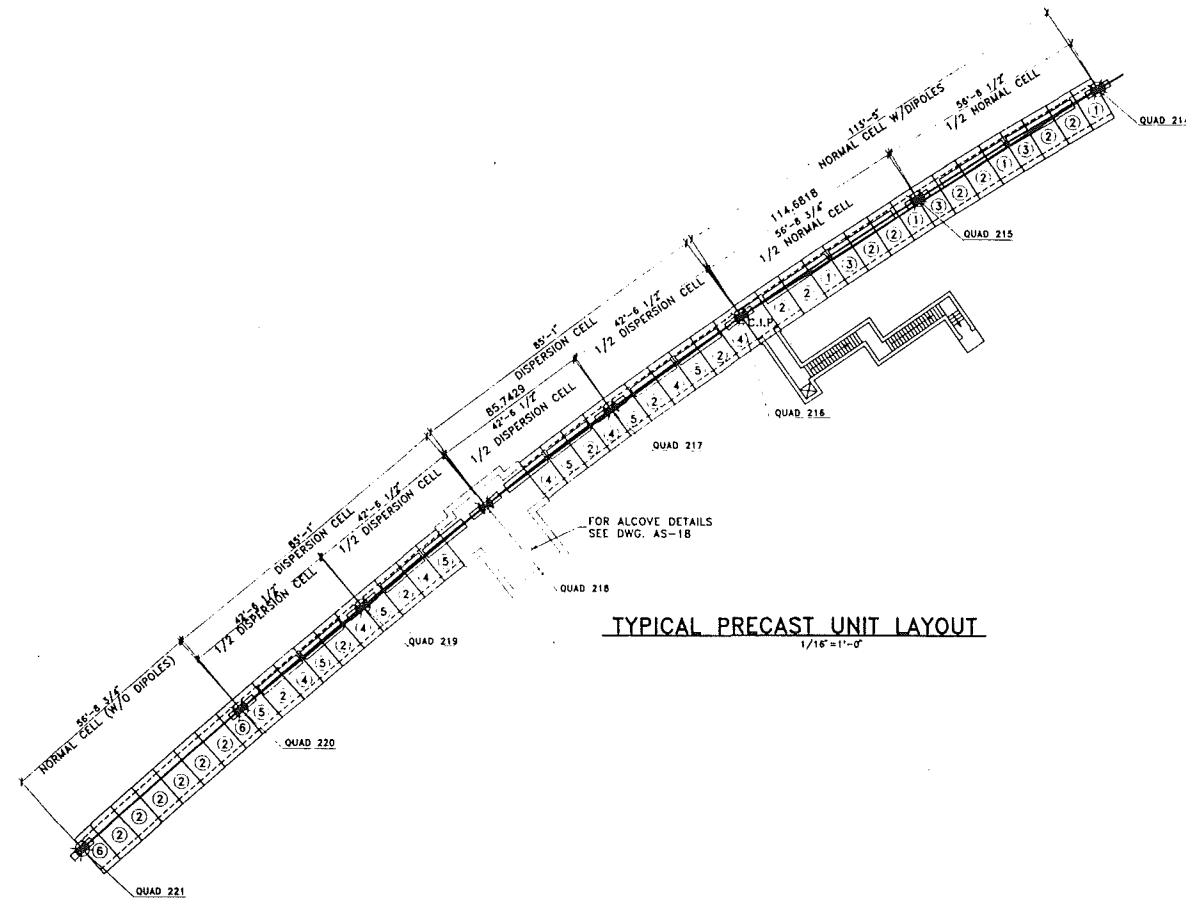
FLUOR DANIEL PROJECT NO. - 21842300			
DESIGNED	R. JEDZINIAK	DATE	JULY, 1992
DRAWN	I. MASIS	DATE	JULY, 1992
CHECKED	A. VASOHS	DATE	JULY, 1992
APPROVED			

DESIGNED	T. LACKOWSKI	DATE	
DRAWN	T. LACKOWSKI/T. BURKE	DATE	
CHECKED		DATE	
APPROVED		DATE	
SUBMITTED		DATE	

SCALE:	1/2"=1'-0"
SCALE	1 2 3 4 5 FEET

FERMI NATIONAL ACCELERATOR LABORATORY	
UNITED STATES DEPARTMENT OF ENERGY	
FERMILAB MAIN INJECTOR	
INJECTOR ENCLOSURE SECTIONS	
DRAWING NO.	6-6-2 TITLE-1 AS-7 REV.

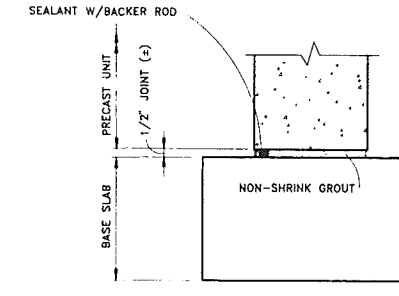
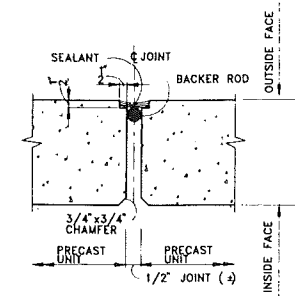
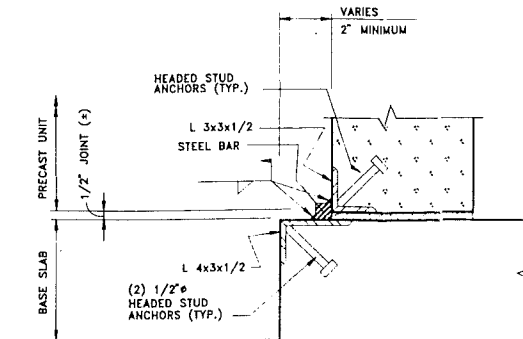
AUG. 1992



TYP. NORMAL CELL (W/O DIPOLES) PRECAST PLACING SCHED.			
ENCLOSURE SEGMENT	WORK POINT #	DISTANCE FROM STATION POINT TO WORK POINT ON REFERENCE LINE	PERPENDICULAR OFFSET FROM REFERENCE LINE TO WORK POINT
QUAD 220 THROUGH 221	220 + 0	0'-0"	2'-5"
	220 + 1	5'-10 1/4"	2'-5"
	220 + 2	13'-4 1/4"	2'-5"
	220 + 3	20'-10 1/4"	2'-5"
	220 + 4	28'-4 1/4"	2'-5"
	220 + 5	35'-10 1/4"	2'-5"
	220 + 6	43'-4 1/4"	2'-5"
	220 + 7	50'-10 1/4"	2'-5"
	221 + 0	58'-8 3/4"	2'-5"

TYP. NORMAL CELL (W/DIPOLES) PRECAST PLACING SCHED.			
ENCLOSURE SEGMENT	WORK POINT #	DISTANCE FROM STATION POINT TO WORK POINT ON REFERENCE LINE	PERPENDICULAR OFFSET FROM REFERENCE LINE TO WORK POINT
QUAD 214 THROUGH 216	214 + 0	0'-0"	2'-5"
	214 + 4	28'-4 1/4"	3'-1 3/4"
	215 + 0	56'-8 1/2"	3'-5 1/4"
	215 + 4	85'-0 3/4"	3'-1 3/4"
	216 + 0	113'-5"	2'-5"

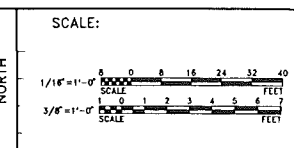
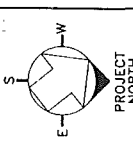
TYP. DISPERSION CELL PRECAST PLACING SCHED.			
ENCLOSURE SEGMENT	WORK POINT #	DISTANCE FROM STATION POINT TO WORK POINT ON REFERENCE LINE	PERPENDICULAR OFFSET FROM REFERENCE LINE TO WORK POINT
QUAD 218 THROUGH 220	218 + 0	0'-0"	2'-5"
	218 + 3	21'-3 1/4"	2'-8 1/4"
	219 + 0	42'-6 1/2"	2'-10"
	219 + 3	63'-9 3/4"	2'-8 1/4"
	220 + 0	85'-1"	2'-5"



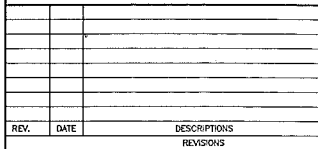
REV	DATE	DESCRIPTIONS

FLUOR DANIEL		
PROJECT NO. - 21842300		
DESIGNED	R. JEDZINIAK	JULY, 1992
DRAWN	A. SKUZA	JULY, 1992
CHECKED	A. VASONIS	JULY, 1992
APPROVED		

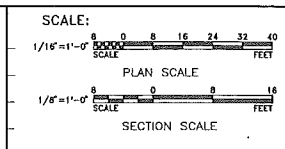
DESIGNED	NAME	DATE
TOMSKI, MIKE GRIMSON		
DRAWN	MIKE GRIMSON	
CHECKED		
APPROVED		
SUBMITTED		




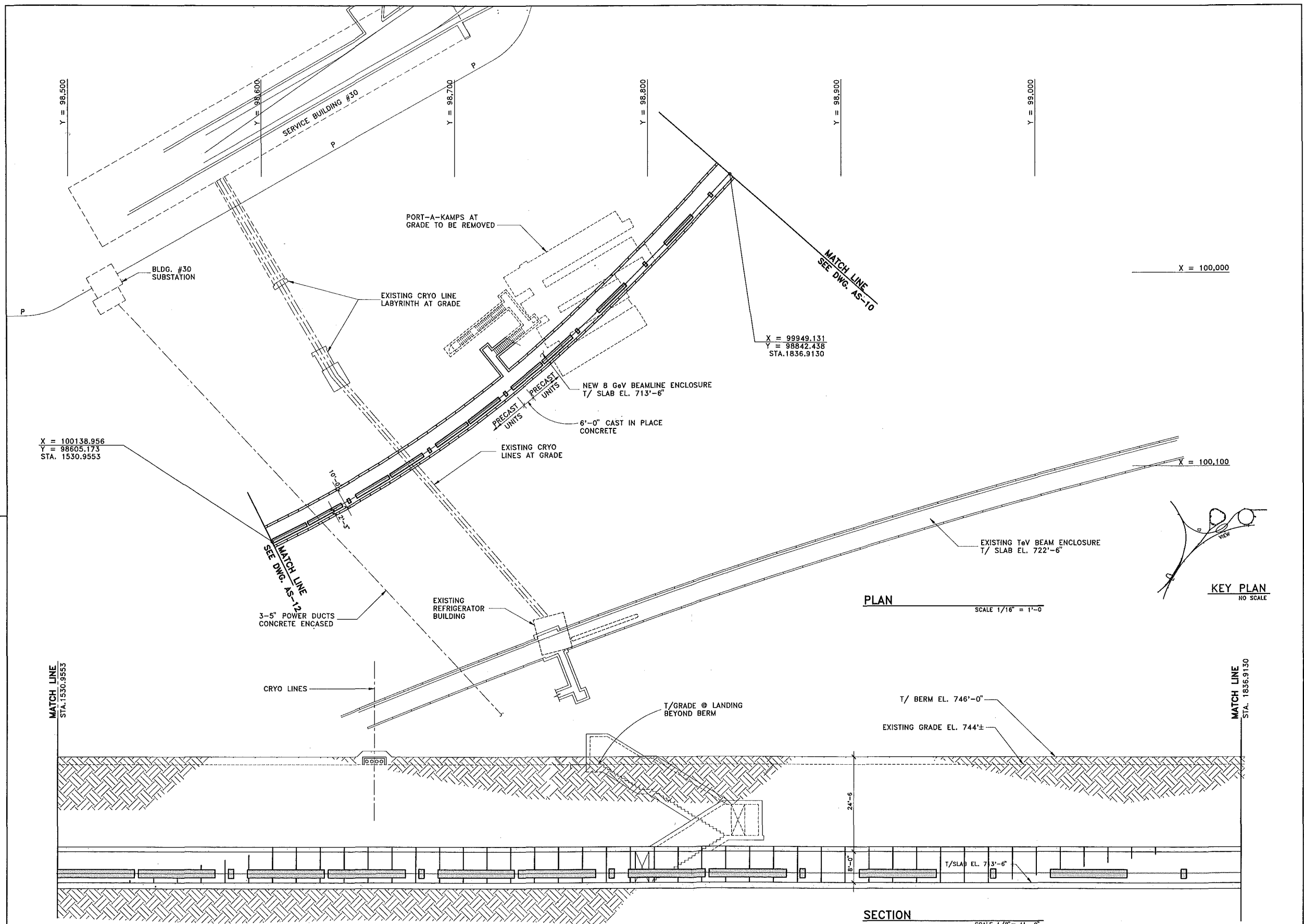
FERMI NATIONAL ACCELERATOR LABORATORY		
UNITED STATES DEPARTMENT OF ENERGY		
FERMILAB MAIN INJECTOR		
PRECAST ENCLOSURE DETAILS		
DRAWING NO.	6-6-2 TITLE-1	AS-8
REV.		



NAME		DATE
DESIGNED	TOMSKI	
DRAWN	JONSKI	
CHECKED		
APPROVED		
SUBMITTED		



FERMI NATIONAL ACCELERATOR LABORATORY			
UNITED STATES DEPARTMENT OF ENERGY			
	FERMILAB MAIN INJECTOR		
	8 GeV BEAMLINE SHT. 1		
DRAWING NO.	6-6-2	TITLE-1	AS-9 REV.

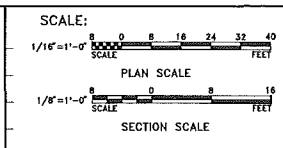
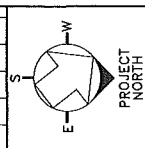


REV.	DATE	DESCRIPTIONS

AS-11

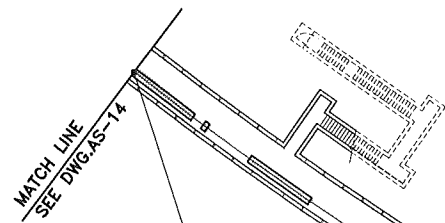
FLUOR DANIEL <small>CHICAGO ILLINOIS</small> PROJECT NO. - Z1842300		
DESIGNED	R. JEDZINIAK	JULY, 1992
DRAWN	I. MASIS	JULY, 1992
CHECKED	D. ABRAHAM	JULY, 1992
APPROVED		

NAME	DATE
DESIGNED	T. LACKOWSKI
DRAWN	J. HACKEMER
CHECKED	
APPROVED	
SUBMITTED	



FERMI NATIONAL ACCELERATOR LABORATORY	
UNITED STATES DEPARTMENT OF ENERGY	
FERMILAB MAIN INJECTOR 8 GeV BEAMLINE SHT. 3	
DRAWING NO.	6-6-2 TITLE-1 AS-11

AUG. 1992



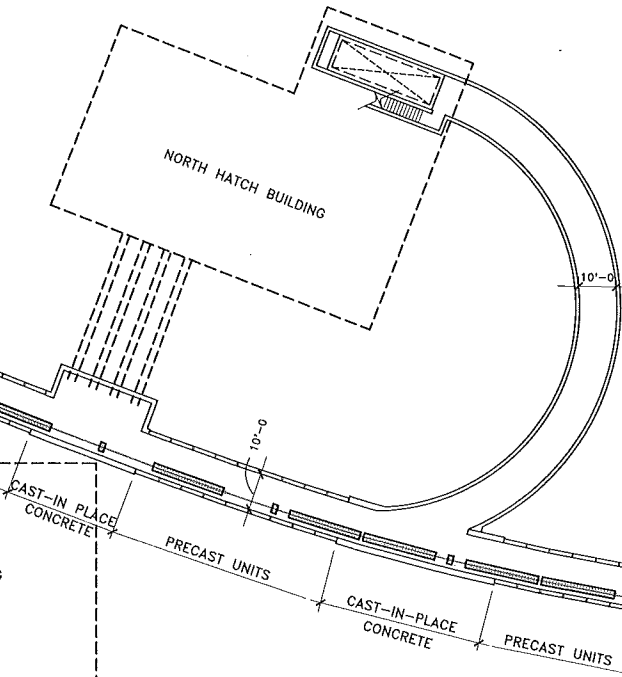
X = 100032.694
Y = 97565.869
STA. 419.1242

NEW 8 GeV BEAMLINE ENCLOSURE
T/SLAB EL. 713'-6"

PLAN

1/16" = 1'-0"

10'-0" WIDE x 8'-0" HIGH
PRECAST UNITS



MATCH LINE
SEE DWG. AS-12

X = 100,100

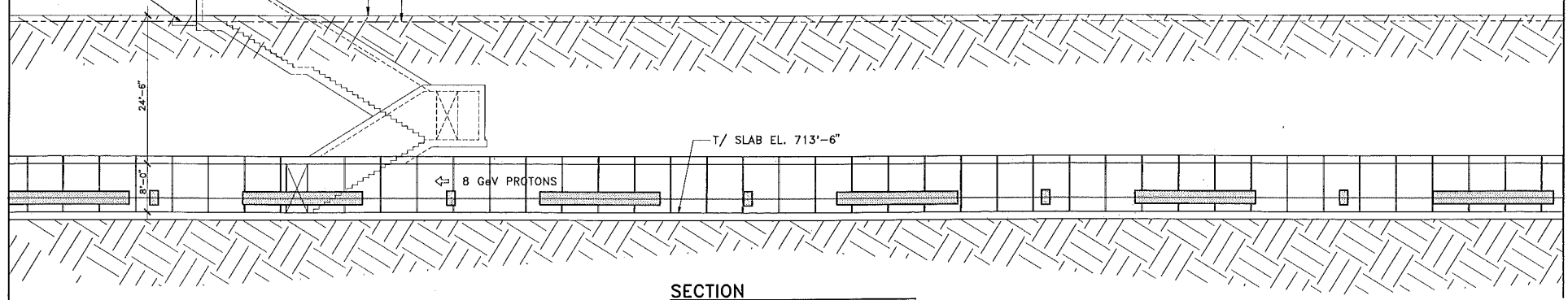
X = 100,200

X = 100251.642
Y = 98033.549
STA. 939.9568

MATCH LINE
STA. 419.1242

MATCH LINE A
SEE SECTION
BELOW

TOP/GRADE @ LANDING
BEYOND BERM



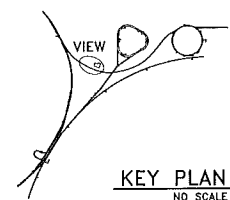
SECTION

SCALE: 1/8" = 1'-0"

SECTION

SCALE: 1/8" = 1'-0"

MATCH LINE
STA. 939.9568



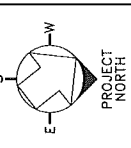
KEY PLAN
NO SCALE

REV.	DATE	DESCRIPTIONS REVISIONS

AS-13

FLUOR DANIEL		
PROJECT NO. - 21842300		
DESIGNED	R. JEDZINIAK	JULY, 1992
DRAWN	I. MASIS	JULY, 1992
CHECKED	A. VASONIS	JULY, 1992
APPROVED		

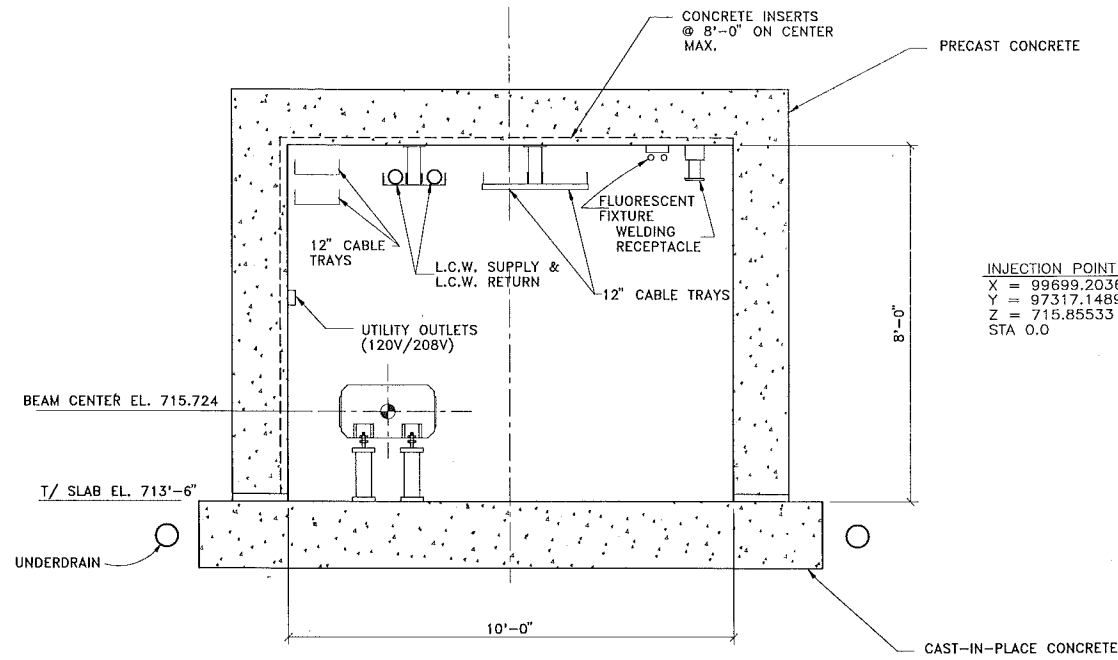
DESIGNED	DATE
T. LACKOWSKI	
DRAWN	DATE
J. HACKEMER	
CHECKED	DATE
APPROVED	DATE
SUBMITTED	DATE



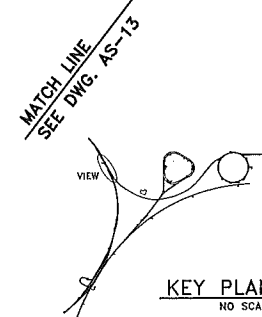
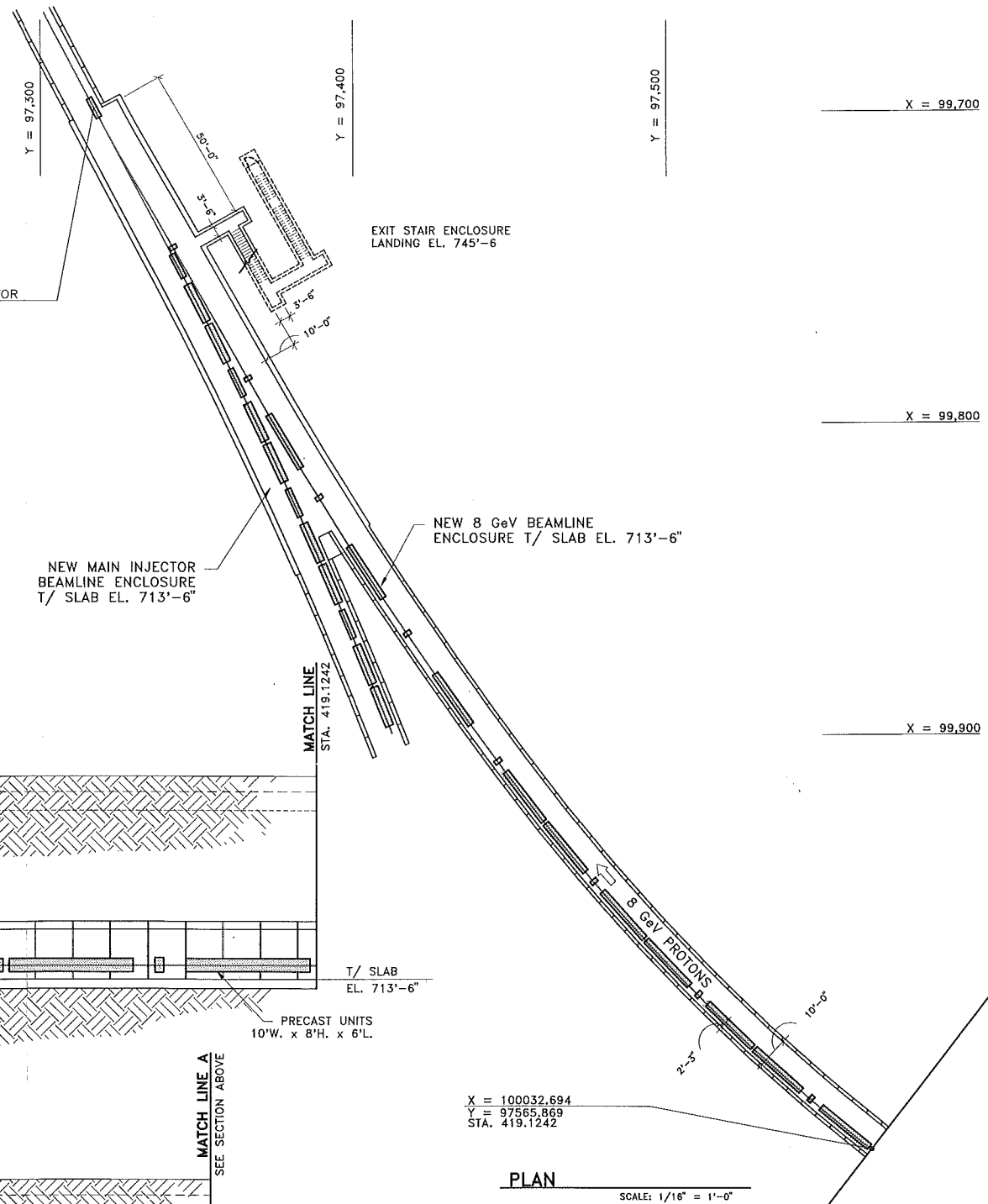
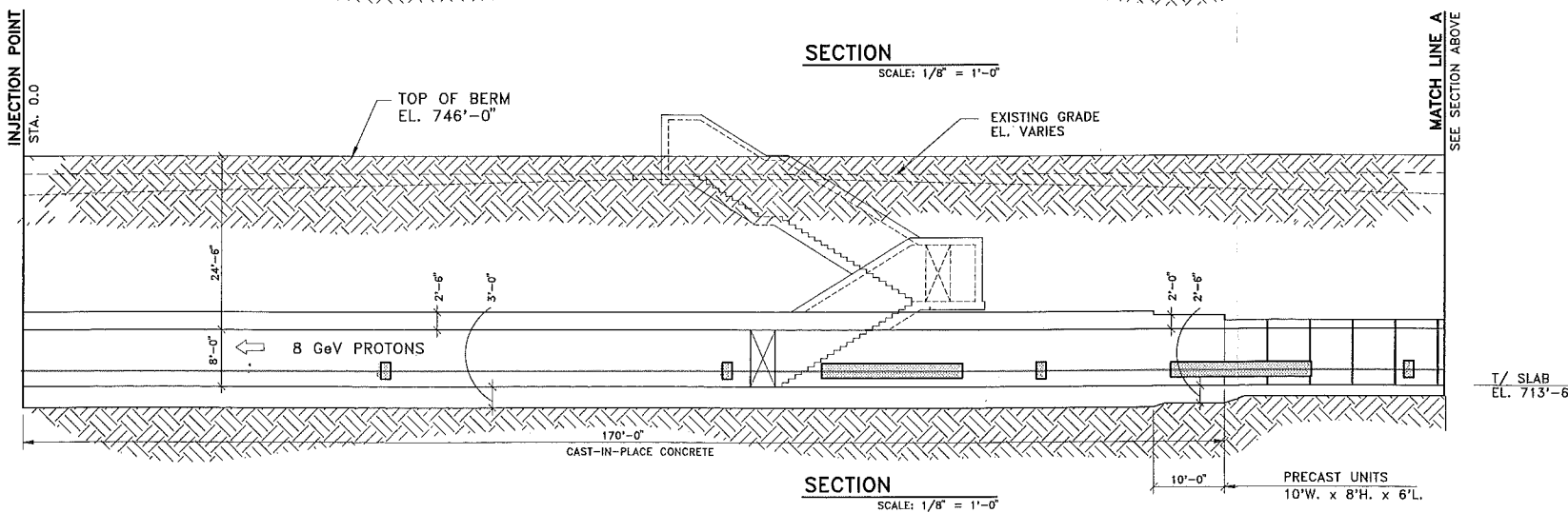
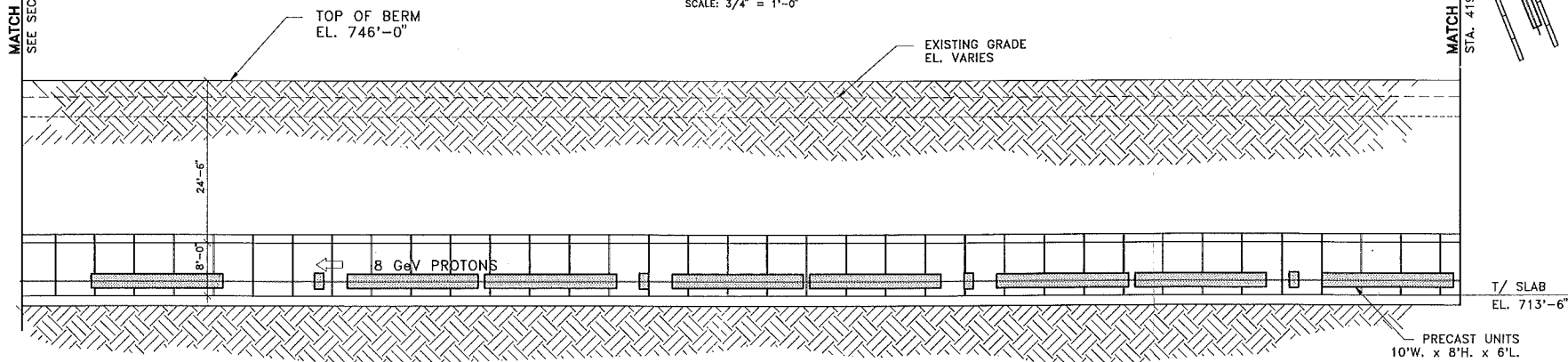
SCALE:
1/16" = 1'-0"
1/8" = 1'-0"
PLAN SCALE
SECTION SCALE

FERMI NATIONAL ACCELERATOR LABORATORY	
UNITED STATES DEPARTMENT OF ENERGY	
FERMILAB MAIN INJECTOR	
8 GeV BEAMLINE SHT. 5	
DRAWING NO.	6-6-2 TITLE-1 AS-13
REV.	

AUG. 1992



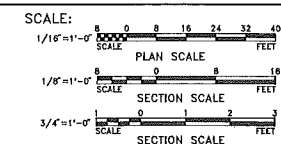
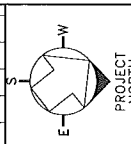
**TYPICAL CROSS SECTION
8 GeV BEAMLINE ENCLOSURE**
SCALE: 3/4" = 1'-0"



REV.	DATE	DESCRIPTION

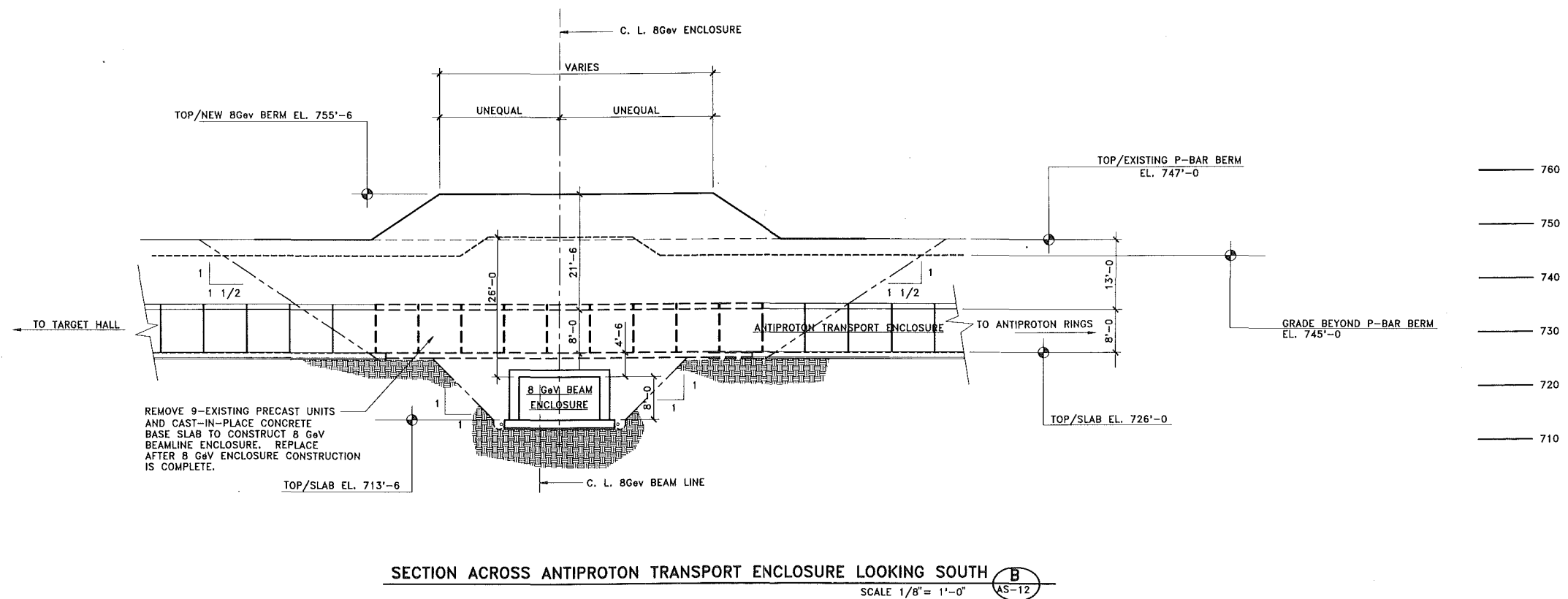
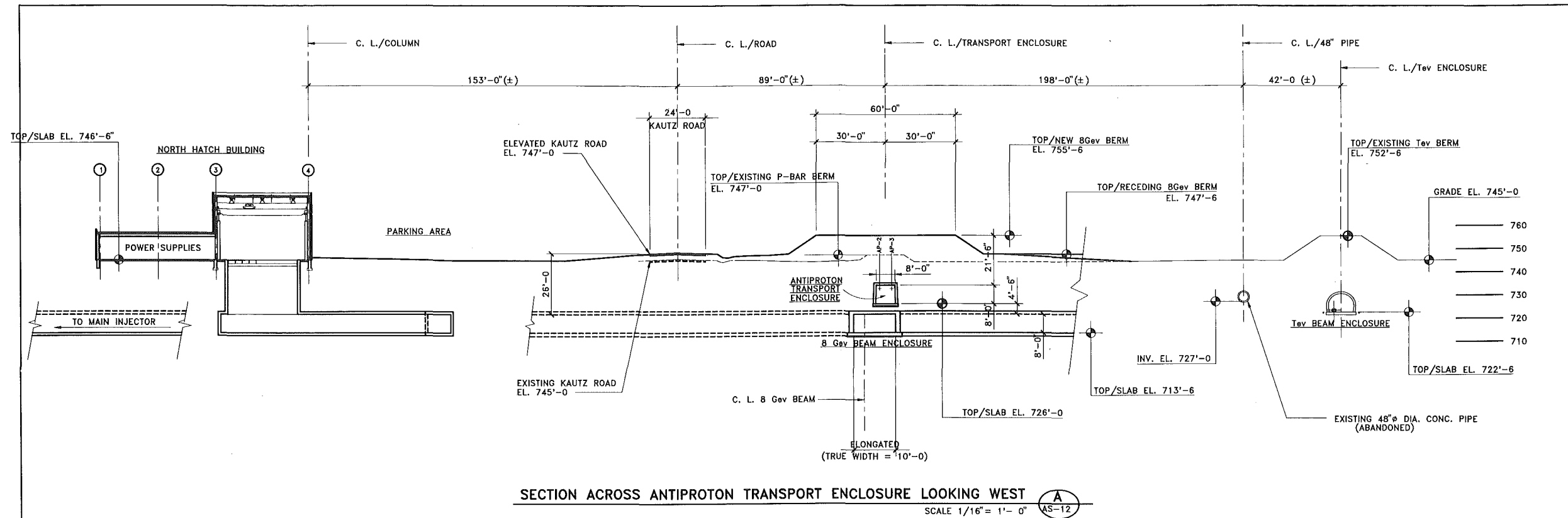
FLUOR DANIEL		
PROJECT NO. - 21842300		
DESIGNED	R. JEDZINIAK	JULY, 1992
DRAWN	R. DELA CRUZ	JULY, 1992
CHECKED	A. VASONIS	JULY, 1992
APPROVED		

DESIGNED	T. LACKOWSKI	DATE	
DRAWN	J. HACKEMER		
CHECKED			
APPROVED			
SUBMITTED			



FERMI NATIONAL ACCELERATOR LABORATORY			
UNITED STATES DEPARTMENT OF ENERGY			
FERMILAB MAIN INJECTOR			
8 GeV BEAMLINE SHT. 6			
DRAWING NO.	6-6-2	TITLE-1	AS-14
REV.			

AUG. 1992

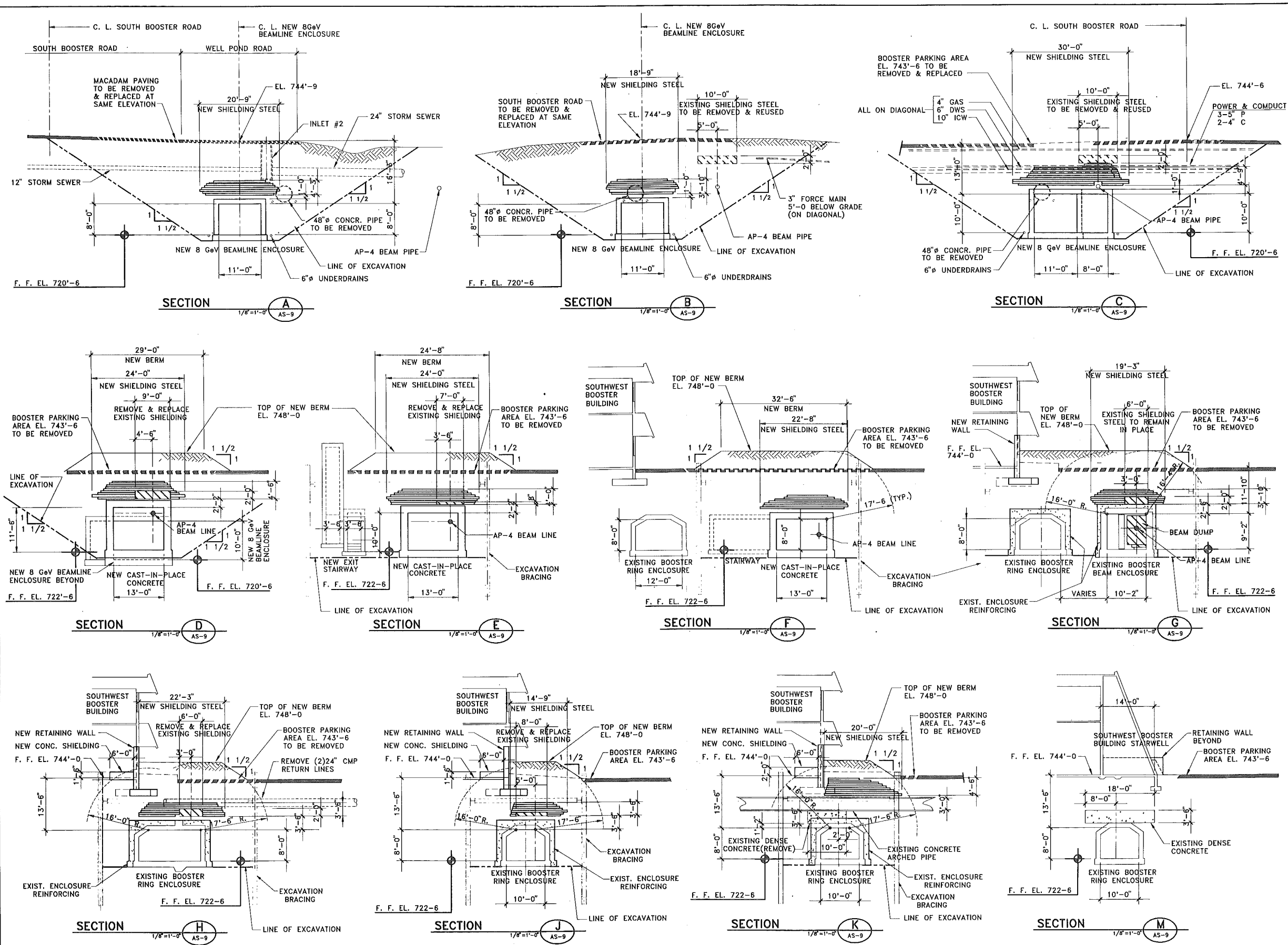


REV. DATE DESCRIPTIONS 1 7/19/92 2 7/19/92 3 7/19/92 4 7/19/92		FLUOR DANIEL PROJECT NO. - 21842300 NAME DATE DESIGNED R. JEDZINIAK JULY, 1992 DRAWN RAY DELA CRUZ JULY, 1992 CHECKED A. VASONIS JULY, 1992 APPROVED		DESIGNED T. LACKOWSKI/J. HACKEMER DRAWN J. HACKEMER CHECKED APPROVED SUBMITTED		SCALE: 1/16" = 1'-0" 1/8" = 1'-0" UPPER SECTION LOWER SECTION		FERMILAB MAIN INJECTOR 8 GeV SECTION SHT. 1 DRAWING NO. 6-6-2 TITLE-1 AS-15 REV.	
--	--	---	--	--	--	---	--	--	--

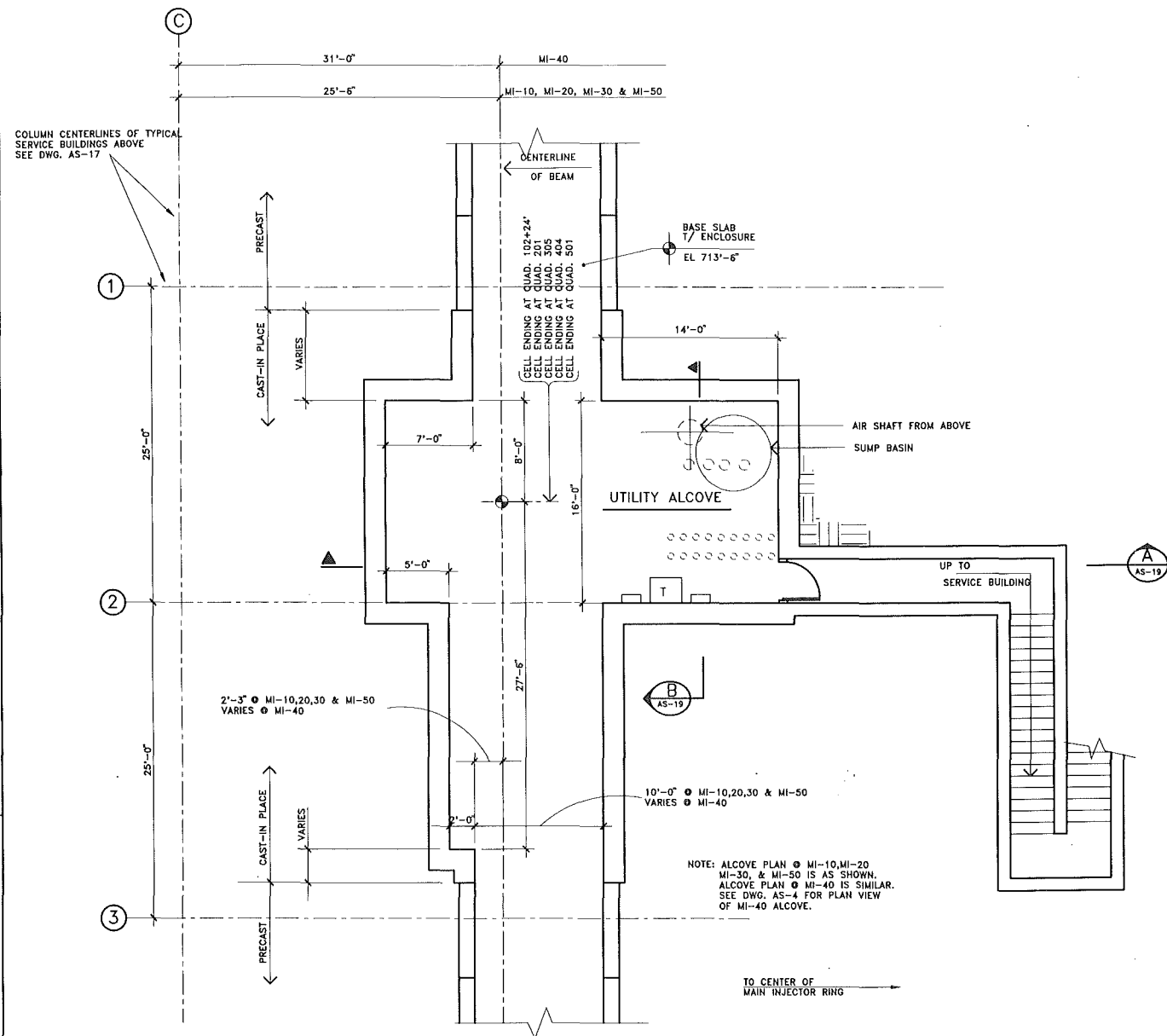
AS-15

PROJECT NORTH

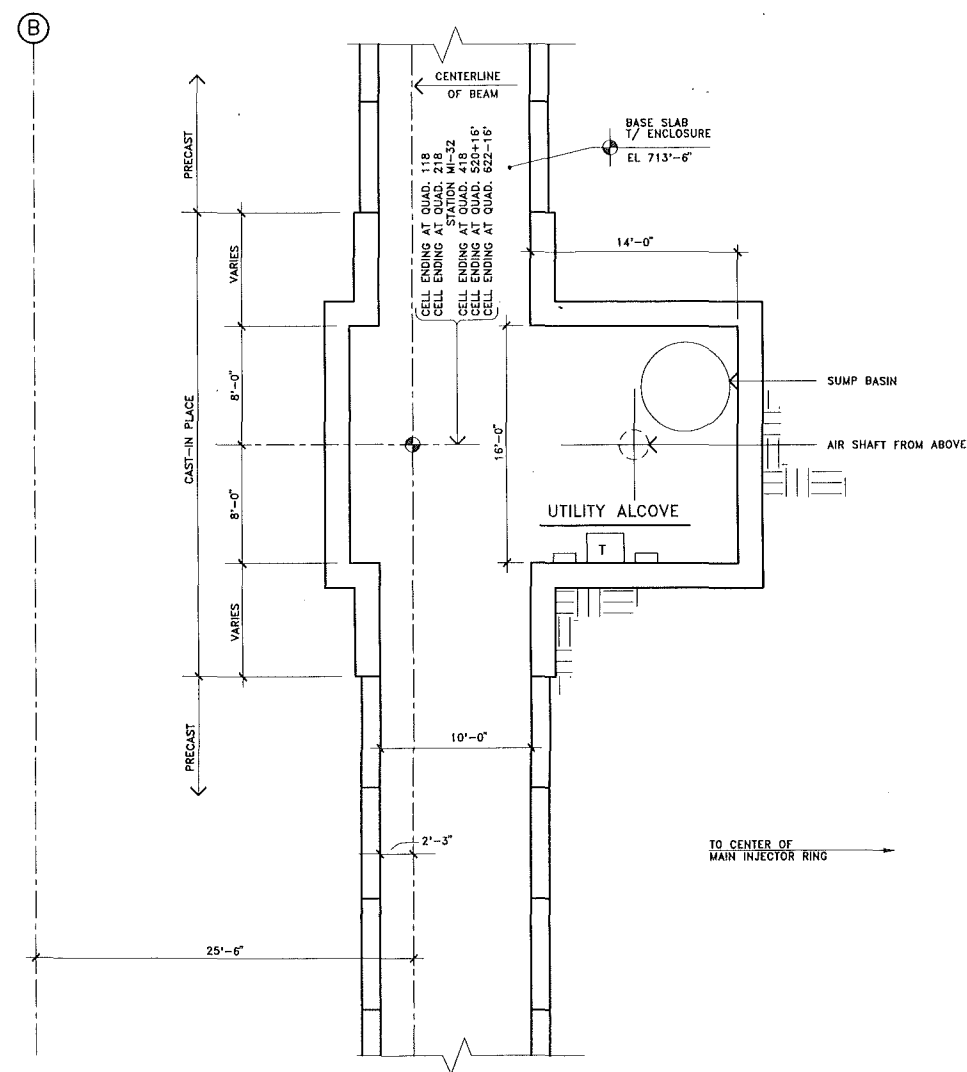
AUG. 1992



FLUOR DANIEL PROJECT NO. - 21842300		DESIGNED: T. LACKOWSKI DRAWN: J. HACKEMER, J. GEHARD CHECKED: A. VASONIS APPROVED:		SCALE: 1/8" = 1'-0" SCALE	FERMILAB MAIN INJECTOR 8 GeV SECTIONS SHIT. 2 DRAWING NO. 6-6-2 TITLE-1 AS-16 REV.
DESIGNED: R. JEDZINIAK DRAWN: R. DELA CRUZ CHECKED: A. VASONIS APPROVED:		NAME: _____ DATE: _____ NAME: _____ DATE: _____ NAME: _____ DATE: _____ NAME: _____ DATE: _____		AUG. 1992	

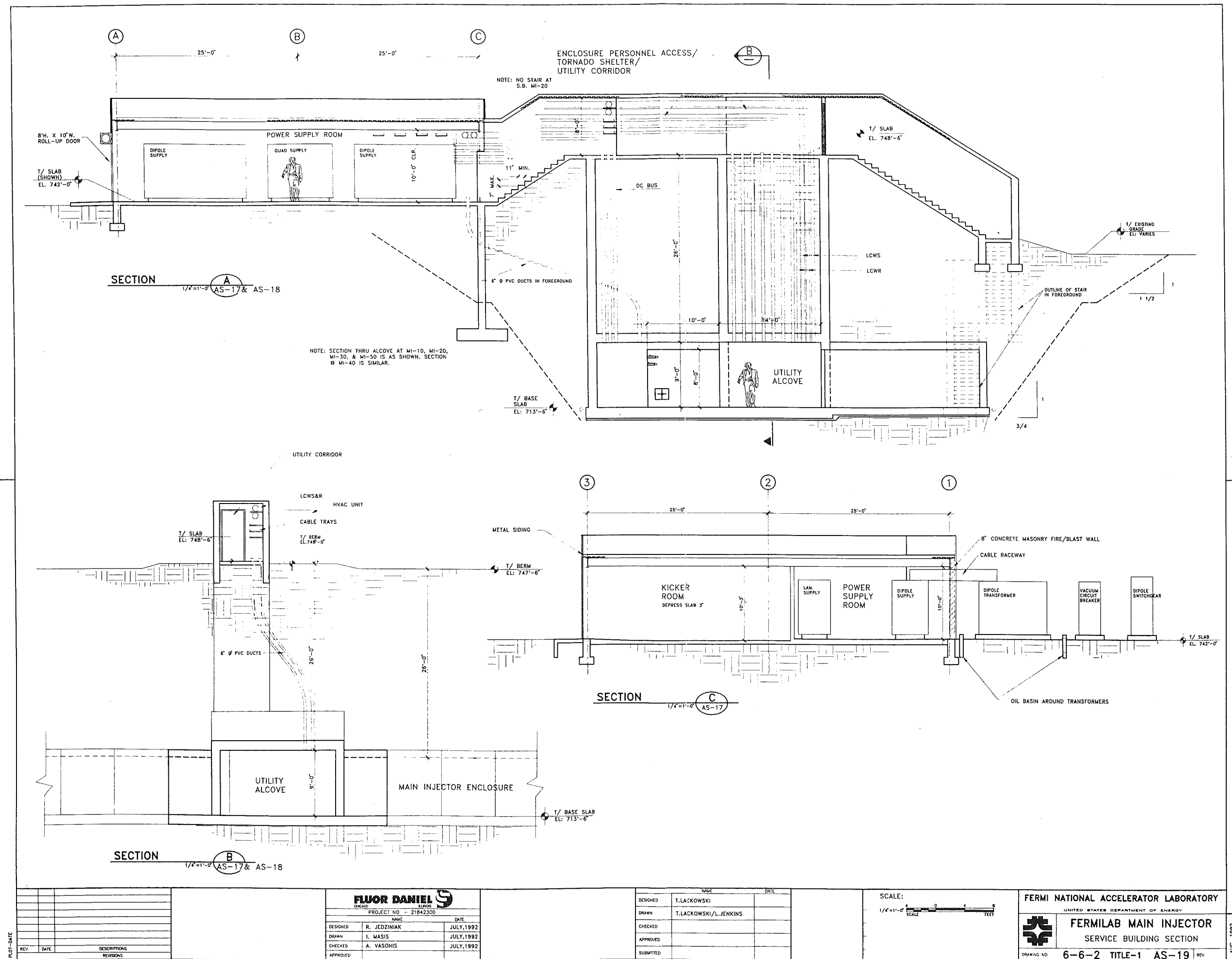


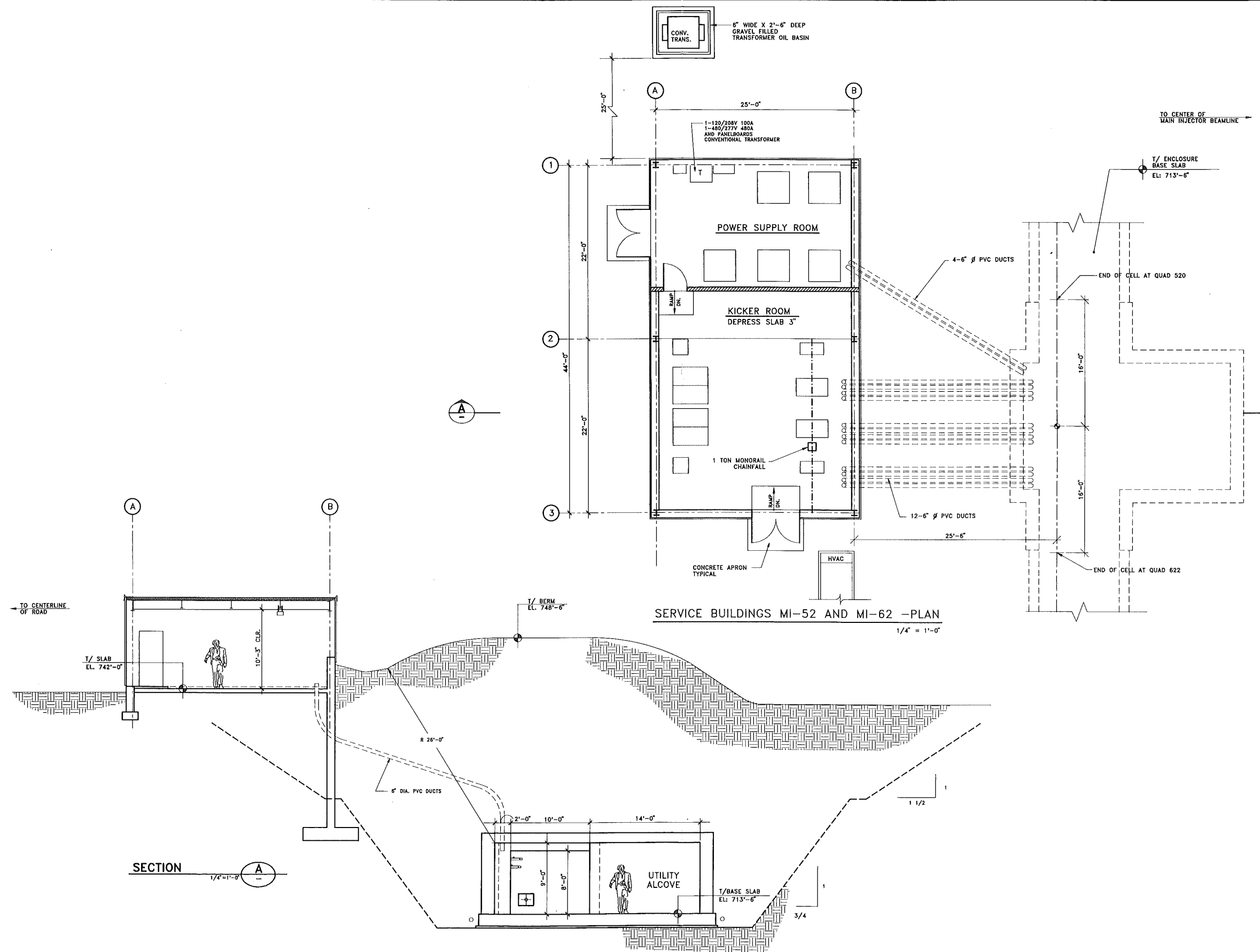
ALCOVE PLAN AT TYPICAL SERVICE BUILDINGS
1/4" = 1'-0"



ALCOVE PLAN AT KICKER BUILDINGS
AND BETWEEN TYPICAL SERVICE BUILDINGS
1/4" = 1'-0"

PLT-DATE REV. DATE DESCRIPTIONS REVISIONS		FLUOR DANIEL CHICAGO ILLINOIS PROJECT NO. 21842300 NAME DATE DESIGNED R. JEDZINIAK JULY, 1992 DRAWN R. DELA CRUZ JULY, 1992 CHECKED A. VASONIS JULY, 1992 APPROVED		DESIGNED TOMSKI DRAWN TOMSKI CHECKED APPROVED SUBMITTED		SCALE: 1/4" = 1'-0" SCALE FEET		FERMILAB MAIN INJECTOR ALCOVE PLANS DRAWING NO. 6-6-2 TITLE-1 AS-18 REV.		AUG. 1992
---	--	--	--	---	--	--------------------------------------	--	--	--	-----------





SERVICE BUILDINGS MI-52 AND MI-62 -PLAN

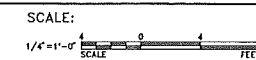
1/4" = 1'-0"

REV.	DATE	DESCRIPTIONS

AS-20

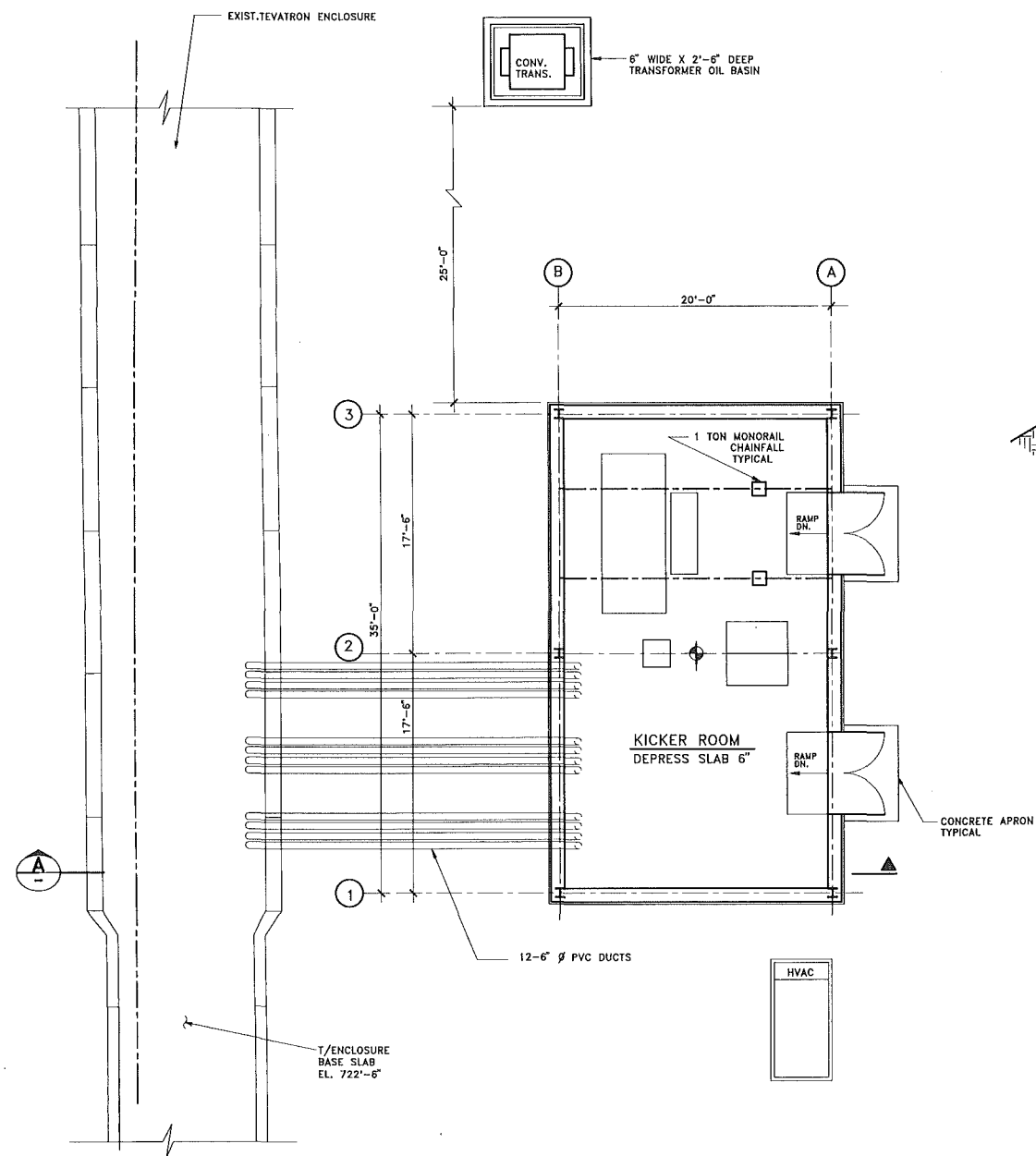
FLUOR DANIEL CHICAGO ILLINOIS PROJECT NO. - Z1842300		
DESIGNED	R. JEDZINIAK	JULY, 1992
DRAWN	A. SKUZA	JULY, 1992
CHECKED	A. VASONIS	JULY, 1992
APPROVED		

NAME	DATE
DESIGNED	TOMSKI
DRAWN	TOMSKI
CHECKED	
APPROVED	
SUBMITTED	

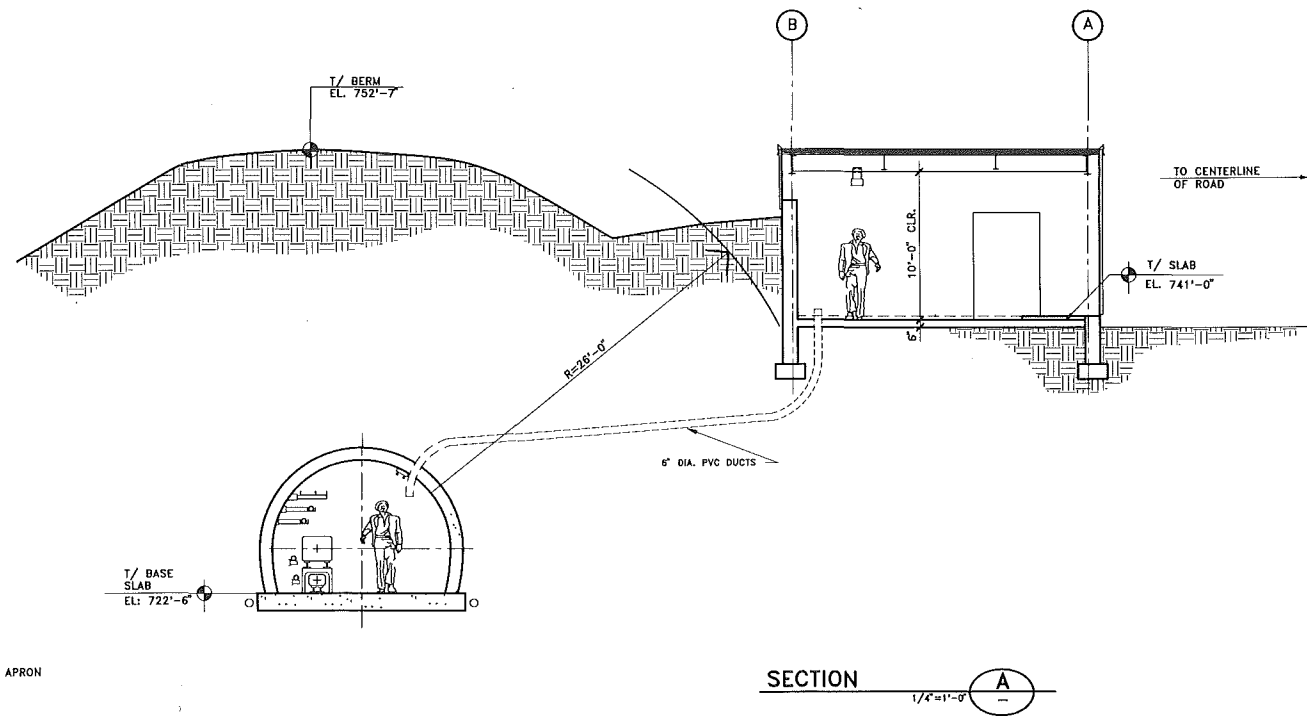


FERMILAB MAIN INJECTOR KICKER SERV. BLDG'S MI-52 & MI-62		
DRAWING NO.	6-6-2	TITLE-1 AS-20
REV.		

AUG. 1992



KICKER SERVICE BUILDING F-17
1/4" = 1'-0"

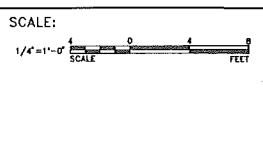
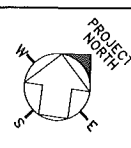


SECTION A-A
1/4" = 1'-0"

REV.	DATE	DESCRIPTIONS

FLUOR DANIEL <small>CHICAGO ILLINOIS</small> PROJECT NO. - 21842300		
DESIGNED	R. JEDZINIAK	JULY, 1992
DRAWN	R. DELA CRUZ	JULY, 1992
CHECKED	A. VASONIS	JULY, 1992
APPROVED		

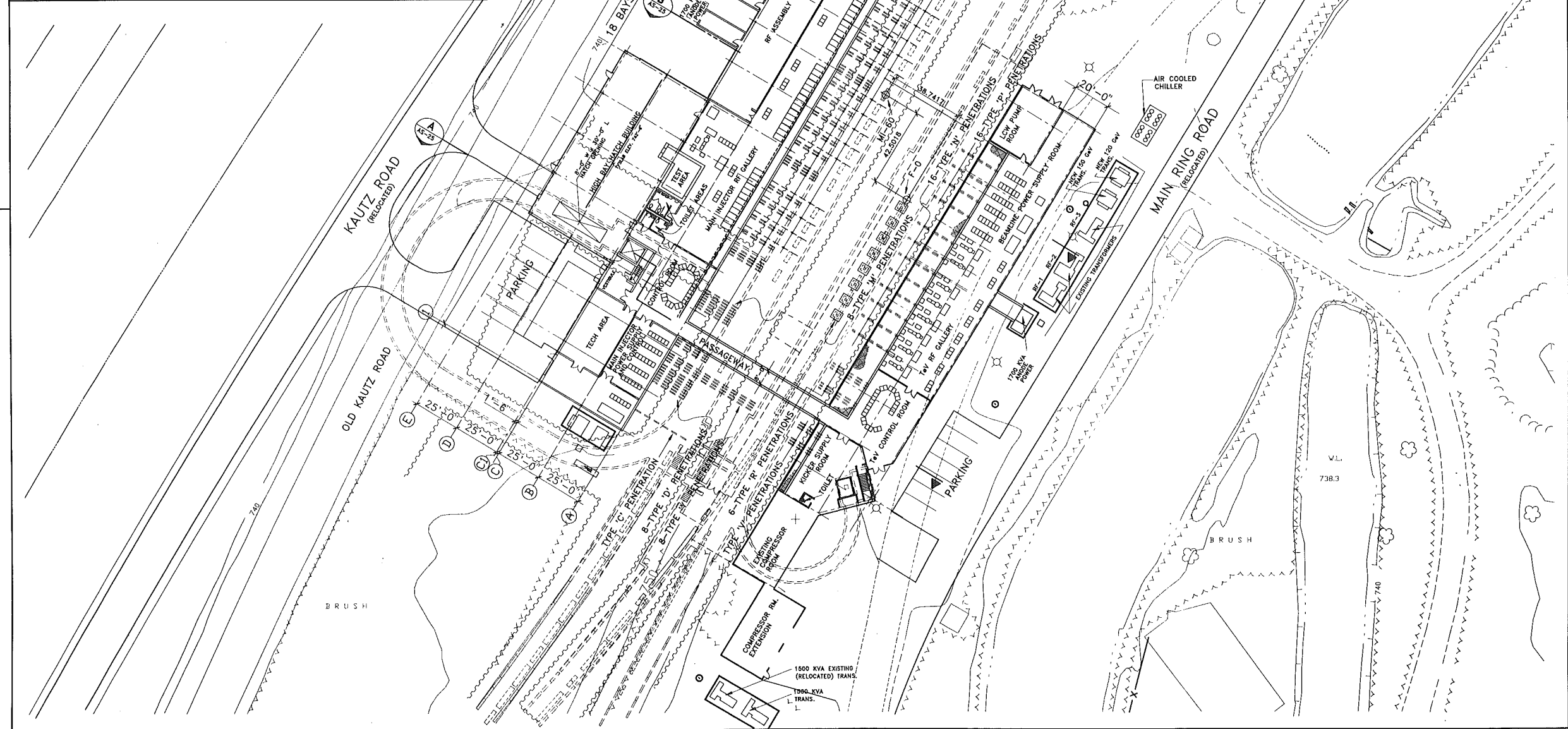
	NAME	DATE
DESIGNED	FLUOR DANIEL	
DRAWN	FLUOR DANIEL	
CHECKED		
APPROVED		
SUBMITTED		



FERMI NATIONAL ACCELERATOR LABORATORY <small>UNITED STATES DEPARTMENT OF ENERGY</small> FERMILAB MAIN INJECTOR KICKER SERVICE BUILDING F-17		
DRAWING NO.	6-6-2 TITLE-1	AS-21
REV.		

AUG. 1992

PENETRATION SCHEDULE						
MARK	FUNCTION	SIZE	MATERIAL	QUANTITY	LOCATION	
MI-60 SERVICE BUILDING TO MI-RF ENCLOSURE	TYPE A	WAVE GUIDE	TS 6X2	STEEL	18	AT DOWNSTREAM END OF EACH CAVITY
	TYPE B	RF POWER AND DIAGNOSTICS	6" Ø	PVC	64	2 PER CAVITY + 4 PER QUAD IN MI-60 STR.
	TYPE C	MI MAGNET BUS	TS 10X6	STEEL	3	1 AT SOUTH END + 2 AT NORTH END
	TYPE D	MI COMM. DUCT	6" Ø	PVC	16	8 EA. AT NORTH AND SOUTH END
	TYPE E	RF CONTROL	6" Ø	PVC	8	AT CONTROL ROOM
	TYPE F	COALESCING CAVITIES	6" Ø	PVC	8	AT COALESCING RACKS
	TYPE G	RF 55" LCW	6" Ø	STAINLESS	2	SEE DRAWING M-2
	TYPE H	RF 95" LCW	6" Ø	STAINLESS	2	SEE DRAWING M-2
	TYPE J	MI LCW	6" Ø	STAINLESS	2	SEE DRAWING M-2
RF SERVICE BUILDING TO T-9V-RF ENCLOSURE	TYPE M	WAVE GUIDE	14" Ø	STEEL	8	1 PER CAVITY
	TYPE N	RF POWER	6" Ø	PVC	16	2 PER CAVITY
	TYPE P	BEAMLINE	6" Ø	PVC	16	NEAR BEAMLINE POWER SUPPLY
	TYPE R	RF CONTROL	6" Ø	PVC	6	AT CONTROL ROOM
	TYPE S	RF LCW	6" Ø	PVC	2	SEE DRAWING M-2
	TYPE T	H ₂ LOW PRESSURE	8" Ø	STAINLESS	2	E-49 AND F-11
	TYPE U	N LOW PRESSURE	3" Ø	STAINLESS	2	E-49 AND F-11
MI-60 SER. BLDG. TO BEAMLINES	TYPE X	CONTROL CABLES	6" Ø	PVC	8	NORTH END OF MI-60 TO A-150 ENCLOSURE
	TYPE Y	CONTROL CABLES	6" Ø	PVC	8	SOUTH END OF MI-60 TO P-150 ENCLOSURE

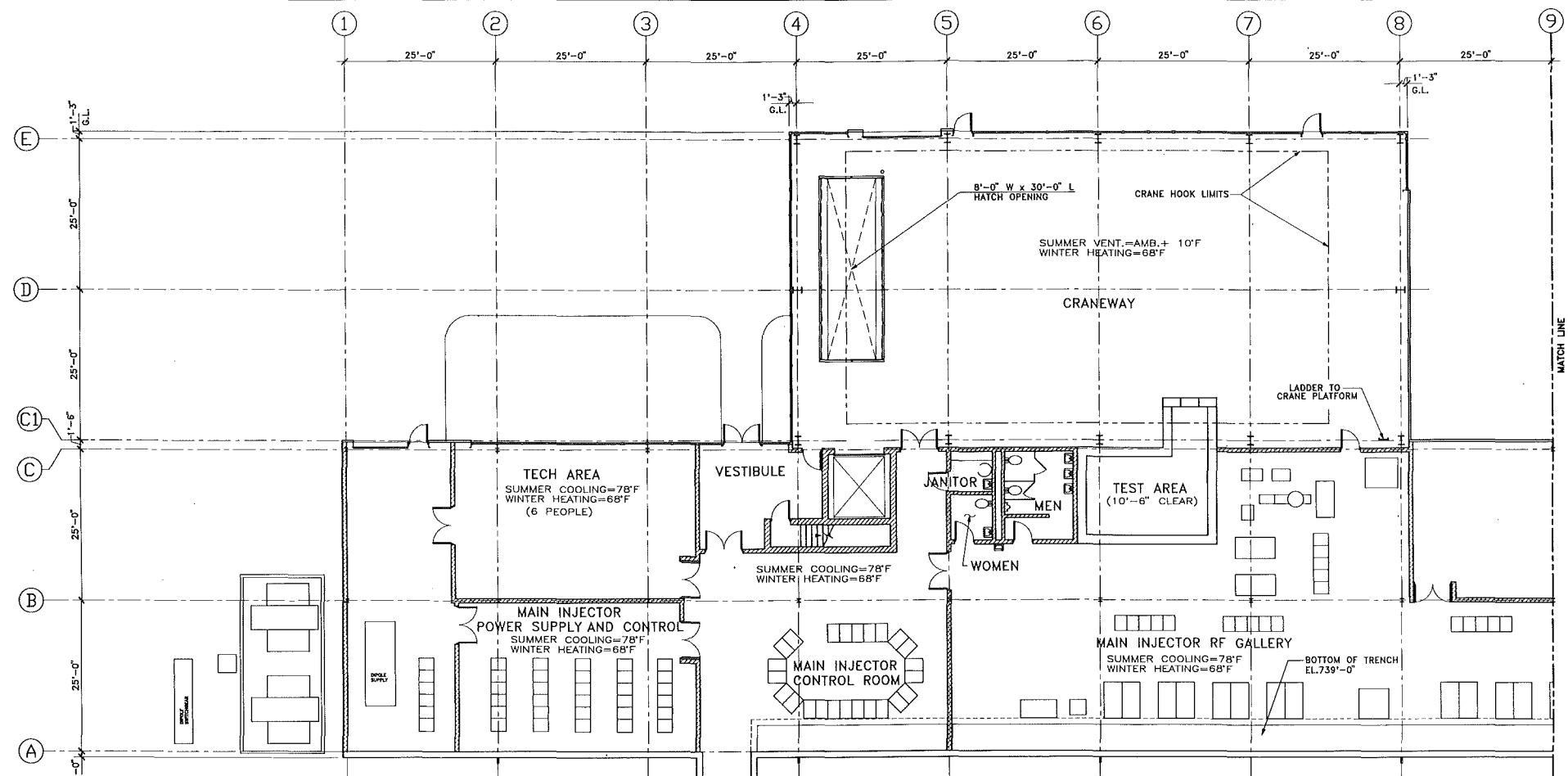


FLUOR DANIEL PROJECT NO. - 21842300		DESIGNED: R. JEDZINIAK DRAWN: REY DELA CRUZ CHECKED: A. VASONIS APPROVED:		DATE: JULY, 1992 DATE: JULY, 1992 DATE: JULY, 1992	
DESIGNED: T. LACKOWSKI DRAWN: T. LACKOWSKI/T. BURKE CHECKED: APPROVED: SUBMITTED:		NAME: T. LACKOWSKI DATE:		SCALE: 1" = 20'-0" SCALE: 0 20 40 FEET	

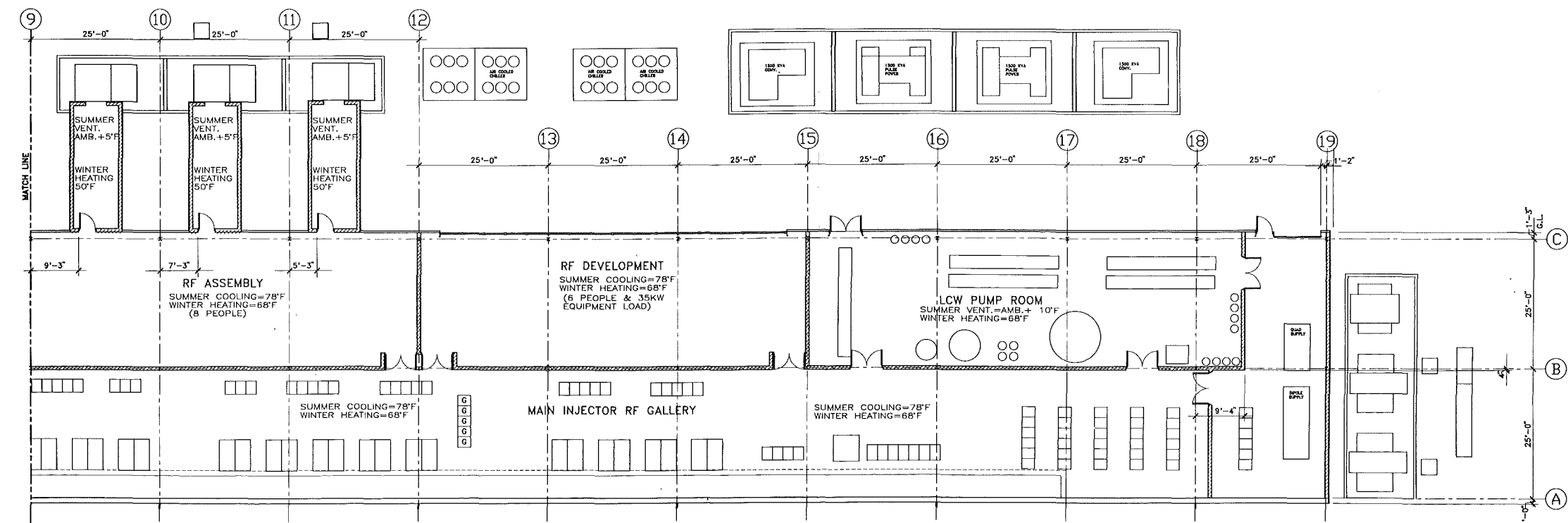
PROJECT NORTH

FERMI NATIONAL ACCELERATOR LABORATORY
 UNITED STATES DEPARTMENT OF ENERGY
FERMILAB MAIN INJECTOR
 F-0 / MI-60 PLAN
 DRAWING NO. 6-6-2 TITLE-1 AS-22 REV.

AUG. 1992



PLAN
1/CONCRETE EL. 742'-5" 1/8"=1'-0"

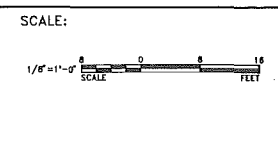
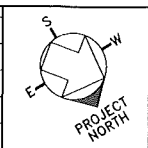


PLAN
1/CONCRETE EL. 742'-5" 1/8"=1'-0"

REV.	DATE	DESCRIPTIONS

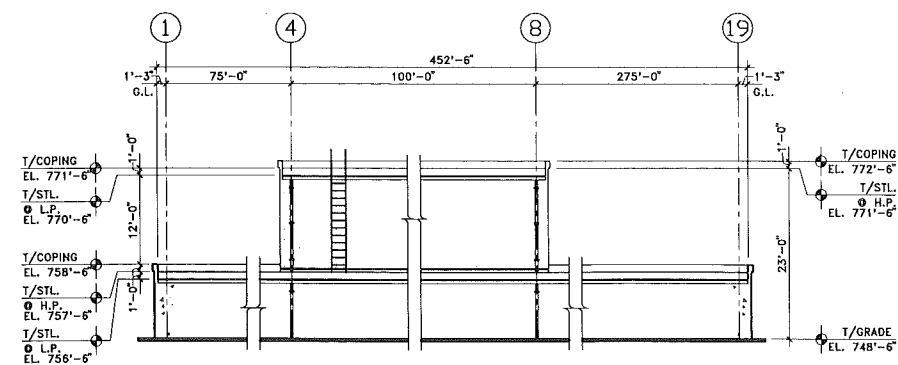
FLUOR DANIEL PROJECT NO. - 21842300 NAME DATE DESIGNED T. LAREN JULY, 1992 DRAWN R. DELA CRUZ JULY, 1992 CHECKED A. VASONIS JULY, 1992 APPROVED		
--	--	--

DESIGNED	FLUOR DANIEL	DATE
DRAWN	FLUOR DANIEL	
CHECKED		
APPROVED		
SUBMITTED		



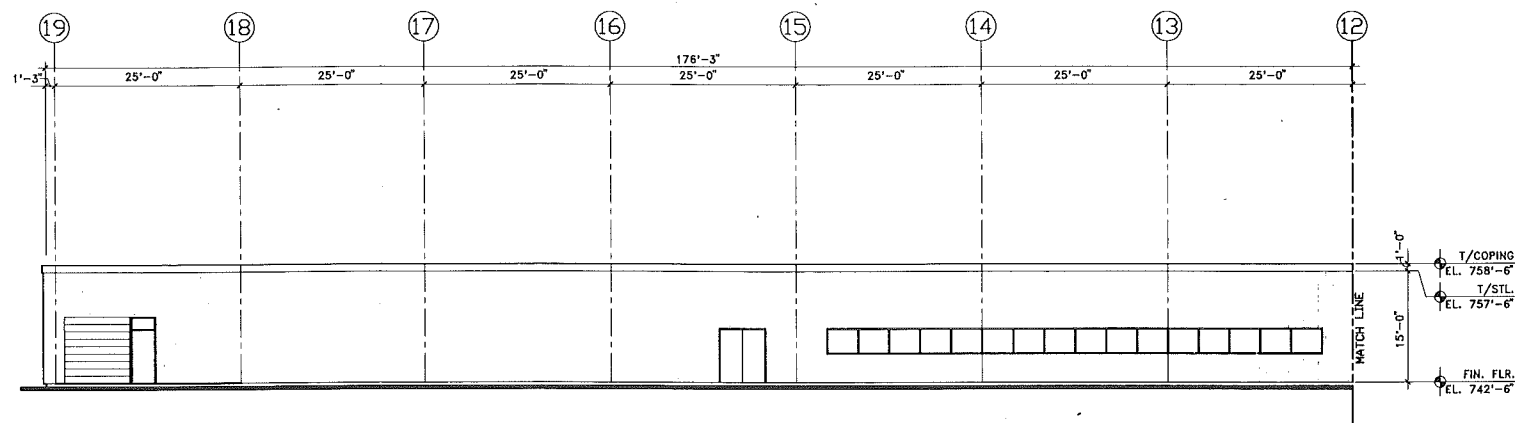
FERMI NATIONAL ACCELERATOR LABORATORY	
UNITED STATES DEPARTMENT OF ENERGY	
FERMILAB MAIN INJECTOR MI-60 FLOOR PLAN	
DRAWING NO. 6-6-2 TITLE-1 AS-23	REV.

AUG. 1992



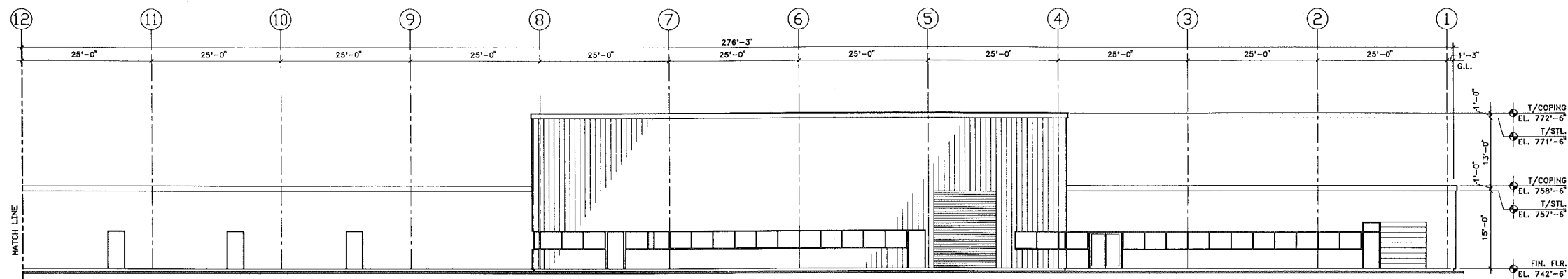
NORTHEAST WALL ELEVATION

1/8"=1'-0"



SOUTHWEST WALL ELEVATION

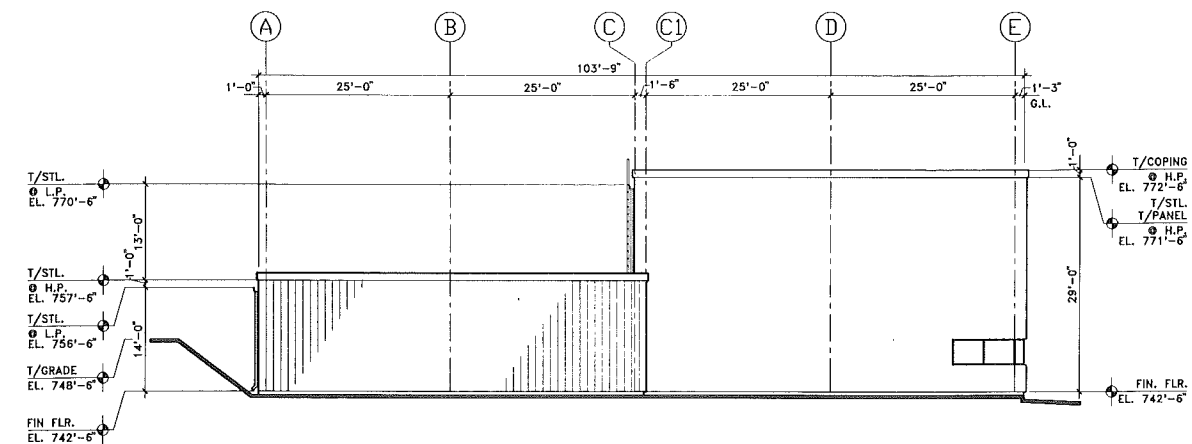
1/8"=1'-0"



NOTE:
ANODE SHELTERS NOT
SHOWN FOR CLARITY

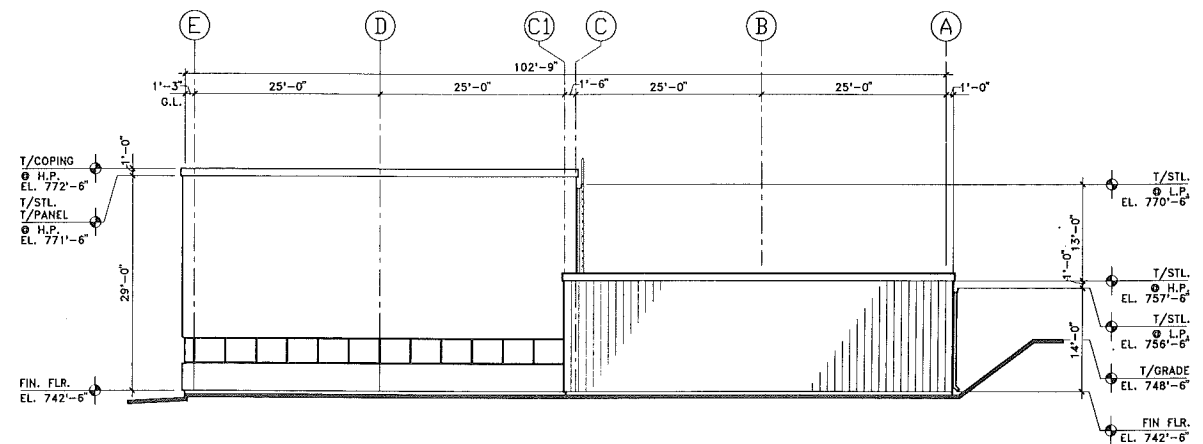
SOUTHWEST WALL ELEVATION

1/8"=1'-0"



NORTHWEST WALL ELEVATION

1/8"=1'-0"



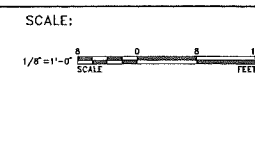
SOUTHEAST WALL ELEVATION

1/8"=1'-0"

REV.	DATE	DESCRIPTIONS

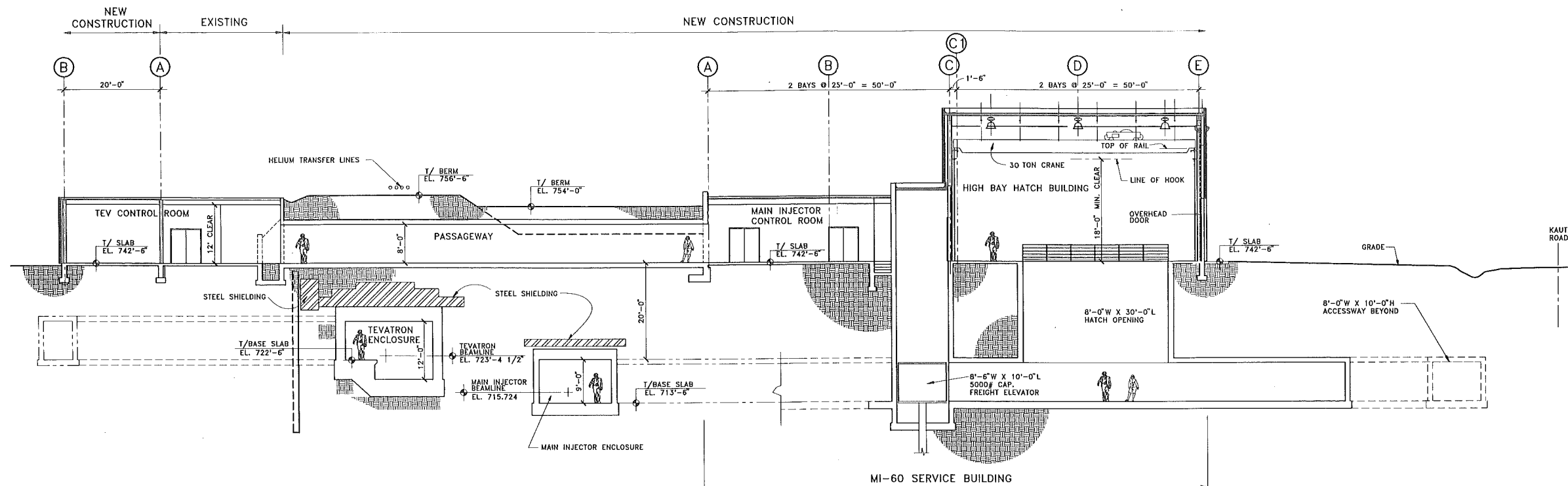
FLUOR DANIEL CHICAGO ILLINOIS PROJECT NO. - 21842300		
DESIGNED	T.LAREN/J.REDEKER	JULY, 1992
DRAWN	J.REDEKER	JULY, 1992
CHECKED	T.LAREN	JULY, 1992
APPROVED		

NAME	DATE
DESIGNED	FLUOR DANIEL INC.
DRAWN	FLUOR DANIEL INC.
CHECKED	FLUOR DANIEL INC.
APPROVED	
SUBMITTED	



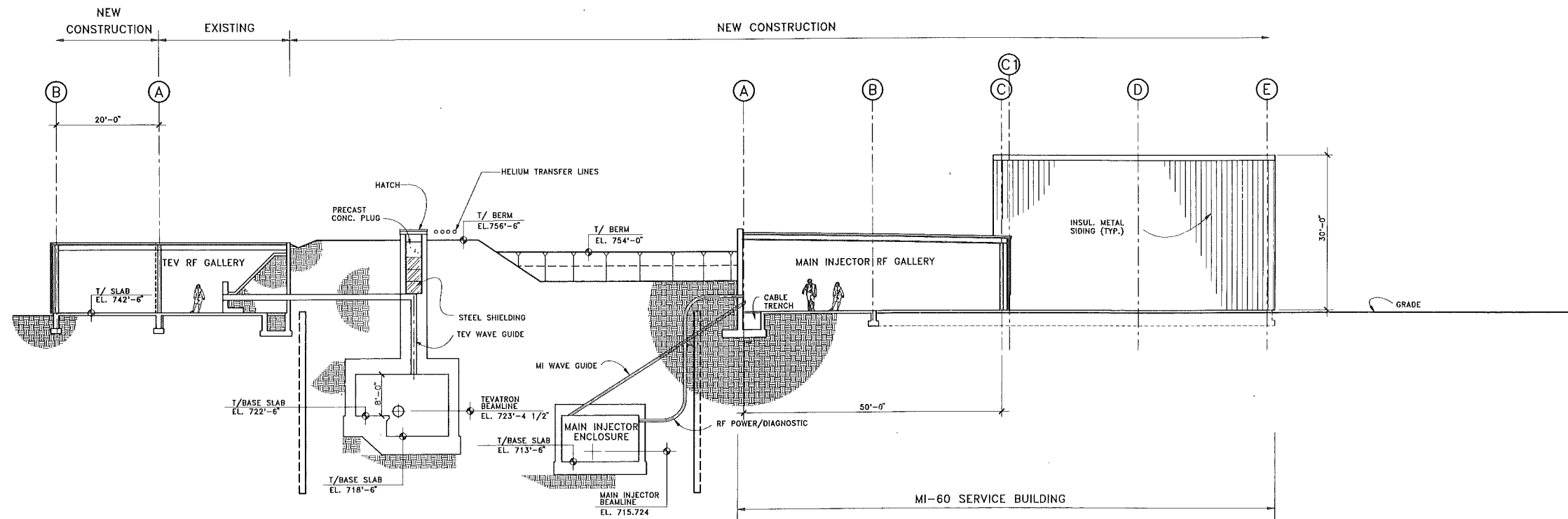
FERMI NATIONAL ACCELERATOR LABORATORY UNITED STATES DEPARTMENT OF ENERGY FERMILAB MAIN INJECTOR MI-60 BUILDING ELEVATIONS		
DRAWING NO.	6-6-2 TITLE-1 AS-24	REV.

AUG. 1992



SECTION

SCALE 1/8" = 1'-0" A AS-22



SECTION

SCALE 1/8" = 1'-0" B AS-22

REV.	DATE	DESCRIPTIONS	REVISIONS

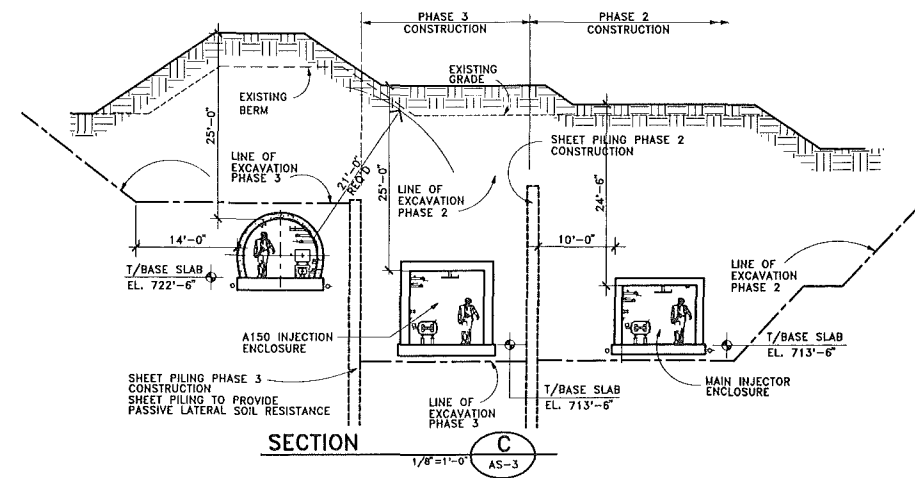
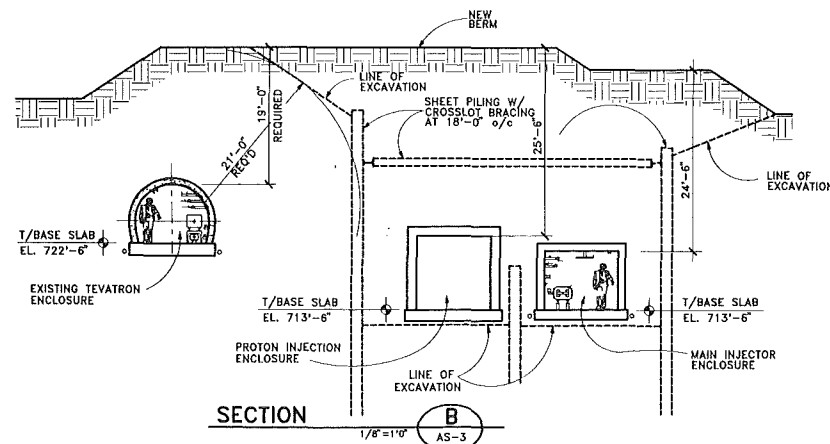
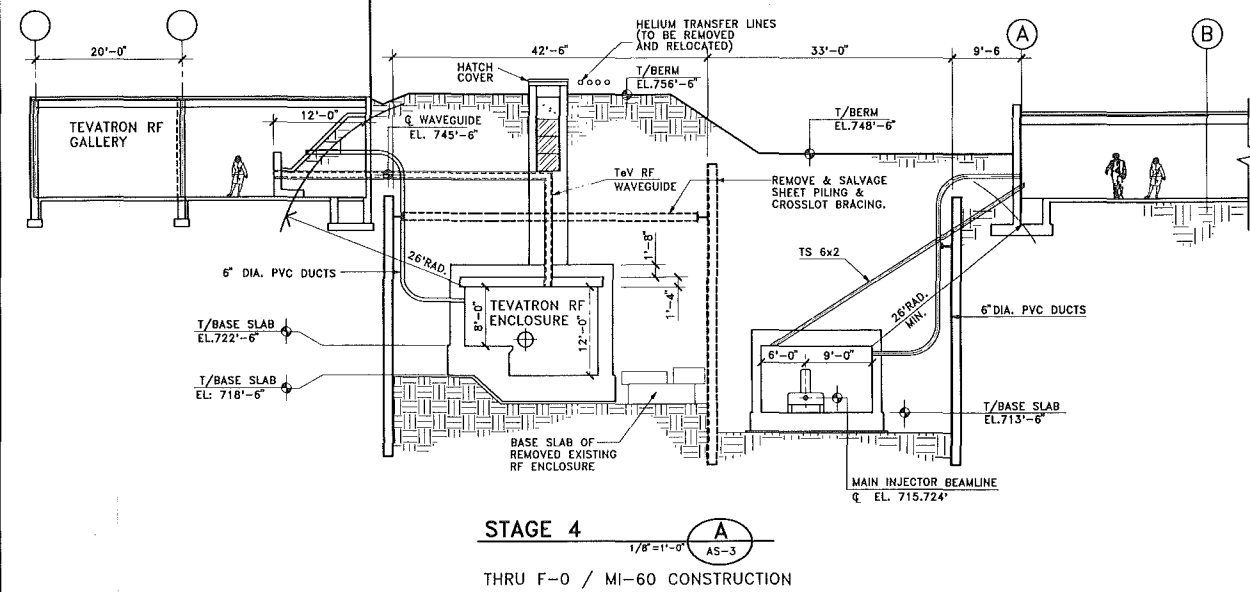
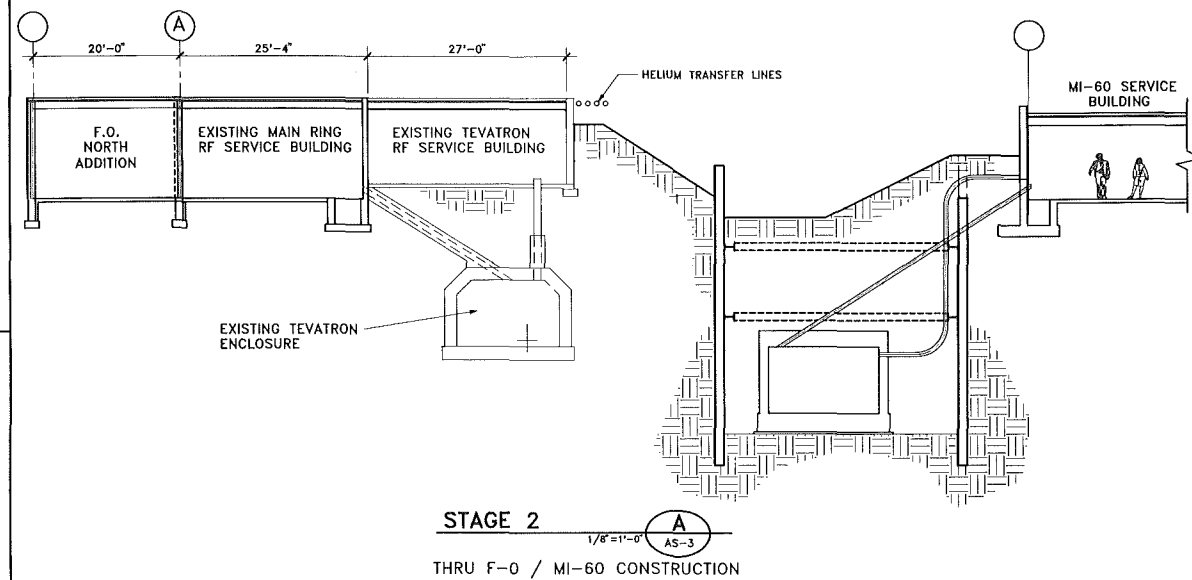
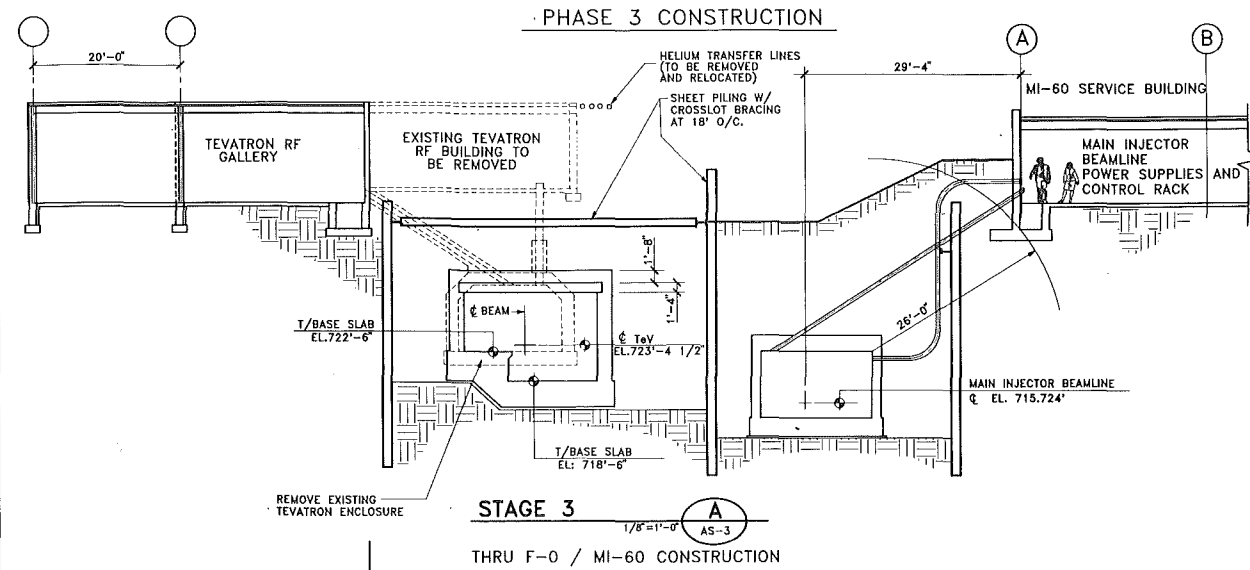
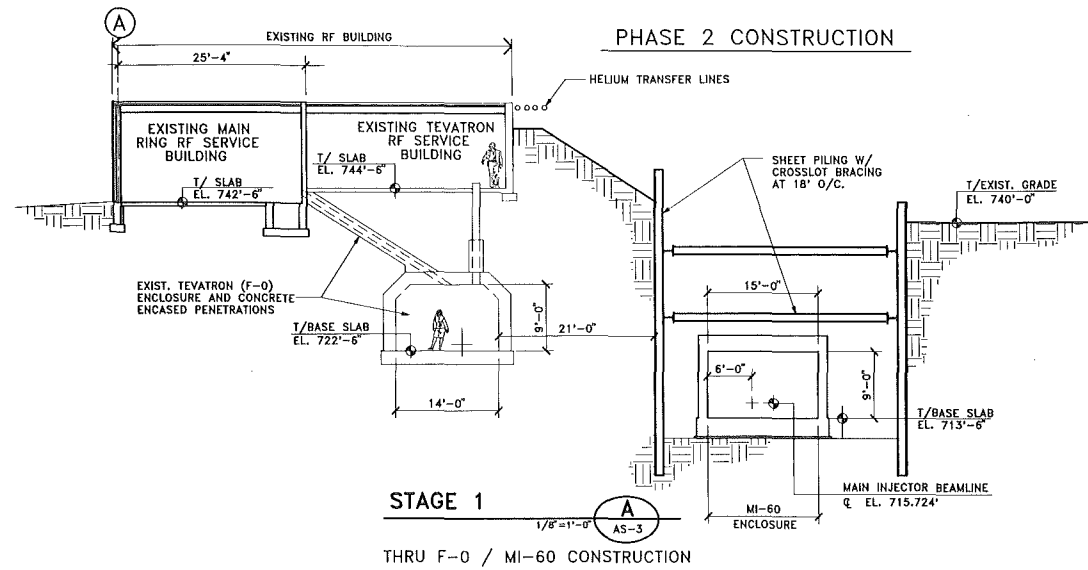
FLUOR DANIEL	
PROJECT NO. - 21842300	
DESIGNED	R. JEDZINIAK
DRAWN	A. SKUZA
CHECKED	A. VASONIS
APPROVED	

DESIGNED	T. LACKOWSKI
DRAWN	J. BANKS/L. JENKINS
CHECKED	
APPROVED	
SUBMITTED	

SCALE:
1/8" = 1'-0"

FERMI NATIONAL ACCELERATOR LABORATORY	
UNITED STATES DEPARTMENT OF ENERGY	
FERMILAB MAIN INJECTOR	
MI-60 BUILDING SECTIONS	
DRAWING NO.	6-6-2 TITLE-1 AS-25
REV.	

AUG. 1992



REV.	DATE	DESCRIPTIONS	REVISIONS

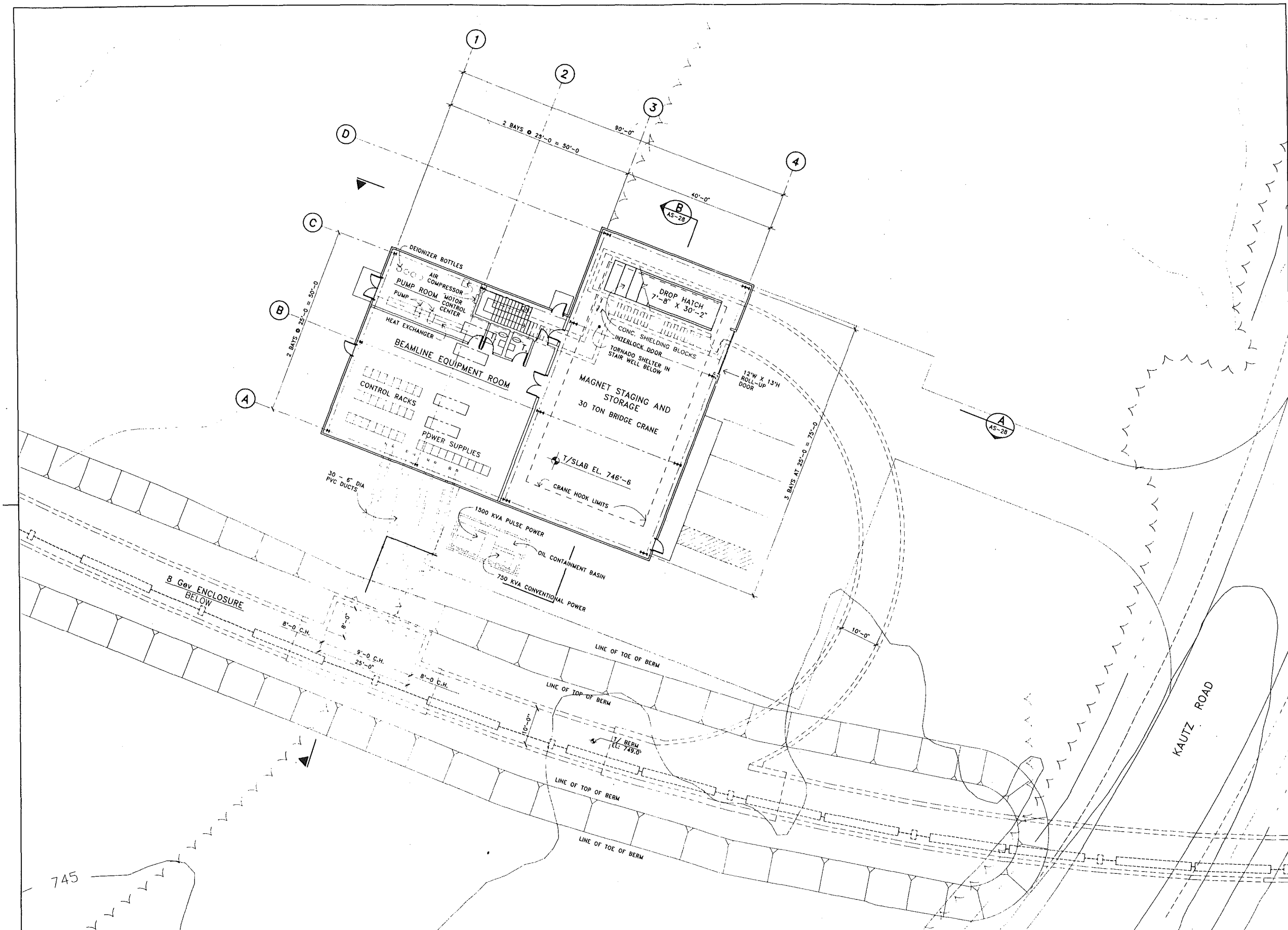
FLUOR DANIEL		
PROJECT NO. - 21842300		
DESIGNED	R. JEDZINIAK	JULY, 1992
DRAWN	A. SKUZA	JULY, 1992
CHECKED	A. VASONIS	JULY, 1992
APPROVED		

DESIGNED	NAME	DATE
TOMSKI		
DRAWN	NAME	DATE
TOMSKI		
CHECKED	NAME	DATE
APPROVED	NAME	DATE
SUBMITTED	NAME	DATE

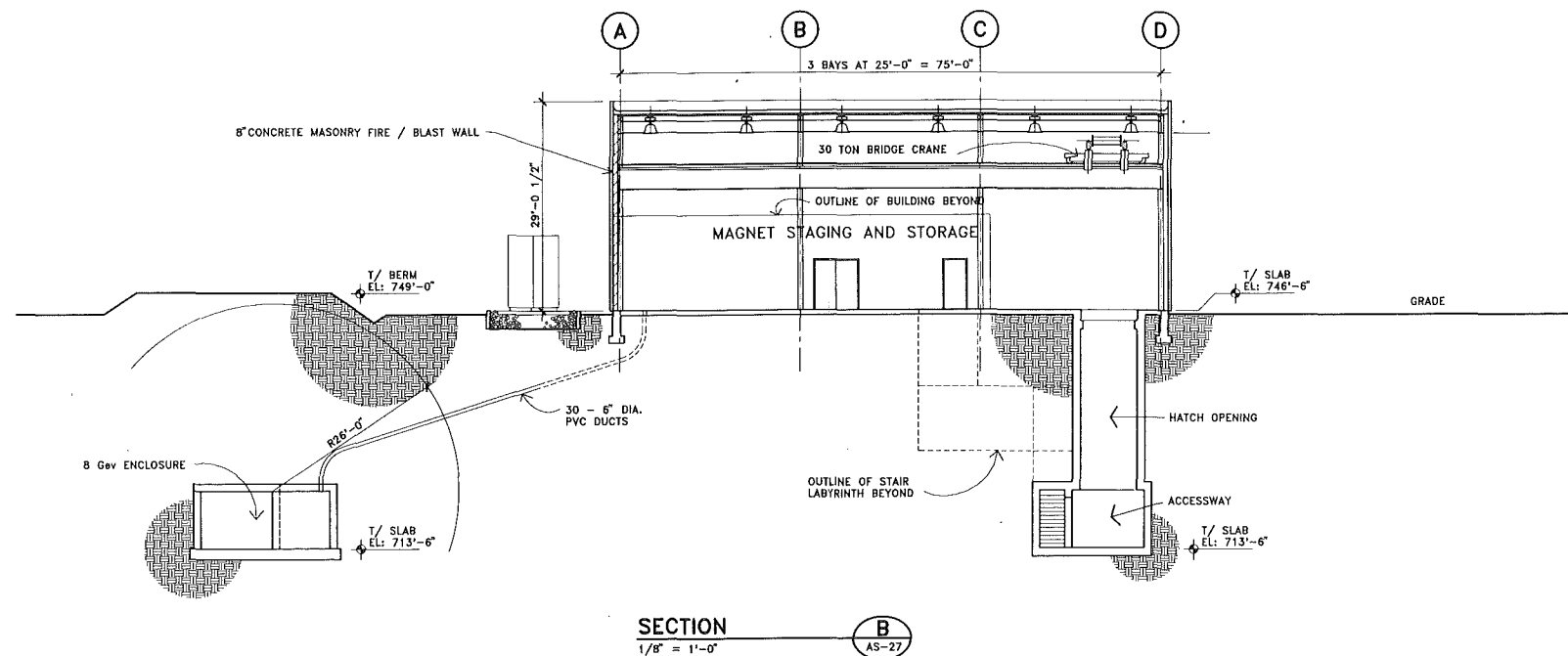
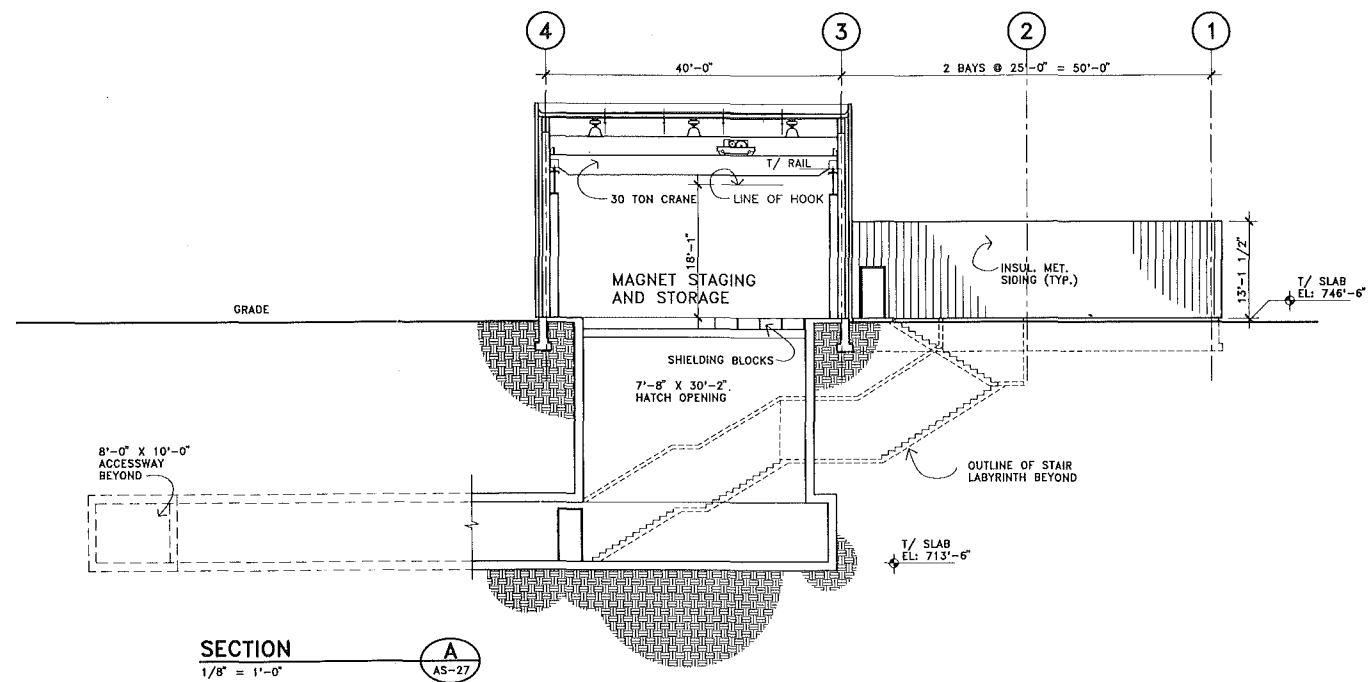
SCALE:
1/8"=1'-0"
SCALE
0 5 10
FEET

FERMI NATIONAL ACCELERATOR LABORATORY	
UNITED STATES DEPARTMENT OF ENERGY	
FERMILAB MAIN INJECTOR	
MI-60 CONSTRUCTION SECTIONS	
DRAWING NO.	6-6-2 TITLE-1 AS-26
REV.	

AUG. 1992



FLUOR DANIEL CHICAGO ILLINOIS PROJECT NO. - 21842300		DESIGNED: TOWSKI DRAWN: T. SURKE, J.W.B. CHECKED: APPROVED: SUBMITTED:		SCALE: 1/8" = 1'-0" SCALE	FERMILAB NATIONAL ACCELERATOR LABORATORY UNITED STATES DEPARTMENT OF ENERGY FERMILAB MAIN INJECTOR NORTH HATCH BUILDING PLAN DRAWING NO. 6-6-2 TITLE-1 AS-27 REV.
DESIGNED: R. JEDZINIAK DRAWN: A. SKUZA CHECKED: A. VASONIS APPROVED:	DATE: JULY, 1992 DATE: JULY, 1992 DATE: JULY, 1992	PROJECT NORTH		AUG. 1992	

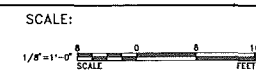


REV.	DATE	DESCRIPTIONS

AS-28

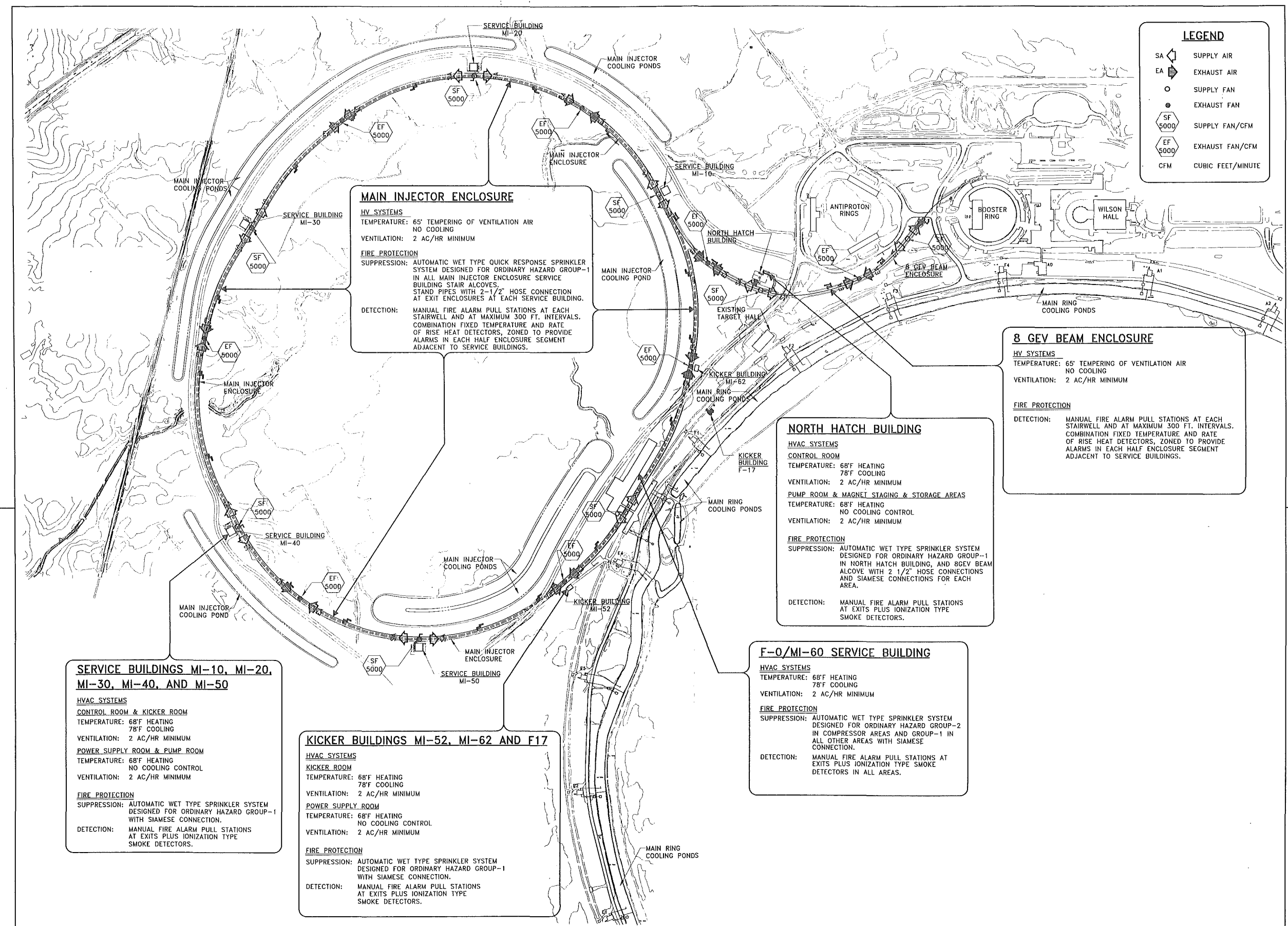
FLUOR DANIEL <small>CHICAGO ILLINOIS</small> PROJECT NO. - 21842300		
DESIGNED	R. JEDZINIAK	JULY, 1992
DRAWN	I. MASIS	JULY, 1992
CHECKED	A. VASONIS	JULY, 1992
APPROVED		

DESIGNED	TOMSKI	
DRAWN	T. BURKE, J.W.B.	
CHECKED		
APPROVED		
SUBMITTED		

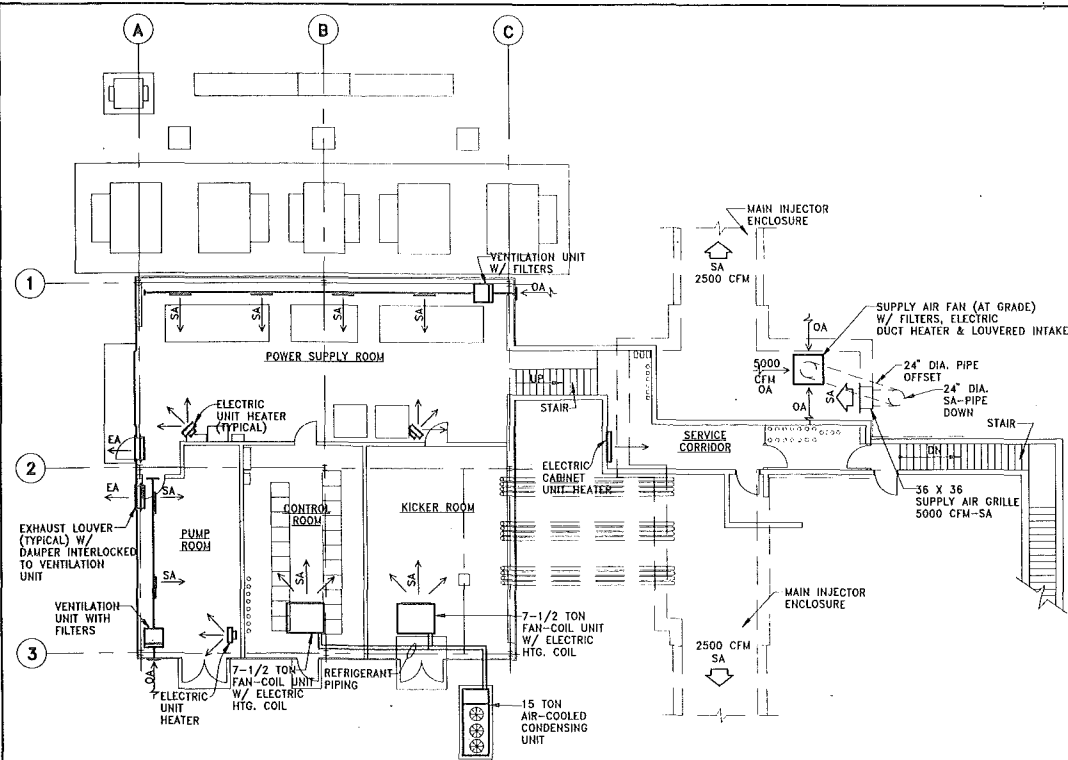


FERMILAB NATIONAL ACCELERATOR LABORATORY <small>UNITED STATES DEPARTMENT OF ENERGY</small> FERMILAB MAIN INJECTOR NORTH HATCH BUILDING SECTIONS		
DRAWING NO.	6-6-2 TITLE-1 AS-28	REV.

AUG. 1992

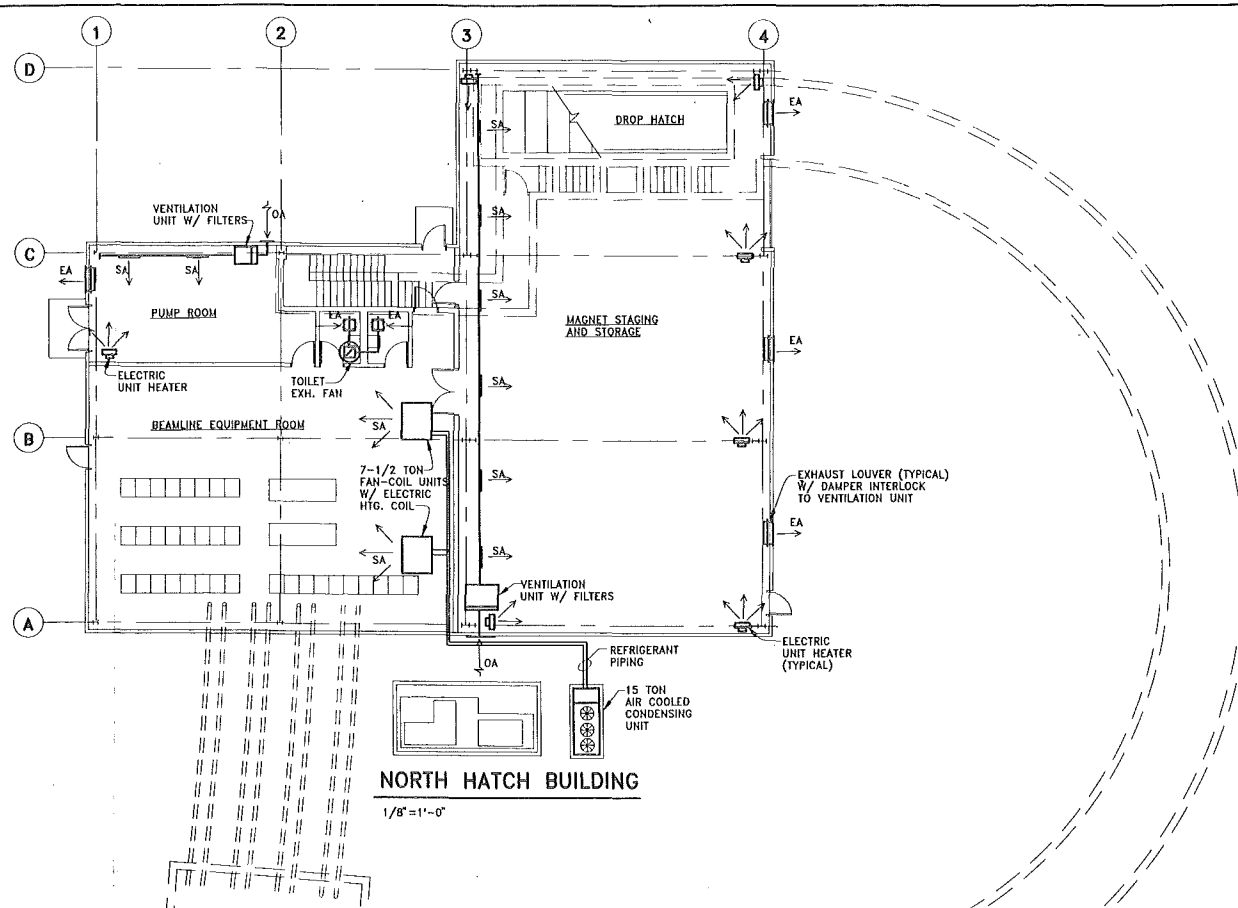


PLOT-DATE				DESIGNED: S. KRSTULOVICH/M. OLSON DRAWN: E. HUEDEM CHECKED: APPROVED: SUBMITTED:		NAME: _____ DATE: _____ SCALE: 1" = 200'-0" SCALE 		FERMILAB MAIN INJECTOR HVAC & FIRE PROTECTION CRITERIA DRAWING NO. 6-6-2 TITLE-1 M-1 REV.	
PROJECT NO. - 21842300 NAME: _____ DATE: _____ DESIGNED: B.A.H. JULY, 1992 CHECKED: G.O./R.K. JULY, 1992 APPROVED:		M-1		AUG. 1992					



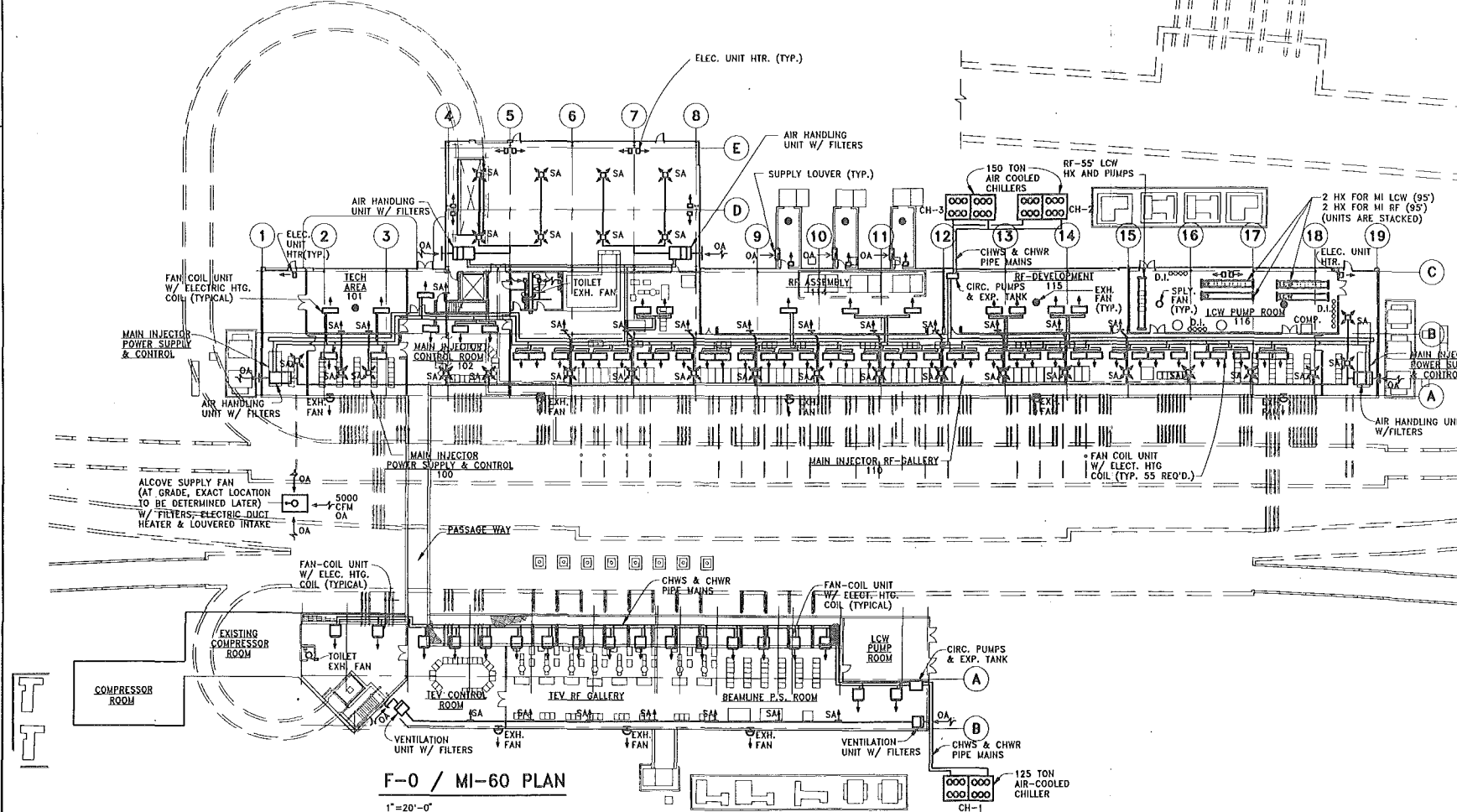
SERVICE BUILDINGS MI-10, MI-20, MI-30, MI-40 AND MI-50 PLAN

1/8"=1'-0" NOTE: SERVICE BUILDINGS MI-10, MI-20, MI-30 AND MI-50 PLANS AS SHOWN. MI-40 SIMILAR NOT SHOWN.



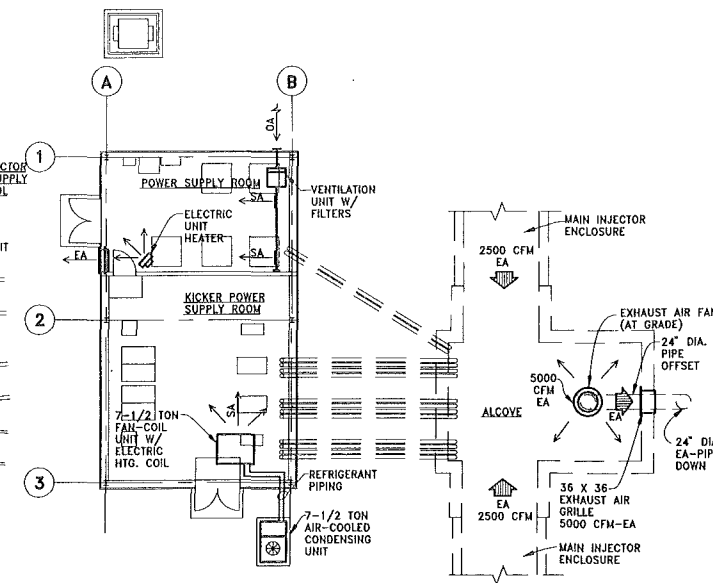
NORTH HATCH BUILDING

1/8"=1'-0"



F-0 / MI-60 PLAN

1"=20'-0"



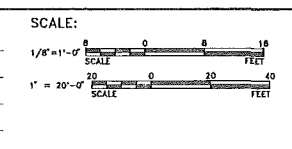
SERVICE BUILDINGS MI-52, MI-62 AND F-17 PLAN

1/8"=1'-0"

REV.	DATE	DESCRIPTION	REVISIONS

FLUOR DANIEL	
PROJECT NO. - 21842300	DATE
DESIGNED	NAME
DRAWN	B.A.H.
CHECKED	G.O./R.K.
APPROVED	JULY, 1992

DESIGNED	S. KRSTULOVICH/M. OLSON	DATE
DRAWN	E. HUEDEM	
CHECKED		
APPROVED		
SUBMITTED		



FERMI NATIONAL ACCELERATOR LABORATORY

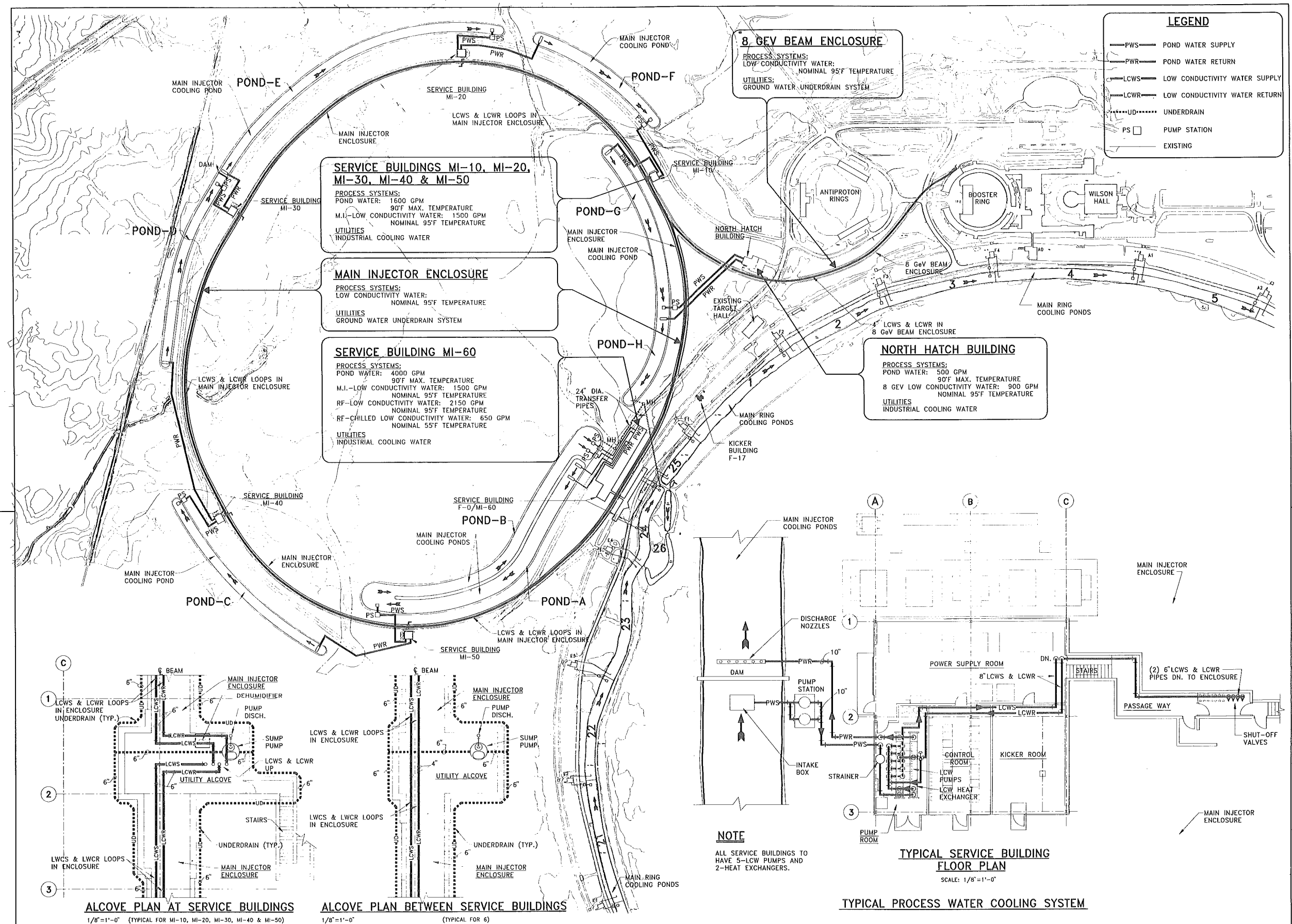
UNITED STATES DEPARTMENT OF ENERGY

FERMILAB MAIN INJECTOR

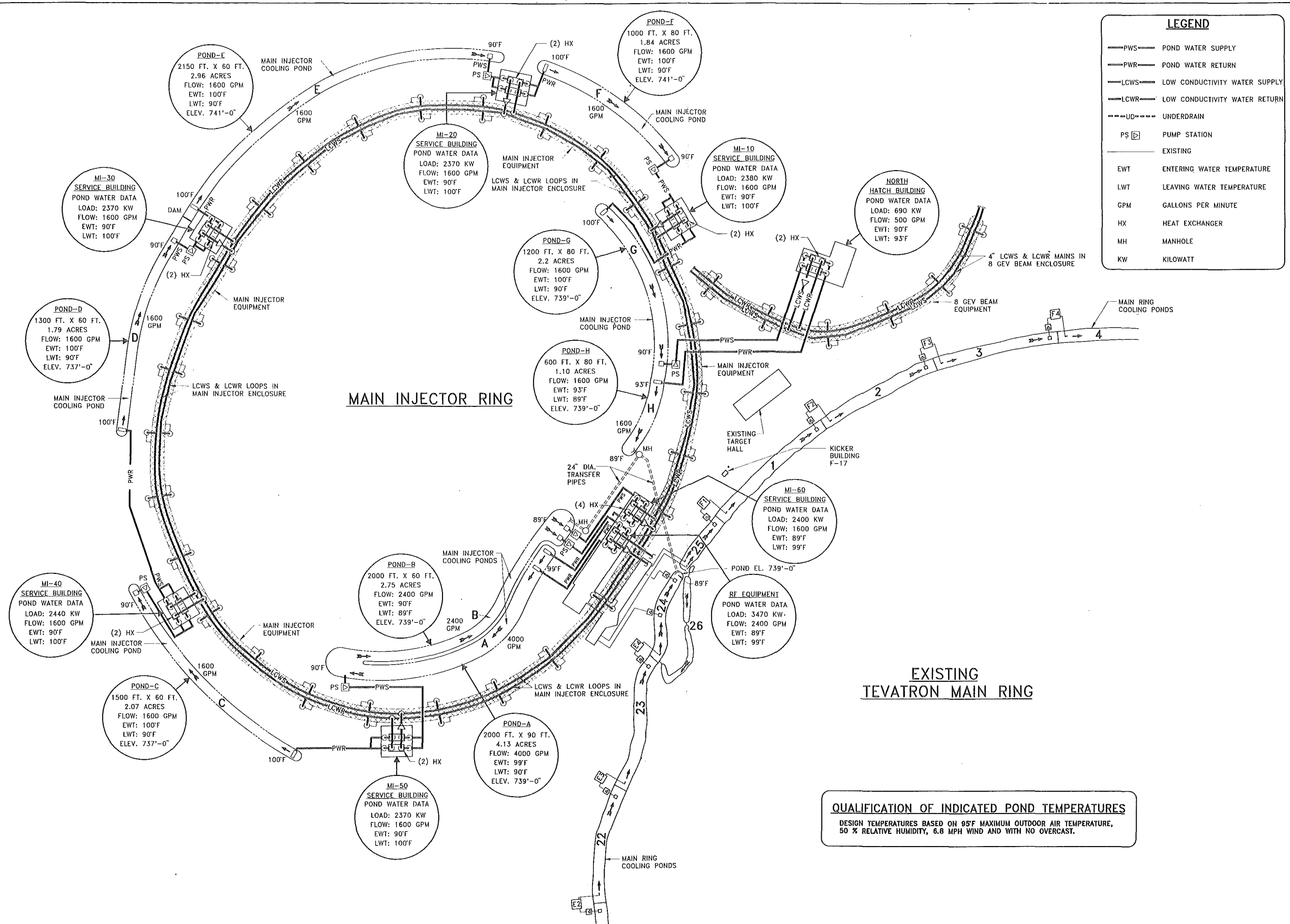
HVAC PLANS

DRAWING NO. 6-6-2 TITLE-1 M-2

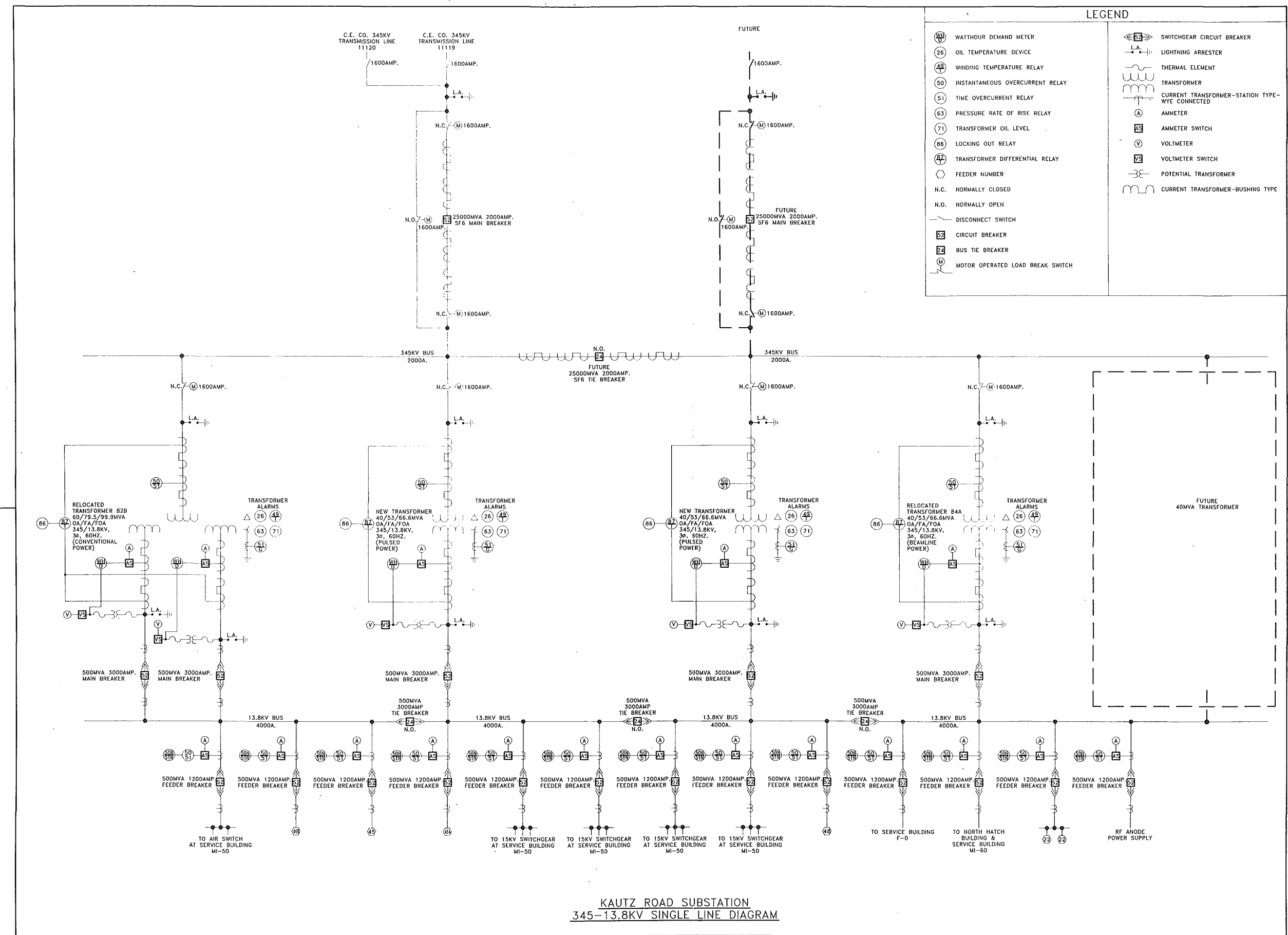
AUG. 1992



FLUOR DANIEL PROJECT NO. - 21842300 NAME _____ DATE _____ DESIGNED B.A.H. JULY, 1992 DRAWN G.O./R.K. JULY, 1992 CHECKED _____ APPROVED _____			NAME _____ DATE _____ DESIGNED S. KRSTULOVICH/M. OLSON DRAWN E. HUEDEM CHECKED _____ APPROVED _____ SUBMITTED _____	SCALE: 1" = 200'-0" 1/8" = 1'-0" SCALE	PROJECT NORTH 	FERMILAB NATIONAL ACCELERATOR LABORATORY UNITED STATES DEPARTMENT OF ENERGY FERMILAB MAIN INJECTOR PROCESS SYSTEM-CRITERIA DRAWING NO. 6-6-2 TITLE-1 M-3 REV. _____
---	--	--	--	---	-------------------	--



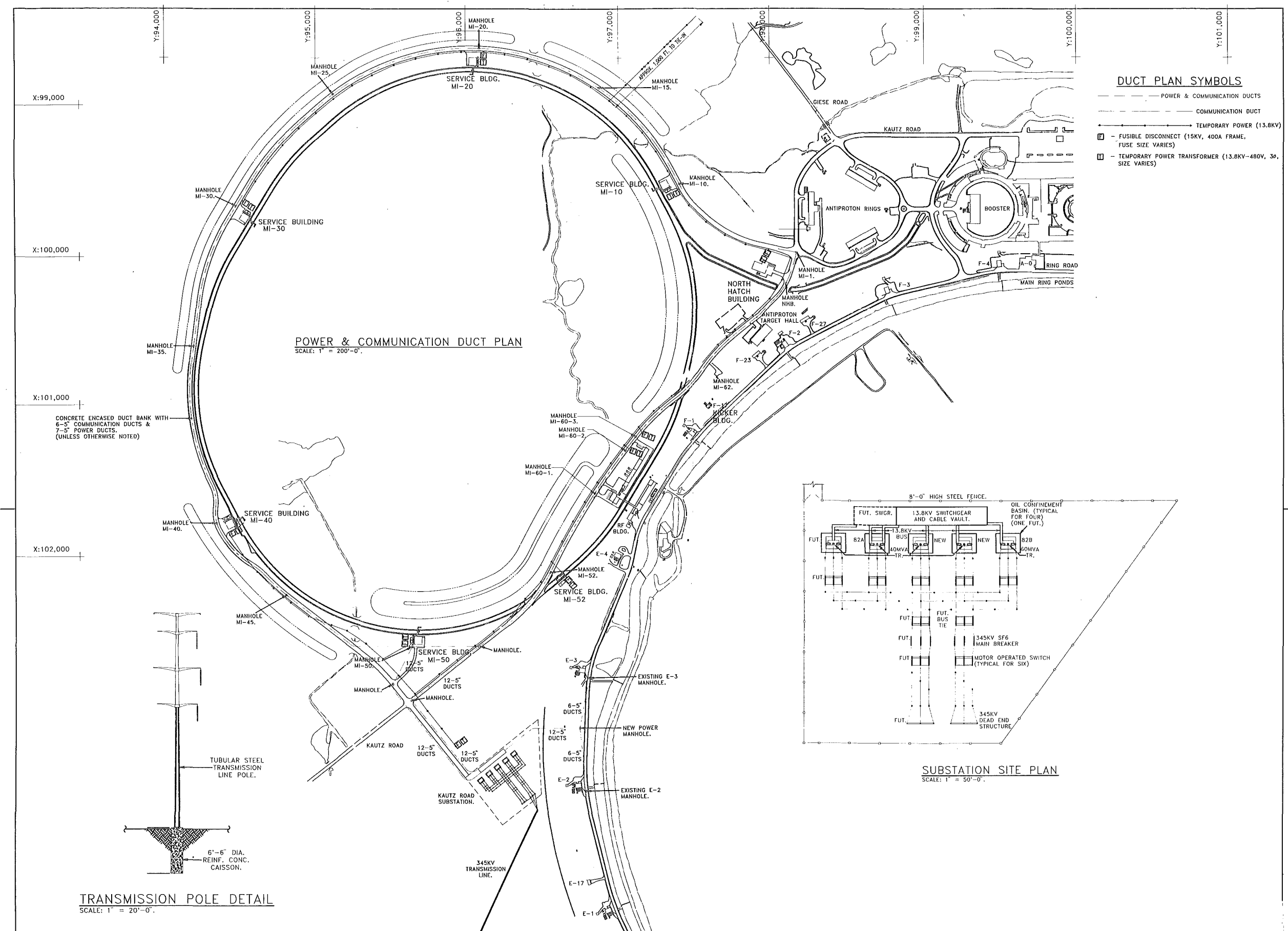
REV. DATE DESCRIPTIONS _____ _____ _____		FLUOR DANIEL <small>CHICAGO</small> PROJECT NO. - 21842300		DESIGNED S. KRSTULOVICH/M. OLSON DRAWN E. HUEDEM CHECKED APPROVED SUBMITTED		SCALE: NONE 	FERMILAB MAIN INJECTOR PROCESS SYSTEMS - FLOW DIAGRAM DRAWING NO. 6-6-2 TITLE-1 M-4 REV.	
		PROJECT NO. - 21842300						
		DESIGNED B.A.H. DRAWN G.O./R.K. CHECKED APPROVED						
		DATE JULY, 1992 DATE JULY, 1992						



KAUTZ ROAD SUBSTATION
345-13.8KV SINGLE LINE DIAGRAM

07/24/92

																																																																																																																																																																																																																																																																																																																																																																																																																																																																																																																																																																																																																																																																																																																																																																																																																																																																																																																																																																																																																																																																																																																																																																																																																																																																																																																																																																																																																																																																												</
--	--	--	--	--	--	--	--	--	--	--	--	--	--	--	--	--	--	--	--	--	--	--	--	--	--	--	--	--	--	--	--	--	--	--	--	--	--	--	--	--	--	--	--	--	--	--	--	--	--	--	--	--	--	--	--	--	--	--	--	--	--	--	--	--	--	--	--	--	--	--	--	--	--	--	--	--	--	--	--	--	--	--	--	--	--	--	--	--	--	--	--	--	--	--	--	--	--	--	--	--	--	--	--	--	--	--	--	--	--	--	--	--	--	--	--	--	--	--	--	--	--	--	--	--	--	--	--	--	--	--	--	--	--	--	--	--	--	--	--	--	--	--	--	--	--	--	--	--	--	--	--	--	--	--	--	--	--	--	--	--	--	--	--	--	--	--	--	--	--	--	--	--	--	--	--	--	--	--	--	--	--	--	--	--	--	--	--	--	--	--	--	--	--	--	--	--	--	--	--	--	--	--	--	--	--	--	--	--	--	--	--	--	--	--	--	--	--	--	--	--	--	--	--	--	--	--	--	--	--	--	--	--	--	--	--	--	--	--	--	--	--	--	--	--	--	--	--	--	--	--	--	--	--	--	--	--	--	--	--	--	--	--	--	--	--	--	--	--	--	--	--	--	--	--	--	--	--	--	--	--	--	--	--	--	--	--	--	--	--	--	--	--	--	--	--	--	--	--	--	--	--	--	--	--	--	--	--	--	--	--	--	--	--	--	--	--	--	--	--	--	--	--	--	--	--	--	--	--	--	--	--	--	--	--	--	--	--	--	--	--	--	--	--	--	--	--	--	--	--	--	--	--	--	--	--	--	--	--	--	--	--	--	--	--	--	--	--	--	--	--	--	--	--	--	--	--	--	--	--	--	--	--	--	--	--	--	--	--	--	--	--	--	--	--	--	--	--	--	--	--	--	--	--	--	--	--	--	--	--	--	--	--	--	--	--	--	--	--	--	--	--	--	--	--	--	--	--	--	--	--	--	--	--	--	--	--	--	--	--	--	--	--	--	--	--	--	--	--	--	--	--	--	--	--	--	--	--	--	--	--	--	--	--	--	--	--	--	--	--	--	--	--	--	--	--	--	--	--	--	--	--	--	--	--	--	--	--	--	--	--	--	--	--	--	--	--	--	--	--	--	--	--	--	--	--	--	--	--	--	--	--	--	--	--	--	--	--	--	--	--	--	--	--	--	--	--	--	--	--	--	--	--	--	--	--	--	--	--	--	--	--	--	--	--	--	--	--	--	--	--	--	--	--	--	--	--	--	--	--	--	--	--	--	--	--	--	--	--	--	--	--	--	--	--	--	--	--	--	--	--	--	--	--	--	--	--	--	--	--	--	--	--	--	--	--	--	--	--	--	--	--	--	--	--	--	--	--	--	--	--	--	--	--	--	--	--	--	--	--	--	--	--	--	--	--	--	--	--	--	--	--	--	--	--	--	--	--	--	--	--	--	--	--	--	--	--	--	--	--	--	--	--	--	--	--	--	--	--	--	--	--	--	--	--	--	--	--	--	--	--	--	--	--	--	--	--	--	--	--	--	--	--	--	--	--	--	--	--	--	--	--	--	--	--	--	--	--	--	--	--	--	--	--	--	--	--	--	--	--	--	--	--	--	--	--	--	--	--	--	--	--	--	--	--	--	--	--	--	--	--	--	--	--	--	--	--	--	--	--	--	--	--	--	--	--	--	--	--	--	--	--	--	--	--	--	--	--	--	--	--	--	--	--	--	--	--	--	--	--	--	--	--	--	--	--	--	--	--	--	--	--	--	--	--	--	--	--	--	--	--	--	--	--	--	--	--	--	--	--	--	--	--	--	--	--	--	--	--	--	--	--	--	--	--	--	--	--	--	--	--	--	--	--	--	--	--	--	--	--	--	--	--	--	--	--	--	--	--	--	--	--	--	--	--	--	--	--	--	--	--	--	--	--	--	--	--	--	--	--	--	--	--	--	--	--	--	--	--	--	--	--	--	--	--	--	--	--	--	--	--	--	--	--	--	--	--	--	--	--	--	--	--	--	--	--	--	--	--	--	--	--	--	--	--	--	--	--	--	--	--	--	--	--	--	--	--	--	--	--	--	--	--	--	--	--	--	--	--	--	--	--	--	--	--	--	--	--	--	--	--	--	--	--	--	--	--	--	--	--	--	--	--	--	--	--	--	--	--	--	--	--	--	--	--	--	--	--	--	--	--	--	--	--	--	--	--	--	--	--	--	--	--	--	--	--	--	--	--	--	--	--	--	--	--	--	--	--	--	--	--	--	--	--	--	--	--	--	--	--	--	--	--	--	--	--	--	--	--	--	--	--	--	--	--	--	--	--	--	--	--	--	--	--	--	--	--	--	--	--	--	--	--	--	--	--	--	--	--	--	--	--	--	--	--	--	--	--	--	--	--	--	--	--	--	--	--	--	--	--	--	--	--	--	--	--	--	--	--	--	--	--	--	--	--	--	--	--	--	--	--	--	--	--	--	--	--	--	--	--	--	--	--	--	--	--	--	--	--	--	--	--	--	--	--	--	--	--	--	--	--	--	--	--	--	--	--	--	--	--	--	--	--	--	--	--	--	--	--	--	--	--	--	--	--	--	--	--	--	--	--	--	--	--	--	--	--	--	--	--	--	--	--	--	--	--	--	--	--	--	--	--	--	--	--	--	--	--	--	--	--	--	--	--	--	--	--	--	--	--	--	--	--	--	--	--	--	--	--	--	--	--	--	--	--	--	--	--	--	--	--	--	--	--	--	--	--	--	--	--	--	--	--	--	--	--	--	--	--	--	--	--	--	--	--	--	--	--	--	--	--	--	--	--	--	--	--	--	--	--	--	--	--	--	--	--	--	--	--	--	--	--	--	--	--	--	--	--	--	--	--	--	--	--	--	--	--	--	--	--	--	--	--	--	--	--	--	--	--	--	--	--	--	--	--	--	--	--	--	--	--	--	--	--	--	--	--	--	--	--	--	--	--	--	--	--	--	--	--	--	--	--	--	--	--	--	--	--	--	--	--	--	--	--	--	--	--	--	--	--	--	--	--	--	--	--	--	--	--	--	--	--	--	--	--	--	--	--	--	--	--	--	--	--	--	--	--	--	--	--	--	--	--	--	--	--	--	--	--	--	--	--	--	--	--	--	--	--	--	--	--	--	--	--	--	--	--	--	--	--	--	--	--	--	--	--	--	--	--	--	--	--	--	--	--	--	--	--	--	--	----




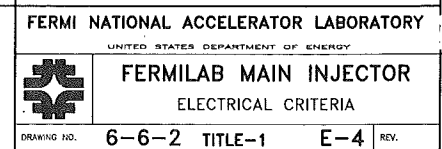
FLUOR DANIEL PROJECT NO. - 21842300		DESIGNED: E. VALDES DRAWN: A. R. FLOWERS CHECKED: [] APPROVED: [] SUBMITTED: []		DATE: 07/07/92 DATE: 07/07/92 DATE: 07/09/92	
REV. DATE DESCRIPTION REVISIONS		FERMILAB MAIN INJECTOR POWER & COMMUNICATION DUCT PLAN DRAWING NO. 6-6-2 TITLE-1 E-3 REV.			

07/23/92

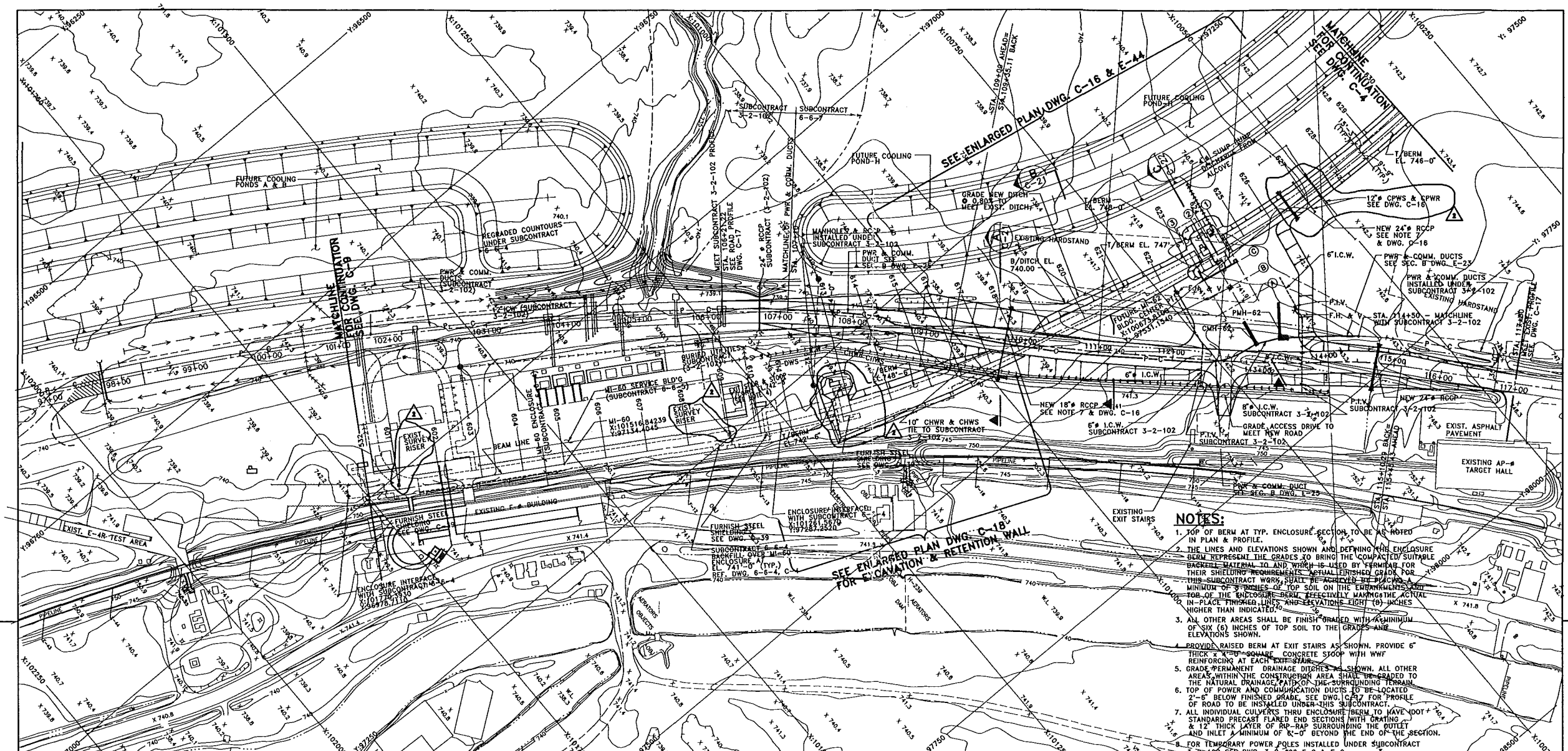
AUG. 1992



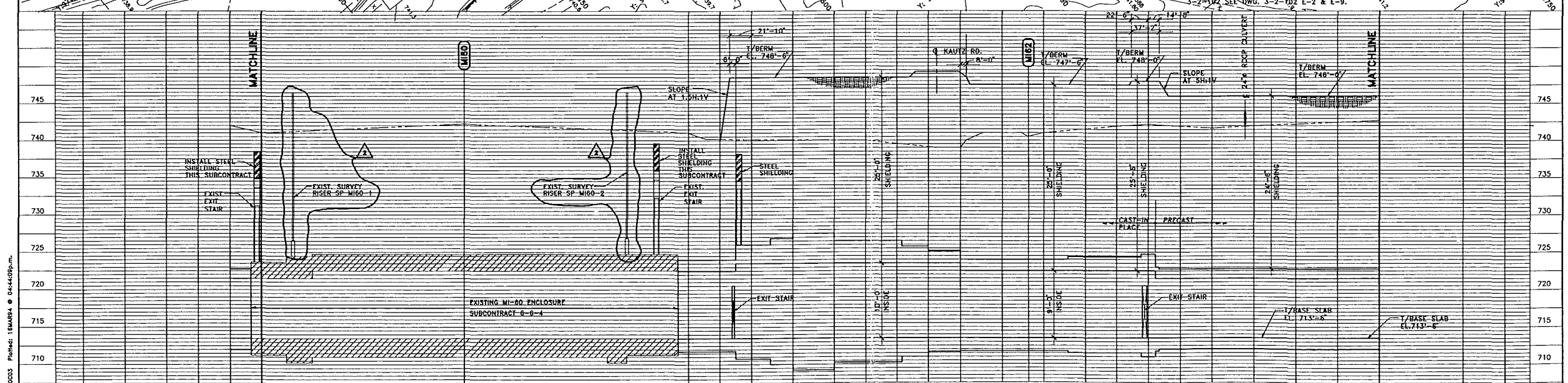
	
CHICAGO	EL PASO
PROJECT NO. - 21842300	
NAME	DATE
DESIGNED R.S.M.	07/07/97
DRAWN R.S.M.	07/07/97
CHECKED Z.S.	07/10/97
APPROVED	



AUG.1992



- NOTES:**
1. TOP OF BERM AT TYP. ENCLOSURE SECTION TO BE AS NOTED IN PLAN & PROFILE.
 2. THE LINES AND ELEVATIONS SHOWN AND DEFINING THE ENCLOSURE BERM REPRESENT THE GRADES TO BRING THE COMPACTED/SUITABLE BERM TO THE GRADE TO WHICH IT IS USED BY THE OWNER FOR THEIR SHIELDING REQUIREMENTS. ACTUAL FINISHED GRADE FOR THIS SUBCONTRACT WORK SHALL BE ACCURATELY PLACED A MINIMUM OF 3 INCHES OF TOP SOIL ON THE EXISTING BERM TO BRING THE BERM TO THE ACTUAL GRADE. RESPECTIVELY, MARKING THE ACTUAL IN-PLACE FINISHED LINES AND ELEVATIONS FIFTY (50) INCHES HIGHER THAN INDICATED.
 3. ALL OTHER AREAS SHALL BE FINISH GRADED WITH A MINIMUM OF SIX (6) INCHES OF TOP SOIL TO THE GRADES AND ELEVATIONS SHOWN.
 4. PROVIDE RAISED BERM AT EXIT STAIRS AS SHOWN. PROVIDE 6" THICK $\times 4'-0"$ SQUARE CONCRETE SLOOP WITH WWF REINFORCING AT EACH EXIT STAIR.
 5. GRADE PERMANENT DRAINAGE DITCHES AS SHOWN. ALL OTHER AREAS WITHIN THE CONSTRUCTION AREA SHALL BE GRADED TO THE NATURAL DRAINAGE PATTERNS OF THE SURROUNDING TERRAIN.
 6. TOP OF POWER AND COMMUNICATION DUCTS TO BE LOCATED 2'-6" BELOW FINISHED GRADE. SEE DWG. C-16 FOR PROFILE OF ROAD TO BE INSTALLED UNDER THIS SUBCONTRACT.
 7. ALL INDIVIDUAL CULVERTS THRU ENCLOSURE BERM TO HAVE 100% STANDARD PRECAST FLARED END SECTIONS WITH 12" \times 12" THICK LAYER OF RCP SURROUNDING THE OUTLET AND INLET A MINIMUM OF 6'-0" BEYOND THE END OF THE SECTION.
 8. FOR TEMPORARY POWER POLES INSTALLED UNDER SUBCONTRACT 3-2-102 SEE DWG. 3-2-102 E-2 & E-9.



FLUOR DANIEL		PROJECT NO. - 21842300		DATE	
CHICAGO		ILLINOIS			
DESIGNED	R. JEDZINIAK	DATE	8/13/93	CONCEPT	T. LACKOWSKI
DRAWN	A. SKUZA	DATE	8/13/93	REVIEWED	C. FEDEROWICZ
CHECKED	B. ZEJNSKI	DATE	8/13/93	REVIEWED	E. CRUMPLEY
APPROVED	R. BRUNTON			APPROVED	TO: I. PAWIAK
				SUBMITTED	WAYNE NESTANDER

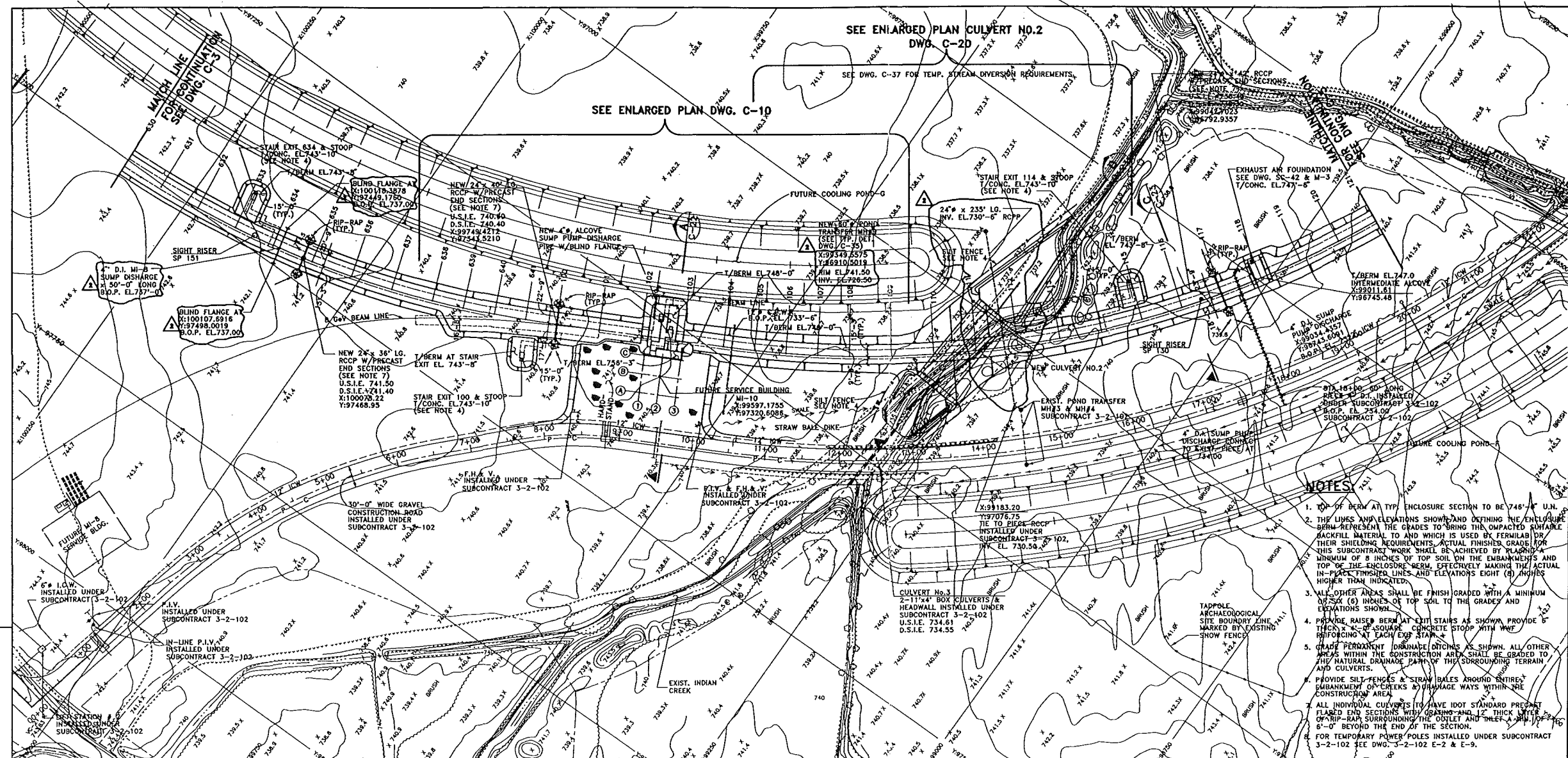
REV.	DATE	DESCRIPTION
2	3/25/94	NOTED EXIST. SIGHT RISERS, MOD. BERM AT STAIR, AND ADDED CPWS & CPWS LINES

FERMI NATIONAL ACCELERATOR LABORATORY	
UNITED STATES DEPARTMENT OF ENERGY	
MAIN INJECTOR ENCLOSURE	
PLAN & PROFILE	
DRAWING NO.	6-6-7
REV.	2

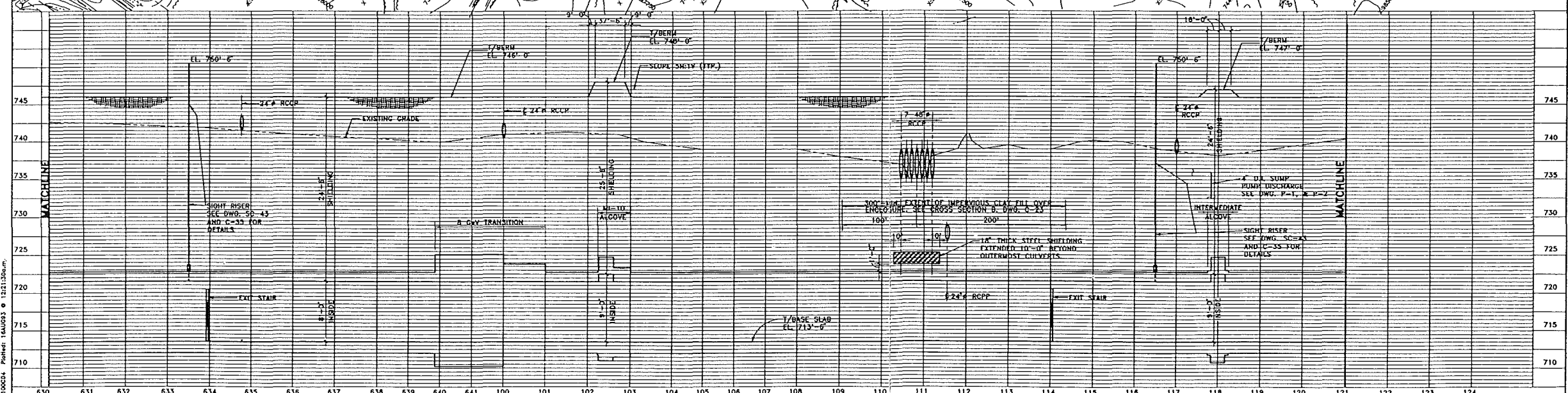
SCALE: HORIZONTAL 1" = 50'-0" VERTICAL 1" = 5'-0"

PROJECT NORTH

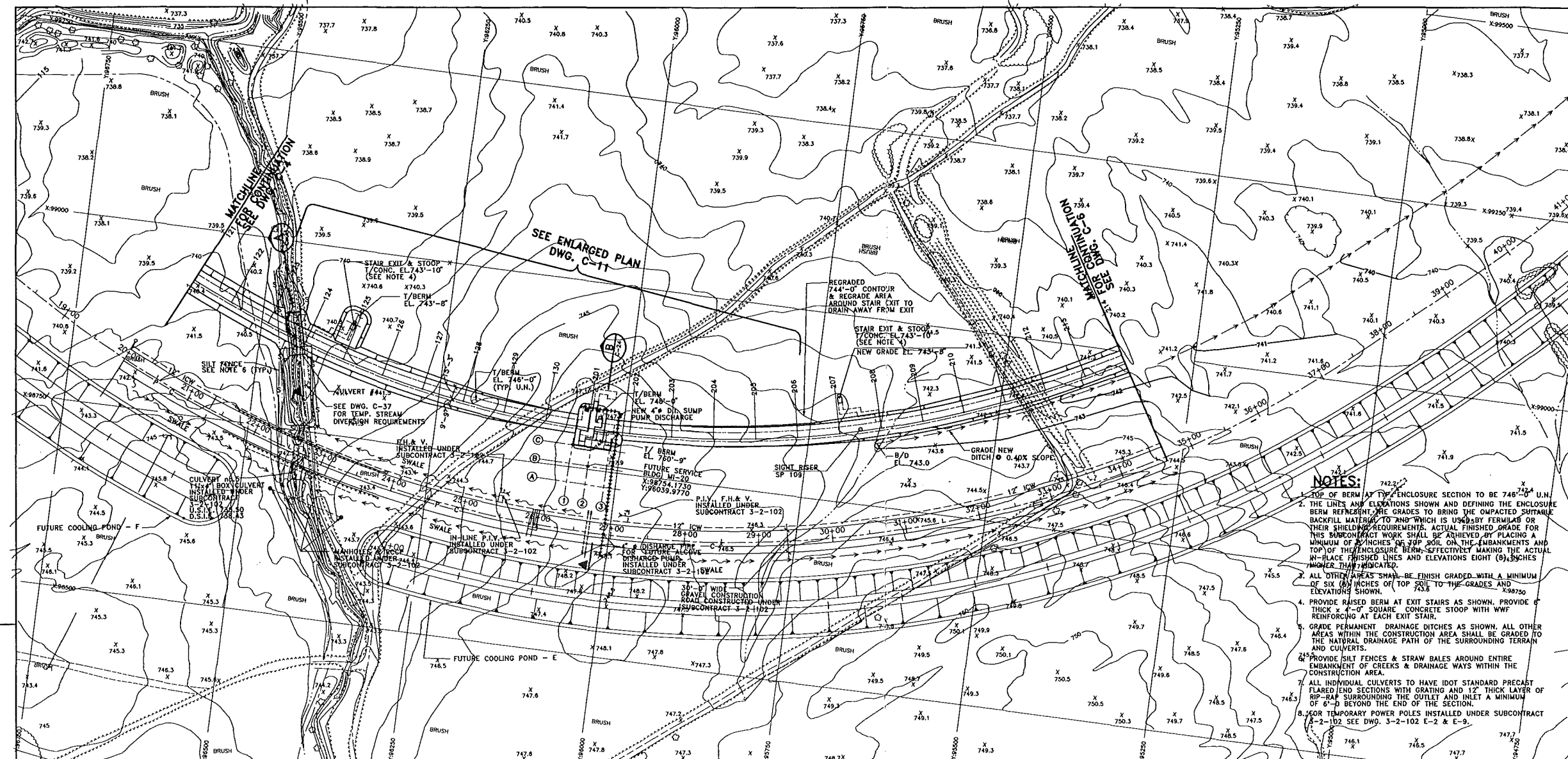
25 MAR. 1994



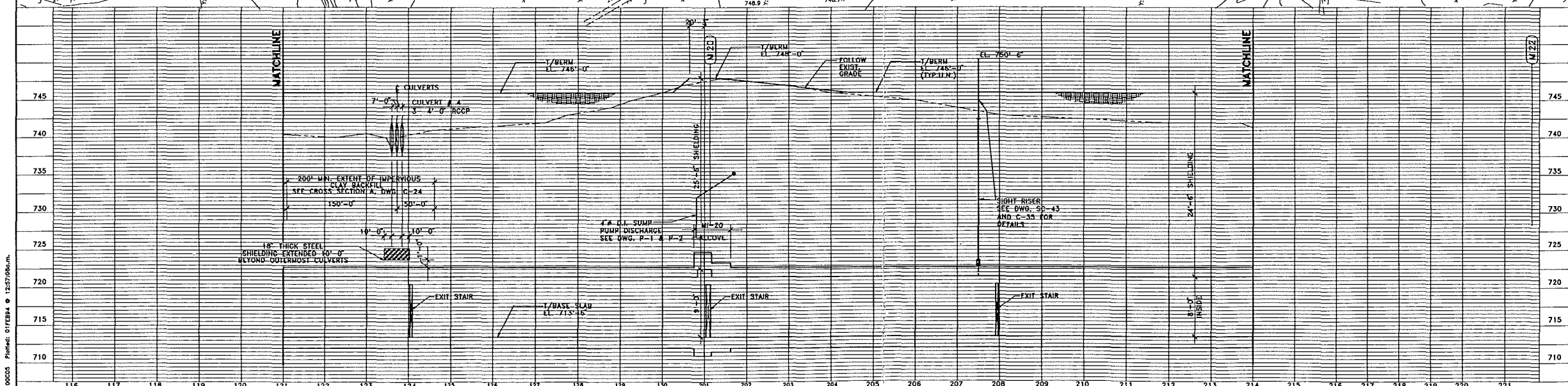
- NOTES**
1. TOP OF BERM AT TYP. ENCLOSURE SECTION TO BE 7'48" U.N.
 2. THE LINES AND ELEVATIONS SHOWN AND DEFINING THE ENCLOSURE BERM REPRESENT THE GRADES TO BE BRING THE COMPACTED SUITABLE BACKFILL MATERIAL TO AND WHICH IS USED BY FERMILAB OR THEIR SHELTERING REQUIREMENTS. ACTUAL FINISHED GRADES FOR THIS SUBCONTRACT WORK SHALL BE ACHIEVED BY PLACING A MINIMUM OF 8 INCHES OF TOP SOIL ON THE EMBANKMENTS AND TOP OF THE ENCLOSURE BERM, EFFECTUALLY MAKING THE ACTUAL IN-PLACE FINISHED LINES AND ELEVATIONS EIGHT (8) INCHES HIGHER THAN INDICATED.
 3. ALL OTHER AREAS SHALL BE FINISH GRADED WITH A MINIMUM OF SIX (6) INCHES OF TOP SOIL TO THE GRADES AND ELEVATIONS SHOWN.
 4. PROVIDE RAISED BERM AT EXIT STAIRS AS SHOWN. PROVIDE 6" THICK 4" x 4" SQUARE CONCRETE STOOP WITH W/WF REINFORCING AT EACH EXIT STAIR.
 5. GRADY PERMANENT DRAINAGE DITCHES AS SHOWN. ALL OTHER AREAS WITHIN THE CONSTRUCTION AREA SHALL BE GRADED TO THE NATURAL DRAINAGE PATTERN OF THE SURROUNDING TERRAIN AND CULVERTS.
 6. PROVIDE SILT-FENCES & STRAW BALES AROUND ENTIRE EMBANKMENT OF CREEKS & DRAINAGE WAYS WITHIN THE CONSTRUCTION AREA.
 7. ALL INDIVIDUAL CULVERTS TO HAVE 10" STANDARD PREPARED FLARED END SECTIONS WITH GRASS AND 12" THICK LAYER OF RIP-RAP SURROUNDING THE OUTLET AND INLET A MIN. OF 50' 6" BEYOND THE END OF THE SECTION.
 8. FOR TEMPORARY POWER POLES INSTALLED UNDER SUBCONTRACT 3-2-102 SEE DWG. 3-2-102 E-2 & E-9.



FLUOR DANIEL PROJECT NO. - 21842300		CONCEPT: T. LACK/WSKI REVIEWED: C. FEDEROWICZ REVIEWED: E. CRUMPLEY APPROVED: TOM PAWLAK SUBMITTED: DIXON BOGERT		SCALE: HORIZONTAL: 1" = 50'-0" VERTICAL: 1" = 5'-0"	FERMI NATIONAL ACCELERATOR LABORATORY UNITED STATES DEPARTMENT OF ENERGY MAIN INJECTOR ENCLOSURE PLAN & PROFILE DRAWING NO. 6-6-7 C-4 REV. 2
DESIGNED: R. JEDZINIAK DRAWN: A. SKUZA CHECKED: B. ZELINSKI APPROVED: R. BRUNTON	DATE: 8/13/93 DATE: 8/13/93 DATE: 8/13/93	PROJECT NORTH		23 MAR. 1994	



- NOTES:**
1. TOP OF BERM AT TYP. ENCLOSURE SECTION TO BE 746'-0" U.N.
 2. THE LINES AND ELEVATIONS SHOWN AND DEFINING THE ENCLOSURE BERM REPRESENT THE GRADES TO BRING THE IMPACTED SUITABLE BACKFILL MATERIAL TO AND WHICH IS USED BY FERMILAB OR THEIR SHIELDING REQUIREMENTS. ACTUAL FINISHED GRADE FOR THIS SUBCONTRACT WORK SHALL BE ACHIEVED BY PLACING A MINIMUM OF 2 INCHES OF TOP SOIL ON THE EMBANKMENTS AND TOP OF THE ENCLOSURE BERM, EFFECTIVELY MAKING THE ACTUAL FINISHED GRADE LINES AND ELEVATIONS EIGHT (8) INCHES LOWER THAN INDICATED.
 3. ALL OTHER AREAS SHALL BE FINISH GRADED WITH A MINIMUM OF SIX (6) INCHES OF TOP SOIL TO THE GRADES AND ELEVATIONS SHOWN.
 4. PROVIDE RAISED BERM AT EXIT STAIRS AS SHOWN. PROVIDE 6" THICK x 4'-0" SQUARE CONCRETE STOOP WITH WWF REINFORCING AT EACH EXIT STAIR.
 5. GRADE PERMANENT DRAINAGE DITCHES AS SHOWN. ALL OTHER AREAS WITHIN THE CONSTRUCTION AREA SHALL BE GRADED TO THE NATURAL DRAINAGE PATH OF THE SURROUNDING TERRAIN AND CULVERTS.
 6. PROVIDE SILT FENCES & STRAW BALES AROUND ENTIRE EMBANKMENT OF CREEKS & DRAINAGE WAYS WITHIN THE CONSTRUCTION AREA.
 7. ALL INDIVIDUAL CULVERTS TO HAVE IDOT STANDARD PRECAST FLARED END SECTIONS WITH GRATING AND 12" THICK LAYER OF RIP-RAP SURROUNDING THE OUTLET AND INLET A MINIMUM OF 6'-0" BEYOND THE END OF THE SECTION.
 8. FOR TEMPORARY POWER POLES INSTALLED UNDER SUBCONTRACT 3-2-102 SEE DWG. 3-2-102 E-2 & E-9.



FLUOR DANIEL CHICAGO		PROJECT NO. - 21842300	
DESIGNED	R. JEDZINIAK	DATE	8/13/93
DRAWN	A. SOUZA		8/13/93
CHECKED	B. TELINSKI		8/13/93
APPROVED	R. BRUNTON		

CONCEPT	T. LACKOWSKI	DATE	
REVIEWED	C. FEDEROWICZ		
REVIEWED	E. CRUMPLEY		
APPROVED	TOM PAWLAK WAYNE NESTANDER		
SUBMITTED	DIXON BOGERT		

SCALE:

HORIZONTAL
1" = 50'-0"
SCALE

VERTICAL
1" = 5'-0"
SCALE

PROJECT NORTH

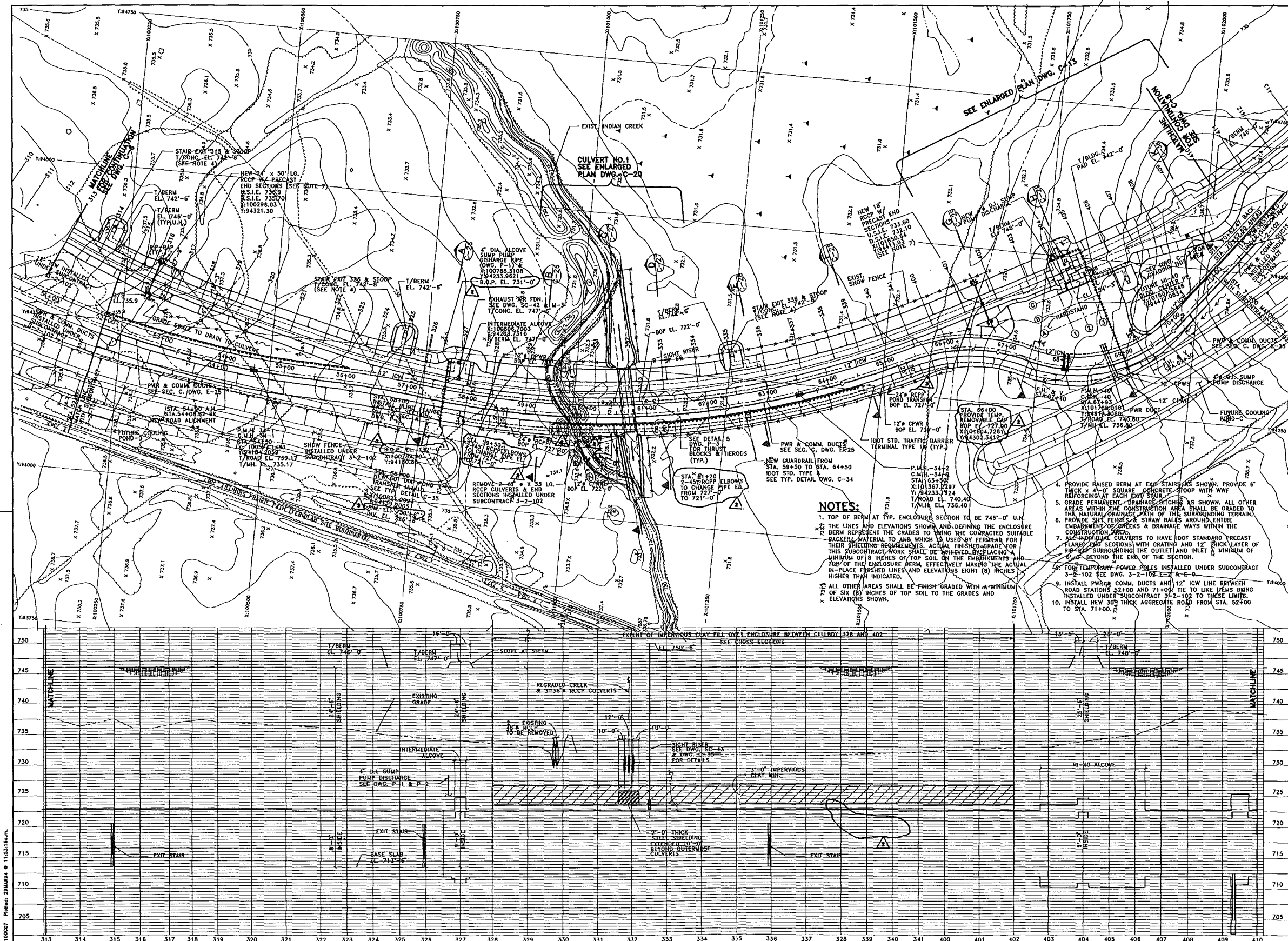
FERMI NATIONAL ACCELERATOR LABORATORY
UNITED STATES DEPARTMENT OF ENERGY

MAIN INJECTOR ENCLOSURE
PLAN & PROFILE

DRAWING NO. **6-6-7** **C-5** REV. **1**

Dwg. F:\P\A\642303\ETRA\2100005.dwg Plotfile: 01FERM4 2/27/98m.

11 FEB. 1994



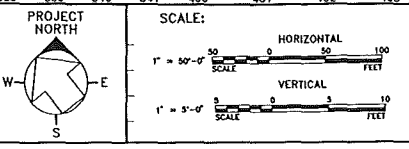
NOTES:

1. TOP OF BERM AT TYP. ENCLOSURE SECTION TO BE 745'-0" U.N.
2. THE LINES AND ELEVATIONS SHOWN AND DEFINING THE ENCLOSURE BERM REPRESENT THE GRADES TO BEING THE CONTRACTED SUITABLE BACKFILL MATERIAL TO AND WHICH IS USED BY FERMILAB FOR THEIR SHIELDING REQUIREMENTS. ACTUAL FINISHED GRADE FOR THIS SUBCONTRACT WORK SHALL BE ACHIEVED BY REPLACING A MINIMUM OF 8 INCHES OF TOP SOIL ON THE EMBANKMENTS AND TOP OF THE ENCLOSURE BERM, EFFECTIVELY MAKING THE ACTUAL IN-PLACE FINISHED LINES AND ELEVATIONS EIGHT (8) INCHES HIGHER THAN INDICATED.
3. ALL OTHER AREAS SHALL BE FINISH GRADED WITH A MINIMUM OF SIX (6) INCHES OF TOP SOIL TO THE GRADES AND ELEVATIONS SHOWN.
4. PROVIDE RAISED BERM AT EXIST. STAIRS AS SHOWN. PROVIDE 6" THICK REINFORCING AT EACH EXIST. STAIR.
5. GRADE PERMANENT DRAINAGE DITCHES AS SHOWN. ALL OTHER AREAS WITHIN THE CONSTRUCTION AREA SHALL BE GRADED TO THE NATURAL DRAINAGE PATH OF THE SURROUNDING TERRAIN.
6. PROVIDE SIX FIBER & STRAW BALES AROUND EXIST. EMBANKMENT OF CREEKS & DRAINAGE WAYS WITHIN THE CONSTRUCTION AREA.
7. ALL ENDS OF CULVERTS TO HAVE 100' STANDARD PRECAST PLATE AND TWO SECTIONS WITH GRATING AND 12" THICK LAYER OF RIB-ROOF SURROUNDING THE OUTLET AND INLET A MINIMUM OF 6" BEYOND THE END OF THE SECTION.
8. FOR TEMPORARY POWER POLES INSTALLED UNDER SUBCONTRACT 3-2-102 SEE DWG. 3-2-102-2-4-6-9.
9. INSTALL PWR & COMM. DUCTS AND 12" ICW LINE BETWEEN ROAD STATIONS 52+00 AND 71+00. TIE TO LIKE ITEMS BEING INSTALLED UNDER SUBCONTRACT 3-2-102 TO THESE LIMITS.
10. INSTALL NEW 30" THICK AGGREGATE ROAD FROM STA. 52+00 TO STA. 71+00. 7'

REV.	DATE	DESCRIPTION
2	3/25/94	DEL. GEOTECHNICAL CALLOUT IN PROFILE. REV. FROM TO RCP. DEL. WYS 11, 12 & 13. ADDED 18\"/>

FLUOR DANIEL CHICAGO	
PROJECT NO. - 21842300	
DESIGNED	R. JEDZINIAK 8/13/93
DRAWN	A. SKUZA 8/13/93
CHECKED	B. ZELINSKI 8/13/93
APPROVED	R. BRUNTON

CONCEPT	T. LACKOWSKI
REVIEWED	C. FEDEROWICZ
REVIEWED	E. CRUMLEY
APPROVED	TOM PAVLAK WAYNE HESTANDER
SUBMITTED	DIXON BOCERT

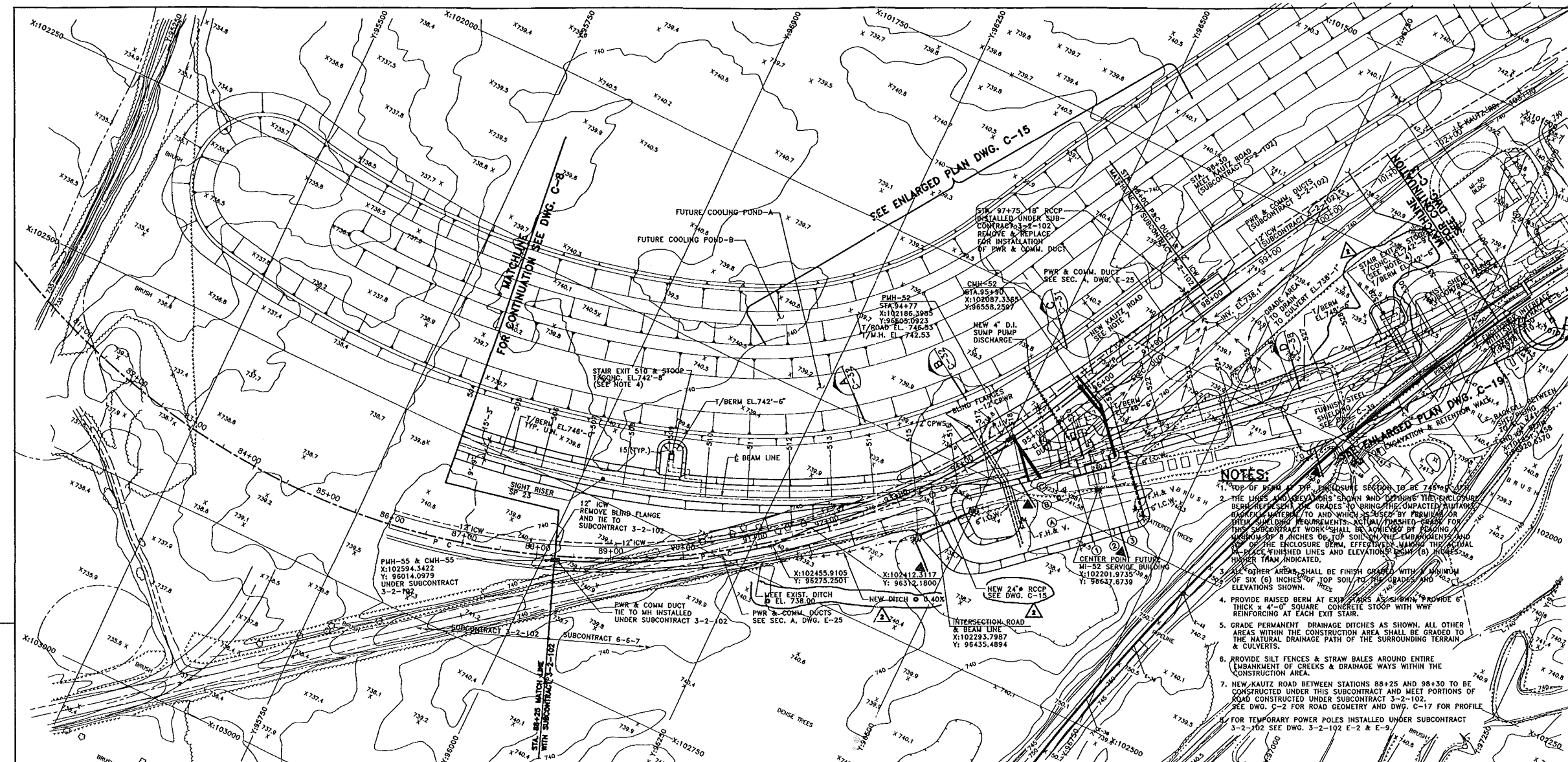


FERMI NATIONAL ACCELERATOR LABORATORY
UNITED STATES DEPARTMENT OF ENERGY

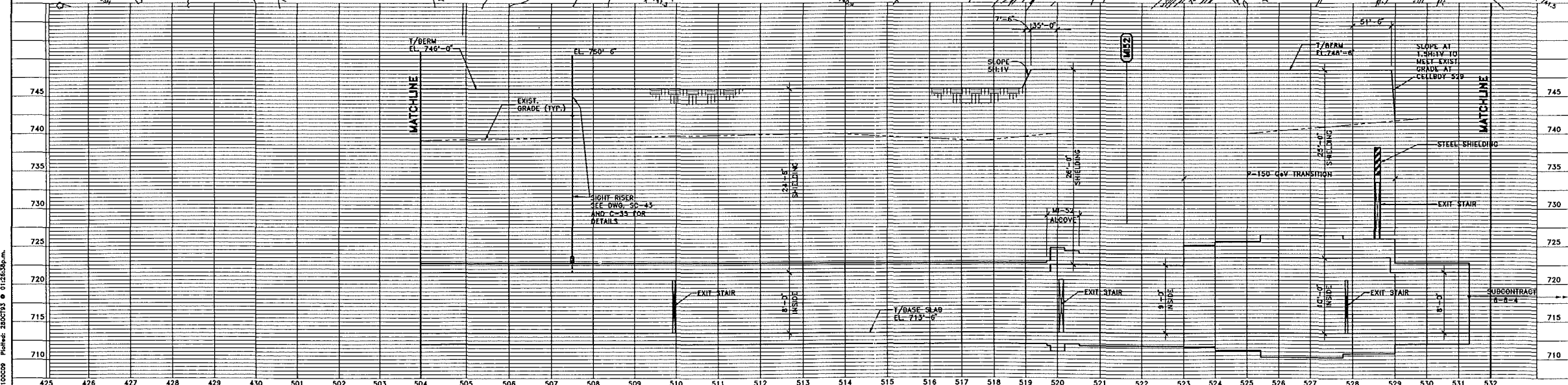
MAIN INJECTOR ENCLOSURE
PLAN & PROFILE

DRAWING NO. **6-6-7** **C-7** REV. **2**

Drawn: FL 942300, STRU 21842300, P 11/25/94m.



- NOTES:**
1. TOP OF BERM AT THE ENCLOSURE SECTION TO BE 740.00'.
 2. THE LINES AND ELEVATIONS SHOWN AND DEFINING THE ENCLOSURE BERM REPRESENT THE GRADES TO BE BRINGING THE COMPACTED SUBGRADE TO THE GRADES TO WHICH THE BERM IS TO BE CONSTRUCTED. THE BERM SHALL BE CONSTRUCTED TO THE GRADES SHOWN AND TO WHICH THE BERM IS TO BE CONSTRUCTED. THE BERM SHALL BE CONSTRUCTED TO THE GRADES SHOWN AND TO WHICH THE BERM IS TO BE CONSTRUCTED.
 3. ALL OTHER AREAS SHALL BE FINISH GRADED WITH A MINIMUM OF SIX (6) INCHES OF TOP SOIL TO THE BERM AND TO THE ELEVATIONS SHOWN.
 4. PROVIDE RAISED BERM AT EXIT STAIRS AS SHOWN. PROVIDE 6" THICK 4'-0" SQUARE CONCRETE STOOP WITH WWF REINFORCING AT EACH EXIT STAIR.
 5. GRADE PERMANENT DRAINAGE DITCHES AS SHOWN. ALL OTHER AREAS WITHIN THE CONSTRUCTION AREA SHALL BE GRADED TO THE NATURAL DRAINAGE PATH OF THE SURROUNDING TERRAIN & CULVERTS.
 6. PROVIDE SILT FENCES & STRAW BALES AROUND ENTIRE PERIMETER OF CREEKS & DRAINAGE WAYS WITHIN THE CONSTRUCTION AREA.
 7. NEW KAUTZ ROAD BETWEEN STATIONS 88+25 AND 98+30 TO BE CONSTRUCTED UNDER THIS SUBCONTRACT AND MEET PORTIONS OF ROAD CONSTRUCTED UNDER SUBCONTRACT 3-2-102. SEE DWG. C-2 FOR ROAD GEOMETRY AND DWG. C-17 FOR PROFILE.
 8. FOR TEMPORARY POWER POLES INSTALLED UNDER SUBCONTRACT 3-2-102 SEE DWG. 3-2-102 E-2 & E-9.



FLUOR DANIEL PROJECT NO. - 21842300		FERMI NATIONAL ACCELERATOR LABORATORY UNITED STATES DEPARTMENT OF ENERGY MAIN INJECTOR ENCLOSURE PLAN & PROFILE	
DESIGNED	R. JEDZINIAK	DATE	8/13/93
DRAWN	A. SKUZA	DATE	8/13/93
CHECKED	B. ZELINSKI	DATE	8/13/93
APPROVED	R. BRUNTON	DATE	8/13/93
CONCEPT	T. LACKOWSKI	DATE	
REVIEWED	C. FEDEROWICZ	DATE	
REVIEWED	E. LRUIMPLEY	DATE	
APPROVED	TOM PAWLAK WAYNE NESTANDER	DATE	
SUBMITTED	DIXON BOGERT	DATE	

SCALE: HORIZONTAL 1" = 50'-0" VERTICAL 1" = 5'-0"

PROJECT NORTH

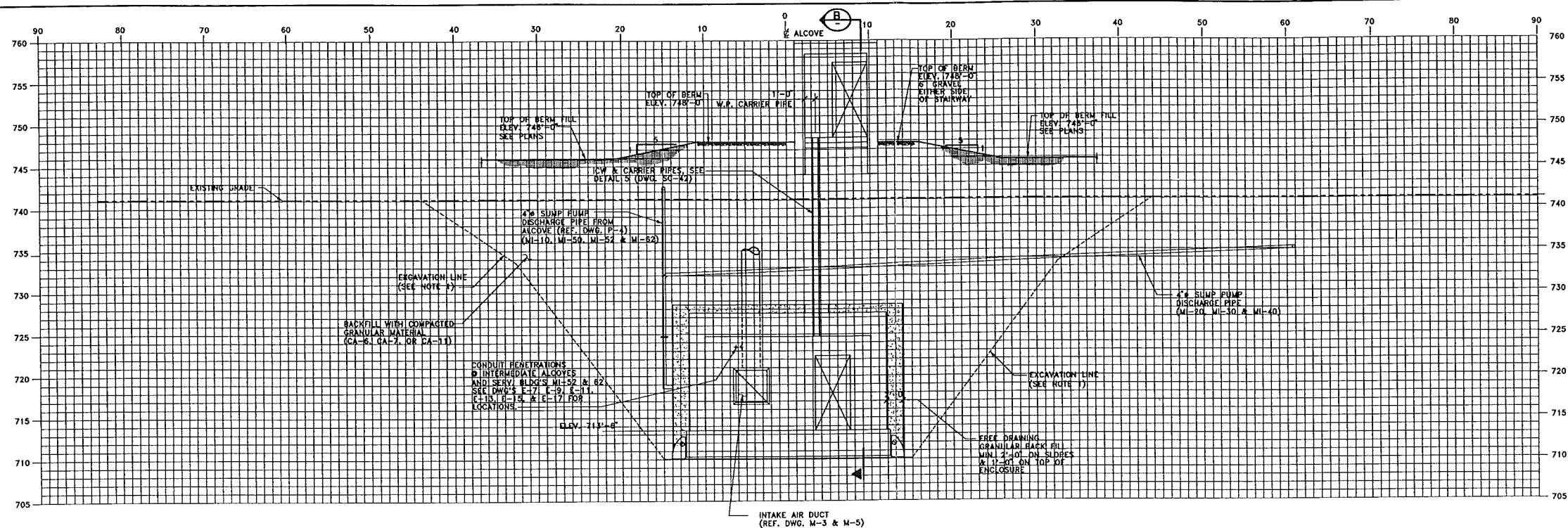
REV. 2 3/25/94

DATE 3/25/94

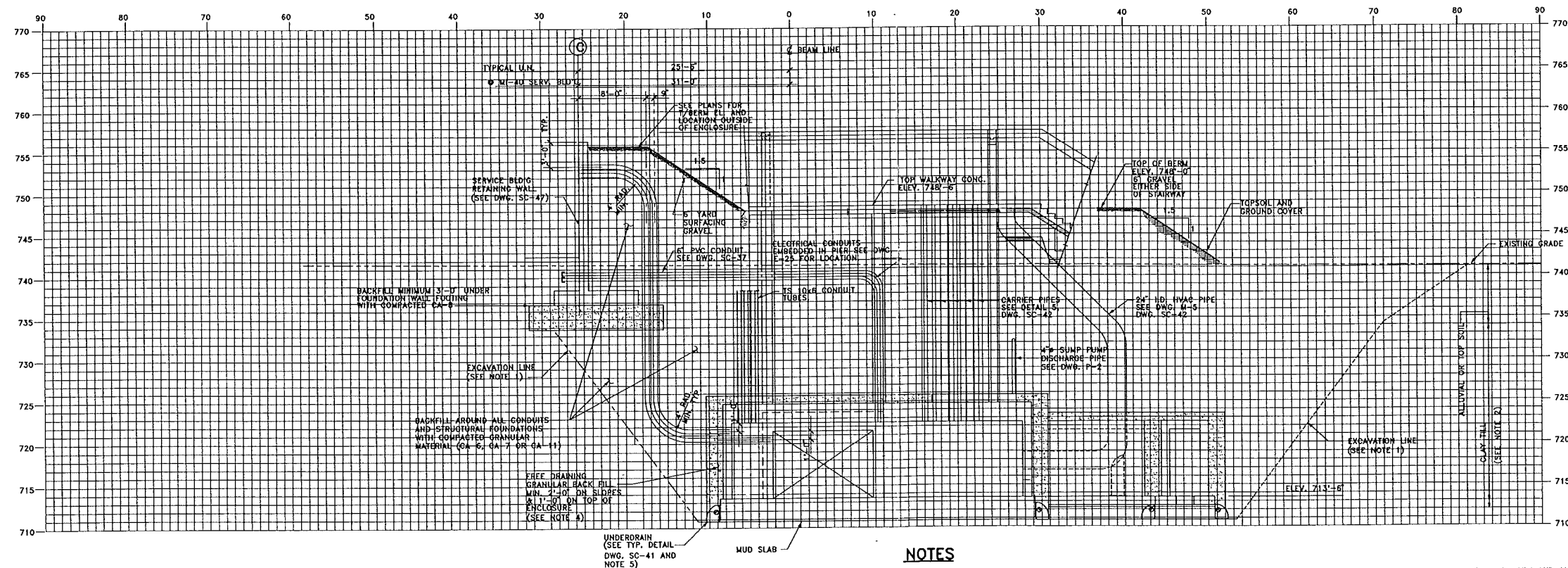
DESCRIPTIONS

REVISIONS

35 MAR. 1994



SECTION A
TYP. AT ALL SERVICE BUILDING C-10 THRU C-16

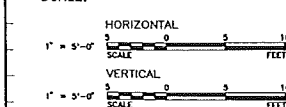


SECTION B
TYP. AT ALL SERVICE BUILDING

NOTES

- EXCAVATION SLOPES INDICATED ARE BASED ON THE STS RECOMMENDED SLOPES OF 0.75H:1.0V IN CLAY TILL AND 1.5H:1.0V IN THE ALLUVIAL SOILS AND ARE MEANT TO INDICATE THE STEEPEST SLOPES THAT WILL BE ACCEPTABLE TO FERMILAB. BENCHES, OR OTHER REQUIRED MEASURES SUCH AS SHALLOWER SLOPES, WHICH MAY BE REQUIRED AS DETERMINED BY THE SUBCONTRACTOR'S ENGINEER, ARE NOT SHOWN BUT SHALL BE ACCOUNTED FOR BY THE SUBCONTRACTOR.
- IDENTIFICATION AND LOCATION OF EXISTING SOIL LAYERS IS AN ESTIMATE INTERPOLATED FROM THE STS SOIL BORINGS.
- SUITABLE FILL SHALL BE SUITABLE EXCAVATED MATERIALS COMPACTED TO 95% STANDARD PROCTOR; EXCEPT UNDER ALL EXIT STAIRS, SERVICE BUILDING FOUNDATION WALLS, AND AROUND PENETRATION CONDUITS, WHERE THE BACKFILL SHALL BE GRANULAR COMPACTED TO 95% MODIFIED PROCTOR.
- THE LIMIT OF FREE DRAINING GRANULAR MATERIAL SHOWN AROUND THE ENCLOSURE IS THE MINIMUM DESIGN REQUIREMENT. ADDITIONAL GRANULAR MATERIAL PLACED TO ACHIEVE THIS REQUIREMENT SHALL BE AT THE SUBCONTRACTOR'S EXPENSE.
- THE UNDERDRAIN PIPE SHALL BE INSTALLED CONTINUOUSLY AROUND THE ENTIRE PERIMETER OF THE ENCLOSURE AND ALCOVES. SEE THE STRUCTURAL FOUNDATION DRAWINGS AND MECHANICAL PIPING DRAWINGS FOR DETAILED ROUTING OF THE UNDERDRAIN AT ALCOVES AND OTHER SPECIALIZED AREAS.

SCALE:



FERMI NATIONAL ACCELERATOR LABORATORY

UNITED STATES DEPARTMENT OF ENERGY

MAIN INJECTOR ENCLOSURE
CROSS SECTIONS - SHT. 13

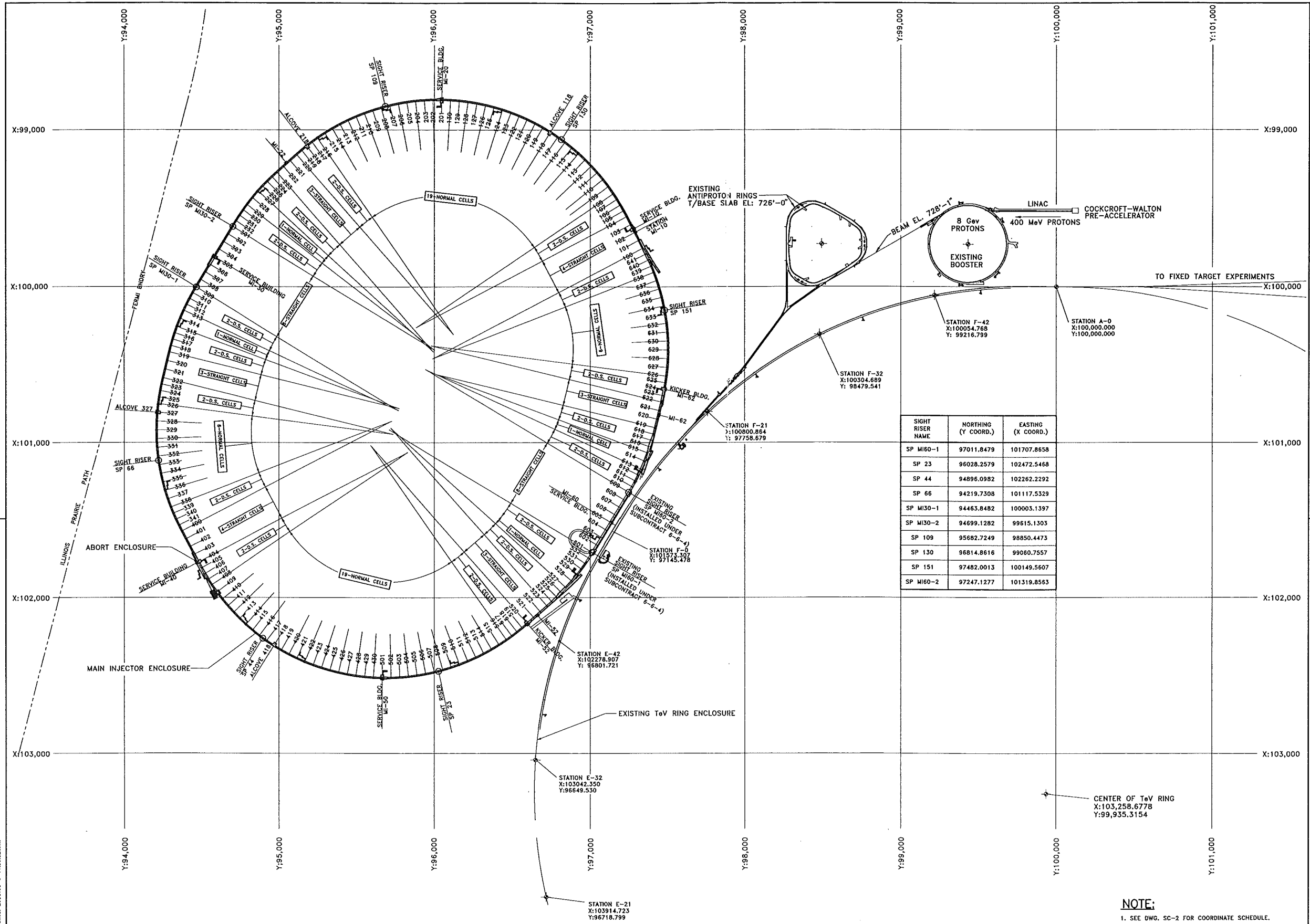
DRAWING NO. 6-6-7 C-33 REV. 1

11 FEB. 1984

REV.	DATE	DESCRIPTION
1	2/11/94	POSTED AMENDMENT 1

FLUOR DANIEL	
PROJECT NO. - 21842300	
DESIGNED	R. JEDZIMIAK 7/16/93
DRAWN	R. DELA CRUZ 7/16/93
CHECKED	B. ZELINSKI 7/16/93
APPROVED	R. BRUNTON

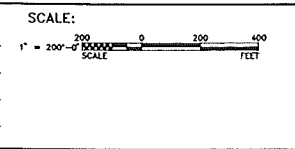
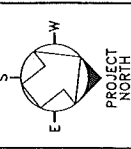
CONCEPT	T. LACKOWSKI
REVIEWED	C. FEDEROWICZ
REVIEWED	E. CRUMPLEY
APPROVED	TOM PAWLAK WAYNE NESTANDER
SUBMITTED	DIXON BOGERT



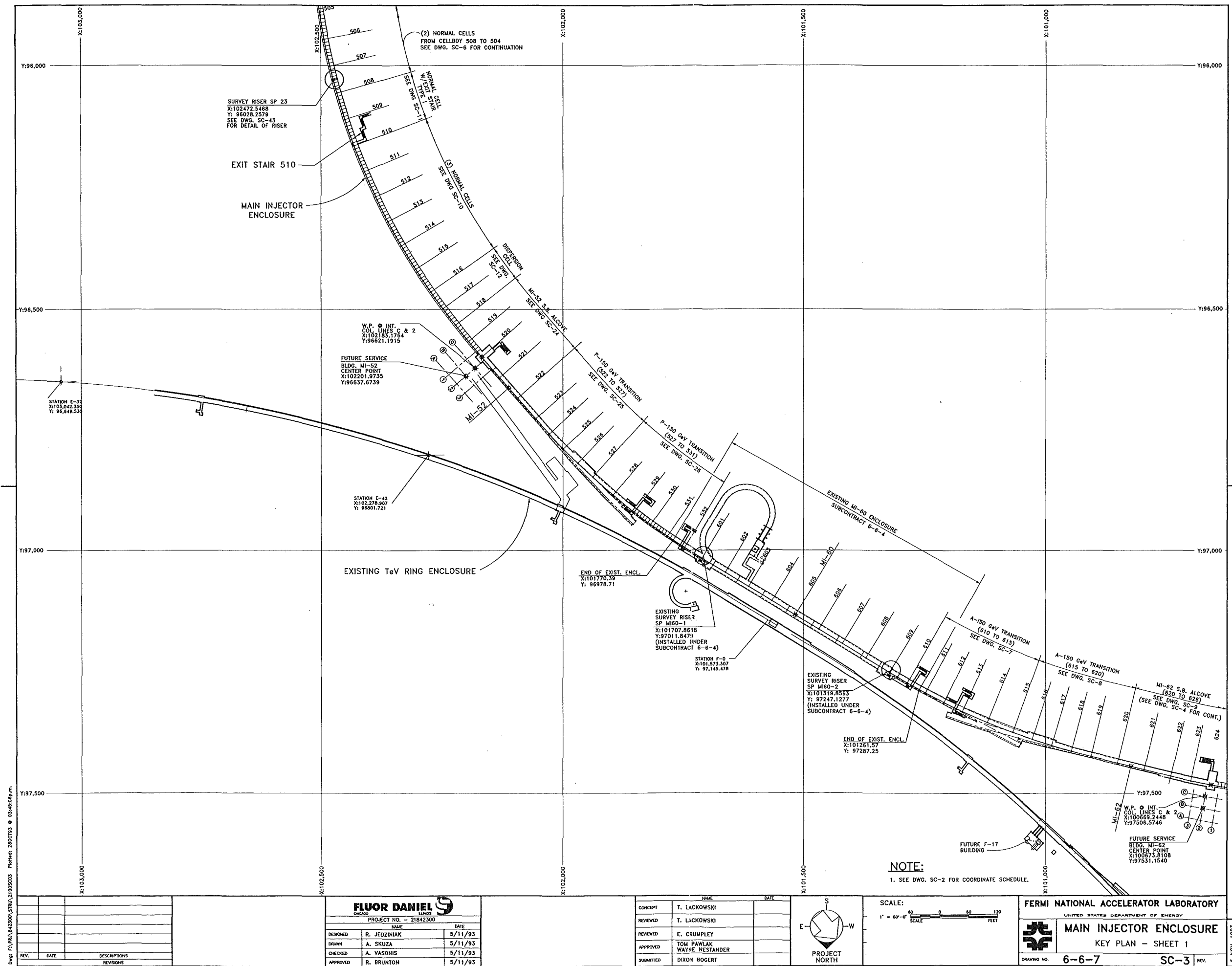
REV.	DATE	DESCRIPTIONS

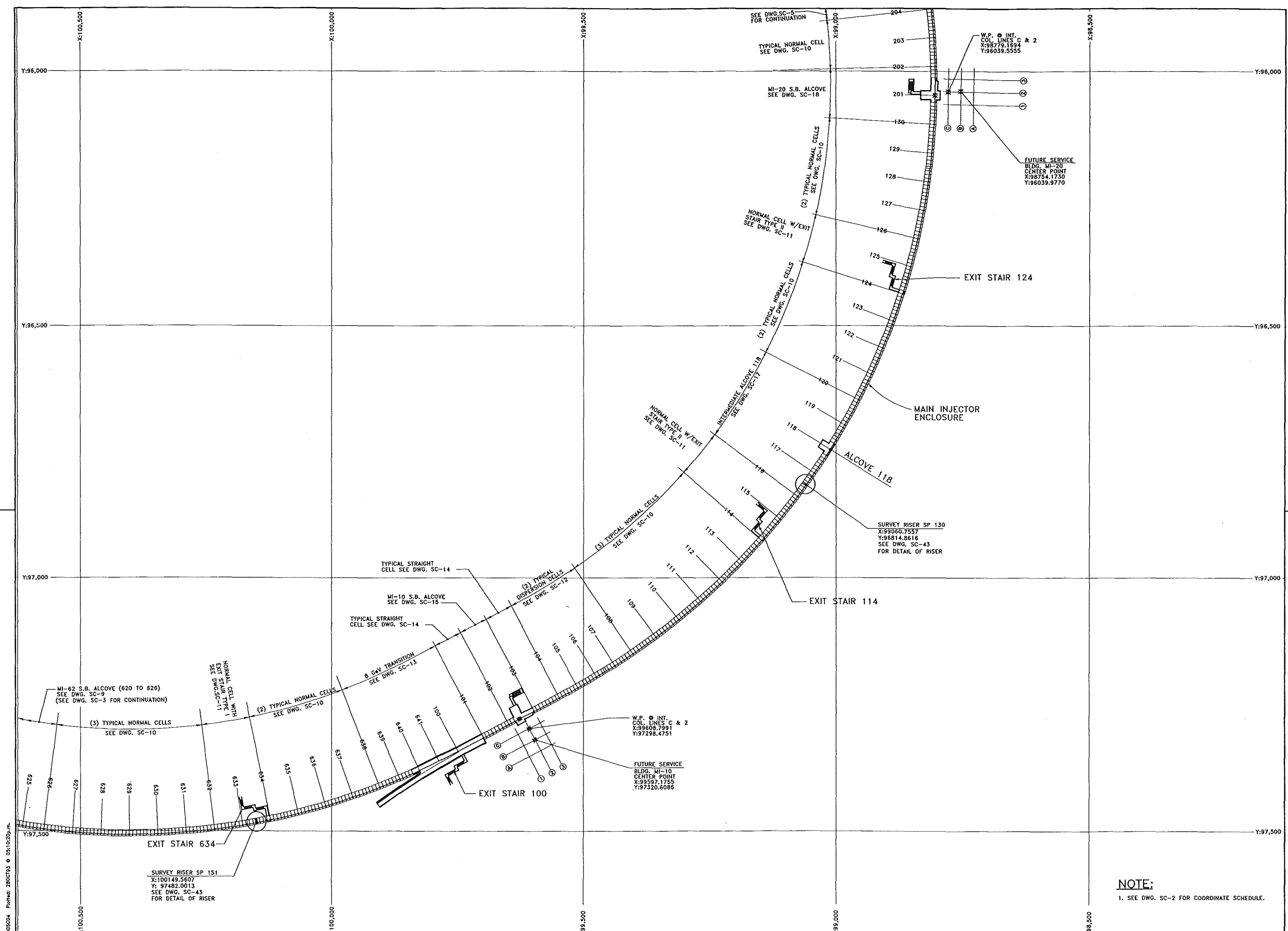
FLUOR DANIEL CHICAGO ILLINOIS PROJECT NO. - 21642300		
DESIGNED	R. JEDZINIAK	7/16/93
DRAWN	A. DELACRUZ	7/16/93
CHECKED	A. VASONIS	7/16/93
APPROVED	R. BRUNTON	7/16/93

CONCEPT	NAME	DATE
REVIEWED	T. LACKOWSKI	
REVIEWED	E. GRUMPLEY	
APPROVED	TOM PAWLAK WAYNE NESTANDER	
SUBMITTED	DIXON BOGERT	



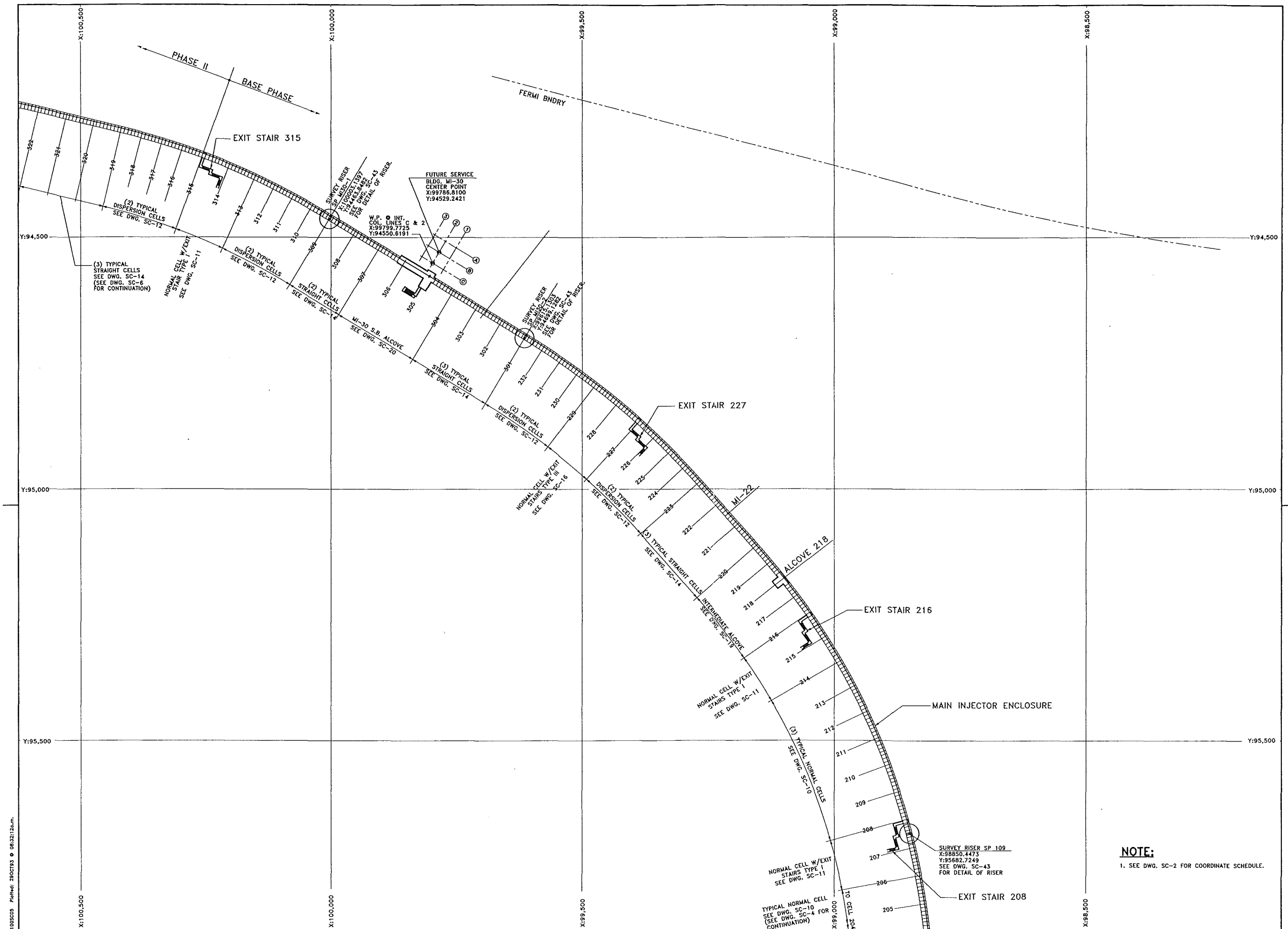
Fermi National Accelerator Laboratory
 UNITED STATES DEPARTMENT OF ENERGY
MAIN INJECTOR ENCLOSURE
 BEAMLINE GEOMETRICS
 DRAWING NO. 6-6-7 SC-1 REV. 5 NOV. 1993





NOTE:
1. SEE DWG. SC-2 FOR COORDINATE SCHEDULE.

<table border="1" style="width: 100%; border-collapse: collapse;"> <tr><th>REV.</th><th>DATE</th><th>DESCRIPTION</th></tr> <tr><td> </td><td> </td><td> </td></tr> <tr><td> </td><td> </td><td> </td></tr> <tr><td> </td><td> </td><td> </td></tr> </table>		REV.	DATE	DESCRIPTION										FLUOR DANIEL <small>CHICAGO ILLINOIS</small> PROJECT NO. - 21842300		<table border="1" style="width: 100%; border-collapse: collapse;"> <tr><th>NAME</th><th>DATE</th></tr> <tr><td>DESIGNED</td><td>R. JEDZINIAK 4/29/93</td></tr> <tr><td>DRAWN</td><td>A. SKUZA 4/29/93</td></tr> <tr><td>CHECKED</td><td>A. VASONIS 4/29/93</td></tr> <tr><td>APPROVED</td><td>R. BRUNTON 4/29/93</td></tr> </table>		NAME	DATE	DESIGNED	R. JEDZINIAK 4/29/93	DRAWN	A. SKUZA 4/29/93	CHECKED	A. VASONIS 4/29/93	APPROVED	R. BRUNTON 4/29/93	<table border="1" style="width: 100%; border-collapse: collapse;"> <tr><th>NAME</th><th>DATE</th></tr> <tr><td>CONCEPT</td><td>T. LACKOWSKI</td></tr> <tr><td>REVIEWED</td><td>T. LACKOWSKI</td></tr> <tr><td>REVIEWED</td><td>E. CRUMPLEY</td></tr> <tr><td>APPROVED</td><td>TOM PAWLAK WAYNE NESTANDER</td></tr> <tr><td>SUBMITTED</td><td>DIXON BOGERT</td></tr> </table>		NAME	DATE	CONCEPT	T. LACKOWSKI	REVIEWED	T. LACKOWSKI	REVIEWED	E. CRUMPLEY	APPROVED	TOM PAWLAK WAYNE NESTANDER	SUBMITTED	DIXON BOGERT	 PROJECT NORTH	SCALE: 1" = 60'-0" SCALE	Fermi National Accelerator Laboratory <small>UNITED STATES DEPARTMENT OF ENERGY</small> MAIN INJECTOR ENCLOSURE KEY PLAN - SHEET 2 DRAWING NO. 6-6-7 SC-4 REV.		5 NOV. 1993
		REV.	DATE	DESCRIPTION																																										
NAME	DATE																																													
DESIGNED	R. JEDZINIAK 4/29/93																																													
DRAWN	A. SKUZA 4/29/93																																													
CHECKED	A. VASONIS 4/29/93																																													
APPROVED	R. BRUNTON 4/29/93																																													
NAME	DATE																																													
CONCEPT	T. LACKOWSKI																																													
REVIEWED	T. LACKOWSKI																																													
REVIEWED	E. CRUMPLEY																																													
APPROVED	TOM PAWLAK WAYNE NESTANDER																																													
SUBMITTED	DIXON BOGERT																																													



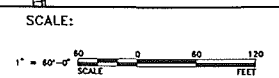
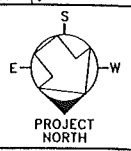
NOTE:
1. SEE DWG. SC-2 FOR COORDINATE SCHEDULE.

DWG. FL-PR-043200-STR-01050005 Plotfile: 2900793 © 08/30/2005

REV.	DATE	DESCRIPTIONS

FLUOR DANIEL <small>CHICAGO ILLINOIS</small>		
PROJECT NO. - Z1842300		
DESIGNED	R. JEDZINIAK	7/13/93
DRAWN	A. SKUZA	7/13/93
CHECKED	A. VASONIS	7/13/93
APPROVED	R. BRUNTON	7/23/93

	NAME	DATE
CONCEPT	T. LACKOWSKI	
REVIEWED	T. LACKOWSKI	
REVIEWED	E. CRUMPLEY	
APPROVED	TOM PAWLAK WAYNE NESTANDER	
SUBMITTED	DIXON BOGERT	

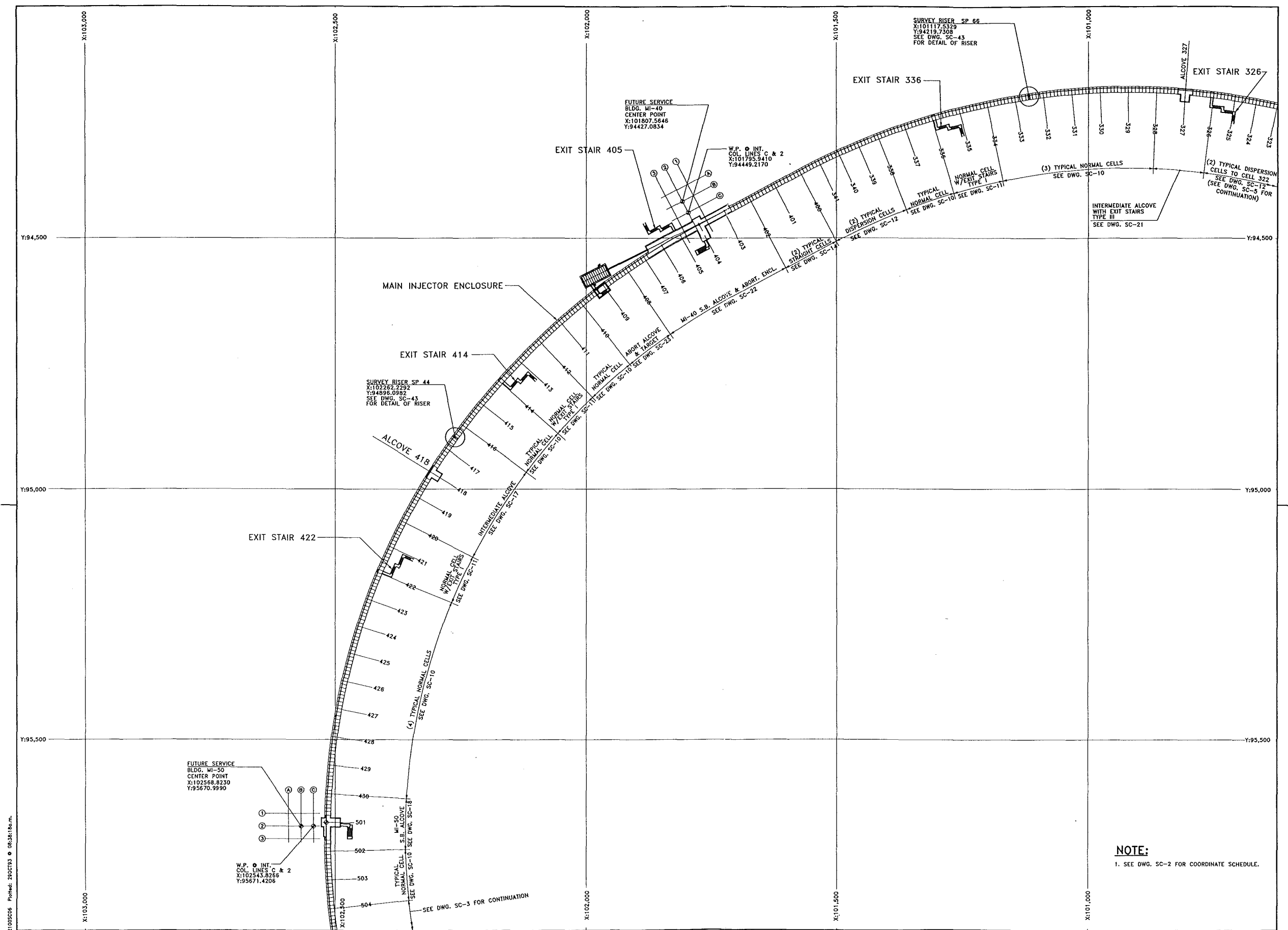


FERMI NATIONAL ACCELERATOR LABORATORY
 UNITED STATES DEPARTMENT OF ENERGY

MAIN INJECTOR PROJECT
 KEY PLAN - SHEET 3

DRAWING NO. **6-6-7** **SC-5** REV.

5 NOV. 1993



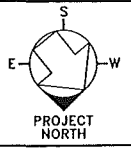
NOTE:
1. SEE DWG. SC-2 FOR COORDINATE SCHEDULE.

Dwg: F:\P\A\642300\STRN\2100SC06 Plot: 2001193 08/31/1993

REV.	DATE	DESCRIPTIONS

FLUOR DANIEL <small>DESIGN</small>		
PROJECT NO. - 21842300		
DESIGNED	R. JEDZINIAK	4/29/93
DRAWN	A. SKUZA	4/29/93
CHECKED	A. VASONIS	4/30/93
APPROVED	R. BRUNTON	4/30/93

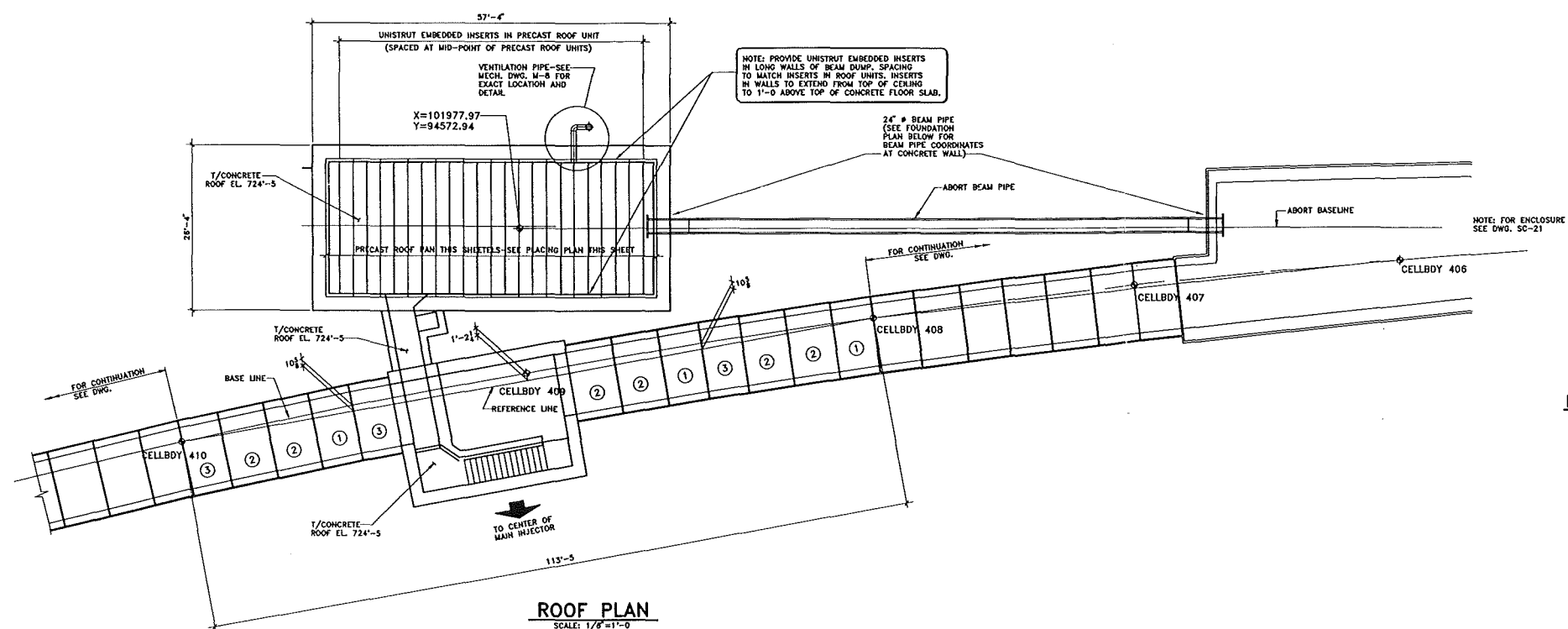
NAME	DATE
CONCEPT	T. LACKOWSKI
REVIEWED	T. LACKOWSKI
REVIEWED	E. CRUMPLEY
APPROVED	TOM PAWLAK WAYNE NESTANDER
SUBMITTED	DIXON BOGERT



Fermi National Accelerator Laboratory
 UNITED STATES DEPARTMENT OF ENERGY

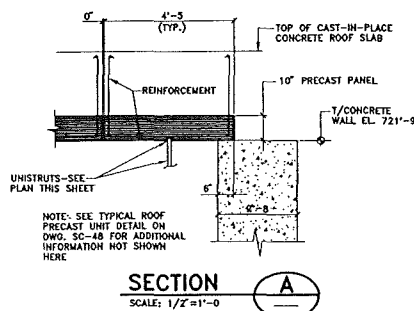
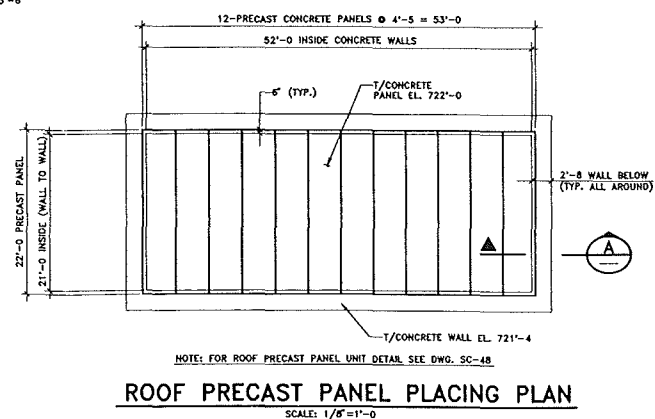
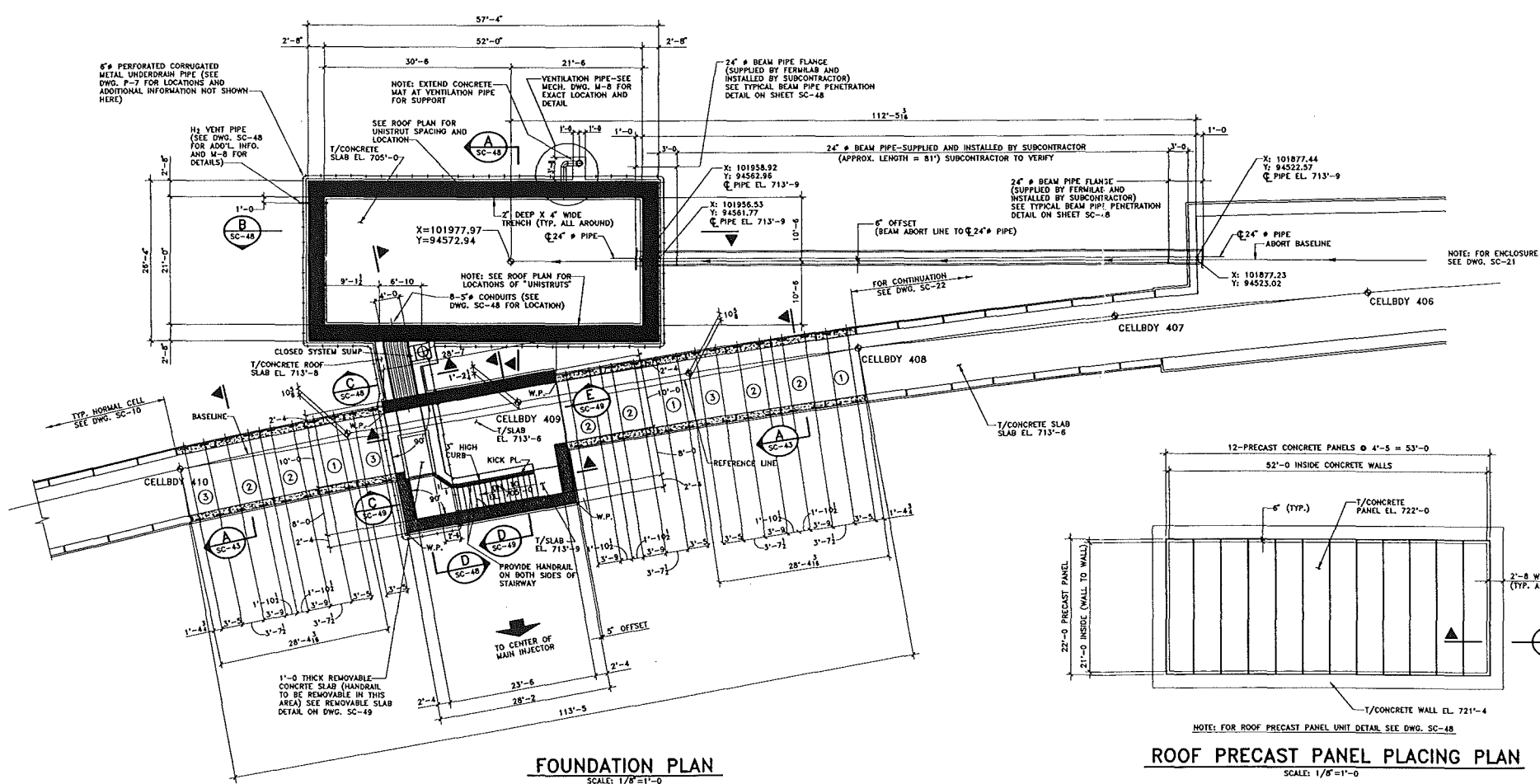
MAIN INJECTOR ENCLOSURE
 KEY PLAN - SHEET 4

DRAWING NO. **6-6-7** SC-6 REV. 5 NOV. 1993

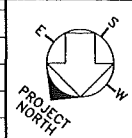


- NOTES:**

1. FOR LOCATION, SEE KEY PLAN ON DWG. SC-6.
2. FOR UNDERDRAINS REFER TO DWG. P-7.
3. FOR DETAILS NOT SHOWN RELATED TO THE PRECAST INCLUDING BASE SLAB, EMBEDDED ATTACHMENT ANGLE, AND PRECAST JOINTS, SEE THE SLAB AND ROOF PLAN FOR A TYPICAL NORMAL CELL ON DWG. SC-10.
4. EDGE OF SLAB, CAST-IN-PLACE WALLS AND PRECAST ELEMENTS SHALL BE OFFSET FROM THE BASELINE THE DISTANCE SHOWN ON THE DRAWING. REFER TO THE WALLS, WHERE INDICATED, SHALL BE USED WITH THE CELLBOY COORDINATES TO LOCATE BASE AND CENTERLINES.
5. TRANSVERSE CONSTRUCTION JOINTS IN CAST-IN-PLACE CONCRETE SHALL BE SPACED AS SHOWN ON THE PLANS AS A MINIMUM, SPACING SHALL NOT EXCEED 6'-0" WHERE JOINTS ARE NOT SHOWN.
6. ALL CAST-IN-PLACE CONSTRUCTION JOINTS SHALL BE DOVEILED IN ACCORDANCE WITH THE TYPICAL CONCRETE SECTIONS AND DETAILS.
7. UNDERDRAINS SHALL BE CONTINUOUS AND SHALL BE INSTALLED ON EACH SIDE OF THE ENCLOSURE AS SHOWN ON THE TYPICAL UNDERDRAIN DETAIL ON DWG. SC-41. UNDERDRAIN PIPING SHALL BE ROUTED TO THE ALCOHOL TANK AS SHOWN ON DWG. P-7.
8. SEE PLANS ON DWG'S E-15 AND E-29 FOR INFORMATION ON THE UNDERDRAIN SYSTEM. EMBEDDED ATTACHMENT ANGLE

[illegible]

	NAME	DATE
DESIGNED	M. GRIMSON	
DRAWN	D. KILLIAN	
CHECKED	LACKOWSKI/CRUMPLEY	
APPROVED	NESTANDER/PAWLAK	
SUBMITTED	DIXON BOGERT	



SCALE:

$1/2" = 1'-0"$

1 0 1 2 3 4 5
SCALE FEET

$1/8" = 1'-0"$

0 8 16
SCALE FEET

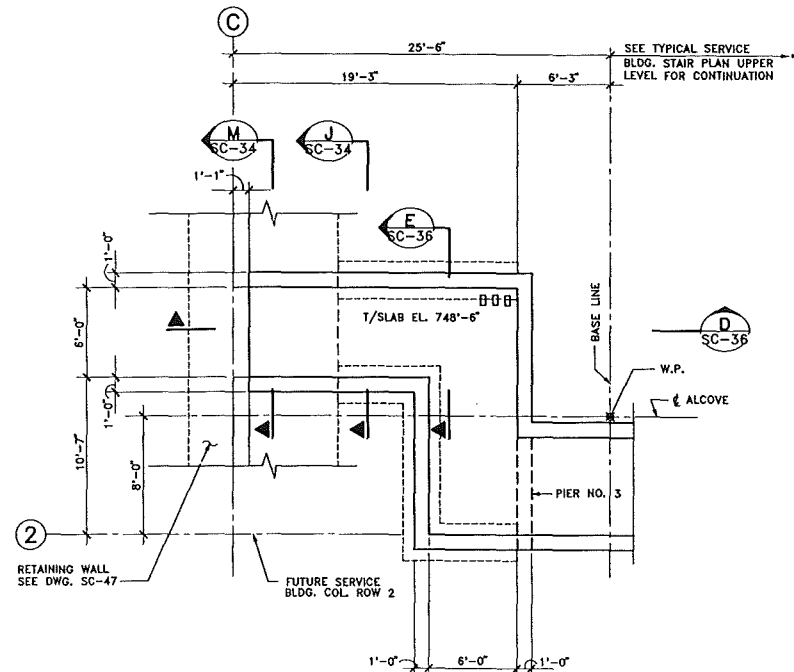
FERMI NATIONAL ACCELERATOR LABORATORY

UNITED STATES DEPARTMENT OF ENERGY

MAIN INJECTOR ENCLOSURE

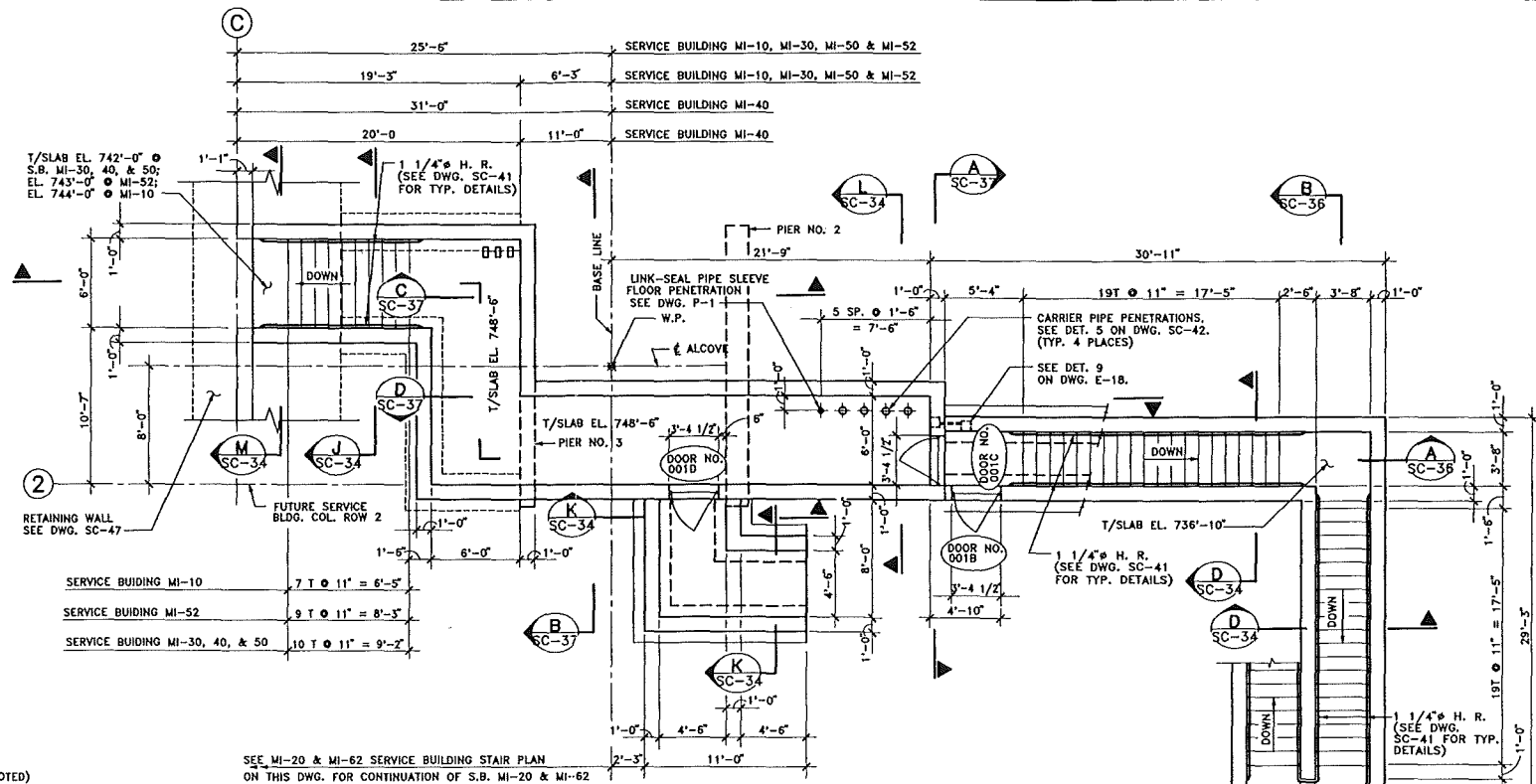
MAIN INJECTOR ENCLOSURE

	ABORT ALCOVE & BEAM DUMP		
	DRAWING NO.	6-6-7	SC-23 REV.



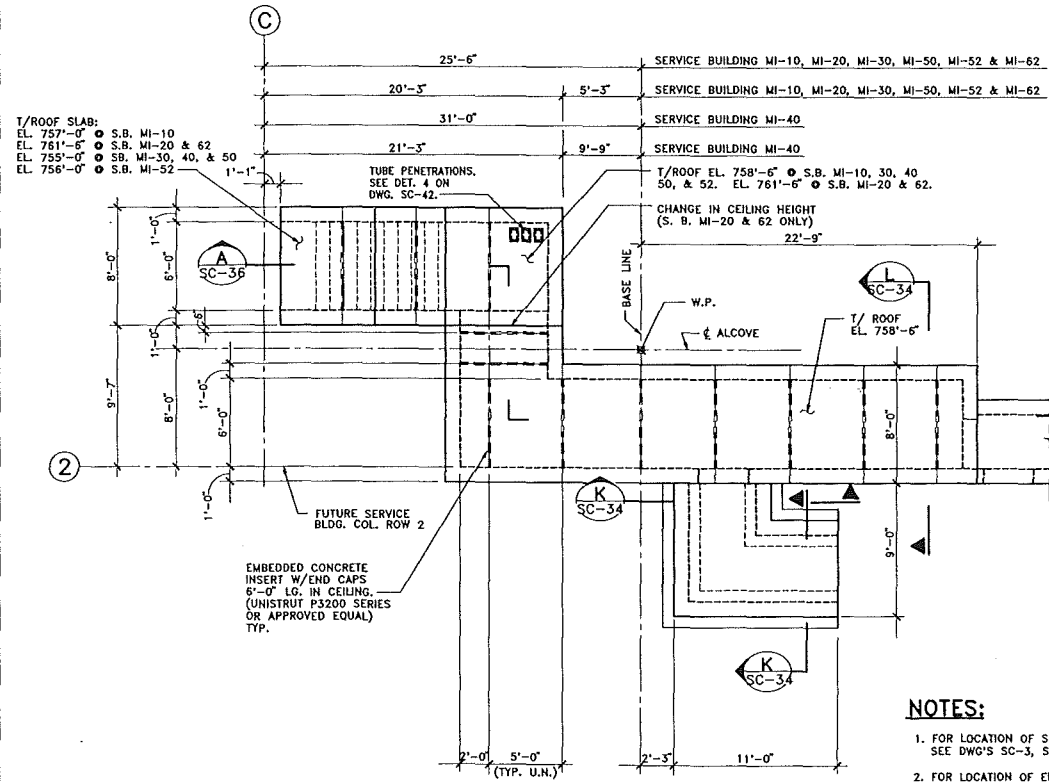
MI-20 SERVICE BUILDING STAIR PLAN (AS SHOWN & AS NOTED)

MI-62 SERVICE BUILDING STAIR PLAN (OPP. HAND ABOUT & ALCOVE & AS NOTED)



TYPICAL SERVICE BUILDING STAIR PLAN

(MI-10, MI-20, MI-30, MI-40, MI-50 & MI-62 AS SHOWN & NOTED)
(MI-62 OPPOSITE HAND ABOUT & ALCOVE & AS NOTED)

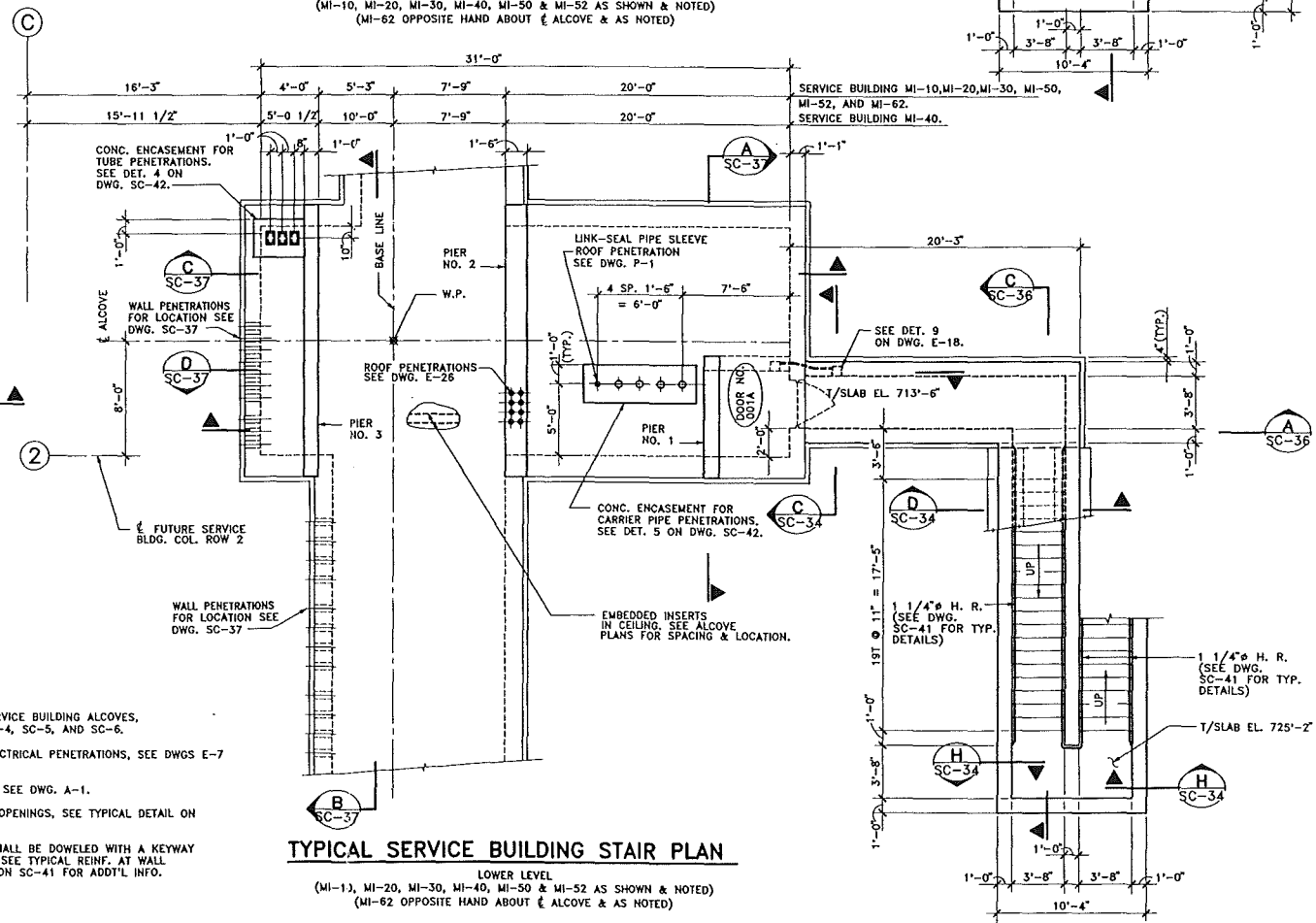


TYPICAL SERVICE BUILDING STAIR ROOF PLAN

(MI-10, MI-20, MI-30, MI-40, MI-50 & MI-62 AS SHOWN & NOTED)
(MI-62 OPPOSITE HAND ABOUT & ALCOVE & AS NOTED)

NOTES:

1. FOR LOCATION OF SERVICE BUILDING ALCOVES, SEE DWG'S SC-3, SC-4, SC-5, AND SC-6.
2. FOR LOCATION OF ELECTRICAL PENETRATIONS, SEE DWGS E-7 THRU E-19.
3. FOR DOOR SCHEDULE, SEE DWG. A-1.
4. FOR REINF. AT DOOR OPENINGS, SEE TYPICAL DETAIL ON DWG. SC-41.
5. ALL CONST. JOINTS SHALL BE DOWELED WITH A KEYWAY AND 6" WATERSTOP. SEE TYPICAL REINF. AT WALL INTERSECTION DETAIL ON SC-41 FOR ADD'L INFO.



TYPICAL SERVICE BUILDING STAIR PLAN

(MI-10, MI-20, MI-30, MI-40, MI-50 & MI-62 AS SHOWN & NOTED)
(MI-62 OPPOSITE HAND ABOUT & ALCOVE & AS NOTED)

DWG. NO. 642300, STRUC. 2105235, PLOT: 27JUL93, 07:09:49am

FLUOR DANIEL		
PROJECT NO. - 21842300		
DESIGNED	DATE	
A. VASONIS	7/23/93	
DRAWN	DATE	
I. MASIS	7/23/93	
CHECKED	DATE	
S. SETLUR	7/23/93	
APPROVED	DATE	
R. BRUNTON	7/23/93	

DATE	DATE
CONCEPT	T. LACKOWSKI
REVIEWED	T. LACKOWSKI
REVIEWED	E. CRUMPLEY
APPROVED	TOM PAWLAK
SUBMITTED	WAYNE NESTANDER
	DIXON BOGERT

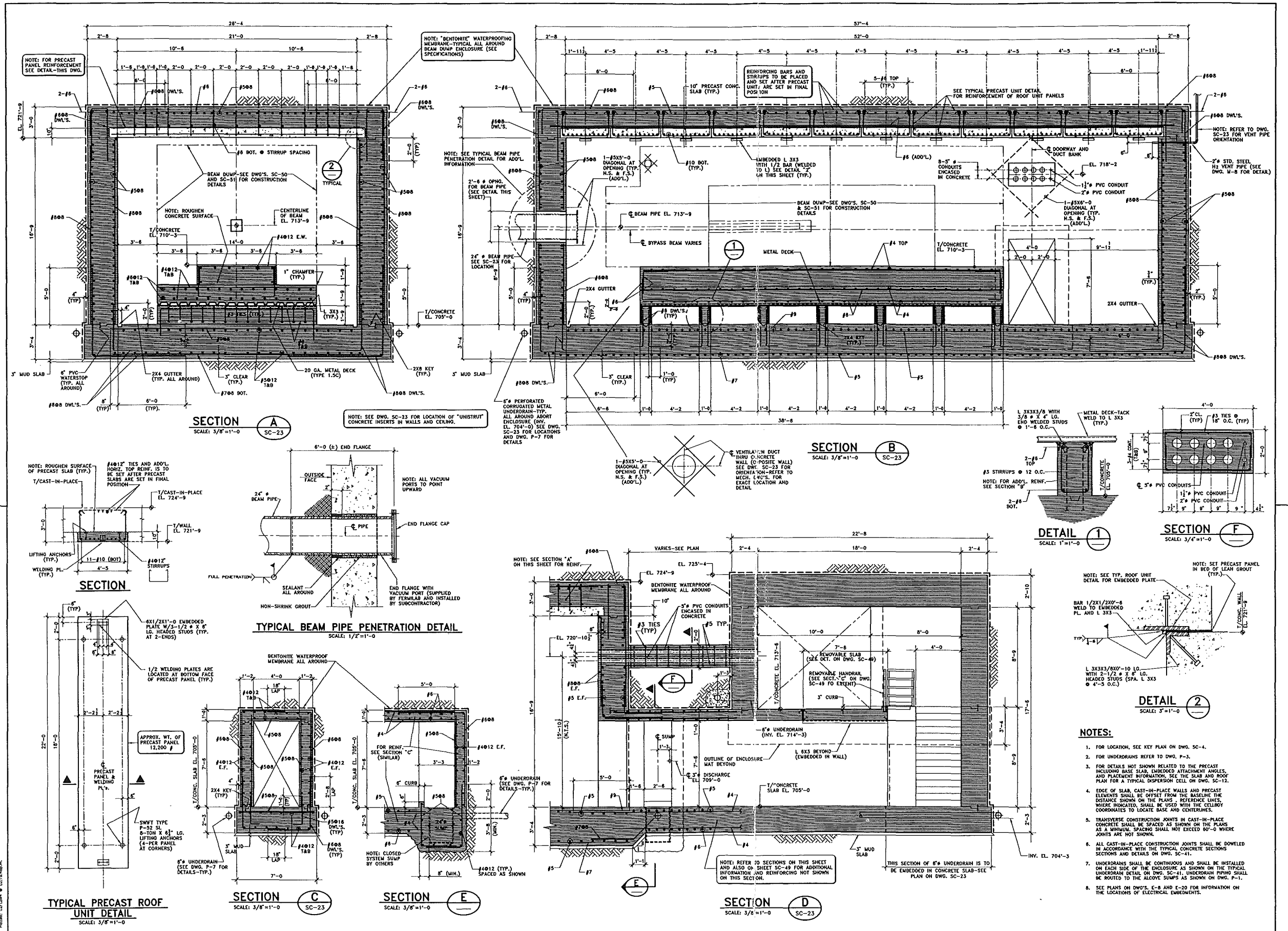


FERMI NATIONAL ACCELERATOR LABORATORY
UNITED STATES DEPARTMENT OF ENERGY

MAIN INJECTOR ENCLOSURE
SERVICE BLDG. EXIT STAIR PLANS

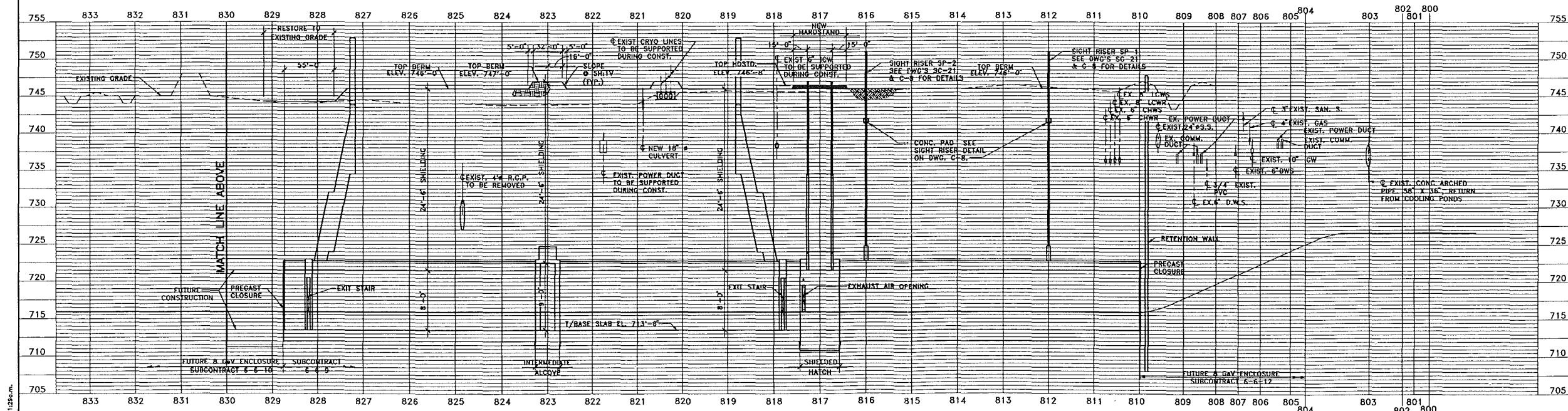
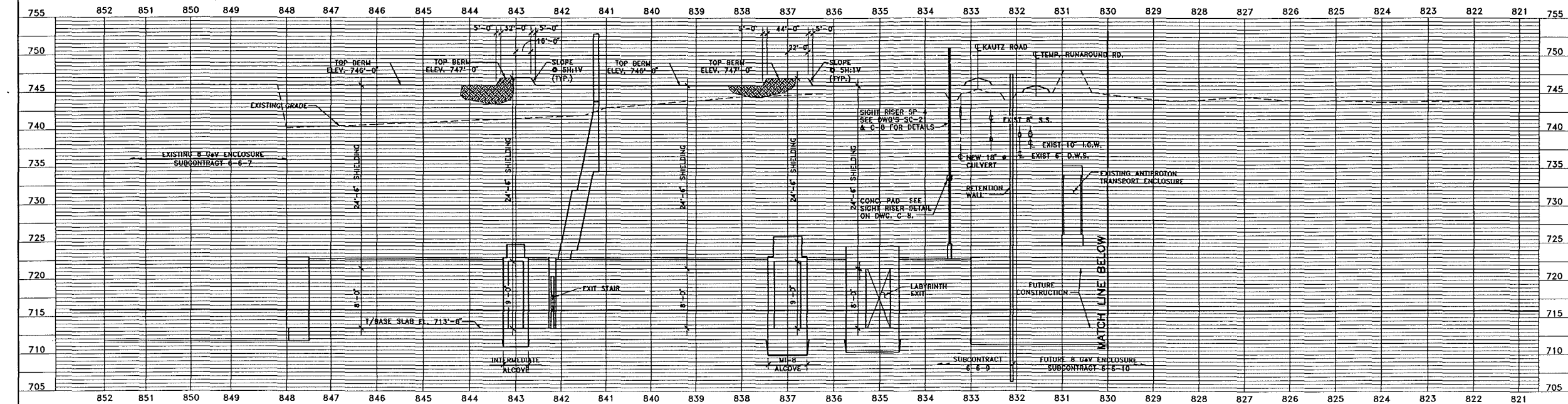
DRAWING NO. 6-6-7 SC-35 REV.

5 NOV. 1993



DESIGNED: M. GRIMSON DRAWN: D. KILLIAN CHECKED: LACKOWSKI/CRUMPLEY APPROVED: NESTANDER/PAWLAK SUBMITTED: DIXON BOGERT		NAME: _____ DATE: _____ SCALE: 0 1 2 3 4 5 6 7 8 9 10 FEET 1"=1'-0" 3/8"=1'-0" 1/2"=1'-0" 3/4"=1'-0" 1"=1'-0"		FERMILAB NATIONAL ACCELERATOR LABORATORY UNITED STATES DEPARTMENT OF ENERGY MAIN INJECTOR ENCLOSURE BEAM DUMP SECTIONS-SHT 1 DRAWING NO. 6-6-7 SC-48 REV. 1	
---	--	--	--	--	--

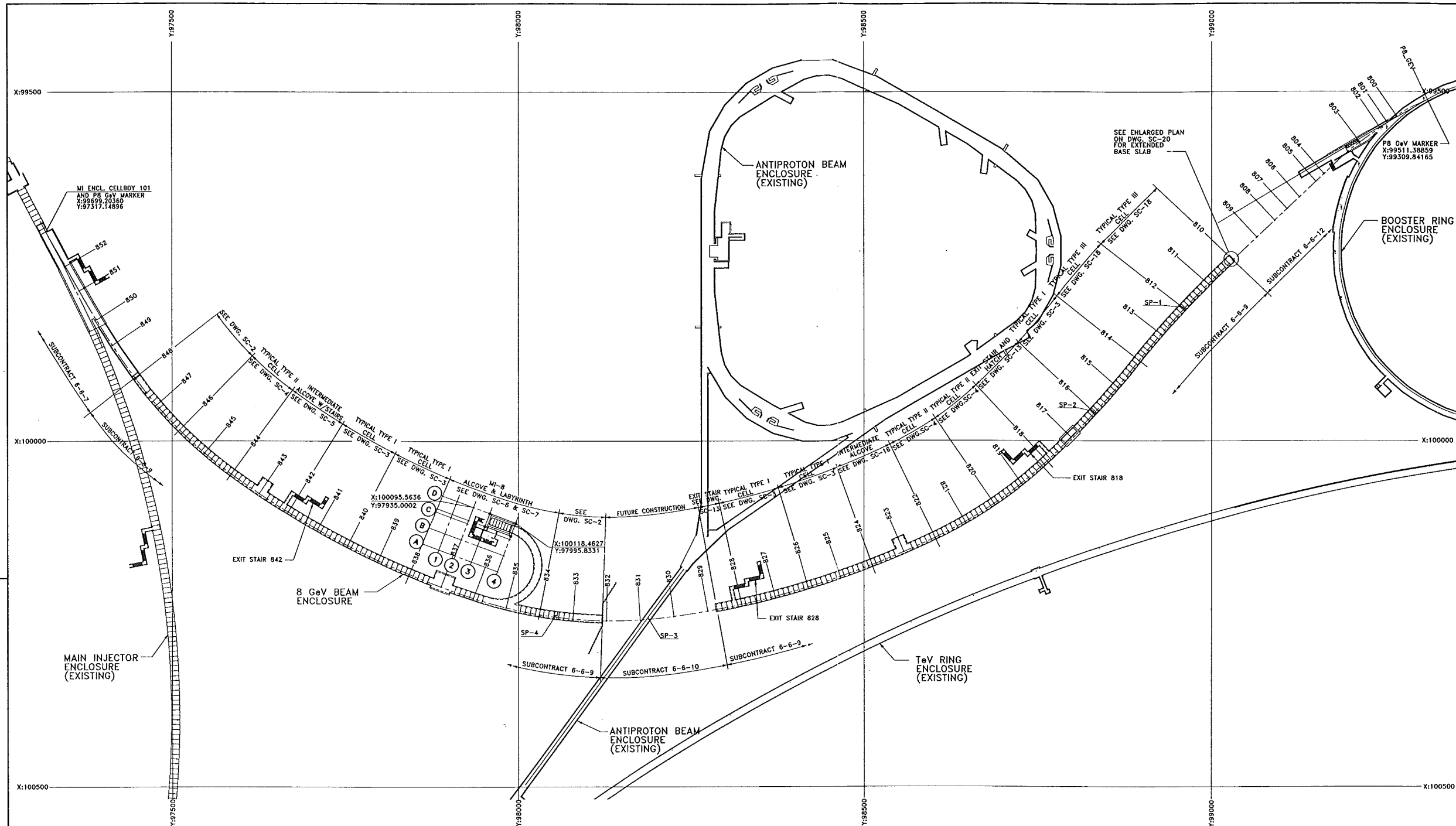
11 FEB. 1994	0
--------------	---



NOTES
 1. WORK THIS DRAWING WITH FINISHED SITE PLAN ON DRAWING C-3.

D:\VIA\44330\3RD\3700002 Plotted: 12AUG94 @ 09:41:28a.m.

<table border="1" style="width: 100%; border-collapse: collapse;"> <tr> <th>REV.</th> <th>DATE</th> <th>DESCRIPTIONS</th> </tr> <tr> <td> </td> <td> </td> <td> </td> </tr> <tr> <td> </td> <td> </td> <td> </td> </tr> <tr> <td> </td> <td> </td> <td> </td> </tr> </table>		REV.	DATE	DESCRIPTIONS										FLUOR DANIEL <small>CHICAGO ILLINOIS</small> PROJECT NO. - 21842300		NAME DESIGNED S. SETLUR DRAWN R. JEDZINIAK CHECKED A. VASONIS APPROVED R. BRUNTON		DATE 12/30/93 12/30/93 2/09/94		NO. & DATE T. LACKOWSKI C. FEDEROWICZ E. CRUMPLEY TOM PAWLAK DAVID HEVIN DIXON BOGERT		SCALE: 1" = 40'-0" HORIZONTAL SCALE 1" = 3'-0" VERTICAL SCALE		Fermi National Accelerator Laboratory <small>UNITED STATES DEPARTMENT OF ENERGY</small> 8 GeV BEAM ENCLOSURE ENCLOSURE LONGITUDINAL SECTION DRAWING NO. 6-6-9 C-2 REV.	
		REV.	DATE	DESCRIPTIONS																					



COORDINATE SCHEDULE			
CELLBODY	X:	Y:	REMARKS
800	99535.00488	99265.99848	
801	99544.31973	99252.82566	
802	99551.66173	99242.44437	
803	99572.14337	99213.48416	
804	99617.24125	99161.69294	
805	99628.08936	99150.12639	
806	99650.20776	99126.54315	
807	99666.86177	99108.78619	
808	99683.51579	99091.02923	
809	99707.51258	99065.44321	
810	99740.01070	99030.79283	
811	99774.06574	98995.21941	
812	99809.46194	98960.98019	
813	99846.14706	98926.12570	

COORDINATE SCHEDULE			
CELLBODY	X:	Y:	REMARKS
814	99884.06696	98896.70443	
815	99922.28763	98865.65284	
816	99959.28749	98833.15621	
817	99995.01195	98799.26249	
818	100029.40828	98764.02170	
819	100061.73896	98726.88723	
820	100091.12390	98687.38068	
821	100117.38971	98645.73516	
822	100140.38141	98602.19639	
823	100160.79902	98557.38410	
824	100179.48045	98511.82088	
825	100196.39813	98465.57337	
826	100211.52709	98418.71043	
827	100224.84502	98371.30100	

COORDINATE SCHEDULE			
CELLBODY	X:	Y:	REMARKS
828	100236.33225	98323.41505	
829	100245.97184	98275.12323	
830	100253.74956	98226.49682	
831	100258.74765	98177.51457	
832	100259.97123	98128.29318	
833	100257.41306	98079.12309	
834	100251.08826	98030.29442	
835	100241.03413	97982.09529	
836	100227.31001	97934.81008	
837	100210.84991	97888.39795	
838	100192.61938	97842.65225	
839	100172.64535	97797.64048	
840	100150.95727	97753.42908	

COORDINATE SCHEDULE			
CELLBODY	X:	Y:	REMARKS
841	100127.58716	97710.08327	
842	100102.56950	97667.66703	
843	100075.94120	97626.24295	
844	100047.74157	97585.87214	
845	100017.29590	97547.17714	
846	99983.96991	97510.93324	
847	99947.96024	97477.35429	
848	99910.62086	97447.47742	
849	99861.59988	97413.02004	
850	99825.01230	97389.49859	
851	99783.67756	97364.93656	
852	99744.10526	97342.35413	

SIGHT RISER SCHEDULE			
MARK	X:	Y:	REMARKS
SP-1	99807.7751	98959.1350	
SP-2	99957.6007	98831.3111	
SP-3	100255.3909	98188.7149	FUTURE CONST.
SP-4	100252.2003	98054.0636	

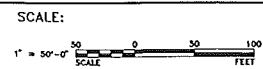
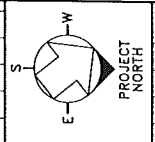
NOTE:
1. THE COORDINATES OF THE CELL BOUNDARIES (CELLBODY'S)
INDICATED ABOVE ARE BASED ON THE FERMILAB SCRIPT FILES
DATED 5-6-94

Dwg: I:\P\1\412300\STRU\27050001 Plotfile: 09AUG94 12:42:27a.m.

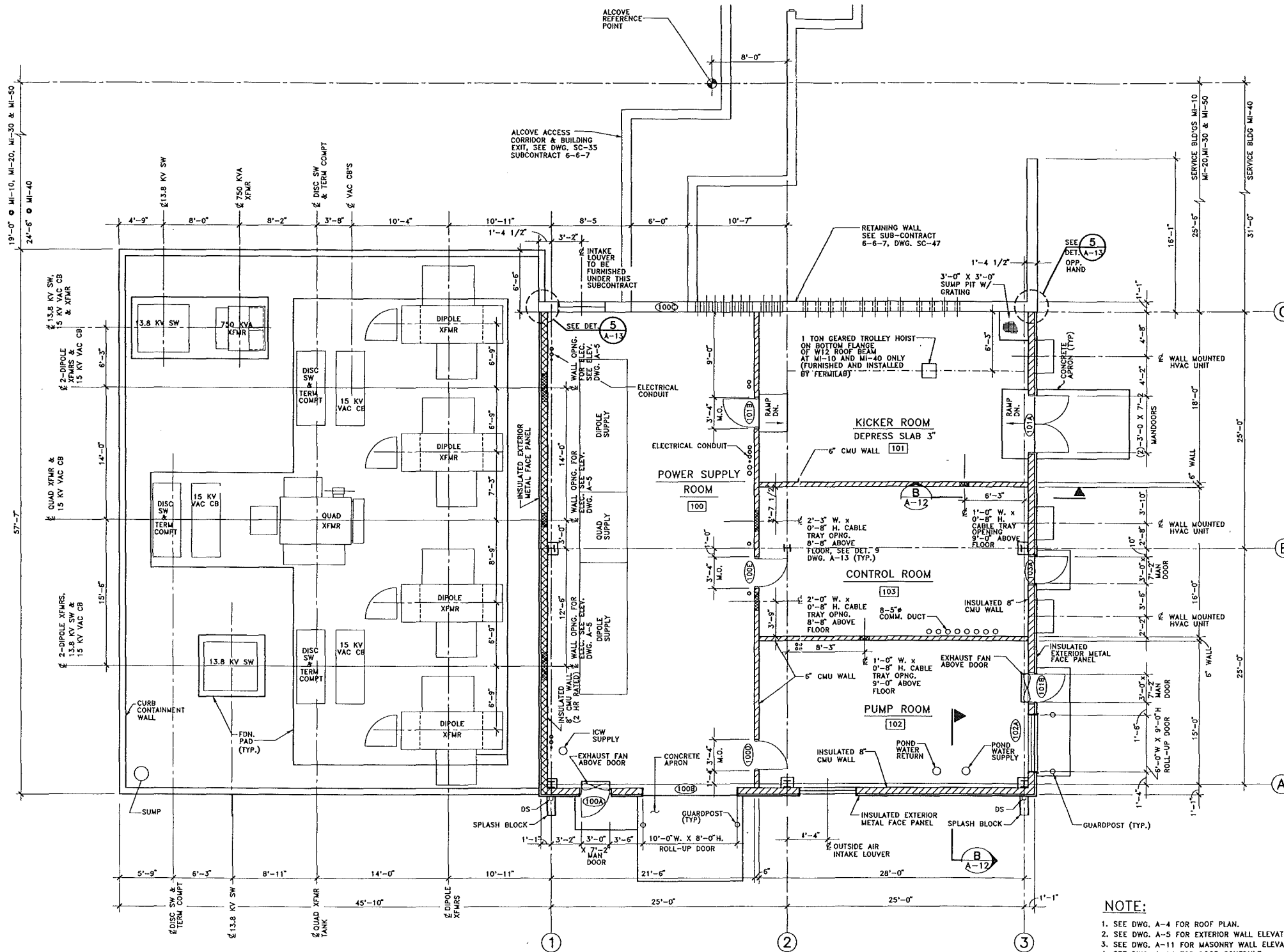
REV.	DATE	DESCRIPTIONS

FLUOR DANIEL		
PROJECT NO. - 21842300		
DESIGNED	S. SETLUR	DATE 11/22/93
DRAWN	I. MASIS	DATE 11/22/93
CHECKED	A. VASONIS	DATE 2/17/94
APPROVED	R. BRUNTON	

	NAME	DATE
CONCEPT	T. LACKOWSKI	
REVIEWED	T. LACKOWSKI	
REVIEWED	E. CRUMPLEY	
APPROVED	TOM PAWLAK DAVID HEVIN	
SUBMITTED	DIXON BOGERT	



FERMI NATIONAL ACCELERATOR LABORATORY		
UNITED STATES DEPARTMENT OF ENERGY		
8 GeV BEAM ENCLOSURE		
KEY PLAN & COORDINATE SCHEDULE		
DRAWING NO.	6-6-9	SC-1 REV.

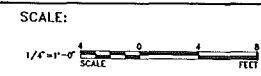


FLOOR PLAN
SERVICE BUILDINGS MI-10, MI-20, MI-30, MI-40, & MI-50

SERVICE BUILDING	T/FLOOR ELEVATION
MI-10	744'-0"
MI-20	748'-5"
MI-30	742'-0"
MI-40	742'-0"
MI-50	742'-0"

- LEGEND:**
- CMU-2HR. RATED
 - CMU-NON RATED
 - METAL SIDING
 - CONCRETE WALL
 - DS = DOWN SPOUT
 - ACT = ACTIVE DOOR
 - XXX = ROOM NUMBER
 - XXX = DOOR NUMBER

- NOTE:**
- SEE DWG. A-4 FOR ROOF PLAN.
 - SEE DWG. A-5 FOR EXTERIOR WALL ELEVATIONS.
 - SEE DWG. A-11 FOR MASONRY WALL ELEVATIONS.
 - SEE DWG. A-14 FOR DOOR SCHEDULE.
 - ALL ELEC. TRANSFORMERS, SWITCHES, CABINETS, ETC., SHOWN IN BACKGROUND ARE CONCEPTUAL AND PRELIMINARY AND WILL BE FURNISHED BY OTHERS. SEE ELECTRICAL DRAWINGS FOR SUBCONTRACTOR INSTALLATION REQUIREMENTS.
 - CONDUIT PENETRATIONS ARE CONCEPTUAL. SEE ELECTRICAL DRAWINGS FOR EXACT NUMBER AND LOCATION.
 - SUBCONTRACTOR SHALL PROVIDE OPENINGS IN MASONRY WALL FOR CABLE TRAYS AS SHOWN. SEE DWGS. E-13, E-20, E-27, E-34, AND E-41 FOR CABLE TRAYS.
 - SUBCONTRACTOR SHALL FIELD DRILL OPENINGS IN CMU WALL FOR SPRINKLER PIPING AND ELECTRICAL CONDUITS. SEE MECH. AND ELEC. DRAWINGS FOR LOCATION AND SIZE.
 - SUBCONTRACTOR TO DEVELOP & SUBMIT FOR APPROVAL ALL DETAILS FOR SEALING OF FIRE-RATED WALLS TO ADJACENT CONSTRUCTION AND SEALING OF ALL PENETRATIONS.



FERMI NATIONAL ACCELERATOR LABORATORY
 UNITED STATES DEPARTMENT OF ENERGY

SERVICE BUILDINGS
 MI-10,20,30,40 & 50 - FLOOR PLAN

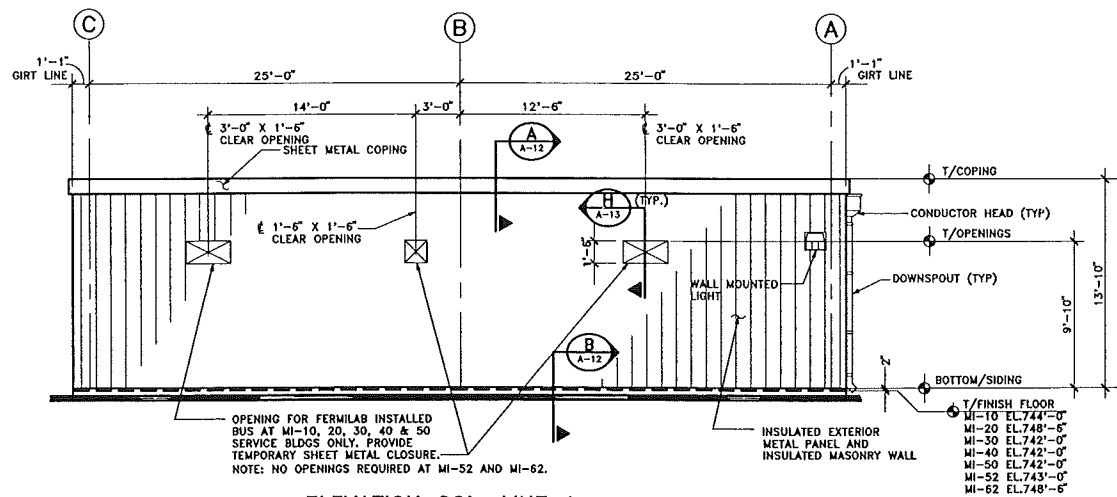
DRAWING NO. **6-6-8** **A-1** REV.

FLUOR DANIEL		
PROJECT NO. - 21842300		
DESIGNED	M. BELLAGAMBA	7/15/93
DRAWN	M. BELLAGAMBA	7/15/93
CHECKED	B. ZELINSKI	9/2/93
APPROVED	R. BRUNTON	

CONCEPT	T. LACKOWSKI	DATE	
REVIEWED	A. TUBINAS S. DIXON		
REVIEWED	E. CRUMPLEY		
APPROVED	TOM PAWLAK DAVID NEVIN		
SUBMITTED	DIXON BOGERT		

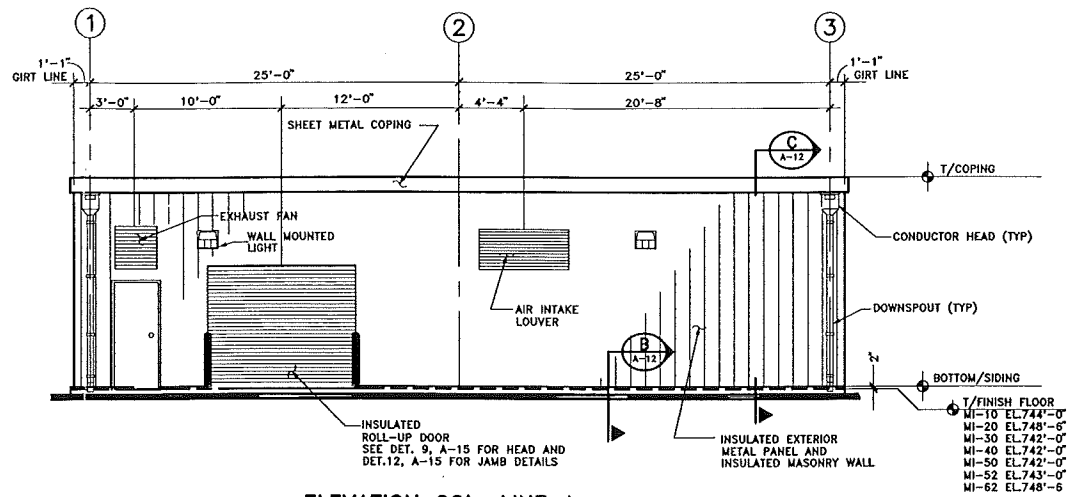
Dwg: F:\PRA\642300\STRU\2455A01 Plotfile: 18APR94 09:37:52Z.m

8 APRIL 1994



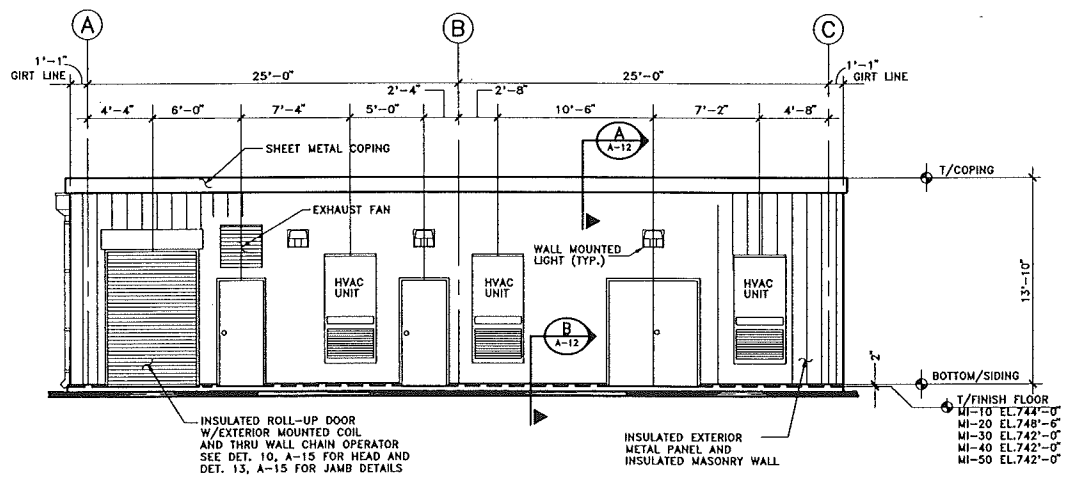
ELEVATION COL. LINE 1

TYP. FOR SERVICE BUILDINGS
MI-10,20,30,40,50,52 & 62



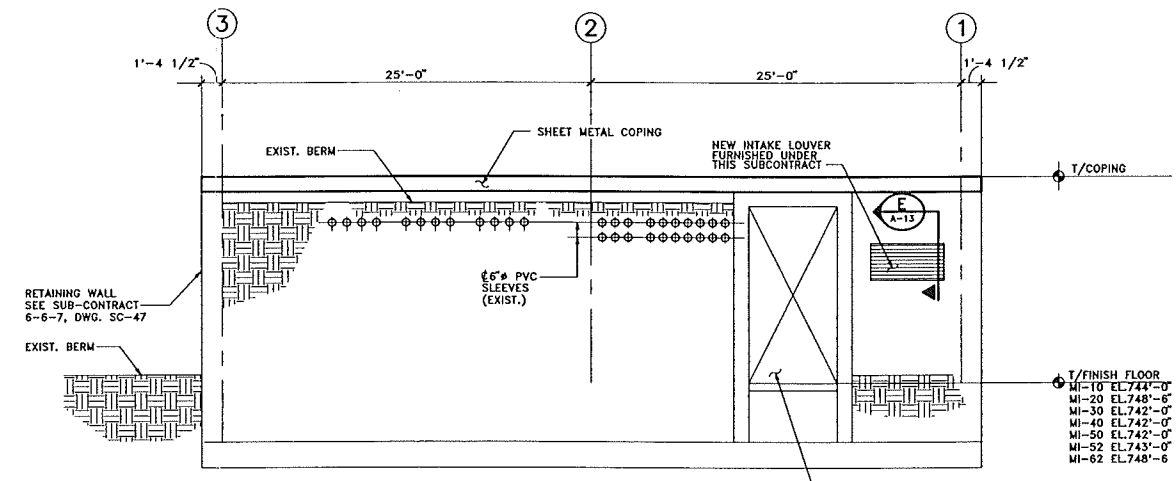
ELEVATION COL. LINE A

TYP. FOR SERVICE BUILDINGS
MI-10,20,30,40,50,52 & 62



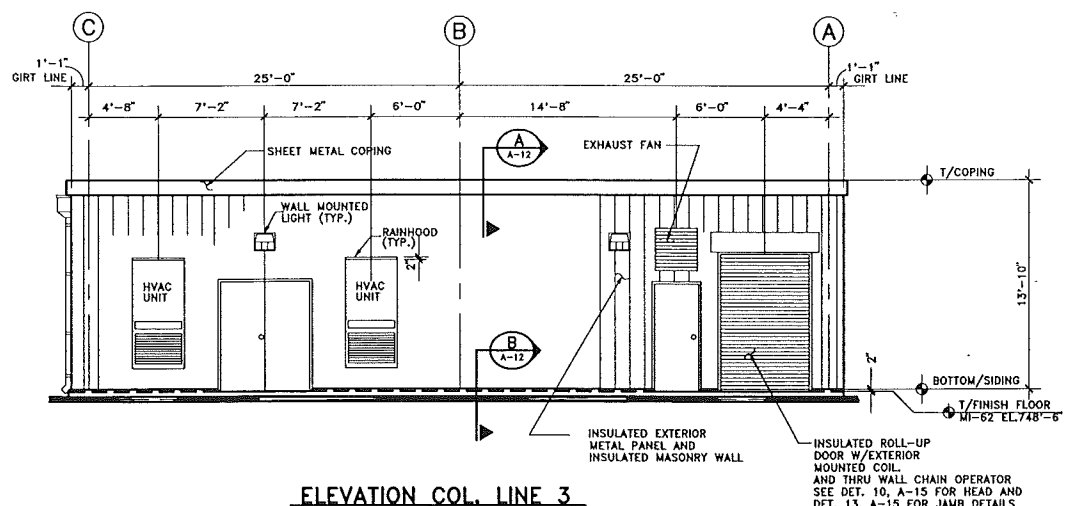
ELEVATION COL. LINE 3

TYP. FOR SERVICE BUILDINGS
MI-10,20,30,40 & 50



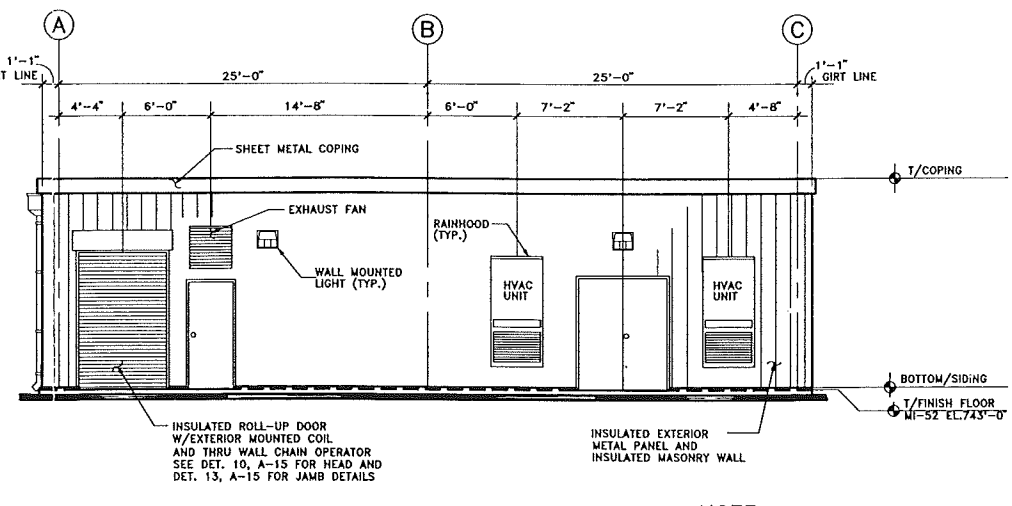
ELEVATION COL. LINE C

TYP. FOR SERVICE BUILDINGS
MI-10,20,30,40,50,52 & 62



ELEVATION COL. LINE 3

SERVICE BUILDING MI-62



ELEVATION COL. LINE 3

SERVICE BUILDING MI-52

NOTE:

1. SEE DWG. A-11 FOR ELEVATIONS OF MASONRY WALL.

DWG: P:\P\A\42300\STUD\2458A03 Plotfile: 11APR94 09:53:28am

REV.	DATE	DESCRIPTIONS

FLUOR DANIEL PROJECT NO. - 21842300		
DESIGNED	M. BELLAGAMBA	7/15/93
DRAWN	M. BELLAGAMBA	7/15/93
CHECKED	B. ZELINSKI	9/2/93
APPROVED	R. BRUNTON	

CONCEPT	NAME	DATE
REVIEWED	T. LACKOWSKI	
REVIEWED	A. TUBINAS	
REVIEWED	S. DIXON	
REVIEWED	E. CRUMPLEY	
APPROVED	TOM PAWLAK	
APPROVED	DAVID HEVIN	
SUBMITTED	DIXON BOGERT	

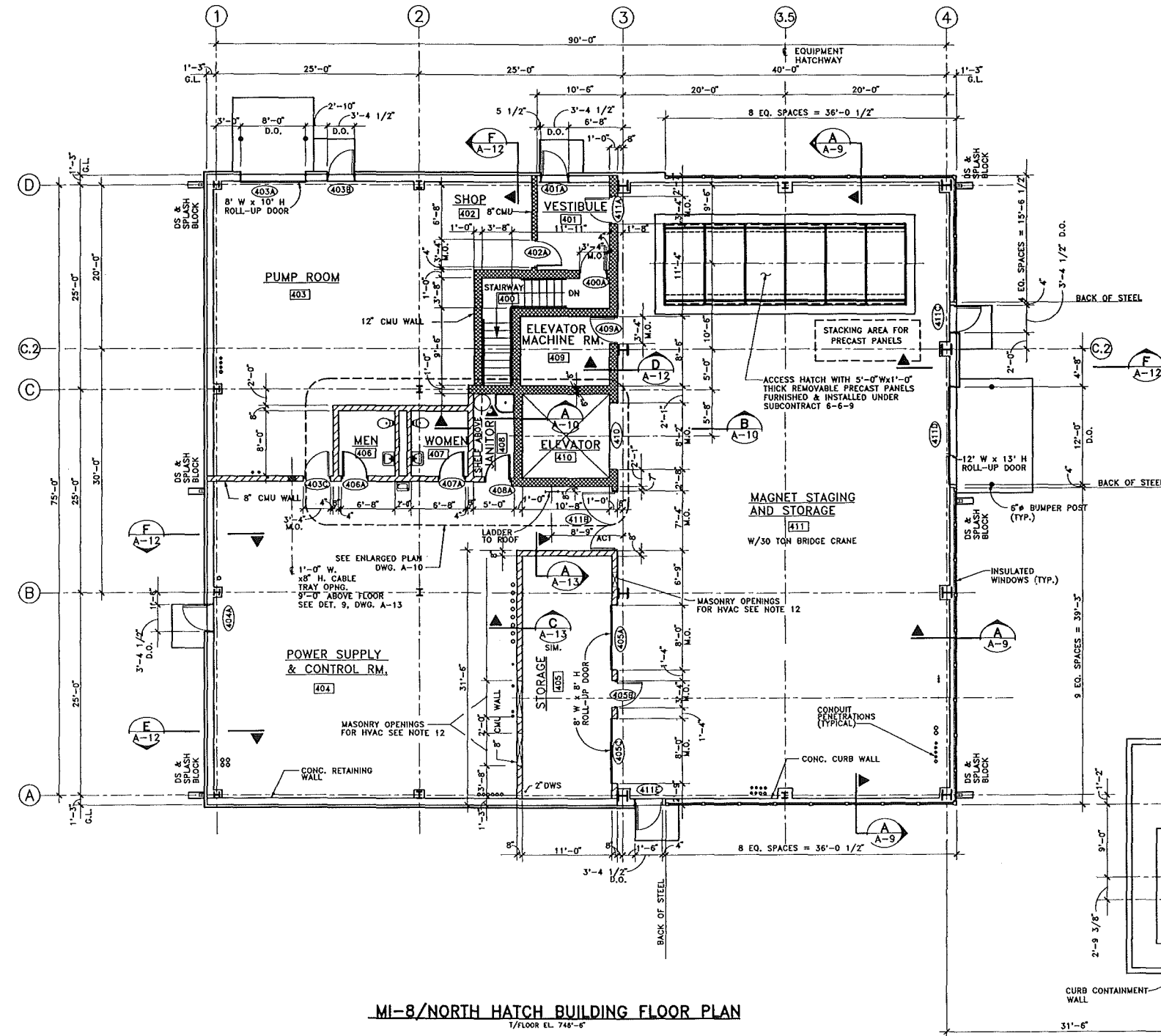
SCALE:
1/4"=1'-0"
SCALE

FERMI NATIONAL ACCELERATOR LABORATORY
UNITED STATES DEPARTMENT OF ENERGY

SERVICE BUILDINGS
MI-10 THRU MI-62 ELEVATIONS

DRAWING NO. **6-6-8** **A-5** REV.

8 APRIL 1994



NOTES:

- SEE DWG'S A-8 & A-9 FOR WALL ELEVATIONS.
- SEE DWG. A-7 FOR ROOF PLAN.
- ALL MASONRY DIMENSIONS ARE NOMINAL.
- ALL CMU WALLS SHALL HAVE HORIZONTAL JOINT REINFORCEMENT @ 16" O.C.
- ALL WALLS ENCLOSING VESTIBULE (401), STAIRWAY (400), ELEVATOR MACHINE ROOM (409) AND THE ELEVATOR (410) SHALL BE 2 HR. FIRE RATED CONSTRUCTION.
- ALL FIRE RATED CONSTRUCTION SHALL BE IN ACCORDANCE WITH U.L. AND F.M. LISTED DETAILS & MATERIALS.
- ALL ELEC. TRANSFORMERS, SWITCHES, CABINETS, ETC., SHOWN IN BACKGROUND ARE CONCEPTUAL AND PRELIMINARY AND WILL BE FURNISHED BY OTHERS. SEE ELECTRICAL DRAWINGS FOR SUBCONTRACTOR INSTALLATION REQUIREMENTS.
- CONDUIT PENETRATIONS ARE CONCEPTUAL. SEE ELECTRICAL DRAWINGS FOR EXACT NUMBER AND LOCATION.
- SUBCONTRACTOR SHALL PROVIDE OPENINGS IN MASONRY WALL FOR CABLE TRAYS AS SHOWN. SEE DWG. E-64 FOR CABLE TRAY.
- SUBCONTRACTOR SHALL FIELD DRILL OPENINGS IN CMU WALL FOR SPRINKLER PIPING AND ELECTRICAL CONDUITS. SEE MECH. AND ELEC. DRAWINGS FOR LOCATION AND SIZE.
- SUBCONTRACTOR TO DEVELOP & SUBMIT FOR APPROVAL ALL DETAILS FOR SEALING OF FIRE-RATED WALLS TO ADJACENT CONSTRUCTION AND SEALING OF ALL PENETRATIONS.
- SUBCONTRACTOR TO FINALIZE AND COORDINATE SIZE AND LOCATION OF WALL OPENINGS IN MASONRY WALL FOR HVAC. SEE DWG. M-7 AND M-9 FOR HVAC LAYOUT. FURNISH GROUTED UNTEL BEAM OVER EACH OPENING WITH 1 #5 REINFORCING BAR.

LEGEND:

- CMU-2HR. RATED (SEE NOTE 11)
- CMU-NON RATED
- METAL SIDING
- WINDOWS
- CONCRETE WALL
- DS = DOWN SPOUT
- ACT = ACTIVE DOOR
- XXX = ROOM NUMBER
- XXX = DOOR NUMBER

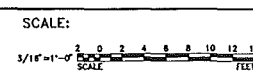
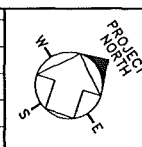
MI-8/NORTH HATCH BUILDING FLOOR PLAN
1/FLOOR EL. 748'-6"

Dwg: F:\P\A\642300\STRN\2458A05 Plotted: 13APR94 @ 02:08:06p.m.

REV.	DATE	DESCRIPTION	REVISIONS

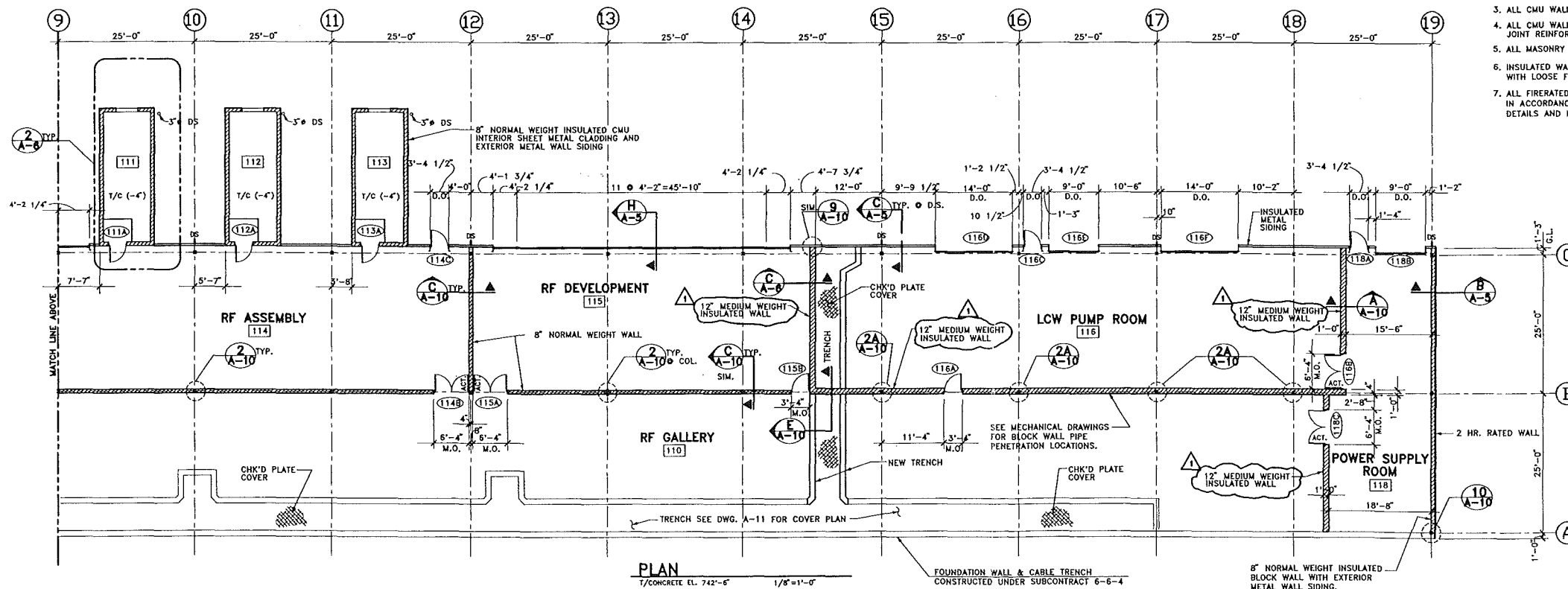
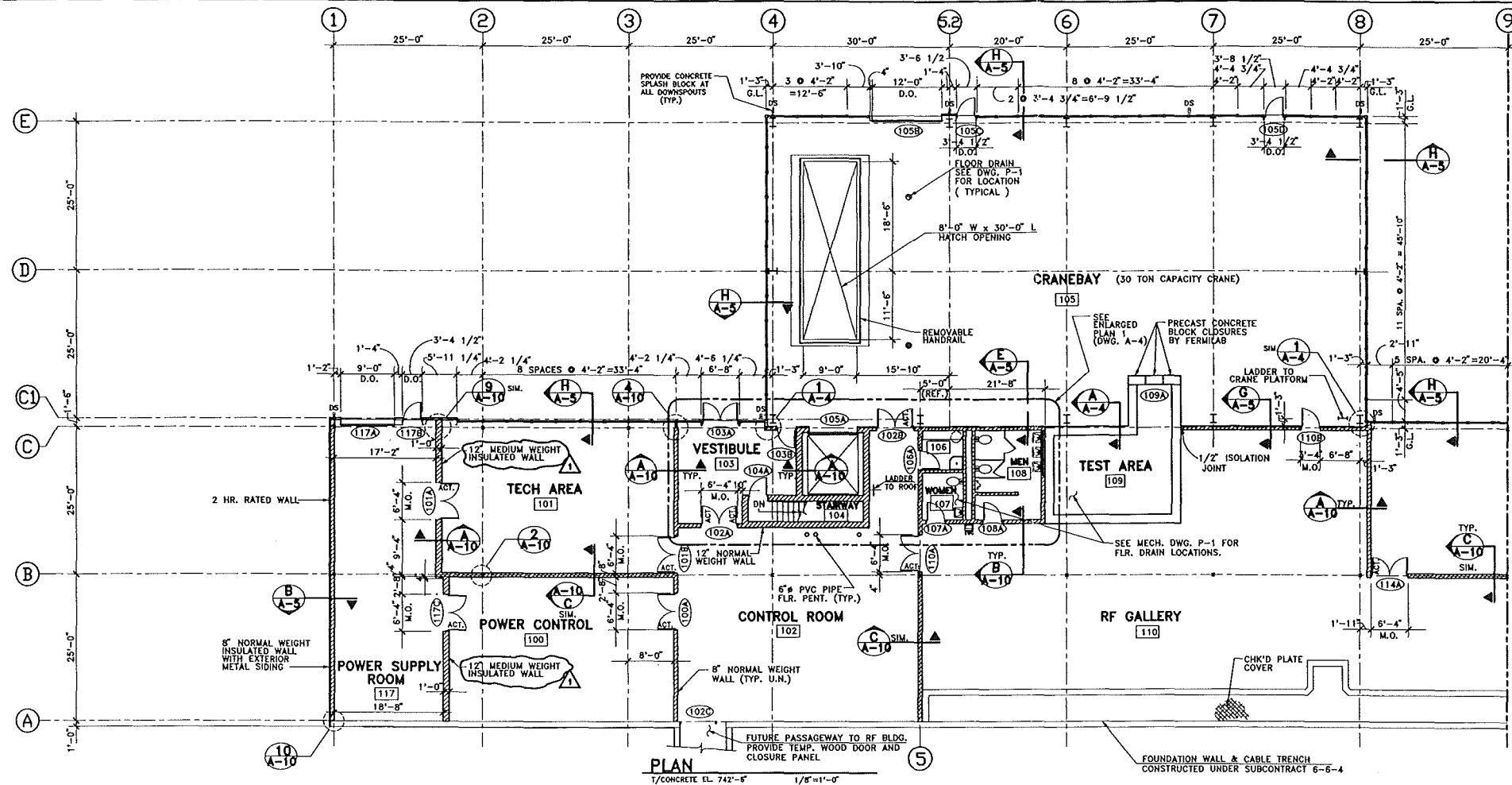
FLUOR DANIEL			
PROJECT NO. - 21642300			
DESIGNED	S. BARADI	DATE	7/19/93
DRAWN	R. DELA CRUZ		7/19/93
CHECKED	D. TALUKDER		10/14/94
APPROVED	R. BRUNTON		

CONCEPT	NAME	DATE
REVIEWED	T. LACKOWSKI	
REVIEWED	A. TUBINAS	
REVIEWED	S. DIXON	
REVIEWED	E. CRUMPLEY	
APPROVED	TOM PAWLAK	
APPROVED	DAVID NEVIN	
SUBMITTED	DIXON BOGERT	



FERMI NATIONAL ACCELERATOR LABORATORY	
UNITED STATES DEPARTMENT OF ENERGY	
SERVICE BUILDINGS	
MI-8/NORTH HATCH BLDG. FLOOR PLAN	
DRAWING NO. 6-6-8	REV. A-6

8 APRIL 1994

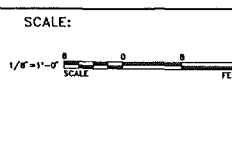
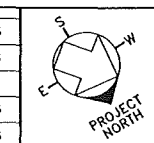


Drawn: J. PAUL, 8/23/93, STRO/321141, Project: 232P93, 1129356.m.

REV.	DATE	DESCRIPTION
1	9/21/93	REV. LIGHTWEIGHT CMU TO MEDIUM WT.
2	4/9/93	POSTED AMENDMENT 1

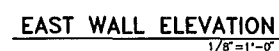
FLUOR DANIEL		
DESIGNED	T. LAREH/J. REDEKER	2/9/93
DRAWN	J. REDEKER	2/9/93
CHECKED	T. LAREH	2/9/93
APPROVED	R. BRUNTON	2/9/93

NAME	DATE
CONCEPT	T. LACKOWSKI
REVIEWED	A. TUBINAS
REVIEWED	S. DIXON
REVIEWED	E. CRUMPLEY
APPROVED	TOM PAWLAK
APPROVED	WAYNE HESTANDER
SUBMITTED	DIXON BOBERT



FERMI NATIONAL ACCELERATOR LABORATORY	
UNITED STATES DEPARTMENT OF ENERGY	
MI-60 SERVICE BUILDING	
FLOOR PLAN	
DRAWING NO.	6-6-5
REV.	A-1

21 SEPT. 1993




\\P8\B42300\STRU\2311A03.DWG

REV.	DATE	DESCRIPTIONS

FLUOR DANIEL CHICAGO ILLINOIS		
PROJECT NO. - 21842300		
NAME		DATE
DESIGNED	T.LAREN/J.REDEKER	4/1/92
DRAWN	J.REDEKER	4/1/92
CHECKED	T.LAREN	4/1/92
APPROVED	R.DRINTON	5/1/92

NAME		DATE
CONCEPT	T.LACKOWSKI	
REVIEWED	A.TUBINAS S.DIXON	
REVIEWED	E.CRUMPLEY	
APPROVED	TOM PAWLAK WAYNE NESTANDER	
SUBMITTED	DIXON BOGERT	


SCALE:



1/8" = 1'-0"

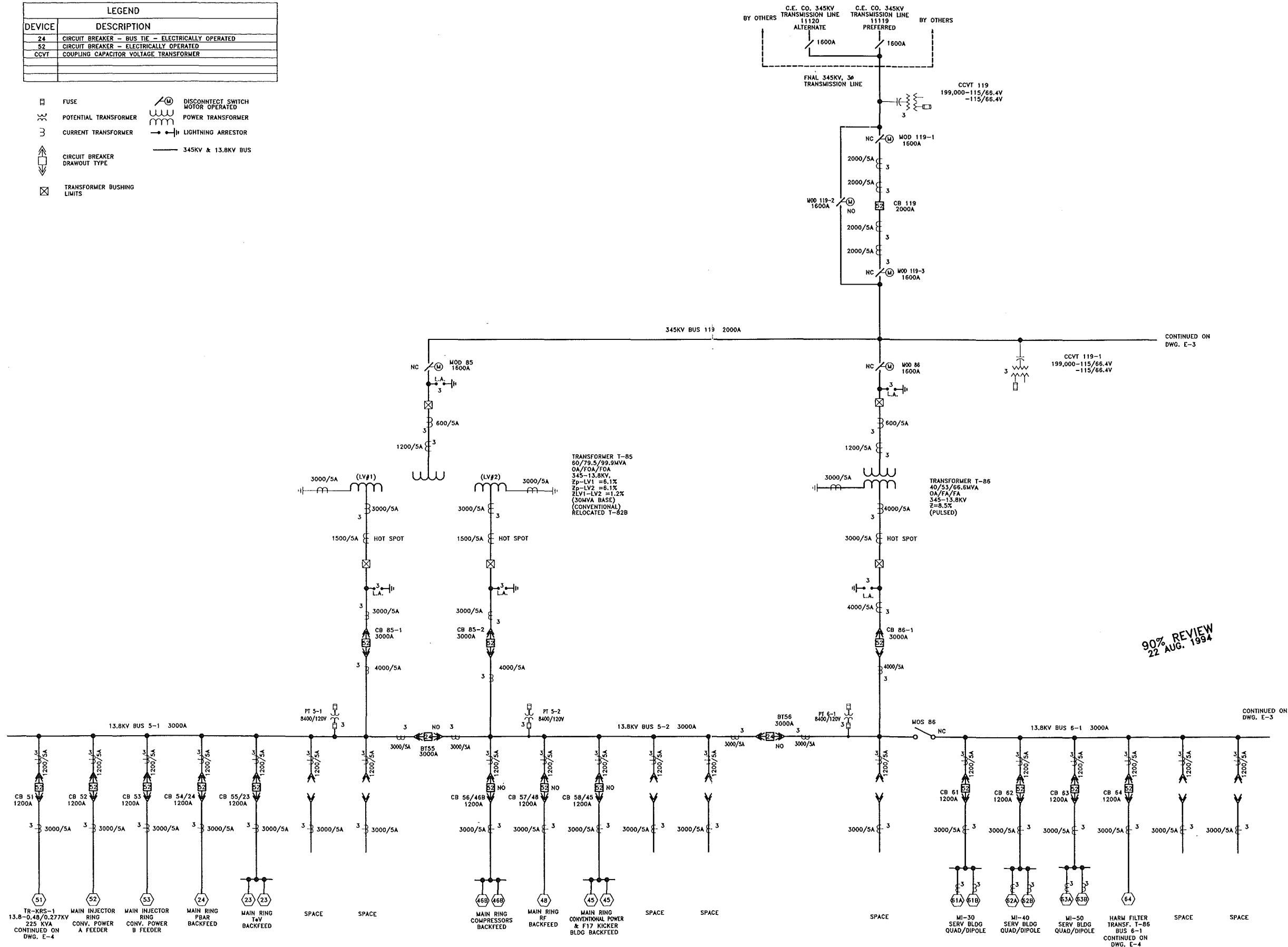
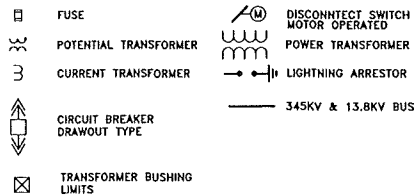
0 4 8 16

SCALE FEET

FERMI NATIONAL ACCELERATOR LABORATORY	
UNITED STATES DEPARTMENT OF ENERGY	
	MI-60 SERVICE BUILDING ELEVATIONS
DRAWING NO. 6-6-5	A-3 REV.

	9 FEB 1993
--	------------

LEGEND	
DEVICE	DESCRIPTION
24	CIRCUIT BREAKER - BUS TIE - ELECTRICALLY OPERATED
52	CIRCUIT BREAKER - ELECTRICALLY OPERATED
CCVT	COUPLING CAPACITOR VOLTAGE TRANSFORMER



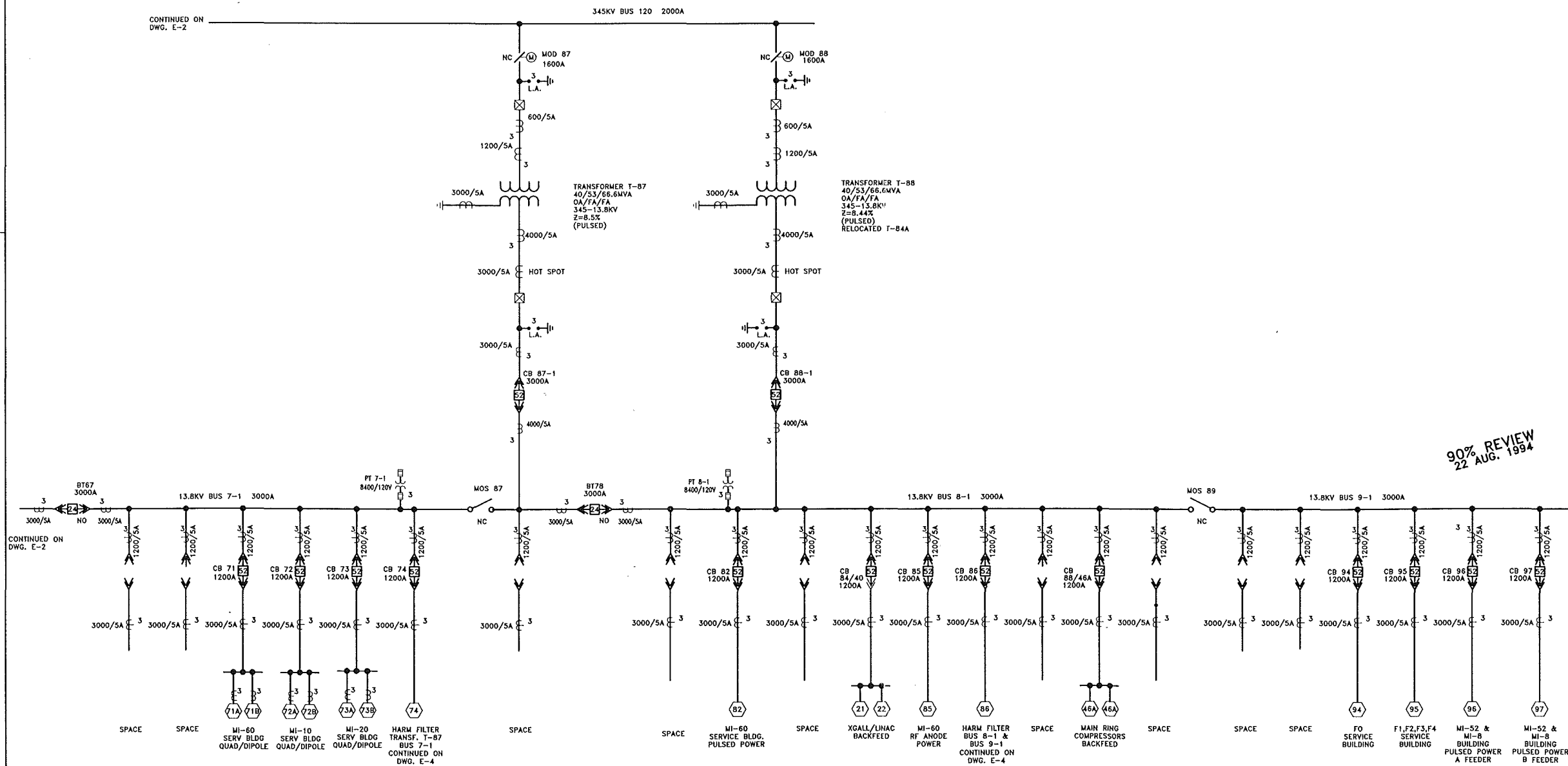
90% REVIEW
22 AUG. 1994

DWG: FL/PRA/442300/LLC/3000102 Plotter: 16AUG94 01:40:14p.m.

FLUOR DANIEL PROJECT NO. - 21842300		NAME: T. LACKOWSKI DATE: 8/17/92		SCALE: NONE		FERMI NATIONAL ACCELERATOR LABORATORY UNITED STATES DEPARTMENT OF ENERGY	
DESIGNED: Z. SILJKOVIC DATE: 8/17/92		REVIEWED: E. MORLAN		KAUTZ ROAD SUBSTATION 345-13.8KV SINGLE LINE SHT. 1		DRAWING NO. 3-6-17 E-2 REV.	
DRAWN: F. LATZKO		REVIEWED: E. CRUMPLEY					
CHECKED: J. SANTIC		APPROVED: TOM PAWLAK DAVID NEVIN					
APPROVED: J. SANTIC		SUBMITTED: DIXON BOGERT					

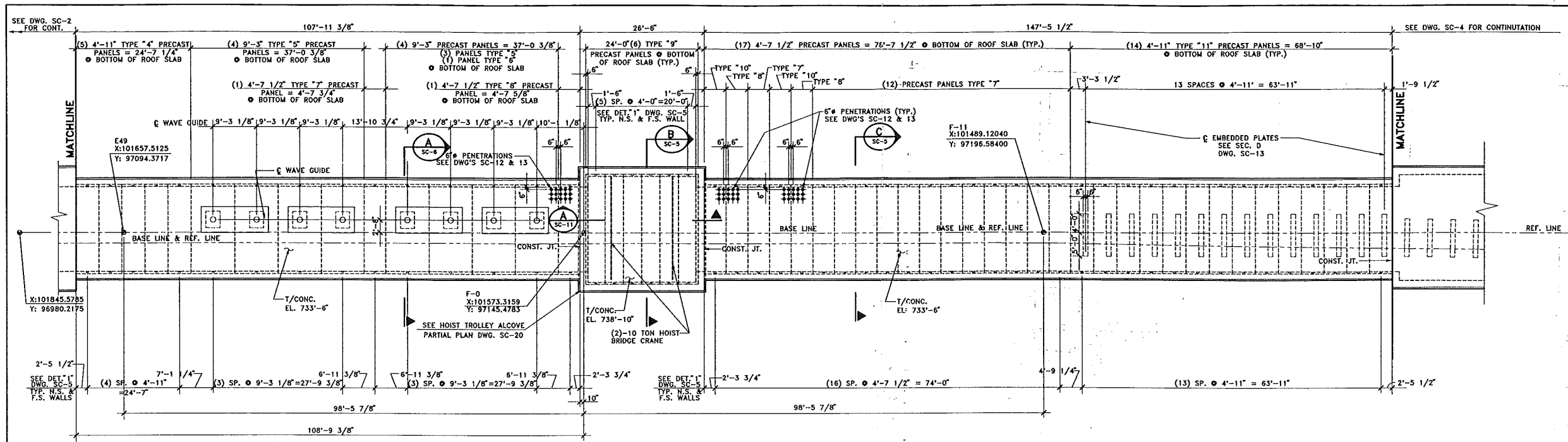
LEGEND	
DEVICE	DESCRIPTION
24	CIRCUIT BREAKER - BUS TIE - ELECTRICALLY OPERATED
52	CIRCUIT BREAKER - ELECTRICALLY OPERATED
CCVT	COUPLING CAPACITOR VOLTAGE TRANSFORMER

	FUSE		DISCONNECT SWITCH
	POTENTIAL TRANSFORMER		MOTOR OPERATED
	CURRENT TRANSFORMER		POWER TRANSFORMER
	CIRCUIT BREAKER		LIGHTNING ARRESTOR
	DRAWOUT TYPE		345KV & 13.8KV BUS
	TRANSFORMER BUSHING LIMITS		



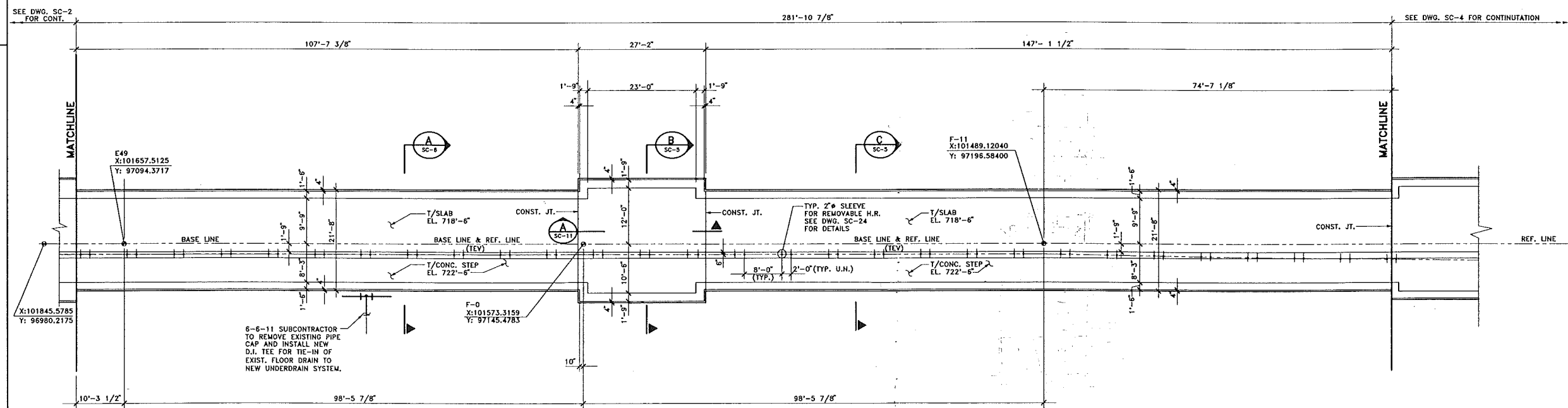
90% REVIEW
22 AUG. 1994

FLUOR DANIEL PROJECT NO. - 21842300		NAME T. LACKOWSKI		SCALE: NONE		FERMILAB NATIONAL ACCELERATOR LABORATORY UNITED STATES DEPARTMENT OF ENERGY	
DESIGNED Z. SILJKOVIC		REVIEWED E. MORLAN		DATE 8/17/92		KAUTZ ROAD SUBSTATION 345-13.8KV SINGLE LINE SH. 2	
DRAWN F. LATZKO		REVIEWED E. CRUMPLEY		DATE 8/17/92		DRAWING NO. 3-6-17	
CHECKED J. SANTIC		APPROVED TOM PAWLAK DAVID NEVIN		DATE 8/17/92		E-3	
APPROVED J. SANTIC		SUBMITTED DIXON BOGERT		DATE 8/17/92		REV.	



ROOF PLAN

1/8"=1'-0"



SLAB PLAN

1/8"=1'-0"

90% REVIEW
8 SEPT. 1994

DESIGNED: S. BARADI DRAWN: R. DELA CRUZ CHECKED: A. VASONIS APPROVED:		PROJECT NO. 21842300 DATE: 6/1/94 DATE: 6/1/94 DATE: 9/8/94		CONCEPT: T. LICKOWSKI REVIEWED: T. LICKOWSKI REVIEWED: E. CRUMPLEY APPROVED: TOM PAWLAK SUBMITTED: DIXON BOGERT		SCALE: 1/8"=1'-0" 		FERMILAB NATIONAL ACCELERATOR LABORATORY UNITED STATES DEPARTMENT OF ENERGY F-0 ENCLOSURE SLAB PLAN & ROOF PLAN - SHEET 2 DRAWING NO. 6-6-11 SC-3 REV.	
--	--	--	--	---	--	-----------------------	--	---	--

